Multicatalytic Cerium Photoredox Reactions for the Activation of O–H Bonds and Total Synthesis of (±)-Hyperolactone C

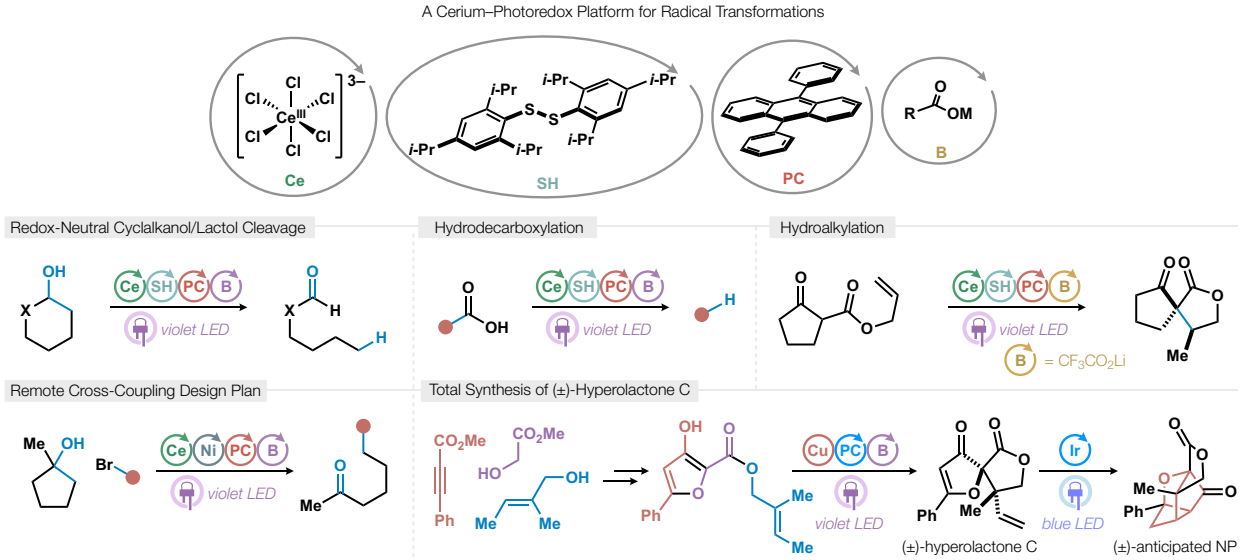
Avery Morris

Thesis submitted to the University of Ottawa
in partial Fulfillment of the requirements for the
Doctorate in Philosophy degree in Chemistry

Department of Chemistry and Biomolecular Sciences
Faculty of Science
University of Ottawa

© Avery Morris, Ottawa, Canada, 2026

Abstract



Radical chemistry enables a wealth of valuable organic transformations in organic synthesis. Photoredox catalysis has made entry into this high-energy radical regime more appealing and often reveals unique reactivity and functional-group tolerance. **Chapter 1** presents an overview of radical chemistry and the key role of photoredox catalysis in modern approaches to chemical synthesis. This thesis focused on the development of new photoredox platforms to access radical intermediates and their application in the synthesis of complex molecules.

In **Chapter 2**, a cerium photoredox platform was used to generate high energy *O*-centered radical intermediates from the native O–H bonds of common chemical feedstocks including alcohols, carboxylic acids, and 1,3-dicarbonyls. The multicatalytic system enabled a variety of redox-neutral transformations including fragmentation of lactols and cycloalkanols to the corresponding formate esters and ketones and hydrodecarboxylation. Synergistic application of cerium photoredox and nickel catalysis enabled a remote arylation reaction that furnished distal aryl and alkyl ketones *via* C(sp^2)–C(sp^3) and C(sp^3)–C(sp^3) cross-coupling in moderate to high yields without reliance on cycloalkanol ring-strain or redox-auxiliaries.

In **Chapter 3**, the photoredox platform was adapted to activate 1,3-dicarbonyl C(sp^3)–H acids, forming radical intermediates that performed a plethora of reactions including hydroalkylation, oxidative cyclization, and cross-coupling. The discovery of both cerium-containing and cerium-free conditions prompted detailed mechanistic experiments that gave insight into important reaction. Exploration of reaction scope and mechanistic studies helped to develop our understanding of the platform. NMR and UV/Vis spectroscopy revealed ground-state equilibria between

reaction components and the kinetics of thermal oxidation processes. Stern-Volmer fluorescence quenching experiments were used to elucidate the dominant photochemical events from catalyst excited states. Competition experiments and isotope studies helped determine the reaction path of organic substrates. Computational modelling was used to rationalize reaction outcomes including regio- and stereoselectivity, guided us in devising strategies for synthesis of more complex products, and ultimately enabled a total synthesis.

In **Chapter 4**, total synthesis of the natural product hyperolactone C displayed the utility of the photoredox platform in complex molecule synthesis. The hydroxyfuranoate intermediate was quickly assembled from abundant building blocks and enabled a 4-step synthesis, the shortest route to date. A Au(I)-catalyzed addition of glycolate esters to unsymmetrical propiolate esters, a previously underdeveloped hydroetherification reaction, and a Dieckmann condensation of the resulting *Z*-enol ether were developed to access hydroxyfuranoate esters. The densely functionalized spirolactone core with two contiguous stereocentres was constructed in the key final step using the oxidative photoredox cyclization that demonstrated remarkable tolerance for the oxidation-sensitive π-excessive furan heterocycle. Using the complementary redox-neutral hydroalkylation, we have also generated several analogues of this bioactive natural product. Inspired by the biosynthetic hypothesis for formation of biyouyanagin natural products, we performed an intramolecular [2+2] reaction to yield a 2-oxatricyclo[3.2.1.$0^{3,6}$]octane-bearing compound that may represent an undiscovered natural product.

Contribution to Original Research

Contributions to work described in this thesis

Chapter 2

The work towards redox-neutral ring scission and hydrodecarboxylation described in this chapter was carried out independently, with guidance from Louis Barriault. The initial investigations into the β-scission cross-coupling reaction were performed with some assistance from Tegan O'Brien (whose reactions are indicated by superscript symbol ***§***). Further work on the cross-coupling reaction was carried out by Dr. Timothée Stoerkler. Key contributions include:

- Conceptualization of the reaction and working catalytic hypothesis
- Initial screening, hit discovery, and optimization.
- Exploration of applicable chemical space & discovery of the $C(sp^3)$–$C(sp^3)$ cross-coupling
- Devised key control and competition reactions to probe the reaction mechanism & substrate tolerances

Chapter 3

The work described in this chapter was carried out in equal collaboration with Tegan O'Brien (whose reactions are indicated by superscript symbol ***§***), with guidance from Louis Barriault. Key contributions include:

- Conceptualization of reactions
- Initial screening, hit discovery, and optimization
- Substrate synthesis
- Exploration of reaction scope
- Design and execution of mechanistic studies (UV/vis, Stern-Volmer kinetics, isotopic labelling, KIE studies)

Chapter 4

The work described in this chapter was carried out in equal collaboration with Tegan O'Brien (whose reactions are indicated by superscript symbol ***§***), with guidance from Louis Barriault. Key contributions include:

- Identification of hyperolactone C as a target for synthesis
- Use of computational chemistry to predict regio- and diastereoselectivity in the key dearomative spirocyclization reaction, aiding synthetic design
- Retrosynthetic analysis, design and execution of synthetic sequence

- Optimization of Dieckmann condensation and transesterification
- Conceptualization and optimization of novel oxidative dearomative cyclization reaction
- Identification of distannoxane conditions necessary for transesterification of sensitive hydroxyfuranoate ester
- Identification of chromatography-free purification of silica-unstable hydroxyfuranoate esters
- Fully characterization of hydroxyfuranoate esters by NMR spectroscopy for the first time, as their instability/interconversion on the NMR timescale had eluded previous efforts
- Proposal and completion of natural product anticipation experiments

Published material related to the contents of this thesis

Articles published or accepted in peer-reviewed journals

Morris, A. O. and Barriault, L. (2024) Redox-Neutral Multicatalytic Cerium Photoredox-Enabled Cleavage of O–H Bearing Substrates. *Chemistry – A European Journal. 30*: e202400642. (Original research; PhD work; published 4 March, 2024; Contribution: 81–90% – designed project, planned and performed all experiments, prepared manuscript and supporting information)

Morris, A. O., O'Brien, T. E., Barriault, L. (2025) Photoredox-Catalyzed Hydroalkylation of C(sp^3)–H Acids. *Chemistry – A European Journal.*, e202501148. ((Original research; PhD work; published 7 April, 2025; Contribution: 50% – in equal collaboration with TO: designed project, planned and performed all experiments, prepared manuscript and supporting information)

Other peer-reviewed contributions

O'Brien T. E.,† **Morris A. O.**,† Villela, L. F.,† and Barriault, L. (2023) Synthetic Applications of Photochemically Generated Radicals from Protic C(sp3)−H Bonds *ChemCatChem*. *15*: e202300989. (Review; published 6 November, 2023; Contribution: 31–40% – searched primary literature, organized and analyzed articles, prepared manuscript) †these authors contributed equally

Non-peer-reviewed contributions

Morris, A. O.,† O'Brien, T. E.,† and Barriault, L. (2024) Photoredox-Catalyzed Activation of C(sp^3)–H Acids and Total Synthesis of Hyperolactone C. *ChemRxiv.* (Original research, PhD work, pre-print article; Contribution: 41–50% – designed project, planned and performed experiments, prepared manuscript and supporting information) †these authors contributed equally

Presentations

106th Canadian Chemistry Conference and Exhibition (CCCE/CSC 2023) (National) **Morris, A. O.,*** and Barriault, L. *Remote Arylation of Cycloalkanols through Cerium and Nickel Metallaphotoredox Catalysis*. Poster Presentation

CCRI – Centre for Catalysis Research and Innovation Seminar Series (2022) (Institutional) **Morris, A. O.,*** O'Brien, T. E., and Barriault, L. *Multicatalytic Redox-Neutral Transformations Enabled by Cerium Photoredox.* Oral Presentation

32nd Quebec-Ontario Mini-Symposium for Synthetic and Bioorganic Chemistry (QOMSBOC 2022) (Interprovincial) **Morris, A. O.,*** O'Brien, T. E., and Barriault, L. *A Mulitcatalytic Cerium-Based Photoredox Platform for Redox Neutral Transformations.* Poster Presentation

105th Canadian Chemistry Conference and Exhibition (CCCE/CSC 2022) (National) **Morris, A. O.,*** O'Brien, T. E., and Barriault, L. *Multicatalytic Redox-Neutral Transformations Enabled by Cerium Photoredox.* Oral Presentation

31st Quebec-Ontario Mini-Symposium for Synthetic and Bioorganic Chemistry (QOMSBOC 2021) (Interprovincial) **Morris, A. O.,*** and Barriault, L. *Multicatalytic Cerium–HAT Photoredox Catalyzed C–C Cleavage of Lactols.* Poster Presentation

Material unrelated to the contents of this thesis

Articles published or accepted in peer-reviewed journals

Zidan, M., **Morris, A. O.**, McCallum, T., and Barriault, L. (2020) The Alkylation and Reduction of Heteroarenes with Alcohols Using Photoredox Catalyzed Hydrogen Atom Transfer via Chlorine Atom Generation. *European Journal of Organic Chemistry* 1453–1458. (Original research; BSc/MSc work prior to transfer to PhD; published 18 July, 2019; Contribution: 31–40% – planned and performed experiments, prepared manuscript and supporting information)

Rohe, S.,† **Morris, A. O.,**† McCallum, T.,† and Barriault, L. (2018) Hydrogen Atom Transfer Reactions via Photoredox Catalyzed Chlorine Atom Generation. *Angewandte Chemie International Edition. 57* (48): 15664–15669. (Original research; BSc/MSc work prior to transfer to PhD; published 8 October, 2018; Contribution: 41–50% –

planned and performed experiments, prepared manuscript and supporting information) †these authors contributed equally

Rohe, S., McCallum, T., **Morris, A. O.**, and Barriault, L. (2018) Transformations of Isonitriles with Unactivated Bromoalkanes using Photoredox Gold Catalysis. *Journal of Organic Chemistry. 83* (17): 10015–10024. (Original research; BSc work; published 6 July, 2018; Contribution: 31–40% – planned and performed all experiments, prepared manuscript and supporting information)

Non-peer-reviewed contributions

O'Brien, T. E.,† **Morris, A. O.**,† and Barriault, L. (2024) 1.10 - Selected Diastereoselective Reactions: Ionic and Zwitterionic Cyclizations. in *Comprehensive Chirality (Second Edition)* (Ed.: J. Cossy), Academic Press, Oxford, 295-311. (Textbook chapter; published 17 May, 2024; Contribution: 41–40% – searched primary literature, organized and analyzed articles, prepared manuscript) †these authors contributed equally

Presentations

30th Quebec-Ontario Mini-Symposium for Synthetic and Bioorganic Chemistry (QOMSBOC 2019) (Interprovincial) **Morris, A. O.,*** Zidan, M., McCallum, T., and Barriault, L. *Photoredox-Mediated Alkylation and Reduction of Heteroarenes.* Poster Presentation

102nd Canadian Chemistry Conference and Exhibition (CCCE/CSC 2019) (National) **Morris, A. O.,*** Rohe, S., McCallum, T., and Barriault, L. *Hydrogen Atom Transfer Through Dual Photoredox and Atomic Chlorine Catalysis.* Poster Presentation

101st Canadian Chemistry Conference and Exhibition (CCCE/CSC 2018) (National) **Morris, A. O.,*** Zidan, M., McCallum, T., and Barriault, L. *Photoredox-Mediated Alkylation and Reduction of Heteroarenes.* Poster Presentation (Prize Winner)

Acknowledgements

Louis, thank you for the opportunity to begin my synthesis journey in your lab. Your mentorship and passion for chemistry have shaped me into the scientist I am today. The environment you have created was the perfect place to begin my career by stoking curiosity and creativity. I am especially grateful for the patience and support with which you have fostered independent research pursuits.

To my thesis advisory committee: Professors Gagosz, Beauchemin, and Scaiano, I thank you for your guidance and your time over the years. I have had the pleasure of learning from each of you. I wish to thank Fabien, in particular, for years of valuable discussions in and out of group meetings, including conference presentation preparations and career advice. Your wealth of scientific knowledge is inspiring and you have taught me a great deal about critical thinking and mechanistic understanding. I also wish to thank Professor Collins for serving as my external examiner.

A huge thank you goes out to all the excellent uOttawa technical and support staff, without whom this thesis would be devoid of data: Jeff Ovens, Sara Osterholm, Glenn Facey, Peter Pallister, Patrick Szell, Vincent Morin, Volodymyr Semeniuchenko, Sharon Curtis, Roxanne Clément, Nicholas Mrazek, and Ian Myers. A special thank you to Dr. Neeraj Joshi for teaching me practical skills and guiding me through some of the pitfalls of fluorimetry and UV-vis spectroscopy. Thank you to Patrick Szell and Volodymyr Semeniuchenko for helping Tegan and I to get beautiful NMR spectra of 3-hydroxyfuranoate esters for the first time, and for assisting us in obtaining unlocked acetonitrile experiments.

To all my lab mates past and present, thank you for making this experience so enjoyable. Doctors Terry M^{c}Callum and Montserrat Zidan, thank you both for teaching me the way of chemistry and photoredox catalysis. You both exposed me to so many new ideas and techniques and guided me into the world of research which has become my passion. Alyson Poyser, thank you for making the beginning of this journey so fun, it was nice to share it with someone! Martin Hébert, thank you for the numerous discussions about chemistry and synthesis, I learned a lot that I would not have been exposed to otherwise. Huy Tran, thank you for being a rockstar and a calming and wise presence in the chaos that is my approach. Julie Brousseau, thank you for bringing such vivacious energy to the lab each day and for sharing your chemical expertise and intuition, and for the cat pictures/stories. André Costisella, thank you for the insightful discussions about science, careers and life, it was a joy to work alongside such an excellent chemist/human being. Lucas Facuri Villela, thank you for bringing so much levity to every situation, you have a talent

for cheering people up and it has been a pleasure watching you grow as a scientist. Christopher Grant Wicks, thank you for being such an all-around great person and for bringing your social skills to our group/department, also for your enthusiasm and insights into all things chemistry. Vamika Kaushal, thank you for being such a stellar student and for always brightening my day, it has been a great joy to see you transform from a new student in the research lab to a confident and independent professional at the dawn of your career. Special thanks to Dr. Timothée Stoerkler for carrying on the cross-coupling project with such skill and vigor. Thanks to all the other Barriault students I have shared the lab with, it has been a pleasure, and I have learned something from each of you: Mathieu Morin, Philippe McGee, Michael Forberg, Sam Rohe, Victor Borba, Jason Crema, Chad Normandin, Soufian Tibouti, Joshua Tapp, and others who have passed through here!

Tegan O'Brien deserves extra thanks for being my partner in crime throughout my studies. I can honestly say that I could not have done this without you. You have been an ally and supporter and a tireless collaborator with which to discuss, plan, and execute scientific ideas. You have made each part of our collaboration fun and exciting. I am grateful to have experienced this journey with you and cannot imagine this degree without your guidance, enthusiasm, or jokes. I look forward to our continued collaboration in the future.

Thank you to all the Barriault lab undergraduate students I have had the pleasure of interacting with over the years: Britt Halvorsen, Elliot Jackson, Victor Boddy, Kian Mansour, Akvilė Mažeikaitė, Eleni Karaiskos, Kiara Britto, Patrick Ferrari, Weldon Blastorah, Kéliane Levesque, Anna Korobkow, Ève Bergeron. I would like to thank those students I have personally supervised who inspired a love for teaching in me including Vamika, Britt, Kéliane, Kiara, Victor, Eleni, and Weldon.

Thanks to our Gagosz lab kin for many scientific discussions, celebrations, and shared trips; our door is eternally locked for you, but you may always knock. I want to give special thanks to Dominic Campeau, Karim Muratov, and Alice Pommainville, you guys made this degree a treat with conference trip movie nights and adventures in exotic locales. Thanks again to Dom for being a humble genius, DFT guru, and funny guy.

To the friends and family that have helped me to retain some semblance of normality through this challenging time. Thank you for getting me out of the lab to play games and go on adventures Olivier & Lindsay, and Faith. To my sister Mackenzie, thank you for reminding me of what's important and for grounding me. Your adventures have inspired me to look forward to a balanced life post-graduate studies. Along with Dustin, thank you both for the fun times playing games, having chats, and sharing holidays, you brightened each of them. To my Mother and Father,

Nancy & Kevin, thank you for your constant support, it has kept me going and I don't know where I would be without your help. You two have instilled in me a deep sense of responsibility for the commitments I make and taught me diligence, and I believe these lessons have served me well throughout my studies and will continue to do so for the rest of my life. To all the feline fur-riends who have helped me to this point, I am indebted eternally: Aura, Ivy, Pekoe, Raphael, Nova, Zora, Smokey, and Boogey. A huge thank you to Jerome and Annette for your hospitality and support over the years, I can officially say this degree is almost complete. To my partner and best-friend Sara Sparks whose unwavering support has gotten me through countless times of tumult and centered me for those of calm, I cannot express all that you have done for me. Your grounding presence has brought me back to reality more times than I can count and has kept me laughing through it all. I look forward to our continued adventures together.

Table of Contents

Abstract ii

Contribution to Original Research iv

Acknowledgements viii

Table of Contents xi

List of Figures xiii

List of Schemes xv

List of Tables xvii

List of Abbreviations xix

Chapter 1 Introduction 1

1.1 Introduction to Photochemistry 1

1.2 Introduction to Photoredox Catalysis 3

1.3 Introduction to Radical Chemistry 16

Chapter 2 Redox-Neutral Cerium Photoredox-Enabled Cleavage of O−H Bearing Substrates 22

2.1 Introduction 22

2.2 Initial Studies & Optimization 27

2.3 Hydroxyl Ring β-Scission Scope 33

2.4 Mechanistic Investigations 44

2.5 B-Scission Cross-Coupling Investigations 47

2.6 Direct Photoredox Catalyzed Hydrodecarboxylations 59

2.7 Hydrodecarboxylation Scope 60

2.8 Conclusions & Future Directions 61

Chapter 3 Photoredox-Catalyzed Hydroalkylation of C(sp^3)–H Acids 62

3.1 Introduction 62

3.2 Project Motivation 74

3.3 Initial Investigations and Optimization 77

3.4 Intramolecular Hydroalkylation Scope 84

3.5 Intermolecular Hydroalkylation Scope 90

3.6 Mechanistic Investigations 94

3.7 Computational Investigations 104

Chapter 4 Total Synthesis of Hyperolactone C 111

4.1 Introduction 111

4.2 Retrosynthetic Analyses for the Redox-Neutral Hydroalkylative Synthesis of (±)-Hyperolactone C 114

4.3 Synthesis of Diene-Containing Fragments 117

4.4 Synthesis of Enol Ether Derivatives 124

4.5 Furanoate Ester Synthesis and Derivatizations 136

4.6 Rethinking the Dearomative Radical Spirocyclization 143

4.7 Oxidative Cyclization Reaction Development....147
4.8 Completion of the Total Synthesis of (±)-Hyperolactone C and Derivatives....150
4.9 Application of (±)-Hyperolactone C towards Natural Product Anticipation....152
4.10 Comparison of Hyperolactone C Total Syntheses....157
Conclusions....161
Chapter 5 Experimental....165
5.1 General Information....165
5.2 Chapter 2 Experimental Details....166
5.3 Chapter 3 Experimental Details....210
5.4 Chapter 4 Experimental Details....288
5.5 Supplemental Experimental Details....309
References....314
Appendix A Computational Data....354
Appendix B Crystallographic Data....416
Appendix C NMR Spectra....418

List of Figures

Figure 1. Generic Jablonski diagram illustrating some photophysical processes. 1
Figure 2. A general overview of photocatalysis. 4
Figure 3. Photocatalysts and their excited states. 7
Figure 4. Redox potential diagram for relevant species. 9
Figure 5. Cerium(III) photochemistry. 10
Figure 6. Ce(IV) Photochemistry and LMCT catalysis. 11
Figure 7. Cerium LMCT photoredox reaction timeline and examples. 12
Figure 8. PCET Theory and an example. 15
Figure 9. Timeline of a selection of notable advances in synthetic organic radical chemistry. 17
Figure 10. Radical structure and reactivity. 20
Figure 11. Hemiacetal ring-chain tautomerism and factors affecting alkoxyl radical β-scission propensity. 22
Figure 12. β-scission of hydroxyl-containing molecules. 24
Figure 13. Principles and applications of cycloalkanol ring scission. 26
Figure 14. Preparation of lactones used to access lactol substrates. 34
Figure 15. Lactol substrate preparations. 37
Figure 16. Redox-neutral lactol/cycloalkanol ring β-scission scope 39
Figure 17. Ring-scission product derivatizations. 42
Figure 18. Attempted synthesis of phoracantholide I by redox-neutral ring-scission and comparison to oxidative conditions. 43
Figure 19. Unsuccessful substrates in the redox-neutral ring-scission reaction. 44
Figure 20. Tentative multicatalytic cycle for the redox-neutral lactol/cycloalkanol ring β-scission reaction. 45
Figure 21. Mechanistic investigations. 46
Figure 22. Photoredox catalyzed ring-cleaving remote arylation of cycloalkanols. 48
Figure 23. Catalytic hypothesis. 49
Figure 24. Direct photoredox-catalyzed proto- and deuterodecarboxylations. 60
Figure 25. Substrate scope for the cerium photoredox catalyzed hydrodecarboxylation of native carboxylic acids. 61
Figure 26. Radical activation of C(sp^3)–H acids. 62
Figure 27. A brief timeline (1940s – 2000s) of landmark publications for radical generation from C(sp^3)–H acids and their hydroalkylation. 65
Figure 28. Radical polarity examples and considerations. 67
Figure 29. Direct photoexcitation α-alkylations of carbon acids with olefins. 69
Figure 30. Indirect photo-initiated α-alkylations of carbon acids. 71
Figure 31. Photoredox catalyzed α-alkylations of carbon acids using olefins. 73
Figure 32. Project inspiration. 75
Figure 33. Product inhibition investigation. 82
Figure 34. Intramolecular hydroalkylation reaction scope 87

Figure 35. Failed intramolecular hydroalkylation substrates. 89
Figure 36. Intermolecular hydroalkylation reaction scope..... 92
Figure 37. Reaction variants and mechanistic probes based on the photocatalytic hydroalkylation reaction. 93
Figure 38. Assessing the fate of LiTFA under stoichiometric and catalytic photolysis conditions through ^{19}F NMR spectroscopy. All resonances present in the spectra are shown. 95
Figure 39. 9,10-DPA steady-state emission quenching. 99
Figure 40. NMR binding studies of hydroalkylation reaction components. 100
Figure 41. UV-vis Ce(IV)thermal decay profiles over time in the dark at room temperature. 101
Figure 42. UV-vis Ce(IV)thermal decay profiles over time in the dark at room temperature. 102
Figure 43. Conformers of the ketolactone diastereomers **3.59a**. Searched for at the uM06-2X/LanL2DZ level.... 105
Figure 44. Reaction coordinate for the spirocyclizing hydroalkylation of allyl 2-oxocyclopentane carboxylate (**3.59a**). 109
Figure 45. Hyperolactone C Background. 113
Figure 46. Elimination of the 1,4-dibromoolefin. 119
Figure 47. Ketoester enolate alkylation intricacies. 126
Figure 48. O-alkylation of ethyl benzoylacetate. 128
Figure 49. Early attempts at enol ether synthesis through coinage-metal catalysis. 130
Figure 50. Z-Selective Mizoroki-Heck coupling of β-alkoxy acrylate esters. 132
Figure 51. Dieckmann condensation success and 3-hydroxyfuranoate ester characteristics. 139
Figure 52. Transesterifications of furanoate esters..... 142
Figure 53. Redox-neutral hydroalkylation prospects. 143
Figure 54. uM06-2X/LanL2DZ reaction coordinate for the redox-neutral hydroalkylation of diene furanoate ester 145
Figure 55. Alternative radical cyclization strategies for the preparation of hyperolactone C. 147
Figure 56. Tentative catalytic cycle for the oxidative cyclization reaction. 148
Figure 57. Böttcher complexity score plotted against steps until hyperolactone C. 158
Figure 58. Representative ^{1}H NMR spectrum for the KIE experiment (mixture of rotamers of 6a & 6a-d). 209
Figure 59. Absorbance of $[Et_4N]_2[Ce^{IV}Cl_6]$ at 378 nm with varying concentration 277
Figure 60. Complexity of synthetic intermediates (Böttcher Score, C_m) against normalized step count (step/max. step)..... 305
Figure 61. Complexity of synthetic intermediates (Böttcher Score, C_m) against total step count, expressed as steps remaining until target..... 306

List of Schemes

Scheme 1. Neophyl rearrangement reaction mechanism and approximate rearrangement rate. 28
Scheme 2. Synthesis of authentic cross-coupling target compound. 50
Scheme 3. Remote arylation reaction benchmark using Zuo's conditions for dehydroymethylation arylation. 56
Scheme 4. Attempted remote arylation under Knowles-like photoredox-catalyzed PCET activation conditions. 58
Scheme 5. Remote arylation optimized conditions. 58
Scheme 6. Unoptimized attempt at remote $C(sp^3)$–$C(sp^3)$ cross-coupling of methylcyclopentanol and 1-bromo-3-phenylpropane. 59
Scheme 7. Redox schemes for the spirocyclizing addition in Andre Costisella's approach towards the penostatins. 76
Scheme 8. β-ketoesters keto-enol tautomerism and application of Ce-photoredox catalysis for mesomeric O-radical generation. 76
Scheme 9. General synthesis of β-ketoester substrates through transesterification or Claisen condensation. 84
Scheme 10. A) Synthesis of the bicyclic diene ketoester **3.59f** through a Stork-Danheiser transposition approach; B) Stereochemical considerations for the radical cyclization; C) Curran and Rakiewicz's radical cyclization cascade in the synthesis of (±)-hirsutene. 85
Scheme 11. Synthesis of 3-hydroxy-benzofuran-2-oate esters through Dieckmann condensation of salicylate diesters. 86
Scheme 12. Proposed Ce-containing hydroalkylation catalytic cycles. 103
Scheme 13. Proposed Ce-free hydroalkylation catalytic cycles. 104
Scheme 14. Retrosynthetic analysis tree for the total synthesis of (±)-hyperolactone C via redox-neutral hydroalkylation key step. 114
Scheme 15. A) diene glycolate ester and B) diene carbonate/carbamate retrosynthetic analyses. 116
Scheme 16. Preparation of diene glycolate ester via isoprene bromination. 118
Scheme 17. Substitution regioselectivity assessment using potassium glycolate and 1,4-dibromoolefin. 120
Scheme 18. Synthesis of diene glycolate ester via 3-methylsulfolene route. 121
Scheme 19. Preliminary attempts to synthesize 2-(hydroxymethyl)-1,3-butadiene. 122
Scheme 20. Alternative synthetic sequences utilizing 3-(bromomethyl)sulfolane. 124
Scheme 21. Synthesis of 5-phenyl-3(2H)-furanone and attempted elaborations. 129
Scheme 22. Au(I)-catalyzed addition of glycolate esters on methyl phenylpropiolate. 136
Scheme 23. Attempted synthesis of (±)-hyperolactone C through a redox-neutral hydroalkylation/SO_2 extrusion cascade. 143
Scheme 24. Four-step total synthesis of (±)-hyperolactone C through oxidative cyclization. 150
Scheme 25. Synthesis of unnatural analogues of (±)-hyperolactone C through redox-neutral hydroalkylation. 151
Scheme 26. Nicolaou, Sarlah, and Shaw's biomimetic [2+2]-photocycloaddition in the synthesis of (–)-biyouyanagin A. [238d] 153
Scheme 27. Intramolecular [2+2]-photocycloaddition of (±)-hyperolactone C and other photochemical syntheses of tricyclo[3.2.1.$0^{3,6}$]octanes. 156

Scheme 28. Total synthesis of hyperolactone C by Kinoshita and coworkers (2001) [238b] with computed Böttcher scores (C_m) 307
Scheme 29. Total synthesis of hyperolactone C by Kraus and coworkers (2004) [238c] with computed Böttcher scores (C_m) 307
Scheme 30. Total synthesis of hyperolactone C by Hodgson and coworkers (2008) [238e] with computed Böttcher scores (C_m) 307
Scheme 31. Total synthesis of hyperolactone C by Nicolaou and coworkers (2000)[238d] with computed Böttcher scores (C_m) 308
Scheme 32. Total synthesis of hyperolactone C by Xie and coworkers (2009 [238g] with computed Böttcher scores (C_m) 308
Scheme 33. Total synthesis of hyperolactone C by Hodgson and coworkers (2011)[238i] with computed Böttcher scores (C_m) 308
Scheme 34. Total synthesis of hyperolactone C by Xie and coworkers (2018)[238m] with computed Böttcher scores (C_m) 309

List of Tables

Table 1. Preliminary redox-neutral lactol ring scission attempt and control reactions. 27
Table 2. Reaction optimization: solvent study. 29
Table 3. Reaction optimization: secondary photocatalyst, inorganic base additive, and halide salt studies. 30
Table 4. Reaction optimization: Ce-loading and reaction concentration studies. 30
Table 5. Reaction optimization: miscellaneous screening. 32
Table 6. Reaction optimization: weak base additive screening. 32
Table 7. Reaction optimization: initial investigations. 52
Table 8. Reaction optimization: Solvent study. 53
Table 9. Reaction optimization: aryl carboxylate/sulfonate additive study. 54
Table 10. Reaction optimization: nickel ligand study. 55
Table 11. Reaction optimization: superstoichiometric base study. 56
Table 12. Reaction optimization: miscellaneous reactions using methyl cyclopentanol and methyl 4-bromobenzoate. 57
Table 13. Controls and optimization of the redox-neutral hydroalkylation 77
Table 14. Optimization of redox-neutral hydroalkylation: solvent. 79
Table 15. Optimization of redox-neutral hydroalkylation: Catalyst loadings and concentrations 79
Table 16. Optimization of redox-neutral hydroalkylation: Additives and reaction duration 81
Table 17. Optimization of redox-neutral hydroalkylation: Light source comparisons 83
Table 18. Photon flux determination using potassium ferrioxalate chemical actinometry. 96
Table 19. Ce-containing conditions (A) quantum yield – Assuming no IFE from $(TRIPS)_2$. 97
Table 20. Ce-free conditions (B) quantum yield – Assuming no IFE from $(TRIPS)_2$ 97
Table 21. Reaction component solubilities in acetonitrile at room temperature. 98
Table 22. Ce-containing conditions (A) quantum yield – Assuming supersaturated $(TRIPS)_2$. 98
Table 23. Ce-free conditions (B) quantum yield - Assuming supersaturated $(TRIPS)_2$. 98
Table 24. Z-selective Heck-coupling investigations 133
Table 25. Optimization of the Au(I)-catalyzed 1,4-addition of allyl glycolate to methyl phenylpropiolate 134
Table 26. Dieckmann condensation investigations with mixed diesters. 138
Table 27. Oxidative cyclization optimization 149
Table 28. Photon flux determined by actinometry 273
Table 29. Quencher solutions prepared for fluorescence quenching experiments 275
Table 30. Results of Stern–Volmer quenching experiments 276
Table 31. Solutions prepared for thermal Ce^{IV} decay studies 277
Table 32. Results of thermal Ce^{IV} decay studies in acetonitrile solution 277
Table 33. Results of thermal Ce^{IV} decay studies in acetonitrile solutions including TBACl (0.2 M) 279
Table 34. Results of UV/Vis spectroscopy of reaction components in acetonitrile at various concentrations 280
Table 35. Titration solutions prepared for NMR studies 283

Table 36. NMR signals of interest for reaction component titrations 283
Table 37. Results of NMR titrations 284
Table 38. LiTFA fate studies 287

List of Abbreviations

°C	degrees Celsius
Å	angstrom(s)
δ	chemical shift in parts per million downfield from tetramethylsilane
Δ	heat
μ	micro
Abs	absorption
Ac	acetyl
Acac	acetylacetonate
Ad	adamantyl
AIBN	2,2'-azobisisobutyronitrile
anh	anhydrous
AO	atomic orbital
approx.	approximate(ly)
aq	aqueous
Ar	aryl
ATRA	atom transfer radical addition
atm	atmosphere(s)
BDE	bond dissociation enthalpy
BET	back electron transfer
BHT	2,6-di-*tert*-butyl-4-methylphenol
BINAP	2,2'-bis(diphenylphosphino)-1,1'-binaphthyl
BiOX	bioxazoline
Bn	benzyl
Boc	*tert*-butoxycarbonyl
BOM	benzyloxymethyl
BOX	Bis(oxazoline)
bp	boiling point
br	broad (spectral)
Bu, *n*-Bu	normal (primary) butyl
BVO	Baeyer–Villiger oxidation
Bz	benzoyl
cal	calorie (unit)
CAM	cerium ammonium molybdate stain
CAN	ceric ammonium nitrate
cat.	catalytic
Cbz	benzyloxycarbonyl
CCDC	Cambridge Crystallographic Data Centre
CD	circular dichroism
CDI	1,1'-carbonyldiimidazole
CI	configuration interaction
CIF	crystallographic information file
cm	centimeter(s)
cm^{-1}	wavenumber(s)
cod	1,5-cyclooctadiene
conc	concentration
conv.	conversion
COSY	correlation spectroscopy
Cp	cyclopentadienyl
CSA	camphorsulfonic acid
CT	charge transfer
CV	cyclic voltammetry
Cy	cyclohexyl
d	day(s); doublet (spectral); deci
d	density
DA	Diels–Alder
DABCO	1,4-diazabicyclo[2.2.2]octane
dba	dibenzylideneacetone
DBU	1,8-diazabicyclo[5.4.0]undec-7-ene
DCC	*N,N'*-dicyclohexylcarbodiimide
DCE	1,2-dichloroethane
DCM	dichloromethane
DDQ	2,3-dichloro-5,6-dicyano-1,4-benzoquinone
de	diastereomeric excess
DEAD	diethyl azodicarboxylate
DEPT	distortionless enhancement by polarization transfer

DFT	density functional theory
DIBAL	diisobutylaluminum hydride
dil	dilute
DIPEA	diisopropylethylamine
DMA	dimethylacetamide
DMAP	4-(*N,N*-dimethylamino)pyridine
DMDO	dimethyldioxirane
DME	1,2 -dimethoxyethane
DMF	dimethylformamide
DMP	Dess-Martin periodinane
DMPU	1,3-dimethyl-3,4,5,6-tetrahydro-2(1*H*)-pyrimidinone
DMSO	dimethylsulfoxide
DNA	deoxyribonucleic acid
DPA	diphenylanthracene
dr	diastereomeric ratio
E	entgegen olefin geometry
E1	unimolecular elimination
E2	bimolecular elimination
EC50	half maximal effective concentration
EDTA	ethylenediaminetetraacetic acid
ee, er	enantiomeric excess, enantiomeric ratio
e.g.	for example
EI	electron impact
equil.	equilibrium
equiv	equivalent
ESI	electrospray ionization
ESR, EPR	electron spin resonance, electron paramagnetic resonance
Et	ethyl
ET	electron transfer
et al.	and others
etc.	and so forth
eV	electron volt (unit)
Fc	ferrocene
FID	flame ionization detector
Fmoc	9-fluorenylmethoxycarbonyl
FRET	Förster resonance energy transfer
g	gram (unit)
GC	gas chromatography
[H]	reduction
h	hour (unit)
hν	light
HAT	hydrogen atom transfer
HBA	hydrogen bond acceptor
HBD	hydrogen bond donor
HF	Hartree–Fock
HMBC	heteronuclear multiple bond correlation
HMDS	hexamethyldisilazane
HMPA	hexamethylphosphoramide
HMQC	heteronuclear multiple quantum correlation
HOMO	highest occupied molecular orbital
HPLC	high-performance liquid chromatography
HRMS	high-resolution mass spectrometry
HSQC	heteronuclear single quantum correlation
Hz	hertz (cycles/sec) (unit)
IBX	2-iodoxybenzoic acid
IC	internal conversion
ID	inhibitory dose
IP	ionization potential
iPr	isopropyl
IR	infrared
ISC	intersystem crossing
J	coupling constant (spectral)
K	kelvin (unit)
k	kilo
L	liter (unit)
LAH	lithium aluminium hydride
LC	liquid chromatography
LD	lethal dose
LDA	lithium diisopropylamide

LED	light emitting diode
LFER	linear free energy relationship
lit.	literature value
LLS	longest linear sequence
LMCT	ligand to metal charge transfer
LTA	Lead tetraacetate
LUMO	lowest unoccupied molecular orbital
m	meter (unit); multiplet (spectral); milli
m	*meta*
M	molar (unit), parent molecular ion, mega, metal
m/z	mass-to-charge ratio
max.	maximum
*m*CPBA	*meta*-chloroperoxybenzoic acid
Me	methyl
Mes	2,4,6-trimethylphenyl (mesityl)
min	minute (unit)
min.	minimum(s)
misc.	miscellaneous
MLCT	metal-to-ligand charge transfer
MO	molecular orbital
mol	mole (unit)
MOM	methoxymethyl
m.p.	melting point
MS	mass spectrometry
Ms	methanesulfonyl (mesyl)
M.S.	molecular sieves
MS-PCET	multi-site proton coupled electron transfer
MW	molecular weight
n	nano, number
NBS	*N*-bromosuccinimide
NCS	*N*-chlorosuccinimide
NHE	normal hydrogen electrode
NHPI	*N*-hydroxyphthalimide
NICS	nucleus-independent chemical shift
NMO	*N*-methylmorpholine-*N*-oxide
NMP	*N*-methylpyrrolidone
NMR	nuclear magnetic resonance
nOe	nuclear Overhauser effect
NOESY	2D nuclear Overhauser effect spectroscopy
NP	natural product
NRCC	National Research Council of Canada
Nu	nucleophile
[O]	oxidation
o	*ortho*
org.	organic
p	pico
p	*para*
Pa	pascal (unit)
PAH	polyaromatic hydrocarbons
PAN	9-cyano-10-phenylanthracene
PC	photocatalyst
PCC	pyridinium chlorochromate
PCET	proton-coupled electron transfer
PDC	pyridinium dichromate
PET	photoinduced electron transfer
Ph	phenyl
Phth	phthalamidyl
PMB	p-methoxybenzyl
ppb	parts per billion (unit)
ppm	parts per million (unit)
ppt.	precipitate
PPTS	pyridinium para-toluenesulfonate
Pr, *n*-Pr	propyl (normal)
psi	pounds per square inch (unit)
PT	proton transfer
PTC	phase transfer catalysis
py	pyridine
PyBOX	Pyridine bisoxazoline
PyOX	Pyridine oxazoline
q	quartet (spectral)
qual.	qualitative(ly)

quant.	quantitative(ly)
R	rectus (configurational)
RDS	rate-determining step
Red-Al	sodium bis(2-methoxyethoxy)aluminum hydride
redox	reduction–oxidation
ref.	reference
R_f	retention factor
RCM	ring-closing metathesis
ROESY	rotating frame Overhauser effect spectroscopy
rpm	revolutions per minute (unit)
rt	room temperature
s	second (unit), singlet (spectral)
S	sinister (configurational)
S_n	singlet energy level
SAR	structure–activity relationship
sat.	saturate, saturated
sBu	*sec*-butyl
SCE	saturated calomel electrode
SCXRD	single crystal X-ray diffraction
SET	single electron transfer
SM	starting material
SN1	unimolecular nucleophilic substitution
SN2	bimolecular nucleophilic substitution
sol.	soluble
soln.	solution
SOMO	singly-occupied molecular orbital
std.	standard
stoich.	stoichiometric
t	triplet (spectral)
t	time, tertiary
$t_{1/2}$	half-life
T_n	triplet energy level
TBA	tetrabutylammonium
TBS	*tert*-butyldimethylsilyl
tBu	*tert*-butyl
TEA	tetraethylammonium
temp	temperature
Tf	trifluoromethanesulfonyl
TFA	trifluoroacetic acid
THF	tetrahydrofuran
TIPS	triisopropylsilyl
TLC	thin-layer chromatography
TMEDA	tetramethylethylenediamine
TMG	tetramethylguanidine
TMP	2,2,6,6-tetramethylpiperidine
TMS	trimethylsilyl
TRIP	2,4,6-triisopropylphenyl
Ts	p-toluenesulfonyl or p-toluenesulfonic
UV	ultraviolet
V	volt (unit)
v/v	volume per unit volume
Vis	visible
vol.	volume
VR	vibrational relaxation
vs	*versus*
W	watt (unit)
w/w	weight per unit weight
wk	week (unit)
yr	year (unit)
XAT	X-atom transfer
XRD	X-ray diffraction
Z	zusammen olefin geometry

Chapter 1

Introduction

1.1 Introduction to Photochemistry

A full account of the intricacies of photochemistry is well beyond the scope of this thesis and the interested reader is directed to Turro, Scaiano, and Ramamurthy's textbook *Modern Molecular Photochemistry of Organic Molecules*.[1] Herein, are detailed only the principles and theory necessary to have a workable knowledge of photochemistry for the purposes of this thesis.

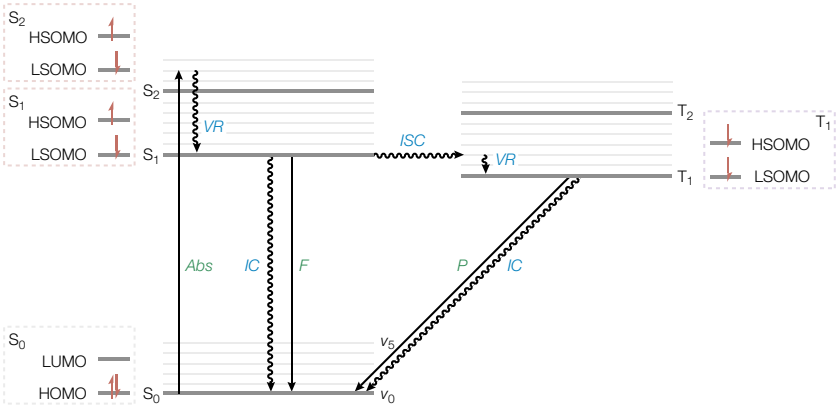


Figure 1. *Generic Jablonski diagram illustrating some photophysical processes.*
Abs (absorption); VR = vibrational relaxation; ISC = intersystem crossing; IC = internal conversion; F = fluorescence; P = phosphorescence; S_0 = singlet ground state; S_1 = first singlet excited state; S_2 = second singlet excited state; T_1 = first triplet excited state; v_0 = 0^{th} vibrational energy level; v_5 = 5^{th} vibrational energy level. Electronic configurations for each state are illustrated in dashed boxes.

Energy-state (Jablonski) diagrams are a powerful tool to illustrate a molecule's electronic configurations and vibrational energy levels in its available ground and excited states, as well as the possible thermal, photophysical, and photochemical transitions (**Figure 1**). The ground state of a molecule is the lowest energy electronic and nuclear configuration for that system at a given temperature whilst an excited state refers to any higher energy permutation of that system at the same temperature. Through Jablonski diagrams, one can quickly gain insight into the key photophysical characteristics of a given molecule.

Excitation occurs through the absorption (*Abs*) of a photon resulting in the promotion of an electron from one molecular orbital (MO) into a higher energy MO. In **Figure 1**, this is shown as the promotion of an electron from the HOMO to the LUMO of the singlet ground-state (S_0). Since electrons are much less massive than nuclei, and due to the disproportionate acceleration of electrons relative to nuclei resulting from their mutual Coulombic attraction,

electronic motions are significantly faster than nuclear motion. The Born-Oppenheimer approximation states that the atomic nuclei in a molecule can be considered stationary relative to electronic motion, allowing separation of the nuclear and electronic components of a molecular wavefunction for any configuration. The photophysical implication of this approximation is that nuclei remain relatively unchanged upon absorption of a photon and the promotion of an electron from one MO into another, a concept known as the Franck-Condon principle. From the perspective of the atomic nuclei in a molecule, during photoexcitation an electron jumps from one MO into another instantaneously. As a result, electronic transitions are more favourable when the ground and excited states have similar relative nuclear configurations and momenta. In the Jablonski diagram, from the 0^{th} vibrational energy level of a ground-state molecule, absorption of photons can result in excitation to a set of distinct vibrational energy levels (a single excitation is shown in **Figure 1**, from S_0v_0 to S_2v_2) resulting in fine structure in the absorption spectra (*e.g.* if S_0v_0 to S_nv_m are also available transitions and are suitably energetically disparate as to be distinct).

The promoted electron now occupies a different MO (HSOMO) and there is a hole in the former LUMO (now LSOMO). The new excited state molecular configuration may not be the lowest energy vibrational state. As a result, vibrational relaxation (VR), a thermal dissipation of energy (typically denoted by wavy lines), causes decay to the lowest vibrational energy state of the excited-state, in this case the first singlet excited-state (S_1). This VR decay is so rapid that photophysical and photochemical processes typically only occur from the lowest energy excited state (Kasha's rule), with few exceptions (see azulene for a classic example of an outlier). From S_1v_0, two relaxation processes to return to the ground-state are illustrated: 1) internal conversion (IC), a thermal decay process; or 2) fluorescence, a radiative process in which energy is lost as a photon emitted from the excited molecule. Each of these transitions show a 0-0 transition, from the v_0 of the excited to v_0 of the ground state, however emission to upper vibrational energy levels of the ground state is common (e.g. 0-n, where $n \geq 1$), resulting in fine structure in the fluorescence emission spectra. The energy lost upon VR from upper singlet excited states to S_1v_0 results in emission of longer wavelength photons than those that have been absorbed, causing a shift of the emission spectrum relative to the absorbance spectrum (Stokes shift).

Each of the transitions discussed thus far have conserved multiplicity, *i.e*. all the states concerned are singlet states, making them so-called 'allowed' transitions. Transitions between states of different multiplicity are dubbed 'forbidden' transitions, though this is a misnomer as these transitions may occur but are typically slow and disfavoured. Intersystem crossing (ISC) from the S_1 to the triplet state is a thermal process, illustrated as a horizontal transition

between states of different multiplicity. As with excitation and relaxation processes, this transition may occur to one, or several, vibrational energy levels in the triplet regime, and VR dissipates thermal energy to allow relaxation to the lowest energy triplet excited state (T_1). Often, ISC is depicted as a radiationless diagonal transition from S_1 directly to T_1v_0, for brevity. As ISC involves a change in multiplicity, it is formally a forbidden process, however a change in molecular orbital (MO) occupancy (*e.g.* change from an n,π* excited state to a π,π* excited state) increases the rate of ISC which can render it quite facile (El-Sayed's rule).

Transitions from T_1 to S_0 are also forbidden and, correspondingly, quite slow. For this reason, the lifetimes of triplet excited states are much longer than singlet states. Radiationless IC relaxation from this state, depicted here as a diagonal transition can enable return to S_0. Alternatively, the spin forbidden radiative transition, phosphorescence (P), results in the emission of a photon with concomitant return to S_0. As with fluorescence, decay to various higher level S_0 vibrational states is common, with subsequent VR resulting in further relaxation to S_0. The decrease in energy over the course of ISC from S_1 to T_1 means that phosphorescence emissions occur at longer wavelengths than fluorescence and with greater Stokes shifts. It should be noted that fluorescence and phosphorescence describe radiative relaxations with conservation and inversion of spin, respectively, not necessarily whether a triplet or singlet state is involved. While not shown in the above diagram, Jablonski diagrams can also be used to illustrate intermolecular photochemical processes like SET or energy transfer.

1.2 Introduction to Photoredox Catalysis

Outer-Sphere SET Photoredox Catalysis

Photocatalysis occurs when a light-absorbing species effects a photochemical change on a reaction component from the excited state to enable reaction processes, while returning to their original state over the course of the reaction.[2] Through photochemistry, light energy can be harnessed to achieve quite challenging, high-energy processes considering the ~71 kcal/mol provided by 400 nm light. Photoredox catalysis uses light energy to perform reduction/oxidation reactions (redox) through single electron transfer reactions. Photoexcitation renders any species both a better oxidant and reductant than its ground state, which is evident when one considers that a lower lying hole and high energy electron are both generated upon promotion of an electron to a higher energy MO. In the excited state, a photocatalyst can either undergo reductive or oxidative quenching depending on its thermodynamic propensity to either accept or donate an electron to another reaction component and the rates at which it does so (**Figure 2**, **A**). A

reductive quench SET reduces the photocatalyst by a single electron and oxidizes the quenching species whilst an oxidative quench oxidizes the photocatalyst by a single electron with concomitant reduction of the quencher species.

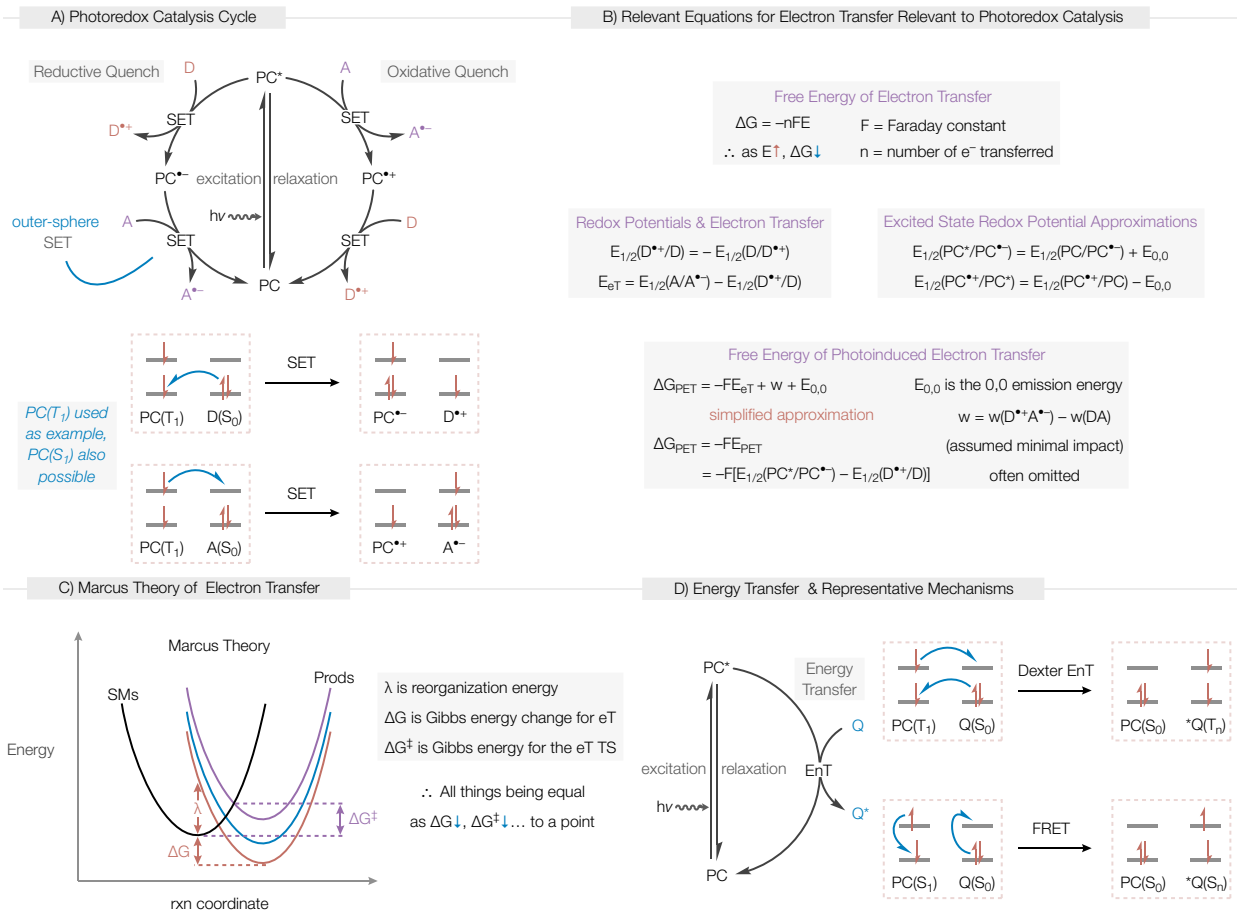


Figure 2. *A general overview of photocatalysis.*

A) Photoredox catalysis; B) Relevant equations for electron transfer relevant to photoredox catalysis; C) Marcus Theory of electron transfer; D) Energy transfer & representative mechanisms.

The thermodynamics of electron transfers are governed by the redox potentials of both species (**Figure 2**, **B**). The Gibbs free energy for electron transfer is proportional to the difference in potential (E) of the donor and acceptor, with larger potential differences resulting in more exergonic reactions. *E* for a redox reaction is given by the difference in the reduction potential of the acceptor and the donor (written as a reduction potential for its oxidation). In a photoredox reaction, the photocatalyst excited state acts as either the donor or acceptor. This poses a problem, as the redox potentials of fleeting excited states are difficult to determine experimentally. As an approximation, the excited state potentials for photocatalysts can be derived from the sum of the ground state potentials and the relevant excited state energy. Note: the excited state energy in eV is used interchangeably with V. Altogether, the Gibbs free energy for photoinduced electron transfer (PET) can be used to determine whether a photocatalyst/quencher pair SET is

spontaneous. Using Marcus theory, we can begin to understand how the rates of photoredox reactions are influenced through thermodynamics.

The 1992 Nobel prize in chemistry was awarded to Rudolph A. Marcus for "his contributions to the theory of electron transfer reactions in chemical systems". Marcus theory, as it is now known, was developed between 1956 and 1965 to define the mechanism by which electron transfers occur between two species in solution, accounting for changes in reactant structure and solvation before and after the electron transfer event. Applying Marcus theory allows for the prediction of the rate of electron transfer for a given system (**Figure 2**, **C**).[2c] Along an electron transfer reaction coordinate, the pre-and post-transfer complexes can be illustrated as parabola whose minima are offset by ΔG. As ΔG for the electron transfer becomes more negative, the successor complex shifts to lower and lower energy relative to the precursor. The intersection between the two parabola indicates the intrinsic barrier (transition state, TS) for electron transfer with an energy of $\Delta G^{\ddagger}$. Shifting the relative height of the parabola necessarily causes the intersection point between these curves to change. As a result, shifts in the thermodynamics for electron transfer have a proportional effect on the barrier to this process. As an electron transfer becomes more favourable, the barrier decreases proportionally, resulting in a rate increase. This barrier is derived from the solvent reorganization (λ_s) and the change in vibrational modes (λ_v) to give the total reorganization penalty denoted as λ. In a beautiful example of theory predicting an unobserved phenomenon, Marcus theory predicted that as electron transfers became increasingly exergonic there would come a point where the rate of electron transfer began to increase rather than decrease. As the successor parabola shifts lower and lower, the crossing point begins to shift from the right to the left side of the precursor parabola, resulting in a $\Delta G^{\ddagger}$ increase. This theoretical prediction sparked a search for the "Marcus inverted region" which took almost 30 years to validate experimentally![3] The decrease in the rate of electron transfer as the reaction becomes exceedingly exergonic has been rationalized on the basis of a decreasing overlap in the vibrational wavefunctions in the pre- and post-electron transfer states, in accord with the Franck-Condon principle.

Photocatalysts can also perform energy transfers to promote reaction components into excited states at wavelengths where their direct excitation may not be possible, or for compounds without reasonable mechanisms to access these excited states (**Figure 2**, **D**). As with all chemical reactions, these energy transfers are favourable when exergonic, meaning it is desirable for the donor excited state to be higher in energy than that of the acceptor. The two fundamental mechanisms for energy transfer are the Dexter and Förster resonance mechanisms. In Dexter, or electron exchange, energy transfer, the HSOMO electron from the photoexcited species is transferred into the LUMO of an

acceptor species whilst an electron from the HOMO of the quencher is transferred to the LSOMO of the photocatalyst. This results in the excitation of the energy acceptor with concomitant production of the ground state photocatalyst. This process can occur from singlet and triplet excited states of the photocatalyst and the multiplicity is transferred to the quencher species, *i.e.* triplet–triplet or singlet–singlet energy transfer. Dexter energy transfer requires spectral overlap between donor emission and acceptor absorption, as well as orbital wavefunction overlap, meaning it can only occur across short separations (<10 Å). In Förster, or dipole–dipole, resonance energy transfer (FRET), the oscillating dipole of the excited donor species induces a dipole in an acceptor species which deactivates the donor and excites the acceptor. As with Dexter energy transfer, spectral overlap between the donor emission and acceptor absorption is required for FRET. The proximity requirements for FRET are less stringent than Dexter energy transfer, with the interaction strength between point dipoles dropping off at $1/r^6$. This results for an effective dipole–dipole resonance energy transfer range of ~10–100 Å between donor and acceptor. Additionally, FRET is a singlet-only process resulting from spin conservation and the low rates associated with two simultaneous spin-forbidden transitions required for triplet–triplet FRET.

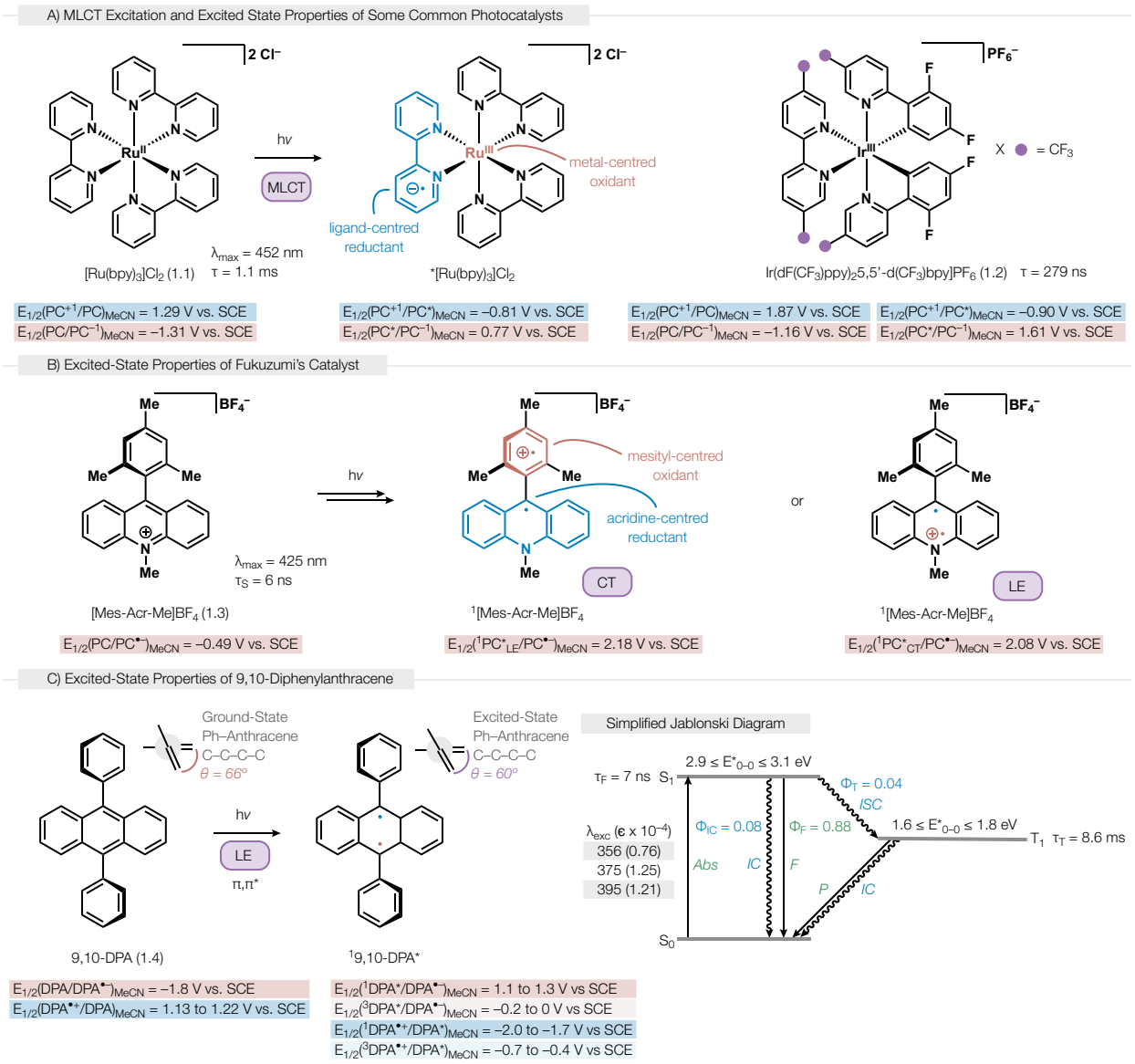


Figure 3. *Photocatalysts and their excited states.*

A) MLCT excitation and excited-state properties of some common photocatalysts; B) excited-state properties of Fukuzumi's catalyst; C) excited-state properties of 9,10-diphenylanthracene.

There are a variety of light-absorbing species that can be used as photocatalysts including a variety of transition metal complexes and organic dyes.[2b] A very popular class of transition metal photocatalysts are ruthenium- and iridium-based polypyridyl complexes like $[Ru(bpy)_3]^{2+}$ (**1.1**) and $[Ir(dF(CF_3)ppy)_2dtbbpy]^+$ (**1.2**, **Figure 3**, **A**).[4] These noble metal photocatalysts are popular due to their long-lived triplet excited states and the high efficiency with which these states are accessed, facilitated by spin–orbit coupling. Additionally, the modular preparation of these complexes allows for their excited state properties to be tuned through ligand effects. The triplet excited states of these

catalysts are metal-to-ligand charge transfer (MLCT) states in which an electron has been promoted from a metal centred orbital into a ligand centred orbital. This results in an oxidized metal centre and reduced ligand that acts as the oxidant or reductant in a SET quench, respectively.

A popular series of acridinium dyes like Fukuzumi's catalyst, [Mes-Acr-Me]BF_4 (**1.3**), are a proven class of strong photooxidants (**Figure 3**, **B**).[2b, 5] While there has been much debate about the nature of the excited state for Fukuzumi's catalyst, the putative quenching mechanism for these dyes occurs from the singlet excited states.[5a-e] In the singlet excited state regime, these dyes have access to both charge transfer (CT) and locally excited (LE) states, both of which are exceptionally strong oxidants. The major drawbacks of this class of catalysts are their typically short excited-state lifetimes and their poor reducing capabilities after reduction to $PC^{\bullet-}$.

While there are many other popular photocatalysts that could be discussed here, one dye that is notably less popular, but more relevant herein, is 9,10-diphenylanthracene (**1.4**, 9,10-DPA, **Figure 3**, **C**). 9,10-DPA (**1.4**) is a simple polyaromatic hydrocarbon that has been studied extensively due to its high quantum yield of fluorescence ($\Phi_F \geq 0.88$) and potential for applications as an electrochemiluminescent compound.[6] Recently, the Zuo group demonstrated its usefulness as a secondary photocatalyst in cerium photoredox reactions, and it is in the same context that it appears here. Despite the large number of studies on this compound, it is not commonly employed in the modern period of photoredox catalysis research and, as such, its photophysical and photochemical properties have not been compiled into a single resource before. To remedy this issue, I have constructed a Jablonski diagram annotated with the ground and excited state redox potentials for 9,10-DPA (**1.4**). The 9,10-DPA (**1.4**) absorption spectrum resembles that of anthracene in that it has well defined fine structure, with absorbance maxima at 356, 375, and 395 nm. Photoexcitation produces a ^{1}LE (π,π^*) state in which the appended phenyl rings lie at a 60º dihedral angle (θ) relative to the anthracene core.[7] The ^{1}LE singlet excited state has an exceptionally short lifetime (τ_0 = 7 ns) with an energy between 2.9 and 3.1 eV (66.9 to 72.7 kcal/mol).[6c, e, g, j, 8] IC from S_1 is a minor pathway (Φ_{IC} = 0.08) and an upper limit for ISC shows that transition to the triplet state is minimal (Φ_{ISC} = 0.04).[6a, b] Estimates of the triplet state energy for 9,10-DPA (**1.4**) place it in a low lying range of 1.6 to 1.8 eV (36.9 to 41.5 kcal/mol) with a long 8.6 ms lifetime.[6c, j] 9,10-DPA (**1.4**) is a good photooxidant and photoreductant in the singlet excited state, but is quite weak in the disfavoured triplet state. Following oxidative or reductive quenching, the radical ions of 9,10-DPA are potent oxidants and reductants, respectively.[6e-l]

With a firm grasp on the underlying theories on photoredox reactions, it seems prudent to include here the redox potentials for some compounds relevant to this thesis (**Figure 4**).[9] Altogether, this diagram can illustrate the anticipated spontaneity of a given redox reaction with more reducing species appearing further to the left of the number line and more oxidizing species appearing further to the right. It should be noted that each redox potential here is written as the reduction potential.

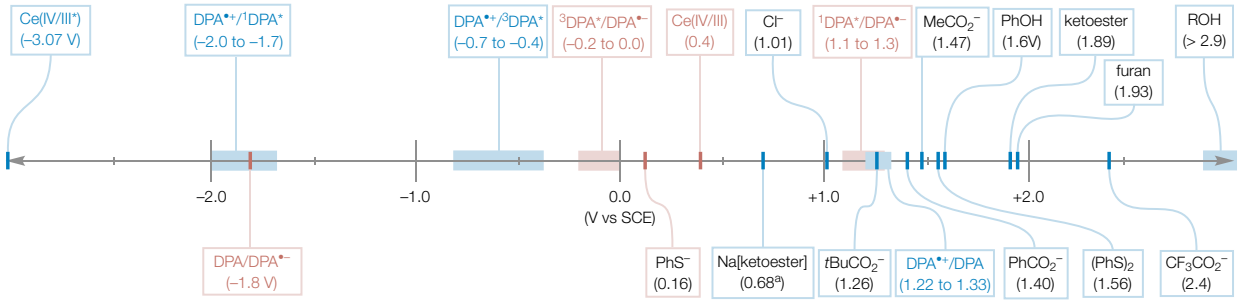


Figure 4. *Redox potential diagram for relevant species.*
[a]Redox potential vs SCE in DMSO rather than MeCN.[9a] See the following references for redox potential sources.[9b-h] Ce(IV/III) potential was converted from Fc/Fc$^+$ to SCE using Addison's conversion (+ 0.38 V).[10]*

Cerium Photochemistry and LMCT Photoredox Catalysis

In addition to outer-sphere electron transfer photoredox catalysis, this thesis deals in large part with the inner-sphere photochemistry of cerium complexes. Ce(0) has an electronic configuration of [Xe]4f^{1}5d^{1}6s^2 and the most stable configuration of Ce(III) is [Xe]4f^1. Kunkley and Vogler reported the interesting photochemical behaviour of cerium(III) halides in the early 2000s (**Figure 5**, **A**).[11] They showed that the lowest E transition (metal-centred, MC) for Ce(III) is 4f to 5d and the configurations in both the ground and excited state are spin doublets (paramagnetic), making all transitions allowed. They suggest that down the halide series ($Cl^- < Br^- < I^-$) there is a greater contribution of unoccupied halide *n*d-orbitals in the excitation of Ce(III) such that the excitation has less MC and more MLCT character upon moving from chloride to iodide and a bathochromic shift in excitation wavelength occurs down the group. The better overlap between the 5d orbital of I with the 5d orbital of Ce results in improved mixing and greater stabilization than the mismatched d orbitals from earlier group members.

In acetonitrile solution, the hexachlorocerate((III) anion (**1.5**) was shown to exist in equilibrium with the bridged dimer $[Ce_2Cl_9]^{3+}$ (**1.6**) when in the absence of excess supporting chloride (**Figure 5**, **B**).[9b] With sufficient supporting chloride, the hexachlorocerate(III) anion (**1.5**) is the dominant species in acetonitrile solution. Excitation of hexachlorocerate(III) (**1.5**, λ_{max} = 329 nm) results in an f,d excitation with some MLCT character that has a lifetime

of 22.1 ns. Ce(III) excited states result from f,d transitions and both the ground and excited states of Ce(III) are spin doublet states, making their transitions spin allowed and facile and leading to their unusually short lifetimes relative to the other lanthanides. Emission maxima from the hexachlorocerate(III) (**1.5**) anion occur at 356 and 395 nm.

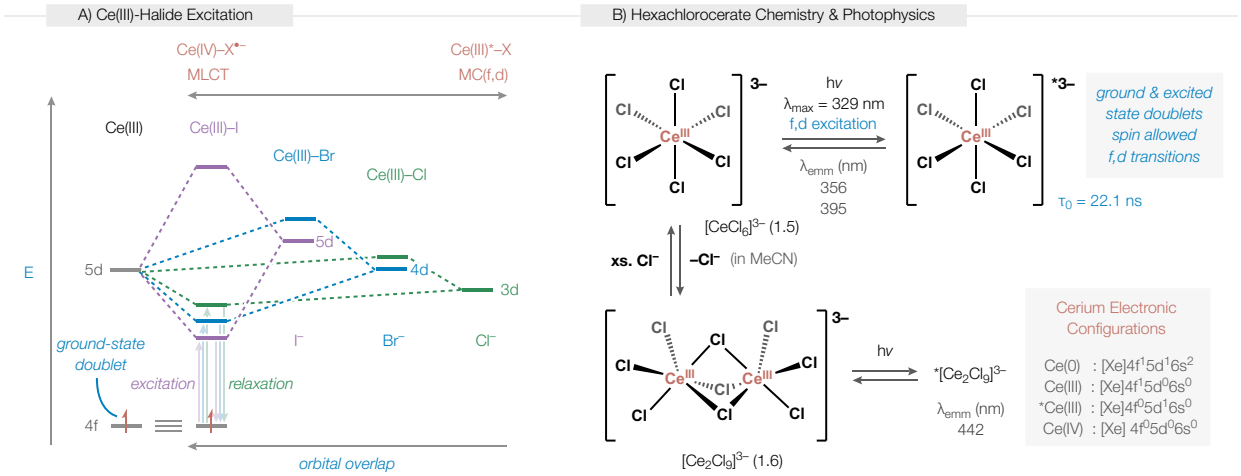


Figure 5. *Cerium(III) photochemistry.*
A) Ce(III)-halide excitation; B) hexachlorocerate chemistry & photophysics.

Ce(IV) photochemistry is dominated by ligand-to-metal charge transfer (LMCT) excited states. In 2001, Vogler and Kunkley showed that $Ce(TMDH)_4$ (**1.7**) is an f^0 Ce(IV) complex with fluorescence emission (**Figure 6**, **A**).[12] They suggested that an upper Ce(III) d^1 LMCT state emits to give a lower energy f^1 LMCT excited state. The authors also noted that excitation into a higher energy intra ligand (IL) excited state which relaxes to a lower energy LMCT state may occur, but these excitations were not resolved enough to conclude definitively. Altogether, the d^1 LMCT excited state can be considered a MC excited state of a Ce(III) complex with an oxidized ligand ($L^{\bullet+}$). Relaxation of the MC(f,d) state would give a Ce(III)–$L^{\bullet+}$ complex which may undergo a relaxation back down to the ground state S_0 configuration or undergo homolysis to liberate Ce(III) and $L^{\bullet}$.[13] Schelter and Zuo have studied the photochemistry of hexa- and pentachlorocerium(IV) dianions since Costanzo's seminal report.[9b, 14] Excitation of these Ce(IV) species promotes an electron from a ligand *n*p orbital into the Ce(4f) orbital, resembling a Ce(III) centre with an oxidized ligand still associated. Zuo measured a lifetime for the LMCT excited state of less than 1 ps,[15] and relaxation by homolysis liberates Ce(III) and $X^{\bullet}$. Zuo also measured quantum yields for the liberation of $L^{\bullet}$ and showed that alkoxy ligands underwent homolysis more efficiently than chloride ($\Phi_{Ce\text{–}O\ homolysis} \leq 0.39$ using aliphatic alcohols and $\Phi_{Ce\text{–}Cl\ homolysis} = 0.05$) and that the rate of back electron transfer (BET) decreases along the series $Cl^{\bullet} > ArCO_2^{\bullet} > RO^{\bullet}$.[15]

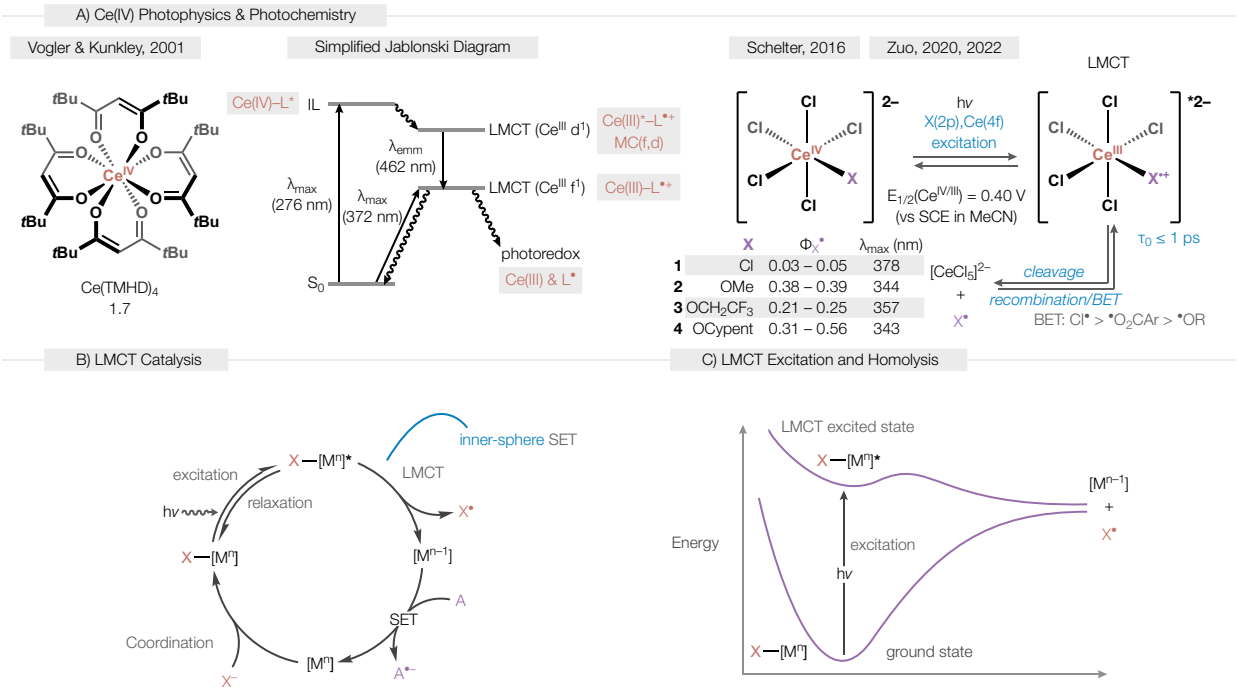


Figure 6. *Ce(IV) Photochemistry and LMCT catalysis.*

A) Ce(IV) photophysics & photochemistry; B) LMCT catalysis; C) LMCT excitation and homolysis.

LMCT photoredox catalysis cycles differ from their outer-sphere SET counterparts in that a coordination event must precede excitation to the excited state, where an inner-sphere electron transfer occurs (**Figure 6**, **B**).[16] The reduced LMCT photoredox catalyst must then lose an electron to return to the oxidation state capable of further LMCT excitation. Although LMCT excited states are typically short-lived, there is a barrier to homolysis resulting in a non-unity quantum yields for production of L•, particularly when considering the potential for BET prior to cage escape (**Figure 6**, **C**).

Ce LMCT photoredox reactions have a long history, beginning in 1908 with Baur's identification of oxygen as a byproduct of photolytic ceric ions (Ce^{IV}),[17] which was later confirmed by Weiss and Porret (**Figure 7**).[18] The quantum yield for this process was later measured by Heidt and Smith in 1948, [19] and the mechanism of this process was investigated by Sworski in 1955.[20]

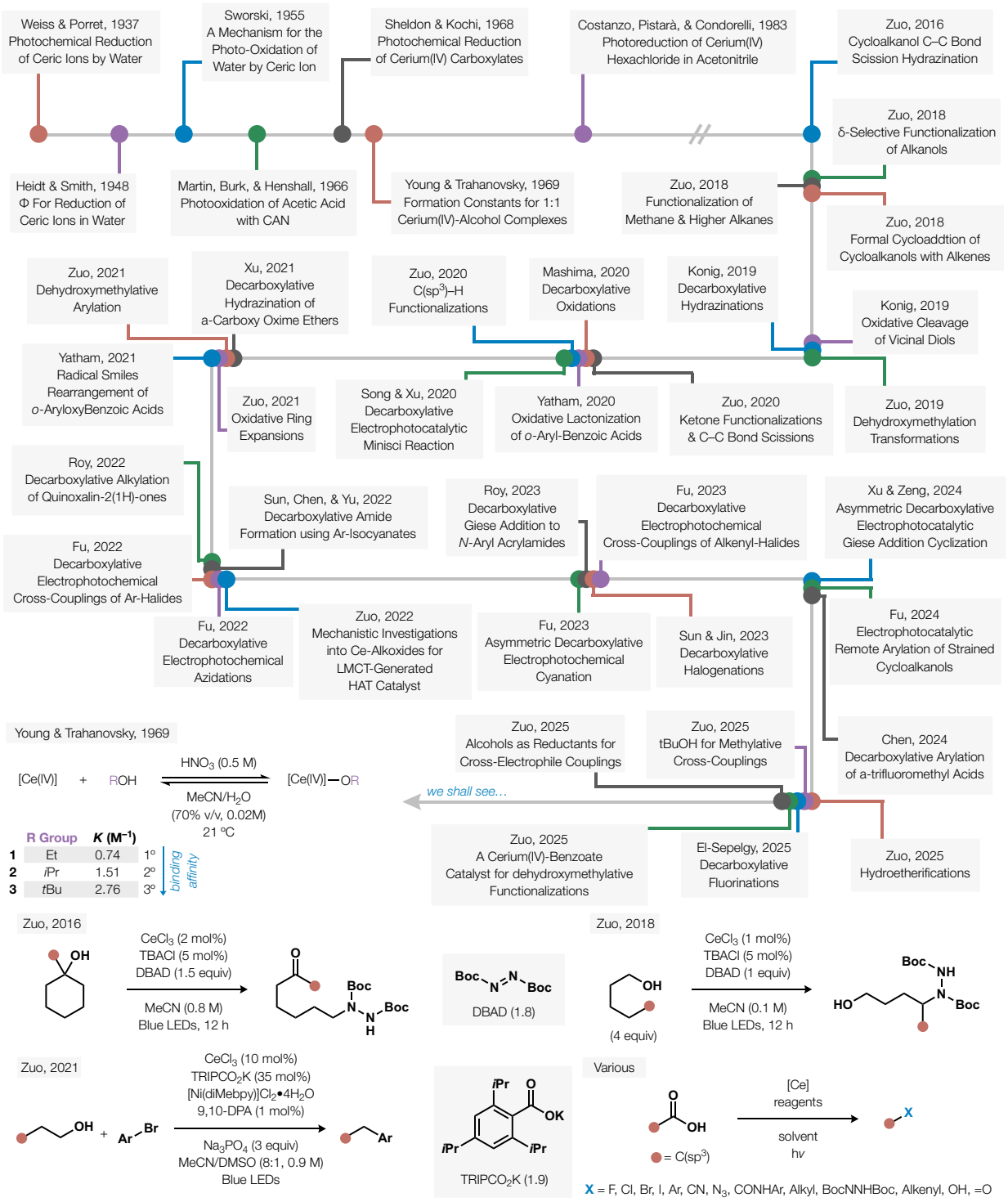


Figure 7. *Cerium LMCT photoredox reaction timeline and examples.*

Bringing this concept into the realm of organic chemistry, Martin, Burk, and Henshall studied the photoreduction of ceric ammonium nitrate (CAN) in glacial acetic acid and measured the quantum yields for the

formation of numerous products.[21] Similarly, Kochi and Sheldon studied the photoreduction of Ce(IV)-carboxylates and measured the quantum yields for decarboxylation and oxidations of the ensuing C-centred radicals.[22]

While not photoredox reactions, Trahanovsky studied the behaviour of Ce(IV) oxidants extensively in the 1960s and 1970s with several key insights into their action as single electron oxidants.[23] One of key insight from this series comes from the 1969 publication by Young and Trahanovsky on the binding affinity for a variety of alcohols in 1:1 ratio in MeCN/H_2O solution.[23e] The authors found that binding affinity increases going from 1º to 2º to 3º alcohols. This counterintuitive result was rationalized on a steric basis, wherein solvation of 1º alcohols is easier than 2º and easier than 3º. As such, the authors concluded that binding affinity increases in the series 1º < 2º < 3º simply because there is a greater entropic penalty to pay for having free alcohols that are more hindered.

A 1983 report by Costanzo, Pistarà, and Condorelli showed the interesting behaviour of the hexachlorocerate(IV) ion to liberate $Cl^{\bullet}$ upon LMCT excitation and homolysis.[14] Almost 40 years later, this work would spark an intriguing series of investigations into the mechanism for Ce-photoredox catalyzed HAT functionalization reactions.[24]

Interest in cerium(IV) LMCT excitation waned until an influential 2016 report by Zuo on the use of $CeCl_3$ as a photoredox catalyst for the ring-scission hydrazination of cycloalkanols.[25] What followed was an explosion of reports. Entries by Zuo in 2018 included the aforementioned HAT functionalization reactions of methane and higher alkanes,[24a] 1,5-HAT-enabled functionalizations of primary alcohols,[26] and a formal cycloaddition reaction of strained cycloalkanols.[6e] Konig later published a Ce-photoredox catalyzed diol cleavage and a decarboxylative hydrazination reaction in 2019, and Zuo demonstrated several dehydroxymethylation reactions of primary alcohols.[27] 2020 saw several entries into this renaissance of Ce-photoredox catalysis including work by Zuo,[15, 28] Mashima,[29] Yatham,[30] as well as Song and Xu.[31] The year 2021 saw more entries from Xu[32] and Yatham[33] along with standout publication by Zuo on a dehydroxymethylation cross-coupling through Ce/Ni metallaphotoredox catalysis,[6k] and the oxidative ring expansion of bicyclic hemiketals into medium-sized and macrolactones.[34] The year 2022 saw multiple reports on cerium photoredox catalysis from Roy,[35] Sun, Chen and Yu,[36] Zuo,[24d] and dual reports from Fu on electrophotocatalytic Ce-based systems for decarboxylative cross-coupling and azidation reactions.[37] In 2023, there were dual entries to this field from the Fu group on electrophotocatalytic alkenylations[38] and asymmetric cyanation,[39] as well as a report from Roy on a decarboxylative Giese addition cyclization using *N*-aryl acrylamides,[40] and a report from Sun and Jin on decarboxylative halogenation.[41] In 2024, the Fu group reported a remote arylation of strained

cycloalkanols through metallaelectrophotocatytic cross-coupling,[42] the Chen group achieved a decarboxylative arylation of α-fluoroalkyl-α-C(sp^3) carboxylic acids,[43] the Xu and Xeng groups jointly published an asymmetric Giese addition cyclization,[44] and our first entry into this field on the redox-neutral cleavage of cycloalkanols and carboxylic acids was reported.[45] 2025 has already shown 6 reports concerning Ce-photoredox catalysis just halfway into the year. Zuo has published four papers on this topic including alkene hydroetherification,[6l] the use of *tert*-butanol as a methyl radical source for cross-coupling,[46] a bench-stable Ce(IV)-benzoate catalyst for dehydroxymethylative transformations,[47] and the activation and application of alcohols as reductants under Ce-metallaphotoredox catalysis to enable reductive cross-coupling reactions.[48] A decarboxylative fluorination reaction has also been reported by El-Sepelgy[49] as well as our report on the hydroalkylation of 1,3-dicarbonyls by our group, the topic of chapter 3 of this thesis.[8]

Alternatives to LMCT Activation of strong O–H bonds: Proton-Coupled Electron Transfer (PCET)

The activation of O–H bonds through LMCT activation can be considered a subset of proton-coupled electron transfer (PCET) reactions, as a special case of proton-transfer electron-transfer (PTET) activation. PCET is a mechanistic archetype that has been highly useful for the activation of a variety of X–H bonds and is utilized in chapters 3 and 4 of this thesis. PCET is an umbrella term for all the possible reaction schemes in which a proton and electron are transferred to or from a substrate to arrive at an open shell species (**Figure 8**, **A**).[50] The combination of oxidant/base, or reductant/acid, pairs can effect sequential proton and electron transfers in either order (*i.e.* PTET or ETPT) depending on the identity of the reactant pair and the substrate. Additionally, concerted PCET reactions transfer the electron and proton in a single kinetic step and occur whenever the intermediate in the corresponding stepwise processes are higher in energy than the single concerted TS. When the pair performing the concerted PCET reaction are spatially or stereoelectronically separated, these reactions may be referred to as multi-site proton-coupled electron transfer (MS-PCET) reactions. HAT reactions are another subset of PCET reactions in which the proton/electron pair are transferred in a single kinetic step to and from the same MO. All examples here are for the formal loss of a hydrogen atom from the substrate as these are most relevant to this thesis, however, acid/reductant pairs can achieve the reverse process through the same analysis.

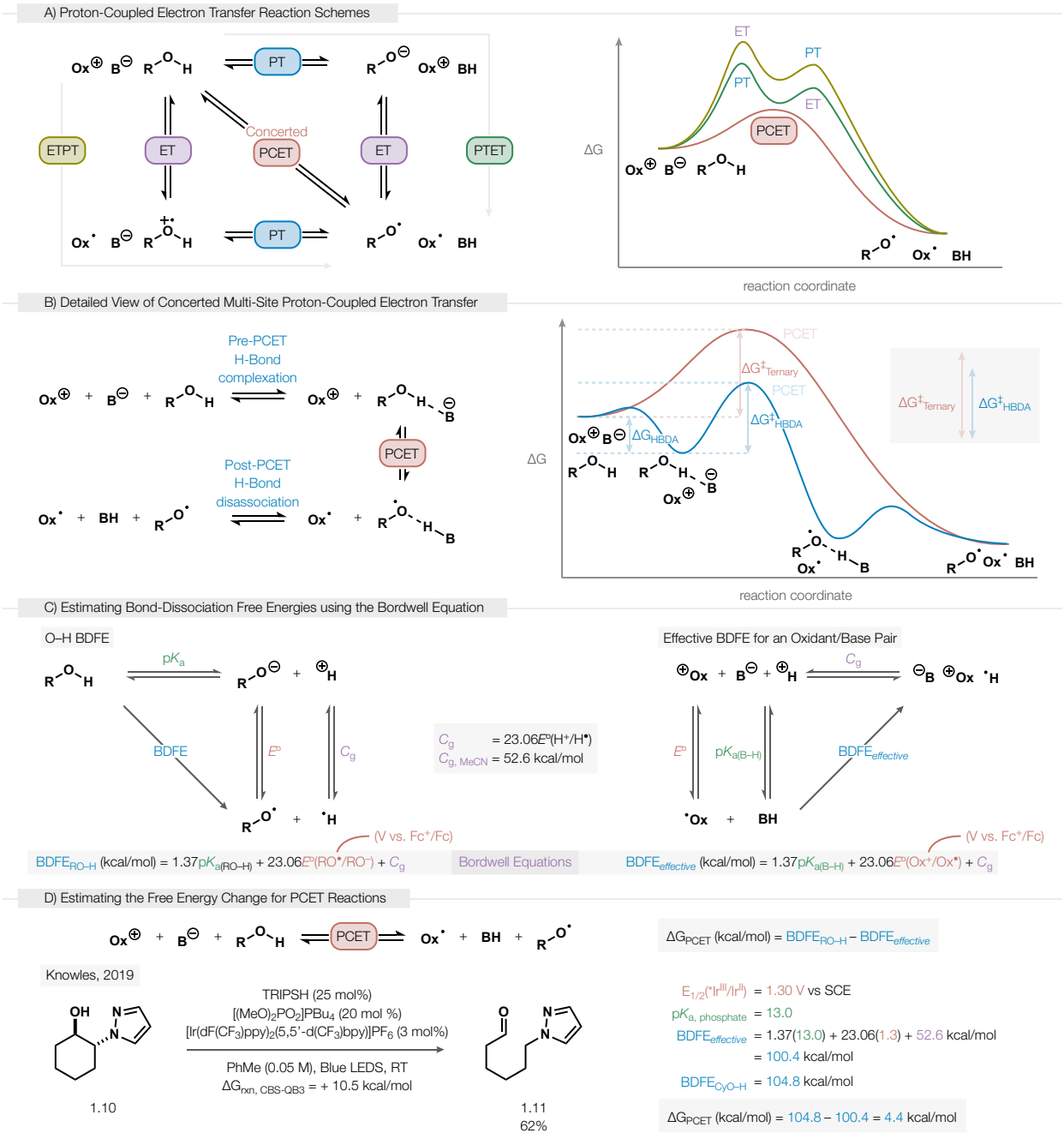


Figure 8. *PCET Theory and an example.*

A) Proton-Coupled Electron Transfer Reaction Schemes; B) Detailed View of Multi-Site Proton-Coupled Electron Transfer; C) Estimating Bond-Dissociation Free Energies using the Bordwell Equation; D) Estimating the Free Energy Change for PCET Reactions.

While a concerted MS-PCET reaction involves three species, it is not a termolecular process (**Figure 8**, **B**). In the example of PCET activated alcohols for O-centred radical generation, a hydrogen bond donor-acceptor complex (HBDA), a metastable intermediate, is first formed under a pre-PCET equilibrium defined by ΔG_{HBDA}. Subsequently,

the oxidant can effect the MS-PCET event on the binary substrate•base complex through a single transition state, with energy $\Delta G^{\ddagger}_{HBDA}$, to result in a post-PCET HBDA$^{\bullet+}$ complex. Disassociation of this post-PCET complex liberates the free O-centred radical and the conjugate acid of the basic species. The single transition state of the ternary PCET reaction ($\Delta G^{\ddagger}_{Ternary}$) is likely to be much higher in energy and would only contribute to the PCET process if it was kinetically competitive with the HBDA process (*i.e.* if $\Delta G^{\ddagger}_{Ternary} \simeq \Delta G^{\ddagger}_{HBDA}$).

The strength of X–H bond that can be activated by a given a base/oxidant pair can be approximated using the Bordwell equation to calculate an effective bond dissociation free energy ($BDFE_{effective}$, **Figure 8**, **C**). If $BDFE_{effective}$ is greater than the BDFE of the X–H bond, then the PCET reaction is exergonic and thermodynamically favourable. The Bordwell equation makes use of the state function nature of Gibbs free energy to evaluate the strength of an X–H bond *via* its p*K*a (heterolytic cleavage) in summation with the oxidation potential of the anion formed upon deprotonation and the reduction potential for the proton/hydrogen atom half-cell reaction. Similarly, the effective BDFE for a given base/oxidant pair can be evaluated using the same approach. The Knowles groups' 2019 report on contrathermodynamic redox-neutral formal rearrangement of cycloalkanols (*e.g.* **1.10**) to linear aldehydes (*e.g.* **1.11**) and ketones provides an example of this analysis (**Figure 8**, **D**).[51] The reduction potential of the excited state of the Ir(III) photocatalyst (1.30 V *vs* Fc/Fc^{+}) and the p*K*a of the phosphate base (13.0 in MeCN) result in an effective BDFE of 100.4 kcal/mol against the estimated BDFE for the substrate of 104.8 kcal/mol. Overall, this analysis results in the prediction of an endergonic 4.4 kcal/mol PCET reaction which may proceed due to an irreversible HAT step subsequent to the PCET, although it is plausible that this is an overestimate of ΔG_{PCET}. It should be noted that the value for the reduction potential for the redox reaction $H^{+/\bullet}$ was revised recently to the 52.6 kcal/mol given above,[50a] and as such these estimates are less than those predicted in the original publication by Knowles and co-workers.

1.3 Introduction to Radical Chemistry

Central to this thesis is the use of radical intermediates to achieve new synthetic transformations. A complete account of radical chemistry is well beyond the scope of any thesis and so a brief timeline of some notable advances in synthetic radical chemistry will have to suffice (**Figure 9**).

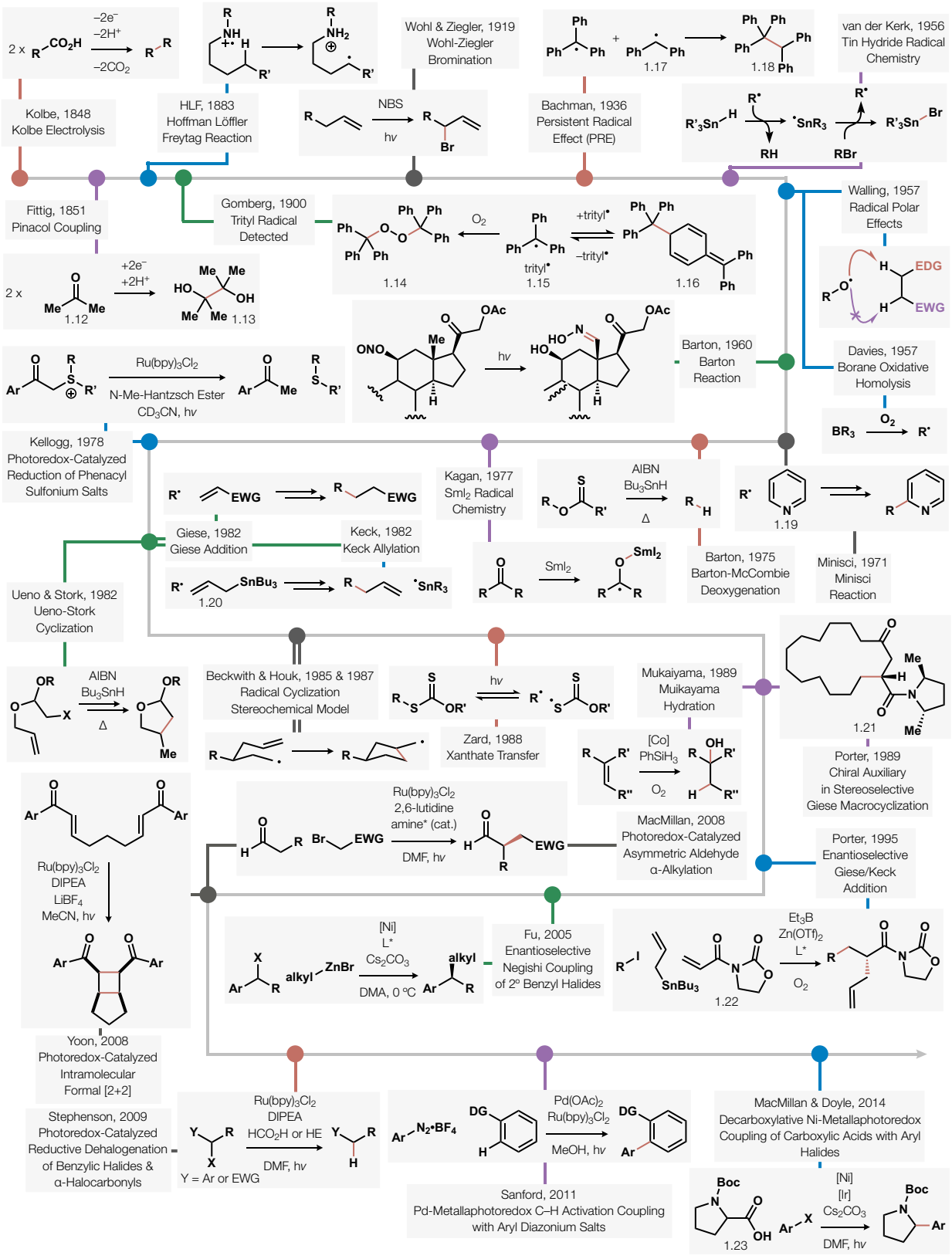


Figure 9. *Timeline of a selection of notable advances in synthetic organic radical chemistry.*

In the mid to late 1800s, some well-known radical reactions including the Kolbe electrolysis, [52] Hoffman-Löffler-Freytag reaction,[53] and pinacol coupling were all reported.[54] In 1900, Gomberg detected a persistent C-centered free radical (**1.15**) and its dimerization (**1.16**) and oxidative dimerization (**1.14**) products.[55] 1919 was marked by the discovery of the Wohl-Ziegler bromination,[56] an excellent method for allylic oxidation that will make an appearance in **Chapter 4** of this thesis. In 1936, Bachman investigated the persistent radical effect and described how this phenomenon can lead to excellent cross-coupling efficiencies despite the high reactivity of most free radical species.[57] In 1956, van der Kerk described the uses of tin hydrides, leading to their applications in radical chain reactions using organohalides and thereby delivering methods that have found exceptionally broad applications.[58] In the 1950s, Walling studied polar effects of free radicals, and especially O-centred radicals, which has informed modern radical reaction development by providing necessary insight into radical reaction kinetics.[59] In 1967, Davies and Roberts reported the use of trialkyl boranes as radical initiators under oxygen;[60] this initiation method has found widespread use for its ability to be run at low temperatures, providing later opportunities for stereoselective radical reactions.[61] In 1960, the eponymous Barton reaction was reported, a landmark method for remote C–H functionalizations.[62] The year 1971 saw the first report of the Minisci reaction, an excellent method for the formal C–H functionalization of heteroarenes.[63] In 1975, Barton and McCombie reported their similarly excellent method for radical deoxygenations utilizing thionoesters to activate hydroxyl groups.[64] 1977 saw Kagan's seminal report on the use of SmI_2 as a SET reductant for carbonyls to generate Sm-ketyl radicals, a highly useful intermediate.[65] Kellog's 1978 publication on the photoredox catalyzed reduction of phenacyl sulfonium salts marks the earliest report of synthetic photoredox catalysis.[66] This landmark achievement is especially notable given the nearly 30 years between this publication and the explosion in photoredox methodology interest that began in 2008. 1982 saw reports of three prominent free radical reactions, the Giese addition,[67] Ueno-Stork cyclization,[68] and the Keck allylation.[69] In the mid-1980s, the Beckwith-Houk model was developed for radical cyclizations and the rationalization of stereoselectivity in these transformations.[70] In 1988, Zard reported on the use of xanthates as a reversible reservoir for C-centred free radicals, which has found widespread use.[71] 1989 saw the first report of an asymmetric radical reaction using a chiral auxiliary (**1.22**) from Porter in a macrocyclizing Giese addition reaction,[72] as well as the first report on the Mukaiyama hydration, a reaction that has sparked much recent work in metal hydrogen atom transfer (MHAT) chemistry.[73] In 1995, Porter reported an asymmetric Giese addition/Keck allylation reaction using a chiral zinc(II)•bisoxazoline catalyst system.[74] In 2005, the Fu group reported one of the first asymmetric radical cross-coupling reactions using a

nickel catalyst for an enantioselective Negishi coupling of 2º benzylic halides.[75] The renaissance of photoredox catalysis began in 2008 with influential publications by MacMillan and Yoon,[76] followed closely by a report from the Stephenson group on the reduction of alkyl halides.[77] In 2011, one of the first publications on the now ubiquitous field of metallaphotoredox catalysis was reported by the Sanford lab, using dual $Ru(bpy)_3Cl_2$ (**1.1**) and $Pd(OAc)_2$ catalysts for C–H activation cross-coupling of arenes with aryl diazonium salts.[78] In 2014, MacMillan and Doyle jointly authored a landmark publication on the use of a metallaphotoredox platform for the decarboxylative cross-coupling of α-C(sp^3)-carboxylic acids and aryl halides.[79] These two publications have sparked a significant amount of work on the use of photoredox catalysis to generate free radicals from both nucleophilic and electrophilic partners in cross-coupling chemistry.[80] While not a complete account of all the subfields that utilize free radicals for synthesis, I believe these constitute many of the touchstone publications necessary to get a feel for how this field has developed since the 1800s until the modern day.

Central to understanding the reactivity of radical intermediates is an appreciation for their structure.[59m, 81] C-centred radicals can be divided into two main classes, p-type and s-type, depending on their hybridization (**Figure 10**, **A**). P-type radicals reside in p-orbitals, with pyramidalization possible depending on the flanking substituents (*e.g.* $^{\bullet}CF_3$), and are lower in energy than s-type radicals which reside in sp^2 hybridized orbitals. The increased s-character of s-type radicals increases their electron affinity, thereby destabilizing them relative to p-type radicals. O-centred radicals are very high energy intermediates that reside in p-orbitals. The increased reactivity of O-centred radicals is the result of their localization on oxygen which has a greater electronegativity than carbon, resulting in a less stable electron-deficient open-shell species. Some common classes of reactions available to free radicals include: addition to unsaturations or metals; α- and β-scissions to generate unsaturations; atom transfer reactions including HAT (homolytic substitutions, S_H2); disproportionation or combination with other open-shell species; and redox reactions (**Figure 10**, **B**).

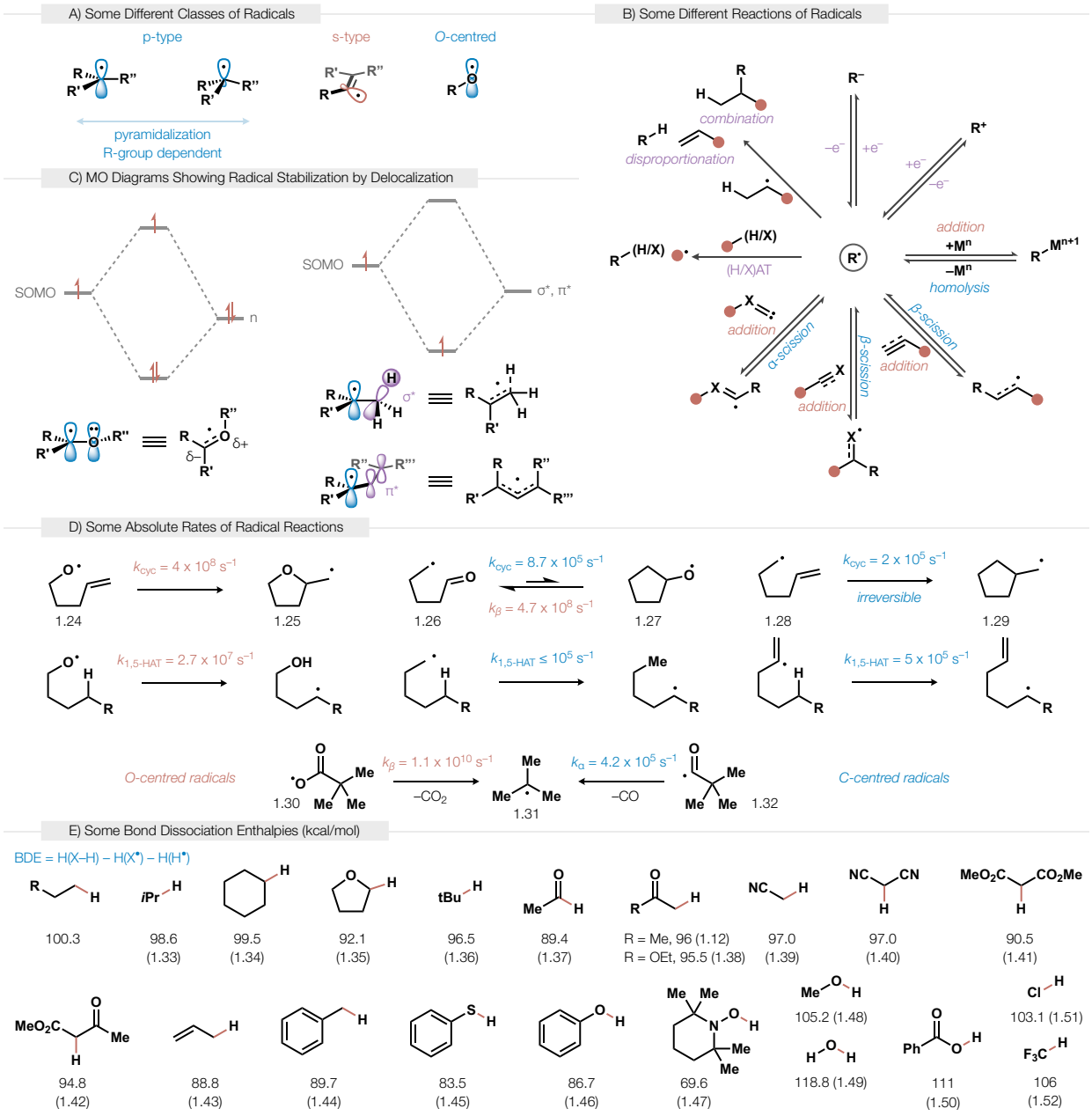


Figure 10. *Radical structure and reactivity.*

A) Some Different Classes of Radicals; B) Some Different Reactions of Radicals; C) Some MO Diagrams Showing Radical Stabilization by Delocalization; D) Some Absolute Rates of Radical Reactions; E) Some Bond Dissociation Enthalpies (kcal/mol).

Radicals can be stabilized or destabilized based on adjacent substituents and the stereoelectronic and inductive effects they impart (**Figure 10**, **C**). Conjugation of a radical with vicinal lone pairs can result in net stabilization by lowering the energy of two electrons in the delocalized system whilst only increasing the energy of one electron. A

single electron in a SOMO may also be stabilized through (hyper)conjugation with empty adjacent orbitals like π* or σ* antibonding orbitals. Each of these scenarios delocalize the spin system to result in net stabilization.

This thesis is concerned with the reactions of both C- and O-centred radicals and so it is prudent to briefly compare their reactivities (**Figure 10**, **D**). The difference in reactivity of C- *vs*. O-centred radicals is well-demonstrated by the difference in 5-*exo-trig* cyclization rates of the 4-pentene-methyl (**1.29**) and -oxyl (**1.25**) compounds, with the latter reaction occurring more than 1000 times faster.[82] The differing propensity for β-scission in C- *vs*. O-centred radicals is evident when comparing the equilibrium behaviour of aldehyde/cycloalkoxy radical (**1.27**/**1.28**) and the lack of appreciable ring-scission in the cyclopentanemethyl (**1.30**) and tetrahydrofuranmethyl radicals (**1.26**). 1,5-HAT to the O-centred radical **1.31** is ~50 times faster than to the high energy s-type radical,[83] representing an upper limit to HAT for the p-type radical. Decarboxylative β-scission of pivaloxyl radical[84] **1.31** is nearly 5 orders of magnitude faster than the corresponding α-scission from the acyl radical **1.33**.[85]

Bond dissociation enthalpies (BDE) give a thermodynamic metric for the homolytic cleavage of a chemical bond (**Figure 10**, **E**). The stability of the radicals formed upon homolysis is reflected in the strength of a chemical bond, where higher BDEs mean stronger bonds and higher energy radicals upon homolysis. **Figure 10**, E gives some BDEs relevant to the work in this thesis; [86] in general, effects that stabilize radicals like delocalization, hyperconjugation, and the identity of the radical centre result in lower BDEs.

Chapter 2

Redox-Neutral Cerium Photoredox-Enabled Cleavage of O–H Bearing Substrates

2.1 Introduction

Ring-chain tautomerism in lactols describes the relationship between the cyclic hemiacetal and open hydroxyaldehyde forms which differ in the location of a proton and a C–O bond (**Figure 11**, **A**). The equilibrium distribution between these two forms is impacted by medium effects (solvent, polarity, H-bond donor-acceptor complexes, *etc*.) and structure effects (ring-size, ring-strain, conformation).[87e] Ring-strain causes the equilibrium distribution for cyclic isomers to be lower in the 5-membered ring than in the 6-membered ring. The greater degrees of freedom in larger ring systems confers a greater entropic penalty to cyclization and results in a substantially lower proportion of cyclic hemiacetal in the 7-membered *vs*. 5/6-membered ring systems.

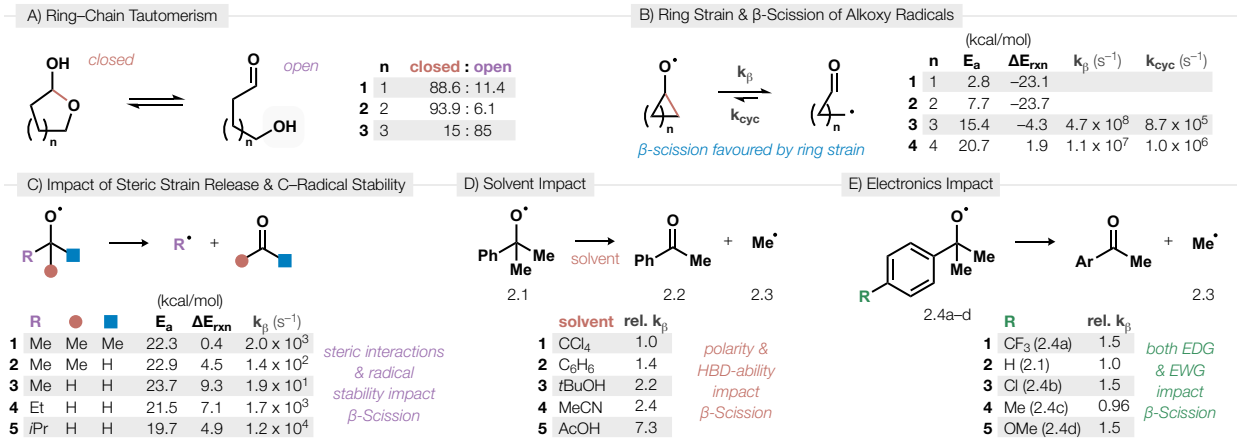


Figure 11. *Hemiacetal ring-chain tautomerism and factors affecting alkoxyl radical β-scission propensity.*

When it comes to the β-scission of alkoxy radicals, there are a number of well-studied factors that impact selectivity and cleavage rates.[59d, j, 86h, 87a–d] Ring-strain and alkoxy radical β-scission activation energy show an inverse correlation, and this strain significantly impacts the extent to which β-scission is reversible (**Figure 11**, **B**). Steric strain release can also influence the selectivity and rate of alkoxy radical β-scission wherein more sterically congested α-carbons will more readily cleave a substituent (**Figure 11**, **C**).

The stability of the ejected radical also influences the rate of cleavage with more stable radicals cleaving at faster rates. Hyperconjugative and delocalizing stabilizations of the incipient C-centred radical serve to favour cleavage towards the imparting substituents. Zavitsas and Seltzer demonstrated through secondary D-isotope effects that the liberation of Me$^{\bullet}$ (**2.3**) and acetophenone (**2.2**) from the precursor O-radical (**2.1**) has a product-resembling

late TS.[88] It should be noted that effects rendering the β-scission more exothermic, such as significant ring-strain release, can make product-stabilizing effects less important in determining selectivity.[89]

The reaction medium also impacts the rate of alkoxy radical β-scission (**Figure 11**, **D**). More polar solvents result in a faster rate of β-scission due to stabilizing solvation of the polar β-scission TS. This has been explained as the result of a greater stabilization of the incipient carbonyl product which is prominent at these late TSs.[90] Hydrogen bond-donor/acceptor pairing also impacts the β-scission rate for the same reasons. Finally, electronic effects also influence the rate of β-scission, with both electron-withdrawing and electron donating groups serving to increase the rate of cleavage due to delocalization of nascent radical species and/or stabilization of the incipient carbonyl (**Figure 11**, **E**).

In 1961, Barton demonstrated a ring β-scission reaction of a steroid-derived alkyl nitrite **2.5** (**Figure 12**, **A**).[91] Light-induced N–O bond homolysis to generate the alkoxyl radical, β-scission to the more stable tertiary C-centred radical, nitrosyl radical capture, nitrogen attack at the newly formed aldehyde, and tautomerization yield the corresponding hydroxamic acid **2.6**. Overall, this represents a redox-neutral reaction from the pre-functionalized starting material **2.5**. The Hunsdiecker-Borodine reaction is a ubiquitous reaction also operating on the principle of O-activation through oxidation with a stoichiometric oxidant.[92] Intermediate acyl hypohalites undergo thermal or photolytic homolysis to generate carboxyl radicals which may undergo β-scission to liberate CO_2 and generate a C-centred radical. Subsequent XAT generates the corresponding organohalide product in a net-oxidative process. Barton-decarboxylation, and many of its recent variations, requires the prefunctionalization of the carboxylic acid as a redox-active ester.[93] In Barton's seminal works, a thiohydroximate ester is treated with tributyltin hydride at elevated temperature. A radical chain reaction liberating CO_2 and aromatic 2-thiopyridine leaving groups generate the desired closed-shell alkanes through a formal β-scission of intermediate acyloxy radicals.

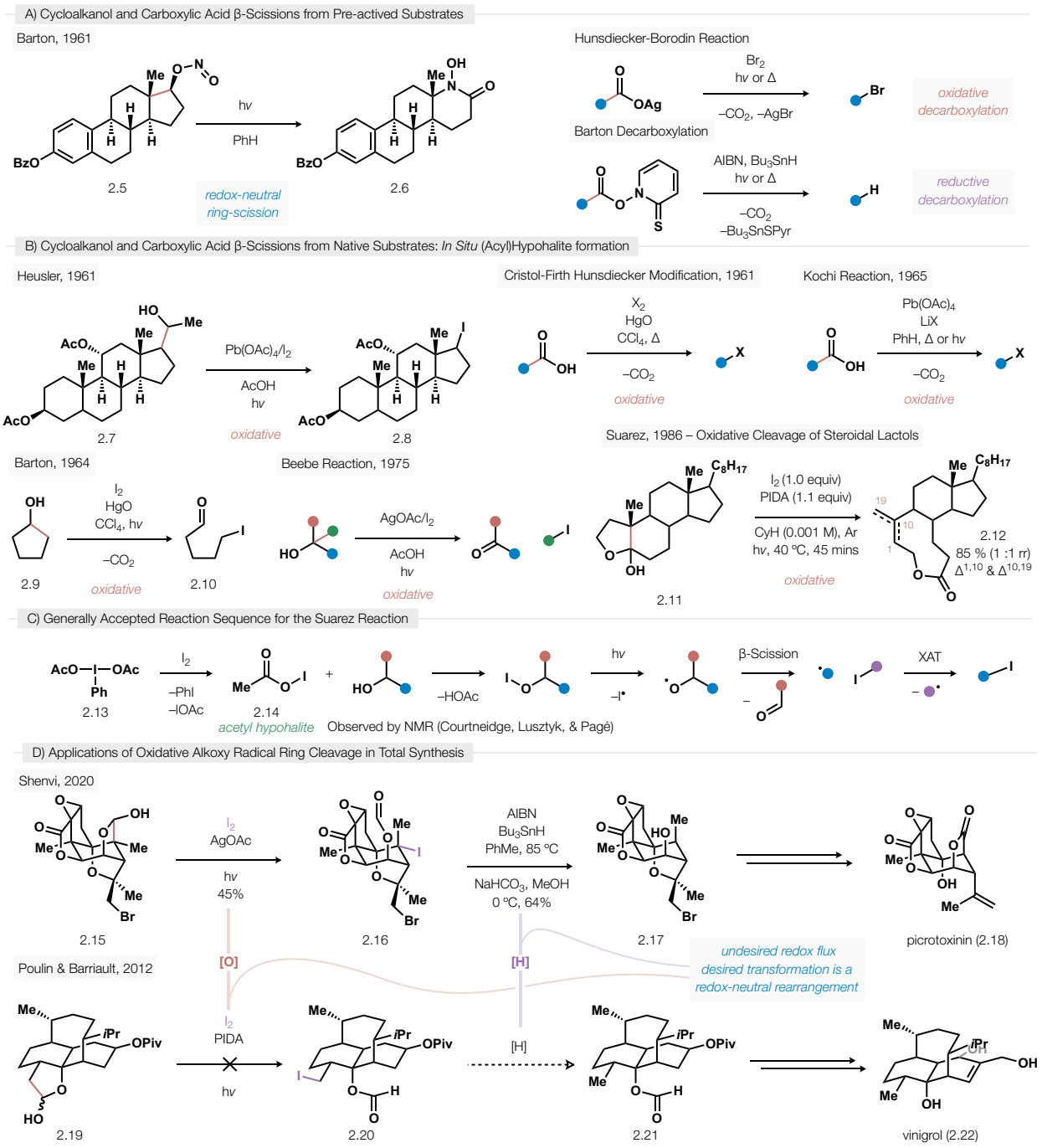


Figure 12. *β-scission of hydroxyl-containing molecules.*

A) β-scission of pre-activated cycloalkanols and carboxylic acids; B) Native substrate β-scission of cycloalkanols and carboxylic acids through hypohalite intermediates; C) Putative reaction scheme for the Suaréz cleavage; D) Applications of oxidative lactol ring cleavage in total synthesis.

β-Scission reactions from native alcohol or carboxylic acids have traditionally been oxidative transformations (**Figure 12**, **B**). Most prominent examples utilize intermediate hypo(acyl)halites generated *in situ*. Seminal works

include: Heusler's LTA/I_2 photolytic β-scission of steroidal alcohols (**2.7**),[94] the Cristol-Firth modification of the Hunsdiecker reaction,[95] the Kochi reaction,[96] Barton's oxidative ring cleavage,[97] the Beebe reaction,[98] and the Suaréz cleavage.[99] The putative reaction sequence for the Suaréz cleavage first involves the formation of acetyl hypoiodite (**2.14**) from the reaction of iodine and di(acetoxy)iodobenzene (**2.13**, **Figure 12**, **C**). This intermediate was first observed by NMR spectroscopy under these conditions and those of the Beebe reaction by Courtneidge, Lusztyk and Pagé at the NRCC.[100] Oxidation of the alcohol substrate to the cycloalkyl hypoiodite ensues, followed by photolytic homolysis of the O–I bond. Finally, iodine atom transfer generates the closed-shell iodide product.

Applications of lactol C–C β-scission reactions in total synthesis are often performed oxidatively due to the lack of redox-neutral variants available (**Figure 12**, **D**). In Shenvi's synthesis of picrotoxinin (**2.18**), cleavage of lactol **2.15** under Beebe conditions yielded iodide **2.16** in 45% yield.[101] Subsequently, the authors reduced the 3º iodide under AIBN/Bu_3SnH conditions to give **2.17** in 64% yield. During one approach towards vinigrol (**2.22**) by Barriault and Poulin, a Suaréz cleavage of lactol **2.19** with subsequent 1º alkyl iodide (**2.20**) reduction to yield **2.21** was attempted.[102] Each of these sequences show undesired redox flux and demonstrate a need for a redox-neutral formal rearrangement of lactols to formate esters *via* C–C bond β-scission.

The thermodynamics of oxidative and redox-neutral ring scission reactions differ significantly (**Figure 13**, **A**). Oxidative cleavage reactions are typically exothermic due to the reduction of the (super)stoichiometric co-oxidant. In contrast, the redox-neutral transformation constitutes a formal rearrangement where the strengths of the bonds formed in the products are typically weaker than the bonds broken in the starting materials. To achieve a contrathermodynamic rearrangement reaction, photoredox multicatalysis can enable irreversible reaction mechanisms driven by light. The decoupling of activation and termination events in a multicatalytic reaction scheme enables paired elementary steps that make the overall process irreversible.

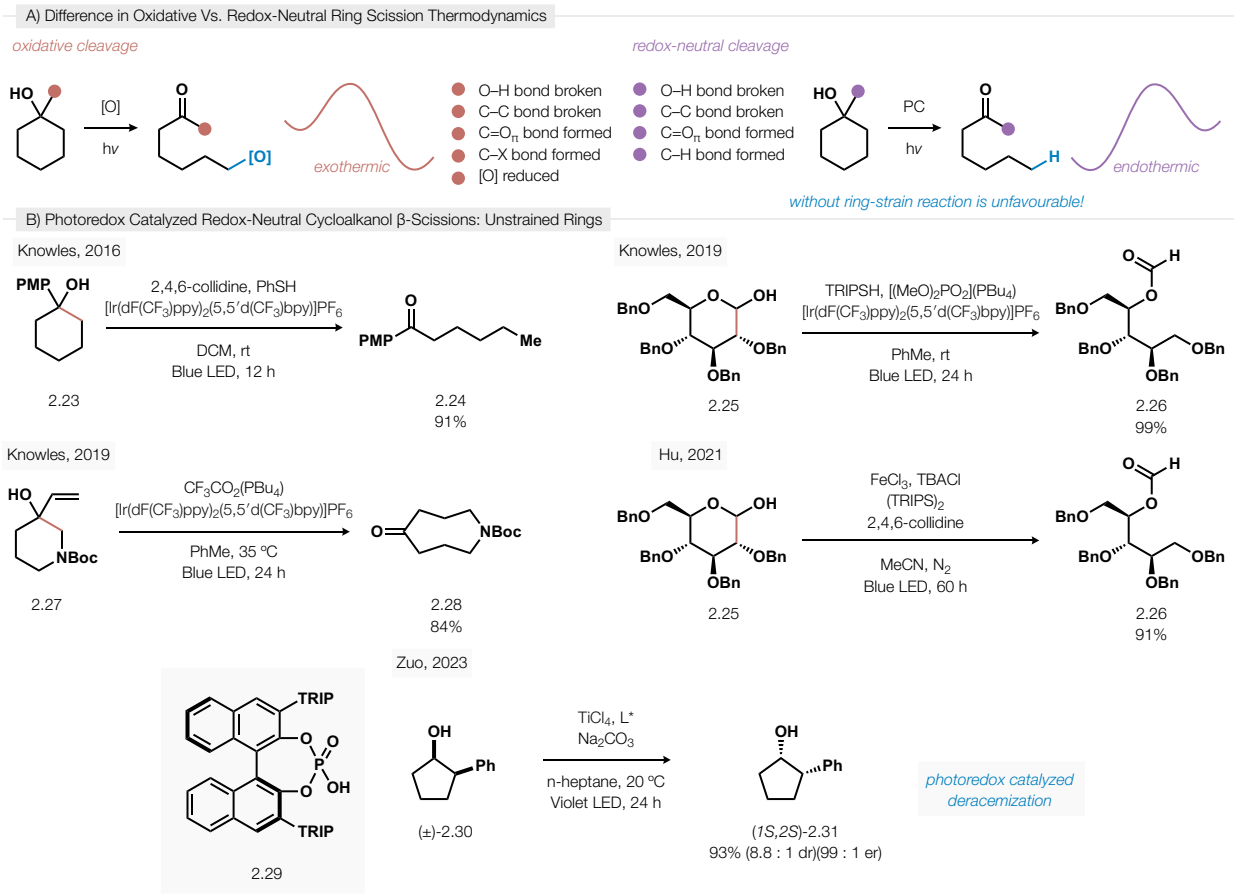


Figure 13. *Principles and applications of cycloalkanol ring scission.*
A) Thermodynamics of oxidative and redox-neutral cycloalkanol ring scission reactions; B) Photoredox catalyzed redox-neutral β-scission reactions of unstrained cycloalkanols.

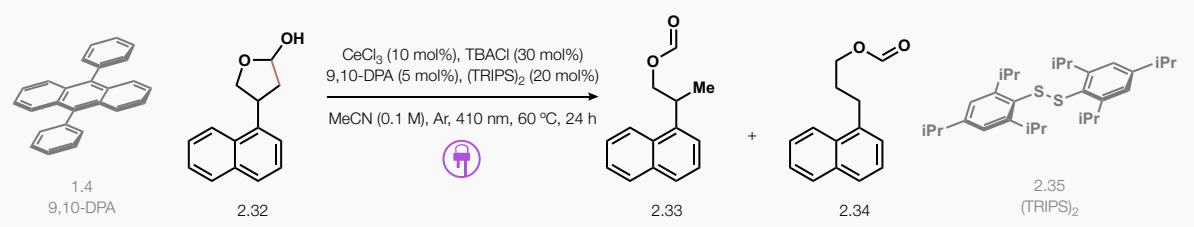
In 2016, the Knowles group published the PCET-enabled photoredox-catalyzed rearrangement of 3º benzylic cyclic alcohols (e.g. **2.23**) to the corresponding aryl ketones (e.g. **2.24**, **Figure 13**, **B**).[103] The substrate scope for this transformation was severely limited by the requirement for an oxidizable aryl group, typically *p*-methoxyphenyl, bound directly to the 3º alcohol centre. Photoinduced single electron transfer oxidation of the redox-auxiliary generates an aryl radical cation which acts as a strong intramolecular oxidant for a subsequent PCET event to generate the O-centred radical. Later revisiting this strategy, the Knowles group improved upon their conditions with an anionic base catalyst to facilitate stronger HBD–HBA association, enabling an efficient MS-PCET to generate O-centred radicals without the need for a covalent redox auxiliary.[51] This work demonstrates an efficient contrathermodynamic reaction process driven by an irreversible photocatalytic reaction. The Knowles group later applied this photoredox catalyzed PCET activation mode to the ring expansion of cyclic allylic alcohols (e.g. **2.27**).[104] While these publications are excellent and insightful, the main drawback of these methods is the use of rare and expensive Ir-based photocatalysts.

Shortly after we embarked on our own efforts to realize a redox-neutral cycloalkanol/lactol ring-scission reaction, the Hu group reported an iron trichloride photoredox-catalyzed LMCT-enabled cleavage of cyclic alcohols & lactols (e.g. **2.25**).[105] Finally, Zuo demonstrated a photoredox catalyzed deracemization of cyclic alcohols (e.g. **2.30** to **2.31**). *O*-Centred radicals are generated by Ti(IV) LMCT activation, ring cleavage generates a prochiral aldehyde and C-centred radical, and subsequent cyclization and reduction regenerates both stereogenic centres (**2.31**).[106] A chiral phosphoric acid ligand (**2.29**) bound to titanium enforces substrate discrimination prior to LMCT activation, thereby resulting in a build-up of the more slowly activated enantiomer.

2.2 Initial Studies & Optimization

Our initial forays into the redox-neutral β-scission reaction showed modest success, yielding 35% of the naphthyl formate esters **2.33** and **2.34** in a 1:1 ratio (**Table 1**, **entry 1**). Control reactions excluding $CeCl_3$, tetrabutylammonium chloride, bis(2,4,6-triisopropylphenyl)disulfide (**2.35**), or violet LED irradiation all failed to deliver ring cleavage products **2.33** or **2.34** (**entries 2–5**). In contrast, exclusion of the 9,10-diphenylanthracene (**1.4**) photocatalyst delivered the separable products in a 1:1 ratio and a diminished 8% overall yield. This control suggests 9,10-DPA (**1.4**) is not necessary for productive reaction, but its inclusion results in an improved conversion to the desired products. Based on this result, we believe 9,10-DPA (**1.4**) serves to increase the rate of global turnover frequency and mediate the cerium and disulfide catalytic cycles to more effectively match the relative rates of radical and thiol production. Overall, this intermediary catalytic cycle results in a more efficient and selective reaction profile.

Table 1. *Preliminary redox-neutral lactol ring scission attempt and control reactions.*

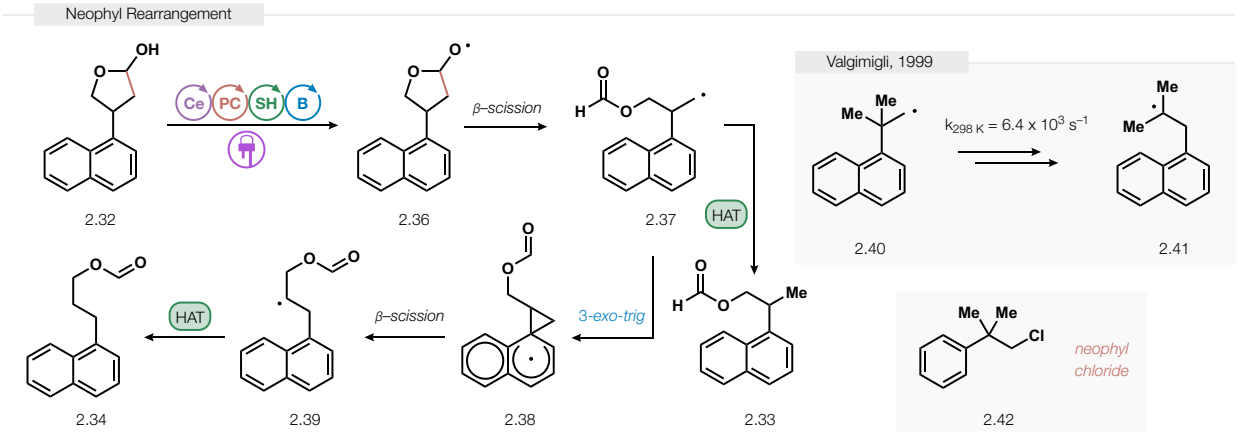


Entry	Control	% Yield (2.33:2.34)	% SM (2.32)
1	**none**	**35 (1:1)**	**29**
2	No $CeCl_3$	0	87
3	No TBACl	0	32
4	No $(TRIPS)_2$	0	76
5	No light	0	93
6	No 9,10-DPA	8 (1:1)	42

The origin of product **2.34** warrants some discussion on radical 1,2-aryl migrations, sometimes referred to as the neophyl rearrangement (**Scheme 1**).[107] The neophyl rearrangement is so named due to its initial observation in the

rearrangement of neophyl chloride (**2.42**) with PhMgBr and $CoCl_2$ in ether by Kharasch and Urry in 1944.[108] This 1,2-aryl shift rearrangement likely occurs through the intermediacy of a spirocyclopropyl cyclohexadienyl radical of the type **2.38** with subsequent β-scission leading to the more stable 2º C-centred radical **2.39**. The presence of the cyclohexadienyl radical **2.38** as a discrete intermediate, or the presence of a single 1,2-shift transition state, has been the subject of many studies by Fischer, Ingold, Scaiano, Leardini, and more.[107, 108b, 109] There is now a general consensus that such an intermediate (**2.38**) is likely present in these reactions, if very short-lived, with lifetimes varying based on the degree of radical stabilization.

Likewise there has been numerous studies seeking to establish the absolute rate for radical 1,2-aryl shift reactions for use as radical clocks/probes.[82, 110] In 1999, Valgimigli measured the rate for the rearrangement of the naphthyl-derived 1º radical **2.40** into the 3º radical **2.41**.[111] The authors established a radical aryl migration rate of 6.4 × 10^3 s^{-1} using a radical clock approach wherein the concentration of an H-atom donor (2,4,6-trimethylphenol) was varied under $(Bu_3Sn)_2$ radical initiation. Of course, the substrate **2.32** used under our reaction conditions does not bear the same 4º benzylic C-centre as the substrate used by Valgimigli and colleagues. As such, our substrate does not benefit as significantly from a Thorpe-Ingold effect in the initial spirocyclization step and also experiences less stabilization after β-scission to the less stabilized 2º (**2.39**), rather than 3º, C-centred radical. For these reasons, the rate measured by Valgimigli likely represents an upper limit for the rearrangement of radical **2.37**.

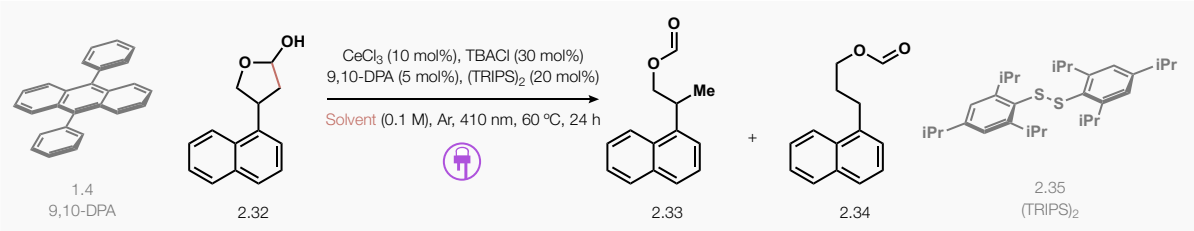


Scheme 1. *Neophyl rearrangement reaction mechanism and approximate rearrangement rate.*

A survey of solvents performed with DCE, THF, DMSO and $PhCF_3$ failed to yield any of the desired product (**2.33**, **Table 2**, **entries 2**, **4**, **6–7**). THF gave minimal conversion of starting material (**2.32**), an unsurprising result given the propensity for photoactivated Ce(III) species to oligomerize and form inactive compounds in ethereal

solvents (**entry 4**).[112] Toluene, acetone, benzonitrile, ethyl acetate and acetonitrile/acetone all yielded products in inferior yield to acetonitrile (entries **1**, **3**, **5**, **8–10**).

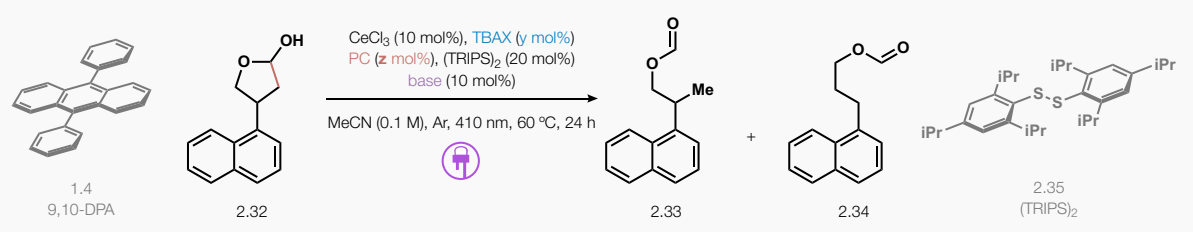
Table 2. *Reaction optimization: solvent study.*



Entry	Solvent	% Yield (2.33:2.34)	% SM (2.32)
1	**MeCN**	**35 (1:1)**	**29**
2	DCE	0	58
3	PhMe	13 (0:1)	76
4	THF	0	95
5	MeAc	24 (1.7:1)	35
6	DMSO	0	36
7	$PhCF_3$	0	55
8	PhCN	18 (1:1)	16
9	EtOAc	13 (0:1)	74
10	MeCN/MeAc (1:1)	19 (3:1)	33

Subsequently, we assessed the identities and loadings of the photocatalyst and tetrabutylammonium halide salt, as well as the effects of some inorganic bases. 9,10-DPA (**1.4**) remained the best photocatalyst surveyed, with **2.33** and **2.34** formed in 56% yield and 2:1 ratio at 5 mol% loading (**Table 3**, **entries 1–6**). The inorganic bases tested showed either no significant impact or were detrimental to the reaction, prompting a small survey (**entries 7–9**). Next, the halide source and loadings were assessed with 1 equivalent of tetrabutylammonium chloride proving superior to the bromide or iodide salts (**entries 12**, **14–15**). We observed a marked increase in yield on increasing the halide loading from 30 to 60 mol%, no significant improvement on increasing to 1 equivalent, and detrimental effects on increasing to 160 mol% (**entries 1**, **10–13**). Despite indistinguishable yields upon increasing to 1 equivalent, we maintained this loading for the remainder of the study. We reasoned that optimal halide concentration may vary based on substate–Ce binding equilibria and that a higher concentration might inhibit the formation of potentially inactive polyalkoxy-Ce species across the broadest possible set of substrates.

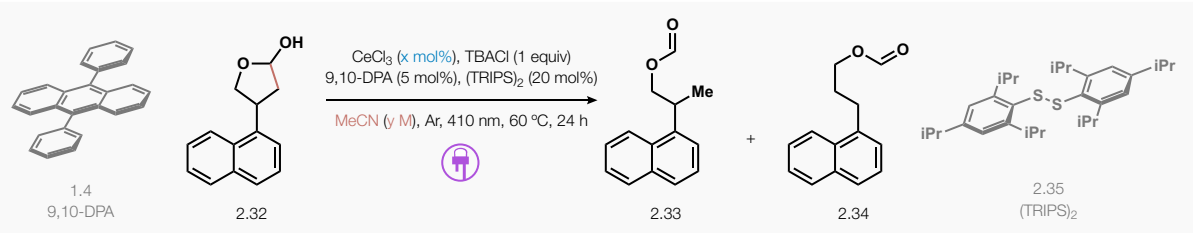
Table 3. *Reaction optimization: secondary photocatalyst, inorganic base additive, and halide salt studies.*



Entry	TBAX (mol%)	PC (mol%)	base	% Yield (2.33:2.34)	% SM (2.35)
1	TBACl (60)	9,10-DPA (5)	–	56 (2:1)	15
2	TBACl (60)	9,10-DPA (10)	–	51 (1.5:1)	10
3	TBACl (60)	9,10-DPA (15)	–	43 (1.66:1)	13
4	TBACl (60)	4CzIPN (5)	–	0	46
5	TBACl (60)	5CzBN (5)	–	17 (2:1)	36
6	TBACl (60)	$[Ru(bpy)_3](PF_6)_2$	–	0	73
7	TBACl (60)	9,10-DPA (5)	K_2CO_3	43 (1:1)	9
8	TBACl (60)	9,10-DPA (5)	$KHCO_3$	51 (1.4:1)	9
9	TBACl (60)	9,10-DPA (5)	K_2HPO_4	54 (1.25:1)	9
10	TBACl (30)	9,10-DPA (5)	–	35 (1:1)	29
11	TBACl (40)	9,10-DPA (5)	–	47 (1.75:1)	11
12	**TBACl (100)**	**9,10-DPA (5)**	**–**	**57 (1.25:1)**	**11**
13	TBACl (160)	9,10-DPA (5)	–	31 (1:1)	17
14	TBABr (100)	9,10-DPA (5)	–	23 (1.33:1)	26
15	TBAI (100)	9,10-DPA (5)	–	0	67

Next, we assessed the Ce loading and overall reaction concentration (**Table 4**). Halving the Ce loading appeared to slightly diminish the reaction yield, whilst doubling it conferred no benefit (**entries 1–3**). Doubling the reaction concentration to 0.2 M showed no impact and further increasing it to 0.4 M proved detrimental to the reaction (**entries 4–5**). Reaction concentration will also impact Ce–substrate binding equilibria and optimal concentrations are likely to be substrate dependent.

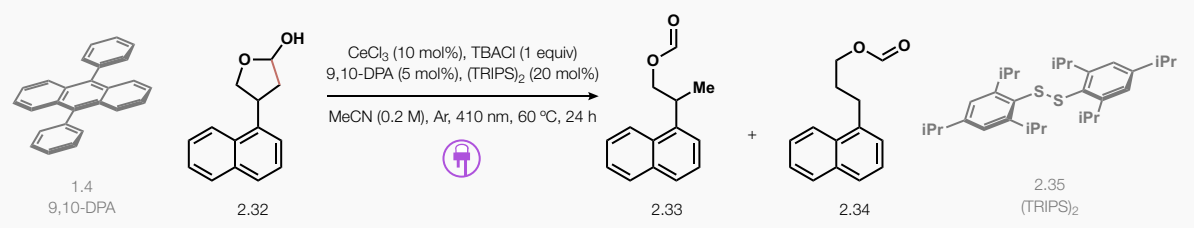
Table 4. *Reaction optimization: Ce-loading and reaction concentration studies.*



Entry	$mol\%_{Ce}$	$Conc._{2.32}$ (M)	% Yield (2.33:2.34)	% SM (2.32)
1	10	0.1	57 (1.25:1)	11
2	5	0.1	53 (3.5:1)	21
3	20	0.1	58 (1.8:1)	17
4	**10**	**0.2**	**58 (1.5:1)**	**16**
5	10	0.4	44 (4.5:1)	17

We next assessed the impacts of the remaining additives and reaction conditions (**Table 5**). With the purpose of improving selectivity for unrearranged (**2.33**) *vs* rearranged products (**2.34**), we cooled the reaction to ~45 ºC internal temperature using fan cooling and found improvement in both the total yield and selectivity (**entry 1**). We hypothesized a diselenide with its weaker Se–H bond might result in a faster HAT reaction and further increase selectivity, however only trace products were observed with the majority of SM (**2.32**) remaining (**entry 2**). Given the number of roles that this species must play in the catalytic cycle (oxidant, H-atom donor, base), it is not surprising that a change in identity failed to improve our conditions. Neither halving nor doubling the disulfide loading resulted in a better reaction than the existing conditions (**entries 3 & 4**). The erosion in selectivity at lower disulfide loading might imply that there is a non-infinitesimal steady state concentration of TRIPSH. Inclusion of 45 mol% sodium benzoate resulted in a significant enhancement, providing product in 86% yield and an unrearranged to rearranged (**2.33:2.34**) ratio of 7:1 with just 8% SM (**2.32**) remaining (**entry 5**). We reasoned that a weak carboxylate base ($pKa^{\text{benzoic acid}} = 4.2$) could facilitate substrate–Ce binding while still engaging in the necessary PT to thiolate ($pKa^{\text{PhSH}} = 7$) for its subsequent role as a thiol H-atom donor. A few short days after obtaining this result, the Zuo group published a dehydroxymethylation arylation reaction in which a high throughput screen of ligands for Ce identified aryl carboxylates as a privileged ligand class.[47] To see the impact of BHT on the reaction conditions, we included it as a 20 mol% additive where it appeared to decrease conversion (**compare entries 1 & 6**). As we do not anticipate radical chain contribution in this reaction, the impact of BHT might be due to Ce-ligation or slowed conversion due to increased HAT (PCET) quenching of O-centred substrate radicals with the higher concentration of H-atom donor now present. It should be noted that BHT could plausibly substitute disulfide/thiol and fulfill the same role. Cs_2CO_3 as a base additive and diethyl phenylmalonate as an alternative to $(TRIPS)_2$ (**2.35**) both failed to improve upon the previously identified best conditions (**compare entries 1**, **7–8**).

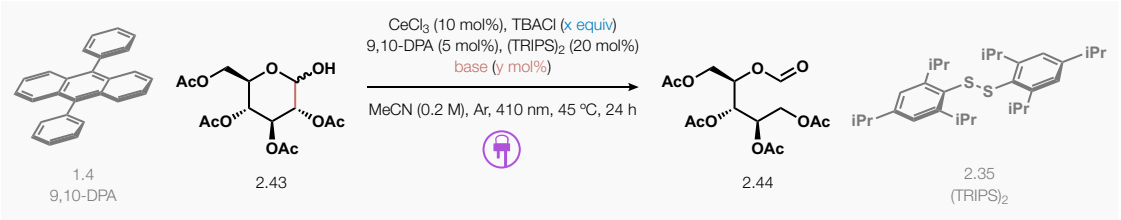
Table 5. *Reaction optimization: miscellaneous screening.*



Entry	Deviation from above	% Yield (2.33:2.34)	% SM (2.32)
1	45 °C (fan cooled)	69 (5:1)	10
2	$(TRIPSe)_2$ in place of $(TRIPS)_2$ (**2.35**)	trace	84
3	10 mol% $(TRIPS)_2$ (**2.35**)	63 (2:1)	31
4	40 mol% $(TRIPS)_2$ (**2.35**)	43 (3:1)	15
5	**45 °C, with 10 mol% $PhCO_2Na$**	**86 (7:1)**	**8**
6	+ 20 mol% BHT additive	60 (2:1)	24
7	+ 10 mol% Cs_2CO_3 additive	57 (2.5:1)	20
8	+ 20 mol% diethyl phenylmalonate additive	63 (8:1)	4

After discovering the marked improvement conferred by the addition of sodium benzoate, we surveyed more weakly-basic additives in the fragmentation of **2.43** to **2.44** (**Table 6**). Sodium trifluoroacetate, sodium 2,4,6-triisopropylphenyl thiolate, and dibutyl sodium phosphate all proved inferior to sodium benzoate (**entries 1–5**). 10 mol% loading of sodium benzoate proved optimal (**entries 5–8**). Maintaining 1 equivalent of tetrabutylammonium chloride also appeared to be optimal (**entries 9–10**).

Table 6. *Reaction optimization: weak base additive screening.*



Entry	equiv.$_{TBACl}$	base (mol%)	% Yield (2.44 : 2.44')	% SM
1	1.0	none	33	58
2	1.0	CF_3CO_2Na (20)	30	57
3	1.0	TRIPSNa (20)	40	60
4	1.0	$(n\text{-}BuO)_2PO_2Na$ (20)	46	52
5	1.0	$PhCO_2Na$ (20)	76	15
6	**1.0**	**$PhCO_2Na$ (10)**	**82**	**17**
7	1.0	$PhCO_2Na$ (40)	73	23
8	1.0	$PhCO_2Na$ (5)	67	33
9	0.9	$PhCO_2Na$ (10)	80	15
10	1.1	$PhCO_2Na$ (10)	71	20

2.3 Hydroxyl Ring β-Scission Scope

As our efforts were primarily focused on the cleavage of lactol rings, we first had to synthesize several lactones for subsequent reduction prior to use under the reaction conditions (**Figure 14**). (–)-Menthol (**2.45**) was first converted to menthone (**2.46**) under PCC oxidation in 73% yield followed by Baeyer–Villiger oxidation (BVO) using mCPBA in 78% yield to furnish the desired 7-membered lactone (**2.47**, **Figure 14**, **A**). These conventional BVO conditions were used to oxidize 6-membered cyclic ketones 2-adamantanone (**2.48**), cyclohexanone (**2.50a**), 4-*tert*-butylcyclohexanone (**2.50b**), and 4-phenylcyclohexanone (**2.50c**), providing the corresponding 7-membered lactones (**2.51a**–**c**) in excellent yields.

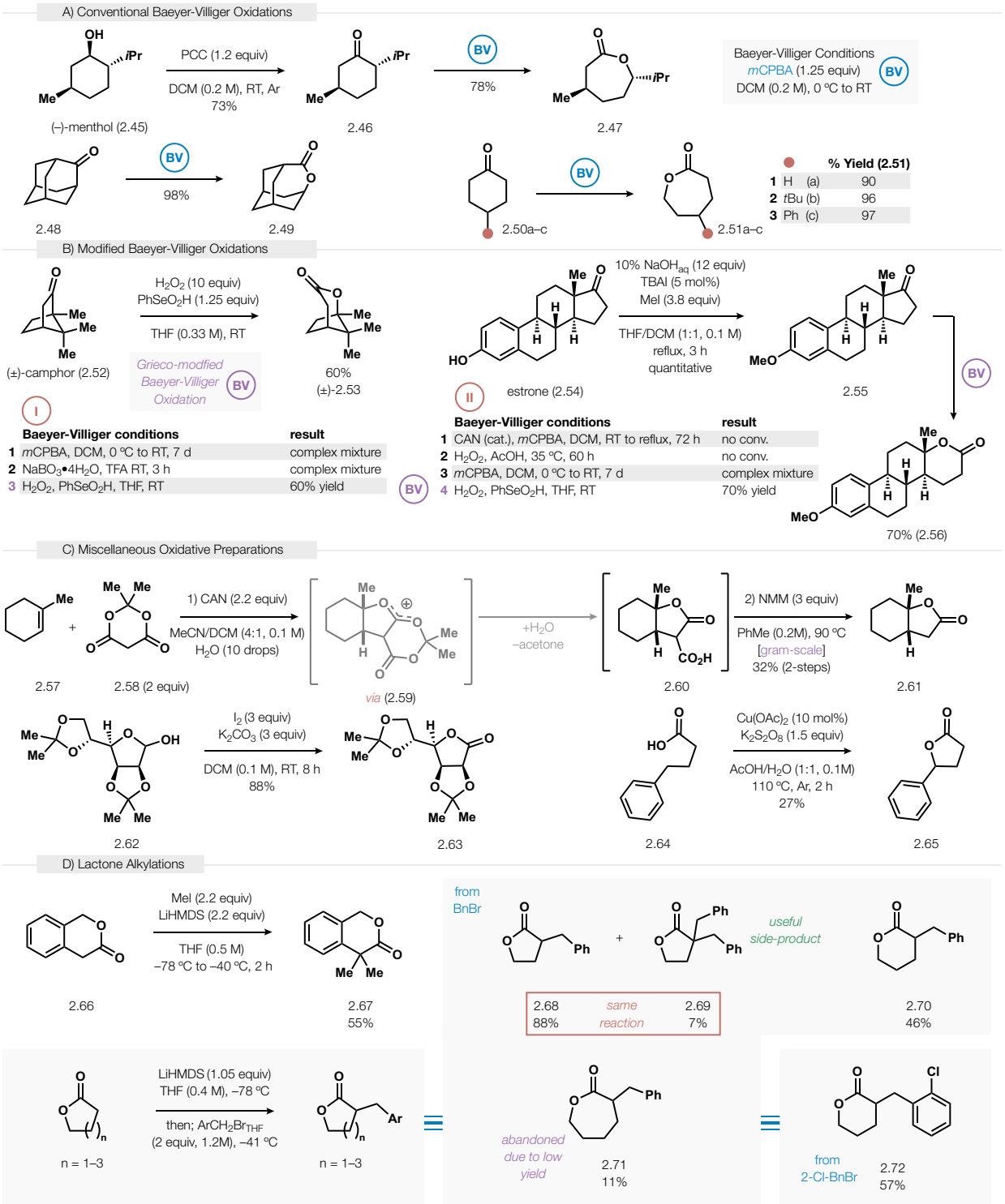


Figure 14. *Preparation of lactones used to access lactol substrates.*

A) Conventional Baeyer-Villiger ketone oxidations; B) Baeyer-Villiger oxidations under Grieco modification conditions; C) Miscellaneous oxidative lactone preparations; D) Alkylative lactone derivatizations.

Unfortunately, conventional BVOs failed on the more sterically congested ketones (±)-camphor (**2.52**) and Me-estrone (**2.55**, **Figure 14**, **B**). Oxidation of camphor (**2.52**) under Tarbin and McKillop's conditions using sodium perborate failed to yield derivative **2.53**, giving an intractable mixture (**Figure 14**, **B**, **table I**).[113] Fortunately, Grieco's modification of the BVO using benzeneseleninic acid with hydrogen peroxide cleanly converted **2.52** to **2.53** in 60% isolated yield.[114] Grieco's BVO conditions were traditionally thought to produce benzeneperoxyseleninic acid *in situ* as the active oxidant, however, a more recent report challenges this mechanism.[115] Back and colleagues found that the combination of benzeneseleninic acid and hydrogen peroxide can produce benzeneperoxyselenonic acid, a Se(VI) species, which acts as the active oxidizing agent under these conditions.

Me-estrone (**2.55**) was synthesized from estrone (**2.54**) in quantitative yield under phase transfer catalysis conditions reported by Li and colleagues.[116] Conventional BVO conditions, Jacobsen's AcOH/H_2O_2 conditions,[117] and conditions employing CAN as a catalyst[118] all failed to yield the desired steroid-derived lactone **2.56**, with the latter two conditions showing no conversion (**Figure 14**, **B**, **table II**). Gratifyingly, Grieco's modification once again proved viable and delivered lactone **2.56** in 70% isolated yield.

γ-Lactones **2.61**, **2.63** and **2.65** were prepared through a variety of oxidative transformations (**Figure 14**, **C**). Ceric ammonium nitrate promoted formal [3+2] cycloaddition between methylcyclohexene (**2.57**) and Meldrum's acid (**2.58**) produced intermediate carboxylactone **2.60** after *in situ* hydrolysis of the oxocarbenium **2.59** according to procedures by Szumny & Wawrzenczyk,[119] and Mane *et al.*.[120] Subsequent decarboxylation of the crudely worked-up carboxylactone **2.60** using *N*-methylmorpholine in toluene at elevated temperature yielded bicyclic lactone **2.61** in 32% yield over 2 steps. Mannofuranose diacetonide **2.62** underwent anomeric carbon oxidation using iodine and potassium carbonate at room temperature to yield lactone **2.63** in 88% isolated yield. Simple γ-phenyl-γ-lactone **2.65** was prepared in a single step from 4-phenylbutyric acid (**2.64**) using Dubois and Sathyamoorthy's benzylic C–H oxidation lactonization procedure in a modest 27% isolated yield.[121]

Several commercially available lactones were alkylated under basic conditions (**Figure 14**, **D**). Dimethylation of isochroman-3-one (**2.66**) was accomplished in 55% yield using excess LiHMDS and methyl iodide. Addition of benzyl halides to γ-, δ-, and caprolactones using LiHMDS produced lactones **2.68**, **2.69**, **2.70**, **2.71**, and **2.72** under the same reaction conditions. Gram-scale alkylation of γ-lactone gave monoalkylated product **2.68** as the major product in 88% yield and 7% of dialkylated product **2.69** in separable fractions. Fortuitously, dialkylated product **2.69**, although isolated in modest yield as a side-product from the intended reaction, could be reduced to a lactol for use in

the photochemical reaction. The low yield of caprolactam derivative **2.71** (11%), in addition to the ring-chain tautomerism challenges associated with 7-membered hemiacetals, precluded its further conversion to a lactol substrate. 6-membered lactones **2.70** and **2.72** were prepared in moderate yields for elaboration into lactols.

The prepared lactones were reduced to their corresponding lactols using DIBAL (**2.73**, Figure 15, **A**). Reduction of 5-membered and 6-membered lactones proceeded in high yields, except for dihydrocoumarin and isochroman-2-one which gave compounds 2.82 and 2.83 in 20% and 35% yields, respectively. Estrone-derived lactone 2.56 was reduced to lactol 2.84, present in DMSO-d6 solution exclusively as the α-anomer. 7-membered lactones were all reduced in high to excellent yields. Interestingly, *t*Bu-compound (±)-**2.88** was observed as a single anomer in chloroform-*d* by ^{1}H NMR.

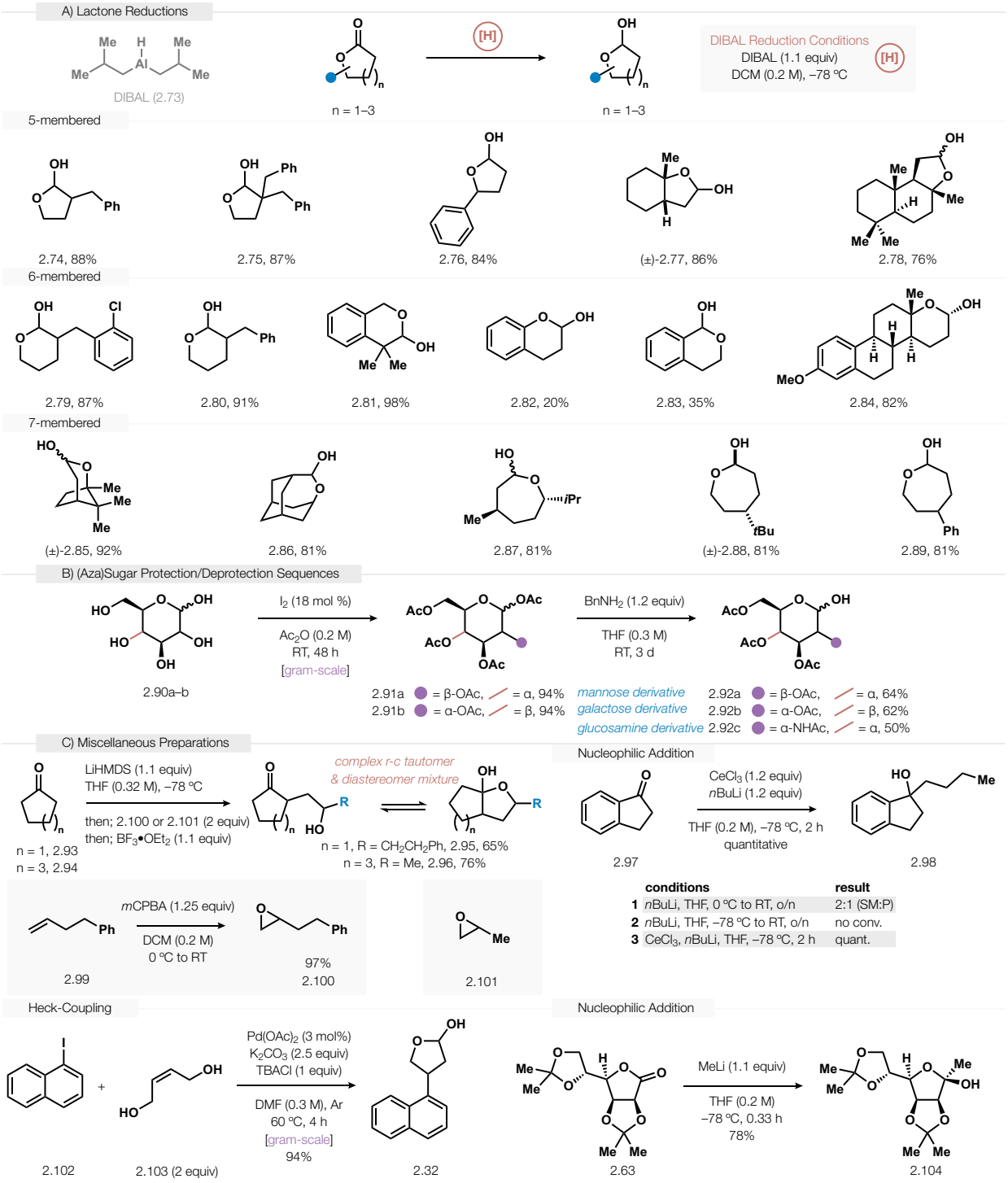


Figure 15. *Lactol substrate preparations.*

A) Lactone reductions with DIBAL; B) (Aza)sugar protections/deprotections; C) Miscellaneous preparations.

In addition to lactone reductions, a few (aza)sugar substrates were prepared by protection/deprotection sequences

Figure 15, **B**). Iodine catalyzed peracetylation of D-galactose (**2.90a**) and D-mannose (**2.90b**) yielded protected compounds **2.91a** and **2.91b** in identical 94% yields on gram-scale. Benzylamine-enabled deprotection on

2.91a, **2.91b** and commercially available peracetyl glucosamine, provided substrates **2.92a**, **2.92b**, and **2.92c** in good yields. Hemiketals **2.95** and **2.96** were prepared through BF_3•OEt_2 promoted addition of Li-enolates of cyclopentanone (**2.93**) or cycloheptanone (**2.94**) to epoxides **2.100** and **2.101** in 65% and 76% yields, respectively (

Figure 15, **C**). The complex diastereomeric and ring-chain tautomeric mixture of these compounds precludes full assignment of their NMR spectral features. Epoxide **2.100** was prepared through Prilezhaev oxidation of terminal olefin **2.99** in 97% isolated yield.

Synthesis of indanol derivative **2.98** by nucleophilic addition of *n*BuLi was hampered by a competing deprotonation pathway. Addition of *n*BuLi to indanone (**2.97**) at –78 ºC showed no conversion even after allowing the mixture to warm to room temperature overnight. Addition of *n*BuLi to indanone (**2.97**) at 0 ºC showed incomplete conversion over the course of several hours, and slow warming of this solution to room temperature and reaction overnight resulted in a 2:1 mixture of **2.97**/**2.98** that was difficult to separate by column chromatography. In the 1980s, Imamoto and co-workers demonstrated the easy preparation of organocerium(III) reagents from Grignard reagents or organolithiums.[122] The authors further showed the enhanced nucleophilic rather than basic behaviour of organocerium(III) reagents, particularly in the addition to enolizable carbonyl substrates.[122c] Gratifyingly, treatment of indanone (**2.97**) with the organocerium nucleophile provided indanol derivative **2.98** in quantitative yield under cryogenic conditions.

Heck coupling between 1-iodonaphthalene (**2.102**) and *cis*-butene-1,4-diol (**2.103**) furnished naphthyl lactol substrate **2.32** in 94% yield.[123] Lactone **2.63** was converted into hemiacetal **2.104**, as a single anomer, by nucleophilic addition of MeLi at –78 ºC in 78% isolated yield.

Application of the optimized conditions produced the following substrate scope

Figure 16). 5-Membered ring lactols underwent redox-neutral β-scission reactions in poor to excellent yields (21–91%). Benzyl protected D-arabino- (**2.107a**), and D-ribofuranose (**2.107b**) underwent scission in nearly identical yields of 68% and 72% respectively, showing no sensitivity to the stereochemistry of the vicinal stereocentre.

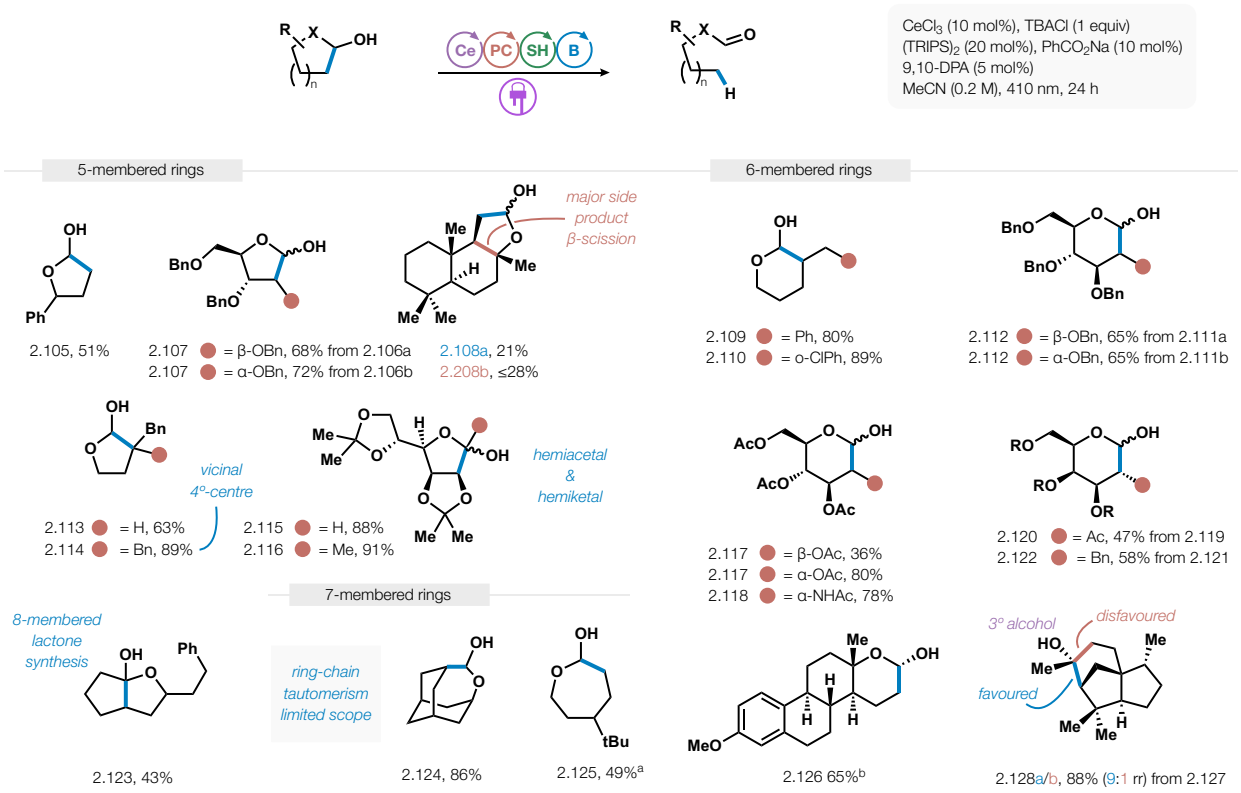


***Figure 16**. Redox-neutral lactol/cycloalkanol ring β-scission scope.*

[a]Two-step yield following saponification. [b]Reaction concentration 0.05 M in acetonitrile.

Sclaral (**2.78**) yielded the desired β-scission product (**2.108a**) in only 21% isolated yield with the major side product derived from cleavage of the C–C bond at the B/C (6,5) ring junction (**2.108b**). The most likely explanation for the unexpected ring-scission product comes from the LMCT activation of the 3° alcohol present in the ring-opened hydroxyaldehyde tautomer of the SM. As the 6,5-ring system in **2.78** is *trans* fused, there is considerable ring strain in the 5-membered lactol, likely shifting the equilibrium towards the open hydroxyaldehyde form. Alternative explanations include a concerted process of β-C–O_σ bond scission with concomitant γ-δ-C–C_σ bond scission from the lactol-derived O-centred radical or *via* a stepwise β-scission cascade. The stereoelectronic requirements necessary for the concerted process serve to make this an unlikely process. The strain present in this ring system may make a C–O β-scission more exothermic with an earlier TS and therefore kinetically favoured, regardless of the anticipated stability of a O-centred radical intermediate *vs* a C-centred radical intermediate.[89b] Stereoelectronic alignment of the cleaving Ce–O and C–C_σ or C–O_σ bonds may play a significant role in dictating product distributions.[46] The Knowles group also reported the β-scission of compound **2.78** under PCET activation to obtain the expected product in 48% yield, with no mention made of the 5/6-ring junction cleavage product (**2.108b**) nor other side products.[51] As a result, we

cannot draw any conclusions about the origin of this side product (**2.108b**) under PCET *vs* LMCT activation modes or the likelihood of side product derivation due to a stepwise β-scission cascade *vs* open form ring scission.

Lactols **2.74** and **2.75** underwent ring scission in 63% and 89% yields, with **2.75** demonstrating remarkable tolerance to the β-quaternary centre (to **2.114**). Mannofuranose diacetonide **2.62** and the corresponding hemiketal **2.104** were both cleaved in excellent yields, showing an insignificant difference in the activation of both hemiacetals and hemiketals. Fused bicyclic hemiketal **2.95** underwent ring-junction C–C$_\sigma$ bond cleavage to deliver 8-membered ring lactone **2.123** in 48% yield that may be difficult to form otherwise.

6-Membered ring lactols were also cleaved in modest to excellent yields. Substrates **2.70** and **2.72** bearing an aryl group at the γ-position were cleaved in 80% and 89% yields, with substrate **2.72** demonstrating a tolerance for aryl chlorides. Aryl chlorides are typically not a functionality of great concern, however, their photocatalytic reduction from the Ce(III) excited state has been demonstrated.[9b, 124] Benzyl protected glucose and galactose species **2.111a** and **2.111b** were cleaved to give **2.112** in identical yields of 65%, further demonstrating a tolerance for variable steric profiles at the β-position. Acetyl protected galactose, glucose, and glucosamine derivatives **2.91a**, **2.91b**, and **2.91c** underwent β-scission in 36%, 80%, and 78% yields. Acetyl or benzyl protected mannopyranoses **2.119** and **2.121** yielded cleaved compounds **2.120** and **2.122** in 47% and 58% yields, respectively. Estrone derivative **2.84** underwent β-scission to give **2.126** in 65% yield, requiring more dilute reaction conditions to afford better solubility to the starting material. 3º alcohol α-cedrol (**2.127**) underwent cleavage of the bridging 6-membered ring in 88% yield as a 9:1 mixture resulting from cleavage to the 2º (**2.128a**) *versus* 1º (**2.128b**) C-centred radical intermediates. This substrate was also reported by the Knowles group with the 2º-cleavage product (**2.128a**) obtained in 68% yield, however no mention was made of cleavage to the 1º C-centre.[51]

7-Membered lactols were also amenable to the desired reaction, so long as they possessed sufficient ring-closed form at equilibrium (see below). Caged adamantanone derived compound **2.86** underwent efficient β-scission to bridged bicyclo[3.3.1]nonane formate ester **2.124** in 87% isolated yield, demonstrating that these compounds are not as unbreakable as their name would imply. Simple 7-membered ring lactol **2.88** underwent cleavage to formate ester **2.125**, which was subsequently saponified to form alcohol **2.130** in 49% yield over two steps in order to combat volatility.

Some products of the redox-neutral ring β-scission reaction required further derivatization to aid isolation and characterization (**Figure 17**). Formate esters **2.124** and **2.125** each required saponification to their corresponding

alcohols **2.129** and **2.130** in 61% and 49% 2-step yields (**Figure 17**, **A**). Although formate ester **2.124** could be isolated in 86% yield and characterized by NMR spectroscopy, obtaining a HRMS of this compound proved challenging due to its volatility, small size, and minimal functionality. Interestingly, the α-oxo methine proton at C3 of the bicyclo[3.3.1]nonane **2.124** experiences a high 3-bond coupling with adjacent protons, indicating a near antiperiplanar diaxial relationship. The only way for this proton to align antiperiplanar to vicinal protons is through population of a boat conformer at equilibrium, or if a radical epimerization of the 3º centre resulted in the formation of an *exo*-formate ester substituent. A survey of the literature looking at simple 3-*endo*-functionalized bicyclo[3.3.1]nonane systems showed a tendency to adopt the boat-chair-like conformers depicted that minimizes 1,3- or extended flagpole interactions with the bridging ring system.[125] Formate ester **2.125** proved exceptionally volatile with significant losses incurred when isolated directly. Hydrolysis in a two-step procedure provided the product as the less volatile primary alcohol **2.130**. Estrone derivative **2.84** was cleaved to afford 3º formate ester **2.126** in 65% isolated yield. Crystallization of **2.126** proved challenging, and while saponification proceeded in an excellent 93% yield, growing a crystal suitable of **2.131** for X-ray diffraction remained elusive with the limited quantities of **2.126** available.

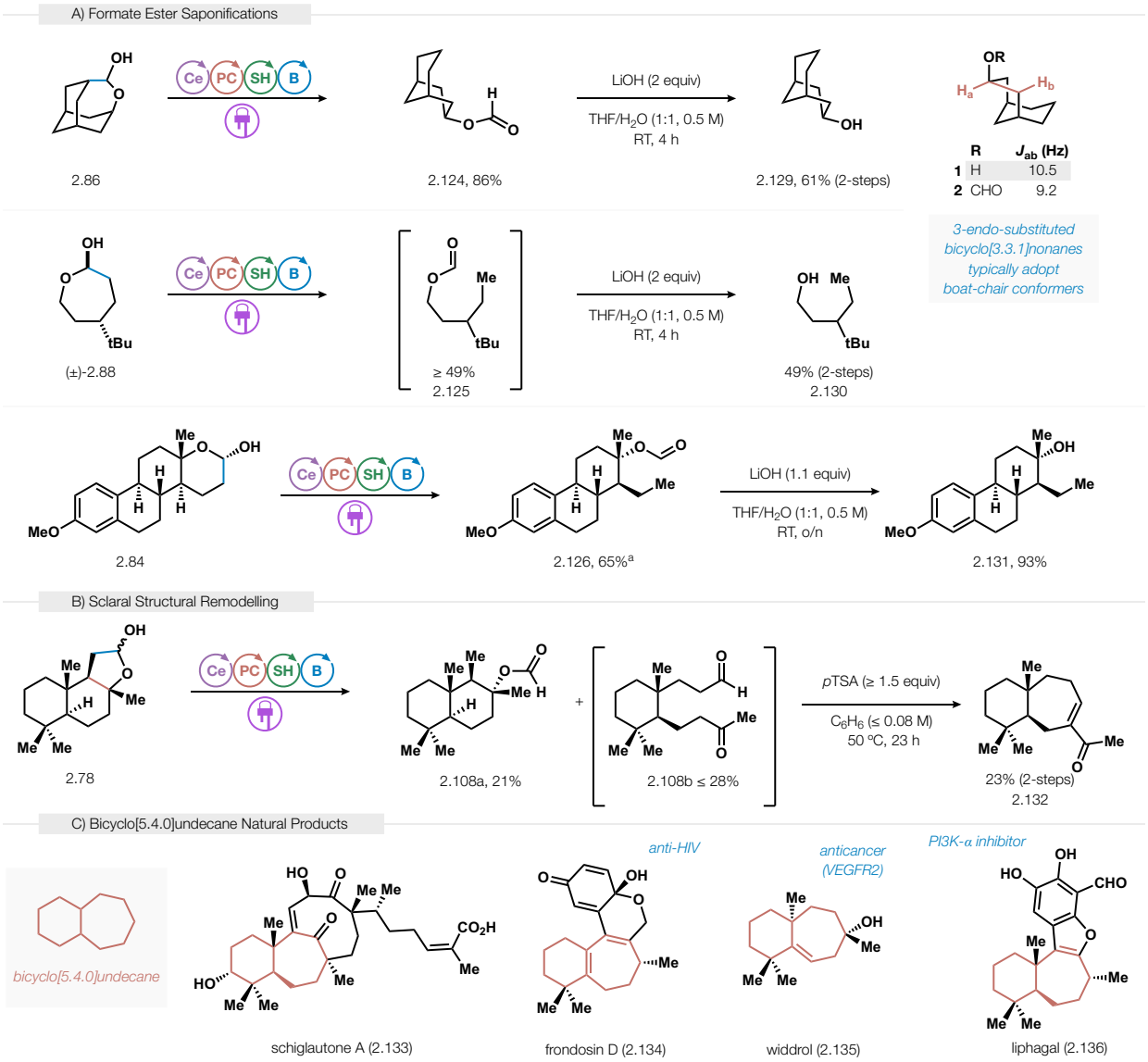


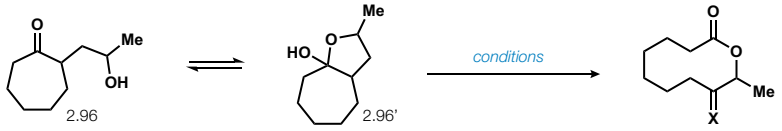
Figure 17. *Ring-scission product derivatizations.*

A) Formate ester saponifications; B) Sclaral structural remodelling through a ring-scission aldol condensation sequence; C) bicyclo[5.4.0]undecane containing natural products.

Of the two compounds formed upon cleavage of sclaral (**2.78**), the ketoaldehyde **2.108b** proved to be moderately unstable to silica and during storage which made HRMS acquisition challenging (**Figure 17**, **B**). Reasoning that the aldehyde functionality represented the greatest liability, crudely isolated compound **2.108b** was treated with *p*-toluenesulfonic acid in benzene at elevated temperature and formed fused 6/7-ring compound **2.132** in 23 % yield over two steps. ^{1}H NMR spectroscopy of the crude material from the ring scission reaction indicated an approximate 28% yield for ketoaldehyde **2.108b** and therefore the aldol condensation appears to work in estimated 92% yield. Interestingly, this a bicyclo[5.4.0]undecane system[126] is a key structural feature of several natural products

including: the triterpenoid schiglautone A (**2.133**),[127] the *p*-quinone sesquiterpene frondosin D (**2.134**),[128] widdrol (**2.135**),[129] liphagal (**2.136**),[130] and the icetexanes.[131] With improvements to selectivity, yield, and scalability in the C–C bond cleavage step, this novel scaffold remodelling of sclareolide (**3.1**) as a chiral pool SM could find application in the total synthesis of such complex natural products.[132]

7/5-Lactol **2.96'** showed poor conversion of starting material with only trace product detected, which was an unfortunate result as this reaction would have represented a 2-step total synthesis of phoracantholide I (**2.138**, **Figure 18**).[133] The Zuo group performed an oxidative cleavage of the same substrate (**2.96'**) to form **2.137** under Ce photoredox catalysis conditions, which I was able to replicate using their conditions.[34]



	conditions	result
1	$CeCl_3$, TBACl, $(TRIPS)_2$, $PhCO_2Na$, 9.10-DPA, MeCN, 410 nm, Ar	poor conversion
2	$Ce(OTf)_3$, TBACl, $(TRIPS)_2$, $PhCO_2Na$, 9.10-DPA, MeCN, 410 nm, Ar	poor conversion
3	$CeCl_3$, TBACl, $(TRIPS)_2$, $PhCO_2Na$, 9.10-DPA, EtOAc, 410 nm, Ar	poor conversion
4	$CeCl_3$, TBACl, $(TRIPS)_2$, $PhCO_2Na$, 9.10-DPA, MeCN, 390 nm, Ar	poor conversion
5	$CeCl_3$, TBACl, $(TRIPS)_2$, $PhCO_2Na$, 9.10-DPA, MeCN, 427 nm, Ar	poor conversion
6	$CeCl_3$, TBACl, $(TRIPS)_2$, CF_3CO_2Na, 9.10-DPA, MeCN, 410 nm, Ar	poor conversion
7	$CeCl_3$, TBACl, PAN, EtOAc, 390 nm, O_2	33% (2.137)
8	$Ce(OTf)_3$, TBPCl, PAN, EtOAc, Blue LED, O_2 (Zuo's report)	60% (2.137)

X = O (2.137)
X = H, H (2.138) phoracantholide I

Figure 18. *Attempted synthesis of phoracantholide I by redox-neutral ring-scission and comparison to oxidative conditions.*

Several other substrates failed to convert to desired products under the optimized conditions for ring scission (Figure 19). Fused 6/5-lactol **2.77** showed poor conversion of starting material and appeared to give multiple products with little formate ester present. Indanol compound **2.98** appeared to yield the desired ring-cleaved ketone in only ~20% yield with a significant proportion of the material converting back into indanone (**2.97**), presumably through homolysis of the exocyclic C–C bond to liberate *n*Bu$^{\bullet}$.[87c] 6-Membered lactols **2.79** and **2.82** showed minimal conversion of SM with a complex reaction profile observed for substrate **2.79**. The lack of conversion observed for substrate **2.82** was not surprising as β-scission to the stabilized phenoxyl radical was expected to predominate C–C bond scission. Formal H-atom transfer to the phenoxyl radical generates the phenol with a tethered aldehyde and subsequent hemiacetalization re-forms the SM **2.82**. As such, we anticipated irreversible conversion of **2.82** to the ring-cleaved product may be slow due to an undesired and more favourable activation that regenerates **2.82**. Compound **2.83** simply showed decomposition to an intractable mixture of products under the reaction conditions. β-Scission to the corresponding aryl radical was not expected to be a favourable process. Camphor-derived lactol **2.85** showed no conversion under the reaction conditions which we attributed to the steric congestion present in this bridged

ring system. 7-membered ring lactols **2.87** and **2.89** both failed to provide the desired formate ester products. Menthone-derived compound **2.87** appeared to show cleavage of the isopropyl subunit to generate a dial product (see compound **5.11** in section **5.5**). We suspect this is due to activation of the 2º alcohol in the open hydroxyaldehyde form, a natural consequence of the decreased tendency of this larger ring system to adopt the lactol form in solution. Phenyl-containing lactol **2.89** produced a complex mixture of compounds under the reaction conditions with little evidence of significant quantities of any one product.

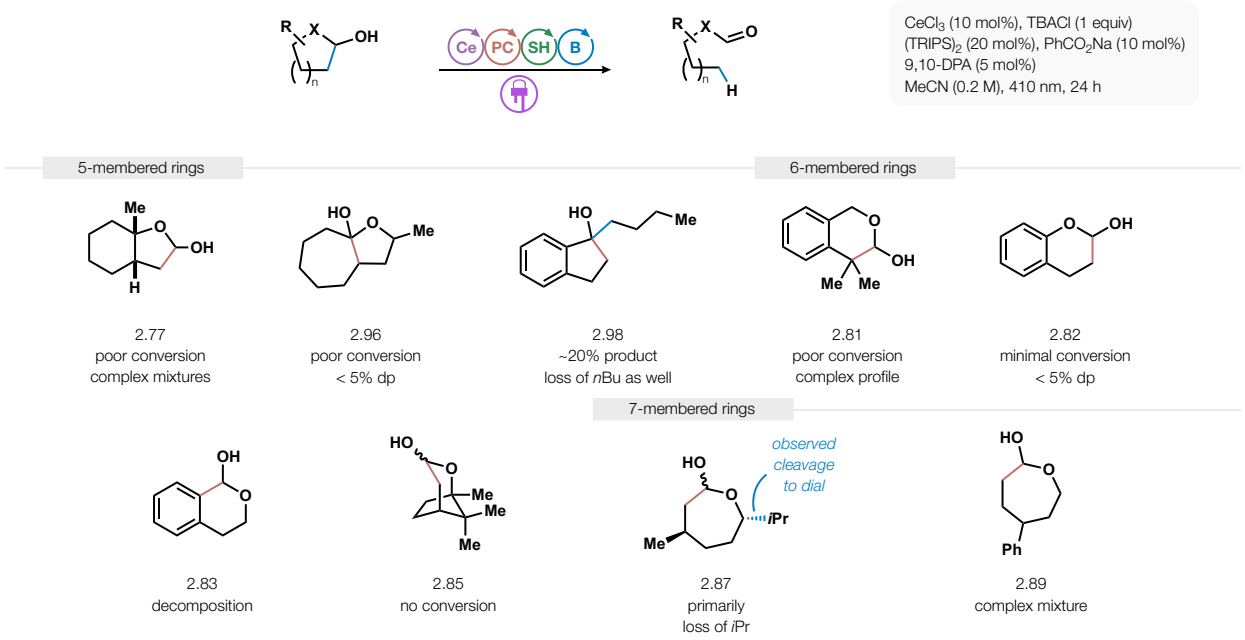


Figure 19. *Unsuccessful substrates in the redox-neutral ring-scission reaction.*

2.4 Mechanistic Investigations

Below is the tentative catalytic hypothesis for the cerium photoredox catalyzed β-scission reaction for O–H bond activations (**Figure 20**). Based on work by Zuo, we suspect that carboxylate ligation to Ce(III) produces a Ce-carboxylate.[6k] Subsequently, X-ligand exchange yields the key Ce-alkoxy species Ce–X. SET oxidation of Ce(III) ($E_{1/2}(Ce^{IV/III})$ = 0.35 V *vs*. SCE in MeCN)[34] by photoexcited 9,10-DPA ($E_{1/2}(DPA^{*/\bullet-})$ = 1.28 V *vs*. SCE in MeCN)[6f] is expected to be favourable, producing the requisite Ce(IV)-alkoxy species and $DPA^{\bullet-}$ simultaneously. The Ce(IV)-alkoxide may then undergo photoexcitation to an LMCT excited state with subsequent Ce–O bond homolysis to regenerate Ce(III) with concomitant liberation of the O-centred radical **III**. C–C_σ β-scission generates C-centred radical **IV**, primed for HAT with a suitable donor.

Simultaneously, $DPA^{\bullet-}$ ($E_{1/2}(DPA/DPA^{\bullet-})$ = –1.80 V *vs* SCE in MeCN)[6f] may reduce thiyl radical **IV** ($E_{1/2}(PhS^{\bullet/-})$ = 0.16 V *vs* SCE),[134] generated upon disulfide S–S bond homolysis. This SET event regenerates ground-

state 9,10-DPA and produces thiolate **V**. Thiolate **V** ($pKa_{aq}^{S–H}$ = 7) may then deprotonate the benzoic acid (pKa_{aq} = 4.2) liberated during X-ligand exchange at Ce, to return the carboxylate co-catalyst and give thiol **VI**. Thiol **VI** with its relatively weak S–H bond (83.5 kcal/mol)[86d] may then act as an H-atom donor to C-centred radical **VII** (k_{HAT} ~$10^{7–8}$ M^{-1} s^{-1})[86d] to yield the rearranged product **VIII** ($BDE_{1°\ C–H}$ = 100.3 kcal/mol)[86b] along with thiyl radical **IV**. Based on this hypothesis, 4 distinct catalytic cycles operate synergistically under a two-photon excitation regime to effect a contrathermodynamic rearrangement of cyclic alcohols utilizing an irreversible HAT in the cycle-closing step.

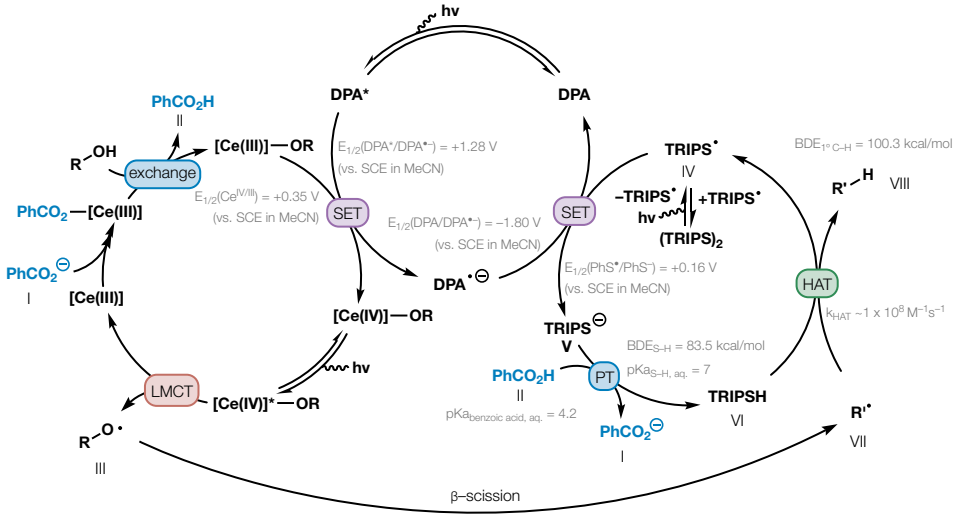


Figure 20. *Tentative multicatalytic cycle for the redox-neutral lactol/cycloalkanol ring β-scission reaction.*

The breadth of reactions promoted by hypohalite chemistry like dehydroxymethylation and decarboxylation inspired us to push this catalytic system further. With the ring-scission reaction established, we felt it was prudent to demonstrate the utility of this catalytic platform to effect β-scission reactions for a series of homologous compounds differing in their oxidation state (**Figure 21**, **A**). Cbz-protected proline (**2.139**) underwent decarboxylation under the standard conditions in 93% isolated yield and prolinol derivative **2.140** was defunctionalized in 97% yield (**entries 1–2**). Interestingly, Cbz-prolinal (**2.141**) underwent decarbonylation in a modest 24% yield (**entry 3**). While carboxylic acid substrate **2.139** and 1° alcohol **2.140** each have obvious free O–H functionalities that could result in ligation to Ce, aldehyde **2.141** lacks such a straightforward activation mode. This prompted a brief investigation into the mechanism for decarbonylation. Exclusion of the sodium benzoate co-catalyst under otherwise standard conditions yielded the defunctionalized Cbz-pyrrolidine product (**2.143**) in an identical 24% yield (**entry 4**). This control suggests that LMCT activation of a $PhCO_2$–Ce bond to liberate an HAT-competent carboxyl radical is likely not responsible for the observed reactivity. We suspected that LMCT liberation of atomic chlorine (Cl•) was producing an HAT catalyst capable of abstracting the acyl hydrogen atom from **2.141**. Supplying *d*-prolinal derivative **2.142** to the same

carboxylate-free conditions resulted in the isolation of **2.143** in a diminished 13% yield with less than 5% deuterium incorporation. The diminished yield points to an isotope-induced impact on the activation of the substrate whilst the lack of deuterium incorporation suggests that adventitious water in the reaction medium likely exchanges with TRIPS–D to generate TRIPS–H as the key H-atom donor catalyst. The lack of incorporation also suggests that an HAT propagated radical chain reaction is likely not operative in the decarbonylation conditions, at least in the case of the deuteroaldehyde **2.142**. The presence of adventitious water under the reaction conditions does raise the question about whether hydrate formation (*gem*-diol) and subsequent ligation by Ce to form a Ce–O bond is in fact the activation mode for aldehydes.

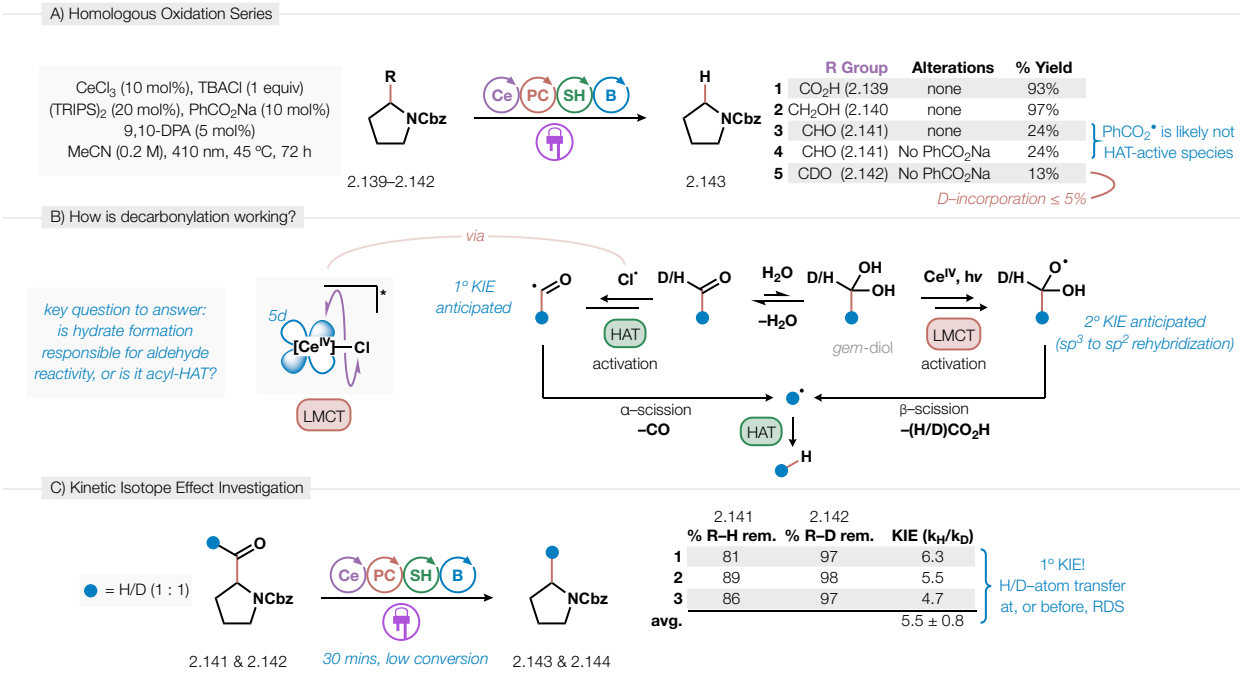


Figure 21. *Mechanistic investigations.*

A) Cerium photoredox multicatalysis β-scission of a homologous oxidation series of proline derivatives, and control reactions; B) Potential mechanisms for the decarbonylative reaction and anticipated effects of acyl deuteration on KIE; C) Kinetic isotope effect study, suggesting decarbonylation via LMCT-generated atomic chlorine HAT.

Left with two different hypotheses for substrate activation, Cl• HAT or *gem*-diol ligation and LMCT, we needed an approach to distinguish these two mechanisms (**Figure 21**, **B**). Under a competitive KIE experiment, protio- and deutero-aldehydes **2.141** and **2.142** were supplied in equimolarity and the reaction durations limited to promote minimal conversion. The conversions of **2.141** and **2.142** were compared to assess their relative activation rates. Under the HAT activation mechanism, we anticipated a primary KIE due to the transfer of the key H/D bond. In contrast, the acyl proton/deuteron is not transferred in the LMCT activation of a *gem*-diol intermediate. In a hydrate activation,

there would be a rehybridization of the isotope-bearing carbon from sp^3 to sp^2 that results in a secondary KIE. Carrying out this competition experiment under the standard reaction conditions resulted in an average 1º KIE of 5.5 (± 0.8), indicative of acyl C–H/D bond breaking (**Figure 21**, **C**). As this is a competition KIE experiment, it is not necessarily the case that this bond-breaking event occurs at or before the RDS.[135] Based on these results, we believe the HAT activation of aldehydes by atomic chlorine generated from Ce–Cl LMCT is consistent with the available information.

2.5 B-Scission Cross-Coupling Investigations

Overview & Precedent

With a redox-neutral cycloalkanol ring β-scission reaction achieved, the logical next extension was to perform a ring cleavage remote arylation reaction by replacing the disulfide catalyst with a nickel catalytic cycle to terminate by cross-coupling. At the time we embarked on this project, there were few reports on metallaphotoredox-catalyzed remote arylation reactions on fragmented cyclic alcohols (**Figure 22**). As with ground-state transition metal catalyzed alcohol β-scission cross-couplings,[136] ring-strain has been used to aid cleavage to C-centred radicals for subsequent coupling (**Figure 22**, **A**). In 2021, Hurski and colleagues reported the metallaphotoredox $Ti(OiPr)_4$/4CzIPN/Ni-catalyzed arylation and alkenylation of cyclopropanols (not shown).[137] In 2022, Li *et al.* demonstrated an asymmetric metallaphotoredox β-arylation of cyclopropanols.[138] In that same year, the Shenvi group reported the β-arylation of cyclopropyl silyl ether **2.145** with tetrahydronaphthalene derivative **2.146** to yield **2.147** in 57% yield during the total synthesis of the GB-alkaloids.[139] While these are highly enabling transformations, their reliance on ring strain may limit their application in synthesis.

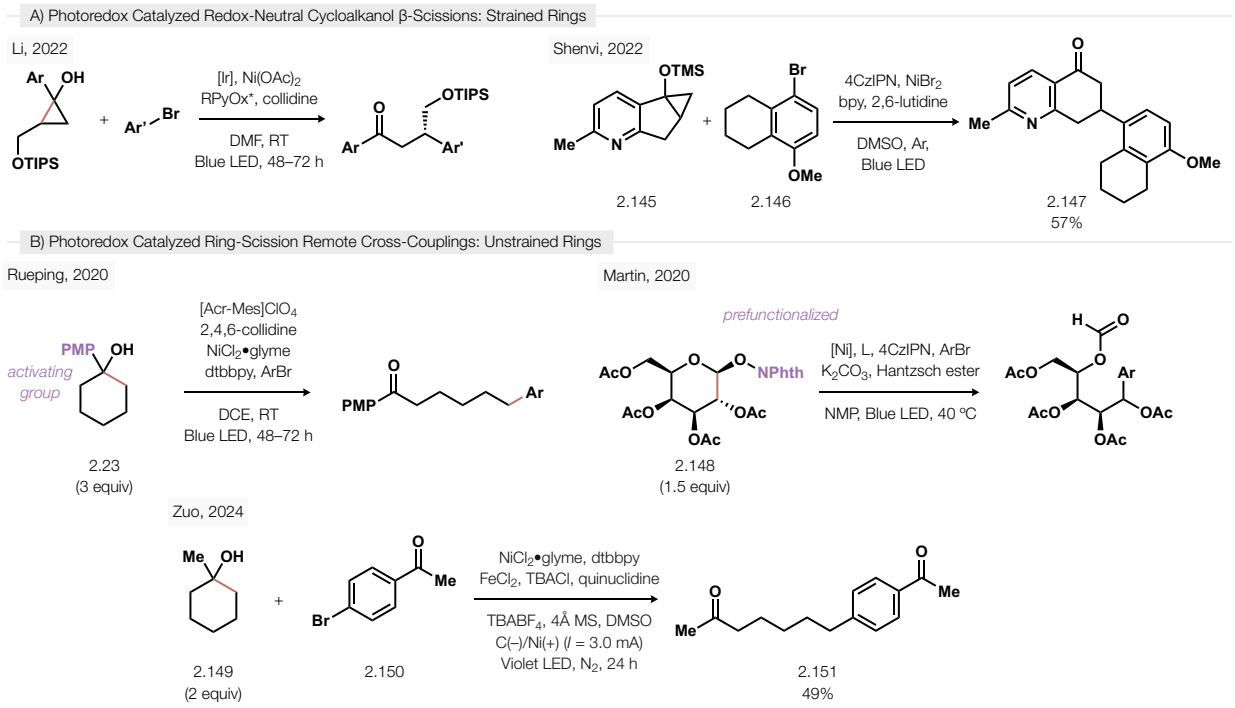


Figure 22. *Photoredox catalyzed ring-cleaving remote arylation of cycloalkanols. A) Strained ring systems; B) Unstrained ring systems.*

Activation of unstrained cycloalkanol ring systems under metallaphotoredox catalysis has typically relied on auxiliary activation to achieve the necessary reactivity (**Figure 22**, **B**). In 2020, the Rueping group reported a remote arylation reaction using a redox auxiliary approach to PCET activation, similar to Knowles earlier 2016 approach (see **Figure 13**, **B**).[103, 140] As with Knowles' work, the requirement for a redox auxiliary in this reaction severely limits the amenable substrate scope. The same year, the Martin group reported the ring cleavage remote arylation of *N*-hydroxyphthalimide ethers (*e.g.* **2.148**) through a reductive metallaphotoredox cross-coupling reaction.[141] Despite the broad array of substrates employed by the authors in this reaction, its major limitation is the need to pre-functionalize the native O–H functionality, not to mention the reductant and redox-active leaving group byproducts generated as waste.

When we embarked on our research into the activation of unstrained and unaltered cycloalkanols for a nickel metallaphotoredox cross coupling, there were no examples that fit all these criteria. During our endeavours, the Lu group,[142] the Zuo and Mei groups,[143] and the Fu group[42] published metallaelectrophotocatalytic versions of this transformation using either Fe or Ce LMCT activation. An undivided electrolytic cell was used to shuttle electrons between catalysts in each of these reports, thereby replacing 9,10-DPA (**1.4**). More recently, the Zuo group reported

a C(sp^3)–C(sp^3) dehydroxymethylative alkylation reaction using a Ce/9,10-DPA/Ni-bipyridine metallaphotoredox system.[46]

Catalytic Hypothesis

Our working hypothesis for how this multicatalytic cycle might operate to deliver cross-coupled ring-cleavage products is shown in **Figure 23**. The cerium and 9,10-DPA (**1.4**) catalytic cycles were expected to operate in essentially the same manner as in the redox-neutral formal rearrangement reaction, excepting the turnover SET from $DPA^{\bullet-}$ which we reasoned could reduce the requisite Ni(I) catalytic intermediate.

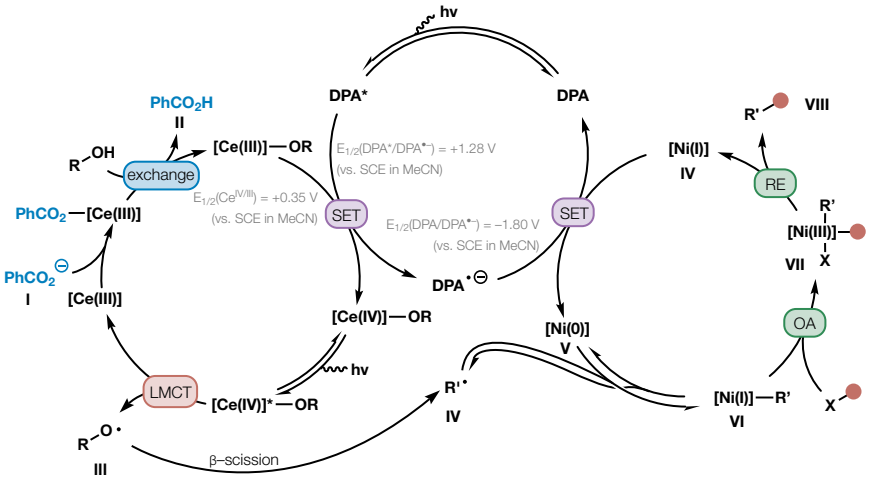


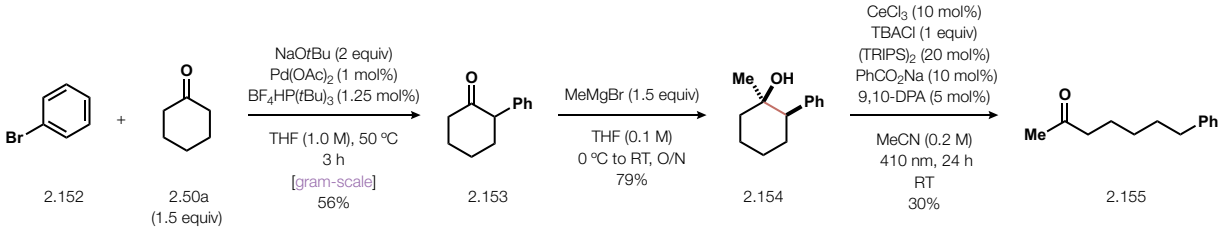
Figure 23. *Catalytic hypothesis.*
Direct redox-neutral ring-cleaving remote arylation of cycloalkanols/lactols via nickel/cerium/9,10-diphenylanthracene cooperative catalysis.

LMCT activation and β-scission of the alcohol substrate was expected to give C-centred radical **IV**, predisposed to reversible capture by an active Ni(0) catalytic intermediate. The Ni(I) intermediate formed therein was expected to undergo oxidative addition to the aryl or alkyl halide electrophiles to generate key Ni(III) species **VII**. Intermediate **VII** could reductively eliminate our desired cross-coupled product (**VIII**) and yield a Ni(I) species that continues through subsequent catalytic turnovers.

While our first hypothesis revolved around a Ni(0/I/III) catalytic cycle, an orthogonal Ni(0/II/III) cycle in which oxidative addition precedes radical capture was also considered. A 2015 report by the Molander and Kozlowski groups on the Ni-bipyridine catalyzed metallaphotoredox coupling of alkyl potassium trifluoroborate salts with aryl bromides supported a low energy Ni(0/I/III) cycle in competition with a less favourable Ni(0/II/III) cycle.[144] Later

work revisiting the effect of the radical structure on such systems by the Molander and Gutierrez groups corroborated earlier findings.[145]

Initial Investigations



Scheme 2. *Synthesis of authentic cross-coupling target compound.*

Synthesis of the target product provided an authentic sample that could assist in TLC and NMR comparisons during reaction screening (**Scheme 2**). A Pd-catalyzed α-arylation of cyclohexanone (**2.50a**) with bromobenzene (**2.152**) reported by Kawatsura and Hartwig[146] provided desired product **2.153** in 56% yield on gram-scale. Next, addition of MeMgBr yielded cyclohexanol **2.154** in 79% yield, with the major diastereoisomer confirmed by an nOe correlation between the methyl and benzylic protons. Finally, application of our redox-neutral ring-scission conditions to cycloalkanol **2.154** gave linear ketone **2.155** in 30% yield, along with substantial quantities of the undesired ring-scission ketone isomer.

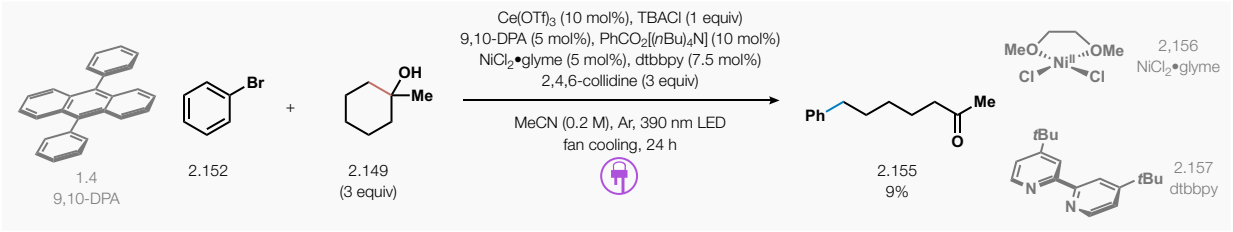
Our initial cross-coupling investigations centred on identifying a reaction hit under homogeneous conditions (**Table 7**). We began using $Ce(OTf)_3$ as a soluble Ce(III) precatalyst source, TBACl as a supporting halide ion source/electrolyte, 9,10-DPA (**1.4**) as an electron-shuttling photocatalyst, $PhCO_2TBA$ as a carboxylate base/ligand for cerium, $NiCl_2$•glyme (**2.156**) as a Ni(II) pre-catalyst source, di(*tert*-butyl)bipyridine (**2.157**) as a ligand for nickel, and 2,4,6-collidine as a superstoichiometric weak hindered base in acetonitrile under 390 nm LED irradiation for 24 hours using bromobenzene (**2.152**) as the limiting reagent and 3 equivalents of methylcyclohexanol (**2.149**). The choice of 2,4,6-collidine was dictated by the need for a base that could effectively quench the formation of HBr generated during each global turnover whilst also being hindered enough to minimize ligation of this species to either the Ni- or Ce-centres, which we suspected might impede their desired catalytic action. Additionally, there was precedent for 2,4,6-collidine as the stoichiometric base used in the Rueping groups' earlier report on the metallaphotoredox catalyzed remote arylation of cycloalkanols.[140] These initial conditions furnished a 9% yield of the desired cross-coupled product **2.155** (**entry 1**). Tripling the reaction duration to 72 hours resulted in an identical 9% yield of **2.155** (**entry 2**). Trading the tetrabutylammonium cation on the benzoate salt for sodium had no significant impact on the reaction outcome

(**entry 3**). Initially, we had suspected the high chloride concentrations imparted by the TBACl additive were saturating Ni coordination sites and diminishing its catalytic activity due to a noticeable colour change upon its addition to solutions of Ni(II)-dtbbpy solutions in acetonitrile. Removal of TBACl with concomitant increase in carboxylate loading resulted in no detectable product (**entry 4**). Likewise, increasing the carboxylate loading whilst decreasing the TBACl loading resulted in only trace product observed, a high loading of TBA-benzoate proved inferior to the starting conditions, and high loading of TBA-benzoate with decreased TBACl loading resulted in no detectable product (**entries 5–7**). This experiment was performed to more closely mimic Zuo's earlier conditions for dehydroxymethylative arylation.[6k] Exchanging bromobenzene (**2.152**) with the chloro-, iodo-, or trifluoromethanesulfonate ester electrophiles all resulted in diminished yields (**entries 8–10**).

Replacing collidine with the stronger hindered base TMP did not prove beneficial (**entry 11**). The reaction did prove sensitive to lowering the number of equivalents of the alcohol (**2.149**) and inverting the initial relative equivalents of alcohol (**2.149**) and bromobenzene (**2.152**) proved detrimental (**entries 12 & 13**).

Exchanging TBA-benzoate with the more hindered potassium 2,4,6-tri(isopropyl)benzoate (**1.9**, $TRIPCO_2K$) resulted in the first substantial improvement to give **2.155** in 21% NMR yield (**entry 14**) and this result proved reproducible (**entry 15**). Exchanging Ce(III) trifluoromethanesulfonate for Ce(III) chloride proved detrimental (**entry 16**). Further attempts to alter the stoichiometric base using K_3PO_4, Cs_2CO_3, or DBU in place of collidine all resulted in no detectable product (**entries 17–19**). Finally, running the reaction under the current best conditions using longer wavelength 440 nm LEDs substantially decreased the yield to only 6% product **2.155** (**entry 20**).

Table 7. *Reaction optimization: initial investigations.*

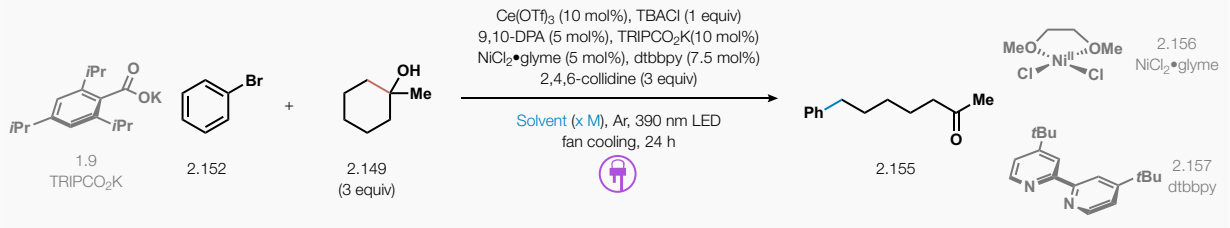


Entry	Deviation from above conditions	% Yield 2.153
1	none	9
2	72 h	9
3	72 h, $PhCO_2Na$ in place of $PhCO_2TBA$	8
4	72 h, 35 mol% $PhCO_2Na$, no TBACl	0
5[§]	72 h, 30 mol% $PhCO_2TBA$ and 30 mol% TBACl	≤ 5
6	30 mol% $PhCO_2TBA$	6
7	30 mol% $PhCO_2TBA$, no TBACl	0
8	72 h, PhCl in place of PhBr (**2.152**)	≤ 5
9	72 h, PhI in place of PhBr (**2.152**)	≤ 5
10	72 h, PhOTf in place of PhBr (**2.152**)	≤ 5
11	2,2,6,6-tetramethylpiperidine in place of 2,4,6-collidine	≤ 5
12	1 equivalent of 1-methylcyclohexanol (**2.149**)	≤ 5
13	3 equivalents PhBr (**2.152**), 1 equivalent 1-methylcyclohexanol (**2.149**)	≤ 5
14	Potassium 2,4,6-triisopropylbenzoate (**1.9**) in place of $PhCO_2TBA$	21
15	**Potassium 2,4,6-triisopropylbenzoate (1.9) in place of $PhCO_2TBA$**	**23**
16	$CeCl_3$ in place of $Ce(OTf)_3$	≤ 5
17[§]	K_3PO_4 in place of 2,4,6-collidine	0
18	Cs_2CO_3 in place of 2,4,6-collidine	0
19	DBU in place of 2,4,6-collidine	0
20	Potassium 2,4,6-triisopropylbenzoate in place of $PhCO_2TBA$, 440nm LED	6

Yields determined by ^1H NMR analysis of crude mixtures relative to PhTMS internal standard by integrating 2.59 (t, J = 7.7 Hz) ppm. [§]Reactions performed by Tegan O'Brien.

Next, we studied the impact of the solvent on reaction efficiency (**Table 8**). Replacing acetonitrile with DCE, ethyl acetate, DMF, DMSO, PhMe, or THF all failed to provide desired product **2.155** (**entries 2–7**). Binary solvent mixtures of MeCN/DMSO or MeCN/DMF yielded **2.155** in only trace quantities (**entries 8 & 9**). Doubling or halving the volume of acetonitrile each proved detrimental to the yield of **2.155** (**entries 10 & 11**).

Table 8. *Reaction optimization: Solvent study.*

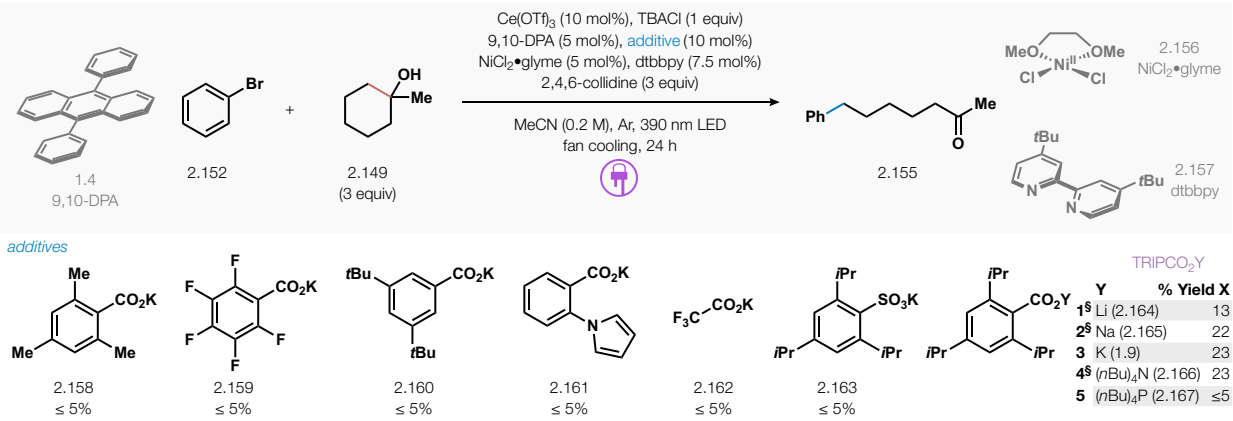


Entry	Solvent (M)	% Yield 2.155
1	**MeCN (0.2)**	**23**
2[§]	DCE (0.2)	0
3	EtOAc (0.2)	0
4	DMF (0.2)	0
5[§]	DMSO (0.2)	0
6[§]	PhMe (0.2)	0
7	THF (0.2)	0
8	MeCN/DMSO [9:1] (0.2)	≤ 5
9[§]	MeCN/DMF [9:1]	≤ 5
10	MeCN (0.1)	16
11	MeCN (0.4)	18

[§]*Reactions performed by Tegan O'Brien.*

Next, we wished to study the impact of the weak anionic base/cerium ligand identity on the remote coupling reaction (**Table 9**). Substituting the aryl carboxylate TRIPCO$_2$K (**1.9**) with the potassium salts of: mesitylene carboxylic acid (**2.158**), pentafluorobenzoic acid (**2.159**), 3,5-di(*tert*-butyl)benzoic acid (**2.160**), 2-(1-pyrrolyl)benzoic acid (**2.161**), trifluoroacetic acid (**2.162**), or 2,4,6-tri(isopropyl)benzene sulfonic acid (**2.163**) all delivered product in only trace quantities. Surveying counterions for 2,4,6-tri(isopropyl)benzoate showed similar efficiency for sodium (**2.165**), potassium (**1.9**), and tetrabutylammonium (**2.166**) counterions, whilst lithium (**2.164**) and tetrabutylphosphonium (**2.167**) cations each proved inferior (**entries 1–5**).

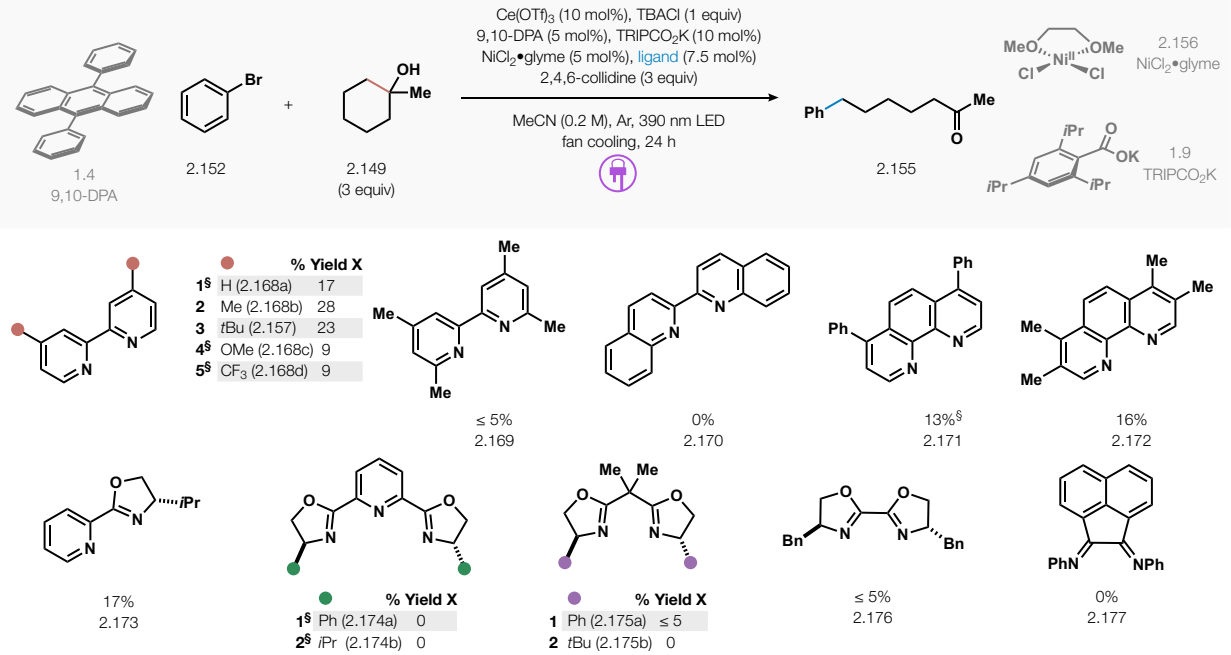
Table 9. *Reaction optimization: aryl carboxylate/sulfonate additive study.*



§*Reactions performed by Tegan O'Brien.*

After establishing TRIPCO$_2$K (**1.9**) as the optimal carboxylate, we turned to a study on the identity of the ligand for the nickel catalyst (**Table 10**). Surveying 2,2'-bipyridine derivatives showed that the 4,4'-dimethyl ligand (**2.168b**) resulted in the most efficient reaction (**entry 2**). A 4,4'-EDG (**2.168c**) or -EWG (**2.168d**) on the bipyridine ligand resulted in diminished yields (**entries 4 & 5**). 2,2'-biquinoline (**2.170**) failed to deliver any detectable quantities of product **2.155**. Bathophenanthroline (**2.171**) and 3,4,7,8-tetramethyl-1,10-phenanthroline (**2.172**) both yielded product **2.155** in lower yields than the *t*Bu- and Me-bipyridine ligands. PyOX ligand **2.173** delivered product **2.155** in 17% yield which may prove promising for future investigation into an asymmetric coupling reaction. PyBOX (**2.174a & b**), BOX (**2.175a & b**), and BiOX (**2.176**) ligands were all inferior ligands for the desired transformation with only **2.175a** and **2.176** showing any trace of product. Finally, acenaphthenediimine ligand **2.177** failed to yield any detectable cross-coupled product (**2.155**).

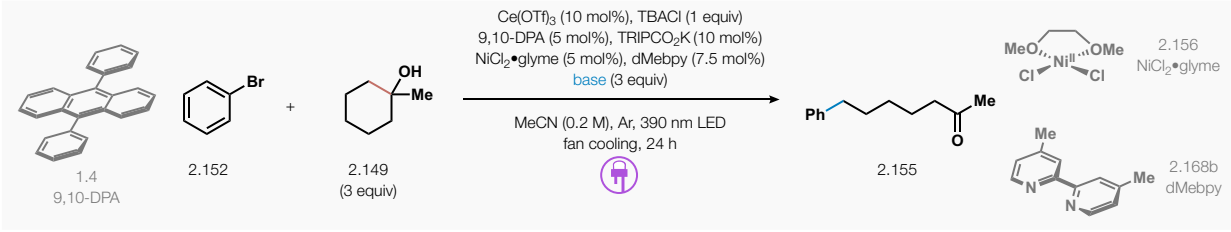
Table 10. *Reaction optimization: nickel ligand study.*



§Reactions performed by Tegan O'Brien.

Optimization of the superstoichiometric base covered an array of organic and inorganic species with a range of pKb values. (**Table 11**). Organic amine bases TMG, 2-*tert*-butyl-1,1,3,3-tetramethylguanidine, DBU, 2,6-di-*tert*-butylpyridine, lutidine, 2,6-diphenylpyridine, pyridine, DABCO, 3-acetoxyquinuclidine, TMP, and imidazole all failed to deliver **2.155** in the same quantity as collidine (**entries 1–12**). Inorganic sodium phosphate, carbonate, bicarbonate, tri(isopropyl)benzoate (**2.165**), and acetate stoichiometric bases were also all inferior to 2,4,6-collidine (**entries 13–19**).

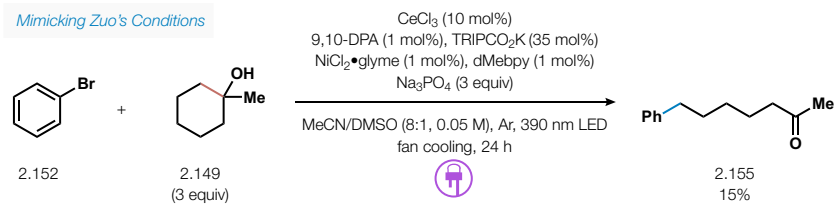
Table 11. *Reaction optimization: superstoichiometric base study.*



Entry	Base	$pKa_{aq.}$[c.a.]	pKa_{DMSO}[c.a.]	% Yield 2.153
1	**2,4,6-collidine**		**4.5**	**28**
2	Tetramethylguanidine (TMG)		13.6	0
3	2-*tert*-Butyl-1,1,3,3-tetramethylguanidine	–	–	≤ 5
4	DBU		12	≤ 5
5	2,6-Di-*tert*-butylpyridine		0.9	≤ 5
6	Lutidine		4.5	14
7	2,6-Diphenylpyridine			≤ 5
8	Pyridine	5.2		≤ 5
9	DABCO		8.9, 3.0	≤ 5
10	3-Acetoxyquinuclidine		9.8	≤ 5
11	TMP		11	≤ 5
12[§]	Imidazole		7	0
13	Na_3PO_4	12.3		≤ 5
14	Na_2HPO_4	7.2		7
15	NaH_2PO_4	2.1		0
16	Na_2CO_3	10.3		≤ 5
17[§]	$NaHCO_3$	3.6		≤ 5
18[§]	$TRIPCO_2Na$ **2.165** (1 eq.)			18
19[§]	NaOAc		12	≤ 5

[§]*Reactions performed by Tegan O'Brien.*

At this stage, we wanted to see whether our optimization campaign had led us in the correct direction. As a comparison, we tested Zuo's conditions for dehydroxymethylation arylation under cerium/nickel metallaphotoredox catalysis (**Scheme 3**).[6k] These conditions were significantly more heterogeneous than those we had optimized to and resulted in a diminished 15% yield of product (**2.155**) relative to our best of 28%.

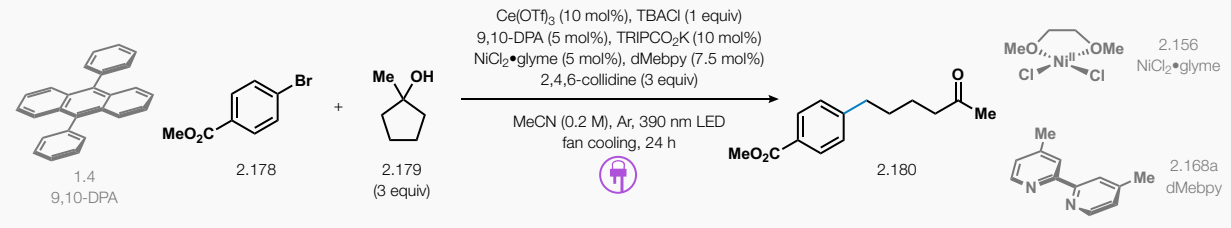


Scheme 3. *Remote arylation reaction benchmark using Zuo's conditions for dehydroymethylation arylation.*

Reassured that our optimization campaign was trending in the correct direction, we chose to see how the reaction fared with a more strained cycloalkanol (**2.179**) and a more activated, and easier to quantify, aryl bromide

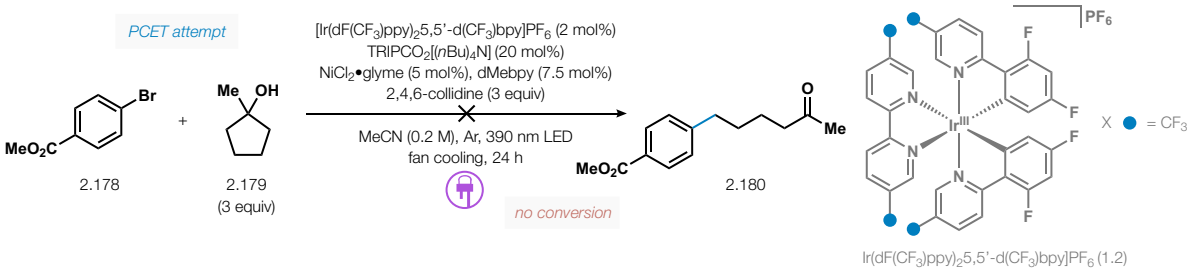
(**2.178**, **Table 12**). To our dismay, our best conditions provided the cross-coupled product **2.180** in only 26% yield with 51% aryl bromide (**2.178**) remaining after 24 h (**entry 1**, 53% brsm). Doubling the loading of methylcyclopentanol (**2.179**) significantly improved the reaction, providing **2.180** in 47% yield with 37% SM **2.178** remaining (**entry 2**, 75% brsm). Halving the nickel and bipyridine ligand loadings simultaneously decreased the conversion to approximately 60% of that previously seen after 24 h (**compare entries 1 & 3**, 53% brsm). The reaction did not prove sensitive to halving the loading of tetrabutylammonium chloride (**entry 1 *vs.* 4**), however at the higher alcohol (**2.179**) loading of 6 equivalents the conversion and efficiency were significantly impeded (**entry 2 *vs.* entry 5**). Increasing the alcohol (**2.179**) loading to 10 equivalents did not further improve the reaction, and in fact resulted in a diminished conversion to **2.180** relative to 6 equivalents (**entry 6**, 72% brsm). Taken together, it appears that there is an equilibrium range wherein cycloalkanol (**2.179**) and halide concentrations are optimal, facilitating formation of catalytically active species. Higher halide concentrations or lower alcohol (**2.179**) concentrations may result in disfavoured substrate binding, which therefore retards conversion. Conversely, higher alcohol (**2.179**) or lower halide concentrations may favour the formation of catalytically inactive polyalkoxy-cerium species.

Table 12. *Reaction optimization: miscellaneous reactions using methyl cyclopentanol and methyl 4-bromobenzoate.*



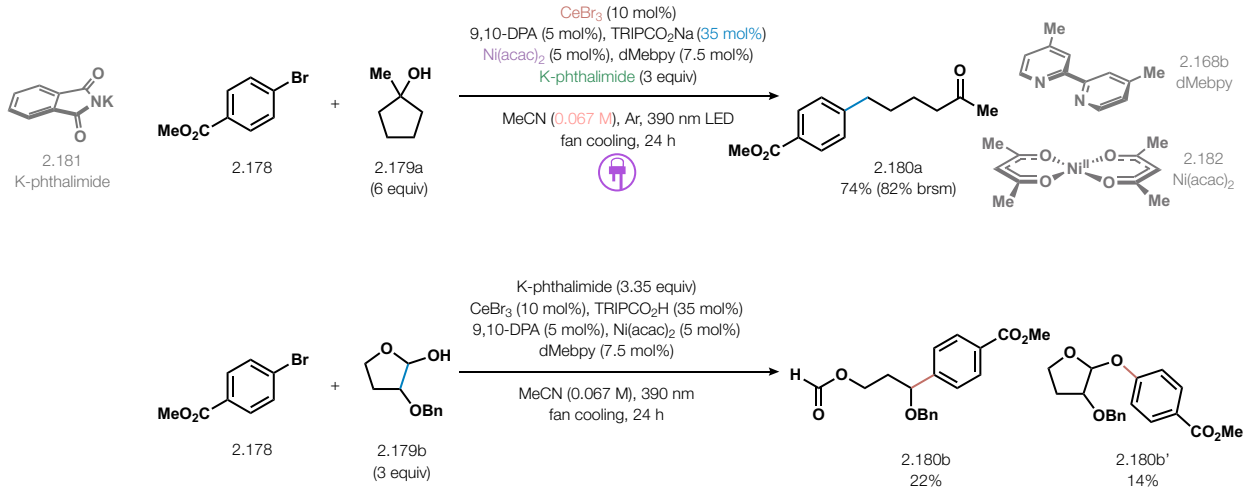
Entry	Deviation from above	% Yield 2.178	% SM 2.176 Remaining
1	none	26	51
2	**6 equiv alcohol**	**47**	**37**
3	2.5 mol% $NiCl_2$•glyme, 3.75 mol% dMebpy	16	70
4	0.5 equiv TBACl	28	56
5	6 equiv alcohol, 0.5 equiv TBACl	10	78
6	10 equiv alcohol	33	54

To convince ourselves that a simpler and already established activation method would not immediately give better results, we ran a reaction using the Knowles groups' improved PCET conditions with the thiol catalyst replaced by a nickel/ligand system, and with the inclusion of collidine as a superstoichiometric base (**Scheme 4**).[51] Under the initial conditions tested, there was no conversion of starting aryl bromide **2.178** after 24 hours of irradiation.



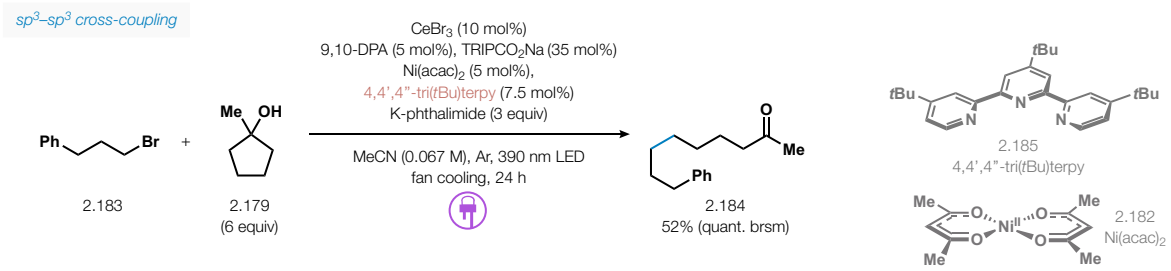
Scheme 4. *Attempted remote arylation under Knowles-like photoredox-catalyzed PCET activation conditions.*

Ultimately, we arrived at conditions capable of effecting the desired ring-scission arylation reaction in an isolated yield of 74% **2.180** (**Scheme 5**). To arrive at these conditions, Dr. Timothée Stoerkler increased the carboxylate loading, changed the Ce(III) species from the $Ce(OTf_3)$ to $CeBr_3$, changed the Ni(II) pre-catalyst to $Ni(acac)_2$ (**2.182**), and decreased the reaction concentration from 0.2 M to 0.067 M. Ultimately, I found that potassium phthalimide (**2.181**) was superior to K_3PO_4 for the conversion of cycloalkanols. I chose this base for its purported ability to stabilize bipyridine•Ni(II)-aryl halide oxidative addition complexes[147] and for its appearance in related cerium/nickel decarboxylative metallaphotoredox cross-couplings.[37a, 38]



Scheme 5. *Remote arylation optimized conditions.*

With effective conditions for ring-cleaving $C(sp^3)$–$C(sp^2)$ cross-coupling in hand, I wished to assess the feasibility of $C(sp^3)$–$C(sp^3)$ cross-coupling. Fortunately, prior work by the Martin group had shown successful ring-scission coupling of NHPI ethers and alkyl bromides using 4,4',4''-tri(*tert*-butyl)terpyridine (**2.185**) as an enabling ligand for nickel. Exchanging the bipyridine ligand in our system for the terpyridine **2.185** yielded cross coupled product **2.184** in 52% isolated yield after 24 hours (**Scheme 6**). In contrast, arylation of lactol **2.179b** gave formate ester **2.180b** in a poor yield of 22% along with a 14% yield of C–O arylation side product **2.180b'**.



Scheme 6. *Unoptimized attempt at remote C(sp^3)–C(sp^3) cross-coupling of methylcyclopentanol and 1-bromo-3-phenylpropane.*

Shortly after obtaining these results, the Zuo group published their report on the direct ring-scission arylation of cycloalkanols.[143] More recently, the Zuo group has also reported a C(sp^3)–C(sp^3) dehydroxymethylation cross-coupling reaction.[47] Dr. Timothée Stoerkler has continued to investigate the ring-scission cross-coupling of lactols, the results of which will be published in due course.

2.6 Direct Photoredox Catalyzed Hydrodecarboxylations

Mechanistic investigation into the dehydroxymethylation reaction revealed the competence of the catalytic system in a hydrodecarboxylation reaction (**Figure 21**). Looking back at hypo(acyl)halite chemistry, there is obvious overlap between conditions that can effect decarboxylation and ring scission reactions (see **Figure 12**). The rapid decarboxylation rates from alkyl acyloxy radicals (10^9–10^{10} s^{-1})[84, 148] have served to enable many hydrodecarboxylation reactions.

Photoredox catalyzed hydrodecarboxylation reactions represent a highly enabling defunctionalization reaction for the direct removal of free carboxy groups without the need for prior functionalization (**Figure 24**). The earliest example of a direct photoredox catalyzed hydrodecarboxylation comes from Yoshimi and Hatanaka in 2007 and used phenanthrene and dicyanobenzene with superstoichiometric *t*-dodecanethiol.[149] In 2014, the Wallentin group published a hydrodecarboxylation reaction using an acridinium and disulfide catalytic system.[150] The Nicewicz group next published their hydrodecarboxylation, also using a disulfide and acridinium multicatalysis system. [151] Later work by Zhu and co-workers demonstrated a decarboxylative deuteration of carboxylic acids using an acridinium photocatalyst with D_2O as the source of deuterium.[152] In 2022, Lu and West reported the iron-photoredox catalyzed proto- and deuterodecarboxylation of free carboxylic acids utilizing LMCT activation.[153]

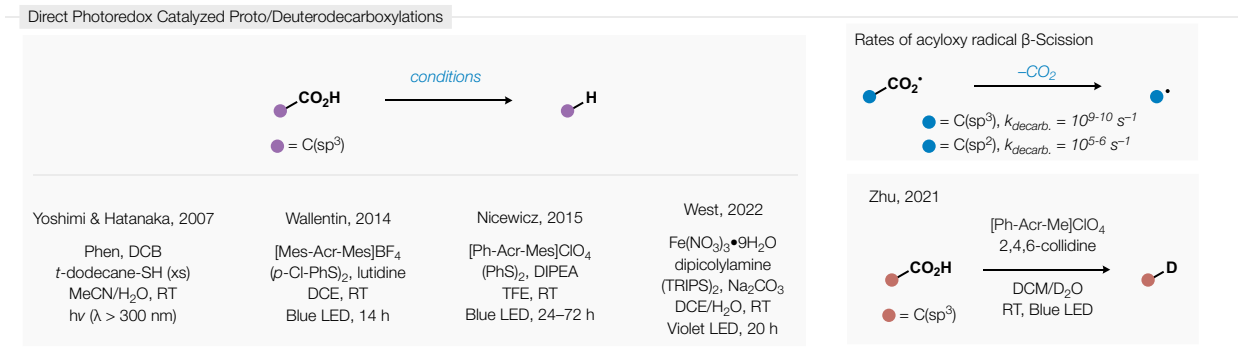


Figure 24. *Direct photoredox-catalyzed proto- and deuterodecarboxylations.*

2.7 Hydrodecarboxylation Scope

Fortunately, our conditions for the formal rearrangement of lactols to formate esters were readily applicable to the direct hydrodecarboxylation of α-C(sp^3) carboxylic acids (**Figure 25**). The sole modification necessary was to increase the reaction duration from 24 to 72 h to ensure complete conversion of SM for this new class of substrates. With this minor modification, Cbz-proline (**2.139**) underwent the transformation in an excellent 94% isolated yield with a diminished efficiency when increased to 1 mmol scale (71%). *N*-Protected α-amino acids **2.186a**–**2.190a** all underwent hydrodecarboxylation in good to excellent yields, except for tyrosine derivative **2.189a**. We reasoned that the free phenolic O–H in **2.189a** was competitively activated by Ce-LMCT in an unproductive process as the remaining mass balance from the decarboxylation of was remaining SM. Fortunately, protection of the phenol as the acetyl ester (**2.190a**) restored reactivity, delivering tyramine derivative **2.190b** in 81% yield.

Treatment of α-2º-acid **2.191a** and bridgehead 3º acid **2.192a** both proceeded in good yields. Decarboxylation of α-1º γ-ketoacids **2.193a** and **2.194a** provided ketones **2.193b** and **2.194b** in 98% and 64% yields, respectively. The diminished yield from biaryl **2.194a** may be due to its lower solubility under the reaction conditions, resulting in lower conversion after 72 hours relative to **2.193a**. Gemfibrozil (**2.195a**) was efficiently defunctionalized in 87% yield. Decarboxylation to a 1º C-centred radical in **2.196a** occurred smoothly, furnishing the product **2.196b** in 70% yield. Indomethacin (**2.197a**) underwent hydrodecarboxylation in 41% isolated yield, showing a tolerance for cleavage to heterobenzylic stabilized radicals. Indole succinate monoamide **2.198a** furnished 39% yield of product **2.198b** that showed a propensity to sublime at room temperature under reduced pressure. (*S*)-naproxen (**2.199a**) efficiently decarboxylated to a benzylic radical prior to HAT to give **2.199b** in 79% isolated yield. Dehydrocholic acid (**2.200a**), a bile acid, was decarboxylated in 73% isolated yield but required dilution to improve SM solubility. Compounds

2.197 and **2.200** highlight the utility of this reaction to perform late-stage defunctionalization of complex drug or NP-like compounds.

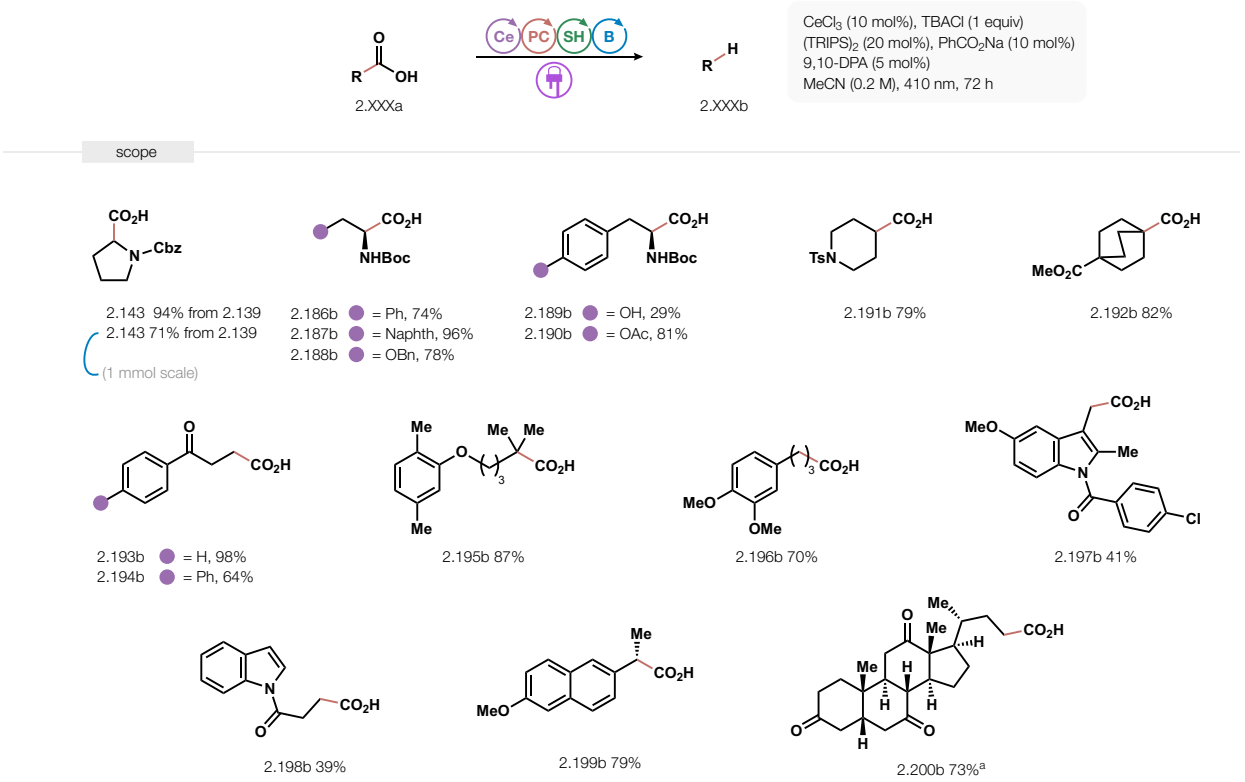


Figure 25. *Substrate scope for the cerium photoredox catalyzed hydrodecarboxylation of native carboxylic acids.* [a]*Reaction concentration 0.05 M in acetonitrile.*

2.8 Conclusions & Future Directions

The present chapter details the development of multicatalytic Ce-photoredox reactions to perform redox-neutral β-scission reactions from native hydroxyl- and carboxyl-bearing substrates. We successfully achieved the contrathermodynamic formal rearrangement of lactols into formate esters and hydrodecarboxylation of free acids. Additionally, we made significant progress in realizing a ring-scission cross-coupling of cycloalkanols with aryl and alkyl bromides using an altered metallaphotoredox platform. Each of these transformations required careful tuning of reaction conditions to effectively match relative rates of radical generation and termination and result in productive reactions.

Chapter 3

Photoredox-Catalyzed Hydroalkylation of C(sp^3)–H Acids

3.1 Introduction

The direct functionalization of C–H bonds remains a key challenge in modern synthesis, and new methodologies that address this challenge are essential to accelerate exploration of chemical space and the development of new chemical tools, biological probes, and pharmaceuticals.[154] C(sp^3)–H acids are a ubiquitous functionality, but methods for their catalytic activation towards radical chemistry have lagged-behind those aimed at hydridic C(sp^3)–H or protic X–H bonds.[86g] This disparity can be attributed to the relative scarcity of systems with the requisite polarity to promote efficient activation.[155] Consequently, protic C–H bonds have been underutilized in radical chemistry despite the potential application of these feedstocks towards the synthesis of complex architectures.

In contrast to the use of protic 1,3-dicarbonyls in anionic chemistry, their use in radical chemistry is less prolific. Over 50 years ago, Julia demonstrated the feasibility of hydrogen atom transfer (HAT) radical cyclizations using C(sp^3)–H acids.[156] Despite this demonstration, a persistent sentiment in the field is that "hydrogen atom transfer cyclizations are of only limited value for organic synthesis".[81i] Many early methods relied on short, inefficient radical chains with limited substrate generality, leading to their reputation as capricious systems of little synthetic value.[157]

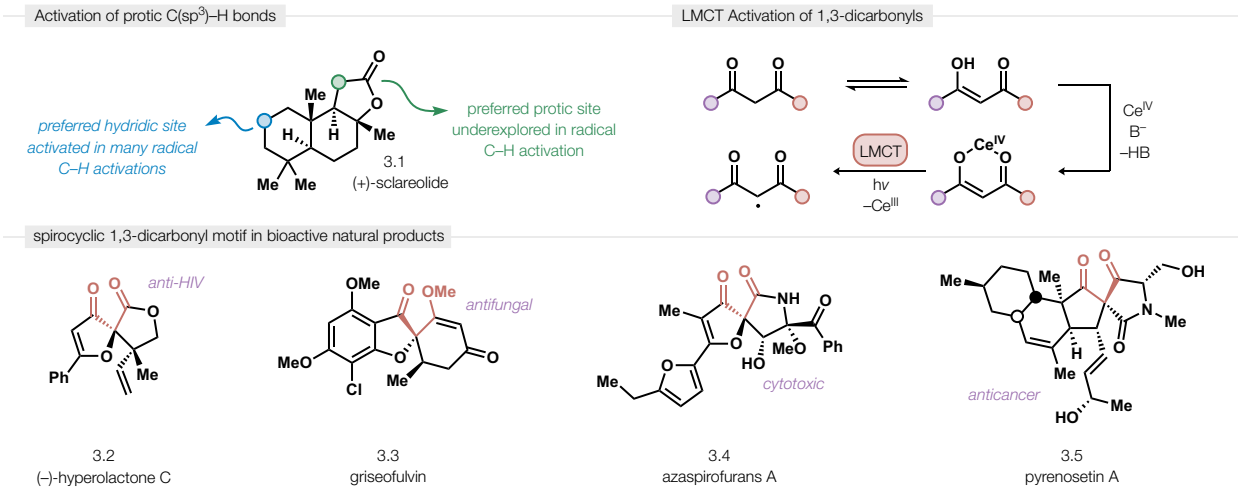


Figure 26. *Radical activation of C(sp^3)–H acids.*

We envisioned a strategy for photocatalytic activation of C(sp^3)–H acids based on ligand-to-metal charge-transfer (LMCT).[16a, 158] We reasoned that this activation mode has the potential to greatly expand the scope of amenable substrates by capitalizing on the dynamics of keto-enol tautomerism. The expected interaction with the enol tautomer allowed us to envision substrate activation for the entire catalogue of 1,3-dicarbonyl substrates in addition

to substrates that exclusively adopt the enol form in solution. This blueprint led us to explore Ce-photoredox catalysis to perform the requisite LMCT, and focus the transformation primarily on the creation of spirocycles. Spirocyclic compounds with a 1,3-dicarbonyl motif separated by the spirocentre are prevalent in bioactive compounds like hyperolactone C (**3.2**), griseofulvin (**3.3**), azaspirofurans A (**3.4**), and pyrenosetin A (**3.5**, **Figure 26**).[159] The wealth of literature detailing the use of Ce(IV) salts as single electron oxidants for 1,3-dicarbonyls suggested that a system comprised of a ground-state Ce(IV/III) cycle mediated by photocatalytic turnover might also prove viable.[160] These varied yet convergent catalytic proposals served to convince us that such a system could be identified quickly.

This chapter presents a detailed study on the use of a Ce-photoredox catalysis platform that directly engages 1,3-dicarbonyl C(sp^3)–H acids towards radical reactions. This platform enables redox-neutral hydroalkylation and cross-coupling, as well as oxidative transformations that demonstrably improve on the prior state of the art. Interrogations of this platform through kinetic, thermodynamic, and computational studies provide a model for diastereoselectivity and catalytic turnover. The present investigations also demonstrate the key role of lithium trifluoroacetate under complementary Ce-containing and Ce-free photoredox conditions to enable ligand-to-metal charge transfer (LMCT) or multi-site proton coupled electron transfer (MS-PCET) activations, respectively.

Conventional Radical Additions of C(sp^3)–H Acids to Olefins

The reaction we wished to realize was formally a hydrogen atom transfer radical addition (ATRA) or, more broadly, a radical hydroalkylation reaction of a 1,3-dicarbonyl. Consequently, it is necessary to discuss the historical context for these reactions using C(sp^3)–H acids. The activation of protic C(sp^3)–H bonds towards radical reactivity has a prolific history in organic chemistry that has been summarized as a timeline in **Figure 27**.

Discovered by Kharasch in 1937,[161] ATRA reactions are a powerful method for the anti-Markovnikov 1,2-halo- or hydroalkylation of olefins. Kharasch later demonstrated ATRA reactions using chloroform (**3.6**),[162] carbon tetrachloride (**3.7**), and α-bromoesters (**Figure 27**, **1940s**).[163] While our desired net-reaction conforms to an ATRA, historically this term is restricted to instances in which the chain-transfer and product formation steps are the same, hence the "atom transfer" portion of ATRA.[157] To ensure ample thermodynamic driving force, and favourable kinetics, ATRA reactions are restricted to cases in which the X–R bond strength increases from the starting material to the product.

Significant advances in radical generation from protic C–H bonds were made in the 1960s. In back-to-back articles, Heiba & Dessau[164] and Bush & Finkbeiner[165] reported the use of $Mn(OAc)_3$ to oxidize acetic acid (**3.9**) and

add it to olefins in a formal [3+2] lactonization reaction. These reports sparked significant attention by the organic chemistry community into the oxidative addition of carbon acids to olefins promoted by a variety of single electron metal oxidants.[160, 166]

The same decade saw landmark publications from Trahanovsky on the use of Ce(IV) reagents as single electron oxidants. In Trahanovsky and Young's seminal note,[167] the authors demonstrated the oxidation of benzylic alcohols with ceric ammonium nitrate (CAN, not shown).[23c] Later, benzylic C–H oxidation was reported by Trahanovsky[23b] and Syper,[168] independently (not shown). Trahanovsky later showed the peculiar behaviour of 2-aryl-1-phenylethanols that underwent oxidation and β-scission to give benzaldehydes (**3.15**) and benzyl alcohols (**Figure 27**, **1960s**). [23d] This work demonstrated through Hammett analysis that a significant degree of positive charge character is built up on the β-carbon during bond cleavage ($\rho = -2.0$). In 1969, Trahanovsky, Flash, and Smith demonstrated another oxidative β-scission process on bridge bicyclic 2º alcohols (not shown).[23g] In another thought-provoking early contribution, Trahanovsky and colleagues demonstrated the oxidative cyclization of 1-pentanol (**3.10**) to form 2-Me-THF (**3.14s**) using CAN.[23f]

Beginning in the 1960s, and continuing into the 1970s, Julia demonstrated the feasibility of hydrogen atom transfer (HAT) radical cyclizations using C(sp^3)–H acids. Using ester, β-ketoester, malonate diester, and β-cyanoester substrates, Julia studied regioselectivity in 5-*exo-trig vs*. 6-*endo-trig* cyclizations of their corresponding radicals.[156, 169] This work demonstrated the potential for redox-neutral formal hydrogen-ATRA reactions on a limited set of substrates. Julia and colleagues also showed that cyclizations of this type are reversible under their reaction conditions and the resulting product distribution was substrate dependent. The authors surmised that 5-*exo-trig* cyclization has a lower activation energy but leads to a high energy 1º C–centred radical (**3.16**), whilst 6-*endo-trig* cyclization has a higher energy TS but leads to a more stabilized 2º radical (**3.18**). Thus, as the open form radical (**3.17**) becomes more stabilized through the addition of stronger EWGs, 1º cyclopentylmethyl radicals (**3.16**) undergo more facile ring opening and the proportion of 6-*endo* product increases. This effect could be further accentuated by the addition of a methyl group at the internal position of the olefin that increases the barrier to 5-*exo* cyclization and stabilizes the 6-*endo* cyclized species as a 3º radical. Despite this success, these reactions were shown to operate on short and inefficient radical chains, making their synthetic application daunting.[157] Further work in the 1970s by Heiba and Dessau showed that Ce(IV) reagents could be used to effect the SET-initiated oxidative additions akin to $Mn(OAc)_3$ (not shown).[170]

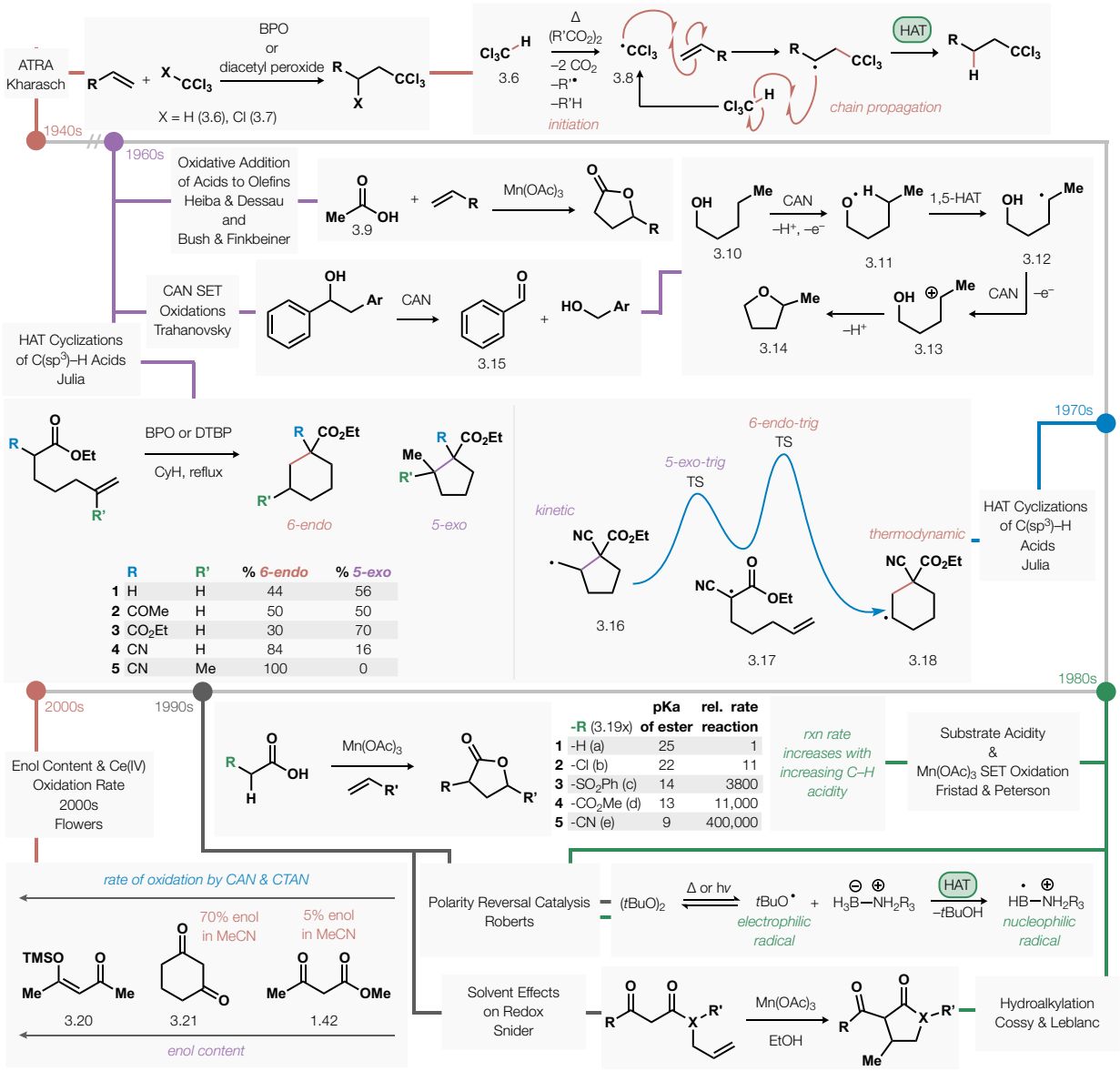


Figure 27. *A brief timeline (1940s – 2000s) of landmark publications for radical generation from C(sp³)–H acids and their hydroalkylation.*

In 1985, Fristad and Peterson showed that the rate of oxidation of C(sp³)–H acids with $Mn(OAc)_3$ increased with increased enolizability, or C–H acidity, of the substrate. This report used a Hammett kinetic analysis (LFER) on the oxidation of various α-functionalized acids in their reaction with $Mn(OAc)_3$.[171] They compared the relative individual reaction rates of these different species with acetic acid and plotted the logarithm of the relative reaction rate against the difference in pKa (ΔpKa) of the corresponding esters. This gave a linear plot ($R^2 = 0.999$) with $\rho = 0.344$. They went on to compare the rate of $Mn(OAc)_3$ reactions with acetic acid and acetic anhydride, claiming that anhydride could not be compared on the same scale because it did not have a free carboxylate with which to ligate

Mn^{III}. Acetic anhydride had a relative reaction rate 30-fold greater than acetic acid and a 250-fold greater relative reactivity was calculated based on their Hammett analysis (the difference in these values might reflect the difference made by having a free acid that can ligate the metal centre). The authors noted that increasing the concentration of KOAc increased reaction rates, suggesting that it behaves as a Brønsted base to perform deprotonation.

The 1980s also saw significant application of oxidative $Mn(OAc)_3$ cyclizations of enolizable 1,3-dicarbonyls, beginning with entries from Corey[172] and closely followed by Snider (not shown).[173] During this time period, Cossy and Leblanc reported a redox-neutral cyclization reaction promoted by $Mn(OAc)_3$ in ethanol (**Figure 27**, **1980s**).[174] Subsequent work by Snider investigated the impact of ethanol solvent compared to the more commonly used acetic acid. [175] The authors found that ethanol acts as a hydrogen atom donor for vinyl and 1º alkyl radicals to result in a redox-neutral transformation.

The 1980s and 1990s saw significant interest from the synthesis community in the use of alternative SET oxidants like Ce(IV),[176] Fe(III),[177] and Co(II)[178] to act upon 1,3-dicarbonyls. During this time period, Roberts described polarity reversal catalysis (PRC) and demonstrated the utility of amine-boranes to act as HAT catalysts that were particularly effective for abstractions from protic positions.[179]

In the early 2000s, Flowers studied the rate of 1,3-dicarbonyl oxidations by Ce(IV) reagents in MeCN.[180] Silyl enol esters and 1,3-diketones were found to be oxidized faster than β-ketoesters which they attributed to differences in the enol content of these species. Tautomerization of the ketoesters was thought to be rate-limiting.

While this is certainly not an exhaustive list of reports relevant to the development of radical generation from protic C–H bonds, it sets the stage for more modern developments. During these time periods, there was a reliance on the combination of stoichiometric oxidants and reductants to accomplish redox-neutral transformations. Alternatives to such systems relied on inefficient radical chain reactions. The lessons learned from these studies would prove invaluable for the development of modern methods that employ catalytic activations of $C(sp^3)$–H acids.

Radical Polarity

Radicals are related to anions and cations through the gain, or loss, of an electron and likewise are stabilized by effects that stabilize either ion. The thermodynamic stabilization of radicals certainly impacts the overall outcome of reactions proceeding through these intermediates, however, the chemical environment surrounding a radical can have a similarly profound impact on the kinetics of radical reactivity. In addition to sterics, the polarity of each radical

intermediate and reaction partner affect reaction kinetics and lead to different selectivity across the polarity spectrum. These polarity effects can often override enthalpic considerations for reaction selectivity prediction.[181]

Radical polarity refers to the degree of electrophilicity or nucleophilicity of a given radical, and is influenced by the effects of nearby substituents and functionalities as well as the identity of the atom(s) on which the radical is located. Radicals located on electronegative atoms are electrophilic whilst those located on more electropositive atoms are nucleophilic. Inductive and (hyper)conjugative effects of nearby substituents can serve to alter the polarity of a given radical species. Nearby electron withdrawing groups will render a radical more electrophilic whilst nearby electron donating groups will serve to increase nucleophilicity. The polarity of a given radical can be crudely assessed by deciding which corresponding ion would be more stable, cation or anion, from the hypothetical removal or addition of an electron. If the addition of an electron would be preferred and form a stabilized anion, then the radical is electrophilic. Conversely, if the removal of an electron results in a stabilized cation, then the radical is nucleophilic. In instances where both electron donating and electron withdrawing effects are present the relative influence of the effects can make assessment of the overall polarity of a given radical more challenging.

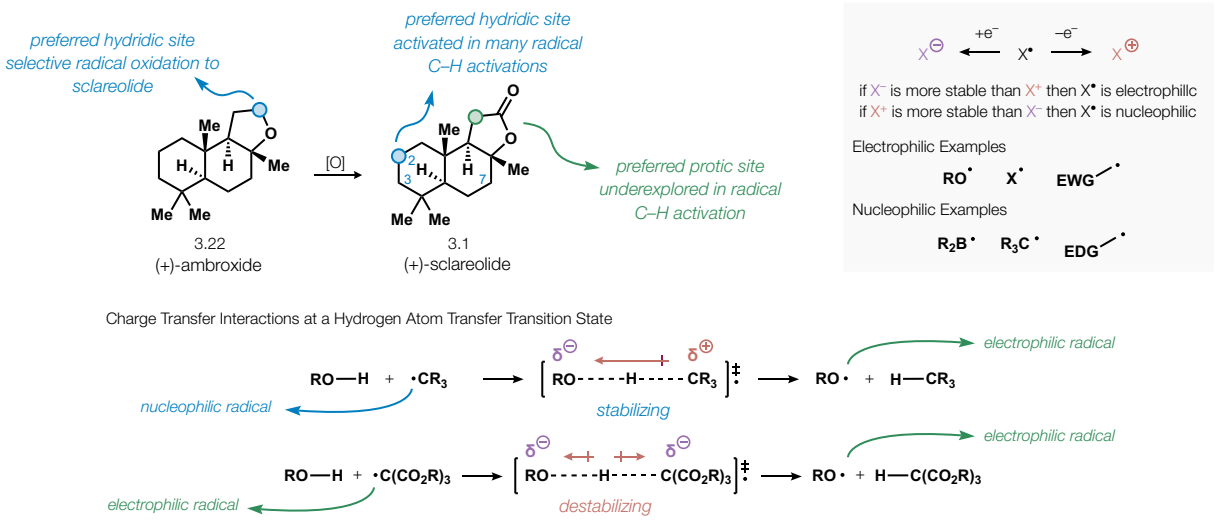


Figure 28. *Radical polarity examples and considerations.*

Just as in ionic chemistry, the careful consideration of the nucleophilicity and electrophilicity of reaction components can mean the difference between facile, selective, desired reactions and those that are undesirable, slow, and/or unselective. Radical polarity exerts an impact on reaction kinetics through stabilizing and destabilizing electrostatic charge transfer interactions at the transition state activated complex. In instances with paired polarity — *e.g.* the Giese addition of a nucleophilic radical to an electron poor olefin — complementarity serves to stabilize the

activated complex, resulting in a lower TS energy barrier and thus a faster reaction. If the radical employed in the same reaction were instead electrophilic, the addition of the radical to the electron poor olefin might still be a thermodynamically favoured reaction, but the polar interactions at the TS would be destabilizing and result in a higher barrier and a slower addition step relative to the nucleophilic radical. These considerations apply to all the elementary reactions of radicals whether it be addition, substitution, or elimination.

In the context of radical generation from C–H bonds, historically there has been a bias towards the study of reactions that activate hydridic sites and therefore result in nucleophilic radicals. This tendency is a natural consequence of the electrophilic hydrogen at transfer reagents and catalysts that are most available and often used to activate these hydridic C–H bonds. There is a plethora of reactions that rely on electron poor halogen-, oxygen-, and nitrogen-centred radicals to activate a given substrate through HAT. In contrast, there are relatively few nucleophilic HAT reagent and catalyst systems that can selectively abstract H$^{\bullet}$ from electrophilic C–H sites. As a consequence, many transformations that involve C-centred radicals at electrophilic sites proceed through alternative, non-HAT activation mechanisms that can be broadly described as proton-coupled electron transfers (*e.g.* ETPT, PTET, or MS-PCET).

Recently, Garwood, Chen, and Nagib quantified the polarity of a variety of organic radicals to create a database that can aid chemists in predicting reaction viability and outcomes.[155a] The authors found that computed radical electrophilicity, derived from the computed ionization potential and electron affinity, correlated well with reaction kinetics across a broad array of radicals. By default, most C-centred radicals tend to be nucleophilic in nature.[182] Resonant delocalization of a C-centred radical into adjacent carbonyl groups does not always render these species electrophilic relative to H$^{\bullet}$, but they are rendered less nucleophilic by this environment.

Under the ionic regime, an alkyl carbonyl with an α C–H bond would be considered an electron-rich site that could react as a nucleophile either from an enol or enolate intermediate. The corresponding radical at that site, from the formal loss of H$^{\bullet}$, is an electrophilic radical and as such is kinetically biased towards reaction with nucleophilic reaction partners. As such, the change from closed to open shell chemistry inverts the reactivity of these sites resulting in umpolung reactivity.[183] Phenol hydroxyl groups, close cousins of enols, behave as π-electron donors that increase the nucleophilicity of ortho/para sites when neutral ($\sigma_p^- = -0.37$) or anionic.[184] When converted to phenoxyl radicals, they become exceptionally strong electron withdrawing groups ($\sigma_p^- = 2.79$; *cf.* $\sigma_p^-(NO_2) = 1.27$). For further reading

on radical polarity and its impact on reaction efficiency and selectivity, the interested reader is directed to reviews by Leonori[185] and Welin.[155b]

Photochemical α-Alkylation of C(sp^3)–H Acids with Olefins

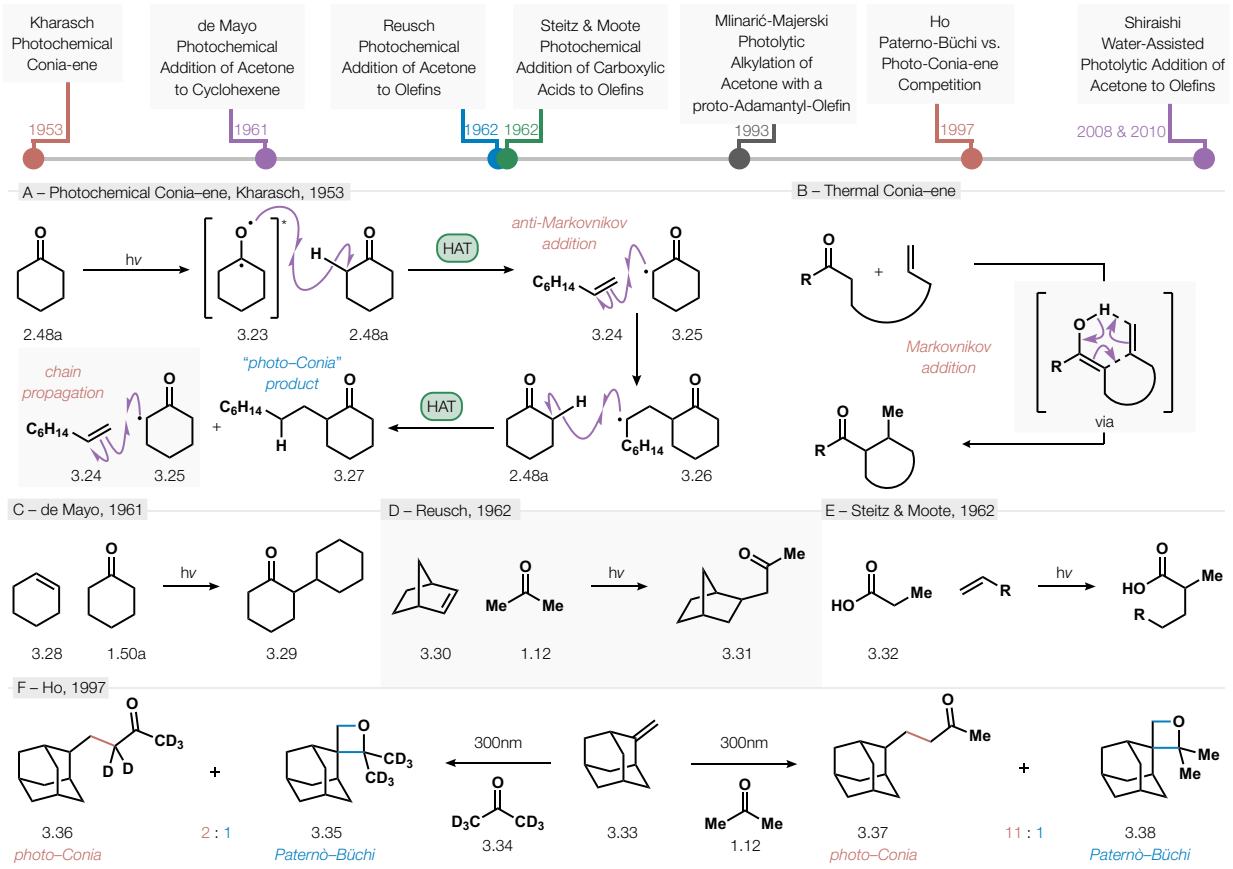


Figure 29. *Direct photoexcitation α-alkylations of carbon acids with olefins.*

Early radical α-alkylations with olefins relied on the innate reactivity of the ketone excited state as a HAT radical initiator. Kharasch was the first to report this type of reaction in 1953, where it was found that UV irradiation of a solution of cyclohexanone (**2.48a**) in 1-octene (**3.24**) gave the adduct (**3.27**, **Figure 29**, **A**). A plausible mechanism for this transformation begins with initiation by excitation of cyclohexanone to give biradical **3.23** and hydrogen abstraction from the α-position of a second equivalent of cyclohexanone (**2.48a**) to give **3.25**. From the electrophilic α-keto radical **3.25**, radical chain propagation can occur *via* anti-Markovnikov addition to the terminus of 1-octene to give **3.26**. The chain can then transfer through HAT from another equivalent of cyclohexanone (**2.48a**) to the 2º C-centred radical **3.25**. This process represents an intermolecular hydrogen atom transfer radical addition (ATRA)

reaction, which some have deemed a 'photo Conia-ene' reaction for its similarity to the thermal Conia-ene reaction, despite the regiochemical differences (**Figure 29**, **B**).[186]

Following Kharasch's discovery, in 1961 de Mayo noted a similar adduct formed between cyclohexanone (**2.48a**) and cyclohexene (**3.28**, **Figure 29**, **C**).[187] In 1962, Reusch reported the same behaviour when acetone (**1.12**)/norbornene (**3.30**) mixtures were irradiated to give adduct **3.31** as a single stereoisomer (**Figure 29**, **D**).[188] In the same year, Steitz and Moote reported the α-alkylation of aliphatic carboxylic acids with olefins under photolysis conditions (**Figure 29**, **E**).[189] In 1993, Mlinarić-Majerski reported the direct photolytic addition of acetone (**1.12**) to 4-methylene-2-protoadamantanone (not shown).[190]

In 1997, Ho reported on the photolytic addition of acetone (**1.12**) to 2-methyleneadamantane (**3.33**) (**Figure 29**, **F**). The authors noted an 11:1 preference for Kharasch-like photo-Conia addition (**3.37**) relative to the anticipated Paterno-Büchi [2+2] product (**3.38**).[186] The preference for hydroalkylation could be reduced to 2:1 (**3.36**/**3.35**) when using acetone-d_6 (**3.34**), leveraging a kinetic isotope effect to decrease the rate of HAT necessary for the photo-Conia reaction.

In 2008, the Shiraishi group reported a water-assisted Kharasch-addition of acetone to olefins.[191] The authors suggested that the use of water as the reaction medium results in the hydration of α-keto radicals and discourages radical-radical combination events, leading to a higher proportion of Kharasch addition product (not shown). In 2010, Shiraishi and colleagues followed up this work with the acetone addition to olefins assisted by a Mg-exchanged zeolite Y (not shown).[192]

Later, strategies emerged that rely on the excitation of radical chain initiators like peroxides, metals which behave as single electron oxidants or HAT initiators, as well as several photoredox approaches that can be described as photoredox initiated radical chains (**Figure 30**).

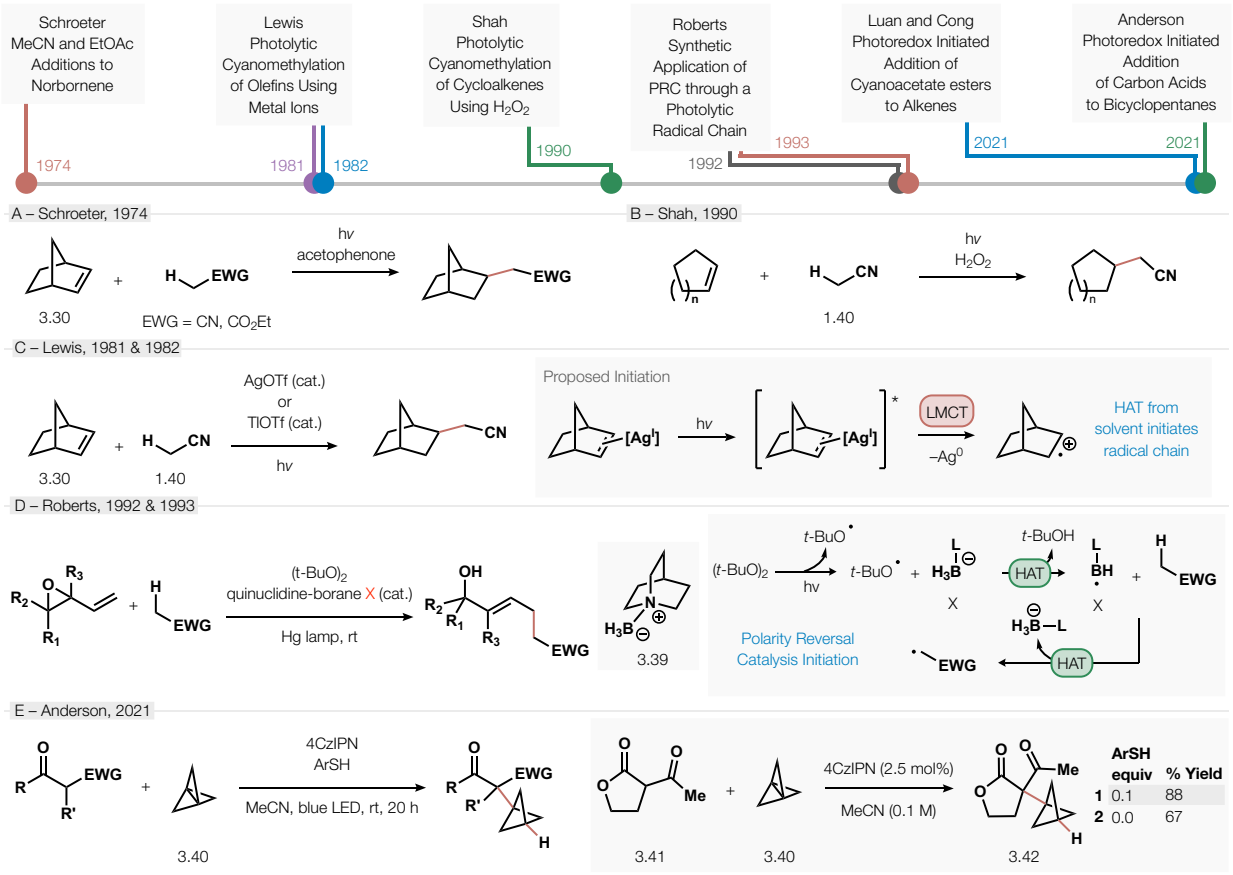


Figure 30. *Indirect photo-initiated α-alkylations of carbon acids.*

In 1974, Schroeter reported an indirect photo-initiated α-alkylation of acetonitrile (**1.40**) and ethyl acetate with norbornene (**3.30**) using acetophenone as a photoinitiator (**Figure 30**, **A**). In the early 1980s, Lewis detailed the cyanomethylation of norbornene (**3.30**) with Ag(I) and Tl(I) ions under irradiation (**Figure 30**, **C**).[193] In contrast to all of the studies discussed in this section so far, Lewis does not propose the excitation of a carbonyl to initiate a radical chain. Rather, the authors propose a π-acid complex of Ag(I) and norbornene (**3.30**) undergoes LMCT upon excitation to precipitate Ag(0) and liberate a norbornene radical cation. The radical cation is thought to be the key HAT agent that initiates a radical chain reaction through abstraction from the α-position of the acetonitrile solvent.

In 1990, Shah reported the cyanomethylation of olefins using hydrogen peroxide as a radical initiator under photolysis conditions (**Figure 30**, **B**).[194] In 1992 and 1993, Roberts' demonstrated polarity reversal catalysis (PRC) for the α-allylation of carbon acids using di-*tert*-butyl peroxide as a photoinitiator with a quinuclidine-borane (**3.39**) HAT catalyst (**Figure 30**, **D**). Under the PRC paradigm, slow polarity-mismatched HAT between the electrophilic C(sp^3)–H and the electrophilic O-centred radicals during initiation and propagation are circumvented through the intermediacy of a polarity-matched cycle. In this instance, Roberts' employed an amino borane catalyst as a

nucleophilic hydrogen atom donor and acceptor species that can give H• to electrophilic O-centred radicals and abstract H• from the carbon acid starting material.

In 2021, Luan and Cong reported the photoredox initiated addition of cyanoacetate esters to alkenes which is proposed to proceed through a radical chain mechanism.[195] Later that year, Anderson reported a photoredox catalyzed addition of [1.1.1]-propellane (**3.40**) to 1,3-dicarbonyls to give bicyclopentanes (**3.42**) with a quaternary bridgehead (**Figure 30**, **E**).[196] The authors show that in the absence of thiol co-catalyst the reaction proceeds in 67% yield compared to 88% with thiol. Although the authors do not report a quantum yield for this reaction, it seems reasonable to suggest there is some contribution from a radical chain under the optimized conditions.

Naturally, there have also been reports on photocatalytic α-alkylations of carbon acids with olefins, purportedly proceeding through closed catalytic cycles (**Figure 31**). In 2017, MacMillan reported the asymmetric α alkylation of aldehydes with alkenes through a triple catalysis system (**Figure 31**, **A**). This system, comprised of a chiral amine organocatalyst, a thiol HAT/base catalyst, and an iridium photocatalyst operates through a reductive PET from a transient enamine intermediate to photoexcited [Ir(III)]* to generate a radical cation predisposed to addition to olefins with facial selectivity dictated by the chiral amine moiety.

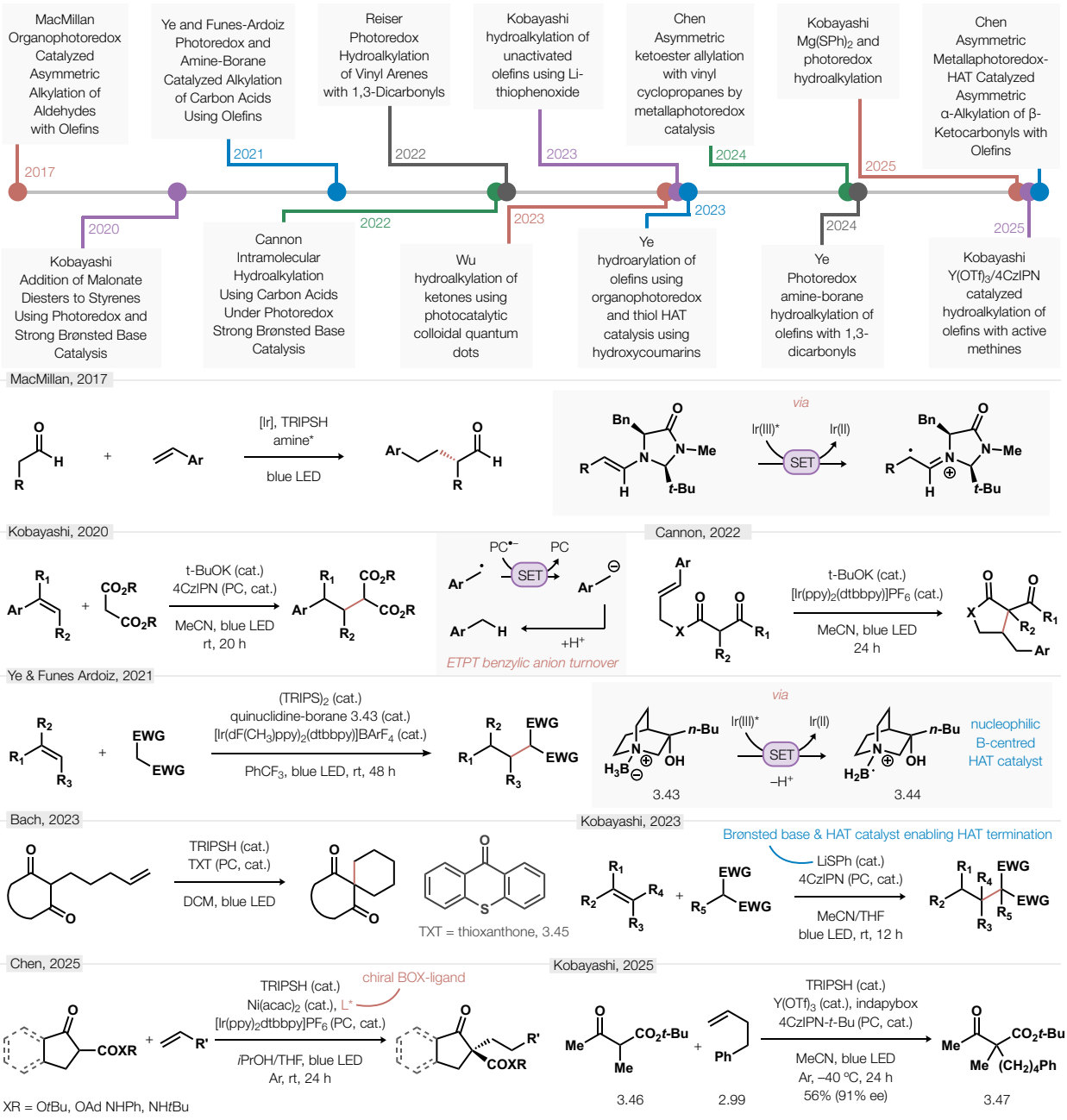


Figure 31. *Photoredox catalyzed α-alkylations of carbon acids using olefins.*

Kobayashi[197] and Cannon[198] each reported α-alkylations of carbon acids with olefins through photoredox/strong base catalysis (**Figure 31**, **B**). These reactions achieve turnover through an ETPT sequence that limits the amenable substrate scope to olefins that produce stabilized benzylic radicals and thus benzylic anions. A related strategy was employed by Reiser in 2022 for the α-alkylation of malonate diesters with vinyl arenes using 4CzIPN and K_3PO_4 (not shown).[199]

In 2021, Funes-Ardoiz and Ye employed an amine-borane HAT catalyst for the intermolecular hydroalkylation of olefins using 1,3-dicarbonyls (**Figure 31**, **D**). Just as Roberts demonstrated in the 1990s, the authors employ an amine-borane HAT catalyst to use the intermediate B-centred radicals as the key agent to abstract a hydrogen atom from the electrophilic α-position of 1,3-dicarbonyls in a polarity-matched step.

The year 2023 saw several reports on the α-alkylation of carbon acids using olefins under photocatalysis. Wu and colleagues reported the visible light-induced hydroalkylation of cyclic ketones using colloidal quantum dots (not shown).[200] Kobayashi reported an improved hydroalkylation reaction using lithium thiophenoxide as a base and HAT catalyst, thereby expanding the scope of alkene acceptors to unactivated olefins (**Figure 31**, **F**).[201] Bach, Franziska, and Johannes reported a spirocyclizing hydroalkylation of cyclic 1,3-diones onto tethered olefins using a thioxanthone photocatalyst (**3.45**) and 2,4,6-triisopropylthiophenol as an HAT catalyst (**Figure 31**, **E**).

Chen reported in 2024 the asymmetric allylation of ketoesters with vinyl cyclopropanes using a photoredox catalyst in conjunction with a nickel catalyst bearing a chiral BOX ligand (not shown).[202] The authors did not supply an HAT catalyst to this reaction, limiting the substrate scope to those that fragment to electrophilic α-malonate radicals that could undergo subsequent reduction to stabilized enolate anions. In the same year, Ye and colleagues reported an improved quinuclidine-borane catalyst for the α-alkylation of 1,3-dicarbonyls with olefins (not shown).[203] The authors demonstrated that the introduction of an amide functionality at C3 of the quinuclidine core results in stronger substrate-catalyst hydrogen bonding and an improved yield.

Recently, Kobayashi and Chen have described more α-alkylations using photoredox catalysis. Kobayashi demonstrated hydroalkylation using $Mg(SPh)_2$ as a highly efficient base/HAT catalyst under photoredox catalysis.[204] They also reported a system comprised of TRIPSH, organic dye 4CzIPN-*t*Bu, and a $Y(OTf)_3$ Lewis acid to α-alkylate active methine 1,3-dicarbonyls.[205] Impressively, they demonstrated enantioselective addition of ketoester **3.46** to olefin **2.99** in 56% yield and 91% ee using a chiral indapybox ligand (**Figure 31**, **H**). Building upon their earlier report with the inclusion of a TRIPSH HAT catalyst, Chen and colleagues reported an asymmetric α-alkylation of 1,3-dicarbonyls with olefins mediated by a nickel co-catalyst bearing a chiral BOX ligand (**Figure 31**, **G**).[206]

3.2 Project Motivation

Moving on from our interest in the activation of strong O–H bond activations applied to C–C bond cleavage, this project focuses on weak O–H bond activations applied towards C–C bond formation. We became interested in these reactions following a discussion with another lab member on a troublesome step in their total synthesis. Andre

Costisella was attempting to perform a spirocyclizing anionic Michael addition reaction (**3.48** to **3.51**) during his studies towards the penostatin family of natural products (**Figure 32**, **A**).[207] Early attempts under basic conditions proved fruitless and prompted discussions about the likely culprits. We initially hypothesized that the formation of the 4º spirocentre might be challenging due to the steric interactions present at the transition state. We also expected that the ambiphilic nature of the Michael acceptor might discourage cyclization, as it has both the necessary π-acceptor carbonyl functionality that would suit anionic addition as well as a detrimental π-donor endocyclic oxygen. These problems might be readily solved through a radical cyclization (**Figure 32**, **B**). Our reasoning was two-fold: first, the earlier transition state of a radical cyclization should display longer bond lengths at the cyclization TS when compared to comparable ionic processes, thereby mitigating the impact of steric interactions, and; second, we anticipated that the captodative stabilization of the cyclized radical intermediate would render the radical cyclization more favourable than the corresponding anionic process.

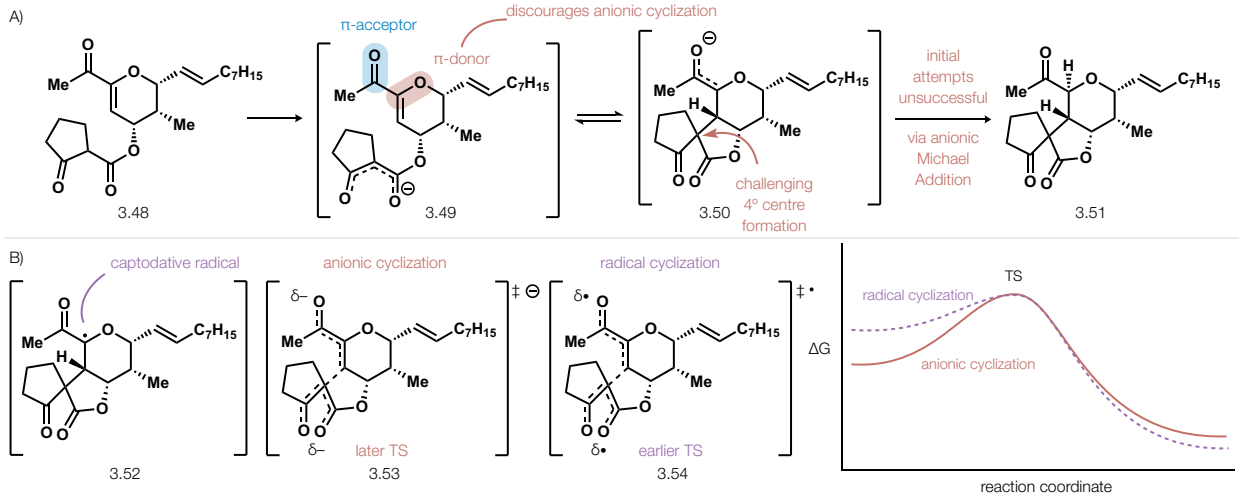
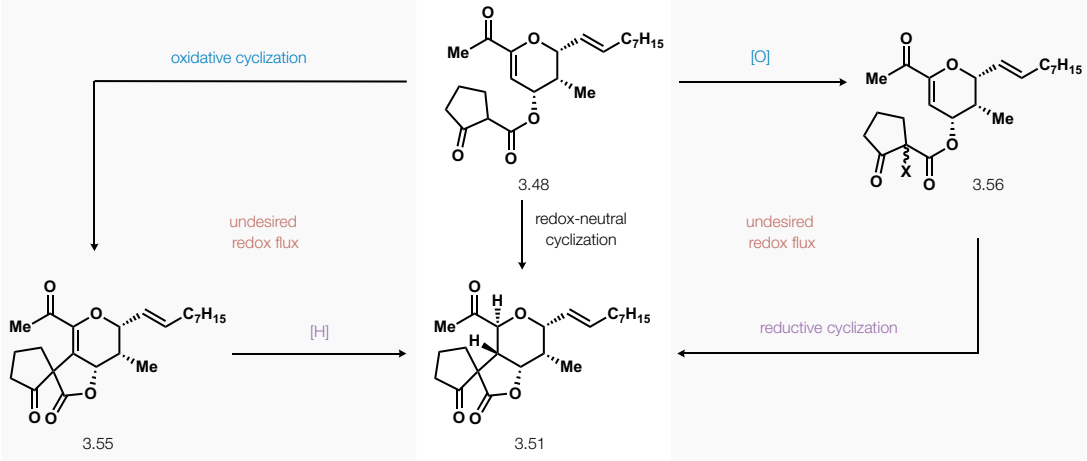


Figure 32. *Project inspiration.*
A) Challenging anionic Michael addition in Andre Costisella's penostatin synthesis studies; B) Comparison of anionic and radical cyclizations.

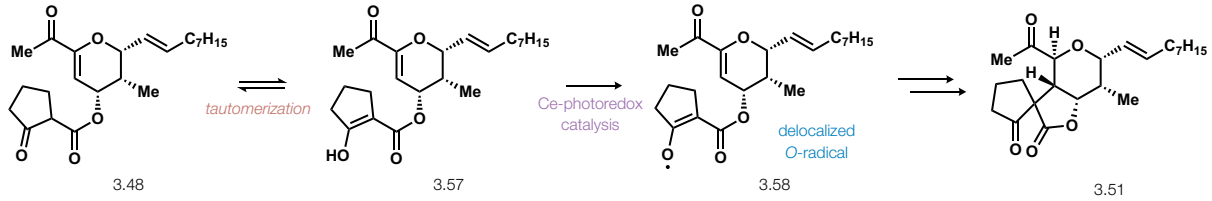
Next came discussions about how such a radical transformation might be accomplished. As this step used advanced material in Andre's synthesis, the most desirable starting material for a radical cyclization would be the ketoester (**3.48**) used in the anionic cyclization attempts (**Scheme 7**). Known ketoester cyclizations that would suit this substrate were net-oxidative or net-reductive. A net-oxidative cyclization would allow André to use his existing substrate but would yield the product in a higher oxidation state than intended (**3.55**, **Scheme 7**, **left**). A net-reductive cyclization would require André to supply the starting material in a higher oxidation state and add a superfluous step

(**3.56**, **Scheme 7**, **right**). The most suitable redox-neutral cyclizations of such ketoesters, in a hydroalkylation/Kharasch-type addition reaction, were far less developed (**Scheme 7**, **centre**).



Scheme 7. *Redox schemes for the spirocyclizing addition in Andre Costisella's approach towards the penostatins.*

Modifications to net-oxidative conditions existed that render them redox-neutral from the perspective of the substrate,[208] however, they do nothing to quell the impacts of supplying a stoichiometric single electron oxidant to an oxidatively-sensitive substrate or product. Additionally, the modification of these net-oxidative methods, such as the use of ethanol as solvent and reductant in $Mn(OAc)_3$ reactions, does not reduce the waste byproducts formed from a stoichiometric reaction. In fact, this strategy intensifies waste production as waste derived from the terminal reductant is produced in addition to the waste produced by the stoichiometric oxidant. We believed that catalysis could solve the issues of waste intensity as well as provide milder conditions that tolerate more sensitive substrates.



Scheme 8. *β-ketoesters keto-enol tautomerism and application of Ce-photoredox catalysis for mesomeric O-radical generation.*

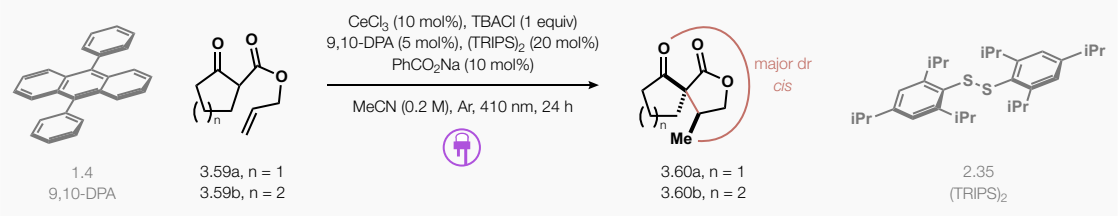
Recognizing that the desired transformation was formally a hydrogen atom transfer radical addition, we surmised that photoredox catalysis would be an effective tool to realize this transformation. Further, recognition of the reactive motif in André's starting material not as simply a ketoester (**3.48**), but as an enol (**3.57**), caused us to prioritize exploration of Ce-photoredox catalysis to this challenge (**Scheme 8**). Given the successes of Ce photoredox catalysis in O-radical generation, and the history of Ce(IV) ground state SET of active methylene and methine $C(sp^3)$–

H acids,[160] we surmised that our conditions would readily generate the requisite radical for cyclization (**3.58**). From here, mesomeric reaction from carbon could allow cyclization *via* radical intermediates and might mitigate the issues encountered in the anionic transformation. During these studies, Dr. André Costisella identified conditions for the anionic Michael addition process that permitted access to the desired spirocyclic product. The interested reader is directed to Dr. Costisella's thesis for further discussion of this problem and its solution.[207]

3.3 Initial Investigations and Optimization

To realize the spirocyclizing hydroalkylation, we began with our previously identified conditions for the redox-neutral β-scission of lactols and hydrodecarboxylation reactions.[45] Gratifyingly, violet LED irradiation of a suspension of β-ketoester **3.59a**, cerium(III) chloride, bis(2,4,6-triisopropylphenyl)disulfide (**2.33**, $(TRIPS)_2$), tetrabutylammonium chloride (TBACl), sodium benzoate and 9,10-diphenylanthracene (**1.4**, 9,10-DPA) for 16 hours under argon atmosphere delivered the desired [4.4]-spirocyclic ketolactone **3.60a** in 83% yield and 3.8:1 diastereomeric ratio (**Table 13**, **entry 1**).

Table 13. *Controls and optimization of the redox-neutral hydroalkylation*



Entry	n	Deviation	% Yield 3.60	d.r.	% SM 3.59
1	1	none	83	3.8:1	0
2	1	no light, heated to 55 ºC	n.d.	–	64
3	1	no $(TRIPS)_2$	20	3.0:1	42
4	1	no TBACl	33	2.0:1	26
5	1	no $CeCl_3$	0	–	74
6	1	no 9,10-DPA	8	2.0:1	70
7	1	no Ce, no TBACl	57	3.0:1	36
8	1	air atmosphere instead of argon	36	3.0:1	35
9	1	no $PhCO_2Na$	86	3.0:1	0
10	1	no $PhCO_2Na$, $Ce(OTf)_3$ in place of $CeCl_3$	91	3.5:1	0
11	1	no $PhCO_2Na$, $(Et_4N)_2CeCl_6$ in place of $CeCl_3$	59	2.0:1	34
12	1	$Ce(OTf)_3$ & CF_3CO_2Na in place of $CeCl_3$ & $PhCO_2Na$	90*	4.0:1	0
13	1	$Ce(OTf)_3$ & CF_3CO_2Li in place of $CeCl_3$ & $PhCO_2Na$	85	3.1:1	0
14	1	no Ce, no TBACl, CF_3CO_2Li instead of $PhCO_2Na$	90 (80*)	3.4:1	–
15	2	no Ce, no TBACl, CF_3CO_2Li instead of $PhCO_2Na$	78	2.5:1	n.d.
16	2	no Ce, no TBACl, CF_3CO_2Na instead of $PhCO_2Na$	13	2.0:1	n.d.

*[a] ^1H NMR spectroscopy yields using PhTMS as internal standard; *Isolated yield; d.r. were obtained by ^1H NMR spectroscopy of the crude reaction mixture.*

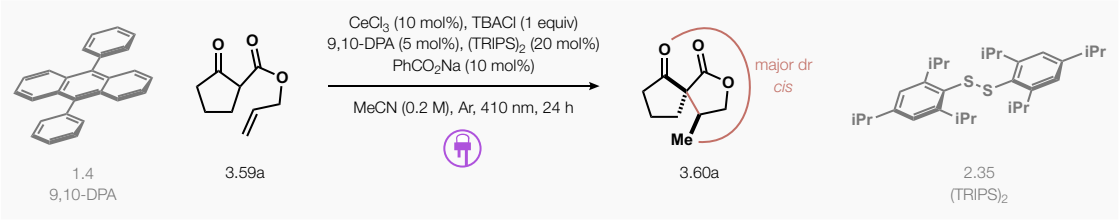
A thermal control reaction showed that the reaction was photoinduced, excluding thermal Conia-ene reactivity as the origin of product formation (**Table 13**, **entry 2**). Removal of $(TRIPS)_2$ (**2.33**) resulted in severely reduced conversion to **3.60a** (**Table 13**, **entry 3**). Conversion to **3.60a** in the absence of disulfide co-catalyst may arise from an HAT-propagated background radical chain reaction. Omission of TBACl significantly reduced the yield, aligning with previous findings that high halide concentrations are imperative for efficient Ce reactivity (**Table 13**, **entry 4**).[9b, 209] Exclusion of $CeCl_3$ did not result in detectable conversion of **3.59a** to **3.60a** (**Table 13**, **entry 5**). Without 9,10-DPA (**1.4**) present, conversion to **3.60a** occurs in just 8% yield with 70% **3.59a** remaining, suggesting a profound impact on turnover frequency (**Table 13**, **entry 6**). Curiously, simultaneous exclusion of $CeCl_3$ and TBACl saw a revival in catalytic turnover towards **3.60a** (**Table 13**, **entry 7**). We reasoned that in the absence of both Ce(III) and excess chloride, a background PCET oxidation of **3.59a** by photoexcited 9,10-DPA* (**1.4***) is likely operative ($E_{1/2}$(ketoester/ketoester$^{\bullet+}$) = +1.89 V *vs* SCE; E(DPA*/DPA$^{\bullet-}$) = +1.28 V *vs* SCE in MeCN).[6f, 9d] Running the reaction under ambient atmosphere instead of an argon purged solution impacted the reaction negatively, furnishing **3.60a** in only 36% yield with 35% starting material remaining (**Table 13**, **entry 8**). Removal of $PhCO_2Na$ led to a slight improvement in yield (**Table 13**, **entry 9**), and use of $Ce(OTf)_3$ in place of $CeCl_3$ gave a further 5% improvement in yield (**Table 13**, **entry 10**). This unexpected result prompted us to further investigate the identity of the carboxylate additive.

After extensive screening, we identified trifluoroacetate salts as the superior additive to accomplish hydroalkylation. Screening Ce(III) sources identified $Ce(OTf)_3$ as the most effective pre-catalyst, likely a result of its superior solubility in MeCN. Bis(tetraethylammonium) hexachlorocerate as a Ce(IV) LMCT photocatalyst gave only a 59% yield of desired product (**3.60a**) with 34% SM (**3.59a**) remaining after a 24-hour reaction period (**Table 13**, **entry 11**). When used in conjunction with CF_3CO_2Na additive, $Ce(OTf)_3$ delivered **3.60a** in 90% isolated yield (**Table 13**, **entry 12**). Comparison of CF_3CO_2Na to CF_3CO_2Li showed no substantial difference between the two cations (**Table 13**, **entries 12 & 13**).

Building upon the Ce/TBACl-free control (**Table 13**, **entry 7**), we explored the viability of cerium-free conditions. A significant cation effect was observed, wherein CF_3CO_2Li, 9,10-DPA (**1.4**), and $(TRIPS)_2$ (**2.33**) yielded [4.5]-spirocycle **3.60b** in 78% yield (**Table 13**, **entry 15**), while use of CF_3CO_2Na resulted in just a 13% yield (**Table 13**, **entry 16**). Application of the CF_3CO_2Li and Ce-free conditions to synthesis of [4.4]-spirocycle **3.60a** results in an

80% isolated (90% NMR) yield (**Table 13**, **entry 14**). With two sets of optimized hydroalkylation conditions in hand, we sought to demonstrate the utility of this redox-neutral photocatalytic hydroalkylation reaction.

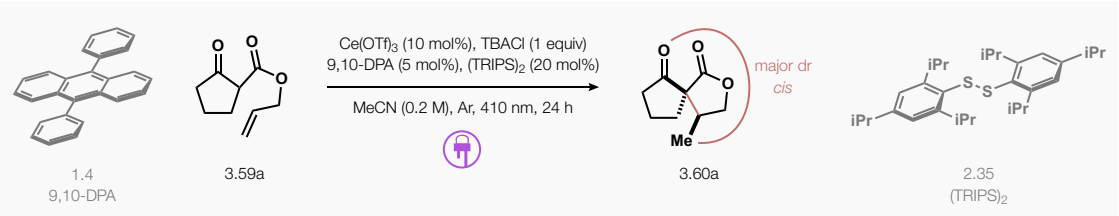
Table 14. *Optimization of redox-neutral hydroalkylation: solvent.*



Entry	Deviation	% Yield 3.60a	% SM 3.59a
1	none	83	0
2	Methyl ethyl ketone instead of MeCN	43	28
3	DCE instead of MeCN	15	65
4	TFE instead of MeCN	trace	49
5	NMP instead of MeCN	18	44
6	MeCN/DMSO (98:2)	67	trace
7	MeCN/DMSO (9:1)	78	trace
8	MeCN/DMSO (8:2)	62	18

Early in the optimization campaign, we assessed reaction efficiency in a variety of solvents (**Table 14**). Compared to acetonitrile (**Table 14**, **entry 1**), DCE, TFE, NMP and binary MeCN/DMSO solvent mixtures all provided inferior conversion of ketoester **3.59a** into ketolactone **3.60a** (**Table 14**, **entries 1–8**).

Table 15*. Optimization of redox-neutral hydroalkylation: Catalyst loadings and concentrations*

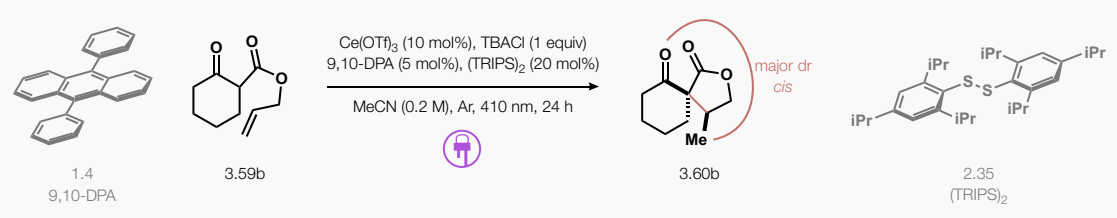


Entry	Deviation	% Yield 3.60a	% SM 3.59a
1	DPA (2.5 mol%)	81	0
2	DPA (10 mol%)	91	0
3	$Ce(OTf)_3$ (5 mol%)	77	0
4	$Ce(OTf)_3$ (20 mol%)	53	30
5	$(TRIPS)_2$ (10 mol%)	75	0
6	$(TRIPS)_2$ (40 mol%)	88	0
7	TBACl (0.5 equiv)	62	15
8	TBACl (2.0 equiv)	84	0
9	Halved all catalyst loadings	87	0
10	Doubled all catalyst loadings	88	0
11	0.4 M concentration	80	0
12	0.1 M concentration	88	0

We also assessed the catalyst loadings and global concentration (**Table 15**). Halving the 9,10-DPA (**1.4**) loading showed a ~10% decrease in yield while doubling the loading showed no improvement relative to standard conditions (**Table 15**, **entries 1 & 2**). Halving or doubling the $Ce(OTf)_3$ catalyst loading both led to lower yields than the initial loading of 10 mol% (**Table 15**, **entries 3 & 4**). Decreasing the disulfide loading from 20 mol% down to 10 mol% led to a significant drop in yield, whilst increasing the loading to 40 mol% had almost no impact (**Table 15**, **entries 5 & 6**). Likewise, halving or doubling the loading of tetrabutylammonium chloride both resulted in a diminished conversion to desired product (**Table 15**, **entries 7 & 8**). The reaction was not very sensitive to halving or doubling the loading of all the catalysts simultaneously, resulting in nearly identical yields of **3.60a** with a nearly indistinguishable efficiency to the standard conditions (**Table 15**, **entries 9 & 10**). Taken together with the previous results in this table, the reaction is more sensitive to the relative concentrations of the catalysts than it is to the overall concentration of the multicatalytic network.

Doubling the reaction concentration to 0.4 M (with respect to ketoester **3.59a**) resulted in a slightly diminished 80% yield (**Table 15**, **entry 11**), whilst halving the concentration showed an insignificant impact (**Table 15**, **entry 12**). When considered in the context of entries **9** and **10**, these results suggest that although the reaction is insensitive to overall catalyst loading (within solubility limits), increased substrate concentration has a minor negative impact on reaction efficiency. We speculate that the most likely deleterious impact on yield is through an increase in minor side-product formation at higher substrate concentrations.

Table 16. *Optimization of redox-neutral hydroalkylation: Additives and reaction duration*



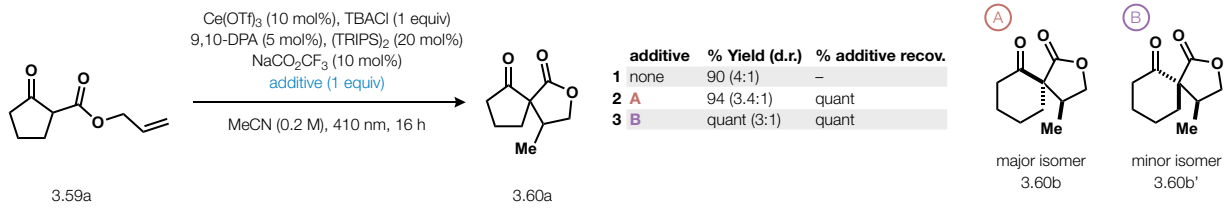
Entry	Deviation	% Yield	% SM
1	none	41	59
2	16 h, then 24 h (attempt 1)	56	36
3	16 h, then 24 h (attempt 2)	62	37
4	88 h	66	27
5	16 h, then + additional $Ce(OTf)_3$ (10 mol%), then 24 h	57	39
6	16 h, then + additional 9,10-DPA (5 mol%), then 24 h	62	36
7	16 h, then + additional $(TRIPS)_2$ (20 mol%), then 24 h	66	34
8	16 h, then + additional doses of $Ce(OTf)_3$, 9,10-DPA, & $(TRIPS)_2$, then 24 h	66	34
9	+ 2,4,6-collidine (10 mol%)	38	59
10	+ DABCO (10 mol%)	10	87
11	+ $PhCO_2H$ (10 mol%)	30	61
12	+ $(BuO)_2P(O)ONa$ (10 mol%)	46	41
13	+ MsONa (10 mol%)	60	36
14	+ TsONa (10 mol%)	47	50
15	+ $TRIPCO_2Na$ (10 mol%)	22	71
16	+ $F_5C_6CO_2Na$ (10 mol%)	53	47
17	+ TRIPSNa (10 mol%)	35	62
18	+ CF_3CO_2Na (10 mol%)	74	26
19	+ CF_3CO_2Na (5 mol%)	58	42
20	+ CF_3CO_2Na (20 mol%)	54	31
21	+ CF_3CO_2Na (10 mol%) & LiCl (0.5 equiv)	79	20
22	+ CF_3CO_2Na (10 mol%) & KCl (0.5 equiv)	69	35
23	+ CF_3CO_2Na (10 mol%) & $MgCl_2$ (0.5 equiv)	64	15
24	+ CF_3CO_2Na (10 mol%) & $ZnCl_2$ (0.5 equiv)	35	53
25	+ CF_3CO_2Li (10 mol%)	83	10
26	+ CF_3CO_2Li (5 mol%)	75	25
27	+ CF_3CO_2Li (20 mol%)	85	9
28	72 h + CF_3CO_2Li (10 mol%)	90	trace
29	+ CF_3CO_2Li (10 mol%) – $Ce(OTf)_3$	54	29
30	+ CF_3CO_2Li (10 mol%) – $Ce(OTf)_3$ – TBACl	78	10
31	+ CF_3CO_2Na (10 mol%) – $Ce(OTf)_3$	8	83
32	+ CF_3CO_2Na (10 mol%) – $Ce(OTf)_3$ – TBACl	13	73

We also explored the effects of various Lewis acid and base additives at different loadings as well as the effect of subsequent catalyst additions and extended durations on yield of [4.5]-spirocycle **3.60b** (**Table 16**). Early attempts to synthesize **3.60b** were thwarted by reactions that appeared to stall prior to full conversion. Under the standard conditions at that time, we observed that after 24 h there was a 41% yield of **3.60b** with 59% **3.59b** remaining

(**entry 1**). At 40 h of irradiation, we saw 56–62% yield with 36–37% starting material remaining (**entries 2 & 3**). Crucially, running a reaction for 88 h of irradiation resulted in no significant improvement in conversion to product **3.60b** when compared to the 40-hour reactions (**compare entries 2 & 3 to 4**). Based on these results, we had three hypotheses for why the reaction would cease to convert: 1) one or more catalysts were decomposing under the reaction conditions, 2) the product inhibits one or more of the catalytic cycles such that the reaction shuts down as the concentration of **3.59b** approaches or exceeds a critical threshold, or 3) under these conditions the concentration of substrate **3.59b** falls below a critical threshold for a productive forward reaction to take place.

To assess the first possibility, we ran reactions under the standard conditions for 16 h of irradiation. After 16 h, a subsequent loading of catalyst was added to the reaction, the solution was sparged with argon, sealed, and irradiated for another 24 h (**entries 5–8**). Comparing these catalyst addition treatments with the 40-hour control reactions (**entries 2 & 3**) showed no improvement in conversion with any of the reaction components. These results suggested it was unlikely that catalyst decomposition was responsible for the lack of conversion in the reaction with substrate **3.59b**.

To probe the second possibility, we examined the impact of the [4.5]spirocyclic lactone **3.60b** on the reaction efficiency for the formation of the [4.4]-spirocyclic ketolactone **3.60a** (**Figure 33**). Supplying 1 equivalent of either diastereoisomer of the ketolactone **3.60b** to the reaction conditions had no impact on the conversion of **3.59a** to **3.60a**. While it is plausible that the [4.5]spirocycle (**3.60b**) only inhibits reaction of its own SM (**3.59b**) due to competitive binding, or some alternative poisoning mechanism, these results seemed to suggest to us that further improving substrate binding for the cyclohexanone ketoester **3.59b** might broaden our substrate scope.



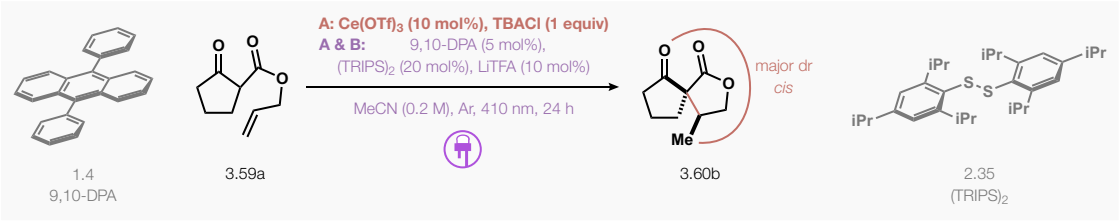
	additive	% Yield (d.r.)	% additive recov.
1	none	90 (4:1)	–
2	A	94 (3.4:1)	quant
3	B	quant (3:1)	quant

Figure 33. *Product inhibition investigation.*

In the event the third possibility was responsible for incomplete conversion, we hypothesized that we could overcome this issue using catalytic base additives to further favour substrate activation (**entries 9–32**). Among the additives screened, sodium methanesulfonate ($pKa_{MeCN}^{c.a.} \simeq 9.97$, **entry 13**),[210] sodium pentafluorobenzoate, and sodium trifluoroacetate ($pKa_{MeCN}^{c.a.} \simeq 12.65$, **entry 18**)[211] showed promising improvements in conversion to **3.60b** after 24 hours. As sodium trifluoroacetate improved the yield the most, we proceeded to employ this base in

combination with some salt additives (**entries 21–24**). Supplying 50 mol% of lithium chloride appeared to provide a slight benefit to the reaction, prompting us to examine the efficacy of lithium trifluoroacetate. We hypothesized that the greater Lewis acidity of the lithium counterion might aid substrate activation. Gratifyingly, LiTFA further improved the reaction, resulting in 83% yield of **3.60b** after 24 hours. Altering the loading of LiTFA did not meaningfully improve the desired reaction (**entries 26 & 27**), while increasing the duration under these conditions enabled complete conversion of **3.60b** for the first time (**entry 28**).

Table 17. *Optimization of redox-neutral hydroalkylation: Light source comparisons.*

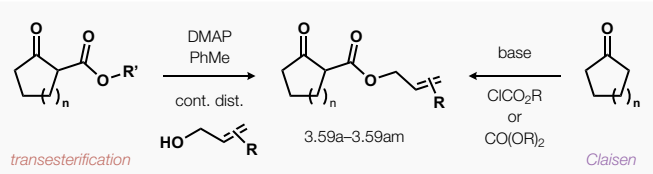


Entry	Condition	Light Source	3.60a (%)	dr	3.59a (%)
1	A	410 nm LED	90	4.0:1	–
2	B	410 nm LED	80	3.4:1	–
3	A	Kessil PR160L 390 nm	45	3.7:1	41
4	B	Kessil PR160L 390 nm	51	4.0:1	43
5	A	Kessil PR160L 427 nm	30	3.8:1	57
6	B	Kessil PR160L 427 nm	37	3.7:1	60

In addition to the above optimizations, we wished to study the impact of the light source on reaction efficiency (**Table 17**). We compared both of our optimized conditions, with cerium (**entry 1**) and without cerium (**entry 2**), when irradiated with LEDs with emission centred at 410 nm that were attached to heat sinks and wired to power switches in-house as well as with commonly used, commercially available Kessil LED lamps. Both conditions (A & B) saw marked decreases in reaction efficiency when irradiated with 390 and 427 nm Kessil LEDs. The Ce-containing conditions (A) showed a slightly greater impact from the change in light source than Ce-free conditions (B). The decrease in reaction efficiency when using disparate light sources could be due to differences in light intensity and/or in absorbance at the given wavelength. Given the need to balance many reaction rates in a multi-catalytic system, it likely that a change in light source would require a re-optimization of the loadings of individual catalyst components.

Intramolecular Hydroalkylation Scope

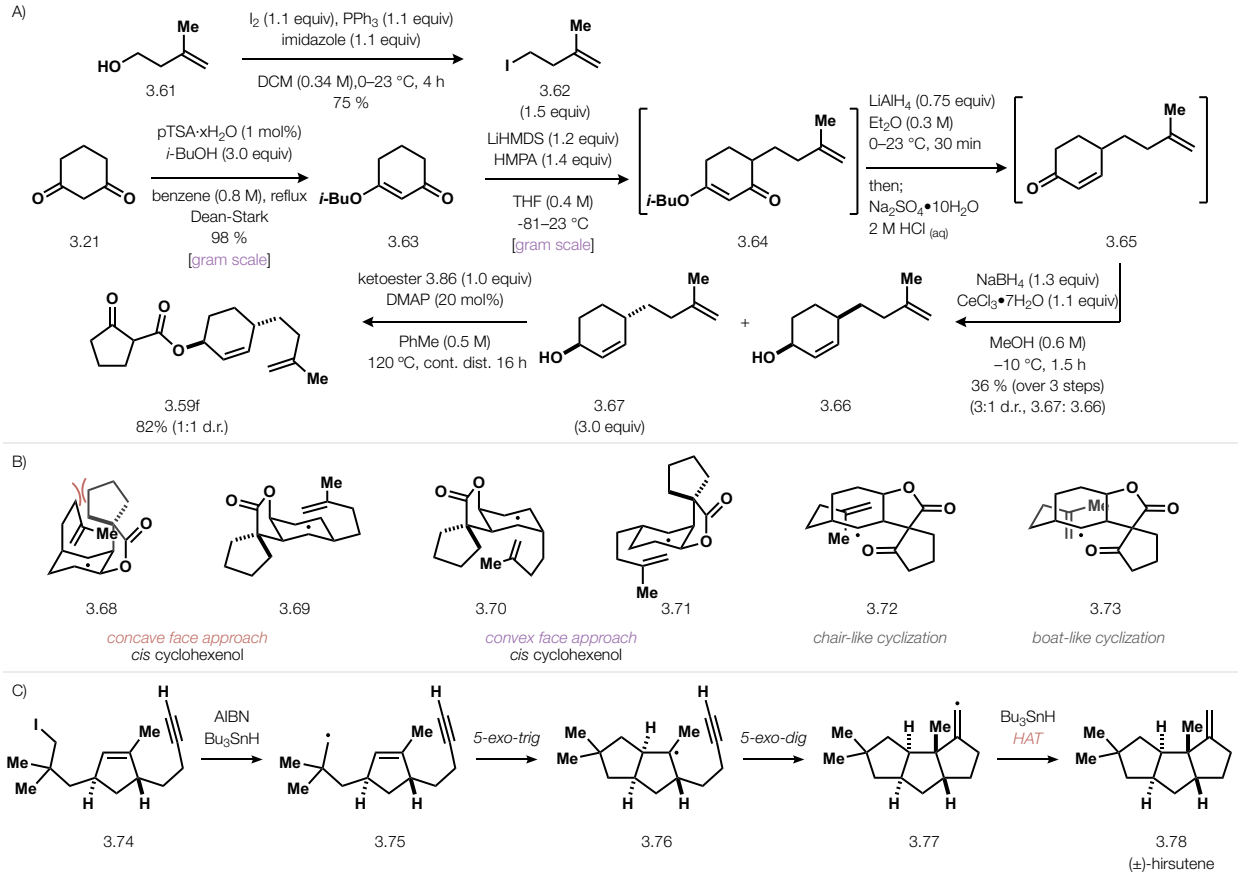
Most substrates (**3.59**) used in this chapter were prepared by transesterification of a ketoester using an allylic alcohol. Occasionally, we first had to prepare the ketoesters from the corresponding ketone through Claisen alkoxycarbonylation using carbonate or chloroformate electrophiles (**Scheme 9**).



Scheme 9. *General synthesis of β-ketoester substrates through transesterification or Claisen condensation.*

Ketoester **3.59f** required the preparation of cyclohexadienol **3.67** through a 4-step longest linear sequence (LLS), 5-step total, synthesis through a Stork-Danheiser transposition (**Scheme 10**, **A**).[212] Condensation of isobutanol on 1,3-cyclohexanedione (**3.21**) with azeotropic removal of water furnished enol ether **3.63** in 98% yield on gram scale. Enol ether **3.63** was α-alkylated using homoallylic iodide **3.62**, prepared in 75% yield *via* Appel reaction from 3-methyl-3-buten-1-ol (**3.61**). Purification of the alkylated enol ether **3.64** was challenging, prompting a crude purification by flash chromatography and submission to the next reaction. Hydride reduction followed by acidic hydrolysis of the intermediate β-hydroxyenol furnished enone **3.65** which was used in the next step without further purification. Luche reduction of crude enone **3.65** delivered cyclohexadienol **3.67/3.66** in 36% yield (over 3 steps) in a 3:1 *trans* to *cis* ratio. The major *trans* diastereoisomer was submitted to DMAP-catalyzed transesterification with methyl 2-oxocyclopentanecarboxylate (**3.86**) to give ketoester **3.59f** in 82% yield as a 1:1 mixture of epimers at the active methine. This synthetic sequence was performed in a single pass without any attempt to optimize reactions. While the *trans*-cyclohexadienol **3.67** was the major product of Luche reduction, it was also the desired substrate for hydroalkylation as we believed it would result in a more favourable cyclization cascade than the corresponding *cis* isomer (**Scheme 10**, **B**). We expected that the initial 5-*exo*-*trig* cyclization would establish a *cis* ring junction between the newly formed lactone ring and the cyclohexyl ring. This *cis* ring junction establishes concave and convex faces for the tethered alkene to approach. In the *trans* isomer, a kinetically favoured *cis* approach of the alkene occurs on the less sterically hindered convex face of the bicyclic ring system. Conversely, the *cis* isomer would require alkene approach on the more hindered concave face of the nascent bicyclic system. While comprised of different functionalities and scaffolding, a classic example of a pendant radical cyclization onto a cyclic olefin followed by

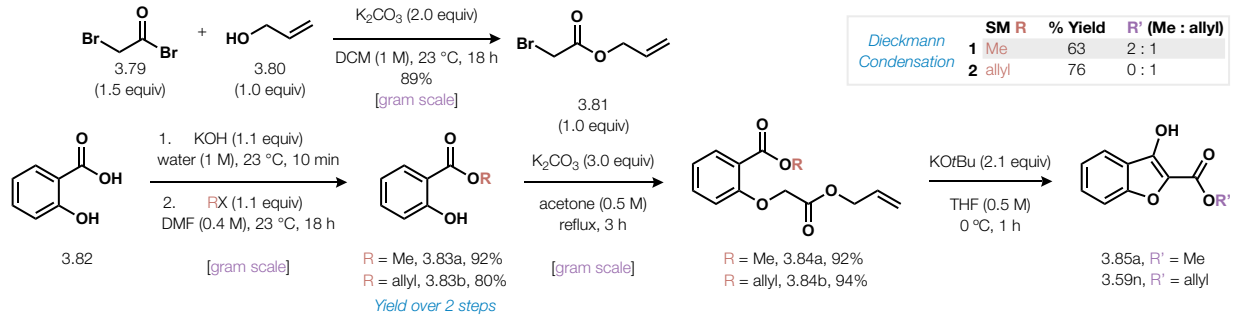
cyclization of the cycloalkyl radical onto a tethered radical acceptor features in Curran and Rakiewicz's landmark synthesis of (±)-hirsutene (**3.78**, **Scheme 10**, **C**).[213]



Scheme 10. *A) Synthesis of the bicyclic diene ketoester* ***3.59f*** *through a Stork-Danheiser transposition approach; B) Stereochemical considerations for the radical cyclization; C) Curran and Rakiewicz's radical cyclization cascade in the synthesis of (±)-hirsutene.*

Allyl 3-hydroxy-benzofuran-2-oate (**3.59n**) was prepared through a 4-step sequence akin to that described by Leatherbarrow and colleagues (**Scheme 11**).[214] We began with the preparation of methyl salicylate (**3.83a**) in 92% yield (over 2 steps) through the alkylation of the potassium carboxylate of salicylic acid (**3.82**). Next, Williamson ether synthesis using allyl bromoacetate (**3.81**) gave mixed diester **3.84a** in 92% yield. Dieckmann condensation of mixed diester **3.84a** was accomplished using KO*t*Bu in THF at 0 ºC. To our surprise, we obtained the desired allyl benzofuranoate **3.59n** as the minor product in only 21% yield while the major product was the methyl ester **3.85**. Clearly, transesterification during the Dieckmann condensation resulted in scrambling of the ester and significantly diminished our yield of the desired product. A low yield of **3.59n** might have been tolerable if it weren't for the sensitivity of the 3-hydroxybenzofuranoate ester core. 2D TLC revealed that the products decompose significantly

when exposed to silica gel. Additionally, we found that the white, paste-like material obtained after purification and drying decomposed to yellow paste upon exposure to ambient atmosphere over the course of a few hours. We wished to use short column path lengths to minimize decomposition caused by silica gel which was not viable for the separation of the two esters **3.59n** and **3.85**.



Scheme 11. *Synthesis of 3-hydroxy-benzofuran-2-oate esters through Dieckmann condensation of salicylate diesters.*

To circumvent the purification issues, we chose to begin the synthesis with an allylation rather than methylation. This change would result in a Dieckmann substrate with two allyl esters, meaning that cyclization would liberate the same alkoxide leaving group as is desired in the final product. Allylation by the same two-step procedure proceeded in 80% yield to furnish allyl salicylate (**3.83b**). Etherification with allyl bromoacetate (**3.81**) proceeded in 94% yield to give diallyl ester substrate **3.84b**. To our delight, Dieckmann cyclization of this compound provided allyl benzofuranoate **3.59n** in 76% yield as the sole identifiable product. The improved reaction profile allowed for purification with a short pad of silica, thereby minimizing exposure to silica gel. Product **3.59n** was stored under argon atmosphere at –20 ºC with only minor yellowing observed over the course of a few weeks.

Application of cerium-containing conditions (A) and cerium-free conditions (B) to intramolecular hydroalkylation of 1,3-dicarbonyls with tethered alkenes gave a variety of spirocyclic products (**Figure 34**). Cyclic β-ketoesters of increasing ring size from 5- to 8-membered gave the corresponding spirocycles **3.59a–d** in excellent yields and with good stereoselectivity. Formation of **3.59d** using condition A was also performed on 1-gram scale and delivered the product in 57% yield and 3.4:1 dr after 72 h (69% brsm). Spirocycle **3.59d** was crystalline and SCXRD analysis confirmed the *cis* relationship between methyl and ketone groups in the major diastereomer.

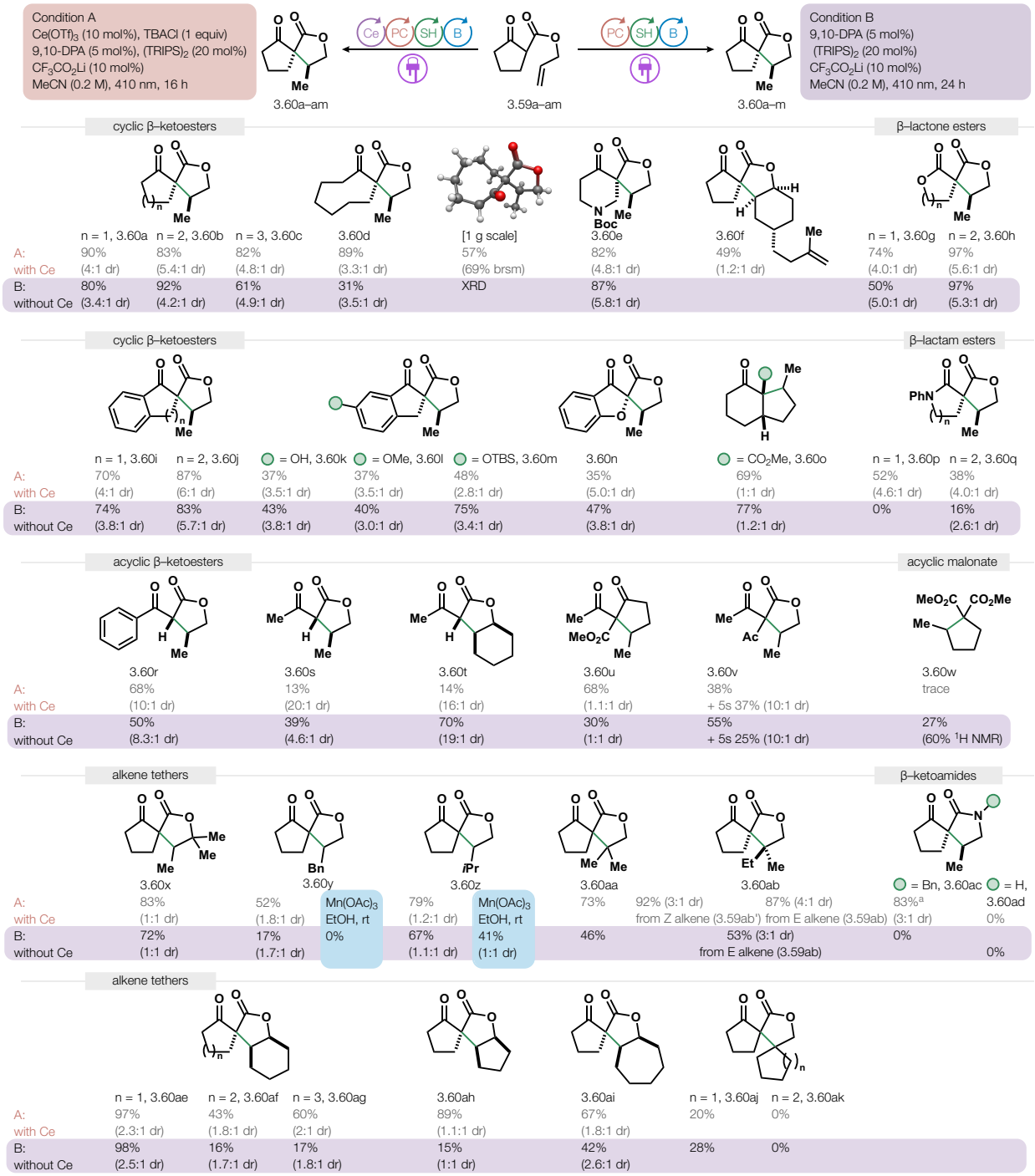


Figure 34. *Intramolecular hydroalkylation reaction scope.*

Substrates ***3.59i–m, 3.59r–w, 3.59z–ad*** *prepared and tested by Tegan E. O'Brien, excluding redox-neutral* $Mn(OAc)_3$ *reactions.*

Boc-protected piperidone derivative **3.59e** was well tolerated by both conditions, yielding ketolactone **3.60e** in 82% (A) and 87% (B) yield and ~ 5:1 diastereomeric ratio. Bicyclic substrate **3.59f** gave only monocyclized tricycle

3.60f under condition A with moderate yield and low diastereoselectivity. β-Lactone esters also proved to be competent substrates; 5-membered spiro[4.4] bis-lactone **3.60g** was formed in good yield and the corresponding spiro[5.4] bis-lactone **3.60h** was formed in excellent yield under both conditions with both substrates giving moderate diastereoselectivity (~5:1).

Benzo-fused indanone and tetralone derivatives also gave spirocyclic products **3.60i–m** in fair to excellent yields with moderate dr (35–87%). Unprotected phenol **3.59k** was tolerated by both conditions to give **3.60k**, albeit in lower yields. Methyl-ether protected phenol spirocycle **3.60l** was produced in comparable yields, suggesting that the diminished yields observed for this substrate series are not due to the free phenol O–H. Surprisingly, silyl protecting groups were tolerated, with TBDMS-protected phenol **3.60m** formed in 48% using conditions A and an excellent yield of 75% using conditions B. We suspect that the high chloride concentration under conditions A may render the phenolic silyl ether labile and result in the diminished yield under conditions A. Benzofuranone **3.60n** was formed in lower yield, likely due to the instability of precursor **3.59n** to acid and oxygen that necessitated its immediate preparation and use. Fused ring systems were also accessible through either hydroalkylation conditions, with ketolactone **3.60o** furnished in high yield and poor diastereoselectivity. Lactam esters were also competent substrates, with 5- and 6-membered spiro lactams **3.60p** and **3.60q** formed in 52% and 38% yield, respectively, under condition A. Under cerium-free conditions (B), the 5-membered lactam failed to undergo conversion and the 6-membered **3.60q** was obtained in only 16% yield.

Acyclic β-ketoesters performed the hydroalkylation comparably to their cyclic counterparts. Acetophenone-type substrate **3.59r** gave lactone **3.60r** in good yield under both conditions, with good diastereoselectivity and trans stereochemistry, presumably due to epimerization. Cyclization of the simplest allyl β-ketoester gave **3.60s** in low isolated yields due to volatility, and cyclization onto a cyclic alkene gave fused bicyclic lactone **3.60t** in comparable yields. Acyclic tricarbonyl substrates were also competent, though their cyclized products **3.60u** and **3.60v** were plagued by retro-Claisen reactions, leading to diminished yields. Malonate-derived product **3.60w** was formed under cerium-free conditions, though cerium-containing conditions gave **3.60w** in only trace amounts.

Varying the allyl ester substitution furnished various spiro[4.4] ketolactones through 5-*exo-trig* cyclization. Dimethyl-substituted lactone **3.60x** was produced in high yields under both conditions. Cyclization to form a secondary, benzylic radical was possible under both conditions, forming lactone **3.60y** in moderate yield after HAT. The diminished yield here could be attributed to the slower HAT from benzylic radicals (~10^5 $M^{-1}s^{-1}$) to thiol when

compared to less stabilized C-centred radicals (~10^7 – 10^8 $M^{-1}s^{-1}$).[82] Similarly, cyclization to form a tertiary alkyl radical intermediate proceeded readily under both conditions to give isopropyl-substituted lactone **3.60z** in high yields. In comparison, redox-neutral $Mn(OAc)_3$ cyclization conditions failed to deliver **3.60y** and delivered **3.60z** in a diminished yield. We anticipated that these substrates would be susceptible to degradation under conditions employing stoichiometric oxidants. Geminally-disubstituted products **3.60aa** and **3.60ab** were formed in high yield, demonstrating the strength of this radical cyclization in accessing sterically congested products.

Benzyl-protected ketoamide **3.59ac** underwent the hydroalkylation under condition A in 83% yield with a 3:1 dr but did not react under the cerium-free conditions (B). In contrast, secondary amide **3.59ad** failed to react under either set of conditions, presumably due to the lower proportion of the reactive s-*trans* conformer adopted by the 2º amide relative to the 3º amide (**3.59c**). Esters derived from secondary, cyclic allyl alcohols performed well in the hydroalkylation. Varying ring sizes led to formation of spirocycles **3.60ae–ai** in low to excellent yields. Ester **3.59aj** gave dispiro ketolactone **3.60aj** in low yields under both conditions, likely due to increased steric strain during the cyclization. Similarly, ester **3.59ak** failed to cyclize under either condition.

Attempts at 6-*exo-trig* or 7-*endo-trig* cyclizations with substrate **3.59al** were unproductive under both conditions. Attempts to induce cyclization by leveraging the Thorpe-Ingold effect in substrate **3.59am** also failed to yield product.

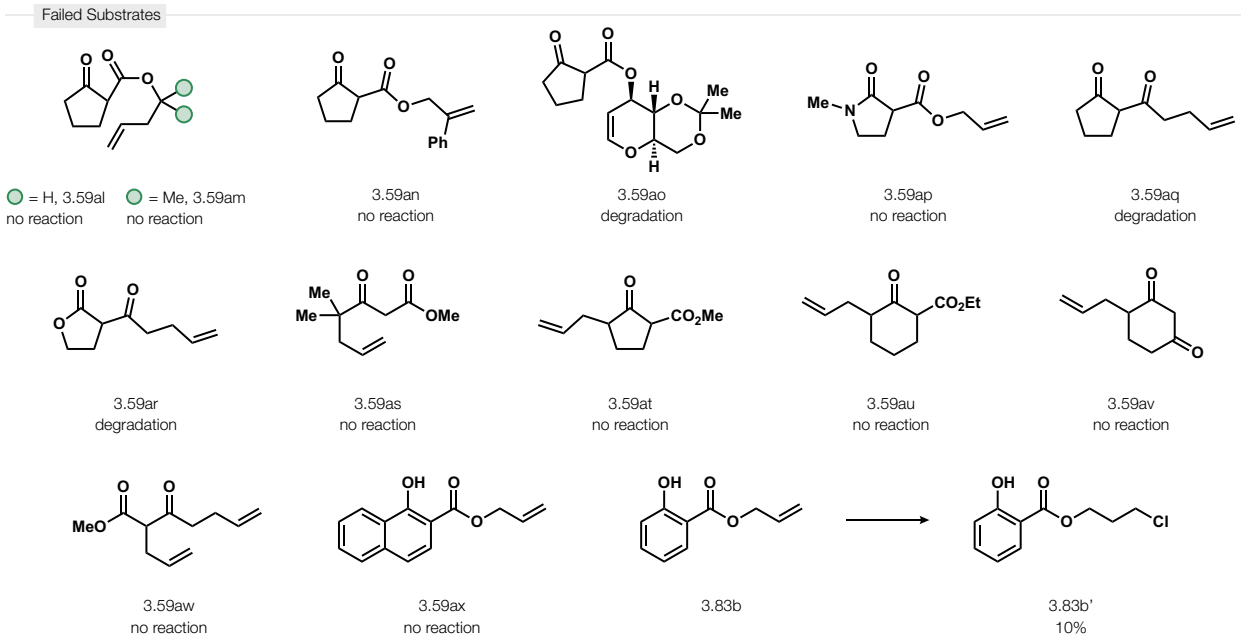


Figure 35. *Failed intramolecular hydroalkylation substrates.*

Sterically congested substrate **3.59an**, primed for 6-*endo-trig* cyclization, showed no conversion under the reaction conditions. The glucal acetonide substrate **3.59ao** showed significant decomposition under the reaction conditions which was not mitigated by shorter reaction durations. The high polarity of many of the products formed led us to conclude that deprotection of the acetonide protecting group and subsequent cleavages may be responsible for the messy reaction profile.

N-Methyl lactam ester **3.59ap** failed to convert under the reaction conditions. We hypothesized that the lactam may not be electron withdrawing enough to pass the pKa or enol content thresholds necessary to elicit the desired activation. Based on this hypothesis, we later synthesized *N*-Ph derivatives (**3.59p** & **3.59q**) which restored reactivity.

1,3-Diketone **3.59aq** and ketolactone **3.59ar** each showed incomplete conversion to intractable mixtures upon submission to the reaction conditions. We suspect that the greater conformational freedom afforded by the methylene linkers, relative to the typical *O*-linkers used in the allyl ester substrates, resulted in intramolecular photo-[2+2] & 6-*endo-trig* side products, which could not be separated from the typical [4.4]-spirocyclic products. Acyclic ketoester **3.59as** showed no reaction under both Ce-containing and Ce-free reaction conditions.

Substrates **3.59at–av** all failed to show conversion under either reaction condition. We suspected that the higher energy TSs necessary to form the bridged ring system could not be achieved at the reaction temperature. Removal of the cooling fan from the reaction setup (internal temperatures ~60 ºC) also failed to induce any productive conversion to bridged ring products.

Unsurprisingly, dearomatization of napthol and phenol esters **3.59aw** and **3.83b** failed to proceed under either reaction condition. Interestingly, prolonged reaction of phenol **3.83b** resulted in an appreciable conversion to anti-Markovnikov hydrochlorination product **3.59b'**, providing further support for the presence of Cl˙ under the Ce-photoredox conditions.

3.4 Intermolecular Hydroalkylation Scope

Intermolecular addition reactions were also achieved by this method (**Figure 36**). β-Ketoester **3.86** and β-lactone ester **3.88** added readily to ethyl vinyl ether (**3.87**) at the terminal position to give linear adducts **3.98** and **3.99** in high to quantitative yields under both Ce-containing conditions (C) and Ce-free conditions (D). A range of dicarbonyl species successfully added to ethyl vinyl ether (**3.87**) in this umpolung combination, where a nucleophilic carbon is coupled with an electron-rich alkene in a formal cross-nucleophile coupling. β-ketolactone **3.41** gave adduct **3.99** in only 45% yield by ^{1}H NMR under conditions C, but cerium-free conditions achieved quantitative yield.

Dimethyl malonate (**1.47**) showed a complete lack of reactivity under conditions C but performed the addition to ethyl vinyl ether (**3.87**) in quantitative yield under conditions D. A significant difference in reactivity was observed between dimethyl malonate (**1.46**) and dimethyl methylmalonate (**3.90**), which forms adduct **3.101** in 18% yield under conditions C and 11% yield under conditions D. Malonate-derived methine substrates appear to struggle in this reaction, though it is notable that reactivity is observed under cerium-containing conditions where no reactivity is observed for the corresponding methylene. Diketones **3.90** and **3.91** and methyl cyanoacetate (**3.92**) exhibited limited reactivity under conditions C. Under cerium-free conditions (D), these substrates showed improved reactivity. Acetylacetone (**3.91**) produced the double addition product **3.106** as the major product, though reducing the ethyl vinyl ether (**3.87**) loading to 1.2 equivalents enabled isolation of the mono-addition adduct **3.107** in 42% yield. Methyl cyanoacetate (**3.92**) gave adduct **3.108** in 35% yield by ^{1}H NMR, with reduced isolated yield due to volatility. Additionally, intermolecular hydroalkylation was attempted with a range of alkene acceptors. Dimethyl malonate (**1.47**) was able to add to silyl enol ether **3.94** under conditions D to give trimethylsilyl ether adduct **3.101** in 61% yield as the *trans* isomer predominantly. Addition to unactivated alkenes was not productive under either condition. A notable exception was the addition of ketoester **3.86** and lactone ester **3.88** to β-pinene (**3.95**) to form bicyclic products **3.103** and **3.104** in high to quantitative yields under both conditions. We hypothesized that the formation of these adducts benefits from a strain-releasing radical fragmentation upon addition. This suggests that, under the reaction conditions, addition to other unactivated alkenes may be possible but reversible, leading to unproductive regeneration of the starting material. Addition of dimethyl malonate (**1.47**) to α-cyclopropylstyrene (**3.96**) yielded fragmented product **3.108** in 58% yield under conditions D as a 10:1 *E/Z* mixture. A formal [3+2] reaction was achieved *via* an addition-cyclization sequence between dimethyl allylmalonate (**3.93**) and ethyl vinyl ether (**3.87**), yielding cyclopentane **3.109** in 37% yield under cerium-free conditions.

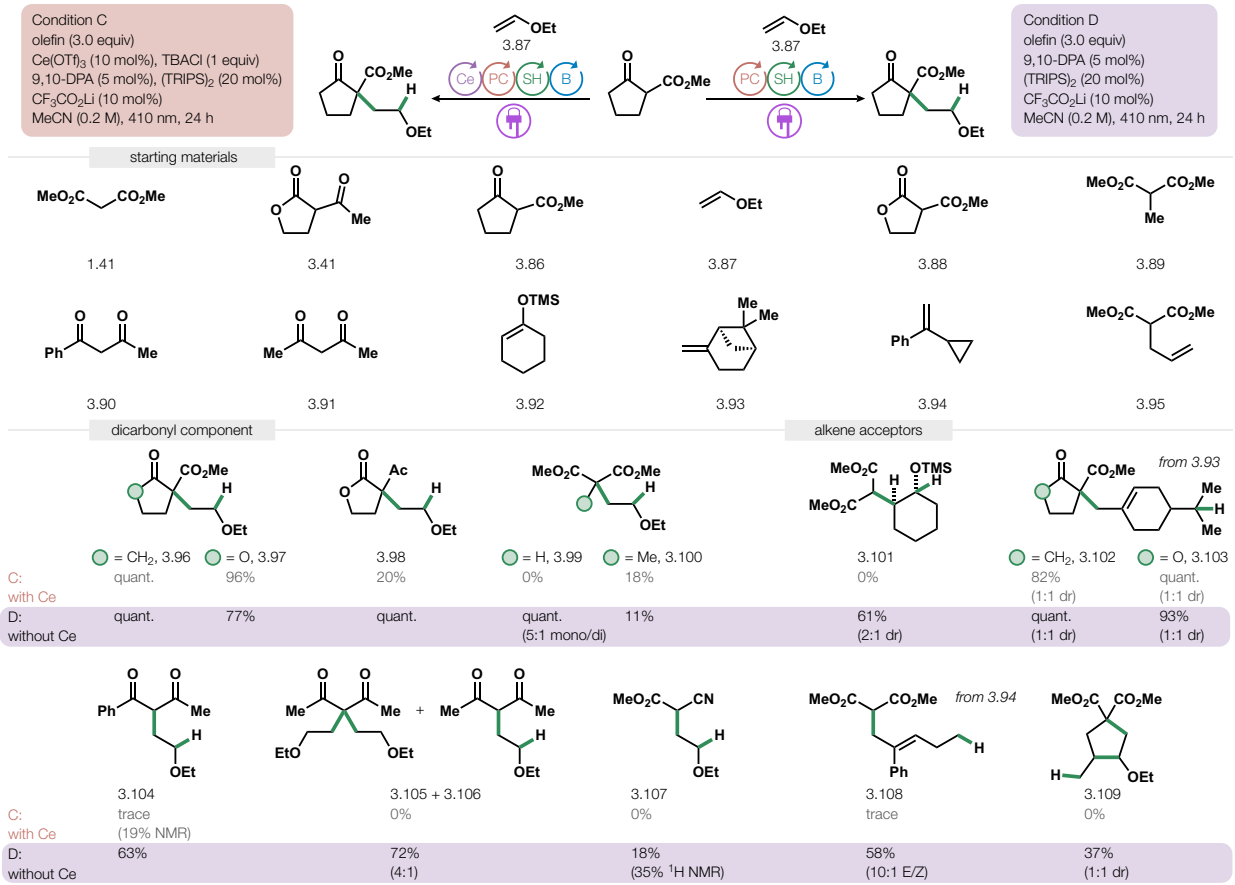


Figure 36. *Intermolecular hydroalkylation reaction scope.*
Substrate ***3.58*** *and products* ***3.96–3.107*** *prepared by Tegan E. O'Brien.*

Reaction Variants & Mechanistic Probes

Beyond the redox-neutral hydroalkylation, orthogonal transformations of the cyclized C-centred radical intermediate were successfully demonstrated (**Figure 37**). Cross-coupling was achieved with bromobenzene (**2.150**), catalyzed by 9,10-DPA (**1.4**), CF_3CO_2Li, $NiBr_2$•glyme, 4,4'-dimethyl-2,2'-bipyridine (**2.166b**), and 2,4,6-collidine to afford spiroketolactone **3.60y** in 46% yield, without optimization. Amination was achieved by addition to di-*tert*-butyl azodicarboxylate (**1.8**, DBAD) in the absence of HAT catalyst, yielding amination product **3.110** in 41% yield under cerium-containing conditions and 34% yield under cerium-free conditions, without optimization.

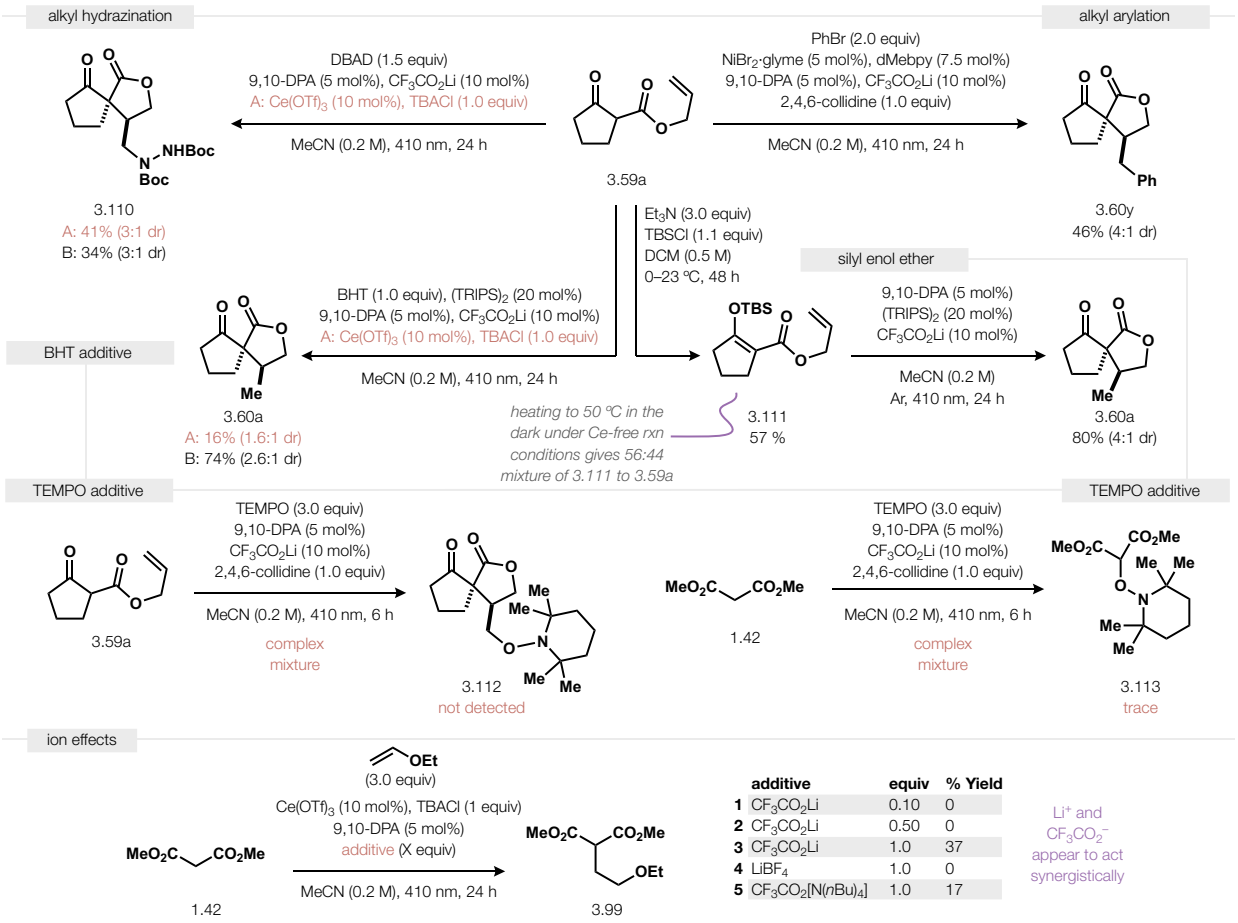


Figure 37. *Reaction variants and mechanistic probes based on the photocatalytic hydroalkylation reaction. Results obtained by Tegan E. O'Brien, excluding silyl enol ether preparation and experimentation.*

Mechanistic probe reactions were also devised and executed. Employing silyl enol ether derivative **3.112** under the Ce-free reaction conditions gave spiroketolactone **3.60a** in 80% yield and 4:1 dr. We had hoped this reaction would provide evidence for direct PET enol oxidation to give a radical cation intermediate, however, a subsequent thermal control reaction demonstrated the lability of the TBS-group under the reaction conditions. Without kinetic data, or a less labile protecting group, we cannot know whether deprotection precedes the photoredox cyclization or whether spiroketolactone **3.60a** is formed following an initial cyclization of a radical cation intermediate.

Reactions including TEMPO failed to give detectable spirocyclic adduct **3.113** and gave malonate adduct **3.114** isolated in trace amounts, consistent with the presence of radical intermediates. TEMPO additives could have several impacts on such a complex system, acting as an oxidant, reductant, or radical trap. The detection of TEMPO adducts are typically reported as evidence of radical involvement, however this is not always the case, [9a] and the implications of such adducts should be considered cautiously.

BHT additives were found to attenuate the yield under both conditions, with a greater impact on condition A. BHT inhibits radical chain processes and particularly autoxidation through its behaviour as an H-atom donor with a weak phenolic O–H bond and poor chain propagation kinetics it might be able to take on the role filled by thiol/disulfide in these reactions, albeit with altered efficiency. The impact that BHT had on these reactions could be the result of competitive activation by the photocatalytic system or through an alteration of the termination/turnover kinetics. Curiously, the impact of the additive on the diastereomeric ratio, although modest, may be indicative in a change in the mechanism for diastereoinduction. The greater impact on the Ce-containing conditions might additionally be due to competitive complexation of BHT over substrate to the Ce-centre.

Since the cerium-free conditions are a subset of the cerium-containing conditions, it might be expected that the cerium-free activation would operate in the background and would therefore be general to all substrates. However, the intermolecular reaction scope showed that dimethyl malonate (**1.41**), acetylacetone (**3.91**), and methyl cyanoacetate (**3.92**) add to ethyl vinyl ether (**3.87**) under cerium-free conditions but not under cerium-containing conditions (**Figure 36**). In the formation of dimethyl malonate adduct **3.99** under cerium-containing conditions (C), increasing the LiTFA loading from 10 to 50 mol% gave no trace of product. However, supplying one equivalent of LiTFA gave **3.99** in 37% yield (**Figure 37**). This restoration of reactivity could be attributed to saturation of Ce with carboxylate ligand, such that unbound LiTFA is available to activate **1.41** towards oxidation by 9,10-DPA* (**1.4***). To decouple the roles of the lithium cation and trifluoroacetate anion, we introduced each separately using salts with innocent counterions. Supplying one equivalent of $LiBF_4$ resulted in no formation of **3.99**, while [*n*Bu_4N][O_2CCF_3] yielded 17% of **3.99**. As no reactivity was restored with stoichiometric Li^+, and only partial reactivity returned with TFA^-, it is clear that neither ion is wholly responsible for the effectiveness of LiTFA. Rather, Li^+ and the weak trifluoroacetate base may act in synergy. This cooperative effect lends support to a concerted MS-PCET activation of a LiTFA•substrate complex.

3.5 Mechanistic Investigations

The Role and Fate of LiTFA

We undertook further investigations to refute potential reaction mechanisms and to elucidate key steps in the catalytic cycles. Firstly, we wished to assess whether the LiTFA additive was consumed during the reaction to assess its potential to act as a radical chain initiator (**Figure 38**). We presumed that carboxylates bind to Ce centres,[6k, 29] and our NMR studies suggest that trifluoroacetate indeed interacts with Ce(III) and Ce(IV) (refer to **Figure 40**). This

complexation permits the possibility of Ce(IV)–O_2CCF_3 bond homolysis *via* photoinduced LMCT. The resultant $CF_3CO_2^{\bullet}$ radical could then act as an HAT catalyst and directly activate substrates. Alternatively, $CF_3CO_2^{\bullet}$ could undergo decarboxylation to form a trifluoromethyl radical ($^{\bullet}CF_3$), which could abstract hydrogen from the dicarbonyl (BDE(C–H)[9d] ~88 kcal/mol; BDE(F_3C–H)[86a] ~106 kcal/mol) and initiate a radical chain reaction. We reasoned that the catalytic application of LiTFA in our system, coupled with the slow decarboxylation of $CF_3CO_2^{\bullet}$ (1.59×10^5 s^{-1} at 45 ºC)[215] and potential for BET ($E_{1/2}$ ($Ce^{IV/III}$) = +0.35 V *vs* SCE in MeCN; $E_{1/2}(CF_3CO_2^{\bullet}/CF_3CO_2^{-})$ = –2.4 V *vs* SCE in MeCN),[216] would likely limit these pathways to minor or unproductive outcomes, competing with more direct substrate activation modes.

To probe the fate of trifluoroacetate, a stoichiometric photolysis of LiTFA and $[Et_4N]_2[Ce^{IV}Cl_6]$ (1:1) was performed. After 5 minutes of irradiation, Ce(IV) was fully consumed based on loss of the characteristic colouration, yielding only a single ^{19}F resonance (**Figure 38**). The same resonance was maintained throughout all subsequent manipulations, suggesting that there is no appreciable conversion of trifluoroacetate to fluoroform or any other fluorine-containing byproduct. Given the kinetics of trifluoromethyl radical production, we reasoned that decarboxylation might still occur provided sufficient catalytic turnover events and such a possibility needed to be tested.

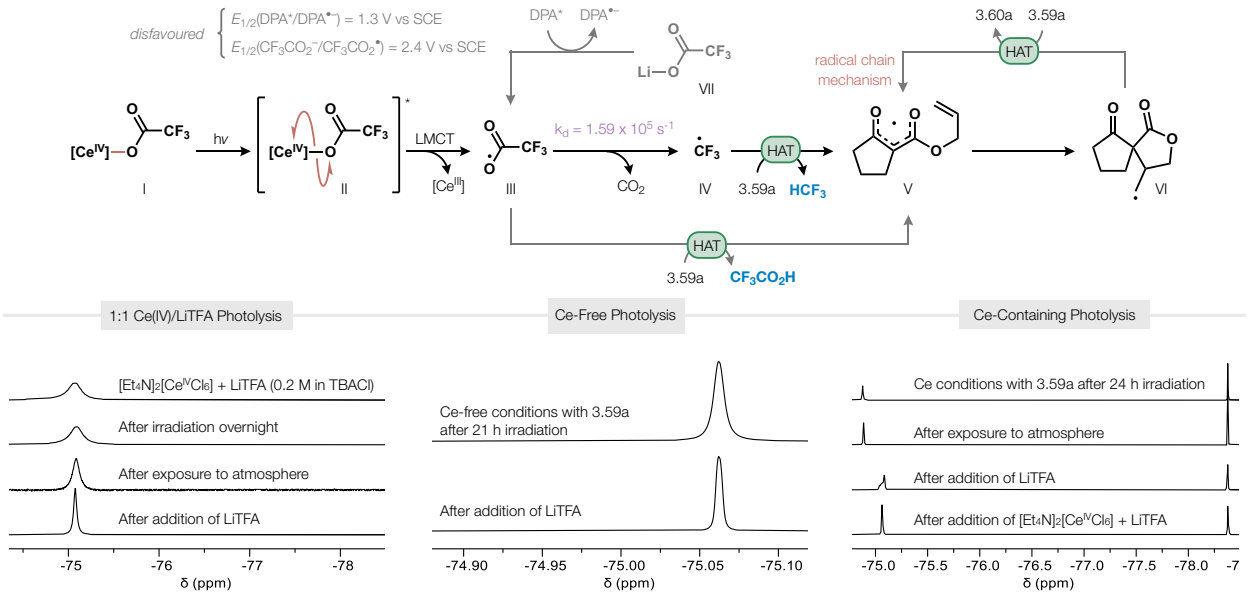


Figure 38. *Assessing the fate of LiTFA under stoichiometric and catalytic photolysis conditions through ^{19}F NMR spectroscopy. All resonances present in the spectra are shown.*

To determine whether $^{\bullet}CF_3$ was produced under either reaction condition (A or B), we chose to monitor the ^{19}F NMR profile upon complete conversion of ketoester **3.59a** to ketolactone **3.60a**. Both conditions resulted in a ^{19}F

spectrum containing only a single resonance that subsequently coalesced with an additional LiTFA dose, suggesting that trifluoroacetate is not appreciably deteriorated and is not a precursor to a chain-initiating trifluoromethyl radical.

Quantum Yield

While the above analysis ruled out the possibility of trifluoroacetate salts as photogenerated chain initiators, we still wished to probe the likelihood of a radical chain reaction. Controls omitting the disulfide co-catalyst $(TRIPS)_2$ maintained productive conversion (**Table 13**, **entry 3**). Given prior reports of formal HAT radical cyclizations proceeding *via* chain mechanisms, we deemed it prudent to examine whether such a process was contributing to our reaction.[81i, 156]

To assess chain contribution, potassium ferrioxalate actinometry was used to determine the photon flux of our setup (**Table 18**) and the quantum yield (Φ) for each reaction.[217] Quantum yield is a measure of a photochemical reaction's efficiency, defined as the quotient of the amount of product formed per number of photons absorbed ($\Phi = n_{Prod}/n_{Photon}$). $\Phi > 1$ indicates more than 1 equivalent of product is formed per photon absorbed, typically suggesting a chain process.

Chemical actinometry is a technique used to determine the photon flux of a particular photochemical apparatus.[218] A chemical actinometer is a compound which has a known quantum yield at a specified wavelength. Knowledge of Φ for a chemical actinometer and irradiation time allows for the determination of photon flux. Potassium ferrioxalate was first described as an actinometer by Hatchard and Parker in 1956 to replace the uranium-based actinometers typically employed at the time.[217c] The easy preparation of potassium ferrioxalate coupled with the well characterized absorption at numerous wavelengths of interest have made it a very popular chemical actinometer. Using this actinometer, we determined the average photon flux of our setup to be 8.6 (±0.5) nE/s (**Table 18**). Having established the number of photons passing through our reaction tube per unit time, measuring the yield of reactions run for known durations allows for calculation of Φ.

Table 18. *Photon flux determination using potassium ferrioxalate chemical actinometry.*

Entry	$\Delta Abs_{510\ nm}$ ($A_{light} - A_{dark}$)	$n_{Fe(II)}$ (mol)	Photon Flux (nE/s)
1	1.92	5.41E-07	7.91
2	2.10	5.89E-07	8.62
3	2.22	6.24E-07	9.12
4	2.13	5.97E-07	8.73
	Average		8.6 (± 0.5)

Using the same photoreactor setup, we irradiated reactions under our standard Ce-containing and Ce-free conditions in triplicate for exactly 1 hour before internal standard was added and an aliquot of the reaction mixture was analyzed by unlocked ^{1}H NMR spectroscopy in acetonitrile.

Table 19. *Ce-containing conditions (A) quantum yield – Assuming no IFE from (TRIPS)$_2$.*

Entry	Mass Balance (%)	nmol$_{3.59a}$	Φ
1	100	54.90	0.00177
2	100	90.35	0.00292
3	100	113.62	0.00368
	Average		0.0028 ± 0.0009

Under the Ce-containing conditions (A), reaction of ketoester **3.59a** for 1 hour and analysis by ^{1}H NMR spectroscopy showed 100% mass balance in each reaction and gave an average ϕ = 0.0028 ± 0.0009, assuming no inner filter effect from competitive absorption by (TRIPS)$_2$ (**Table 20**).

Table 20. *Ce-free conditions (B) quantum yield – Assuming no IFE from (TRIPS)$_2$*

Entry	Mass Balance (%)	nmol$_{3.59a}$	Φ
1	99	41.65	0.00135
2	99	37.62	0.00122
3	99	36.48	0.00118
	Average		0.00125 ± 0.00009

Under Ce-free conditions (B), reaction of ketoester **3.59a** showed Φ = 0.00125 ± 0.00009, assuming no inner filter effect from (TRIPS)$_2$. Given the overlap in absorbance spectra of 9,10-DPA and (TRIPS)$_2$, it is likely that some light was being absorbed by (TRIPS)$_2$ which would serve to diminish the observed Φ. To correct for this inner filter effect, we needed to determine the fraction of light absorbed by 9,10-DPA with (TRIPS)$_2$ present and absorbing some incident light. The maximum correction to ϕ would occur when we assume 9,10-DPA is present up to its solubility limit in MeCN whilst (TRIPS)$_2$ is at its maximum concentration as determined by the reaction condition loadings.

To determine the solubility of 9,10-DPA, (TRIPS)$_2$, and $[Et_4N]_3[Ce^{III}Cl_6]$, supersaturated solutions were prepared in volumetric flasks, filtered through submicron syringe filters, and the resulting filtrate concentrated and dried until a constant mass was obtained. We repeated this for each component in triplicate to arrive at the solubility in acetonitrile at room temperature (**Table 21**). From this analysis we determined the solubility of 9,10-DPA = 1.5 mM, (TRIPS)$_2$ = 16 mM, and $[Et_4N]_3[Ce^{III}Cl_6]$ = 130 mM at room temperature in acetonitrile.

Table 21. *Reaction component solubilities in acetonitrile at room temperature.*

Entry	Compound	V_{MeCN} (mL)	$m_{component}$ (mg)	Average Solubility (mg/mL)	Average Solubility (M)
1	9,10-DPA (**1.4**)	5.0	2.4	0.49 ± 0.01	0.0015 ± 0.00003
2	9,10-DPA (**1.4**)	5.0	2.4		
3	9,10-DPA (**1.4**)	5.0	2.5		
4	$(TRIPS)_2$ (**2.33**)	2.0	15.0	7.7 ± 0.2	0.016 ± 0.001
5	$(TRIPS)_2$ (**2.33**)	2.0	15.9		
6	$(TRIPS)_2$ (**2.33**)	2.0	15.2		
7	$[Et_4N]_3[Ce^{III}Cl_6]$	1.0	94.6	98 ± 12	0.13 ± 0.02
8	$[Et_4N]_3[Ce^{III}Cl_6]$	1.0	87.5		
9	$[Et_4N]_3[Ce^{III}Cl_6]$	1.0	111.3		

The scenario where all the $(TRIPS)_2$ (**2.33**) has been solubilized under the reaction conditions and 9,10-DPA (**1.4**) is at its saturation concentration would require in the largest correction to Φ. This correction resulted in a Φ_{Ce} = 0.004 and $\Phi_{Ce\text{-}free}$ = 0.0020 under $(TRIPS)_2$ (**2.33**) supersaturation and 9,10-DPA (**1.4**) saturation (**Table 22** and **Table 23**).

Table 22. *Ce-containing conditions (A) quantum yield – Assuming supersaturated* $(TRIPS)_2$.

Entry	Mass Balance (%)	$nmol_{3.59a}$	Φ
1	100	54.90	0.00289
2	100	90.35	0.00476
3	100	113.62	0.00599
	Average		0.004 ± 0.002

Table 23. *Ce-free conditions (B) quantum yield - Assuming supersaturated* $(TRIPS)_2$.

Entry	Mass Balance (%)	$nmol_{3.59a}$	Φ
1	99	41.65	0.00220
2	99	37.62	0.00198
3	99	36.48	0.00192
	Average		0.0020 ± 0.0001

Julia's pioneering work on HAT cyclizations of $C(sp^3–H)$ acids shows that short, inefficient chains are possible for these substrates.[156, 169, 219] However, the low quantum yields ($\Phi \ll 1$), under even the most generous assumptions, suggest that a chain reaction is unlikely under our conditions. Of course, a radical chain cannot be ruled out based on these experiments alone as a chain process with poor photoinitiation could also account for these low Φ values.[217b]

Stern-Volmer Kinetics Studies

After establishing that our reaction most likely proceeds through a closed catalytic cycle, we turned to Stern-Volmer studies to elucidate the identity of the quencher species. The change in steady state emission intensity of a

fluorophore as the concentration of a quencher increases can be used to determine the Stern-Volmer quenching constant (K_{sv}). This constant provides a metric for the efficiency of excited state quenching between the fluorophore and quencher. Coupled with a known excited state lifetime, the 2nd order quenching rate between fluorophore and quencher can be determined ($K_{SV} = k_q\tau$).

$$\frac{I}{I_0} = 1 + k_q\tau_0[Q] = 1 + K_{SV}[Q]$$

Initial forays proved challenging due to 9,10-DPA's short excited-state lifetime (9 ns in MeCN)[6e] and insignificant quenching rates when employing individual reaction components, up to their solubility limits. Direct oxidation of ketoester **3.86** by the DPA excited state was not observed ($E_{1/2}$(DPA*/DPA$^{\bullet-}$) = +1.28 V *vs* SCE in MeCN),[6f] in accordance with the inaccessible oxidation potential of neutral ketoesters ($E_{1/2}$(ketoester/ketoester$^{\bullet+}$ = 1.89 V *vs* SCE in MeCN).[9d] This analysis was further complicated by the complex equilibria involved in generation of the active quencher entities.[220] Titration of two-component quencher mixtures such as $[Et_4N]_3[Ce^{III}Cl_6]$/ketoester **3.86** (1:10) or $[Et_4N]_3[Ce^{III}Cl_6]$/LiTFA (1:10) showed no discernable quenching. In contrast, titrating a 1:1 mixture of LiTFA and ketoester **3.86** caused a notable decrease in emission intensity, as did titration of a 10:10:1 mixture of LiTFA, ketoester and Ce(III) (**Figure 39**). The quenching rate was comparable in both cerium-containing and cerium-free systems. Altogether, these results suggested that Ce•ketoester or LiTFA•ketoester complexes are the most likely quencher of the 9,10-DPA excited state.

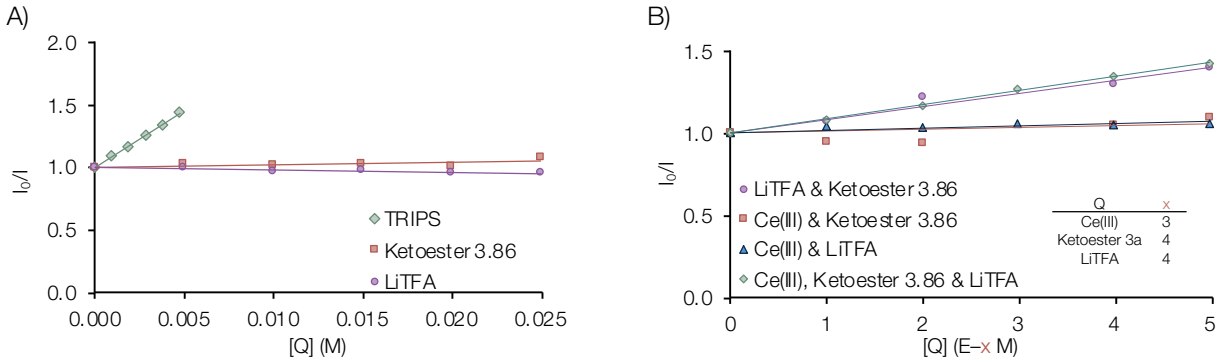


Figure 39. *9,10-DPA steady-state emission quenching. Individual reaction components (left) and mixtures (right).*

NMR Binding Equilibria

To gain further insight into the identity of the active quencher species, we studied the binding equilibria between reaction components by NMR. Titration of ketoester **3.86** and malonate **1.41** with LiTFA revealed a nearly

identical normalized response, suggesting that both substrates bind with LiTFA with similar thermodynamic drive (**Figure 40**, **A**). This finding aligns with the observation that both substrates participate in hydroalkylation in the absence of Ce. A similar response was observed upon addition of LiTFA to $[Et_4N]_3[Ce^{III}Cl_6]$, though this effect was diminished in the presence of 0.2 M tetraethylammonium chloride (**Figure 40**, **B**). Titration of $[Et_4N]_2[Ce^{IV}Cl_6]$ with LiTFA produced a more immediate response, suggesting stronger binding.

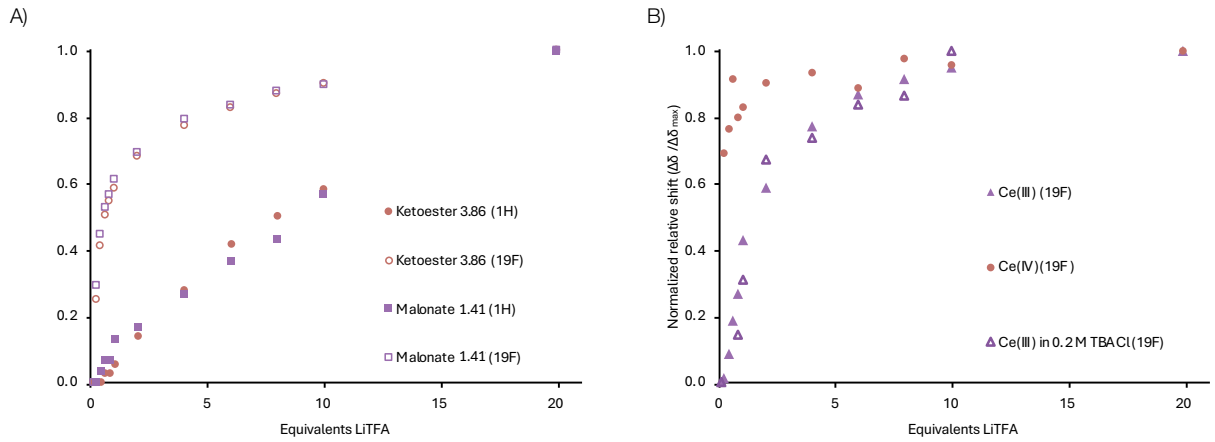


Figure 40. *NMR binding studies of hydroalkylation reaction components.*
*^1H or ^{19}F shift in MeCN when ketoester **3.86**, malonate **1.41**, $[Et_4N]_2CeCl_6$, or $[Et_4N]_3CeCl_6$ was titrated with LiTFA (relative to initial shift and normalized to maximum difference in shift). A) Ketoester **3.86** and malonate **1.41** titrated with LiTFA; B) $[Et_4N]_2CeCl_6$, $[Et_4N]_3CeCl_6$, or $[Et_4N]_3CeCl_6$ in 0.2 M TBACl in MeCN. Performed by Tegan E. O'Brien.*

Titration of Ce(III) analyte solutions with ketoester **3.86** or malonate **1.41** showed no discernable binding isotherm, while the corresponding Ce(IV) studies were thwarted by thermal decay. These results, taken together with the thermal Ce(IV) decay studies, suggest that substrate•Ce complexation is probable, but could not be reliably detected by NMR spectroscopy.

In light of these mechanistic studies, substrate activation in the absence of Ce(III) could occur by a proton transfer/electron transfer (PT/ET) mechanism or by multi-site proton-coupled electron transfer (MS-PCET). Given the pK_a difference between ketoester enols and LiTFA (10.5 *vs* –0.25 in water),[221] the concentration of lithium enolate would be infinitesimal (~8.9×10^{-15} M at the highest quencher concentration 5×10^{-4} M in both ketoester and LiTFA), and would imply a fluorescence quenching rate well beyond the diffusion limit (~5.6×10^{21} s^{-1}), making the PT/ET sequence implausible. This makes MS-PCET activation of a ketoester•LiTFA complex the more plausible quenching event. Despite the similarity in excited-state quenching kinetics between the cerium-free and cerium-containing

systems, our synthetic studies showed instances in which the cerium-containing conditions outperformed reactions run without it, suggesting a subtle substrate dependence for Ce and LiTFA binding.

Ce(IV) Thermal Decay Studies

Next, we sought to investigate the differences between Ce-containing and Ce-free conditions. Given the established precedent for Ce(IV) single electron oxidation of β-ketoesters in the ground state,[160] we first aimed to understand the action of putative complex $[Et_4N]_2[Ce^{IV}Cl_6]$ in the presence of ketoester **3.86**. To this end, we examined the single-electron reduction of Ce(IV) to Ce(III) in solution that is easily observed as a disappearance of the strong absorbance band at 378 nm and appearance of a weaker band at 328 nm.[14, 24b]

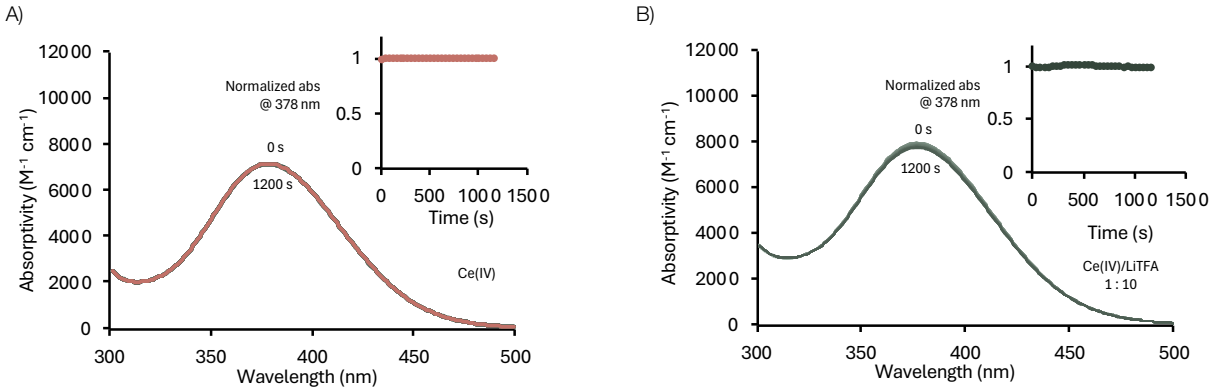


Figure 41. *UV-vis Ce(IV)thermal decay profiles over time in the dark at room temperature. Normalized absorbance at 378 nm shown in insets. A) $[Et_4N]_2[Ce^{IV}Cl_6]$ (0.33 mM); B) $[Et_4N]_2[Ce^{IV}Cl_6]$/LiTFA (0.33 mM). Performed by Tegan E. O'Brien.*

Solutions of $[Et_4N]_2[Ce^{IV}Cl_6]$ and LiTFA/$[Et_4N]_2[Ce^{IV}Cl_6]$ (10:1) mixed in the dark showed negligible decay in Ce(IV) absorbance at 328 nm over 20 minutes (**Figure 41**). In contrast, thermally promoted decay in the dark at room temperature occurred at an initial rate of 3×10^{-7} M•s^{-1} in a mixture of ketoester **3.86**/$[Et_4N]_2[Ce^{IV}Cl_6]$ (10:1) (**Figure 42**, **A**), which accelerated to 1×10^{-6} M•s^{-1} with the inclusion of LiTFA (ketoester **3.86**/LiTFA/$[Et_4N]_2[Ce^{IV}Cl_6]$, 10:10:1) (**Figure 42**, **C**). The pronounced effect of LiTFA on the thermal reduction of Ce(IV) in the presence of ketoester **3.86** suggests an increased propensity for substrate–Ce(IV) complexation and oxidation, or potentially a stabilization of post-oxidation products. The addition of TBACl in the ketoester **3.86**/LiTFA/$[Et_4N]_2[Ce^{IV}Cl_6]$ (10:10:1) solution led to a sigmoidal depletion of absorbance at 378 nm over time (**Figure 42**, **B**). This sigmoidal behaviour suggests a lag phase in which slow complexation between the components limits reduction, with an increase in rate as equilibrium approaches. Near the inflection point, the rate of Ce(IV)

reduction occurs more rapidly than that of the corresponding mixture without supporting chloride (**Figure 42**, **A**). The greater rate of thermal decay in the presence of excess chloride could be attributed to suppression of back electron transfer (BET), either by stabilizing the resulting oxidized species or by occupying a newly formed coordination site.

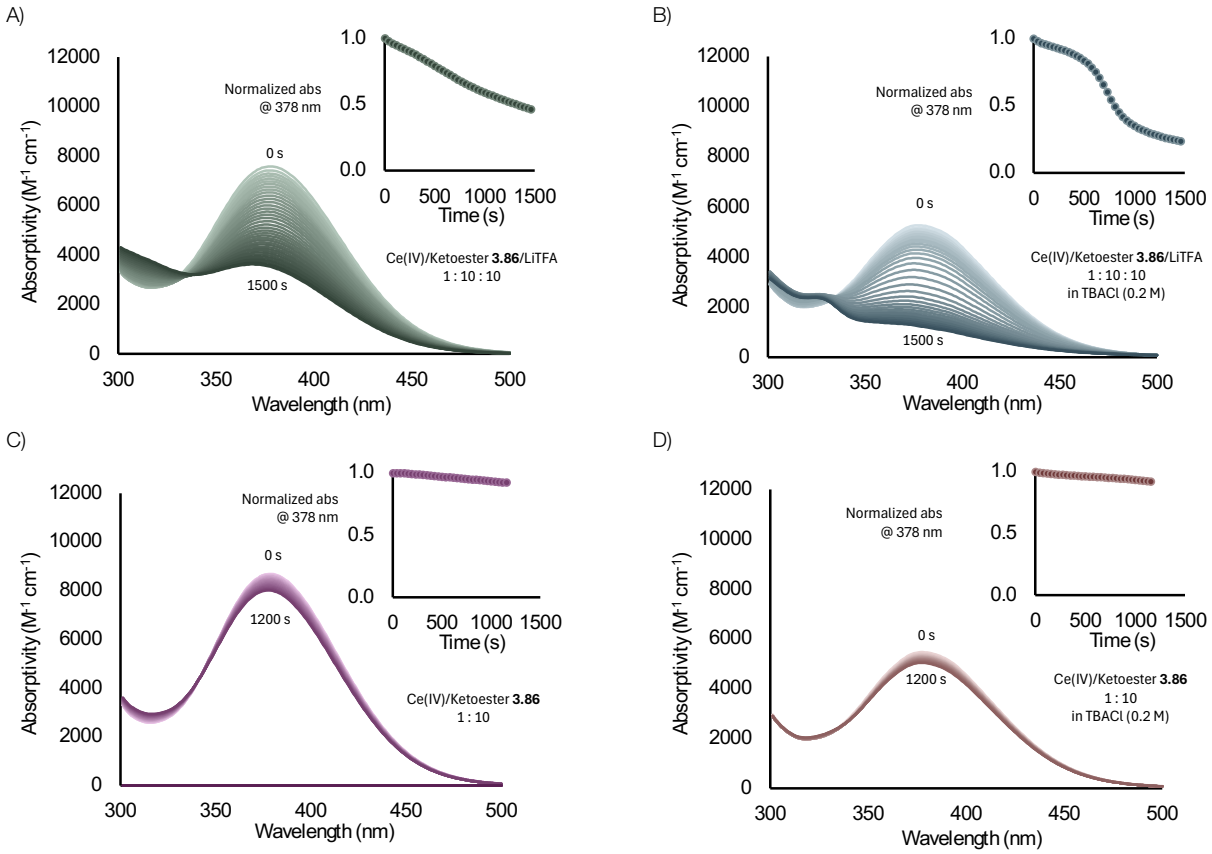
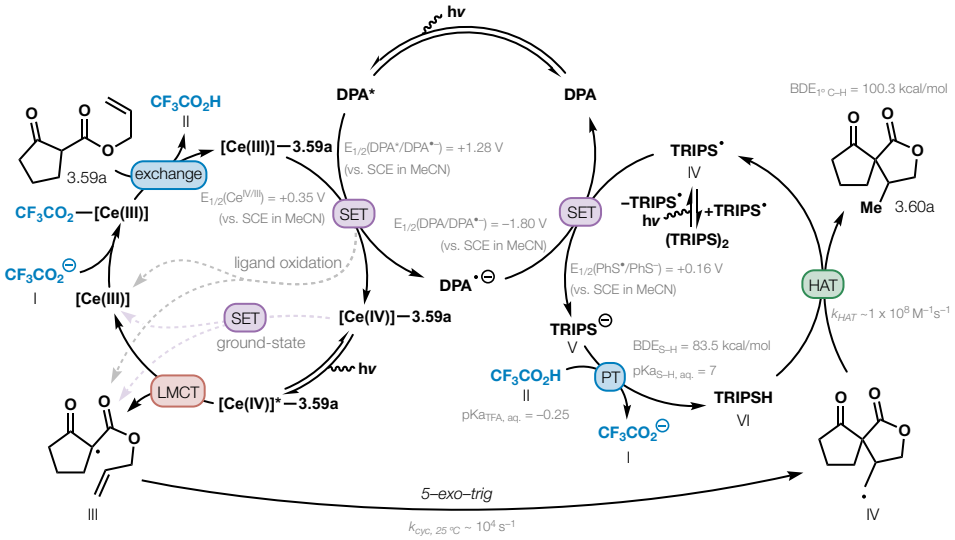


Figure 42. *UV-vis Ce(IV)thermal decay profiles over time in the dark at room temperature. Normalized absorbance at 378 nm shown in insets). A) $[Et_4N]_2[Ce^{IV}Cl_6]$/ketoester **3.86**/LiTFA (1:10:10, 0.33 mM); B) $[Et_4N]_2[Ce^{IV}Cl_6]$/ketoester **3.86**/LiTFA (1:10:10, 0.33 mM, 0.2 M in TBACl); C) $[Et_4N]_2[Ce^{IV}Cl_6]$/ketoester **3.86** (1:10, 0.33 mM); D) $[Et_4N]_2[Ce^{IV}Cl_6]$/ketoester **3.86** (1:10, 0.33 mM, 0.2 M in TBACl). Performed by Tegan E. O'Brien.*

Altogether, these data suggest a two-photon system is not necessary for Ce-catalyzed activation of ketoester substrates and may simply proceed through a ground-state SET event. This does not exclude the possibility of a two-photon cycle as this may still prove to be a faster process. These experiments also demonstrate the significant rate-accelerating effect of LiTFA on Ce(IV) oxidation of ketoester **3.86**.

Catalytic Proposal

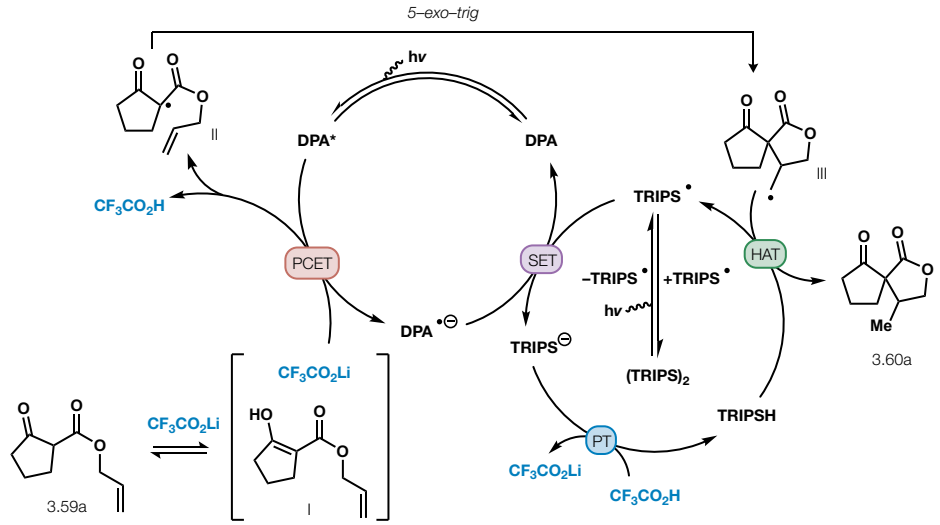
Based on these mechanistic investigations, we propose the following tentative catalytic scheme (**Scheme 12**). Under cerium-employing conditions (A), we propose an initial formation of a Ce(III)•LiTFA complex, which then facilitates formation of a Ce(III)•ketoester complex (**I**). **I** is subsequently oxidized by 9,10-DPA* to give a ketoester•Ce(IV) complex and radical anion 9,10-DPA$^{\bullet-}$ ($E_{1/2}$(DPA*/DPA$^{\bullet-}$) = +1.28 V *vs* SCE in MeCN).[6f] The Ce(IV)•ketoester complex may then undergo thermal or photochemical LMCT, oxidizing the ketoester to furnish radical **II** and reducing Ce(IV) to Ce(III). Alternatively, a ligand-centred oxidation of complex **I** could result in the liberation of radical **II** and Ce(III) directly ($E_{1/2}$(ketoester-Na/ketoester$^{\bullet}$ = 0.68 V *vs* SCE in DMSO).[9a] 5-*exo-trig* cyclization ($k_{cyc,\ 25\ °C}$ ~ 10^4 s^{-1})[222] gives a diastereomeric pair of [4.4]-spirocyclic radicals (**III**). Concurrent with cyclization, 9,10-DPA$^{\bullet-}$ reduces thiyl radical **IV**, simultaneously regenerating the 9,10-DPA ground state and producing thiolate **V** ($E_{1/2}$(DPA/DPA$^{\bullet-}$) = –1.80 V *vs* SCE in MeCN;[6f] $E_{1/2}$(PhS$^{\bullet}$/PhS^{-}) = +0.16 V *vs* SCE in MeCN).[134] Thiolate **V** then deprotonates trifluoroacetic acid, regenerating trifluoroacetate and yielding TRIPSH (**VI**) (pKa(S–H) ~7 in water, pKa(CF_3COO–H) –0.25 in water). HAT from TRIPSH (**VI**) to C-centred radical **III** regenerates thiyl **IV**, simultaneously producing closed-shell ketolactone product **3.60a** (BDE(TRIPS–H) ~83.5 kcal/mol, BDE(1º alkyl C–H) ~100.3 kcal/mol, k_{HAT} ~1 × 10^8 $M^{-1}s^{-1}$).[86b, d]



Scheme 12. *Proposed Ce-containing hydroalkylation catalytic cycles.*

Under Ce-free conditions, we propose that dicarbonyl substrates bind LiTFA to form a PCET-competent substrate•LiTFA complex **VII** (**Scheme 13**). This complex (**VII**) can undergo a MS-PCET with photoexcited 9,10-DPA*, transferring a proton to LiTFA with concomitant photocatalyst reduction (BDE(PhO–H) ~86.7 kcal/mol,[86e]

effective BDFE ~89.8 kcal/mol).[50a, e] The remaining steps to complete the multi-catalytic cycle operate identically to the cycles described for conditions A.



Scheme 13. *Proposed Ce-free hydroalkylation catalytic cycles.*

With a reasonable understanding of the catalytic system, we turned to computational chemistry to understand the radical cyclization mechanism, with a focus on understanding the origin of the observed modest diastereoselectivity.

3.6 Computational Investigations

Methods

The conformer rotamer ensemble sampling tool (CREST) was used to explore the low energy regions of the PES for various intermediates and TSs. CREST is an open-source software created by Prof. Stefan Grimme and colleagues.[223] From an initially supplied molecular geometry, CREST seeks to identify an ensemble of conformers and rotamers within a specified energetic span from the lowest energy conformer identified. The program explores the low energy PES about this minimum through semiempirical GFN-xTB (extended tight binding) optimizations of ensemble members. The ensemble is created through the application of metadynamics simulations using history-dependent biasing potential which drives conformational change. Crucially, CREST uses atomic Cartesian RMSD as the collective variable to bias exploration towards unique structures. Once structures are identified, the ensemble is algorithmically pruned to avoid duplicates by comparing the energy of conformers, the RMSD in atomic Cartesian coordinates, and molecular rotational constants with individual thresholds for each of these parameters to dictate what is deemed a duplicate structure. The program ranks members of the ensemble based on energy relative to the lowest

energy member that has been identified. In addition to the exploration of conformers at minima, it can also be used to probe conformational freedom at transition states by constraining key interatomic distances and orientations.

DFT computations were performed in pursuit of more accurate description of the reaction coordinate. Initial optimizations were performed in the Gaussian 16[224] software package at the uM06-2X/LanL2DZ for its reasonable accuracy in describing activation energies for free radical processes.[225] Subsequent optimizations of select species along the reaction coordinate were performed at the CBS-QB3 level to obtain highly accurate energies.[226] Frequency calculations were performed on all species to verify stationary points and TSs. IRC calculations were performed on TSs to justify their inclusion on the PES. Optimized structure models were created using CYLview20.[227]

Approach

To begin our computational investigation, we set about identifying stationary points for species preceding, during, and following the cyclization transition state. To accomplish this, we looked for an array of possible conformers at the uM06-2X/LanL2DZ level in the Gaussian 16 software package (**Figure 43**).[224] This array was comprised of all possible conformers made by the combination of pseudoequatorially or pseudoaxially oriented: methyl groups, ketone carbonyls, and lactone carbonyls (3 descriptors with two options each = 2^3 or 8 possibilities).

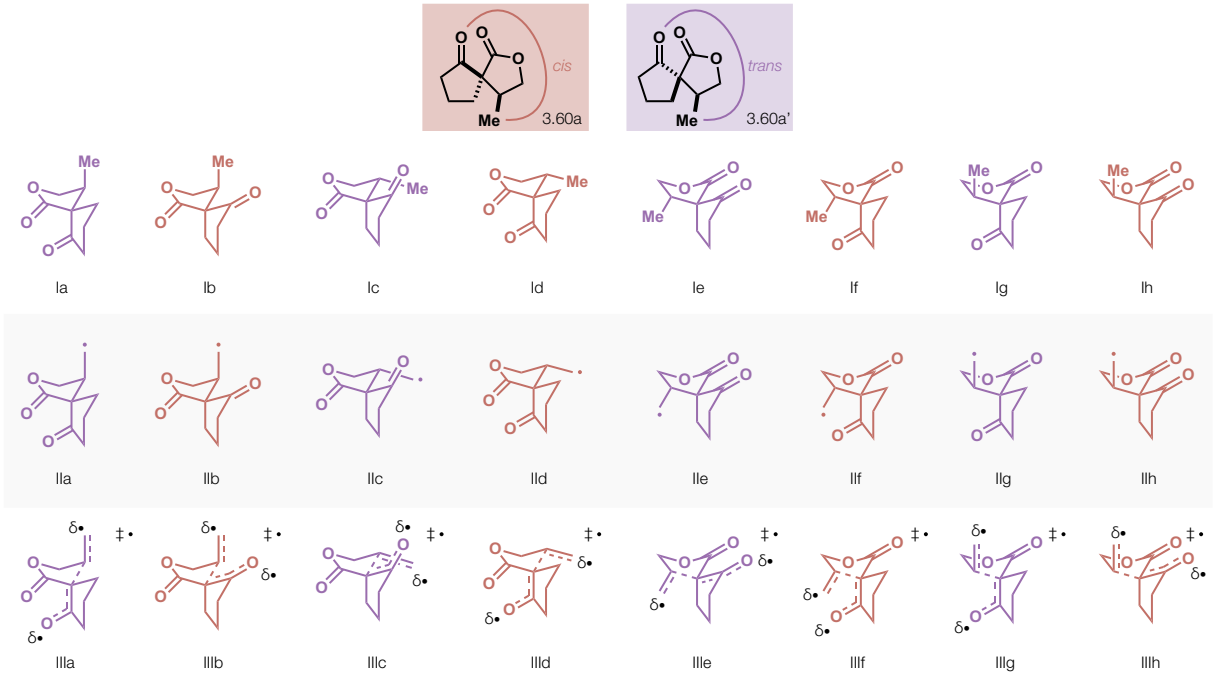


Figure 43. *Conformers of the ketolactone diastereomers* ***3.59a****. Searched for at the uM06-2X/LanL2DZ level. Similar conformers were searched for at the cyclized radical intermediate and the cyclization transition states.*

In addition, initial guess conformations for the closed-shell starting material and open-shell uncyclized radicals were optimized at the uM06-2X/LanL2DZ level. From these optimized structures, CREST[223a, 228] searches were performed to identify the lowest energy conformers/tautomers of each intermediate along the reaction coordinate. All structures within 1.5 kcal/mol of the CREST-identified minimum were optimized at the uM06-2X/LanLD2DZ level with GD3. The lowest energy intermediates and TSs at this level were then optimized at the CBS-QB3 level of theory.

Intermolecular HAT transition states were first identified at the uM06-2X/LanLD2DZ level with GD3 by relaxed coordinate scan for the transferred hydrogen atom, followed by a CREST search with constrained C--H--S interatomic distances. HAT TS conformers within 1.5 kcal/mol of the lowest energy structure were then taken to TS optimization at the uM06-2X/LanLD2DZ level with GD3. The lowest energy TSs leading to each diastereoisomer were then optimized at the CBS-QB3 level of theory. All transition states were found to have a single imaginary frequency. IRC calculations were performed from all TSs at the uM06-2X/LanLD2DZ level with GD3 level to find pre- and post-TS conformers which were subsequently optimized at this level.

Construction of the reaction coordinate diagram that spanned both the closed- and open-shell regimes required a number of other thermodynamic values whose calculations are described below.

Energy of the excited state of 9,10-DPA

$$\begin{aligned} \Delta G_{excited\ state} &= \Delta G_{ground\ state} + E_{DPA*} \\ &= 0 + 70.1\ \text{kcal/mol} \\ &= 70.1\ \text{kcal/mol} \end{aligned}$$

Where:

- E_{DPA*} = 70.1 kcal/mol, based on the estimated λ^{DPA}_{0-0} = 408 nm from the measured emission spectrum
- O–H BDE_{phenol} = 86.7 kcal/mol,[86b, 229] used as an estimate of the O–H BDFE for the enol tautomer of the allyl β-ketoester **3.59a**

Effective BDFE of PCET System Using Bordwell Equation

$$\begin{aligned} \text{BDFE} &= 1.37\text{p}K_{a\ c.a.} + 23.06E^0_{DPA*/DPA^{\cdot+}} + C_g \\ &= 1.37(12.65) + 23.06(0.86\ \text{V}) + 52.6\ \text{kcal/mol} \\ &= 89.7621\ \text{kcal/mol} \end{aligned}$$

Where:

- C_g is the reduction potential for $H^+/H^{\bullet}$, 52.6 kcal/mol in MeCN[230]
- pKa^{TFA}_{MeCN} = 12.65[231]

- $E^{\circ}(DPA^{*}/DPA^{\bullet-})$ = 0.86V *vs* Fc^{+}/Fc, excited state reduction potential for DPA calculated according to the conversion term reported by Addison[232]

$$E^{0}_{DPA*/DPA^{\cdot+}} vs\ \mathrm{Fc}^{+}/\mathrm{Fc} = E^{0}_{DPA*/DPA^{\cdot+}} vs\ \mathrm{SCE} - 0.38\ \mathrm{V}$$
$$= 1.24\ \mathrm{V} - 0.38\ \mathrm{V}$$
$$= 0.86\ \mathrm{V}\ vs\ \mathrm{Fc}^{+}/\mathrm{Fc}$$

- $E^{\circ}(DPA^{*}/DPA^{\bullet-})$ *vs* SCE = 1.24 V, calculated according to the conversion term reported by Addison[232]

$$E^{0}_{DPA*/DPA^{\cdot+}} vs\ \mathrm{SCE} = E^{0}_{DPA*/DPA^{\cdot+}} + E^{*}_{0-0}$$
$$= -1.80\ \mathrm{V} + 3.04\ \mathrm{V}$$
$$= 1.24\ \mathrm{V}\ vs\ \mathrm{SCE}$$

- $E(DPA/DPA^{\bullet-})$ = –1.80 V[6g, 233]

- E_{0-0}^{*} = –3.04 eV, based our emission spectrum 0–0 band estimate of 408 nm and in good agreement with Bard[6j]

Difference in Free Energy Following MS–PCET

$$\Delta\Delta G_{MS-PCET} = \mathrm{BDE}^{substrate}_{O-H} - \mathrm{BDFE}_{effective}$$
$$= 86.7 - 89.7621\ \mathrm{kcal/mol}$$
$$= -3.0621\ \mathrm{kcal/mol}$$
$$= -3.1\ \mathrm{kcal/mol}$$

This is the change in free energy between the pre- and post-PCET substrate/catalyst ensemble that links the closed- and open-shell ketoesters of the same conformation. *Assuming negligible entropic change in this process.

$$\Delta G_{open\ shell} = \Delta G_{excited\ state} + \Delta\Delta G_{MS-PCET}$$
$$= 70.1 + (-3.1)\ \mathrm{kcal/mol}$$
$$= 67.0\ \mathrm{kcal/mol}$$

Using this as the starting point for the open-shell cyclization pathway, all conformational changes and transition states are made relative to the CBS-QB3 Free Energy of this radical species.

Example Calculation for a Radical Species (5-*exo* TS **3.59a-Va**)

$$\Delta G_{3.59a-Va} = G^{CBSQB3}_{3.59a-Va} - G^{CBSQB3}_{open\ shell} + \Delta G_{open\ shell} \quad (1)$$
$$= -360367.0205 - (-360377.562) + 67.0\ \mathrm{kcal/mol}$$
$$= 77.6\ \mathrm{kcal/mol}$$

Where:

- $G^{CBSQB3}_{\mathbf{3.59a}}$ = -360367.0205, the computed CBS-QB3 free energy for the open-shell species of interest
- $G^{CBSQB3}_{\text{open-shell}}$ = -360377.562, the computed CBS-QB3 free energy for the open-shell species following MS–PCET in the same conformation as the closed-shell starting material
- $\Delta G_{\text{open-shell}}$ = 67.0 kcal/mol, calculated above is the normalization constant for the open-shell regime
- Hartree values were transformed to kcal/mol using the relationship 1 Hartree = 627.509474 kcal/mol

Example Calculation for the Energy of Closed-Shell Product (3.59a-IXa) Prior to Complete Catalyst Turnover

$$\Delta G_{3.59a-IXa} = G^{CBSQB3}_{3.59a-IXa} - G^{CBSQB3}_{open\ shell} + \Delta G_{open\ shell} + \Delta\Delta G_{1^\circ HAT}$$
$$= -360799.3877 - (-360780.6823) + 67.0 + (-16.8)\ \text{kcal/mol}$$
$$= 31.50947009\ \text{kcal/mol}$$
$$= 31.5\ \text{kcal/mol}$$

Where:

- $G^{CBSQB3}_{\mathbf{IXa}} = -360799.3877$ kcal/mol, the computed CBS-QB3 free energy for the open-shell species of interest
- $G^{CBSQB3}_{\text{closed-shell SM}} = -360780.6823$ kcal/mol, the computed CBS-QB3 free energy of the closed-shell starting material
- $\Delta\Delta G_{1^\circ \text{HAT}} = -16.8$ kcal/mol

Calculation of $\Delta\Delta G_{1^\circ \text{HAT}}$ and $\Delta\Delta G_{2^\circ \text{HAT}}$

The difference in Gibbs free energy before and after the hydrogen atom transfer was estimated based on the difference in bond dissociation enthalpy for primary C–H and secondary C–H bonds and the thiophenol S–H bond and assuming negligible entropy change.

$$\Delta\Delta G_{1^\circ HAT} = BDE_{PhS-H} - BDE_{1^\circ C-H,neopentane}$$
$$= 83.5\ \text{kcal/mol} - 100.3\ \text{kcal/mol}$$
$$= -16.8\ \text{kcal/mol}$$
$$\Delta\Delta G_{2^\circ HAT} = BDE_{PhS-H} - BDE_{2^\circ C-H,cyclohexane}$$
$$= 83.5\ \text{kcal/mol} - 99.5\ \text{kcal/mol}$$
$$= -16.0\ \text{kcal/mol}$$

Where:

- $BDE_{\text{PhS–H}} = 83.5$ kcal/mol;[86b] $BDE_{1^\circ \text{ C–H, neopentane}} = 100.3$ kcal/mol;[86b] $BDE_{2^\circ \text{ C–H, cyclohexane}} = 99.5$ kcal/mol[86b]

**Assuming negligible entropic change across the HAT*

Example Calculation for the Energy of Closed-Shell Product (3.59a-Xa) Following Complete Catalyst Turnover

$$\Delta G_{3.59a-Xa} = G^{CBSQB3}_{3.59a-Xa} - G^{CBSQB3}_{closed-shellSM}$$
$$= -360799.3877 - (-360780.6823)\ \text{kcal/mol}$$
$$= -18.8\ \text{kcal/mol}$$

This computational approach resulted in the given reaction coordinate for the conversion of allyl ketoester **3.59a** into diastereomeric ketolactones **3.60a** and **3.60a'** (**Figure 44**). Excitation of 9,10-DPA results in a ~70.0 kcal/mol increase in energy of the system from the lowest energy conformer I. PCET liberates free radical **II** which is exergonic by ~3 kcal/mol, and a dipole-minimizing conformational change to radical **III** further stabilizes the system by 1.7 kcal/mol. IRC calculations located minima **IVa** and **IVb** *en route* to cyclization TSs, differing in the direction

of cyclopentanone ring puckering relative to the ester chain. Given the ~4–5 kcal/mol activation energy to envelope flipping,[234] it is plausible that these conformers may equilibrate without reversion back to **III**, making a pre-cyclization bifurcation towards diastereomers unlikely.

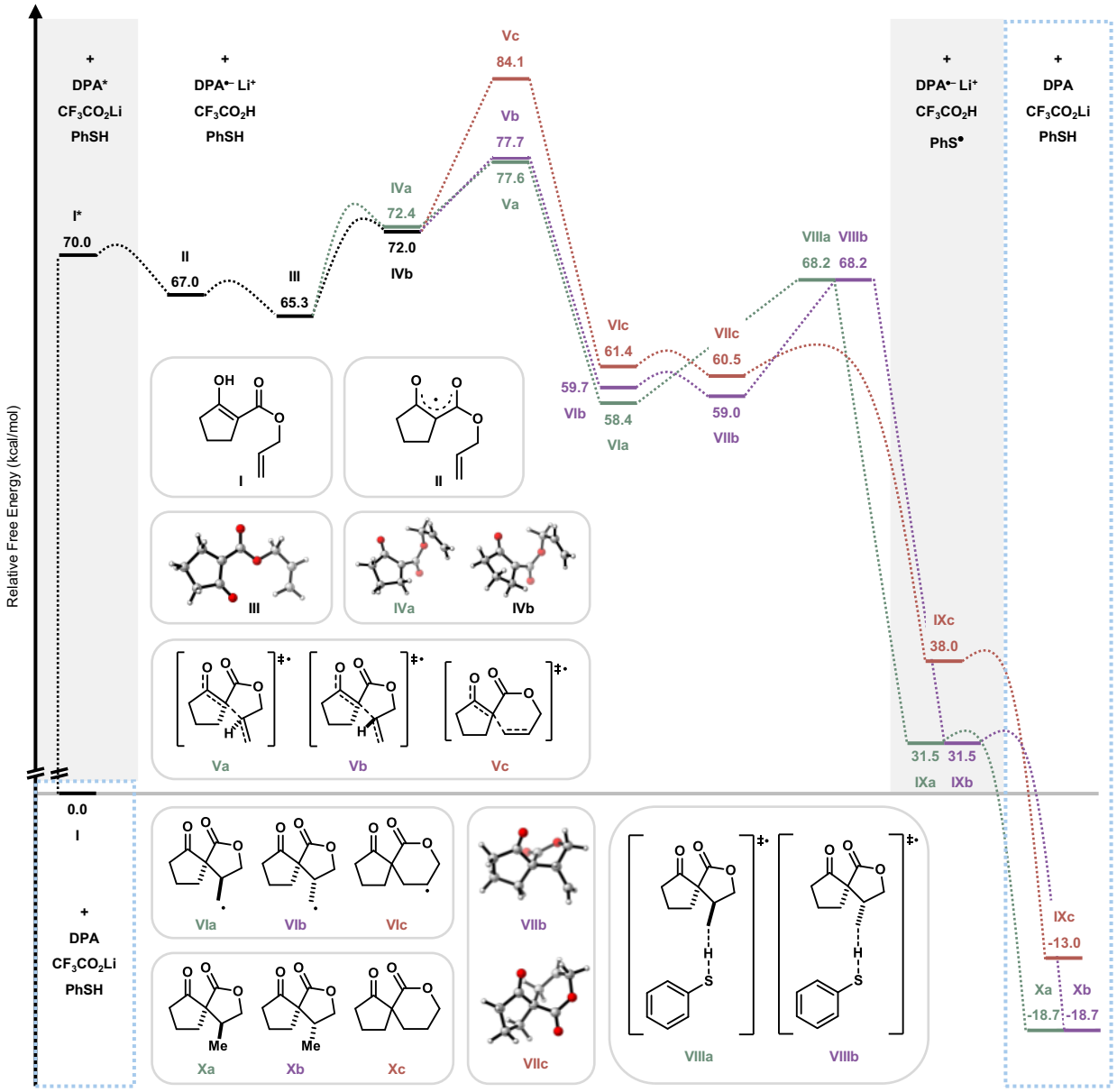


Figure 44. *Reaction coordinate for the spirocyclizing hydroalkylation of allyl 2-oxocyclopentane carboxylate (**3.59a**). (CBS-QB3 optimized structures, see Appendix A).*

Cyclization can occur through 5-*exo-trig* modes **Va** and **Vb** from **IVa** and **IVb**, respectively, and these TSs differ by only 0.1 kcal/mol. This small difference in energy does not account for the experimentally observed 3:1 diastereomeric ratio. The lowest energy 6-*endo-trig* cyclization **Vc** was found to have a global energy of 84.1 kcal/mol

resulting in an 18.8 kcal/mol activation energy from radical **III**. Given the 6.4 kcal/mol $\Delta\Delta G^{\ddagger}$ between the high energy 5-*exo-trig* (**Vb**) and 6-*endo-trig* (**Vc**) cyclizations, it is unsurprising that we do not observe any [4.5]-ketolactone product under the reaction conditions.

5-Exo-trig cyclization gives radicals **VIa** and **VIb**, and intermediate **VIb** undergoes a conformational change to **VIIb**. Primary radicals **VIa** and **VIIb** differ in energy by 0.6 kcal/mol which matches the experimentally observed ~4:1 dr, assuming free equilibration. Equilibration between cyclized radicals **VIa** and **VIIb** through retrocyclization/cyclization appears to be supported by the impact of BHT on the diastereomeric ratio (**Figure 37**). Under this model for diastereoselectivity, the inclusion of a stoichiometric H-atom donor like BHT could increase the rate of HAT termination. Increasing the rate of termination would diminish equilibration between diastereoisomers and result in a product distribution more dictated by the $\Delta\Delta G^{\ddagger}_{cycl}$. We hypothesize that although the computed intrinsic barrier for HAT is lower than the barriers for cyclization or fragmentation (**Va/b** vs. **VIIIa/b**), the concentration of thiol under the reaction conditions is likely to be infinitesimally small, thereby allowing equilibration between the diastereomeric cyclized radicals **VIa** and **VIb**, in agreement with findings by Sung and Wang.[235]

For the difference in **VIa** and **VIIb** energies to be reflected in the product distribution, there must be a negligible energy difference between the HAT transition states, and indeed the located TSs **VIIIa** and **VIIIb** are isoenergetic. HAT gives isoenergetic products **IXa** and **IXb** with thiyl radical. ETPT to close catalytic cycles for thiol, 9,10-DPA and LiTFA can be computed *via* a formal PCET reaction using the Bordwell equation. This treatment results in spirocycles **Xa** and **Xb** which are both –18.7 kcal/mol from the starting material **I**. The computed reaction coordinate for substrate **3.59a** suggests that the rate determining step for the intramolecular hydroalkylation reactions is the cyclization and that diastereoselectivity is dictated by the difference in energy between the cyclic radicals. Of course, the minor differences in diastereoselectivity observed in the reaction and the correspondingly small energy differences that lead to those selectivities, paired with the sensitivity of DFT results to computational conditions, likely puts the energy values generated here below the limit of precision/reliability. As such, the DFT approach performed herein may be an imperfect tool for the purpose and the results fall below a realistic confidence threshold for true prediction.

Chapter 4
Total Synthesis of Hyperolactone C

4.1 Introduction

Hypericum L. species are rich sources of bioactive compounds whose use in medicine has been documented as early as the 1st century CE.[236] *Hypericum chinense* L. has been used in folk medicine in Japan and is primarily known as a source of acylphloroglucinol natural products.[237] The hyperolactone and related biyouyanagin natural product families found in *H. chinense* L. have unique spirolactone cores and have shown promising activity against HIV, as well as broader anti-inflammatory and anti-cancer properties. Their structural complexity has made hyperolactones attractive targets for total synthesis[238] and derivatization as analogues,[238f,j] some of which have shown markedly improved biological activity. While synthetic interest in the last two decades has revealed routes to these natural products and their unnatural relatives, the hyperolactone scaffold is yet to be transformed into a viable medicinal agent despite the wealth of avenues left for exploration.

The hyperolactones were discovered with the isolation of hyperolactone A (**4.1**) in the methanol extract of the leaves and stems of *Hypericum chinense* L. in 1989 by Tada and coworkers (**Figure 45**, **A**).[239] Its structure was elucidated by mass spectrometry and NMR spectroscopy, along with chemical tests, to give the structure **4.1** with the given *trans* stereochemistry. Key structural features include the spirocyclic [4.4] core, β-ketoester, cyclic enol ether, and vinyl substituent. Further analysis of these extracts revealed hyperolactones B–D (**4.2, 3.2, 4.3**) as other abundant components, reported in 1995.[159a] The family is unified by a common β-ketoester core, in spirocyclic enol ether form for members A–C (**4.1, 4.2, 3.2**), and the conserved stereochemistry and substitution at the C4 quaternary centre. Each family member is defined by its substitution at C7: hyperolactone A (**4.1**) has an (*S*)-*sec*-butyl group, hyperolactone B (**4.2**) has an isopropyl group, and hyperolactones C (**3.2**) and D (**4.3**) have phenyl groups. The absolute stereochemistry of these four natural products has been confirmed by total synthesis from chiral starting materials,[238b] X-ray crystallographic diffraction,[240] and comparison of computational simulations to circular dichroism (CD) spectra.[241] While the configuration at C3 is conserved in the family, the C4 spirocentre is (*S*)-configured in A (**4.1**) and C (**3.2**) and (*R*)-configured in B (**4.2**). 4-hydroxyhyperolactone D (**4.5**) and 5,6-dihydrohyperolactone D (**4.6**) were isolated by Tanaka in 2009[242] and numerous other family members have been reported and reviewed elsewhere.[237]

The biyouyanagin family is one such structurally related group, named for the Japanese name "Biyouyanagi" for *Hypericum chinense* L., whose members contain a unit of hyperolactone C as the eastern fragment. Biyouyanagin A (**4.4**) was first isolated in 2005 and contains a cyclobutane ring linking C6 and C7 of hyperolactone C to a unit of the terpenoid *ent*-zingibrene (**4.121**).[243] A stereochemical reassignment was made following the total synthesis of biyouyanagin A (**4.4**) and other stereoisomers by Nicolaou to confirm the *exo* relationship between the spiroketone ring and 6-membered ring and the *trans* relationship between the cyclobutane and C24 methyl.[238d] Similarly, biyouyanagin B (**4.7**) was also isolated by Tanaka in 2009[242] and underwent structural reassignment by Nicolaou in 2010.[238h]

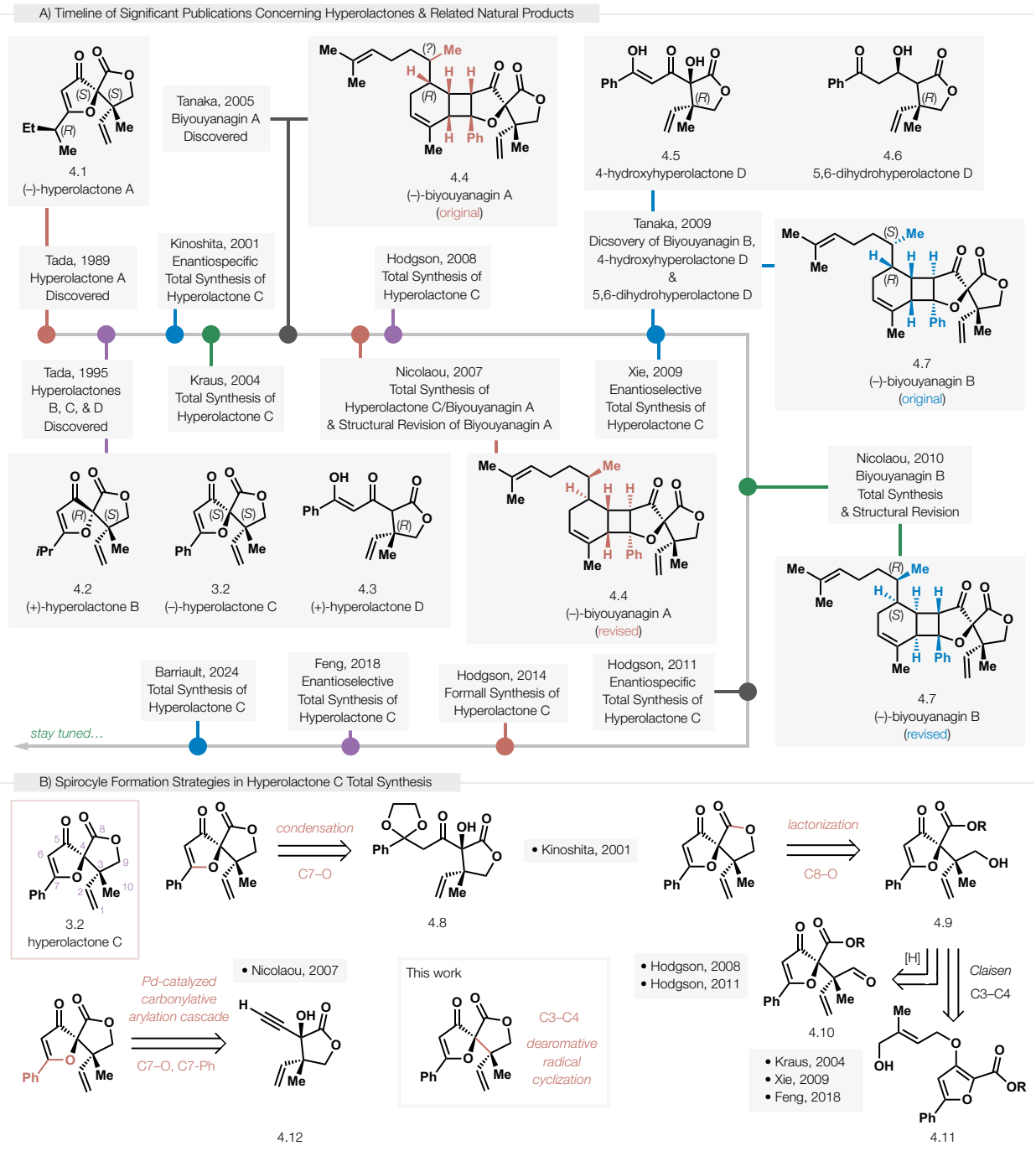


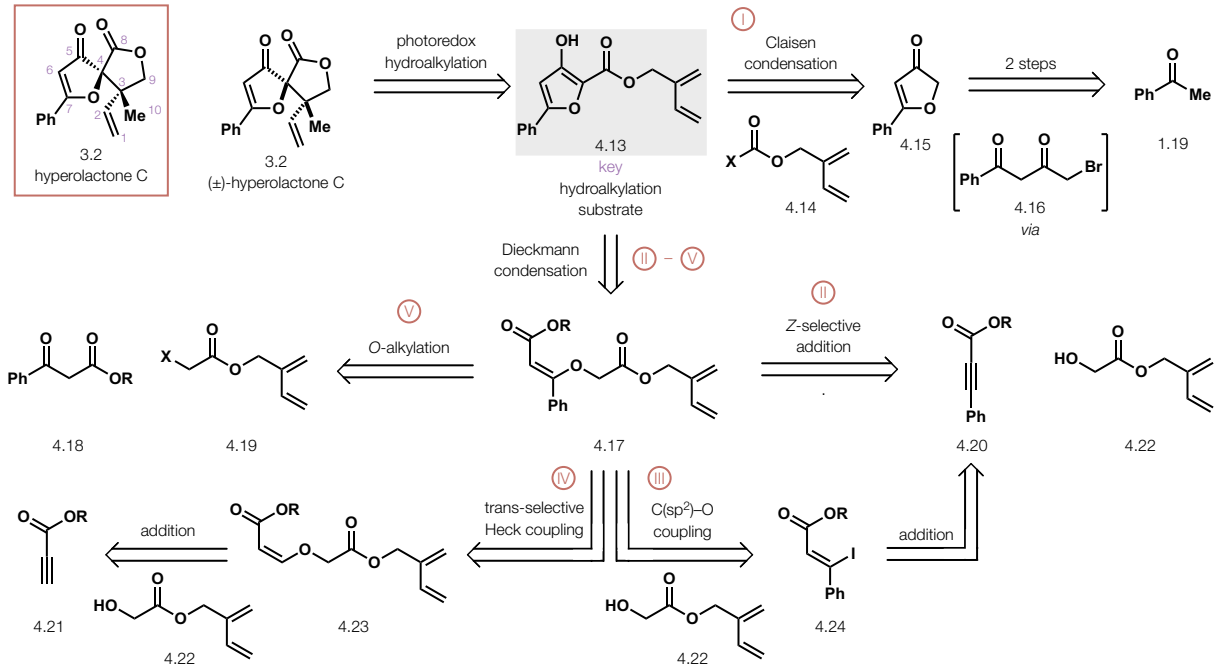
Figure 45. *Hyperolactone C Background.*

A) Timeline of Significant Publications Concerning Hyperolactones & Related Natural Products; B) Spirocycle Formation Strategies in Hyperolactone C Total Synthesis.

With the attention placed on hyperolactone C (**3.2**) from the synthesis community, it is worth mentioning the strategies for spirocycle formation that have led to productive syntheses (**Figure 45**, **B**). The first total synthesis of hyperolactone C (**3.2**) by Kinoshita and co-workers utilized a C4-hydroxyl condensation onto C7 from the ketal-

protected 4-hydroxyhyperolactone D analogue **4.8**.[238b] The majority of synthetic approaches have formed the [4.4]-spirocyclic system through a lactonization between C8–O,[238c, e, g, i, 238k-m] with several approaches using a Claisen rearrangement to access the requisite γ-hydroxyester from furanyl ether **4.11**.[238c, g, m] Nicolaou's approach utilized a carbonylative arylation cascade reaction to forge the C7–Ph, C7–O bonds and reforge the C4–O bond from the α-hydroxylactone **4.12**.[238d] We opted for an entirely different approach to spirocycle formation through the strategic disconnection of the C3–C4 bond in a novel dearomative radical cyclization from a 3-hydroxy-2-furanoate ester precursor (**4.13**). This chapter will deal with our efforts to realize this synthetic approach.

4.2 Retrosynthetic Analyses for the Redox-Neutral Hydroalkylative Synthesis of (±)-Hyperolactone C



Scheme 14. *Retrosynthetic analysis tree for the total synthesis of (±)-hyperolactone C via redox-neutral hydroalkylation key step.*

We envisioned a total synthesis of (±)-hyperolactone C (**3.2**) that would employ our redox-neutral hydroalkylation to forge the C3–C4 bond in a dearomative spirocyclization (**Scheme 14**). Given the relatively early transition states of most *C*-radical cyclizations, we imagined that our hydroalkylation would excel at generating the vicinal quaternary stereocenters of this highly congested core. Additionally, we had already demonstrated that similarly congested compounds could be prepared using our method (see **Figure 34**, compounds **3.60aa** and **3.60ab**). Simultaneously establishing both stereocenters of **3.2** through hydroalkylation of achiral furanoate ester **4.13** represents a major leap in molecular complexity, further demonstrating the power of this transformation.

Retrosynthetic analysis of precursor **4.13** resulted in several viable sequences which demanded empirical validation. At the outset, we discounted any routes requiring late-stage transesterifications to append the dienallyl moiety due to the anticipated sensitivity of the hydroxyfuran/3(2*H*)-furanone core of **4.15**. To maximize convergency, we reasoned that the requisite allylic dienol motif could be pre-installed in the ester in each sequence.

Route I sought to access **4.13** *via* Claisen condensation between the known compound 5-phenyl-3(2*H*)-furanone (**4.15**) and the carbonate or carbamate diene derivative **4.14**.[244] Furanone **4.15** could be accessed through the base-promoted cyclization of bromobenzoylacetone (**4.16**),[245] that could, in turn, be derived from benzoylacetone (**3.91**) in a bromination/debromination protocol.[246] Benzoylacetone (**3.91**) is easily prepared by the Claisen condensation of acetophenone (**2.2**) with ethyl acetate under basic conditions.

An alternative branch of retrosyntheses disconnect the furan ring between C4 and C5 through a Claisen condensation transform, leading to *Z*-enol ether diester **4.17**. ***Routes II*** through ***V*** all diverge from enol ether **4.17**, which we imagined could be prepared through several viable sequences.

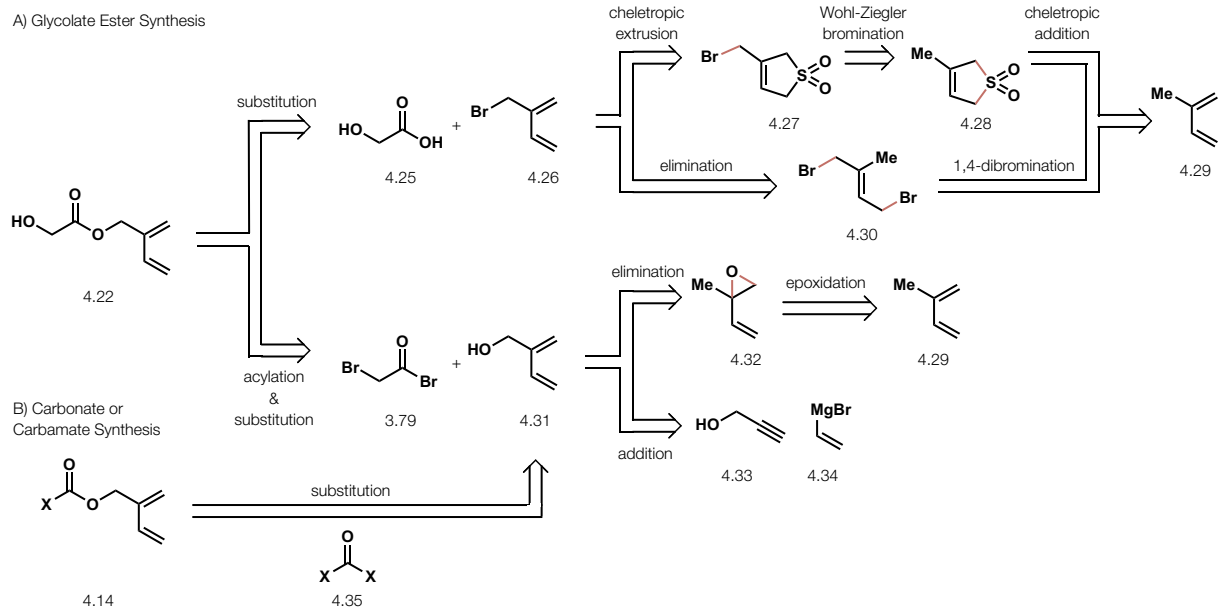
In ***route II***, we envisaged a gold(I)-catalyzed *Z*-selective *trans*-addition of glycolate ester **4.21** on to a phenylpropiolate ester **4.20**.[273] Given that the initial addition of nucleophiles to alkynes is stereospecific, the major challenge is avoiding subsequent isomerization to the undesired *E*-enol ether.

Route III sees the C7–O bond constructed *via* C(sp^2)–O coupling between *Z*-iodo alkene **4.24** and glycolate ester **4.22**, either by metal-catalyzed means or through a Michael addition/elimination sequence. Iodoalkene **4.24** could be prepared by the hydroiodination of phenylpropiolate ester **4.20**. Unforunately, this route would be less direct than ***route II*** as it would require prefunctionalization of the propiolate ester before coupling to the glycolate ester.

Route IV uses a *trans*-selective Heck coupling to add the characteristic phenyl group while dictating the *Z*-olefin configuration required for cyclization. The Heck coupling transform leads back to enol ether **4.23**, which we imagined could be easily derived from an unselective addition of glycolate **4.22** to propiolate ester **4.21**. Naturally, this approach was also less direct than ***route II*** as a step is required to transform enol ether **4.23** into another enol ether with the desired phenyl substituent. Of course, an analogous sequence is possible wherein the unsubstituted enol ether **4.23** cyclized in a Dieckmann condensation followed by Heck coupling to add the necessary phenyl substituent. In any case, we expected that enol ether **4.23** could be accessed through a 1,4-addition of glycolate ester **4.22** onto a propiolate ester (**4.21**).

In our fifth envisioned route (***V***), a *Z*-selective *O*-alkylation transform allows us to use the glycolic ester fragment as an electrophilic partner rather than a nucleophile. Using a benzoylacetate ester (**4.18**) nucleophile and a (pseudo)haloacetate ester (**4.19**) electrophile, we imagined that an intermediate enolate might be persuaded to react at oxygen to forge the C4–O single bond and C6=C7 double bond simultaneously. This route would also be highly convergent as it would furnish enol ether **4.17** in a single step from starting materials of nearly equal complexity.

The above retrosynthetic analyses rely on the preparation of diene glycolate ester **4.22**, or the carbonate or carbamate compounds **4.14** (**Scheme 14**). Four routes for the synthesis of glycolate **4.22**, and two routes for the synthesis of carbonate/carbamate **4.14**, were deemed promising enough for investigation (**Scheme 15**).



Scheme 15. *A) diene glycolate ester and B) diene carbonate/carbamate retrosynthetic analyses.*

We imagined that glycolate ester **4.22** could be derived from glycolic acid (**4.25**) and 2-(bromomethyl)-1,3-butadiene (**4.26**) through an S_N2' transform. Bromomethyl diene **4.26** is a compound with known sequences for preparation. The first sequence proceeds by a cheletropic sulfur dioxide extrusion transform to give the bromomethyl sulfolene precursor **4.27**. A Wohl-Ziegler allylic bromination transform traces back to 3-methylsulfolene (**4.28**) which, in turn, can be accessed through a cheletropic [4+1] addition of SO_2 with isoprene (**4.29**).[247]

Alternatively, bromomethyl diene **4.26** might be accessed through a known elimination leading back to 1,4-dibromoolefin **4.30**, which could be prepared from isoprene through bromination.[248] Isoprene (**4.28**) represents an ideal 5-carbon starting material for the preparation of hyperolactone C (**3.2**) due to its abundance and low cost ($19.64 CAD/mol, MilliporeSigma, 15/01/2025).

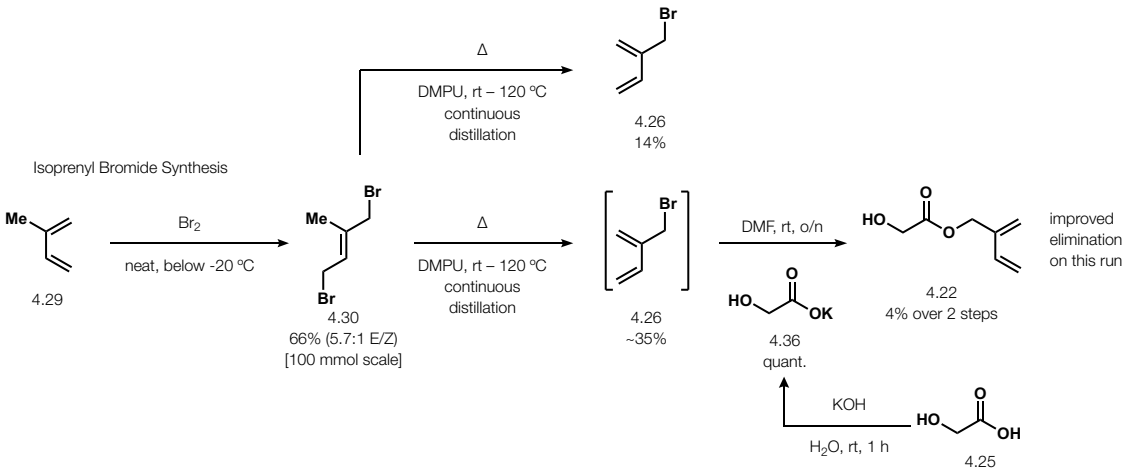
In addition to the S_N2' transform, we envisioned an alternative synthesis of glycolate ester **4.22** derive from an acylation transform to give bromoacetyl bromide (**3.79**) and dienol **4.31** as precursors. **4.31** is a known compound which could be prepared through two distinct sequences. The first sequence traces back to isoprene oxide (**4.32**) through a known elimination transform, and isoprene oxide (**4.32**) has been accessed by epoxidation of isoprene (**4.29**).[244] Hydroxydiene **4.31** might alternatively be accessed through cuprate-mediated addition of vinylmagnesium bromide to propargyl alcohol (**4.33**).[249]

2-(Hydroxymethyl)-1,3-butadiene (**4.31**) was also a key intermediate in the synthesis of the electrophiles (**4.14**) that would be required for the synthesis of **4.13** by late-stage Claisen condensation (**Scheme 14**, ***route I***). As such, we imagined that **4.14** might be prepared through a substitution transform with a suitable 1-carbon synthon (a phosgene derivative, haloformate, CDI, etc.).[244]

With these plans devised, we commenced our simultaneous exploration of all routes. To divide labour appropriately, I was primarily responsible for investigations into the diene ester/carbonate/carbamate synthesis and the *O*-alkylation route (***V***) towards the enol ether **4.17**, while Tegan focused on exploring the beginnings of the other four remaining routes towards enol ether **4.17**.

4.3 Synthesis of Diene-Containing Fragments

I first explored the synthesis of the diene-containing subunit with the 1,4-dibromination of isoprene.[250] Dropwise treatment of neat isoprene (**4.29**) with liquid bromine at –20–0 ºC, over the course of three hours, created an orange solution which could be distilled *in vacuo* to give the 1,4-dibromide **4.30** as a clear colourless oil in 66% yield as a 5.7:1 mixture of *E*/*Z* isomers (**Scheme 16**). Contrary to the original report,[250] temperatures as low as –20 ºC could not be maintained over the course of the entire addition of bromine as the mixture would begin to freeze into a single solid mass. As such, it was necessary to allow the temperature of the cooling bath to increase gradually over the course of the addition and to carefully monitor the state of the contents in the reaction flask. If the mixture had frozen solid, addition of bromine would be stopped, the reaction flask would be removed from the cooling bath until it had melted, and then the flask would be returned to a slightly warmer cooling bath to continue the reaction. While this procedure proved reliable for large-scale preparation of 1,4-dibromoolefin **4.30** (routinely performed on 100 mmol scale), its capricious behaviour made for variable product distributions and yields and required constant manipulation over the duration of the addition (≥3 hours).



Scheme 16. *Preparation of diene glycolate ester via isoprene bromination.*

After 1,4-dibromination, the reported elimination to yield 2-(bromomethyl)-1,3-butadiene (**4.26**) was attempted.[250] The initial effort to perform the elimination in DMPU at 120 ºC under continuous distillation using a diaphragm vacuum pump gave a disappointing 14% yield of the desired product (**4.26**) and caused the remaining solution in the reaction flask to go from clear and colourless to opaque black, suggesting major decomposition (**Scheme 16**). Unsurprisingly, the product **4.26** proved to be quite volatile prompting its direct use in the substitution reaction in subsequent attempts.

Distillate from this subsequent attempt was employed in a substitution reaction with potassium glycolate (**4.36**). ^{1}H NMR analysis of the distillate showed a better yield of the desired dienyl bromide **4.26** (~35% w/w) which, upon reaction with potassium glycolate (**4.36**), gave the diene glycolate ester **4.22** in only 4% yield over two steps (**Scheme 16**). The poor performance of these attempts prompts a brief discussion of the intricacies of this reaction.

We surmised that this elimination reaction likely occurs through an E1 mechanism, with possible anchimeric stabilization and/or assistance through bromonium ion formation (**Figure 46**, **C**, **pathways C & D**).[248] E1 nucleofugality of each bromide in 1,4-dibromoolefin **4.30** can be distinguished based on the resonance contributors available to the allylic cations formed upon heterolytic cleavage of the C–Br bond at either the 1- or 4-position. 4-position cleavage generates an allylic cation comprised of delocalized 3º (**4.37**) and 1º (**4.37'**) resonance contributors (**Figure 46**, **A**), whilst 1-position cleavage results in 2º (**4.38**) and 1º (**4.38'**) carbocation resonance contributors (**Figure 46**, **B**). As such, 4-position heterolysis results in a more stable allyl cation (**4.37**) and should be the thermodynamically favoured intermediate.

Subsequently, the delocalized carbocation **4.37** has numerous reaction pathways it may progress through (**Figure 46**, **C**). The desired pathway (**A**) requires proton loss from the C5-methyl group *α* to the allyl cation and this pathway is rendered irreversible by distillation of bromomethyl diene **4.26** out of the reaction solution. Alternatively, proton loss from the 1-position *via* pathway **B** could generate diastereomeric bromodienes (**4.41**) that may also be distilled out of the reaction, producing undesired side products. Additionally, we surmised that the allylic cation **4.37** would be prone to cross- and self-adduct formation through electrophilic capture by olefinic species present within the reaction medium. It is likely that these adducts formed homo- and hetero- -dimers, -oligomers and -polymers as decomposition products that imparted the opaque black tar-like characteristics to the reaction mixtures upon prolonged heating.

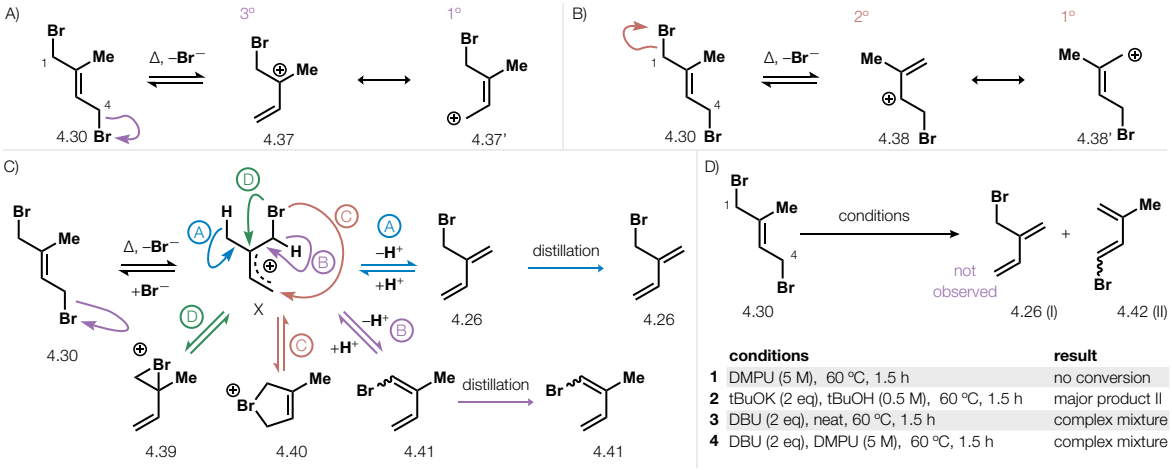


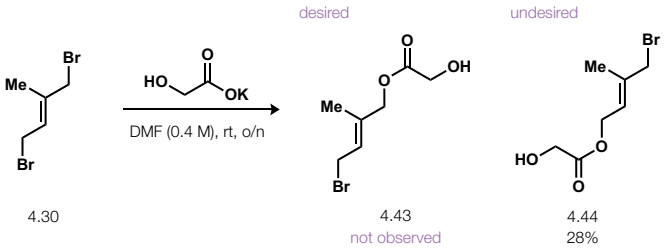
Figure 46. *Elimination of the 1,4-dibromoolefin.*
A) Heterolytic cleavage at the 4-position and resonance structures; B) 1-Position heterolytic cleavage and resonance structures C) E1 elimination mechanism and anchimeric stabilization; D) A brief exploration of 1,4-dibromoolefin elimination conditions.

The harsh conditions and poor selectivity afforded by the E1 elimination prompted a brief investigation into milder elimination conditions that could be carried out at lower temperatures (**Figure 46**, **D**). Lower temperatures were desirable for two reasons: a lower temperature distillation ($bp^{\mathbf{4.26}}_{10\ mmHg}$ = 25 ºC)[251] might provide better resolution between product isomers while also mitigating losses due to volatility, and; potential reduction in side product formation as compared with the harsh, acidic conditions.

We began these investigations into milder conditions by first establishing that the elimination reaction did require a temperature of 120 ºC. Heating the reaction to 60 ºC did not result in any conversion to product as determined by analysis of the distillate (**Figure 46**, **D**, **entry 1**). Increasing the reaction temperature by 20 ºC every 30 minutes

resulted in distillate formation only at ~120 ºC and failed to diminish decomposition in the reaction flask, validating the initial reaction temperature. Subsequently, we investigated the use of strong Brønsted base to promote E2 elimination at lower temperatures. This change in elimination mechanism brings about regioselectivity concerns as there are three competent sites for deprotonation at C1, C4 and C5. Use of potassium *tert*-butoxide in *t*-BuOH at 60 ºC for 1.5 h resulted in full conversion of SM with bromodiene **4.42** (**product II**) as the major identifiable product (**entry 2**). We suspected that this selectivity is governed by sterics and that deprotonation from the 4-position occurs because it is the most accessible site. In any case, this regioselectivity did not bode well for further E2 eliminations. Regardless, we also tested elimination conditions using DBU base under neat and solvated conditions, each time the reactions produced complex mixtures which were not investigated further (**entries 3 and 4**).

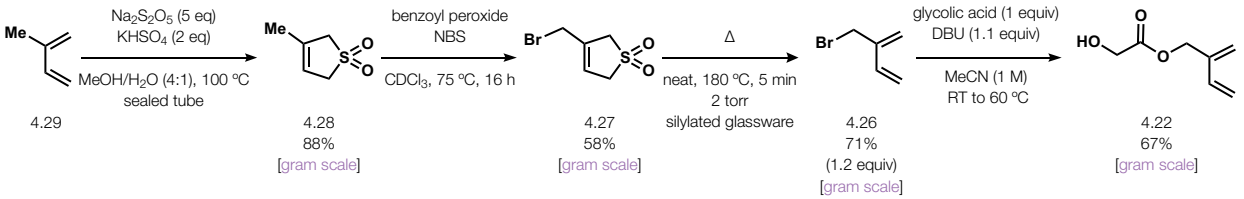
As a final attempt to make use of the 1,4-dibromoalkene **4.30**, we sought to assess the regioselectivity in nucleophilic capture using potassium glycolate (**Scheme 17**). We had hoped that substitution might occur at the desired 1-position of **4.30** and that subsequent dehydrobromination from the glycolate ester might prove more productive than it had from the dibromide. Unfortunately, the same regioselectivity observed for the E2 elimination was observed in our S_N2 attempt as undesired compound **4.43** was produced in 28% yield as the major isolable product while the desired isomer **4.44** was not observed. A survey of the literature shows that substitutions on **4.30** tend towards the same undesired site selectivity with a variety of nucleophiles.[252] While we had considered subjecting glycolate ester **4.43** to high temperature E1 conditions in an attempt at one-pot isomerization and dehydrobromination, parallel experiments caused us to set aside dibromoolefin-based sequences in favour of other routes.



Scheme 17. *Substitution regioselectivity assessment using potassium glycolate and 1,4-dibromoolefin.*

Contemporaneously, we explored the synthesis of 2-(bromomethy)-1,3-butadiene (**4.26**) through a sulfolene-based sequence (**Scheme 15**, **A**). In 2018, Larionov and colleagues reported the cheletropic [4+1] reaction between dienes and sulfur dioxide liberated *in situ* from sodium metabisulfite under acidic conditions.[247a] These conditions were readily applicable to the gram-scale preparation of 3-methylsulfolene (**4.28**), routinely giving the desired product in 80% yield, or higher, as a brilliant white powder (**Scheme 18**). In agreement with the original authors' report, we

found that after a simple liquid–liquid extraction, the material was sufficiently pure for further elaboration. For the sake of reagent availability, we found that potassium bisulfate could be prepared in the reaction flask using a pre-mixed solution potassium hydroxide and sulfuric acid in water. This change in procedure had no impact on the reaction outcome over several trials. While this reaction proved exceptionally reliable, its scalability was limited by the need for a high-pressure flask of sufficient size and as a result we were limited to 35 mmol scale reactions on a single pass.



Scheme 18. *Synthesis of diene glycolate ester via 3-methylsulfolene route.*
4.22 *prepared by Tegan E. O'Brien*

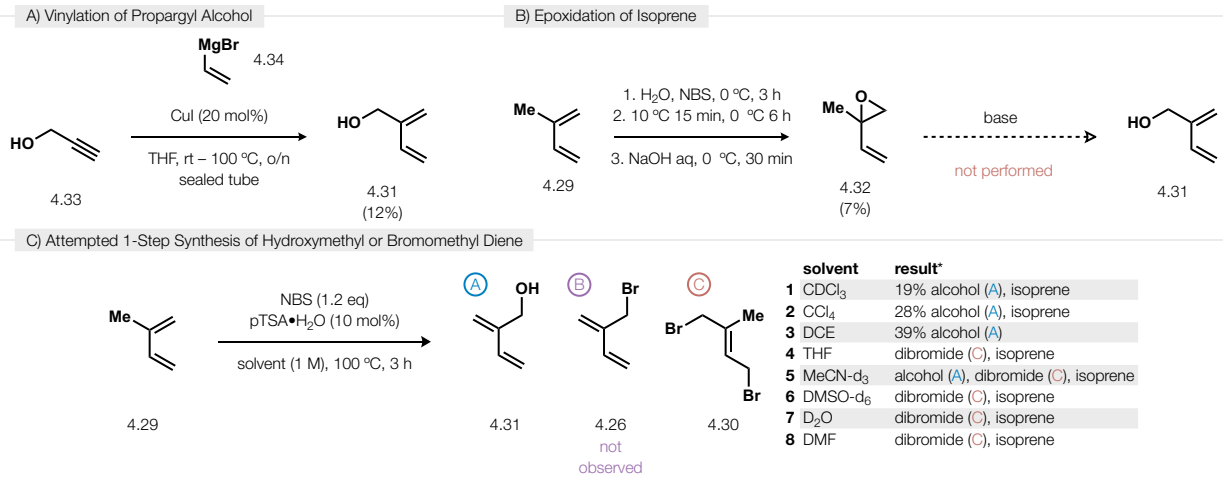
With reliable access to **4.28**, we next sought to perform a site-selective Wohl-Ziegler allylic bromination. Fortunately, the literature reported procedure[250b] employing benzoyl peroxide (BPO) and NBS reliably provided 3-(bromomethyl)sulfolene (**4.27**) in 40–50% yields. Despite several attempts, we were unable to attain complete consumption of the starting material in this bromination. Increased loadings of BPO and NBS had no beneficial impact, nor did additions of either reagent at various intervals throughout the reaction. While we typically employed freshly recrystallized NBS to the reaction, this appeared to be of little consequence to the overall outcome. Isolation of pure bromosulfolene **4.27** proved challenging as it shared similar retention times with the remaining starting material (**4.28**) and several side-products from the radical halogenation in a variety of eluent systems. Fortunately, we found that crude purification by flash column chromatography (25–60% EtOAc/hexanes), followed by recrystallization from hot ethanol, yielded sufficiently pure **4.27** for further elaboration.

Flash vacuum pyrolysis to extrude SO_2 was required to reveal bromomethyl diene **4.26**.[250b] With minimal experimentation, we were able to isolate **4.26** in 71% yield as a clear and colourless volatile oil. Key factors that resulted in high-yielding vacuum pyrolysis reactions included: the use of silylated glassware;[253] the use of a flask of minimal volume to contain the neat bromosulfolene **4.27**, and; repeated brief introductions of the pyrolysis flask to the pre-heated oil bath. Glassware was silylated to create an inert reaction vessel surface to minimize decomposition. Minimum volume flasks were employed to maximize rapid heat transfer by maximizing the surface area to volume ratio ($SA_{sphere} = 4\pi r^2$ and $V_{sphere} = (4\pi r^3)/3$). Prolonged exposure of the pyrolysis flask to the 180 ºC wax bath resulted in extensive decomposition of material as determined by a change in appearance from an off-white powder to a brown-

black tar-like syrup. As such, we found it beneficial to expose the neat sulfolene solution to the high temperatures for short durations repeatedly.

Finally, we needed to form glycolate ester **4.22** from 2-(bromomethyl)-1,3-butadiene (**4.26**) through substitution. Fortunately, Tegan found that conditions using stoichiometric DBU in acetonitrile at 60 ºC for 18 h afforded the requisite ester (**4.22**) in 67% yield on gram scale and allowed for isolation without losses due to volatility or water-solubility of **4.22**.[254] Conditions employing potassium carbonate in acetone were markedly less efficient.

In addition to the synthesis of the bromide derivatives, we also undertook brief investigations into the synthesis of 2-(hydroxymethyl)-1,3-butadiene (**4.31**). Two reported sequences caught our attention: addition of a vinyl subunit to propargyl alcohol,[249b] and base-induced isomerization of isoprene oxide (**Scheme 15**, **A**).[244] While the reported synthesis was high-yielding, our initial attempt to prepare dienol **4.31** through direct vinylation was met with a poor ^{1}H NMR yield of 12% (**Scheme 19**, **A**). Similarly, our first attempt to prepare isoprene oxide (**4.32**) through epoxidation of isoprene was low yielding (7% ^{1}H NMR yield) which we attributed to the volatility of the product (**Scheme 19**, **B**).

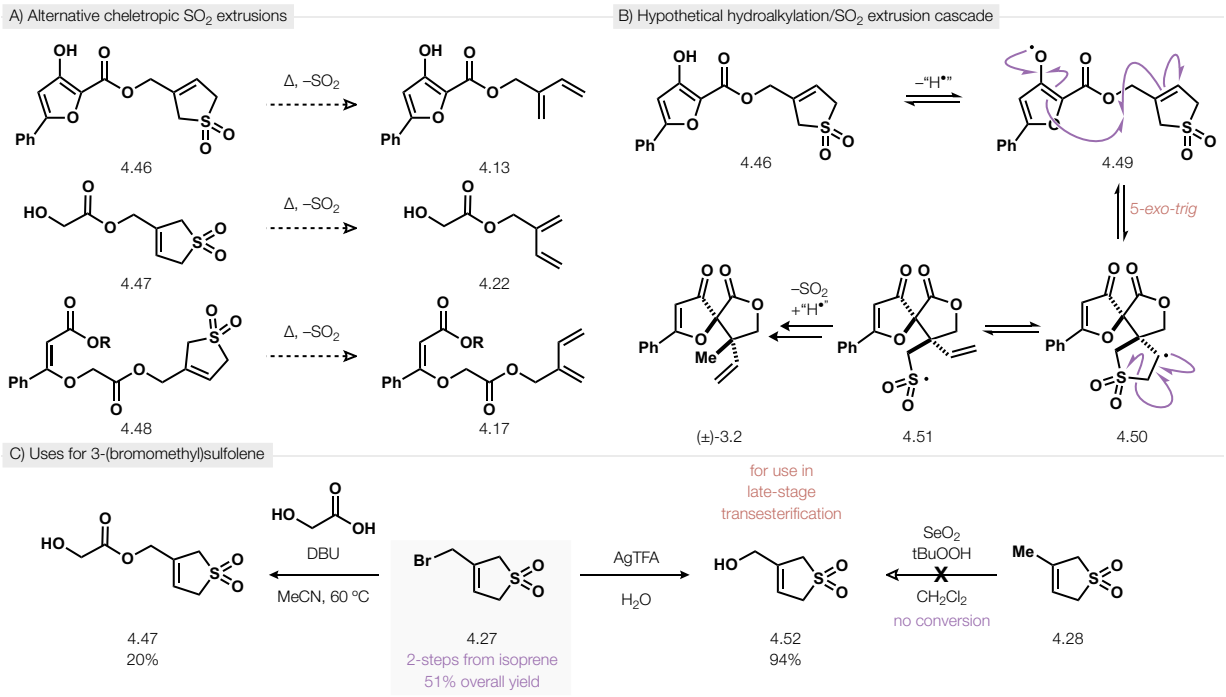


Scheme 19. *Preliminary attempts to synthesize 2-(hydroxymethyl)-1,3-butadiene.*
*A) Vinylation of propargyl alcohol; B) Epoxidation of isoprene; C) Attempted 1-step preparation of hydroxymethyl or bromomethyl diene. *^{1}H NMR spectroscopy yields using PhTMS as internal standard.*

Dissatisfied with the number of steps required to prepare bromomethyl diene **4.26**, we reasoned that it might be possible to effect a formal allylic bromination of isoprene using NBS and an acid catalyst. At high temperature, and in the absence of bromide counterions, we reasoned that allylic cation/bromonium ion intermediates (*e.g.* **4.37**, **4.39**, or **4.40**, **Figure 46**, **C**) could be engaged in deprotonation to give the desired compound **4.26** in a single step. A brief investigation into this reaction employing *p*TSA and NBS in various solvents at 100 ºC in a sealed tube showed

early promise (**Scheme 19**, **C**). Rather than leading to the desired bromomethyl diene **4.26**, our attempts in chlorinated solvents ($CDCl_3$, CCl_4, DCE) produced the hydroxymethyl diene **4.31** in low to moderate yields (19–39%) as the major identifiable product. Conversely, polar aprotic and protic solvents primarily yielded the dibromide **4.30** and leftover isoprene (**4.29**) following a 3-hour reaction period. While these results were intriguing and may have led to the development of a novel single-step synthesis of alcohol **4.31**, time constraints led us to instead focus on the more precedented route *via* bromomethylsulfolene **4.27**.

Two alternatives to the direct substitution of 2-(bromomethyl)-1,3-diene (**4.26**) with glycolate were available to us that warranted exploration: 1) changing the reaction sequence order to alkylate the glycolate first, and then performing the cheletropic SO_2 extrusion at a later stage, or; 2) attempting a hydroalkylation/SO_2 extrusion cascade on a furanoate-sulfolene substrate (**4.46**) (**Scheme 20**, **A & B**). To evaluate these sequences, we prepared sulfolene glycolate (**4.47**) in 20% yield through a DBU-promoted substitution (**Scheme 20**, **C**, **left**). As this reaction would occur at step three in a hypothetical 6-7 step synthesis of hyperolactone C (**3.2**), we surmised that it would not be feasible to use this sequence without significant improvement in yield. This result instead prompted us to explore a conversion of bromomethyl sulfolene **4.27** into hydroxymethyl sulfolene **4.52**, in anticipation of a late-stage esterification to join the sulfolene and enol ether subunits. Gratifyingly, aqueous silver(I) trifluoroacetate-promoted solvolysis yielded the desired alcohol (**4.52**) in 94% isolated yield (**Scheme 20**, **C-right**). Direct access to hydroxymethyl sulfolene **4.52** by allylic hydroxylation using selenium dioxide showed no conversion under standard, or forcing, conditions.



Scheme 20. *Alternative synthetic sequences utilizing 3-(bromomethyl)sulfolane.*
A) Alternative cheletropic SO_2 extrusions; B) Hypothetical hydroalkylation/SO_2 extrusion cascade for the synthesis of (±)-hyperolatonce C; C) Uses for 3-(bromomethyl)sulfolene. ***4.47*** *and* ***4.52*** *prepared by Tegan E. O'Brien*

Having established a reliable route to synthesize the diene subunit *via* the intermediate sulfolene, I will turn our attention towards our contemporaneous investigations into the synthesis of enol ether **4.17**.

4.4 Synthesis of Enol Ether Derivatives

While exploring synthesis of the diene motif in the hyperolactone C precursor **4.13**, we also commenced investigations into the synthesis of the key enol ether **4.17**. My work in this realm first centred on assessing the feasibility of an *O*-selective alkylation of ethyl benzoylacetate (**4.18**) with (pseudo)halo acetate esters. The major concerns with this transformation are stereoselectivity and the site of enolate reactivity. We required a system demonstrating a high-degree of *O*-alkylation over *C*-alkylation, with high selectivity for the formation of the *Z*-enol ether derivative over the undesired *E*-isomer.

Enolates are ambiphilic nucleophiles and may react through alkylation at carbon or at oxygen.[255] More negative charge resides on *O* than on *C* in these delocalized anions. Analysis of this system through the lens of hard and soft acid base (HSAB) theory shows that the *C*-centre is the softer site of reactivity, whilst the *O*-centre is the harder site of reactivity due to its higher charge density. This means that *O*-centred reactivity is more heavily

influenced by electrostatic interactions than at the *C*-terminus. As a result of this, *O*-alkylation can be favoured by increasing the localized anionic charge on oxygen and by increasing the hardness of the electrophile.

Higher localized anionic charge is favoured through the creation of a more "naked" enolate anion, *i.e*. through greater ion pair dissociation. Ion pair dissociation can be increased using more weakly associating cations derived from the choice of base,[256] through cation-sequestering additives like crown ethers,[257] and through the choice of solvent and its ability to solvate cations whilst minimally associating with the enolate anion.[256a]

Increasing the electrophile hardness will increase the electrostatic interaction present at the S_N2 transition state, thereby decreasing the activation energy and increasing reaction rate for the *O*-alkylation. This contribution can be influenced by changing the identity of the leaving group on the alkylating agent.[256, 258] Harder and less polarizable leaving groups will favour these electrostatic interactions. Using these principles, *O*- vs. *C*-alkylation selectivity can be influenced through several controllable variables.[256b, 259]

Rhoads and Hasbrouck studied the kinetics of *O*- and *C*-alkylation of cyclic β-ketoesters.[259a] In this study, they saw the proportion of *O*-alkylation products increase as temperature was increased (20 to 40 ºC), suggesting the *O*-alkylation reaction has a higher enthalpy of activation ($\Delta H^{\ddagger}$) and comparable, or more favourable, entropy of activation ($\Delta S^{\ddagger}$). This work suggests that improved *O*-selectivity might be attained in our desired system by increasing the reaction temperature.

Le Noble and Puerta studied the alkylation of the alkali metal enolates of ethyl acetoacetate in DMSO with *n*-propyl halides.[258] They found that the proportion of *O*-alkylation product increased in the order I < Br < Cl, matching the expected effects of leaving group hardness. They also observed that the enolate counterion had a significant impact on selectivity with the order $Li^+ < Na^+ \sim K^+$, consistent with the expected trend in ion pair dissociation.

A later report by Reutov and colleagues corroborated these findings using alkali ethyl acetoacetate enolates under strictly anhydrous conditions (**Figure 47**, **A**).[256a] This manuscript demonstrates several trends to favour *O*-alkylation, chiefly that *O*-alkylation proportion increases as cation polarizability increases and as leaving group hardness increases. Unfortunately, no mention of the stereochemical outcome of these reactions was reported. In a follow-up study, Reutov and co-workers demonstrated the leaving group trend $I^- < Br^- < Cl^- < {}^-OTs$ for 1º alkyl electrophiles.[256b]

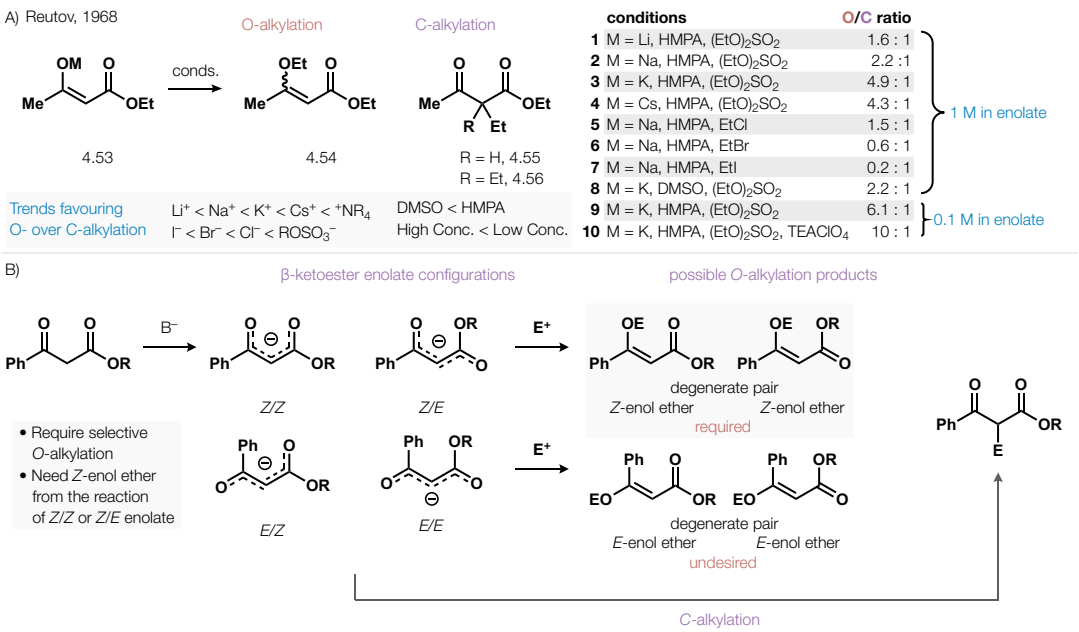


Figure 47. *Ketoester enolate alkylation intricacies.*

A) Reutov and colleagues' investigations into C- vs. O-alkylation; B) Enolate geometries and corresponding products.

Enolates that bear two different substituents at *C* have the additional complexity afforded by *E*/*Z*-configurational stereoisomerism. That is, the enolate can exist in either the *E* or *Z* geometry which can have significant impacts on site-selectivity and stereoselectivity. β-Ketoester enolates add an additional layer of complexity on top of this because the anion is delocalized across 5-centres rather than the 3-centres of a typical enolate. This means that the benzoylacetate ester enolates we wanted to employ can exist in four distinct configurations, the *Z*/*Z*-, *Z*/*E*-, *E*/*Z*- and *E*/*E*-conformers (**Figure 47**, **B**).[259b] Jackman and Lange suggested that these four enolate configurations should readily interconvert faster than reaction with an electrophile and should therefore be considered conformers.[260] Each of these conformers can react *via* the undesired *C*-alkylation pathway or the desired *O*-alkylation. From these different enolates, reaction at the ketonic oxygen can produce an enol ether. The *Z*/*Z* and *Z*/*E*-enolates would both furnish the *Z*-enol ether required for our proposed Dieckmann condensation, whilst the *E*/*Z*- and *E*/*E*-enolates would produce the undesired *E*-enol ether that could not be used in a subsequent Dieckmann condensation. Thankfully, in the 1960s this topic garnered interest from several groups who sought to understand selectivity in the alkylation of ketoester enolates.[256-260]

Rhoads and Holder performed a comparative study of the alkylation of cyclic and acyclic β-ketoesters.[259b] The authors show that acyclic β-ketoester enolates are more reactive than analogous cyclic enolates as a consequence of their greater dissociation in solution which, they suggest, arises from their ability to adopt a dipole-minimized *E*/*E*

geometry. The ability to adopt this configuration in acyclic β-ketoesters would allow a greater ion pair separation and thus greater localized anionic character on the enolate. A greater degree of cation dissociation allows the polar aprotic solvent to stabilize the cationic charge and leave the anion more free, a scenario that is less favourable to the *Z*/*Z*-configuration that has the ability to chelate the metal, and form aggregates.[261] Correspondingly, the authors suggest that the *O*-alkylation product is the *E*-enol ether based on NMR spectral comparisons to unpublished works.

Altogether these considerations seemed to present us with a paradox: it appeared that the dissociated ion pair effect that favoured *O*-alkylation would disfavour the formation of the *Z*/*Z*-enolate. This suggested that the most likely scenarios we would encounter were reactions with an undesirable *E/Z* selectivity but a high proportion of *O*-alkylation, or reactions with undesirable *O*/*C*-selectivity but favouring the formation of the *Z*-enol ether. When faced with such a paradox, the only recourse is to investigate at the fumehood.

This study began with an investigation into the effects of solvent identity on the alkylation of **4.18** with allyl bromoacetate (**3.81**), which could be prepared in a single step from bromoacetyl bromide (**3.79**) and allyl alcohol (**3.80**, **Figure 48**, **A & C**). A survey of solvents with varying polarity (**Figure 48**, **A**) failed to deliver the desired *O*-alkylation product **4.57**, however, higher polarity solvents (e.g. higher dielectric constants) resulted in a lower proportion of *C*-alkylation products **4.58** and **4.59** and unknown compounds began to predominate.

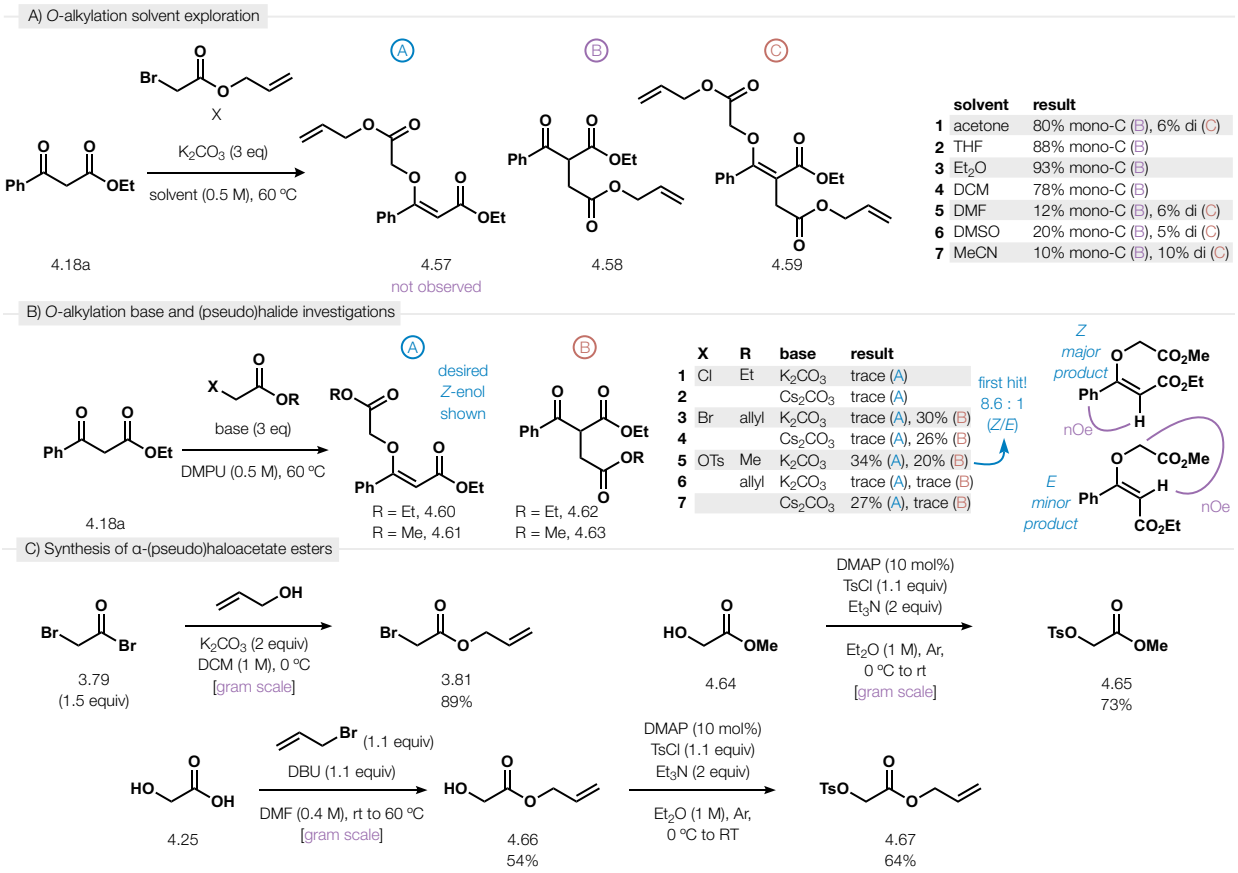


Figure 48. *O-alkylation of ethyl benzoylacetate.*

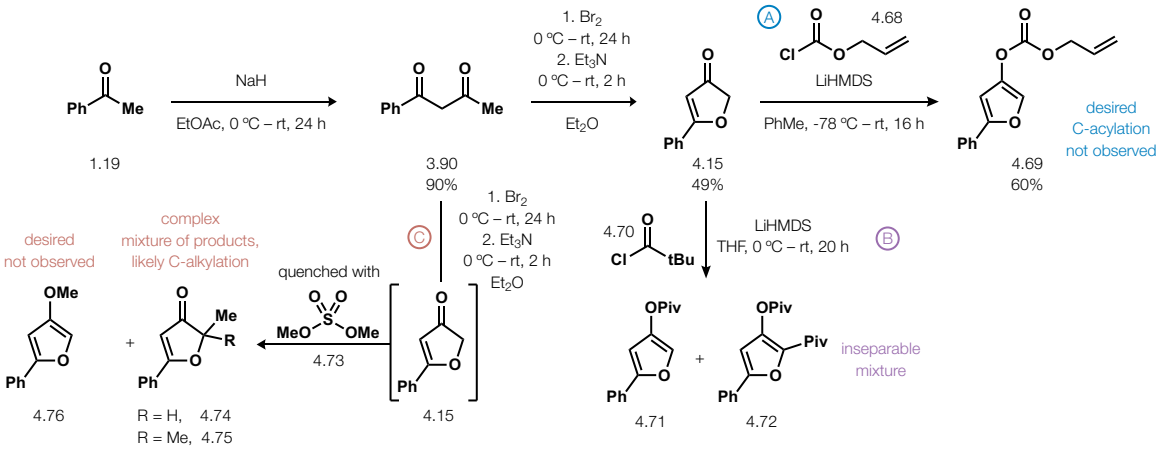
A) Solvent exploration; B) Base & (pseudo)halide investigations; C) Synthesis of α-(pseudo)halodacetate esters.

In parallel, potassium and cesium carbonate bases with α-chloro, -bromo, and -tosylate acetate esters were screened, using DMPU as a highly polar, aprotic solvent (**Figure 48**, **B**). Switching from soft bromoacetate to harder chloroacetate esters did not provide the desired selectivity, as each produced enol ether products in only trace quantities. Fortunately, as demonstrated by Reutov,[256] tosylates provided even greater selectivity for the *O*-alkylation of enolates, prompting the synthesis of tosylacetate esters **4.65** and **4.66** (**Figure 48**, **C**).

Gratifyingly, alkylation of ethyl benzoylacetate (**4.18**) with methyl α-tosylate acetate (**4.65**) in DMPU at 60 ºC using K_2CO_3 gave us our first appreciable access to enol ether **4.61** in a 34% yield. Pleasingly, the reaction furnished a mixture of *O*-alkylated products **4.61** and **4.61'** in an 8.6:1 (*Z*/*E*) ratio (**Figure 48**, **B**). A 2D NOESY experiment showed alkenyl methine correlation to the phenyl ring in the major product, but not in the minor. In contrast, there is a NOESY correlation between the methine and the methylene protons in the minor product that is not present in the major. This selectivity is remarkable given the literature precedent on the *O*-alkylation of ketoester enolates. Whether

this unexpected distribution was kinetically determined or is the product of equilibration is currently unknown and would require further experimentation to elucidate.

To prepare an allyl ester model substrate for the photoredox hydroalkylation, I employed allyl α-tosylate acetate (**4.66**) under the same conditions. Unfortunately, this reaction failed to give *O*-alkylation products in synthetically useful quantities. Changing the cation of the carbonate base from potassium to cesium provided the allyl enol ether derivative **4.57** in 27% yield. While this showed early promise, the additional step required to prepare the tosylglycolate ester, coupled with more promising results from Tegan's forays into enol ether synthesis, caused us to abandon this route without further exploration. Future efforts to improve this transformation could assess more polar aprotic solvents, more base identities, dilution effects, temperature effects, and additives such as crown ethers or tetraalkylammonium or tetraalkylphosphonium salts. After concluding these explorations, we became aware of an analogous Mitsunobu reaction which, if successful, could prove valuable for any future studies in this chemical space.[262]



Scheme 21. *Synthesis of 5-phenyl-3(2H)-furanone and attempted elaborations.*
Performed by Tegan E. O'Brien.

Simultaneously, Tegan explored the synthesis and elaboration of 5-phenyl-3(2*H*)-furanone (**4.15**). The sequence began with preparation of benzoylacetone (**3.90**) through Claisen condensation of acetophenone (**4.19**) with ethyl acetate, which gave the desired 1,3-dione (**3.90**) in 90% isolated yield (**Scheme 21**). Subsequent bromination and cyclization proved difficult, owing to the unselective halogenation of the diketone (**3.90**) and the susceptibility of furanone **4.15** to decomposition,[246] particularly under the oxidizing and acidic conditions employed. These challenges led to complex reaction profiles with correspondingly difficult isolations and a resulting high variability in the preparation of furanone **4.15**. Nevertheless, with access to furanone **4.15** Claisen condensation was attempted with

allyl chloroformate (**4.67**) at –78 ºC using LiHMDS. Unfortunately, none of the desired *C*-acylated product was observed and instead carbonate derivative **4.68** was isolated in 60% yield as the major product of the reaction (**Scheme 21**, **A**). Similar behaviour was observed when attempting acylation using pivaloyl chloride (**4.69**) and in this case the major *O*-acylation product **4.70** was obtained as an inseparable mixture with a minor *O*/*C*-diacylated product **4.71** (**Scheme 21**, **B**). At this juncture we thought that fighting the *O*-centred selectivity of this ambident nucleophile might be a daunting task, and that protection of the oxygen would allow us to lithiate C2 of the furan for use as the nucleophile instead. This prompted an attempted synthesis of the methyl ether derivative **4.75** by quenching the furanone annulation reaction with dimethyl sulphate. Dimethyl sulphate was chosen as a hard electrophilic methyl source to favour selective *O*-alkylation.[256a] Surprisingly, this reaction did not produce the intended methyl ether derivative **4.75** but yielded a mixture of mono- and dimethylated furanone products **4.73** and **4.74** *via* reaction at the C-terminus of the enolate (**Scheme 21**, **C**). This confounding result certainly warranted further investigation, but our attentions were drawn to more promising routes explored simultaneously.

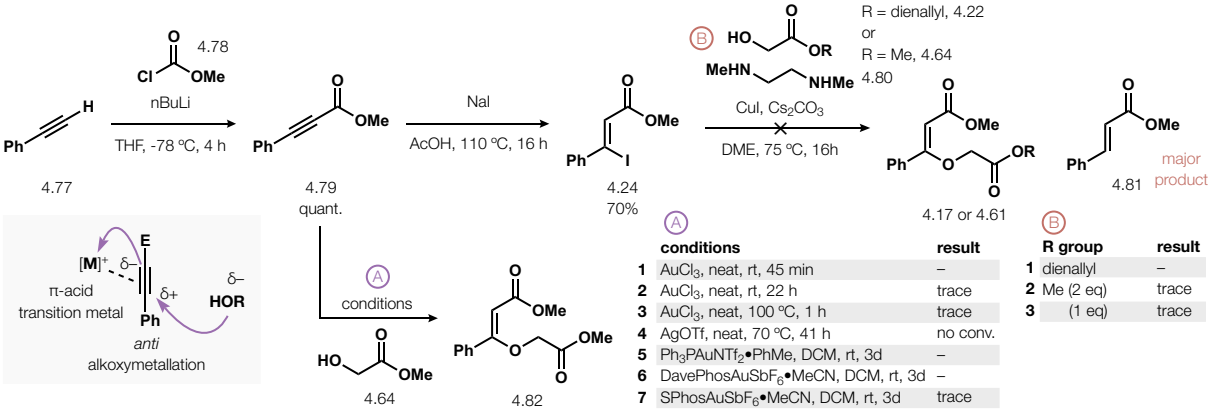


Figure 49. *Early attempts at enol ether synthesis through coinage-metal catalysis.*
Performed by Tegan E. O'Brien

Early investigations into coinage-metal catalyzed enol ether synthesis were fruitless (**Figure 49**). Beginning from phenylacetylene (**4.76**), we prepared methyl phenylpropiolate (**4.79**) in quantitative yield *via* lithiation and subsequent acylation with methyl chloroformate (**4.78**, **Figure 49**). From the ynoate ester **4.79**, two pathways were investigated. Pathway A endeavoured to prepare the enol ether **4.81** through direct hydroalkoxylation methyl glycolate (**4.64**) and gold(I), gold(III), or silver(I) π-acid catalysts. Pathway B sought to prepare the enol ether through C(sp^2)–O coupling of the intermediate iodide **4.24** with glycolate esters through copper catalysis.

Direct hydroalkoxylation was expected to deliver the desired regioisomer based on a polar bond disconnection analysis wherein the electropositive metal should be placed at the higher electron density α-position of the ynoate system whilst the alcohol nucleophile attacks the more electron-poor β-carbon (**Figure 49**, **box**). We also predicted that the desired stereochemistry should be the major product of the reaction given the *antiperiplanar* addition of the metal and nucleophile in the alkoxymetallation step. Given a stereoretentive protodemetallation step, the desired *Z*-enol ether stereochemistry should be established by the *anti*-addition.

These early efforts to conduct a direct addition of methyl glycolate (**4.64**) showed trace conversion to the desired product (**4.82**) when employing $AuCl_3$ as a catalyst in neat methyl glycolate (**4.64**) for extended duration at room temperature or at 100 ºC for 1 h (**Figure 49**, **A table**, **entries 1–3**). AgOTf failed to provide any conversion after an extended reaction period at 70 ºC in neat methyl glycolate (**4.64**, **entry 4**). Reactions using phosphine-ligated Au(I)-complexes on very small scale gave trace formation of the desired adduct (**4.82**) after 3 days of reaction at room temperature (**entries 5–7**), and this route was later revisited.

Contemporaneously, iodide **4.24** was prepared *via* hydroiodination of alkyne **4.79** in 70% yield. From this intermediate, we explored McDonald's conditions for C–O cross-coupling through copper catalysis.[263] While the diene-bearing glycolate ester **4.22** failed to yield any of the desired enol ether, methyl glycolate (**4.64**) appeared to give trace product. This route was similarly abandoned as it was not the most expedient access to the furanoate core, and it had not yielded an immediate positive result. As a result, we turned our attention towards the investigation of our envisioned ***route IV***, the Heck-coupling approach.

We surmised that Mizoroki-Heck coupling of a *trans*-β-alkoxyacrylate ester (**4.87**) with bromobenzene (**2.150**) could be a rapid entry point to our desired *Z*-enol ether **4.89** and that such a transformation would likely have already been reported in the literature. Once again, this transformation brings forth questions about regioselectivity and stereoselectivity.

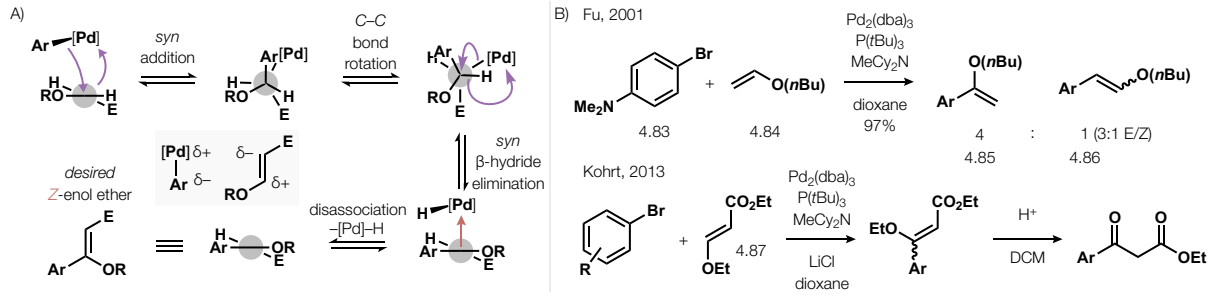


Figure 50. *Z-Selective Mizoroki-Heck coupling of β-alkoxy acrylate esters.*
A) Regiochemical and stereochemical analyses; B) Literature precedents.

We believed that the regioselectivity of this reaction would be ensured by the electron donating effect of the enol, and the electron withdrawing effect of the acrylate ester, motifs that would synergistically dictate the preferred orientation of the carbopalladation step. Through a polar bond analysis of an isolated enol ether, the electron donating effect should serve to direct arylation *α* to oxygen and place the electropositive [Pd^{II}] centre at the nucleophilic carbon *β* to oxygen (**Figure 50**, **A**, **box**). Additionally, in an isolated acrylate ester, carbopalladation should arylate *β* to the ester carbonyl and place the electropositive metal at the more electron-rich α-position. These two effects would work in concert to influence the sense of carbopalladative addition and reinforce the desired regioselectivity.

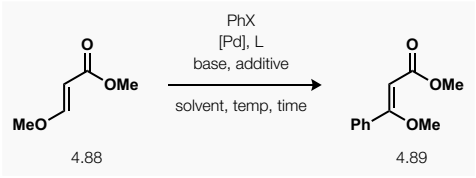
To understand the anticipated stereochemical outcome of this transformation, we must consider the underlying mechanisms for the Heck-coupling (**Figure 50**, **A**). We anticipated that the desired *Z*-enol ether (**4.88**) could be prepared from the *trans*-enol acrylate (**4.87**) because carbopalladation and β-hydride elimination are both *syn* processes. Based on these considerations, a *trans*-configured enol acrylate ester (**4.87**) starting material will undergo *syn* carbopalladation and a C–C bond rotation is required to orient the β-hydrogen and Pd-centres *syn* for β-hydride elimination. β-Hydride elimination then sets the olefin stereochemistry with the aryl group and ester moieties *trans* to one another, as desired. Of course, β-hydride elimination is reversible and subsequent hydropalladation and β-hydride eliminations can cause scrambling of the olefin geometry and establish a thermodynamic mixture.

In 2007, Doucet, Santenelli, *et. al* reported the coupling of (*E*)-3-methoxyacrylate (**4.87**) with aryl bromides followed by hydrolysis to give the corresponding β-ketoesters.[264] While this work looked promising initially, giving the expected β-aryl-β-alkoxyacrylate regioisomer, a few drawbacks quickly came to light. First and foremost, this Pd-catalyzed cross-coupling reaction utilizes a ligand that is not commercially available, Tedicyp (*cis,cis,cis*-1,2,3,4-tetrakis(diphenylphosphanylmethyl)cyclo-pentane) and requires a multi-step synthesis to prepare.[265] Moreover, the Mizoroki-Heck condition they employed were quite harsh (150 ºC in DMF for 20 h) and the authors

noted 1:1 *E/Z*-enol ether mixtures with accompanying premature hydrolysis, and the creation of several unidentified side products.

Fortunately, Kohrt and colleagues at Pfizer also developed a Mizoroki-Heck coupling on β-alkoxyacrylate esters (**Figure 50**, **B**, **bottom**).[266] Based on conditions originally identified by Fu in 2001 (**Figure 50**, **B**, **top**),[267] the Pfizer team found they could effectively couple (hetero)aryl bromides and iodides by including a lithium chloride additive.[268] This work suggested that our desired regioselectivity could be attained, however, the only note about stereoselectivity within this article described *E*/*Z*-olefin mixtures that were not further elucidated because the enol ether intermediates were immediately hydrolyzed. Given the milder conditions presented in this article (110 ºC in dioxane for 2.5 h), we were hopeful that enol ether hydrolysis would be minimal and high *Z*-selectivity could be realized. These conditions, along with several other reports[269] on Heck-couplings of acrylate esters,[270] and enol ethers,[271] gave us clear indications for where to begin.

Table 24. *Z-selective Heck-coupling investigations*



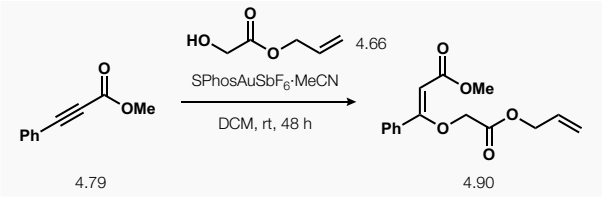
4.88 4.89

Entry	X	[Pd]	L	base	additive	solvent	T (º C)	t (h)	% yield 4.89
1	Br	$Pd(OAc)_2$	dppp	Et_3N	–	DMF	80	15	–
2	I	$Pd(OAc)_2$	dppp	Et_3N	–	DMF	120	17	–
3	I	$Pd(OAc)_2$	dppp	K_2CO_3	–	DMF	120	17	trace
4	I	Pd/C (5%)	–	K_2CO_3	–	MeCN	120	17	–
5	I	$Pd_2(dba)_3$	dppp	Et_3N	LiCl	dioxane	120	17	trace
6	I	$Pd_2(dba)_3$	dppp	Et_3N	LiCl	dioxane	80, 100	17, 4	trace
7	I	$Pd_2(dba)_3$	dppp	Et_3N	KCl	dioxane	80, 100	17, 4	trace
8	I	$Pd_2(dba)_3$	dppp	Et_3N	–	dioxane	80, 100	17, 4	trace
9	I	$Pd_2(dba)_3$	dppp	$MeCy_2N$	LiCl	dioxane	80, 100	17, 4	trace
10	I	$Pd_2(dba)_3$	*t*-BuPHBF$_4$	Et_3N	LiCl	dioxane	120	13	–
11	I	$Pd_2(dba)_3$	*t*-BuPHBF$_4$	Et_3N	LiCl	dioxane	80, 100	17, 4	–
12	I	$Pd_2(dba)_3$	*t*-BuPHBF$_4$	$MeCy_2N$	LiCl	dioxane	80, 100	17, 4	trace
13	OTf	$Pd_2(dba)_3$	dppp	Et_3N	LiCl	dioxane	80	17	–
14	OTf	$Pd_2(dba)_3$	dppp	Et_3N	KCl	dioxane	80, 100	17, 4	13
15	OTf	$Pd_2(dba)_3$	dppp	Et_3N	–	dioxane	80, 100	17, 4	15
16	OTf	$Pd_2(dba)_3$	dppp	$MeCy_2N$	LiCl	dioxane	80, 100	17, 4	–
17	OTf	$Pd_2(dba)_3$	*t*-BuPHBF$_4$	Et_3N	LiCl	dioxane	80, 100	17, 4	–
18	OTf	$Pd_2(dba)_3$	*t*-BuPHBF$_4$	$MeCy_2N$	LiCl	dioxane	80, 100	17, 4	9

Reactions performed by Tegan O'Brien

Heck couplings using methyl *trans*-3-methoxyacrylate (**4.88**) as a model substrate were explored (**Table 24**).[270a, 272] Use of bromobenzene (**2.150**) did not yield any product after 15 h at 80 ºC, prompting us to screen with the more reactive iodobenzene (**entry 1**). Similarly, iodobenzene delivered only trace product under a variety of conditions. Only when using phenyl triflate as the aryl source did we observe any significant product formation. Conditions using $Pd_2(dba)_3$ with dppp ligand and triethylamine base without any additives appeared to give the desired product **4.89** in 15% NMR yield. Potassium chloride had no beneficial effect on the efficiency of this reaction whilst 3 equivalents of lithium chloride completely suppressed the desired transformation. Interestingly, Fu/Kohrt-like conditions were not sufficiently effective at promoting this transformation.[266, 270b] This hit may have delivered a successful entry to hyperolactone C (**3.2**) with further optimization. However, we surmised that direct addition of glycolate ester to alkyne **4.79** facilitated a more direct synthesis of hyperolactone C (**3.2**), and that this approach warranted further investigation.

Table 25. *Optimization of the Au(I)-catalyzed 1,4-addition of allyl glycolate to methyl phenylpropiolate*



Entry	Alkyne Equiv.	Glycolic Ester Equiv.	[Au] (mol%)	t (h)	% yield (*Z*/*E*)
1	1	2	0.5	42	44 (20:1)
2	2	1	0.5	24	51 (6:1)
3	2	1	0.5	16	38 (2.8:1)
4	2	1	2.5	24	62 (1.7:1)
5	2	1	1.5	13	45 (2.2:1)
6[a]	2	1	2.0	96	no conv.
7[b]	2	1	2.0	168	24 (1:2.5)
8[c]	2	1	0.5	48	72 (>20:1)
9[d]	2	1	0.5	48	63 (>20:1)

[a.] Reactions run on 1 mmol scale in DCM at a concentration of 2 M, unless otherwise stated. [a]activated 4Å MS included; [b]activated 3Å MS included; [c]reaction run on 3 mmol scale and purified by flash column chromatography without work-up; [d]reaction run with SPhosAuNTf₂ on 2 mmol scale and purified by flash column chromatography without work-up. Performed by Tegan E. O'Brien

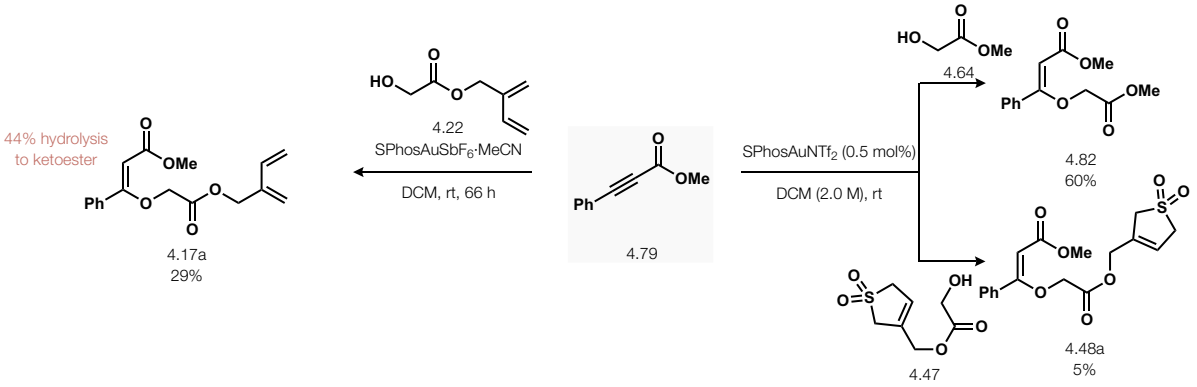
Due to the expected expediency that a Au(I)-catalyzed 1,4-addition would provide, we returned to the optimization of this reaction. Work by Corma and co-workers on the regio- and stereoselective hydroalkoxylation of alkynes suggested that such a reaction should be feasible through cationic Au(I)-catalysis.[273] These authors demonstrated a substantial ligand effect on the stereochemical outcome of the reaction, with a high proportion of *Z*-

enol ether formed from the reaction of alcohols with dimethyl acetylenedicarboxylate using SPhosAuNTf$_2$. The authors demonstrate that Z-enol ethers are formed kinetically and may undergo subsequent isomerization with more electrophilic catalysts. Despite this promising precedent, the authors had not demonstrated any reactions using unsymmetrical internal ynoate ester systems of the kind required here.

Using two equivalents of allyl glycolate (**4.66**) we obtained **4.90** in 44% NMR yield and 20:1 *Z/E* ratio on 1 mmol scale after 42 h using SPhosAuSbF$_6$ catalyst (**Table 25**, **entry 1**). The major side products observed from these reactions were ketal formation and hydrolysis to methyl benzoylacetate (**4.18**). Swapping the limiting and excess reagents resulted in a faster reaction with slightly improved overall yield to the detriment of the *Z*/*E*-ratio (**entry 2**). To limit hydrolysis and ketal side product formation, a reaction was terminated prior to full conversion, however, the yield and diastereoselectivity were both inferior to the 24-hour reaction (**entry 3**). Greatly increased catalyst loading (2.5 mol%) resulted in an improved yield and worse selectivity whilst a moderate loading increase (1.5 mol%) appeared to have little effect on the yield while still diminishing selectivity (**entries 4 & 5**). To limit hydrolysis, two reactions were run in the presence of activated 4Å or 3Å molecular sieves (**entries 6 & 7**, respectively). 4Å Molecular sieves completely suppressed the reaction, likely through adsorption of the glycolic ester nucleophile while 3Å sieves slowed conversion significantly. Despite our efforts to control the reaction conditions, we surmised that adventitious water was likely responsible for the large proportions of hydrolysis product we were observing. As our efforts to mitigate hydrolysis were fruitless, we hypothesized that this problem might be less impactful on larger scale and could be limited through direct isolation of the product **4.90** from the reaction mixture without prior work-up or manipulations. To our delight, when we applied our best conditions to a 3 mmol scale reaction run without interruption for 48 hours and then directly loaded onto a prepared silica gel column for flash chromatography, we obtained **4.90** in 72% isolated yielded with excellent selectivity (>20:1 *Z/E,* **entry 8**). This entry finally cemented our entry to the hyperolactone C scaffold and enabled the most convergent route we had devised. As a final test, we employed SPhosAu(I) with an $^{-}$NTf$_2$ counterion due to reagent availability. SPhosAuNTf$_2$ provided **4.90** in a slightly diminished 63% yield with a maintained >20:1 *E/Z* ratio, which we deemed efficient enough for further use in the preparation of hyperolactone C (**Table 25**, **entry 9**). From here we targeted a suitably functionalized enol ether by using derivatized glycolate esters in this Au(I)-catalyzed addition.

Attempting to apply this hydroalkoxylation to the synthesis of key enol ether substrate **4.17** proved troubling as the desired adduct (**4.90**) was formed in only 29% yield along with 44% hydrolysis side product (**4.18**, **Scheme**

22). This low yield coming at the end of an already low-yielding 4-step sequence to prepare the diene glycolate ester **4.22** caused us to explore orthogonal sequences.



Scheme 22. *Au(I)-catalyzed addition of glycolate esters on methyl phenylpropiolate. Performed by Tegan E. O'Brien*

Preparation of the sulfolene-bearing glycolate ester **4.47** was similarly plagued by a low-yielding glycolate alkylation and, unfortunately, the addition of this glycolate ester by Au(I)-catalysis was also too inefficient for further use (**Scheme 22**, **bottom right**). Finally, we observed that addition of simple methyl glycolate (**4.64**) occurred with similar efficiency to the allyl ester, furnishing **4.82** in 60% yield as the *Z*-enol ether, exclusively (**Scheme 22**, **top right**). At this point, we were not sure what role the dimethyl ester **4.82** would play in the overall synthesis as we were concerned that transesterification at this point or later in the sequence would not be tolerated by such apparently sensitive substrates.

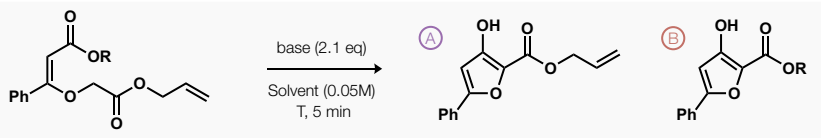
Having prepared a number of enol ether derivatives that could plausibly be elaborated into hyperolactone C (**3.2**), I was next tasked with identifying suitable conditions for the Dieckmann condensation needed to synthesize the key furanoate ester intermediates.

4.5 Furanoate Ester Synthesis and Derivatizations

Tegan's reliable access to the mixed diester substrate **4.90** enabled investigation into Dieckmann condensation conditions (**Table 26**). Given our earlier experience preparing the benzofuranoate ester **3.59n**, it was no great surprise that the use of mixed diesters in this transformation resulted in product distributions composed of the desired allyl furanoate ester **4.92** as well as the transesterified product **4.93**. Investigations into this condensation began by screening bis(trimethylsilyl)amide bases with Li^+, Na^+, and K^+ cations to see if counterion identity had a significant impact on the reaction (**Table 26**, **entries 1–3**). The lithium and potassium bases produced similar reaction profiles that favoured the formation of the undesired transesterified product **4.93** at –81 ºC after 5 minutes of reaction in THF

(**entries 1 & 3**). In contrast, NaHMDS performed much worse under the same conditions, giving the furanoate products in combined yield of 14% with 33% starting material remaining (**entry 2**). Potassium *tert*-butoxide provided a nearly identical reaction profile to KHMDS, and the remaining investigations were carried out with this base (**entry 4**). Hypothesizing that the transesterification product might be arising *via* a high-energy ketene intermediate (**4.95**), I chose to cool the reaction further than –81 ºC to see the effects on product distribution (**entry 5**). Applying a reaction temperature near the melting point of tetrahydrofuran (–108 ºC) had little impact on the product ratio, with ~1.3:1 **4.93**/**4.92** observed at –81 ºC and ~1.5:1 **4.93**/**4.92** at –108ºC, both favouring the undesired compound (**entry 4** *vs.* **5**). The lower temperature did appear to influence overall mass balance recovery as the furanoate esters were obtained in a combined overall yield of 77% at –108 ºC versus 64% at –81 ºC. Cooling the reaction further required a change in solvent to anhydrous diethyl ether (**entry 6**). Running the reaction in Et_2O cooled using a liquid nitrogen-ethanol bath gave a combined yield of 76% with an improved 1:1 **4.92**/**4.93** ratio of esters. Despite this improvement, we were unhappy with the prospect of losing half of our suitably functionalized material as a methyl furanoate ester. To further dissuade transesterification, we reasoned that a less nucleophilic leaving group would provide better selectivity. Replacing the methyl ester with a phenyl ester would liberate an equivalent of phenoxide, rather than methoxide, which we expected to improve our product distribution. Application of this allyl/phenyl mixed diester **4.91** did indeed improve our selectivity from 1:1 up to 4.3:1 **4.92**/**4.94** with an overall yield of 69% (**entry 7**). While we were satisfied with this improvement, the fact that phenyl phenylpropiolate is not commercially available whilst methyl phenylpropiolate (**4.79**) is meant that this route would require us to count an additional step in our sequence. This was unacceptable to us as we now had our sights set on a 4-step LLS, and 5-step total, synthesis of (±)-hyperolactone C (**3.2**).

Table 26. *Dieckmann condensation investigations with mixed diesters.*



Entry	Base	Solvent	T (ºC)	R	% yield A (4.92)	% yield B
1	LiHMDS	THF	–81	Me	23	33
2[a]	NaHMDS	THF	–81	Me	9	5
3	KHMDS	THF	–81	Me	27	36
4	KO*t*Bu	THF	–81	Me	28	36
5	KO*t*Bu	THF	–108	Me	31	46
6	KO*t*Bu	Et_2O	–116	Me	37	39
7	KO*t*Bu	Et_2O	–116	Ph	56	13

[a]*33% starting material remaining.*

The projected two-step access to the methyl furanoate **4.93** by way of the dimethyl diester **4.82**, along with the observed ester scrambling during Dieckmann condensation, served to convince us that there would be some way to promote a transesterification, either during Dieckmann condensation or after it. Such a transesterification would represent a point of diversification allowing us to employ a variety of alcohols in a convergent coupling of two fragments of equal complexity.

As starting point we assessed the condensation of the diester **4.82** at –81 ºC using KO*t*Bu base (**Figure 51**, **A**, **entry 1**). Gratifyingly, the overall yield for the transformation was maintained when compared to the mixed diesters, but now the material was obtained as a single product. In fact, running the reaction at a higher temperature of –10 ºC and higher concentration was not only tolerated but gave an improved isolated yield of 85% of the methyl furanoate **4.93** (**entry 2**). It is worth noting that these hydroxyfuranoate esters are indeed unstable on silica gel, as confirmed by 2D TLC, and upon prolonged exposure to ambient atmosphere or acidic conditions. When preparing methyl furanoate **4.93** *via* Dieckmann condensation of dimethyl ester **4.82**, I found that pure material could be obtained by recrystallization of the crude residue from hot hexanes, thereby avoiding any chromatography-related decomposition (**Figure 51**, **B**). Despite the sensitivity of these compounds, we did not observe decomposition when the material was stored in crystalline form under argon atmosphere at –20 ºC for several months.

Crystals suitable for SCXRD were prepared *via* slow evaporation of a solution of recrystallized **4.93** in hexanes (**Figure 51**, **C**). The X-ray structure demonstrates a significant contrast between the furanol C16–O8 bond length of 1.339 Å and a typical carbonyl bond length in the ester C14=O6 (1.238 Å). As well, the C15=C16 and

C17=C18 bond lengths are nearly identical at 1.376 Å and 1.373 Å, respectively. Taken together, these characteristics suggest the furanol tautomeric form is dominant in the solid phase rather than 3(2*H*)-furanone.

Several reports detail the preparation of 3-hydroxy-2-furanoate esters, however, few of these reports include complete NMR-spectral characterizations.[238g, 274] As a result, these compounds are occasionally portrayed in the furanone tautomeric form, despite no evidence that this is the major species in solution or the solid state.[238g, 274c] Where these compounds do appear in literature, they are often used promptly, likely as a consequence of their reputation for instability.[274c, 275] Additionally, most spectra that are included in the literature were taken in *d*-chloroform solutions.[276] In our experience, even chloroform-*d* shaken over solid K_2CO_3 or passed through basic alumina proved acidic enough to decompose some of the pure material during NMR spectra collection (**Figure 51**, **D**). Additionally, we found that several carbon signals could not be reliably distinguished from the baseline in chloroform-*d*, C_6D_6, or toluene-d_8, regardless of concentration or temperature (**Figure 51**, **E**). Satisfyingly, acquisition in DMSO-d_6 provided NMR spectra adequate for full analysis and characterization.

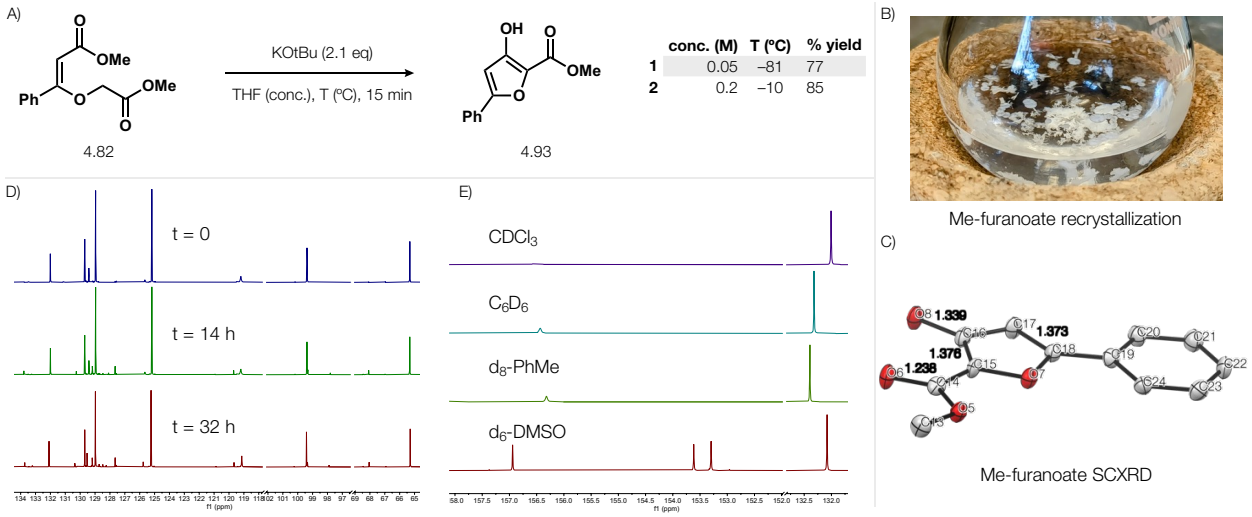


Figure 51. *Dieckmann condensation success and 3-hydroxyfuranoate ester characteristics.*
*A) Dieckmann condensation of dimethyl ester; B) Recrystallization of methyl furanoate product from hot hexanes; C) X-ray diffraction ORTEP structure of methyl furanoate product (hydrogens omitted for clarity, bond lengths in Å); D) Decomposition of allyl furanoate over time in K_2CO_3-stabilized $CDCl_3$ in a freeze-pump-thawed and flame-sealed NMR tube (featureless portions of spectra excised for clarity, 1 h 10 min ^{13}C acquisition at 151 MHz); E) NMR solvent impact on allyl furanoate quaternary ^{13}C signal strength (~152–133 ppm excised for clarity, 1 h 10 min ^{13}C acquisition at 151 MHz, *missing signals could not be located elsewhere in the spectra).*

With the methyl furanoate (**4.93**) material in hand, we thought about how we might accomplish a transesterification on such a potentially unstable substrate. First, we sought insight into the mechanism for the ester

scrambling that was occurring under the Dieckmann condensation conditions (**Figure 52**, **A**). If transesterification occurs after Dieckmann condensation, then the desired furanoate ester (**4.13**) could be formed under Dieckmann conditions using an excess of the desired alcohol to push the equilibrium forward.

If transesterification precedes Dieckmann condensation, then we imagined two underlying mechanistic possibilities. The first is that transesterification occurs in the open enol ether form *via* addition of an alkoxide nucleophile to the glycolate-like ester to give a tetrahedral intermediate. This tetrahedral intermediate may collapse to give the new ester or return the original starting material. If this mechanism is operative with the starting material, then it is also plausible with the furan product as the ester functionality is conserved. As the anionic furanoxide **4.97** is likely the dominant species under the reaction conditions, this pathway may be disfavoured due to anion delocalization decreasing the carbonyl electrophilicity. Such anionic character will cause the carbonyl to bear a higher energy π^* LUMO orbital that may prohibit nucleophile capture. An alternative possibility is that transesterification in the starting material might occur through a highly reactive ketene intermediates (**4.95**) — species commonly invoked in ester enolate chemistry, particularly at higher temperatures. For this reason, we employed cryogenic conditions throughout our screening and optimization of the Dieckmann condensation and sought even colder temperatures as a method to dissuade ester scrambling. If ketenes were necessary intermediates for transesterification, then submission of furanoate ester products to the same conditions for Dieckmann condensation with an excess alcohol would not result in the production of a transesterified product. The only way transesterification could be possible under this mechanistic paradigm is in the unlikely event that the aromatizing Dieckmann condensation itself were reversible, or if an α-furanone ketene could form as an intermediate under the cryogenic conditions.

To test these possibilities, we submitted methyl furanoate **4.93** to Dieckmann conditions with 10 equivalents of allyl alcohol (**Figure 52**, **B**, **entry 1**). Unfortunately, this did not result in any conversion after several hours, suggesting that the mechanism for transesterification during the Dieckmann condensation involves the starting material (**4.93**). This single experiment does not allow us to distinguish between attenuated product reactivity due to anion character, or increased starting material reactivity due to ketene intermediacy, as the factor that dictates transesterification feasibility. In any event, this result did mean we would need to identify alternative transesterification conditions to continue our synthesis.

Attempts to transesterify **4.93** using DMAP in toluene at high temperature — conditions we typically employed for transesterification of β-ketoesters — caused the solution to rapidly turn an opaque black. TLC and a ^{1}H NMR spectrum of the crude residue each showed a complex mixture of products (**Figure 52**, **B**, **entry 2**).

Finally, we came across the class of distannoxane catalysts popularized by Otera that have proven highly effective for transesterifications, especially in the case of β-ketoesters and sensitive substrates.[277] We were emboldened by reports from Schreiber[278] and Trost[279] who found Otera's catalyst to be uniquely effective in the preparation of iodoacrylate ester **4.100** and diketopiperazine **4.104**, respectively (**Figure 52**, **D**). While putatively "Otera's catalyst" refers to 1,1,3,3-tetrabutyl-1,3-diisothiocyanatodistannoxane, we did not possess the reagents necessary to prepare it or the time necessary to acquire those reagents.[280] Otera's original report describes a related distannoxane **4.98** that showed similar effectiveness and was easily prepared from dibutyltin(IV) chloride and dibutyltin(IV) oxide in 40% yield after recrystallization (**Figure 52**, **C**).[277a] To our relief, use of 10 mol% of **4.98** accomplished the transesterification of methyl furanoate **4.93** into allyl furanoate **4.92** in 58% isolated yield (**Figure 52**, **B**, **entry 3**). Otera and colleagues showed that distannoxanes are highly effective transesterification catalysts for their ability to template the alcohol and ester in close proximity, and that this effect is magnified in non-polar solvents due to "reverse micelle" behaviour.[277a, 281] The realization of this transformation marked another key convergency point in our synthesis of hyperolactone C (**3.2**), and should allow for the preparation of various analogues bearing the same core scaffold.

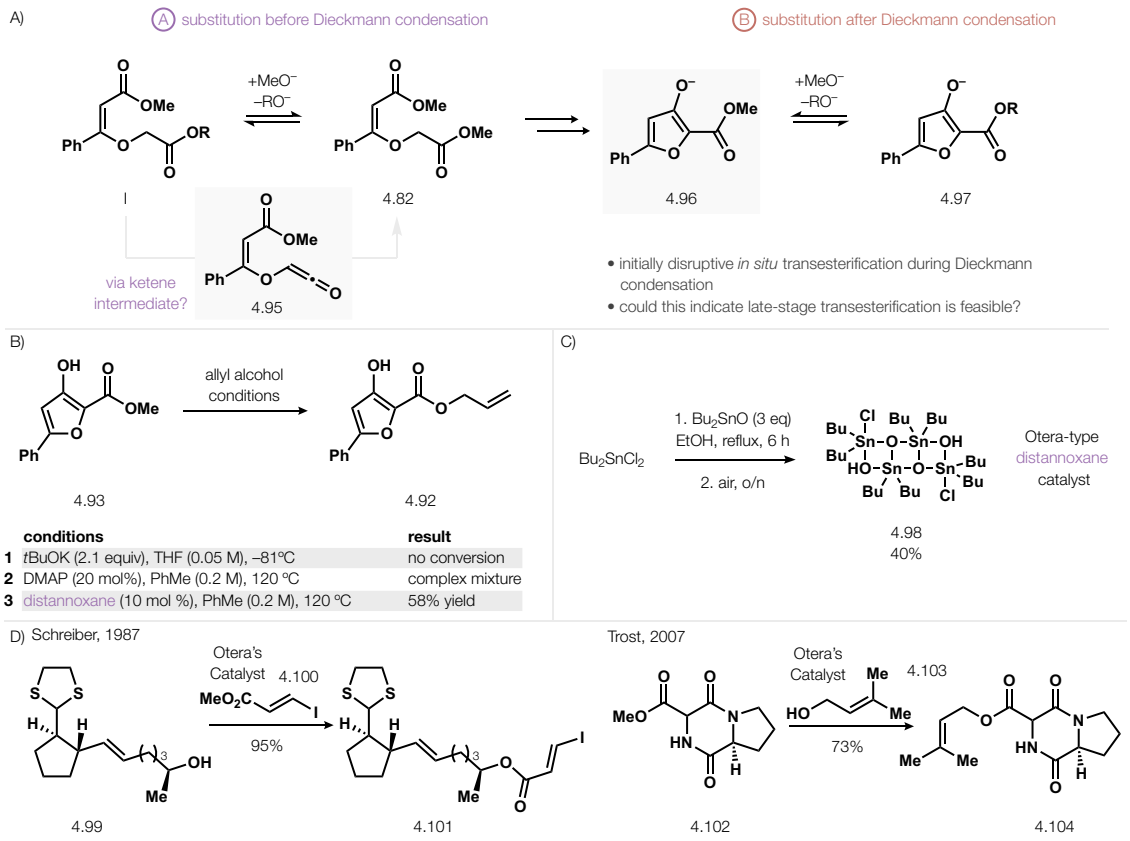
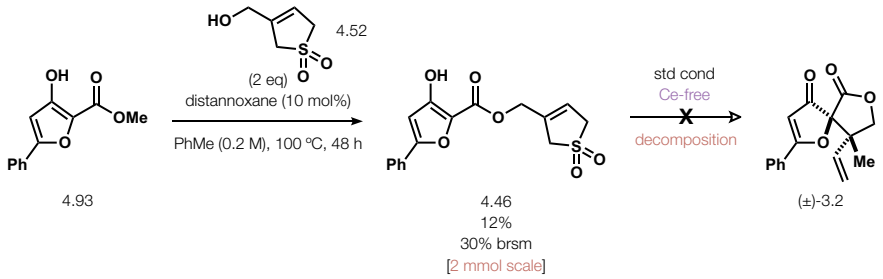


Figure 52. *Transesterifications of furanoate esters.*

A) Dieckmann condensation mechanisms for ester scrambling; B) Attempted transesterifications of methyl furanoate to allyl; C) Synthesis of distannoxane catalyst; D) Inspirational literature precedents.

Using this highly enabling transesterification, we attempted to quickly bring an end to the synthesis through the hypothesized cyclization SO_2 extrusion cascade (see **Scheme 20**, **B**). To this end, transesterification of **4.93** with hydroxymethyl sulfolene **4.52** under distannoxane conditions yielded the desired ester (**4.46**) in only 12% isolated yield (30% brsm, **Scheme 23**). Regardless, we obtained enough material for a test reaction employing our Ce-free redox-neutral photoredox catalysis conditions for hydroalkylation. This test showed significant decomposition, and the components of this mixture could not be identified by ^{1}H NMR spectroscopy. This test, coupled with the difficulties we had experienced in the preparation of the diene substrates, convinced us we needed to rethink the final step of the synthesis. Principally, we were concerned with amount of effort needed to supply the alkene/diene subunit in the oxidation state necessary for a redox-neutral cyclization.



Scheme 23. *Attempted synthesis of (±)-hyperolactone C through a redox-neutral hydroalkylation/SO_2 extrusion cascade.*

4.6 Rethinking the Dearomative Radical Spirocyclization

From the standpoint of synthetic burden, our redox-neutral hydroalkylation approach as the final step of the synthesis required us to supply the substrate in the same oxidation state as the desired product, hyperolactone C (**3.2**). To reliably achieve this required a multi-step sequence to effect an allylic C–H oxidation of isoprene (**Figure 53**, **A**). However, this was not the only difficulty we foresaw with a redox-neutral hydroalkylation for the final step of the reaction.

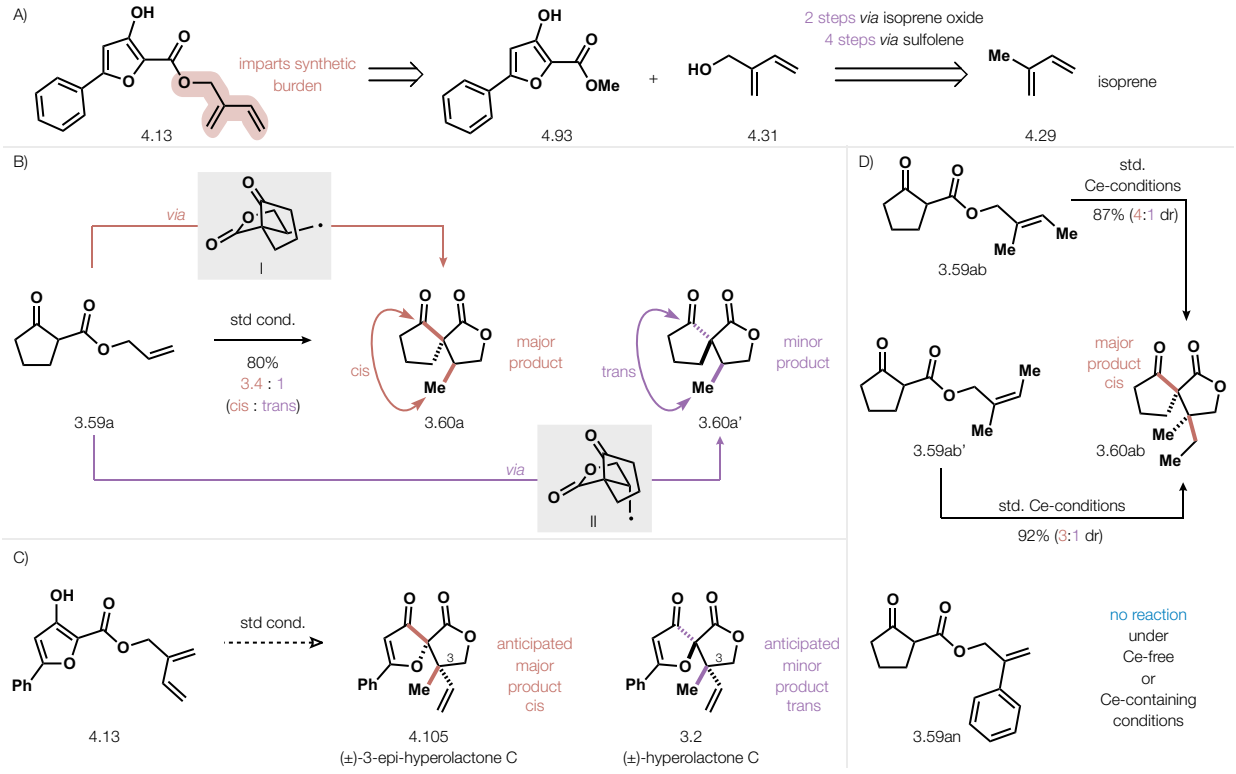


Figure 53. *Redox-neutral hydroalkylation prospects.*
A) Stereochemical outcome on typical hydroalkylation substrates; B) Anticipated diastereoselectivity for redox-neutral hydroalkylation of diene furanoate towards hyperolactone C; C) Relevant scope examples.

Previously, we had observed that the stereochemical outcome of the hydroalkylation reactions was the result of the difference in stability of the cyclized radicals, since the 5-*exo-trig* cyclizations were reversible and the computed

HAT TS energies were identical for each diastereomer (of course, this assumed that the final selectivity holds for a Boltzmann-weighted TS conformer analysis). Additionally, we found during our substrate scope that in cases where some diastereoselectivity was observed, that the major product has *cis* relative stereochemistry (**3.60a**) while the minor product had *trans* (**3.60a'**) relative stereochemistry (**Figure 53**, **B**). In the context of (±)-hyperolactone C (**3.2**), the implication for this was that cyclization of a diene substrate (**4.13**) would likely deliver undesired (±)-3-*epi*-hyperolactone C (**4.105**) as the major product of 5-*exo*-*trig* cyclization, while the natural diastereomer **3.2** would be produced as the minor product (**Figure 53**, **C**). As we had seen in our hydroalkylation substrate scope, diastereoselectivity ranged from moderate ~5:1 to completely unselective 1:1 (excluding cases where product epimerization impacted dr). Given how concise the projected synthesis of **3.2** was, we were willing to risk producing the NP as the minor diastereomer in the final reaction while hoping for a completely unselective 1:1 reaction. Compounds **3.59ab** and **3.59ab'** initially bolstered our confidence that this reaction could work sufficiently well, while the failure of substrate **3.59an** to react was cause for concern (**Figure 53**, **D**). While exploring the various routes outlined in the preceding subchapters, we also applied a computational analysis to predict what the selectivity might be on substrate **4.13**.

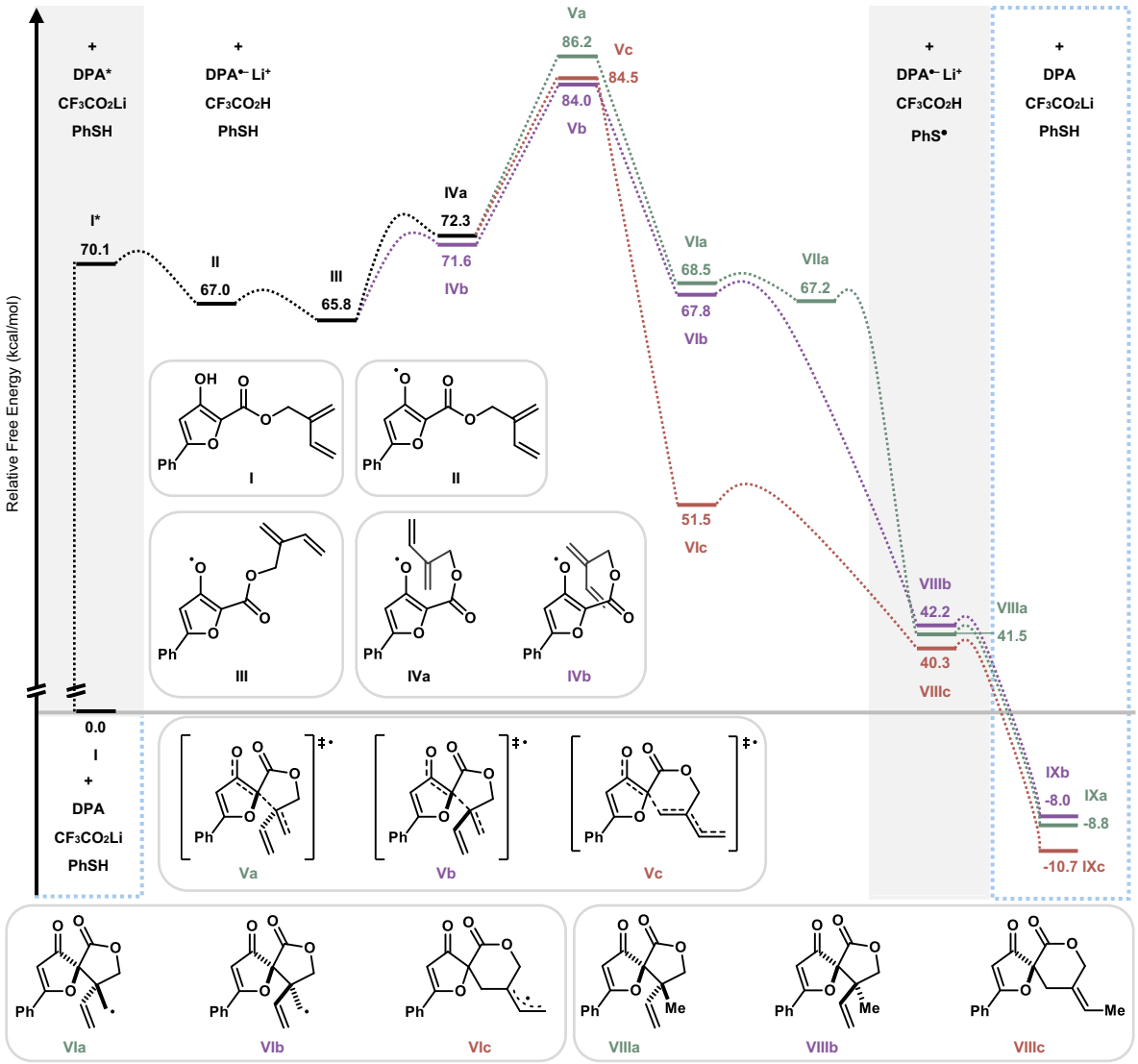


Figure 54. *uM06-2X/LanL2DZ reaction coordinate for the redox-neutral hydroalkylation of diene furanoate ester (relative energies in kcal/mol).*

Using the same computational workflow as for the spirocyclizing hydroalkylation of substrate **3.59a** (**section 3.6**), we assessed the various reactive conformers that might participate in the redox-neutral hydroalkylation of **4.13** (**Figure 54**). We unfortunately discovered a kinetically competitive 6-*endo-trig* cyclization to give [4.5]-spirocylic intermediate **VIc**, which bears a delocalized allylic radical. Unsurprisingly, this intermediate radical species was significantly lower in energy (> 16 kcal/mol) than the corresponding 1º radicals derived from the 5-*exo-trig* cyclization (**VIa** and **VIb**). This predicted selectivity was both unsurprising and disheartening as we had not observed substantial quantities of 6-*endo-trig*-derived [4.5]-spirocycles from any substrate in our methodology scope, even in cases where they might be expected to predominate (see **Figure 34**, compounds **3.60aa** and **3.60ab**). Yet, the evidence for

reversible cyclization of these substrates, coupled with radical cyclization first principles, suggested we should be observing these [4.5]-spirocycles as significant contributors to our product distribution. Our computational work on base substrate **3.59a** suggested the reason we had not seen such products before was due to the high barrier to 6-*endo-trig* cyclization, resulting in a kinetically controlled reaction. As the 6-*endo-trig* TS (**Vc**) now appeared to be kinetically competitive with the undesired 5-*exo* (**Vb**), and drastically preferable to the desired 5-*exo* (**Va**), we were now greatly concerned about the validity of our earlier gamble on diastereoselectivity.

The combination of these factors made it unlikely that we would isolate substantial quantities of (±)-hyperolactone C (**3.2**), if we managed to progress all through this redox-neutral hydroalkylation route using the diene-bearing substrate **4.13**. These concerns, coupled with our difficulty in preparing enough of substrate **4.13**, caused us to consider alternative S_H2' cyclization strategies (**Figure 55**, **A**). While formation of dispiro compounds had proven unreliable in our hydroalkylation method (**3.60aj** and **3.60ak**) we hypothesized that this could be due to the reversibility of the cyclization caused by the formation of such a sterically congested core. As such, we thought that SO_2 extrusion might provide an irreversible drive towards product formation and render the reaction much more efficient in the case of substrate **4.46**. Of course, the diastereoselectivity in the cyclization of dispirocyclic compound **4.46** was unknown. As we learned experimentally, the hydroalkylation of compound **4.46** did not prove viable and major decomposition of the starting material was instead observed (**Scheme 23**). Contemporaneously, we had imagined that a substrate with an alkene bearing a radical leaving group at C4 could be prepared from the 1,4-dibromoolefin **4.30** and that this compound would benefit from the same diastereo- and regioselectivity benefits as the sulfolene compound **4.46**. Based on this, several S_H2' cyclization substrates were imagined that might have been worth investigating. Overall, we found that installation of 1,4-distributed functionalities was step intensive and time constraints once again caused us to prioritize a more direct route to the natural product.

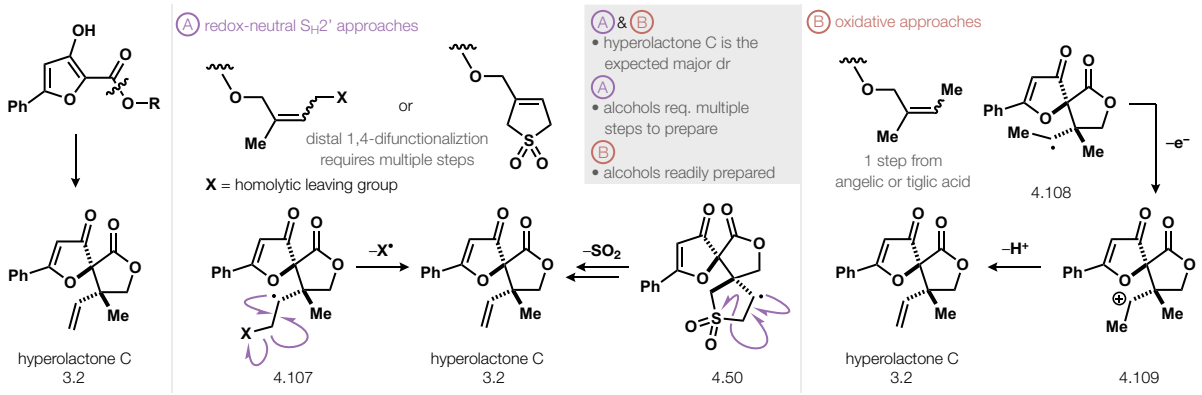


Figure 55. *Alternative radical cyclization strategies for the preparation of hyperolactone C. A) Redox-neutral S_H2' approaches; B) Oxidative approaches.*

We were also aware that an oxidative cyclization of tiglyl- or angelyl-furanoate esters (**4.114 or 4.114'**) could yield hyperolactone C (**3.2**, **Figure 55**, **B**). In contemplating what would constitute an ideal synthesis of hyperolactone C (**3.2**), we considered efficiency in terms of step count, starting material availability, and use of steps that represented significant leaps in complexity. The alcohols required to access a substrate for oxidative spirocyclization could be obtained from simple reduction of the commercially available tiglic (**4.111**) or angelic acids. Cyclization of such substrates had already been tested under our redox-neutral conditions (**3.59ab & 3.59ab'**) and the observed diastereo- and regioselectivities suited the formation of the natural product. Of course, an oxidative cyclization was not what we had initially developed and could potentially be performed using existing $Mn(OAc)_3$ systems, but we anticipated that a mild photoredox method to perform such cyclizations may have greater substrate tolerance and see broader applicability beyond the hyperolactone family. As a result, we decided to develop a net-oxidative reaction from our redox-neutral conditions and evaluate it against existing methods.

4.7 Oxidative Cyclization Reaction Development

To realize the desired oxidative transformation, we imagined using a single electron oxidant in place of the disulfide co-catalyst. At the top of our list of single electron oxidants were copper(II) salts due to their history of success in the context of C-centred radical oxidation and elimination.[282] This is a rich area of redox chemistry that was pioneered by Kochi, has been extensively studied, but in this context, it is appropriate and sufficient to regard Cu(II) species as single electron oxidants that can convert C-centred radicals to alkenes either by oxidation and elimination or by β-hydride elimination.[282-283] Under this reaction regime, we imagined the modified catalytic cycle in which turnover of the 9,10-DPA radical anion and the oxidation of the cyclized radical IV are accomplished using Cu(II) (**Figure 56**).

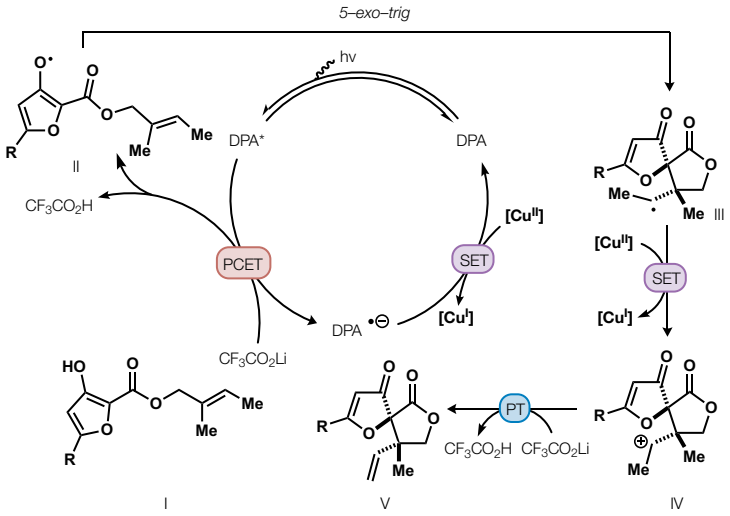
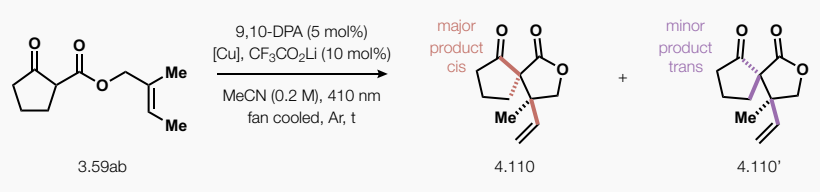


Figure 56. *Tentative catalytic cycle for the oxidative cyclization reaction.*

To realize an oxidative cyclization based on our Ce-free photoredox platform, we began with the model substrate **3.59ab** and set about screening common Cu(II) sources and reaction conditions (**Table 27**). While one could imagine a system in which the Cu(II) oxidant is turned over by another terminal oxidant to render copper catalytic, we reasoned that the low cost of most Cu(II) salts made this unnecessary at the outset. Additionally, we imagined that use of oxygen or some alternative terminal oxidant could drastically alter the reaction profile, producing side products.

Table 27. *Oxidative cyclization optimization*



Entry	[Cu] (equiv)	Time (h)	% SM Remaining (3.59ab)	% Product (dr, cis:trans)
1[a]	$Cu(OTf)_2$ (2)	22	–	10 (n.d.)
2[a]	$Cu(OTf)_2$ (2)	2	trace	10 (n.d.)
3[b]	$Cu(OTf)_2$ (2)	2	8	10 (n.d.)
4[a]	$Cu(OTf)_2$ (2)	0.17	12	9 (n.d.)
5[a]	$Cu(OAc)_2$ (2)	15	62	25 (> 20:1)
6[a]	$Cu(EH)_2$ (2)	18	68	8 (n.d.)
7[b]	$Cu(hfac)_2$ (2)	15	50	11 (n.d.)
8[a]	$CuCl_2$ (2)	2	27	trace
9[a]	$CuBr_2$ (2)	2	0	0
10[a]	$Cu(BF_4)_2$•xH_2O (2)	15	20	20 (8:1)
11[a]	$CuSO_4$ (2)	16	74	12 (n.d.)
12[a]	$Cu(TFA)_2$•xH_2O (2)	16	31	60 (4:1)
13[a]	$Cu(TFA)_2$•xH_2O (2)	48	26	60 (4:1)
14[a, c]	$Cu(TFA)_2$•xH_2O (3)	16	8	79 (3.8:1)

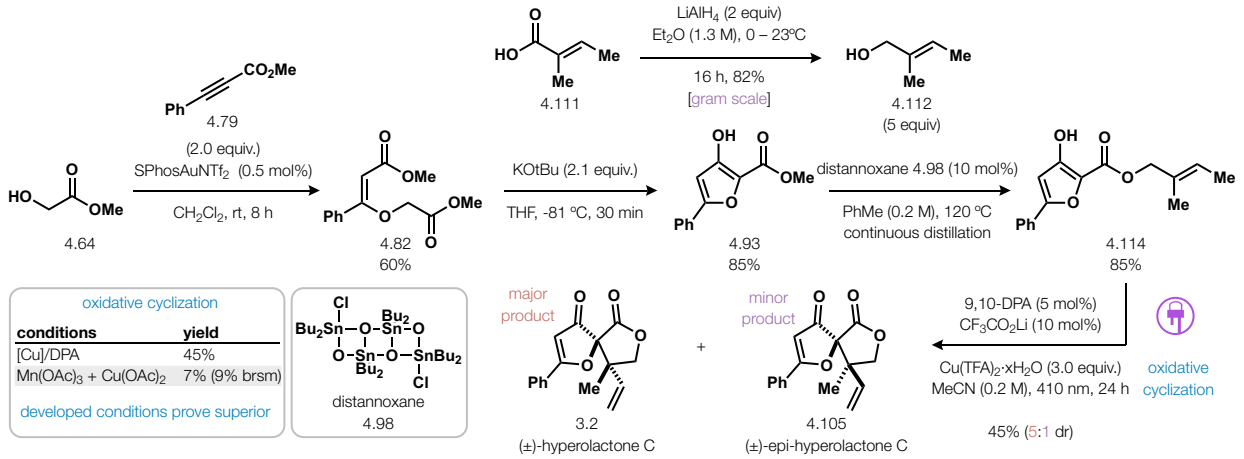
[a]aqueous NH_4Cl work-up; [b]aqueous EDTA work-up; [c]isolated yield; n.d. = not determined. $Cu(TFA)_2$•xH_2O prepared and tested by Tegan E. O'Brien.

We began with $Cu(OTf)_2$ under the assumption that its higher solubility in acetonitrile might be beneficial to the reaction. Running the reaction for 22 hours of irradiation at 410 nm with 10 mol% LiTFA and 5 mol% 9,10-DPA resulted in a 10% ^{1}H NMR yield of the desired spirocyclic product **4.110** with complete consumption of the starting material (**entry 1**). Fearing the low yield might be the result of product decomposition, we repeated the same conditions for a 2-hour reaction period and obtained the same result (**entry 2**). The poor mass balance obtained from the short reaction caused us to revise our work-up strategy. Changing our washing solution from NH_4Cl to EDTA to remove copper waste had little impact on our ability to recover and identify more of the mass balance from this reaction (**entry 3**). Once more we tried to decrease the reaction duration, this time to just 10 minutes and once more we obtained a poor mass balance accounting for only 21% of the material used (**entry 4**). At this point we found it difficult to believe that shorter reaction times would drastically improve the yield or mass balance of the reaction. These results prompted us to continue exploring the identity of the copper species.

Immediately we saw marked increases in mass balance recovery and the yield of desired product **4.110**. $Cu(OAc)_2$ gave a 25% yield with 62% remaining starting material (**entry 5**). Copper(II) 2-ethylhexanoate ($Cu(EH)_2$) gave a similar return of starting material **3.59ab** (68%) but with a diminished yield of product **4.110** (8%) (**entry 6**).

Copper(II) hexafluoroacetylacetonate gave a poor yield of 11% with only 50% starting material (**3.59ab**) recovered after 15 hours of irradiation and this reaction required EDTA washes in the work-up to sufficiently remove copper impurities for analysis (entry 7). Copper(II) chloride, copper(II) bromide, and copper(II) tetrafluoroborate all performed poorly under the reaction conditions (**entries 8–10**). Copper(II) sulfate gave an excellent 86% recovery of mass balance but gave only a 12% yield of the desired product (**4.110**, **entry 11**). The major breakthrough came from the use of copper(II) trifluoracetate as the stoichiometric oxidant (**entry 12**). Using $Cu(TFA)_2 \bullet xH_2O$, we obtained a 60% ^1H NMR yield of the desired product after 16 hours of reaction with 30% unreacted starting material remaining. The superior effectiveness of the $Cu(TFA)_2$ system reinforces the privileged status of the trifluoroacetate anion in our 9,10-DPA catalyzed oxidation of enols. Increasing the reaction time from 16 to 48 hours did not result in a greater conversion of starting material to product (**entry 13**). Increasing the Cu(II) oxidant loading from 2 to 3 equivalents gave an improved yield of 79% **4.110** with 92% consumption of starting material **3.59ab** (**entry 14**). With these optimized conditions in hand, we were confident we could accomplish our concise synthesis of hyperolactone C (**3.2**).

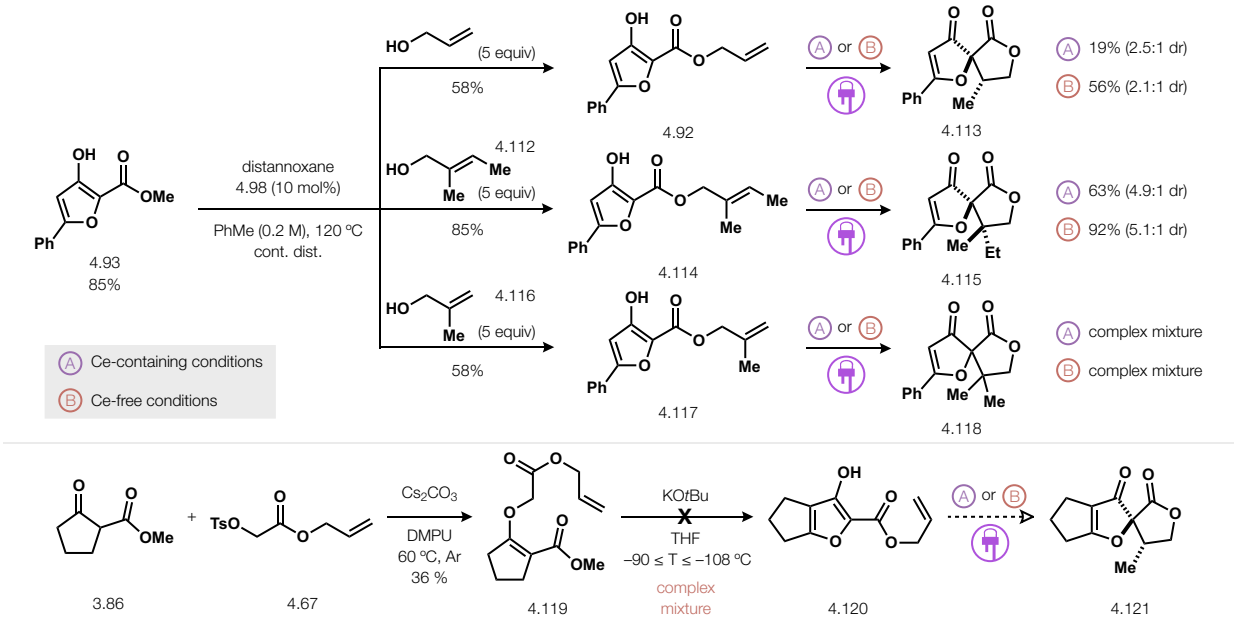
4.8 Completion of the Total Synthesis of (±)-Hyperolactone C and Derivatives



Scheme 24. *Four-step total synthesis of (±)-hyperolactone C through oxidative cyclization.*

Our synthesis commenced with the gold(I)-catalyzed 1,4-addition of commercially available methyl glycolate (**4.64**) on to methyl phenylpropiolate (**4.79**), producing the *Z*-enol ether (**4.82**) in 60% yield (**Scheme 24**). The subsequent Dieckmann condensation of *Z*-enol ether **4.82** delivered methyl hydroxyfuranoate **4.93** in 85% yield. Transesterification using Otera-type distannoxane catalyst **4.98** under continuous distillation conditions with tiglyl alcohol (**4.112**) delivered key substrate **4.114** in 85% yield.

With precursor **4.114** in hand, we applied our oxidative cyclization conditions to yield (±)-hyperolactone C (**3.2**) and (±)-3-*epi*-hyperolactone C (**4.112**) in 45% yield and 5:1 ratio favouring the natural product. For comparison, we also attempted oxidative cyclization of **4.105** using $Mn(OAc)_3/Cu(OAc)_2$ conditions,[356] which resulted in only a 7% NMR yield (9% brsm) with the remaining mass balance unidentifiable. This new route, featuring a key dearomative photocatalytic oxidative spirocyclization, resulted in the concise 4-step synthesis of hyperolactone C (**3.2**), the shortest synthesis to date.



Scheme 25. *Synthesis of unnatural analogues of (±)-hyperolactone C through redox-neutral hydroalkylation.*

Our modular approach using a distannoxane-catalyzed transesterification also allowed for rapid diversification of the substituents on the lactone ring (**Scheme 25**, **top**). Transesterification with allyl alcohol gave allyl furanoate **4.92** in 58% yield which could be elaborated to *des*-vinyl-hyperolactone C (**4.113**) in 19% or 56% yields under Ce-containing and Ce-free conditions, respectively (**Scheme 25**, **top**). Dihydro-hyperolactone C derivative **4.115** could be obtained from the same furanoate ester used for hyperolactone C (**4.114**) by employing our redox-neutral conditions. In this case, Ce-containing conditions (**A**) gave **4.115** in 63% yield and 4.9:1 dr while the Ce-free conditions (**B**) resulted in an excellent 92% isolated yield of product **4.115** with a 5.1:1 dr (**Scheme 25**). We then prepared methallyl furanoate derivative **4.117** in 58% yield for use under hydroalkylation conditions. Unfortunately, all attempts to prepare the simplified *gem*-dimethyl hyperolactone derivative **4.118** resulted in complex mixtures. We suspect that the absence of a methyl group at the terminus of the olefin results in less steric hindrance

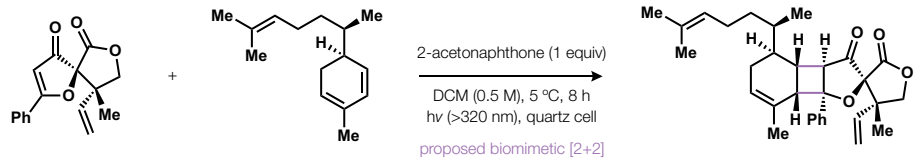
in the *6-endo-trig* TS making this process competitive with *5-exo-trig* cyclization, producing an inseparable mixture of compounds.

Additionally, we prepared mixed diester **4.119** in 36% yield through *O*-alkylation of methyl 2-oxocyclopentanecarboxylate (**3.86**) with allyl α-tosylglycolate (**4.67**) under our previously used conditions (**Scheme 25**, **bottom**). Unfortunately, all attempts to effect Dieckmann condensation on this substrate produced complex mixtures with only trace product observed. We suspect this furanoate product (**4.120**) degrades more readily than the above derivatives due to the increased angular strain present in the furanone system imposed by the 4,5-ring fusion. This hypothesis is congruent with earlier observations showing the benzofuranone derivative **3.59o** was less stable than the corresponding styrenone derivative **4.93**. This would result in the following tentative trend for stability of 3-hydroxy-2-furanoate ester derivatives: 4,5-cycloalkyl fused << 4,5-benzo fused < non-fused, although more investigation is necessary to establish this. Ultimately, this caused us to abandon the pursuit for the *des*-vinyl fused cyclopentafuranone derivative **4.121**.

Overall, this concise sequence provides a valuable opportunity to develop structure-activity relationship (SAR) studies on this bioactive natural product.[238f] As my journey in the lab was coming to an end, however, I only had time for one more elaboration on this strategy.

4.9 Application of (±)-Hyperolactone C towards Natural Product Anticipation

Once we had completed its synthesis, we were drawn to explore the photochemical behaviour of hyperolactone C. Our interest in this arose because of a biosynthetic hypothesis put forth by Lee and colleagues for the related natural product biyouyanagin A (**4.4**).[243] The authors proposed that an intermolecular [2+2] photocycloaddition between hyperolactone C and the monocyclic sesquiterpene *ent*-zingiberene occurs to forge the cyclobutane ring system. Later work from Sarlah, Shaw, and Nicolaou revised the structure of biyouyanagin A (**4.4**), and supported its biosynthetic proposal, by synthesis of the natural product through the [2+2] photocycloaddition of hyperolactone C (**3.2**) and *ent*-zingiberene (**4.122**) under UV irradiation sensitized by 2-acetonaphthone (**Scheme 26**).[238d]



Scheme 26. *Nicolaou, Sarlah, and Shaw's biomimetic [2+2]-photocycloaddition in the synthesis of (–)-biyouyanagin A.* [238d]

If this natural product is indeed produced *via* an intermolecular [2+2] photocycloaddition, are there other natural products in the literature that are suspected, or known, to be derived from such a transformation? To date, I have not found any other examples where an intermolecular biosynthetic [2+2] photocycloaddition has been proposed. I also wondered if there might be undiscovered natural products that arise from this kind of photochemical intermolecular coupling, including coupling of hyperolactone C (**3.2**) with other olefinic natural products. Hyperolactone C (**3.2**) is likely the photoactive species in the coupling with *ent*-zingibrene (**4.122**) due to the greater conjugation present in its 4-phenylenone chromophore. In this case, other competent coupling partners may exist aside from *ent*-zingibrene (**3.2**). There were three cases I considered for how this coupling selectivity might arise.

The first case is an argument for specificity rather than selectivity. In this scenario, the [2+2] photocycloaddition could be mediated by an enzyme that imposes a substrate specificity on this reaction, though finding no other examples of natural products derived from intermolecular [2+2] photocycloadditions I found this to be an unlikely scenario. There have been recent reports on Diels-Alderase enzymes that demonstrate competitive [2+2] activity,[284] however, along with reaction promiscuity these Diels-Alderases have also documented substrate promiscuity.[285] These studies suggest that even if this [2+2] is catalyzed by a Diels-Alderase enzyme it might not confer substrate or product specificity.

The second case would rely on a kinetics-dictated model for selectivity in which the pairing of (–)-hyperolactone C (**3.2**) and *ent*-zingiberene (**4.122**) results in the most facile photo-[2+2] reaction. Under this model, alkene coupling partners cannot react with excited state (–)-hyperolactone C (**3.2***) before *ent*-zingiberene (**4.122**) does, which leads to selective coupling. *A priori,* I cannot imagine a mechanistic reason why this cross-coupling would outcompete other potential cross-couplings with similar olefin partners to a degree significant enough for (–)-biyouyanagin A (**4.4**) to be the sole product of this reaction. The only other way to improve the cross-coupling selectivity through a kinetic rationale would be to ensure that the *ent*-zingiberene (**4.122**) coupling partner is present in sufficient excess to alternative coupling partners, such that the rate of adduct formation with **4.122** is greater than

all other coupling partners. This rationale is subject to the biochemical conditions present within the plant. Even assuming these factors favour the selective formation of (–)-biyouyanagin A (**4.4**), it is plausible that trace natural products might be produced alongside it by the same [2+2] process. Isolation of such trace natural product components would provide support for the proposed photo-[2+2] biosynthetic step.

The third possibility is a thermodynamics-dictated model for selectivity. Under this model, the [2+2]-photocycloadditions of (–)-hyperolactone C (**3.2**) with a variety of alkenes would need to be a reversible process *and* (–)-biyouyanagin A (**4.4**) would have to be the lowest energy adduct to be the sole product of this reaction. As the chromophoric 4-phenylenone π-system present in hyperolactone C (**3.2**) is absent in (–)-biyouyanagin A (**4.4**), the forward and reverse of the [2+2] reaction would have to occur through different mechanisms. The loss of this chromophore would result in the need for higher energy light to effect the reverse reaction, or for a thermal mechanism to operate. This leads to a scenario wherein a photostationary state, rather than a true thermodynamic equilibrium, dictates the product distribution under competition/crossover conditions. While photostationary states arising from photo-[2+2] reactions are not unknown,[286] to the best of my knowledge, this would be the first report of such a scenario in the context of natural product biosynthesis. Even if this selectivity model were at play, the biyouyanagins are unlikely to be the only compounds produced in this way. Given the bioactivities of (–)-biyouyanagin A (**4.4**) and (–)-hyperolactone C (**3.2**),[238f, j] it is possible that an even more active member of this natural product family remains to be discovered. Even if these missing compounds are produced in infinitesimal quantities, if their activity is high enough, they may confer an evolutionary benefit to the producing species.

Many biyouyanagin natural products may currently remain undiscovered. Nicolaou and Sarlah explored the breadth of products formed upon [2+2]-photocycloaddition of (–)-hyperolactone C (**3.2**) and various zingiberene stereoisomers discretely, and in competition experiments, towards their revision of the structure of (–)-biyouyanagin B (**4.6**).[238h, 242] Unfortunately, the authors did not perform a crossover experiment, so it remains to be seen whether these products can equilibrate to a photostationary state. In any case, we were more concerned with any new natural products outside of the biyouyanagin family that might be formed *via* the photo-[2+2] of hyperolactone C (**3.2**) with some other alkene partner that might be present in the same plant species.

Importantly, we questioned whether hyperolactone C (**3.2**) could dimerize with itself. After all, **3.2** has both an olefin moiety in the C1=C2 vinyl group as well as the necessary chromophore for excitation. A photo-[2+2] dimerization does not require prior knowledge about other olefinic compounds that might be produced by the same

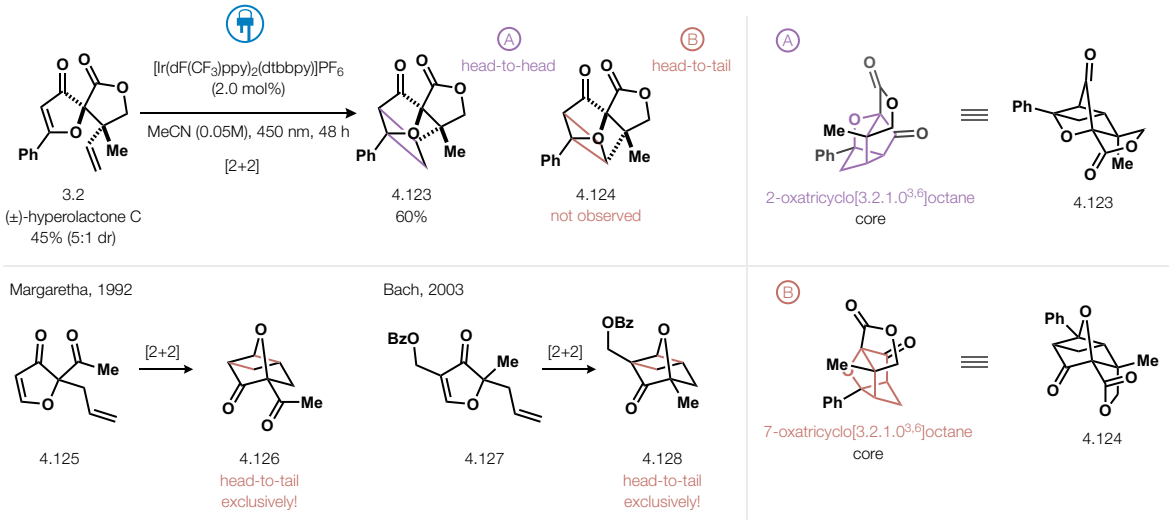
plant species that produces **3.2**, or which compounds might be produced in the same tissues or cellular compartments. We could, however, be confident that hyperolactone C (**3.2**) is produced in the same location as itself!

Based on this, we decided to simply set up a photo-[2+2] reaction with the material we had obtained from our initial synthesis of hyperolactone C (**3.2**). As this material was a 5:1 mixture of diastereoisomers, and racemic, we anticipated that the reaction would likely be an isomeric mess of various dimers and oligomers. There existed the possibility of homo- and heterochiral dimers, arranged in head-to-head or head-to-tail fashion, with *endo* or *exo* diastereomeric additions, and approach of vinyl group to the α or β faces of the enone. Based purely upon combinatorial consideration, this material could produce up to $2^5 = 32$ different stereoisomers, just from the dimerization of the racemic hyperolactone C (**3.2**) material, without accounting for the racemic epimer present in our starting material. Regardless, we had hoped that some homochiral product might be formed in significant enough excess for isolation and characterization. If such a compound could be prepared, then it is plausible that it could form in nature where hyperolactone C (**3.2**) is produced as a single enantiomer.[241]

Submitting our material to blue light irradiation with an iridium(III) photosensitizer in anhydrous acetonitrile under an atmosphere of argon for 48 hours gave the delightful result of a single major compound (**Scheme 27**). Upon isolation we discovered that the product had much simpler NMR spectra than anticipated, corresponding to compound **4.123**. Extensive 2D NMR analysis suggested that we had formed head-to-head dimer **4.123** exclusively and in 60% isolated yield.

There is precedent for oxatricyclo[3.2.1.$0^{3,6}$]octane or tricyclo[3.2.1.$0^{3,6}$]octane cores prepared through intramolecular photo-[2+2] cycloaddition (**Scheme 27**).[287] Margaretha and colleagues had previously studied the photochemical preparation of many such systems, including the photo-[2+2] of allylated furanone derivatives **4.125**.[288] The authors obtained exclusively the head-to-tail regioisomer in these furanone systems, in direct contrast to our observed selectivity though we are awaiting SCXRD analysis to confirm our assignment. Crucially, Margaretha and colleagues demonstrated that the allyl furanones (**4.125**) could form oxatricyclo[3.2.1.$0^{3,6}$]octane (**4.126**) products through direct excitation using UVA light (350 nm). Additionally, the authors demonstrated that a phenyl substituent is not necessary for excitation and reaction of these furanone derivatives occurs under direct excitation at this wavelength. This demonstration of reactivity strongly suggests that hyperolactones A (**4.1**) and B (**4.2**) might also undergo photo-[2+2] reactions (**Figure 45**). Later work form Bach and colleagues corroborated Margaretha's findings and further demonstrated the impacts of alkene tether length on the regioselectivity obtained from the photo-[2+2] of

2-alkenyl-3(2*H*)-furanones.[289] In this work, Bach and colleagues showed that the head-to-tail photoproduct (**4.128**) was formed exclusively with allylic substrates (**4.127**), while the head-to-head product forms exclusively from homoallylic substrates. In this work, Bach also claims that McMurry *et. al* demonstrated an instance of equilibration during a photo-[2+2] reaction.[290] McMurry does indeed show a 2:1 regioisomeric ratio that changes to 19:1 upon further irradiation. McMurry even claims that no alternative photoproducts from the minor regioisomers could be identified which would suggest it had equilibrated to the major isomer. However, as McMurry could not separate the two regioisomers to submit the minor to individual photolysis conditions or to determine the mass balance of this process, we cannot be sure whether photochemical equilibration or a photochemical resolution (*via* minor isomer reaction/decomposition) is the mechanism by which this enrichment occurs.



Scheme 27. *Intramolecular [2+2]-photocycloaddition of (±)-hyperolactone C and other photochemical syntheses of tricyclo[3.2.1.0^{3,6}]octanes.*

Given the remarkable selectivity and efficiency with which product **4.123** was formed, it is worth reflecting on the potential biosynthetic implications. *A priori*, we can expect intramolecular reactions to proceed more rapidly than intermolecular reactions. Critically, Nicolaou's biyouyanagin formation *via* intermolecular photo-[2+2] was performed at high concentrations (≥0.5 M) with a large excess of *ent*-zingiberene (**4.122**). These conditions would serve to increase the rate of intermolecular reaction to the point where it could outcompete the intramolecular reaction. Given our demonstration of this intramolecular [2+2], we can be reasonably confident that it would occur as a background reaction and is favoured when zingiberene concentrations are low. As such, it is highly plausible that the product **4.123** is a hyperolactone natural product family member that has yet to be isolated![291] Analogously, caged

compounds derived from the intramolecular photo-[2+2] of hyperolactones A and B might one day be discovered in nature.

4.10 Comparison of Hyperolactone C Total Syntheses

Having prepared (±)-hyperolactone C (**3.2**) in short order, we wished to compare the present approach to those already reported in the literature. We identified seven total syntheses of hyperolactone C (**3.2**) prior to ours, beginning with the 2001 report by Kinoshita.[238b, c, 238e-g, i, m] To broadly compare our synthesis to previous reports, our 4-step approach is the shortest synthesis of this natural product, to date. However, our approach produces racemic material whilst the Kinoshita,[238b] Nicolaou,[238d] and 2011 Hodgson[238i] approaches are enantiospecific, and Xie[238g] and Feng's[238m] approaches are enantioselective. As both stereocenters are set in the final step of our synthesis, we would need to develop an asymmetric oxidative cyclization to achieve an enantioselective synthesis. In lieu of a detailed comparison of the benefits and shortcomings of all 8 syntheses, we opted to compare all the approaches simultaneously by plotting the Böttcher complexity scores of each intermediate against the step number in that synthesis (**Figure 57**).[292]

The Böttcher complexity scoring system was created by Thomas Böttcher and reported in 2016 as a method to quantify intrinsic chemical complexity using chemical structure information.[292] In synthetic chemistry, we typically think about the extrinsic complexity of a compound of interest.[293] That is, we most often think about the structural features that are easily cleared and those that impart significant synthetic burden — subjective criteria. As new and enabling chemical methods are developed, extrinsic complexity for compounds will decrease. Intrinsic complexity metrics attempt to objectively quantify the information content of a molecule based on its structure without consideration of the synthetic difficulty these features impart. There have been many approaches to compute intrinsic molecular complexity and to discuss them all would be outside the scope of this section.[294]

Briefly, Böttcher's approach to computing molecular complexity (C_m) assesses the information content of the individual atoms within a compound and then uses the sum of these individual values as the complexity score for the molecule in molecular bits of information (mcbits).[292] As a result of this approach, the addition of new substituents to a compound does not alter the complexity of the original subunits and *vice versa*. Bonds to hydrogen atoms are considered the default state within this approach and so do no contribute to the information content of an atom. This approach describes the complexity at each atom using five variables; one describes the valence shell of the element while the remaining four describe the bonding environment around that atom. The bonding environment of an atom

is described by the number of bonds, the number of bonds that are chemically distinct, the array of elements that are bound to the atom of interest, and the stereochemistry at this atom. Molecular symmetry is accounted for such that chemically identical atoms contribute information content to C_m to a lesser degree than non-identical atoms.

This metric allows us to compare many syntheses graphically to see how C_m changes over each sequence *en route* to the target compound. With respect to hyperolactone C (**3.2**) total syntheses we can now see how our synthesis compares to those that came before by measuring C_m as a function of the steps remaining until hyperolactone C (**3.2**) is formed (**Figure 57**).

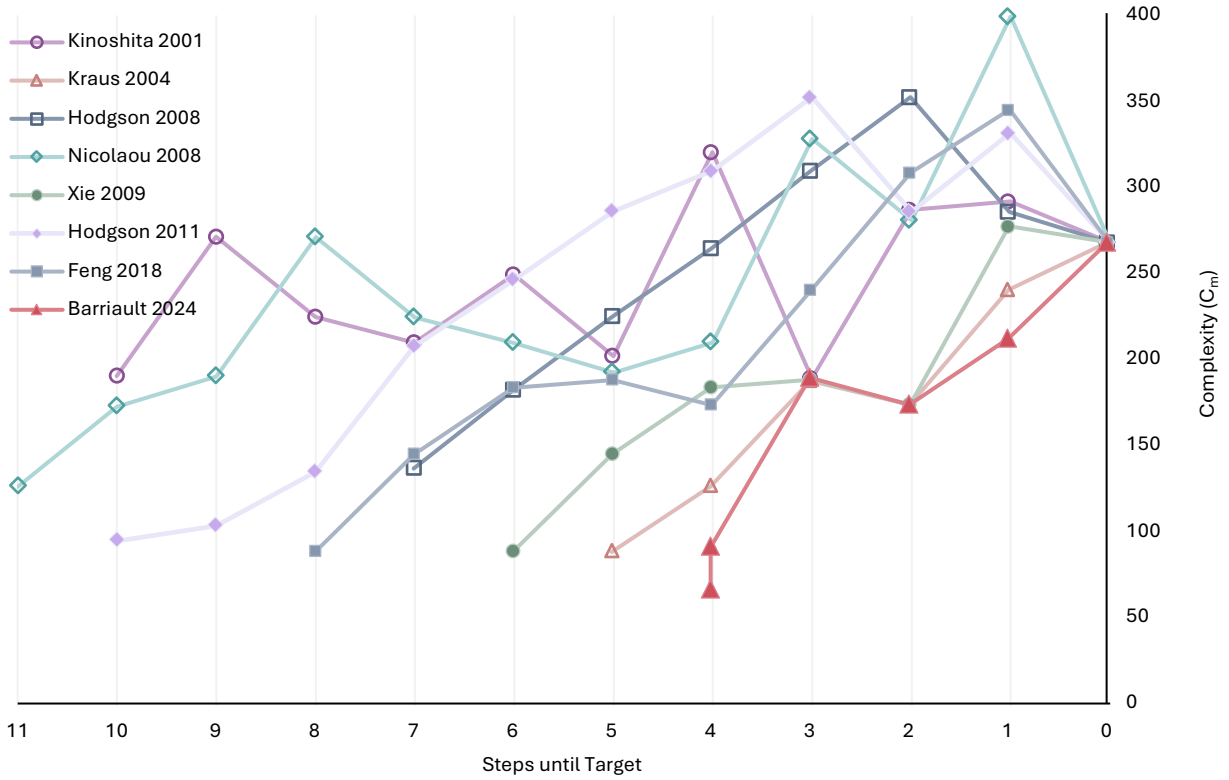


Figure 57. *Böttcher complexity score plotted against steps until hyperolactone C.*
See Chapter 4 Experimental Details for synthetic sequences and complexity scores for each intermediate. Calculated by Tegan E. O'Brien

The shortest syntheses, ours and Kraus' 2004 synthesis, both have relatively linear increases in C_m towards hyperolactone C (**3.2**) without ever surpassing the complexity of the final target (268.28 mcbits). Our syntheses converge in complexity 3-steps from hyperolactone C (**3.2**) and share a common intermediate, methyl furanoate **4.93**, at 2-steps from hyperolactone C (**3.2**). The decrease in complexity in these two syntheses between step –3 and –2 corresponds to the aromatizing condensations in both syntheses. From the methyl furanoate intermediate **4.93** at step

–2, Kraus' synthesis has a more substantial jump in complexity than in our synthesis. This is because Kraus incorporates the remaining 5-carbon unit as a more complex and higher oxidation state compound, (*E*)-4-chloro-2-methylbut-2-en-1-ol prepared from isoprene oxide. Our sequence approaches the target C_m more linearly from step –2 which allowed us to make use of a less complex 5-C subunit, tiglyl alcohol (**4.112**), and a final step that increases complexity more drastically than the final step of Kraus' synthesis.

Böttcher's analysis allows us to determine the complexity change for a given reaction class (ΔC_m^{rxn}) and it has been shown to be structure-independent within a homologous series. From this analysis we can see that $\Delta C_m^{ox.cyc.} = +55.83$ for our oxidative cyclization reaction, imparting a great deal of information content within a single step. For comparison, Böttcher demonstrates that in aldol additions $\Delta C_m^{aldol\ add.} = +40.68$, in aldol condensations $\Delta C_m^{aldol\ cond.} = +8.00$, and in azide alkyne cycloadditions $\Delta C_m^{a.a.\ cyc.\ add.} = +47.80$.

Critically, this analysis shows us that all the remaining syntheses exceed the target complexity at some point, with larger overshoots typically correlating to longer overall sequences. This is a natural consequence of incorporating superfluous substituents to facilitate synthesis which need to be removed to arrive at the target compound (protecting groups, auxiliaries, etc.).

By plotting C_m against steps until the target, we can also quickly see where two or more syntheses converge, diverge, or share common sequences. Nodes of identical complexity often share a common structure (or require a greater resolution in the y-axis). We can also observe and compare how complexity changes between different segments of a synthesis given that ΔC_m is constant for identical reactions. This representation nicely reflects how steps –9 to –6 of Nicolaou's 2008 approach and Kinoshita's 2001 approach pass through identical intermediates in an identical sequence. Similarly, the complexity change between steps –6 to –3 for Kinoshita's synthesis and steps –3 to 0 for Nicolaou's synthesis reflects the same 3-step sequence being performed within both syntheses: benzyl-ether deprotection followed by a two-step Grieco elimination sequence (alcohol to selenide substitution followed by selenide oxidation/*syn* elimination) to transform a C1-benzyl ether into the C1=C2 vinyl substituent. Comparing these two portions of the plot shows that despite this sequence being performed with substrates that bear different substituents, the relative change in complexity is the same.

Aside from providing a quick graphical representation of synthetic sequences without structural detail, what value might be derived from complexity metrics? For this one needs to consider the concepts of complexity density ($C_m/Å^3$) and the emergent properties of molecules.[295] These concepts contend that the whole is greater than the sum

of its parts and that compounds with a high complexity density tend to elicit unprecedented biological responses based on their underlying components, and often with a higher degree of selectivity. This makes sense intuitively as increasing the number of ligand-receptor contacts for a given target-substrate pair can only be increased within the limits of what can be accommodated by the target. Accordingly, reactions which significantly increase molecular complexity density could hold value in their ability to produce new compounds with emergent properties.[296] Complexity density analysis provides a platform to assess the efficiency of synthetic sequences and individual reactions as well as the potential value of molecular targets or structural motifs in their ability to store information and convey that information to biological systems. In this context, I believe that our approach to hyperolactone C (**3.2**) and photo-[2+2] product **4.123** (C_m = 297.21), presents a synthetically accessible and diversity-oriented system to probe for new emergent properties.[296a, c]

Conclusions

In **Chapter 2**, our first foray into cerium photoredox platforms demonstrated the ability to generate high energy O-centered radical intermediates capable of delivering a wealth of reactivity. Our system, comprised of cerium, a hydrogen atom transfer catalyst, base, and photocatalyst, enabled a variety of redox-neutral transformations including fragmentation of lactols and cycloalkanols to the corresponding formate esters and ketones and hydrodecarboxylation. Single-step hydrodecarboxylation using readily available catalysts on native carboxylic acids represents a highly enabling reaction for defunctionalization and peripheral SAR. Likewise, redox-neutral cycloalkanol ring-scission can aid in the SAR of bioactive compounds through a formal scaffold hop approach. Combining cerium photoredox[6k, 297] and nickel catalysis enabled a remote arylation reaction that is not reliant on cycloalkanol ring-strain[136c, d, 298] or redox-auxiliaries.[86h, 87a, 136b, 140] To date, this work has furnished distal aryl and alkyl ketones *via* $C(sp^2)$–$C(sp^3)$ and $C(sp^3)$–$C(sp^3)$ cross-coupling moderate to high yields. Prior to Zuo's recent reports,[47, 143] these reactions had not previously existed on native unactivated cycloalkanols.

Future work in this area requires a better understanding of the substrate–cerium interactions that determine reactivity. Application of this radical generation method in complex contexts such as multicatalytic cross-coupling reactions requires careful matching of radical formation rates and cycle turnover to ensure productive coupling. Better understanding the rates of substrate activation will allow for these applications. In particular, the ring-chain tautomerism of lactol substrates, and their anomeric orientations, adds an extra dimension to reactivity that is likely a source of scope variability. Sugars are abundant chiral pool starting materials with lactol functionality, but are also highly oxygenated species that likely have other, undesired interactions with cerium that should be elucidated. We have long suspected that stereoelectronic effects are at play in β-scission reactions promoted by Ce-complexation that remain to be uncovered, mapped, and manipulated to achieve regioselective transformations.

While the logical extension of these transformations, to effect redox-neutral cross-coupling reactions, has been demonstrated by Zuo, other avenues for exploration in Ce/metallaphotoredox catalysis remain. Though nickel cross-couplings are exceptionally useful, metals more distinctly suited to other types of reactivity could be combined with Ce-photoredox radical generation methods to create a variety of reactions. For example, Cu-additives applied stoichiometrically (or with a co-oxidant) could be used to achieve cycloalkanol ring-scission or decarboxylative olefinations through intermediate C-centred radical oxidation. The same might be realized through use of catalytic cobalt in a dehydrogenative manner. Cu-catalysts with co-oxidants might be capable of coupling a variety of

nucleophiles (amines, amides, anilines, acetylides, etc.) with C-centred radicals. Redox-active Au-catalysts might enable coupling of these C-centred radicals with vinyl-Au intermediates generated through a variety of conventional Au-catalyzed alkyne activations.

In **Chapter 3**, we applied the photoredox catalyst platform to the activation of 1,3-dicarbonyl C(sp^3)–H acids and performed divergent C-centred radical reactions that offer new opportunities for building molecular complexity. A wide range of substrates were activated under both cerium-containing and cerium-free conditions, and we highlighted the various interception strategies available for these radicals.

Our scope studies revealed that subtle variations in substrate properties confer a preference for different reaction conditions. We attribute this divergence in activation to differences in binding equilibria, which lead to the formation of LMCT- and PCET-competent complexes. This was further supported by mechanistic investigations, including Stern-Volmer and NMR binding studies, which emphasized the critical role of carboxylate catalysts. In the cerium-containing conditions, we propose carboxylates act as ligands that facilitate substrate–Ce binding, whereas in cerium-free conditions, LiTFA serves as both a base and activator in a formal PCET process with photoexcited 9,10-DPA*. CBS-QB3 computational studies provided insight into the regio- and diastereoselectivity in these reactions, which arise from a pre-rate determining step (RDS) equilibrium. This computational approach also guided us in devising strategies for synthesis of more complex substrates.

Future work centres around a deeper mechanistic understanding of this reaction with an understanding of the key role of the Li-carboxylates in activation being essential. PCET mechanisms are difficult to prove and require careful collection of kinetic data. Expanding our NMR and UV/Vis binding studies could help develop a clearer picture of the key complexes formed under the reaction conditions and explain limitations in substrate scope. Advancing this activation mode to include mono-carbonyl species, masked carbonyls such as enol ethers, or the enols embedded in phenols could create a powerful tool for synthesis. Our most intriguing finding during hydroalkylation mechanistic studies was the discovery of the privileged role of LiTFA and the synergistic action of Li cations and TFA anions in substrate activation. Insight into the influence of Li could open new avenues for the development of this reaction. We imagine that there is a counterion-specific effect that creates an improved HBDA complex that may speed PCET reactions and potentially broaden the range of substrates amenable to this activation mode (*e.g.* widen the accessible pKa range). A predictive model for such effects to complement the Bordwell equation would be a valuable contribution. If metals remain coordinated to the post-PCET complex during cyclization, it's possible that they could

influence stereoselectivity in the cyclization when armed with chiral ligands. This effect would be even more powerful since the coordinated radical cations should react more quickly than the corresponding neutral species. Advancing this activation mode to include mono-carbonyl species, masked carbonyls such as enol ethers, or the enols embedded in phenols could create a powerful tool for synthesis.

In **Chapter 4**, our enhanced understanding of the catalytic system enabled a concise synthesis of anti-HIV natural product hyperolactone C (**3.2**) using a novel retrosynthetic disconnection. Computational chemistry allowed us to predict regio- and diastereoselectivity in the key dearomative spirocyclization reaction. We developed a Au(I)-catalyzed addition of glycolate esters to unsymmetrical propiolate esters, a previously underdeveloped hydroetherification reaction, and a Dieckmann condensation of the resulting *Z*-enol ether as a useful way to access hydroxyfuranoate esters. Mild transesterification conditions and chromatography-free purifications were optimized to allow us to manipulate these tricky heterocycles and characterize them by NMR spectroscopy for the first time. Our oxidative cyclization step was tolerated well by the oxidation-sensitive substrate that was found to degrade under classic radical generation conditions, which demonstrated the value of photoredox methods as an entry point to radical reactivity.

Simply accessing the natural product is only the starting point for this investigation. Inspired by the related biyouyanagin NP family, we performed natural product anticipation experiments that gave access to a highly caged 2-oxatricyclo[3.2.1.$0^{3,6}$]octane derivative by an intramolecular photo-[2+2]. This synthetic route also enabled the synthesis of unnatural analogues and sets the stage for future SAR studies, expanding the potential for therapeutic development.

Future work in this area is underway. The oxidative cyclization conditions are still underdeveloped, and further optimization, scope exploration, and mechanistic studies are currently being performed by Tegan O'Brien. While Cu(II) salts are relatively abundant and inexpensive oxidants, even more desirable oxidants could improve the reaction by rendering the copper catalytic. The known photoactivity of Cu(II) species and their propensity to perform LMCT processes may hint at a simpler reaction system possible under these conditions. Similarly, the base and copper species present in the reaction offer opportunities to create an enantioselective variant of the cyclization to perform a synthesis of (–)-hyperolactone C (**3.2**) and related analogues. Such analogues could possess superior medicinal properties, and evaluation of the photoredox method through the lens of analogue synthesis could further demonstrate its value. In particular, the dearomative nature of the reaction could be explored through preparation of analogues

derived from heteroaromatic substrates with differing aromaticity and stability. Understanding the breadth of dearomative reactions possible using this system could allow us to create sp^3-rich drug-like molecules from a wealth of existing heteroaromatic substrates.

Chapter 5
Experimental

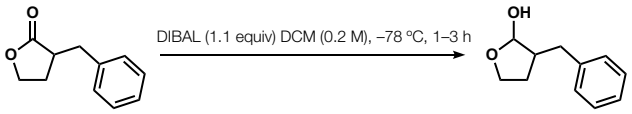
5.1 General Information

^{1}H NMR spectra were recorded in chloroform–*d*, benzene–d_6, acetone–d_6, or DMSO–d_6 at 400 MHz using a Bruker AMX400 spectrometer, 500 MHz using a Bruker AVANCE III HD 500 spectrometer, or 600 MHz using a Bruker Avance III HD 600 spectrometer. Residual chloroform (δ 7.26 ppm), benzene (δ 7.16 ppm), acetone (δ 2.05 ppm), or DMSO (δ 2.50 ppm) signals were used as an internal reference for ^{1}H NMR spectra recorded in these solvents. Coupling constants (*J*) are quoted to the nearest 0.1 Hz. ^{13}C NMR spectra were recorded in chloroform–*d*, benzene–d_6, acetone–d_6, or DMSO–d_6 at 76 MHz, 101 MHz, 126 MHz, or 151 MHz using the same Bruker instruments. Chloroform (δ 77.16 ppm), benzene (δ 128.06 ppm), acetone (δ 29.84 ppm), or DMSO (δ 39.52 ppm) signals were used as an internal reference for ^{13}C NMR spectra. Assignment of carbon signals was assisted by DEPT–90, DEPT–135, COSY, HSQC, HMBC, and NOESY experiments where necessary. The following abbreviations (or combinations thereof) were used to explain ^{1}H NMR multiplicities: s = singlet, d = doublet, t = triplet, q = quartet, m = multiplet, br = broad. Signals corresponding to different compounds in mixtures were denoted by **M** = major and **m** = minor. High–resolution mass spectra (HRMS) were recorded on a Kratos Analytical Concept – Magnetic Sector Electron Impact Mass Spectrometer instrument or Micromass Q-TOF I-TOF Electrospray Ionisation mass spectrometer (University of Ottawa, John L. Holmes Mass Spectrometry Facility). UV/Vis spectroscopy was performed using an Agilent Cary 7000 universal measurement spectrophotometer in 10 mm quartz cuvettes. Fluorimetry experiments were performed using a Photon Technology International (PTI) spectrofluorometer. Analytical thin layer chromatography (TLC) was performed using SiliCycle SiliaPlate aluminum-backed silica gel plates, pre–coated with silica gel F254 (0.2 mm) and visualised using UV fluorescence (λ_{max} = 254 nm) and developed using *p*-anisaldehyde and/or potassium permanganate stains following heating. Flash chromatography was conducted using SiliCycle SiliaFlash irregular silica gel, F60, 40-63 μm (230-400 mesh). Reactions were conducted in flame-dried Pyrex glassware equipped with a magnetic stir bar, capped with a septum, and under a positive pressure of dry argon unless otherwise stated. Solvent compositions are given in (%v/v). All commercial reagents were used without further purification, unless otherwise noted. Yields refer to products isolated after purification, unless otherwise stated.

5.2 Chapter 2 Experimental Details

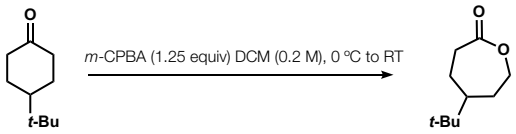
General Procedures for Chapter 2

GP1 Reduction of Lactones to Hemiacetals



A flame-dried round bottom flask under argon and equipped with stir bar was charged with lactone (1 equivalent) and DCM (0.2 M), and then cooled to –78 ºC with a dry-ice acetone bath. After equilibrating at –78 ºC, a solution of diisobutylaluminum hydride (DIBAL) was added dropwise over 15 minutes (1.1 equivalents, 25% w/w in hexanes). The resulting solution was then stirred at –78 ºC until complete consumption of the lactone starting material as judged by TLC (~1–3 h). Upon complete consumption of the starting material, excess DIBAL was quenched at –78 ºC by addition of acetone and stirred for an additional 10 minutes. The resulting mixture was allowed to warm to room temperature slowly following removal of the cryogenic bath. A saturated aqueous solution of Rochelle's salt was added and biphasic mixture stirred vigorously at room temperature until the layers clarified. The layers were then separated and the aqueous phase extracted with additional DCM (× 3). Combined organic phases were then washed with brine, dried over Na_2SO_4, filtered, and concentrated under reduced pressure. Crude residues were purified by flash column chromatography (0–100% EtOAc/hexanes unless otherwise stated).

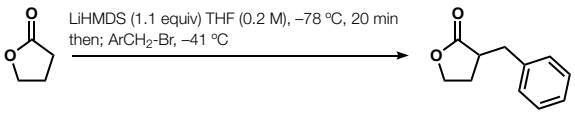
GP2 Baeyer-Villiger Oxidation of Cyclic Ketones or Epoxidation of Alkenes



A flame-dried round bottom flask under argon and equipped with stir bar was charged with ketone (1 equivalent) and DCM (0.2 M), and then cooled to 0 ºC with an ice–water bath. Next, *meta*-chloroperoxybenzoic acid (mCPBA, 1.25 equivalents) was added in 3 equal portions at 5-minute intervals. After the final addition of mCPBA, the resulting solution was stirred for an additional 10 minutes at 0 ºC before the ice-bath was removed and the solution allowed to warm to room temperature. The solution was stirred at room temperature until complete consumption of the ketone starting material as determined by TLC. Upon complete consumption of the ketone, excess mCPBA was quenched with $Na_2S_2O_3$ (sat. aq.) followed by $NaHCO_3$ (sat. aq.). The layers were then separated and the aqueous

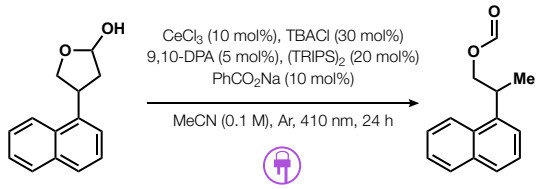
phase extracted with additional DCM (× 3). The combined organic extracts were washed with brine, dried over Na_2SO_4, filtered, and concentrated under reduced pressure. The crude residues were then purified by flash column chromatography (0–100% EtOAc/hexanes unless otherwise stated).

GP3 Benzylation of Lactones



A flame-dried round bottom flask under argon and equipped with stir bar was charged with a solution of lithium bis(trimethylsilyl)amide (LiHMDS) in THF (1.0 M, 1.05 equivalents) and cooled to –78 ºC with a dry-ice acetone bath. After thermally equilibrating for 10 minutes, a solution of lactone in THF (0.6 M, 1 equivalent) was added dropwise over 2 minutes. Upon complete addition of the lactone, the solution is allowed to stir at –78 ºC for an additional 10 minutes. Next, a solution of the benzyl bromide in THF (1.2 M, 2 equivalents) was added by syringe before the mixture was warmed to –41 ºC by placing it in a dry-ice acetonitrile bath. The resulting solution was allowed to stir at this temperature until complete consumption of the lactone starting material by TLC. Upon complete consumption of the lactone, a solution of NH_4Cl (sat. aq.) was added and the cryogenic bath removed to allow the solution to warm to room temperature. The layers are separated and the aqueous phase extracted with EtOAc (× 3). The combined organic extracts were washed with distilled water (× 1), then brine (× 1), dried over Na_2SO_4, filtered, and concentrated under reduced pressure. The crude material was purified by flash column chromatography (0–100% EtOAc/hexanes unless otherwise stated).

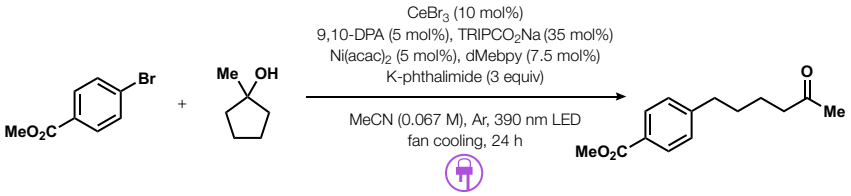
GP4 Photochemical Ring Scission or Decarboxylation



Inside a nitrogen-filled glovebox, an 8 mL oven-dried screw-top Pyrex tube was charged with sodium benzoate (0.02 mmol, 10 mol%), 9,10-diphenylanthracene (0.01 mmol, 5 mol%), $CeCl_3$ (0.02 mmol, 10 mol%, anhydrous), 2,4,6-bis(triisopropylphenyl)disulfide (0.04 mmol, 20 mol%), tetrabutylammonium chloride (0.2 mmol, 1 equivalent), and either hemiacetal or carboxylic acid substrate (0.2 mmol, 1 equivalent). Once all components were

charged, the tube was sealed with a Teflon-septum screw-cap, transferred out of the glovebox, and immediately placed under a positive pressure of argon. Next, anhydrous acetonitrile (1 mL) was added and the resulting suspension sparged with argon for 5 minutes. After sparging, the septum cap was quickly exchanged with a hard plastic cap and the vessel was further sealed with electrical tape and then parafilm. The reaction mixture was then sonicated (90 s) before irradiating with a violet LED (2–2.4 W, 405 nm) at a distance of 1–5 mm for 24–72 h. Upon complete conversion of starting material as determined by TLC, or if conversion had stalled, the reaction solution was passed through a silica plug (3 cm^3 in a 6 mL syringe barrel) eluting with Et_2O (~25 mL). The resulting solution was concentrated under reduced pressure and purified by flash column chromatography on silica gel (0–100% EtOAc/hexanes unless otherwise stated).

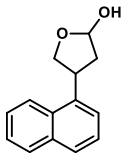
GP5 Photochemical Ring Scission Cross-Coupling



Inside a nitrogen-filled glovebox, an 8 mL oven-dried screw-top Pyrex tube was charged with $TRIPCO_2H$ or $TRIPCO_2K$ (0.07 mmol, 35 mol%), 9,10-diphenylanthracene (0.01 mmol, 5 mol%), $CeBr_3$ (0.02 mmol, 10 mol%, anhydrous), $Ni(acac)_2$ (0.01 mmol, 5 mol%), diMebpy (0.015 mmol, 7.5 mol%), K-phthalimide (3 equivalents when using $TRIPCO_2K$ or 3.35 equivalents when using $TRIPCO_2H$, 0.6 – 0.67 mmol) and solid hydroxyl substrate (0.6 mmol, 3 equivalents). Once all components were charged, the tube was sealed with a Teflon-septum screw-cap, transferred out of the glovebox, and immediately placed under a positive pressure of argon. Next, anhydrous acetonitrile (3 mL) was added followed by any liquid hydroxyl substrate (0.6 mmol, 3 equivalents) and the resulting suspension was sparged with argon for 5 minutes. After sparging, the septum cap was quickly exchanged with a hard plastic cap and the vessel was further sealed with electrical tape and then parafilm. The reaction mixture was then sonicated (90 s) before irradiating with a violet LED (2–2.4 W, 390 nm) at a distance of 1–5 mm for 24 h. Upon complete conversion of starting material as determined by TLC, or if conversion had stalled, the reaction solution was diluted with Et_2O (25 mL) and washed with sat. NH_4Cl (3 x 5 mL) and brine (1 x 5 mL) before being dried over Na_2SO_4 and filtered. The filtrate was concentrated under reduced pressure and purified by flash column chromatography on silica gel (0–100% EtOAc/hexanes unless otherwise stated).

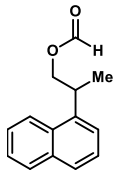
Procedures and Data

4-(naphthalen-1-yl)tetrahydrofuran-2-ol (2.32)



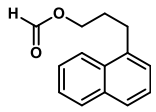
Prepared according to the following adapted literature procedure.[300] A solution of $Pd(OAc)_2$ (67.3 mg, 3 mol%) in dimethylformamide (DMF, 11 mL) was prepared and added *via* syringe to a stirred solution of 1-iodonaphthalene (**2.102**, 1.5 mL, 10 mmol, 1 equivalent), *cis*-2-butene-1,4-diol (**2.103**, 1.6 mL, 20 mmol, 2 equivalents), K_2CO_3 (3.45 g, 25 mmol, 2.5 equivalents), and tetrabutylammonium chloride (2.78g, 10 mmol, 1 equivalent) in DMF (22 mL, for 33 mL total). The resulting solution was stirred and sparged with argon for 15 minutes. After sparging, the solution was stirred and heated to 60 ºC until complete consumption of the iodonaphthalene by TLC (~ 4 h). Upon complete conversion of starting material, the mixture was diluted with distilled water (30 mL) and extracted with ethyl acetate (EtOAc, 3 × 30 mL). The combined extracts were washed with distilled water (3 × 30 mL), brine (1 × 50 mL), dried over Na_2SO_4, filtered, and concentrated under reduced pressure. The crude residue was purified by flash column chromatography (10–50% EtOAc/hexanes) to deliver purified product as a white amorphous powder as a ~2:1 mixture of anomers (94%, 2.01 g). R_f 0.34 (40% EtOAc/hexanes); **^{1}H NMR** (500 MHz, C_6D_6) δ 7.90 – 7.84 (m, 1H, **M**), 7.84 – 7.80 (m, 0.5H, **m**) 7.68 – 7.62 (m, 1.5H, **M** & **m**), 7.57 – 7.49 (m, 2H, **M** & 2 × **m**), 7.33 – 7.16 (m, 5.5H, 4 × **M** & 3 × **m**), 5.52 – 5.44 (m, 1H, **M** & **m**), 4.43 (td, J = 8.1, 2.4 Hz, 1H, **M**), 4.27 – 4.17 (m, 1H, **M**), 4.17 – 4.10 (m, 0.5H, **m**), 4.10 – 4.01 (m, 0.5H, **m**), 3.93 – 3.77 (m, 1.5H, **M** & **m**), 2.72 – 2.38 (m, 1.5H, **M** & **m**), 2.33 – 2.19 (m, 1.5H, **M** & **m**), 2.12 – 1.95 (m, 1.5H, **M** & **m**) ppm; **^{13}C NMR** (101 MHz, C_6D_6) δ 138.8 (C, **M**), 137.7 (C, **m**), 134.6 (C, **M**), 134.5 (C, **m**), 132.8 (C, **m**), 132.6 (C, **M**), 129.3 (CH, **m**), 129.2 (CH, **M**), 127.4 (CH, **M** & **m**), 126.3 (CH, **M**), 126.2 (CH, **m**), 126.0 (CH, **m**), 125.8 (CH, **M**), 125.8 (CH, **M**), 125.7 (CH, **m**), 123.9 (CH, **M**), 123.8 (CH, **m**), 123.7 (CH, **m**), 123.0 (CH, **M**), 99.5 (CH, **m**), 99.1 (CH, **M**), 72.9 (CH_2, **M**), 72.5 (CH_2, **m**), 41.3 (CH_2, **m**), 41.1 (CH_2, **M**), 40.0 (CH, **m**), 38.8 (CH, **M**) ppm; **HRMS** (EI): *m/z* calculated for $C_{14}H_{14}O_2$ $[M]^+$ 214.09938, found 214.09729.

2-(naphthalen-1-yl)propyl formate (2.33)



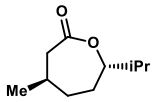
Prepared according to GP4 as a yellow oil (75%, 0.2 mmol scale, 32 mg isolated). Purified by flash column chromatography (2–8% EtOAc/hexanes). Characterized according to NMR comparison. [301] R_f 0.29 (8% EtOAc/hexanes); **^{1}H NMR** (400 MHz, $CDCl_3$) δ 8.16 (d, J = 8.4 Hz, 1H), 8.07 (s, 1H), 7.88 (dd, J = 8.0, 1.6 Hz, 1H), 7.77 (d, J = 7.9 Hz, 1H), 7.61 – 7.38 (m, 4H), 4.55 (dd, J = 10.9, 6.1 Hz, 1H), 4.32 (dd, J = 10.9, 7.9 Hz, 1H), 4.13 – 3.97 (m, 1H), 1.49 (d, J = 6.9 Hz, 3H) ppm; **^{13}C NMR** (101 MHz, $CDCl_3$) δ 161.2 (CH), 138.6 (C), 134.1 (C), 131.7 (C), 129.2 (CH), 127.5 (CH), 126.4 (CH), 125.7 (CH), 125.6 (CH), 123.3 (CH), 123.0 (CH), 68.7 (CH_2), 33.2 (CH), 18.2 (CH_3) ppm; **HRMS** (EI): *m/z* calculated for $C_{14}H_{14}O_2$ $[M]^+$: 214.09938, found 214.09647.

3-(naphthalen-1-yl)propyl formate (2.34)



Prepared according to GP4 as a yellow oil (11%, 0.2 mmol scale, 5 mg isolated). Purified by flash column chromatography (2–8% EtOAc/hexanes). R_f 0.19 (5% EtOAc/hexanes); **^{1}H NMR** (400 MHz, $CDCl_3$) δ 8.14 (s, 1H), 8.03 (dd, J = 8.4, 1.4 Hz, 1H), 7.88 (dd, J = 7.7, 1.7 Hz, 1H), 7.75 (d, J = 8.2 Hz, 1H), 7.58 – 7.45 (m, 2H), 7.41 (dd, J = 8.2, 7.0 Hz, 1H), 7.34 (dd, J = 7.1, 1.3 Hz, 1H), 4.27 (t, J = 6.4 Hz, 2H), 3.23 – 3.14 (m, 2H), 2.20 – 2.08 (m, 2H) ppm; **^{13}C NMR** (101 MHz, $CDCl_3$) δ 161.3 (CH), 137.1 (C), 134.1 (C), 131.8 (C), 129.0 (CH), 127.1 (CH), 126.3 (CH), 126.1 (CH), 125.7 (CH), 125.7 (CH), 123.6 (CH), 63.6 (CH_2), 29.5 (CH_2), 29.3 (CH_2) ppm; **HRMS** (EI): *m/z* calculated for $C_{14}H_{14}O_2$ $[M]^+$: 214.09938, found 214.09660.

(4R,7S)-7-isopropyl-4-methyloxepan-2-one (2.47)



Prepared according to GP2 on 3.4 mmol scale to give a white powder in quantitative yield (0.45 g, 78%). Purified by flash column chromatography (10–30% EtOAc in hexanes). Characterized according to NMR comparison. [302] **^{1}H NMR** (400 MHz, $CDCl_3$) δ 4.03 (dd, J = 9.2, 4.5 Hz, 1H), 2.58 – 2.42 (m, 2H), 2.05 – 1.75 (m, 4H), 1.60 (dddd, J = 15.2, 13.2, 9.2, 3.0 Hz, 1H), 1.28 (tdd, J = 13.1, 11.4, 3.4 Hz, 1H), 1.04 (d, J = 6.7 Hz, 3H), 0.98 (d, J = 5.3 Hz,

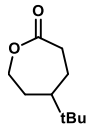
3H), 0.96 (d, J = 5.3 Hz, 3H) ppm; **^{13}C NMR** (101 MHz, $CDCl_3$) δ 175.1 (C), 84.9 (CH), 42.7 (CH_2), 37.6 (CH_2), 33.5 (CH), 31.1 (CH_2), 30.6 (CH), 24.1 (CH_3), 18.5 (CH_3), 17.3 (CH_3) ppm.

(±)–(1R,3r,6s,8S)-4-oxatricyclo[4.3.1.1^{3,8}]undecan-5-one (2.49)



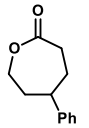
Prepared according to GP2 from 2-adamantanone as a white powder in quantitative yield (13.3 mmol scale, 2.22 g isolated). Purified by flash column chromatography (10–30% EtOAc in hexanes). Characterized according to NMR comparison.[303] ***R$_f$*** 0.29 (20% EtOAc/hexanes); **^{1}H NMR** (400 MHz, $CDCl_3$) δ 4.48 (tt, J = 4.3, 2.4 Hz, 1H), 3.07 (tt, J = 5.8, 2.0 Hz, 1H), 2.14 – 1.90 (m, 8H), 1.88 – 1.79 (m, 2H), 1.78 – 1.68 (m, 2H) ppm; **^{13}C NMR** (101 MHz, $CDCl_3$) δ 179.1 (C), 73.3 (CH), 41.4 (CH), 35.9 (2 × CH_2), 34.0 (CH_2), 31.1 (2 × CH_2), 26.0 (2 × CH) ppm.

5-(tert-butyl)oxepan-2-one (2.51b)



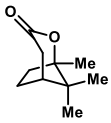
Prepared according to GP2 from 4-*tert*-butylcyclohexanone as a white powder (96%, 6.5 mmol scale, 1.06 g isolated). Purified by flash column chromatography (5–20% EtOAc in hexanes). Characterized according to NMR comparison.[302] ***R$_f$*** 0.31 (20% EtOAc/hexanes); **^{1}H NMR** (400 MHz, $CDCl_3$) δ 4.34 (ddd, J = 12.8, 5.9, 1.8 Hz, 1H), 4.15 (ddt, J = 12.9, 10.4, 0.7 Hz, 1H), 2.71 (ddd, J = 14.2, 7.5, 1.5 Hz, 1H), 2.63 – 2.51 (m, 1H), 2.12 – 1.98 (m, 2H), 1.59 – 1.47 (m, 1H), 1.42 – 1.27 (m, 2H), 0.90 (s, 9H) ppm; **^{13}C NMR** (101 MHz, $CDCl_3$) δ 176.5 (C), 68.8 (CH_2), 51.0 (CH), 33.6 (CH_2), 33.2 (C), 30.5 (CH_2), 27.6 (3 × CH_3), 23.9 (CH_2) ppm.

5-phenyloxepan-2-one (2.51c)



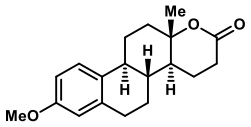
Prepared according to GP2 on 5.7 mmol scale and used without further purification (1.05 g, 97%). Characterized according to NMR comparison.[304] **^{1}H NMR** (400 MHz, DMSO-d_6) δ 7.28 (ddd, J = 14.4, 8.1, 6.5 Hz, 4H), 7.24 – 7.15 (m, 1H), 4.43 (dd, J = 12.9, 10.4 Hz, 1H), 4.24 (ddd, J = 13.0, 5.5, 1.9 Hz, 1H), 3.02 – 2.82 (m, 2H), 2.57 – 2.48 (m, 1H), 2.07 – 1.96 (m, 1H), 1.96 – 1.79 (m, 2H), 1.68 (dtd, J = 14.0, 12.5, 1.5 Hz, 1H) ppm; **^{13}C NMR** (101 MHz, DMSO-d_6) δ 175.4 (C), 145.8 (C), 128.5 (2 × CH), 126.7 (2 × CH), 126.3 (CH), 67.5 (CH_2), 45.8 (CH), 36.4 (CH_2), 33.2 (CH_2), 29.8 (CH_2) ppm.

(±)–(1R,5R)-1,8,8-trimethyl-2-oxabicyclo[3.2.1]octan-3-one (2.53)



Prepared according to the following adapted literature procedure.[305] A 50 mL round bottom flask under argon and equipped with stir bar was charged with benzeneseleninic acid (1.6 g, 8.2 mmol, 1.25 equivalents) and THF (20 mL) followed by H_2O_2 (30% w/w in water, 6.8 mL, 66 mmol, 10 equivalents) at room temperature. The resulting suspension was stirred vigorously until homogeneous (~10 minutes) at which point camphor (1.0 g, 6.6 mmol, 1 equivalent) was added and the solution continued to stir until complete consumption of the starting material (~1 h as determined by TLC). Upon complete conversion, the solution was cooled to 0 ºC with an ice bath and quenched by addition of saturated $Na_2S_2O_3$ (sat. aq., 20 mL). Next, additional distilled water was added (20 mL) followed by EtOAc (40 mL). The layers were separated and the aqueous phase was extracted with additional EtOAc (3 × 30 mL). The combined organic phases were washed with $NaHCO_3$ (sat. aq., 2 × 30 mL), and brine (1 × 40 mL), then dried over Na_2SO_4, filtered and concentrated *in vacuo*. The resulting crude material was purified by flash column chromatography (5–20% EtOAc in hexanes) to give a white solid (60%, 680 mg). R_f 0.30 (21% EtOAc/hexanes); **^{1}H NMR** (400 MHz, $CDCl_3$) δ 2.86 – 2.75 (m, 1H), 2.40 (dd, J = 18.7, 1.4 Hz, 1H), 2.24 – 2.14 (m, 1H), 2.13 – 1.92 (m, 3H), 1.61 – 1.49 (m, 1H), 1.29 (s, 3H), 1.06 (s, 3H), 1.00 (s, 3H) ppm; **^{13}C NMR** (101 MHz, $CDCl_3$) δ 172.0 (C), 93.1 (C), 43.5 (C), 42.6 (CH), 38.7 (CH_2), 37.2 (CH_2), 28.0 (CH_2), 24.0 (CH_3), 18.5 (CH_3), 17.6 (CH_3) ppm;

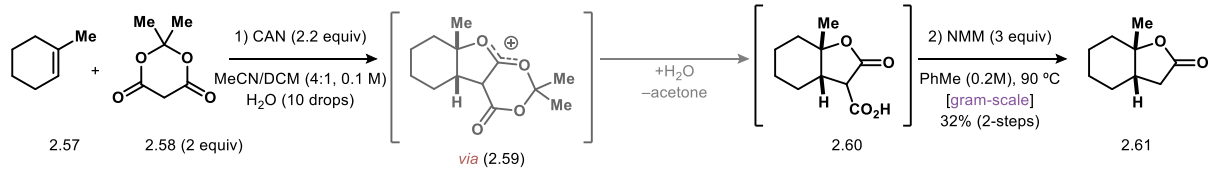
(4aS,4bR,10bS,12aS)-8-methoxy-12a-methyl-3,4,4a,4b,5,6,10b,11,12,12a-decahydro-2H-naphtho[2,1-f]chromen-2-one (2.56)



Prepared according to the following adapted literature procedure.[305] A 50 mL round bottom flask under argon and equipped with stir bar was charged with benzeneseleninic acid (622 mg, 3.3 mmol, 1.25 equivalents) and THF (8 mL) followed by H_2O_2 (30% w/w in water, 2.7 mL, 26.3 mmol, 10 equivalents) at room temperature. The resulting suspension was stirred vigorously until homogeneous (~10 minutes) at which point estrone 3-methyl ether (750 mg, 2.6 mmol, 1 equivalent) was added and the solution continued to stir until complete consumption of the starting material (~1 h as determined by TLC). Upon complete conversion, the solution was cooled to 0 ºC with an ice bath and quenched by addition of saturated $Na_2S_2O_3$ (sat. aq., 10 mL). Next, additional distilled water was added (10 mL)

followed by EtOAc (20 mL). The layers were separated and the aqueous phase was extracted with additional EtOAc (3 × 15 mL). The combined organic phases were washed with $NaHCO_3$ (sat. aq., 2 × 15 mL), and brine (1 × 20 mL), then dried over Na_2SO_4, filtered and concentrated *in vacuo*. The resulting crude material was purified by flash column chromatography (10–40% EtOAc in hexanes) to give the lactone as a white solid (70%, 557 mg). Characterized according to NMR comparison.[305b] ***R**f* 0.33 (43% EtOAc/hexanes); **^{1}H NMR** (400 MHz, $CDCl_3$) δ 7.20 (dd, J = 8.7, 1.0 Hz, 1H), 6.73 (dd, J = 8.6, 2.8 Hz, 1H), 6.64 (dd, J = 2.6, 1.1 Hz, 1H), 3.78 (s, 3H), 2.94 – 2.80 (m, 2H), 2.79 – 2.56 (m, 2H), 2.54 – 2.39 (m, 2H), 2.17 – 2.01 (m, 3H), 1.88 (ddd, J = 13.3, 13.2, 3.6 Hz, 1H), 1.71 – 1.54 (m, 2H), 1.48 – 1.36 (m, 2H), 1.35 (s, 3H), 1.30 – 1.18 (m, 1H) ppm; **^{13}C NMR** (101 MHz, $CDCl_3$) δ 171.5 (C), 158.0 (C), 137.6 (C), 131.5 (C), 126.5 (CH), 113.8 (CH), 112.0 (CH), 83.5 (C), 55.4 (CH_3), 45.3 (CH), 42.9 (CH), 41.6 (CH), 39.4 (CH_2), 30.0 (CH_2), 28.8 (CH_2), 27.6 (CH_2), 26.3 (CH_2), 20.3 (CH_3), 19.9 (CH_2) ppm; **HRMS** (EI): *m/z* calculated for $[M]^+$: 300.17254, found 300.17463.

(cis)-7a-methylhexahydrobenzofuran-2(3H)-one (2.61)

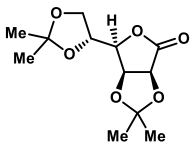


To a solution of 1-methylcyclohexene (1 mL, 8.4 mmol, 1.0 equiv.) in MeCN/DCM (42 mL, 4:1, 0.2 M) was added 10 drops of water, followed by Meldrum's acid (1.34 g, 9.3 mmol, 1.1 equiv.) and then cerium ammonium nitrate (10.2 g, 18.6 mmol, 2.2 equiv.) at 0 °C. The mixture was stirred until complete consumption of alkene (1 hour). The reaction was diluted with EtOAc (50 mL) and water (50 mL) were added and the phases separated. The aqueous phase was extracted with EtOAc (3 x 50 mL) and the combined organic phases were dried over Na_2SO_4, filtered, and concentrated under reduced pressure. The crude intermediate **2.60** was used without further purification.

A solution of ketoacid **2.60** and NMM (2.8 mL, 25 mmol, 3.0 equiv.) in PhMe (42 mL, 0.2 M) was heated to 80 °C until the ketoacid was consumed. The reaction was diluted with EtOAc (50 mL) and water (50 mL) were added and the phases separated. The aqueous phase was extracted with EtOAc (3 × 50 mL) and the combined organic phases were dried over $MgSO_4$, filtered, and concentrated under reduced pressure. The crude residue was purified by silica gel flash column chromatography (0–16% EtOAc/hexanes) and isolated as a clear colourless oil (38%, 492 mg). Characterized according to NMR comparison.[306] ***R**f* 0.35 (20% EtOAc/hexanes); **^{1}H NMR** (400 MHz, $CDCl_3$) δ 2.60 (dd, J = 17.3, 7.7 Hz, 1H), 2.39 (dd, J = 17.2, 8.0 Hz, 1H), 2.25 (tt, J = 7.8, 5.6 Hz, 1H), 1.78 (ddd, J = 13.3, 9.0, 4.1

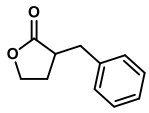
Hz, 1H), 1.74 – 1.64 (m, 2H), 1.64 – 1.29 (m, 7H) ppm; **^{13}C NMR** (101 MHz, $CDCl_3$) δ 176.8 (C), 85.2 (C), 40.4 (CH), 35.3 (CH_2), 34.8 (CH_2), 26.6 (CH_2), 25.7 (CH_3), 22.1 (CH_2), 21.4 (CH_2) ppm.

(3aS,6R,6aS)-6-((R)-2,2-dimethyl-1,3-dioxolan-4-yl)-2,2-dimethyldihydrofuro[3,4-d][1,3]dioxol-4(3aH)-one (2.63)



Prepared according to the following adapted literature procedure.[307] A flame-dried 50 mL round bottom flask under argon and equipped with stir bar was charged with 2,3:5,6-di-*O*-isopropylidene-α-D-mannofuranose (**2.62**, 500 mg, 1.9 mmol, 1 equivalent) and DCM (19 mL) at room temperature. Upon complete dissolution, freshly ground K_2CO_3 (1.46 g, 5.8 mmol, 3 equivalents) was added followed by I_2 (800 mg, 5.8 mmol, 3 equivalents). The mixture is stirred vigorously at room temperature until complete consumption of the mannofuranose derivative by TLC (~8 h). The suspension was then cooled to 0 ºC with an ice bath and excess iodine was quenched by addition of $Na_2S_2O_3$ (sat. aq.) under vigorous stirring until the colour change was complete. Additional distilled water was added to homogenize the aqueous phase and the layers were then separated. The aqueous phase was extracted with DCM (3 × 20 mL). The combined organic extracts were washed with brine (1 × 40 mL), dried over Na_2SO_4, filtered and concentrated under reduced pressure. The crude residue was purified by silica gel flash column chromatography (10–30% EtOAc/hexanes) and isolated as a white powder (88%, 436 mg). Characterized according to NMR comparison.[308] ***R$_f$*** 0.35 (30% EtOAc/hexanes); **^{1}H NMR** (400 MHz, $CDCl_3$) δ 4.88 (dd, J = 5.3, 3.3 Hz, 1H), 4.83 (d, J = 5.3 Hz, 1H), 4.44 (ddd, J = 8.1, 5.9, 3.9 Hz, 1H), 4.37 (dd, J = 8.0, 3.3 Hz, 1H), 4.15 (dd, J = 9.2, 5.9 Hz, 1H), 4.07 (dd, J = 9.2, 3.9 Hz, 1H), 1.55 (s, 1H), 1.51 – 1.48 (m, 3H), 1.47 (d, J = 0.7 Hz, 3H), 1.43 (d, J = 0.7 Hz, 3H), 1.39 (d, J = 0.7 Hz, 3H) ppm; **^{13}C NMR** (101 MHz, $CDCl_3$) δ 173.5 (C), 114.7 (C), 110.1 (C), 78.3 (CH), 76.2 (CH), 76.0 (CH), 72.8 (CH), 66.6 (CH_2), 27.1 (CH_3), 26.9 (CH_3), 26.1 (CH_3), 25.3 (CH_3) ppm.

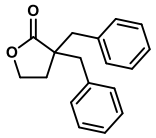
.3-benzyldihydrofuran-2(3H)-one (2.68)



Prepared according to GP3 from γ-butyrolactone and benzyl bromide as a white powder (73%, 15 mmol scale, 1.92 g isolated). Purified by flash column chromatography (10–30% EtOAc/hexanes). Spectral data were consistent with those previously reported.[309] ***R$_f$*** 0.47 (27% EtOAc/hexanes); **^{1}H NMR** (400 MHz, $CDCl_3$) δ 7.35 – 7.29 (m, 2H),

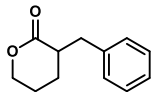
7.28 – 7.19 (m, 3H), 4.23 (ddd, *J* = 8.8, 8.6, 3.0 Hz, 1H), 4.15 (ddd, *J* = 9.3, 9.2, 6.7 Hz, 1H), 3.26 (dd, *J* = 13.6, 4.0 Hz, 1H), 2.90 – 2.80 (m, 1H), 2.76 (dd, *J* = 13.6, 9.5 Hz, 1H), 2.31 – 2.19 (m, 1H), 2.07 – 1.92 (m, 1H) ppm; **^{13}C NMR** (101 MHz, $CDCl_3$) *δ* 178.8 (C), 138.5 (C), 129.0 (2 × CH), 128.8 (2 × CH), 126.8 (CH), 66.7 (CH_2), 41.2 (CH), 36.2 (CH_2), 28.1 (CH_2) ppm.

3,3-dibenzyldihydrofuran-2(3H)-one (2.69)



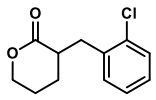
Prepared according to GP3 from γ-butyrolactone and benzyl bromide and isolated as a white powder (7%, 15 mmol scale, 294 mg, isolated as a side product from the alkylation of γ-butyrolactone). Purified by flash column chromatography (10–30% EtOAc/ hexanes). Characterized according to NMR comparison.[310] ***R$_f$*** 0.73 (27% EtOAc/ hexanes); **^{1}H NMR** (400 MHz, $CDCl_3$) *δ* 7.33 – 7.26 (m, 6H), 7.25 – 7.19 (m, 4H), 3.37 (t, *J* = 7.4 Hz, 2H), 3.20 (d, *J* = 13.4 Hz, 2H), 2.79 (d, *J* = 13.5 Hz, 2H), 2.15 (t, *J* = 7.4 Hz, 2H) ppm; **^{13}C NMR** (101 MHz, $CDCl_3$) *δ* 181.3 (C), 136.6 (2 × C), 130.3 (4 × CH), 128.7 (4 × CH), 127.3 (2 × CH), 65.4 (CH_2), 49.9 (C), 44.0 (2 × CH_2), 29.2 (CH_2) ppm.

3-benzyltetrahydro-2H-pyran-2-one (2.70)



Prepared according to GP3 from *δ*-valerolactone and benzyl bromide as a yellow oil (46%, 16 mmol scale, 1.43 g isolated). Purified by flash column chromatography (50–90% DCM/hexanes). Characterized according to NMR comparison.[309] ***R$_f$*** 0.28 (84% DCM/hexanes); **^{1}H NMR** (400 MHz, $CDCl_3$) *δ* 7.35 – 7.27 (m, 2H), 7.26 – 7.17 (m, 3H), 4.34 – 4.21 (m, 2H), 3.45 – 3.29 (m, 1H), 2.80 – 2.64 (m, 2H), 1.97 – 1.73 (m, 3H), 1.61 – 1.42 (m, 1H) ppm; **^{13}C NMR** (101 MHz, $CDCl_3$) *δ* 174.2 (C), 139.0 (C), 129.3 (2 × CH), 128.6 (2 × CH), 126.6 (CH), 68.6 (CH_2), 41.6 (CH), 37.3 (CH_2), 24.2 (CH_2), 22.0 (CH_2) ppm.

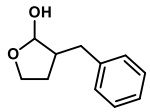
3-(2-chlorobenzyl)tetrahydro-2H-pyran-2-one (2.72)



Prepared according to GP3 from *δ*-valerolactone and 2-chlorobenzyl bromide as a white powder (57%, 3.9 mmol scale, 496 mg isolated). Purified by flash column chromatography (5–20% EtOAc/hexanes). ***R$_f$*** 0.31 (20% EtOAc/hexanes); **^{1}H NMR** (400 MHz, $CDCl_3$) *δ* 7.39 – 7.33 (m, 1H), 7.31 – 7.27 (m, 1H), 7.23 – 7.15 (m, 2H), 4.36

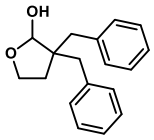
– 4.23 (m, 2H), 3.57 – 3.44 (m, 1H), 2.95 – 2.75 (m, 2H), 1.98 – 1.73 (m, 3H), 1.63 – 1.52 (m, 1H) ppm; **^{13}C NMR** (101 MHz, $CDCl_3$) δ 174.2 (C), 136.9 (C), 134.4 (C), 131.9 (CH), 129.8 (CH), 128.2 (CH), 127.0 (CH), 68.3 (CH_2), 39.8 (CH), 34.8 (CH_2), 24.2 (CH_2), 22.0 (CH_2) ppm; **HRMS** (EI): *m/z* calculated for $C_{12}H_{13}O_2^+$ $[M - Cl]^+$ 189.09155, found 189.09633.

3-benzyltetrahydrofuran-2-ol (2.74)



Prepared according to GP1 from **2.68** as a white powder as a 4:3 mixture of anomers (88%, 5.7 mmol scale, 894 mg isolated). Purified by flash column chromatography (15–30% EtOAc/hexanes). R_f 0.32 (30% EtOAc/hexanes); **^{1}H NMR** (400 MHz, C_6D_6) δ 7.20 – 7.14 (m, 2.25H, 3 × **m**), 7.14 – 7.09 (m, 3H, 3 × **M**), 7.09 – 7.02 (m, 1.5H, 2 × **m**), 7.01 – 6.95 (m, 2H, 2 × **M**), 5.12 (d, J = 1.7 Hz, 1H, **M**), 5.09 (d, J = 4.4 Hz, 0.75H, **m**), 3.94 (ddd, J = 9.2, 8.1, 2.6 Hz, 0.75H, **m**), 3.88 (td, J = 8.2, 6.4 Hz, 1H, **M**), 3.73 (td, J = 8.0, 5.9 Hz, 1H, **M**), 3.54 (dt, J = 9.4, 7.7 Hz, 1H, **m**), 2.95 – 2.76 (m, 2.5H, **M** & 2 × **m**), 2.63 (dd, J = 13.6, 7.6 Hz, 0.75H, **m**), 2.55 (dd, J = 13.5, 7.3 Hz, 1H, **M**), 2.43 – 2.32 (m, 1H, **M**), 2.24 (dd, J = 13.5, 8.7 Hz, 1H, **M**), 2.07 – 1.94 (m, 1H, **m**), 1.91 – 1.80 (m, 1H, **M**), 1.68 (tt, J = 11.7, 9.3 Hz, 1H, **m**), 1.52 – 1.41 (m, 1H, **m**), 1.24 (dddd, J = 12.3, 7.8, 6.3, 4.4 Hz, 1H, **M**) ppm; **^{13}C NMR** (101 MHz, C_6D_6) δ 141.7 (C, **m**), 140.6 (C, **M**), 129.2 (CH, 2 × **M** & 2 × **m**), 128.7 (CH, 2 × **M**), 128.6 (CH, 2 × **m**), 126.4 (CH, **M**), 126.2 (CH, **m**), 102.5 (CH, **M**), 98.1 (CH, **m**), 67.0 (CH_2, **m**), 66.6 (CH_2, **M**), 47.8 (CH, **M**), 46.8 (CH, **m**), 38.4 (CH_2, **M**), 35.2 (CH_2, **m**), 29.6 (CH_2, **M**), 29.1 (CH_2, **m**) ppm; **HRMS** (EI): *m/z* calculated for $C_{11}H_{14}O_2$ $[M]^+$: 178.09938, found 178.09829.

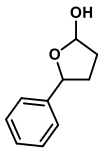
3,3-dibenzyltetrahydrofuran-2-ol (2.75)



Prepared according to GP1 from **2.69** as a white powder (87%, 0.75 mmol scale, 174 mg isolated). Purified by flash column chromatography (20% EtOAc/hexanes). R_f 0.32 (21% EtOAc/hexanes); **^{1}H NMR** (500 MHz, C_6D_6) δ 7.31 (d, J = 7.0 Hz, 2H), 7.21 (dd, J = 7.6, 7.6 Hz, 2H), 7.15 – 7.05 (m, 6H), 5.03 (d, J = 2.4 Hz, 1H), 3.87 (ddd, J = 9.6, 8.2, 3.2 Hz, 1H), 3.51 (ddd, J = 8.2, 8.2, 8.2 Hz, 1H), 3.06 (d, J = 14.2 Hz, 1H), 2.82 (d, J = 14.2 Hz, 1H), 2.55 (d, J = 13.8 Hz, 1H), 2.51 (d, J = 13.8 Hz, 1H), 2.31 – 2.22 (m, 1H), 1.84 (dt, J = 12.3, 9.1 Hz, 1H), 1.47 (ddd, J = 12.3, 7.8, 3.2 Hz, 1H) ppm; **^{13}C NMR** (126 MHz, C_6D_6) δ 139.9 (C), 138.7 (C), 131.0 (2 × CH), 130.9 (2 × CH),

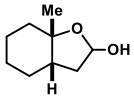
128.5 (2 × CH), 128.4 (2 × CH), 126.5 (CH), 126.4 (CH), 101.9 (CH), 66.0 (CH_2), 51.8 (C), 39.7 (CH_2), 38.9 (CH_2), 33.4 (CH_2) ppm; **HRMS** (EI): *m/z* calculated for $C_{18}H_{20}O_2$ $[M]^+$: 268.14633, found 268.14609.

5-phenyltetrahydrofuran-2-ol (2.76)



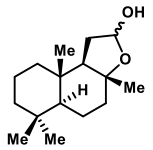
Prepared according to GP1 from γ-phenyl-γ-butyrolactone as a white solid as a 1.35:1 mixture of anomers (84%, 1.8 mmol scale, 256 mg isolated). Purified by flash column chromatography (30% EtOAc/hexanes). Product was characterized by NMR comparison.[311] R_f 0.31 (25% EtOAc/hexanes); **^{1}H NMR** (400 MHz, C_6D_6) δ 7.48 – 7.40 (m, 1.6H, 2 × **m**), 7.27 – 7.22 (m, 3H, 3 × **M**), 7.21 – 7.17 (m, 2.4H, 3 × **m**), 7.15 – 7.04 (m, 2H, 2 × **M**), 5.53 – 5.46 (m, 1H, **M**), 5.41 – 5.35 (m, 0.8H, **m**), 5.17 (dd, J = 7.0, 7.0 Hz, 1H, **M**), 4.77 (dd, J = 9.7, 6.2 Hz, 0.8H, **m**), 3.04 (dd, J = 3.3, 1.6 Hz, 0.8H, **m**), 2.92 (d, J = 3.0 Hz, 1H, **M**), 2.14 (ddt, J = 12.1, 8.2, 7.1 Hz, 1H, **M**), 1.97 – 1.87 (m, 0.8H, **m**), 1.86 – 1.68 (m, 3.6H, 2 × **M** & 2 × **m**), 1.60 – 1.49 (m, 0.8H, **m**), 1.44 (ddt, J = 12.1, 8.7, 6.8 Hz, 1H, **M**) ppm; **^{13}C NMR** (101 MHz, C_6D_6) δ 144.0 (C, **m**), 143.4 (C, **M**), 128.6 (2 × CH, **m**), 128.6 (2 × CH, **M**), 127.6 (CH, **m**), 127.4 (CH, **M**), 126.7 (2 × CH, **m**), 126.0 (2 × CH, **M**), 99.2 (CH, **M**), 98.9 (CH, **m**), 82.9 (CH, **m**), 79.6 (CH, **M**), 34.7 (CH_2, **m**), 33.3 (CH_2, **M**), 33.2 (CH_2, **M**), 33.2 (CH_2, **m**) ppm; **HRMS** (EI): *m/z* calculated for $C_{10}H_{12}O_2$ $[M]^+$: 164.08373, found 164.08316.

(cis)-7a-methyloctahydrobenzofuran-2-ol (2.77)



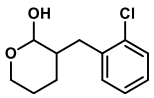
Prepared according to GP1 on 9.7 mmol scale and purified by flash column chromatography (10–30% EtOAc/hexanes) to give a clear colourless oil (1.3 g, 86%). R_f 0.15 (10% EtOAc/DCM); **^{1}H NMR** (400 MHz, MeOD) δ 5.43 (dd, J = 6.2, 5.0 Hz, 0.36H, **m**), 5.38 (dd, J = 5.0, 2.5 Hz, 0.64H, **M**), 2.29 – 2.17 (m, 0.36H, **m**), 2.19 – 2.07 (m, 1.36H), 2.06 – 1.75 (m, 1.64H), 1.77 – 1.10 (m, 11.64H) ppm; **^{13}C NMR** (101 MHz, MeOD) δ 98.8 (CH, **m**), 98.1 (CH, **M**), 83.4 (C, **M**), 82.8 (C, **m**), 44.4 (CH, **m**), 42.4 (CH, **M**), 39.9 (CH_2, **M**), 39.5 (CH_2, **m**), 36.8 (CH_2, **m**), 36.8 (CH_2, **M**), 27.5 (CH_2, **M**), 27.4 (CH_3, **M**), 26.9 (CH_2, **m**), 26.1 (CH_3, **m**), 24.6 (CH_2, **m**), 24.0 (CH_2, **M**), 22.8 (CH_2, **M**), 22.3 (CH_2, **m**) ppm.

(3aR,5aS,9aS,9bR)-3a,6,6,9a-tetramethyldodecahydronaphtho[2,1-b]furan-2-ol, sclaral (2.78)



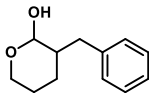
Prepared according to GP1 from sclareolide (**3.1**) as a white powder containing a mixture of anomers and open hydroxy aldehyde forms (99%, 4 mmol scale, 999 mg isolated). Purified by flash column chromatography (5–30% EtOAc/hexanes). Spectral data matched those previously reported.[312] ***R**f* 0.33 (30% EtOAc/hexanes); **^{1}H NMR** (400 MHz, $CDCl_3$) δ 5.46 – 5.21 (m, 1H), 2.09 – 1.96 (m, 1H), 1.99 – 1.84 (m, 1H), 1.79 – 1.56 (m, 3H), 1.49 – 1.22 (m, 6H), 1.24 – 1.04 (m, 4H), 1.07 – 0.89 (m, 2H), 0.88 – 0.79 (m, 9H) ppm; **^{13}C NMR** (101 MHz, $CDCl_3$) δ 102.0, 100.6, 82.7, 81.3, 60.4, 57.2, 57.2, 57.2, 42.6, 40.4, 40.1, 40.0, 39.9, 36.2, 36.1, 33.7, 33.6, 33.3, 33.2, 31.0, 31.0, 23.7, 23.1, 21.2, 20.9, 20.6, 18.5, 18.5, 15.5, 15.4, 15.3 ppm.

3-(2-chlorobenzyl)tetrahydro-2H-pyran-2-ol (2.79)



Prepared according to GP1 from **2.72** as a white powder containing a 1:1 mixture of anomers (91%, 2 mmol scale, 411 mg isolated). Purified by flash column chromatography (5–25% EtOAc in hexanes). ***R**f* 0.40 (30% EtOAc/hexanes); **^{1}H NMR** (400 MHz, $CDCl_3$) δ 7.36 – 7.32 (m, 2H), 7.26 – 7.09 (m, 6H), 5.00 (dd, J = 3.0, 2.8 Hz, 1H), 4.57 (dd, J = 6.1, 6.1 Hz, 1H), 4.06 – 3.92 (m, 2H), 3.61 – 3.46 (m, 2H), 3.20 (dd, J = 13.5, 4.7 Hz, 1H), 2.89 – 2.76 (m, 2H), 2.66 (dd, J = 13.5, 8.0 Hz, 1H), 2.54 (dd, J = 13.5, 9.5 Hz, 1H), 2.47 (s, 1H), 2.13 – 2.02 (m, 1H), 1.89 – 1.41 (m, 8H), 1.34 – 1.20 (m, 1H) ppm; **^{13}C NMR** (101 MHz, $CDCl_3$) δ 137.9 (C), 137.9 (C), 134.5 (C), 134.4 (C), 131.6 (CH), 131.6 (CH), 129.7 (CH × 2), 127.6 (CH × 2), 126.7 (CH), 126.6 (CH), 99.2 (CH), 93.7 (CH), 65.4 (CH_2), 59.9 (CH_2), 42.3 (CH), 39.8 (CH), 35.9 (CH_2), 35.0 (CH_2), 26.6 (CH_2), 25.5 (CH_2), 24.6 (CH_2), 23.4 (CH_2) ppm; **HRMS** (EI): *m/z* calculated for $C_{12}H_{15}ClO_2$ $[M]^+$: 226.07606, found 226.07710.

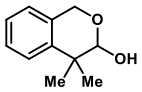
3-benzyltetrahydro-2H-pyran-2-ol (2.80)



Prepared according to GP1 from **2.70** as a white powder containing a 1:1 mixture of anomers (87%, 2.6 mmol scale, 438 mg isolated). Purified by flash column chromatography (5–25% EtOAc/hexanes). Characterized according to NMR comparison.[313] ***R**f* 0.33 (25% EtOAc/hexanes); **^{1}H NMR** (400 MHz, $CDCl_3$) δ 7.33 – 7.26 (m, 4H), 7.24 –

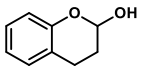
7.14 (m, 6H), 4.97 (dd, J = 3.1, 3.0 Hz, 1H), 4.52 (dd, J = 6.8, 5.1 Hz, 1H), 4.03 – 3.93 (m, 2H), 3.60 – 3.54 (m, 1H), 3.50 (ddd, J = 11.4, 10.0, 3.3 Hz, 1H), 3.07 (dd, J = 13.5, 4.5 Hz, 1H), 2.85 (s, 1H), 2.72 (dd, J = 13.5, 7.3 Hz, 1H), 2.51 (dd, J = 13.6, 8.0 Hz, 1H), 2.45 (s, 1H), 2.41 (dd, J = 13.5, 9.4 Hz, 1H), 2.02 – 1.91 (m, 1H), 1.81 – 1.41 (m, 8H), 1.28 – 1.13 (m, 1H) ppm; **^{13}C NMR** (101 MHz, $CDCl_3$) δ 140.3 (C), 139.9 (C), 129.5 (CH × 2), 129.2 (CH × 2), 128.4 (CH × 4), 126.1 (CH), 126.1 (CH), 99.0 (CH), 93.7 (CH), 65.4 (CH_2), 60.0 (CH_2), 43.5 (CH), 41.9 (CH), 38.2 (CH_2), 37.5 (CH_2), 26.6 (CH_2), 25.5 (CH_2), 24.7 (CH_2), 23.6 (CH_2) ppm; **HRMS** (EI): calculated for $C_{12}H_{16}O_2$ $[M]^+$: 192.11503, found 192.11562.

4,4-dimethylisochroman-3-ol (2.81)



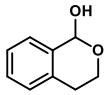
Prepared according to GP1 on 2.8 mmol scale and purified by flash column chromatography (2–5% EtOAc/hexanes) to give the title compound (490 mg, 98%). Characterized according to NMR comparison.[314] ***R$_f$*** 0.50 (10% EtOAc/DCM); **^{1}H NMR** (400 MHz, MeOD) δ 7.34 (dd, J = 7.9, 1.3 Hz, 1H), 7.19 (tdt, J = 8.0, 1.5, 0.8 Hz, 1H), 7.12 (td, J = 7.5, 1.4 Hz, 1H), 6.97 (ddq, J = 7.5, 1.5, 0.8 Hz, 1H), 4.94 (d, J = 15.0 Hz, 1H), 4.83 (s, 1H), 4.78 (d, J = 15.1 Hz, 1H), 1.27 (s, 3H), 1.26 (s, 3H) ppm; **^{13}C NMR** (101 MHz, MeOD) δ 143.2 (C), 133.8 (C), 127.9 (CH), 126.9 (CH), 126.7 (CH), 124.5 (CH), 100.1 (CH), 65.2 (CH_2), 38.9 (C), 27.8 (CH_3), 23.7 (CH_3) ppm.

chroman-2-ol (2.82)



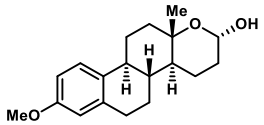
Prepared according to GP1 on 7.9 mmol scale and purified by flash column chromatography (3–40% EtOAc/hexanes) to give a clear colourless oil (240 mg, 20%). Characterized according to NMR comparison.[315] ***R$_f$*** 0.38 (20% EtOAc/hexanes); **^{1}H NMR** (400 MHz, $CDCl_3$) δ 7.12 (dddt, J = 8.0, 7.3, 1.6, 0.7 Hz, 1H), 7.08 (dq, J = 8.5, 1.1 Hz, 1H), 6.89 (td, J = 7.4, 1.3 Hz, 1H), 6.83 (dd, J = 8.1, 1.2 Hz, 1H), 5.62 (dd, J = 3.9, 2.6 Hz, 1H), 2.99 (ddd, J = 16.6, 10.5, 6.3 Hz, 1H), 2.71 (dt, J = 16.4, 5.3 Hz, 1H), 2.10 – 1.93 (m, 2H); **^{13}C NMR** (101 MHz, $CDCl_3$) δ 152.1 (C), 129.4 (CH), 127.6 (CH), 122.1 (C), 121.0 (CH), 117.0 (CH), 92.2 (CH), 27.1 (CH_2), 20.4 (CH_2) ppm.

isochroman-1-ol (2.83)



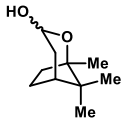
Prepared according to GP1 on 6.7 mmol scale and purified by flash column chromatography (15–40% EtOAc/hexanes) to give a white solid (352 mg, 35%). Characterized according to NMR comparison.[316] $\boldsymbol{R_f}$ 0.25 (15% EtOAc/DCM); **^{1}H NMR** (400 MHz, DMSO-d_6) δ 7.26 – 7.09 (m, 4H), 6.64 (d, J = 5.8 Hz, 1H), 5.74 (d, J = 5.6 Hz, 1H), 4.06 (td, J = 11.0, 3.8 Hz, 1H), 3.79 (ddd, J = 11.3, 5.8, 2.8 Hz, 1H), 2.82 (ddd, J = 16.6, 10.7, 5.8 Hz, 1H), 2.63 (dt, J = 16.7, 3.3 Hz, 1H) ppm; **^{13}C NMR** (101 MHz, DMSO-d_6) δ 136.7 (C), 133.9 (C), 128.2 (CH), 127.4 (CH), 127.2 (CH), 125.8 (CH), 90.3 (CH), 57.1 (CH_2), 27.6 (CH_2) ppm.

(2S,4aS,4bR,10bS,12aS)-8-methoxy-12a-methyl-3,4,4a,4b,5,6,10b,11,12,12a-decahydro-2H-naphtho[2,1-f]chromen-2-ol (2.84)



Prepared according to GP1 from **2.56** as a white powder (82%, 1.7 mmol scale, 413 mg isolated). Purified by flash column chromatography (20% EtOAc/DCM). $\boldsymbol{R_f}$ 0.27 (15% EtOAc/DCM); **^{1}H NMR** (500 MHz, DMSO–d_6) δ 7.17 (d, J = 8.6 Hz, 1H), 6.68 (dd, J = 8.6, 2.8 Hz, 1H), 6.60 (d, J = 2.8 Hz, 1H), 5.98 (d, J = 6.6 Hz, 1H), 4.90 (ddd, J = 9.2, 6.6, 2.4 Hz, 1H), 3.68 (s, 3H), 2.84 – 2.66 (m, 2H), 2.43 – 2.32 (m, 1H), 2.28 (ddd, J = 11.6, 11.4, 4.1 Hz, 1H), 1.95 (ddd, J = 12.3, 5.9, 2.9 Hz, 1H), 1.83 – 1.68 (m, 3H), 1.59 (ddd, J = 13.2, 12.9, 4.3 Hz, 1H), 1.37 – 1.16 (m, 5H), 1.13 (s, 3H), 1.02 (dddd, J = 11.2, 11.2, 11.0, 2.5 Hz, 1H) ppm; **^{13}C NMR** (126 MHz, DMSO-d_6) δ 157.1 (C), 137.3 (C), 131.9 (C), 126.2 (CH), 113.1 (CH), 111.6 (CH), 89.5 (CH), 74.9 (C), 54.9 (CH_3), 47.9 (CH), 43.0 (CH), 39.7 (CH_2), 39.7 (CH), 34.2 (CH_2), 29.6 (CH_2), 27.1 (CH_2), 25.6 (CH_2), 21.1 (CH_2), 16.9 (CH_3) ppm; **HRMS** (ESI+): *m/z* calculated for $C_{19}H_{26}O_3Na$ $[M + Na]^+$: 325.1780, found 325.1804.

(1R,5R)-1,8,8-trimethyl-2-oxabicyclo[3.2.1]octan-3-ol (2.85)



Prepared according to GP1 on 1.78 mmol scale and purified by flash column chromatography (10–30% EtOAc/hexanes) to give a white solid (280 mg, 92%). **^{1}H NMR** (500 MHz, MeOD) δ 5.15 (d, J = 6.3 Hz, 0.2H), 5.06 (dd, J = 9.3, 4.1 Hz, 0.8H), 2.42 – 2.31 (m), 2.26 – 2.18 (m), 2.02 – 1.71 (m), 1.62 – 1.45 (m), 1.39 – 1.22 (m), 1.08

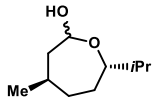
(d, J = 7.3 Hz), 1.01 – 0.93 (m), 0.93 – 0.81 (m) ppm; Integration of the anomeric protons for a total of 1H results in a slight over-integration of the total spectrum, likely due to minor component impurities lacking a signal at this chemical shift. **^{13}C NMR** (126 MHz, MeOD, **Major lactol**) δ 92.4 (CH), 86.2 (C), 45.8 (CH), 44.7 (C), 37.9 (CH_2), 35.3 (CH_2), 27.4 (CH_2), 24.3 (CH_3), 19.5 (CH_3), 18.6 (CH_3) ppm. **^{13}C NMR** (126 MHz, MeOD, **minor lactol**) δ 92.1 (CH), 85.8 (C), 44.9 (CH), 43.2 (C), 36.2 (CH_2), 32.7 (CH_2), 24.9 (CH_3), 23.7 (CH_2), 19.9 (CH_3), 18.8 (CH_3) ppm. Additional constituents appear to include the hydroxyaldehyde form as a minor component, though its complete assignment cannot be confidently made.

(1R,3r,6s,8S)-4-oxatricyclo[4.3.1.13,8]undecan-5-ol (2.86)



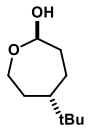
Prepared according to GP1 from **2.49** as a white powder (98%, 6 mmol scale, 993 mg isolated). Purified by flash column chromatography (5–20% EtOAc in hexanes). ***R**$_f$* 0.17 (10% EtOAc/hexanes); **^{1}H NMR** (400 MHz, $CDCl_3$) δ 5.28 (t, J = 3.4 Hz, 1H), 4.23 – 4.12 (m, 1H), 2.99 – 2.85 (m, 1H), 2.25 – 2.10 (m, 2H), 2.01 – 1.91 (m, 3H), 1.89 – 1.76 (m, 4H), 1.67 – 1.53 (m, 4H) ppm; **^{13}C NMR** (101 MHz, $CDCl_3$) δ 100.2 (CH), 72.4 (CH), 38.5 (CH_2), 38.2 (CH), 37.3 (CH_2), 35.8 (CH_2), 33.1 (CH_2), 29.4 (CH_2), 26.8 (CH), 26.7 (CH) ppm; **HRMS** (EI): *m/z* calculated for C_9H_{14} $[M - CH_2O_2]^+$: 122.10955, found 122.10802.

(4R,7S)-7-isopropyl-4-methyloxepan-2-ol (2.87)



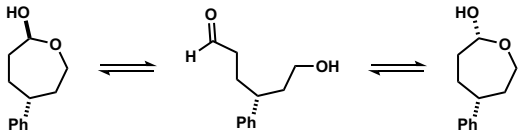
Prepared according to GP1 to give a white powder (81%, 1.8 mmol scale, 247 mg isolated). Purified by flash column chromatography (10–30% EtOAc in hexanes). **^{1}H NMR** (400 MHz, DMSO-d_6) δ 5.64 (d, J = 4.7 Hz, 1H), 4.96 (dt, J = 9.6, 5.1 Hz, 1H), 3.51 (dd, J = 10.4, 5.0 Hz, 1H), 1.76 – 1.62 (m, 2H), 1.62 – 1.38 (m, 4H), 1.28 (tdd, J = 13.6, 10.5, 4.4 Hz, 1H), 1.06 (tdd, J = 13.1, 10.7, 4.5 Hz, 1H), 0.86 (d, J = 6.7 Hz, 3H), 0.85 (d, J = 4.0 Hz, 3H), 0.83 (d, J = 4.0 Hz, 3H) ppm; **^{13}C NMR** (101 MHz, DMSO-d_6) δ 92.8 (CH), 73.3 (CH), 44.5 (CH_2), 38.1 (CH_2), 33.1 (CH), 31.6 (CH_2), 28.7 (CH), 24.3 (CH_3), 19.2 (CH_3), 18.0 (CH_3) ppm.

(±)-(2R,5S)-5-(tert-butyl)oxepan-2-ol (2.88)



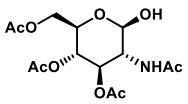
Prepared according to GP1 from **2.51b** as a white powder containing a 14:1.7:1 mixture *trans*/*cis*/hydroxy aldehyde forms (89%, 2.9 mmol scale, 453 mg isolated). Purified by flash column chromatography (10–30% EtOAc/hexanes). R_f 0.33 (25% EtOAc/hexanes); **^{1}H NMR** (400 MHz, C_6D_6) δ 5.17 (dd, J = 9.1, 5.3 Hz, 1H), 3.96 (ddd, J = 13.0, 11.3, 1.5 Hz, 1H), 3.65 (dt, J = 12.8, 3.6 Hz, 1H), 3.16 (s, 1H), 2.10 (dddd, J = 14.9, 8.4, 5.4, 1.1 Hz, 1H), 1.77 – 1.61 (m, 1H), 1.61 – 1.47 (m, 2H), 1.47 – 1.33 (m, 1H), 1.21 – 1.09 (m, 1H), 1.08 – 0.96 (m, 1H), 0.86 (s, 9H) ppm; **^{13}C NMR** (101 MHz, C_6D_6) δ 96.6 (CH), 60.2 (CH_2), 51.7 (CH), 34.8 (CH_2), 33.0 (C), 31.9 (CH_2), 27.7 (3 × CH_3), 23.5 (CH_2) ppm; **HRMS** (EI): *m/z* calculated for $C_{10}H_{20}O_2$ $[M - OH]^+$: 155.14359, found 155.14582.

5-phenyloxepan-2-ol (2.89)



Prepared according to GP1 on 2.6 mmol scale and purified by flash column chromatography (30–50% EtOAc/hexanes) to give a clear colourless oil (408 mg, 81%). Characterized according to NMR comparison.[317] **^{1}H NMR** (400 MHz, DMSO-d_6) δ 9.55 (dt, J = 5.0, 1.6 Hz), 7.35 – 6.93 (m, 5H), 5.92 (d, J = 4.6 Hz), 5.68 – 5.58 (m), 5.09 – 4.94 (m), 4.49 (s), 4.39 – 4.17 (m), 3.89 (t, J = 12.1 Hz), 3.53 – 3.33 (m), 3.31 – 3.11 (m), 3.10 – 2.97 (m), 2.91 (s), 2.75 – 2.52 (m), 2.35 – 2.07 (m), 1.97 – 1.39 (m), 1.14 (d, J = 1.0 Hz) ppm (total integration gives 16H based on aryl region of 5H); **^{13}C NMR** (101 MHz, DMSO-d_6) δ 203.1, 203.1, 145.4, 144.5, 128.4, 128.3, 128.2, 127.6, 127.5, 126.6, 126.2, 126.1, 125.8, 96.8, 96.4, 94.9, 58.8, 58.7, 47.4, 41.3, 41.3, 40.9, 34.9, 31.5, 28.4 ppm.

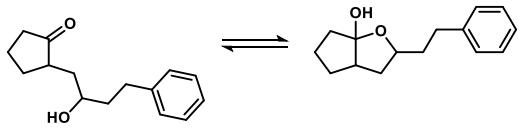
2-Acetamido-3,4,6-tri-O-acetyl-2-deoxy-D-glucopyranose (2.92c)



Prepared according to the following adapted literature procedure.[318] A flame-dried 50mL round bottom flask under argon and equipped with stir bar was charged with 2-acetamido-1,3,4,6-tetra-*O*-acetyl-2-deoxy-D-glucopyranose (1 g, 2.6 mmol, 1 equivalent) and anhydrous THF (8.5 mL) followed by benzylamine (0.34 mL, 3.1 mmol, 1.2 equivalents). The resulting suspension was stirred at room temperature for 3 days at which point it was

concentrated *in vacuo*. The crude residue was purified by flash column chromatography (0–8% MeOH in DCM) giving **2.92c** as a white solid as a single anomer (50%, 466 mg isolated). The isolated product was characterized by NMR comparison.[319] ***R**f* 0.26 (5% MeOH/DCM); **^{1}H NMR** (400 MHz, $CDCl_3$) δ 5.84 (d, J = 9.3 Hz, 1H), 5.34 – 5.25 (m, 2H), 5.14 (t, J = 9.5 Hz, 1H), 4.30 (ddd, J = 10.8, 9.4, 3.6 Hz, 1H), 4.26 – 4.10 (m, 3H), 2.10 (s, 3H), 2.04 (s, 3H), 2.03 (s, 3H), 1.96 (s, 3H) ppm; **^{13}C NMR** (101 MHz, $CDCl_3$) δ 171.5 (C), 170.9 (C), 170.3 (C), 169.4 (C), 91.7 (CH), 70.9 (CH), 68.2 (CH), 67.7 (CH), 62.1 (CH_2), 52.2 (CH), 23.2 (CH_3), 20.8 (CH_3), 20.8 (CH_3), 20.7 (CH_3) ppm.

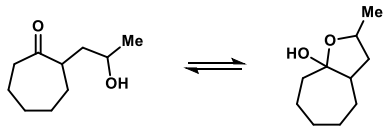
2-(2-hydroxy-4-phenylbutyl)cyclopentan-1-one (2.95 & 2.95')



Prepared according to the following adapted literature procedure.[320] A flame-dried 50 mL round bottom flask under argon and equipped with stir bar was charged with a solution of LiHMDS in THF (1.0 M, 3.7 mL, 3.7 mmol, 1.1 equivalents) and additional anhydrous THF (6.8 mL) and cooled to –78 ºC with a dry ice acetone bath under vigorous stirring. After thermal equilibration, cyclopentanone (0.3 mL, 3.4 mmol, 1 equivalent) was added dropwise and the resulting solution stirred for 30 minutes maintaining –78 ºC. After this interval, the epoxide **2.100** (1.0 g, 6.8 mmol, 2 equivalents) was added followed by dropwise addition of BF_3•OEt_2 (48%, 0.47 mL, 3.7 mmol, 1.1 equivalents). This solution was then stirred at –78 ºC until complete consumption of cyclopentanone (~1.5 h after addition of BF_3•OEt_2). The mixture is then quenched at –78 ºC upon addition of NH_4Cl (sat. aq., 15 mL) and the cryogenic bath was removed to allow the solution to slowly warm to room temperature. The biphasic mixture was poured into a separatory funnel and the aqueous phase extracted with Et_2O (3 × 20 mL). The combined organic extracts were washed with $NaHCO_3$ (sat. aq., 2 × 10 mL), brine (1 × 20 mL), dried over Na_2SO_4, filtered and concentrated *in vacuo*. The crude material was then purified by flash column chromatography (15–75% EtOAc/hexanes) to deliver **2.95** (65%, 510 mg) as a yellow oil composed of a complex mixture of adducts as hemiketals and their ring-chain tautomeric hydroxy ketones. ***R**f* ≈ 0.44 (25% EtOAc/hexanes); **^{1}H NMR** (500 MHz, C_6D_6) δ 7.23 – 7.00 (m, 16.70H), 4.16 – 4.03 (m, 0.36H), 3.99 – 3.86 (m, 0.50H), 3.74 – 3.60 (m, 1H), 3.53 – 3.46 (m, 0.42H), 3.20 – 3.08 (m, 0.36H), 2.98 – 2.84 (m, 0.63H), 2.86 – 2.67 (m, 3.00H), 2.67 – 2.54 (m, 2.22H), 2.48 – 2.32 (m, 0.88H), 2.18 – 1.46 (m, 20.26H), 1.48 – 1.26 (m, 4.19H), 1.26 – 1.05 (m, 5.05H), 0.97 – 0.86 (m, 1.59H) ppm; **^{13}C NMR** (126 MHz, C_6D_6) δ 142.9, 142.8, 142.6, 142.5, 129.0, 128.9, 128.9, 128.8, 128.7, 128.7, 128.4, 126.1, 126.1, 126.1, 117.2, 116.9, 79.9, 78.6, 69.9, 69.3, 49.2, 48.6, 47.9, 46.2, 40.9, 40.5, 40.2, 40.0, 39.8, 39.0, 38.2, 38.1, 37.8, 37.6, 37.5, 37.3, 33.1, 33.0,

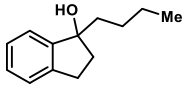
33.0, 32.6, 32.4, 31.9, 30.7, 30.4, 25.0, 24.9, 21.0, 20.9 ppm; **HRMS** (EI): *m/z* calculated for $[M]^+$: 232.14633, found 232.14617.

2-(2-hydroxypropyl)cycloheptan-1-one (2.96 & 2.96')



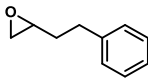
Prepared according to a procedure by Posner.[320] **^{1}H NMR** (400 MHz, $CDCl_3$) δ 4.40 – 4.15 (m, 0.63H), 3.76 (s, 0.37H), 2.87 – 2.67 (m, 0.37H), 2.59 – 2.39 (m, 0.63H), 2.34 – 1.02 (m, 16H) ppm; **^{13}C NMR** (101 MHz, $CDCl_3$) δ 217.7, 217.5, 151.4, 110.5, 109.6, 107.5, 107.3, 107.0, 75.7, 75.7, 75.3, 73.0, 72.9, 66.8, 65.6, 51.0, 50.9, 49.8, 48.8, 47.0, 44.4, 44.3, 43.0, 43.0, 42.5, 42.1, 41.9, 41.8, 41.7, 40.7, 40.6, 40.5, 39.4, 39.0, 33.3, 33.1, 32.2, 31.9, 31.7, 31.3, 31.2, 30.9, 30.4, 29.5, 29.5, 29.4, 28.8, 28.7, 28.6, 28.6, 28.4, 27.0, 26.9, 26.7, 26.4, 26.2, 25.8, 25.8, 25.6, 25.3, 25.2, 24.5, 24.4, 24.4, 24.0, 23.7, 23.3, 23.3, 23.2, 22.7, 22.2, 20.5 ppm.

1-butyl-2,3-dihydro-1H-inden-1-ol (2.98)



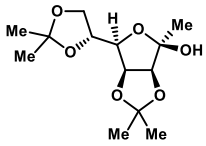
To a solution of $CeCl_3$ (1.1 g, 4.6 mmol, 1.2 equiv.) in THF (9.5 mL) was added nBuLi (1.9 mL, 4.6 mmol. 1.2 equiv., 2.5 M in hexanes) at -78 °C and stirred for 30 minutes at the same temperature. A solution of indanone (0.5 g, 3.8 mmol, 1.0 equiv.) in THF (19 mL, 0.2 M) was added slowly at -78 °C and the mixture allowed to stir at -78 °C until the indanone was consumed (2 hours). Excess nBuLi was quenched at 0 °C with addition of NH4Cl (saturated aqueous, 10 mL) and the solution was concentrated under reduced pressure, then extracted with EtOAc (3 × 10 mL). The combined organic extracts were washed with brine, dried over Na_2SO_4, filtered, and concentrated under reduced pressure. The crude residue was purified by flash column chromatography (SiO_2, 15% EtOAc/hexanes) to give the title compound (721 mg, quantitative). Characterized according to NMR comparison.[321] **^{1}H NMR** (400 MHz, DMSO-d_6) δ 7.24 (tq, J = 3.7, 2.1 Hz, 1H), 7.20 – 7.13 (m, 3H), 4.84 (s, 1H), 2.87 (ddd, J = 15.8, 8.7, 4.4 Hz, 1H), 2.71 (dt, J = 15.7, 7.5 Hz, 1H), 2.11 (ddd, J = 12.6, 8.1, 4.4 Hz, 1H), 1.96 (ddd, J = 12.8, 8.6, 7.1 Hz, 1H), 1.71 (ddd, J = 13.3, 11.6, 4.6 Hz, 1H), 1.57 (ddd, J = 13.3, 11.5, 4.2 Hz, 1H), 1.40 – 1.11 (m, 4H), 0.84 (t, J = 7.0 Hz, 3H) ppm; **^{13}C NMR** (101 MHz, DMSO-d_6) δ 149.0 (C), 142.3 (C), 127.2 (CH), 126.0 (CH), 124.4 (CH), 123.1 (CH), 81.8 (C), 40.3 (CH_2), 39.3 (CH_2), 29.1 (CH_2), 26.1 (CH_2), 22.7 (CH_2), 14.0 (CH_3) ppm.

2-phenethyloxirane (2.100)



Prepared according to GP2 from 4-phenyl-1-butene as a clear and colourless oil (97%, 8.5 mmol scale, 1.22 g isolated). Purified by flash column chromatography (2–8% EtOAc in hexanes). Characterized according to NMR comparison.[322] R_f 0.49 (15% EtOAc/hexanes); **^{1}H NMR** (400 MHz, $CDCl_3$) δ 7.33 – 7.27 (m, 2H), 7.24 – 7.17 (m, 3H), 3.00 – 2.92 (m, 1H), 2.89 – 2.71 (m, 3H), 2.48 (dd, J = 5.0, 2.7 Hz, 1H), 1.94 – 1.78 (m, 2H) ppm; **^{13}C NMR** (101 MHz, $CDCl_3$) δ 141.4 (C), 128.6 (2 × CH), 128.5 (2 × CH), 126.2 (CH), 51.9 (CH), 47.4 (CH_2), 34.4 (CH_2), 32.4 (CH_2) ppm.

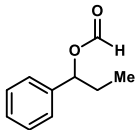
(3aS,4R,6R,6aS)-6-((R)-2,2-dimethyl-1,3-dioxolan-4-yl)-2,2,4-trimethyltetrahydrofuro[3,4-d][1,3]dioxol-4-ol (2.104)



A flame-dried 50 mL round bottom flask under argon and equipped with stir bar was charged with the lactone **2.63** (500 mg, 1.9 mmol, 1 equivalent) and anhydrous THF (10 mL) and the resulting solution was cooled to –78ºC with a dry ice acetone bath with vigorous stirring. Upon thermal equilibration, a solution of MeLi was added (1.6 M in Et_2O, 1.3 mL, 1.1 equivalents) dropwise over 2 minutes. The resulting solution was stirred at –78 ºC until the lactone was completely consumed as determined by TLC (~20 minutes). Excess MeLi was quenched at –78 ºC by the addition of acetone (2 mL) before the cooling bath was removed and the solution was allowed to warm to room temperature. After warming to room temperature, a phosphate buffer solution (pH ~7, aqueous) was added followed by EtOAc (10 mL). The resulting layers were separated, and the aqueous phase was extracted with additional EtOAc (3 × 15 mL). The combined organic extracts were washed with brine (1 × 30 mL), dried over Na_2SO_4, filtered, and concentrated under reduced pressure. The crude residue was then purified by flash column chromatography (20% EtOAc/hexanes) to deliver hemiketal **2.104** as a single anomer (78%, 405mg). Isolated product was characterized according to NMR comparison.[323] R_f 0.14 (15% EtOAc/hexanes); **^{1}H NMR** (400 MHz, DMSO–d_6) δ 6.05 (s, 1H), 4.71 (dd, J = 5.9, 3.7 Hz, 1H), 4.26 (d, J = 5.9 Hz, 1H), 4.21 (ddd, J = 6.6, 6.6, 5.7 Hz, 1H), 3.96 (dd, J = 11.0, 6.6 Hz, 1H), 3.95 (dd, J = 6.5, 6.5 Hz, 1H), 3.78 (dd, J = 8.3, 5.7 Hz, 1H), 1.35 (s, 3H), 1.32 (s, 3H), 1.30 (s, 3H), 1.26 (s, 3H), 1.23 (s, 3H) ppm;

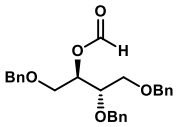
^{13}C NMR (101 MHz, DMSO–d_6) δ 111.3 (C), 107.8 (C), 104.3 (C), 85.5(CH), 80.1 (CH), 78.0 (CH), 72.7 (CH), 65.9 (CH_2), 26.6 (CH_3), 25.8 (CH_3), 25.2 (CH_3), 24.4 (CH_3), 22.0 (CH_3) ppm.

1-phenylpropyl formate (2.105)



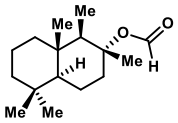
Prepared according to GP4 as a clear, and colourless oil (51%, 0.2 mmol scale, 17 mg isolated). Purified by flash column chromatography (3% Et_2O/hexanes). R_f 0.61 (40% EtOAc/hexanes); **^{1}H NMR** (400 MHz, $CDCl_3$) δ 8.15 – 8.08 (m, 1H), 7.39 – 7.27 (m, 5H), 5.79 (ddd, J = 7.4, 6.4, 1.1 Hz, 1H), 2.05 – 1.92 (m, 1H), 1.92 – 1.81 (m, 1H), 0.91 (t, J = 7.4 Hz, 3H) ppm; **^{13}C NMR** (101 MHz, $CDCl_3$) δ 160.6 (CH), 139.9 (C), 128.6 (2 × CH), 128.2 (CH), 126.8 (2 × CH), 77.4 (CH), 29.3 (CH_2), 10.0 (CH_3) ppm; **HRMS** (EI): *m/z* calculated for $C_{10}H_{12}O_2$ $[M]^+$: 164.08373, found 164.98532.

(2R,3S)-1,3,4-tris(benzyloxy)butan-2-yl formate (2.107)



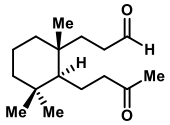
Prepared according to GP4 as a clear, and colourless oil in 72% from ribofuranose derivative **2.106b** and 68% yield from arabinofuranose derivative **2.106a** (0.2 mmol scale, 71 and 57 mg isolated, respectively). Purified by flash column chromatography (5–22% EtOAc/hexanes). Characterized according to NMR comparison.[324] R_f 0.25 (15% EtOAc/hexanes); **^{1}H NMR** (400 MHz, $CDCl_3$) δ 8.08 (d, J = 0.9 Hz, 1H), 7.42 – 7.27 (m, 15H), 5.37 (dddd, J = 5.3, 5.3, 4.1, 0.9 Hz, 1H), 4.70 (d, J = 11.6 Hz, 1H), 4.63 (d, J = 11.6 Hz, 1H), 4.58 – 4.47 (m, 4H), 3.93 (ddd, J = 5.5, 5.5, 4.0 Hz, 1H), 3.80 – 3.74 (m, 2H), 3.68 (dd, J = 10.5, 4.0 Hz, 1H), 3.60 (dd, J = 10.5, 5.4 Hz, 1H) ppm; **^{13}C NMR** (101 MHz, $CDCl_3$) δ 160.6 (CH), 138.1(C), 138.1 (C), 137.9 (C), 128.5 (n × CH), 128.5 (n × CH), 128.0 (n × CH), 127.8 (CH), 127.8 (CH), 127.8 (n × CH), 127.8 (n × CH), 76.7 (CH), 73.5 (CH_2), 73.3 (CH_2), 72.9 (CH_2), 72.3 (CH), 69.3 (CH_2), 68.4 (CH_2) ppm.

(1R,2R,4aS,8aS)-1,2,5,5,8a-pentamethyldecahydronaphthalen-2-yl formate (2.108a)



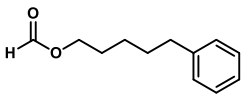
Prepared according to GP4 as a white solid (21%, 0.2 mmol scale, 10 mg isolated). Purified by flash column chromatography (0–15% EtOAc/hexanes). Characterized according to NMR comparison.[324] R_f 0.48 (5% EtOAc/hexanes); **^{1}H NMR** (400 MHz, $CDCl_3$) δ 8.05 (s, 1H), 2.55 (ddd, J = 12.5, 3.4, 3.4 Hz, 1H), 1.82 (dddd, J = 13.6, 12.6, 4.5, 1.1 Hz, 1H), 1.74 (q, J = 7.0 Hz, 1H), 1.72 – 1.53 (m, 3H), 1.45 (s, 3H), 1.43 – 1.32 (m, 2H), 1.31 – 1.22 (m, 1H), 1.15 (ddd, J = 13.5, 13.5, 4.4 Hz, 1H), 1.00 (dd, J = 12.3, 2.3 Hz, 1H), 0.97 – 0.90 (m, 1H), 0.88 (d, J = 7.0 Hz, 3H), 0.88 (s, 3H), 0.84 (d, J = 1.0 Hz, 3H), 0.80 (s, 3H) ppm; **^{13}C NMR** (101 MHz, $CDCl_3$) δ 160.8 (CH), 88.2 (C), 55.7 (CH), 52.6 (CH), 41.9 (CH_2), 39.9 (CH_2), 39.8 (CH_2), 38.3 (C), 33.5 (CH_3), 33.3 (C), 21.7 (CH_3), 20.6 (CH_3), 20.2 (CH_2), 18.6 (CH_2), 14.8 (CH_3), 7.8 (CH_3) ppm.

3-((1R,2S)-1,3,3-trimethyl-2-(3-oxobutyl)cyclohexyl)propanal (2.108b)



Prepared according to GP4 as a yellow oil (28%, 0.2 mmol scale, 14 mg isolated, unstable). Purified by flash column chromatography (0–20% EtOAc/hexanes). R_f 0.32 (20% EtOAc/hexanes); **^{1}H NMR** (400 MHz, C_6D_6) δ 9.38 (t, J = 1.6 Hz, 1H), 2.20 – 2.04 (m, 2H), 1.88 – 1.73 (m, 2H), 1.70 (s, 3H), 1.59 – 1.42 (m, 3H), 1.42 – 1.31 (m, 3H), 1.31 – 1.19 (m, 3H), 1.14 – 1.04 (m, 2H), 0.80 (s, 3H), 0.74 (s, 3H), 0.61 (s, 3H) ppm; **^{13}C NMR** (101 MHz, C_6D_6) δ 206.3 (C), 201.1 (CH), 54.5 (CH), 47.3 (CH_2), 42.3 (CH_2), 38.5 (CH_2), 38.1 (CH_2), 37.0 (C), 35.5 (CH_2), 35.2 (C), 33.5 (CH_3), 29.4 (CH_3), 21.8 (CH_3), 20.6 (CH_2), 19.0 (CH_2), 18.6 (CH_3) ppm; Molecular ion peak could not be found for this compound, as a result it was further elaborated to compound **2.132** and this compound was fully characterized.

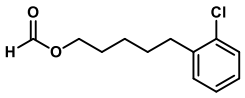
5-phenylpentyl formate (2.109)



Prepared according to GP4 as a white solid (80%, 0.2 mmol scale, 31 mg isolated). Purified by flash column chromatography (0–5% Et_2O/hexanes). R_f 0.30 (6% Et_2O/hexanes); **^{1}H NMR** (400 MHz, $CDCl_3$) δ 8.06 (t, J = 0.8 Hz, 1H), 7.32 – 7.26 (m, 2H), 7.22 – 7.16 (m, 3H), 4.17 (td, J = 6.7, 0.9 Hz, 2H), 2.68 – 2.59 (m, 2H), 1.76 – 1.63 (m, 4H), 1.48 – 1.37 (m, 2H) ppm; **^{13}C NMR** (101 MHz, $CDCl_3$) δ 161.2 (CH), 142.4 (C), 128.5 (2 × CH), 128.4 (2 ×

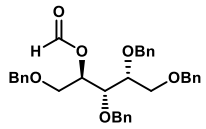
CH), 125.9 (CH), 64.1 (CH_2), 35.9 (CH_2), 31.1 (CH_2), 28.5 (CH_2), 25.6 (CH_2) ppm; **HRMS** (EI): *m/z* calculated for $C_{12}H_{16}O_2$ $[M]^+$: 192.11503, found 192.11305.

5-(2-chlorophenyl)pentyl formate (2.110)



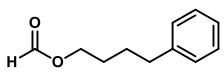
Prepared according to GP4 as a white solid (89%, 0.2 mmol scale, 41 mg isolated). Purified by flash column chromatography (10–40% DCM/hexanes). R_f 0.34 (5% EtOAc/hexanes); **^{1}H NMR** (400 MHz, $CDCl_3$) δ 8.06 (t, J = 0.7 Hz, 1H), 7.36 – 7.31 (m, 1H), 7.23 – 7.10 (m, 3H), 4.18 (td, J = 6.7, 0.9 Hz, 2H), 2.77 – 2.71 (m, 2H), 1.77 – 1.61 (m, 4H), 1.50 – 1.40 (m, 2H) ppm; **^{13}C NMR** (101 MHz, $CDCl_3$) δ 161.3 (CH), 140.0 (C), 134.0 (C), 130.5 (CH), 129.6 (CH), 127.4 (CH), 126.8 (CH), 64.1 (CH_2), 33.6 (CH_2), 29.4 (CH_2), 28.5 (CH_2), 25.7 (CH_2) ppm; **HRMS** (EI): *m/z* calculated for $C_{12}H_{15}ClO_2$ $[M]^+$: 226.07606, found 226.07430.

(2R,3S,4R)-1,3,4,5-tetrakis(benzyloxy)pentan-2-yl formate (2.112)



Prepared according to GP4 as a white solid in 65% yield from the mannose (**2.111a**) and glucose (**2.111b**) derivatives (0.2 mmol scale, 71 mg isolated for both). Purified by flash column chromatography (5–20% EtOAc/hexanes). Characterized according to NMR comparison.[324] R_f 0.42 (20% EtOAc/hexanes); **^{1}H NMR** (400 MHz, $CDCl_3$) δ 7.93 (d, J = 0.6 Hz, 1H), 7.38 – 7.26 (m, 18H), 7.25 – 7.21 (m, 2H), 5.30 (dddd, J = 5.6, 5.5, 2.6, 0.7 Hz, 1H), 4.67 – 4.43 (m, 8H), 3.94 (dd, J = 6.0, 3.7 Hz, 1H), 3.84 – 3.71 (m, 3H), 3.64 (dd, J = 9.8, 5.4 Hz, 1H), 3.59 (dd, J = 9.7, 6.2 Hz, 1H) ppm; **^{13}C NMR** (101 MHz, $CDCl_3$) δ 160.6 (CH), 138.2 (C), 138.1 (2 × C), 138.0 (C), 128.6 (n × CH), 128.5 (n × CH), 128.5 (n × CH), 128.4 (n × CH), 128.4 (n × CH), 128.3 (n × CH), 127.9 (CH), 127.9 (n × CH), 127.9 (CH), 127.8 (n × CH), 77.9 (CH), 77.6 (CH), 74.7 (CH_2), 73.6 (CH_2), 73.3 (2 × CH_2), 72.9 (CH), 69.6 (CH_2), 68.5 (CH_2) ppm.

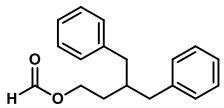
4-phenylbutyl formate (2.113)



Prepared according to GP4 as a clear, and colourless oil (63%, 0.2 mmol scale, 22 mg isolated). Purified by flash column chromatography (2–4% EtOAc in hexanes). Characterized according to NMR comparison.[325] R_f 0.53 (10% EtOAc/hexanes); **^{1}H NMR** (400 MHz, $CDCl_3$) δ 8.06 (s, 1H), 7.33 – 7.27 (m, 2H), 7.23 – 7.15 (m, 3H), 4.24 –

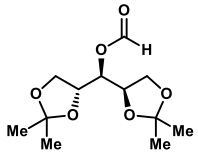
4.15 (m, 2H), 2.70 – 2.62 (m, 2H), 1.75 – 1.68 (m, 4H) ppm; **^{13}C NMR** (101 MHz, $CDCl_3$) δ 161.2 (CH), 142.0 (C), 128.5 (4 × CH), 126.0 (CH), 63.9 (CH_2), 35.5 (CH_2), 28.2 (CH_2), 27.7 (CH_2) ppm.

3-benzyl-4-phenylbutyl formate (2.114)



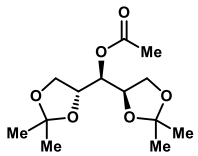
Prepared according to GP4 as a clear, and colourless oil (89%, 0.2 mmol scale, 48 mg isolated). Purified by flash column chromatography (2–8% EtOAc/hexanes). R_f 0.41 (10% EtOAc/hexanes); **^{1}H NMR** (400 MHz, $CDCl_3$) δ 7.99 (s, 1H), 7.36 – 7.26 (m, 4H), 7.24 – 7.18 (m, 2H), 7.18 – 7.10 (m, 4H), 4.17 (t, J = 6.9 Hz, 2H), 2.70 – 2.54 (m, 4H), 2.21 – 2.03 (m, 1H), 1.65 (dt, J = 6.8, 6.8 Hz, 2H) ppm; **^{13}C NMR** (101 MHz, $CDCl_3$) δ 161.2 (CH), 140.5 (2 × C), 129.3 (4 × CH), 128.5 (4 × CH), 126.2 (2 × CH), 62.3 (CH_2), 40.4 (2 × CH_2), 39.0 (CH), 31.8 (CH_2) ppm; **HRMS** (EI): *m/z* calculated for $C_{18}H_{20}O_2$ $[M]^+$: 268.14633, found 268.14549.

bis((R)-2,2-dimethyl-1,3-dioxolan-4-yl)methyl formate (2.115)



Prepared according to GP4 as a white solid (88%, 0.2 mmol scale, 46 mg isolated). Purified by flash column chromatography (5–20% EtOAc/hexanes). R_f 0.37 (20% EtOAc/hexanes); **^{1}H NMR** (400 MHz, $CDCl_3$) δ 8.17 (s, 1H), 5.19 – 4.97 (m, 1H), 4.31 (ddd, J = 6.3, 6.3, 4.2 Hz, 1H), 4.23 (ddd, J = 6.3, 6.3, 6.3 Hz, 1H), 4.11 – 4.01 (m, 2H), 3.85 (dd, J = 8.8, 6.0 Hz, 1H), 3.79 (dd, J = 8.8, 5.9 Hz, 1H), 1.40 (s, 3H), 1.39 (s, 3H), 1.34 (s, 6H) ppm; **^{13}C NMR** (101 MHz, $CDCl_3$) δ 160.4 (CH), 109.8 (2 × C), 74.9 (CH), 74.8 (CH), 72.7 (CH), 66.4 (CH_2), 65.9 (CH_2), 26.6 (CH_3), 26.2 (CH_3), 25.4 (CH_3), 25.4 (CH_3) ppm; **HRMS** (EI): *m/z* calculated for $C_{11}H_{17}O_6$ $[M - CH_3]^+$: 245.10251, found 245.10248.

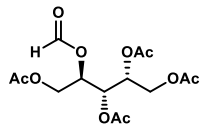
bis((R)-2,2-dimethyl-1,3-dioxolan-4-yl)methyl acetate (2.116)



Prepared according to GP4 as a white solid (91%, 0.2 mmol scale, 50 mg isolated). Purified by flash column chromatography (5–20% EtOAc/hexanes). R_f 0.35 (20% EtOAc/hexanes); **^{1}H NMR** (400 MHz, $CDCl_3$) δ 5.02 (dd, J = 6.7, 3.4 Hz, 1H), 4.32 (ddd, J = 6.2, 6.2, 3.4 Hz, 1H), 4.23 (ddd, J = 6.4, 6.4, 6.4 Hz, 1H), 4.08 – 4.00 (m, 2H), 3.84

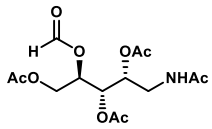
(ddd, J = 8.5, 6.0, 0.7 Hz, 1H), 3.78 (ddd, J = 8.8, 5.7, 0.7 Hz, 1H), 2.11 (s, 3H), 1.41 (s, 3H), 1.38 (s, 3H), 1.35 (s, 3H), 1.34 (s, 3H) ppm; **^{13}C NMR** (101 MHz, $CDCl_3$) δ 170.6 (C), 109.7 (C), 109.6 (C), 75.0 (CH), 74.9 (CH), 72.7 (CH), 66.5 (CH_2), 66.0 (CH_2), 26.7 (CH_3), 26.1 (CH_3), 25.5 (CH_3), 25.5 (CH_3), 21.0 (CH_3) ppm; **HRMS** (EI): *m/z* calculated for $C_{12}H_{19}O_6$ $[M - CH_3]^+$: 259.11816, found 259.11716.

(2R,3R,4R)-4-(formyloxy)pentane-1,2,3,5-tetrayl tetraacetate (2.117)



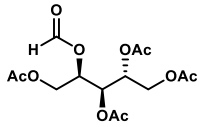
Prepared according to GP4 as a white solid in 36% yield from mannose derivative **2.92a** and 80% yield from glucose derivative 2,3,4,5-tetra-*O*-acetyl-D-glucose (0.2 mmol scale, 25 & 56 mg isolated, respectively). Purified by flash column chromatography (10–40% EtOAc/hexanes). R_f 0.28 (35% EtOAc/hexanes); **^{1}H NMR** (400 MHz, $CDCl_3$) δ 7.98 (s, 1H), 5.40 (dd, J = 8.1, 2.8 Hz, 1H), 5.37 – 5.27 (m, 2H), 4.30 – 4.21 (m, 2H), 4.15 (dd, J = 12.6, 5.4 Hz, 1H), 3.94 (dd, J = 11.7, 6.9 Hz, 1H), 2.11 (s, 3H), 2.06 (s, 3H), 2.03 (s, 3H), 2.02 (s, 3H) ppm; **^{13}C NMR** (101 MHz, $CDCl_3$) δ 170.5 (C), 170.5 (C), 170.1 (C), 169.6 (C), 159.5 (CH), 68.4 (CH), 68.2 (CH), 67.9 (CH), 61.9 (CH_2), 61.7 (CH_2), 20.8 (CH_3), 20.7 (2 × CH_3), 20.6 (CH_3) ppm; **HRMS** (ESI+): *m/z* calculated for $C_{14}H_{20}O_{10}Na$ $[M + Na]^+$: 371.0954, found 371.0953.

(2R,3S,4R)-5-acetamido-2-(formyloxy)pentane-1,3,4-triyl triacetate (2.118)



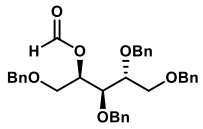
Prepared according to GP4 as a yellow oil (78%, 0.2 mmol scale, 54 mg isolated). Purified by flash column chromatography (2–4% MeOH/DCM). R_f 0.33 (5% MeOH/DCM); **^{1}H NMR** (400 MHz, $CDCl_3$) δ 8.00 (d, J = 0.6 Hz, 1H), 5.83 (dd, J = 5.9, 5.9 Hz, 1H), 5.36 – 5.31 (m, 2H), 5.22 – 5.15 (m, 1H), 4.31 – 4.25 (m, 1H), 4.23 – 4.16 (m, 1H), 3.54 (ddd, J = 14.0, 7.0, 7.0 Hz, 1H), 3.23 (ddd, J = 14.2, 5.6, 5.6 Hz, 1H), 2.16 (s, 3H), 2.09 (s, 3H), 2.06 (s, 3H), 1.97 (s, 3H) ppm; **^{13}C NMR** (101 MHz, $CDCl_3$) δ 170.6 (C), 170.6 (C), 170.4 (C), 170.4 (C), 159.6 (CH), 69.3 (CH), 68.9 (CH), 68.0 (CH), 61.8 (CH_2), 39.6 (CH_2), 23.3 (CH_3), 20.9 (CH_3), 20.8 (CH_3), 20.8 (CH_3) ppm; **HRMS** (EI): *m/z* calculated for $C_{14}H_{21}NO_9Na$ $[M + Na]^+$: 370.1114, found 370.1108.

(2R,3S,4R)-4-(formyloxy)pentane-1,2,3,5-tetrayl tetraacetate (2.120)



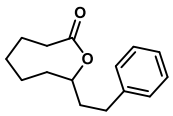
Prepared according to GP4 as a yellow oil (47%, 0.2 mmol scale, 33 mg isolated). Purified by flash column chromatography (10–40% EtOAc/hexanes). R_f 0.27 (35% EtOAc/hexanes); **^{1}H NMR** (400 MHz, $CDCl_3$) δ 8.05 (dd, J = 0.9, 0.9 Hz, 1H), 5.53 (dddd, J = 7.4, 4.5, 2.8, 1.0 Hz, 1H), 5.42 (ddd, J = 8.5, 2.8, 0.9 Hz, 1H), 5.12 (ddd, J = 8.5, 4.6, 2.8 Hz, 1H), 4.32 (dd, J = 11.9, 4.5 Hz, 1H), 4.25 (dd, J = 12.6, 2.8 Hz, 1H), 4.15 (dd, J = 12.6, 4.6 Hz, 1H), 3.97 (dd, J = 11.9, 7.5 Hz, 1H), 2.12 (s, 3H), 2.06 (s, 3H), 2.05 (s, 3H), 2.04 (s, 3H) ppm; **^{13}C NMR** (101 MHz, $CDCl_3$) δ 170.6 (C), 170.5 (C), 169.9 (C), 169.7 (C), 159.8 (CH), 68.3 (CH), 68.3 (CH), 67.9 (CH), 62.2 (CH_2), 61.6 (CH_2), 20.9 (CH_3), 20.8 (CH_3), 20.7 (CH_3), 20.6 (CH_3) ppm; **HRMS** (EI): *m/z* calculated for $C_{14}H_{20}O_{10}$ $[M]^+$: 371.0954, found 371.0916.

(2R,3R,4R)-1,3,4,5-tetrakis(benzyloxy)pentan-2-yl formate (2.122)



Prepared according to GP4 as a white solid (58%, 0.2 mmol scale, 63 mg isolated). Purified by flash column chromatography (5–15% EtOAc/hexanes). Characterized according to NMR comparison.[324] R_f 0.35 (20% EtOAc/hexanes); **^{1}H NMR** (400 MHz, $CDCl_3$) δ 8.03 (s, 1H), 7.36 – 7.27 (m, 18H), 7.25 – 7.19 (m, 2H), 5.50 (ddd, J = 5.5, 5.5, 2.8 Hz, 1H), 4.67 – 4.61 (m, 2H), 4.59 – 4.53 (m, 3H), 4.51 – 4.47 (m, 3H), 4.00 (dd, J = 6.6, 3.4 Hz, 1H), 3.84 – 3.76 (m, 1H), 3.71 – 3.62 (m, 3H), 3.57 (dd, J = 10.1, 5.6 Hz, 1H) ppm; ^{13}C NMR (101 MHz, $CDCl_3$) δ 160.8 (CH), 138.2 (C), 138.1 (C), 138.0 (C), 137.8 (C), 128.5 (n × CH), 128.5 (n × CH), 128.5 (n × CH), 128.3 (n × CH), 128.0 (n × CH), 127.9 (CH), 127.9 (n × CH), 127.9 (CH), 127.9 (CH), 127.8 (CH), 77.4 (CH), 76.4 (CH), 74.7 (CH_2), 73.5 (CH_2), 73.3 (CH_2), 72.3 (CH_2), 72.0 (CH), 68.4 (CH_2), 68.1 (CH_2) ppm.

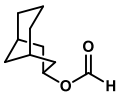
8-phenethyloxocan-2-one (2.123)



Prepared according to GP4 as a yellow oil (43%, 0.2 mmol scale, 20 mg isolated). Purified by flash column chromatography (10–20% Et_2O in hexanes). R_f 0.42 (15% EtOAc/hexanes); **^{1}H NMR** (400 MHz, $CDCl_3$) δ 7.31 –

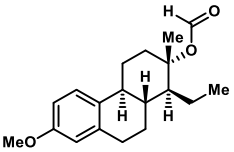
7.25 (m, 2H), 7.22 – 7.13 (m, 3H), 4.42 (dddd, J = 11.8, 9.4, 3.2, 3.2 Hz, 1H), 2.81 (ddd, J = 13.8, 8.9, 4.9 Hz, 1H), 2.66 (ddd, J = 13.8, 8.3, 8.3 Hz, 1H), 2.41 (ddd, J = 12.3, 6.0, 4.3 Hz, 1H), 2.31 (ddd, J = 12.3, 11.9, 4.3 Hz, 1H), 2.01 (dddd, J = 14.1, 9.3, 8.5, 4.8 Hz, 1H), 1.92 – 1.67 (m, 5H), 1.67 – 1.54 (m, 2H), 1.52 – 1.29 (m, 2H) ppm; **^{13}C NMR** (101 MHz, $CDCl_3$) δ 177.0 (C), 141.4 (C), 128.7 (2 × CH), 128.6 (2 × CH), 126.2 (CH), 77.5 (CH), 37.4 (CH_2), 37.2 (CH_2), 32.4 (CH_2), 31.9 (CH_2), 28.8 (CH_2), 26.4 (CH_2), 23.9 (CH_2) ppm; **HRMS** (EI): *m/z* calculated for $C_{15}H_{20}O_2$ $[M]^+$: 232.14633, found 232.14508.

(1R, 3s, 5S)-bicyclo[3.3.1]nonan-3-yl formate (2.124)



Prepared according to GP4 as a clear and colourless oil (86%, 0.2 mmol scale, 29 mg isolated). Purified by flash column chromatography (5–40% DCM in hexanes). ***R**$_f$* 0.33 (41% DCM/hexanes); **^{1}H NMR** (400 MHz, $CDCl_3$) δ 8.03 (d, J = 1.0 Hz, 1H), 5.12 (ttd, J = 9.2, 6.8, 1.1 Hz, 1H), 2.25 – 2.14 (m, 2H), 2.14 – 2.05 (m, 2H), 1.99 – 1.85 (m, 1H), 1.66 – 1.59 (m, 1H), 1.53 – 1.32 (m, 7H), 1.24 – 1.15 (m, 1H) ppm; **^{13}C NMR** (101 MHz, $CDCl_3$) δ 161.0 (CH), 68.8 (CH), 32.6 (2 × CH_2), 32.4 (2 × CH_2), 29.7 (CH_2), 26.2 (2 × CH), 16.4 (CH_2) ppm; Molecular ion peak could not be found for this compound, as a result saponification was performed to give compound **2.129** which was then fully characterized.

(1S,2S,4aS,10aR)-1-ethyl-7-methoxy-2-methyl-1,2,3,4,4a,9,10,10a-octahydrophenanthren-2-yl formate (2.126)



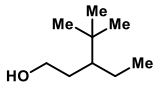
Prepared according to modified GP4 in which 4 mL of MeCN was used, and isolated as a white solid (65%, 0.2 mmol scale, 39 mg isolated). Purified by flash column chromatography (1–10% Et_2O/hexanes). ***R**$_f$* 0.11 (5% Et_2O/hexanes); **^{1}H NMR** (400 MHz, $CDCl_3$) δ 8.10 (s, 1H), 7.18 (dd, J = 8.7, 1.0 Hz, 1H), 6.72 (dd, J = 8.6, 2.8 Hz, 1H), 6.63 (dd, J = 2.7, 1.0 Hz, 1H), 3.78 (s, 3H), 2.94 – 2.79 (m, 2H), 2.58 (ddd, J = 12.6, 3.4, 3.4 Hz, 1H), 2.46 – 2.36 (m, 2H), 2.14 (dddd, J = 12.6, 5.4, 2.8, 2.8 Hz, 1H), 2.07 – 1.96 (m, 1H), 1.75 – 1.61 (m, 2H), 1.47 (s, 3H), 1.44 – 1.22 (m, 4H), 1.03 (t, J = 7.5 Hz, 3H) ppm; **^{13}C NMR** (101 MHz, $CDCl_3$) δ 160.8 (CH), 157.8 (C), 137.9 (C), 131.9 (C), 126.7 (CH), 113.7 (CH), 111.9 (CH), 88.0 (C), 55.4 (CH_3), 51.8 (CH), 43.2 (CH), 42.9 (CH), 37.6 (CH_2), 30.6 (CH_2), 28.2 (CH_2), 27.4 (CH_2), 21.0 (CH_2), 19.2 (CH_3), 15.6 (CH_3) ppm; **HRMS** (EI): *m/z* calculated for $C_{19}H_{26}O_3$ $[M]^+$: 302.18819, found 302.18897.

(1R,3s,5S)-bicyclo[3.3.1]nonan-3-ol (2.129)



Prepared according to GP4 wherein, after passing the crude photochemical reaction through a silica plug eluting with Et_2O and concentration of the resulting solution in vacuo at low temperature, the resulting residue was taken up in a THF/H_2O mixture (1:1, 0.5 M, 2 mL) and LiOH (84 mg, 2 mmol, 2 equivalents) was added. The solution was stirred at room temperature until complete consumption of the intermediate formate ester by TLC (~4 h). Upon complete conversion, HCl (aq., 1.0 M, 1 mL) was added followed by distilled water (4 mL) and Et_2O (5 mL). The layers were separated, and the aqueous phase extracted with more Et_2O (3 × 5 mL). The combined extracts were dried over $MgSO_4$, filtered, and concentrated in vacuo. The crude residue was purified by silica gel flash column chromatography (20– 40% Et_2O/hexanes) to deliver the alcohol **2.129** as a white crystalline solid in 61% yield over two steps (61%, 1 mmol scale, 86 mg isolated). R_f 0.23 (35% Et_2O/hexanes); **^{1}H NMR** (400 MHz, $CDCl_3$) δ 3.94 (tt, J = 10.5, 6.4 Hz, 1H), 2.23 – 2.04 (m, 4H), 1.97 – 1.79 (m, 1H), 1.60 (dtt, J = 12.4, 3.9, 2.0 Hz, 1H), 1.51 – 1.32 (m, 6H), 1.15 (ddd, J = 13.1, 10.4, 2.2 Hz, 2H), 1.08 (dt, J = 12.8, 2.5 Hz, 1H) ppm; **^{13}C NMR** (101 MHz, $CDCl_3$) δ 65.7 (CH), 36.0 (2 × CH_2), 33.1(2 × CH_2), 29.3 (CH_2), 26.5 (CH_2), 16.3 (2 × CH) ppm; **HRMS** (EI): *m/z* calculated for C_9H_{14} $[M - H_2O]^+$ 122.10955, found 122.11015.

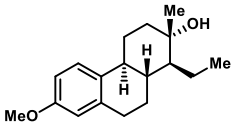
3-ethyl-4,4-dimethylpentan-1-ol (2.130)



Prepared according to GP4 wherein, after passing the crude photochemical reaction through a silica plug eluting with Et_2O and concentration of the resulting solution *in vacuo* at low temperature, the resulting residue was taken up in a THF/H_2O mixture (1:1, 0.5 M, 1 mL) and LiOH (42 mg, 1 mmol, 2 equivalents) was added. The solution was stirred at room temperature until complete consumption of the intermediate formate ester by TLC (~4 h). Upon complete conversion, HCl (aq., 1.0 M, 1 mL) was added followed by distilled water (4 mL) and Et_2O (5 mL). The layers were separated and the aqueous phase extracted with more Et_2O (3 × 5 mL). The combined extracts were dried over $MgSO_4$, filtered, and concentrated *in vacuo*. The crude residue was purified by silica gel flash column chromatography (15–30% Et_2O/hexanes) to deliver the alcohol **2.130** as a yellow oil in 49% yield over two steps (0.5 mmol scale, 35 mg isolated). Characterized according to NMR comparison.[326] R_f 0.5 (25% EtOAc/hexanes); **^{1}H NMR** (400 MHz, $CDCl_3$) δ 3.75 – 3.54 (m, 2H), 1.96 – 1.79 (m, 1H), 1.80 – 1.69 (m, 1H), 1.62 – 1.49 (m, 1H), 1.39 – 1.28

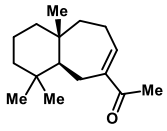
(m, 1H), 1.14 – 0.98 (m, 1H), 0.91 (t, J = 7.4 Hz, 3H), 0.89 – 0.80 (m, 10H) ppm; **^{13}C NMR** (101 MHz, $CDCl_3$) δ 63.6 (CH_2), 46.9 (CH), 34.5 (CH_2), 33.9 (C), 27.8 (3 × CH_3), 24.1 (CH_2), 14.2 (CH_3) ppm;

(1S,2S,4aS,10aR)-1-ethyl-7-methoxy-2-methyl-1,2,3,4,4a,9,10,10a-octahydrophenanthren-2-ol (2.131)



Compound **2.126** (16.8 mg, 0.05 mmol, 1 equivalent) was dissolved in a THF/H_2O mixture (1:1, 200 µL) in a 1 mL HPLC vial equipped with stir bar and stirred vigorously. To this biphasic mixture was added LiOH•H_2O (2.4 mg, 0.057 mmol, 1.1 equivalents) and the resulting mixture was stirred at room temperature overnight. Upon complete conversion, HCl (aq., 1.0 M, 1 mL) was added followed by Et_2O (1 mL). The layers were separated, and the aqueous phase extracted with more Et_2O (3 × 1 mL). The combined extracts were dried over $MgSO_4$, filtered, and concentrated *in vacuo*. The crude residue was purified by silica gel flash column chromatography (10–20% EtOAc/hexanes) to deliver the alcohol **2.131** as a white crystalline solid (93%, 0.05 mmol scale, 13 mg isolated). **^{1}H NMR** (600 MHz, $CDCl_3$) δ 7.20 (d, J = 8.7 Hz, 1H), 6.72 (dd, J = 8.6, 2.8 Hz, 1H), 6.63 (d, J = 2.8 Hz, 1H), 3.78 (s, 3H), 2.91 – 2.80 (m, 2H), 2.42 – 2.32 (m, 2H), 2.13 (ddt, J = 12.8, 5.5, 2.7 Hz, 1H), 1.91 (dt, J = 12.5, 3.2 Hz, 1H), 1.74 (dqd, J = 15.5, 7.8, 2.9 Hz, 1H), 1.63 (td, J = 13.3, 3.9 Hz, 1H), 1.45 – 1.24 (m, 4H), 1.22 (qd, J = 11.1, 2.5 Hz, 1H), 1.13 (s, 3H), 1.13 – 1.08 (m, 1H), 1.04 (t, J = 7.6 Hz, 3H) ppm; **^{13}C NMR** (151 MHz, $CDCl_3$) δ 157.7 (C), 138.0 (C), 132.4 (C), 126.7 (CH), 113.6 (CH), 111.9 (CH), 74.0 (C), 55.3 (CH_3), 54.8 (CH), 43.8 (CH), 43.3 (CH), 42.9 (CH_2), 30.7 (CH_2), 28.8 (CH_2), 27.6 (CH_2), 21.4 (CH_3), 20.8 (CH_2), 16.2 (CH_3) ppm; **HRMS** (EI): *m/z* calculated for $C_{18}H_{24}O$ $[M - H_2O]^+$ 256.18272, found 256.18574.

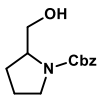
1-((4aS,9aR)-4,4,9a-trimethyl-2,3,4,4a,5,8,9,9a-octahydro-1H-benzo[7]annulen-6-yl)ethan-1-one (2.132)



Prepared as a clear and colourless oil according to the following procedure. Inside a nitrogen-filled glovebox, an 8 mL oven-dried screw-top Pyrex tube was charged with sodium benzoate (0.1 mmol, 10 mol%), 9,10-diphenylanthracene (0.05 mmol, 5 mol%), $CeCl_3$ (0.1 mmol, 10 mol%, anhydrous), 2,4,6-bis(triisopropylphenyl)disulfide (0.2 mmol, 20 mol%), tetrabutylammonium chloride (1 mmol, 1 equivalent), and sclaral (**2.78**, 1 mmol, 252 mg, 1 equivalent). Once all components were charged, the tube was sealed with a Teflon-

septum screw-cap, transferred out of the glovebox, and immediately placed under a positive pressure of argon. Next, anhydrous acetonitrile (5 mL) was added and the resulting suspension sparged with argon for 5 minutes. After sparging, the septum cap was quickly exchanged with a hard plastic cap and the vessel was further sealed with electrical tape and then parafilm. The reaction mixture was then sonicated (90 s) before irradiating with a violet LED (2–2.4 W, 405 nm) at a distance of 1–5 mm for 72 h. The resulting solution was concentrated under reduced pressure and purified by flash column chromatography on silica gel (5–20% EtOAc/hexanes) to isolate compound **2.108b** as a yellow oil which was immediately used in the following procedure. Compound **2.108b** was dissolved in benzene (13 mL) in a 50 mL round-bottom flask equipped with stir bar under ambient atmosphere and charged with *p*-toluenesulfonic acid (1.5 mmol, 285 mg). The resulting solution was then capped with a plastic cap and sealed with parafilm before being heated to 50 ºC using an oil bath until complete consumption of **2.108b** as judged by TLC (23 h). Upon complete consumption of **2.108b**, the mixture was removed from the oil bath and allowed to cool to room temperature. After cooling to room temperature, the reaction mixture was poured into ice cooled $NaHCO_3$ (aq., saturated, 30 mL) and then the aqueous phase was extracted with Et_2O (3 × 20 mL). Combined organic extracts were then washed with brine (1 × 30 mL), dried over $MgSO_4$, filtered, and concentrated in vacuo. The crude residue was purified by flash column chromatography (1–3% EtOAc/hexanes) to deliver compound **2.132** as a clear and colourless oil (23% over two steps, 53 mg isolated). ***R_f*** 0.36 (5% EtOAc/hexanes); **^{1}H NMR** (600 MHz, $CDCl_3$) δ 7.02 (dddd, J = 7.6, 5.4, 2.3, 1.2 Hz, 1H), 2.90 (d, J = 15.5 Hz, 1H), 2.41 (dddd, J = 16.5, 8.6, 4.3, 1.6 Hz, 1H), 2.29 (s, 3H), 2.25 – 2.15 (m, 1H), 1.89 (dddt, J = 15.3, 9.9, 2.6, 1.4 Hz, 1H), 1.63 (qt, J = 13.4, 3.6 Hz, 1H), 1.43 – 1.32 (m, 3H), 1.32 – 1.09 (m, 4H), 1.05 (s, 3H), 0.93 (s, 3H), 0.91 (d, J = 9.9 Hz, 1H), 0.85 (s, 3H) ppm; **^{13}C NMR** (151 MHz, $CDCl_3$) δ 198.9 (C), 147.2 (C), 145.6 (CH), 53.0 (CH), 44.0 (CH_2), 42.6 (CH_2), 42.5 (CH_2), 38.0 (C), 34.7 (C), 33.6 (CH_3), 25.6 (CH_3), 24.2 (CH_2), 21.9 (CH_2), 21.5 (CH_3), 20.1 (CH_3), 19.1 (CH_2) ppm; **HRMS** (EI): m/z calculated for $C_{16}H_{26}O^{\bullet+}$ $[M]^{\bullet+}$: 234.19837, found 234.20128.

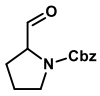
benzyl 2-(hydroxymethyl)pyrrolidine-1-carboxylate (2.140)



A flame dried 50 mL round bottom flask under argon atmosphere and equipped with stir bar was charged with *N*-benzyloxycarbonyl-L-proline (1 g, 4 mmol, 1 equivalent) and anhydrous THF (5.8 mL) and cooled to 0 ºC with an ice bath. Next, BH_3•DMS (0.76 mL, 8 mmol, 2 equivalents) was added dropwise to the solution under vigorous

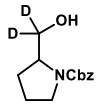
stirring. The resulting solution was allowed to stir at 0 ºC for 3 h, at which point the cooling bath was removed and the solution allowed to warm to room temperature slowly. After 22 h of stirring at room temperature, the solution was cooled again to 0 ºC and quenched by addition of H_2O (15 mL). The aqueous phase was extracted with EtOAc (3 × 15 mL). Combined organic extracts were washed with saturated $NaHCO_3$ (sat. aq., 3 × 10 mL), and brine (1 × 20 mL), dried over Na_2SO_4, filtered and concentrated *in vacuo*. The crude material was run through a silica plug (60% EtOAc/hexanes) to deliver alcohol **2.140** as a clear & colourless oil in quantitative yield (938 mg). Characterized according to NMR comparison.[327] ***R**f* 0.30 (50% EtOAc/hexanes); **^{1}H NMR** (400 MHz, $CDCl_3$) δ 7.41 – 7.29 (m, 5H), 5.20 – 5.09 (m, 2H), 4.40 (dd, J = 7.8, 3.2 Hz, 1H), 4.08 – 3.89 (m, 1H), 3.73 – 3.48 (m, 3H), 3.45 – 3.33 (m, 1H), 2.10 – 1.73 (m, 3H), 1.67 – 1.52 (m, 1H) ppm; **^{13}C NMR** (101 MHz, $CDCl_3$) δ 157.3 (C), 136.6 (C), 128.6 (2 × CH), 128.2 (CH), 128.0 (2 × CH), 67.4 (CH_2), 67.3 (CH_2), 60.9 (CH), 47.5 (CH_2), 28.8 (CH_2), 24.2 (CH_2) ppm;

benzyl 2-formylpyrrolidine-1-carboxylate (2.141)



A flame dried 50 mL round bottom flask under argon atmosphere and equipped with stir bar was charged with alcohol **2.140** (300 mg, 1.3 mmol, 1 equivalent), activated 3Å molecular sieves (200 mg), and DCM (4 mL) and the resulting mixture was stirred at room temperature for 20 minutes. Afterwards, pyridinium chlorochromate (PCC, 411 mg, 1.9 mmol, 1.5 equivalents) was added and the resulting suspension stirred at room temperature for 4 h. Next, Celite (500 mg) was added followed by Et_2O (15 mL) and the resulting slurry was filtered through a Celite-topped silica pad. The resulting filtrate was concentrated *in vacuo* and purified by column chromatography (15–30% EtOAc/hexanes). The final aldehyde **2.141** was isolated as a clear and colourless oil (55%, 163 mg) and characterized by NMR comparison, appearing as a 1:1 mixture of rotamers.[328] ***R**f* 0.45 (50% EtOAc/hexanes); **^{1}H NMR** (400 MHz, $CDCl_3$) δ 9.59 (d, J = 1.8 Hz, 1H), 9.49 (d, J = 2.4 Hz, 1H), 7.42 – 7.27 (m, 5H), 5.22 – 5.10 (m, 2H), 4.30 (ddd, J = 7.8, 5.3, 1.8 Hz, 1H), 4.20 (ddd, J = 8.2, 5.4, 2.4 Hz, 1H), 3.68 – 3.20 (m, 2H), 2.26 – 1.71 (m, 4H) ppm; **^{13}C NMR** (101 MHz, $CDCl_3$) δ 200.2 (CH), 155.5 (C, rotamer), 154.6 (C, rotamer), 136.6 (C, rotamer), 136.4 (C, rotamer), 128.6 (2 × CH, both rotamers), 128.2 (CH, both rotamers), 128.1 (2 × CH, both rotamers), 67.4 (CH_2, rotamer), 67.4 (CH_2, rotamer), 65.4 (CH, rotamer), 65.0 (CH, rotamer), 47.4 (CH_2, rotamer), 46.8 (CH_2, rotamer), 28.0 (CH_2, rotamer), 26.7 (CH_2, rotamer), 24.6 (CH_2, rotamer), 23.9 (CH_2, rotamer) ppm.

benzyl 2-(hydroxymethyl-d$_2$)pyrrolidine-1-carboxylate (5.13)



A suspension of $LiAlD_4$ (LAD, 126 mg, 3 mmol, 1 equivalent) in anhydrous THF (15 mL) was prepared in a 50 mL round-bottom flask under argon atmosphere and equipped with a stir bar and was cooled to –10 ºC using an ice/acetone bath for 15 minutes under vigorous stirring. After 15 minutes, **2.141** (790 mg, 3 mmol, 1 equivalent) was added dropwise over the course of 10 minutes. The solution was kept at –10ºC for 1 h and then quenched by addition of Rochelle's salt solution (sat. aq., 15 mL). Note that the reaction was quenched at incomplete conversion to avoid reductive cleavage of the Cbz protecting group. The resulting mixture was allowed to warm to room temperature, EtOAc was added (10 mL) and the layers were separated. The aqueous phase was then extracted with EtOAc (3 × 10 mL). The combined organic extracts were washed with brine (20 mL), dried over Na_2SO_4, filtered, and concentrated in vacuo. The crude residue was purified by flash column chromatography (25–60% EtOAc/hexanes) $\boldsymbol{R_f}$ 0.24 (50% EtOAc/hexanes); **^{1}H NMR** (400 MHz, $CDCl_3$) δ 7.39 – 7.27 (m, 5H), 5.20 – 5.09 (m, 2H), 4.35 (s, 1H, rotamer), 4.01 (t, J = 7.0 Hz, 1H, rotamer), 3.93 (s, 1H, rotamer), 3.60 – 3.49 (m, 1H), 3.44 – 3.34 (m, 1H), 2.09 – 1.96 (m, 1H), 1.95 – 1.72 (m, 2H), 1.59 (dq, J = 13.3, 6.8 Hz, 1H) ppm; **^{13}C NMR** (101 MHz, $CDCl_3$) δ 157.3 (C), 136.6 (C), 128.6 (2 × CH), 128.2 (2 × CH), 128.0 (CH), 67.4 (CH_2), 60.8 (CH), 47.5 (CH_2), 28.7 (CH_2), 24.2 (CH_2) ppm; **HRMS** (EI): *m/z* calculated for $C_{12}H_{14}NO_2$ $[M - CD_2OH]^+$ 204.10245, found 204.10082

benzyl 2-(formyl-d)pyrrolidine-1-carboxylate (2.142)



A flame dried 50 mL round bottom flask under argon atmosphere and equipped with stir bar was charged with alcohol **5.13** (380 mg, 1.6 mmol, 1 equivalent) and DCM (8 mL) and the resulting mixture was stirred at 0 ºC for 10 minutes. After 10 minutes, Dess-Martin periodinane (DMP, 1.019 g, 2.4 mmol, 1.5 equivalents) was added and the resulting suspension stirred and allowed to warm to room temperature slowly. After 2 hours, the reaction was again cooled to 0 ºC and quenched by addition of $Na_2S_2O_3$ (sat. aq., 10 mL) followed by $NaHCO_3$ (sat. aq. 10 mL) and water (10 mL). The resulting layers were separated, and the aqueous phase was extracted with DCM (3 × 15 mL). The combined organic extracts were washed with brine (1 × 20 mL), dried over Na_2SO_4, filtered, and concentrated in vacuo. The crude residue was purified by column chromatography (15–40% EtOAc/hexanes). The final aldehyde was

isolated as a clear and colourless oil (70%, 262 mg), appearing as a 1:1 mixture of rotamers. R_f 0.23 (30% EtOAc/hexanes) **^{1}H NMR** (600 MHz, $CDCl_3$) δ 7.41 – 7.27 (m, 5H), 5.21 – 5.09 (m, 2H), 4.30 (dd, J = 8.4, 5.1 Hz, 0.51H, rotamer), 4.20 (dd, J = 8.6, 5.4 Hz, 0.54H, rotamer), 3.64 – 3.48 (m, 2H), 2.18 – 1.98 (m, 2H), 1.96 – 1.81 (m, 2H) ppm; **^{13}C NMR** (151 MHz, $CDCl_3$) δ 199.8 (t, J = 27.1 Hz, CDO) 155.5 (C, rotamer), 154.6 (C, rotamer), 136.6 (C, rotamer), 136.4 (C, rotamer), 128.7 (CH, both rotamers), 128.3 (CH, both rotamers), 128.1 (CH, both rotamers), 67.4 (CH_2, rotamer), 67.4 (CH_2, rotamer), 65.3 (t, J = 3.6 Hz, CH, rotamer), 64.9 (t, J = 3.6 Hz, CH, rotamer), 47.4 (CH_2, rotamer), 46.8 (CH_2, rotamer), 28.0 (CH_2, rotamer), 26.7 (CH_2, rotamer), 24.6 (CH_2, rotamer), 23.9 (CH_2, rotamer) ppm; **HRMS** (EI): *m/z* calculated for $C_{12}H_{14}NO_2$ $[M - CDO]^+$ 204.10245, found 204.10089.

benzyl pyrrolidine-1-carboxylate (2.143)



Prepared according to GP4 as a clear, colourless oil (94%, 0.2 mmol scale, 35 mg isolated). Purified by flash column chromatography (10–20% EtOAc/hexanes). Characterized according to NMR comparison.[329] R_f 0.22 (15% EtOAc/hexanes); **^{1}H NMR** (400 MHz, $CDCl_3$) δ 7.41 – 7.27 (m, 5H), 5.14 (s, 2H), 3.50 – 3.27 (m, 4H), 1.93 – 1.78 (m, 4H) ppm; ^{13}C NMR (101 MHz, $CDCl_3$) δ 155.1 (C), 137.3 (C), 128.6 (2 × CH), 128.0 (3 × CH), 66.7 (CH_2), 46.4 (CH_2), 45.9 (CH_2), 25.9 (CH_2), 25.1 (CH_2) ppm.

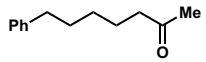
1-methyl-2-phenylcyclohexan-1-ol (2.154)



A flame-dried 100 mL round bottom flask under argon and equipped with a magnetic stir bar was charged with a solution of MeMgBr (3.0 M in Et_2O, 1.5 equiv, 4.3 mmol, 1.5 mL) and THF (20 mL, anhydrous). The solution was stirred and cooled to 0 ºC with an ice water bath. Next, 2-phenylcyclohexanone (2.9 mmol, 1 equiv, 500 mg) dissolved in THF (9 mL, anhydrous) was added dropwise, maintaining 0 ºC. After complete addition, the solution was allowed to stir and slowly warm to room temperature overnight (16 hours). The mixture was then quenched with saturated NH_4Cl (aqueous, 20 mL). The aqueous phase was extracted with EtOAc (3 x 30 mL). Combined extracts were washed with brine (1 x 20 mL) before being dried over Na_2SO_4, filtered, and concentrated *in vacuo*. The resulting residue was purified by flash column chromatography (8 % EtOAc in hexanes). Characterized according to NMR comparison.[330] R_f 0.38 (10% EtOAc/hexanes); **^{1}H NMR** (500 MHz, $CDCl_3$) δ 7.40 – 7.27 (m, 5H), 2.56 (dd, J = 13.0, 3.5 Hz, 1H), 2.12 (qd, J = 13.0, 3.6 Hz, 1H), 1.89 (tdd, J = 13.7, 5.2, 2.5 Hz, 2H), 1.79 (tt, J = 13.4, 3.8 Hz, 1H), 1.74

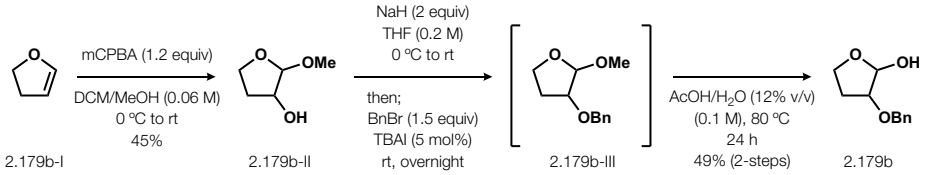
– 1.63 (m, 2H), 1.55 (td, J = 13.4, 4.2 Hz, 1H), 1.42 (qt, J = 13.0, 3.7 Hz, 1H), 1.30 (s, 1H), 1.05 (s, 3H) ppm; **^{13}C NMR** (126 MHz, $CDCl_3$) δ 143.0 (C), 129.2 (2 × CH), 128.2 (2 × CH), 126.6 (CH), 70.8 (C), 53.3 (CH), 40.2 (CH_2), 30.2 (CH_3), 28.5 (CH_2), 26.6 (CH_2), 22.1 (CH_2) ppm.

7-phenylheptan-2-one (2.155)



Prepared according to GP4 on cycloalkanol **2.154** and purified by flash column chromatography (2 – 4% EtOAc/hexanes) to give **2.155** as a clear, colourless oil (31 mg, 61 % yield, 1 mmol scale). Characterized according to NMR comparison.[331] **^{1}H NMR** (400 MHz, $CDCl_3$) δ 7.32 – 7.24 (m, 2H), 7.20 – 7.13 (m, 3H), 2.61 (t, J = 7.7 Hz, 2H), 2.42 (t, J = 7.4 Hz, 2H), 2.13 (s, 3H), 1.69 – 1.55 (m, 5H), 1.39 – 1.27 (m, 2H) ppm; **^{13}C NMR** (101 MHz, $CDCl_3$) δ 209.3 (C), 142.6 (C), 128.5 (2 × CH), 128.4 (2 × CH), 125.8 (CH), 43.8 (CH_2), 35.9 (CH_2), 31.4 (CH_2), 30.0 (CH_3), 28.9 (CH_2), 23.8 (CH_2) ppm.

3-(benzyloxy)tetrahydrofuran-2-ol (2.179b)

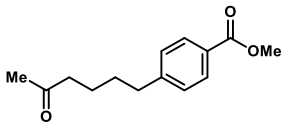


To a solution of *m*CPBA (≤77% w/w, 73 mmol, 1.1 equiv,16.36 g) in DCM/MeOH (1:1, 660 mL total, 0.1 M) at 0 ºC was added 2,3-dihydrofuran (**2.179b-I**, 66 mmol, 1 equiv, 5 mL) dropwise. The resulting solution was stirred at 0 ºC for 30 minutes before the ice bath was removed and the mixture was allowed to slowly warm to room temperature and stir overnight (16 h). After 16 h, saturated $NaHCO_3$ (100 mL, aqueous) followed by saturated $Na_2S_2O_3$ (100 mL, aqueous) solutions were added and the mixture was stirred vigorously for 10 minutes. The mixture was then concentrated *in vacuo* to remove MeOH and DCM. The aqueous phase was extracted with EtOAc (5 x 200 mL). Combined extracts were dried over Na_2SO_4, filtered and concentrated *in vacuo*. The resulting white paste containing **2.179b-II** was used without further purification (3.51 g, 45 % yield).

A hexanes-rinsed suspension of NaH (60% w/w in mineral oil, 16.8 mmol, 2 equiv, 644 mg) in THF (anhydrous, 32 mL) under argon was prepared and cooled in an ice/water bath under vigorous stirring. After thermal equilibration, a slurry of **2.179b-II** (8.4 mmol, 1 equiv, 1 g) in THF (anhydrous, 10 mL) was added dropwise, maintaining 0 ºC. The cooling bath was subsequently removed and the mixture was allowed to warm to room temperature and stir until bubbling subsided. Tetra-*n*-butylammonium iodide (0.42 mmol, 5 mol %, 155.1 mg) and

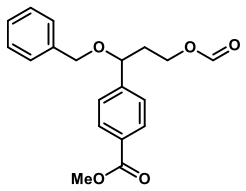
benzyl bromide (12.7 mmol, 1.5 equiv, 1.5 mL) were added, sequentially. The resulting mixture was stirred overnight (17 h). The mixture was then quenched with an AcOH/H_2O mixture (12% v/v, 2 M in AcOH, 84 mL) and the mixture was concentrated *in vacuo* to remove THF (e.g. removal of ~1/3 of the volume). The resulting mixture was heated to 80 ºC for 24 h. After 24 h the solution was allowed to cool to room temperature before it was diluted with water (50 mL) and quenched by portionwise addition of Na_2CO_3 until gas evolution ceased. The aqueous phase was then extracted with EtOAc (4 x 70 mL). Combined extracts were washed with brine (1 x 50 mL), dried over Na_2SO_4, filtered, and concentrated *in vacuo*. The crude residue was purified by flash column chromatography (SiO_2, 20–40% EtOAc/hexanes) to give **2.179b** as an amorphous white powder (49% 2-steps, 4.1 mmol, 796 mg isolated). $\boldsymbol{R_f}$ (40% EtOAc/hexanes); **^{1}H NMR** (400 MHz, $CDCl_3$) δ 7.40 – 7.25 (m, 8H), 7.24 (d, J = 0.8 Hz, 1H), 5.43 (d, J = 2.9 Hz, 1H), 5.31 (dd, J = 7.9, 4.1 Hz, 1H), 4.63 (d, J = 11.6 Hz, 1H), 4.58 (d, J = 11.7 Hz, 1H), 4.59 – 4.51 (m, 3H), 4.08 (dd, J = 8.1, 6.1 Hz, 2H), 4.05 – 3.97 (m, 2H), 3.85 – 3.79 (m, 1H), 3.77 (d, J = 7.9 Hz, 1H), 2.61 (d, J = 2.9 Hz, 1H), 2.22 (dtd, J = 13.7, 8.2, 5.7 Hz, 1H), 2.14 – 1.93 (m, 3H) ppm; **^{13}C NMR** (101 MHz, $CDCl_3$) δ 138.0, 137.3, 128.7, 128.6, 128.3, 128.0, 127.9, 127.8, 100.8, 96.5, 83.5, 78.2, 77.5, 77.2, 76.8, 72.6, 71.6, 67.2, 64.9, 30.0, 30.0 ppm; **HRMS** (EI+) *m/z* calculated for $C_{10}H_{13}O_2^+$ [*M–CHO*•]$^+$ 165.09101, found 165.09413.

methyl 4-(5-oxohexyl)benzoate (2.180a)



Prepared according to GP5 in 74% isolated yield. **^{1}H NMR** (600 MHz, $CDCl_3$) δ 7.97 – 7.89 (m, 2H), 7.23 (d, J = 8.3 Hz, 2H), 3.89 (s, 3H), 2.71 – 2.61 (m, 2H), 2.44 (t, J = 6.6 Hz, 2H), 2.12 (s, 3H), 1.62 (dq, J = 6.7, 3.0 Hz, 5H) ppm; **^{13}C NMR** (151 MHz, $CDCl_3$) δ 208.9 (C), 167.3 (C), 147.8 (C), 129.8 (2 × CH), 128.5 (2 × CH), 128.0 (C), 52.1 (CH_3), 43.6 (CH_2), 35.9 (CH_2), 30.7 (CH_2), 30.0 (CH_3), 23.5 (CH_2) ppm; **HRMS** (EI): *m/z* calculated for $C_{14}H_{18}O_3$ $[M]^+$: 243.12559, found 243.12575.

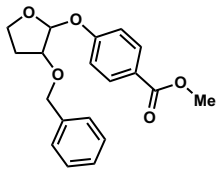
methyl 4-(1-(benzyloxy)-3-(formyloxy)propyl)benzoate (2.180b)



Prepared according to GP5 using methyl bromobenzoate **2.178** and lactol **2.179b** and purified by flash column chromatography (SiO_2, 5–10% EtOAc/hexanes) to give a clear and colourless oil (22%, 0.2 mmol scale, 14 mg

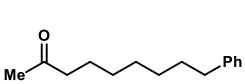
isolated). ***R_f*** 0.31 (15% EtOAc/hexanes); **^{1}H NMR** (400 MHz, $CDCl_3$) δ = 8.10 – 8.04 (m, 2H), 8.00 (s, 1H), 7.46 – 7.41 (m, 2H), 7.37 – 7.30 (m, 3H), 7.30 – 7.26 (m, 2H), 4.52 (dd, *J* = 9.1, 4.4 Hz, 1H), 4.46 (d, *J* = 11.6 Hz, 1H), 4.37 (ddd, *J* = 11.1, 8.2, 5.5 Hz, 1H), 4.25 (d, *J* = 11.6 Hz, 1H), 4.20 (dt, *J* = 11.2, 5.7 Hz, 1H), 3.93 (s, 3H), 2.16 (ddt, *J* = 14.5, 9.0, 5.4 Hz, 1H), 1.99 (dddd, *J* = 14.4, 8.2, 6.1, 4.4 Hz, 1H) ppm; **^{13}C NMR** (101 MHz, $CDCl_3$) δ = 167.0 (C), 161.0 (CH), 147.0 (C), 137.9 (C), 130.2 (2 × CH), 130.0 (C), 128.6 (2 × CH), 128.0 (2 × CH), 128.0 (CH), 126.7 (2 × CH), 77.4 (CH), 71.0 (CH_2), 60.8 (CH_2), 52.3 (CH_3), 37.2 (CH_2) ppm; **HRMS** (ESI-QTOF): *m/z* calculated for $C_{19}H_{20}O_5Na$ $[M + Na]^+$: 351.1208, found 351.1207.

methyl 4-((3-(benzyloxy)tetrahydrofuran-2-yl)oxy)benzoate (2.180b')



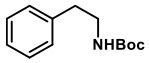
Prepared according to GP5 and purified by flash column chromatography (5–10% EtOAc/hexanes) to give a clear and colourless oil (14%, 0.2 mmol scale, 10 mg isolated). **^{1}H NMR** (400 MHz, $CDCl_3$) *δ* 8.01 – 7.93 (m, 2H), 7.41 – 7.26 (m, 5H), 7.05 – 6.97 (m, 2H), 5.78 (s, 1H), 4.61 (s, 2H), 4.29 (dd, J = 5.8, 2.3 Hz, 1H), 4.19 (q, *J* = 7.7 Hz, 1H), 4.08 (td, *J* = 8.5, 4.9 Hz, 1H), 3.88 (s, 3H), 2.40 – 2.26 (m, 1H), 2.20 – 2.02 (m, 1H) ppm; **^{13}C NMR** (101 MHz, $CDCl_3$) *δ* 166.9 (C), 160.5 (C), 137.7 (C), 131.6 (2 × CH), 128.7 (2 × CH), 128.1 (CH), 127.9 (2 × CH), 123.6 (C), 115.9 (2 × CH), 104.1 (CH), 83.2 (CH), 71.8 (CH_2), 68.1 (CH_2), 52.0 (CH_3), 30.2 (CH_2) ppm; **HRMS** (ESI-QTOF): *m/z* calculated for $C_{19}H_{20}O_5Na$ $[M + Na]^+$: 351.1208, found 351.1195.

9-phenylnonan-2-one (2.184)



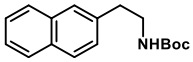
Prepared according to GP5 and purified by flash column chromatography on silica gel (0–100% EtOAc/hexanes unless otherwise stated). Characterized according to NMR comparison. [332] **^{1}H NMR** (400 MHz, $CDCl_3$) *δ* 7.27 (dd, *J* = 8.2, 7.0 Hz, 2H), 7.20 – 7.14 (m, 3H), 2.59 (dd, *J* = 8.7, 6.8 Hz, 2H), 2.41 (t, *J* = 7.5 Hz, 2H), 2.13 (s, 3H), 1.68 – 1.49 (m, 4H), 1.44 – 1.19 (m, 6H) ppm; **^{13}C NMR** (101 MHz, $CDCl_3$) δ 209.5 (C), 143.0 (C), 128.5 (2 × CH), 128.4 (2 ×CH), 125.7 (CH), 43.9 (CH_2), 36.1 (CH_2), 31.6 (CH_2), 30.0 (CH_3), 29.4 (CH_2), 29.3 (CH_2), 29.2 (CH_2), 24.0 (CH_2) ppm.

tert-butyl pyrrolidine-1-carboxylate (2.186b)



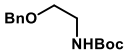
Prepared according to GP4 as a tan solid (74%, 0.2 mmol scale, 33 mg isolated). Purified by flash column chromatography (5–10% EtOAc/hexanes). Characterized according to NMR comparison. [333] $\boldsymbol{R_f}$ 0.41 (15% EtOAc/hexanes); **^{1}H NMR** (400 MHz, $CDCl_3$) δ 7.35 – 7.28 (m, 2H), 7.25 – 7.16 (m, 3H), 4.55 (s, 1H), 3.38 (dt, J = 6.8, 6.7 Hz, 2H), 2.80 (t, J = 7.1 Hz, 2H), 1.44 (s, 9H) ppm; **^{13}C NMR** (101 MHz, $CDCl_3$) δ 156.0 (C), 139.2 (C), 128.9 (2 × CH), 128.7 (2 × CH), 126.5 (CH), 79.3 (C), 41.9 (CH_2), 36.3 (CH_2), 28.5 (3 × CH_3) ppm;

tert-butyl phenethylcarbamate (2.187b)



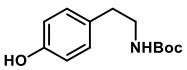
Prepared according to GP4 as a white powder (96%, 0.2 mmol scale, 52 mg isolated). Purified by flash column chromatography (5–10% in hexanes). $\boldsymbol{R_f}$ 0.39 (16% EtOAc/hexanes); **^{1}H NMR** (400 MHz, $CDCl_3$) δ 7.87 – 7.74 (m, 3H), 7.64 (s, 1H), 7.53 – 7.40 (m, 2H), 7.34 (dd, J = 8.4, 1.7 Hz, 1H), 4.55 (br s, N*H*, 1H), 3.56 – 3.35 (m, 2H), 2.97 (t, J = 7.0 Hz, 2H), 1.43 (s, 9H); **^{13}C NMR** (101 MHz, $CDCl_3$) δ 156.0 (C), 136.6 (C), 133.7 (C), 132.4 (C), 128.4 (CH), 127.8 (CH), 127.6 (CH), 127.4 (CH), 127.3 (CH), 126.2 (CH), 125.6 (CH), 79.4 (C), 41.8 (CH_2), 36.4 (CH_2), 28.5 (3 × CH_3) ppm; **HRMS** (EI): *m/z* calculated for $C_{17}H_{21}NO_2$ $[M]^+$ 271.1572, found 271.1576 ppm.

tert-butyl (2-(naphthalen-2-yl)ethyl)carbamate (2.188b)



Prepared according to GP4 and purified by flash column chromatography (7–14% EtOAc/hexanes) to give a yellow oil (78%, 0.2 mmol scale, 40 mg isolated). Characterized according to NMR comparison. [334] $\boldsymbol{R_f}$ 0.26 (15% EtOAc/hexanes); **^{1}H NMR** (400 MHz, $CDCl_3$) δ 7.39 – 7.27 (m, 5H), 4.52 (s, 2H), 3.54 (t, J = 5.1 Hz, 2H), 3.42 – 3.27 (m, 2H), 1.44 (s, 9H) ppm; **^{13}C NMR** (101 MHz, $CDCl_3$) δ 156.1 (C), 138.1 (C), 128.6 (2 × CH), 127.9 (CH), 127.8 (2 × CH), 79.4 (C), 73.2 (CH_2), 69.4 (CH_2), 40.6 (CH_2), 28.5 (3 × CH_3) ppm; **HRMS** (EI): *m/z* calculated for $[M]^+$ 271.1572, found 271.1576

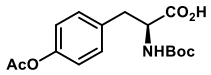
tert-butyl (4-hydroxyphenethyl)carbamate (2.189b)



Prepared according to GP4 and purified by flash column chromatography (20–35% EtOAc/hexanes) to give a yellow oil (29%, 0.2 mmol scale, 14 mg isolated). Characterized according to NMR comparison. [333] $\boldsymbol{R_f}$ 0.44 (40%

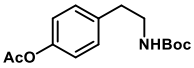
EtOAc/hexanes); **^{1}H NMR** (400 MHz, $CDCl_3$) δ 7.05 – 6.97 (m, 2H), 6.81 – 6.74 (m, 2H), 5.95 (s, 1H), 4.60 (s, 1H), 3.47 – 3.21 (m, 2H), 2.70 (t, J = 7.2 Hz, 2H), 1.44 (s, 9H) ppm; **^{13}C NMR** (101 MHz, $CDCl_3$) δ 156.3 (C), 154.7 (C), 130.7 (C), 130.0 (2 × CH), 115.6 (2 × CH), 79.7 (C), 42.2 (CH_2), 35.4 (CH_2), 28.6 (3 × CH_3) ppm.

(S)-3-(4-acetoxyphenyl)-2-((tert-butoxycarbonyl)amino)propanoic acid (2.190a)



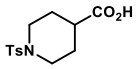
Prepared according to the following adapted literature procedure.[335] A 25 mL round bottom flask under ambient atmosphere and equipped with a stir bar was charged with *N*-(*tert*-butoxycarbonyl)-L-tyrosine (500 mg, 1.78 mmol, 1 equivalent) and NaOH (aq., 15% w/v, 1.8 mL) followed by ice chips. Next, acetic anhydride was added and the solution stirred vigorously for 40 minutes. The mixture was then cooled to 0 ºC with an ice bath and HCl (aq., 3 M) was added to acidify (brought to pH ~3). The aqueous phase was then extracted with EtOAc (3 × 10 mL). The combined organic extracts were then dried over Na_2SO_4, filtered, and concentrated by rotary evaporation and the crude residue purified by column chromatography (5% MeOH/DCM). The protected tyrosine derivative **2.190a** was isolated as a white solid (93%, 538 mg). R_f 0.77 (20% MeOH/DCM); **^{1}H NMR** (500 MHz, DMSO–d_6) δ 12.65 (s, 1H), 7.27 (d, J = 8.1 Hz, 2H), 7.11 (d, J = 8.4 Hz, 1H), 7.03 (d, J = 8.1 Hz, 2H), 4.09 (ddd, J = 9.5, 9.4, 4.5 Hz, 1H), 3.02 (dd, J = 14.0, 4.5 Hz, 1H), 2.83 (dd, J = 13.9, 10.4 Hz, 1H), 2.25 (s, 3H), 1.33 (s, 9H) ppm; **^{13}C NMR** (126 MHz, DMSO) δ 173.5 (C), 169.2 (C), 155.5 (C), 149.0 (C), 135.5 (C), 130.0 (2 × CH), 121.4 (2 × CH), 78.1 (C), 55.1 (CH), 35.7 (CH_2), 28.1 (3 × CH_3), 20.8 (CH_3) ppm; **HRMS** (ESI+): *m/z* calculated for $C_{16}H_{21}NO_6Na$ $[M + Na]^+$: 346.1267, found 346.1267.

4-(2-((tert-butoxycarbonyl)amino)ethyl)phenyl acetate (2.190b)



Prepared according to GP4 as a white powder (81%, 0.2 mmol scale, 46 mg isolated). Purified by flash column chromatography (18–25% EtOAc/hexanes). R_f 0.17 (18% EtOAc/hexanes); **^{1}H NMR** (400 MHz, $CDCl_3$) δ 7.22 – 7.17 (m, 2H), 7.04 – 6.99 (m, 2H), 4.55 (s, 1H), 3.37 (q, J = 6.7 Hz, 2H), 2.79 (t, J = 7.0 Hz, 2H), 2.29 (s, 3H), 1.43 (s, 9H) ppm; **^{13}C NMR** (101 MHz, $CDCl_3$) δ 169.8 (C), 156.0 (C), 149.4 (C), 136.8 (C), 129.9 (2 × CH), 121.8 (2 × CH), 41.8 (CH_2), 35.7 (CH_2), 28.5 (3 × CH_3), 21.3 (CH_3) ppm; **HRMS** (EI): *m/z* calculated for $C_{15}H_{21}NO_4$ $[M]^+$: 279.14706, found 279.14764.

1-tosylpiperidine-4-carboxylic acid (2.191a)



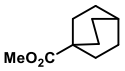
Prepared according to the following adapted literature procedure.[336] A 50 mL round bottom flask equipped with stir bar and under ambient atmosphere was charged with 4-piperidinecarboxylic acid (1 g, 7.7 mmol, 1 equivalent), NaOH (616 mg, 15.4 mmol, 2 equivalents), Et_2O (7.7 mL), and H_2O (7.7 mL). The resulting mixture was stirred at room temperature for 24 h. After 24 h the white suspension was diluted with Et_2O and H_2O until the precipitate had completely dissolved (~15 mL each). The layers were then separated and the aqueous phase was adjusted to a pH ~3 by addition of HCl (aq., 6 M). The resulting precipitate was then filtered out of the aqueous solution, dissolved in EtOAc, dried over Na_2SO_4, filtered and concentrated *in vacuo*. The crude material was clean enough for use without further purification, delivering **2.191a** as a fluffy white solid (68%, 1.49 g). Characterized according to NMR comparison.[336] **^{1}H NMR** (400 MHz, $CDCl_3$) δ 7.63 (d, J = 8.3 Hz, 2H), 7.32 (d, J = 8.0 Hz, 2H), 3.65 (dt, J = 11.5, 4.0 Hz, 2H), 2.51 – 2.36 (m, 5H), 2.27 (tt, J = 10.8, 4.0 Hz, 1H), 2.04 – 1.93 (m, 2H), 1.87 – 1.74 (m, 2H) ppm; **^{13}C NMR** (101 MHz, $CDCl_3$) δ 180.1 (C), 143.8 (C), 133.1 (C), 129.8 (2 × CH), 127.8 (2 × CH), 45.5 (2 × CH_2), 39.9 (CH_3), 27.3 (2 × CH_2), 21.7 (CH) ppm.

1-tosylpiperidine (2.191b)



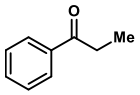
Prepared according to GP4 as a white powder (79%, 0.2 mmol scale, 38 mg isolated). Purified by flash column chromatography (5–10% EtOAc/hexanes). Characterized according to NMR comparison.[337] R_f 0.32 (10% EtOAc/hexanes); **^{1}H NMR** (400 MHz, $CDCl_3$) δ 7.63 (d, J = 8.3 Hz, 2H), 7.31 (d, J = 8.1 Hz, 2H), 3.00 – 2.91 (m, 4H), 2.43 (s, 3H), 1.68 – 1.59 (m, 4H), 1.45 – 1.36 (m, 2H) ppm; **^{13}C NMR** (101 MHz, $CDCl_3$) δ 143.4 (C), 133.4 (C), 129.7 (2 × CH), 127.9 (2 × CH), 47.1 (2 × CH_2), 25.3 (2 × CH_2), 23.7 (CH_2), 21.7 (CH_3) ppm.

methyl bicyclo[2.2.2]octane-1-carboxylate (2.192b)



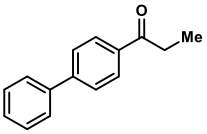
Prepared according to GP4 as a yellow oil (82%, 0.2 mmol scale, 44 mg isolated). Purified by flash column chromatography (2–4% Et_2O in hexanes). Characterized according to NMR comparison.[338] R_f 0.26 (5% Et_2O/hexanes); **^{1}H NMR** (400 MHz, $CDCl_3$) δ 3.62 (s, 3H), 1.78 – 1.67 (m, 6H), 1.64 – 1.52 (m, 7H) ppm; **^{13}C NMR** (101 MHz, $CDCl_3$) δ 178.8 (C), 51.7 (CH_3), 38.4 (C), 28.2 (3 × CH_2), 25.5 (3 × CH_2), 23.9 (CH) ppm.

propiophenone (2.193b)



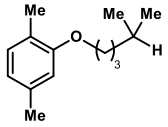
Prepared according to GP4 as a yellow oil (98%, 0.2 mmol scale, 26 mg isolated). Purified by flash column chromatography (1–3% Et_2O/hexanes). Characterized according to NMR comparison.[339] $\boldsymbol{R_f}$ 0.38 (5% Et_2O/hexanes); **^{1}H NMR** (400 MHz, $CDCl_3$) δ 8.00 – 7.94 (m, 2H), 7.59 – 7.51 (m, 1H), 7.49 – 7.42 (m, 2H), 3.01 (q, J = 7.3 Hz, 2H), 1.23 (t, J = 7.3 Hz, 3H) ppm; **^{13}C NMR** (101 MHz, $CDCl_3$) δ 201.0 (C), 137.0 (C), 133.0 (CH), 128.7 (2 × CH), 128.1 (2 × CH), 31.9 (CH_2), 8.4 (CH_3) ppm.

1-([1,1'-biphenyl]-4-yl)propan-1-one (2.194b)



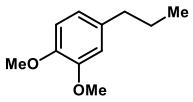
Prepared according to GP4 as a tan solid (64%, 0.2 mmol scale, 27 mg isolated). Purified by flash column chromatography (2–4% EtOAc/hexanes). Characterized according to NMR comparison.[340] $\boldsymbol{R_f}$ 0.55 (15% EtOAc/hexanes); **^{1}H NMR** (400 MHz, $CDCl_3$) δ 8.08 – 8.02 (m, 2H), 7.71 – 7.66 (m, 2H), 7.66 – 7.61 (m, 2H), 7.51 – 7.44 (m, 2H), 7.43 – 7.37 (m, 1H), 3.05 (q, J = 7.3 Hz, 2H), 1.26 (t, J = 7.3 Hz, 3H) ppm; **^{13}C NMR** (101 MHz, $CDCl_3$) δ 200.6 (C), 145.7 (C), 140.1 (C), 135.8 (C), 129.1 (2 × CH), 128.7 (2 × CH), 128.3 (CH), 127.4 (2 × CH), 127.4 (2 × CH), 32.0 (CH_2), 8.5 (CH_3) ppm.

1,4-dimethyl-2-((4-methylpentyl)oxy)benzene (2.195b)



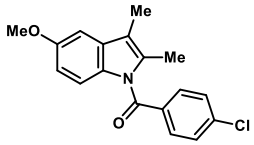
Prepared according to GP4 as a clear, colourless oil (87%, 0.2 mmol scale, 36 mg isolated). Purified by flash column chromatography (100% hexanes). Characterized according to NMR comparison.[341] $\boldsymbol{R_f}$ 0.30 (100% hexanes); **^{1}H NMR** (400 MHz, $CDCl_3$) δ 7.02 (d, J = 7.4 Hz, 1H), 6.67 (dd, J = 7.3, 1.6 Hz, 1H), 6.64 (d, J = 1.6 Hz, 1H), 3.94 (t, J = 6.5 Hz, 2H), 2.32 (s, 3H), 2.19 (s, 3H), 1.86 – 1.75 (m, 2H), 1.70 – 1.57 (m, 1H), 1.42 – 1.32 (m, 2H), 0.94 (d, J = 6.6 Hz, 6H) ppm; **^{13}C NMR** (101 MHz, $CDCl_3$) δ 157.3 (C), 136.6 (C), 130.4 (CH), 123.8 (C), 120.7 (CH), 112.1 (CH), 68.3 (CH_2), 35.5 (CH_2), 27.9 (CH_3), 27.4 (CH_2), 22.7 (2 × CH_3), 21.6 (CH), 15.9 (CH_3) ppm.

1,2-dimethoxy-4-propylbenzene (2.196b)



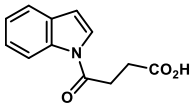
Prepared according to GP4 as a clear and colourless oil (70%, 0.2 mmol scale, 25 mg isolated). Purified by flash column chromatography (10% EtOAc/hexanes). Characterized according to NMR comparison.[342] $\boldsymbol{R_f}$ 0.39 (10% EtOAc/hexanes); **^{1}H NMR** (400 MHz, $CDCl_3$) δ 6.83 – 6.78 (m, 1H), 6.76 – 6.69 (m, 2H), 3.88 (s, 3H), 3.87 (s, 3H), 2.60 – 2.48 (m, 2H), 1.69 – 1.57 (m, 2H), 0.95 (t, J = 7.3 Hz, 3H) ppm; **^{13}C NMR** (101 MHz, $CDCl_3$) δ 148.8 (C), 147.1 (C), 135.5 (C), 120.3 (CH), 111.9 (CH), 111.2 (CH), 56.1 (CH_3), 55.9 (CH_3), 37.8 (CH_2), 24.9 (CH_2), 14.0 (CH_3) ppm.

(4-chlorophenyl)(5-methoxy-2,3-dimethyl-1H-indol-1-yl)methanone (2.197b)



Prepared according to GP4 as a yellow oil (41%, 0.2 mmol scale, 26 mg isolated). Purified by flash column chromatography (2–5% EtOAc/hexanes). Characterized according to NMR comparison.[341] $\boldsymbol{R_f}$ 0.29 (6% EtOAc/hexanes); **^{1}H NMR** (400 MHz, $CDCl_3$) δ 7.71 – 7.58 (m, 2H), 7.52 – 7.41 (m, 2H), 6.91 (d, J = 11.9 Hz, 1H), 6.90 (s, 1H), 6.66 (dd, J = 9.0, 2.6 Hz, 1H), 3.85 (s, 3H), 2.31 (s, 3H), 2.19 (s, 3H) ppm; **^{13}C NMR** (101 MHz, $CDCl_3$) δ 168.4 (C), 156.1 (C), 139.0 (C), 134.5 (C), 133.9 (C), 132.1 (C), 131.2 (2 × CH), 131.0 (C), 129.2 (2 × CH), 115.6 (C), 115.1 (CH), 111.3 (CH), 101.4 (CH), 55.8 (CH_3), 13.4 (CH_3), 8.9 (CH_3) ppm.

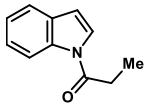
4-(1H-indol-1-yl)-4-oxobutanoic acid (2.198a)



A 25 mL high-pressure flask under argon and equipped with stir bar was charged with indole (500 mg, 4.3 mmol, 1 equivalent), succinic anhydride (762 mg, 6.4 mmol, 1.5 equivalents), and 4-dimethylaminopyridine (53 mg, 0.4 mmol, 10 mol%) followed by DCM (8.6 mL) and freshly distilled triethylamine (1.8 mL). The high-pressure flask was then sealed with a screw top and heated to 40 ºC for 24 h. After 24 h the tube was cooled in an ice bath and opened, HCl (aq., 1 M, 25 mL) was added followed by EtOAc (40 mL) and the layers were separated. The organic phase was then washed with 1 M $HCl_{(aq)}$ (3 × 10 mL), and brine (1 × 20 mL), dried over Na_2SO_4, filtered and concentrated by rotary evaporation. The crude material was purified by flash column chromatography (5%

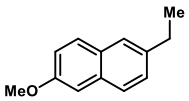
MeOH/DCM) to deliver **2.198a** as a white solid (35%, 327 mg). Characterized according to NMR comparison.[343] R_f 0.19 (5% MeOH/DCM); **^{1}H NMR** (400 MHz, $CDCl_3$) δ 8.43 (d, J = 8.3 Hz, 1H), 7.57 (ddd, J = 7.7, 1.4, 0.8 Hz, 1H), 7.48 (d, J = 3.8 Hz, 1H), 7.35 (ddd, J = 8.4, 7.2, 1.4 Hz, 1H), 7.29 (dd, J = 7.6, 1.1 Hz, 1H), 6.67 (dd, J = 3.8, 0.8 Hz, 1H), 3.27 (dd, J = 7.2, 5.9 Hz, 2H), 2.91 (dd, J = 7.2, 5.9 Hz, 2H) ppm; **^{13}C NMR** (101 MHz, $CDCl_3$) δ 177.5 (C), 169.7 (C), 135.8 (C), 130.5 (C), 125.4 (CH), 124.4 (CH), 124.0 (CH), 121.1 (CH), 116.7 (CH), 109.8 (CH), 30.6 (CH_2), 28.4 (CH_2) ppm;

1-(1H-indol-1-yl)propan-1-one (2.198b)



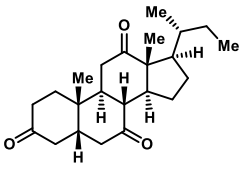
Prepared according to GP4 and purified by flash column chromatography (SiO_2, 3–6% EtOAc/hexanes) to give a beige solid (39%, 0.2 mmol scale, 13 mg isolated). Characterized according to NMR comparison.[344] R_f 0.26 (5% EtOAc/hexanes); **^{1}H NMR** (400 MHz, $CDCl_3$) δ 8.48 (d, J = 8.3 Hz, 1H), 7.57 (ddd, J = 7.7, 1.4, 0.8 Hz, 1H), 7.47 (d, J = 3.8 Hz, 1H), 7.36 (ddd, J = 8.4, 7.2, 1.4 Hz, 1H), 7.31 – 7.23 (m, 1H), 6.64 (dd, J = 3.8, 0.8 Hz, 1H), 2.97 (q, J = 7.3 Hz, 2H), 1.35 (t, J = 7.3 Hz, 3H) ppm; **^{13}C NMR** (101 MHz, $CDCl_3$) δ 172.4 (C), 135.8 (C), 130.4 (C), 125.2 (CH), 124.6 (CH), 123.7 (CH), 120.9 (CH), 116.7 (CH), 109.2 (CH), 29.3 (CH_2), 8.9 (CH_3) ppm.

2-ethyl-6-methoxynaphthalene (2.199b)



Prepared according to GP4 and purified by flash column chromatography (0–1% EtOAc/hexanes) to give a white solid (79%, 0.2 mmol scale, 29 mg isolated). Characterized according to NMR comparison.[338] R_f 0.28 (1% EtOAc/hexanes); **^{1}H NMR** (400 MHz, $CDCl_3$) δ 7.72 – 7.64 (m, 2H), 7.56 (dd, J = 1.7, 0.8 Hz, 1H), 7.32 (dd, J = 8.4, 1.8 Hz, 1H), 7.15 – 7.09 (m, 2H), 3.92 (s, 3H), 2.78 (q, J = 7.6 Hz, 2H), 1.31 (t, J = 7.6 Hz, 3H) ppm; **^{13}C NMR** (101 MHz, $CDCl_3$) δ 157.2 (C), 139.6 (C), 133.0 (C), 129.3 (C), 129.0 (CH), 127.7 (CH), 126.8 (CH), 125.6 (CH), 118.7 (CH), 105.8 (CH), 55.4 (CH_3), 29.0 (CH_2), 15.8 (CH_3) ppm.

(5S,8R,9S,10S,13R,14S,17R)-17-((R)-sec-butyl)-10,13-dimethyldodecahydro-3H-cyclopenta[a]phenanthrene3,7,12(2H,4H)-trione (2.200b)

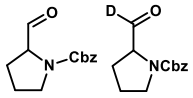


Prepared according to modified GP4 in which 4 mL MeCN was used and the product isolated as a beige solid (73%, 0.2 mmol scale, 52 mg isolated). Purified by flash column chromatography (20–50% EtOAc/hexanes). Characterized according to NMR comparison.[341] R_f 0.33 (35% EtOAc/hexanes); **^{1}H NMR** (400 MHz, $CDCl_3$) δ 2.97 – 2.79 (m, 3H), 2.39 – 2.18 (m, 6H), 2.17 – 2.09 (m, 2H), 2.10 – 1.91 (m, 4H), 1.84 (ddd, J = 11.1, 11.0, 7.0 Hz, 1H), 1.61 (ddd, J = 14.3, 14.3, 5.0 Hz, 1H), 1.54 – 1.43 (m, 1H), 1.40 (s, 3H), 1.34 – 1.10 (m, 4H), 1.07 (s, 3H), 0.86 (t, J = 7.2 Hz, 3H), 0.83 (d, J = 6.4 Hz, 3H) ppm; **^{13}C NMR** (101 MHz, $CDCl_3$) δ 212.2 (C), 209.3 (C), 209.0 (C), 57.0 (C), 51.9 (CH), 49.2 (CH), 47.0 (CH), 45.7 (CH), 45.6 (CH), 45.2 (CH_2), 43.0 (CH_2), 38.8 (CH_2), 37.6 (CH), 36.6 (CH_2), 36.2 (C), 35.4 (CH_2), 28.0 (CH_2), 27.8 (CH_2), 25.4 (CH_2), 22.1 (CH_3), 18.6 (CH_3), 12.0 (CH_3), 11.0 (CH_3) ppm.

Mechanistic Studies

Kinetic Isotope Effect Experiment

Competition KIE experiment



Inside a nitrogen-filled glovebox, an 8 mL oven-dried screw-top Pyrex tube was charged with 9,10-diphenylanthracene (0.01 mmol, 5 mol%), $CeCl_3$ (0.02 mmol, 10 mol%, anhydrous), 2,4,6-bis(triisopropylphenyl)disulfide (0.04 mmol, 20 mol%) and tetrabutylammonium chloride (0.2 mmol, 1 equivalent). Once all components were charged, the tube was sealed with a Teflon-septum screw-cap, transferred out of the glovebox, and immediately placed under a positive pressure of argon. Next, stock solutions of **2.141** (0.2 mmol, 1 equivalent) and **2.142** (0.2 mmol, 1 equivalent) in acetonitrile were added followed by anhydrous acetonitrile to bring the reaction volume to 1 mL. The resulting suspension was sparged with argon for 5 minutes. After sparging, the septum cap was quickly exchanged with a hard plastic cap and the vessel was further sealed with electrical tape and then parafilm. The reaction mixture was then sonicated (90 s) before irradiating with a violet LED (2–2.4 W, 405 nm) at a distance of 1 mm for 30 minutes. This procedure was performed in triplicate. After 30 minutes, the reaction

solution was passed through a silica plug (3 cm^3 in a 6 mL syringe barrel) eluting with Et_2O (25 mL). The resulting solution was concentrated under reduced pressure, accurately weighed phenyltrimethylsilane (~8 mg) internal standard was added, the entire residue was dissolved in *d*-chloroform and the composition analyzed through ^1H NMR spectroscopy using a Bruker Avance III HD 500 spectrometer. Analysis of the ratio of remaining **2.141**/**2.142** at low conversion delivered the following results:

Trial	% 2.141 remaining	% 2.142 remaining	KIE obtained
1	81	97	6.3
2	89	98	5.5
3	86	97	4.7

KIE average: 5.5 ± 0.8

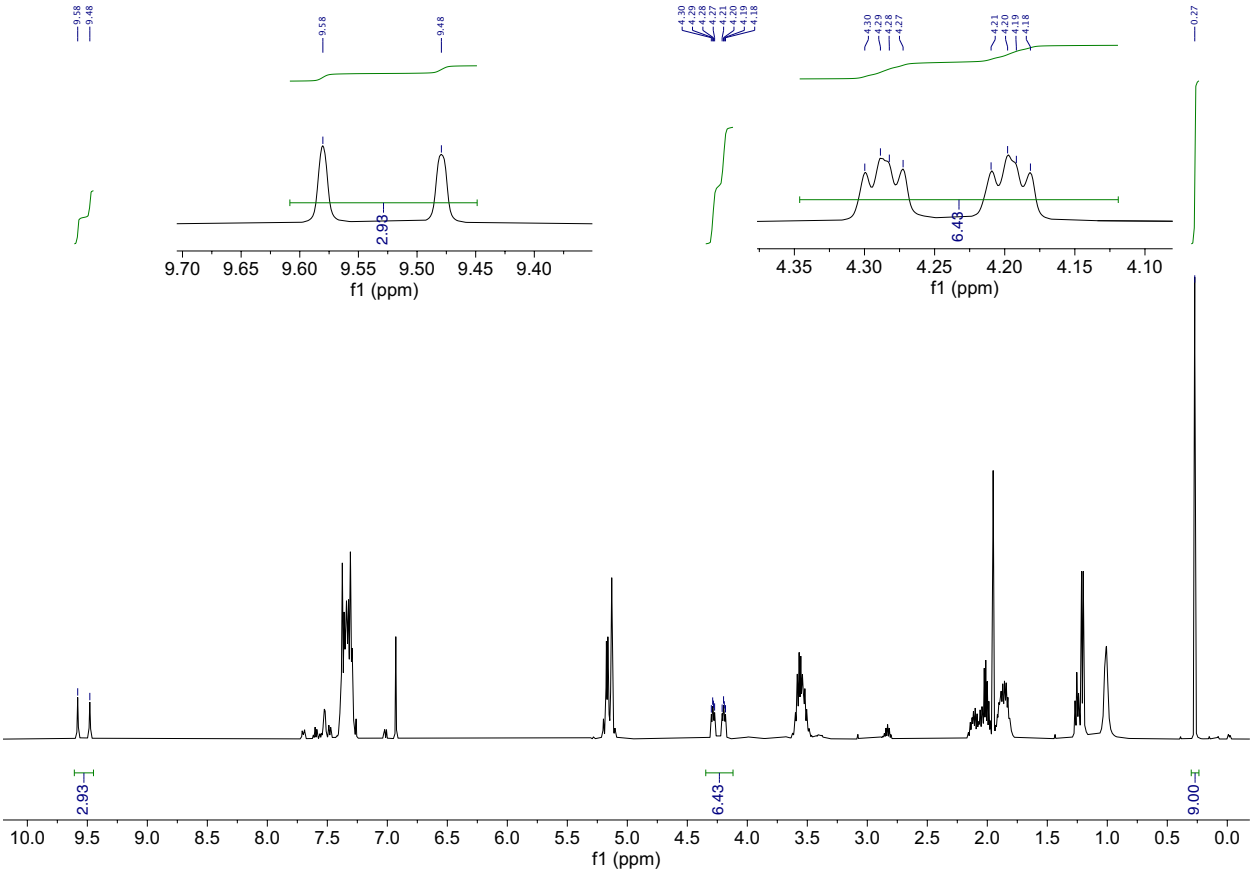


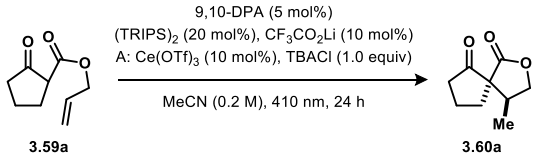
Figure 58. *Representative ^1H NMR spectrum for the KIE experiment (mixture of rotamers of 6a & 6a-d).*

The insert regions above showcase the asserted KIE wherein the signals at 9.58–9.48 ppm correspond to **2.141** (CHO) solely, whilst the signals at 4.30–4.18 ppm correspond to both **2.141** and **2.142** ($CHNCH_2C{=}O$). The signal at 0.27 ppm corresponds to the phenyltrimethylsilane internal standard ($PhSi(CH_3)_3$) with all integrations referenced to this signal.

5.3 Chapter 3 Experimental Details

General Procedures for Chapter 3

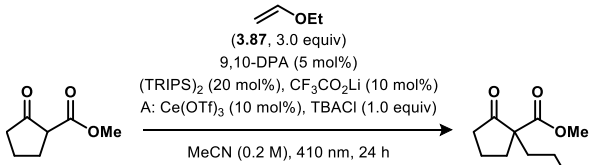
GP6 Photoredox hydroalkylation – Intramolecular



3.59a **3.60a**

Inside a nitrogen-filled glovebox, an 8 mL oven-dried screw-top Pyrex tube (12 mm diameter) was charged with lithium trifluoroacetate (0.020 mmol, 10 mol%), 9,10-diphenylanthracene (0.010 mmol, 5 mol%), $Ce(OTf)_3$ (0.020 mmol, 10 mol%, anhydrous), 2,4,6-bis(triisopropylphenyl)disulfide (0.040 mmol, 20 mol%), tetrabutylammonium chloride (TBACl, 0.20 mmol, 1 equiv., anhydrous), and the dicarbonyl substrate (0.20 mmol, 1 equiv.). $Ce(OTf)_3$ and TBACl were omitted for cerium-free conditions (B). Once all components were added, the tube was sealed with a Teflon-septum screw cap, transferred out of the glovebox, and immediately placed under a positive pressure of argon. Anhydrous acetonitrile (1.0 mL, 0.2 M) was added and the resulting suspension sparged with argon for 5 minutes. After sparging, the septum cap was quickly exchanged with a hard plastic cap and the vessel sealed with electrical tape and then Parafilm. The reaction mixture was then sonicated (90 s) before irradiating with a violet LED (2–2.4 W, 410 nm) at a distance of 1–5 mm for 24 h. Upon complete conversion of starting material as determined by TLC, or if conversion had stalled, the reaction solution was passed through a silica plug (3 cm^3 in a 6 mL syringe barrel) eluting with Et_2O (~25 mL). The resulting solution was concentrated under reduced pressure and purified by flash column chromatography.

GP7 Photoredox hydroalkylation – Intermolecular

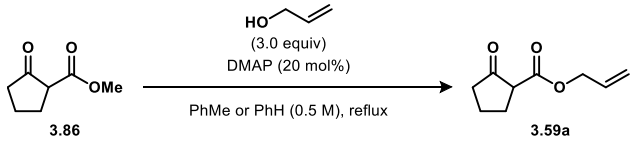


3.86 **3.96**

Inside a nitrogen-filled glovebox, an 8 mL oven-dried screw-top Pyrex tube (12 mm diameter) was charged with lithium trifluoroacetate (0.020 mmol, 10 mol%), 9,10-diphenylanthracene (0.010 mmol, 5 mol%), $Ce(OTf)_3$ (0.020 mmol, 10 mol%, anhydrous), 2,4,6-bis(triisopropylphenyl)disulfide (0.040 mmol, 20 mol%) and tetrabutylammonium chloride (TBACl, 0.20 mmol, 1 equiv., anhydrous). $Ce(OTf)_3$ and TBACl were omitted for

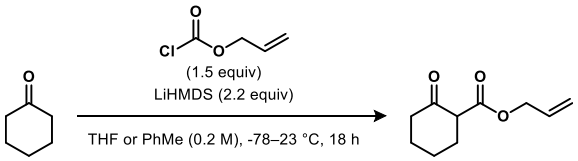
cerium-free conditions (B). Once all components were added, the tube was sealed with a Teflon-septum screw cap, transferred out of the glovebox, and immediately placed under a positive pressure of argon. Anhydrous acetonitrile (1.0 mL, 0.2 M) was added and the resulting suspension sparged with argon for 5 minutes. The dicarbonyl substrate (0.20 mmol, 1 equiv.). and alkene acceptor (0.6 mmol, 3.0 equiv.) were added, the septum cap was quickly exchanged with a hard plastic cap, and the vessel sealed with electrical tape and then Parafilm. The reaction mixture was then sonicated (90 s) before irradiating with a violet LED (2–2.4 W, 410 nm) at a distance of 1–5 mm for 24 h. Upon complete conversion of starting material as determined by TLC, or if conversion had stalled, the reaction solution was passed through a silica plug (3 cm^3 in a 6 mL syringe barrel) eluting with Et_2O (~25 mL). The resulting solution was concentrated under reduced pressure and purified by flash column chromatography.

GP8 Transesterification



To a solution of ketoester (1.0 equiv.) in toluene or benzene (0.5 M) was added the desired allylic alcohol (3.0 equiv.) and 4-dimethylaminopyridine (DMAP, 20 mol%) in a round-bottom flask fitted with a one-piece distillation apparatus with a collection flask and condenser cooled with tap water. The mixture was heated to reflux until consumption of the ketoester was observed by TLC (approximately 48 h), then allow to cool to room temperature, filtered through a pad of Celite eluting with DCM, and the filtrate concentrated under reduced pressure. The crude residue was purified by flash column chromatography (SiO_2, EtOAc/hexanes).

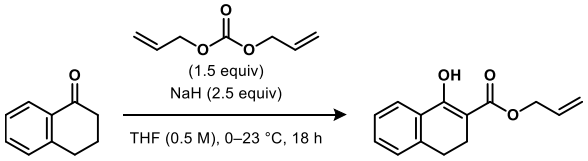
GP9 Allyl esterification with LiHMDS and allyl chloroformate



To a solution of ketone (1.0 equiv.) in THF or toluene (0.2 M) was added lithium bis(trimethylsilyl)amide (LiHMDS, 2.2 equiv., 1.0 M in THF) dropwise over 5 minutes at –78 °C in a dry ice/acetone bath. The reaction was stirred at –78 °C for 15 minutes. Allyl chloroformate (1.5 equiv.) was then added dropwise over 2 minutes at –78 °C and the reaction stirred overnight and allowed to reach room temperature. The mixture was cooled to 0 °C in an ice bath, quenched with NH_2Cl (saturated aqueous), and the phases separated. The aqueous phase was extracted with

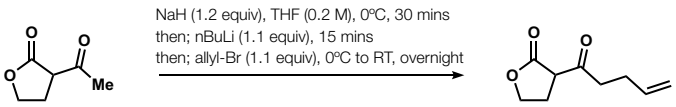
EtOAc (× 3). The combined organic phases were washed with water and brine, dried over $MgSO_4$, filtered, and concentrated under reduced pressure. The crude residue was purified by flash column chromatography (SiO_2, EtOAc/hexanes).

GP10 Allyl esterification with NaH and diallylcarbonate



To a suspension of NaH (2.5 equiv, 60% w/w dispersion in mineral oil) in THF (0.67 M) was added a solution of ketone (1.0 equiv.) in THF (2.0 M) dropwise over 5 minutes at 0 °C in an ice bath. The reaction was stirred for 30 minutes and allowed to reach room temperature. Diallylcarbonate (1.5 equiv.) was then added dropwise over 2 minutes at room temperature and the reaction stirred overnight. The mixture was cooled to 0 °C in an ice bath, quenched with NH_4Cl (saturated aqueous), and the phases separated. The aqueous phase was extracted with EtOAc (× 3). The combined organic phases were washed with water and brine, dried over $MgSO_4$, filtered, and concentrated under reduced pressure. The crude residue was purified by flash column chromatography (SiO_2, EtOAc/hexanes).

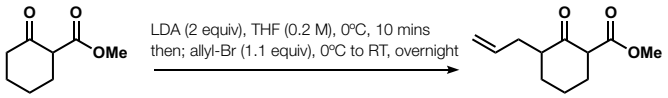
GP11 1,3-Dicarbonyl Dianion Alkylation – NaH/nBuLi



A flame-dried round bottom flask under argon atmosphere and equipped with a magnetic stir bar was charged with NaH (60% w/w in mineral oil, 1.2 equiv) and anhydrous THF (0.2 M) and the resulting suspension was stirred and cooled to 0 ºC with an ice bath. Next, the 1,3-dicarbonyl (1 equiv) was added dropwise over 5 minutes, maintaining 0 ºC. The resulting mixture was stirred at 0 ºC for an additional 30 minutes before *n*-butyllithium was added dropwise (2.5 M in hexanes, 1.1 equiv) over 10 minutes, maintaining 0 ºC. After 5 minutes of further stirring, allyl bromide (1.1 equiv) was added dropwise at 0 ºC. The resulting mixture was allowed to warm to room temperature gradually, without removal of the ice bath, and stir overnight. After complete consumption of the 1,3-dicarbonyl as judged by TLC analysis, the mixture was quenched with saturated NH_4Cl (aqueous) and diluted with distilled water and then EtOAc. The biphasic mixture was then transferred to a separatory funnel and the layers were separated. The aqueous phase

was extracted with EtOAc (3 x). The combined extracts were washed with brine (1 x), dried over $NaSO_4$, filtered, and concentrated *in vacuo*. The resulting crude residue was purified by flash column chromatography.

GP12 1,3-Dicarbonyl Dianion Alkylation – LDA

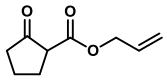


A flame-dried round bottom flask under argon atmosphere and equipped with a magnetic stir bar was charged with anhydrous THF (0.2 M) and LDA (2.0 M in THF/heptane/benzene, 2.0 equiv) the resulting solution was stirred and cooled to 0 ºC with an ice bath for 10 minutes. Next, the 1,3-dicarbonyl (1 equiv) was added dropwise over 5 minutes, maintaining 0 ºC. The resulting mixture was stirred at 0 ºC for an additional 15 minutes before allyl bromide (1.1 equiv) was added dropwise. The resulting mixture was allowed to warm to stir at 0 ºC until complete consumption of the 1,3-dicarbonyl as judged by TLC analysis. Once complete, the mixture was quenched with pH 7 phosphate buffer and concentrated *in vacuo*. Distilled water and EtOAc were added and the biphasic mixture was then transferred to a separatory funnel and the layers were separated. The organic phase was washed with 1M HCl (aqueous, 3 x), then brine (1 x), before being dried over Na_2SO_4, filtered, and concentrated *in vacuo*. The resulting crude residue was purified by flash column chromatography.

Procedures and Data

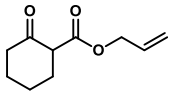
Intramolecular Hydroalkylation Substrates

allyl 2-oxocyclopentane-1-carboxylate (3.59a)



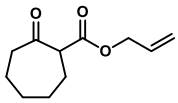
Prepared according to GP8 with ketoester **3.86** and allyl alcohol on 5.0 mmol scale and purified by flash column chromatography (SiO_2, 4–8% EtOAc/hexanes) to give **3.59a** as a clear, colourless oil (711 mg, 85%). $\mathbf{R_f}$ 0.39 (15 % EtOAc/hexanes); **^{1}H NMR** (400 MHz, $CDCl_3$) δ 5.99 – 5.83 (m, 1H), 5.38 – 5.27 (m, 1H), 5.27 – 5.19 (m, 1H), 4.69 – 4.57 (m, 2H), 3.22 – 3.13 (m, 1H), 2.40 – 2.21 (m, 4H), 2.21 – 2.06 (m, 1H), 1.94 – 1.78 (m, 1H) ppm; **^{13}C NMR** (101 MHz, $CDCl_3$) δ 212.3 (C), 169.2 (C), 131.8 (CH), 118.7 (CH_2), 66.0 (CH_2), 54.9 (CH), 38.2 (CH_2), 27.5 (CH_2), 21.1 (CH_2) ppm; **HRMS** (EI+) *m/z* calculated for $C_9H_{12}O_3^{\bullet+}$ $[M]^{\bullet+}$ 168.07810, found 168.07876.

allyl 2-oxocyclohexane-1-carboxylate (3.59b)



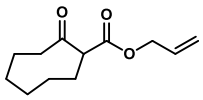
Prepared according to GP9 with cyclohexanone on 20 mmol scale and purified by flash column chromatography (SiO_2, 3–5% Et_2O/hexanes) to give **3.59b** as a clear, colourless oil (2.8 g, 77%). $\mathbf{R_f}$ 0.25 (5% Et_2O/hexanes); **^{1}H NMR** (500 MHz, $CDCl_3$) δ 12.14 (s, 1H, **e**), 6.00 – 5.87 (m, 1H, **k** + **e**), 5.41 – 5.21 (m, 2H, **k** + **e**), 4.71 – 4.57 (m, 2H, **k** + **e**), 3.41 (ddd, J = 9.7, 6.0, 1.3 Hz, 1H, **k**), 2.55 – 2.48 (m, 1H, **k**), 2.41 – 2.33 (m, 1H, **k**), 2.26 (dtt, J = 7.9, 6.3, 1.6 Hz, 4H, **e**), 2.22 – 2.08 (m, 3H, **k**), 2.02 – 1.94 (m, 1H, **k**), 1.92 – 1.77 (m, 2H, **k**), 1.77 – 1.65 (m, 2H, **k** + **e**), 1.65 – 1.55 (m, 2H, **k** + **e**) ppm; **^{13}C NMR** (126 MHz, $CDCl_3$) δ 172.6 (C), 172.5 (C), 132.4 (CH), 118.0 (CH_2), 97.8 (C), 64.8 (CH_2), 29.3 (CH_2), 22.5 (CH_2), 22.5 (CH_2), 22.0 (CH_2) ppm; **HRMS** (EI+) *m/z* calculated for $C_{10}H_{14}O_3^{\bullet+}$ $[M]^{\bullet+}$ 182.09375, found 182.09262

allyl 2-oxocycloheptane-1-carboxylate (3.59c)



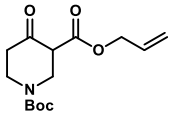
Prepared according to GP10 with cycloheptanone on 4.2 mmol scale and purified by flash column chromatography (SiO_2, 5–10% EtOAc/hexanes) to give **3.59c** as a clear, colourless oil (647 mg, 79%, 5:1 keto/enol). $\mathbf{R_f}$ 0.55 (30% Et_2O/hexanes); **^{1}H NMR** (400 MHz, $CDCl_3$) δ 12.65 (s, 0.2H, **e**), 5.90 (ddt, J = 17.2, 10.4, 5.7 Hz, 1.2H, **k** + **e**), 5.32 (dq, J = 17.2, 1.5 Hz, 1.2H, **k** + **e**), 5.23 (dq, J = 10.4, 1.3 Hz, 1.2H, **k** + **e**), 4.65 (dt, J = 5.5, 1.5 Hz, 0.4H, 2 × **e**), 4.62 (dq, J = 5.8, 1.2 Hz, 2H, 2 × **k**), 3.57 (dd, J = 10.3, 3.9 Hz, 1H, **k**), 2.68 – 2.57 (m, 2H, 2 × **k**), 2.58 – 2.53 (m, 0.2H, **e**), 2.48 – 2.38 (m, 0.8H, 4 × **e**), 2.17 – 2.05 (m, 1H, **k**), 2.00 – 1.78 (m, 4H, 4 × **k**), 1.78 – 1.68 (m, 0.4H, 2 × **e**), 1.68 – 1.53 (m, 1.8H, 1 × **k** + 4 × **e**), 1.51 – 1.38 (m, 2.6H, 2 × **k** + 3 × **e**) ppm; **^{13}C NMR** (101 MHz, $CDCl_3$) δ 209.0 (C, **k**), 180.2 (C, **e**), 172.8 (C, **e**), 170.4 (C, **k**), 132.5 (CH, **e**), 131.9 (CH, **k**), 118.7 (CH_2, **k**), 117.9 (CH_2, **e**), 101.7 (C, **e**), 65.8 (CH_2, **k**), 65.0 (CH_2, **e**), 59.0 (CH, **k**), 43.3 (CH_2, **k**), 35.5 (CH_2, **e**), 32.1 (CH_2, **e**), 29.8 (CH_2, **k**), 28.2 (CH_2, **k**), 27.7 (CH_2, **k** + **e**), 27.5 (CH_2, **e**), 24.8 (CH_2, **e**), 24.5 (CH_2, **k**); **HRMS** (ESI+) *m/z* calculated for $C_{11}H_{16}O_3Na^+$ $[M + Na]^+$ 219.0997, found 219.0995

allyl 2-oxocyclooctane-1-carboxylate (3.59d)



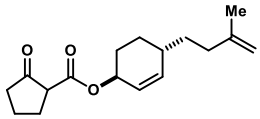
Prepared according to GP9 with cyclooctanone on 10 mmol scale and purified by flash column chromatography (SiO_2, 2–5% EtOAc/hexanes) to give **3.59d** as a clear, colourless oil (1.93 g, 92%, 3:2 enol/keto). $\mathbf{R_f}$ 0.32 (5% EtOAc/hexanes); **^{1}H NMR** (500 MHz, $CDCl_3$) δ 12.49 (t, J = 1.3 Hz, 0.6H, **e**), 6.02 – 5.81 (m, 1H, **k** + **e**), 5.39 – 5.16 (m, 2H, **2k** + **2e**), 4.66 (dt, J = 5.4, 1.5 Hz, 1.2H, **2e**), 4.58 (dt, J = 5.7, 1.4 Hz, 0.8H, **2e**), 3.61 (dd, J = 10.7, 4.5 Hz, 0.4H, **k**), 2.60 (ddd, J = 13.9, 11.4, 4.2 Hz, 0.4H, **k**), 2.53 – 2.44 (m, 0.4H, **k**), 2.44 – 2.33 (m, 2.4H, **4e**), 2.20 – 2.04 (m, 0.8H, **2k**), 1.97 – 1.82 (m, 1H, **2k**), 1.80 – 1.60 (m, 2.2H, **4k** + **1e** or **k** + **3e**), 1.60 – 1.34 (m, 4.6H, **4k** + **5e** or **7k** + **3e**) ppm; **^{13}C NMR** (126 MHz, $CDCl_3$) δ 212.1 (C, **k**), 176.7 (C, **e**), 172.6 (C, **e**), 169.9 (C, **k**), 132.5 (CH, **e**), 131.8 (CH, **k**), 118.6 (CH_2, **k**), 117.6 (CH_2, **e**), 99.2 (C, **e**), 65.8 (CH_2, **k**), 64.8 (CH_2, **e**), 57.0 (CH, **k**), 42.0 (CH_2, **k**), 32.5 (CH_2, **e**), 30.0 (CH_2, **e**), 29.2 (CH_2, **k**), 28.8 (CH_2, **e**), 27.2 (CH_2, **k**), 26.7 (CH_2, **e**), 26.2 (CH_2, **e**), 25.5 (CH_2, **k**), 25.3 (CH_2, **k**), 24.6 (CH_2, **k**), 24.0 (CH_2, **e**) ppm; **HRMS** (EI+) *m/z* calculated for $C_{12}H_{18}O_3^{\bullet+}$ $[M]^{+\bullet}$ 210.12505, found 210.12328.

3-allyl 1-(tert-butyl) 4-oxopiperidine-1,3-dicarboxylate (3.59e)



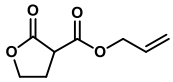
Prepared according to GP9 with *N*-Boc-4-piperidone on 5.0 mmol scale and purified by flash column chromatography (SiO_2, 5–10% EtOAc/hexanes) to give **3.59e** as an amorphous white powder (479 mg, 34%). $\mathbf{R_f}$ 0.27 (10% EtOAc/hexanes); **^{1}H NMR** (400 MHz, $CDCl_3$) δ 11.96 (s, 1H), 5.93 (ddt, J = 16.9, 11.7, 6.0 Hz, 1H), 5.39 – 5.29 (m, 1H), 5.25 (d, J = 10.5 Hz, 1H), 4.68 (d, J = 5.5 Hz, 2H), 4.09 (s, 2H), 3.57 (t, J = 6.0 Hz, 2H), 2.46 – 2.29 (m, 2H), 1.47 (s, 9H) ppm; **^{13}C NMR** (101 MHz, $CDCl_3$) δ 202.7 (C), 170.4 (C), 154.7 (C), 131.9 (CH), 118.4 (CH_2), 80.3 (C), 65.1 (CH_2), 56.6 (CH), 40.8 (CH_2), 40.4 (CH_2), 29.0 (CH_2), 28.5 (3 × CH_3) ppm; **HRMS** (EI+) *m/z* calculated for $C_{14}H_{21}NO_5^{\bullet+}$ $[M]^{\bullet+}$ 283.14142, found 283.14185.

4-(3-methylbut-3-en-1-yl)cyclohex-2-en-1-yl 2-oxocyclopentane-1-carboxylate (3.59f)



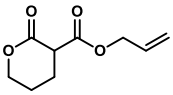
Prepared according to GP8 with ketoester **3.86** and alcohol **3.67** on 0.16 mmol scale and purified by flash column chromatography (SiO_2, 4–8% EtOAc/hexanes) to give **3.59f** as a clear, colourless oil (36.4 mg, 82%, 1:1 mixture of epimers). $\mathbf{R_f}$ 0.52 (16% EtOAc/hexanes); **^{1}H NMR** (400 MHz, $CDCl_3$) δ 5.85 – 7.76 (m, 1H), 5.68 – 5.57 (m, 1H), 5.36 – 5.27 (m, 1H), 4.70 (s, 1H), 4.67 (s, 1H), 3.13 (t, J = 9.0 Hz, 1H), 2.40 – 2.21 (m, 4H), 2.19 – 2.00 (m, 5H), 1.95 – 1.79 (m, 2H), 1.71 (s, 3H), 1.70 – 1.53 (m, 1H), 1.48 (ddd, J = 13.5, 9.0, 6.7 Hz, 1H), 1.42 – 1.21 (m, 2H) ppm; **^{13}C NMR** (101 MHz, $CDCl_3$) δ 212.5 (C), 212.5 (C), 169.4 (C), 169.4 (C), 145.8 (2 × C), 136.8 (CH), 136.6 (CH), 126.0 (CH), 125.8 (CH), 110.2 (2 × CH_2), 70.8 (CH), 70.7 (CH), 55.1 (CH), 55.1 (CH), 38.2 (2 × CH_2), 35.1 (CH_2), 35.1 (CH_2), 34.7 (CH), 34.7 (CH), 33.6 (CH_2), 33.5 (CH_2), 27.6 (CH_2), 27.5 (CH_2), 27.5 (CH_2), 27.5 (CH_2), 26.4 (CH_2), 26.2 (CH_2), 22.5 (2 × CH_3), 21.1 (CH_2), 21.1 (CH_2) ppm; **HRMS** (EI+) *m/z* calculated for $C_{11}H_{18}O^{\bullet+}$ [M – $C_6H_7O_2$]$^{\bullet+}$ 166.13522, found 166.13420.

allyl 2-oxotetrahydrofuran-3-carboxylate (4g)



Prepared according to GP9 with γ-butyrolactone on 4.6 mmol scale and purified by flash column chromatography (SiO_2, 15% EtOAc/hexanes) to give **3.59g** as a pale-yellow oil (598.4 mg, 76%). $\mathbf{R_f}$ 0.4 (35% EtOAc/hexanes); **^{1}H NMR** (400 MHz, $CDCl_3$) δ 5.91 (ddt, J = 17.2, 10.5, 5.7 Hz, 1H), 5.35 (dq, J = 17.2, 1.5 Hz, 1H), 5.26 (dq, J = 10.5, 1.3 Hz, 1H), 4.75 – 4.61 (m, 2H), 4.46 (ddd, J = 9.0, 8.1, 5.3 Hz, 1H), 4.32 (dt, J = 9.0, 7.4 Hz, 1H), 3.57 (dd, J = 9.3, 7.8 Hz, 1H), 2.67 (dtd, J = 13.1, 8.0, 7.2 Hz, 1H), 2.51 (dddd, J = 13.0, 9.4, 7.6, 5.3 Hz, 1H) ppm; **^{13}C NMR** (101 MHz, $CDCl_3$) δ 172.3 (C), 167.5 (C), 131.3 (CH), 119.2 (CH_2), 67.4 (CH_2), 66.7 (CH_2), 46.0 (CH), 26.5 (CH_2) ppm; **HRMS** (EI+) *m/z* calculated for $[M]^+$ 193.0477, found 193.0459.

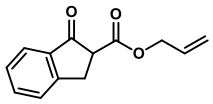
allyl 2-oxotetrahydro-2H-pyran-3-carboxylate (3.59h)



Prepared according to GP10 with δ-valerolactone on 4.6 mmol scale and purified by flash column chromatography (SiO_2, 50–75% Et_2O/hexanes) to give **3.59h** as an amorphous white solid (496.4 mg, 59%). $\mathbf{R_f}$ 0.6 (50% EtOAc/hexanes); **^{1}H NMR** (400 MHz, $CDCl_3$) δ 5.92 (ddt, J = 17.2, 10.4, 5.7 Hz, 1H), 5.36 (dq, J = 17.2, 1.5

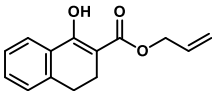
Hz, 1H), 5.27 (dq, *J* = 10.5, 1.3 Hz, 1H), 4.75 – 4.61 (m, 2H), 4.44 – 4.31 (m, 2H), 3.59 (dd, *J* = 8.5, 7.5 Hz, 1H), 2.35 – 2.12 (m, 2H), 2.07 – 1.82 (m, 2H) ppm; **^{13}C NMR** (101 MHz, $CDCl_3$) δ 168.9 (C), 167.3 (C), 131.5 (CH), 119.1 (CH_2), 69.5 (CH_2), 66.5 (CH_2), 47.4 (CH), 22.9 (CH_2), 21.0 (CH_2) ppm; **HRMS** (ESI+) *m/z* calculated for $C_9H_{12}O_4Na^+$ $[M + Na]^+$ 207.0633, found 207.0644.

allyl 1-oxo-2,3-dihydro-1H-indene-2-carboxylate (3.59i)[§]



Prepared according to GP9 with indanone on 5.0 mmol scale and purified by flash column chromatography (SiO_2, 5% EtOAc/hexanes) to give **3.59i** as a clear, colourless oil (742 mg, 69%, 4:1 keto/enol). **R_f** 0.79 (30% EtOAc/hexanes); **^{1}H NMR** (400 MHz, $CDCl_3$) δ 7.78 (keto, ddq, *J* = 7.7, 1.2, 0.5 Hz, 1H), 7.68 – 7.59 (m, 1H), 7.54 – 7.36 (m, 2H), 6.09 – 5.88 (m, 1H), 5.39 (enol, dq, *J* = 17.2, 1.5 Hz, 1H), 5.37 (keto, dq, *J* = 17.2, 1.5 Hz, 1H), 5.33 – 5.23 (m, 1H), 4.81 – 4.64 (m, 2H), 3.76 (keto, dd, *J* = 8.3, 4.1 Hz, 1H), 3.60 (enol, d, *J* = 4.2 Hz, 2H), 3.57 – 3.54 (m, 1H), 3.44 – 3.35 (m, 1H) ppm; **^{13}C NMR** (101 MHz, $CDCl_3$) δ **keto** 199.5 (C), 168.9 (C), 153.7 (C), 135.6 (CH), 135.4 (C), 131.8 (CH), 128.0 (CH), 126.7 (CH), 124.9 (CH), 118.8 (CH_2), 66.3 (CH_2), 53.4 (CH), 30.4 (CH_2) **enol** 199.5 (C), 168.9 (C), 153.7 (C), 143.4 (C), 132.5 (CH), 129.6 (CH), 127.0 (CH), 124.9 (CH), 120.9 (CH), 118.3 (CH_2), 102 (C), 64.8 (CH_2), 32.7 (CH_2) ppm; **HRMS** (ESI+) *m/z* calculated for $C_{13}H_{12}O_3Na^+$ $[M + Na]^+$ 239.0679, found 239.0686;

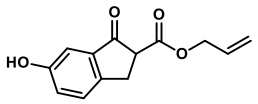
allyl 1-oxo-1,2,3,4-tetrahydronaphthalene-2-carboxylate (3.59j)[§]



Prepared according to GP10 with tetralone on 2.0 mmol scale and purified by flash column chromatography (SiO_2, 5% EtOAc/hexanes) to give **3.59j** as a clear, colourless oil (236 mg, 51%). **R_f** 0.75 (25% EtOAc/hexanes); **^{1}H NMR** (400 MHz, $CDCl_3$) δ 12.40 (s, 1H), 8.05 (ddd, *J* = 7.9, 1.3, 0.5 Hz, 1H), 7.80 (ddd, *J* = 7.7, 1.4, 0.5 Hz, 1H), 7.50 (td, *J* = 7.5, 1.5 Hz, 1H), 7.36 – 7.24 (m, 4H), 7.20 – 7.15 (m, 1H), 6.00 (ddt, *J* = 15.9, 9.1, 5.6 Hz, 1H), 5.93 (ddt, *J* = 17.2, 10.5, 5.6 Hz, 1H), 5.36 (ddd, *J* = 16.2, 3.1, 1.6 Hz, 2H), 5.26 (ddq, *J* = 14.4, 10.5, 1.3 Hz, 2H), 4.73 (dt, *J* = 5.6, 1.4 Hz, 2H), 4.70 (tt, *J* = 5.7, 1.4 Hz, 2H), 3.68 – 3.60 (m, 1H), 3.08 (dt, *J* = 16.4, 5.1 Hz, 1H), 3.04 – 2.95 (m, 1H), 2.82 (dd, *J* = 9.0, 6.6 Hz, 2H), 2.64 – 2.56 (m, 2H), 2.56 – 2.46 (m, 1H), 2.38 (ddt, *J* = 13.5, 5.7, 4.7 Hz, 1H) ppm; **^{13}C NMR** (101 MHz, $CDCl_3$) δ 193.2 (C), 172.5 (C), 170.0 (C), 165.5 (C), 143.8 (C), 139.6 (C), 134.1 (CH), 132.3 (CH), 131.9 (CH), 130.7 (CH), 130.1 (C), 128.9 (CH), 127.9 (CH), 127.6 (CH), 127.1 (CH), 126.7 (CH), 124.5

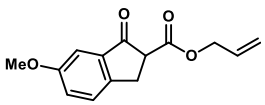
(CH), 118.6 (CH_2), 118.3 (CH_2), 96.9 (C), 66.0 (CH_2), 65.2 (CH_2), 54.7 (CH), 27.9 (CH_2), 27.8 (CH_2), 26.5 (CH_2), 20.6 (CH_2) ppm; **HRMS** (ESI+) *m/z* calculated for $C_{14}H_{14}O_3Na^+$ $[M + Na]^+$ 253.0835, found 253.0811;

allyl 6-hydroxy-1-oxo-2,3-dihydro-1H-indene-2-carboxylate (3.59k)[§]



To a solution of **3.59m** (173 mg, 0.5 mmol, 1.0 equiv.) in THF (2.5 mL, 0.2 M) was added tetrabutylammonium fluoride (TBAF, 0.55 mL, 1.1 equiv., 1 M in THF) dropwise over 2 minutes at room temperature. The reaction was stirred at room temperature for 1 hour. The mixture was diluted with EtOAc (20 mL), quenched with dropwise addition of NH_4Cl (5 mL, saturated aqueous), and the phases separated. The organic phase was washed with water (3 × 10 mL) and brine (10 mL), dried over $MgSO_4$, filtered, and concentrated under reduced pressure. The crude residue was purified by flash column chromatography (SiO_2, 30% EtOAc/hexanes) to give **3.59k** as an amorphous beige solid (126 mg, quantitative, 7.5:1.2:1 keto/enol/enol). ; **^{1}H NMR** (400 MHz, $CDCl_3$) δ 10.31 (s, 1H, **e**), 9.81 (s, 1H, **e**), 7.41 – 7.34 (m, 1H, **k** + **e**), 7.32 (d, J = 8.1 Hz, 1H, **e**), 7.23 – 7.13 (m, 2H, **k** + **e**), 7.09 (d, J = 2.5 Hz, 1H, **e**), 6.93 (dd, J = 8.1, 2.5 Hz, 1H, **e**), 6.07 – 5.77 (m, 1H, **k** + **2e**), 5.66 (s, 1H, **e**), 5.53 (s, 1H, **k**), 5.39 (dq, J = 17.2, 1.6 Hz, 1H, **e**), 5.36 (dq, J = 17.2, 1.5 Hz, 1H, **k**), 5.32 – 5.19 (m, 1H, **k** + **e**), 5.08 (s, 1H, **e**), 4.77 (dt, J = 5.6, 1.4 Hz, 2H, **e**), 4.75 – 4.62 (m, 2H, **k** + **e**), 3.78 (dd, J = 8.1, 3.9 Hz, 1H, **k**), 3.61 (d, J = 17.4 Hz, 1H, **e**), 3.52 – 3.42 (m, 2H, **k** + **3e**), 3.31 (dd, J = 16.9, 8.1 Hz, 1H, **k**) ppm; **^{13}C NMR** (101 MHz, $CDCl_3$) δ 200.0, 169.2, 168.8, 156.3, 156.2, 156.0, 146.3, 145.0, 144.4, 136.6, 135.2, 134.9, 131.7, 130.9, 127.7, 127.6, 127.6, 125.5, 125.2, 124.6, 119.6, 119.2, 119.0, 110.3, 110.2, 109.6, 91.2, 81.3, 67.1, 66.9, 66.5, 54.2, 38.9, 36.3, 29.8 ppm; **HRMS** (EI+) *m/z* calculated for $C_{13}H_{12}O_4^{\bullet+}$ $[M]^{\bullet+}$: 232.07301, found 232.07553

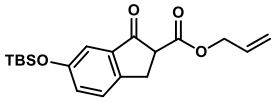
allyl 6-methoxy-1-oxo-2,3-dihydro-1H-indene-2-carboxylate (3.59l)[§]



Prepared according to GP9 with 6-methoxyindanone on 5.0 mmol scale and purified by flash column chromatography (SiO_2, 5–30% EtOAc/hexanes) to give **3.59l** as a clear, colourless oil (230 mg, 19%). $\mathbf{R_f}$ 0.39 (20% EtOAc/hexanes); **^{1}H NMR** (400 MHz, $CDCl_3$) δ 7.39 (dq, J = 8.3, 0.8 Hz, 1H, **k**), 7.35 (dd, J = 8.2, 0.7 Hz, 1H, **e**), 7.25 – 7.17 (m, 2H, **k**), 7.15 (d, J = 2.5 Hz, 1H, **e**), 7.00 (dd, J = 8.3, 2.5 Hz, 1H, **e**), 6.07 – 5.87 (m, 1H, **k + e**), 5.43 – 5.32 (m, 1H, **k** + **e**), 5.32 – 5.20 (m, 1H, **k** + **e**), 4.77 (dt, J = 5.6, 1.5 Hz, 2H, **e**), 4.69 (ddt, J = 13.2, 5.6, 1.5 Hz, 2H,

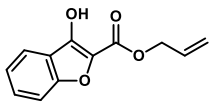
k), 3.86 (s, 3H, **e**), 3.83 (s, 3H, **k**), 3.78 (dd, *J* = 8.1, 3.9 Hz, 1H, **k** + **e**), 3.52 – 3.43 (m, 1H, **k** + **e**), 3.32 (dd, *J* = 16.9, 8.0 Hz, 1H, **k** + **e**) ppm; **^{13}C NMR** (101 MHz, $CDCl_3$) δ **keto** 199.4 (C), 169.0 (C), 159.9 (C), 146.6 (C), 136.6 (C), 131.8 (CH), 127.3 (CH), 125.1 (CH), 118.8 (CH_2), 105.8 (CH), 66.3 (CH_2), 55.8 (CH_3), 54.1 (CH), 29.8 (CH_2) **enol** 159.3 (C), 138.1 (C), 135.6 (C), 132.4 (CH), 125.6 (C), 118.3 (C), 117.4 (CH), 104.6 (CH), 103.4 (C), 64.8 (CH_2), 55.7 (CH_3), 31.9 (CH_2) ppm; **HRMS** (EI+) *m/z* calculated for $C_{14}H_{14}O_4^{\bullet+}$ $[M]^{\bullet+}$ 246.08866, found 246.08813

allyl 6-((tert-butyldimethylsilyl)oxy)-1-oxo-2,3-dihydro-1H-indene-2-carboxylate (3.59m)[§]



Prepared according to GP9 with indanone-derived **5.10** on 3.0 mmol scale and purified by flash column chromatography (SiO_2, 2–10% EtOAc/hexanes) to give **3.59m** as a clear, colourless oil (400 mg, 38%, 6.7:1 keto/enol). $\mathbf{R_f}$ 0.65 (20% EtOAc/hexanes); **^{1}H NMR** (400 MHz, $CDCl_3$) δ 7.35 (ddd, *J* = 8.1, 0.9, 0.9 Hz, 1H, **k**), 7.30 (d, *J* = 8.1 Hz, 1H, **e**), 7.16 (d, *J* = 2.3 Hz, 1H, **k**), 7.12 (dd, *J* = 8.1, 2.4 Hz, 1H, **k**), 7.09 (d, *J* = 2.3 Hz, 1H, **e**), 6.91 (dd, *J* = 8.1, 2.4 Hz, 1H, **e**), 6.08 – 5.86 (m, 1H), 5.43 – 5.31 (m, 1H), 5.31 – 5.21 (m, 1H), 4.80 – 4.61 (m, 2H), 3.76 (dd, *J* = 8.1, 4.0 Hz, 1H, **k**), 3.48 – 3.46 (m, 2H, **e**), 3.47 (dd, *J* = 16.8, 4.0 Hz, 1H, **k**), 3.30 (dd, *J* = 17.0, 8.2 Hz, 1H, **k**), 0.99 (s, 9H, **e**), 0.98 (s, 9H, **k**), 0.21 (s, 6H, **e**), 0.20 (s, 6H, **k**) ppm; **^{13}C NMR** (101 MHz, $CDCl_3$) δ 199.3 (C, **k**), 169.0 (C), 155.8 (C, **k**), 155.1 (C, **e**), 146.7 (C, **k**), 138.2 (C, **e**), 136.7 (C, **k**), 136.2 (C, **e**), 132.5 (CH, **e**), 131.8 (CH, **k**), 128.8 (CH, **k**), 127.3 (CH, **k**), 125.5 (CH, **e**), 122.1 (CH, **e**), 118.7 (CH_2, **k**), 118.2 (CH_2, **e**), 114.3 (CH, **k**), 112.1 (CH, **e**), 103.3 (C, **e**), 66.3 (CH_2, **k**), 64.7 (CH_2, **e**), 54.1 (CH), 32.0 (CH_2, **e**), 29.8 (CH_2, **k**), 25.8 (3 × CH_3, **e**), 25.7 (3 × CH_3, **k**), 18.3 (C, **e**), 18.3 (C, **k**), -4.3 (2 × CH_3, **e**), -4.4 (2 × CH_3, **k**) ppm; **HRMS** (EI+) *m/z* calculated for $C_{14}H_{14}O_4^{\bullet+}$ $[M]^{\bullet+}$ 346.15949, found 346.16252

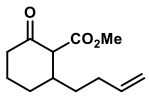
allyl 3-oxo-2,3-dihydrobenzofuran-2-carboxylate (3.59n)



Prepared according to the following literature adapted procedure.[345] To a solution of KOtBu (471.3 mg, 4.2 mmol, 2.1 equiv) in THF (anhydrous, 3 mL) was added a solution of diester **3.84b** (552.6 mg, 2 mmol, 1.0 equiv) in anhydrous THF (1 mL) dropwise over 5 minutes at 0 ºC in an ice bath. The resulting solution was stirred at 0 ºC until complete conversion of the starting material was observed by TLC (~30 mins). Once complete, the mixture was quenched by addition of NH_4Cl (saturated aqueous, 10 mL) and diluted with Et_2O (10 mL) and the layers were

separated. The aqueous phase was extracted with Et_2O (2 × 10 mL). Combined extracts were washed with brine (15 mL), dried over $MgSO_4$, filtered and concentrated *in vacuo*. The crude residue was rapidly purified by flash column chromatography (SiO_2, 1:15:84 AcOH/EtOAc/hexanes) to give **3.59n** as an amorphous white solid (329.8 mg, 76%). Note: 2D TLC showed the product is unstable on silica gel, to minimize degradation short column path lengths and rapid elution was prioritized; this compound was also unstable under air and decomposes to a yellow paste upon prolonged exposure, necessitating storage under argon at –20 ºC. $\mathbf{R_f}$ 0.52 (20% EtOAc/hexanes); **^{1}H NMR** (500 MHz, $CDCl_3$) δ 7.74 (dt, J = 8.0, 1.1 Hz, 1H), 7.53 – 7.43 (m, 2H), 7.30 (ddd, J = 8.0, 6.6, 1.4 Hz, 1H), 6.07 (ddt, J = 17.3, 10.4, 5.9 Hz, 1H), 5.47 (dq, J = 17.1, 1.4 Hz, 1H), 5.36 (dq, J = 10.3, 1.2 Hz, 1H), 4.92 (dt, J = 5.9, 1.3 Hz, 2H) ppm; **^{13}C NMR** (126 MHz, $CDCl_3$) δ 153.9 (C), 138.8 (C), 131.6 (CH), 131.1 (C), 129.6 (CH), 126.1 (C), 123.3 (CH), 120.8 (CH), 120.2 (C), 119.8 (CH_2), 112.8 (CH), 65.9 (CH_2) ppm; **HRMS** (EI+) *m/z* calculated for $C_{12}H_{10}O_4^{\bullet+}$ $[M]^{\bullet+}$ 218.05736, found 218.06010.

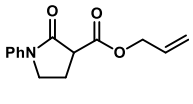
methyl 2-(but-3-en-1-yl)-6-oxocyclohexane-1-carboxylate (3.59o)



Prepared according to the following literature adapted procedure.[346] A flame-dried 100 mL round-bottom flask under a positive pressure of argon was charged with magnesium powder (1.25 g, 51.4 mmol, 4.9 equiv.), iodine flakes (0.1 g, 0.39 mmol, 0.04 equiv.), a magnetic stir bar, and a reflux condenser, and the two components were dry-stirred together overnight. The next morning, anhydrous THF (40 mL) was added followed by a solution of 4-bromo-1-butene (4.2 g, 3.2 mL, 31.1 mmol, 3 equiv.) in anhydrous THF (7.5 mL). The resulting solution was stirred and brought to a gentle reflux for 1.5 hours. After 1.5 hours at reflux, the solution was allowed to cool to room temperature. Once at room temperature, the Grignard reagent solution was transferred by cannula dropwise over 10 minutes to a pre-cooled (–20 ºC, ice/acetone bath) solution of CuBr•DMS (0.550 g, 2.68 mmol, 0.26 equiv.) in anhydrous THF (5 mL) inside of a flame-dried 250 mL round-bottom flask under argon and equipped with a stir bar, to give a purple solution. The resulting solution was stirred at –20 ºC for 30 minutes before a solution of 2-cyclohexen-1-one (1 g, 10.4 mmol, 1 equiv.) in anhydrous THF (5 mL) was added dropwise over 10 minutes. This solution was allowed to stir at –20 ºC for 30 minutes (cyclohexenone consumed according to TLC) before HMPA (freshly distilled from CaH_2, 6.4 mL, 36.8 mmol, 3.5 equiv.) was added. Next, methyl cyanoformate (2.9 mL, 36.5 mmol, 3.5 equiv.) was added and the mixture was allowed to stir at –20 ºC for a further 3 hours. After 3 hours, brine (100 mL) was added, and the

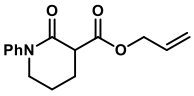
mixture was transferred to a separatory funnel with EtOAc (30 mL). The layers were mixed and separated, and the aqueous phase was extracted with more EtOAc (2 × 50 mL). The combined extracts were washed with water (2 × 30 mL) and brine (50 mL) and dried over Na_2SO_4, filtered, and concentrated *in vacuo*. The crude residue was filtered through a pad of silica eluting with 10% EtOAc/Hexanes and concentrated by rotary evaporation. The residue was then further purified by flash column chromatography (SiO_2, 4–30% EtOAc/hexanes) to give **3.59o** as a complex mixture of diastereomers and keto/enol tautomers (903 mg, 41 %). $\mathbf{R_f}$ 0.33 (10% EtOAc/hexanes); **^{1}H NMR** (400 MHz, $CDCl_3$) δ 12.33 (s, 0H), 5.89 – 5.65 (m, 1H), 5.14 – 4.97 (m, 1H), 5.01 – 4.88 (m, 2H), 3.84 (s, 1H), 3.78 – 3.65 (m, 3H), 2.56 – 2.35 (m, 1H), 2.37 – 1.10 (m, 8H) ppm; **^{13}C NMR** (101 MHz, $CDCl_3$) δ 206.2, 176.0, 173.3, 172.7, 170.4, 139.0, 138.0, 137.9, 137.5, 121.3, 115.3, 115.3, 115.2, 115.2, 114.7, 114.4, 102.7, 67.9, 63.8, 61.0, 57.1, 55.3, 52.7, 52.2, 52.1, 51.6, 51.5, 42.1, 41.7, 41.2, 40.7, 39.6, 35.7, 35.5, 34.3, 34.2, 34.1, 33.5, 33.3, 32.3, 32.1, 31.2, 31.1, 30.8, 30.6, 30.5, 30.2, 29.6, 29.2, 28.9, 28.6, 28.0, 26.5, 25.4, 25.3, 24.8, 20.7, 19.3, 17.1 ppm; **HRMS** (EI+) *m/z* calculated for $C_{12}H_{18}O_3^{\bullet+}$ $[M]^{\bullet+}$ 210.12505, found 210.12489.

allyl 2-oxo-1-phenylpyrrolidine-3-carboxylate (3.59p)



Prepared according to GP10 with *N*-phenylpyrrolidone on 5.0 mmol scale and purified by flash column chromatography (SiO_2, 15–40% EtOAc/hexanes) to give **3.59p** as a waxy beige solid (377 mg, 31%). $\mathbf{R_f}$ 0.36 (30% EtOAc/hexanes); **^{1}H NMR** (400 MHz, $CDCl_3$) δ 7.65 – 7.57 (m, 2H), 7.44 – 7.32 (m, 2H), 7.17 (ddt, J = 8.6, 7.4, 1.2 Hz, 1H), 5.95 (ddt, J = 17.3, 10.5, 5.7 Hz, 1H), 5.38 (dq, J = 17.3, 1.5 Hz, 1H), 5.26 (dq, J = 10.4, 1.3 Hz, 1H), 4.71 (ddt, J = 5.8, 4.3, 1.4 Hz, 2H), 4.00 (ddd, J = 9.3, 8.4, 5.2 Hz, 1H), 3.86 (ddd, J = 9.4, 8.1, 6.2 Hz, 1H), 3.69 (dd, J = 9.2, 7.1 Hz, 1H), 2.56 (dddd, J = 13.1, 8.4, 7.0, 6.2 Hz, 1H), 2.41 (dddd, J = 13.1, 9.1, 8.1, 5.2 Hz, 1H) ppm; **^{13}C NMR** (101 MHz, $CDCl_3$) δ 169.7 (C), 168.8 (C), 139.0 (C), 131.7 (CH), 129.0 (2 × CH), 125.2 (CH), 120.3 (2 × CH), 118.9 (CH_2), 66.4 (CH_2), 50.1 (CH), 47.4 (CH_2), 22.4 (CH_2) ppm; **HRMS** (EI+) *m/z* calculated for $C_{14}H_{15}NO_3$ $[M]^+$ 245.10519, found 245.10553.

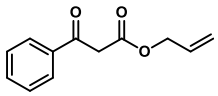
allyl 2-oxo-1-phenylpiperidine-3-carboxylate (3.59q)



Prepared according to GP10 with *N*-phenyl-2-piperidone (**5.1**) on 5.0 mmol scale at 0 °C and purified by flash column chromatography (SiO_2, 15–40% EtOAc/hexanes) to give **3.59q** as a pale-yellow oil (397 mg, 31%). $\boldsymbol{R_f}$ 0.23

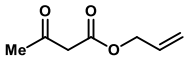
(35% EtOAc/hexanes); **^{1}H NMR** (400 MHz, $CDCl_3$) δ 7.44 – 7.34 (m, 2H), 7.31 – 7.22 (m, 3H), 6.01 – 5.87 (m, 1H), 5.41 – 5.32 (m, 1H), 5.31 – 5.20 (m, 1H), 4.81 – 4.58 (m, 2H), 3.80 – 3.57 (m, 3H), 2.38 – 2.02 (m, 3H), 2.01 – 1.83 (m, 1H) ppm; **^{13}C NMR** (101 MHz, $CDCl_3$) δ 171.8 (C, **e**), 170.7 (C, **k**), 168.6 (C, **e**), 166.0 (C, **k**), 142.9 (C, **k**), 142.3 (C, **e**), 131.9 (CH, **k**), 131.3 (CH, **e**), 129.4 (2 × CH, **e**), 129.2 (2 × CH, **k**), 127.3 (CH, **e**), 127.0 (CH, **k**), 126.1 (2 × CH, **k**), 125.7 (2 × CH, **e**), 119.2 (CH_2, **e**), 118.6 (CH_2, **k**), 75.6 (C, **e**), 66.8 (CH_2, **e**), 66.0 (CH_2, **k**), 51.5 (CH_2, **e**), 51.4 (CH_2, **k**), 49.7 (CH, **k**), 31.8 (CH_2, **e**), 25.3 (CH_2, **k**), 21.5 (CH_2, **k**), 19.7 (CH_2, **e**) ppm; **HRMS** (EI+) *m/z* calculated for $C_{15}H_{17}NO_3^{\bullet+}$ $[M]^{\bullet+}$ 259.12029, found 259.12178.

allyl 3-oxo-3-phenylpropanoate (3.59r)[§]



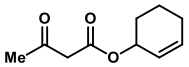
To a solution of allyl acetate (1.0 g, 1.1 mL, 10 mmol, 1.0 equiv.) in THF (50 mL, 0.2 M) was added lithium bis(trimethylsilyl)amide (LiHMDS, 22 mL, 22 mmol, 2.2 equiv., 1.0 M in THF) dropwise over 5 minutes at –78 °C in a dry ice/acetone bath. The reaction was stirred at –78 °C for 15 minutes. Benzoyl chloride (1.6 g, 1.3 mL, 11 mmol, 1.1 equiv.) was then added dropwise over 2 minutes at –78 °C and the reaction stirred overnight and allowed to reach room temperature. The mixture was cooled to 0 °C in an ice bath, quenched with NH_2Cl (50 mL, saturated aqueous), and the phases separated. The aqueous phase was extracted with EtOAc (3 × 30 mL). The combined organic phases were washed with water (50 mL) and brine (50 mL), dried over $MgSO_4$, filtered, and concentrated under reduced pressure. The crude residue was purified by flash column chromatography (SiO_2, 10% Et_2O/hexanes) to give **4r** as a pale pink oil (1.82 g, 89%). R_f 0.28 (5% Et_2O/hexanes); **^{1}H NMR** (400 MHz, $CDCl_3$) δ **k** 7.99 – 7.91 (m, 2H), 7.60 (tt, J = 6.9, 1.3 Hz, 1H), 7.53 – 7.46 (m, 2H), 5.90 (ddt, J = 17.2, 10.4, 5.8 Hz, 1H), 5.31 (dq, J = 17.2, 1.5 Hz, 1H), 5.23 (dq, J = 10.4, 1.3 Hz, 1H), 4.66 (dt, J = 5.8, 1.5 Hz, 2H), 4.04 (s, 2H) **e** 12.48 (s, 1H), 7.82 – 7.76 (m, 2H), 7.46 – 7.39 (m, 3H), 5.99 (ddt, J = 16.3, 10.8, 5.7 Hz, 1H), 5.71 (s, 1H), 5.38 (dd, J = 17.3, 1.6 Hz, 1H), 5.31 – 5.26 (m, 1H), 4.74 – 4.69 (m, 2H) ppm; **^{13}C NMR** (101 MHz, $CDCl_3$) δ **k** 192.5 (C), 167.3 (C), 136.0 (C), 133.9 (CH), 131.7 (CH), 129.0 (2 × CH), 128.7 (2 × CH), 118.9 (CH_2), 66.2 (CH_2), 46.0 (CH_2) **e** 172.9 (C), 171.9 (C), 133.5 (C), 132.2 (CH), 131.5 (CH), 128.7 (2 × CH), 126.2 (2 × CH), 118.6 (CH_2), 87.3 (CH), 65.1 (CH_2) ppm; **HRMS** (ESI+) *m/z* calculated for $C_{12}H_{12}O_3Na^+$ $[M + Na]^+$ 227.0679, found 227.0693;

allyl 3-oxobutanoate (3.59s)[§]



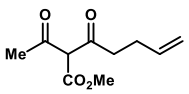
A neat mixture of methyl acetoacetate (2.3 g, 2.1 mL, 10 mmol, 1.0 equiv.) and allyl alcohol (1.7 g, 2.0 mL, 30 mmol, 3.0 equiv.) was stirred at 110 °C for 24 hours. The crude mixture was purified by flash column chromatography (SiO_2, 10% EtOAc/hexanes) to give **4s** as a clear, colourless oil (1.6 g, 50%). R_f 0.43 (20% EtOAc/hexanes); **^{1}H NMR** (400 MHz, $CDCl_3$) δ 12.00 (s, 1H, **e**), 6.00 – 5.82 (m, 1H, **k** + **e**), 5.39 – 5.19 (m, 2H, **k** + **e**), 5.02 (s, 1H, **e**), 4.64 (dt, J = 5.8, 1.3 Hz, 2H, **k** + **e**), 3.48 (s, 2H, **k**), 2.27 (s, 3H, **k**), 1.96 (s, 3H, **e**) ppm; **^{13}C NMR** (101 MHz, $CDCl_3$) δ **keto** 200.5 (C), 166.9 (C), 131.6 (CH), 119.1 (CH_2), 66.1 (CH_2), 50.1 (CH_2), 30.3 (CH_3) **enol (*E*/*Z*)** 176.0 (C), 132.3 (CH), 118.3 (CH_2), 89.7 (CH), 64.7 (CH_2), 60.5 (CH_2), 21.4 (C), 21.2 (CH), 14.3 (CH_3) ppm; **HRMS** (EI+) *m/z* calculated for $C_7H_{10}O_3^{\bullet+}$ $[M]^{\bullet+}$ 142.06245, found 142.06529

cyclohex-1-en-1-ylmethyl 3-oxobutanoate (3.59t)[§]



Prepared according to GP8 with methyl acetoacetate and cyclohex-2-enol (**5.3**) on 5.0 mmol scale and purified by flash column chromatography (SiO_2, 10% EtOAc/hexanes) to give **3.59t** as a clear, colourless oil (850 mg, 93%). R_f 0.47 (20% EtOAc/hexanes); **^{1}H NMR** (400 MHz, $CDCl_3$) δ 12.14 (s, 1H, **e**), 5.98 (dddd, J = 10.1, 4.3, 3.5, 1.2 Hz, 1H, **k** + **e**), 5.71 (ddt, J = 10.0, 4.0, 2.2 Hz, 1H, **k** + **e**), 5.32 (dtq, J = 5.3, 3.6, 1.7 Hz, 1H, **k** + **e**), 4.98 (s, 1H, **e**), 3.44 (s, 2H, **k**), 2.26 (s, 3H, **k**), 2.15 – 1.96 (m, 2H, **k** + **e**), 1.94 (d, J = 0.7 Hz, 3H, **e**), 1.93 – 1.82 (m, 1H, **k** + **e**), 1.82 – 1.56 (m, 3H, **k** + **e**) ppm; **^{13}C NMR** (101 MHz, $CDCl_3$) δ **k** 200.8 (C), 166.9 (C), 133.5 (CH), 125.1 (CH), 69.4 (CH), 50.6 (CH_2), 30.3 (CH_3), 28.2 (CH_2), 24.9 (CH_2), 18.8 (CH_2) **e** 175.5 (C), 133.0 (CH), 125.7 (CH), 90.2 (C), 67.8 (CH), 28.5 (CH_2), 25.0 (CH_2), 21.3 (CH_3), 18.9 (CH_2) ppm; **HRMS** (EI+) *m/z* calculated for $C_{10}H_{14}O_3^{\bullet+}$ $[M]^{\bullet+}$ 182.09375, found 182.09256

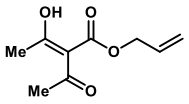
methyl 2-acetyl-3-oxohept-6-enoate (3.59u)[§]



Adapted from a procedure by Rathke.[347] To a solution of pent-4-enoic acid in DCM (1.0 M) was added oxalyl chloride (0.55 g, 0.56 mL, 5.5 mmol, 1.1 equiv.) and DMF (2 drops) dropwise at 0 °C in an ice bath. The reaction was stirred until gas evolution was complete (~1 hour) and then concentrated under reduced pressure to give pent-4-enoyl chloride. To a suspension of magnesium chloride (0.48 g, 5.0 mmol, 1.0 equiv., anhydrous) in DCM (5 mL, 1.0 M)

was added methyl acetoacetate (0.58 g, 0.54 mL, 5.0 mmol, 1.0 equiv.) in one portion at room temperature. The mixture was cooled to 0 °C in an ice bath and pyridine (0.79 g, 0.81 mL, 10 mmol, 2.0 equiv.) added dropwise over 1 minute at 0 °C. The mixture was stirred at 0 °C for 15 minutes. Pent-4-enoyl chloride was added dropwise at 0 °C over 1 minute at 0 °C and the reaction stirred at 0 °C for 15 minutes, then removed from the ice bath and stirred at room temperature for 1 hour. The reaction was quenched at 0 °C by dropwise addition of HCl (2 mL, 6 M aqueous). The mixture was extracted with Et_2O (3 × 10 mL) and the combined organic layers dried over $MgSO_4$, filtered, and concentrated under reduced pressure. The crude residue was purified by flash column chromatography (SiO_2, 10% Et_2O/hexanes) to give methyl 2-acetyl-3-oxohept-6-enoate as a clear, colourless oil (**4u**, 280 mg, 28%). $\mathbf{R_f}$ 0.69 (50% Et_2O/hexanes); **^{1}H NMR** (400 MHz, $CDCl_3$) δ 5.83 (ddt, J = 16.8, 10.2, 6.5 Hz, 1H), 5.05 (dq, J = 17.1, 1.6 Hz, 1H), 5.00 (ddt, J = 10.2, 1.8, 1.3 Hz, 1H), 3.80 (s, 3H), 2.82 – 2.73 (m, 2H), 2.45 – 2.35 (m, 2H), 2.34 (s, 3H) ppm; **^{13}C NMR** (101 MHz, $CDCl_3$) δ 198.8 (C), 195.7 (C), 167.8 (C), 137.0 (CH), 115.6 (CH_2), 108.5 (enol, C), 51.8 (CH_3), 37.5 (CH_2), 29.5 (CH_2), 25.7 (CH_3) ppm; **HRMS** (EI+) *m/z* calculated for $C_{10}H_{14}O_4^{\bullet+}$ $[M]^{\bullet+}$ 198.08866, found 198.08907

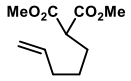
allyl 2-acetyl-3-oxobutanoate (3.59v)[§]



Adapted from a procedure by Rathke.[347] To a suspension of magnesium chloride (0.48 g, 5.0 mmol, 1.0 equiv., anhydrous) in DCM (5 mL, 1.0 M) was added methyl acetoacetate (0.58 g, 0.54 mL, 5.0 mmol, 1.0 equiv.) in one portion at room temperature. The mixture was cooled to 0 °C in an ice bath and pyridine (0.79 g, 0.81 mL, 10 mmol, 2.0 equiv.) added dropwise over 1 minute at 0 °C. The mixture was stirred at 0 °C for 15 minutes. Acetyl chloride (0.39 g, 0.36 mL, 5.0 mmol, 1.0 equiv., freshly distilled from quinoline) was added dropwise over 1 minute at 0 °C and the reaction stirred at 0 °C for 15 minutes, then removed from the ice bath and stirred at room temperature for 1 hour. The reaction was quenched at 0 °C by dropwise addition of NH_4Cl (2 mL, saturated aqueous). The mixture was extracted with Et_2O (3 × 10 mL) and the combined organic layers dried over $MgSO_4$, filtered, and concentrated under reduced pressure. The crude residue was purified by flash column chromatography (SiO_2, 10% Et_2O/hexanes) to give allyl 2-acetyl-3-oxobutanoate as a clear, colourless oil (**4v**, 680 mg, 74%). $\mathbf{R_f}$ 0.69 (20% EtOAc/hexanes); **^{1}H NMR** (400 MHz, $CDCl_3$) δ 5.96 (ddt, J = 17.3, 10.4, 6.0 Hz, 1H), 5.35 (dq, J = 17.2, 1.5 Hz, 1H), 5.27 (dq, J = 10.4, 1.2 Hz, 1H), 4.69 (dt, J = 6.0, 1.4 Hz, 2H), 2.36 (s, 6H) ppm; **^{13}C NMR** (101 MHz, $CDCl_3$) δ 196.9 (C), 166.9 (C),

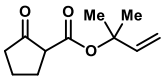
132.0 (CH), 119.2 (CH_2), 108.5 (C), 65.7 (CH_2), 26.2 (2 × CH_3) ppm; **HRMS** (EI+) *m/z* calculated for $C_9H_{12}O_4^{\bullet+}$ $[M]^{\bullet+}$ 184.07301, found 184.07240

dimethyl 2-(pent-4-en-1-yl)malonate (3.59w)[§]



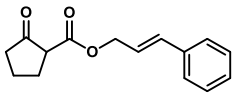
Adapted from a procedure by Deslongchamps.[348] To a solution of 5-bromopentene (0.75 g, 0.60 mL, 5.0 mmol, 1.0 equiv.) and dimethyl malonate (3.3 g, 2.9 mL, 25 mmol, 5.0 equiv.) in THF/DMF (20 mL, 0.25 M, 1:1) was added K_2CO_3 (3.5 g, 25 mmol, 5.0 equiv.) in one portion at room temperature. The reaction was stirred for 15 hours at room temperature. The mixture was diluted with hexanes (10 mL), filtered over a pad of Celite eluting with hexanes, and the filtrate concentrated under reduced pressure. The crude residue was purified by flash column chromatography (SiO_2, 10% EtOAc/hexanes) to give **3.59w** as a clear, colourless oil (570 mg, 57%). $\mathbf{R_f}$ 0.60 (20% EtOAc/hexanes); **^{1}H NMR** (400 MHz, $CDCl_3$) δ 5.77 (ddt, J = 16.9, 10.2, 6.7 Hz, 1H), 5.01 (dq, J = 17.2, 1.6 Hz, 1H), 4.96 (ddt, J = 10.2, 2.0, 1.2 Hz, 1H), 3.74 (s, 6H), 3.37 (t, J = 7.5 Hz, 1H), 2.12 – 2.04 (m, 2H), 1.95 – 1.88 (m, 2H), 1.46 – 1.36 (m, 2H) ppm; **^{13}C NMR** (101 MHz, $CDCl_3$) δ 170.0 (C), 138.0 (CH), 115.2 (CH_2), 52.6 (CH_3), 51.7 (CH), 33.4 (CH_2), 28.4 (CH_2), 26.7 (CH_2) ppm; **HRMS** (EI+) *m/z* calculated for $C_9H_{13}O_3^+$ $[M - OCH_3]^+$ 169.08592, found 169.08468

2-methylbut-3-en-2-yl 2-oxocyclopentane-1-carboxylate (3.59x)



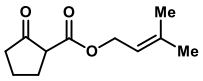
Prepared according to GP8 with ketoester **3.86** and 2-methyl-3-buten-2-ol on 5.0 mmol scale at 100 °C and to incomplete conversion to avoid a competing Ireland–Claisen reaction that gave inseparable prenyl ester product **4z**. The crude residue was purified by flash column chromatography (SiO_2, 6–12% EtOAc/hexanes) to give **3.59x** as a pale pink oil (196 mg, 20%). $\mathbf{R_f}$ 0.34 (15% EtOAc/hexanes); **^{1}H NMR** (400 MHz, $CDCl_3$) δ 6.10 – 6.00 (m, 1H), 5.22 – 5.13 (m, 1H), 5.10 – 5.03 (m, 1H), 3.07 (t, J = 9.0 Hz, 1H), 2.32 – 2.20 (m, 4H), 2.16 – 2.04 (m, 1H), 1.90 – 1.76 (m, 1H), 1.52 (s, 6H) ppm; **^{13}C NMR** (101 MHz, $CDCl_3$) δ 212.8 (C), 168.4 (C), 142.2 (CH), 113.1 (CH_2), 82.1 (C), 55.6 (CH), 38.2 (CH_2), 27.4 (CH_2), 26.6 (CH_3), 26.5 (CH_3), 21.0 (CH_2) ppm; **HRMS** (EI+) *m/z* calculated for $C_{10}H_{16}O_2^{\bullet+}$ $[M - CO]^{+\bullet}$ 168.11448, found 168.11386.

cinnamyl 2-oxocyclopentane-1-carboxylate (3.59y)



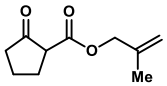
Prepared according to GP8 with ketoester **3.86** and cinnamyl alcohol on 5.0 mmol scale and purified by flash column chromatography (SiO_2, 5–20% EtOAc/hexanes) to give **3.59y** as an amorphous pink solid (994.0 mg, 81%). $\mathbf{R_f}$ 0.37 (20% EtOAc/hexanes); **^{1}H NMR** (400 MHz, $CDCl_3$) δ 7.42 – 7.37 (m, 2H), 7.36 – 7.30 (m, 2H), 7.29 – 7.23 (m, 1H), 6.68 (ddd, J = 15.8, 1.4, 1.4 Hz, 1H), 6.28 (ddd, J = 15.9, 6.4, 6.4 Hz, 1H), 4.81 (dd, J = 6.4, 1.4 Hz, 2H), 3.21 (dd, J = 9.1, 9.1 Hz, 1H), 2.42 – 2.25 (m, 4H), 2.20 – 2.10 (m, 1H), 1.95 – 1.80 (m, 1H) ppm; **^{13}C NMR** (101 MHz, $CDCl_3$) δ 212.4 (C), 169.3 (C), 136.3 (C), 134.6 (CH), 128.7 (2 × CH), 128.2 (CH), 126.8 (2 × CH), 122.8 (CH), 66.1 (CH_2), 54.9 (CH), 38.2 (CH_2), 27.6 (CH_2), 21.1 (CH_2) ppm; **HRMS** (ESI+) *m/z* calculated for $C_{15}H_{16}O_3Na^+$ [M + Na]$^+$ 267.0997, found 267.0977.

3-methylbut-2-en-1-yl 2-oxocyclopentane-1-carboxylate (3.59z)[§]



Prepared according to GP8 with ketoester **3.86** and prenol on 10 mmol scale and purified by flash column chromatography (SiO_2, 5–25% EtOAc/hexanes) to give **3.59z** as a clear, colourless oil (1.3 g, 68%). $\mathbf{R_f}$ 0.44 (20% EtOAc/hexanes); **^{1}H NMR** (500 MHz, $CDCl_3$) δ 5.34 (ddq, J = 8.6, 5.7, 1.4 Hz, 1H), 4.68 – 4.59 (m, 2H), 3.15 (t, J = 8.9 Hz, 1H), 2.36 – 2.23 (m, 4H), 2.19 – 2.06 (m, 1H), 1.93 – 1.79 (m, 1H), 1.76 (d, J = 1.3 Hz, 3H), 1.71 (d, J = 1.3 Hz, 3H) ppm; **^{13}C NMR** (126 MHz, $CDCl_3$) δ 212.5 (C), 169.6 (C), 139.6 (C), 118.4 (CH), 62.5 (CH_2), 54.9 (CH), 38.2 (CH_2), 27.6 (CH_2), 25.9 (CH_3), 21.1 (CH_2), 18.2 (CH_3) ppm; **HRMS** (ESI+) *m/z* calculated for $C_{11}H_{16}O_3Na^+$ [M + Na]$^+$ 219.0992, found 219.0991.

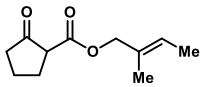
2-methylallyl 2-oxocyclopentane-1-carboxylate (4aa)[§]



Prepared according to GP8 with ketoester **3.86** and methallyl alcohol on 5.0 mmol scale and purified by flash column chromatography (SiO_2, 5–25% EtOAc/hexanes) to give **3.59aa** as a clear, colourless oil (1.1 g, 62%). $\mathbf{R_f}$ 0.44 (20% EtOAc/hexanes); **^{1}H NMR** (300 MHz, $CDCl_3$) δ 5.04 – 4.98 (m, 1H), 4.98 – 4.90 (m, 1H), 4.66 – 4.57 (m, 1H), 4.57 – 4.48 (m, 1H), 3.27 – 3.13 (m, 1H), 2.39 – 2.25 (m, 4H), 2.25 – 2.07 (m, 1H), 1.97 – 1.80 (m, 1H), 1.80 – 1.73 (m, 3H) ppm; **^{13}C NMR** (101 MHz, $CDCl_3$) δ 212.3 (C), 169.2 (C), 139.7 (C), 113.4 (CH_2), 68.6 (CH_2), 54.9 (CH),

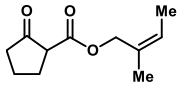
38.2 (CH_2), 27.6 (CH_2), 21.1 (CH_2), 19.5 (CH_3) ppm; **HRMS** (EI+) *m/z* calculated for $C_{10}H_{14}O_3^{\bullet+}$ $[M]^{\bullet+}$ 182.09375, found 182.09279

(E)-2-methylbut-2-en-1-yl 2-oxocyclopentane-1-carboxylate (3.59ab)[§]



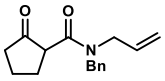
Prepared according to GP8 with ketoester **3.86** and tiglyl alcohol (**4.112**) on 5.0 mmol scale and purified by flash column chromatography (SiO_2, 15% Et_2O/hexanes) to give **3.59ab** as a clear, colourless oil (616 mg, 63%). $\mathbf{R_f}$ 0.25 (10% Et_2O/hexanes); **^{1}H NMR** (500 MHz, $CDCl_3$) δ 5.56 (qq, J = 6.6, 1.3 Hz, 1H), 4.58 – 4.46 (m, 2H), 3.17 (t, J = 8.9 Hz, 1H), 2.37 – 2.24 (m, 4H), 2.19 – 2.09 (m, 1H), 1.92 – 1.81 (m, 1H), 1.65 (s, 3H), 1.63 (dq, J = 6.8, 1.1 Hz, 3H) ppm; **^{13}C NMR** (126 MHz, $CDCl_3$) δ 212.4 (C), 169.5 (C), 130.6 (C), 124.6 (CH), 71.3 (CH_2), 55.0 (CH), 38.2 (CH_2), 27.6 (CH_2), 21.1 (CH_2), 13.7 (CH_3), 13.4 (CH_3) ppm; **HRMS** (EI+) calculated for $C_{11}H_{16}O_3$ $[M]^{\bullet+}$ 196.10940, found 196.10993.

(Z)-2-methylbut-2-en-1-yl 2-oxocyclopentane-1-carboxylate (3.59ab')[§]



Prepared according to GP8 with ketoester **3.86** and angelyl alcohol on 5.0 mmol scale and purified by flash column chromatography (SiO_2, 15% Et_2O/hexanes) to give **3.59ab'** as a clear, colourless oil (640 mg, 65%). $\mathbf{R_f}$ 0.25 (10% Et_2O/hexanes); **^{1}H NMR** (500 MHz, $CDCl_3$) δ 5.52 – 5.42 (m, 1H), 4.67 (s, 2H), 3.17 (t, J = 9.1 Hz, 1H), 2.38 – 2.23 (m, 4H), 2.18 – 2.09 (m, 1H), 1.92 – 1.81 (m, 1H), 1.74 (p, J = 1.5 Hz, 3H), 1.66 (dq, J = 6.9, 1.6 Hz, 3H) ppm; **^{13}C NMR** (126 MHz, $CDCl_3$) δ 212.3 (C), 169.6 (C), 130.3 (C), 125.4 (CH), 63.9 (CH_2), 54.9 (CH), 38.2 (CH_2), 27.6 (CH_2), 21.4 (CH_3), 21.1 (CH_2), 13.4 (CH_3) ppm;

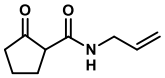
N-allyl-N-benzyl-2-oxocyclopentane-1-carboxamide (3.59ac)[§]



Prepared according to a procedure by Bezzenine-Lafollée and Gandon[349] on 5.0 mmol scale with ketoester **3.86** and *N*-allylbenzylamine **5.2** and purified by flash column chromatography (SiO_2, 15–25% EtOAc/hexanes) to give ketoamide **3.59ac** as an amber oil (1.03 g, 80%). $\mathbf{R_f}$ 0.30 (30% EtOAc/hexanes); **^{1}H NMR** (400 MHz, $CDCl_3$) mixture of rotamers (58:42) δ 7.40 – 7.15 (m, 5H, **M** + **m**), 5.85 – 5.69 (m, 1H, **M** + **m**), 5.27 – 5.11 (m, 2H, **M** + **m**), 5.04 (d, J = 15.1 Hz, 1H, **M**), 4.99 (d, J = 17.6 Hz, 1H, **m**), 4.50 – 4.40 (m, 2H, **m**), 4.29 (dddt, J = 18.2, 4.6, 3.1, 1.5

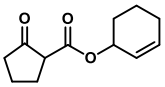
Hz, 1H, **M**), 4.22 (d, *J* = 15.1 Hz, 1H, **M**), 3.77 (ddt, *J* = 18.1, 4.7, 1.9 Hz, 1H, **M**), 3.60 (ddt, *J* = 15.6, 6.1, 1.4 Hz, 1H, **m**), 3.48 – 3.36 (m, 1H, **M** + **m**), 2.62 – 2.48 (m, 1H, **M** + **m**), 2.38 – 2.27 (m, 2H, **M** + **m**), 2.26 – 2.07 (m, 2H, **M** + **m**), 1.93 – 1.72 (m, 1H, **M** + **m**) ppm; **^{13}C NMR** (101 MHz, $CDCl_3$) δ **M** 214.9 (C), 169.6 (C), 137.2 (C), 133.1 (CH), 128.7 (2 × CH), 127.8 (2 × CH), 127.4 (CH), 116.7 (CH_2), 52.2 (CH), 49.3 (CH_2), 48.8 (CH_2), 38.8 (CH_2), 27.7 (CH_2), 21.2 (CH_2) **m** 214.8 (C), 169.4 (C), 136.9 (C), 132.5 (CH), 129.1 (2 × CH), 127.7 (CH), 126.3 (2 × CH), 117.3 (CH_2), 52.3 (CH), 50.3 (CH_2), 48.5 (CH_2), 38.8 (CH_2), 27.7 (CH_2), 21.1 (CH_2) ppm; **HRMS** (ESI+) *m/z* calculated for $C_{16}H_{19}NO_2Na^+$ $[M + Na]^+$ 280.1308, found 280.1313

N-allyl-2-oxocyclopentane-1-carboxamide (3.59ad)[§]



A mixture of ketoester **3.86** (1.4 g, 10 mmol, 1.0 equiv.) and allyl amine (2.3 g, 40 mmol, 4.0 equiv.) was heated to 180 °C in a microwave reactor for 3 hours with stirring. The mixture was diluted with THF (10 mL) and HCl (6 mL, 6 M aqueous) and stirred for 1 hour. The mixture was then diluted with EtOAc (20 mL), the phases separated, and the aqueous phase extracted with EtOAc (3 × 20 mL). The combined organic phases were washed with water (20 mL) and brine (20 mL), dried over $MgSO_4$, filtered, and concentrated under reduced pressure. The crude residue was purified by flash column chromatography (SiO_2, 10-50% EtOAc/hexanes) to give ketoamide **3.59ad** as a clear, colourless oil (760 mg, 45%). **^{1}H NMR** (400 MHz, $CDCl_3$) δ 6.83 (s, 1H), 5.84 (ddt, *J* = 17.2, 10.2, 5.5 Hz, 1H), 5.19 (dq, *J* = 17.1, 1.6 Hz, 1H), 5.13 (dq, *J* = 10.2, 1.4 Hz, 1H), 3.90 (tq, *J* = 5.7, 1.8 Hz, 2H), 2.99 (t, *J* = 9.2 Hz, 1H), 2.46 – 2.20 (m, 5H), 2.07 (dddt, *J* = 12.7, 8.5, 6.7, 4.2 Hz, 1H), 1.92 – 1.76 (m, 1H) ppm; **^{13}C NMR** (101 MHz, $CDCl_3$) δ 216.9 (C), 166.6 (C), 134.1 (CH), 116.5 (CH_2), 54.3 (CH), 42.1 (CH_2), 39.1 (CH_2), 26.0 (CH_2), 20.6 (CH_2) ppm; **HRMS** (EI+) *m/z* calculated for $C_9H_{13}NO_2^{\bullet+}$ $[M]^{\bullet+}$ 167.09408, found 167.09557.

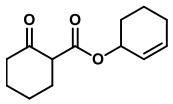
cyclohex-2-en-1-yl 2-oxocyclopentane-1-carboxylate (3.59ae)



Prepared according to GP8 with ketoester **3.86** and cyclohex-2-enyl alcohol (**5.3**) on 5.0 mmol scale and purified by flash column chromatography (SiO_2, 8–15% EtOAc/hexanes) to give **3.59ae** as a clear colourless oil (604 mg, 58%, 1:1 dr). **R_f** 0.50 (20% EtOAc/hexanes); **^{1}H NMR** (400 MHz, $CDCl_3$) δ 6.01 – 5.91 (m, 1H), 5.77 – 5.64 (m, 1H), 5.33 – 5.24 (m, 1H), 3.18 – 3.08 (m, 1H), 2.39 – 2.20 (m, 4H), 2.19 – 1.54 (m, 8H) ppm; **^{13}C NMR** (101 MHz, $CDCl_3$) δ 212.5 (C), 212.5 (C) 169.3 (C), 169.3 (C), 133.3 (CH), 133.1 (CH), 125.5 (CH), 125.3 (CH), 69.3 (CH),

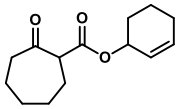
69.2 (CH), 55.1 (CH), 55.1 (CH), 38.2 (CH_2), 38.2 (CH_2), 28.3 (CH_2), 28.3 (CH_2), 27.7 (CH_2), 27.5 (CH_2), 25.0 (CH_2), 24.9 (CH_2), 21.1 (CH_2), 21.1 (CH_2), 19.0 (CH_2), 18.8 (CH_2) ppm; **HRMS** (EI+) *m/z* calculated for $C_{11}H_{16}O_2^{\bullet+}$ [*M* – CO]$^{\bullet+}$ 180.11448, found 180.11652.

cyclohex-2-en-1-yl 2-oxocyclohexane-1-carboxylate (3.59af)



Prepared according to GP8 with ketoester **3.86** and cyclohex-2-enyl alcohol (**5.3**) on 5.0 mmol scale and purified by flash column chromatography (SiO_2, 0–8% EtOAc/hexanes) to give **3.59af** as a clear colourless oil (732 mg, 66%, 2:1:1 enol/dr). $\mathbf{R_f}$ 0.76 (25% EtOAc/hexanes); **^{1}H NMR** (500 MHz, $CDCl_3$) δ 12.26 (s, 0.5H, **e**), 6.04 – 5.91 (m, 1H, **k** + **e**), 5.78 – 5.68 (m, 1H, **k** + **e**), 5.42 – 5.27 (m, 1H, **k** + **e**), 3.41 – 3.29 (m, 0.5H, **k**), 2.55 – 2.45 (m, 0.5H, **k** + **e**), 2.42 – 2.30 (m, 0.5H, **k** + **e**), 2.29 – 1.54 (m, 13H, **k** + **e**) ppm; **^{13}C NMR** (126 MHz, $CDCl_3$) δ 206.4 (C, **k**), 206.4 (C, **k**), 172.5 (C, **e**), 172.0 (C, **e**), 169.8 (C, **k**), 169.8 (C, **k**), 133.3 (CH, **k**), 133.0 (CH, **k**), 132.9 (CH, **e**), 125.9 (CH, **e**), 125.5 (CH, **k**), 125.4 (CH, **k**), 98.1 (C, **e**), 69.0 (CH, **k**), 68.9 (CH, **k**), 67.9 (CH, **e**), 57.5 (CH, **k**), 57.4 (CH, **k**), 41.7 (CH_2, **k**), 41.6 (CH_2, **k**), 30.2 (CH_2, **k**), 30.1 (CH_2, **k**), 29.2 (CH_2, **e**), 28.5 (CH_2, **e**), 28.3 (CH_2, **k**), 28.3 (CH_2, **k**), 27.3 (CH_2, **k**), 27.2 (CH_2, **k**), 25.0 (CH_2, **e**), 25.0 (CH_2, **k**), 24.9 (CH_2, **k**), 23.4 (CH_2, **k**), 23.3 (CH_2, **k**), 22.6 (CH_2, **e**), 22.5 (CH_2, **e**), 22.1 (CH_2, **e**), 19.0 (CH_2, **e**), 18.9 (CH_2, **k**), 18.8 (CH_2, **k**) ppm; **HRMS** (EI+) *m/z* calculated for $C_{13}H_{18}O_3^{\bullet+}$ [*M*]$^{\bullet+}$ 222.12505, found 222.12599.

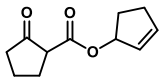
cyclohex-2-en-1-yl 2-oxocycloheptane-1-carboxylate (3.59ag)



Prepared according to GP8 with ketoester × and cyclohex-2-enyl alcohol (**5.3**) on 5.0 mmol scale and purified by flash column chromatography (SiO_2, 0–10% EtOAc/hexanes) to give **3.59ag** as a pale-yellow oil (791 mg, 67%, 2:2:1 dr/enol mixture). $\mathbf{R_f}$ 0.42 (10% EtOAc/hexanes); **^{1}H NMR** (500 MHz, $CDCl_3$) δ 12.78 (s, 0.2H, **e**), 6.00 – 5.91 (m, 1H, **all**), 5.77 – 5.64 (m, 1H, **all**), 5.36 – 5.26 (m, 1H, **all**), 3.52 (t, J = 10.2 Hz, 0.4H, $\mathbf{k_a}$), 3.51 (t, J = 10.2 Hz, 0.4H, $\mathbf{k_b}$), 2.73 – 2.52 (m, 1.6H), 2.45 – 2.41 (m, 0.4H), 2.41 – 2.36 (m, 0.4H), 2.17 – 1.52 (m, 11.6H), 1.52 – 1.35 (m, 2H) ppm; **^{13}C NMR** (126 MHz, $CDCl_3$) δ 209.2 (2 × C, **k**), 179.6 (C, **e**), 172.9 (C, **e**), 170.4 (C, **k**), 170.4 (C, **k**), 133.3 (CH, **k**), 133.0 (CH, **k**), 132.8 (CH, **e**), 126.1 (CH, **e**), 125.4 (CH, **k**), 125.4 (CH, **k**), 102.0 (C, **e**), 69.0 (CH, **k**), 68.9 (CH, **k**), 68.2 (CH, **e**), 59.3 (CH, **k**), 59.1 (CH, **k**), 43.3 (2 × CH_2, **k**), 35.6 (CH_2, **e**), 32.1 (CH_2, **e**), 29.8 (CH_2, **k**),

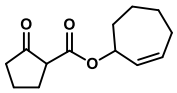
29.8 (CH_2, **k**), 28.6 (CH_2, **e**), 28.3 (CH_2, **k**), 28.2 (CH_2, **k**), 28.2 (CH_2, **k**), 28.1 (CH_2, **k**), 27.8 (CH_2, **k**), 27.7 (CH_2, **k**), 27.5 (CH_2, **e**), 25.1 (CH_2, **e**), 25.0 (CH_2, **k**), 25.0 (CH_2, **k**), 24.8 (CH_2, **e**), 24.6 (CH_2, **e**), 24.5 (CH_2, **k**), 24.5 (CH_2, **k**), 19.1 (CH_2, **e**), 19.0 (CH_2, **k**), 18.8 (CH_2, **k**) ppm; **HRMS** (EI+) *m/z* calculated for $C_{13}H_{20}O_2^{\bullet+}$ $[M - CO]^{+\bullet}$ 208.14578, found 208.14689.

cyclopent-2-en-1-yl 2-oxocyclopentane-1-carboxylate (3.59ah)



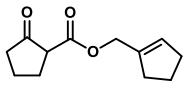
Prepared according to GP8 with ketoester **3.86** and cyclopent-2-enyl alcohol (**5.4**) on 4.0 mmol scale and purified by flash column chromatography (SiO_2, 0–15% EtOAc/hexanes) to give **3.59ah** as clear colourless oil (442 mg, 57%, 1:1 dr). $\mathbf{R_f}$ 0.45 (15% EtOAc/hexanes); **^{1}H NMR** (500 MHz, $CDCl_3$) δ 6.14 – 6.08 (m, 1H), 5.86 – 5.77 (m, 1H), 5.77 – 5.70 (m, 1H), 3.15 – 3.05 (m, 1H), 2.59 – 2.44 (m, 1H), 2.36 – 2.21 (m, 6H), 2.17 – 2.06 (m, 1H), 1.91 – 1.77 (m, 2H) ppm; **^{13}C NMR** (126 MHz, $CDCl_3$) δ 212.6 (C), 212.6 (C), 169.6 (C), 169.6 (C), 138.2 (CH), 138.0 (CH), 129.1 (CH), 129.0 (CH), 81.7 (2 × CH), 55.1 (CH), 55.0 (CH), 38.2 (CH_2), 38.2 (CH_2), 31.2 (CH_2), 31.2 (CH_2), 30.0 (CH_2), 29.9 (CH_2), 27.6 (CH_2), 27.5 (CH_2), 21.1 (CH_2), 21.1 (CH_2) ppm; **HRMS** (EI+) *m/z* calculated for $C_{10}H_{14}O_2^{\bullet+}$ $[M - CO]^{+\bullet}$ 166.09883, found 166.09883.

cyclohept-2-en-1-yl 2-oxocyclopentane-1-carboxylate (3.59ai)



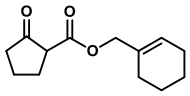
Prepared according to GP8 with ketoester **3.86** and cyclohept-2-enyl alcohol (**5.5**) on 5.0 mmol scale and purified by flash column chromatography (SiO_2, 0–20% EtOAc/hexanes) to give **3.59ai** as a clear colourless oil (892 mg, 80%). $\mathbf{R_f}$ 0.43 (16% EtOAc/hexanes); **^{1}H NMR** (400 MHz, $CDCl_3$) δ 5.87 – 5.77 (m, 1H), 5.70 – 5.58 (m, 1H), 5.49 – 5.37 (m, 1H), 3.18 – 3.10 (m, 1H), 2.35 – 2.25 (m, 4H), 2.25 – 2.01 (m, 3H), 1.98 – 1.79 (m, 3H), 1.78 – 1.58 (m, 3H), 1.47 – 1.33 (m, 1H) ppm; **^{13}C NMR** (101 MHz, $CDCl_3$) δ 212.5 (C), 212.5 (C), 169.0 (C), 168.9 (C), 133.4 (CH), 133.2 (CH), 132.1 (CH), 131.9 (CH), 75.3 (CH), 75.3 (CH), 55.0 (2 × CH), 38.2 (2 × CH_2), 32.8 (CH_2), 32.8 (CH_2), 28.5 (2 × CH_2), 27.5 (2 × CH_2), 26.7 (2 × CH_2), 26.6 (CH_2), 26.5 (CH_2), 21.1 (2 × CH_2) ppm; **HRMS** (EI+) *m/z* calculated for $C_{13}H_{18}O_3^{\bullet+}$ $[M]^{+\bullet}$ 222.12505, found 222.12452.

cyclopent-1-en-1-ylmethyl 2-oxocyclopentane-1-carboxylate (3.59aj)



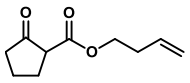
Prepared according to GP8 with ketoester **6a** and cyclopent-1-en-1-ylmethanol (**5.6**) alcohol on 5.0 mmol scale and purified by flash column chromatography (SiO_2, 0–20% EtOAc/hexanes) to give **3.59aj** as a clear colourless oil (699 mg, 67%). **R**$_f$ 0.43 (15% EtOAc/hexanes); **^{1}H NMR** (400 MHz, $CDCl_3$) δ 5.73 – 5.63 (m, 1H), 4.77 – 4.63 (m, 2H), 3.18 (t, J = 9.0 Hz, 1H), 2.41 – 2.29 (m, 8H), 2.22 – 2.07 (m, 1H), 1.97 – 1.79 (m, 3H) ppm; ^{13}C NMR (101 MHz, $CDCl_3$) δ 212.4 (C), 169.3 (C), 138.8 (C), 128.9 (CH), 64.2 (CH_2), 54.9 (CH), 38.2 (CH_2), 32.9 (CH_2), 32.5 (CH_2), 27.6 (CH_2), 23.4 (CH_2), 21.1 (CH_2) ppm; **HRMS** (EI+) *m/z* calculated for $C_{12}H_{16}O_3^{\bullet+}$ $[M]^{\bullet+}$ 208.10940, found 208.11157.

cyclohex-1-en-1-ylmethyl 2-oxocyclopentane-1-carboxylate (3.59ak)



Prepared according to GP8 with ketoester **3.86** and alcohol **5.7** on 5.0 mmol scale and purified by flash column chromatography (SiO_2, 3–8% EtOAc/hexanes) to give **3.59ak** as a clear, colourless oil (1.05 g, 95%). ***R$_f$*** 0.55 (20% EtOAc/hexanes); **^{1}H NMR** (400 MHz, $CDCl_3$) δ 5.78 – 5.70 (m, 1H), 4.57 – 4.43 (m, 2H), 3.17 (dd, J = 9.1, 9.1 Hz, 1H), 2.39 – 2.22 (m, 4H), 2.19 – 2.08 (m, 1H), 2.06 – 1.94 (m, 4H), 1.93 – 1.79 (m, 1H), 1.69 – 1.51 (m, 4H) ppm; **^{13}C NMR** (101 MHz, $CDCl_3$) δ 212.5 (C), 169.5 (C), 132.7 (C), 126.7 (CH), 69.9 (CH_2), 55.0 (CH), 38.2 (CH_2), 27.6 (CH_2), 25.8 (CH_2), 25.1 (CH_2), 22.4 (CH_2), 22.2 (CH_2), 21.1 (CH_2) ppm; **HRMS** (EI+) *m/z* calculated for $C_{13}H_{18}O_3^{\bullet+}$ $[M]^{+\bullet}$ 222.12505, found 222.12318.

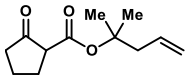
but-3-en-1-yl 2-oxocyclopentane-1-carboxylate (3.59al)



Prepared according to GP8 with ketoester **3.86** and but-3-en-1-ol on 5.0 mmol scale and purified by flash column chromatography (SiO_2, 7–15% EtOAc/hexanes) to give **3.59al** as a pale pink oil (607.4 mg, 67%). ***R$_f$*** 0.37 (15% EtOAc/hexanes); **^{1}H NMR** (400 MHz, $CDCl_3$) δ 5.78 (dddd, J = 17.1, 10.2, 6.8, 6.8 Hz, 1H), 5.16 – 5.02 (m, 2H), 4.24 – 4.14 (m, 2H), 3.15 (dd, J = 9.0, 9.0 Hz, 1H), 2.46 – 2.36 (m, 2H), 2.34 – 2.25 (m, 4H), 2.19 – 2.06 (m, 1H), 1.93 – 1.79 (m, 1H) ppm; **^{13}C NMR** (101 MHz, $CDCl_3$) δ 212.4 (C), 169.5 (C), 133.9 (CH), 117.5 (CH_2), 64.5

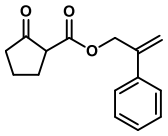
(CH_2), 54.9 (CH), 38.2 (CH_2), 33.1 (CH_2), 27.6 (CH_2), 21.1 (CH_2) ppm; **HRMS** (EI+) *m/z* calculated for $C_{10}H_{14}O_3^{\bullet+}$ $[M]^{\bullet+}$ 182.09375, found 182,09303.

2-methylpent-4-en-2-yl 2-oxocyclopentane-1-carboxylate (3.59am)



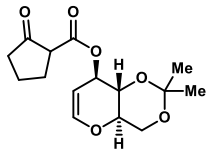
Prepared according to GP8 with ketoester **3.86** and 2-methylpent-4-en-2-ol (**5.8**) on 5.0 mmol scale and purified by flash column chromatography (SiO_2, 0–15% EtOAc/hexanes) to give **3.59am** as a clear colourless oil (228 mg, 22%). R_f 0.30 (10% EtOAc/hexanes); **^{1}H NMR** (400 MHz, $CDCl_3$) δ 5.80 (ddt, J = 16.6, 10.4, 7.3 Hz, 1H), 5.12 – 5.03 (m, 2H), 3.04 (t, J = 8.8 Hz, 1H), 2.53 (d, J = 7.3 Hz, 2H), 2.33 – 2.19 (m, 4H), 2.19 – 2.02 (m, 1H), 1.84 (ddddd, J = 12.7, 8.5, 8.4, 8.4 Hz, 1H), 1.44 (s, 6H) ppm; **^{13}C NMR** (101 MHz, $CDCl_3$) δ 212.9,(C) 168.7 (C), 133.4 (CH), 118.5 (CH_2), 83.2 (C), 55.8 (CH), 45.1 (CH_2), 38.2 (CH_2), 27.6 (CH_2), 26.0 (CH_3), 26.0 (CH_3), 21.1 (CH_2) ppm; **HRMS** (EI+) *m/z* calculated for $C_9H_{13}O_3^{\bullet+}$ $[M - C_3H_5]^{\bullet+}$ 169.08592, found 169.08504.

2-phenylallyl 2-oxocyclopentane-1-carboxylate (3.59an)



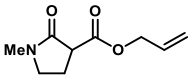
Prepared according to GP8 with ketoester **3.86** and 3-hydroxy-2-phenylpropene on 5.0 mmol scale and purified by flash column chromatography (SiO_2, 7–15% EtOAc/hexanes) to give a clear, colourless oil (1.0 g, 82%). Characterized according to NMR spectra comparison.[350] R_f 0.49 (20% EtOAc/hexanes); **^{1}H NMR** (400 MHz, $CDCl_3$) δ 7.48 – 7.39 (m, 2H), 7.37 – 7.27 (m, 3H), 5.56 (d, J = 0.9 Hz, 1H), 5.40 (d, J = 1.1 Hz, 1H), 5.09 – 4.99 (m, 2H), 3.18 (t, J = 9.0 Hz, 1H), 2.38 – 2.16 (m, 4H), 2.13 – 2.01 (m, 1H), 1.91 – 1.76 (m, 1H) ppm; **^{13}C NMR** (101 MHz, $CDCl_3$) δ 212.2 (C), 169.2 (C), 142.2 (C), 138.0 (C), 128.6 (2 × CH), 128.2 (CH), 126.1 (2 × CH), 115.4 (CH_2), 66.5 (CH_2), 54.8 (CH), 38.1 (CH_2), 27.5 (CH_2), 21.0 (CH_2) ppm.

(4aR,8R,8aS)-2,2-dimethyl-4,4a,8,8a-tetrahydropyrano[3,2-d][1,3]dioxin-8-yl 2-oxocyclopentane-1-carboxylate (3.59ao)



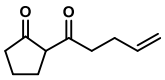
Prepared according to GP8 using ketoester **3.86** on 2.7 mmol scale and purified by flash column chromatography (SiO_2, 10–30% EtOAc/hexanes) to give a white solid (429 mg, 54%, 55:45 epimeric ratio). $\boldsymbol{R_f}$ 0.36 (20% EtOAc/hexanes); **^{1}H NMR** (400 MHz, $CDCl_3$) δ 6.35 (dt, J = 6.1, 1.6 Hz, 1H, **M + m**), 5.45 (dt, J = 7.7, 1.8 Hz, 0.45H, **m**), 5.40 (dt, J = 7.8, 1.8 Hz, 0.55H, **M**), 4.75 (dd, J = 6.1, 2.0 Hz, 0.55H, **M**), 4.71 (dd, J = 6.1, 2.1 Hz, 0.45H, **m**), 4.11 (dd, J = 10.1, 7.8 Hz, 0.55H, **M**), 4.05 (dd, J = 10.2, 7.6 Hz, 0.45H, **m**), 4.00 – 3.94 (m, 1H, **M + m**), 3.89 – 3.76 (m, 2H, **2M + 2m**), 3.21 (dd, J = 9.3, 9.3 Hz, 0.55H, **M**), 3.16 (dd, J = 8.8, 8.8 Hz, 0.45H, **m**), 2.37 – 2.26 (m, 4H, **4M + 4m**), 2.19 – 2.08 (m, 1H, **M + m**), 1.94 – 1.80 (m, 1H, **M + m**), 1.53 (s, 1.35H, **3m**), 1.52 (s, 1.65H, **3M**), 1.41 (s, 1.65H, **3M**), 1.40 (s, 1.35H, **3m**) ppm;**^{13}C NMR** (101 MHz, $CDCl_3$) δ 212.2 (C, **M**), 211.7 (C, m), 169.4 (C, M), 169.2 (C, m), 145.8 (CH, m), 145.7 (CH, M), 100.6 (CH, M), 100.5 (CH, m), 100.0 (C, m), 100.0 (C, M), 70.5 (CH, M), 70.1 (CH, m), 70.1 (CH, m), 70.0 (CH, m), 69.8 (CH, M), 69.7 (CH, M), 61.8 (CH_2, m), 61.7 (CH_2, M), 54.9 (CH, m), 54.8 (CH, M), 38.2 (CH_2, M), 38.1 (CH_2, m), 29.0 (CH_3, M), 29.0 (CH_3, m), 27.6 (CH_2, m), 27.3 (CH_2, M), 21.1 (CH_2, m), 21.0 (CH_2, M), 19.1 (CH_3, M), 19.0 (CH_3, m) ppm.

allyl 1-methyl-2-oxopyrrolidine-3-carboxylate (3.59ap)



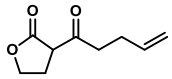
Prepared according to GP9 using *N*-methyl pyrrolidone on 4.6 mmol scale and purified by flash column chromatography (SiO_2, 45–90% EtOAc/hexanes) to give an amber oil (333 mg, 40% yield). $\boldsymbol{R_f}$ 0.22 (60% EtOAc/hexanes); **^{1}H NMR** (400 MHz, $CDCl_3$) δ 5.91 (dddd, J = 17.2, 10.4, 5.6, 5.6 Hz, 1H), 5.35 (dddd, J = 17.2, 1.5, 1.5, 1.5 Hz, 1H), 5.23 (dddd, J = 10.5, 1.3, 1.3, 1.3 Hz, 1H), 4.71 – 4.60 (m, 2H), 3.53 – 3.41 (m, 2H), 3.35 (ddd, J = 9.5, 8.4, 5.8 Hz, 1H), 2.86 (d, J = 0.8 Hz, 3H), 2.40 (dddd, J = 13.1, 8.7, 6.6, 5.8 Hz, 1H), 2.26 (dddd, J = 13.3, 9.5, 8.4, 5.1 Hz, 1H) ppm; **^{13}C NMR** (101 MHz, $CDCl_3$) δ 170.2 (C), 169.7 (C), 131.8 (CH), 118.7 (CH_2), 66.2 (CH_2), 48.3 (CH), 48.0 (CH_2), 30.1 (CH_3), 22.3 (CH_2) ppm; **HRMS** (EI): *m/z* calculated for $C_9H_{13}NO_3Na^+$ $[M+Na]^+$: 206.0793, found 206.0775.

2-(pent-4-enoyl)cyclopentan-1-one (3.59aq)



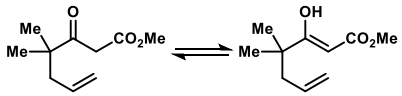
Prepared according to GP12 using 2-acetylcyclopentanone and allyl bromide on 5.0 mmol scale and purified by flash column chromatography (SiO_2, 5–10% EtOAc/hexanes) to give a pink oil (250 mg, 30%). R_f 0.37 (10% EtOAc/hexanes); **^{1}H NMR** (400 MHz, $CDCl_3$) δ 13.57 (s, 0.55H, **e**), 5.89 – 5.72 (m, 1H, **k + e**), 5.11 – 4.92 (m, 2H, **2k + 2e**), 3.37 (td, J = 8.0, 1.0 Hz, 0.45H, **k**), 3.02 – 2.89 (m, 0.45H, **k**), 2.64 – 2.49 (m, 2H, **k & e**), 2.49 – 2.12 (m, 6H, **k & e**), 2.13 – 1.77 (m, 3H, **k & e**) ppm; **^{13}C NMR** (101 MHz, $CDCl_3$) δ 213.2 (C, k), 204.8 (C, k), 203.9 (C, e), 178.7 (C, e), 137.1 (CH, k), 137.1 (CH, e), 115.6 (CH_2, e), 115.4 (CH_2, k), 109.7 (C, e), 62.1 (CH, k), 42.2 (CH_2), 38.9 (CH_2), 36.9 (CH_2), 34.0 (CH_2), 29.5 (CH_2), 27.4 (CH_2), 25.8 (CH_2), 25.4 (CH_2), 20.9 (CH_2), 20.4 (CH_2) ppm; **HRMS** (EI): *m/z* calculated for $C_{10}H_{14}O_2^{\bullet+}$ $[M]^{+\bullet}$: 166.09883, found 166.09936.

3-(pent-4-enoyl)dihydrofuran-2(3H)-one (3.59ar)



Prepared according to GP11 using 3-acetyldihydrofuran-2(3H)-one **3.41** and allyl bromide on 5.0 mmol scale. The crude residue was purified by flash column chromatography (10–25% EtOAc/hexanes) to give a clear colourless oil (309 mg, 1.85 mmol, 37% yield). R_f 0.47 (35% EtOAc/hexanes); **^{1}H NMR** (400 MHz, $CDCl_3$) δ 5.89 – 5.70 (m, 1H), 5.12 – 5.00 (m, 1H), 5.04 – 4.95 (m, 1H), 4.43 – 4.26 (m, 2H), 3.69 (dd, J = 9.2, 6.6 Hz, 1H), 3.17 – 3.04 (m, 1H), 2.91 – 2.62 (m, 2H), 2.44 – 2.23 (m, 3H) ppm; **^{13}C NMR** (101 MHz, $CDCl_3$) δ 201.8 (C), 172.9 (C), 136.6 (CH), 115.7 (CH_2), 67.7 (CH_2), 52.4 (CH), 41.3 (CH_2), 27.4 (CH_2), 24.0 (CH_2) ppm; **HRMS** (EI): *m/z* calculated for $C_9H_{12}O_3^{\bullet+}$ $[M]^{+\bullet}$: 168.07810, found 168.07637.

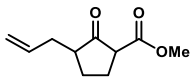
methyl 4,4-dimethyl-3-oxohept-6-enoate (3.59as)



Prepared according to GP12 using methyl isobutyrylacetate on 5.0 mmol scale and purified by flash column chromatography (5–10% EtOAc/hexanes) to give an orange oil (479 mg, 52% yield, 4:1 keto to enol mixture). R_f 0.35 (10% EtOAc/hexanes); **^{1}H NMR** (400 MHz, $CDCl_3$) δ 12.27 (s, 0.2H, **e**), 5.74 – 5.61 (m, 1H, **k + e**), 5.10 – 4.98 (m, 2.2H, **2k + 3e**), 3.72 (s, 3H, **3k + 3e**), 3.53 (s, 1.6H, **2k**), 2.29 – 2.23 (m, 2H, **2k + 2e**), 1.14 (s, 4.8H, **6k**), 1.10 (s, 1.2H, **6e**) ppm; **^{13}C NMR** (101 MHz, $CDCl_3$) δ 207.4 (C, **k**), 184.6 (C, **e**), 173.6 (C, **e**), 168.2 (C, **k**), 134.4 (CH, **e**),

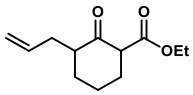
133.5 (CH, **k**), 118.7 (CH_2, **k**), 117.8 (CH_2, **e**), 86.8 (CH, **e**), 52.4 (CH_3, **k**), 51.3 (CH_3, **e**), 48.2 (C, **k**), 44.6 (CH_2, **e**), 44.5 (CH_2, **k**), 43.8 (CH_2, **k**), 39.9 (C, **e**), 25.2 (2 × CH_3, **e**), 23.9 (2 × CH_3, **k**) ppm; **HRMS** (EI): *m/z* calculated for $C_{10}H_{16}O_3^{\bullet+}$ $[M]^{+\bullet}$: 184.10940, found 184.10951.

methyl 3-allyl-2-oxocyclopentane-1-carboxylate (3.59at)



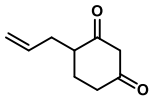
Prepared according to GP11 using ketoester **3.86** and allyl bromide on a 5 mmol scale reaction. The crude residue was purified by flash column chromatography (5–10% EtOAc/hexanes) to give 164.9 mg of the title compound as a yellow oil (0.9 mmol, 18% yield) in a 55_k:$35_{k'}$:10_e ratio of ketoester diastereoisomers to enol. R_f 0.47 (20 % EtOAc/hexanes); **^{1}H NMR** (400 MHz, $CDCl_3$) δ 5.73 (ddt, J = 17.1, 10.1, 7.0 Hz, 1H), 5.14 – 4.96 (m, 2H), 3.77 – 3.69 (m, 3H), 3.34 – 3.24 (m, 0.35H, $\mathbf{m_k}$), 3.12 (dd, J = 10.9, 8.4 Hz, 0.55H, $\mathbf{M_k}$), 2.57 – 2.42 (m, 1H), 2.41 – 2.04 (m, 5H), 1.92 – 1.81 (m, 0.35H, $\mathbf{m_k}$), 1.66 – 1.44 (m, 1H) ppm; **^{13}C NMR** (101 MHz, $CDCl_3$) δ 213.2 (C, m), 212.4 (C, M), 170.0 (C, M), 169.8 (C, m), 135.5 (CH, m), 135.3 (CH, M), 117.1 (CH_2, M), 117.0 (CH_2, m), 55.0 (CH, M), 54.2 (CH, m) 54.2 (CH_3, m), 52.6 (CH_3, M), 49.0 (CH, M), 48.4 (CH, m), 34.3 (CH_2, m), 33.8 (CH_2, M), 27.0 (CH_2, m), 26.8 (CH_2, M), 25.2 (CH_2, M), 25.0 (CH_2, m) ppm;

ethyl 3-allyl-2-oxocyclohexane-1-carboxylate (3.59au)



Prepared according to GP12 on a 5 mmol scale reaction. The crude residue was purified by flash column chromatography (4% EtOAc/hexanes) to give 440 mg of the title compound as a clear, colourless oil (2.1 mmol, 42% yield) as a mixture of tautomers and diastereoisomers. Characterized according to literature comparison of NMR spectra.[351] R_f 0.35 (5% EtOAc/hexanes); **^{1}H NMR** (400 MHz, $CDCl_3$) δ 12.43 (s, 0.55H), 12.24 (s, 0.15H), 5.85 – 5.69 (m, 1H), 5.11 – 4.97 (m, 2H), 4.28 – 4.14 (m, 2.45H), 3.44 – 3.34 (m, 0.45H), 2.70 – 2.45 (m, 1H), 2.45 – 2.33 (m, 1H), 2.30 – 2.12 (m, 3H), 2.12 – 1.89 (m, 1H), 1.88 – 1.56 (m, 2H), 1.56 – 1.43 (m, 1H), 1.39 (dd, J = 13.0, 3.8 Hz, 0.3H), 1.34 – 1.22 (m, 3H) ppm; **^{13}C NMR** (101 MHz, $CDCl_3$) δ 207.6, 206.9, 173.9, 173.1, 172.9, 172.1, 170.1, 136.6, 136.1, 136.0, 116.8, 116.6, 98.3, 97.9, 61.4, 61.1, 60.4, 60.3, 58.0, 57.4, 56.4, 50.7, 49.1, 41.7, 38.4, 36.4, 33.9, 33.9, 33.6, 33.2, 30.9, 30.4, 30.1, 29.2, 27.2, 26.9, 24.2, 23.4, 23.0, 22.5, 22.5, 22.1, 21.8, 20.1, 14.4, 14.3, 14.3 ppm.

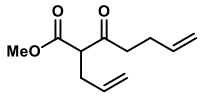
4-allylcyclohexane-1,3-dione (3.59av)



Prepared according to the following literature adapted procedure.[352] To a solution of LiHMDS (1.7 mL, 6.6 mmol, 1.1 equiv., 0.8 M in THF) was added enol ether **3.63** (1 g, 6 mmol, 1.0 equiv.) at -78 °C. The solution was stirred for 1 hour, then allyl bromide (0.7 mL, 8.0 mmol, 1.3 equiv.) was added and the solution was allowed to warm slowly to room temperature and stirring was continued overnight. Brine (50 mL) was added and the resulting mixture was extracted with Et_2O (3 × 20 mL). The combined extracts were washed with brine, dried over $MgSO_4$, filtered, and concentrated. The crude residue was purified by flash column chromatography (SiO_2, 2–10% EtOAc/hexanes) to give an orange solid (662 mg, 53%).

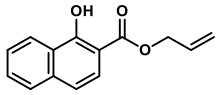
To a solution of the resulting enol ether (400 mg, 1.9 mmol) in acetone (7 mL, 0.38 M) was added hydrochloric acid (2.6 mL, 1 N aqueous) at room temperature with vigorous stirring. The resulting solution was stirred for 6 hours, then most of the acetone was removed under reduced pressure. The mixture was diluted with brine (10 mL) and extracted with DCM (3 × 10 mL). The combined extracts were dried over $MgSO_4$, filtered, and concentrated under reduced pressure. The crude materials was purified by flash column chromatography (SiO_2, 50–80% EtOAc/hexanes) to give a yellow oil (310 mg, quantitative yield). $\boldsymbol{R_f}$ 0.15 (50% EtOAc/hexanes); **^{1}H NMR** (400 MHz, $CDCl_3$) δ 5.80 (dddd, J = 16.7, 10.1, 7.9, 6.3 Hz, 1H), 5.16 – 5.05 (m, 2H), 3.51 – 3.36 (m, 2H), 2.76 – 2.41 (m, 4H), 2.29 – 2.11 (m, 2H), 1.57 (dtd, J = 14.1, 12.2, 4.6 Hz, 1H) ppm; Characterized according to NMR comparison.[353]

methyl 2-allyl-3-oxohex-5-enoate (3.59aw)



Prepared according to GP9 using methyl pent-4-enoate and omitting allyl chloroformate on 7.5 mmol scale and purified by flash column chromatography (SiO_2, 5–10% EtOAc/hexanes) to give a yellow oil (603 mg, 82%). $\boldsymbol{R_f}$ 0.54 (12% EtOAc/hexanes); **^{1}H NMR** (400 MHz, $CDCl_3$) δ 5.87 – 5.61 (m, 2H), 5.13 – 4.94 (m, 4H), 3.72 (s, 3H), 3.55 (t, J = 7.4 Hz, 1H), 2.73 – 2.51 (m, 4H), 2.36 – 2.29 (m, 2H) ppm; **^{13}C NMR** (101 MHz, $CDCl_3$) δ 203.8 (C), 169.8 (C), 136.8 (CH), 134.3 (CH), 117.7 (CH_2), 115.6 (CH_2), 58.5 (CH), 52.6 (CH_3), 41.5 (CH_2), 32.4 (CH_2), 27.5 (CH_2) ppm. Characterized according to NMR comparison.[354]

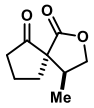
allyl 1-hydroxy-2-naphthoate (3.59ax)



1-hydroxy-2-naphthoic acid (997 mg, 5.3 mmol, 1.0 equiv) was added to a stirring solution of KOH (325 mg, 5.8 mmol, 1.1 equiv) dissolved in distilled water (5.3 mL, 1 M). The mixture was stirred at room temperature for 1 hour, then concentrated to dryness by rotary evaporation. The resulting white powder was ground in a mortar and pestle then suspended in toluene (15 mL) and concentrated (Å~ 3) to remove water by azeotropic distillation. The dried white powder was then dissolved in DMF (anhydrous, 25 mL, 0.4 M) and allyl bromide (0.47 mL, 5.8 mmol, 1.1 equiv) was added in one portion at room temperature. The resulting solution was stirred vigorously at room temperature overnight. The solution was diluted with brine (30 mL) and Et_2O (20 mL, inhibitor-free) and the layers separated. The aqueous phase was extracted with Et_2O (2 × 20 mL). Combined extracts were washed with distilled water (3 × 15 mL) and brine (20 mL), dried over $MgSO_4$, filtered, and concentrated under reduced pressure. The crude residue was purified by flash column chromatography (4% EtOAc/hexanes) to give a crystalline white solid (544 mg, 45% yield). **^{1}H NMR** (400 MHz, $CDCl_3$) δ 11.97 (s, 1H), 8.42 (ddt, J = 8.3, 1.5, 0.8 Hz, 1H), 7.81 (d, J = 8.8 Hz, 1H), 7.77 (dt, J = 8.2, 1.0 Hz, 1H), 7.61 (ddd, J = 8.2, 6.9, 1.4 Hz, 1H), 7.53 (ddd, J = 8.2, 6.9, 1.3 Hz, 1H), 7.29 (dd, J = 8.9, 0.9 Hz, 1H), 6.08 (ddt, J = 17.2, 10.4, 5.7 Hz, 1H), 5.47 (dq, J = 17.2, 1.5 Hz, 1H), 5.35 (dq, J = 10.4, 1.3 Hz, 1H) ppm; **^{13}C NMR** (101 MHz, $CDCl_3$) δ 170.8 (C), 161.3 (C), 137.4 (C), 131.9 (CH), 129.6 (CH), 127.6 (CH), 125.9 (CH), 124.9 (C), 124.4 (CH), 124.0 (CH), 119.0 (CH_2), 118.8 (CH), 105.7 (C), 66.0 (CH_2) ppm. Characterized according to NMR comparison.[355]

Intramolecular Hydroalkylation Products

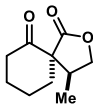
4-methyl-2-oxaspiro[4.4]nonane-1,6-dione (3.60a/a')



Prepared according to GP6 with substrate **3.59a** on 0.2 mmol scale and using CF_3CO_2Na and purified by flash column chromatography (SiO_2, 15–50% Et_2O/hexanes) to give **3.60a/a'** as a clear, colourless oil (condition A: 30 mg, 90%, 4:1 dr; condition B: 27 mg, 80%, 3.4:1 dr). R_f 0.38 (50% Et_2O/hexanes); **^{1}H NMR** (500 MHz, $CDCl_3$) δ 4.63 (dd, J = 8.7, 6.7 Hz, 0.2H, **m**), 4.30 (dd, J = 8.2, 8.2 Hz, 0.8H, **M**), 4.18 (dd, J = 10.9, 8.5 Hz, 0.8H, **M**), 3.89 (dd, J = 8.6, 4.7 Hz, 0.2H, **m**), 2.76 (ddddd, J = 7.0, 7.0, 7.0, 7.0, 4.7 Hz, 0.2H, **m**), 2.65 – 2.17 (m, 4.8H, **5M** + **4m**), 2.10 –

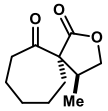
1.89 (m, 2H, **2M** + **2m**), 1.09 (d, J = 6.9 Hz, 2.4H, **3M**), 1.05 (d, J = 7.1 Hz, 0.6H, **3m**) ppm; **^{13}C NMR** (126 MHz, $CDCl_3$) δ **M** 213.8 (C), 175.8 (C), 71.8 (CH_2), 60.2 (C), 41.3 (CH), 39.7 (CH_2), 32.6 (CH_2), 20.4 (CH_2), 11.1 (CH_3) **m** 213.9 (C), 175.4 (C), 73.1 (CH_2), 61.1 (C), 37.6 (CH_2), 36.7 (CH), 28.4 (CH_2), 19.4 (CH_2), 14.6 (CH_3) ppm; **HRMS** (ESI+) *m/z* calculated for $C_9H_{12}O_3Na^+$ $[M + Na]^+$ 191.0684, found 191.0699.

4-methyl-2-oxaspiro[4.5]decane-1,6-dione (3.60b/b')



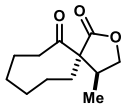
Prepared according to GP6 with substrate **3.59b** on 0.2 mmol scale and purified by flash column chromatography (SiO_2, 40–50% Et_2O/hexanes) to give **3.60b/b'** as a clear, colourless oil (condition A: 30 mg, 83%, 5.4:1 dr; condition B: 33.1 mg, 92%, 4.2:1 dr). R_f 0.35 (50% Et_2O/hexanes); **^{1}H NMR** (400 MHz, $CDCl_3$) δ **M** 4.30 (dd, J = 8.7, 7.5 Hz, 1H), 3.92 (dd, J = 9.8, 8.6 Hz, 1H), 2.61 (dtd, J = 16.2, 5.6, 1.0 Hz, 1H), 2.51 (dp, J = 9.8, 7.1 Hz, 1H), 2.34 – 2.22 (m, 2H), 2.14 – 2.04 (m, 1H), 1.98 – 1.82 (m, 3H), 1.80 – 1.66 (m, 1H), 1.16 (d, J = 7.1 Hz, 3H) **m** 4.34 (dd, J = 8.8, 7.2 Hz, 1H), 3.82 (dd, J = 8.8, 7.6 Hz, 1H), 3.19 (h, J = 7.1 Hz, 1H), 2.98 (ddd, J = 14.0, 11.5, 5.8 Hz, 1H), 2.53 – 2.44 (m, 1H), 2.25 – 2.03 (m, 3H), 1.85 – 1.64 (m, 3H), 1.03 (d, J = 7.0 Hz, 3H) ppm; **^{13}C NMR** (101 MHz, $CDCl_3$) δ **M** 206.6 (C), 176.5 (C), 71.6 (CH_2), 60.5 (C), 42.4 (CH_2), 41.6 (CH), 34.6 (CH_2), 24.8 (CH_2), 21.0 (CH_2), 13.2 (CH_3) **m** 205.8 (C), 175.2 (C), 71.7 (CH_2), 60.2 (C), 39.8 (CH_2), 34.9 (CH), 29.9 (CH_2), 26.9 (CH_2), 20.5 (CH_2), 12.3 (CH_3) ppm; **HRMS** (EI+) *m/z* calculated for $C_{10}H_{14}O_3^{\bullet+}$ $[M]^{\bullet+}$ 182.09375, found 182.09357.

4-methyl-2-oxaspiro[4.6]undecane-1,6-dione (3.60c/c')



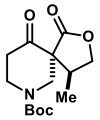
Prepared according to GP6 with substrate **3.59c** on 0.2 mmol scale and purified by flash column chromatography (SiO_2, 10–30% EtOAc/hexanes) to give **3.60c/c'** as a clear, colourless oil (condition A: 32.2 mg, 82%, 4.8:1 dr; condition B: 23.6 mg, 61%, 4.9:1 dr). R_f 0.35 (25% EtOAc/hexanes); **^{1}H NMR** (400 MHz, $CDCl_3$) δ 4.29 (dd, J = 8.7, 7.6 Hz, 1H), 3.85 (dd, J = 10.8, 8.7 Hz, 1H), 2.63 – 2.52 (m, 2H), 2.45 (ddddd, J = 10.8, 7.2, 7.1, 7.1 Hz, 1H), 2.15 – 2.01 (m, 2H), 1.98 – 1.77 (m, 4H), 1.65 – 1.44 (m, 2H), 1.09 (d, J = 7.1 Hz, 3H) ppm; **^{13}C NMR** (101 MHz, $CDCl_3$) δ 210.7 (C), 177.4 (C), 70.8 (CH_2), 62.5 (C), 44.6 (CH_2), 42.9 (CH), 33.3 (CH_2), 31.0 (CH_2), 26.2 (CH_2), 24.6 (CH_2), 11.8 (CH_3) ppm; **HRMS** (ESI+) *m/z* calculated for $C_{11}H_{16}O_3Na^+$ $[M + Na]^+$ 219.0997, found 219.0982.

4-methyl-2-oxaspiro[4.7]dodecane-1,6-dione (3.60d/d')



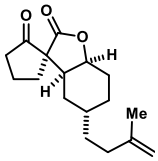
Prepared according to GP6 with substrate **3.59d** on 0.2 mmol scale and purified by flash column chromatography (SiO_2, 10–20% EtOAc/hexanes) to give **3.60d/d'** as crystalline white solids (condition A: 37.6 mg, 89%, 3.3:1 dr; condition B: 12.4 mg, 31%, 3.5:1 dr). Synthesis on 1.0 g/4.75 mmol scale under condition A gave **3.60d/d'** (567.3 mg, 57%, 88% brsm, 3.4:1 dr). $\boldsymbol{R_f}$ major 0.44, minor 0.72 (30% EtOAc/hexanes); **^{1}H NMR** (500 MHz, $CDCl_3$) δ **M** 4.29 (dd, J = 8.7, 7.4 Hz, 1H), 3.86 (dd, J = 9.7, 8.7 Hz, 1H), 2.61 – 2.45 (m, 3H), 2.33 – 2.19 (m, 2H), 2.12 – 2.00 (m, 1H), 1.90 – 1.75 (m, 2H), 1.72 – 1.62 (m, 1H), 1.62 – 1.38 (m, 4H), 1.15 (d, J = 7.1 Hz, 3H) **m** 4.38 (dd, J = 8.6, 5.7 Hz, 1H), 3.86 (dd, J = 8.6, 2.0 Hz, 1H), 3.14 – 3.04 (m, 2H), 2.63 (ddd, J = 15.7, 12.1, 3.6 Hz, 1H), 2.23 (ddd, J = 11.9, 6.2, 3.8 Hz, 1H), 1.97 – 1.86 (m, 2H), 1.82 – 1.61 (m, 4H), 1.55 – 1.41 (m, 2H), 1.13 (d, J = 7.4 Hz, 3H), 1.12 – 1.02 (m, 1H) ppm; **^{13}C NMR** (126 MHz, $CDCl_3$) δ **M** 212.1 (C), 175.2 (C), 71.2 (CH_2), 62.3 (C), 42.0 (CH), 40.0 (CH_2), 32.3 (CH_2), 30.4 (CH_2), 26.5 (CH_2), 25.2 (CH_2), 25.1 (CH_2), 12.6 (CH_3) **m** 210.3 (C), 174.5 (C), 73.8 (CH_2), 64.7 (C), 37.5 (CH_2), 34.4 (CH), 29.8 (CH_2), 26.1 (CH_2), 25.8 (CH_2), 24.8 (CH_2), 24.8 (CH_2), 15.3 (CH_3) ppm; **HRMS** (EI+) *m/z* calculated for $C_{12}H_{18}O_3^{\bullet+}$ $[M]^{+\bullet}$ 210.12505, found **M** 210.12851, **m** 210.12851.

tert-butyl 4-methyl-1,10-dioxo-2-oxa-7-azaspiro[4.5]decane-7-carboxylate (3.60e/e')



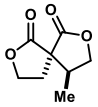
Prepared according to GP6 with substrate **3.59e** on 0.2 mmol scale and purified by flash column chromatography (SiO_2, 15–40% EtOAc/hexanes) to give **3.60e/e'** as an amorphous beige solid (condition A: 46.5 mg, 82%, 4.8:1 dr; condition B: 49.3 mg, 87%, 5.8:1 dr). $\boldsymbol{R_f}$ 0.36 (40% EtOAc/hexanes); **^{1}H NMR** (600 MHz, DMSO-d_6) δ 4.40 (dd, J = 8.7, 7.6 Hz, 1H), 4.32 (dd, J = 8.9, 7.2 Hz, 0.1H, **m**), 4.17 (d, J = 14.0 Hz, 1H), 4.08 – 3.94 (m, 1H), 3.69 (dd, J = 9.8, 8.7 Hz, 1H), 3.66 – 3.59 (m, 1H), 3.42 – 3.33 (m, J = 13.4 Hz, 1H), 2.86 – 2.77 (m, 1H), 2.60 – 2.46 (m, 2H), 1.44 (s, 8H, **9M**), 1.41 (s, 1H, **9m**), 1.01 (d, J = 7.1 Hz, 0.31H, **3m**), 0.96 (d, J = 7.0 Hz, 2.69H, **3M**) ppm; ^{13}C NMR (151 MHz, DMSO-d_6) δ 204.4, 173.8, 173.1, 153.5, 79.6, 79.5, 71.0, 70.9, 60.6, 27.8, 12.7 ppm; **HRMS** (EI+) *m/z* calculated for $C_{10}H_{12}NO_5^{\bullet+}$ $[M - C_4H_9]^{\bullet+}$ 226.07100, found 226.07205.

5-(3-methylbut-3-en-1-yl)hexahydro-2H-spiro[benzofuran-3,1'-cyclopentane]-2,2'-dione (3.60f/f')



Prepared according to GP6 with substrate **3.59f** on 0.11 mmol scale and purified by flash column chromatography (SiO_2, 6–20% EtOAc/hexanes) to give **3.60f/f'** as a pale-yellow oil (condition A: 15.5 mg, 49%, 1.2:1 dr). $\boldsymbol{R_f}$ major 0.33 minor 0.16 (16% EtOAc/hexanes); **^{1}H NMR** (600 MHz, $CDCl_3$) δ **M** 4.96 (ddd, J = 5.1, 5.1, 5.1 Hz, 1H), 4.74 – 4.69 (m, 1H), 4.69 – 4.64 (m, 1H), 2.65 (ddd, J = 9.1, 6.0, 6.0 Hz, 1H), 2.54 – 2.45 (m, 1H), 2.39 – 2.26 (m, 3H), 2.06 – 1.86 (m, 5H), 1.84 – 1.78 (m, 1H), 1.71 (t, J = 1.1 Hz, 3H), 1.70 – 1.62 (m, 1H), 1.52 – 1.33 (m, 4H), 1.33 – 1.20 (m, 2H) **m** 4.73 – 4.68 (m, 1H), 4.68 – 4.63 (m, 1H), 4.55 (ddd, J = 6.3, 6.2, 6.2 Hz, 1H), 2.53 (ddd, J = 6.8, 6.7, 6.7 Hz, 1H), 2.49 – 2.31 (m, 3H), 2.24 – 2.13 (m, 2H), 2.07 – 1.91 (m, 4H), 1.88 (ddd, J = 14.8, 7.3, 4.6 Hz, 1H), 1.76 – 1.67 (m, 1H), 1.70 (dd, J = 1.0, 1.0 Hz, 3H), 1.63 – 1.57 (m, 1H), 1.43 – 1.19 (m, 4H), 1.18 – 1.09 (m, 1H) ppm; **^{13}C NMR** (151 MHz, $CDCl_3$) δ **M** 213.8 (C), 175.3 (C), 145.7 (C), 110.2 (CH_2), 77.2 (CH), 63.1 (C), 37.9 (CH), 37.6 (CH_2), 35.6 (CH_2), 31.3 (CH), 30.4 (CH_2), 29.7 (CH_2), 28.3 (CH_2), 24.4 (CH_2), 24.2 (CH_2), 22.5 (CH_3), 19.4 (CH_2) **m** 213.4 (C), 176.6 (C), 145.9 (C), 110.1 (CH_2), 77.8 (CH), 61.2 (C), 43.1 (CH), 39.1 (CH_2), 35.5 (2 × CH_2), 31.7 (CH_2), 30.9 (CH), 29.3 (CH_2), 25.6 (CH_2), 25.5 (CH_2), 22.6 (CH_3), 20.0 (CH_2) ppm; **HRMS** (EI+) *m/z* calculated for $C_{17}H_{24}O_3^{\bullet+}$ $[M]^{\bullet+}$ 276.17200, found 276.17201.

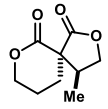
4-methyl-2,7-dioxaspiro[4.4]nonane-1,6-dione (3.60g/g')



Prepared according to GP6 with substrate **3.59g** on 0.2 mmol scale and purified by flash column chromatography (SiO_2, 25–50% EtOAc/hexanes) to give **3.60g/g'** as a white solid (condition A: 25.2 mg, 74%, 4:1 dr; condition B: 17.1 mg, 50%, 5:1 dr). $\boldsymbol{R_f}$ 0.32 (40% EtOAc/hexanes); **^{1}H NMR** (400 MHz, $CDCl_3$) δ 4.78 (dd, J = 8.8, 6.6 Hz, 0.2H, **m**), 4.62 (td, J = 9.1, 6.9 Hz, 0.2H, **m**), 4.55 (td, J = 8.8, 6.2 Hz, 0.8H, **M**), 4.45 – 4.33 (m, 1.8H, **2M** + **m**), 4.30 (dd, J = 11.0, 8.7 Hz, 0.8H, **M**), 3.98 (dd, J = 8.8, 4.4 Hz, 0.2H, **m**), 3.02 – 2.91 (m, 0.2H, **m**), 2.88 (ddd, J = 13.3, 8.6, 6.3 Hz, 0.8H, **M**), 2.78 – 2.63 (m, 0.8H, **M**), 2.55 – 2.45 (m, 0.2H, **m**), 2.45 – 2.35 (m, 0.2H, **m**), 2.27 (ddd, J = 13.4, 8.3, 6.2 Hz, 0.8H, **M**), 1.21 (d, J = 6.9 Hz, 2.4H, **3M**), 1.13 (d, J = 7.2 Hz, 0.6H, **3m**) ppm; **^{13}C NMR** (101 MHz, $CDCl_3$) δ **M** 174.0 (C), 171.9 (C), 71.8 (CH_2), 67.0 (CH_2), 54.4 (C), 40.5 (CH), 30.7 (CH_2), 10.9

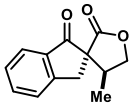
(CH_3) **m** 173.8 (C), 173.7 (C), 73.6 (CH_2), 66.7 (CH_2), 54.6 (C), 36.8 (CH), 27.8 (CH_2), 14.6 (CH_3) ppm; **HRMS** (EI+) *m/z* calculated for $C_8H_{10}O_4^{\bullet+}$ $[M]^{+\bullet}$ 170.05736, found 170.05666.

4-methyl-2,7-dioxaspiro[4.5]decane-1,6-dione (3.60h)



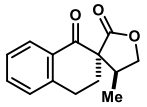
Prepared according to GP6 with substrate **3.59h** on 0.2 mmol scale and purified by flash column chromatography (SiO_2, 70–90% Et_2O/hexanes) to give **3.60h/h'** as a white solid (condition A: 35.7 mg, 97%, 5.6:1 dr; condition B: 35.8 mg, 97%, 5.3:1 dr). R_f 0.22 (50% EtOAc/hexanes); **^{1}H NMR** (400 MHz, $CDCl_3$) δ 4.61 (dd, J = 8.8, 7.0 Hz, 0.15H, **m**), 4.57 (dddd, J = 11.2, 6.7, 4.7, 1.1 Hz, 0.15H, **m**), 4.54 – 4.45 (m, 0.85H, **M**), 4.45 – 4.37 (m, 1H, **M** + **m**), 4.34 (dd, J = 8.2, 8.2 Hz, 0.85H, **M**), 4.22 (dd, J = 10.7, 8.5 Hz, 0.85H, **M**), 3.91 (dd, J = 8.8, 6.4 Hz, 0.15H, **m**), 3.24 (ddddd, J = 7.0, 7.0, 7.0 Hz, 0.15H, **m**), 2.56 (ddddd, J = 10.7, 8.1, 6.8, 6.8, 6.8 Hz, 0.85H, **M**), 2.49 – 2.37 (m, 0.85H, **M**), 2.34 – 2.17 (m, 1H, **M** + **m**), 2.13 (dddd, J = 14.2, 7.9, 4.2, 1.0 Hz, 0.15H, **m**), 2.07 – 1.81 (m, 2H, **2M** + **2m**), 1.19 (d, J = 6.8 Hz, 2.55H, **3M**), 1.11 (d, J = 7.2 Hz, 0.45H, **3m**) ppm; **^{13}C NMR** (101 MHz, $CDCl_3$) δ 175.6 (C, **M**), 166.5 (C, **M**), 72.2 (CH_2, **M**), 71.1 (CH_2, **M**), 54.2 (C, **M**), 44.0 (CH, **M**), 30.6 (CH_2, **M**), 20.7 (CH_2, **M**), 12.1 (CH_3, **M**) ppm; **HRMS** (ESI+) *m/z* calculated for $C_9H_{12}O_4Na^+$ $[M + Na]^+$ 207.0633, found 207.0631.

4-methyl-4,5-dihydro-2H-spiro[furan-3,2'-indene]-1',2(3'H)-dione (3.60i/i')[§]



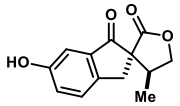
Prepared according to GP6 with substrate **3.59i** on 0.2 mmol scale and purified by flash column chromatography (SiO_2, 10–30% EtOAc/hexanes) to give **3.60i/i'** as an amber oil (condition A: 30 mg, 70%, 4.0:1 dr; condition B: 32 mg, 74%, 3.8:1 dr). R_f 0.43 (30% EtOAc/hexanes); **^{1}H NMR** (400 MHz, $CDCl_3$) δ 7.74 (ddd, J = 7.8, 1.3, 0.7 Hz, 1H, **M + m**), 7.65 (td, J = 7.5, 1.3 Hz, 1H, **M + m**), 7.51 (dp, J = 7.7, 1.0 Hz, 1H, **M + m**), 7.42 (ddq, J = 8.0, 7.3, 0.9 Hz, 1H, **M + m**), 4.94 (dd, J = 8.6, 6.5 Hz, 1H, **m**), 4.51 (dd, J = 11.2, 8.5 Hz, 1H, **M**), 4.42 (dd, J = 8.2, 8.2 Hz, 1H, **M**), 4.05 (dd, J = 8.6, 3.9 Hz, 1H, **m**), 3.78 (d, J = 17.4 Hz, 1H, **M**), 3.44 (d, J = 17.2 Hz, 1H, **m**), 3.28 (minor, d, J = 17.2 Hz, 1H, **m**), 3.05 (d, J = 17.4 Hz, 1H, **M**), 3.01 – 2.95 (m, 1H, **m**), 2.85 (ddq, J = 11.2, 8.0, 6.9 Hz, 1H, **M**), 1.17 (d, J = 7.2 Hz, 2H, **m**), 1.03 (d, J = 6.9 Hz, 3H, **M**) ppm; **^{13}C NMR** (101 MHz, $CDCl_3$) δ 200.7 (C), 175.7 (C), 153.7 (C), 136.0 (CH), 135.3 (C), 128.3 (CH), 126.5 (CH), 124.8 (CH), 71.9 (CH_2), 60.8 (C), 41.7 (CH), 36.0 (CH_2), 10.6 (CH_3) ppm; **HRMS** (EI+) *m/z* calculated for $C_{13}H_{12}O_3^{\bullet+}$ $[M]^{+\bullet}$ 216.07810, found 216.07983.

4-methyl-3',4,4',5-tetrahydro-1'H,2H-spiro[furan-3,2'-naphthalene]-1',2-dione (3.60j/j')[§]



Prepared according to GP6 with substrate **3.59j** on 0.2 mmol scale and purified by flash column chromatography (SiO_2, 10–30% EtOAc/hexanes) to give **3.60j/j'** as an amber oil (condition A: 40 mg, 87%, 6:1 dr; condition B: 38.2 mg, 83%, 6.2:1 dr). R_f 0.33 (60% Et_2O/hexanes); **^{1}H NMR** (600 MHz, $CDCl_3$) δ 8.09 – 8.00 (m, 1H, **M + m**), 7.53 (qd, J = 7.2, 1.5 Hz, 1H, **M + m**), 7.39 – 7.33 (m, 1H, **M + m**), 7.29 – 7.27 (m, 1H, **M + m**), 4.53 (dd, J = 8.8, 6.8 Hz, 1H, **m**), 4.41 (dd, J = 8.7, 7.9 Hz, 1H, **M**), 4.05 (dd, J = 10.5, 8.8 Hz, 1H, **M**), 3.95 (dd, J = 8.8, 6.1 Hz, 1H, **m**), 3.33 – 3.25 (m, 1H, **m**), 3.25 – 3.16 (m, 1H, **M + m**), 3.16 – 3.06 (m, 1H, **M**), 3.02 – 2.95 (m, 1H, **m**), 2.81 – 2.71 (m, 2H, **M**), 2.46 – 2.40 (m, 1H, **m**), 2.26 – 2.17 (m, 1H, **m**), 2.15 (dt, J = 13.9, 4.5 Hz, 1H, **M**), 1.14 (d, J = 7.1 Hz, 3H, **m**), 0.98 (d, J = 6.9 Hz, 3H, **M**) ppm; **^{13}C NMR** (151 MHz, $CDCl_3$) δ **M** 194.5 (C), 177.1 (C), 143.5 (C), 134.5 (CH), 132.1 (C), 129.0 (CH), 127.8 (CH), 127.4 (CH), 71.7 (CH_2), 57.7 (C), 41.9 (CH), 31.8 (CH_2), 25.4 (CH_2), 13.2 (CH_3) **m** 193.5 (C), 175.2 (C), 143.8 (C), 134.3 (CH), 131.0 (C), 128.9 (CH), 128.6 (CH), 127.1 (CH), 72.3 (CH_2), 57.5 (C), 36.1 (CH), 25.3 (CH_2), 25.2 (CH_2), 13.6 (CH_3) ppm; **HRMS** (EI+) *m/z* calculated for $C_{14}H_{14}O_3^{\bullet+}$ $[M]^{\bullet+}$ 230.09375, found 230.09617.

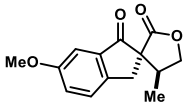
6'-hydroxy-4-methyl-4,5-dihydro-2H-spiro[furan-3,2'-indene]-1',2(3'H)-dione (3.60k/k')[§]



Prepared according to GP6 with substrate **3.59k** on 0.2 mmol scale and purified by flash column chromatography (SiO_2, 50% EtOAc/hexanes) to give **3.60k/k'** as an amorphous tan solid (condition A: 17 mg, 37%, 3.5:1 dr; condition B: 19.6 mg, 43%, 3.8:1 dr). R_f 0.47 (50% EtOAc/hexanes); **^{1}H NMR** (400 MHz, acetone-d_6) δ 8.93 (s, 1H, **M + m**), 7.48 (dq, J = 8.3, 0.9 Hz, 1H, **M + m**), 7.25 (dd, J = 8.4, 2.5 Hz, 1H, **M**), 7.24 (dd, J = 8.3, 2.4 Hz, 1H, **m**), 7.08 (d, J = 2.5 Hz, 1H, **m**), 7.06 (d, J = 2.5 Hz, 1H, **M**), 4.79 (dd, J = 8.6, 6.7 Hz, 1H, **m**), 4.45 (t, J = 8.2 Hz, 1H, **M**), 4.32 (dd, J = 11.0, 8.3 Hz, 1H, **M**), 4.06 (dd, J = 8.6, 5.2 Hz, 1H, **m**), 3.54 (dd, J = 17.2, 0.9 Hz, 1H, **M**), 3.35 (d, J = 17.1 Hz, 1H, **m**), 3.20 (d, J = 17.1 Hz, 1H, **m**), 3.10 (dd, J = 17.2, 0.9 Hz, 1H, **M**), 3.05 – 2.93 (m, 1H, **M + m**), 1.14 (d, J = 7.1 Hz, 3H, **m**), 0.98 (d, J = 6.8 Hz, 3H, **M**) ppm; **^{13}C NMR** (101 MHz, acetone-d_6) δ **M** 201.9 (C), 176.2 (C), 158.5 (C), 146.4 (C), 137.4 (C), 128.3 (CH), 125.4 (CH), 108.9 (CH), 72.3 (CH_2), 62.3 (C), 41.7 (CH), 35.8 (CH_2), 10.6 (CH_3) **m** 202.5 (C), 176.3 (C), 158.4 (C), 145.8 (C), 137.0 (C), 128.4 (CH), 125.3 (CH), 109.3 (CH),

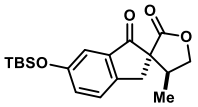
73.9 (CH_2), 63.0 (C), 38.6 (CH), 31.6 (CH_2), 14.7 (CH_3) ppm; **HRMS** (ESI+) *m/z* calculated for $C_{13}H_{13}O_4^+$ $[M + H]^+$ 233.0808, found 233.0796.

6'-methoxy-4-methyl-4,5-dihydro-2H-spiro[furan-3,2'-indene]-1',2(3'H)-dione (3.60l/l')[§]



Prepared according to GP6 with substrate **3.59l** on 0.2 mmol scale and purified by flash column chromatography (SiO_2, 15–30% Et_2O/hexanes) to give **3.60l/l'** as an amorphous tan solid (condition A: 18.7 mg, 37%, 2.4:1 dr; condition B: 19.9 mg, 40%, 3.7:1 dr). R_f 0.34 (30% EtOAc/hexanes); **^{1}H NMR** (400 MHz, $CDCl_3$) δ 7.41 (d, J = 8.5 Hz, 1H, **m**), 7.40 (d, J = 8.4 Hz, 1H, **M**), 7.25 (dd, J = 8.4, 2.8 Hz, 1H, **m**), 7.24 (dd, J = 8.4, 2.5 Hz, 1H, **M**), 7.18 (d, J = 2.5 Hz, 1H, **m**), 7.14 (d, J = 2.5 Hz, 1H, **M**), 4.91 (dd, J = 8.6, 6.6 Hz, 1H, **m**), 4.50 (dd, J = 11.1, 8.4 Hz, 1H, **M**), 4.42 (t, J = 8.2 Hz, 1H, **M**), 4.03 (dd, J = 8.6, 4.2 Hz, 1H, **m**), 3.84 (s, 3H, **M+m**), 3.69 (d, J = 17.1 Hz, 1H, **M**), 3.34 (d, J = 16.9 Hz, 1H, **m**), 3.21 (d, J = 16.8 Hz, 1H, **m**), 3.06 – 2.94 (m, 1H, **m**), 2.96 (d, J = 17.1 Hz, 1H, **M**), 2.91 – 2.78 (m, 1H, **M**), 1.16 (d, J = 7.2 Hz, 3H, **m**), 1.03 (d, J = 6.9 Hz, 3H, **M**) ppm; **^{13}C NMR** (151 MHz, $CDCl_3$) δ **M** 200.6 (C), 175.7 (C), 160.1 (C), 146.7 (C), 136.5 (C), 127.1 (CH), 125.5 (CH), 105.6 (CH), 71.9 (CH_2), 61.6 (C), 55.8 (CH_3), 41.6 (CH), 35.3 (CH_2), 10.6 (CH_3) **m** 201.5 (C), 175.6 (C), 160.1 (C), 146.0 (C), 135.9 (C), 127.3 (CH), 125.5 (CH), 106.0 (CH), 73.7 (CH_2), 62.6 (C), 55.8 (CH_3), 37.7 (CH), 31.3 (CH_2), 15.5 (CH_3) ppm; **HRMS** (EI+) *m/z* calculated for $C_{14}H_{14}O_4^{\bullet+}$ $[M]^{\bullet+}$ 246.08866, found 246.08853.

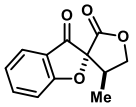
6'-((tert-butyldimethylsilyl)oxy)-4-methyl-4,5-dihydro-2H-spiro[furan-3,2'-indene]-1',2(3'H)-dione (3.60m/m')[§]



Prepared according to GP6 with substrate **3.59m** on 0.2 mmol scale and purified by flash column chromatography (SiO_2, 10–20% EtOAc/hexanes) for 72 h to give **3.60m/m'** as amorphous beige solid (condition A: 33 mg, 48%, 2.8:1 dr; condition B: 52 mg, 75%, 3.4:1 dr). R_f 0.33 (20% EtOAc/hexanes); **^{1}H NMR** (400 MHz, $CDCl_3$) δ 7.39 – 7.34 (m, 1H, **M** + **m**), 7.16 – 7.09 (m, 2H, **M** + **m**), 4.91 (dd, J = 8.6, 6.5 Hz, 1H, **m**), 4.49 (dd, J = 11.1, 8.5 Hz, 1H, **M**), 4.40 (dd, J = 8.2, 8.2 Hz, 1H, **M**), 4.02 (dd, J = 8.6, 4.1 Hz, 1H, **m**), 3.68 (dd, J = 17.0, 0.9 Hz, 1H, **M**), 3.34 (d, J = 17.0 Hz, 1H, **m**), 3.20 (d, J = 17.0 Hz, 1H, **m**), 3.02 – 2.89 (m, 1H, **m**), 2.95 (d, J = 17.0 Hz, 1H, **M**), 2.83 (ddd, J = 11.1, 7.7, 6.9 Hz, 1H, **M**), 1.16 (d, J = 7.1 Hz, 3H, **m**), 1.02 (d, J = 6.9 Hz, 3H, **M**), 0.98 (s, 9H, **M** + **m**), 0.21 (s, 6H, **M + m**) ppm; **^{13}C NMR** (126 MHz, $CDCl_3$) δ **M** 200.5 (C), 175.8 (C), 156.1 (C), 146.7 (C), 136.6 (C),

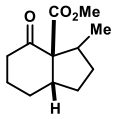
129.2 (CH), 127.1 (CH), 114.0 (CH), 71.8 (CH_2), 61.6 (C), 41.7 (CH), 35.4 (CH_2), 25.7 (CH_3, 3C), 18.3 (C), 10.5 (CH_3), -4.3 (CH_3), -4.4 (CH_3) **m** 201.4 (C), 175.6 (C), 156.0 (C), 146.1 (C), 136.0 (C), 129.2 (CH), 127.2 (CH), 114.4 (CH), 73.7 (CH_2), 62.6 (C), 37.8 (CH), 31.3 (CH_2), 25.7 (CH_3, 3C), 18.3 (C), 15.6 (CH_3), -4.3 (CH_3), -4.4 (CH_3) ppm; **HRMS** (EI+) *m/z* calculated for $C_{19}H_{26}O_4Si^{\bullet+}$ $[M]^{\bullet+}$ 346.15949, found 346.16075.

4'-methyl-4',5'-dihydro-2'H,3H-spiro[benzofuran-2,3'-furan]-2',3-dione (3.60n/n')



Prepared according to GP6 with substrate **3.59n** on 0.2 mmol scale and purified by flash column chromatography (SiO_2, 10–20% EtOAc/hexanes) to give **3.60n/n'** as an amorphous beige solid (condition A: 15.1 mg, 35%, 5:1 dr; condition B: 20.7 mg, 47%, 3.8:1 dr). R_f 0.33 (25% EtOAc/hexanes); **^{1}H NMR** (500 MHz, $CDCl_3$) δ 7.71 – 7.64 (m, 2H, **2M** + **2m**), 7.26 – 7.22 (m, 1H, **M** + **m**), 7.20 – 7.14 (m, 1H, **M** + **m**), 4.85 (dd, J = 8.8, 6.7 Hz, 0.15H, **m**), 4.57 – 4.42 (m, 2H, **2M**), 4.17 (dd, J = 8.8, 5.0 Hz, 0.15H, **m**), 3.21 (ddq, J = 10.8, 8.7, 6.8 Hz, 1H, **M**), 3.04 (qdd, J = 7.0, 7.0, 5.0 Hz, 0.15H, **m**), 1.21 (d, J = 7.1 Hz, 0.45H, **3m**), 1.12 (d, J = 6.9 Hz, 3H, **3M**) ppm; **^{13}C NMR** (101 MHz, $CDCl_3$) δ **M** 195.2 (C), 173.5 (C), 169.5 (C), 139.1 (CH), 125.0 (CH), 123.4 (CH), 119.9 (C), 113.8 (CH), 90.2 (C), 70.3 (CH_2), 39.3 (CH), 9.7 (CH_3) **m** 196.2 (C), 172.7 (C), 169.5 (C), 139.0 (CH), 125.1 (CH), 123.4 (CH), 119.8 (C), 113.8 (CH), 89.4 (C), 72.4 (CH_2), 38.0 (CH), 12.2 (CH_3) ppm; **HRMS** (EI+) *m/z* calculated for $C_{12}H_{10}O_4^{\bullet+}$ $[M]^{+\bullet}$ 218.05736, found 218.05562.

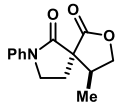
methyl 3-methyl-4-oxooctahydro-3aH-indene-3a-carboxylate (3.60o/o')



Prepared according to GP6 with substrate **3.59o** on 0.2 mmol scale and purified by flash column chromatography (SiO_2, 2–5% EtOAc/hexanes) to give **3.60o/o'** as an amber oil (condition A: 29 mg, 69%, 1:1 dr; condition B: 32 mg, 77%, 1.2:1 dr). R_f 0.41 (10% EtOAc/hexanes, visualized with *p*-anisaldehyde stain); **^{1}H NMR** (400 MHz, $CDCl_3$) δ 3.73 (s, 1.71H, **3M**), 3.70 (s, 1.29H, **3m**), 3.10 – 2.95 (m, 0.86H, **2m**), 2.92 – 2.81 (m, 0.57H, **M**), 2.52 – 2.28 (m, 2H **2M** + **2m**), 2.26 – 2.17 (m, 0.57H, **M**), 2.06 – 1.62 (m, 5H, **5M** + **5m**), 1.62 – 1.44 (m, 2H, **2M** + **2m**), 1.33 – 1.18 (m, 1H, **M** + **m**), 1.16 (d, J = 7.2 Hz, 1.71H, **3M**), 0.85 (d, J = 7.2 Hz, 1.29H, **3m**) ppm; **^{13}C NMR** (101 MHz, $CDCl_3$) δ 209.7 (C), 207.7 (C), 173.6 (C), 171.4 (C), 69.6 (C), 68.2 (C), 52.6 (CH_3), 52.3 (CH_3), 47.8 (CH), 45.4 (CH), 43.8 (CH), 42.3 (CH_2), 40.9 (CH_2), 36.7 (CH), 32.0 (CH_2), 31.2 (CH_2), 28.4 (CH_2), 27.5 (CH_2),

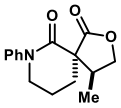
26.6 (CH_2), 25.6 (CH_2), 23.5 (CH_2), 23.2 (CH_2), 17.9 (CH_3), 15.8 (CH_3) ppm; **HRMS** (EI+) *m/z* calculated for $C_{12}H_{18}O_3^{\bullet+}$ $[M]^+$ 210.12505, found 210.12366.

4-methyl-7-phenyl-2-oxa-7-azaspiro[4.4]nonane-1,6-dione (3.60p/p')



Prepared according to GP6 with substrate **3.59p** on 0.2 mmol scale and purified by flash column chromatography (SiO_2, 20–40% EtOAc/hexanes) to give **3.60p/p'** as a crystalline white solid (condition A: 25.3 mg, 52%, 4.5:1 dr; condition B: 0%). R_f 0.32 (40% EtOAc/hexanes); **^{1}H NMR** (600 MHz, $CDCl_3$) δ 7.67 – 7.56 (m, 2H, **2M** + **2m**), 7.44 – 7.34 (m, 2H, **2M** + **2m**), 7.24 – 7.17 (m, 1H, **M** + **m**), 4.83 (dd, J = 8.6, 6.7 Hz, 0.2H, **m**), 4.43 – 4.34 (m, 1.6H, **2M**), 4.21 (ddd, J = 9.3, 8.4, 7.3 Hz, 0.2H, **m**), 4.05 (td, J = 9.2, 5.2 Hz, 0.8H, **M**), 3.98 (dd, J = 8.6, 4.6 Hz, 0.2H, **m**), 3.88 (ddd, J = 9.5, 8.6, 5.9 Hz, 0.8H, **M**), 3.82 (td, J = 9.0, 2.8 Hz, 0.2H, **m**), 3.06 (ddddd, J = 7.1, 7.1, 4.5 Hz, 0.2H, **m**), 2.79 (ddd, J = 13.2, 8.9, 5.9 Hz, 0.8H, **M**), 2.73 – 2.62 (m, 0.8H, **M**), 2.42 (ddd, J = 12.9, 7.3, 2.8 Hz, 0.2H, **m**), 2.28 (dt, J = 13.0, 8.5 Hz, 0.2H, **m**), 2.12 (ddd, J = 13.5, 8.6, 5.2 Hz, 0.8H, **M**), 1.24 (d, J = 6.9 Hz, 2.4H, **3M**), 1.15 (d, J = 7.2 Hz, 0.6H, **3m**) ppm; **^{13}C NMR** (151 MHz, $CDCl_3$) δ **M** 176.3 (C), 168.7 (C), 138.6 (C), 129.1 (2 × CH), 125.6 (CH), 120.5 (2 × CH), 72.2 (CH_2), 57.3 (C), 46.7 (CH_2), 41.4 (CH), 26.7 (CH_2), 10.7 (CH_3) **m** 176.0 (C), 170.2 (C), 138.9 (C), 129.1 (2 × CH), 125.5 (CH), 120.4 (2 × CH), 73.8 (CH_2), 57.7 (C), 46.3 (CH_2), 36.6 (CH), 23.9 (CH_2), 14.6 (CH_3) ppm; **HRMS** (EI+) *m/z* calculated for $C_{14}H_{15}NO_3^{\bullet+}$ $[M]^{\bullet+}$ 245.10464, found 245.10772.

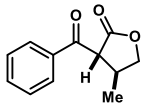
4-methyl-7-phenyl-2-oxa-7-azaspiro[4.5]decane-1,6-dione (3.60q/q')



Prepared according to GP6 with substrate **3.59q** on 0.2 mmol scale and purified by flash column chromatography (SiO_2, 4–8% EtOAc/DCM) to give **3.60q/q'** as an amorphous beige solid (condition A: 19.8 mg, 38%, 4.0:1 dr; condition B: 8.5 mg, 22%, 2.6:1 dr). R_f 0.38 (10% EtOAc/DCM); **^{1}H NMR** (600 MHz, $CDCl_3$) δ 7.44 – 7.36 (m, 3H, **M** + **m**), 7.30 – 7.26 (m, 1H, **M** + **m**), 7.26 – 7.21 (m, 2H, **M** + **m**), 4.64 (dd, J = 8.5, 7.1 Hz, 0.3H, **m**), 4.33 (dd, J = 8.2, 8.2 Hz, 1H, **M**), 4.25 (dd, J = 10.7, 8.2 Hz, 1H, **M**), 3.90 (dd, J = 8.5, 6.8 Hz, 0.3H, **m**), 3.79 – 3.56 (m, 3.3H, **M** + **m**), 3.39 – 3.32 (m, 0.3H, **m**), 2.62 – 2.52 (m, 1H, **M**), 2.49 (ddd, J = 13.5, 9.6, 3.5 Hz, 1H, **M**), 2.41 (ddtd, J = 13.4, 9.9, 6.6, 3.3 Hz, 0.3H, **m**), 2.38 – 2.25 (m, 1.3H, **M** + **m**), 2.25 – 1.98 (m, 2.27H, **M** + **m**), 1.93 (ddd, J = 13.8, 8.3, 3.4 Hz, 1.3H, **M** + **m**), 1.27 (d, J = 6.8 Hz, 3H, **3M**), 1.12 (d, J = 7.1 Hz, 0.9H, **3m**) ppm; **^{13}C**

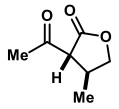
NMR (151 MHz, $CDCl_3$) δ **M** 177.5 (C), 166.2 (C), 142.7 (C), 129.5 (2 × CH), 127.5 (CH), 126.4 (2 × CH), 72.7 (CH_2), 54.2 (C), 52.1 (CH_2), 43.8 (CH), 32.2 (CH_2), 20.5 (CH_2), 12.3 (CH_3) **m** 176.7 (C), 167.6 (C), 143.0 (C), 129.4 (2 × CH), 127.3 (CH), 126.3 (2 × CH), 73.0 (CH_2), 54.2 (C), 51.7 (CH_2), 38.1 (CH), 24.6 (CH_2), 19.4 (CH_2), 13.4 (CH_3) ppm; **HRMS** (EI+) *m/z* calculated for $C_{15}H_{17}NO_3^{\bullet+}$ $[M]^{\bullet+}$ 259.12029, found 259.11864.

3-benzoyl-4-methyldihydrofuran-2(3H)-one (3.60r/r')[§]



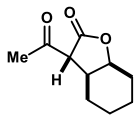
Prepared according to GP6 with substrate **3.59r** on 0.2 mmol scale and purified by flash column chromatography (SiO_2, 45–55% Et_2O/hexanes) to give **3.60r/r'** as an amber oil (condition A: 27.8 mg, 68%, 10:1 dr; condition B: 21 mg, 50%, 8.3:1 dr). R_f 0.23 (50% Et_2O/hexanes); **^{1}H NMR** (500 MHz, $CDCl_3$) δ 8.09 – 8.01 (m, 2H), 7.66 – 7.59 (m, 1H), 7.56 – 7.47 (m, 2H), 4.60 (dd, J = 8.8, 7.2 Hz, 1H), 4.18 (d, J = 7.1 Hz, 1H), 3.99 (dd, J = 8.7, 6.7 Hz, 1H), 3.25 (hept, J = 6.9 Hz, 1H), 1.24 (d, J = 6.8 Hz, 3H) ppm; **^{13}C NMR** (126 MHz, $CDCl_3$) δ 192.9 (C), 172.7 (C), 135.9 (C), 134.2 (CH), 129.5 (CH, 2C), 129.0 (CH, 2C), 73.8 (CH_2), 56.2 (CH), 34.4 (CH), 17.5 (CH_3) ppm; **HRMS** (EI+) *m/z* calculated for $C_{12}H_{12}O_3^{\bullet+}$ $[M]^{\bullet+}$: 204.07810, found 204.07851.

3-acetyl-4-methyldihydrofuran-2(3H)-one (3.60s/s')[§]



Prepared according to GP6 with substrate **3.59s** on 0.4 mmol scale and purified by flash column chromatography (SiO_2, 20–50% Et_2O/hexanes) to give **3.60s/s'** as an amorphous white solid (condition A: 7.3 mg, 13%, 20:1 dr; condition B: 11 mg, 39%, 4.6:1 dr). R_f 0.20 (30% Et_2O/hexanes); **^{1}H NMR** (400 MHz, $CDCl_3$) δ 4.43 (dd, J = 8.8, 7.6 Hz, 1H), 3.82 (dd, J = 8.8, 7.8 Hz, 1H), 3.26 (d, J = 8.5 Hz, 1H), 3.14 – 3.00 (m, 1H), 2.42 (s, 3H), 1.14 (d, J = 6.8 Hz, 3H) ppm; **^{13}C NMR** (101 MHz, $CDCl_3$) δ 200.3 (C), 172.5 (C), 73.3 (CH_2), 60.7 (CH_3), 32.3 (CH), 30.0 (CH), 17.1 (CH_3) ppm; **HRMS** (EI+) *m/z* calculated for $C_7H_{10}O_3^{\bullet+}$ $[M]^{\bullet+}$ 142.06245, found 142.06254.

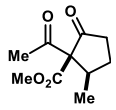
3-acetylhexahydrobenzofuran-2(3H)-one (3.60t/t')[§]



Prepared according to GP6 with substrate **3.59t** on 0.4 mmol scale and purified by flash column chromatography (SiO_2, 30–40% Et_2O/hexanes) to give **3.60t/t'** as a clear, colourless oil (condition A: 6 mg, 14%, 16:1

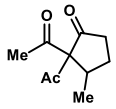
dr; condition B: 25.5 mg, 70%, 19:1 dr). R_f 0.26 (30% Et_2O/hexanes); **^{1}H NMR** (600 MHz, $CDCl_3$) δ 4.67 – 4.57 (m, 1H), 3.44 (d, J = 4.4 Hz, 1H), 2.91 – 2.83 (m, 1H), 2.41 (s, 3H), 1.95 – 1.86 (m, 1H), 1.84 – 1.77 (m, 1H), 1.77 – 1.70 (m, 1H), 1.62 – 1.58 (m, 1H), 1.55 – 1.44 (m, 2H), 1.43 – 1.34 (m, 2H) ppm; **^{13}C NMR** (101 MHz, $CDCl_3$) δ 200.4 (C), 172.7 (C), 78.8 (CH), 61.8 (CH), 36.7 (CH_3), 29.7 (CH), 28.1 (CH_2), 26.3 (CH_2), 22.4 (CH_2), 20.3 (CH_2) ppm;

methyl 1-acetyl-2-methyl-5-oxocyclopentane-1-carboxylate (3.60u/u')[§]



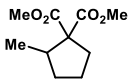
Prepared according to GP6 with substrate **3.59u** on 0.2 mmol scale and purified by flash column chromatography (SiO_2, 10–50% Et_2O/hexanes) to give **3.60u/u'** as an amber oil (condition A: 24.9 mg, 64%, 1.1:1 dr; condition B: 11.7 mg, 30%, 1:1 dr). R_f 0.31 (20% Et_2O/hexanes); **^{1}H NMR** (400 MHz, C_6D_6) δ 3.39 (s, 3H), 2.80 – 2.65 (m, 1H), 2.32 – 2.20 (m, 1H), 2.06 (s, 3H), 1.97 – 1.84 (m, 1H), 1.56 – 1.46 (m, 2H), 1.05 (d, J = 7.0 Hz, 3H) ppm; **^{13}C NMR** (101 MHz, C_6D_6) δ 207.8 (C), 201.6 (C), 168.4 (C), 77.4 (C), 52.3 (CH_3), 40.6 (CH), 38.3 (CH_2), 30.6 (CH_3), 27.6 (CH_2), 15.6 (CH_3) ppm; **HRMS** (EI+) *m/z* calculated for $C_8H_{12}O_3^{\bullet+}$ [M – C_2H_2O]$^{\bullet+}$ 156.07810, found 156.07855.

1,1'-(4-methyl-2-oxotetrahydrofuran-3,3-diyl)bis(ethan-1-one) (3.60v/v')[§]



Prepared according to GP6 with substrate **3.59v** on 0.2 mmol scale and purified by flash column chromatography (SiO_2, 40–50% Et_2O/hexanes) to give **3.60v/v'** as an amber oil (condition A: 13.7 mg, 38% + **5s** 10.6 mg, 37%, 10:1 dr; condition B: 20 mg, 55% + **5s** 7 mg, 25%, 10:1 dr). R_f 0.39 (50% Et_2O/hexanes); **^{1}H NMR** (400 MHz, $CDCl_3$) δ 4.42 (dd, J = 8.9, 7.5 Hz, 1H), 3.91 (dd, J = 9.0, 8.0 Hz, 1H), 3.43 – 3.30 (m, 1H), 2.37 (s, 3H), 2.33 (s, 3H), 1.06 (d, J = 7.1 Hz, 3H) ppm; **^{13}C NMR** (101 MHz, $CDCl_3$) δ 200.3 (C), 197.7 (C), 171.4 (C), 72.4 (CH_2), 36.3 (CH_3), 30.6 (CH_3), 28.1 (CH), 13.6 (CH_3) ppm; **HRMS** (EI+) *m/z* calculated for $C_9H_{12}O_4^{\bullet+}$ [M]$^{\bullet+}$: 184.07301, found 184.07143.

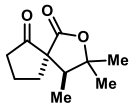
dimethyl 2-methylcyclopentane-1,1-dicarboxylate (3.60w/w')[§]



Prepared according to GP6 with substrate **3.59w** on 0.2 mmol scale and purified by flash column chromatography (SiO_2, 5–20% Et_2O/hexanes) to give **3.60w/w'** as a clear, colourless oil (condition A: trace; condition

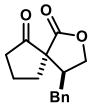
B: 10.8 mg, 27% isolated, 60% ^{1}H NMR). ***R**f* 0.34 (20% Et_2O/hexanes); **^{1}H NMR** (600 MHz, $CDCl_3$) δ 3.71 (dd, J = 8.1, 0.5 Hz, 6H), 2.68 (dp, J = 8.9, 7.1 Hz, 1H), 2.43 (ddd, J = 13.7, 8.8, 7.6 Hz, 1H), 2.02 (ddd, J = 14.0, 9.4, 4.8 Hz, 1H), 1.96 – 1.88 (m, 1H), 1.86 – 1.77 (m, 1H), 1.61 – 1.52 (m, 1H), 1.40 (dq, J = 12.5, 8.7 Hz, 1H), 0.97 (dd, J = 7.1, 0.4 Hz, 3H) ppm; **^{13}C NMR** (151 MHz, $CDCl_3$) δ 173.2 (C), 172.0 (C), 63.9 (C), 52.5 (CH_3), 52.1 (CH_3), 41.0 (CH), 34.1 (CH_2), 33.6 (CH_2), 23.0 (CH_2), 16.6 (CH_3) ppm; Characterized according to literature comparison. [356]

3,3,4-trimethyl-2-oxaspiro[4.4]nonane-1,6-dione (3.60x/x')



Prepared according to GP6 with substrate **3.59x** on 0.2 mmol scale and purified by flash column chromatography (SiO_2, 20–40% Et_2O/hexanes) to give **3.60x/x'** as a pale-yellow oil (condition A: 32.5 mg, 83%, 1:1 dr; condition B: 28.1 mg, 72%, 1:1 dr). ***R**f* 0.26 (40% Et_2O/hexanes); **^{1}H NMR** (400 MHz, $CDCl_3$) δ 2.88 (q, J = 7.3 Hz, 1H), 2.69 – 2.52 (m, 2H), 2.49 – 2.08 (m, 8H), 2.09 – 1.88 (m, 3H), 1.47 (s, 3H), 1.47 (s, 3H), 1.41 (s, 3H), 1.27 (s, 3H), 1.03 (d, J = 7.3 Hz, 3H), 0.90 (d, J = 7.3 Hz, 3H) ppm; **^{13}C NMR** (101 MHz, $CDCl_3$) δ 214.2 (C), 213.3 (C), 175.1 (C), 175.1 (C), 86.1 (C), 86.1 (C), 61.8 (C), 61.0 (C), 50.3 (CH), 45.3 (CH), 39.7 (CH_2), 37.4 (CH_2), 36.8 (CH_2), 29.9 (CH_2), 29.2 (CH_3), 27.3 (CH_3), 23.7 (CH_3), 23.5 (CH_3), 20.1 (CH_2), 19.3 (CH_2), 10.2 (CH_3), 9.8 ppm (CH_3); **HRMS** (EI+) *m/z* calculated for $C_{11}H_{16}O_3^{\bullet+}$ $[M]^{+\bullet}$ 196.10940, found 196.11185.

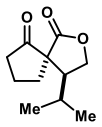
4-benzyl-2-oxaspiro[4.4]nonane-1,6-dione (3.60y/y')



Prepared according to GP6 with substrate **3.59y** on 0.2 mmol scale and purified by flash column chromatography (SiO_2, 10–20% EtOAc/hexanes) to give **3.60y/y'** as a clear, colourless oil (condition A: 25.1 mg, 52%, 1.8:1 dr; condition B: 8.2 mg, 17%, 1.7:1 dr). ***R**f* 0.23 (20% EtOAc/hexanes); **^{1}H NMR** (400 MHz, $CDCl_3$) δ 7.35 – 7.21 (m, 3H, **3M** + **3m**), 7.18 – 7.11 (m, 2H, **2M** + **2m**), 4.43 (dd, J = 9.0, 6.8 Hz, 0.33H, **m**), 4.34 (dd, J = 10.3, 8.6 Hz, 0.66H, **M**), 4.17 (dd, J = 8.6, 7.5 Hz, 0.66H, **M**), 3.99 (dd, J = 9.0, 5.6 Hz, 0.33H, **m**), 3.08 (dddd, J = 11.0, 6.8, 5.5, 5.5 Hz, 0.33H, **m**), 2.93 – 2.72 (m, 2.33H, **3M + m** or **2M + 3m**), 2.62 – 2.12 (m, 4.66H, **5M** + **4m**), 2.03 – 1.93 (m, 0.33H, **m**), 1.92 – 1.72 (m, 1.33H, **M** + **2m** or **2M**) ppm; **^{13}C NMR** (101 MHz, $CDCl_3$) δ 214.0 (C), 175.5 (C), 137.7 (C), 129.1 (2 × CH), 128.7 (2 × CH), 127.2 (CH), 71.1 (CH_2), 59.8 (C), 47.7 (CH), 39.9 (CH_2), 33.3 (CH_2), 33.0 (CH_2), 20.1 (CH_2) **m** 213.6 (C), 175.3 (C), 137.5 (C), 129.0 (2 × CH), 128.9 (2 × CH), 127.1 (CH), 70.5

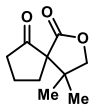
(CH_2), 60.6 (C), 43.1 (CH), 37.5 (CH_2), 34.7 (CH_2), 28.7 (CH_2), 19.4 (CH_2) ppm; **HRMS** (ESI+) *m/z* calculated for $C_{15}H_{16}O_3Na^+$ $[M + Na]^+$ 267.0997, found 267.1010.

4-isopropyl-2-oxaspiro[4.4]nonane-1,6-dione (3.60z/z')[§]



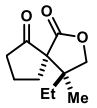
Prepared according to GP6 with substrate **3.59z** on 0.2 mmol scale and purified by flash column chromatography (SiO_2, 20–40% Et_2O/hexanes) to give **3.60z/z'** as a clear, colourless oil and the minor diastereomer as an amorphous white solid (condition A: 31 mg, 79%, 1.2:1 dr; condition B: 26.1 mg, 67%, 1.1:1 dr). R_f 0.40 (40% Et_2O/hexanes); **^{1}H NMR** (400 MHz, $CDCl_3$) δ **M** 4.37 (t, J = 8.4 Hz, 1H), 4.25 (dd, J = 10.8, 8.6 Hz, 1H), 2.58 – 2.29 (m, 4H), 2.27 – 2.01 (m, 4H), 0.95 (d, J = 6.6 Hz, 3H), 0.88 (d, J = 6.6 Hz, 3H) **m** 4.51 (dd, J = 8.9, 7.5 Hz, 1H), 3.99 (dd, J = 8.9, 7.8 Hz, 1H), 2.67 – 2.51 (m, 2H), 2.38 – 2.27 (m, 3H), 2.19 – 1.97 (m, 3H), 1.75 (dt, J = 7.9, 6.7 Hz, 1H), 0.87 (d, J = 6.7 Hz, 3H), 0.82 (d, J = 6.7 Hz, 3H) ppm; **^{13}C NMR** (101 MHz, $CDCl_3$) δ **M** 214.0 (C), 176.1 (C), 71.3 (CH_2), 59.8 (C), 52.1 (CH), 39.4 (CH_2), 34.1 (CH_2), 27.4 (CH), 22.4 (CH_3), 21.0 (CH_3), 19.9 (CH_2) **m** 214.2 (C), 175.9 (C), 69.5 (CH_2), 59.7 (C), 47.9 (CH), 37.4 (CH_2), 27.7 (CH_2), 27.3 (CH), 21.6 (CH_3), 19.2 (CH_2), 18.9 (CH_3) ppm; **HRMS** (EI+) *m/z* calculated for $C_{11}H_{16}O_3^{\bullet+}$ $[M]^{\bullet+}$ 196.10940, found 196.10695.

4,4-dimethyl-2-oxaspiro[4.4]nonane-1,6-dione (3.60aa/aa')[§]

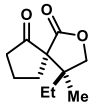


Prepared according to GP6 with substrate **3.59aa** on 0.2 mmol scale and purified by flash column chromatography (SiO_2, 20–40% Et_2O/hexanes) to give **3.60aa/aa'** as a yellow oil (condition A: 26.2 mg, 73%; condition B: 16.7 mg, 46%). R_f 0.20 (10% EtOAc/hexanes); **^{1}H NMR** (400 MHz, $CDCl_3$) δ 4.53 (dd, J = 8.2, 0.9 Hz, 1H), 3.90 (d, J = 8.2 Hz, 1H), 2.48 – 2.29 (m, 2H), 2.29 – 2.10 (m, 2H), 2.06 – 1.91 (m, 2H), 1.08 (d, J = 0.8 Hz, 3H), 1.05 (s, 3H) ppm; **^{13}C NMR** (101 MHz, $CDCl_3$) δ 213.7 (C), 175.2 (C), 77.32 (CH2), 64.9 (C), 42.9 (C), 39.5 (CH_2), 27.9 (CH_2), 25.0 (CH_3), 19.7 (CH_2), 18.9 (CH_3) ppm; **HRMS** (EI+) *m/z* calculated for $C_{10}H_{14}O_3^{\bullet+}$ $[M]^{\bullet+}$ 182.09375, found 182.09256

4-ethyl-4-methyl-2-oxaspiro[4.4]nonane-1,6-dione (3.60ab/ab')[§]

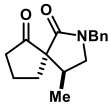


Prepared according to GP6 with substrate **3.59ab** on 0.2 mmol scale and purified by flash column chromatography (SiO_2, 20% Et_2O/hexanes) to give **3.60ab/ab'** as a yellow oil (condition A: 34 mg, 87%, 4:1 dr; condition B: 20.5 mg, 53%, 3:1 dr).



Prepared according to GP6 under cerium-containing conditions with substrate **3.59ab'** on 0.2 mmol scale and purified by flash column chromatography (SiO_2, 20% Et_2O/hexanes) to give **3.60ab/ab'** as a yellow oil (condition A: 38 mg, 92%, 3:1 dr). R_f 0.40 (30% Et_2O/hexanes); **^{1}H NMR** (500 MHz, $CDCl_3$) δ 4.53 (dq, J = 8.3, 1.0 Hz, 1H, **M**), 4.41 (dt, J = 8.7, 0.8 Hz, 1H, **m**), 4.10 (d, J = 8.6 Hz, 1H, **m**), 3.92 (d, J = 8.2 Hz, 1H, **M**), 2.47 – 2.29 (m, 2H, **M** + **m**), 2.29 – 2.10 (m, 2H, **M** + **m**), 2.04 – 1.92 (m, 2H, **M** + **m**), 1.58 (q, J = 7.5 Hz, 1H, **m**), 1.57 (q, J = 7.5 Hz, 1H, **M**), 1.47 (q, J = 7.5 Hz, 1H, **M**), 1.45 (q, J = 7.6 Hz, 1H, **m**), 1.08 (d, J = 0.9 Hz, 3H, **M**), 0.99 (s, 3H, **m**), 0.89 (t, J = 7.5 Hz, 3H, **m**), 0.87 (t, J = 7.6 Hz, 3H, **M**) ppm; **^{13}C NMR** (126 MHz, $CDCl_3$) δ **M** 213.9 (C), 175.4 (C), 76.7 (CH_2), 65.5 (C), 46.4 (C), 39.8 (CH_2), 28.5 (CH_2), 25.6 (CH_2), 20.9 (CH_3), 19.6 (CH_2), 8.6 (CH_3) **m** 214.0 (C), 175.6 (C), 73.5 (CH_2), 64.8 (C), 45.8 (C), 39.6 (CH_2), 29.5 (CH_2), 27.5 (CH_2), 19.7 (CH_2), 17.0 (CH_3), 8.6 (CH_3) ppm; **HRMS** (EI+) *m/z* calculated for $C_{11}H_{14}O_5^{\bullet+}$ $[M]^{\bullet+}$ 196.10940, found 196.10851.

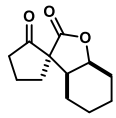
2-benzyl-4-methyl-2-azaspiro[4.4]nonane-1,6-dione (3.60ac/ac')[§]



Prepared according to GP6 with substrate **3.59ac** on 0.2 mmol scale and purified by flash column chromatography (SiO_2, 100% EtOAc) to give **3.60ac/ac'** as an amorphous white solid (condition A: 42.9 mg, 83%, 3:1 dr). R_f 0.33 (70% Et_2O/hexanes); **^{1}H NMR** (400 MHz, $CDCl_3$) δ 7.37 – 7.30 (m, 2H, **M** + **m**), 7.30 – 7.20 (m, 3H, **M** + **m**), 4.55 (d, J = 14.9 Hz, 1H, **M**), 4.48 (d, J = 14.8 Hz, 1H, **m**), 4.44 (d, J = 14.9 Hz, 1H, **M**), 4.41 (d, J = 14.8 Hz, 1H, **m**), 3.60 (dd, J = 9.4, 7.2 Hz, 1H, **m**), 3.22 (t, J = 9.6 Hz, 1H, **M**), 3.11 (dd, J = 9.2, 8.0 Hz, 1H, **M**), 2.73 (dd, J = 9.4, 4.4 Hz, 1H, **m**), 2.67 – 2.58 (m, 1H, **M**), 2.58 – 2.16 (m, 4H, **M** + **m**), 2.08 – 1.86 (m, 2H, **M** + **m**), 1.03 (d, J = 6.9 Hz, 3H, **M**), 0.94 (d, J = 7.1 Hz, 3H, **m**) ppm; **^{13}C NMR** (101 MHz, $CDCl_3$) δ **M** 217.0 (C), 173.7 (C), 136.3

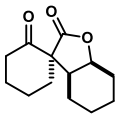
(C), 128.8 (2 × 2C), 128.0 (2 × CH), 127.6 (CH), 62.1 (CH), 51.2 (CH_2), 47.0 (CH_2), 40.0 (CH_2), 38.7 (C), 32.7 (CH_2), 20.6 (CH_2), 12.7 (CH_3) **m** 217.5 (C), 173.0 (C), 128.8 (2 × CH), 128.1 (2 × CH), 127.7 (CH), 62.9 (CH), 52.0 (CH_2), 46.9 (CH_2), 40.0 (CH_2), 38.0 (CH_2), 33.2 (CH), 28.3 (CH_2), 19.7 (CH_2), 15.8 (CH_3) ppm; **HRMS** (EI+) *m/z* calculated for $C_{16}H_{19}NO_2^{\bullet+}$ $[M]^{\bullet+}$ 257.14103, found 257.1424.

hexahydro-2H-spiro[benzofuran-3,1'-cyclopentane]-2,2'-dione (3.60ae/ae')



Prepared according to GP6 with substrate **3.59ae** on 0.2 mmol scale and purified by flash column chromatography (SiO_2, 30–40% Et_2O/hexanes) to give **3.60ae** as a clear colourless oil and **3.60ae'** as an amorphous beige solid (condition A: 40.4 mg, 97%, 2.3:1 dr; condition B: 41 mg, 98%, 2.5:1 dr). R_f major 0.3 minor 0.1 (20% EtOAc/hexanes); **^{1}H NMR** (400 MHz, $CDCl_3$) δ **M** 5.13 – 5.06 (m, 1H), 2.50 – 2.17 (m, 6H), 2.11 – 1.96 (m, 1H), 1.97 – 1.81 (m, 1H), 1.80 – 1.66 (m, 2H), 1.67 – 1.50 (m, 2H), 1.43 – 1.29 (m, 1H), 1.28 – 1.02 (m, 2H) **m** 4.57 (ddd, J = 3.9, 3.8, 3.8 Hz, 1H), 2.45 – 2.20 (m, 6H), 2.22 – 2.09 (m, 1H), 2.01 – 1.85 (m, 1H), 1.79 – 1.55 (m, 3H), 1.59 – 1.33 (m, 3H), 1.21 – 1.04 (m, 1H) ppm; **^{13}C NMR** (101 MHz, $CDCl_3$) δ **M** 213.5 (C), 175.4 (C), 76.6 (CH), 64.9 (C), 41.2 (CH), 37.9 (CH_2), 28.7 (CH_2), 27.4 (CH_2), 24.4 (CH_2), 23.5 (CH_2), 19.6 (CH_2), 19.5 (CH_2) **m** 212.4 (C), 176.8 (C), 77.2 (CH), 62.8 (C), 44.6 (CH), 38.5 (CH_2), 33.6 (CH_2), 27.7 (CH_2), 24.2 (CH_2), 23.1 (CH_2), 20.0 (CH_2), 19.5 (CH_2) ppm; **HRMS** (EI+) *m/z* calculated for $C_{12}H_{16}O_3^{\bullet+}$ $[M]^{+\bullet}$ 208.10940, found 208.10805.

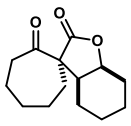
hexahydro-2H-spiro[benzofuran-3,1'-cyclohexane]-2,2'-dione (3.60af/af')



Prepared according to GP6 with substrate **3.59af** on 0.2 mmol scale and purified by flash column chromatography (SiO_2, 10–30% EtOAc/hexanes) to give **3.60af/af'** as an amorphous beige solid (condition A: 19.1 mg, 43%, 1.8:1 dr; condition B: 6.9 mg, 16%, 1.7:1 dr). R_f major 0.30 minor 0.15 (25% EtOAc/hexanes); **^{1}H NMR** (400 MHz, $CDCl_3$) δ **M** 4.43 (ddd, J = 3.5, 3.5, 3.5 Hz, 1H), 2.61 – 2.45 (m, 3H), 2.28 – 2.07 (m, 3H), 1.99 – 1.82 (m, 3H), 1.82 – 1.67 (m, 2H), 1.65 – 1.49 (m, 3H), 1.45 – 1.29 (m, 1H), 1.28 – 1.06 (m, 2H) **m** 4.58 (ddd, J = 3.8, 3.6, 3.6 Hz, 1H), 2.65 (dddd, J = 14.3, 4.0, 4.0, 1.5 Hz, 1H), 2.53 – 2.40 (m, 1H), 2.30 – 2.09 (m, 3H), 2.07 – 1.45 (m, 9H), 1.46 – 1.31 (m, 1H), 1.29 – 1.10 (m, 2H) ppm; **^{13}C NMR** (101 MHz, $CDCl_3$) δ **M** 206.8 (C), 176.0 (C), 76.1 (CH), 66.2 (C), 41.0 (CH), 39.7 (CH_2), 30.1 (CH_2), 27.4 (CH_2), 27.2 (CH_2), 23.6 (CH_2), 23.1 (CH_2), 21.5 (CH_2), 19.7 (CH_2)

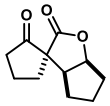
m 205.2 (C), 175.3 (C), 74.9 (CH), 64.2 (C), 41.6 (CH_2), 41.2 (CH), 32.1 (CH_2), 27.7 (CH_2), 26.6 (CH_2), 23.7 (CH_2), 23.4 (CH_2), 22.0 (CH_2), 19.5 (CH_2) ppm; **HRMS** (EI+) *m/z* calculated for $C_{13}H_{18}O_3^{\bullet+}$ $[M]^{\bullet+}$ 222.12505, found 222.12353.

hexahydro-2H-spiro[benzofuran-3,1'-cycloheptane]-2,2'-dione (3.60ag/ag')



Prepared according to GP6 with substrate **3.59ag** on 0.2 mmol scale and purified by flash column chromatography (SiO_2, 10–30% EtOAc/hexanes) to give **3.60ag/ag'** as an amber oil (condition A: 28.3 mg, 60%, 2:1 dr; condition B: 8.0 mg, 17%, 1.8:1 dr). R_f 0.34 (21% EtOAc/hexanes); **^{1}H NMR** (400 MHz, $CDCl_3$) δ **M** 4.52 (ddd, J = 3.6, 3.6, 3.5 Hz, 1H), 2.76 – 2.64 (m, 1H), 2.60 – 2.50 (m, 1H), 2.47 (ddd, J = 12.0, 6.0, 3.9 Hz, 1H), 2.25 – 2.07 (m, 2H), 1.87 – 1.48 (m, 11H), 1.43 – 1.27 (m, 1H), 1.26 – 1.07 (m, 2H) **m** 4.59 (ddd, J = 4.3, 4.2, 4.2 Hz, 1H), 2.62 – 2.46 (m, 2H), 2.42 – 2.26 (m, 2H), 2.15 (dqd, J = 14.8, 4.0, 1.5 Hz, 1H), 1.91 (ddddd, J = 15.0, 13.7, 12.3, 5.2, 2.0 Hz, 2H), 1.87 – 1.74 (m, 1H), 1.71 – 1.53 (m, 3H), 1.54 – 1.30 (m, 4H), 1.27 – 1.09 (m, 1H) ppm; **^{13}C NMR** (101 MHz, $CDCl_3$) δ **M** 208.3 (C), 176.4 (C), 76.2 (CH), 68.6 (C), 41.3 (CH), 40.7 (CH_2), 30.6 (CH_2), 27.3 (3 × CH_2), 24.7 (CH_2), 23.7 (CH_2), 23.6 (CH_2), 19.7 (CH_2) **m** 208.4 (C), 175.7 (C), 75.0 (CH), 65.3 (C), 45.9 (CH), 42.5 (CH_2), 33.0 (CH_2), 30.5 (CH_2), 27.6 (CH_2), 26.6 (CH_2), 24.5 (CH_2), 24.3 (CH_2), 22.9 (CH_2), 19.9 (CH_2) ppm; **HRMS** (EI+) *m/z* calculated for $C_{14}H_{20}O_3^{\bullet+}$ $[M]^{+\bullet}$ 236.14070, found **M** 236.14810, **m** 236.14188.

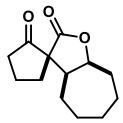
tetrahydro-2'H,4'H-spiro[cyclopentane-1,3'-cyclopenta[b]furan]-2,2'-dione (3.60ah/ah')



Prepared according to GP6 with substrate **3.59ah** on 0.2 mmol scale and purified by flash column chromatography (SiO_2, 10–40% EtOAc/hexanes) to give **3.60ah/ah'** as an amber oil (condition A: 34.6 mg, 89%, 1.1:1 dr; condition B: 5.8 mg, 15%, 1:1 dr). R_f major 0.33, minor 0.11 (22% EtOAc/hexanes); **^{1}H NMR** (400 MHz, $CDCl_3$) δ **M** 5.18 (ddd, J = 5.8, 5.8, 1.7 Hz, 1H), 2.73 (ddd, J = 9.0, 6.1, 6.1 Hz, 1H), 2.53 – 2.27 (m, 4H), 2.08 – 1.49 (m, 8H) **m** 4.97 (ddd, J = 6.7, 4.9, 1.9 Hz, 1H), 2.74 – 2.63 (m, 1H), 2.46 – 2.31 (m, 3H), 2.26 – 2.12 (m, 2H), 2.07 – 1.86 (m, 2H), 1.88 – 1.74 (m, 3H), 1.69 – 1.49 (m, 2H) ppm; **^{13}C NMR** (101 MHz, $CDCl_3$) δ **M** 214.3 (C), 174.9 (C), 84.7 (CH), 62.6 (C), 47.4 (CH), 37.4 (CH_2), 33.2 (CH_2), 30.4 (CH_2), 27.9 (CH_2), 24.1 (CH_2), 19.8 (CH_2) **m** 213.3 (C),

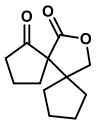
176.8 (C), 84.8 (CH), 60.6 (C), 49.9 (CH), 38.3 (CH_2), 37.4 (CH_2), 32.6 (CH_2), 27.9 (CH_2), 24.3 (CH_2), 20.1 (CH_2) ppm; **HRMS** (EI+) *m/z* calculated for $C_{11}H_{14}O_3^{\bullet+}$ $[M]^{+\bullet}$ 194.09375, found **M** 194.09580, **m** 194.09311.

hexahydro-2H,4H-spiro[cyclohepta[b]furan-3,1'-cyclopentane]-2,2'-dione (3.60ai/ai')



Prepared according to GP6 with substrate **3.59ai** on 1.0 mmol scale under condition A and 0.2 mmol scale under condition B and purified by flash column chromatography (SiO_2, 5–15% EtOAc/hexanes) to give **3.60ai/ai'** as a pale-yellow oil (condition A: 148 mg, 67%, 1.8:1 dr; condition B: 18.7 mg, 42%, 2.6:1 dr). R_f 0.38 (20% EtOAc/hexanes); **^{1}H NMR** (400 MHz, $CDCl_3$) δ 5.00 (ddd, J = 10.7, 7.2, 4.6 Hz, 0.59H, **M**), 4.67 (ddd, J = 10.5, 10.4, 4.4 Hz, 0.41H, **m**), 2.66 (ddd, J = 11.1, 7.2, 3.7 Hz, 0.59H, **M**), 2.62 – 2.54 (m, 0.41H, **m**), 2.54 – 2.12 (m, 5H, **M** & **m**), 2.12 – 1.16 (m, 11H, **M** & **m**) ppm; **^{13}C NMR** (101 MHz, $CDCl_3$) δ 214.4 (C), 214.3 (C), 175.0 (C), 174.7 (C), 82.6 (CH), 82.3 (CH), 62.8 (C), 62.4 (C), 52.6 (CH), 46.5 (CH), 40.0 (CH_2), 37.1 (CH_2), 33.4 (CH_2), 32.7 (CH_2), 31.3 (CH_2), 30.8 (CH_2), 29.7 (CH_2), 28.3 (CH_2), 27.3 (CH_2), 25.5 (CH_2), 25.4 (CH_2), 24.6 (CH_2), 24.5 (CH_2), 23.2 (CH_2), 20.4 (CH_2), 19.5 (CH_2) ppm; **HRMS** (EI+) *m/z* calculated for $C_{13}H_{18}O_3^{\bullet+}$ $[M]^{+\bullet}$ 222.12505, found 222.12413.

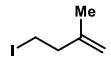
12-oxadispiro[4.0.46.35]tridecane-1,13-dione (3.60aj/aj')



Prepared according to GP6 with substrate **3.59aj** on 0.2 mmol scale and purified by flash column chromatography (SiO_2, 6–12% EtOAc/hexanes) to give **3.60aj/aj'** as an amorphous beige solid (condition A: 14.5 mg, 20%; condition B: 15.1 mg, 28%). R_f 0.24 (15% EtOAc/hexanes); **^{1}H NMR** (400 MHz, $CDCl_3$) δ 4.56 (dd, J = 8.1, 1.8 Hz, 1H), 3.99 (d, J = 8.1 Hz, 1H), 2.51 – 2.32 (m, 2H), 2.34 – 2.14 (m, 2H), 2.09 – 1.85 (m, 2H), 1.88 – 1.40 (m, 8H) ppm; **^{13}C NMR** (101 MHz, $CDCl_3$) δ 213.7 (C), 175.1 (C), 77.2 (CH_2), 63.2 (C), 53.9 (C), 39.2 (CH_2), 34.6 (CH_2), 30.2 (CH_2), 28.8 (CH_2), 24.1 (CH_2), 23.7 (CH_2), 19.6 (CH_2) ppm; **HRMS** (EI+) *m/z* calculated for $C_{12}H_{16}O_3^{\bullet+}$ $[M]^{\bullet+}$ 208.10940, found 208.11388.

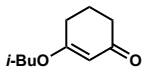
Synthetic Intermediates

4-iodo-2-methylbut-1-ene (3.62)



Prepared according to the following literature adapted procedure.[357] To a solution of triphenylphosphine (14.4 g, 55 mmol, 1.1 equiv, freshly-ground) and imidazole (3.7 g, 55 mmol, 1.1 equiv) in dichloromethane (170 mL, 0.34 M) were added iodine flakes (14.0 g, 55 mmol, 1.1 equiv) at 0 ºC with vigorous stirring. The mixture transformed from a clear, colourless solution into an orange suspension upon addition of iodine. The resulting orange suspension was stirred for 15 minutes before dropwise addition of 3-methyl-3-buten-1-ol (**3.61**, 5 mL, 50 mmol, 1.0 equiv) over 10 minutes at 0 ºC. Upon complete addition of the alcohol, the ice-water bath was removed, and the suspension was allowed to stir at room temperature for 4 hours. The mixture was concentrated to a thick slurry (~1/5 of the original volume) *in vacuo* at 10 ºC, then diluted with pentane (350 mL) and filtered through a pad of Celite. The resulting solution was concentrated *in vacuo* at 10 ºC to give the crude residue as a yellow oil. The crude material was purified by distillation under vacuum (40–44 °C/5 torr) to give **3.62** as a clear colourless oil (7.36 g, 75%). **^{1}H NMR** (400 MHz, $CDCl_3$) δ 4.86 (tq, J = 2.1, 1.3 Hz, 1H), 4.78 – 4.72 (m, 1H), 3.26 (t, J = 7.5 Hz, 2H), 2.63 – 2.53 (m, 2H), 1.79 – 1.69 (m, 3H) ppm; **^{13}C NMR** (101 MHz, $CDCl_3$) δ 144.0 (C), 112.4 (CH_2), 42.0 (CH_2), 21.8 (CH_3), 3.7 (CH_2) ppm; Characterized according to literature comparison.[358]

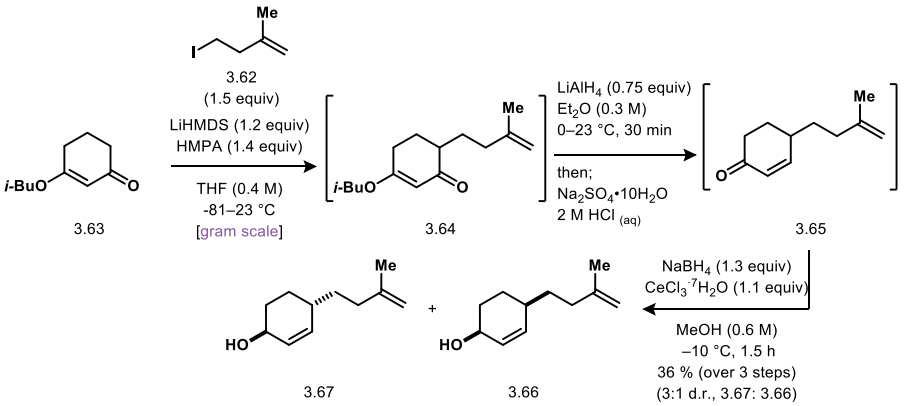
3-isobutoxycyclohex-2-en-1-one (3.63)



Prepared according to the following literature adapted procedure.[359] A mixture of 1,3-cyclohexanedione (**3.21**, 3.0 g, 26.8 mmol, 1.0 equiv.), isobutanol (7.4 mL, 80.4 mmol, 3 equiv.), and benzene (34 mL, 0.8 M) and pTSA•H_2O (51.0 mg, 0.27 mmol, 1 mol%) was heated to reflux with vigorous stirring until the dione starting material was completely consumed. Once complete, the heating bath was removed and the mixture was allowed to cool to room temperature before Et_3N (1.5 mL) was added. The resulting solution was concentrated under reduced pressure. The crude residue was purified by flash column chromatography (30% EtOAc/hexanes) to yield enol ether **3.63** as a yellow oil (4.42 g, 98%). R_f 0.38 (30% EtOAc/hexanes); **^{1}H NMR** (400 MHz, $CDCl_3$) δ 5.33 (s, 1H), 3.58 (d, J = 6.5 Hz, 2H), 2.40 (t, J = 6.3 Hz, 2H), 2.33 (dd, J = 7.2, 6.0 Hz, 2H), 2.09 – 1.92 (m, 3H), 0.96 (d, J = 6.7 Hz, 6H) ppm;

^{13}C NMR (101 MHz, $CDCl_3$) δ 199.9 (C), 178.3 (C), 102.8 (CH), 74.8 (CH_2), 36.9 (CH_2), 29.1 (CH_2), 27.8 (CH), 21.4 (CH_2), 19.2 (2 × CH_3) ppm; **HRMS** (ESI+) *m/z* calculated for $C_{10}H_{16}O_2Na^+$ $[M + Na]^+$ 191.1048, found 191.1041.

trans-4-(3-methylbut-3-en-1-yl)cyclohex-2-en-1-ol (3.67)



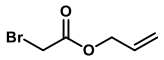
A flame-dried 100 mL round-bottom flask under argon atmosphere and equipped with a stir bar was charged with 1.0 M LiHMDS in THF (12.5 mL, 12.5 mmol, 1.2 equiv) and further anhydrous THF (9 mL) and cooled to –81 ºC with a liquid nitrogen/EtOAc bath under vigorous stirring. After equilibrating at this temperature for 10 minutes, a solution of enol ether **3.63** (1.75 g, 10.2 mmol, 1 equiv) in THF (9 mL) was added dropwise over 30 minutes. After complete addition of the enol ether, the solution was stirred for 5 minutes longer before the LN_2–EtOAc bath was replaced with a –36 ºC LN_2–H_2O/MeOH (60:40) bath. The solution was allowed to stir and warm to –36 ºC for 5 minutes before a solution of anhydrous HMPA (2.5 mL, 14.6 mmol, 1.4 equiv, freshly refluxed over and distilled from CaH_2 under reduced pressure) in anhydrous THF (9 mL) was added. After stirring at this temperature for 5 minutes, 4-iodo-2-methylbut-1-ene **3.62** (3.05 g, 15.6 mmol, 1.5 equiv) was added dropwise. The resulting solution was allowed to stir and warm to room temperature slowly over 1 hour without removing the cooling bath. The mixture was allowed to stir for another hour once at room temperature. The mixture was then cooled to 0 ºC with an ice-water bath before being quenched with NH_4Cl (50 mL, saturated aqueous). The mixture was then diluted with 100 mL of Et_2O (100 mL) and the layers separated. The organic phase was washed with water (5 × 20 mL) and brine (30 mL), dried over $MgSO_4$, filtered, and concentrated *in vacuo*. The crude residue was then rapidly purified by flash column chromatography (SiO_2, 0–20% EtOAc/hexanes). R_f 0.60 (25% EtOAc/hexanes)

The dried, purified material from the previous step was dissolved in anhydrous Et_2O (3 mL) and added dropwise to a stirring suspension of $LiAlH_4$ (111 mg, 2.9 mmol, ~0.75 equiv) in anhydrous Et_2O (10 mL) under argon atmosphere pre-cooled to 0 ºC with an ice–water bath. Upon complete addition of enol ether **3.64**, the cooling bath

was removed, and the suspension was allowed to warm to room temperature and stir for 30 minutes. After 30 minutes at room temperature, Na_2SO_4•$10H_2O$ was added in three portions at two-minute intervals (~ 2 g total). After stirring for 5 minutes, 10 mL of distilled water was added slowly, followed by 2 N HCl (~ 0.5 mL). This mixture was stirred vigorously at room temperature for 30 minutes before being diluted with 10 mL of Et_2O and transferred into a separatory funnel. The layers were separated, and the organic phase was washed twice with $NaHCO_3$ (10 mL, saturated aqueous), distilled water (10 mL), and brine (10 mL) before being dried over Na_2SO_4, filtered and concentrated *in vacuo*. The crude residue was used in the next reaction without further purification.

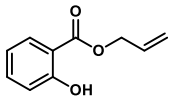
In a 50 mL round-bottom flask, the dried crude residue from the previous reaction was dissolved in methanol (6.5 mL) and stirred at –10 ºC (ice–acetone bath). Next, freshly-ground $CeCl_3$•$7H_2O$ (1.6 g, 4.3 mmol) was added and the mixture was stirred until homogeneous. After stirring at –10 ºC for 10 minutes, $NaBH_4$ (193 mg, 5.1 mmol) was added in three portions at 5-minute intervals, and the resulting mixture was stirred until complete by TLC (~ 1.5 h). Once complete, the mixture was quenched by addition of NH_4Cl (10 mL, saturated aqueous), stirred for 15 minutes and then concentrated *in vacuo*. The resulting residue was diluted with 10 mL of distilled water and transferred to a separatory funnel with 15 mL of Et_2O. The layers were separated, and the aqueous phase was extracted with 15 mL of Et_2O two more times. The combined extracts were washed with brine (10 mL), dried over $MgSO_4$, filtered and concentrated *in vacuo*. The crude residue was purified by flash column chromatography (SiO_2, 10–20% EtOAc/hexanes) to give **3.67** as a clear colourless oil with a scent similar to citronella (231 mg, 36% over 3 steps, 3:1 dr). $\boldsymbol{R_f}$ 0.63 (100% hexanes); **^{1}H NMR** (400 MHz, $CDCl_3$) δ 5.80 – 5.63 (m, 2H), 4.72 – 4.69 (m, 1H), 4.67 (dq, J = 2.2, 1.1 Hz, 1H), 4.26 – 4.17 (m, 1H), 2.14 – 1.97 (m, 4H), 1.93 – 1.82 (m, 1H), 1.71 (t, J = 1.0 Hz, 3H), 1.59 – 1.16 (m, 4H) ppm; **^{13}C NMR** (101 MHz, $CDCl_3$) δ 146.0 (C), 134.5 (CH), 130.5 (CH), 110.1 (CH_2), 67.2 (CH), 35.1 (CH_2), 35.0 (CH), 33.9 (CH_2), 32.0 (CH_2), 26.8 (CH_2), 22.6 (CH_3) ppm; **HRMS** (EI+) *m/z* calculated for $C_{11}H_{18}O^{\bullet+}$ $[M]^{+\bullet}$ 166.13522, found 166.13700. Note: Diastereoisomers assigned by comparison of ^{13}C shifts to 4-substituted cyclohexenols prepared by Wickham and coworkers.[360] This publication shows the cis isomer has a larger difference in ^{13}C chemical shifts for C2 *vs* C3 and C5 *vs* C6. It also shows the trans isomer has a more deshielded ^{13}C shift for the CHOH (C1), C5, and C6 positions, whilst the cis isomer C4 3º methine is more deshielded. Based on these characteristics, the major isomer obtained was assigned as the trans isomer and this was used in further transformations. C5 and C6 positions were assigned based on HSQC and HMBC correlations on the mixture of isomers.

allyl bromoacetate (3.81)



To a suspension of freshly-ground K_2CO_3 (11.06 g, 80 mmol, 2 equiv) in dry DCM (40 mL, 1M) was added allyl alcohol (2.8 mL, 40 mmol, 1.0 equiv.), then bromoacetyl bromide (5.2 mL, 60 mmol, 1.5 equiv.) dropwise over 10 minutes. The mixture was stirred vigorously for 17 hours at room temperature. The salts were filtered, rinsed with DCM (~40 mL), and the resulting filtrate was concentrated *in vacuo*. The amber-coloured crude reside was purified by distillation under reduced pressure (38–40 ºC/5 Torr) to give **3.81** as a clear, colourless oil (6.38 g, 89%). **^{1}H NMR** (400 MHz, $CDCl_3$) δ 5.93 (ddt, J = 17.1, 10.4, 5.8 Hz, 1H), 5.37 (dddd, J = 17.2, 1.5, 1.5, 1.5 Hz, 1H), 5.29 (dddd, J = 10.4, 1.2, 1.2, 1.2 Hz, 1H), 4.67 (ddd, J = 5.8, 1.4, 1.4 Hz, 2H), 3.86 (s, 2H) ppm; **^{13}C NMR** (101 MHz, $CDCl_3$) δ 167.1 (C), 131.3 (CH), 119.4 (CH_2), 66.9 (CH_2), 25.9 (CH_2) ppm; Characterized according to literature comparison.[361]

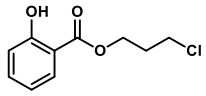
allyl 2-hydroxybenzoate (3.83b)



Salicylic acid (1.5 g, 10 mmol, 1.0 equiv) was added to a stirring solution of KOH (0.75 g, 11 mmol, 1.1 equiv) dissolved in distilled water (10 mL, 1 M). The mixture was stirred at room temperature until homogeneous (~10 mins), then concentrated to dryness by rotary evaporation. The resulting white powder was powdered and suspended in toluene (15 mL) and concentrated (× 3) to remove water by azeotropic distillation. The dried white powder was then dissolved in DMF (anhydrous, 25 mL, 0.4 M) and allyl bromide (0.9 mL, 11 mmol, 1.1 equiv) was added in one portion at room temperature. The resulting solution was stirred vigorously at room temperature overnight. The solution was diluted with brine (30 mL) and Et_2O (20 mL, inhibitor-free) and the layers separated. The aqueous phase was extracted with Et_2O (2 × 20 mL). Combined extracts were washed with distilled water (3 × 15 mL) and brine (20 mL), dried over $MgSO_4$, filtered, and concentrated under reduced pressure. The crude residue was purified by flash column chromatography (15% EtOAc/hexanes) to give **3.83b** as a clear, colourless oil (1.43 g, 80%). R_f 0.88 (25% EtOAc/hexanes); **^{1}H NMR** (400 MHz, $CDCl_3$) δ 10.75 (d, J = 0.4 Hz, 1H), 7.88 (ddd, J = 7.9, 1.8, 0.5 Hz, 1H), 7.46 (dddd, J = 8.4, 7.2, 1.8, 0.4 Hz, 1H), 6.99 (ddd, J = 8.4, 1.1, 0.4 Hz, 1H), 6.89 (ddd, J = 8.2, 7.2, 1.2 Hz, 1H), 6.04 (ddt, J = 17.1, 10.4, 5.7 Hz, 1H), 5.43 (dddd, J = 17.2, 1.5, 1.5, 1.5 Hz, 1H), 5.33 (dqd, J = 10.4, 1.3, 0.1 Hz, 1H), 4.85 (ddd, J = 5.7, 1.4, 1.4 Hz, 2H) ppm; **^{13}C NMR** (101 MHz, $CDCl_3$) δ 170.0 (C), 161.8 (C), 135.9 (CH), 131.7

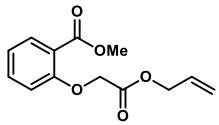
(CH), 130.1 (CH), 119.3 (CH), 119.0 (CH_2), 117.7 (CH), 112.5 (C), 65.9 (CH_2) ppm; **HRMS** (EI+) *m/z* calculated for $C_{10}H_{10}O_3^{\bullet+}$ $[M]^{\bullet+}$ 178.06245, found 178.06225.

3-chloropropyl 2-hydroxybenzoate (3.83b')



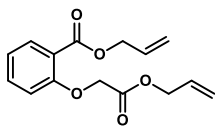
Prepared according to GP6 on a 0.2 mmol scale reaction from compound **3.83b** to give the title product as a yellow oil (3.4 mg, 0.02 mmol, 10% yield) after flash column chromatography (1.5% Et_2O/hexanes). Characterized according to literature comparison.[362] R_f 0.36 (5% Et_2O/hexanes). **^{1}H NMR** (400 MHz, $CDCl_3$) δ 10.73 (s, 1H), 7.83 (ddd, J = 8.0, 1.8, 0.5 Hz, 1H), 7.50 – 7.44 (m, 2H), 6.99 (ddd, J = 8.4, 1.2, 0.4 Hz, 1H), 6.89 (ddd, J = 8.3, 7.2, 1.2 Hz, 1H), 4.52 (t, J = 6.0 Hz, 2H), 3.71 (t, J = 6.3 Hz, 2H), 2.26 (p, J = 6.2 Hz, 2H) ppm; **^{13}C NMR** (101 MHz, $CDCl_3$) δ 170.1 (C), 161.9 (C), 136.0 (CH), 129.9 (CH), 119.3 (CH), 117.8 (CH), 112.4 (C), 62.2 (CH_2), 41.2 (CH_2), 31.7 (CH_2) ppm.

methyl 2-(2-(allyloxy)-2-oxomethoxy)benzoate (3.84a)



Prepared according to a procedure by Leatherbarrow and co-workers on 5 mmol scale to give a clear colourless oil (1.16 g, 92%).[363] R_f 0.23 (20% EtOAc/hexanes); **^{1}H NMR** (400 MHz, $CDCl_3$) δ 7.83 (dd, J = 7.7, 1.8 Hz, 1H), 7.44 (ddd, J = 8.4, 7.4, 1.8 Hz, 1H), 7.05 (ddd, J = 7.6, 7.5, 1.0 Hz, 1H), 6.89 (dd, J = 8.4, 1.0 Hz, 1H), 5.92 (dddd, J = 17.2, 10.4, 5.8, 5.8 Hz, 1H), 5.33 (dddd, J = 17.2, 1.5, 1.5, 1.5 Hz, 1H), 5.26 (dddd, J = 10.4, 1.2, 1.2, 1.2 Hz, 1H), 4.75 (s, 2H), 4.70 (ddd, J = 5.8, 1.4, 1.4 Hz, 2H), 3.90 (s, 3H) ppm; **^{13}C NMR** (101 MHz, $CDCl_3$) δ 168.4 (C), 166.5 (C), 157.5 (C), 133.5 (CH), 132.1 (CH), 131.5 (CH), 121.8 (CH), 121.4 (C), 119.2 (CH_2), 114.3 (CH), 66.7 (CH_2), 66.0 (CH_2), 52.3 (CH_3) ppm; **HRMS** (EI): *m/z* calculated for $C_{13}H_{14}O_5^{\bullet+}$ $[M]^{+\bullet}$: 250.08357, found 250.08423.

allyl 2-(2-(allyloxy)-2-oxoethoxy)benzoate (3.84b)

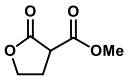


Adapted from the following literature procedure.[363] A mixture of freshly-ground K_2CO_3 (2.49 g, 18 mmol, 3 equiv), acetone (12 mL, 0.5 M), allyl 2-hydroxybenzoate (**3.83b**, 1.06 g, 6 mmol, 1.0 equiv.) and allyl bromoacetate (**3.81**, 750 µL, 6 mmol, 1.0 equiv.) was stirred at reflux for 3 hours. The solution was allowed to cool to room

temperature before being concentrated under reduced pressure. The resulting slurry was diluted with distilled water (25 mL) and EtOAc (30 mL). The layers were separated, and the aqueous phase was extracted with EtOAc (2 × 30 mL). The combined extracts were washed with brine (30 mL), dried over Na_2SO_4, filtered, and concentrated *in vacuo.* The crude residue was purified by flash column chromatography (SiO_2, 7–20% EtOAc/hexanes) to give **3.84b** as a clear colourless oil (1.82 g, 94%). R_f 0.28 (15% EtOAc/hexanes); **^{1}H NMR** (400 MHz, $CDCl_3$) δ 7.86 (dd, J = 7.7, 1.8 Hz, 1H), 7.45 (ddd, J = 8.1, 7.4, 1.8 Hz, 1H), 7.05 (td, J = 7.5, 1.0 Hz, 1H), 6.89 (dd, J = 8.4, 1.0 Hz, 1H), 6.04 (ddt, J = 17.1, 10.2, 5.6 Hz, 1H), 5.91 (ddt, J = 17.2, 10.3, 5.8 Hz, 1H), 5.42 (dq, J = 17.2, 1.6 Hz, 1H), 5.33 (dq, J = 17.2, 1.5 Hz, 1H), 5.31 – 5.22 (m, 2H), 4.85 – 4.78 (m, 2H), 4.75 (s, 2H), 4.73 – 4.66 (m, 2H) ppm; **^{13}C NMR** (101 MHz, $CDCl_3$) δ 168.4 (C), 165.6 (C), 157.6 (C), 133.6 (CH), 132.4 (CH), 132.1 (CH), 131.5 (CH), 121.8 (CH), 121.3 (C), 119.2 (CH_2), 118.3 (CH_2), 114.4 (CH), 66.7 (CH_2), 66.0 (CH_2), 65.7 (CH_2) ppm; **HRMS** (EI+) *m/z* calculated for $C_{15}H_{16}O_5^{\bullet+}$ $[M]^{\bullet+}$ 276.09923, found 276.10166.

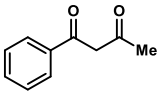
Intermolecular Hydroalkylation Substrates

methyl 2-oxotetrahydrofuran-3-carboxylate (3.88)[§]



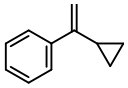
To a solution of γ-butyrolactone (0.43 g, 0.38 mL, 5.0 mmol, 1.0 equiv.) in toluene (25 mL, 0.2 M) was added lithium bis(trimethylsilyl)amide (LiHMDS, 11 mL, 11 mmol, 2.2 equiv., 1.0 M in THF) dropwise over 5 minutes at 0 °C in an ice bath. The reaction was stirred at 0 °C for 15 minutes. Dimethylcarbonate (0.72 g, 0.63 mL, 6.0 mmol, 1.2 equiv.) was then added dropwise over 2 minutes at 0 °C and the reaction stirred overnight and allowed to reach room temperature. The mixture was cooled to 0 °C in an ice bath, quenched with NH_2Cl (20 mL, saturated aqueous), and the phases separated. The aqueous phase was extracted with EtOAc (3 × 30 mL). The combined organic phases were washed with water (30 mL) and brine (30 mL), dried over $MgSO_4$, filtered, and concentrated under reduced pressure. The crude residue was purified by flash column chromatography (SiO_2, 40–50% EtOAc/hexanes) to give **6b** as a clear, colourless oil (304 mg, 42%). R_f 0.32 (40% EtOAc/hexanes); **^{1}H NMR** (400 MHz, $CDCl_3$) δ 4.48 (ddd, J = 9.0, 8.1, 5.4 Hz, 1H), 4.38 – 4.27 (m, 1H), 3.81 (d, J = 1.7 Hz, 3H), 3.57 (dd, J = 9.3, 7.7 Hz, 1H), 2.76 – 2.62 (m, 1H), 2.51 (dddd, J = 13.0, 9.3, 7.6, 5.4 Hz, 1H) ppm; **^{13}C NMR** (126 MHz, $CDCl_3$) δ 172.3 (C), 168.3 (C), 67.5 (CH_3), 53.2 (CH_2), 45.9 (CH_2), 26.5 (CH) ppm; Characterized according to literature comparison. [364]

1-phenylbutane-1,3-dione (3.90)[§]



Adapted from a procedure by Deng and coworkers.[365] To a suspension of NaH (6.4 g, 160 mmol, 4.0 equiv., 60% w/w mineral oil dispersion) in EtOAc (40 mL, 1 M, anhydrous) was added a solution of acetophenone (4.8 g, 4.6 mL, 40 mmol, 1.0 equiv.) in EtOAc (40 mL, 1 M, anhydrous) over 10 minutes at 0 °C in an ice bath. The mixture was stirred at 0 °C for 2 hours and allowed to reach room temperature overnight. The reaction was diluted with EtOAc (60 mL) and quenched with careful addition of NH_4Cl (60 mL, sat. aq.) at 0 °C in an ice bath then acidified to pH 5 with HCl (3 M). The aqueous phase was separated and extracted with EtOAc (3 × 50 mL). The combined organic phases were dried over $MgSO_4$, filtered, and concentrated under reduced pressure. The crude product was recrystallized (EtOH) to give **3.90** as a peach solid (4.26 g, 66%, 14:1 mixture of enol/keto). R_f 0.82 (30% EtOAc/hexanes); **^{1}H NMR** (400 MHz, $CDCl_3$) δ 7.91 – 7.84 (m, 2H), 7.57 – 7.48 (m, 1H), 7.48 – 7.39 (m, 2H), 6.18 (s, 1H), 2.19 (s, 3H) ppm; **^{13}C NMR** (101 MHz, $CDCl_3$) δ 193.9 (C), 183.4 (C), 134.9 (C), 132.4 (CH), 128.7 (2 × CH), 127.1 (2 × CH), 96.8 (CH), 25.9 (CH_3) ppm; **HRMS** (EI+) *m/z* calculated for $C_{10}H_{10}O_2^{\bullet+}$ $[M]^{\bullet+}$ 162.06753, found 162.06765

(1-cyclopropylvinyl)benzene (3.94)

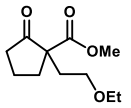


Adapted from a literature procedure.[366] To a solution of $MePPh_3I$ (4.04 g, 10 mmol, 2 equiv) in THF (anhydrous, 30 mL, 0.15 M) was added nBuLi (4.0 mL, 10 mmol, 2 equiv., 2.5 M in hexanes) dropwise over 5 minutes at –78 ºC in a dry-ice/acetone bath and the resulting mixture was stirred for 10 minutes at –78 ºC following complete addition. The cooling bath was removed and the mixture allowed to slowly warm to room temperature. A solution of cyclopropyl phenyl ketone (0.73 g, 5 mmol, 1.0 equiv.) in THF (anhydrous, 3 mL) was added dropwise over 5 minutes at room temperature, and the resulting mixture stirred until complete consumption of the ketone was observed by TLC (~3 hours). The mixture was diluted with brine (25 mL), water (10 mL), and pentane (20 mL). The layers were separated and the aqueous phase extracted with pentane (2 × 20 mL). The combined extracts were dried over $MgSO_4$, filtered into a round-bottom flask containing ~2 g of Celite, and concentrated *in vacuo* at 10 ºC. The resulting adsorbed material was poured onto a silica pad and the product was eluted with pentane. The resulting solution was concentrated *in vacuo* to give **3.94** as a clear colourless oil (593 mg, 82%). R_f 0.63 (100% hexanes); **^{1}H NMR** (400 MHz, $CDCl_3$) δ 7.65 – 7.57 (m, 2H), 7.40 – 7.31 (m, 2H), 7.33 – 7.25 (m, 1H), 5.31 – 5.27 (m, 1H), 4.95 (t, J = 1.1 Hz, 1H), 1.72 –

1.61 (m, 1H), 0.88 – 0.82 (m, 2H), 0.63 – 0.57 (m, 2H) ppm; **^{13}C NMR** (101 MHz, $CDCl_3$) δ 149.5 (C), 141.8 (C), 128.3 (2 × CH), 127.6 (CH), 126.3 (2 × CH), 109.1 (CH_2), 15.8 (CH), 6.8 (CH_2) ppm; Characterized according to literature comparison.[367]

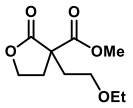
Intermolecular Hydroalkylation Products

methyl 1-(2-ethoxyethyl)-2-oxocyclopentane-1-carboxylate (3.96)[§]



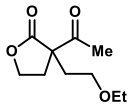
Prepared according to GP7 with ketoester **3.86** and ethyl vinyl ether (**3.87**) on 0.2 mmol scale and purified by flash column chromatography (SiO_2, 20–40% Et_2O/hexanes) to give **3.96** as an amber oil (condition C: 46 mg, quantitative; condition D: 44 mg, quantitative). ***R$_f$*** 0.30 (35% Et_2O/hexanes); **^{1}H NMR** (400 MHz, $CDCl_3$) δ 3.66 (s, 3H), 3.53 – 3.41 (m, 2H), 3.41 – 3.29 (m, 2H), 2.56 – 2.43 (m, 1H), 2.42 – 2.21 (m, 2H), 2.16 (dt, J = 14.3, 6.0 Hz, 2H), 2.03 – 1.87 (m, 4H), 1.10 (t, J = 7.0 Hz, 3H) ppm; **^{13}C NMR** (101 MHz, $CDCl_3$) δ 214.7 (C), 171.7 (C), 66.7 (CH_2), 66.2 (CH_2), 58.8 (C), 52.6 (CH_3), 37.8 (CH_2), 33.7 (CH_2), 32.7 (CH_2), 19.8 (CH_2), 15.1 (CH_3) ppm; **HRMS** (EI+) *m/z* calculated for $C_{11}H_{18}O_4^{\bullet+}$ $[M]^{\bullet+}$ 214.11996, found 214.12121.

methyl 3-(2-ethoxyethyl)-2-oxotetrahydrofuran-3-carboxylate (3.97)[§]



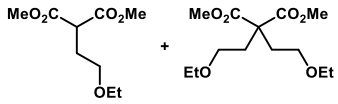
Prepared according to GP7 with lactone ester **3.86** and ethyl vinyl ether (**3.87**) on 0.4 mmol scale under condition A and 0.2 mmol scale under condition B and purified by flash column chromatography (SiO_2, 30–35% Et_2O/hexanes) to give **3.97** as an amber oil (condition C: 83 mg, 96%; condition D: 33.2 mg, 77%). ***R$_f$*** 0.30 (30% EtOAc/hexanes); **^{1}H NMR** (600 MHz, $CDCl_3$) δ 4.37 – 4.30 (m, 2H), 3.76 (s, 3H), 3.58 – 3.47 (m, 2H), 3.41 (q, J = 7.0 Hz, 2H), 2.77 (ddd, J = 13.1, 6.2, 4.2 Hz, 1H), 2.45 – 2.36 (m, 2H), 2.06 (ddd, J = 14.5, 6.7, 5.2 Hz, 1H), 1.14 (t, J = 7.0 Hz, 3H) ppm; **^{13}C NMR** (151 MHz, $CDCl_3$) δ 175.0 (C), 170.1 (C), 66.6 (CH_2), 66.5 (CH_2), 66.5 (CH_2), 53.2 (CH_3), 52.9 (C), 33.9 (CH_2), 31.8 (CH_2), 15.1 (CH_3) ppm; **HRMS** (EI+) *m/z* calculated for $C_{10}H_{16}O_5^{\bullet+}$ $[M]^{\bullet+}$: 216.09923, found 216.09777.

3-acetyl-3-(2-ethoxyethyl)oxolan-2-one (3.98)[§]



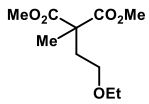
Prepared according to GP7 with ketolactone **3.41** and ethyl vinyl ether (**3.87**) on 0.2 mmol scale and purified by flash column chromatography (SiO_2, 30% Et_2O/hexanes) to give **3.98** as an amber oil (condition C: 14.7 mg, 20%; condition D: 40 mg, quantitative). $\boldsymbol{R_f}$ 0.29 (30% Et_2O/hexanes); **^{1}H NMR** (400 MHz, $CDCl_3$) δ 4.30 (td, J = 8.9, 2.7 Hz, 1H), 4.17 (ddd, J = 9.6, 8.9, 7.0 Hz, 1H), 3.53 (dt, J = 10.1, 5.2 Hz, 1H), 3.44 – 3.27 (m, 3H), 2.95 (ddd, J = 12.8, 7.0, 2.7 Hz, 1H), 2.55 (ddd, J = 14.8, 8.7, 5.0 Hz, 1H), 2.34 (s, 3H), 2.10 (dt, J = 12.8, 9.2 Hz, 1H), 1.98 (ddd, J = 14.7, 5.4, 4.4 Hz, 1H), 1.12 (t, J = 7.0 Hz, 3H) ppm; **^{13}C NMR** (101 MHz, $CDCl_3$) δ 202.1 (C), 175.8 (C), 66.8 (CH_2, 2C), 66.5 (CH_2), 60.2 (C), 35.3 (CH_2), 29.4 (CH_2), 25.8 (CH_3), 14.9 (CH_3) ppm; **HRMS** (EI+) *m/z* calculated for $C_8H_{14}O_3^{\bullet+}$ $[M - C_2H_2O]^{+\bullet}$: 158.09375, found 158.09513.

1,3-dimethyl 2-(2-ethoxyethyl)propanedioate (3.99) & dimethyl 2,2-bis(2-ethoxyethyl)malonate (3.100)[§]



Prepared according to GP7 with dimethyl malonate (**1.41**) and ethyl vinyl ether (**3.87**) on 0.2 mmol scale and purified by flash column chromatography (SiO_2, 20–40% Et_2O/hexanes) to give **3.99/3.100** as a clear, colourless oil (condition C: 0%; condition D: 47.3 mg, quantitative, 5:1 **3.104**/**3.105**). $\boldsymbol{R_f}$ 0.31 (30% Et_2O/hexanes); **^{1}H NMR** (400 MHz, $CDCl_3$) δ 3.74 (s, 6H, **mono**), 3.69 (s, 6H, **di**), 3.58 (t, J = 7.3 Hz, 1H, **mono**), 3.48 – 3.40 (m, 4H **mono**, 4H **di**), 3.38 (q, J = 7.0 Hz, 4H, **di**), 2.25 (t, J = 6.4 Hz, 4H, **di**), 2.18 (dt, J = 7.3, 6.0 Hz, 2H, **mono**), 1.16 (t, J = 7.0 Hz, 3H, **mono**), 1.12 (t, J = 7.0 Hz, 6H, **di**) ppm; **^{13}C NMR** (101 MHz, $CDCl_3$) δ **mono** 170.0 (2 × C), 67.7 (CH_2), 66.4 (CH_2), 52.6 (2 × CH_3), 49.0 (CH), 29.2 (CH_2), 15.2 (CH_3) **di** 172.1 (C), 66.5 (2 × CH_2), 66.4 (2 × CH_2), 54.2 (C), 52.5 (2 × CH_3), 32.7 (2 × CH_2), 15.2 (2 × CH_3) ppm; **HRMS** (EI+) **mono** *m/z* calculated for $C_8H_{13}O_4^+$ $[M - OCH_3]^+$ 173.08084, found 173.07927, **di** *m/z* calculated for $C_{12}H_{21}O_5^+$ $[M - OCH_3]^+$ 245.13835, found 245.13761.

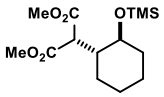
dimethyl 2-(2-ethoxyethyl)-2-methylmalonate (3.100)[§]



Prepared according to GP7 with dimethyl methylmalonate (**3.89**) and ethyl vinyl ether (**3.87**) on 0.4 mmol scale and purified by flash column chromatography (SiO_2, 20–30% Et_2O/hexanes) to give **3.100** as a clear, colourless

oil (condition C: 16 mg, 18%; condition D: 10 mg, 11%). R_f 0.20 (20% Et_2O/hexanes); **^{1}H NMR** (400 MHz, $CDCl_3$) δ 3.71 (s, 6H), 3.47 (t, J = 6.4 Hz, 2H), 3.40 (q, J = 7.0 Hz, 2H), 2.19 (t, J = 6.4 Hz, 2H), 1.45 (s, 3H), 1.14 (t, J = 7.0 Hz, 3H) ppm; **^{13}C NMR** (101 MHz, $CDCl_3$) δ 172.8 (C), 66.4 (CH_2), 66.4 (CH_2), 52.6 (CH_3), 52.1 (CH_3), 35.5 (CH_2), 20.2 (CH_3), 15.2 (CH_3) ppm;

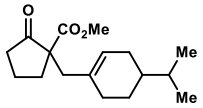
dimethyl 2-(2-((trimethylsilyl)oxy)cyclohexyl)malonate (3.101) [§]



Prepared according to GP7 with dimethyl malonate (**1.42**) and (cyclohex-1-en-1-yloxy)trimethylsilane (**3.92**) on 0.4 mmol scale and purified by flash column chromatography (SiO_2, 10% Et_2O/hexanes) to give **3.101** as a clear, colourless oil (condition C: 0%; condition D: 74 mg, 61% isolated, 2:1 dr). R_f 0.37 (10% Et_2O/hexanes); **^{1}H NMR** (400 MHz, $CDCl_3$) δ 3.97 – 3.92 (m, 1H, **m**), 3.80 (d, J = 4.6 Hz, 1H, **M**), 3.73 – 3.70 (m, 6H, **M**+**m**), 3.52 (td, J = 9.9, 4.2 Hz, 1H, **M**), 3.47 (d, J = 11.0 Hz, 1H, **m**), 2.17 (tt, J = 11.4, 3.0 Hz, 1H, **m**), 2.05 (ddt, J = 11.8, 9.9, 3.9 Hz, 1H, **M**), 1.96 – 1.88 (m, 1H, **M**+**m**), 1.83 – 1.60 (m, 3H, **M**+**m**), 1.60 – 1.13 (m, 4H, **M**+**m**), 0.10 (s, 6H, **M**+**m**), 0.05 (s, 3H, **M**+**m**) ppm; **^{13}C NMR** (151 MHz, $CDCl_3$) δ **M** 170.2 (C), 169.4 (C), 73.1 (CH), 52.4 (CH_3), 52.3 (CH), 52.0 (CH_3), 45.9 (CH), 36.3 (CH_2), 27.4 (CH_2), 25.7 (CH_2), 24.9 (CH_2), 0.5 (3 × CH_3) **m** 169.8 (C), 169.3 (C), 67.7 (CH), 54.6 (CH_3), 52.5 (CH), 52.4 (CH_3), 42.3 (CH), 33.4 (CH_2), 25.5 (CH_2), 24.3 (CH_2), 19.6 (CH_2), 0.2 (3 × CH_3) ppm; **HRMS** (EI+) *m/z* calculated for $C_{13}H_{23}O_5Si^{\bullet+}$ $[M - CH_3]^{\bullet+}$ 287.13093, found 287.13214.

Stereochemistry determined based on axial-axial coupling constant (9.9 Hz) between peaks at each stereocentre (3.52 ppm & 2.05 ppm) in the major diastereomer.

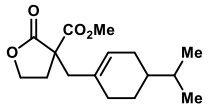
methyl 1-((4-isopropylcyclohex-1-en-1-yl)methyl)-2-oxocyclopentane-1-carboxylate (3.102) [§]



Prepared according to GP7 with ketoester **3.86** and β-pinene (**3.93**) on 0.4 mmol scale under condition C and 0.2 mmol scale under condition D and purified by flash column chromatography (SiO_2, 20% Et_2O/hexanes) to give **3.102** as a clear, colourless oil (condition C: 95 mg, 82%, 1:1 dr; condition D: 55 mg, quantitative, 1:1 dr). R_f 0.38 (30% Et_2O/hexanes); **^{1}H NMR** (400 MHz, $CDCl_3$) δ 5.43 (s, 1H), 3.70 (d, J = 5.3 Hz, 3H), 2.80 – 2.66 (m, 1H), 2.59 – 2.47 (m, 1H), 2.45 – 2.15 (m, 4H), 2.06 – 1.78 (m, 7H), 1.71 (ddt, J = 10.0, 5.6, 2.3 Hz, 2H), 1.43 (dq, J = 13.3, 6.5 Hz, 1H), 1.28 – 1.07 (m, 4H), 0.87 (d, J = 4.3 Hz, 3H), 0.85 (d, J = 4.3 Hz, 3H) ppm; **^{13}C NMR** (101 MHz, $CDCl_3$) δ

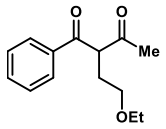
M 214.7 (C), 171.3 (C), 133.3 (C), 126.3 (CH), 60.5 (C), 52.7 (CH_3), 41.9 (CH_2), 39.9 (CH), 37.9 (CH_2), 32.3 (CH), 31.6 (CH_2), 30.3 (CH_2), 29.3 (CH_2), 26.6 (CH_2), 20.1 (CH_2), 19.8 (CH_3), 19.6 (CH_3) **m** 214.9 (C), 171.5 (C), 133.3 (C), 126.4 (CH), 60.7 (C), 52.7 (CH_3), 41.9 (CH_2), 39.9 (CH), 37.9 (CH_2), 32.3 (CH), 32.1 (CH_2), 29.7 (CH_2), 29.3 (CH_2), 26.5 (CH_2), 20.1 (CH_2), 19.8 (CH_3), 19.5 (CH_3) ppm; **HRMS** (EI+) *m/z* calculated for $C_{17}H_{25}O_3^+$ $[M - H]^+$ 277.17982, found 277.18016.

methyl 3-((4-isopropylcyclohex-1-en-1-yl)methyl)-2-oxotetrahydrofuran-3-carboxylate (3.103)[§]



Prepared according to GP7 with lactoneester **3.88** and β-pinene (**3.93**) on 0.4 mmol scale under condition A and 0.2 mmol under condition B and purified by flash column chromatography (SiO_2, 20% Et_2O/hexanes) to give **3.103** as a clear, colourless oil (condition C: 115 mg, quantitative, 1:1 dr; condition D: 52 mg, 93%, 1:1 dr). R_f 0.31 (20% Et_2O/hexanes); **^{1}H NMR** (600 MHz, $CDCl_3$) δ 5.57 – 5.43 (m, 1H, **M** + **m**), 4.33 – 4.28 (m, 2H, **M** + **m**), 3.77 (s, 3H, **M**), 3.78 (s, 3H, **m**), 2.91 – 2.86 (m, 1H, **m**), 2.79 (dd, J = 14.6, 1.4 Hz, 1H, **M**), 2.77 (ddd, J = 13.2, 7.1, 3.4 Hz, 1H, **m**), 2.71 (dt, J = 13.1, 5.3 Hz, 1H, **M**), 2.59 – 2.54 (m, 1H, **M** + **m**), 2.45 (d, J = 13.8 Hz, 1H, **m**), 2.32 (dt, J = 13.2, 8.8 Hz, 1H, **M**), 2.27 (dt, J = 13.2, 8.5 Hz, 1H, **m**), 2.07 – 1.99 (m, 1H, **M** + **m**), 1.92 – 1.85 (m, 2H, **M** + **m**), 1.77 – 1.71 (m, 2H, **M** + **m**), 1.45 (dq, J = 13.2, 6.6 Hz, 1H, **M** + **m**), 1.28 – 1.11 (m, 3H, **M** + **m**), 0.87 (t, J = 6.7 Hz, 6H, **M** + **m**) ppm; **^{13}C NMR** (151 MHz, $CDCl_3$) δ **M** 175.3 (C), 170.2 (C), 132.6 (C), 127.4 (CH), 66.4 (CH_2), 54.0 (C), 53.3 (CH), 42.2 (CH_2), 39.9 (CH), 32.3 (CH), 30.9 (CH_2), 29.9 (CH_2), 29.3 (CH_2), 26.4 (CH_2), 20.0 (CH_3), 19.7 (CH_3) **m** 175.2 (C), 170.1 (C), 132.6 (C) 127.1 (CH), 66.5 (CH_2), 53.9 (C), 53.3 (CH), 42.2 (CH_2), 39.8 (CH), 32.2 (CH), 30.9 (CH_2), 29.6 (CH_2), 29.3 (CH_2), 26.5 (CH_2), 20.1 (CH_3), 19.8 (CH_3) ppm; **HRMS** (EI+) *m/z* calculated for $C_{16}H_{24}O_4^{\bullet+}$ $[M]^{\bullet+}$ 280.16691, found 280.16477.

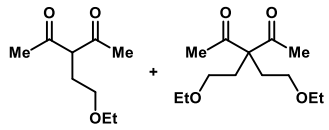
2-(2-ethoxyethyl)-1-phenylbutane-1,3-dione (3.104)[§]



Prepared according to GP7 with 1-phenylbutane-1,3-dione (**3.90**) and 1.2 equivalents of ethyl vinyl ether (**3.87**) on 0.4 mmol scale and purified by flash column chromatography (SiO_2, 15–30% Et_2O/hexanes) to give **3.104** as a clear, colourless oil (condition C: 0%; condition D: 59 mg, 63%). R_f 0.28 (30% Et_2O/hexanes); **^{1}H NMR** (400 MHz, $CDCl_3$) δ 8.07 – 7.99 (m, 2H), 7.65 – 7.54 (m, 1H), 7.54 – 7.44 (m, 2H), 4.72 (t, J = 6.9 Hz, 1H), 3.51 – 3.30

(m, 4H), 2.25 (dddd, J = 9.1, 8.5, 4.7, 2.3 Hz, 2H), 2.16 (s, 3H), 1.11 (t, J = 7.0 Hz, 3H) ppm; **^{13}C NMR** (101 MHz, $CDCl_3$) δ 204.0 (C), 196.9 (C), 136.7 (C), 133.8 (CH), 128.9 (CH, 4C), 67.9 (CH_2), 66.4 (CH_2), 59.8 (CH), 29.4 (CH_3), 28.7 (CH_2), 15.2 (CH_3) ppm; **HRMS** (EI+) *m/z* calculated for $C_{14}H_{18}O_3^{\bullet+}$ $[M]^{\bullet+}$ 234.12505, found 234.12450.

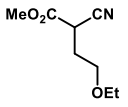
3-(2-ethoxyethyl)pentane-2,4-dione (3.106) & 3,3-bis(2-ethoxyethyl)pentane-2,4-dione (3.105)[§]



Prepared according to GP7 with acetoacetone (**3.91**) and ethyl vinyl ether (**3.87**) on 0.4 mmol scale and purified by flash column chromatography (SiO_2, 15–30% Et_2O/hexanes) to give **3.106** & **3.105** as a clear, colourless oil (condition C: 0%; condition D: 70 mg, 72%, 4:1 **3.106**/**3.105**). R_f 0.39 (30% Et_2O/hexanes); **^{1}H NMR** (400 MHz, $CDCl_3$) δ **3.105** 3.33 (qd, J = 7.1, 0.6 Hz, 4H), 3.32 (t, J = 6.2 Hz, 4H), 2.24 (t, J = 6.3 Hz, 4H), 2.11 (d, J = 0.6 Hz, 6H), 1.09 (td, J = 7.0, 0.6 Hz, 6H) ppm;

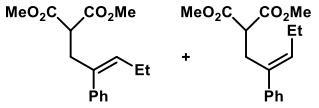
Prepared according to GP7 with acetoacetone (**3.91**) and 1.2 equivalents of ethyl vinyl ether (**3.87**) on 0.4 mmol scale and purified by flash column chromatography (SiO_2, 15–30% Et_2O/hexanes) to give **3.106** as a clear, colourless oil (condition C: 0%; condition D: 29 mg, 42%). R_f 0.39 (30% Et_2O/hexanes); **^{1}H NMR** (400 MHz, $CDCl_3$) δ **3.106** 3.82 (t, J = 7.0 Hz, 1H, **k**), 3.48 (q, J = 7.0 Hz, 2H, **e**), 3.41 (q, J = 7.1 Hz, 4H, **k**), 3.39 (t, J = 5.9 Hz, 2H, **e**), 2.52 (t, J = 7.4 Hz, 2H, **e**), 2.20 (s, 6H, **k**), 2.17 (s, 6H, **e**), 2.11 (dt, J = 7.0, 5.9 Hz, 2H, **k**), 1.20 (t, J = 7.0 Hz, 3H, **e**), 1.15 (t, J = 7.0 Hz, 3H, **k**) ppm; **^{13}C NMR** (101 MHz, C_6D_6) δ 203.3 (C), 192.0 (C), 107.6 (C), 71.0 (CH_2), 68.5 (CH_2), 66.8 (CH_2), 66.5 (CH_2), 66.2 (CH), 32.3 (CH_2), 29.1 (CH), 29.1 (CH_2), 28.6 (CH_2), 23.4 (CH_2), 23.2 (CH_3), 15.7 (CH_3), 15.5 (CH_3), 14.7 (CH_3) ppm; **HRMS** (EI+) *m/z* calculated for $C_9H_{16}O_3^{\bullet+}$ $[M]^{\bullet+}$ 172.10940, found 172.10849.

methyl 2-cyano-4-ethoxybutanoate (3.107)[§]



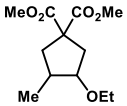
Prepared according to GP7 with methyl 2-cyanoacetate and ethyl vinyl ether (**3.87**) on 0.2 mmol scale and purified by flash column chromatography (SiO_2, 30–40% Et_2O/hexanes) to give **3.107** as a clear, colourless oil (condition C: 0%; condition D: 12.1 mg, 18% isolated, 35% by ^{1}H NMR). R_f 0.26 (30% Et_2O/hexanes); **^{1}H NMR** (400 MHz, $CDCl_3$) δ 3.81 (s, 3H), 3.78 (dd, J = 8.3, 5.8 Hz, 1H), 3.66 – 3.53 (m, 2H), 3.49 (q, J = 7.0 Hz, 2H), 2.34 – 2.08 (m, 2H), 1.18 (t, J = 7.0 Hz, 4H) ppm; Compound degraded before complete characterization data could be collected.

dimethyl 2-(2-phenylpent-2-en-1-yl)malonate (3.108)



Prepared according to GP7 with dimethyl malonate (**1.42**) and 1-cyclopropylvinylbenzene (**3.94**) on 0.2 mmol scale and purified by flash column chromatography (SiO_2, 5–10% EtOAc/hexanes) to give **3.108** as a clear, colourless oil (condition C: 0%; condition D: 32.1 mg, 58%, 10:1 dr). R_f 0.31 (10% EtOAc/hexanes); **^{1}H NMR** (600 MHz, $CDCl_3$) δ 7.35 – 7.30 (m, 2H, **2M** + **2m**), 7.28 – 7.22 (m, 1H, **M** + **m**), 7.15 – 7.11 (m, 2H, **2M** + **2m**), 5.68 (t, J = 7.3 Hz, 0.1H, **m**), 5.52 (tt, J = 7.4, 1.2 Hz, 1H, **M**), 3.68 (s, 6H, **6M**), 3.63 (s, 0.6H, **6m**), 3.37 (t, J = 7.8 Hz, 1H, **M** + **m**), 3.15 (d, J = 7.7 Hz, 0.2H, **2m**), 2.93 (dd, J = 7.9, 1.1 Hz, 2H, **2M**), 2.23 (dddd, J = 7.5, 7.5, 7.5 Hz, 0.2H, **2m**), 1.89 (dddd, J = 7.6, 7.6, 7.6 Hz, 2H, **2M**), 1.04 (t, J = 7.5 Hz, 0.3H, **3m**), 0.89 (t, J = 7.5 Hz, 3H, **3M**) ppm; **^{13}C NMR** (101 MHz, $CDCl_3$) δ 169.6 (2 × C), 139.5 (C), 136.1 (C), 132.5 (CH), 128.8 (2 × CH), 128.3 (2 × CH), 127.1 (CH), 52.5 (2 × CH_3), 50.9 (CH), 38.7 (CH_2), 22.4 (CH_2), 14.6 (CH_3) ppm; **HRMS** (EI+) *m/z* calculated for $C_{16}H_{20}O_4^{\bullet+}$ $[M]^{\bullet+}$ 276.13561, found 276.13688. Note: major diastereomer assigned based on nOE between alkene methine proton and the methylene protons on the malonate side.

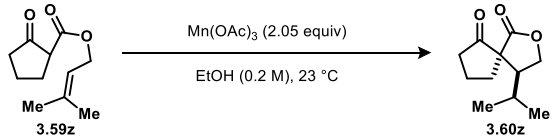
dimethyl 3-ethoxy-4-methylcyclopentane-1,1-dicarboxylate (3.109)



Prepared according to GP7 with dimethyl allylmalonate and ethyl vinyl ether on 0.4 mmol scale and purified by flash column chromatography (SiO_2, 5–10% EtOAc/hexanes) to give **3.109** as a clear, colourless oil (condition C: 0%; condition D: 36 mg, 37%, 1:1 dr). R_f 0.60 (16% EtOAc/hexanes); **^{1}H NMR** (600 MHz, $CDCl_3$) δ **3.109** 3.71 (t, J = 0.8 Hz, 3H), 3.70 (t, J = 0.7 Hz, 3H), 3.68 (q, J = 4.1 Hz, 1H), 3.50 (dq, J = 9.2, 6.8 Hz, 1H), 3.30 (dq, J = 9.2, 7.0 Hz, 1H), 2.57 (dd, J = 14.2, 2.9 Hz, 1H), 2.29 (dd, J = 12.3, 6.6 Hz, 1H), 2.23 (dd, J = 14.2, 4.7 Hz, 1H), 2.17 – 2.06 (m, 2H), 1.12 (t, J = 7.0 Hz, 3H), 0.99 (d, J = 6.4 Hz, 3H) **3.109'** 3.69 (s, 6H), 3.42 – 3.36 (m, 3H), 2.18 (t, J = 6.4 Hz, 2H), 2.17 – 2.12 (m, 1H), 2.05 – 1.96 (m, 1H), 1.58 (dd, J = 13.6, 9.7 Hz, 1H), 1.15 (t, J = 6.6 Hz, 3H), 1.02 (d, J = 6.8 Hz, 3H) ppm; **^{13}C NMR** (151 MHz, $CDCl_3$) δ **3.109** 173.8 (C), 172.8 (C), 81.9 (CH), 64.2 (CH_2), 58.4 (C), 52.9 (CH_3), 52.8 (CH_3), 39.5 (CH_2), 39.3 (CH_2), 38.6 (CH), 15.4 (CH_3), 13.4 (CH_3) **3.109'** 173.2 (C), 172.6 (C), 85.6 (CH), 66.2 (CH_2), 57.4 (C), 52.8 (CH_3), 52.5 (CH_3), 39.7 (CH), 39.3 (CH_2), 32.5 (CH_2), 18.0 (CH_3), 15.6 (CH_3) ppm; **HRMS** (EI+) *m/z* calculated for $C_{12}H_{20}O_5^{\bullet+}$ $[M]^{\bullet+}$ 244.13053, found 244.13053.

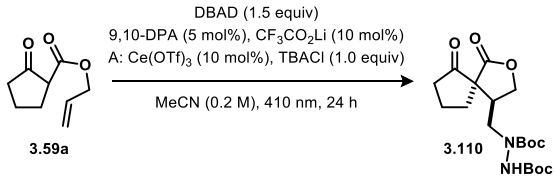
Hydroalkylation Variants

Redox-neutral $Mn(OAc)_3$ cyclization



A suspension of $Mn(OAc)_3$ (anhydrous, 238 mg, 1.03 mmol, 2.05 equiv) in EtOH (anhydrous, 2.5 mL, 0.2 M) was sparged with argon for 15 minutes, then the desired ketoester substrate (0.5 mmol, 1.0 equiv) was added as a solution in EtOH (anhydrous, 0.1 mL, 5 M) in one portion at room temperature. The suspension was stirred at room temperature until consumption of ketoester was observed by TLC. Upon complete conversion, water (4 mL) and $NaHSO_3$ (4 mL, saturated aqueous) were added and the mixture stirred for 5 minutes at room temperature. The mixture was extracted with DCM (3 × 10 mL), The combined extracts were washed with brine (10 mL), dried over Na_2SO_4, filtered, and concentration under reduced pressure. Trimethylsilylbenzene internal standard was added to the concentrated crude residue and conversion was assessed by ^1H NMR spectroscopy. The crude material was then purified by flash column chromatography.

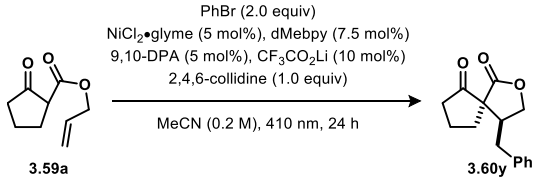
di-tert-butyl 1-((1,6-dioxo-2-oxaspiro[4.4]nonan-4-yl)methyl)hydrazine-1,2-dicarboxylate (3.110)[§]



Inside a nitrogen-filled glovebox, an 8 mL oven-dried screw-top Pyrex tube (12 mm diameter) was charged with lithium trifluoroacetate (0.020 mmol, 10 mol%), 9,10-diphenylanthracene (0.010 mmol, 5 mol%), $Ce(OTf)_3$ (0.020 mmol, 10 mol%, anhydrous), tetrabutylammonium chloride (0.20 mmol, 1 equiv., anhydrous), and dicarbonyl **3.59a** (0.20 mmol, 1 equiv.). $Ce(OTf)_3$ and TBACl were omitted for cerium-free conditions (B). Once all components were added, the tube was sealed with a Teflon-septum screw cap, transferred out of the glovebox, and immediately placed under a positive pressure of argon. Di-tert-butyl azodicarboxylate (DBAD, 0.3 mmol, 1.5 equiv.) and anhydrous acetonitrile (1.0 mL, 0.2 M) were added and the resulting suspension sparged with argon for 5 minutes. After sparging, the septum cap was quickly exchanged with a hard plastic cap and the vessel sealed with electrical tape and then Parafilm. The reaction mixture was then sonicated (90 s) before irradiating with a violet LED (2–2.4 W, 410 nm) at a distance of 1–5 mm for 24 h. The reaction solution was passed through a silica plug (3 cm^3 in a 6 mL syringe barrel)

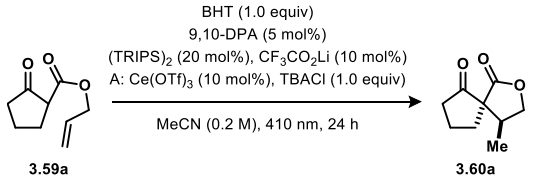
eluting with Et_2O (~25 mL). The resulting solution was concentrated under reduced pressure and purified by flash column chromatography (SiO_2, 30% EtOAc/hexanes) to give **3.110** as an amber oil (condition A: 33 mg, 41%, 3:1 dr; condition B: 27 mg, 34%, 3:1 dr). R_f 0.33 (30% EtOAc/hexanes); **^{1}H NMR** (600 MHz, DMSO-d_6, 80 °C) δ 9.30 – 8.95 (m, 1H), 4.56 – 4.31 (m, 1H), 4.23 – 4.01 (m, 1H), 2.95 – 2.77 (m, 1H), 2.50 – 2.23 (m, 3H), 2.20 – 2.00 (m, 2H), 1.97 – 1.86 (m, 1H), 1.48 – 1.30 (m, 18H) ppm; **^{13}C NMR** (151 MHz, DMSO-d_6, 80 °C) δ 214.2 (C), 174.5 (C), 154.5 (2 × C), 79.7 (C), 79.3 (C), 68.9 (CH_2), 58.1 (C), 46.3 (CH), 36.3 (CH_2), 31.5 (CH_2), 27.4 (CH_3), 27.1 (CH_3), 19.2 (CH_2), 18.6 (CH_2) ppm; **HRMS** (ESI+) *m/z* calculated for $C_{18}H_{30}N_2O_7Na^+$ $[M + Na]^+$: 421.1945, found 421.1951.

Nickel-catalyzed cross-coupling[§]



Inside a nitrogen-filled glovebox, an 8 mL oven-dried screw-top Pyrex tube (12 mm diameter) was charged with lithium trifluoroacetate (2.4 mg, 0.020 mmol, 10 mol%), 9,10-diphenylanthracene (3.3 mg, 0.010 mmol, 5 mol%), $NiCl_2$•glyme (2.2 mg, 0.01 mmol, 5 mol%), 4,4′-dimethyl-2,2′-bipyridine (2.4 mg, 0.015 mmol, 7.5 mol%), and the dicarbonyl substrate (**3.59a**, 0.2 mmol, 1.0 equiv.). The tube was sealed with a Teflon-septum screw cap, transferred out of the glovebox, and immediately placed under a positive pressure of argon. Anhydrous acetonitrile (1.0 mL, 0.2 M) and 2,4,6-collidine (0.2 mmol, 1.0 equiv.) were added and the resulting suspension sparged with argon for 5 minutes. Bromobenzene (0.4 mmol, 2.0 equiv.) was added and then the septum cap was quickly exchanged with a hard plastic cap and the vessel sealed with electrical tape and then Parafilm. The reaction mixture was then sonicated (90 s) before irradiating with a violet LED (2–2.4 W, 410 nm) at a distance of 1–5 mm for 24 h. The reaction solution was passed through a silica plug (3 cm^3 in a 6 mL syringe barrel) eluting with Et_2O (~25 mL). The resulting solution was concentrated under reduced pressure and purified by flash column chromatography (SiO_2, 10–20% EtOAc/hexanes) to give spiro-ketolactone **3.60y** as a clear, colourless oil (22 mg, 46%, 4:1 dr).

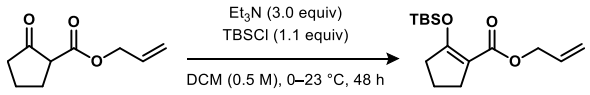
Intramolecular reaction including BHT[§]



3.59a **3.60a**

Performed according to GP6 with addition of 2,6-di-tert-butyl-4-methylphenol (BHT, 44 mg, 0.2 mmol, 1.0 equiv.) on 0.2 mmol scale and purified by flash column chromatography (SiO_2, 15–50% Et_2O/hexanes) to give **3.60a** as a clear, colourless oil (condition A: 5 mg, 16%, 1.6:1 dr; condition B: 25 mg, 74%, 2.6:1 dr).

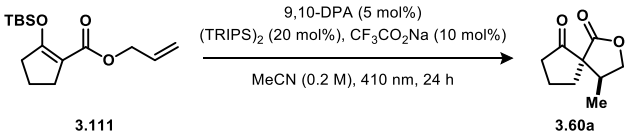
allyl 2-((tert-butyldimethylsilyl)oxy)cyclopent-1-ene-1-carboxylate (3.111)



3.59a **3.111**

To a solution of ketoester **3.59a** (2.0 g, 11.9 mmol, 1.0 equiv) in anhydrous DCM (24 mL, 0.5 M) was added Et_3N (5.0 mL, 35.7 mmol, 3.0 equiv) at 0 °C in an ice bath and the resulting mixture was stirred for 5 minutes at 0 ºC. TBSCl (2.0 g, 13.1 mmol, 1.1 equiv) was added in one portion, the solution was stirred at 0 ºC for 1 hour before being allowed to slowly warm to room temperature. The resulting solution was stirred at room temperature for 38 hours. The resulting suspension was then concentrated *in vacuo* before being re-suspended in hexanes. The resulting slurry was then passed through a medium glass fritted funnel to remove Et_3N•HCl and the filter cake was rinsed with more hexanes. The filtrate was then concentrated *in vacuo* to give a clear colourless oil as the crude residue. The crude residue was then purified by flash column chromatography using a Sepabean machine T (0–10% EtOAc/hexanes) to give **3.111** as a clear and colourless oil (1.93 g, 6.8 mmol, 57%). R_f 0.44 (5% EtOAc/hexanes); **^{1}H NMR** (600 MHz, $CDCl_3$) δ 6.00 – 5.90 (m, 1H), 5.29 (dq, J = 17.2, 1.6 Hz, 1H), 5.19 (dq, J = 10.3, 1.4 Hz, 1H), 4.62 (dt, J = 5.8, 1.5 Hz, 2H), 2.61 – 2.52 (m, 2H), 2.44 (ddd, J = 9.8, 7.0, 1.8 Hz, 2H), 1.97 – 1.76 (m, 2H), 0.96 (s, 9H), 0.20 (s, 6H) ppm; **^{13}C NMR** (151 MHz, $CDCl_3$) δ 165.6 (C), 165.0 (C), 133.3 (CH), 117.7 (CH_2), 108.0 (C), 64.3 (CH_2), 36.2 (CH_2), 29.3 (CH_2), 25.7 (3 × CH_3), 19.5 (CH_2), 18.4 (C), -3.8 (2 × CH_3) ppm; **HRMS** (EI+) *m/z* calculated for $C_{15}H_{26}O_3Si^{\bullet+}$ $[M]^{\bullet+}$ 282.16457, found 282.16621.

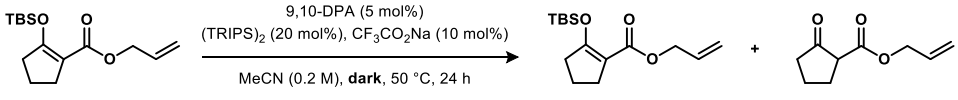
Intramolecular hydroalkylation of silyl enol ether 3.111



3.111 3.60a

Prepared according to GP6 with substrate **3.111** using condition B on 0.2 mmol scale (56.5 mg, 0.2 mmol, 1.0 equiv.) and purified by flash column chromatography (SiO_2, 25% EtOAc/hexanes) to give **3.60a** as a clear, colourless oil (26.8 mg, 80%, 4:1 dr).

Control test for intramolecular hydroalkylation of silyl enol ether 3.111

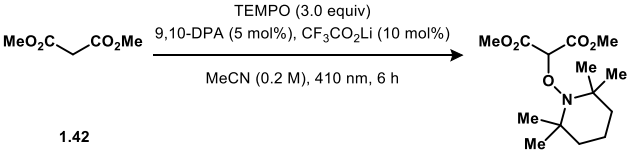


3.111 3.111 56:44 3.59a

Subjecting silyl enol ether **3.111** to GP6 using condition B in the absence of light and with heating to 50 °C led to partial hydrolysis of the silyl enol ether to form substrate **3.59a** (56:44 **3.111**/**3.59a**), indicating that productive hydroalkylation of **3.59a** may be due to hydrolysis under the reaction conditions.

Intramolecular reaction including TEMPO

dimethyl 2-((2,2,6,6-tetramethylpiperidin-1-yl)oxy)malonate (3.113)[§]



1.42 3.113

Inside a nitrogen-filled glovebox, an 8 mL oven-dried screw-top Pyrex tube (12 mm diameter) was charged with lithium trifluoroacetate (7.2 mg, 0.060 mmol, 10 mol%), 9,10-diphenylanthracene (9.9 mg, 0.030 mmol, 5 mol%), and (2,2,6,6-tetramethylpiperidin-1-yl)oxyl (TEMPO, 281 mg, 1.8 mmol, 3.0 equiv.). Once all components were added, the tube was sealed with a Teflon-septum screw cap, transferred out of the glovebox, and immediately placed under a positive pressure of argon. Anhydrous acetonitrile (3.0 mL, 0.2 M) was added and the resulting suspension sparged with argon for 5 minutes. The dimethyl malonate (79 mg, 0.60 mmol, 1.0 equiv.). was added, the septum cap was quickly exchanged with a hard plastic cap, and the vessel sealed with electrical tape and then Parafilm. The reaction mixture was then sonicated (90 s) before irradiating with a violet LED (2–2.4 W, 410 nm) at a distance of 1–5 mm for 6 h. The resulting solution was purified by flash column chromatography (SiO_2, 5–20% Et_2O/hexanes) to give **3.113** as a clear, colourless oil (trace). R_f 0.38 (20% Et_2O/hexanes); **^{1}H NMR** (400 MHz, $CDCl_3$) δ 5.03 (s,

1H), 3.85 (s, 6H), 1.77 – 1.33 (m, 6H), 1.26 (s, 6H), 1.12 (s, 6H) ppm; **^{13}C NMR** (101 MHz, $CDCl_3$) δ 166.4 (2 × C), 85.3 (CH), 59.1 (2 × C), 51.4 (2 × CH_3), 38.9 (2 × CH_2), 31.3 (2 × CH_3), 18.9 (2 × CH_3), 15.8 (CH_2) ppm; Characterized according to literature comparison. [368]

Mechanistic Studies

Reaction Component Solubility

A 1-, 2-, or 5-mL volumetric flask was filled to the line with acetonitrile and then saturated with the desired reaction component. The resulting suspension was sonicated for 6 minutes before being taken up in a syringe and passed through a 0.45 μm filter into a weighed 1-dram vial. The resulting solutions were then concentrated *in vacuo* and dried under high vacuum until a consistent mass was measured.

Entry	Compound	V_{MeCN} (mL)	$m_{component}$ (mg)	Average Solubility (mg/mL)	Average Solubility (M)
1	9,10-DPA	5.0	2.4	0.49 ± 0.01	0.0015 ± 0.00003
2	9,10-DPA	5.0	2.4		
3	9,10-DPA	5.0	2.5		
4	$(TRIPS)_2$	2.0	15.0	7.7 ± 0.2	0.016 ± 0.001
5	$(TRIPS)_2$	2.0	15.9		
6	$(TRIPS)_2$	2.0	15.2		
7	$[Et_4N]_3[Ce^{III}Cl_6]$	1.0	94.6	98 ± 12	0.13 ± 0.02
8	$[Et_4N]_3[Ce^{III}Cl_6]$	1.0	87.5		
9	$[Et_4N]_3[Ce^{III}Cl_6]$	1.0	111.3		

Actinometry and Quantum Yield

Synthesis of potassium ferrioxalate trihydrate actinometer

Preparation of $K_3[Fe(C_2O_4)_3]\bullet 3H_2O$

Adapted from procedures by Parker[369] and by Scaiano. [370] In the dark, solutions of $FeCl_6\bullet 6H_2O$ (1.5M, 4.8928 g, 18.1 mmol, into 12.1 mL) and potassium oxalate monohydrate (1.5M, 10 g, 54.3 mmol, into 36.2 mL) in distilled water were prepared. While still in the dark, the two solutions were combined under vigorous stirring, at room temperature, in air, and allowed to stir for 2 hours. After 2 h, the resulting precipitate was isolated by suction filtration. The material was then purified by three sequential recrystallizations from boiling water in the dark. Following the final suction filtration, the semi-dry recrystallized material was transferred into a 250 mL Erlenmeyer flask which was then submerged in an oil bath pre-heated to 45 ºC. Compressed air was then gently blown over the surface of the green

crystalline material overnight, maintaining the 45 ºC temperature. The next morning, 5.7751 g (73% yield) of green crystalline potassium ferrioxalate trihydrate material was isolated and used in the actinometry experiments.

Actinometry

Preparation of 0.15M $K_3[Fe(C_2O_4)_3]\cdot 3H_2O$ in $H_2SO_{4\,(aq)}$

In the dark, a 25 mL volumetric flask was charged with freshly ground $K_3[Fe(C_2O_4)_3]\cdot 3H_2O$ (1.8422 g, 3.75 mmol) followed by ~12 mL of distilled water. The resulting suspension was shaken before 2.5 mL of 1.0 N $H_2SO_{4\,(aq)}$ was added. This mixture was shaken and sonicated until complete dissolution of the ferrioxalate solute. Upon complete dissolution, the mixture was diluted to 25 mL and the solution was mixed again by inversion until homogeneous. The resulting green solution was transferred to an amber glass bottle and used within the same day it was prepared.

Preparation of 0.1% buffered phenanthroline solution

In the dark, a 25 mL volumetric flask was charged with sodium acetate (5.6250 g, 68.5 mmol) and phenanthroline (25 mg, 0.14 mmol) followed by H_2SO_4 (~12 mL, 0.5 M, aqueous). The resulting mixture was shaken and sonicated until fully dissolved. Upon complete dissolution, more H_2SO_4 (0.5 M, aqueous) was added to dilute to 25 mL and the solution was mixed by inversion. This solution was transferred to an amber glass bottle and used within the same day it was prepared.

Determination of photon flux of the 405 nm LED light source

In the dark, 3 mL of the 0.15 M potassium ferrioxalate solution was added to an 8 mL Pyrex screw-top tube equipped with stir bar and 3 mL of the same solution was transferred into a quartz cuvette equipped with a stir bar. The quartz cuvette was covered with aluminum foil and stirred in the dark whilst the 8 mL Pyrex tube was placed 2 mm from the 405 nm LED and stirred under irradiation for 60 s. After the irradiation is complete, the cuvette control and the irradiation sample are each treated with 0.5 mL of the 0.1% buffered phenanthroline solution in the dark. The resulting solutions are allowed to sit and develop for 5 minutes for 5 minutes. After 5 minutes, the irradiation sample was transferred to a quartz cuvette and the absorbance at 510 nm of both the dark and light solutions was measured using a Cary 7000 spectrophotometer. This procedure was completed four times to give the following results:

***Table 28**. Photon flux determined by actinometry*

Entry	$\Delta Abs_{510\ nm}$ ($A_{light} - A_{dark}$)	$n_{Fe(II)}$ (mol)	Photon Flux (nE/s)
1	1.924081393	5.40906E-07	7.908
2	2.096339956	5.89333E-07	8.61598
3	2.218884244	6.23783E-07	9.11964
4	2.125113018	5.97421E-07	8.73424
Average			8.6 (± 0.5)

Example calculation to determine the amount of Fe(II) produced by photolysis of the potassium ferrioxalate actinometer:

$$n_{Fe(II)} = \frac{V_{total} \cdot \Delta Abs_{510}}{\varepsilon_{510} \cdot l}$$
$$= \frac{(0.0035\ \text{L})(1.924081393)}{(12450\ \text{M}^{-1}\text{cm}^{-1})(1\ \text{cm})}$$
$$= 5.40906^{-7}\ \text{mol}$$

Where:

- ε_{510} = 12,450 $M^{-1}cm^{-1}$ for the $Fe(II)(phen)_3$ analyte[371]
  - The commonly used extinction coefficient of 11,100 $M^{-1}cm^{-1}$ does not have a clear source. It may be from a textbook by Marczenko, *Spectrophotometric Determination of Elements*.[372] The primary source of this number seems to be a 1938 publication by Mellon;[373] however, this publication does not specify the extinction coefficient for this complex and only provides concentration vs. transmittance plots. Transformation of that data may have given the commonly used ε_{510} of 11,100 $M^{-1}cm^{-1}$ that has propagated throughout the literature. Smith *et al.* have measured a new value of 12,450 M^{-1} cm^{-1} and the source can be easily identified.[371] This results in a photon flux of 8.6 (± 0.5) vs 9.6 (± 0.6) nE/s using 11,100 $M^{-1}cm^{-1}$. The overall result using this lower number for photon flux results in larger numbers for the quantum yield, further supporting a non-chain mechanism.
- path length of the cuvette, l = 1 cm
- ΔAbs_{510} is the difference in absorbance between the light and dark samples for each trial
- V_{total} is the volume of potassium ferrioxalate solution (3 mL) plus the volume of phenanthroline solution (0.5 mL)

$$photon\ flux\ (\text{E/s}) = \frac{n_{Fe(II)}}{\phi_{405} \cdot t \cdot F}$$

$$= \frac{(5.40906^{-7}\ \text{mol})}{(1.14)(60\ \text{s})(0.99986)}$$
$$= 7.908^{-9}\ \text{mol/s}$$
$$photon\ flux\ (\text{E/s}) \cdot 10^9\ \text{nE/E} = 7.908\ \text{nE/s}$$

Where:

- 1 mol of photons = 1 Einstein (E)
- ϕ_{405} = 1.14 for ferrioxalate photolysis[369]
- t = 60 s, irradiation time
- F = 0.99986, average fraction of light absorbed for the actinometer, calculated as such:

$$F = 1 - 10^{-Abs_{405}}$$
$$= 1 - 10^{-5.850975513}$$
$$= 0.99986$$

Quantum Yield Experiments

Experiments using Ce-containing conditions (A) and Ce-free conditions (B) were performed in triplicate as follows: Inside a nitrogen filled glovebox, an oven dried 8 mL Pyrex screw-top vial was charged with LiTFA (**SI-3**,7.2 mg, 10 mol%), 9,10-DPA (9.9 mg, 5 mol%), $(TRIPS)_2$ (56.5 mg), and allyl ketoester **3.59a** (100.9 mg, 0.6 mmol, 1 equiv). For reactions using condition A, the tube was also charged with $Ce(OTf)_3$ (35.1 mg, 10 mol%) and TBACl (166.8 mg, 1 equiv). The reaction tubes were then closed with a septum screw cap, exported from the glovebox, and immediately placed under a positive pressure of argon. Next, anhydrous MeCN (3 mL) was added and the resulting mixture was sparged with argon for 5 minutes. The septum cap was rapidly replaced with a plastic cap and sealed with electrical tape followed by parafilm. The resulting mixture was then sonicated for 90 s before being placed in the same LED setup used for the actinometry experiments. The reactions were then irradiated for 1 hour under vigorous stirring. After 1 h, irradiation was stopped and trimethylsilylbenzene internal standard was added (30μL, accurate mass recorded) and the solution was shaken vigorously to mix. Next, a 0.5 mL aliquot was transferred into an NMR tube, the tube was capped and an unlocked MeCN ^{1}H NMR spectrum was acquired. The remaining starting material and product yields were then determined by integration relative to the known internal standard quantity.

Stern-Volmer Kinetics and Fluorimetry(§)

9,10-DPA was expected to act as a redox mediator in the reaction, facilitating turnover between oxidation states of the other reaction components including the ketoester **3.86**, cerium catalyst $[Et_4N]_3[Ce^{III}Cl_6]$, and the

$(TRIPS)_2$ disulfide HAT catalyst. Fluorescence quenching experiments were used to determine the primary quencher of the 9,10-DPA* excited state by testing single components or component mixtures.

Stock solutions of 9,10-DPA and each component were prepared in a nitrogen-filled glovebox using analytical balances, gastight syringes, and volumetric glassware. Analyte solutions were prepared by sequential addition of 9,10-DPA stock, component stock solution(s), and acetonitrile to a 5.0 mL volumetric flask and then transferred to a 1 cm quartz fluorescence cuvette, capped under nitrogen atmosphere, sealed with Parafilm, and exported from the glovebox.

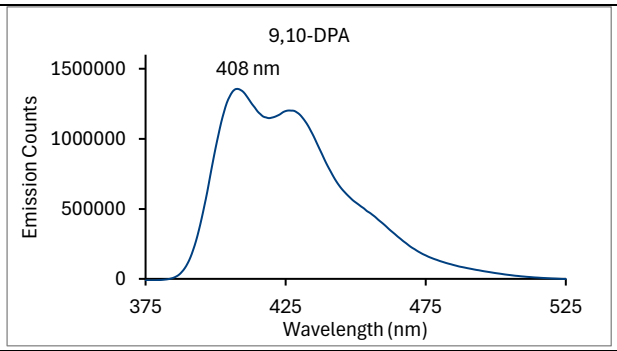
***Table 29**. Quencher solutions prepared for fluorescence quenching experiments*

Trial	[9,10-DPA] (M)	[Ketoester **3.86**] (M)	[LiTFA] (M)	$[(Et_4N)_3(Ce^{III}Cl_6)]$ (M)	$[(TRIPS)_2]$ (M)
1.1–1.3	5E-6	–	–	–	–
2.1–2.5	5E-6	1E-4 to 5E-4	–	–	–
3.1–3.5	5E-6	–	1E-4 to 5E-4	–	–
4.1–4.5	5E-6	–	–	1E-3 to 5E-3	–
5.1–5.4	5E-6	–	–	–	1E-4 to 4E-4
6.1–6.5	5E-6	1E-4 to 5E-4	1E-4 to 5E-4	–	–
7.1–7.5	5E-6	1E-4 to 5E-4	–	1E-3 to 5E-3	–
8.1–8.5	5E-6	–	1E-4 to 5E-4	1E-3 to 5E-3	–
9.1–9.5	5E-6	1E-4 to 5E-4	1E-4 to 5E-4	1E-3 to 5E-3	–

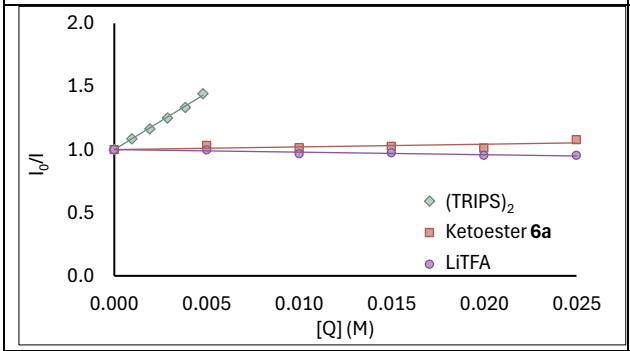
Fluorescence spectra were collected with $\lambda_{excitation}$ = 400 nm, $\lambda_{emission}$ = 600–420 nm in 1 nm steps. Emission intensity measured at 427 nm was plotted as the intensity in the absence of quencher (I_0) over intensity with quencher (I) against quencher concentration.

***Table 30**. Results of Stern–Volmer quenching experiments*

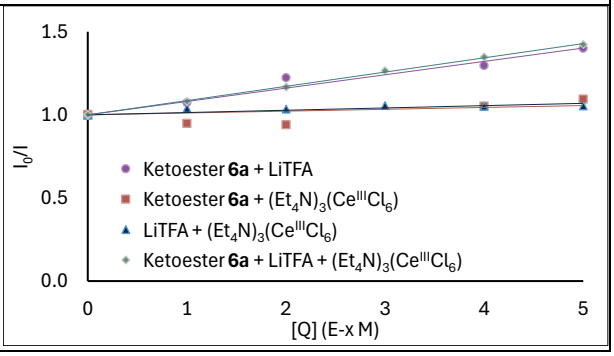
Trial 1: Emission spectrum of 9,10-DPA with no quencher, $\lambda_{0,0}$ = 408 nm



Trials 2–5: Quenching with individual components



Trials 6–9: Quenching with mixtures of components



Despite the appearance of 9,10-DPA quenching in the presence of $(TRIPS)_2$, the attenuation of emission in this case is due to primary inner filter effects as $(TRIPS)_2$ absorbs appreciably at the excitation wavelength of 400 nm (ε_{400} = ~28.8 M^{-1} cm^{-1}, see UV/Vis of Components Section). Ketoester **3.86** activated by LiTFA (Trial 6) or by LiTFA and $[Et_4N]_3[Ce^{III}Cl_6]$ together (Trial 9) are the most likely quenchers of the 9,10-DPA* excited state.

Ce^{IV} Decay Kinetics[§]

Reduction of $[Et_4N]_2[Ce^{IV}Cl_6]$ to $[Et_4N]_3[Ce^{III}Cl_6]$ can be tracked by UV-Vis spectrophotometry,[374] by a loss of signal corresponding to Ce^{IV} (λ = ~380 nm) and a development of signal corresponding to Ce^{III} (λ = ~330 nm). This process was observed visually as a loss of orange colour in solutions containing $[Et_4N]_2[Ce^{IV}Cl_6]$ at room temperature, occurring at different rates depending on the other components in the solution. Quantification of Ce^{IV} decay at room temperature was achieved by mixing solutions of $[Et_4N]_2[Ce^{IV}Cl_6]$ with ketoester **3.86** and/or LiTFA in an Agilent Cary 7000 UV-Vis spectrophotometer and collecting absorbance data over time.

Combination of $[Et_4N]_2[Ce^{IV}Cl_6]$ with the ketoester **3.86** and/or LiTFA had been observed visually to accelerate the decay of $[Et_4N]_2[Ce^{IV}Cl_6]$ at room temperature, so the analyte solutions needed to be mixed directly in the cuvette and in the dark immediately before beginning acquisition. Stock solutions of each component were

prepared using analytical balances, gastight syringes, and volumetric glassware. Analyte solutions were prepared by sequential addition of acetonitrile, then ketoester **3.86** and/or LiTFA solutions to a quartz cuvette in a fumehood in the dark. The cuvette was transferred to the spectrophotometer in the dark and $[Et_4N]_2[Ce^{IV}Cl_6]$ solution was added by syringe immediately before data acquisition was commenced.

Table 31. *Solutions prepared for thermal Ce^{IV} decay studies*

Trial	[TBACl] (M)	[ketoester **3.86**] (M)	[LiTFA] (M)	$[(Et_4N)_2(Ce^{IV}Cl_6)]$ (M)
1	–	–	–	4.3E-4
2	–	–	4.3E-3	4.3E-4
3	–	4.3E-3	–	4.3E-4
4	–	4.3E-3	4.3E-3	4.3E-4
5	0.2	–	–	4.3E-4
6	0.2	–	4.3E-3	4.3E-4
7	0.2	4.3E-3	–	4.3E-4
8	0.2	4.3E-3	4.3E-3	4.3E-4

Spectra were acquired using the Agilent "Scanning Kinetics" software (500–300 nm @ 400 nm/min over 20 minutes (25 minutes for trials 4 and 8)). Raw absorbance data was converted to absorptivity and plotted against wavelength (A). Absorbance at the peak maximum (378 nm) was normalized relative to the t_1 value and plotted against time (B) to show the unimolecular decay rates of the resulting Ce^{IV} complexes. Where significant decay (>10% conversion) was observed over the 20- or 25-minute time frame, absorbance was converted to concentration of Ce^{IV} using the molar extinction coefficients at 378 nm (ε_{378}) determined from UV/Vis absorbance data collected in UV/Vis of Components Section and plotted against time (C) such that the linear slope corresponds to the unimolecular rate constant.

Figure 59. *Absorbance of $[Et_4N]_2[Ce^{IV}Cl_6]$ at 378 nm with varying concentration*

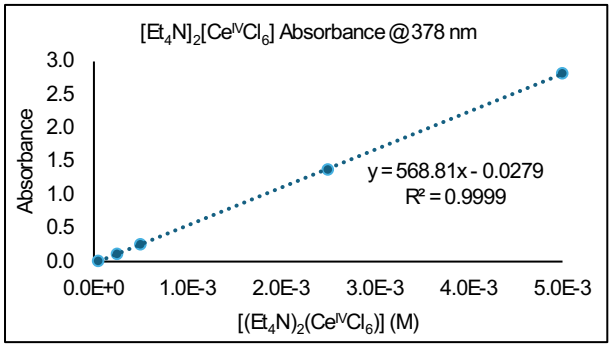
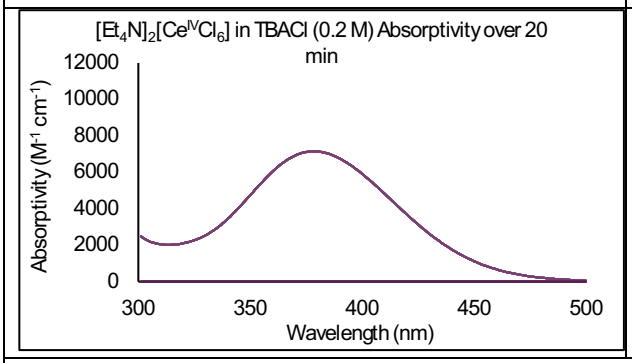


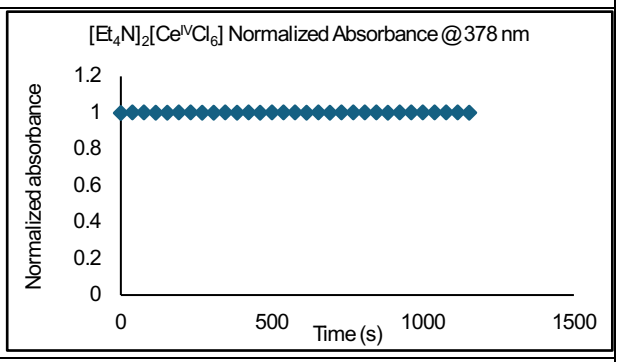
Table 32. *Results of thermal Ce^{IV} decay studies in acetonitrile solution*

Trial 1: $[Et_4N]_2[Ce^{IV}Cl_6]$

1A

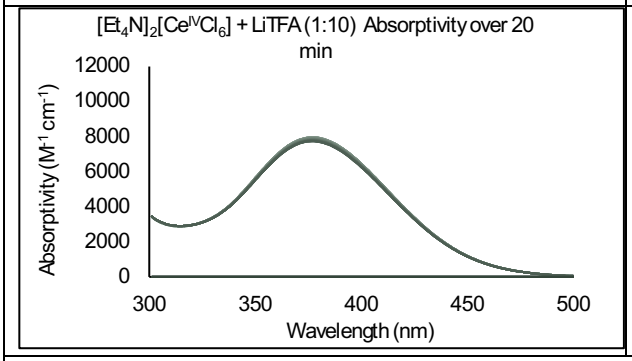


1B

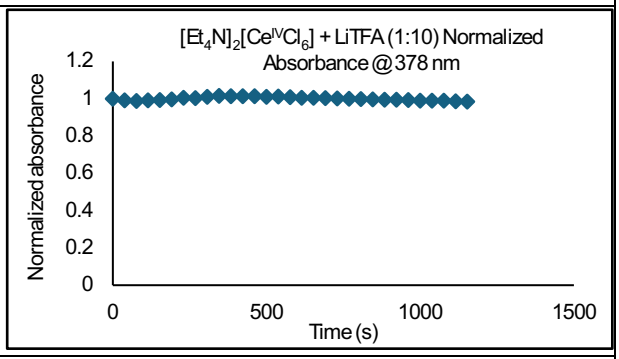


Trial 2: LiTFA + $[Et_4N]_2[Ce^{IV}Cl_6]$ (10:1)

2A

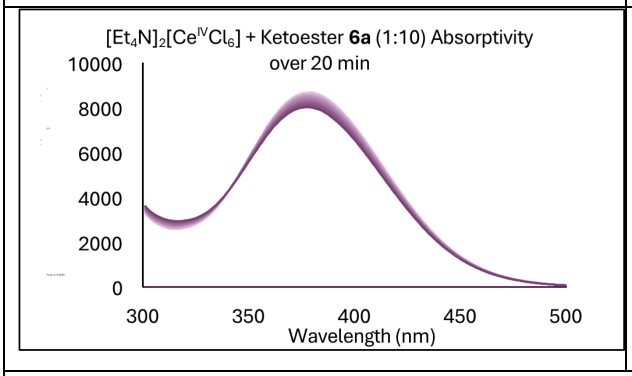


2B

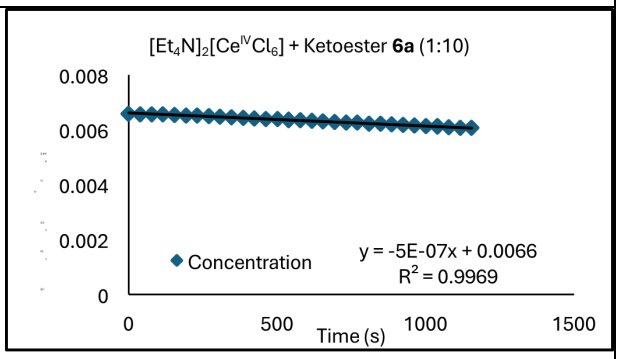


Trial 3: Ketoester **3.86** + $[Et_4N]_2[Ce^{IV}Cl_6]$ (10:1)

3A

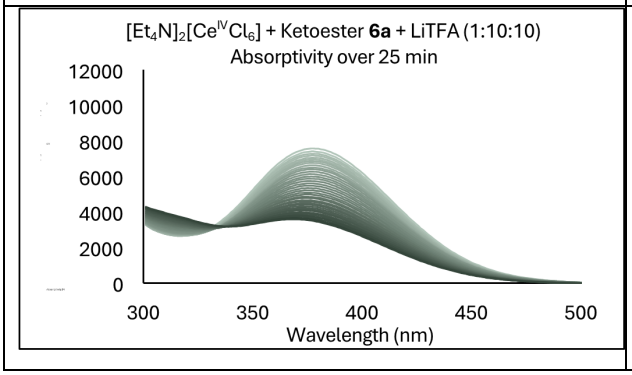


3C



Trial 4: Ketoester **3.86** + LiTFA + $[Et_4N]_2[Ce^{IV}Cl_6]$ (10:10:1)

4A



4C

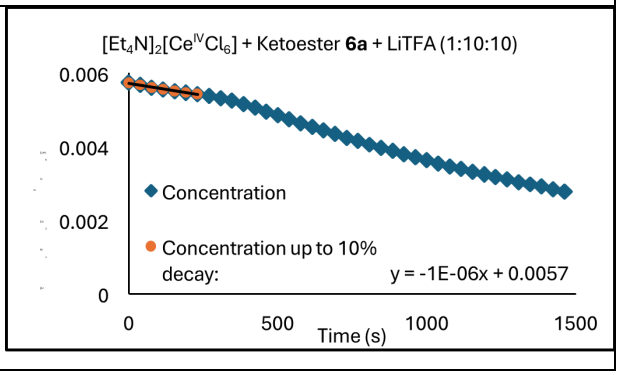
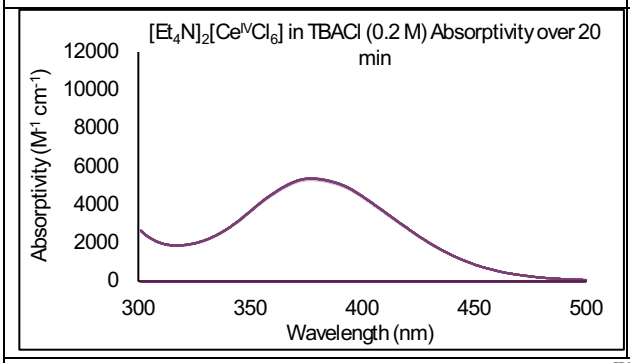
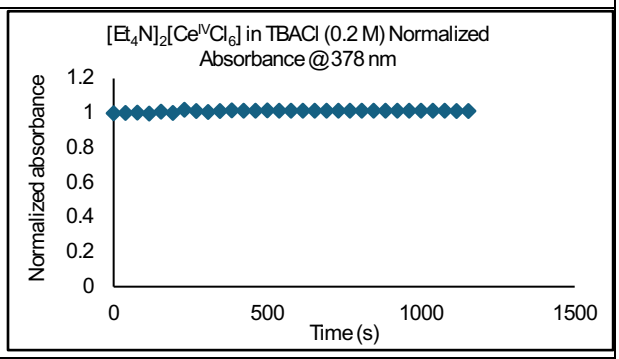
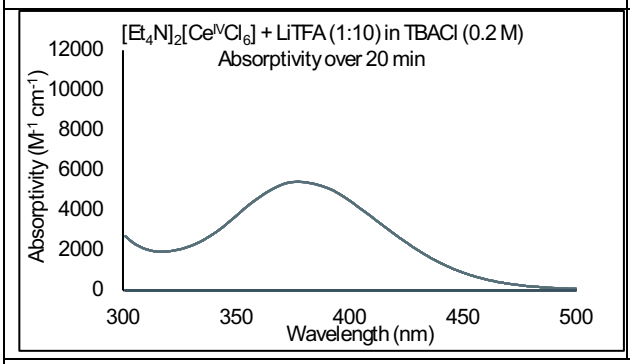
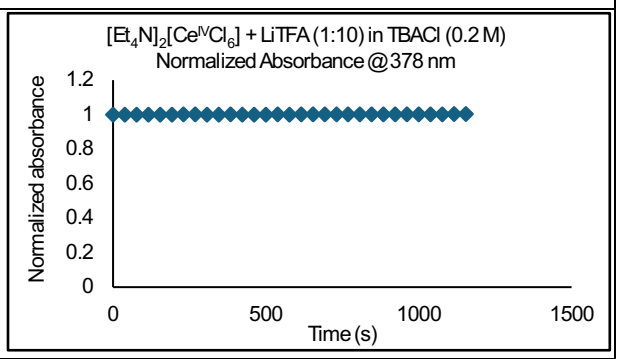
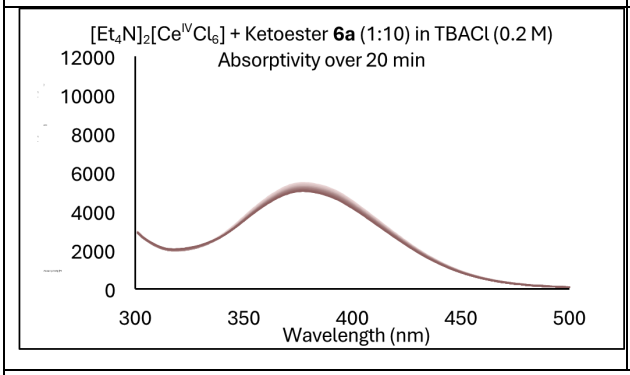
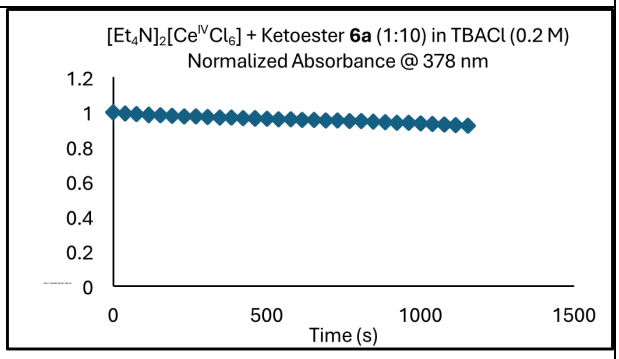
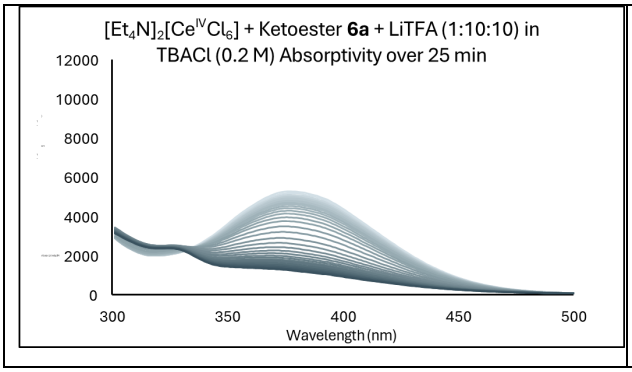
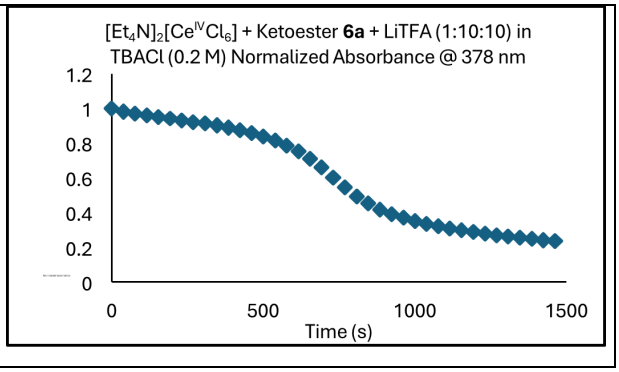


Table 33. *Results of thermal Ce^{IV} decay studies in acetonitrile solutions including TBACl (0.2 M)*

Trial 5: $[Et_4N]_2[Ce^{IV}Cl_6]$ in TBACl (0.2 M)	
5A	**5B**
	
Trial 6: LiTFA + $[Et_4N]_2[Ce^{IV}Cl_6]$ (10:1) in TBACl (0.2 M)	
6A	**6B**
	
Trial 7: Ketoester **3.86** + $[Et_4N]_2[Ce^{IV}Cl_6]$ (10:1) in TBACl (0.2 M)	
7A	**7B**
	
Trial 8: Ketoester **3.86** + LiTFA + $[Et_4N]_2[Ce^{IV}Cl_6]$ (10:10:1) in TBACl (0.2 M)	
8A	**8B**

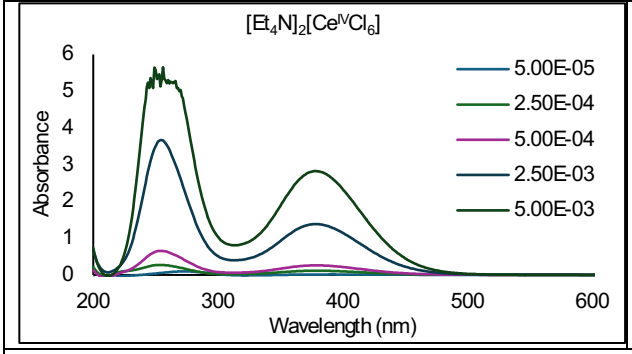
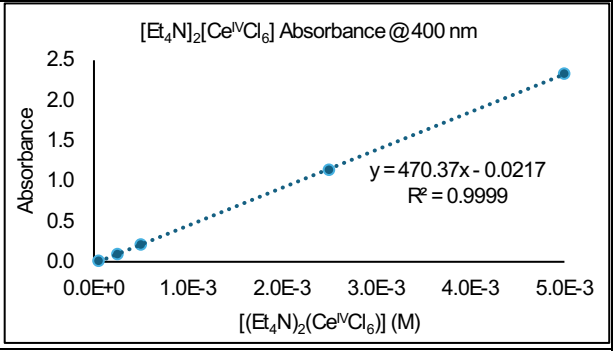


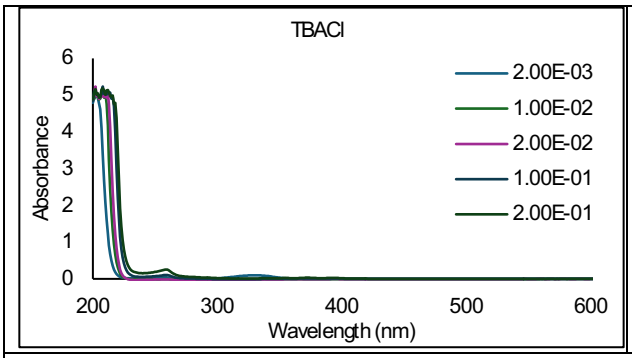


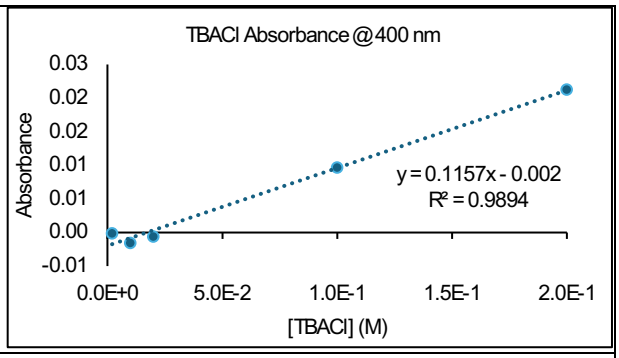
UV/Vis of Components[§]

Solutions of each component were prepared in MeCN at five concentrations spanning two approximately orders of magnitude. Solutions were prepared using analytical balances, gastight syringes, and volumetric glassware. Spectra were recorded in an Agilent Cary 7000 UV-Vis spectrophotometer (200–800 nm). Absorbance data was plotted against wavelength for each concentration (A). Absorbance at 400 nm was plotted against concentration to determine the molar absorption coefficient (ε_{400}) from the linear slope (B) to evaluate the degree of competitive absorption in the Stern–Volmer quenching studies.

Table 34. *Results of UV/Vis spectroscopy of reaction components in acetonitrile at various concentrations*

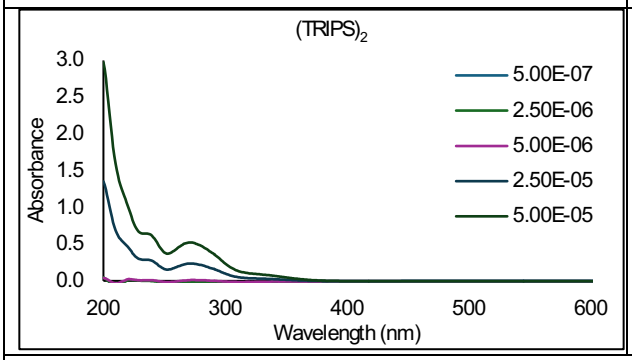
1: $[Et_4N]_2[Ce^{IV}Cl_6]$	
1A	**1B**
	
2: TBACl	
2A	**2B**

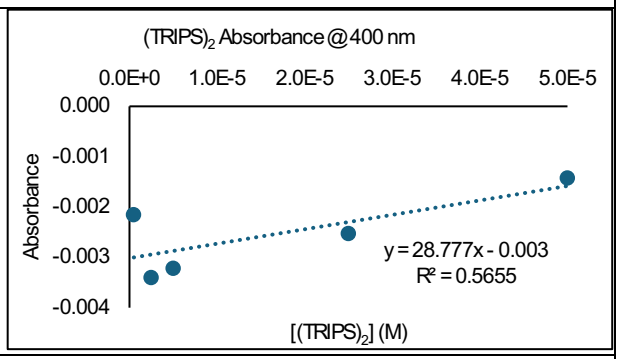




3: $(TRIPS)_2$

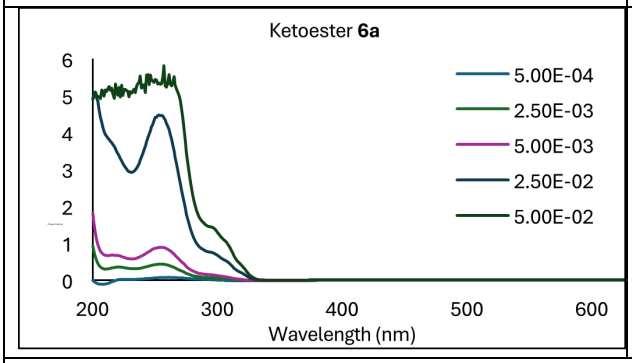
3A **3B**

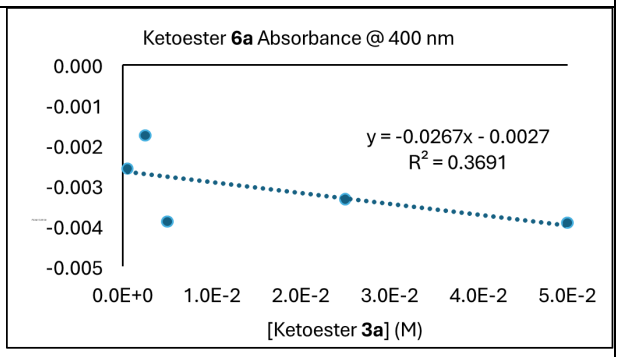




4: Ketoester **3.86**

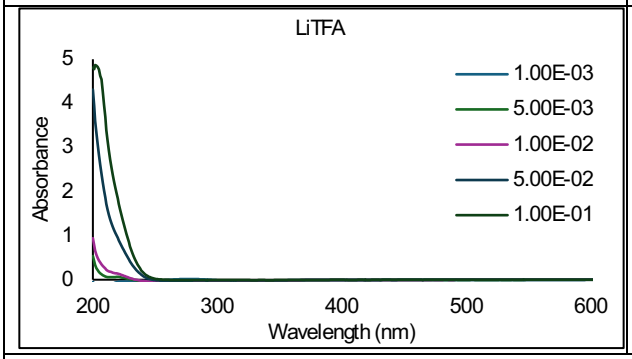
4A **4B**

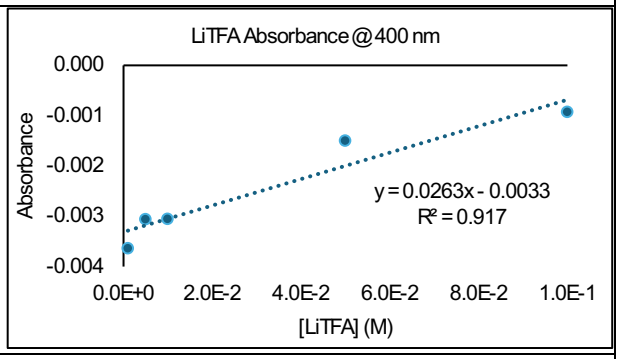




5: LiTFA

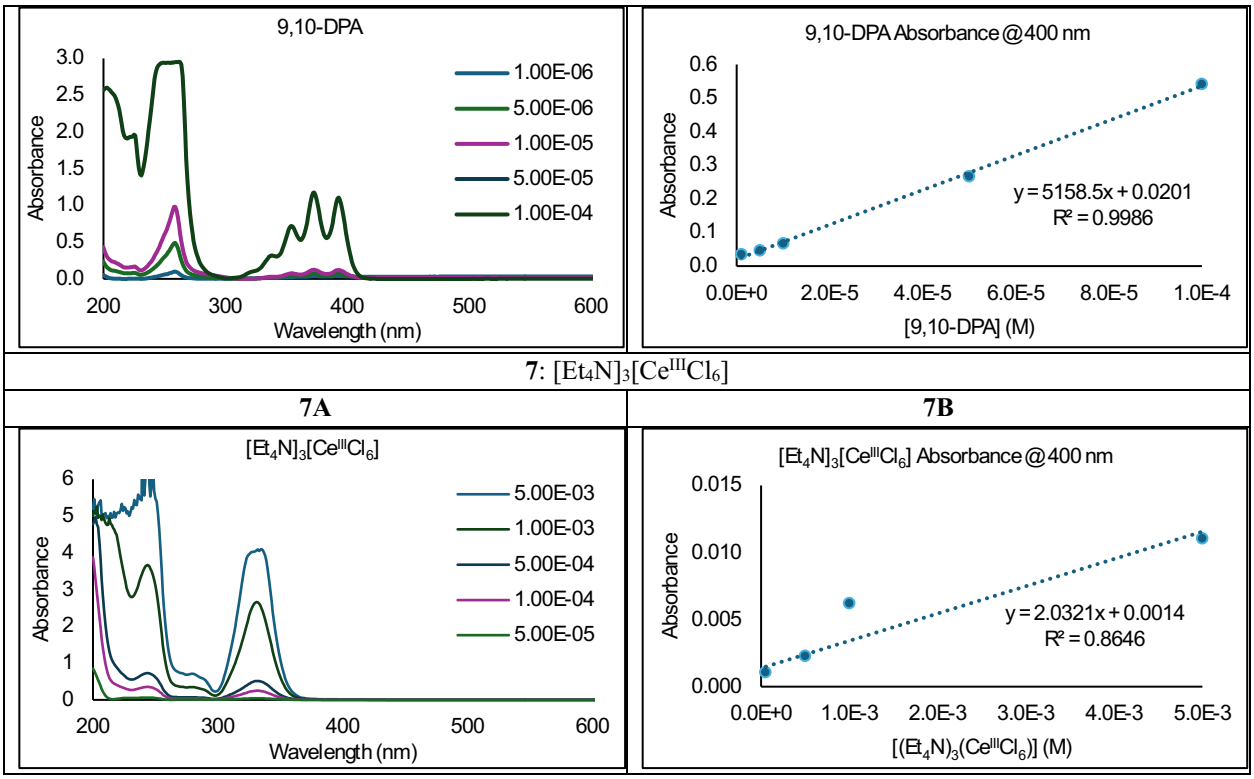
5A **5B**





6: 9,10-DPA

6A **6B**



NMR Titrations[§]

NMR titrations were performed to understand solution-phase interactions between reaction components, namely ketoester **3.86**, dimethylmalonate (**1.42**), LiTFA, and hexachlorocerate species $[Et_4N]_2[Ce^{IV}Cl_6]$ and $[Et_4N]_3[Ce^{III}Cl_6]$. Titrations were performed both in acetonitrile and in solutions of tetraethylammonium chloride (TEACl) in acetonitrile, as hexachlorocerate species are known to form higher order complexes in solution in the absence of supporting chloride.[374] Titrations involving $[Et_4N]_2[Ce^{IV}Cl_6]$ were largely unproductive as thermal decay of the Ce^{IV} species was observed during sample preparation, which was further explored in UV/Vis kinetics studies described in Ce^{IV} Decay Kinetics Section.

Considering known guidelines for host–guest titrations[375] and accounting for the limitations of solubility (see Reaction Component Solubility Section) and stability of the components, the titration experiments were conducted in the following manner. Titrations were performed by preparing individual solutions for each data point. Each series comprised of one "host" species whose concentration remained constant across each data point, and one "guest" species (either one component or a mixture of two components) whose concentration was varied across the series. The

ratios of guest concentration compared to the host concentration ranged between 0.1–20 equivalents with 12 data points collected in this range as given in **Table 35**.

***Table 35**. Titration solutions prepared for NMR studies*

Trial	[Host] (M)	[Guest] (M)	Equivalents of Guest	Volume (Guest) (mL)	Total Volume (mL)
1	0.02	0	0	0	1.0
2	0.02	0.002	0.1	0.002	1.0
3	0.02	0.004	0.2	0.004	1.0
4	0.02	0.008	0.4	0.008	1.0
5	0.02	0.012	0.6	0.012	1.0
6	0.02	0.016	0.8	0.016	1.0
7	0.02	0.020	1.0	0.020	1.0
8	0.02	0.040	2.0	0.040	1.0
9	0.02	0.080	4.0	0.080	1.0
10	0.02	0.12	6.0	0.120	1.0
11	0.02	0.16	8.0	0.160	1.0
12	0.02	0.20	10.0	0.200	1.0
13	0.02	0.40	20.0	0.400	1.0

The titrations would be most representative if they closely resembled the reaction conditions, so the solution concentrations were based on reaction concentrations of each component. Due to the solubility of $[Et_4N]_2[Ce^{IV}Cl_6]$ and $[Et_4N]_3[Ce^{III}Cl_6]$ in acetonitrile, these species were selected for the "host" role so that their concentration could be kept constant at reaction concentration and below their limit of solubility (Section 0). Since the guest species were therefore the NMR-active component, varying their concentration led to dilution effects in some cases. These dilution effects were corrected for by titrating a blank solution with each guest titrant and measuring the effect of dilution on the signal of interest.

***Table 36**. NMR signals of interest for reaction component titrations*

Guest	Signal
Ketoester **3.86**	^{1}H NMR: O*CH*$_3$
Malonate **1.42**	^{1}H NMR: O*CH*$_3$
LiTFA	^{19}F NMR: *CF*$_3$

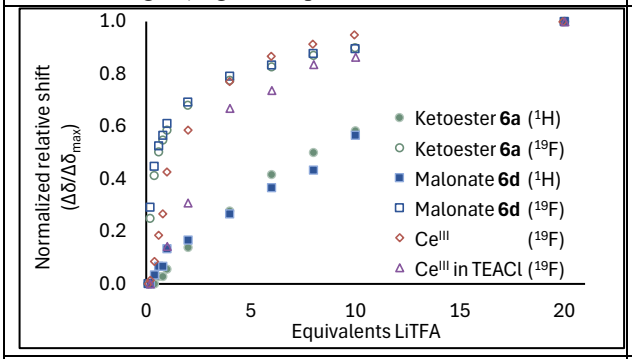
Solutions were prepared using volumetric glassware and gastight syringes, then transferred to NMR tubes and capped. Solutions containing $[Et_4N]_2[Ce^{IV}Cl_6]$ or $[Et_4N]_3[Ce^{III}Cl_6]$ were prepared in the dark. Internal standards were included in each solution to act as a chemical shift reference. They proved unreliable for quantification of the

components in each solution, likely due to their volatility and losses during sample preparation. Phenyltrimethylsilane was used as a ^{1}H NMR reference (0.94 ppm) and hexafluorobenzene as a ^{19}F NMR reference (–164.38 ppm) in MeCN.

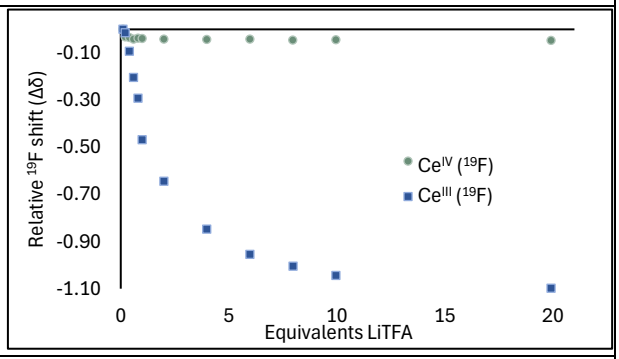
Spectra were acquired on a Bruker AVANCE III HD 500 spectrometer using an experiment that allowed unlocked acquisitions in MeCN (proteated, not deuterated). Sample temperature measured 25 °C consistently. Spectra were processed with MestreNova, using automatic phase correction and baseline correction for ^{1}H NMR and automatic phase correction and Whittaker Smoother baseline correction for ^{19}F NMR. Chemical shift (δ) for signals of interest were collected and expressed relative to their value in trial 2 ($\Delta\delta$). Relative shifts were normalized to the maximum response value from trial 13 ($\Delta\delta/\Delta\delta_{max}$). Relative ($\Delta\delta$) and normalized ($\Delta\delta/\Delta\delta_{max}$) shifts were plotted against added equivalents of the guest species to give titration curves.

Table 37*. Results of NMR titrations*

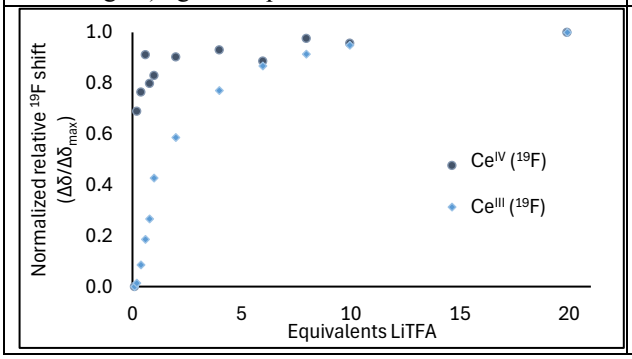
A: Ketoester **3.86**, Malonate **1.42**, and $[Et_4N]_3[Ce^{III}Cl_6]$ titrated with LiTFA, expressed as normalized relative chemical shift ($\Delta\delta/\Delta\delta_{max}$) data from ^{1}H NMR (arising from dicarbonyl signals) and ^{19}F NMR (arising from LiTFA signal) against equivalents of LiTFA added



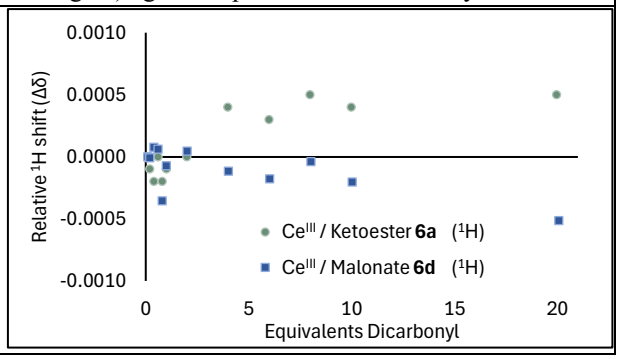
B: $[Et_4N]_3[Ce^{III}Cl_6]$ and $[Et_4N]_2[Ce^{IV}Cl_6]$ titrated with LiTFA, expressed as relative chemical shift ($\Delta\delta$) data from ^{19}F NMR (arising from LiTFA signal) against equivalents of LiTFA added



C: $[Et_4N]_3[Ce^{III}Cl_6]$ and $[Et_4N]_2[Ce^{IV}Cl_6]$ titrated with LiTFA, expressed as normalized relative chemical shift ($\Delta\delta/\Delta\delta_{max}$) data from ^{19}F NMR (arising from LiTFA signal) against equivalents of LiTFA added



D: $[Et_4N]_3[Ce^{III}Cl_6]$ titrated with dicarbonyls ketoester **3.86** and malonate **1.42**, expressed as relative chemical shift ($\Delta\delta$) data from ^{1}H NMR (arising from dicarbonyl signal) against equivalents of dicarbonyl added



Titration of each guest species (ketoester **3.86**, malonate **1.42**, and $[Et_4N]_3[Ce^{III}Cl_6]$) with LiTFA showed a response in ^{19}F NMR shift beyond the background response arising from dilution effects (**Table 36**, A, open shapes). A similar response profile was observed in titration with each of the guests, with approximately half of the maximum change in shift occurring at addition of 1 equivalent of LiTFA. Ketoester **3.86** and malonate **1.42** gave response profiles that appear to overlap, indicating a similar degree of interaction between LiTFA and each dicarbonyl. Titration of $[Et_4N]_3[Ce^{III}Cl_6]$ in acetonitrile with LiTFA indicates an interaction between $[Et_4N]_3[Ce^{III}Cl_6]$ and LiTFA. Inclusion of TEACl in this titration led to a shallower titration curve, suggesting that inclusion of a chloride source in solution attenuates interaction between $[Et_4N]_3[Ce^{III}Cl_6]$ and LiTFA. The interaction between each dicarbonyl and LiTFA was also reflected in the ^1H NMR data (**Table 36**, A, filled shapes).

Titration of $[Et_4N]_2[Ce^{IV}Cl_6]$ or $[Et_4N]_3[Ce^{III}Cl_6]$ with LiTFA showed a response in both cases. The magnitude of the response was greater in titration of Ce^{III} than Ce^{IV} (**Table 36**, B). The titration curve reached a saturation point more rapidly with Ce^{IV} than with Ce^{III} (**Table 36**, C). Overall, this suggests that LiTFA interacts more strongly with Ce^{IV} than with Ce^{III}, though this interaction has less impact on the observed chemical shift of LiTFA.

Titration of $[Et_4N]_3[Ce^{III}Cl_6]$ with either ketoester **3.86** or malonate **1.42** showed little response in ^1H NMR chemical shift across the range of equivalents tested (**Table 36**, D). Any interaction is likely below the limit of detection for NMR.

LiTFA Fate Studies

To assess the fate of the LiTFA additive under the reaction conditions we studied the ^{19}F spectra under a variety of conditions.

Initially, stoichiometric photolysis of a 1:1 mixture of $[Et_4N]_2[Ce^{IV}Cl_6]$ and LiTFA in MeCN was attempted (**Table 38**, A). To this end, 12.8 mg of $[Et_4N]_2[Ce^{IV}Cl_6]$ and 3.2 mg of LiTFA were added to an 8 mL screw top Pyrex tube in the dark followed by 1 mL of anhydrous MeCN. The tube was capped and covered with aluminum foil then sonicated for 90s before being transferred into an oven-dried NMR tube. The tube was sealed with an NMR tube cap with a 20 ga needle piercing through it. The needle was then attached to a closed hi–vac line before the tube was submerged in liquid nitrogen until frozen. Dynamic vacuum was then applied for 45 seconds while still submerged in the LN_2. After 45 seconds of evacuation the manifold was closed to give static vacuum and the tube was removed from the cooling bath. The solution was then allowed to warm to RT under static vacuum. The freeze-pump-thaw procedure was repeated 3 more times. After the fourth cycle, and once the mixture had warmed to RT and while still

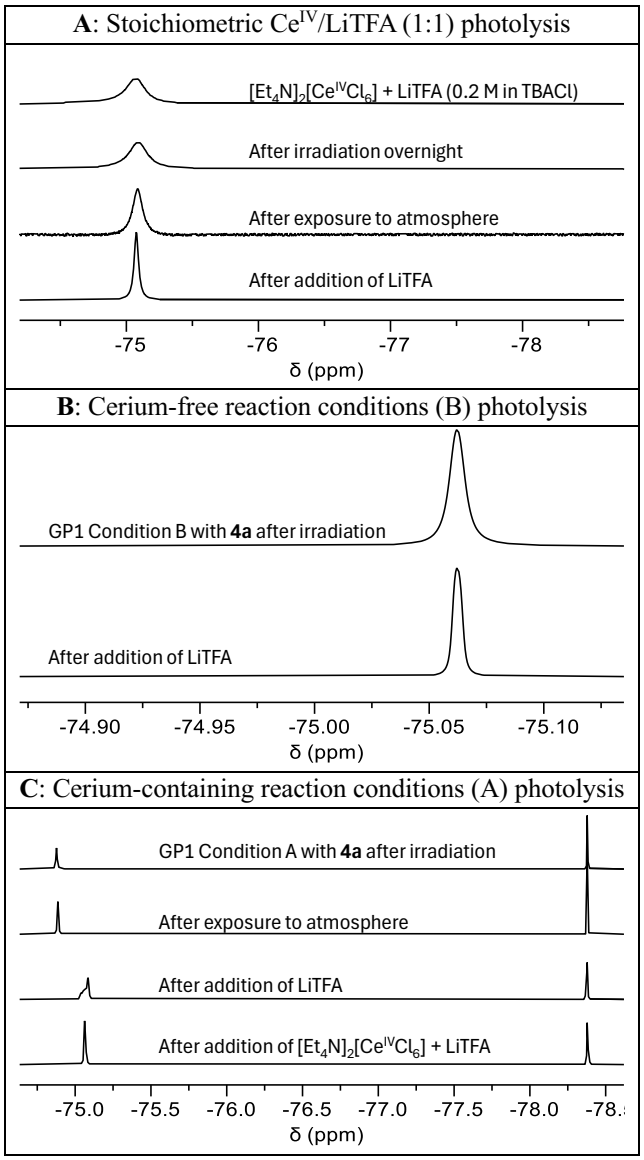
under static vacuum, the top of the tube closest to the needle was heated with a blowtorch and pulled into two closed fragments to flame-seal the reaction into the tube. While still protecting the mixture from ambient light, an 8-scan unlocked MeCN ^{19}F NMR spectrum with 32 second recycle delay was collected on a Bruker Avance III 500 MHz spectrometer revealing only a single ^{19}F resonance. The mixture was then irradiated for 5 minutes using a 405 nm LED (**Table 38**, A). During this time the orange Ce^{IV} colour of the completely faded to give a clear colourless solution. Another ^{19}F spectrum was acquired, again showing only a single fluorine signal. The mixture was then irradiated overnight before another ^{19}F spectrum was acquired, which showed only a single resonance. Re-exposing the tube to ambient atmosphere and transferring to a new NMR tube before acquiring another ^{19}F spectrum showed the same signal was conserved suggesting that it was not due to gaseous fluoroform. Finally, addition of extraneous LiTFA (~ 2 mg) and re-acquisition of ^{19}F spectrum still showed only a single resonance indicating that the LiTFA does not decompose under stoichiometric photolysis conditions in the presence of Ce^{IV}. Under the concern that LiTFA decomposition could occur given longer irradiation time and more potential LMCT events we next chose to perform these NMR studies under the Ce-containing and Ce-free reaction conditions.

For the Ce-free conditions, a reaction mixture was prepared according to GP6, excluding $Ce(OTf)_3$ and TBACl, and without sparging with argon. After sonication, the contents were transferred into an NMR tube and treated to the freeze-pump-thaw procedure described above (4 cycles). The NMR tube was then flame-sealed as described above. The resulting mixture was then studied by unlocked MeCN ^{1}H and ^{19}F NMR spectroscopy before irradiation, following 21 hours of irradiation at 405 nm, after opening to atmosphere, and then after the addition of more LiTFA. The ^{1}H NMR spectra confirmed that full conversion of ketoester **3.59a** had occurred following irradiation, thereby confirming catalyst turnover. Each corresponding ^{19}F spectrum showed only a single resonance, suggesting trifluoroacetate does not undergo decomposition under the reaction conditions to any appreciable extent (**Table 38**, B).

Under the Ce-containing conditions, a reaction mixture was prepared according to GP6 Condition A, excluding ketoester **3.59a**. Following sparging, capping, and sonication, the resulting mixture was irradiated at 405 nm under vigorous stirring and fan cooling for 48 h to solubilize all components completely. After this 48 h period, 33.6 mg of ketoester **3.59a** was added to the homogeneous mixture and this solution was transferred into an NMR tube. This NMR tube sample was treated to the freeze-pump-thaw (4 cycles) and flame sealing procedure described above. Unlocked acetonitrile ^{1}H and ^{19}F NMR spectroscopy of the mixture: before irradiation, after 24 h of irradiation

with a 405 nm LED, after exposure to ambient atmosphere, and after subsequent addition of ~2 mg of LiTFA, showed that irradiation fully converted dicarbonyl **3.59a** and left the LiTFA signal unchanged after each treatment (**Table 38**, A).

***Table 38**. LiTFA fate studies*



Notes:

- C_6F_6 and 1,3,5-tri-*tert*-butylbenzene internal standards were initially included in these experiments in an attempt to quantify the amount of LiTFA, ketoester **3.59a**, and ketolactone **3.60a** after each treatment. However, the C_6F_6 appeared to decompose under the conditions, complicating spectral analysis and quantification. Likewise,

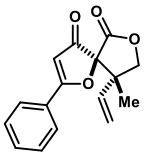
1,3,5-tri-*tert*-butylbenzene appeared to inhibit reaction conversion. For these reasons, the experiments were performed according to the standard reaction conditions.

- The heterogeneous Ce-containing conditions proved challenging for reactions run in NMR tubes. For this reason, we chose to irradiate this solution prior to the introduction of ketoester **3.59a**. This procedure rendered the mixture homogeneous and irradiation of the sample in the flame-sealed NMR tube showed full conversion of **3.59a** into the typically observed product **3.60a** establishing the viability of this pre-irradiation treatment.

5.4 Chapter 4 Experimental Details

Procedures and Data

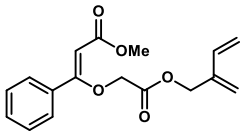
(±)-Hyperolactone C (3.2)



Inside a nitrogen-filled glovebox, an 8 mL oven-dried screw-top Pyrex tube (12 mm diameter) was charged with lithium trifluoroacetate (2.4 mg, 0.020 mmol, 10 mol%), 9,10-diphenylanthracene (3.3 mg, 0.010 mmol, 5 mol%), copper(II) trifluoroacetate hydrate (174 mg, 0.6 mmol, 3.0 equiv.), and tiglyl hydroxyfuranoate **4.114** (54.5 mg, 0.2 mmol, 1.0 equiv.). The tube was sealed with a Teflon-septum screw cap, transferred out of the glovebox, and immediately placed under a positive pressure of argon. Anhydrous acetonitrile (1.0 mL, 0.2 M) was added and the resulting suspension sparged with argon for 5 minutes. After sparging, the septum cap was quickly exchanged with a hard plastic cap and the vessel sealed with electrical tape and then Parafilm. The reaction mixture was then sonicated (90 s) before irradiating with a violet LED (2–2.4 W, 410 nm) at a distance of 1–5 mm for 24 h. The reaction was diluted with EtOAc (20 mL) and washed with NH_4Cl (saturated aqueous, 3 × 20 mL), water (20 mL), and brine (20 mL). The organic phase was dried over Na_2SO_4, filtered, and concentrated under reduced pressure. The crude residue was purified by flash column chromatography (SiO_2, 10–35% EtOAc/hexanes) to give hyperolactone C (**3.2**) as an amber crystalline solid (26.1 mg, 45%, 5:1 dr). $\boldsymbol{R_f}$ 0.30 (20% EtOAc/hexanes); **^{1}H NMR** (400 MHz, $CDCl_3$) δ 7.89 – 7.81 (m, 2H, **2M** + **2m**), 7.65 – 7.56 (m, 1H, **M** + **m**), 7.56 – 7.47 (m, 2H, **2M** + **2m**), 6.12 – 5.93 (m, 2H, **2M** + **2m**), 5.37 (d, J = 9.0 Hz, 0.16H, **m**), 5.33 (d, J = 15.6 Hz, 0.16H, **m**), 5.28 (d, J = 1.8 Hz, 0.84H, **M**), 5.25 (d, J = 8.5 Hz, 0.84H, **M**), 4.96 (dd, J = 8.5, 0.9 Hz, 0.84H, **M**), 4.78 (d, J = 8.7 Hz, 0.16H, **m**), 4.38 (d, J = 8.7 Hz, 0.16H, **m**), 4.11 (d, J = 8.5 Hz, 0.84H, **M**), 1.53 (d, J = 0.8 Hz, 2.52H, **3M**), 1.29 (s, 0.48H, **3m**) ppm; **^{13}C NMR** (101 MHz, $CDCl_3$) δ

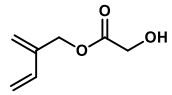
M 196.7 (C), 187.4 (C), 168.2 (C), 134.3 (CH), 133.7 (CH), 129.2 (2 × CH), 127.8 (C), 127.5 (2 × CH), 119.2 (CH_2), 100.4 (CH), 93.2 (C), 74.3 (CH_2), 49.0 (C), 19.7 (CH_3) **m** 196.7 (C), 187.6 (C), 168.3 (C), 136.9 (CH), 133.8 (CH), 129.2 (2 × CH), 127.8 (C), 127.6 (2 × CH), 116.4 (CH_2), 100.5 (CH), 92.4 (C), 73.4 (CH_2), 49.0 (C), 15.6 (CH_3) ppm; **HRMS** (EI+) *m/z* calculated for $C_{16}H_{14}O_4^{\bullet+}$ $[M]^{\bullet+}$ 270.08866, found 270.08947.

methyl (Z)-3-(2-((2-methylenebut-3-en-1-yl)oxy)-2-oxoethoxy)-3-phenylacrylate (4.17)[§]



To a solution of SPhosAuSbF$_6$•MeCN (4.4 mg, 0.015 mmol, 1.0 mol%) in DCM (0.5 mL, 2.0 M) was added methyl phenylpropiolate (**4.79**, 320 mg, 2.0 mmol, 2.0 equiv.) and glycolate **4.22** (142 mg, 1.0 mmol, 1.0 equiv.) at room temperature. The solution was stirred for 72 hours at room temperature. The reaction mixture was purified directly by flash column chromatography (SiO_2, 10–35% EtOAc/hexanes) to give *Z*-enol ether **4.17** with traces of methyl benzoylacetate present as a clear, colourless oil (88 mg, 29%). R_f 0.23 (10% EtOAc/hexanes); **^{1}H NMR** (400 MHz, C_6D_6) δ 7.75 – 7.59 (m, 2H), 7.09 – 6.91 (m, 3H), 6.12 (ddd, J = 17.9, 11.1, 0.8 Hz, 1H), 5.76 (s, 1H), 5.08 – 4.97 (m, 2H), 4.93 – 4.91 (m, 1H), 4.91 – 4.82 (m, 3H), 4.65 (d, J = 1.2 Hz, 2H), 3.43 (s, 3H) ppm.

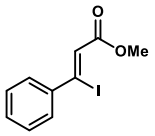
2-methylenebut-3-en-1-yl 2-hydroxyacetate (4.22)



A solution of dibromide **4.30** (5.1 mL, 45 mmol, 1 equiv) in DMPU (freshly distilled over CaH_2, 10.2 mL, 2 volumes) was added to a flame-dried 25 mL round bottom flask equipped with a stir bar and fitted with a short-path distillation piece and collection flask (containing a small crystal of BHT) under argon atmosphere. The solution was stirred and slowly heated in an oil bath slowly from room temperature to 120 ºC over 30 minutes. Once at 120 ºC, a vacuum line attached to a diaphragm pump was switched on to distill crude bromide as a clear colourless oil (**4.26**, 1.36 g, ≤ 9 mmol, ≤ 21% yield). This clear colourless oil was immediately transferred to a solution of potassium glycolate (0.96 g, 8.4 mmol, 1 equiv) in DMF (21 mL, 0.4 M) and the solution was allowed to stir at room temperature overnight. The next morning, the mixture was diluted with distilled water (100 mL) and EtOAc (50 mL) and the layers were separated. The aqueous phase was extracted with EtOAc (3 × 25 mL). The combined organic extracts were washed with water (3 × 20 mL), then brine (1 × 20 mL), and dried over Na_2SO_4, filtered and concentrated *in vacuo*. The crude residue was purified by flash column chromatography (10–25% EtOAc/Hexanes). The title compound

(**4.22**) was obtained as a clear and colourless oil (249 mg, 1.75 mmol, 4% yield over 2 steps). R_f 0.22 (20% EtOAc/hexanes); **^{1}H NMR** (400 MHz, C_6D_6) δ 6.12 (dd, J = 17.9, 11.1 Hz, 1H), 5.03 – 4.97 (m, 2H), 4.94 – 4.85 (m, 2H), 4.61 (d, J = 1.2 Hz, 2H), 3.83 (d, J = 5.3 Hz, 2H) ppm; **^{13}C NMR** (101 MHz, C_6D_6) δ 172.8 (C), 140.3 (C), 135.8 (CH), 118.1 (CH_2), 114.4 (CH_2), 63.7 (CH_2), 60.2 (CH_2) ppm; **HRMS** (EI+) *m/z* calculated for $C_7H_{10}O3^{\bullet+}$ $[M]^{\bullet+}$ 142.06245, found 142.06403.

methyl (Z)-3-iodo-3-phenylacrylate (4.24)[§]



Prepared according to a procedure by Smith. A mixture of methyl phenylpropiolate (1.7 g, 11 mmol, 1.0 equiv), NaI (5.1 g, 34 mmol 3.2 equiv.), and AcOH (7.9 mL, 8.3 g, 138 mmol, 13 equiv.) was heated to 110 °C for 4 hours. The reaction was allowed to cool to room temperature, then diluted with Et_2O (50 mL) and water (50 mL). The phases were separated and the aqueous phase extracted with Et_2O (2 × 20 mL). The combined organic phases were washed with Na_2CO_3 (5% aqueous, 20 mL), $Na_2S_2O_3$ (20 mL, saturated aqueous), then dried over $MgSO_4$, filtered, and concentrated under reduced pressure. The crude residue was purified by flash column chromatography (SiO_2, 0–2% EtOAc/hexanes) to give a clear, colourless oil (2.0 g, 70%). R_f 0.36 (5% EtOAc/hexanes); **^{1}H NMR** (400 MHz, $CDCl_3$) δ 7.60 – 7.45 (m, 2H), 7.43 – 7.29 (m, 3H), 6.64 (s, 1H), 3.82 (s, 3H) ppm; **^{13}C NMR** (101 MHz, $CDCl_3$) δ 165.1 (C), 143.3 (C), 130.1 (CH), 128.9 (2 × CH), 128.5 (2 × CH), 126.5 (CH), 116.8 (C), 51.9 (CH_3) ppm; Characterized by literature comparison. [376]

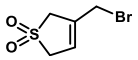
2-(bromomethyl)buta-1,3-diene (4.26)



A 50 mL round bottom flask equipped with a stir bar was charged with 3-(bromomethyl)-2,5-dihydrothiophene 1,1-dioxide (**4.27**, 5.49 g, 26 mmol) and connected to a short path distillation piece and a 25 mL pointed bottom collection flask, then placed under dynamic vacuum. The 50 mL flask was then submerged in a 180 ºC wax bath while the collection flask was submerged into a liquid nitrogen/EtOAc bath until distillation ceased. The title compound was obtained as a volatile clear colourless oil (2.73 g, 18.5 mmol, 71% yield). *All the glassware used in this experiment was silanized before use by placing it into a desiccator with a small open dish of TMSCl and pulling a dynamic vacuum on the desiccator until the TMSCl boiled. Once boiling, the vacuum was switched to static, and the system was left to sit for two minutes. This process was repeated two more times before the glassware was

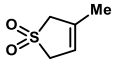
transferred to a 105 ºC oven to bake for several hours. **^{1}H NMR** (400 MHz, $CDCl_3$) δ 6.16 (dd, J = 17.7, 10.9 Hz, 1H), 5.33 (d, J = 17.7 Hz, 1H), 5.17 – 5.04 (m, 1H), 5.02 (s, 1H), 4.91 (s, 1H), 3.72 (s, 2H) ppm; **^{13}C NMR** (101 MHz, $CDCl_3$) δ 142.8 (C), 135.3 (CH), 120.0 (CH_2), 115.9 (CH_2), 30.3 (CH_2) ppm; Characterized according to NMR comparison. [377]

3-(bromomethyl)-2,5-dihydrothiophene 1,1-dioxide (4.27)



A 350 mL high pressure flask equipped with a stir bar was charged with 3-methyl-2,5-dihydrothiophene 1,1-dioxide (**4.28**, 7.6 g, 57 mmol, 1 equiv), recrystallized NBS (12.17 g, 68.4 mmol, 1.2 equiv), and benzoyl peroxide (75% w/w, 1.84 g, 5.7 mmol, 0.1 equiv), and chloroform (85 mL, 0.67 M). Next, the flask was fit with a rubber septum and sparged with argon while it was sonicated for 10 minutes. Afterwards the septum was replaced with a Teflon screw top and the reaction was placed in a 75 ºC oil bath and stirred vigorously at this temperature for 18 hours. After 18 hours, the reaction was removed from the oil bath and allowed to cool to room temperature. Succinimide precipitate was filtered off and rinsed with DCM, the filtrate was concentrated *in vacuo*. The resulting residue was purified by flash column chromatography (25–60% EtOAc/hexanes) to give a yellow powder of moderate purity. The yellow powder was recrystallized twice from a minimum of boiling 95% ethanol to give **4.27** as a brilliant white powder (6.98 g, 33.1 mmol, 58% yield). **m.p.** 77–84 ºC; R_f 0.24 (40% EtOAc/hexanes); **^{1}H NMR** (400 MHz, $CDCl_3$) δ 6.12 – 6.07 (m, 1H), 4.03 (s, 2H), 3.88 (s, 4H) ppm; **^{13}C NMR** (101 MHz, $CDCl_3$) δ 134.6 (C), 122.3 (CH), 57.5 (CH_2), 56.7 (CH_2), 29.8 (CH_2) ppm; **HRMS** (EI+) *m/z* calculated for $C_5H_7Br^{\bullet+}$ $[M–SO_2]^{\bullet+}$ 145.97256, found 145.97296.

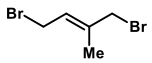
3-methyl-2,5-dihydrothiophene 1,1-dioxide (4.28)



Adapted from work by Larionov and co-workers and characterized according to NMR comparison. [378] A 350 mL high pressure flask equipped with a stir bar was charged with MeOH/H_2O (4:1, 61 & 15.5 mL, 0.4 M) and sparged with argon for 10 minutes. Next, sodium metabisulfite (29.0 g, 155 mmol, 5 equiv) and potassium bisulfate (8.3 g, 62 mmol, 2 equiv often made *in situ* from H_2SO_4/KOH) were added, followed by isoprene (3.1 mL, 31 mmol, 1 equiv). The flask was sealed with a Teflon screw top and placed in a 100 ºC oil-bath under vigorous stirring to react overnight. The next morning the flask is cooled in an ice/water bath before being opened and concentrated *in vacuo*. The resulting residue was diluted with water (100 mL) and EtOAc (100 mL) and the layers were separated. The aqueous phase was extracted with more EtOAc (3 × 50 mL). Combined extracts were washed with brine (1 × 75 mL), dried over Na_2SO_4,

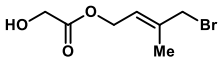
filtered and concentrated *in vacuo*. The resulting material was obtained as a white powder and was used without further purification (3.56 g, 27 mmol, 88% yield). ***R*$_f$** 0.26 (40% EtOAc/hexanes); **^{1}H NMR** (400 MHz, $CDCl_3$) δ 5.71 – 5.63 (m, 1H), 3.80 – 3.77 (m, 2H), 3.68 – 3.65 (m, 2H), 1.90 – 1.86 (m, 3H) ppm; **^{13}C NMR** (101 MHz, $CDCl_3$) δ 134.4 (C), 118.1 (CH), 59.0 (CH_2), 57.5 (CH_2), 19.1 (CH_3) ppm.

(E)-1,4-dibromo-2-methylbut-2-ene (4.30)



A two-neck 50 mL round bottom flask, equipped with a stir bar & thermometer and fitted with a rubber septum, was charged with isoprene (10 mL, 100 mmol, 1 equiv) and the compound was cooled with a 50/50 MeOH/H_2O-dry ice bath. Bromine (5.2 mL, 100 mmol, 1 equiv), pre-cooled in a separate flask using an ice/water bath, was next transferred dropwise to the isoprene flask *via* a PTFE cannula while maintaining an internal temperature of the isoprene flask below –20 ºC. As conversion progressed, the melting point of the resulting mixture rose making it impractical to keep the reaction flask below 0 ºC towards the end of the addition. Upon complete addition of Br_2, the resulting mixture was sparged with argon at ~0 ºC. The crude mixture was then distilled *in vacuo* through a short-path distillation piece. The fractions of distillate boiling between 45 – 75 ºC were collected as a clear and colourless oil for use in subsequent steps (16.7 g, ≤ 66 mmol, ≤ 66% yield, 5.7:1 *E/Z*, material contains a minor impurity). **^{1}H NMR** (400 MHz, $CDCl_3$) δ 5.95 – 5.85 (m, 0.85H, **M**), 5.76 – 5.67 (m, 0.15H, **m**), 4.02 – 3.93 (m, 4H), 1.95 – 1.84 (m, 3H) ppm; **^{13}C NMR** (101 MHz, $CDCl_3$, **Major (*E*)**) δ 138.4 (C), 125.9 (CH), 39.4 (CH_2), 27.7 (CH_2), 14.8 (CH_3); **^{13}C NMR** (101 MHz, $CDCl_3$) δ 138.5 (C), 126.1 (CH), 29.5 (CH_2), 26.7 (CH_2), 22.2 (CH_3) ppm. Characterized according to literature comparison.[379]

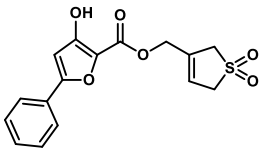
(E)-4-bromo-3-methylbut-2-en-1-yl 2-hydroxyacetate (4.44)



An 8 mL screw-top Pyrex tube equipped with a stir bar was charged with (*E*)-1,4-dibromo-2-methylbut-2-ene (**4.30**, 46 mg, 0.2 mmol, 1 equiv), potassium glycolate (23 mg, 0.2 mmol, 1 equiv), and DMF (0.5 mL, 0.4 M) and the tube was capped. The resulting solution was stirred vigorously at room temperature for 28 hours (incomplete conversion), at which time the reaction was diluted with distilled water (20 mL) and EtOAc (30 mL) and the layers were separated. The organic phase was washed with distilled water (3 × 10 mL) and brine (1 × 10 mL) before being dried over Na_2SO_4, filtered, and concentrated *in vacuo*. The crude residue was purified by flash column chromatography (15–30% EtOAc/hexanes) to give **4.44** as a clear colourless oil (12 mg, 0.06 mmol, 28%). ***R*$_f$** 0.18

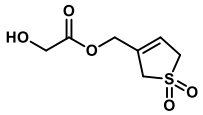
(25% EtOAc/hexanes); **^{1}H NMR** (400 MHz, $CDCl_3$) δ 5.73 (tq, J = 7.0, 1.1 Hz, 1H), 4.73 (d, J = 6.9 Hz, 2H), 4.17 (s, 2H), 3.94 (s, 2H), 2.40 (br s, 1H), 1.87 (s, 3H) ppm; **^{13}C NMR** (101 MHz, $CDCl_3$) δ 173.3 (C), 138.5 (C), 123.3 (CH), 62.0 (CH_2), 60.7 (CH_2), 39.2 (CH_2), 15.3 (CH_3) ppm.

(1,1-dioxido-2,5-dihydrothiophen-3-yl)methyl 3-hydroxy-5-phenylfuran-2-carboxylate (4.46)



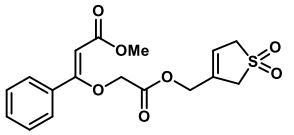
In a round-bottom flask fitted with a short path distillation head and collection flask, a mixture of methyl hydroxyfuranoate **4.93** (436 mg, 2.0 mmol, 1.0 equiv.), alcohol **4.52** (593 mg, 4.0 mmol, 2.0 equiv.), and distannoxane **4.98** (213 mg, 0.20 mmol, 10 mol%) in toluene (10 mL, 0.2 M) and under argon atmosphere was heated to reflux at 120 °C with stirring until completion was determined by TLC. Methanol was continuously removed from the reaction by azeotropic distillation with toluene. Upon complete conversion, the reaction was concentrated *in vacuo* and the crude residue was purified by flash column chromatography (SiO_2, 5–15% EtOAc/hexanesto give a coral-coloured solid (75 mg, 12%). R_f 0.49 (20% EtOAc/hexanes); **^{1}H NMR** (600 MHz, DMSO) δ 7.80 – 7.74 (m, 2H), 7.48 (t, J = 7.7 Hz, 2H), 7.44 – 7.39 (m, 1H), 6.80 (s, 1H), 6.45 (dd, J = 17.9, 11.1 Hz, 1H), 5.41 – 5.32 (m, 2H), 5.28 (d, J = 2.1 Hz, 1H), 5.18 (d, J = 11.1 Hz, 1H), 4.93 (s, 2H) ppm; **^{13}C NMR** (151 MHz, DMSO) δ 157.8 (C), 154.7 (C), 154.5 (C), 140.9 (C), 136.1 (CH), 129.4 (CH), 129.0 (2 × CH), 129.0 (C), 125.9 (C), 124.5 (2 × CH), 117.1 (CH_2), 114.9 (CH_2), 101.5 (CH), 61.9 (CH_2) ppm; **HRMS** (EI+) *m/z* calculated for $C_{16}H_{14}O_4^{\bullet+}$ $[M–SO_2]^{\bullet+}$ 270.08866, found 270.09098.

(1,1-dioxido-2,5-dihydrothiophen-3-yl)methyl 2-hydroxyacetate (4.47)[§]



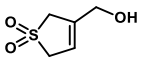
A mixture of glycolic acid (2.3 g, 30 mmol, 1.0 equiv.), bromide **4.27** (7.2 g, 34 mmol, 1.1 equiv.), and DBU (5.1 mL, 5.2 g, 34 mmol, 1.1 equiv.) in MeCN (30 mL, 1.0 M) was heated in a sealed tube to 60 °C for 48 hours. The mixture was concentrated under reduced pressure and the crude residue purified by flash column chromatography (SiO_2, 80–85% EtOAc/hexanes with 1% AcOH) to give a clear, colourless oil (1.2 g, 20%). R_f 0.53 (84:14:1 EtOAc/hexanes/AcOH); **^{1}H NMR** (400 MHz, $CDCl_3$) δ 6.13 – 6.04 (m, 1H), 4.81 – 4.76 (m, 2H), 4.23 (s, 2H), 3.88 – 3.85 (m, 2H), 3.80 – 3.77 (m, 2H) ppm.

methyl (Z)-3-(2-((1,1-dioxido-2,5-dihydrothiophen-3-yl)methoxy)-2-oxoethoxy)-3-phenylacrylate (4.48)[§]



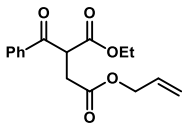
To a solution of SPhosAuNTf$_2$ (17 mg, 0.020 mmol, 0.5 mol%) in DCM (2.0 mL, 0.2 M) was added methyl phenylpropiolate (**4.79**, 1.24 g, 7.8 mmol, 2.0 equiv.) and glycolate **4.64** (0.80 g, 3.9 mmol, 1.0 equiv.) at room temperature. The solution was stirred for 24 hours at room temperature. The reaction mixture was purified directly by flash column chromatography (SiO$_2$, 45–50% EtOAc/hexanes) to give *Z*-enol ether **4.48** as a clear, colourless oil (18 mg, 5%). ***R$_f$*** 0.13 (40% EtOAc/hexanes); **^{1}H NMR** (400 MHz, C$_6$D$_6$) δ 7.66 – 7.55 (m, 2H), 7.10 – 7.01 (m, 3H), 5.76 (s, 1H), 5.00 – 4.83 (m, 1H), 4.75 (s, 2H), 4.01 (tt, *J* = 2.0, 1.0 Hz, 2H), 3.46 (s, 3H), 3.11 (dq, *J* = 2.0, 1.1 Hz, 2H), 3.00 (dt, *J* = 3.2, 1.6 Hz, 2H) ppm; **^{13}C NMR** (101 MHz, C$_6$D$_6$) δ 168.2 (C), 167.5 (C), 165.6 (C), 135.7 (C), 132.8 (C), 131.3 (CH), 129.2 (CH), 128.2 (CH), 121.8 (CH), 99.1 (CH), 70.5 (CH$_2$), 63.4 (CH$_2$), 56.8 (CH$_2$), 55.9 (CH$_2$), 51.4 (CH$_3$) ppm.

3-(hydroxymethyl)-2,5-dihydrothiophene 1,1-dioxide (4.52)[§]



To a solution of AgTFA (2.4 g, 11 mmol, 1.0 equiv.) in water (73 mL, 0.28 M) was added bromide **4.27** (1.7 g, 11 mmol. 1.0 equiv.) at room temperature. The mixture was stirred for 72 h at room temperature, then the resulting suspension filtered over a pad of Celite (eluting with EtOAc) and concentrated under reduced pressure. The crude residue was purified by flash column chromatography (SiO$_2$, 80% EtOAc/hexanes) to give **4.52** (1.5 g, 94%). ***R$_f$*** 0.10 (60% EtOAc/hexanes); **^{1}H NMR** (400 MHz, CDCl$_3$) δ 5.97 (s, 1H), 4.23 (s, 2H), 3.83 (s, 2H), 3.78 (s, 2H), 2.16 (br s, 1H) ppm; **^{13}C NMR** (101 MHz, CDCl$_3$) δ 138.1 (C), 118.1 (CH), 62.2 (CH$_2$), 56.9 (CH$_2$), 56.0 (CH$_2$) ppm; **HRMS** (EI+) *m/z* calculated for $C_5H_8O_3S^{\bullet+}$ $[M]^{\bullet+}$ 148.01887, found 148.01821.

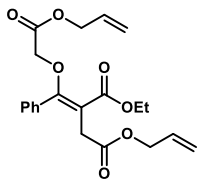
4-allyl 1-ethyl 2-benzoylsuccinate (4.58)



An oven-dried 8 mL pyrex screw-top tube under argon and equipped with a stir bar was charged with K$_2$CO$_3$ (415 mg, 3 mmol, 3 equiv), anhydrous THF (2 mL, 0.5M), ethyl benzoylacetate (**4.18**, 170 µL, 1 mmol, 1 equiv), and allyl bromoacetate (**3.81**, 269 mg, 1.5 mmol, 1.5 equiv). The pyrex tube was capped and sealed with electrical tape

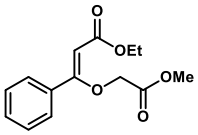
then placed in a 60 ºC oil bath until complete by TLC analysis (~21 h) at which point it was allowed to cool to room temperature. The mixture was diluted with distilled water (10 mL) and EtOAc (10 mL) and the layers were separated. The aqueous phase was extracted with EtOAc (3 × 5 mL). Combined extracts were washed with brine (1 × 10 mL), dried over Na_2SO_4, filtered, and concentrated *in vacuo*. The crude residue was purified by flash column chromatography (6–12% EtOAc/hexanes) to give **4.58** as a yellow oil (17 mg, 0.06 mmol, 6% yield). R_f 0.50 (25% EtOAc/hexanes); **^{1}H NMR** (400 MHz, $CDCl_3$) δ 8.08 – 8.00 (m, 2H), 7.62 – 7.55 (m, 1H), 7.51 – 7.44 (m, 2H), 5.86 (ddt, J = 17.2, 10.4, 5.7 Hz, 1H), 5.35 – 5.25 (m, 1H), 5.24 – 5.10 (m, 1H), 4.86 (dd, J = 7.7, 6.7 Hz, 1H), 4.63 – 4.54 (m, 2H), 4.13 (q, J = 7.1 Hz, 2H), 3.13 (dd, J = 17.4, 7.7 Hz, 1H), 3.05 (dd, J = 17.4, 6.7 Hz, 1H), 1.14 (t, J = 7.1 Hz, 3H) ppm; **^{13}C NMR** (101 MHz, $CDCl_3$) δ 194.2 (C), 171.1 (C), 168.7 (C), 136.0 (C), 133.8 (CH), 131.9 (CH), 129.0 (2 × CH), 128.8 (2 × CH), 118.5 (CH_2), 65.8 (CH_2), 61.9 (CH_2), 49.7 (CH), 33.3 (CH_2), 14.0 (CH_3) ppm.

4-allyl 1-ethyl (Z)-2-((2-(allyloxy)-2-oxoethoxy)(phenyl)methylene)succinate (4.59)



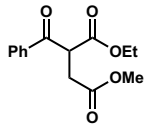
An oven-dried 8 mL pyrex screw top tube under argon was charged with ethyl benzoylacetate (**4.18**, 90 µL, 0.5 mmol, 1 equiv), allyl bromoacetate (**3.81**, 135 mg, 0.75 mmol, 1.5 equiv), K_2CO_3 (208 mg, 1.5 mmol, 3 equiv), and MeCN (1 mL, 0.5 M). The tube was closed with a hard plastic cap and electrical tape and then stirred in a 60 ºC oil bath for 18 hours. After 18 hours the mixture was allowed to cool to room temperature and then concentrated *in vacuo*. The residue was diluted with distilled water (10 mL) and EtOAc (10 mL) and the layers were separates. The aqueous phase was extracted with EtOAc (3 × 10 mL). Combined extracts were washed with brine (1 × 15 mL), dried over Na_2SO_4, filtered, and concentrated *in vacuo*. The crude residue was purified by flash column chromatography (0–30% EtOAc/Hexanes) to give **4.59** as a clear and colourless oil (83 mg, 0.21 mmol, 43% yield). **^{1}H NMR** (400 MHz, $CDCl_3$) δ 7.46 – 7.32 (m, 3H), 7.31 – 7.23 (m, 2H), 6.05 – 5.75 (m, 2H), 5.33 (dq, J = 17.2, 1.6 Hz, 1H), 5.31 – 5.18 (m, 3H), 4.62 (dt, J = 5.6, 1.5 Hz, 2H), 4.57 (dt, J = 5.8, 1.4 Hz, 2H), 4.20 (s, 2H), 3.87 (q, J = 7.1 Hz, 2H), 3.73 (s, 2H), 0.85 (t, J = 7.1 Hz, 3H) ppm.

ethyl (Z)-3-(2-methoxy-2-oxoethoxy)-3-phenylacrylate (4.61)



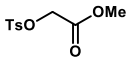
An oven-dried 8 mL pyrex screw-top tube under argon and equipped with a stir bar was charged with K_2CO_3 (263 mg, 1.9 mmol, 3 equiv), freshly distilled DMPU (1.3 mL, 0.5 M), ethyl benzoylacetate (**4.18**, 110 µL, 0.63 mmol, 1 equiv), and methyl 2-(tosyloxy)acetate (**4.65**, 232 mg, 0.95 mmol, 1.5 equiv). The pyrex tube was capped and sealed with electrical tape then placed in a 60 ºC oil bath overnight (~14 h) at which point it was allowed to cool to room temperature. The mixture was diluted with distilled water (20 mL) and EtOAc (20 mL) and the layers were separated. The aqueous phase was extracted with EtOAc (3 × 10 mL). Combined extracts were washed with distilled water (3 × 10 mL) then brine (1 × 10 mL), dried over Na_2SO_4, filtered, and concentrated *in vacuo*. The crude residue was purified by flash column chromatography (9–30% EtOAc/hexanes then a subsequent column at 2–5% EtOAc/PhMe) to give a clear and colourless oil (44 mg, 0.17 mmol, 26% yield). R_f 0.27 (5% EtOAc/PhMe); **^{1}H NMR** (600 MHz, C_6D_6) δ 7.73 – 7.64 (m, 2H), 7.08 – 6.98 (m, 3H), 5.80 (s, 1H), 4.83 (s, 2H), 4.05 (q, J = 7.1 Hz, 2H), 3.23 (s, 3H), 1.03 (t, J = 7.1 Hz, 3H) ppm; **^{13}C NMR** (151 MHz, C_6D_6) δ 168.9 (C), 167.2 (C), 164.8 (C), 13.7 (C), 130.7 (CH), 128.7 (2 × CH), 128.6 (2 × CH), 99.2 (CH), 70.3 (CH_2), 59.9 (CH_2), 51.3 (CH_3), 14.4 (CH_3) ppm. **HRMS** (EI+) *m/z* calculated for $C_{15}H_{16}O_5^{\bullet+}$ $[M]^{\bullet+}$ 264.09923, found 264.09936. NOESY experiment confirms alkenyl methine correlates to aryl ring and not the methylene α to O and the methyl ester while a NOESY spectrum taken on the mixture of major and minor confirms the minor isomer has a methine-methylene correlation. Compound was sensitive to $CDCl_3$ and degraded rapidly within it.

1-ethyl-4-methyl-2-benzoylsuccinate (4.63)



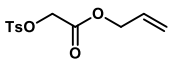
Side product of the above reaction, formed in 20–30% isolated yield. **^{1}H NMR** (400 MHz, $CDCl_3$) δ 8.06 – 8.00 (m, 2H), 7.62 – 7.57 (m, 1H), 7.49 (ddt, J = 8.2, 6.7, 1.1 Hz, 2H), 4.86 (dd, J = 7.7, 6.7 Hz, 1H), 4.14 (q, J = 7.1 Hz, 2H), 3.68 (s, 3H), 3.15 – 2.97 (m, 2H), 1.15 (t, J = 7.1 Hz, 3H) ppm; **^{13}C NMR** (101 MHz, $CDCl_3$) δ 194.3 (C), 171.9 (C), 168.8 (C), 136.0 (C), 133.8 (CH), 129.0 (2 x CH), 128.8 (2 x CH), 62.0 (CH_2), 52.2 (CH_3), 49.8 (CH), 33.1 (CH_2), 14.0 (CH_3) ppm; **HRMS** (EI+) *m/z* calculated for $C_{14}H_{16}O_5^{\bullet+}$ $[M]^{\bullet+}$ 264.09923, found 264.10136.

methyl 2-(tosyloxy)acetate (4.65)



A flame-dried 50 mL round bottom flask under argon and equipped with a stir bar was charged with methyl glycolate (**4.64**, 1.5 mL, 20 mmol, 1 equiv), *p*-toluenesulfonyl chloride (4.2 g, 22 mmol, 1.1 equiv), DMAP (245 mg, 2 mmol, 10 mol%), and anhydrous Et_2O (20 mL, 1 M). The resulting mixture was stirred vigorously and cooled to 0 ºC with an ice/water bath. After equilibrating at 0 ºC for 5 minutes, freshly distilled Et_3N (4.3 mL, 31 mmol, 2 equiv) was added dropwise over 2 minutes. The resulting solution was stirred and allowed to warm to room temperature overnight (~ 15 hours). Once complete, 1M HCl was added (30 mL) and the phases were separated. The aqueous phase was extracted with Et_2O (3 × 40 mL). The combined extracts were washed with brine (1 × 20 mL), dried over $MgSO_4$, filtered, and concentrated *in vacuo*. The crude residue was purified by flash column chromatography (10–20% EtOAc/hexanes) to give **4.65** as a white powder (3.26 g, 14.6 mmol, 73% yield). R_f 0.35 (35% EtOAc/hexanes); **^{1}H NMR** (400 MHz, $CDCl_3$) δ 7.83 (d, J = 8.4 Hz, 2H), 7.40 – 7.32 (m, 3H), 4.59 (s, 2H), 3.73 (s, 3H), 2.45 (s, 3H) ppm; **^{13}C NMR** (101 MHz, $CDCl_3$) δ 166.6 (C), 145.5 (C), 132.7 (C), 130.1 (2 × CH), 128.3 (2 × CH), 64.7 (CH_2), 52.7 (CH_3), 21.8 (CH_3). Characterized according to NMR comparison. [380]

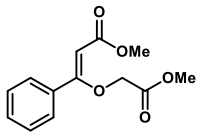
allyl 2-(tosyloxy)acetate (4.67)



A flame-dried 50 mL round bottom flask under argon and equipped with a stir bar was charged with allyl glycolate (**4.66**, 1.34 g, 11.5 mmol, 1 equiv), *p*-toluenesulfonyl chloride (2.40 g, 12.7 mmol, 1.1 equiv), DMAP (147 mg, 1.2 mmol, 10 mol%), and anhydrous Et_2O (11.5 mL, 1 M). The resulting mixture was stirred vigorously and cooled to 0 ºC with an ice/water bath. After equilibrating at 0 ºC for 5 minutes, freshly distilled Et_3N (3.2 mL, 23 mmol, 2 equiv) was added dropwise over 2 minutes. The resulting solution was allowed to stir and slowly warm to room temperature overnight (~16 hours). Once complete, HCl (1 M, aqueous, 30 mL) was added and the phases were separated. The aqueous phase was extracted with Et_2O (3 × 15 mL). The combined extracts were washed with brine (1 × 20 mL), dried over Na_2SO_4, filtered, and concentrated *in vacuo*. The crude residue was purified by flash column chromatography (10–20% EtOAc/hexanes) to give **4.67** as a clear and colourless oil (1.99 g, 7.35 mmol, 64% yield). R_f 0.5 (35% EtOAc/hexanes); **^{1}H NMR** (400 MHz, $CDCl_3$) δ 7.87 – 7.79 (m, 2H), 7.39 – 7.32 (m, 2H), 5.85 (ddt, J = 17.1, 10.4, 5.9 Hz, 1H), 5.31 (dq, J = 17.2, 1.5 Hz, 1H), 5.26 (dq, J = 10.3, 1.2 Hz, 1H), 4.64 – 4.59 (m, 4H), 2.45 (s,

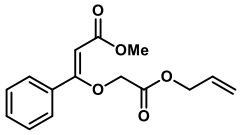
3H) ppm; **^{13}C NMR** (101 MHz, $CDCl_3$) δ 165.9 (C), 145.5 (C), 132.7 (C), 131.1 (CH), 130.0 (2 × CH), 128.3 (2 × CH), 119.6 (CH_2), 66.5 (CH_2), 64.7 (CH_2), 21.8 (CH_3) ppm; **HRMS** (EI+) *m/z* calculated for $C_{12}H_{14}O_5S^{\bullet+}$ $[M]^{\bullet+}$ 270.05565, found 270.05402.

methyl (Z)-3-(2-methoxy-2-oxoethoxy)-3-phenylacrylate (4.82)[§]



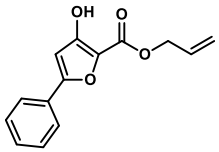
To a solution of $SPhosAuNTf_2$ (4.5 mg, 0.005 mmol, 0.5 mol%) in DCM (0.5 mL, 0.2 M) was added methyl phenylpropiolate (**4.79**, 320 mg, 2.0 mmol, 2.0 equiv.) and methyl glycolate (**4.64**, 90 mg, 1.0 mmol, 1.0 equiv.) at room temperature. The solution was stirred for 8 hours at room temperature. The reaction mixture was purified directly by flash column chromatography (SiO_2, 15% EtOAc/hexanes) to give *Z*-enol ether **4.82** as a clear, colourless oil (150 mg, 60%). R_f 0.29 (15% EtOAc/hexanes); **m.p.** 54–57 °C; **^{1}H NMR** (400 MHz, C_6D_6) δ 7.69 (dd, J = 7.5, 2.2 Hz, 2H), 7.07 – 6.97 (m, 3H), 5.77 (s, 1H), 4.80 (s, 2H), 3.43 (s, 3H), 3.21 (s, 3H) ppm; **^{13}C NMR** (101 MHz, C_6D_6) δ 168.8 (C), 167.4 (C), 165.2 (C), 135.6 (C), 130.8 (2 × CH), 128.7 (3 × CH), 98.7 (CH), 70.3 (CH_2), 51.3 (CH_3), 50.9 (CH_3) ppm; **HRMS** (ESI+) *m/z* calculated for $C_{13}H_{14}O_5Na$ $[M + Na]^+$ 273.0739, found 273.0754.

methyl (Z)-3-(2-(allyloxy)-2-oxoethoxy)-3-phenylacrylate (4.90)[§]



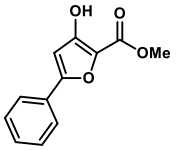
To a solution of $SPhosAuNTf_2$ (4.5 mg, 0.005 mmol, 0.5 mol%) in DCM (0.5 mL, 0.2 M) was added methyl phenylpropiolate (**4.79**, 320 mg, 2.0 mmol, 2.0 equiv.) and allyl glycolate (**4.66**, 116 mg, 1.0 mmol, 1.0 equiv.) at room temperature. The solution was stirred for 24 hours at room temperature. The reaction mixture was purified directly by flash column chromatography (SiO_2, 15% EtOAc/hexanes) to give *Z*-enol ether **4.90** as a clear, colourless oil (243 mg, 44%). R_f 0.29 (15% EtOAc/hexanes); **^{1}H NMR** (400 MHz, $CDCl_3$) δ 7.72 – 7.63 (m, 2H), 7.48 – 7.34 (m, 3H), 5.91 (ddt, J = 17.2, 10.4, 5.9 Hz, 1H), 5.68 (s, 1H), 5.33 (dq, J = 17.2, 1.5 Hz, 1H), 5.25 (dq, J = 10.4, 1.2 Hz, 1H), 4.76 (s, 2H), 4.67 (dt, J = 5.8, 1.4 Hz, 2H), 3.74 (s, 3H) ppm; **^{13}C NMR** (101 MHz, $CDCl_3$) δ 168.5 (C), 167.0 (C), 165.5 (C), 134.5 (C), 131.6 (CH), 130.9 (CH), 128.8 (CH), 127.8 (CH), 119.1 (CH_2), 100.0 (CH), 69.4 (CH_2), 65.9 (CH_2), 51.4 (CH_3) ppm; **HRMS** (ESI+): calculated for $C_{15}H_{16}O_5Na$ $[M]^{\bullet+}$: 299.0925, found 299.0895.

allyl 3-hydroxy-5-phenylfuran-2-carboxylate (4.92)



In a round-bottom flask fitted with one-piece distillation apparatus and collection flask, a mixture of methyl hydroxyfuranoate **4.82** (222 mg, 1.1 mmol, 1.0 equiv.), allyl alcohol (0.75 mL, 11 mmol, 10.0 equiv.), and distannoxane **4.98** (117 mg, 0.11 mmol, 10 mol%) in toluene (5.5 mL, 0.2 M) was heated to reflux at 120 °C with stirring until completion was determined by TLC. Methanol was continuously removed from the reaction by azeotropic distillation with toluene. Upon complete conversion, the reaction was concentrated *in vacuo* and purified by flash column chromatography (SiO_2, 5–10% EtOAc/hexanes) to give a crystalline white solid (42.9 mg, 16%, 27% brsm). Note: 2D TLC showed the product is unstable on silica gel, to minimize degradation short column path lengths and rapid elution was prioritized. 0.24 (25% EtOAc/hexanes); **m.p.** 63–65 °C; **^{1}H NMR** (600 MHz, DMSO–*d*$_6$) δ 10.49 (s, 1H), 7.80 – 7.75 (m, 2H), 7.50 – 7.45 (m, 2H), 7.43 – 7.38 (m, 1H), 6.80 (s, 1H), 6.01 (dddd, J = 17.2, 10.5, 5.3, 5.3 Hz, 1H), 5.40 (dddd, J = 17.2, 1.7, 1.7, 1.7 Hz, 1H), 5.24 (dddd, J = 10.5, 1.5, 1.5, 1.5 Hz, 1H), 4.73 (ddd, J = 5.3, 1.6, 1.6 Hz, 2H) ppm; **^{13}C NMR** (151 MHz, DMSO–*d*$_6$) δ 156.9 (C), 153.6 (C), 153.3 (C), 132.1 (CH), 128.4 (CH), 128.0 (2 × CH), 128.0 (C), 124.9 (C), 123.5 (2 × CH), 116.5 (CH_2), 100.5 (CH), 62.7 (CH_2) ppm; **HRMS** (ESI+) m/z calculated for $C_{14}H_{12}O_4Na$ $[M + Na]^+$ 267.0633, found 267.0621.

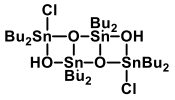
methyl 3-hydroxy-5-phenylfuran-2-carboxylate (4.93)



To a solution of *Z*-enol ether **4.82** (1.30 g, 5.2 mmol, 1.0 equiv.) in THF (22 mL, 0.2 M) was added potassium *tert*-butoxide (11.8 mL, 2.0 equiv., 10% w/v in THF) at –10 °C. The reaction was stirred for 15 minutes at –10 °C, quenched by dropwise addition of AcOH (1 mL) at –10 °C followed by pH 7 phosphate buffer (25 mL), and then allowed to warm to room temperature. The resulting mixture was transferred to a separatory funnel with EtOAc (20 mL) and the layers were separated. The aqueous phase was then extracted with EtOAc (2 × 20 mL). Combined extracts were washed with brine (30 mL), dried over Na_2SO_4, filtered, and concentrated *in vacuo* to give the crude residue as white powder. The resulting crude residue was purified by recrystallization (hexanes) to give **4.93** as a crystalline white solid (960.1 mg, 85%). Note: 2D TLC showed the product is unstable on silica gel. To minimize degradation,

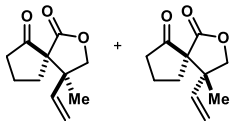
whenever chromatography was necessary, short column path lengths and rapid elution was prioritized. R_f 0.42 (20% EtOAc/hexanes); **m.p.** 94–96 °C; **^{1}H NMR** (600 MHz, DMSO–d_6) δ 10.40 (s, 1H), 7.79 – 7.74 (m, 2H), 7.49 – 7.44 (m, 2H), 7.43 – 7.38 (m, 1H), 6.80 (s, 1H), 3.76 (s, 3H) ppm; **^{13}C NMR** (151 MHz, DMSO–d_6) δ 158.7 (C), 154.5 (C), 154.0 (C), 129.3 (CH), 129.0 (2 × CH), 129.0 (C), 126.0 (C), 124.5 (2 × CH), 101.5 (CH), 50.8 (CH_3) ppm; **HRMS** (ESI+) *m/z* calculated for $C_{12}H_{10}O_4Na$ $[M + Na]^+$ 241.0477, found 241.0460.

1-hydroxy-3-(chloro)tetrabutyldistannoxane (4.98)



Prepared according to the following adapted literature procedure by Otera.[381] A suspension of dibutyltin oxide (7.5 g, 30 mmol, 3.0 equiv), dibutyltin dichloride (3.04 g, 10 mmol, 1.0 equiv), and EtOH (95%, 100 mL, 0.1 M) was vigorously stirred and heated to reflux for 4 hours. The clear, colourless solution was allowed to cool to room temperature and then concentrated under reduced pressure to give a white powder. The white powder was pulverized and left open to ambient atmosphere overnight. The next day, the crude material was recrystallized from boiling hexanes, precipitated at 0 ºC, isolated by suction filtration using a medium porosity fritted funnel, and rinsed with ice-cold hexanes. The recrystallization and washing procedures were repeated twice more. The thrice-recrystallized material was then dried under high vacuum at room temperature overnight to give **4.98** as a white crystalline solid (2.14 g, 40% yield). **m.p.** 109–121 ºC

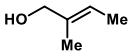
4-methyl-4-vinyl-2-oxaspiro[4.4]nonane-1,6-dione (4.110)



Inside a nitrogen-filled glovebox, an 8 mL oven-dried screw-top Pyrex tube (12 mm diameter) was charged with lithium trifluoroacetate (2.4 mg, 0.020 mmol, 10 mol%), 9,10-diphenylanthracene (3.3 mg, 0.010 mmol, 5 mol%), copper(II) trifluoroacetate hydrate (174 mg, 0.6 mmol, 3 equiv.), and dicarbonyl **3.59ab** (39 mg, 0.2 mmol, 1.0 equiv.). The tube was sealed with a Teflon-septum screw cap, transferred out of the glovebox, and immediately placed under a positive pressure of argon. Anhydrous acetonitrile (1.0 mL, 0.2 M) was added and the resulting suspension sparged with argon for 5 minutes. After sparging, the septum cap was quickly exchanged with a hard plastic cap and the vessel sealed with electrical tape and then Parafilm. The reaction mixture was then sonicated (90 s) before irradiating with a violet LED (2–2.4 W, 410 nm) at a distance of 1–5 mm for 24 h. The reaction was diluted

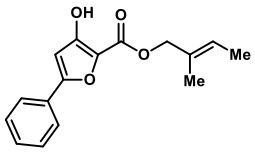
with diluted with EtOAc (20 mL) and washed with NH_4Cl (3 × 20 mL, saturated aqueous), water (20 mL), and brine (20 mL). The organic phase was dried over Na_2SO_4, filtered, and concentrated under reduced pressure. The crude residue was purified by flash column chromatography (SiO_2, 10–15% EtOAc/hexanes) to give spirolactone **4.110** as a clear, colourless oil (30.5 mg, 79%, 3.8:1). R_f 0.28 (17% EtOAc/hexanes); **^{1}H NMR** (600 MHz, $CDCl_3$) δ 5.86 (dd, J = 17.5, 10.9 Hz, 1H, **M**), 5.79 (dd, J = 17.3, 10.8 Hz, 1H, **m**), 5.27 (d, J = 10.9 Hz, 1H, **M**), 5.24 (d, J = 17.2 Hz, 1H, **M**), 5.22 (d, J = 11.1 Hz, 1H, **m**), 5.18 (d, J = 17.3 Hz, 1H, **m**), 4.76 (d, J = 8.4 Hz, 1H, **M**), 4.54 (d, J = 8.5 Hz, 1H, **m**), 4.11 (d, J = 8.5 Hz, 1H, **m**), 3.92 (d, J = 8.5 Hz, 1H, **M**), 2.49 – 2.08 (m, 4H, **M** + **m**), 2.02 – 1.87 (m, 2H, **M** + **m**), 1.21 (s, 3H, **M**), 1.17 (s, 1H, **m**) ppm; **^{13}C NMR** (151 MHz, $CDCl_3$) δ **M** 213.1 (C), 174.6 (C), 136.2 (CH), 118.5 (CH_2), 75.7 (CH_2), 65.8 (C), 48.4 (C), 39.3 (CH_2), 27.7 (CH_2), 20.8 (CH_3), 19.6 (CH_2) **m** 213.5 (C), 175.0 (C), 139.2 (CH), 115.2 (CH_2), 75.2 (CH_2), 63.9 (C), 48.4 (C), 39.6 (CH_2), 29.0 (CH_2), 19.7 (CH_2), 15.3 (CH_3) ppm; **HRMS** (EI+) *m/z* calculated for $C_{11}H_{14}O_3^{\bullet+}$ $[M]^{\bullet+}$ 194.09375, found 194.07967.

(E)-2-methylbut-2-en-1-ol/tiglyl alcohol (4.112)[§]



To a suspension of $LiAlH_4$ (1.5 g, 40 mmol, 2.0 equiv.) in Et_2O (8 mL, 2.5 M) was added tiglic acid (2.0 g, 20 mmol, 1.0 equiv.) in Et_2O (2.5 M) dropwise over 2 minutes at 0 °C in an ice bath. The reaction was stirred for 18 hours and allowed to reach room temperature. Upon completion, the mixture was diluted with Et_2O (40 mL), cooled to 0 °C in an ice bath, and quenched with dropwise addition of water (1.5 mL), NaOH (1.5 mL, 15% aqueous), and then water (4.5 mL). The ice bath was removed, and the mixture allowed to warm to room temperature with stirring over 15 minutes. $MgSO_4$ was added, the suspension stirred for 15 minutes, and then filtered and concentrated at 42 °C and atmospheric pressure. The crude tiglyl alcohol was used without further purification (**4.112**, 1.84 g, 82%).

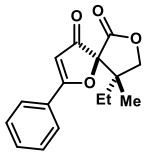
(E)-2-methylbut-2-en-1-yl 3-hydroxy-5-phenylfuran-2-carboxylate (4.114)



In a round-bottom flask fitted with a short path distillation head and collection flask, a mixture of methyl hydroxyfuranoate **4.93** (447.3 mg, 2.05 mmol, 1.0 equiv.), tiglyl alcohol (**4.112**, 882.8 mg, 10.25 mmol, 5.0 equiv.), and distannoxane **4.98** (224.4 mg, 0.21 mmol, 10 mol%) in toluene (10.2 mL, 0.2 M) and under argon atmosphere was heated to reflux at 120 °C with stirring until completion was determined by TLC. Methanol was continuously

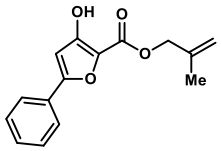
removed from the reaction by azeotropic distillation with toluene. Upon complete conversion, the reaction was concentrated *in vacuo* and the crude residue was purified by flash column chromatography (SiO_2, 5–10% EtOAc/hexanes) and recrystallized (hexanes) to give tiglyl ester **4.114** as a crystalline white solid (459 mg, 85%). Note: 2D TLC showed the product is unstable on silica gel, to minimize degradation short column path lengths and rapid elution was prioritized. R_f 0.63 (25% EtOAc/hexanes); **m.p.** 73–76 ºC ; **^{1}H NMR** (600 MHz, DMSO–d_6) δ 7.78 – 7.74 (m, 2H), 7.50 – 7.45 (m, 2H), 7.43 – 7.38 (m, 1H), 6.79 (s, 1H), 5.59 (dddd, J = 8.1, 6.8, 5.4, 1.4 Hz, 1H), 4.61 (t, J = 1.3 Hz, 2H), 1.65 (t, J = 1.3 Hz, 3H), 1.61 (dq, J = 6.7, 1.1 Hz, 3H) ppm; **^{13}C NMR** (151 MHz, DMSO–d_6) δ 158.2 (C), 154.5 (C), 154.2 (C), 131.1 (C), 129.3 (CH), 129.0 (2 × CH), 129.0 (C), 126.0 (C), 124.5 (2 × CH), 122.4 (CH), 101.5 (CH), 68.3 (CH_2), 13.5 (CH_3), 13.0 (CH_3) ppm; **HRMS** (ESI+) *m/z* calculated for $C_{16}H_{16}O_4Na^+$ [M + Na]$^+$: 295.0946, found 295.0970.

9-ethyl-9-methyl-2-phenyl-1,7-dioxaspiro[4.4]non-2-ene-4,6-dione (4.115)



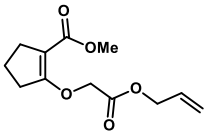
Prepared according to GP6 on 0.2 mmol scale and purified by flash column chromatography (SiO_2, 10–20% EtOAc/hexanes) to give a pale yellow oil (condition A: 34.2 mg, 63%, 4.9:1 dr; condition B: 49.9 mg, 92%, 5.1:1 dr).[382] R_f 0.31 (21% EtOAc/hexanes); **^{1}H NMR** (400 MHz, $CDCl_3$) δ 7.87 – 7.83 (m, 2H, **2M** + **2m**), 7.63 – 7.58 (m, 1H, **M** + **m**), 7.55 – 7.48 (m, 2H, **2M** + **2m**), 6.05 (s, 0.84H, **M**), 6.02 (s, 0.16H, **m**), 4.69 (dq, J = 8.4, 0.8 Hz, 0.84, **M**), 4.62 (d, J = 8.8 Hz, 0.16H, **m**), 4.26 (d, J = 8.8 Hz, 0.16H, **m**), 4.08 (d, J = 8.4 Hz, 0.84H, **M**), 1.84 – 1.70 (m, 1H, **M** + **m**), 1.65 – 1.51 (m, 1H, **M** + **m**), 1.41 (d, J = 0.8 Hz, 2.52H, **3M**), 1.15 (s, 0.48H, **3m**), 1.04 (t, J = 7.5 Hz, 0.48H, **3m**), 0.82 (t, J = 7.6 Hz, 2.52H, **3M**) ppm; **^{13}C NMR** (101 MHz, $CDCl_3$) δ 197.6 (C, **m**), 197.1 (C, **M**), 187.3 (C, **m**), 186.9 (C, **M**), 169.1 (C, **m**), 168.9 (C, **M**), 133.7 (CH, **m**), 133.7 (CH, **M**), 129.2 (4 × CH, **2M** + **2m**), 128.0 (C, **M**), 127.9 (C, **m**), 127.5 (2 × CH, **2m**), 127.5 (2 × CH, **2M**) 100.8 (CH, **M**), 100.4 (CH, **m**), 93.8 (C, **M**), 93.2 (C, **m**), 75.9 (CH_2, **M**), 73.1 (CH_2, **m**), 47.2 (C, **M**), 46.7 (C, **m**), 28.5 (CH_2, **m**), 25.1 (CH_2, **M**), 19.6 (CH_3, **M**), 16.1 (CH_3, **m**), 8.6 (CH_3, **m**), 8.2 (CH_3, **M**) ppm; **HRMS** (EI+) *m/z* calculated for $C_{16}H_{16}O_4^{\bullet+}$ [M]$^{\bullet+}$ 272.10431, found 272.10321.

2-methylallyl 3-hydroxy-5-phenylfuran-2-carboxylate (4.117)



In a round-bottom flask fitted with a short path distillation head and collection flask, a mixture of methyl hydroxyfuranoate **4.93** (961.4 mg, 4.4 mmol, 1.0 equiv.), methallyl alcohol (1.9 mL, 22 mmol, 5.0 equiv.), and distannoxane **4.98** (468 mg, 0.44 mmol, 10 mol%) in toluene (22 mL, 0.2 M) and under argon atmosphere was heated to 130 °C with stirring for 36 h. After 36 h, additional toluene (10 mL) and methallyl alcohol (1 mL, 11.9 mmol, 2.7 equiv) was added and the reaction was continued a further 36 h (reaction incomplete by TLC but stopped and worked up). The reaction was concentrated *in vacuo* and the crude residue was purified by flash column chromatography (SiO_2, 10% EtOAc/hexanes + 1% AcOH) to give a yellow oil. The yellow oil was dissolved in toluene (~20 mL) and concentrated to dryness 3 times to remove acetic acid. The resulting yellow residue was dissolved in hexanes and concentrated to dryness 3 times to yield a yellow powder. The yellow powder was recrystallized (hexanes) to give a crystalline white solid (489.1 mg, 43%). Note: 2D TLC showed the product is unstable on silica gel, to minimize degradation short column path lengths and rapid elution was prioritized. $\boldsymbol{R_f}$ 0.30 (10% EtOAc/hexanes + 1% AcOH); **m.p.** = 62–65 ºC ; **^{1}H NMR** (600 MHz, DMSO-d_6) δ 10.53 (s, 1H), 7.77 (d, J = 7.8 Hz, 2H), 7.48 (t, J = 7.6 Hz, 2H), 7.41 (t, J = 7.4 Hz, 1H), 6.80 (s, 1H), 5.04 (s, 1H), 4.93 (s, 1H), 4.65 (s, 2H), 1.76 (s, 3H) ppm; **^{13}C NMR** (151 MHz, DMSO-d_6) δ 157.9 (C), 154.6 (C), 154.3 (C), 140.4 (C), 129.4 (CH), 129.1 (2 × CH), 129.0 (C), 126.0 (C), 124.5 (2 × CH), 111.9 (CH_2), 101.5 (CH), 66.0 (CH_2), 19.2 (CH_3) ppm; **HRMS** (EI+) *m/z* calculated for $C_{15}H_{14}O_4^{\bullet+}$ $[M]^{\bullet+}$ 258.08866, found 258.08847.

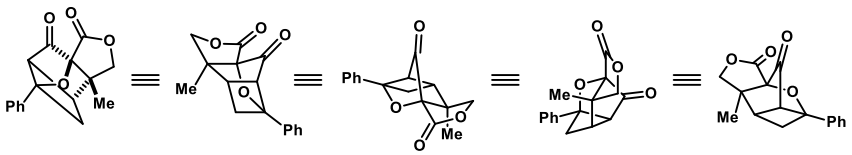
methyl 2-(2-(allyloxy)-2-oxoethoxy)cyclopent-1-ene-1-carboxylate (4.119)



A flame-dried 25 mL round bottom flask under argon atmosphere and equipped with a stir bar was charged with Cs_2CO_3 (3.32 g, 10.2 mmol, 3 equiv) and freshly distilled DMPU (6.8 mL, 0.5 M), followed by allyl 2-(tosyloxy)acetate (**4.67**, 1.09 g, 4 mmol, 1.2 equiv) and methyl 2-oxocyclopentanecarboxylate (**3.86**, 0.42 mL, 3.4 mmol, 1 equiv). The mixture was stirred and heated to 60 ºC in an oil bath until complete consumption of ketoester **3.86** as determined by TLC (≤ 1 hour). Upon complete conversion, the cooled reaction was diluted with distilled water

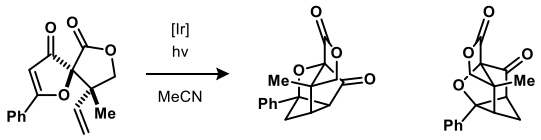
(75 mL) and transferred to a separatory funnel. The aqueous phase was extracted with EtOAc (3 × 25 mL). The combined extracts were washed with distilled water (3 × 15 mL), and brine (1 × 25 mL), before being dried over Na_2SO_4, filtered, and concentrated *in vacuo*. The crude residue was purified by flash column chromatography (15–40% EtOAc/hexanes) to give **4.119** as a white paste (296 mg, 1.2 mmol, 36% yield). R_f 0.37 (31% EtOAc/hexanes); **^{1}H NMR** (400 MHz, C_6D_6) δ 5.58 (ddt, J = 17.2, 10.3, 5.7 Hz, 1H), 5.03 (dq, J = 17.2, 1.6 Hz, 1H), 4.92 (dq, J = 10.4, 1.3 Hz, 1H), 4.35 – 4.28 (m, 4H), 3.49 (s, 2H), 2.65 – 2.58 (m, 2H), 2.09 (ddt, J = 8.2, 6.9, 1.9 Hz, 2H), 1.46 – 1.37 (m, 2H) ppm; **^{13}C NMR** (101 MHz, C_6D_6) δ 168.3 (C), 166.8 (C), 165.0 (C), 132.0 (CH), 118.3 (CH_2), 105.8 (C), 67.2 (CH_2), 65.4 (CH_2), 50.6 (CH_3), 32.3 (CH_2), 30.8 (CH_2), 19.3 (CH_2) ppm; **HRMS** (EI+) *m/z* calculated for $C_{12}H_{16}O_5^{\bullet+}$ $[M]^{\bullet+}$ 240.09923, found 240.10081.

3a-methyl-5-phenylhexahydro-1H,6H-5,6a-epoxycyclobuta[3,4]cyclopenta[1,2-c]furan-1,6-dione (4.123)



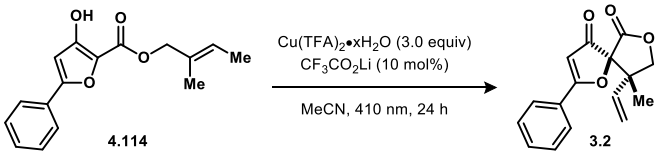
A solution of (±)-hyperolactone C (**3.2**, 16.7 mg, 0.058 mmol, 1.0 equiv.) and $[Ir(dF(CF_3)ppy)_2(dtbbpy)]PF_6$ (1.6 mg, 0.0014 mmol, 2.4 mol%) in acetonitrile (anhydrous, 0.5 mL, 0.12 M) was sparged with argon for 10 minutes before being sealed with parafilm and irradiated at 455 nm and stirred at room temperature for 48 hours. The mixture was concentrated under reduced pressure and the crude residue purified by flash column chromatography (SiO_2, 45% EtOAc/hexanes) to give **4.123** as a white solid (9.4 mg, 60%). R_f 0.41 (40% EtOAc/hexanes); **^{1}H NMR** (600 MHz, C_6D_6) δ 7.16 – 7.08 (m, 5H), 3.83 (d, J = 9.1 Hz, 1H), 3.37 (dd, J = 9.1, 1.0 Hz, 1H), 2.58 (dd, J = 8.2, 4.4 Hz, 1H), 1.89 (ddt, J = 7.3, 4.4, 1.0 Hz, 1H), 1.59 (dtd, J = 12.4, 8.2, 1.0 Hz, 1H), 1.04 (d, J = 12.4 Hz, 1H), 0.83 (s, 3H) ppm; **^{13}C NMR** (151 MHz, C_6D_6) δ 203.2 (C), 163.7 (C), 135.0 (C), 129.3 (CH), 129.0 (2 × CH), 126.0 (2 × CH), 98.7 (C), 94.4 (C), 71.0 (CH_2), 52.6 (C), 51.4 (CH), 49.6 (CH), 23.5 (CH_2), 20.7 (CH_3) ppm; **HRMS** (EI+) *m/z* calculated for $C_{16}H_{14}O_4^{\bullet+}$ $[M]^{\bullet+}$ 270.08866, found 270.08856.

Computational comparison of 2+2 product 20 regioisomers



	3.2	4.123	*4.124*
		60%	*not detected*
relative free energy (kcal/mol)	0	19.2	17.5

Control reaction for oxidative cyclization



4.114 3.2

Prepared as described for Hyperolactone C (**3.2**) using substrate **4.114** in the absence of 9,10-DPA on 0.1 mmol scale to give **3.2** in 8% yield by ^{1}H NMR (3.8:1 dr) with remaining **4.114** in 57% yield.

Complexity Comparison of Hyperolactone C Total Synthesis Routes[§]

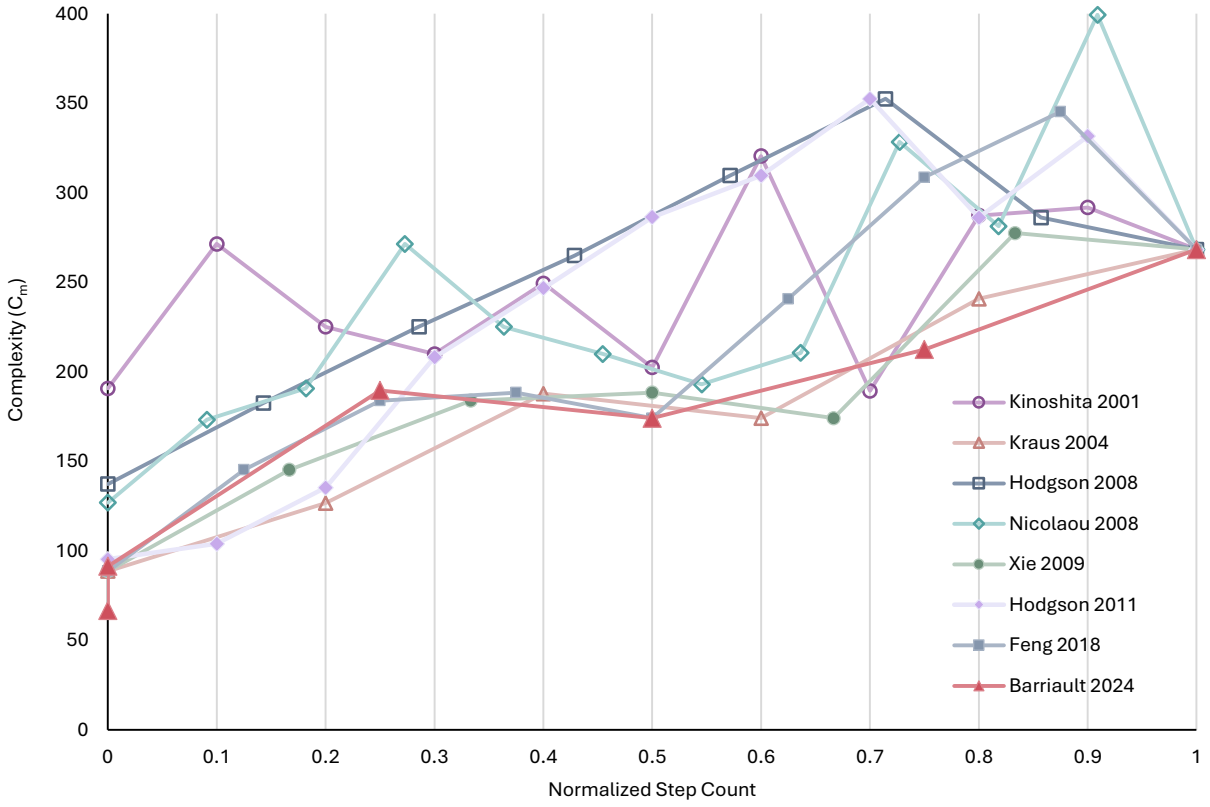


***Figure 60**. Complexity of synthetic intermediates (Böttcher Score, C_m) against normalized step count (step/max. step)*

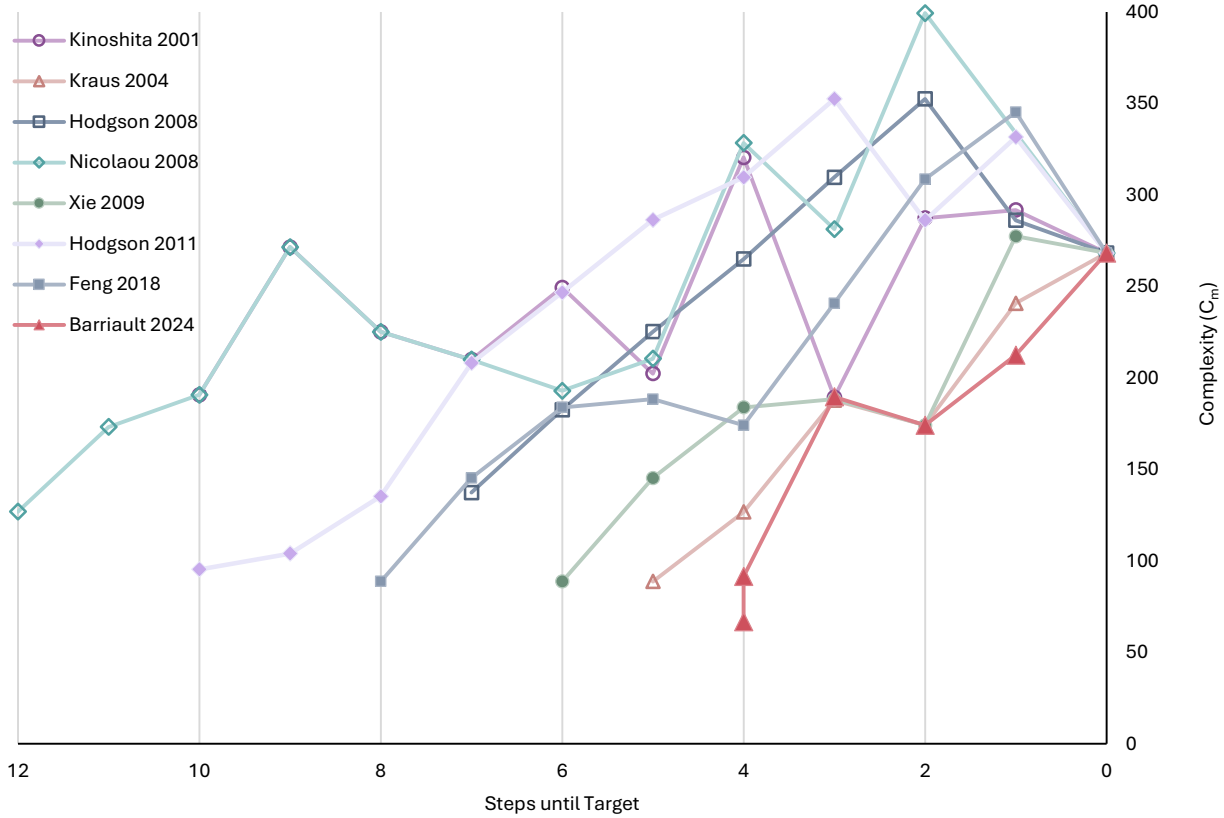
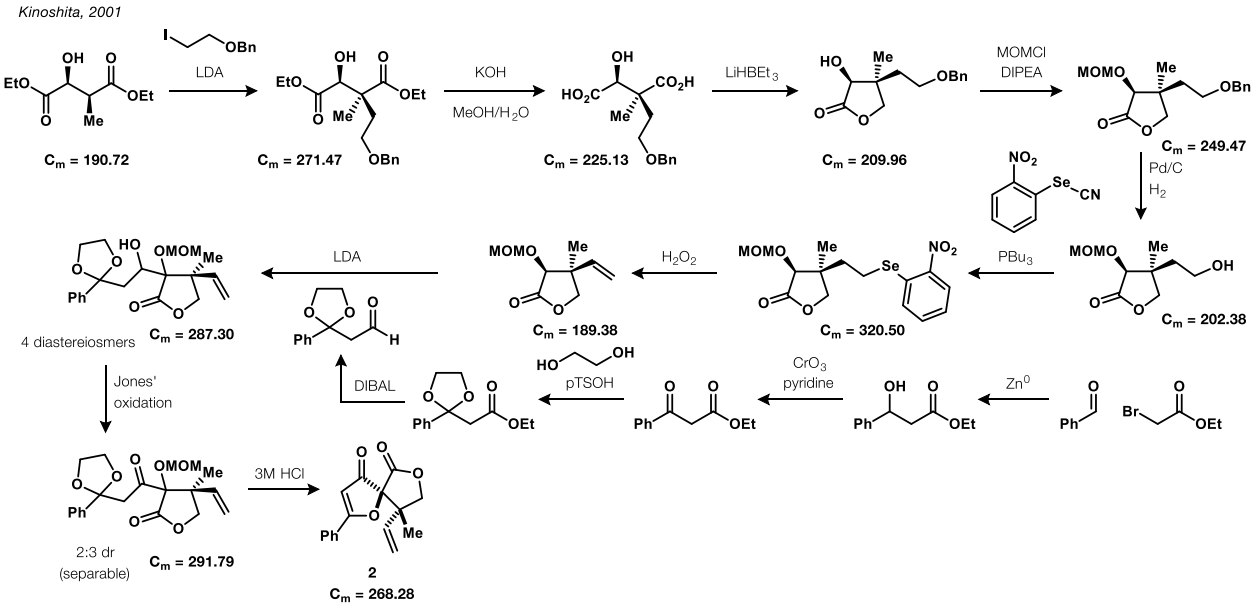
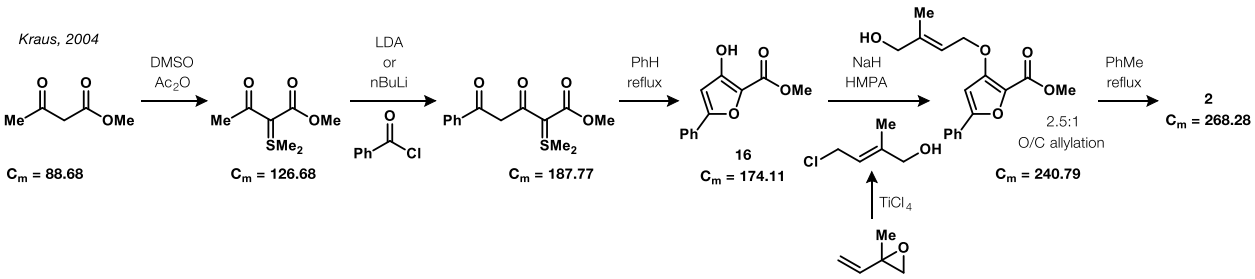


Figure 61. *Complexity of synthetic intermediates (Böttcher Score, C_m) against total step count, expressed as steps remaining until target*

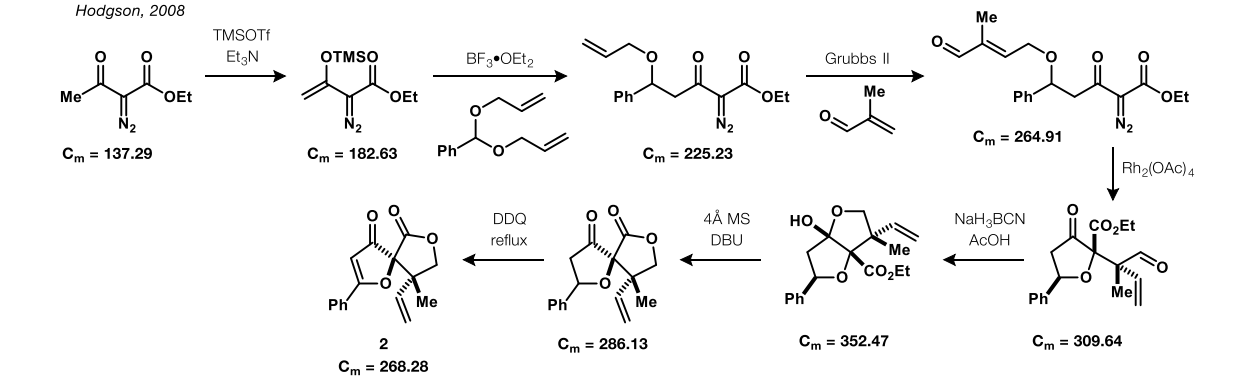
Böttcher complexity scores were computed using the python script bottchscore3.py for starting materials and intermediates *en route* to hyperolactone C (**3.2**) for each synthesis, to date (**Figure 60**).[292, 295a, 299] The corresponding synthetic sequences are illustrated below with each intermediate corresponding to a node on the above plot. The shortest sequences to prepare **3.2**, Barriault 2024 (4 steps), Kraus 2004 (5 steps), and Xie 2009 (6 steps), show gradual increases in complexity toward the target without greatly exceeding it (**Figure 61**). Specifically, our route incorporates substituents in the intended oxidation states and makes no concessions to rearrangements or non-strategic redox steps.



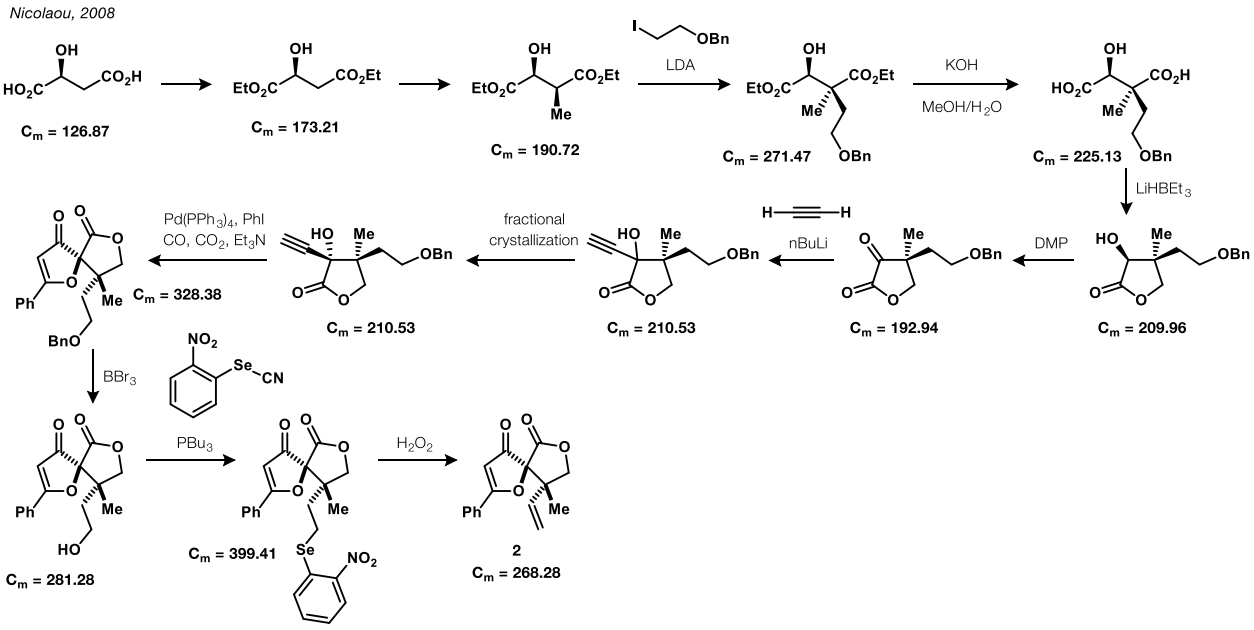
Scheme 28. *Total synthesis of hyperolactone C by Kinoshita and coworkers (2001)* [238b] *with computed Böttcher scores (Cm)*



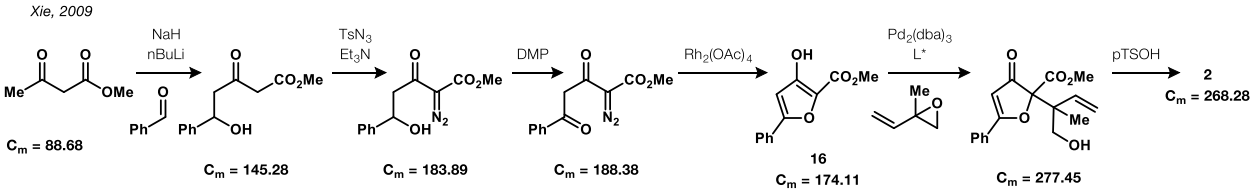
Scheme 29. *Total synthesis of hyperolactone C by Kraus and coworkers (2004)* [238c] *with computed Böttcher scores (Cm)*



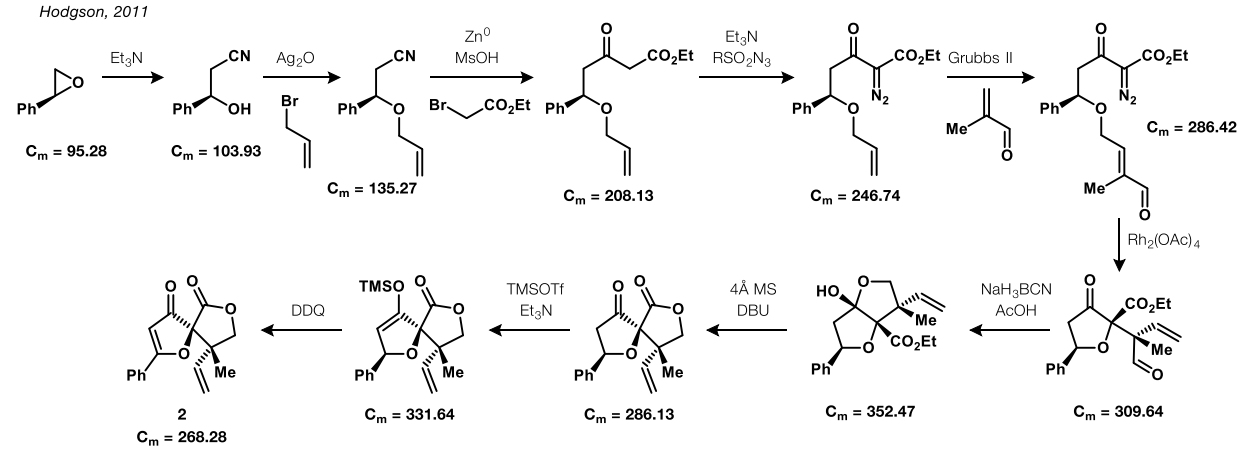
Scheme 30. *Total synthesis of hyperolactone C by Hodgson and coworkers (2008)* [238e] *with computed Böttcher scores (Cm)*



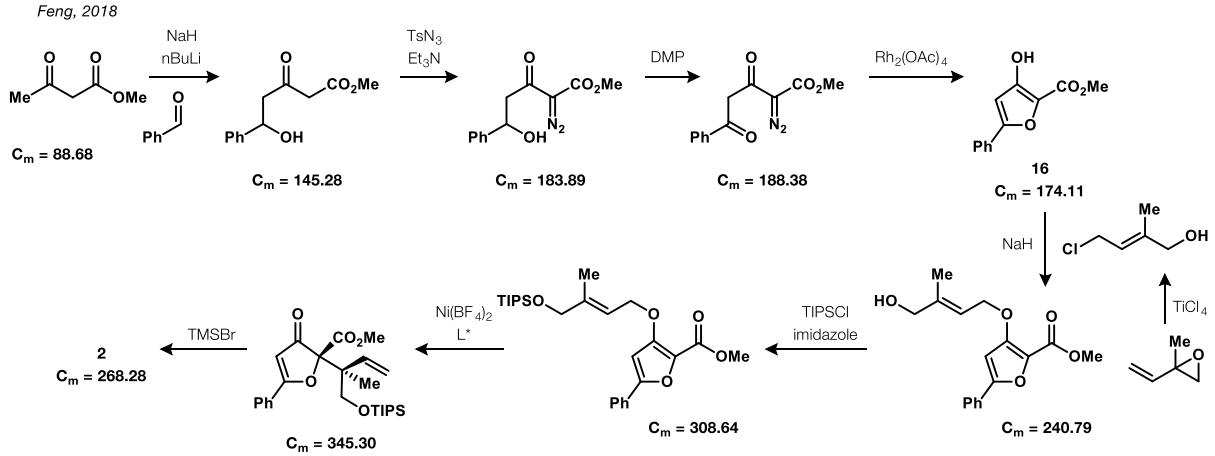
Scheme 31. *Total synthesis of hyperolactone C by Nicolaou and coworkers (2000)[238d] with computed Böttcher scores (C_m)*



Scheme 32. *Total synthesis of hyperolactone C by Xie and coworkers (2009 [238g] with computed Böttcher scores (C_m)*



Scheme 33. *Total synthesis of hyperolactone C by Hodgson and coworkers (2011)[238i] with computed Böttcher scores (C_m)*

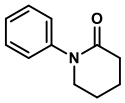


Scheme 34*. Total synthesis of hyperolactone C by Xie and coworkers (2018)[238m] with computed Böttcher scores (Cm)*

5.5 Supplemental Experimental Details

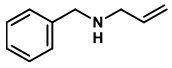
Procedures and Data

N-phenyl-2-piperidone (5.1)



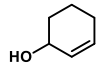
An oven-dried 50 mL high-pressure flask under argon atmosphere and equipped with a magnetic stir bar was charged with freshly-ground K_2CO_3 (2.76 g, 20 mmol, 2.0 equiv), 2-piperidone (1.49 g, 15 mmol, 1.5 equiv), and anhydrous CuI (190.5 mg, 1.0 mmol, 10 mol%). Next, anhydrous toluene (10 mL, 1 M), *N,N'*-dimethylethylenediamine (110 µL, 1.0 mmol, 10 mol%), and iodobenzene (1.1 mL, 10 mmol, 1.0 equiv) were added and the resulting mixture was sparged with argon for 15 minutes. The flask was capped and sealed with electrical tape, sonicated for 90 s, then stirred and heated to 80 ºC for 24 hours in an oil bath. The flask was removed from the oil bath and allowed to cool to room temperature. The room temperature mixture was diluted with distilled water (~25 mL) and EtOAc (30 mL). The layers were separated and the aqueous phase extracted with EtOAc (2 × 30 mL). Combined extracts were washed with NH_4Cl (3 × 25 mL, saturated aqueous), and brine (30 mL) then dried over Na_2SO_4, filtered, and concentrated *in vacuo*. The crude residue was purified by flash column chromatography (70% EtOAc/hexanes) to give a white powder (981.7 mg, 56% yield). R_f 0.29 (80% EtOAc/hexanes); **^{1}H NMR** (400 MHz, $CDCl_3$) δ 7.44 – 7.34 (m, 2H), 7.30 – 7.19 (m, 3H), 3.74 – 3.55 (m, 2H), 2.66 – 2.49 (m, 2H), 2.02 – 1.87 (m, 4H) ppm; **^{13}C NMR** (101 MHz, $CDCl_3$) δ 170.1 (C), 143.5 (C), 129.3 (2 × CH), 126.9 (CH), 126.4 (2 × CH), 51.8 , 33.0, 23.7, 21.6 ppm; Characterized according to literature comparison.[383]

***N*-allylbenzylamine (5.2)[§]**



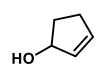
Prepared according to a procedure by Bezzenine-Lafollée and Gandon[349] on 20 mmol scale to give *N*-allylbenzylamine as a clear, colourless oil (2.19 g, 74%). **b.p.** 59–61 °C/5 torr; **^{1}H NMR** (400 MHz, $CDCl_3$) δ 7.35 – 7.32 (m, 4H), 7.29 – 7.23 (m, 1H), 5.94 (ddt, J = 17.2, 10.2, 6.0 Hz, 1H), 5.20 (dq, J = 17.2, 1.7 Hz, 1H), 5.12 (ddt, J = 10.2, 1.8, 1.3 Hz, 1H), 3.80 (s, 2H), 3.29 (dt, J = 6.0, 1.4 Hz, 2H) ppm; **^{13}C NMR** (101 MHz, $CDCl_3$) δ 140.3 (CH), 136.8 (CH), 128.5 (CH), 128.3 (CH), 127.1 (CH), 116.2 (CH_2), 53.4 (CH_2), 51.9 (CH_2) ppm; **HRMS** (EI+) *m/z* calculated for $C_{10}H_{13}N^{\bullet+}$ $[M]^{\bullet+}$ 147.10425, found 147.10544.

cyclohex-2-en-1-ol (5.3)



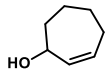
To a solution of 2-cyclohexen-1-one (2.4 mL, 25 mmol, 1.0 equiv) in methanol (42 mL, 0.6 M) was added freshly-ground $CeCl_3$•$7H_2O$ (10.2 g, 27.5 mmol, 1.1 equiv) at 0 ºC (ice–water bath) and the mixture was stirred until homogeneous (~10 min). $NaBH_4$ (1.23 g, 32.5 mmol, 1.3 equiv) was added in three portions at 5-minute intervals and the resulting mixture allowed to warm to room temperature and stirred until complete by TLC (~1.5 h). The mixture was cooled to 0 ºC then quenched by addition of NH_4Cl (100 mL, saturated, aqueous), stirred for 15 minutes, and then concentrated *in vacuo*. The resulting residue was diluted with water (100 mL) and Et_2O (100 mL). The layers were separated, and the aqueous phase extracted with Et_2O (2 × 100 mL). The combined extracts were washed with brine (10 mL), dried over $MgSO_4$, filtered, and concentrated *in vacuo*. The crude material was obtained as a pale-yellow oil and used without further purification (2.07 g, ~84% yield). R_f 0.3 (40% Et_2O/hexanes); **^{1}H NMR** (400 MHz, $CDCl_3$) δ 5.84 – 5.75 (m, 1H), 5.76 – 5.67 (m, 1H), 4.21 – 4.11 (m, 1H), 2.08 – 1.78 (m, 4H), 1.78 – 1.63 (m, 1H), 1.65 – 1.48 (m, 2H) ppm; **^{13}C NMR** (101 MHz, $CDCl_3$) δ 130.5 (CH), 130.0 (CH), 65.5 (CH), 32.0 (CH_2), 25.1 (CH_2), 19.0 (CH_2) ppm; Characterized according to literature comparison.[384]

cyclopent-2-en-1-ol (5.4)



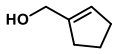
Prepared as described for cyclohex-2-en-1-ol (**5.3**) on 7.5 mmol scale to give a yellow oil that was used without purification (579 mg, 92%). R_f 0.31 (30% EtOAc/hexanes). Characterized according to literature comparison.[385]

cyclohept-2-en-1-ol (5.5)



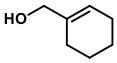
Prepared as described for cyclohex-2-en-1-ol (**5.3**) on 12.5 mmol scale to give a clear colourless oil that was used without purification (1.3 g, 92%). R_f 0.41 (22% EtOAc/hexanes). Characterized according to literature comparison. [386]

cyclopent-1-en-1-ylmethanol (5.6)



To a suspension of $LiAlH_4$ (3.49 g, 92 mmol, 1.0 equiv) and anhydrous THF (230 mL, 0.4 M) was added methyl cyclopent-1-ene-1-carboxylate (12 mL, 92 mmol, 1.0 equiv) dropwise over 10 minutes at 0 °C in an ice bath. The resulting mixture was stirred and allowed to warm to room temperature until consumption of the ester starting material was observed by TLC (~14 h). After complete conversion was achieved, EtOAc (50 mL) was added slowly at 0 ºC to quench excess reductant. Subsequently, Rochelle's salt (saturated aqueous, 250 mL) was added and the mixture was stirred and allowed to warm to room temperature over 30 minutes. The resulting solution was stirred at room temperature until the layers clarified on standing. The mixture was then diluted with EtOAc (50 mL). The layers were separated, and the aqueous phase was extracted with EtOAc (2 × 100 mL). The combined extracts were washed with brine (150 mL), dried over Na_2SO_4, filtered, and concentrated *in vacuo*. The crude residue was obtained as a pale-yellow oil and was used without further purification. Characterized according to literature comparison. [387]

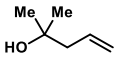
cyclohex-1-en-1-ylmethanol (5.7)



To a solution of methyl cyclohex-1-ene-1-carboxylate (1.35 mL, 10 mmol, 1.0 equiv) in DCM (anhydrous, 50 mL, 0.2 M) was added DIBAL (25% w/w in hexanes, 17.9 mL, 22 mmol, 2.2 equiv) was added dropwise over 10 minutes at to –78 ºC under vigorous stirring using a dry ice/acetone cooling bath. The mixture was allowed to stir at –78 ºC until the starting material was completely consumed according to TLC (~2.5 h). Once complete, excess DIBAL was quenched by addition of MeOH (3 mL) at –78 ºC and the cooling bath was removed to allow the solution to warm up to room temperature. Once at room temperature, Rochelle's salt solution was added (saturated, aqueous, ~ 30 mL) and the biphasic mixture was stirred vigorously until the layers clarified on standing. The mixture was then transferred into a separatory funnel and the layers were separated. The aqueous phase was then extracted with more

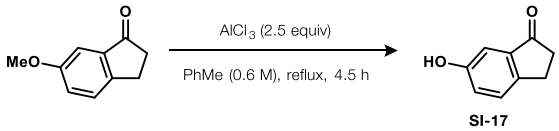
dichloromethane (2 × 30 mL) and the combined extracts were washed with brine (30 mL), dried over Na_2SO_4, filtered, and concentrated *in vacuo*. The crude material was obtained as a clear and colourless deemed pure by TLC analysis and used in the subsequent step without further purification. R_f 0.15 (15% EtOAc/hexanes). Characterized according to literature comparison. [388]

2-methylpent-4-en-2-ol (5.8)



To a solution of allyl magnesium bromide (1.0 M in THF, 16.5 mL, 16.5 mmol, 1.1 equiv) in THF (anhydrous, 13.5 mL) was added acetone (dried over 3 Å molecular sieves for 3 hours prior to use, 1.11 mL, 15 mmol, 1.0 equiv) dropwise over 10 minutes at 0 ºC in an ice-water bath. The resulting mixture was allowed to stir and warm slowly to room temperature overnight (~14 h). The mixture was quenched with NH_4Cl (saturated aqueous, 25 mL) and diluted with Et_2O (20 mL). The layers were separated and the aqueous phase extracted with Et_2O (2 × 25 mL). The combined extracts were washed with brine, dried over $MgSO_4$, filtered and concentrated *in vacuo*. The crude reside was obtained as a clear and colourless oil and used in the next step without further purification (1.5 g, 98% yield).

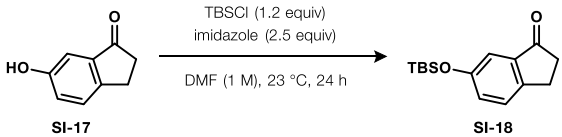
6-hydroxy-2,3-dihydro-1H-inden-1-one (5.9)§



SI-17

Prepared according to a procedure by Luo. [389] A solution of 6-methoxyindanone (0.81 g, 5.0 mmol, 1.0 equiv.) and $AlCl_3$ (1.67 g, 12.5 mmol, 2.5 equiv.) in toluene (9 mL, 0.6 M) was stirred at reflux for 4.5 hours. The mixture was allowed to cool to room temperature, diluted with water (100 mL), and the phases separated. The aqueous phase was extracted with EtOAc (3 × 50 mL). The combined organic phases were washed with brine (60 mL), dried over Na_2SO_4, filtered, and concentrated under reduced pressure. The resulting peach-coloured solid was used without further purification. R_f 0.23 (20% EtOAc/hexanes);

6-((tert-butyldimethylsilyl)oxy)-2,3-dihydro-1H-inden-1-one (5.10)§

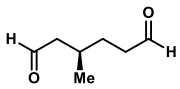


SI-17 SI-18

A solution of indanone **5.9** (0.74 g, 5.0 mmol, 1.0 equiv.), tert-butyldimethylsilylchloride (TBSCl, 0.90 g, 6.0 mmol, 1.2 equiv.), and imidazole (0.85 g, 12.5 mmol, 2.5 equiv.) in DMF (5 mL, 1 M) was stirred at room temperature

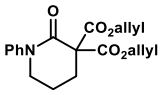
for 24 hours. The reaction was diluted with $NaHCO_3$ (5 mL, saturated aqueous) and the phases separated. The aqueous phase was extracted with Et_2O (3 × 10 mL). The combined organic phases were washed with water (20 mL) and brine (20 mL), dried over $MgSO_4$, filtered, and concentrated under reduced pressure. The crude residue was purified by flash column chromatography (SiO_2, 2–10% EtOAc/hexanes) to give a peach-coloured solid (1.1 g, 80% over two steps). R_f 0.63 (20% EtOAc/hexanes); **^{1}H NMR** (300 MHz, $CDCl_3$) δ 7.33 (ddd, J = 8.2, 0.8, 0.8 Hz, 1H), 7.16 (dd, J = 2.4, 0.6 Hz, 1H), 7.10 (dd, J = 8.2, 2.4 Hz, 1H), 3.12 – 3.00 (m, 2H), 2.74 – 2.67 (m, 2H), 0.98 (s, 9H), 0.20 (s, 6H) ppm; **^{13}C NMR** (101 MHz, $CDCl_3$) δ 207.2 (C), 155.4 (C), 148.4 (C), 138.5 (C), 128.0 (CH), 127.5 (CH), 113.5 (C), 37.2 (CH_2), 25.8 (3 × CH_3), 25.3 (CH_2), 18.3 (C), -4.4 (2 × CH_3) ppm; **HRMS** (EI+) calculated for $C_{15}H_{22}O_2Si^{\bullet+}$ $[M]^{\bullet+}$ 262.13836, found 262.13911.

(R)-3-methylhexanedial (5.11)



Prepared according to GP4 from compound **2.87** giving **5.11** as a clear colourless oil (17 mg, 0.2 mmol scale reaction, 64% yield). **^{1}H NMR** (400 MHz, $CDCl_3$) δ 9.77 (t, J = 1.6 Hz, 1H), 9.75 (t, J = 2.0 Hz, 1H), 2.52 – 2.36 (m, 3H), 2.29 (ddd, J = 16.6, 7.6, 2.2 Hz, 1H), 2.09 (hept, J = 6.8 Hz, 1H), 1.70 (dddd, J = 14.0, 8.6, 6.7, 5.6 Hz, 1H), 1.60 – 1.46 (m, 1H), 0.97 (d, J = 6.7 Hz, 3H) ppm; **^{13}C NMR** (101 MHz, $CDCl_3$) δ 202.1 (C), 202.0 (C), 50.9 (CH_2), 41.6 (CH_2), 28.8 (CH_2), 27.6 (CH), 19.7 (CH_3) ppm. Characterized according to NMR comparison. [390]

diallyl 2-oxo-1-phenylpiperidine-3,3-dicarboxylate (5.12)



Prepared according to GP9 using *N*-phenyl 2-piperidone on 5.0 mmol scale and purified by flash column chromatography (15–40% EtOAc/hexanes) to give a white solid (826 mg, 48%); R_f 0.44 (35% EtOAc/hexanes); **^{1}H NMR** (400 MHz, $CDCl_3$) δ 7.41 – 7.35 (m, 2H), 7.30 – 7.22 (m, 3H), 5.94 (ddt, J = 17.2, 10.5, 5.7 Hz, 2H), 5.37 (dq, J = 17.2, 1.5 Hz, 2H), 5.25 (dq, J = 10.5, 1.3 Hz, 2H), 4.83 – 4.68 (m, 4H), 3.70 (t, J = 6.4 Hz, 2H), 2.69 – 2.60 (m, 2H), 2.01 – 1.90 (m, 2H) ppm; **^{13}C NMR** (101 MHz, $CDCl_3$) δ 167.9 (2 × C), 164.3 (C), 142.7 (C), 131.5 (2 × CH), 129.3 (2 × CH), 127.1 (CH), 125.9 (2 × CH), 119.0 (2 × CH_2), 66.9 (CH_2), 64.3 (C), 50.9 (CH_2), 29.0 (CH_2), 20.0 (CH_2) ppm;

References

(1) Turro, N. J.; Ramamurthy, V.; Scaiano, J. C. *Modern molecular photochemistry of organic molecules*; University Science Books Sausalito, CA, 2010.

(2) (a) Nicewicz, D. A.; Nguyen, T. M. Recent Applications of Organic Dyes as Photoredox Catalysts in Organic Synthesis. *ACS Catal.* **2014**, *4*, 355-360. DOI: 10.1021/cs400956a. (b) Romero, N. A.; Nicewicz, D. A. Organic Photoredox Catalysis. *Chem. Rev.* **2016**, *116*, 10075-10166. DOI: 10.1021/acs.chemrev.6b00057. (c) Tucker, J. W.; Stephenson, C. R. J. Shining Light on Photoredox Catalysis: Theory and Synthetic Applications. *J. Org. Chem.* **2012**, *77*, 1617-1622. DOI: 10.1021/jo202538x. (d) Prier, C. K.; Rankic, D. A.; MacMillan, D. W. C. Visible Light Photoredox Catalysis with Transition Metal Complexes: Applications in Organic Synthesis. *Chem. Rev.* **2013**, *113*, 5322-5363. DOI: 10.1021/cr300503r. (e) Shaw, M. H.; Twilton, J.; MacMillan, D. W. C. Photoredox Catalysis in Organic Chemistry. *J. Org. Chem.* **2016**, *81*, 6898-6926. DOI: 10.1021/acs.joc.6b01449.

(3) Miller, J. R.; Calcaterra, L. T.; Closs, G. L. Intramolecular long-distance electron transfer in radical anions. The effects of free energy and solvent on the reaction rates. *J. Am. Chem. Soc.* **1984**, *106*, 3047-3049. DOI: 10.1021/ja00322a058.

(4) Choi, G. J.; Zhu, Q.; Miller, D. C.; Gu, C. J.; Knowles, R. R. Catalytic alkylation of remote C–H bonds enabled by proton-coupled electron transfer. *Nature* **2016**, *539*, 268-271. DOI: 10.1038/nature19811.

(5) (a) Verhoeven, J. W.; Ramesdonk, H. J. v.; Zhang, H.; Groeneveld, M. M.; Benniston, A. C.; Harriman, A. Long-lived Charge-Transfer States in 9-Aryl-Acridinium Ions; A Critical Reinvestigation. *International Journal of Photoenergy* **2005**, *7*, 596840. DOI: 10.1155/S1110662X05000152. (b) Benniston, A. C.; Harriman, A.; Verhoeven, J. W. Comment: Electron-transfer reactions in the 9-mesityl-10-methylacridinium ion: impurities, triplet states and infinitely long-lived charge-shift states? *Phys. Chem. Chem. Phys.* **2008**, *10*, 5156-5158. DOI: 10.1039/B807893A. (c) Fukuzumi, S.; Kotani, H.; Ohkubo, K. Response: Why had long-lived electron-transfer states of donor-substituted 10-methylacridinium ions been overlooked? Formation of the dimer radical cations detected in the near-IR region. *Phys. Chem. Chem. Phys.* **2008**, *10*, 5159-5162. DOI: 10.1039/B809264H. (d) Zilberg, S. Electronic structure of 9-mesityl-10-methylacridinium in ground and excited states: charge-shift mechanism introduced by counter anion shift. *Phys. Chem. Chem. Phys.* **2010**, *12*, 10292-10294. DOI: 10.1039/C0CP00491J. (e) Hoshino, M.; Uekusa, H.; Tomita, A.; Koshihara, S.-y.; Sato, T.; Nozawa, S.; Adachi, S.-i.; Ohkubo, K.; Kotani, H.; Fukuzumi, S. Determination of the Structural Features of a Long-Lived Electron-Transfer State of 9-Mesityl-10-methylacridinium Ion. *J. Am. Chem. Soc.* **2012**, *134*, 4569-4572. DOI: 10.1021/ja300602h. (f) Tsudaka, T.; Kotani, H.; Ohkubo, K.; Nakagawa, T.; Tkachenko, N. V.; Lemmetyinen, H.; Fukuzumi, S. Photoinduced Electron Transfer in 9-Substituted 10-Methylacridinium Ions. *Chem. Eur. J.* **2017**, *23*, 1306-1317. DOI: 10.1002/chem.201604527.

(6) (a) Suzuki, T.; Nagano, M.; Watanabe, S.; Ichimura, T. Study of the photophysics and energy transfer of 9,10-diphenylanthracene in solution. *J. Photochem. Photobiol. A* **2000**, *136*, 7-13. DOI: 10.1016/S1010-6030(00)00322-1. (b) Chattopadhyay, S. K.; Kumar, C. V.; Das, P. K. Triplet-related photophysics of 9,10-diphenylanthracene. A kinetic study of reversible energy transfer from anthracene triplet by nanosecond laser

flas. *Chem. Phys. Lett.* **1983**, *98*, 250-254. DOI: 10.1016/0009-2614(83)87160-7. (c) Gray, V.; Dzebo, D.; Lundin, A.; Alborzpour, J.; Abrahamsson, M.; Albinsson, B.; Moth-Poulsen, K. Photophysical characterization of the 9,10-disubstituted anthracene chromophore and its applications in triplet–triplet annihilation photon upconversion. *Journal of Materials Chemistry C* **2015**, *3*, 11111-11121. DOI: 10.1039/C5TC02626A. (d) Heinrich, G.; Schoof, S.; Gusten, H. 9,10-diphenylanthracene as a fluorescence quantum yield standard. *J. Photochem.* **1974**, *3*, 315-320. DOI: 10.1016/0047-2670(74)80040-7. (e) Hu, A.; Chen, Y.; Guo, J. J.; Yu, N.; An, Q.; Zuo, Z. Cerium-Catalyzed Formal Cycloaddition of Cycloalkanols with Alkenes through Dual Photoexcitation. *J. Am. Chem. Soc.* **2018**, *140*, 13580-13585. DOI: 10.1021/jacs.8b08781. (f) Sioda, R. E. Electrolytic oxidation of 9,10-diphenylanthracene and properties of its free radical cation and anion. *J. Phys. Chem.* **1968**, *72*, 2322-2330. DOI: 10.1021/j100853a007. (g) Visco, R. E.; Chandross, E. A. Electroluminescence in solutions of aromatic hydrocarbons. *J. Am. Chem. Soc.* **1964**, *86*, 5350-5351. (h) Santhanam, K. S. V.; Bard, A. J. The Electrochemical Reduction of 9,10-Diphenylanthracene. *J. Am. Chem. Soc.* **1966**, *88*, 2669-2675. DOI: 10.1021/ja00964a009. (i) Saraidaridis, J. D.; Suttil, J. A.; Monroe, C. W. High-Voltage Metal-Free Disproportionation Flow Batteries Based on 9, 10-diphenylanthracene. *J. Electrochem. Soc.* **2020**, *167*, 070517. DOI: 10.1149/1945-7111/ab6a8d. (j) Faulkner, L. R.; Bard, A. J. Electrogenerated chemiluminescence. IV. Magnetic field effects on the electrogenerated chemiluminescence of some anthracenes. *J. Am. Chem. Soc.* **1969**, *91*, 209-210. DOI: 10.1021/ja01029a049. (k) Chen, Y.; Wang, X.; He, X.; An, Q.; Zuo, Z. Photocatalytic Dehydroxymethylative Arylation by Synergistic Cerium and Nickel Catalysis. *J. Am. Chem. Soc.* **2021**, *143*, 4896-4902. DOI: 10.1021/jacs.1c00618. (l) Li, P.; Duan, L.; Lin, Y.; Chu, L.; An, Q.; Zuo, Z. Modulating Electron Transfer via Cerium Photocatalysis for Alkoxy Radical-Mediated Selective Hydroetherification. *Angew. Chem. Int. Ed.* **2025**, e202501949. DOI: 10.1002/anie.202501949.

(7) Hamilton, T. D. S. The Effect Of Molecular Shape On The Fluorescent Properties Of 9,10-Diphenylanthracene. *Photochem. Photobiol.* **1964**, *3*, 153-156. DOI: 10.1111/j.1751-1097.1964.tb07864.x.

(8) Morris, A. O.; O'Brien, T. E.; Barriault, L. Photoredox-Catalyzed Hydroalkylation of C(sp3)–H Acids. *Chem. Eur. J.* **2025**, e202501148. DOI: 10.1002/chem.202501148.

(9) (a) Schroll, P.; König, B. Photocatalytic α-Oxyamination of Stable Enolates, Silyl Enol Ethers, and 2-Oxoalkane Phosphonic Esters. *Eur. J. Org. Chem.* **2015**, *2015*, 309-313. DOI: 10.1002/ejoc.201403433. (b) Yin, H.; Jin, Y.; Hertzog, J. E.; Mullane, K. C.; Carroll, P. J.; Manor, B. C.; Anna, J. M.; Schelter, E. J. The Hexachlorocerate(III) Anion: A Potent, Benchtop Stable, and Readily Available Ultraviolet A Photosensitizer for Aryl Chlorides. *J. Am. Chem. Soc.* **2016**, *138*, 16266-16273. DOI: 10.1021/jacs.6b05712. (c) Roth, H. G.; Romero, N. A.; Nicewicz, D. A. Experimental and Calculated Electrochemical Potentials of Common Organic Molecules for Applications to Single-Electron Redox Chemistry. *Synlett* **2016**, *27*, 714-723. DOI: 10.1055/s-0035-1561297. (d) Caldora, H. P.; Zhang, Z.; Tilby, M. J.; Turner, O.; Leonori, D. Dual Photochemical H-Atom Transfer and Cobalt Catalysis for the Desaturative Synthesis of Phenols from Cyclohexanones. *Angew. Chem. Int. Ed.* **2023**, *62*, e202301656. DOI: 10.1002/anie.202301656. (e) Wehlin, S. A. M.; Troian-Gautier, L.; Li, G.; Meyer, G. J. Chloride Oxidation by Ruthenium Excited-States in Solution. *J. Am. Chem. Soc.* **2017**,

139, 12903-12906. DOI: 10.1021/jacs.7b06762. (f) Koppenol, W. H. Oxyradical reactions: from bond-dissociation energies to reduction potentials. *FEBS Lett.* **1990**, *264*, 165-167. DOI: 10.1016/0014-5793(90)80239-F. (g) Cai, X.; Sakamoto, M.; Fujitsuka, M.; Majima, T. One-Electron Oxidation of Alcohols by the 1,3,5-Trimethoxybenzene Radical Cation in the Excited State during Two-Color Two-Laser Flash Photolysis. *J. Phys. Chem. A* **2007**, *111*, 1788-1791. DOI: 10.1021/jp0669658. (h) Pysh, E. S.; Yang, N. C. Polarographic Oxidation Potentials of Aromatic Compounds. *J. Am. Chem. Soc.* **1963**, *85*, 2124-2130. DOI: 10.1021/ja00897a019.

(10) Pavlishchuk, V. V.; Addison, A. W. Conversion constants for redox potentials measured versus different reference electrodes in acetonitrile solutions at 25°C. *Inorg. Chim. Acta* **2000**, *298*, 97-102. DOI: 10.1016/S0020-1693(99)00407-7.

(11) (a) Kunkely, H.; Vogler, A. Optical metal-to-ligand charge transfer in tris(pyrazine-2-carboxylato)cerium(III): Absorption and emission. *J. Photochem. Photobiol. A* **2002**, *151*, 45-47. DOI: 10.1016/S1010-6030(02)00171-5. (b) Vogler, A.; Kunkely, H. Excited state properties of lanthanide complexes: Beyond ff states. *Inorg. Chim. Acta* **2006**, *359*, 4130-4138. DOI: 10.1016/j.ica.2006.05.025.

(12) Kunkely, H.; Vogler, A. Excited state behavior of tetrakis(2,2,6,6-tetramethyl-3,5-heptane-dionato)cerium(IV): Emission and photoredox reaction from ligand-to-metal charge transfer states. *J. Photochem. Photobiol. A* **2001**, *146*, 63-66. DOI: 10.1016/S1010-6030(01)00588-3.

(13) Löble, M. W.; Keith, J. M.; Altman, A. B.; Stieber, S. C. E.; Batista, E. R.; Boland, K. S.; Conradson, S. D.; Clark, D. L.; Lezama Pacheco, J.; Kozimor, S. A.; Martin, R. L.; Minasian, S. G.; Olson, A. C.; Scott, B. L.; Shuh, D. K.; Tyliszczak, T.; Wilkerson, M. P.; Zehnder, R. A. Covalency in lanthanides. An X-ray absorption spectroscopy and density functional theory study of LnCl6x- (x = 3, 2). *J. Am. Chem. Soc.* **2015**, *137*, 2506-2523. DOI: 10.1021/ja510067v.

(14) Costanzo, L. L.; Pistarà, S.; Condorelli, G. Photoreduction of cerium(IV) hexachloride in acetonitrile. *J. Photochem.* **1983**, *21*, 45-51. DOI: 10.1016/0047-2670(83)80006-9.

(15) An, Q.; Wang, Z.; Chen, Y.; Wang, X.; Zhang, K.; Pan, H.; Liu, W.; Zuo, Z. Cerium-Catalyzed C-H Functionalizations of Alkanes Utilizing Alcohols as Hydrogen Atom Transfer Agents. *J. Am. Chem. Soc.* **2020**, *142*, 6216-6226. DOI: 10.1021/jacs.0c00212.

(16) (a) Juliá, F. Ligand-to-Metal Charge Transfer (LMCT) Photochemistry at 3d-Metal Complexes: An Emerging Tool for Sustainable Organic Synthesis. *ChemCatChem* **2022**, *14*, e202200916. DOI: 10.1002/cctc.202200916. (b) Gavelle, S.; Innocent, M.; Aubineau, T.; Guérinot, A. Photoinduced Ligand-to-Metal Charge Transfer of Carboxylates: Decarboxylative Functionalizations, Lactonizations, and Rearrangements. *Adv. Synth. Catal.* **2022**, *364*, 4189-4230. DOI: 10.1002/adsc.202201149. (c) An, Q.; Chang, L.; Pan, H.; Zuo, Z. Ligand-to-Metal Charge Transfer (LMCT) Catalysis: Harnessing Simple Cerium Catalysts for Selective Functionalization of Inert C–H and C–C Bonds. *Acc. Chem. Res.* **2024**, *57*, 2915-2927. DOI: 10.1021/acs.accounts.4c00510.

(17) Baur, E. Über ein Modell der Kohlensäureassimilation. **1908**, *63U*, 683-710. DOI: doi:10.1515/zpch-1908-6344.

(18) Weiss, J.; Porret, D. Photochemical Reduction of Ceric Ions by Water. *Nature* **1937**, *139*, 1019-1020. DOI: 10.1038/1391019a0.

(19) Heidt, L. J.; Smith, M. E. Quantum Yields of the Photochemical Reduction of Ceric Ions by Water and Evidence for the Dimerization of Ceric Ions. *J. Am. Chem. Soc.* **1948**, *70*, 2476-2481. DOI: 10.1021/ja01187a050.

(20) Sworski, T. J. A Mechanism for the Photo-Oxidation of Water by Ceric Ion. *J. Am. Chem. Soc.* **1955**, *77*, 1074-1075. DOI: 10.1021/ja01609a106.

(21) Martin, T. W.; Burk, J. M.; Henshall, A. Ligand Sensitization. I. The Photo- and Oxidation-Reduction Activated Decomposition of Glacial Acetic Acid with Ceric Ammonium Nitrate1. *J. Am. Chem. Soc.* **1966**, *88*, 1097-1104. DOI: 10.1021/ja00958a002.

(22) Sheldon, R. A.; Kochi, J. K. Photochemical and Thermal Reduction of Cerium (IV) Carboxylates. Formation and Oxidation of Alkyl Radicals. *J. Am. Chem. Soc.* **1968**, *90*, 6688-6698. DOI: 10.1021/ja01026a022.

(23) (a) Trofimenko, S.; Mino, G.; Kaizerman, S.; Rasmussen, E.; Trahanovsky, S.; Young, L. H.; Bierman, H.; Richardson, W. H.; Hintz, H. L.; Johnson, D. C.; Russell, G. A.; Williamson, R. C. *Oxidation in Organic Chemistry*; Academic Press, 1965. (b) Trahanovsky, W. S.; Young, L. B. Controlled Oxidation of Organic Compounds with Cerium(IV). II. The Oxidation of Toluenes. *J. Org. Chem.* **1966**, *31*, 2033-2035. DOI: 10.1021/jo01344a544. (c) Trahanovsky, W. S.; Young, L. B.; Brown, G. L. Oxidation of organic compounds with cerium(IV). IV. Oxidation of benzyl and related alcohols. *J. Org. Chem.* **1967**, *32*, 3865-3868. DOI: 10.1021/jo01287a032. (d) Nave, P. M.; Trahanovsky, W. S. Oxidation of organic compounds with cerium(IV). V. The substituent effect on the rate of the one-electron oxidative cleavage of 2-aryl-1-phenylethanols. *J. Am. Chem. Soc.* **1968**, *90*, 4755-4756. DOI: 10.1021/ja01019a060. (e) Young, L. B.; Trahanovsky, W. S. Oxidation of organic compounds with cerium(IV). VII. Formation constants for 1:1 cerium(IV)-alcohol complexes. *J. Am. Chem. Soc.* **1969**, *91*, 5060-5068. DOI: 10.1021/ja01046a021. (f) Trahanovsky, W. S.; Young, M. G.; Nave, P. M. Oxidation of organic compounds with cerium(IV). IX. Formation of 2-methyltetrahydrofuran by oxidation of 1-pentanol. *Tetrahedron Lett.* **1969**, *10*, 2501-2504. DOI: 10.1016/S0040-4039(01)88551-8. (g) Trahanovsky, W. S.; Flash, P. J.; Smith, L. M. Oxidation of organic compounds with cerium(IV). VIII. Oxidation of bicyclo[2.2.1]-2-heptanols and bicyclo[2.2.2]-2-octanol. *J. Am. Chem. Soc.* **1969**, *91*, 5068-5072. DOI: 10.1021/ja01046a022. (h) Eaton, S. S.; Hutchison, J. R.; Holm, R. H.; Muetterties, E. L.; Amer, J.; Eaton, R.; Palozzotto, M. C.; Duffy, D. J.; Edgar, B. L.; Que, L.; Pignolet, L. H.; Porter, G. G.; Chen, S. N.; Schlafer, H. L.; Gausmann, H.; P Kane-Maquire, N. A.; Lang, C. H.; Trahanovsky, W. S.; Fox, N. S. Oxidation of Organic Compounds with Cerium(IV). XIX. Effect of Alkyl Substitution on the Oxidative Cleavage of Alkylphenylmethanols1; *J. Am. Chem. Soc.*, **1971**, 94, 895-895. (i) Trahanovsky, W. S.; Nave, P. M. Oxidation of organic compounds with cerium(IV). XI. Oxidative cleavage of 1,2-diarylethanols and 1-aryl-2,3-diphenylpropan-2-ols by cerium(IV) and chromic acid. *J. Am. Chem. Soc.* **1971**, *93*, 4536-4540. DOI: 10.1021/ja00747a033. (j) Trahanovsky, W. S.; Cramer, J. Oxidation of organic compounds with cerium(IV). XII. Oxidative cleavage and ketone formation of alkylphenylcarbinols. *J. Org. Chem.* **1971**, *36*, 1890-1893. DOI: 10.1021/jo00813a010.

(24) (a) Hu, A.; Guo, J.-J.; Pan, H.; Zuo, Z. Selective functionalization of methane, ethane, and higher alkanes by cerium photocatalysis. *Science* **2018**, *361*, 668-672. DOI: 10.1126/science.aat9750. (b) Yang, Q.; Wang, Y.-H.; Qiao, Y.; Gau, M.; Carroll, P. J.; Walsh, P. J.; Schelter, E. J. Photocatalytic C-H activation and the subtle role of chlorine radical complexation in reactivity. *Science* **2021**, *372*, 847-852. DOI: 10.1126/science.abd8408. (c) Yang, Q.; Song, E.; Wu, Y.; Li, C.; Gau, M. R.; Anna, J. M.; Schelter, E. J.; Walsh, P. J. Mechanistic Investigation of the Ce(III) Chloride Photoredox Catalysis System: Understanding the Role of Alcohols as Additives. *J. Am. Chem. Soc.* **2025**, *147*, 2061-2076. DOI: 10.1021/jacs.4c15627. (d) An, Q.; Xing, Y. Y.; Pu, R.; Jia, M.; Chen, Y.; Hu, A.; Zhang, S. Q.; Yu, N.; Du, J.; Zhang, Y.; Chen, J.; Liu, W.; Hong, X.; Zuo, Z. Identification of Alkoxy Radicals as Hydrogen Atom Transfer Agents in Ce-Catalyzed C-H Functionalization. *J. Am. Chem. Soc.* **2022**. DOI: 10.1021/jacs.2c10126.

(25) Guo, J.-J.; Hu, A.; Chen, Y.; Sun, J.; Tang, H.; Zuo, Z. Photocatalytic C−C Bond Cleavage and Amination of Cycloalkanols by Cerium(III) Chloride Complex. *Angew. Chem.* **2016**, *128*, 15545-15548. DOI: 10.1002/ange.201609035.

(26) Hu, A.; Guo, J. J.; Pan, H.; Tang, H.; Gao, Z.; Zuo, Z. δ-Selective functionalization of alkanols enabled by visible-light-induced ligand-to-metal charge transfer. *J. Am. Chem. Soc.* **2018**, *140*, 1612-1616. DOI: 10.1021/jacs.7b13131.

(27) (a) Schwarz, J.; König, B. Visible-light mediated C-C bond cleavage of 1,2-diols to carbonyls by cerium-photocatalysis. *Chem. Commun.* **2019**, *55*, 486-488. DOI: 10.1039/c8cc09208g. (b) Yatham, V. R.; Bellotti, P.; König, B. Decarboxylative hydrazination of unactivated carboxylic acids by cerium photocatalysis. *Chem. Commun.* **2019**, *55*, 3489-3492. DOI: 10.1039/C9CC00492K. (c) Zhang, K.; Chang, L.; An, Q.; Wang, X.; Zuo, Z. Dehydroxymethylation of alcohols enabled by cerium photocatalysis. *J. Am. Chem. Soc.* **2019**, *141*, 10556-10564. DOI: 10.1021/jacs.9b05932.

(28) Chen, Y.; Du, J.; Zuo, Z. Selective C-C Bond Scission of Ketones via Visible-Light-Mediated Cerium Catalysis. *Chem* **2020**, *6*, 266-279. DOI: 10.1016/j.chempr.2019.11.009.

(29) Shirase, S.; Tamaki, S.; Shinohara, K.; Hirosawa, K.; Tsurugi, H.; Satoh, T.; Mashima, K. Cerium(IV) Carboxylate Photocatalyst for Catalytic Radical Formation from Carboxylic Acids: Decarboxylative Oxygenation of Aliphatic Carboxylic Acids and Lactonization of Aromatic Carboxylic Acids. *J. Am. Chem. Soc.* **2020**, *142*, 5668-5675. DOI: 10.1021/jacs.9b12918.

(30) Wadekar, K.; Aswale, S.; Yatham, V. R. Cerium photocatalyzed dehydrogenative lactonization of 2-arylbenzoic acids. *Organic and Biomolecular Chemistry* **2020**, *18*, 983-987. DOI: 10.1039/c9ob02676b.

(31) Lai, X. L.; Shu, X. M.; Song, J.; Xu, H. C. Electrophotocatalytic Decarboxylative C−H Functionalization of Heteroarenes. *Angew. Chem., Int. Ed.* **2020**, *59*, 10626-10632. DOI: 10.1002/anie.202002900.

(32) Yan, X.; Li, X.; Wang, Y.; Dai, Y.; Yan, X.; Zhao, D.; Xu, X. Iminyl-Radical-Mediated C–C Cleavage/Amination and Alkene Iminoamination Enabled by Visible-Light-Induced Cerium Catalysis. *ACS Sustainable Chemistry & Engineering* **2021**, *9*, 101-105. DOI: 10.1021/acssuschemeng.0c07850.

(33) Tripathy, A. R.; Yedase, G. S.; Yatham, V. R. Cerium photocatalyzed radical smiles rearrangement of 2-aryloxybenzoic acids. *RSC Advances* **2021**, *11*, 25207-25210. DOI: 10.1039/d1ra04130d.

(34) Du, J.; Yang, X.; Wang, X.; An, Q.; He, X.; Pan, H.; Zuo, Z. Photocatalytic Aerobic Oxidative Ring Expansion of Cyclic Ketones to Macrolactones by Cerium and Cyanoanthracene Catalysis. *Angew. Chem., Int. Ed.* **2021**, *60*, 5370-5376. DOI: 10.1002/anie.202012720.

(35) Singh, S.; Dagar, N.; Roy, S. R. Photoinduced ligand to metal charge transfer enabling cerium mediated decarboxylative alkylation of quinoxalin-2(1H)-ones. *Chem. Commun.* **2022**, *58*, 3831-3834. DOI: 10.1039/D2CC00840H.

(36) Li, H.-C.; Li, G.-N.; Sun, K.; Chen, X.-L.; Jiang, M.-X.; Qu, L.-B.; Yu, B. Ce(III)/Photoassisted Synthesis of Amides from Carboxylic Acids and Isocyanates. *Org. Lett.* **2022**, *24*, 2431-2435. DOI: 10.1021/acs.orglett.2c00699.

(37) (a) Yang, K.; Lu, J.; Li, L.; Luo, S.; Fu, N. Electrophotochemical Metal-Catalyzed Decarboxylative Coupling of Aliphatic Carboxylic Acids. *Chem. Eur. J.* **2022**, *28*, e202202370. DOI: 10.1002/chem.202202370. (b) Wang, Y.; Li, L.; Fu, N. Electrophotochemical Decarboxylative Azidation of Aliphatic Carboxylic Acids. *ACS Catal.* **2022**, *12*, 10661-10667. DOI: 10.1021/acscatal.2c02934.

(38) Lu, J.; Yao, Y.; Li, L.; Fu, N. Dual Transition Metal Electrocatalysis: Direct Decarboxylative Alkenylation of Aliphatic Carboxylic Acids. *J. Am. Chem. Soc.* **2023**, *145*, 26774-26782. DOI: 10.1021/jacs.3c08839.

(39) Yang, K.; Wang, Y.; Luo, S.; Fu, N. Electrophotochemical Metal-Catalyzed Enantioselective Decarboxylative Cyanation. *Chem. Eur. J.* **2023**, *29*, e202203962. DOI: 10.1002/chem.202203962.

(40) Dagar, N.; Singh, S.; Roy, S. R. Photoinduced Cerium-Mediated Decarboxylative Alkylation Cascade Cyclization of N-arylacrylamides and N-acryl-2-aryl benzimidazoles. *Chemistry – An Asian Journal* **2023**, *18*, e202300028. DOI: 10.1002/asia.202300028.

(41) Xu, Y.; Huang, P.; Jiang, Y.; Lv, C.; Li, P.; Wang, J.; Sun, B.; Jin, C. Photo-triggered halodecarboxylation of aliphatic carboxylic acids via cerium-mediated ligand-to-metal charge transfer in water. *Green Chemistry* **2023**, *25*, 8741-8747. DOI: 10.1039/D3GC02063K.

(42) Li, W.; Zhang, R.; Zhou, N.; Lu, J.; Fu, N. Dual transition metal electrocatalysis enables selective C(sp3)–C(sp3) bond cleavage and arylation of cyclic alcohols. *Chem. Commun.* **2024**, *60*, 11714-11717. DOI: 10.1039/D4CC04036H.

(43) Wu, Y.; Wang, X.; Wang, Z.; Chen, C. Redox-neutral decarboxylative coupling of fluoroalkyl carboxylic acids via dual metal photoelectrocatalysis. *Chem. Sci.* **2024**, *15*, 18497-18503. DOI: 10.1039/D4SC06057A.

(44) Wang, M.; Wang, D.; Xu, K.; Zeng, C. Electrophotoredox cerium-catalyzed decarboxylative radical cyclization cascade for the synthesis of alkylated benzimidazo-fused isoquinolinones. *Catalysis Science & Technology* **2024**. DOI: 10.1039/D4CY00016A.

(45) Morris, A. O.; Barriault, L. Redox-Neutral Multicatalytic Cerium Photoredox-Enabled Cleavage of O−H Bearing Substrates. *Chem. Eur. J.* **2024**, *30*, e202400642. DOI: 10.1002/chem.202400642.

(46) Duan, L.; Lin, Y.; An, Q.; Zuo, Z. Synergistic LMCT and Ni Catalysis for Methylative Cross-Coupling Using tert-Butanol: Modulating Radical Pathways via Selective Bond Homolysis. *J. Am. Chem. Soc.* **2025**, *147*, 14785-14796. DOI: 10.1021/jacs.5c03711.

(47) Liang, H.; Lai, L.; Zhang, K.; Chen, W.; Li, M.; Yang, Y.; Li, J.; Zuo, Z. Bench-Stable Cerium(IV) Benzoate: A Versatile LMCT Catalyst for Selective Dehydroxymethylative Functionalization. *ACS Catal.* **2025**, *15*, 8069-8077. DOI: 10.1021/acscatal.5c01747.

(48) Wang, S.; Zeng, W.; An, Q.; Duan, L.; Zuo, Z. LMCT-driven electron relay unlocks alcohols as tunable reductants for nickel-catalyzed cross-electrophilic couplings. *Nat. Commun.* **2025**, *16*, 6162. DOI: 10.1038/s41467-025-61414-9.

(49) Azhar, M.; Peng, T.; El-Sepelgy, O. Ligand-Free Cerium-Catalyzed Decarboxylative Fluorination of Carboxylic Acids. *ACS Organic & Inorganic Au* **2025**, *5*, 166-170. DOI: 10.1021/acsorginorgau.5c00024.

(50) (a) Murray, P. R. D.; Cox, J. H.; Chiappini, N. D.; Roos, C. B.; McLoughlin, E. A.; Hejna, B. G.; Nguyen, S. T.; Ripberger, H. H.; Ganley, J. M.; Tsui, E.; Shin, N. Y.; Koronkiewicz, B.; Qiu, G.; Knowles, R. R. Photochemical and Electrochemical Applications of Proton-Coupled Electron Transfer in Organic Synthesis. *Chem. Rev.* **2022**, *122*, 2017-2291. DOI: 10.1021/acs.chemrev.1c00374. (b) Hammes-Schiffer, S. Theoretical perspectives on proton-coupled electron transfer reactions. *Acc. Chem. Res.* **2001**, *34*, 273-281. DOI: 10.1021/ar9901117. (c) Hammes-Schiffer, S.; Stuchebrukhov, A. A. Theory of coupled electron and proton transfer reactions. *Chem. Rev.* **2010**, *110*, 6939-6960. DOI: 10.1021/cr1001436. (d) Mayer, J. M. Understanding Hydrogen Atom Transfer: From Bond Strengths to Marcus Theory. *Acc. Chem. Res.* **2011**, *44*, 36-46. DOI: 10.1021/ar100093z. (e) Gentry, E. C.; Knowles, R. R. Synthetic Applications of Proton-Coupled Electron Transfer. *Acc. Chem. Res.* **2016**, *49*, 1546-1556. DOI: 10.1021/acs.accounts.6b00272. (f) Darcy, J. W.; Koronkiewicz, B.; Parada, G. A.; Mayer, J. M. A Continuum of Proton-Coupled Electron Transfer Reactivity. *Acc. Chem. Res.* **2018**, *51*, 2391-2399. DOI: 10.1021/acs.accounts.8b00319. (g) Agarwal, R. G.; Coste, S. C.; Groff, B. D.; Heuer, A. M.; Noh, H.; Parada, G. A.; Wise, C. F.; Nichols, E. M.; Warren, J. J.; Mayer, J. M. Free Energies of Proton-Coupled Electron Transfer Reagents and Their Applications. In *Chem. Rev.*, American Chemical Society: 2022; Vol. 122, pp 1-49.

(51) Ota, E.; Wang, H.; Frye, N. L.; Knowles, R. R. A Redox Strategy for Light-Driven, Out-of-Equilibrium Isomerizations and Application to Catalytic C-C Bond Cleavage Reactions. *J. Am. Chem. Soc.* **2019**, *141*, 1457-1462. DOI: 10.1021/jacs.8b12552.

(52) Kolbe, H. Zersetzung der Valeriansäure durch den elektrischen Strom. *Justus Liebigs Annalen der Chemie* **1848**, *64*, 339-341. DOI: 10.1002/jlac.18480640346.

(53) (a) Hofmann, A. W. Zur Kenntniss des Piperidins und Pyridins. *Berichte der deutschen chemischen Gesellschaft* **1879**, *12*, 984-990. DOI: 10.1002/cber.187901201254. (b) Hofmann, A. W. Zur Kenntniss der Coniin-Gruppe. *Berichte der deutschen chemischen Gesellschaft* **1885**, *18*, 5-23. DOI: 10.1002/cber.18850180103. (c) Löffler, K.; Freytag, C. Über eine neue Bildungsweise von N-alkylierten Pyrrolidinen. *Berichte der deutschen chemischen Gesellschaft* **1909**, *42*, 3427-3431. DOI: 10.1002/cber.19090420377. (d) Wolff, M. E. Cyclization of N-Halogenated Amines (The Hofmann-Löffler Reaction). *Chem. Rev.* **1963**, *63*, 55-64. DOI: 10.1021/cr60221a004.

(54) Fittig, R. Ueber einige Producte der trockenen Destillation essigsaurer Salze. *Justus Liebigs Annalen der Chemie* **1859**, *110*, 17-23. DOI: 10.1002/jlac.18591100103.

(55) Gomberg, M. An Instance Of Trivalent Carbon: Triphenylmethyl. *J. Am. Chem. Soc.* **1900**, *22*, 757-771. DOI: 10.1021/ja02049a006.

(56) (a) Wohl, A. Bromierung ungesättigter Verbindungen mit N-Brom-acetamid, ein Beitrag zur Lehre vom Verlauf chemischer Vorgänge. *Berichte der deutschen chemischen Gesellschaft (A and B Series)* **1919**, *52*, 51-63. DOI: 10.1002/cber.19190520109. (b) Ziegler, K.; Späth, A.; Schaaf, E.; Schumann, W.; Winkelmann, E. Die Halogenierung ungesättigter Substanzen in der Allylstellung. *Justus Liebigs Annalen der Chemie* **1942**, *551*, 80-119. DOI: 10.1002/jlac.19425510103. (c) Djerassi, C. Brominations with N-Bromosuccinimide and Related Compounds. The Wohl-Ziegler Reaction. *Chem. Rev.* **1948**, *43*, 271-317. DOI: 10.1021/cr60135a004.

(57) Bachmann, W. E.; Wiselogle, F. Y. The Relative Stability Of Pentaarylethanes. III.1 The Reversible Dissociation Of Pentaarylethanes*. *J. Org. Chem.* **1936**, *01*, 354-382. DOI: 10.1021/jo01233a006.

(58) van der Kerk, G. J. M.; Noltes, J. G.; Luijten, J. G. A. Investigations on organo-tin compounds. VII the addition of organo-tin hydrides to olefinic double bonds. *Journal of Applied Chemistry* **1957**, *7*, 356-365. DOI: 10.1002/jctb.5010070703.

(59) (a) Walling, C. *Free Radicals in Solution*; 1957. (b) Walling, C.; Jacknow, B. B. Positive Halogen Compounds. I. The Radical Chain Halogenation of Hydrocarbons by t-Butyl Hypochlorite1. *J. Am. Chem. Soc.* **1960**, *82*, 6108-6112. DOI: 10.1021/ja01508a033. (c) Walling, C.; Padwa, A. Positive Halogen Compounds. V. t-Butyl Hypobromite and Two New Techniques for Hydrocarbon Bromination1. *J. Org. Chem.* **1962**, *27*, 2976-2977. DOI: 10.1021/jo01056a002. (d) Walling, C.; Padwa, A. Positive Halogen Compounds. VI. Effects of Structure and Medium on the β-Scission of Alkoxy Radicals. *J. Am. Chem. Soc.* **1963**, *85*, 1593-1597. DOI: 10.1021/ja00894a012. (e) Walling, C.; Padwa, A. Positive Halogen Compounds. VII. Intramolecular Chlorinations with Long Chain Hypochlorites. *J. Am. Chem. Soc.* **1963**, *85*, 1597-1601. DOI: 10.1021/ja00894a013. (f) Walling, C.; Wagner, P. J. Positive Halogen Compounds. X. Solvent Effects in the Reactions of t-Butoxy Radicals. *J. Am. Chem. Soc.* **1964**, *86*, 3368-3375. DOI: 10.1021/ja01070a032. (g) Wagner, P.; Walling, C. Positive Halogen Compounds. XII.1 Relative Reactivities of Hydrocarbons toward Alkoxy Radicals Determined by Direct and Indirect Methods2. *J. Am. Chem. Soc.* **1965**, *87*, 5179-5185. DOI: 10.1021/ja00950a035. (h) Walling, C.; Heaton, L. Radical Formation in the Reactions of t-Butyl Hydroperoxide with Styrene1. *J. Am. Chem. Soc.* **1965**, *87*, 38-47. DOI: 10.1021/ja01079a009. (i) Walling, C.; Heaton, L.; Tanner, D. D. Positive Halogen Compounds. XI. “Spontaneous” Chain Initiation and the Reaction of t-Butyl Hypohalites with Acetylenes1. *J. Am. Chem. Soc.* **1965**, *87*, 1715-1721. DOI: 10.1021/ja01086a017. (j) Walling, C. Some aspects of the chemistry of alkoxy radicals. **1967**, *15*, 69-80. DOI: 10.1351/pac196715010069. (k) Walling, C. Fenton's reagent revisited. *Acc. Chem. Res.* **1975**, *8*, 125-131. DOI: 10.1021/ar50088a003. (l) Walling, C. Some properties of radical reactions important in synthesis. *Tetrahedron* **1985**, *41*, 3887-3900. DOI: 10.1016/S0040-4020(01)97172-8. (m) Walling, C.; Seeman, J. I. *Fifty Years of Free Radicals: Profiles, Pathways, and Dreams*; 1995. (n) Walling, C.; Huyser, E. S. Free Radical Additions to Olefins to Form Carbon-Carbon Bonds. In *Organic Reactions*, 2011; pp 91-149.

(60) (a) Davies, A. G.; Roberts, B. P. Peroxides of elements other than carbon. Part XII. The autoxidation of optically active 1-phenylethylboronic acid. *Journal of the Chemical Society B: Physical Organic* **1967**, 17-22. DOI:

10.1039/J29670000017. (b) Davies, A. G.; Roberts, B. P. Bimolecular homolytic substitution at a metal center. *Acc. Chem. Res.* **1972**, *5*, 387-392. DOI: 10.1021/ar50059a005.

(61) Ollivier, C.; Renaud, P. Organoboranes as a Source of Radicals. *Chem. Rev.* **2001**, *101*, 3415-3434. DOI: 10.1021/cr010001p.

(62) Barton, D. H. R.; Beaton, J. M.; Geller, L. E.; Pechet, M. M. A NEW PHOTOCHEMICAL REACTION. *J. Am. Chem. Soc.* **1960**, *82*, 2640-2641. DOI: 10.1021/ja01495a061.

(63) Minisci, F.; Bernardi, R.; Bertini, F.; Galli, R.; Perchinummo, M. Nucleophilic character of alkyl radicals—VI: A new convenient selective alkylation of heteroaromatic bases. *Tetrahedron* **1971**, *27*, 3575-3579. DOI: 10.1016/S0040-4020(01)97768-3.

(64) Barton, D. H. R.; McCombie, S. W. A new method for the deoxygenation of secondary alcohols. *J. Chem. Soc., Perkin Trans. 1* **1975**, 1574-1585. DOI: 10.1039/P19750001574.

(65) Namy, J. L.; Girard, P.; Kagan, H. B. A New Preparation Of Some Divalent Lanthanide Iodides And Their Usefulness In Organic Synthesis. **1977**.

(66) Hedstrand, D. M.; Kruizinga, W. H.; Kellogg, R. M. Light induced and dye accelerated reductions of phenacyl onium salts by 1,4-dihydropyridines. *Tetrahedron Lett.* **1978**, *19*, 1255-1258. DOI: 10.1016/S0040-4039(01)94515-0.

(67) (a) Giese, B.; Zwick, W. Reactivity of Alkenes in Free-Radical Additions. *Angew. Chem., Int. Ed.* **1978**, *17*, 66-67. DOI: 10.1002/anie.197800661. (b) Giese, B. Formation of CC Bonds by Addition of Free Radicals to Alkenes. *Angew. Chem., Int. Ed.* **1983**, *22*, 753-764. DOI: 10.1002/anie.198307531.

(68) Ueno, Y.; Chino, K.; Watanabe, M.; Moriya, O.; Okawara, M. Homolytic carbocyclization by use of a heterogeneous supported organotin catalyst. A new synthetic route to 2-alkoxytetrahydrofurans and .gamma.-butyrolactones. *J. Am. Chem. Soc.* **1982**, *104*, 5564-5566. DOI: 10.1021/ja00384a082.

(69) Keck, G. E.; Yates, J. B. A novel synthesis of (.+-.)-perhydrohistrionicotoxin. *J. Org. Chem.* **1982**, *47*, 3590-3591. DOI: 10.1021/jo00139a053.

(70) (a) Beckwith, A. L. J.; Schiesser, C. H. Regio- and stereo-selectivity of alkenyl radical ring closure: A theoretical study. *Tetrahedron* **1985**, *41*, 3925-3941. DOI: 10.1016/S0040-4020(01)97174-1. (b) Spellmeyer, D. C.; Houk, K. N. Force-field model for intramolecular radical additions. *J. Org. Chem.* **1987**, *52*, 959-974. DOI: 10.1021/jo00382a001.

(71) (a) Delduc, P.; Tailhan, C.; Zard, S. Z. A convenient source of alkyl and acyl radicals. *J. Chem. Soc., Chem. Commun.* **1988**, 308-310. DOI: 10.1039/C39880000308. (b) Quiclet-Sire, B.; Zard, S. Z. Fun with radicals: Some new perspectives for organic synthesis. **2010**, *83*, 519-551. DOI: 10.1351/PAC-CON-10-08-07.

(72) (a) Porter, N. A.; Lacher, B.; Chang, V. H. T.; Magnin, D. R. Regioselectivity and diastereoselectivity in free-radical macrocyclization. *J. Am. Chem. Soc.* **1989**, *111*, 8309-8310. DOI: 10.1021/ja00203a059. (b) Porter, N. A.; Scott, D. M.; Lacher, B.; Giese, B.; Zeitz, H. G.; Lindner, H. J. Radical addition to amide-substituted alkenes: stereoselective intermolecular radical additions. *J. Am. Chem. Soc.* **1989**, *111*, 8311-8312. DOI: 10.1021/ja00203a060.

(73) Mukaiyama, T.; Isayama, S.; Inoki, S.; Kato, K.; Yamada, T.; Takai, T. Oxidation-Reduction Hydration of Olefins with Molecular Oxygen and 2-Propanol Catalyzed by Bis(acetylacetonato)cobalt(II). *Chem. Lett.* **1989**, *18*, 449-452. DOI: 10.1246/cl.1989.449.

(74) Wu, J. H.; Radinov, R.; Porter, N. A. Enantioselective Free Radical Carbon-Carbon Bond Forming Reactions: Chiral Lewis Acid Promoted Acyclic Additions. *J. Am. Chem. Soc.* **1995**, *117*, 11029-11030. DOI: 10.1021/ja00149a035.

(75) Arp, F. O.; Fu, G. C. Catalytic Enantioselective Negishi Reactions of Racemic Secondary Benzylic Halides. *J. Am. Chem. Soc.* **2005**, *127*, 10482-10483. DOI: 10.1021/ja053751f.

(76) (a) Ischay, M. A.; Anzovino, M. E.; Du, J.; Yoon, T. P. Efficient Visible Light Photocatalysis of [2+2] Enone Cycloadditions. *J. Am. Chem. Soc.* **2008**, *130*, 12886-12887. DOI: 10.1021/ja805387f. (b) Nicewicz, D. A.; MacMillan, D. W. C. Merging Photoredox Catalysis with Organocatalysis: The Direct Asymmetric Alkylation of Aldehydes. *Science* **2008**, *322*, 77-80. DOI: 10.1126/science.1161976.

(77) Stephenson, N. A.; Zhu, J.; Gellman, S. H.; Stahl, S. S. Catalytic Transamidation Reactions Compatible with Tertiary Amide Metathesis under Ambient Conditions. *J. Am. Chem. Soc.* **2009**, *131*, 10003-10008. DOI: 10.1021/ja8094262.

(78) Kalyani, D.; McMurtrey, K. B.; Neufeldt, S. R.; Sanford, M. S. Room-Temperature C–H Arylation: Merger of Pd-Catalyzed C–H Functionalization and Visible-Light Photocatalysis. *J. Am. Chem. Soc.* **2011**, *133*, 18566-18569. DOI: 10.1021/ja208068w.

(79) Zuo, Z.; Ahneman, D. T.; Chu, L.; Terrett, J. A.; Doyle, A. G.; MacMillan, D. W. C. Merging photoredox with nickel catalysis: Coupling of α-carboxyl sp3-carbons with aryl halides. *Science* **2014**, *345*, 437-440. DOI: 10.1126/science.1255525.

(80) (a) Lipp, A.; Badir, S. O.; Molander, G. A. Stereoinduction in Metallaphotoredox Catalysis. In *Angew. Chem., Int. Ed.*, Wiley-VCH Verlag: 2021; Vol. 60, pp 1714-1726. (b) Chan, A. Y.; Perry, I. B.; Bissonnette, N. B.; Buksh, B. F.; Edwards, G. A.; Frye, L. I.; Garry, O. L.; Lavagnino, M. N.; Li, B. X.; Liang, Y.; Mao, E.; Millet, A.; Oakley, J. V.; Reed, N. L.; Sakai, H. A.; Seath, C. P.; MacMillan, D. W. C. Metallaphotoredox: The Merger of Photoredox and Transition Metal Catalysis. *Chem. Rev.* **2022**, *122*, 1485-1542. DOI: 10.1021/acs.chemrev.1c00383. (c) Zhang, J.; Rueping, M. Metallaphotoredox catalysis for sp3 C–H functionalizations through hydrogen atom transfer (HAT). *Chem. Soc. Rev.* **2023**, *52*, 4099-4120. DOI: 10.1039/D3CS00023K.

(81) (a) Okada, Y.; Chiba, K. Redox-Tag Processes: Intramolecular Electron Transfer and Its Broad Relationship to Redox Reactions in General. In *Chem. Rev.*, American Chemical Society: 2018; Vol. 118, pp 4592-4630. (b) Crespi, S.; Fagnoni, M. Generation of Alkyl Radicals: From the Tyranny of Tin to the Photon Democracy. *Chem. Rev.* **2020**, *120*, 9790-9833. DOI: 10.1021/acs.chemrev.0c00278. (c) Leifert, D.; Studer, A. The Persistent Radical Effect in Organic Synthesis. *Angew. Chem. Int. Ed.* **2020**, *59*, 74-108. DOI: 10.1002/anie.201903726. (d) Julia, M. Free-radical cyclizations. *Acc. Chem. Res.* **1971**, *4*, 386-392. DOI: 10.1021/ar50047a005 (e) Radical Reactions in Organic Synthesis. In *Stereochemistry of Radical Reactions*, 1995; pp 1-22. (f) Curran, D. P.; Porter, N. A.; Giese, B. *Stereochemistry of Radical Reactions: Concepts,*

Guidelines, and Synthetic Applications; 1996. (g) Renaud, P.; Sibi, M. *Radicals in Organic Synthesis*; 2001. (h) Zard, S. Z. *Radical Reactions in Organic Synthesis*; 2003. (i) Giese, B.; Kopping, B.; Göbel, T.; Dickhaut, J.; Thoma, G.; Kulicke, K. J.; Trach, F. Radical Cyclization Reactions. In *Organic Reactions*, Wiley, 2004; pp 301-856.

(82) Newcomb, M. Radical Kinetics and Clocks. In *Encyclopedia of Radicals in Chemistry, Biology and Materials*, 2012.

(83) Gilbert, B. C.; Parry, D. J. Fragmentation, ring-opening, and addition reactions of oxygen-conjugated alkenyl radicals derived by rapid 1,5-hydrogen shifts in vinyl radicals. An electron spin resonance and kinetic investigation. *J. Chem. Soc., Perkin Trans. 2* **1988**, 875-886. DOI: 10.1039/P29880000875.

(84) Hilborn, J. W.; Pincock, J. A. Rates of decarboxylation of acyloxy radicals formed in the photocleavage of substituted 1-naphthylmethyl alkanoates. *J. Am. Chem. Soc.* **1991**, *113*, 2683-2686. DOI: 10.1021/ja00007a049.

(85) Tsentalovich, Y. P.; Fischer, H. Solvent effect on the decarbonylation of acyl radicals studied by laser flash photolysis. *J. Chem. Soc., Perkin Trans. 2* **1994**, 729-733. DOI: 10.1039/P29940000729.

(86) (a) Amphlett, J. C.; Coomber, J. W.; Whittle, E. The C-H Bond Dissociation Energy in Fluoroform. *J. Phys. Chem.* **1966**, *70*, 593-594. DOI: 10.1021/j100874a507. (b) Luo, Y.-R. *Comprehensive handbook of chemical bond energies*; CRC press, 2007. DOI: 10.1201/9781420007282. (c) Banerjee, A.; Lei, Z.; Ngai, M.-Y. Acyl Radical Chemistry via Visible-Light Photoredox Catalysis. *Synthesis* **2019**, *51*, 303-333. DOI: 10.1055/s-0037-1610329. (d) Dénès, F.; Pichowicz, M.; Povie, G.; Renaud, P. Thiyl Radicals in Organic Synthesis. *Chem. Rev.* **2014**, *114*, 2587-2693. DOI: 10.1021/cr400441m. (e) Mulder, P.; Korth, H.-G.; Pratt, D. A.; DiLabio, G. A.; Valgimigli, L.; Pedulli, G. F.; Ingold, K. U. Critical Re-evaluation of the O−H Bond Dissociation Enthalpy in Phenol. *J. Phys. Chem. A* **2005**, *109*, 2647-2655. DOI: 10.1021/jp047148f. (f) Mukherjee, S.; Maji, B.; Tlahuext-Aca, A.; Glorius, F. Visible-Light-Promoted Activation of Unactivated C(sp^3)–H Bonds and Their Selective Trifluoromethylthiolation. *J. Am. Chem. Soc.* **2016**, *138*, 16200-16203. DOI: 10.1021/jacs.6b09970. (g) O'Brien, T. E.; Morris, A. O.; Villela, L. F.; Barriault, L. Synthetic Applications of Photochemically Generated Radicals from Protic C(sp3)−H Bonds. *ChemCatChem* **2023**, *15*, e202300989. DOI: 10.1002/cctc.202300989. (h) Chang, L.; An, Q.; Duan, L.; Feng, K.; Zuo, Z. Alkoxy Radicals See the Light: New Paradigms of Photochemical Synthesis. *Chem. Rev.* **2022**, *122*, 2429-2486. DOI: 10.1021/acs.chemrev.1c00256.

(87) (a) Murakami, M.; Ishida, N. β-scission of alkoxy radicals in synthetic transformations. *Chem. Lett.* **2017**, *46*, 1692-1700. DOI: 10.1246/cl.170834. (b) Aureliano Antunes, C. S.; Bietti, M.; Lanzalunga, O.; Salamone, M. Photolysis of 1-Alkylcycloalkanols in the Presence of (Diacetoxyiodo)benzene and I2. Intramolecular Selectivity in the β-Scission Reactions of the Intermediate 1-Alkylcycloalkoxyl Radicals. *J. Org. Chem.* **2004**, *69*, 5281-5289. DOI: 10.1021/jo049524y. (c) Bietti, M.; Lanzalunga, O.; Salamone, M. Structural effects on the β-scission reaction of alkoxyl radicals. Direct measurement of the absolute rate constants for ring opening of benzocycloalken-1-oxyl radicals. *J. Org. Chem.* **2005**, *70*, 1417-1422. DOI: 10.1021/jo048026m. (d) Salamone, M.; Bietti, M. Reaction pathways of alkoxyl radicals. the role of solvent effects on C-C bond

fragmentation and hydrogen atom transfer reactions. *Synlett* **2014**, *25*, 1803-1816. DOI: 10.1055/s-0033-1341280. (e) Hurd, C. D.; Saunders, W. H., Jr. Ring-Chain Tautomerism of Hydroxy Aldehydes *J. Am. Chem. Soc.* **1952**, *74*, 5324-5329.

(88) Zavitsas, A. A.; Seltzer, S. The Transition State in Methyl Radical Formation. The Secondary α-Deuterium Isotope Effect. *J. Am. Chem. Soc.* **1964**, *86*, 3836-3840. DOI: 10.1021/ja01072a047.

(89) (a) Zhang, W.; Dowd, P. Free radical rearrangement of bicyclo[2.2.2]- and bicyclo[4.2.0]octenones systems. *Tetrahedron* **1993**, *49*, 1965-1978. DOI: 10.1016/S0040-4020(01)86296-7. (b) Wilsey, S.; Dowd, P.; Houk, K. N. Effect of Alkyl Substituents and Ring Size on Alkoxy Radical Cleavage Reactions. *J. Org. Chem.* **1999**, *64*, 8801-8811. DOI: 10.1021/jo990652.

(90) Avila, D. V.; Brown, C. E.; Ingold, K. U.; Lusztyk, J. Solvent effects on the competitive .beta.-scission and hydrogen atom abstraction reactions of the cumyloxyl radical. Resolution of a long-standing problem. *J. Am. Chem. Soc.* **1993**, *115*, 466-470. DOI: 10.1021/ja00055a015.

(91) Robinson, C. H.; Gnoj, O.; Mitchell, A.; Wayne, R.; Townley, E.; Kabasakalian, P.; Oliveto, E. P.; Barton, D. H. R. The Photolysis Of Organic Nitrites. Ii. Synthesis Of Steroidal Hydroxamic Acids. *J. Am. Chem. Soc.* **1961**, *83*, 1771-1772. DOI: 10.1021/ja01468a060.

(92) (a) Borodine, A. Ueber Bromvaleriansäure und Brombuttersäure. *Justus Liebigs Annalen der Chemie* **1861**, *119*, 121-123. DOI: 10.1002/jlac.18611190113. (b) Hunsdiecker, H.; Hunsdiecker, C. Über den Abbau der Salze aliphatischer Säuren durch Brom. *Berichte der deutschen chemischen Gesellschaft (A and B Series)* **1942**, *75*, 291-297. DOI: 10.1002/cber.19420750309.

(93) Barton, D. H. R.; Crich, D.; Motherwell, W. B. New and improved methods for the radical decarboxylation of acids. *J. Chem. Soc., Chem. Commun.* **1983**, 939-941. DOI: 10.1039/C39830000939.

(94) (a) Meystre, C.; Heusler, K.; Kalvoda, J.; Wieland, P.; Anner, G.; Wettstein, A. Neue Substitutionsreaktionen bei Steroiden. *Experientia* **1961**, *17*, 475-480. DOI: 10.1007/BF02158305. (b) Meystre, C. H.; Heusler, K.; Kalvoda, J.; Wieland, P.; Anner, G.; Wettstein, A. Reaktionen von Steroid-Hypojoditen II. Über die Herstellung 18-oxygenierter Pregnanverbindungen. Über Steroide, 187. Mitteilung. *Helv. Chim. Acta* **1962**, *45*, 1317-1343. DOI: 10.1002/hlca.19620450431.

(95) Cristol, S.; Firth, J. W. Communications. A Convenient Synthesis of Alkyl Halides from Carboxylic Acids. *J. Org. Chem.* **1961**, *26*, 280-280. DOI: 10.1021/jo01060a628.

(96) Kochi, J. K. A New Method for Halodecarboxylation of Acids Using Lead(IV) Acetate. *J. Am. Chem. Soc.* **1965**, *87*, 2500-2502. DOI: 10.1021/ja01089a041.

(97) Akhtar, M.; Barton, D. H. R. Reactions at position 19 in the steroid nucleus. A convenient synthesis of 19-norsteroids. *J. Am. Chem. Soc.* **1964**, *86*, 1528-1536.

(98) Beebe, T. R.; Barnes, B. A.; Bender, K. A.; Halbert, A. D.; Miller, R. D.; Ramsay, M. L.; Ridenour, M. W. Oxidation of alcohols with acetyl hypoiodite. *J. Org. Chem.* **1975**, *40*, 1992-1994. DOI: 10.1021/jo00901a028.

(99) (a) Concepción, J. I.; Francisco, C. G.; Hernández, R.; Salazar, J. A.; Suárez, E. Intramolecular hydrogen abstraction. Iodosobenzene diacetate, an efficient and convenient reagent for alkoxy radical generation.

Tetrahedron Lett. **1984**, *25*, 1953-1956. DOI: 10.1016/S0040-4039(01)90085-1. (b) Freire, R.; Marrero, J. J.; Rodríguez, M. S.; Suárez, E. Synthesis of medium-sized lactones: Iodosobenzene diacetate an efficient reagent for β-fragmentation of alkoxy-radicals. *Tetrahedron Lett.* **1986**, *27*, 383-386. DOI: 10.1016/S0040-4039(00)84025-3. (c) Concepcion, J. I.; Francisco, C. G.; Freire, R.; Hernandez, R.; Salazar, J. A.; Suarez, E. Iodosobenzene diacetate, an efficient reagent for the oxidative decarboxylation of carboxylic acids. *J. Org. Chem.* **1986**, *51*, 402-404. DOI: 10.1021/jo00353a026.

(100) Courtneidge, J. L.; Lusztyk, J.; Pagé, D. Alkoxyl Radicals from Alcohols.1 Spectroscopic Detection of Intermediate Alkyl and Acyl Hypoiodites In The Suárez and Beebe Reactions *Tetrahedron Lett.* **1994**, *35*, 1003-1006.

(101) Crossley, S. W. M.; Tong, G.; Lambrecht, M. J.; Burdge, H. E.; Shenvi, R. A. Synthesis of (−)-Picrotoxinin by Late-Stage Strong Bond Activation. *J. Am. Chem. Soc.* **2020**, *142*, 11376-11381. DOI: 10.1021/jacs.0c05042.

(102) Poulin, J.; Ottawa-Carleton Chemistry, I. Formal synthesis of vinigrol and efforts towards the total synthesis of digitoxigenin. University of Ottawa, 2013.

(103) Yayla, H. G.; Wang, H.; Tarantino, K. T.; Orbe, H. S.; Knowles, R. R. Catalytic Ring-Opening of Cyclic Alcohols Enabled by PCET Activation of Strong O-H Bonds. *J. Am. Chem. Soc.* **2016**, *138*, 10794-10797. DOI: 10.1021/jacs.6b06517.

(104) Zhao, K.; Yamashita, K.; Carpenter, J. E.; Sherwood, T. C.; Ewing, W. R.; Cheng, P. T. W.; Knowles, R. R. Catalytic Ring Expansions of Cyclic Alcohols Enabled by Proton-Coupled Electron Transfer. *J. Am. Chem. Soc.* **2019**, *141*, 8752-8757. DOI: 10.1021/jacs.9b03973.

(105) Liu, W.; Wu, Q.; Wang, M.; Huang, Y.; Hu, P. Iron-Catalyzed C-C Single-Bond Cleavage of Alcohols. *Org. Lett.* **2021**, *23*, 8413-8418. DOI: 10.1021/acs.orglett.1c03137.

(106) Wen, L.; Ding, J.; Duan, L.; Wang, S.; An, Q.; Wang, H.; Zuo, Z. Multiplicative enhancement of stereoenrichment by a single catalyst for deracemization of alcohols. *Science* **2023**, *382*, 458-464. DOI: 10.1126/science.adj0040.

(107) Chen, Z.-M.; Zhang, X.-M.; Tu, Y.-Q. Radical aryl migration reactions and synthetic applications. *Chem. Soc. Rev.* **2015**, *44*, 5220-5245. DOI: 10.1039/C4CS00467A.

(108) (a) Urry, W. H.; Kharasch, M. S. Factors Influencing the Course and Mechanism of Grignard Reactions. XV. The Reaction of β,β-Dimethylphenethyl Chloride with Phenylmagnesium Bromide in the Presence of Cobaltous Chloride. *J. Am. Chem. Soc.* **1944**, *66*, 1438-1440. DOI: 10.1021/ja01237a004. (b) Seubold, F. H., Jr. The Rearrangement Of The Neophyl Radical. *J. Am. Chem. Soc.* **1953**, *75*, 2532-2533. DOI: 10.1021/ja01106a535.

(109) (a) Hamilton Jr, E. J.; Fischer, H. Observation of the Neophyl Radical Rearrangement by Electron Spin Resonance Spectroscopy. *Helv. Chim. Acta* **1973**, *56*, 795-799. DOI: 10.1002/hlca.19730560222. (b) Brunton, G.; McBay, H. C.; Ingold, K. U. Kinetic applications of electron paramagnetic resonance spectroscopy. 30. Rearrangement of the benzoylmethyl radical. *J. Am. Chem. Soc.* **1977**, *99*, 4447-4450. DOI: 10.1021/ja00455a038. (c) Effio, A.; Griller, D.; Ingold, K. U.; Scaiano, J. C.; Sheng, S. J. Studies on the spiro[2.5]octadienyl radical and the 2-phenylethyl rearrangement. *J. Am. Chem. Soc.* **1980**, *102*, 6063-6068.

DOI: 10.1021/ja00539a015. (d) Leardini, R.; Nanni, D.; Pedulli, G. F.; Tundo, A.; Zanardi, G.; Foresti, E.; Palmieri, P. On the neophyl-like rearrangement of 2-(9-anthryl)ethyl radicals. *J. Am. Chem. Soc.* **1989**, *111*, 7723-7732. DOI: 10.1021/ja00202a010. (e) Asensio, A.; Dannenberg, J. J. Phenyl-Bridging in the 2-Phenylethyl Radical. A Molecular Orbital Study. *J. Org. Chem.* **2001**, *66*, 5996-5999. DOI: 10.1021/jo0017483.

(110) (a) Griller, D.; Ingold, K. U. Free-radical clocks. *Acc. Chem. Res.* **1980**, *13*, 317-323. DOI: 10.1021/ar50153a004. (b) Newcomb, M. *Competition Methods and Scales for Alkyl Radical Reaction Kinetics*; 1993. (c) Maillard, B.; Ingold, K. U. Kinetic applications of electron paramagnetic resonance spectroscopy. XXIV. Neophyl rearrangements. *J. Am. Chem. Soc.* **1976**, *98*, 1224-1226. DOI: 10.1021/ja00421a028. (d) Lindsay, D. A.; Lusztyk, J.; Ingold, K. U. Kinetics of the 1,2-migration of carbon-centered groups in 2-substituted 2,2-dimethylethyl radicals. *J. Am. Chem. Soc.* **1984**, *106*, 7087-7093. DOI: 10.1021/ja00335a037.

(111) Leardini, R.; Lucarini, M.; Pedulli, G. F.; Valgimigli, L. Synthesis and Calibration of Two Radical Timing Devices: 2-Methyl-2-(1-naphthyl)- and 2-Methyl-2-(2-naphthyl)- 1-bromopropane. *J. Org. Chem.* **1999**, *64*, 3726-3730. DOI: 10.1021/jo9813179.

(112) Wu, S.-H.; Ding, Z.-B.; Li, X.-J. A facile method for preparation of tetrahydrofuran complexes of lanthanide trichlorides. *Polyhedron* **1994**, *13*, 2679-2681. DOI: 10.1016/S0277-5387(00)81320-0.

(113) McKillop, A.; Tarbin, J. A. Functional group oxidation using sodium perborate1. *Tetrahedron* **1987**, *43*, 1753-1758. DOI: 10.1016/S0040-4020(01)81484-8.

(114) (a) Grieco, P. A.; Yokoyama, Y.; Gilman, S.; Ohfune, Y. Conversion of ketones into lactones with benzeneseleninic acid and hydrogen peroxide (benzeneperoxyseleninic acid): a new reagent for the Baeyer-Villiger reaction. *J. Chem. Soc., Chem. Commun.* **1977**, 870-871. DOI: 10.1039/C39770000870. (b) Olmstead, K. K.; Nickon, A. 1,2-Hydrogen shifts in thermal and photic Bamford-Stevens reactions of cyclohexanones. Activation by an endocyclic oxygen. *Tetrahedron* **1998**, *54*, 12161-12172. DOI: 10.1016/S0040-4020(98)00757-1.

(115) Sands, K. N.; Mendoza Rengifo, E.; George, G. N.; Pickering, I. J.; Gelfand, B. S.; Back, T. G. The Unexpected Role of SeVI Species in Epoxidations with Benzeneseleninic Acid and Hydrogen Peroxide. *Angew. Chem. Int. Ed.* **2020**, *59*, 4283-4287. DOI: 10.1002/anie.201913566.

(116) (a) Li, C.; Qiu, W.; Yang, Z.; Luo, J.; Yang, F.; Liu, M.; Xie, J.; Tang, J. Stereoselective synthesis of some methyl-substituted steroid hormones and their in vitro cytotoxic activity against human gastric cancer cell line MGC-803. *Steroids* **2010**, *75*, 859-869. DOI: 10.1016/j.steroids.2010.05.008. (b) Dal Prà, M.; Carta, D.; Szabadkai, G.; Suman, M.; Frión-Herrera, Y.; Paccagnella, N.; Castellani, G.; De Martin, S.; Ferlin, M. G. Targeting RORs nuclear receptors by novel synthetic steroidal inverse agonists for autoimmune disorders. *Biorg. Med. Chem.* **2018**, *26*, 1686-1704. DOI: 10.1016/j.bmc.2018.02.018.

(117) Jacobsen, R. P. Steroid Lactones: I. The Oxidation Of Estrone Acetate To The Lactone Acetate Of Estrolic Acid. *J. Biol. Chem.* **1947**, *171*, 61-70. DOI: 10.1016/S0021-9258(17)41106-9.

(118) *Indian J. Chem., Sect B* **2004**, *43*, 1275–1281.

(119) Szumny, A.; Wawrzenczyk, C. Lactones, Part 28: A New Approach for the Synthesis of α-Methylene Lactones from Alkenes. *Synlett* **2006**, *2006*, 1523-1526. DOI: 10.1055/s-2006-941598.

(120) Solabannavar, S. B.; Helavi, V. B.; Desai, U. V.; Mane, R. B. A novel short synthesis of norbisabolide. *Tetrahedron Lett.* **2002**, *43*, 4535-4536. DOI: 10.1016/S0040-4039(02)00814-6.

(121) Sathyamoorthi, S.; Du Bois, J. Copper-Catalyzed Oxidative Cyclization of Carboxylic Acids. *Org. Lett.*, **2016**, *18*, 6308-6311. DOI: 10.1021/acs.orglett.6b03176.

(122) (a) Imamoto, T.; Kusumoto, T.; Yokoyama, M. Generation and reactivities of organocerium reagents. *J. Chem. Soc., Chem. Commun.* **1982**, 1042-1044. DOI: 10.1039/C39820001042. (b) Imamoto, T.; Kusumoto, T.; Tawarayama, Y.; Sugiura, Y.; Mita, T.; Hatanaka, Y.; Yokoyama, M. Carbon-carbon bond-forming reactions using cerium metal or organocerium(III) reagents. *J. Org. Chem.* **1984**, *49*, 3904-3912. DOI: 10.1021/jo00195a006. (c) Imamoto, T.; Sugiura, Y.; Takiyama, N. Organocerium reagents. Nucleophilic addition to easily enolizable ketones. *Tetrahedron Lett.* **1984**, *25*, 4233-4236. DOI: 10.1016/S0040-4039(01)81404-0. (d) Imamoto, T.; Takiyama, N.; Nakamura, K.; Hatajima, T.; Kamiya, Y. Reactions of carbonyl compounds with Grignard reagents in the presence of cerium chloride. *J. Am. Chem. Soc.* **1989**, *111*, 4392-4398. DOI: 10.1021/ja00194a037. (e) Bartoli, G.; Marcantoni, E.; Marcolini, M.; Sambri, L. Applications of CeCl3 as an Environmental Friendly Promoter in Organic Chemistry. *Chem. Rev.* **2010**, *110*, 6104-6143. DOI: 10.1021/cr100084g.

(123) Arcadi, A.; Bernocchi, E.; Cacchi, S.; Marinelli, F. β-Vinyl-γ-butyrolactones via the palladium-catalysed reaction of vinyl triflates with Z-2-buten-1,4-diol. *Tetrahedron* **1991**, *47*, 1525-1540. DOI: 10.1016/S0040-4020(01)86427-9.

(124) Yin, H.; Carroll, P. J.; Anna, J. M.; Schelter, E. J. Luminescent Ce(III) Complexes as Stoichiometric and Catalytic Photoreductants for Halogen Atom Abstraction Reactions. *J. Am. Chem. Soc.* **2015**, *137*, 9234-9237. DOI: 10.1021/jacs.5b05411.

(125) (a) Schaefer, J. P.; Lark, J. C.; Flegal, C. A.; Honig, L. M. Bicyclo[3.3.1]nonanes. II. Synthesis and reactions of simple derivatives. *J. Org. Chem.* **1967**, *32*, 1372-1378. DOI: 10.1021/jo01280a020. (b) Peters, J. A.; van der Toorn, J. M.; van Bekkum, H. 3,7-disubstituted bicyclo [3.3.1] nonanes—II: Synthesis and conformation of some 3,7-disubstituted 9-oxobicyclo [3.3.1] nonanes. *Tetrahedron* **1974**, *30*, 633-640. DOI: 10.1016/S0040-4020(01)97057-7. (c) Peters, J. A.; Peters-Van Cranenburgh, P. E. J.; Bovée, W. M. M. J.; Rozema, H. P.; van der Toorn, J. M.; Wortel, T. M.; van Bekkum, H. Synthesis and conformation of some 2,4-dioxa- and 2,4-dioxa-3-silabicyclo[3.3.1]nonanes. *Tetrahedron* **1982**, *38*, 3641-3647. DOI: 10.1016/0040-4020(82)80072-0. (d) Duddeck, H.; Wagner, P. Synthese und 13C-NMR-spektroskopische Untersuchungen von brückenkopfsubstituierten endo-Bicyclo[3.3.1]nonan-3-olen und Oxaadamantanen. *Liebigs Ann. Chem.* **1984**, *1984*, 1981-1988. DOI: 10.1002/jlac.198419841208. (e) van Cranenburgh, P. E. J. P.; Peters, J. A.; Baas, J. M. A.; van de Graaf, B.; de Jong, G. Conformational energies and geometries of some oxa- and dioxabicyclo[3.3.1]nonanes from molecular mechanics. *Recl. Trav. Chim. Pays-Bas* **1981**, *100*, 165-168. DOI: 10.1002/recl.19811000409. (f) Marvell, E. N.; Provant, S. Conformations of Bicyclo[3.3.1]nonanes. 3-Methyl-2,4-dioxabicyclo[3.3.1]nonane. *J. Org. Chem.* **1964**, *29*, 3084-3086. DOI: 10.1021/jo01033a513. (g)

Dombi, G.; Mattinen, J.; Pihlaja, K.; Czombos, J. Configurations and conformations of isomeric 3-methyl-2,4-dioxabicyclo [3.3.1]nonanes - their preparation and multinuclear and 2d nmr study. *Tetrahedron* **1986**, *42*, 2359-2367. DOI: 10.1016/S0040-4020(01)90618-0.

(126) (a) Batson, W. A.; Abboud, K. A.; Battiste, M. A.; Wright, D. L. Synthesis of versatile bicyclo[5.4.0]undecane systems from tetrachlorocyclopropene. *Tetrahedron Lett.* **2004**, *45*, 2093-2096. DOI: 10.1016/j.tetlet.2004.01.055. (b) Rigby, J. H.; Sage, J. M.; Raggon, J. A novel entry into the bicyclo[5.4.0]undecane ring system. *J. Org. Chem.* **1982**, *47*, 4815-4816. DOI: 10.1021/jo00145a054.

(127) (a) Meng, F.-Y.; Sun, J.-X.; Li, X.; Yu, H.-Y.; Li, S.-M.; Ruan, H.-L. Schiglautone A, a New Tricyclic Triterpenoid with a Unique 6/7/9-Fused Skeleton from the Stems of Schisandra glaucescens. *Org. Lett.* **2011**, *13*, 1502-1505. DOI: 10.1021/ol200188n. (b) Ma, B.; Zhao, Y.; He, C.; Ding, H. Total Synthesis of an Atropisomer of the Schisandra Triterpenoid Schiglautone A. *Angew. Chem. Int. Ed.* **2018**, *57*, 15567-15571. DOI: 10.1002/anie.201809076.

(128) Hallock, Y. F.; H., C. I. I. J.; and Boyd, M. R. (-)-Frondosins A and D, HIV-Inhibitory Sesquiterpene Hydroquinone Derivatives from Euryspongia sp. *Natural Product Letters* **1998**, *11*, 153-160. DOI: 10.1080/10575639808041212.

(129) (a) Jin, S.; Yun, H. J.; Jeong, H. Y.; Oh, Y. N.; Park, H. J.; Yun, S.-G.; Kim, B. W.; Kwon, H. J. Widdrol, a sesquiterpene isolated from Juniperus chinensis, inhibits angiogenesis by targeting vascular endothelial growth factor receptor 2 signaling. *Oncol Rep* **2015**, *34*, 1178-1184. DOI: 10.3892/or.2015.4075. (b) Erdtman, H.; Thomas, B. R. The chemistry of the natural order Cupressales. XX. Heartwood constituents of the genus Widdringtonia. **1958**.

(130) Marion, F.; Williams, D. E.; Patrick, B. O.; Hollander, I.; Mallon, R.; Kim, S. C.; Roll, D. M.; Feldberg, L.; Van Soest, R.; Andersen, R. J. Liphagal, a Selective Inhibitor of PI3 Kinase α Isolated from the Sponge Aka coralliphaga: Structure Elucidation and Biomimetic Synthesis. *Org. Lett.* **2006**, *8*, 321-324. DOI: 10.1021/ol052744t.

(131) (a) Simmons, E. M.; Sarpong, R. Structure, biosynthetic relationships and chemical synthesis of the icetexane diterpenoids. *Nat. Prod. Rep.* **2009**, *26*, 1195-1217. DOI: 10.1039/B908984E. (b) Naeini, A. A.; Ziegelmeier, A. A.; Chain, W. J. Recent Developments with Icetexane Natural Products. *Chemistry & Biodiversity* **2022**, *19*, e202200793. DOI: 10.1002/cbdv.202200793.

(132) (a) Selka, A.; Abidli, A.; Schiavo, L.; Jeanmart, L.; Hanquet, G.; Lubell, W., D. Recent Advances in Sustainable Total Synthesis and Chiral Pool Strategies with Emphasis on (−)-Sclareol in Natural Products Synthesis. *Eur. J. Org. Chem.* **2025**. DOI: 10.1002/ejoc.202400983. (b) Brill, Z. G.; Condakes, M. L.; Ting, C. P.; Maimone, T. J. Navigating the Chiral Pool in the Total Synthesis of Complex Terpene Natural Products. *Chem. Rev.* **2017**, *117*, 11753-11795. DOI: 10.1021/acs.chemrev.6b00834.

(133) Moore, B. P.; Brown, W. V. The chemistry of the metasternal gland secretion of the eucalypt longicorn Phoracantha synonyma (Coleoptera : Cerambycidae). *Aust. J. Chem.* **1976**, *29*, 1365-1374.

(134) Larsen, A. G.; Holm, A. H.; Roberson, M.; Daasbjerg, K. Substituent Effects on the Oxidation and Reduction Potentials of Phenylthiyl Radicals in Acetonitrile. *J. Am. Chem. Soc.* **2001**, *123*, 1723-1729. DOI: 10.1021/ja003811b.

(135) (a) Gómez-Gallego, M.; Sierra, M. A. Kinetic Isotope Effects in the Study of Organometallic Reaction Mechanisms. *Chem. Rev.* **2011**, *111*, 4857-4963. DOI: 10.1021/cr100436k. (b) Simmons, E. M.; Hartwig, J. F. On the Interpretation of Deuterium Kinetic Isotope Effects in C–H Bond Functionalizations by Transition-Metal Complexes. *Angew. Chem. Int. Ed.* **2012**, *51*, 3066-3072. DOI: 10.1002/anie.201107334.

(136) (a) Murakami, M.; Makino, M.; Ashida, S.; Matsuda, T. Construction of Carbon Frameworks through β-Carbon Elimination Mediated by Transition Metals. *Bull. Chem. Soc. Jpn.* **2006**, *79*, 1315-1321. DOI: 10.1246/bcsj.79.1315. (b) Murakami, M.; Ishida, N. Potential of Metal-Catalyzed C–C Single Bond Cleavage for Organic Synthesis. *J. Am. Chem. Soc.* **2016**, *138*, 13759-13769. DOI: 10.1021/jacs.6b01656. (c) Murakami, M.; Ishida, N. Cleavage of Carbon-Carbon σ-Bonds of Four-Membered Rings. In *Chem. Rev.*, American Chemical Society: 2021; Vol. 121, pp 264-299. (d) McDonald, T. R.; Mills, L. R.; West, M. S.; Rousseaux, S. A. L. Selective Carbon–Carbon Bond Cleavage of Cyclopropanols. *Chem. Rev.* **2021**, *121*, 3-79. DOI: 10.1021/acs.chemrev.0c00346.

(137) Varabyeva, N.; Barysevich, M.; Aniskevich, Y.; Hurski, A. Ti(OiPr)4-Enabled Dual Photoredox and Nickel-Catalyzed Arylation and Alkenylation of Cyclopropanols. *Org. Lett.* **2021**, *23*, 5452-5456. DOI: 10.1021/acs.orglett.1c01795.

(138) Wang, J.; Li, X. Asymmetric β-arylation of cyclopropanols enabled by photoredox and nickel dual catalysis. *Chem. Sci.* **2022**, *13*, 3020-3026. DOI: 10.1039/D1SC07237D.

(139) Landwehr, E. M.; Baker, M. A.; Oguma, T.; Burdge, H. E.; Kawajiri, T.; Shenvi, R. A. Concise syntheses of GB22, GB13, and himgaline by cross-coupling and complete reduction. *Science* **2022**, *375*, 1270-1274. DOI: 10.1126/science.abn8343.

(140) Huang, L.; Ji, T.; Rueping, M. Remote Nickel-Catalyzed Cross-Coupling Arylation via Proton-Coupled Electron Transfer-Enabled C-C Bond Cleavage. *J. Am. Chem. Soc.* **2020**, *142*, 3532-3539. DOI: 10.1021/jacs.9b12490.

(141) Cong, F.; Lv, X.-Y.; Day, C. S.; Martin, R. Dual Catalytic Strategy for Forging sp2–sp3 and sp3–sp3 Architectures via β-Scission of Aliphatic Alcohol Derivatives. *J. Am. Chem. Soc.* **2020**, *142*, 20594-20599. DOI: 10.1021/jacs.0c11172.

(142) Zou, L.; Sun, R.; Tao, Y.; Wang, X.; Zheng, X.; Lu, Q. Photoelectrochemical Fe/Ni cocatalyzed C−C functionalization of alcohols. *Nat. Commun.* **2024**, *15*, 5245. DOI: 10.1038/s41467-024-49557-7.

(143) Liu, Z.-R.; Zhu, X.-Y.; Guo, J.-F.; Ma, C.; Zuo, Z.; Mei, T.-S. Synergistic use of photocatalysis and convergent paired electrolysis for nickel-catalyzed arylation of cyclic alcohols. *Science Bulletin* **2024**, *69*, 1866-1874. DOI: 10.1016/j.scib.2024.04.031.

(144) Gutierrez, O.; Tellis, J. C.; Primer, D. N.; Molander, G. A.; Kozlowski, M. C. Nickel-Catalyzed Cross-Coupling of Photoredox-Generated Radicals: Uncovering a General Manifold for Stereoconvergence in Nickel-Catalyzed Cross-Couplings. *J. Am. Chem. Soc.* **2015**, *137*, 4896-4899. DOI: 10.1021/ja513079r.

(145) Yuan, M.; Song, Z.; Badir, S. O.; Molander, G. A.; Gutierrez, O. On the Nature of C(sp3)–C(sp2) Bond Formation in Nickel-Catalyzed Tertiary Radical Cross-Couplings: A Case Study of Ni/Photoredox Catalytic Cross-Coupling of Alkyl Radicals and Aryl Halides. *J. Am. Chem. Soc.* **2020**, *142*, 7225-7234. DOI: 10.1021/jacs.0c02355.

(146) Kawatsura, M.; Hartwig, J. F. Simple, Highly Active Palladium Catalysts for Ketone and Malonate Arylation: Dissecting the Importance of Chelation and Steric Hindrance. *J. Am. Chem. Soc.* **1999**, *121*, 1473-1478. DOI: 10.1021/ja983378u.

(147) Prieto Kullmer, C. N.; Kautzky, J. A.; Krska, S. W.; Nowak, T.; Dreher, S. D.; MacMillan, D. W. C. Accelerating reaction generality and mechanistic insight through additive mapping. *Science* **2022**, *376*, 532-539. DOI: 10.1126/science.abn1885.

(148) (a) Chateauneuf, J.; Lusztyk, J.; Ingold, K. U. Spectroscopic and kinetic characteristics of aroyloxyl radicals. 1. The 4-methoxybenzoyloxyl radical. *J. Am. Chem. Soc.* **1988**, *110*, 2877-2885. DOI: 10.1021/ja00217a031. (b) Chateauneuf, J.; Lusztyk, J.; Ingold, K. U. Spectroscopic and kinetic characteristics of aroyloxyl radicals. 2. Benzoyloxyl and ring-substituted aroyloxyl radicals. *J. Am. Chem. Soc.* **1988**, *110*, 2886-2893. DOI: 10.1021/ja00217a032.

(149) Yoshimi, Y.; Itou, T.; Hatanaka, M. Decarboxylative reduction of free aliphatic carboxylic acids by photogenerated cation radical. *Chem. Commun.* **2007**, 5244-5246. DOI: 10.1039/B714526H.

(150) Cassani, C.; Bergonzini, G.; Wallentin, C.-J. Photocatalytic Decarboxylative Reduction of Carboxylic Acids and Its Application in Asymmetric Synthesis. *Org. Lett.* **2014**, *16*, 4228-4231. DOI: 10.1021/ol5019294.

(151) Griffin, J. D.; Zeller, M. A.; Nicewicz, D. A. Hydrodecarboxylation of Carboxylic and Malonic Acid Derivatives via Organic Photoredox Catalysis: Substrate Scope and Mechanistic Insight. *J. Am. Chem. Soc.* **2015**, *137*, 11340-11348. DOI: 10.1021/jacs.5b07770.

(152) Li, N.; Ning, Y.; Wu, X.; Xie, J.; Li, W.; Zhu, C. A highly selective decarboxylative deuteration of carboxylic acids. *Chem. Sci.* **2021**, *12*, 5505-5510. DOI: 10.1039/D1SC00528F.

(153) Lu, Y.-C.; West, J. G. Chemoselective Decarboxylative Protonation Enabled by Cooperative Earth-Abundant Element Catalysis. *Angew. Chem. Int. Ed.* **2022**, *62*, e202213055. DOI: 10.1002/anie.202213055.

(154) (a) Dalton, T.; Faber, T.; Glorius, F. C–H Activation: Toward Sustainability and Applications. *ACS Cent. Sci.* **2021**, *7*, 245-261. DOI: 10.1021/acscentsci.0c01413. (b) Capaldo, L.; Ravelli, D. Hydrogen Atom Transfer (HAT): A Versatile Strategy for Substrate Activation in Photocatalyzed Organic Synthesis. *Eur. J. Org. Chem.* **2017**, *2017*, 2056-2071. DOI: 10.1002/ejoc.201601485.

(155) (a) Garwood, J. J. A.; Chen, A. D.; Nagib, D. A. Radical Polarity. *J. Am. Chem. Soc.* **2024**, *146*, 28034-28059. DOI: 10.1021/jacs.4c06774. (b) Parsaee, F.; Senarathna, M. C.; Kannangara, P. B.; Alexander, S. N.; Arche, P. D. E.; Welin, E. R. Radical philicity and its role in selective organic transformations. *Nat. Rev. Chem.* **2021**, *5*, 486-499. DOI: 10.1038/s41570-021-00284-3. (c) Chan, B.; Easton, C. J.; Radom, L. Outcome-Changing Effect of Polarity Reversal in Hydrogen-Atom-Abstraction Reactions. *J. Phys. Chem. A* **2015**, *119*, 3843-3847. DOI: 10.1021/acs.jpca.5b01890.

(156) Julia, M. Free-radical cyclizations. *Acc. Chem. Res.* **1971**, *4*, 386-392. DOI: 10.1021/ar50047a005.

(157) Curran, D. P. The design and application of free radical chain reactions in organic synthesis. Part 2. *Synthesis* **1988**, *1988*, 489-513.

(158) (a) Zhao, R.; Shi, L. A renaissance of ligand-to-metal charge transfer by cerium photocatalysis. *Org. Chem. Front.* **2018**, *5*, 3018-3021. DOI: 10.1039/c8qo00893k. (b) Treacy, S. M.; Rovis, T. Photoinduced Ligand-to-Metal Charge Transfer in Base-Metal Catalysis. *Synthesis* **2023**, *56*, 1967-1978. DOI: 10.1055/s-0042-1751518.

(159) (a) Aramaki, Y.; Chiba, K.; Tada, M. Spiro-lactones, hyperolactone A-D from Hypericum chinense. *Phytochemistry* **1995**, *38*, 1419-1421. DOI: 10.1016/0031-9422(94)00862-N. (b) Grove, J. F.; MacMillan, J.; Mulholland, T. P. C.; Rogers, M. A. T. 762. Griseofulvin. Part IV. Structure. *J. Chem. Soc.* **1952**, 3977-3987. DOI: 10.1039/JR9520003977. (c) Fan, B.; Dewapriya, P.; Li, F.; Blümel, M.; Tasdemir, D. Pyrenosetins A–C, New Decalinoylspirotetramic Acid Derivatives Isolated by Bioactivity-Based Molecular Networking from the Seaweed-Derived Fungus Pyrenochaetopsis sp. FVE-001. In *Mar. Drugs*, 2020; Vol. 18. (d) Ren, H.; Liu, R.; Chen, L.; Zhu, T.; Zhu, W. M.; Gu, Q. Q. Two new hetero-spirocyclic γ-lactam derivatives from marine sediment-derived fungus Aspergillus sydowi D2–6. *Arch. Pharmacal Res.* **2010**, *33*, 499-502. DOI: 10.1007/s12272-010-0401-4.

(160) Nair, V.; Deepthi, A. Cerium(IV) Ammonium Nitrate–A Versatile Single-Electron Oxidant. *Chem. Rev.* **2007**, *107*, 1862-1891. DOI: 10.1021/cr068408n.

(161) Kharasch, M. S.; Engelmann, H.; Mayo, F. R. The Peroxide Effect In The Addition Of Reagents To Unsaturated Compounds. Xv. The Addition Of Hydrogen Bromide To 1- And 2-Bromo- And Chloropropenes. *J. Org. Chem.* **1937**, *02*, 288-302. DOI: 10.1021/jo01226a011.

(162) Kharasch, M. S.; Jensen, E. V.; Urry, W. H. Addition of Carbon Tetrachloride and Chloroform to Olefins. *Science* **1945**, *102*, 128-128. DOI: 10.1126/science.102.2640.128.a.

(163) Kharasch, M. S.; Skell, P. S.; Fisher, P. Reactions of Atoms and Free Radicals in Solution. XII. The Addition of Bromo Esters to Olefins. *J. Am. Chem. Soc.* **1948**, *70*, 1055-1059. DOI: 10.1021/ja01183a053.

(164) Heiba, E. I.; Dessau, R. M.; Koehl, W. J., Jr. Oxidation by metal salts. IV. A new method for the preparation of .gamma.-lactones by the reaction of manganic acetate with olefins. *J. Am. Chem. Soc.* **1968**, *90*, 5905-5906. DOI: 10.1021/ja01023a049.

(165) Bush, J. B., Jr.; Finkbeiner, H. Oxidation reactions of manganese(III) acetate. II. Formation of .gamma.-lactones from olefins and acetic acid. *J. Am. Chem. Soc.* **1968**, *90*, 5903-5905. DOI: 10.1021/ja01023a048.

(166) (a) Iqbal, J.; Bhatia, B.; Nayyar, N. K. Transition Metal-Promoted Free-Radical Reactions in Organic Synthesis: The Formation of Carbon-Carbon Bonds. *Chem. Rev.* **1994**, *94*, 519-564. DOI: 10.1021/cr00026a008. (b) Snider, B. B. Manganese(III)-Based Oxidative Free-Radical Cyclizations. *Chem. Rev.* **1996**, *96*, 339-364. DOI: 10.1021/cr950026m.

(167) Kettle, S. F. A.; de la Mare, P. B. D.; Lomas, J. S.; Pacini, H. A.; Pavlath, A. E.; Cotter, J. L.; Gore, P. H.; Hoskins, J. A.; Wladislaw, B.; Giora, A.; Miller, J. D.; Prince, R. H.; Keen, I. M.; Tuck, D. G.; Faithful, B. D.; Haslam, E.; Marriott, J. E.; Gill, G. B.; Williams, G. H.; Barker, C. C.; Hallas, G.; Thornber, M. N.; Crombie, D. A.; Shaw, S.; Bird, C. W.; Colvin, E. W.; Parker, W.; Fields, E. K.; Leslie, J.; Hamer, D.; Hallas,

G.; Downie, I. M.; Morris, G.; Hiscock, A. K.; Whitehurst, J. S.; Green, M.; Tipping, A. E.; van Es, T.; Staskun, B.; Trahanovsky, W. S.; Young, L. B.; Bristow, P. A.; Khowaja, M.; Tillett, J. G.; Fischer, A.; Hutchinson, R. E. J.; Topsom, R. D.; Carruthers, W.; Watkins, D. A. M.; Knight, J. A.; Roberts, J. C.; Underwood, J. G. Notes. *J. Chem. Soc.* **1965**, 5737-5784. DOI: 10.1039/JR9650005737.

(168) Syper, L. Partial oxidation of aliphatic side chains with cerium (IV). *Tetrahedron Lett.* **1966**, *7*, 4493-4498. DOI: 10.1016/S0040-4039(00)70065-7.

(169) Julia, M. Free radical cyclizations, XVII. Mechanistic studies. *Pure Appl. Chem.* **1974**, *40*, 553-567. DOI: 10.1351/pac197440040553.

(170) (a) Heiba, E.-A. I.; Dessau, R. M. Oxidation by metal salts. VII. Syntheses based on the selective oxidation of organic free radicals. *J. Am. Chem. Soc.* **1971**, *93*, 524-527. DOI: 10.1021/ja00731a042. (b) Heiba, E.-A. I.; Dessau, R. M. Oxidation by metal salts. VIII. Decomposition of ceric carboxylates in the presence of olefins and aromatic hydrocarbons. *J. Am. Chem. Soc.* **1971**, *93*, 995-999. DOI: 10.1021/ja00733a036. (c) Heiba, E. I.; Dessau, R. M. Oxidation by metal salts. IX. Formation of cyclic ketones. *J. Am. Chem. Soc.* **1972**, *94*, 2888-2889. DOI: 10.1021/ja00763a073. (d) Heiba, E. I.; Dessau, R. M.; Rodewald, P. G. Oxidation by metal salts. X. One-step synthesis of .gamma.-lactones from olefins. *J. Am. Chem. Soc.* **1974**, *96*, 7977-7981. DOI: 10.1021/ja00833a024. (e) Dessau, R. M.; Heiba, E. A. I. Oxidation by metal salts. XII. Novel one-step synthesis of 1,4-diketones. *J. Org. Chem.* **1974**, *39*, 3457-3459. DOI: 10.1021/jo00937a053. (f) Heiba, E.-A. I.; Dessau, R. M. Oxidation by metal salts. XI. Formation of dihydrofurans. *J. Org. Chem.* **1974**, *39*, 3456-3457. DOI: 10.1021/jo00937a052.

(171) Fristad, W. E.; Peterson, J. R. Manganese(III)-mediated .gamma.-lactone annulation. *J. Org. Chem.* **1985**, *50*, 10-18. DOI: 10.1021/jo00201a003.

(172) Corey, E. J.; Kang, M. C. A new and general synthesis of polycyclic .gamma.-lactones by double annulation. *J. Am. Chem. Soc.* **1984**, *106*, 5384-5385. DOI: 10.1021/ja00330a076.

(173) Snider, B. B.; Mohan, R.; Kates, S. A. Manganese(III)-based oxidative free-radical cyclization. Synthesis of (.+-.)-podocarpic acid. *J. Org. Chem.* **1985**, *50*, 3659-3661. DOI: 10.1021/jo00219a054.

(174) Cossy, J.; Leblanc, C. New synthesis of lactams and spirolactams radical cyclization induced by manganese(III) acetate. *Tetrahedron Lett.* **1989**, *30*, 4531-4534. DOI: 10.1016/S0040-4039(01)80737-1.

(175) Snider, B. B.; Merritt, J. E.; Dombroski, M. A.; Buckman, B. O. Solvent effects on manganese(III)-based oxidative free-radical cyclizations: ethanol and acetic acid. *J. Org. Chem.* **1991**, *56*, 5544-5553. DOI: 10.1021/jo00019a014.

(176) (a) Nair, V.; Mathew, J.; Alexander, S. Synthesis of Spiroannulated Dihydrofurans by Cerium(IV) Ammonium Nitrate Mediated Addition Of 1,3-Dicarbonyl Compounds to Exocyclic Alkenes. *Synth. Commun.* **1995**, *25*, 3981-3991. DOI: 10.1080/00397919508011474. (b) Nair, V.; Mathew, J.; Radhakrishnan, K. V. Oxidative addition of 1,3-dicarbonyl compounds to alkenes mediated by cerium(IV) ammonium nitrate and manganese(III) acetate: a comparative study. *J. Chem. Soc., Perkin Trans. 1* **1996**, 1487-1492. DOI: 10.1039/P19960001487. (c) Nair, V.; Mathew, J.; Prabhakaran, J. Carbon–carbon bond forming reactions mediated by cerium(IV) reagents. *Chem. Soc. Rev.* **1997**, *26*, 127-132. DOI: 10.1039/CS9972600127. (d)

Baciocchi, E.; Dell'Aira, D.; Ruzziconi, R. Dimethyl arylmalonates from cerium(IV) ammonium nitrate promoted reactions of dimethyl malonate with aromatic compounds in methanol. *Tetrahedron Lett.* **1986**, *27*, 2763-2766. DOI: 10.1016/S0040-4039(00)84638-9. (e) Baciocchi, E.; Ruzziconi, R. 1,2- And 1,4-addition in the reactions of carbonyl compounds with 1,3-butadiene induced by cerium(IV) ammonium nitrate. *J. Org. Chem.* **1986**, *51*, 1645-1649. DOI: 10.1021/jo00360a002. (f) Baciocchi, E.; Ruzziconi, R. Synthesis of 3-Acyl and 3-Carboalkoxyfurans by the Ceric Ammonium Nitrate Promoted Addition of 1,3-Dicarbonyl Compounds to Vinylic Acetates. *Synth. Commun.* **1988**, *18*, 1841-1846. DOI: 10.1080/00397918808060939.

(177) (a) Citterio, A.; Sebastiano, R.; Nicolini, M.; Santi, R. Synthesis of γ-Lactones by Iron(III) Perchlorate Oxidation of Malonic Esters in the Presence of Olefins. *Synlett* **1990**, *1990*, 42-43. DOI: 10.1055/s-1990-20980. (b) Citterio, A.; Sebastiano, R.; Caceres Carvayal, M. Oxidation of diethyl (pyridylmethyl)malonates with manganese(III) acetate, cerium(IV) ammonium nitrate, and iron(III) perchlorate in the presence of alkenes and alkynes. *J. Org. Chem.* **1991**, *56*, 5335-5341. DOI: 10.1021/jo00018a024.

(178) (a) Iqbal, J.; Kumar, T. K. P.; Manogaran, S. Cobalt(II) acetate promoted addition of acetoacetate to terminal olefins: A highly stereoselective synthesis of 5-alkyl-2-hydroxy 2 methyl-3-methoxycarbonyl tetrahydrofurans. *Tetrahedron Lett.* **1989**, *30*, 4701-4702. DOI: 10.1016/S0040-4039(01)80778-4. (b) Iqbal, J.; Bhatia, B.; Nayyar, N. K. Cobalt (II) acetate promoted oxidative addition of 1,3-dicarbonyl compounds to alkenes under aerobic conditions. *Tetrahedron* **1991**, *47*, 6457-6468. DOI: 10.1016/S0040-4020(01)86573-X.

(179) Hai-Shan, D.; Roberts, B. P. Amine-boranes as polarity reversal catalysts for radical chain 2,3-epoxypropanation reactions of esters. *Tetrahedron Lett.* **1992**, *33*, 4621-4624. DOI: 10.1016/S0040-4039(00)61329-1.

(180) Zhang, Y.; Flowers, R. A. Mechanistic Investigation of Substrate Oxidation by Ce(IV) Reagents in Acetonitrile. *J. Org. Chem.* **2003**, *68*, 4560-4562. DOI: 10.1021/jo034384y.

(181) Tedder, J. M. Which Factors Determine the Reactivity and Regioselectivity of Free Radical Substitution and Addition Reactions? *Angew. Chem., Int. Ed.* **1982**, *21*, 401-410. DOI: 10.1002/anie.198204011.

(182) (a) De Vleeschouwer, F.; Van Speybroeck, V.; Waroquier, M.; Geerlings, P.; De Proft, F. Electrophilicity and Nucleophilicity Index for Radicals. *Org. Lett.* **2007**, *9*, 2721-2724. DOI: 10.1021/ol071038k. (b) Héberger, K.; Lopata, A. Assessment of Nucleophilicity and Electrophilicity of Radicals, and of Polar and Enthalpy Effects on Radical Addition Reactions1. *J. Org. Chem.* **1998**, *63*, 8646-8653. DOI: 10.1021/jo971284h.

(183) Lenardon, G. V. A.; Nicchio, L.; Fagnoni, M. Photogenerated electrophilic radicals for the umpolung of enolate chemistry. *Journal of Photochemistry and Photobiology C: Photochemistry Reviews* **2021**, *46*, 100387. DOI: 10.1016/j.jphotochemrev.2020.100387.

(184) Shin, N. Y.; Tsui, E.; Reinhold, A.; Scholes, G. D.; Bird, M. J.; Knowles, R. R. Radicals as Exceptional Electron-Withdrawing Groups: Nucleophilic Aromatic Substitution of Halophenols Via Homolysis-Enabled Electronic Activation. *J. Am. Chem. Soc.* **2022**, *144*, 21783-21790. DOI: 10.1021/jacs.2c10296.

(185) Ruffoni, A.; Mykura, R. C.; Bietti, M.; Leonori, D. The interplay of polar effects in controlling the selectivity of radical reactions. *Nat. Synth.* **2022**, *1*, 682-695. DOI: 10.1038/s44160-022-00108-2.

(186) Chung, W.-S.; Ho, C.-C. Photochemistry of acetone in the presence of exocyclic olefins: an unexpected competition between the photo-Conia and Paternò–Büchi reactions. *Chem. Commun.* **1997**, 317-318. DOI: 10.1039/A607415D.

(187) Mayo, P. d.; Stothers, J. B.; Templeton, W. Photochemical Syntheses: I. The Reaction Of Aldehydes And Ketones With Cycloalkenes. *Can. J. Chem.* **1961**, *39*, 488-497. DOI: 10.1139/v61-058.

(188) Reusch, W. A Stereospecific Photochemical Addition of Acetone to Norbornylene. *J. Org. Chem.* **1962**, *27*, 1882-1883. DOI: 10.1021/jo01052a505.

(189) Steitz, A., Jr.; Moote, T. P., Jr. Photoinitiated Addition of Carboxylic Acids to Higher Olefins. *Industrial & Engineering Chemistry Process Design and Development* **1962**, *1*, 132-137. DOI: 10.1021/i260002a011.

(190) Mlinaric-Majerski, K.; Pavlovic, D.; Sindler-Kulyk, M. Synthesis and photochemistry of 4-methylene-2-protoadamantanone. *J. Org. Chem.* **1993**, *58*, 252-254. DOI: 10.1021/jo00053a047.

(191) Shiraishi, Y.; Tsukamoto, D.; Hirai, T. Highly Efficient Methyl Ketone Synthesis by Water-Assisted C−C Coupling between Olefins and Photoactivated Acetone. *Org. Lett.* **2008**, *10*, 3117-3120. DOI: 10.1021/ol800999s.

(192) Tsukamoto, D.; Shiraishi, Y.; Hirai, T. Highly Efficient Methyl Ketone Synthesis with Photoactivated Acetone and Olefins Assisted by Mg(II)-Exchanged Zeolite Y. *J. Org. Chem.* **2010**, *75*, 1450-1457. DOI: 10.1021/jo902321f.

(193) (a) Bruno, J. W.; Marks, T. J.; Lewis, F. D. Silver(I) photocatalyzed addition of acetonitrile to norbornene. *J. Am. Chem. Soc.* **1981**, *103*, 3608-3609. DOI: 10.1021/ja00402a076. (b) Bruno, J. W.; Marks, T. J.; Lewis, F. D. Metal ion photoinitiated addition of acetonitrile and methanol to olefins. *J. Am. Chem. Soc.* **1982**, *104*, 5580-5585. DOI: 10.1021/ja00385a003.

(194) Sonawane, H. R.; Bellur, N. S.; Shah, V. G. Light-mediated cyanomethylation of cycloalkenes with acetonitrile. *J. Chem. Soc., Chem. Commun.* **1990**, 1603-1605. DOI: 10.1039/C39900001603.

(195) Zhang, Y.; Mao, L.-L.; Hu, S.; Luan, Y.; Cong, H. Photo-induced anti-Markovnikov hydroalkylation of unactivated alkenes employing a dual-component initiator. *Chin. Chem. Lett.* **2021**, *32*, 681-684. DOI: 10.1016/j.cclet.2020.06.026.

(196) Nugent, J.; Sterling, A. J.; Frank, N.; Mousseau, J. J.; Anderson, E. A. Synthesis of α-Quaternary Bicyclo[1.1.1]pentanes through Synergistic Organophotoredox and Hydrogen Atom Transfer Catalysis. *Org. Lett.* **2021**, *23*, 8628-8633. DOI: 10.1021/acs.orglett.1c03346.

(197) Baś, S.; Yamashita, Y.; Kobayashi, S. Development of Brønsted Base–Photocatalyst Hybrid Systems for Highly Efficient C–C Bond Formation Reactions of Malonates with Styrenes. *ACS Catal.* **2020**, *10*, 10546-10550. DOI: 10.1021/acscatal.0c02716.

(198) Forbes, K. C.; Crooke, A. M.; Lee, Y.; Kawada, M.; Shamskhou, K. M.; Zhang, R. A.; Cannon, J. S. Photoredox-Catalyzed Oxidation of Anions for the Atom-Economical Hydro-, Amido-, and Dialkylation of Alkenes. *J. Org. Chem.* **2022**, *87*, 3498-3510. DOI: 10.1021/acs.joc.1c03055.

(199) Paria, S.; Reiser, O. Visible Light and Copper Complexes: A Promising Match in Photoredox Catalysis. In *Visible Light Photocatalysis in Organic Chemistry*, 2018; pp 233-251.

(200) Qiao, J.; Ci, R.-N.; Gan, Q.-C.; Huang, C.; Liu, Z.; Hu, H.-L.; Ye, C.; Chen, B.; Tung, C.-H.; Wu, L.-Z. Amine-Free, Directing-Group-Free and Redox-Neutral α-Alkylation of Saturated Cyclic Ketones. *Angew. Chem. Int. Ed.* **2023**, *62*, e202305679. DOI: 10.1002/anie.202305679.

(201) Yamashita, Y.; Ogasawara, Y.; Banik, T.; Kobayashi, S. Photoinduced Efficient Catalytic α-Alkylation Reactions of Active Methylene and Methine Compounds with Nonactivated Alkenes. *J. Am. Chem. Soc.* **2023**, *145*, 23160-23166. DOI: 10.1021/jacs.3c07436.

(202) Qu, W.-Y.; Zhou, X.-S.; Xiao, W.-J.; Chen, J.-R. Asymmetric radical allylation of β-keto esters with vinyl cyclopropanes by dual photoredox/nickel catalysis. *Science China Chemistry* **2024**, *67*, 3807-3816. DOI: 10.1007/s11426-024-2249-x.

(203) Yang, X.; Ma, M.; Xu, M.; Pang, Y.; Zhao, H.; Ye, J. Enhanced Efficiency of Amide-Substituted Quinuclidine-Boranes as Hydridic Hydrogen Atom Transfer Catalysts for Photoinduced Hydroalkylation of Unactivated Olefins. *Chin. J. Chem* . **2024**, *42*, 3227-3233. DOI: 10.1002/cjoc.202400725.

(204) Yamashita, Y.; Hisada, T.; Sato, Y.; Kobayashi, S. Mg(SPh)2 as a Catalyst for Efficient Photocatalytic Alkylation Reactions of Active Methylene Compounds with Nonactivated Alkenes. *Adv. Synth. Catal.* **2025**, *367*, e202401554. DOI: 10.1002/adsc.202401554.

(205) Yamashita, Y.; Enokijima, R.; Ogasawara, Y.; Hisada, T.; Kobayashi, S. Photoinduced Catalytic Alkylation of Active Methine Compounds with Nonactivated Alkenes Using Yttrium Triflate as a Lewis Acid Catalyst. *Adv. Synth. Catal.* **2025**, e202401568. DOI: 10.1002/adsc.202401568.

(206) Zhou, X.-S.; Li, Z.-Q.; Qu, W.-Y.; Zhang, Z.; Xiao, W.-J.; Chen, J.-R. Direct Asymmetric α-Alkylation of β-Ketocarbonyl Compounds with Simple Olefins by Photoredox-Nickel-Hydrogen Atom Transfer Triple Catalysis. *Angew. Chem. Int. Ed.* **2025**, *n/a*, e202424915. DOI: 10.1002/anie.202424915.

(207) Costisella, A.; Ottawa-Carleton Chemistry, I. Towards the Total Synthesis of Penostatin Natural Products. University of Ottawa, 2023.

(208) Snider, B. B. Manganese(III) Acetate-Mediated Cyclizations. In *Manganese Catalysis in Organic Synthesis*, 2021; pp 293-322.

(209) Friedrich, J.; Schneider, D.; Bock, L.; Maichle-Mössmer, C.; Anwander, R. Cerium(IV) Neopentoxide Complexes. *Inorg. Chem.* **2017**, *56*, 8114-8127. DOI: 10.1021/acs.inorgchem.7b00828.

(210) Kütt, A.; Tshepelevitsh, S.; Saame, J.; Lõkov, M.; Kaljurand, I.; Selberg, S.; Leito, I. Strengths of Acids in Acetonitrile. *Eur. J. Org. Chem.* **2021**, *2021*, 1407-1419. DOI: 10.1002/ejoc.202001649.

(211) Eckert, F.; Leito, I.; Kaljurand, I.; Kütt, A.; Klamt, A.; Diedenhofen, M. Prediction of acidity in acetonitrile solution with COSMO-RS. *J. Comput. Chem.* **2009**, *30*, 799-810. DOI: 10.1002/jcc.21103.

(212) Stork, G.; Danheiser, R. L. Regiospecific alkylation of cyclic .beta.-diketone enol ethers. General synthesis of 4-alkylcyclohexenones. *J. Org. Chem.* **1973**, *38*, 1775-1776. DOI: 10.1021/jo00949a048.

(213) Curran, D. P.; Rakiewicz, D. M. Tandem radical approach to linear condensed cyclopentanoids. Total synthesis of (.+-.)-hirsutene. *J. Am. Chem. Soc.* **1985**, *107*, 1448-1449. DOI: 10.1021/ja00291a077.

(214) Rackham, M. D.; Brannigan, J. A.; Moss, D. K.; Yu, Z.; Wilkinson, A. J.; Holder, A. A.; Tate, E. W.; Leatherbarrow, R. J. Discovery of Novel and Ligand-Efficient Inhibitors of Plasmodium falciparum and Plasmodium vivaxN-Myristoyltransferase. *J. Med. Chem.* **2013**, *56*, 371-375. DOI: 10.1021/jm301474t.

(215) Sawada, H.; Nakayama, M.; Yoshida, M.; Yoshida, T.; Kamigata, N. Trifluoromethylation of aromatic compounds with bis(trifluoroacetyl) peroxide. *J. Fluorine Chem.* **1990**, *46*, 423-431. DOI: 10.1016/S0022-1139(00)82927-9.

(216) Fernández-García, S.; Chantzakou, V. O.; Juliá-Hernández, F. Direct Decarboxylation of Trifluoroacetates Enabled by Iron Photocatalysis**. *Angew. Chem. Int. Ed.* **2024**, *63*, e202311984. DOI: 10.1002/anie.202311984.

(217) (a) Buzzetti, L.; Crisenza, G. E. M.; Melchiorre, P. Mechanistic Studies in Photocatalysis. *Angew. Chem. Int. Ed.* **2019**, *58*, 3730-3747. DOI: 10.1002/anie.201809984. (b) Cismesia, M. A.; Yoon, T. P. Characterizing chain processes in visible light photoredox catalysis. *Chem. Sci.* **2015**, *6*, 5426-5434. DOI: 10.1039/C5SC02185E. (c) Hatchard, C.; Parker, C. A. A new sensitive chemical actinometer-II. Potassium ferrioxalate as a standard chemical actinometer. *Proc. R. Soc. London, Ser. A* **1956**, *235*, 518-536. DOI: 10.1098/rspa.1956.0102. (d) Pitre, S. P.; McTiernan, C. D.; Vine, W.; DiPucchio, R.; Grenier, M.; Scaiano, J. C. Visible-Light Actinometry and Intermittent Illumination as Convenient Tools to Study Ru(bpy)3Cl2 Mediated Photoredox Transformations. *Scientific Reports* **2015**, *5*, 16397. DOI: 10.1038/srep16397.

(218) Rabani, J.; Mamane, H.; Pousty, D.; Bolton, J. R. Practical Chemical Actinometry—A Review. *Photochem. Photobiol.* **2021**, *97*, 873-902. DOI: 10.1111/php.13429.

(219) Curran, D. P.; Morgan, T. M.; Schwartz, C. E.; Snider, B. B.; Dombroski, M. A. Cyclizations of unsaturated .bul.CR(COX)2 radicals. Manganese(III) acetate oxidative cyclizations of unsaturated acetoacetates and atom-transfer cyclizations of unsaturated haloacetoacetates give the same radicals. *J. Am. Chem. Soc.* **1991**, *113*, 6607-6617. DOI: 10.1021/ja00017a037.

(220) (a) Qiu, G.; Knowles, R. R. Understanding Chemoselectivity in Proton-Coupled Electron Transfer: A Kinetic Study of Amide and Thiol Activation. *J. Am. Chem. Soc.* **2019**, *141*, 16574-16578. DOI: 10.1021/jacs.9b08398. (b) Qiu, G.; Knowles, R. R. Rate-Driving Force Relationships in the Multisite Proton-Coupled Electron Transfer Activation of Ketones. *J. Am. Chem. Soc.* **2019**, *141*, 2721-2730. DOI: 10.1021/jacs.8b13451.

(221) Mori, K.; Oshiba, M.; Hara, T.; Mizugaki, T.; Ebitani, K.; Kaneda, K. Michael reaction of 1,3-dicarbonyls with enones catalyzed by a hydroxyapatite-bound La complex. *Tetrahedron Lett.* **2005**, *46*, 4283-4286. DOI: 10.1016/j.tetlet.2005.04.099.

(222) Beckwith, A. L. J.; Schiesser, C. H. Treasures from the Free Radical Renaissance Period – Miscellaneous hexenyl radical kinetic data. *Org. Biomol. Chem.* **2011**, *9*, 1736-1743. DOI: 10.1039/C0OB00708K.

(223) (a) Pracht, P.; Bohle, F.; Grimme, S. Automated exploration of the low-energy chemical space with fast quantum chemical methods. *Phys. Chem. Chem. Phys.* **2020**, *22*, 7169-7192. DOI: 10.1039/C9CP06869D. (b) Pracht, P.; Grimme, S.; Bannwarth, C.; Bohle, F.; Ehlert, S.; Feldmann, G.; Gorges, J.; Müller, M.; Neudecker, T.;

Plett, C.; Spicher, S.; Steinbach, P.; Wesołowski, P. A.; Zeller, F. CREST—A program for the exploration of low-energy molecular chemical space. *J. Chem. Phys.* **2024**, *160*. DOI: 10.1063/5.0197592.

(224) *Gaussian 16 Rev. C.01*; Wallingford, CT, 2016. https://gaussian.com/gaussian16/ (accessed 2024).

(225) Hu, C.; Kuhn, L.; Makurvet, F. D.; Knorr, E. S.; Lin, X.; Kawade, R. K.; Mentink-Vigier, F.; Hanson, K.; Alabugin, I. V. Tethering Three Radical Cascades for Controlled Termination of Radical Alkyne peri-Annulations: Making Phenalenyl Ketones without Oxidants. *J. Am. Chem. Soc.* **2024**, *146*, 4187-4211. DOI: 10.1021/jacs.3c13371.

(226) (a) Montgomery, J. A., Jr.; Frisch, M. J.; Ochterski, J. W.; Petersson, G. A. A complete basis set model chemistry. VI. Use of density functional geometries and frequencies. *J. Chem. Phys.* **1999**, *110*, 2822-2827. DOI: 10.1063/1.477924. (b) Montgomery, J. A., Jr.; Frisch, M. J.; Ochterski, J. W.; Petersson, G. A. A complete basis set model chemistry. VII. Use of the minimum population localization method. *J. Chem. Phys.* **2000**, *112*, 6532-6542. DOI: 10.1063/1.481224.

(227) *CYLview20*; Université de Sherbrooke, 2020. https://www.cylview.org (accessed 2024).

(228) Pracht, P.; Grimme, S.; Bannwarth, C.; Bohle, F.; Ehlert, S.; Feldmann, G.; Gorges, J.; Müller, M.; Neudecker, T.; Plett, C. CREST—A program for the exploration of low-energy molecular chemical space. *J. Chem. Phys.* **2024**, *160*.

(229) Mulder, P.; Korth, H.-G.; Pratt, D. A.; DiLabio, G. A.; Valgimigli, L.; Pedulli, G.; Ingold, K. Critical re-evaluation of the O− H bond dissociation enthalpy in phenol. *J. Phys. Chem. A* **2005**, *109*, 2647-2655.

(230) Wise, C. F.; Agarwal, R. G.; Mayer, J. M. Determining proton-coupled standard potentials and X–H bond dissociation free energies in nonaqueous solvents using open-circuit potential measurements. *J. Am. Chem. Soc.* **2020**, *142*, 10681-10691.

(231) Zhu, Z.; Odagi, M.; Zhao, C.; Abboud, K. A.; Kirm, H. U.; Saame, J.; Lõkov, M.; Leito, I.; Seidel, D. Highly Acidic Conjugate-Base-Stabilized Carboxylic Acids Catalyze Enantioselective oxa-Pictet–Spengler Reactions with Ketals. *Angew. Chem. Int. Ed.* **2020**, *59*, 2028-2032. DOI: 10.1002/anie.201912677.

(232) Pavlishchuk, V. V.; Addison, A. W. Conversion constants for redox potentials measured versus different reference electrodes in acetonitrile solutions at 25 C. *Inorg. Chim. Acta* **2000**, *298*, 97-102.

(233) Sioda, R. Electrolytic oxidation of 9, 10-diphenylanthracene and properties of its free radical cation and anion. *J. Phys. Chem.* **1968**, *72*, 2322-2330.

(234) (a) Saebø, S.; Cordell, F. R.; Boggs, J. E. Structures and conformations of cyclopentane, cyclopentene, and cyclopentadiene. *Journal of Molecular Structure: THEOCHEM* **1983**, *104*, 221-232. DOI: 10.1016/0166-1280(83)80021-9. (b) Baldridge, K. K.; O'Connor, J. M.; Chen, M.-C.; Siegel, J. S. Envelope-Flip Dynamics in CpCo(Diene) Complexes: an ab Initio Quantum Mechanical Study. *J. Phys. Chem. A* **1999**, *103*, 10126-10131. DOI: 10.1021/jp992322z. (c) Carreira, L. A.; Jiang, G. J.; Person, W. B.; Willis, J. N., Jr. Spectroscopic Determination of the Barrier to Planarity in Cyclopentane. *J. Chem. Phys.* **1972**, *56*, 1440-1443. DOI: 10.1063/1.1677386.

(235) Sung, K.; Wang, Y. Y. Mn(III)-Based Oxidative Free-Radical Cyclizations of Substituted Allyl α-Methyl-β-ketoesters: Syntheses, DFT Calculations, and Mechanistic Studies. *J. Org. Chem.* **2003**, *68*, 2771-2778. DOI: 10.1021/jo026681t.

(236) Caldeira, G. I.; Gouveia, L. P.; Serrano, R.; Silva, O. D. Hypericum Genus as a Natural Source for Biologically Active Compounds. *Plants*, **2022**, *11*, 2509.

(237) Tanaka, N.; Kashiwada, Y. Characteristic metabolites of Hypericum plants: their chemical structures and biological activities. *Journal of Natural Medicines* **2021**, *75*, 423-433. DOI: 10.1007/s11418-021-01489-y.

(238) (a) Ichinari, D.; Ueki, T.; Yoshihara, K.; Kinoshita, T. First total synthesis of (±)-hyperolactone A. *Chem. Commun.* **1997**, 1743-1744. DOI: 10.1039/A704159D. (b) Ueki, T.; Doe, M.; Morimoto, Y.; Kinoshita, T.; Tanaka, R.; Yoshihara, K. Synthesis of hyperolactones A and C. *J. Heterocycl. Chem.* **2001**, *38*, 165-172. DOI: 10.1002/jhet.5570380124. (c) Kraus, G. A.; Wei, J. A Direct Synthesis of Hyperolactone C. *J. Nat. Prod.* **2004**, *67*, 1039-1040. DOI: 10.1021/np0498962. (d) Nicolaou, K. C.; Sarlah, D.; Shaw, D. M. Total Synthesis and Revised Structure of Biyouyanagin A. *Angew. Chem. Int. Ed.* **2007**, *46*, 4708-4711. DOI: 10.1002/anie.200701552. (e) Hodgson, D. M.; Angrish, D.; Erickson, S. P.; Kloesges, J.; Lee, C. H. Consecutive Alkene Cross-Metathesis/Oxonium Ylide Formation−Rearrangement: Synthesis of the Anti-HIV Agent Hyperolactone C. *Org. Lett.* **2008**, *10*, 5553-5556. DOI: 10.1021/ol802334y. (f) Nicolaou, K. C.; Wu, T. R.; Sarlah, D.; Shaw, D. M.; Rowcliffe, E.; Burton, D. R. Total Synthesis, Revised Structure, and Biological Evaluation of Biyouyanagin A and Analogues Thereof. *J. Am. Chem. Soc.* **2008**, *130*, 11114-11121. DOI: 10.1021/ja802805c. (g) Du, C.; Li, L.; Li, Y.; Xie, Z. Construction of Two Vicinal Quaternary Carbons by Asymmetric Allylic Alkylation: Total Synthesis of Hyperolactone C and (−)-Biyouyanagin A. *Angew. Chem. Int. Ed.* **2009**, *48*, 7853-7856. DOI: 10.1002/anie.200902908. (h) Nicolaou, K. C.; Sanchini, S.; Wu, T. R.; Sarlah, D. Total Synthesis and Structural Revision of Biyouyanagin B. *Chem. Eur. J.* **2010**, *16*, 7678-7682. DOI: 10.1002/chem.201001474. (i) Hodgson, D. M.; Man, S. Synthesis of the Anti-HIV Agent (−)-Hyperolactone C by Using Oxonium Ylide Formation–Rearrangement. *Chem. Eur. J.* **2011**, *17*, 9731-9737. DOI: 10.1002/chem.201101082. (j) Nicolaou, K. C.; Sanchini, S.; Sarlah, D.; Lu, G.; Wu, T. R.; Nomura, D. K.; Cravatt, B. F.; Cubitt, B.; de la Torre, J. C.; Hessell, A. J.; Burton, D. R. Design, synthesis, and biological evaluation of a biyouyanagin compound library. *PNAS* **2011**, *108*, 6715-6720. DOI: 10.1073/pnas.1015258108. (k) Hodgson, D. M.; Moreno-Clavijo, E.; Day, S. E.; Man, S. An approach to hyperolactone C and analogues using late stage conjugate addition on an oxonium ylide-derived spirofuranone. *Org. Biomol. Chem.* **2013**, *11*, 5362-5369. DOI: 10.1039/C3OB41251B. (l) Hodgson, D. M.; Man, S.; Powell, K. J.; Perko, Z.; Zeng, M.; Moreno-Clavijo, E.; Thompson, A. L.; Moore, M. D. Intramolecular Oxonium Ylide Formation–[2,3] Sigmatropic Rearrangement of Diazocarbonyl-Substituted Cyclic Unsaturated Acetals: A Formal Synthesis of Hyperolactone C. *J. Org. Chem.* **2014**, *79*, 9728-9734. DOI: 10.1021/jo501893r. (m) Zheng, H.; Wang, Y.; Xu, C.; Xu, X.; Lin, L.; Liu, X.; Feng, X. Stereodivergent synthesis of vicinal quaternary-quaternary stereocenters and bioactive hyperolactones. *Nat. Commun.* **2018**, *9*, 1968. DOI: 10.1038/s41467-018-04123-w.

(239) Tada, M.; Nagai, M.; Okumura, C.; Osano, Y.; Matsuzaki, T. Novel spiro-compound, hyperolactone from Hypericum chinese L. *Chem. Lett.* **1989**, *18*, 683-686.

(240) Crockett, S. L.; Schühly, W.; Belaj, F.; Khan, I. A. Hyperolactone C. *Acta Crystallographica Section E* **2004**, *60*, o2174-o2176. DOI: 10.1107/S1600536804026819.

(241) Schühly, W.; Crockett, S. L.; Fabian, W. M. F. Hyperolactone C: Determination of its absolute configuration by comparison of experimental and calculated CD spectra. *Chirality* **2005**, *17*, 250-256. DOI: 10.1002/chir.20164.

(242) Tanaka, N.; Kashiwada, Y.; Kim, S. Y.; Hashida, W.; Sekiya, M.; Ikeshiro, Y.; Takaishi, Y. Acylphloroglucinol, Biyouyanagiol, Biyouyanagin B, and Related Spiro-lactones from Hypericum chinense. *J. Nat. Prod.* **2009**, *72*, 1447-1452. DOI: 10.1021/np900109y.

(243) Tanaka, N.; Okasaka, M.; Ishimaru, Y.; Takaishi, Y.; Sato, M.; Okamoto, M.; Oshikawa, T.; Ahmed, S. U.; Consentino, L. M.; Lee, K.-H. Biyouyanagin A, an Anti-HIV Agent from Hypericum chinense L. var. salicifolium. *Org. Lett.* **2005**, *7*, 2997-2999. DOI: 10.1021/ol050960w.

(244) Hong, A. Y.; Stoltz, B. M. Enantioselective Total Synthesis of the Reported Structures of (−)-9-epi-Presilphiperfolan-1-ol and (−)-Presilphiperfolan-1-ol: Structural Confirmation and Reassignment and Biosynthetic Insights. *Angew. Chem. Int. Ed.* **2012**, *51*, 9674-9678. DOI: 10.1002/anie.201205276.

(245) (a) Shamshina, J. L.; Snowden, T. S. Convergent synthesis of potent COX-2 inhibitor inotilone. *Tetrahedron Lett.* **2007**, *48*, 3767-3769. DOI: 10.1016/j.tetlet.2007.03.166. (b) Inagaki, S.; Saito, K.; Suto, S.; Aihara, H.; Sugawara, A.; Tamura, S.; Kawano, T. Synthesis of 5-Aryl-3(2H)-furanones Using Intramolecular Cyclization of Sulfonium Salts. *J. Org. Chem.* **2018**, *83*, 13834-13846. DOI: 10.1021/acs.joc.8b02153.

(246) Choi, H. Y.; Chi, D. Y. Nonselective Bromination−Selective Debromination Strategy: Selective Bromination of Unsymmetrical Ketones on Singly Activated Carbon against Doubly Activated Carbon. *Org. Lett.* **2003**, *5*, 411-414. DOI: 10.1021/ol0271638.

(247) (a) Dang, H. T.; Nguyen, V. T.; Nguyen, V. D.; Arman, H. D.; Larionov, O. V. Efficient synthesis of 3-sulfolenes from allylic alcohols and 1,3-dienes enabled by sodium metabisulfite as a sulfur dioxide equivalent. *Org. Biomol. Chem.* **2018**, *16*, 3605-3609. DOI: 10.1039/C8OB00745D. (b) Emmett, E. J.; Willis, M. C. The Development and Application of Sulfur Dioxide Surrogates in Synthetic Organic Chemistry. *Asian Journal of Organic Chemistry* **2015**, *4*, 602-611. DOI: 10.1002/ajoc.201500103. (c) Deeming, A. S.; Emmett, E. J.; Richards-Taylor, C. S.; Willis, M. C. Rediscovering the Chemistry of Sulfur Dioxide: New Developments in Synthesis and Catalysis. *Synthesis* **2014**, *46*, 2701-2710. DOI: 10.1055/s-0034-1379042. (d) Desimoni, G.; Faita, G.; Garau, S.; Righetti, P. Solvent effect in pericyclic reactions. X. The cheletropic reaction. *Tetrahedron* **1996**, *52*, 6241-6248. DOI: 10.1016/0040-4020(96)00279-7. (e) Suarez, D.; Sordo, T. L.; Sordo, J. A. A Comparative Analysis of the Mechanisms of Cheletropic and Diels-Alder Reactions of 1,3-Dienes with Sulfur Dioxide: Kinetic and Thermodynamic Controls. *J. Org. Chem.* **1995**, *60*, 2848-2852. DOI: 10.1021/jo00114a039. (f) Deguin, B.; Vogel, P. Hetero-Diels-Alder addition of sulfur dioxide to 1,3-dienes. Suprafaciality, regioselectivity, and stereoselectivity. *J. Am. Chem. Soc.* **1992**, *114*, 9210-9211. DOI: 10.1021/ja00049a076.

(248) Heasley, V. L.; Frye, C. L.; Gore, R. T., Jr.; Wilday, P. S. Bromination of isoprene. *J. Org. Chem.* **1968**, *33*, 2342-2345. DOI: 10.1021/jo01270a034.

(249) (a) Forgione, P.; Wilson, P. D.; Fallis, A. G. Magnesium mediated carbometallation of propargyl alcohols: direct routes to furans and furanones. *Tetrahedron Lett.* **2000**, *41*, 17-20. DOI: 10.1016/S0040-4039(99)01995-4. (b) Schwarz, K. J.; Pearson, C. M.; Cintron-Rosado, G. A.; Liu, P.; Snaddon, T. N. Traversing Steric Limitations by Cooperative Lewis Base/Palladium Catalysis: An Enantioselective Synthesis of α-Branched Esters Using 2-Substituted Allyl Electrophiles. *Angew. Chem. Int. Ed.* **2018**, *57*, 7800-7803. DOI: 10.1002/anie.201803277.

(250) (a) Jing, Y.; Sheares, V. V. Polar, Functionalized Diene-Based Materials. 1. Bulk, Solution, and Emulsion Free Radical Polymerization of 2-Cyanomethyl-1,3-butadiene. *Macromolecules* **2000**, *33*, 6255-6261. DOI: 10.1021/ma9918046. (b) Sheares, V. V. Functionalized diene monomers and polymers containing functionalized dienes and methods for their preparation. United States of America 2002.

(251) Thomas, A. F. Addition of a functionalized isoprene unit to an allyl alcohol. I. The synthesis of .beta.-sinensal and related topics. *J. Am. Chem. Soc.* **1969**, *91*, 3281-3289. DOI: 10.1021/ja01040a032.

(252) (a) Kim, D.; Shi, G.; Kim, Y.; Koo, S. Fast Assembly and High-Throughput Screening of Structure and Antioxidant Relationship of Carotenoids. *Org. Lett.* **2019**, *21*, 714-718. DOI: 10.1021/acs.orglett.8b03915. (b) Sanda, F.; Takata, T.; Endo, T. Radical Ring-Opening Polymerization of Novel Vinylcyclopropanes Designed as Low Shrinkage Monomers. Structure of the Polymer, Mechanism of the Polymerization, and Volume Change on the Polymerization. *Macromolecules* **1995**, *28*, 1346-1355. DOI: 10.1021/ma00109a003. (c) Dugstad, H.; Undheim, K. Preparation of 2-Amino-1,3-butadienes as N-Pyridine Derivatives. *Synth. Commun.* **2008**, *38*, 1846-1854. DOI: 10.1080/00397910801981672. (d) Boutefnouchet, S.; Gaboriaud-Kolar, N.; Minh, N. T.; Depauw, S.; David-Cordonnier, M.-H.; Pfeiffer, B.; Léonce, S.; Pierré, A.; Tillequin, F.; Lallemand, M.-C.; Michel, S. Synthesis, Cytotoxic Activity, and Mechanism of Action of Furo[2,3-c]acridin-6-one and Benzo[b]furo[3,2-h]acridin-6-one Analogues of Psorospermin and Acronycine. *J. Med. Chem.* **2008**, *51*, 7287-7297. DOI: 10.1021/jm8009487. (e) Bode, J. W.; Uesuka, H.; Suzuki, K. Isoxazole → Benzisoxazole Rearrangement Promoted Cascade Reactions Affording Stereodefined Polycycles. *Org. Lett.* **2003**, *5*, 395-398. DOI: 10.1021/ol0272848. (f) Pei, J.; Li, J.; Xie, Y.; Weng, J.; Ge, C.; Wang, S. Large-Scale Synthesis of (E)-4-Amino-2-Methylbut-2-en-1-ol: Key Building Block for the Synthesis of trans-Zeatin. *Asian J. Chem.* **2014**, *26*, 8155–8157. DOI: 10.14233/ajchem.2014.17644.

(253) Glassware was silylated by placing it in a dessicator containing a small quantity of TMSCl in an open beaker and evacuating until the liquid boiled. This was allowed to sit for 5 minutes before the evacuation was repeated. This procedure was repeated once more. The glassware was then removed from the dessicator and baked in an oven at 105 ºC overnight. After cooling to room temperature the silylated glassware was used in the flash vacuum pyrolysis.

(254) Spicer, C. D.; Pujari-Palmer, M.; Autefage, H.; Insley, G.; Procter, P.; Engqvist, H.; Stevens, M. M. Synthesis of Phospho-Amino Acid Analogues as Tissue Adhesive Cement Additives. *ACS Cent. Sci.* **2020**, *6*, 226-231. DOI: 10.1021/acscentsci.9b01149.

(255) Le Noble, W. J. Conditions for the Alkylation of Ambident Anions. *Synthesis* **1970**, *1970*, 1-6. DOI: 10.1055/s-1970-21573.

(256) (a) Kurz, A. L.; Beletskaya, I. P.; Macías, A.; Reutov, O. A. The ratio of C- and O-isomers in the ethylation of alkali enolates of ethyl acetaoacetate in hexamethyl-phosphoramide and dimethyl sulfoxide. *Tetrahedron Lett.* **1968**, *9*, 3679-3682. DOI: 10.1016/S0040-4039(00)89778-6. (b) Kurts, A. L.; Genkina, N. K.; Macias, A.; Beletskaya, L. P.; Reutov, O. A. Reactivity of ambident anions: Hardness of alkyl groups and symbiotic effect in alkylation of ambident anions. *Tetrahedron* **1971**, *27*, 4777-4785. DOI: 10.1016/S0040-4020(01)98183-9.

(257) Whitney, R. R.; Jaeger, D. A. The effect of crown ethers on the alkylation of a cyclic β-keto ester. *Tetrahedron* **1980**, *36*, 769-773. DOI: 10.1016/S0040-4020(01)93692-0.

(258) le Noble, W. J.; Puerta, J. E. The alkyl group effect in the alkylations of ethyl acetoacetate in dimethyl sulfoxide. *Tetrahedron Lett.* **1966**, *7*, 1087-1090. DOI: 10.1016/S0040-4039(00)70244-9.

(259) (a) Rhoads, S. J.; Hasbrouck, R. W. A kinetic study of C- and O-alkylation of some cyclic β-keto esters. *Tetrahedron* **1966**, *22*, 3557-3570. DOI: 10.1016/S0040-4020(01)92544-X. (b) Rhoads, S. J.; Holder, R. W. A comparative study of C- and O-alkylation in cyclic and acyclic β-keto ester systems. *Tetrahedron* **1969**, *25*, 5443-5450. DOI: 10.1016/S0040-4020(01)83046-5.

(260) Jackman, L. M.; Lange, B. C. Structure and reactivity of alkali metal enolates. *Tetrahedron* **1977**, *33*, 2737-2769. DOI: 10.1016/0040-4020(77)80265-2.

(261) (a) Raban, M.; Yamamoto, G. Evidence for a chelated lithium bisacetylacetonate (Li(acac)2−) complex in methanol solution. *Inorganic and Nuclear Chemistry Letters* **1976**, *12*, 949-951. DOI: 10.1016/0020-1650(76)80014-1. (b) Zaugg, H. E.; Schaefer, A. D. Cation and Solvent Effects on the Ultraviolet Spectra of Alkali Salts of Phenols and Enols. *J. Am. Chem. Soc.* **1965**, *87*, 1857-1866. DOI: 10.1021/ja01087a006.

(262) (a) Kurihara, T.; Sugizaki, M.; Kime, I.; Wada, M.; Mitsunobu, O. Stereospecific and Stereoselective Reactions. V. Alkylation of Active Methylene Compounds by the Use of Alcohols, Diethyl Azodicarboxylate, and Triphenylphosphine. *Bull. Chem. Soc. Jpn.* **1981**, *54*, 2107-2112. DOI: 10.1246/bcsj.54.2107. (b) Redman, A. M.; Dumas, J.; Scott, W. J. Preparation of 5-Substituted 3-Aminofuran-2-carboxylate Esters. *Org. Lett.* **2000**, *2*, 2061-2063. DOI: 10.1021/ol0059652.

(263) Pham, S. L.; Kim, T.; McDonald, F. E. Stereospecific Cu(I)-Catalyzed C–O Cross-Coupling Synthesis of Acyclic 1,2-Di- and Trisubstituted Vinylic Ethers from Alcohols and Vinylic Halides. *Org. Lett.* **2023**, *25*, 5297-5301. DOI: 10.1021/acs.orglett.3c01849.

(264) Battace, A.; Feuerstein, M.; Lemhadri, M.; Zair, T.; Doucet, H.; Santelli, M. Heck Reactions of α- or β-Substituted Enol Ethers with Aryl Bromides Catalysed by a Tetraphosphane/Palladium Complex – Direct Access to Acetophenone or 1-Arylpropanone Derivatives. *Eur. J. Org. Chem.* **2007**, *2007*, 3122-3132. DOI: 10.1002/ejoc.200700152.

(265) Laurenti, D.; Feuerstein, M.; Pèpe, G.; Doucet, H.; Santelli, M. A New Tetratertiary Phosphine Ligand and Its Use in Pd-Catalyzed Allylic Substitution. *J. Org. Chem.* **2001**, *66*, 1633-1637. DOI: 10.1021/jo001146j.

(266) Kohrt, J. T.; Conn, E.; Maguire, R.; Wright, S. W.; Singer, R. Expedient synthesis of novel β-ketoesters from the Mizoroki–Heck coupling of ethyl 3-ethoxyacrylate with aryl and pyridyl halides. *Tetrahedron Lett.* **2013**, *54*, 7065-7068. DOI: 10.1016/j.tetlet.2013.10.076.

(267) Littke, A. F.; Fu, G. C. A Versatile Catalyst for Heck Reactions of Aryl Chlorides and Aryl Bromides under Mild Conditions. *J. Am. Chem. Soc.* **2001**, *123*, 6989-7000. DOI: 10.1021/ja010988c.

(268) Johnson, W. S.; Semmelhack, M. F.; Sultanbawa, M. U. S.; Dolak, L. A. A new approach to steroid total synthesis. A nonenzymic biogenetic-like olefinic cyclization involving the stereospecific formation of five asymmetric centers. *J. Am. Chem. Soc.* **1968**, *90*, 2994-2996. DOI: 10.1021/ja01013a066.

(269) Sakamoto, T.; Kondo, Y.; Kashiwagi, Y.; Yamanaka, H. Palladium-Catalyzed Cross-Coupling of Aryl Iodides with Ethyl 2-Ethoxy-and 3-Ethoxyacrylate. *Heterocycles* **1988**, *27*, 257-260.

(270) (a) Fu, G. C. The Development of Versatile Methods for Palladium-Catalyzed Coupling Reactions of Aryl Electrophiles through the Use of P(t-Bu)3 and PCy3 as Ligands. *Acc. Chem. Res.* **2008**, *41*, 1555-1564. DOI: 10.1021/ar800148f. (b) Netherton, M. R.; Fu, G. C. Air-Stable Trialkylphosphonium Salts: Simple, Practical, and Versatile Replacements for Air-Sensitive Trialkylphosphines. Applications in Stoichiometric and Catalytic Processes. *Org. Lett.* **2001**, *3*, 4295-4298. DOI: 10.1021/ol016971g.

(271) (a) Jeffery, T.; David, M. [Pd/Base/QX] catalyst systems for directing Heck-type reactions. *Tetrahedron Lett.* **1998**, *39*, 5751-5754. DOI: 10.1016/S0040-4039(98)01135-6. (b) Fearnley, S. P.; Lory, P. Vinylsilane-mediated synthesis of styryl-lactone frameworks. *Tetrahedron* **2016**, *72*, 1161-1167. DOI: 10.1016/j.tet.2016.01.003. (c) Lei, L.; Zou, P.-S.; Wang, Z.-X.; Liang, C.; Hou, C.; Mo, D.-L. Palladacycle-Catalyzed Regioselective Heck Reaction Using Diaryliodonium Triflates and Aryl Iodides. *Org. Lett.* **2022**, *24*, 663-667. DOI: 10.1021/acs.orglett.1c04120.

(272) Kurandina, D.; Parasram, M.; Gevorgyan, V. Visible Light-Induced Room-Temperature Heck Reaction of Functionalized Alkyl Halides with Vinyl Arenes/Heteroarenes. *Angew. Chem. Int. Ed.* **2017**, *56*, 14212-14216. DOI: 10.1002/anie.201706554.

(273) Corma, A.; Ruiz, V. R.; Leyva-Pérez, A.; Sabater, M. J. Regio- and Stereoselective Intermolecular Hydroalkoxylation of Alkynes Catalysed by Cationic Gold(I) Complexes. *Adv. Synth. Catal.* **2010**, *352*, 1701-1710. DOI: 10.1002/adsc.201000094.

(274) (a) Davey, A. E.; Taylor, R. J. K. A novel 1,3-dithiane-based cyclopenta-annellation procedure: synthesis of the rocaglamide skeleton. *J. Chem. Soc., Chem. Commun.* **1987**, 25-27. DOI: 10.1039/C39870000025. (b) Dong, N.; Li, X.; Wang, F.; Cheng, J.-P. Asymmetric Michael-Aldol Tandem Reaction of 2-Substituted Benzofuran-3-ones and Enones: A Facile Synthesis of Griseofulvin Analogues. *Org. Lett.* **2013**, *15*, 4896-4899. DOI: 10.1021/ol402346c. (c) Liu, W.; Ali, S. Z.; Ammann, S. E.; White, M. C. Asymmetric Allylic C–H Alkylation via Palladium(II)/cis-ArSOX Catalysis. *J. Am. Chem. Soc.* **2018**, *140*, 10658-10662. DOI: 10.1021/jacs.8b05668. (d) Wassereman, H. H.; Lee, G. M. The chemistry of vicinal tricarbonyls. A new synthesis of substituted furans. *Tetrahedron Lett.* **1994**, *35*, 9783-9786. DOI: 10.1016/0040-4039(94)88385-8.

(275) (a) Vojáčková, P.; Chalupa, D.; Prieboj, J.; Nečas, M.; Švenda, J. Enantioselective Conjugate Additions of 2-Alkoxycarbonyl-3(2H)-furanones. *Org. Lett.* **2018**, *20*, 7085-7089. DOI: 10.1021/acs.orglett.8b03039. (b) Truong, P.; Xu, X.; Doyle, M. P. An efficient methodology to substituted furans via oxidation of functionalized α-diazo-β-ketoacetates. *Tetrahedron Lett.* **2011**, *52*, 2093-2096. DOI: 10.1016/j.tetlet.2010.11.166.

(276) Yamamoto, M. Syntheses with carbanions derived from carbonyl-stabilized sulphonium ylides: a novel route to furan-3(2H)-ones. *J. Chem. Soc., Perkin Trans. 1* **1976**, 1688-1691. DOI: 10.1039/P19760001688.

(277) (a) Otera, J.; Danoh, N.; Nozaki, H. Novel template effects of distannoxane catalysts in highly efficient transesterification and esterification. *J. Org. Chem.* **1991**, *56*, 5307-5311. DOI: 10.1021/jo00018a019. (b) Wada, M.; Nishino, M.; Okawara, R. Preparation and properties of dialkyltin isothiocyanate derivatives. *J. Organomet. Chem.* **1965**, *3*, 70-75. DOI: 10.1016/S0022-328X(00)82737-0.

(278) (a) Schreiber, S. L.; Meyers, H. V. Synthetic studies in the brefeldin series: asymmetric enamine-enal cycloaddition and intramolecular Nozaki reactions. *J. Am. Chem. Soc.* **1988**, *110*, 5198-5200. DOI: 10.1021/ja00223a053. (b) Schreiber, S. L.; Desmaele, D.; Porco, J. A. On the use of unsymmetrically substituted furans in the furan-carbonyl photocycloaddition reaction: Synthesis of a kadsurenone-ginkgolide hybrid. *Tetrahedron Lett.* **1988**, *29*, 6689-6692. DOI: 10.1016/S0040-4039(00)82429-6.

(279) Trost, B. M.; Stiles, D. T. Total Synthesis of Spirotryprostatin B via Diastereoselective Prenylation. *Org. Lett.* **2007**, *9*, 2763-2766. DOI: 10.1021/ol070971k.

(280) Driver, T. G. 1,1,3,3-Tetrabutyl-1,3-diisothiocyanatodistannoxane. In *Encyclopedia of Reagents for Organic Synthesis*, 2009.

(281) Otera, J.; Ioka, S.; Nozaki, H. Distannoxane as reverse micelle-type catalyst: novel solvent effect on reaction rate of transesterification. *J. Org. Chem.* **1989**, *54*, 4013-4014. DOI: 10.1021/jo00278a002.

(282) (a) Kochi, J. K. Mechanisms of Organic Oxidation and Reduction by Metal Complexes. *Science* **1967**, *155*, 415-424. DOI: 10.1126/science.155.3761.415. (b) Kochi, J. K.; Bemis, A.; Jenkins, C. L. Mechanism of electron transfer oxidation of alkyl radicals by copper(II) complexes. *J. Am. Chem. Soc.* **1968**, *90*, 4616-4625. DOI: 10.1021/ja01019a018. (c) Kochi, J. K.; Bemis, A. Carbonium ions from alkyl radicals by electron transfer. *J. Am. Chem. Soc.* **1968**, *90*, 4038-4051. DOI: 10.1021/ja01017a022. (d) Jenkins, C. L.; Kochi, J. K. Homolytic and ionic mechanisms in the ligand-transfer oxidation of alkyl radicals by copper(II) halides and pseudohalides. *J. Am. Chem. Soc.* **1972**, *94*, 856-865. DOI: 10.1021/ja00758a025.

(283) (a) Kochi, J. K. The Decomposition of Peroxides Catalyzed by Copper Compounds and the Oxidation of Alkyl Radicals by Cupric Salts. *J. Am. Chem. Soc.* **1963**, *85*, 1958-1968. DOI: 10.1021/ja00896a014. (b) Kochi, J. K.; Subramanian, R. V. Kinetics of Electron-Transfer Oxidation of Alkyl Radicals by Copper(II) Complexes. *J. Am. Chem. Soc.* **1965**, *87*, 4855-4866. DOI: 10.1021/ja00949a033. (c) Jenkins, C. L.; Kochi, J. K. Solvolytic routes via alkylcopper intermediates in the electron-transfer oxidation of alkyl radicals. *J. Am. Chem. Soc.* **1972**, *94*, 843-855. DOI: 10.1021/ja00758a024.

(284) Wang, H.; Zou, Y.; Li, M.; Tang, Z.; Wang, J.; Tian, Z.; Strassner, N.; Yang, Q.; Zheng, Q.; Guo, Y.; Liu, W.; Pan, L.; Houk, K. N. A cyclase that catalyses competing 2 + 2 and 4 + 2 cycloadditions. *Nature Chemistry* **2023**, *15*, 177-184. DOI: 10.1038/s41557-022-01104-x.

(285) Zorn, K.; Back, C. R.; Barringer, R.; Chadimová, V.; Manzo-Ruiz, M.; Mbatha, S. Z.; Mobarec, J.-C.; Williams, S. E.; van der Kamp, M. W.; Race, P. R.; Willis, C. L.; Hayes, M. A. Interrogation of an Enzyme Library Reveals the Catalytic Plasticity of Naturally Evolved [4+2] Cyclases. *ChemBioChem* **2023**, *24*, e202300382. DOI: 10.1002/cbic.202300382.

(286) Asahara, H.; Mochizuki, E.; Oshima, T. Conformational analysis in the reversible intramolecular [2+2] photocycloaddition of diphenylbicyclo[4.2.0]oct-3-ene-2,5-diones. *Tetrahedron Lett.* **2006**, *47*, 7881-7884. DOI: 10.1016/j.tetlet.2006.09.013.

(287) Bakanas, I.; Tang, J. C.; Sarpong, R. Skeletal diversification by C–C cleavage to access bicyclic frameworks from a common tricyclooctane intermediate. *Chem. Commun.* **2023**, *59*, 3858-3861. DOI: 10.1039/D3CC00945A.

(288) (a) Lau, S.; Margaretha, P. Photochemistry of 2,2-Dimethyl-2H-Furo[3,4-b]Pyran-4,7(3H, 5H)-Dione. *Helv. Chim. Acta* **1988**, *71*, 498-501. DOI: 10.1002/hlca.19880710224. (b) Gebel, R.-C.; Margaretha, P. Photochemical Synthesis and Some Reactions of 7-Oxa-and 7-Thiatricyclo[3.2.1.03,6]octan-2-ones. *Helv. Chim. Acta* **1992**, *75*, 1633-1638. DOI: 10.1002/hlca.19920750518.

(289) Bach, T.; Kemmler, M.; Herdtweck, E. Complete Control of Regioselectivity in the Intramolecular [2 + 2] Photocycloaddition of 2-Alkenyl-3(2H)-furanones by the Length of the Side Chain. *J. Org. Chem.* **2003**, *68*, 1994-1997. DOI: 10.1021/jo0264372.

(290) (a) Gowda, G.; McMurry, T. B. H. Photochemistry of substituted cyclic enones. Part 2. 5-[Prop-2-enyl]cyclopentenones. *J. Chem. Soc., Perkin Trans. 1* **1980**, 1516-1522. DOI: 10.1039/P19800001516. (b) McMurry, T. B. H.; Work, A.; McKenna, B. Photochemistry of cyclic enones. Part 8. 5-(But-3-enyl)-3-phenylcyclopent-2-enone and 5-(pent-4-enyl)-3-phenylcyclopent-2-enone. *J. Chem. Soc., Perkin Trans. 1* **1991**, 811-816. DOI: 10.1039/P19910000811.

(291) Hetzler, B. E.; Trauner, D.; Lawrence, A. L. Natural product anticipation through synthesis. *Nat. Rev. Chem.* **2022**, *6*, 170-181. DOI: 10.1038/s41570-021-00345-7.

(292) Böttcher, T. An Additive Definition of Molecular Complexity. *Journal of Chemical Information and Modeling* **2016**, *56*, 462-470. DOI: 10.1021/acs.jcim.5b00723.

(293) Huffman, B. J.; Shenvi, R. A. Natural Products in the “Marketplace”: Interfacing Synthesis and Biology. *J. Am. Chem. Soc.* **2019**, *141*, 3332-3346. DOI: 10.1021/jacs.8b11297.

(294) Méndez-Lucio, O.; Medina-Franco, J. L. The many roles of molecular complexity in drug discovery. *Drug Discov. Today* **2017**, *22*, 120-126. DOI: 10.1016/j.drudis.2016.08.009.

(295) (a) Demoret, R. M.; Baker, M. A.; Ohtawa, M.; Chen, S.; Lam, C. C.; Khom, S.; Roberto, M.; Forli, S.; Houk, K. N.; Shenvi, R. A. Synthetic, Mechanistic, and Biological Interrogation of Ginkgo biloba Chemical Space En Route to (−)-Bilobalide. *J. Am. Chem. Soc.* **2020**, *142*, 18599-18618. DOI: 10.1021/jacs.0c08231. (b) Woo, S.; Shenvi, R. A. Natural Product Synthesis through the Lens of Informatics. *Acc. Chem. Res.* **2021**, *54*, 1157-1167. DOI: 10.1021/acs.accounts.0c00791. (c) Herzon, S. B. Emergent Properties of Natural Products. *Synlett* **2018**, *29*, 1823-1835. DOI: 10.1055/s-0037-1610242.

(296) (a) Gerry, C. J.; Hua, B. K.; Wawer, M. J.; Knowles, J. P.; Nelson Jr, S. D.; Verho, O.; Dandapani, S.; Wagner, B. K.; Clemons, P. A.; Booker-Milburn, K. I.; Boskovic, Z. V.; Schreiber, S. L. Real-Time Biological Annotation of Synthetic Compounds. *J. Am. Chem. Soc.* **2016**, *138*, 8920-8927. DOI: 10.1021/jacs.6b04614. (b) Sauer, W. H. B.; Schwarz, M. K. Molecular Shape Diversity of Combinatorial Libraries: A Prerequisite for Broad Bioactivity. *J. Chem. Inf. Comput. Sci.* **2003**, *43*, 987-1003. DOI: 10.1021/ci025599w. (c) Lee, D.; Sello, J. K.; Schreiber, S. L. Pairwise Use of Complexity-Generating Reactions in Diversity-Oriented Organic Synthesis. *Org. Lett.* **2000**, *2*, 709-712. DOI: 10.1021/ol005574n. (d) Lovering, F.; Bikker, J.; Humblet, C. Escape from Flatland: Increasing Saturation as an Approach to Improving Clinical Success. *J. Med. Chem.* **2009**, *52*, 6752-6756. DOI: 10.1021/jm901241e. (e) Singh, M.; Garza, N.; Pearson, Z.; Douglas, J.; Boskovic, Z. Broad assessment of bioactivity of a collection of spiroindane pyrrolidines through "cell painting". *Biorg. Med. Chem.* **2020**, *28*, 115547. DOI: 10.1016/j.bmc.2020.115547.

(297) An, Q.; Xing, Y.-Y.; Pu, R.; Jia, M.; Chen, Y.; Hu, A.; Zhang, S.-Q.; Yu, N.; Du, J.; Zhang, Y.; Chen, J.; Liu, W.; Hong, X.; Zuo, Z. Identification of Alkoxy Radicals as Hydrogen Atom Transfer Agents in Ce-Catalyzed C–H Functionalization. *J. Am. Chem. Soc.* **2023**, *145*, 359-376. DOI: 10.1021/jacs.2c10126.

(298) Lutz, M. D. R.; Morandi, B. Metal-Catalyzed Carbon-Carbon Bond Cleavage of Unstrained Alcohols. *Chem. Rev.* **2021**, *121*, 300-326. DOI: 10.1021/acs.chemrev.0c00154.

(299) *bottchscore*; https://github.com/forlilab/bottchscore.

(300) Arcadi, A.; Bernocchi, E.; Cacchi, S.; Marinelli, F. β-Vinyl-γ-butyrolactones via the palladium-catalysed reaction of vinyl triflates with Z-2-buten-1,4-diol. *Tetrahedron* **1991**, *47*, 1525-1540. DOI: 10.1016/S0040-4020(01)86427-9.

(301) Liu, C.; Yuan, J.; Zhang, J.; Wang, Z.; Zhang, Z.; Zhang, W. Rh-Catalyzed Asymmetric Hydrogenation of β-Branched Enol Esters for the Synthesis of β-Chiral Primary Alcohols. *Org. Lett.* **2018**, *20*, 108-111. DOI: 10.1021/acs.orglett.7b03469.

(302) Lavinda, O.; Witt, C. H.; Woerpel, K. A. Origin of High Diastereoselectivity in Reactions of Seven-Membered-Ring Enolates. *Angew. Chem. Int. Ed.* **2022**, *61*, e202114183. DOI: https://doi.org/10.1002/anie.202114183.

(303) Yvette, O. M.; Malan, S. F.; Taylor, D.; Kapp, E.; Joubert, J. Adamantane amine-linked chloroquinoline derivatives as chloroquine resistance modulating agents in Plasmodium falciparum. *Bioorg. Med. Chem. Lett.* **2018**, *28*, 1287-1291. DOI: https://doi.org/10.1016/j.bmcl.2018.03.026.

(304) Zhao, J.; Shi, J.; Li, Y. Benzyne-Mediated Esterification Reaction. *Org. Lett.* **2021**, *23*, 7274-7278. DOI: 10.1021/acs.orglett.1c02702.

(305) (a) Grieco, P. A.; Yokoyama, Y.; Gilman, S.; Ohfune, Y. Conversion of ketones into lactones with benzeneseleninic acid and hydrogen peroxide (benzeneperoxyseleninic acid): a new reagent for the Baeyer-Villiger reaction. *J. Chem. Soc., Chem. Commun.* **1977**, 870-871. DOI: 10.1039/C39770000870. (b) Olmstead, K. K.; Nickon, A. 1,2-Hydrogen shifts in thermal and photic Bamford-Stevens reactions of cyclohexanones. Activation by an endocyclic oxygen. *Tetrahedron* **1998**, *54*, 12161-12172. DOI: 10.1016/S0040-4020(98)00757-1.

(306) Lee, G. H.; Choi, E. B.; Lee, E.; Pak, C. S. Reductive Cyclization of Ketones Tethered to Activated Olefins Mediated by Magnesium in Methanol. *J. Org. Chem.* **1994**, *59*, 1428-1443. DOI: 10.1021/jo00085a036.

(307) Fusaro, M. B.; Chagnault, V.; Josse, S.; Postel, D. Metal-free oxidative lactonization of carbohydrates using molecular iodine. *Tetrahedron* **2013**, *69*, 5880-5883. DOI: https://doi.org/10.1016/j.tet.2013.05.021.

(308) Oddo, A.; Holl, R. Design and stereoselective synthesis of a C-aryl furanoside as a conformationally constrained CHIR-090 analogue. *Carbohydr. Res.* **2012**, *359*, 59-64. DOI: https://doi.org/10.1016/j.carres.2012.06.006.

(309) Guo, L.; Ma, X.; Fang, H.; Jia, X.; Huang, Z. A General and Mild Catalytic α-Alkylation of Unactivated Esters Using Alcohols. *Angew. Chem. Int. Ed.* **2015**, *54*, 4023-4027. DOI: https://doi.org/10.1002/anie.201410293.

(310) Miao, L.; Haque, I.; Manzoni, M. R.; Tham, W. S.; Chemler, S. R. Diastereo- and Enantioselective Copper-Catalyzed Intramolecular Carboamination of Alkenes for the Synthesis of Hexahydro-1H-benz[f]indoles. *Org. Lett.* **2010**, *12*, 4739-4741. DOI: 10.1021/ol102233g.

(311) Bates, R. W.; Díez-Martín, D.; Kerr, W. J.; Knight, J. G.; Ley, S. V.; Sakellaridis, A. Assessment of butene-1,4-diols as starting materials for the preparation of π-Allyltricarbonyliron complexes. *Tetrahedron* **1990**, *46*, 4063-4082. DOI: https://doi.org/10.1016/S0040-4020(01)90541-1.

(312) Margaros, I.; Montagnon, T.; Vassilikogiannakis, G. Spiroperoxy Lactones from Furans in One Pot: Synthesis of (+)-Premnalane A. *Org. Lett.* **2007**, *9*, 5585-5588. DOI: 10.1021/ol702575a.

(313) Takacs, J. M.; Newsome, P. W.; Kuehn, C.; Takusagawa, F. Catalytic iron-mediated ene carbocyclizations: formal [4+4]-ene reactions of triene esters. *Tetrahedron* **1990**, *46*, 5507-5522. DOI: https://doi.org/10.1016/S0040-4020(01)87749-8.

(314) Yang, H.; Liu, S.; Dong, H.; Huang, H.; Wang, Y.; Hao, W.; Lan, Y.; Liu, Q. Amplifying the Reactivity of Anionic Mn(I)–H Catalysts via the Cation Effect: Mechanistic Investigation and Application to the Hydrogenation of α-Trisubstituted Carboxylic Esters. *J. Am. Chem. Soc.* **2025**, *147*, 13491-13501. DOI: 10.1021/jacs.5c00362.

(315) Peters, M.; Trobe, M.; Tan, H.; Kleineweischede, R.; Breinbauer, R. A Modular Synthesis of Teraryl-Based α-Helix Mimetics, Part 1: Synthesis of Core Fragments with Two Electronically Differentiated Leaving Groups. *Chem. Eur. J.* **2013**, *19*, 2442-2449. DOI: https://doi.org/10.1002/chem.201203005.

(316) Liu, X.; Sun, B.; Xie, Z.; Qin, X.; Liu, L.; Lou, H. Manganese Dioxide–Methanesulfonic Acid Promoted Direct Dehydrogenative Alkylation of sp3 C–H Bonds Adjacent to a Heteroatom. *J. Org. Chem.* **2013**, *78*, 3104-3112. DOI: 10.1021/jo4000674.

(317) Keck, G. E.; Dougherty, S. M.; Savin, K. A. Intramolecular Allylstannane-Aldehyde Cyclizations: Stereochemical Results with Flexible Tethers for Reactions Forming Vinylcyclohexanols. *J. Am. Chem. Soc.* **1995**, *117*, 6210-6223. DOI: 10.1021/ja00128a007.

(318) Hsu, T.-W.; Hsu, H.-C.; Chan, H.-Y.; Fang, J.-M. A Terpyridine Zinc Complex for Selective Detection of Lipid Pyrophosphates: A Model System for Monitoring Bacterial O- and N-Transglycosylations. *J. Org. Chem.* **2020**, *85*, 12747-12753. DOI: 10.1021/acs.joc.0c01252.

(319) Wang, R.; Chen, J.-Z.; Zheng, X.-A.; Kong, R.; Gong, S.-S.; Sun, Q. Hafnium(IV) triflate as a potent catalyst for selective 1-O-deacetylation of peracetylated saccharides. *Carbohydr. Res.* **2018**, *455*, 114-118. DOI: https://doi.org/10.1016/j.carres.2017.11.015.

(320) Posner, G. H.; Maxwell, J. P.; Kahraman, M. Mild, Fast, and Stereoselective Epoxide Opening by Ketone Enolate Anions. Application to Synthesis of the Norlignan Curculigine. *J. Org. Chem.* **2003**, *68*, 3049-3054. DOI: 10.1021/jo020744q.

(321) Gallego, G. M.; Sarpong, R. Rh(i)-catalyzed enantioselective intramolecular hydroarylation of unactivated ketones with aryl pinacolboronic esters. *Chem. Sci.* **2012**, *3*, 1338-1342. DOI: 10.1039/C2SC01068B.

(322) Yao, Y.-X.; Zhang, H.-W.; Lu, C.-B.; Shang, H.-Y.; Tian, Y.-Y. Highly Selective and Practical Iron-Catalyzed Formal Hydrogenation of Epoxides to Primary Alcohols Using Formic Acid. *Eur. J. Org. Chem.* **2023**, *26*, e202300111. DOI: https://doi.org/10.1002/ejoc.202300111.

(323) Dondoni, A.; Marra, A.; Rojo, I.; Scherrmann, M.-C. Thiazolylketol acetates as glycosyl donors. Stereoselective synthesis of α-linked ketodisaccharides. *Tetrahedron* **1996**, *52*, 3057-3074. DOI: https://doi.org/10.1016/0040-4020(95)01095-5.

(324) Ota, E.; Wang, H.; Frye, N. L.; Knowles, R. R. A Redox Strategy for Light-Driven, Out-of-Equilibrium Isomerizations and Application to Catalytic C-C Bond Cleavage Reactions. *J. Am. Chem. Soc.* **2019**, *141*, 1457-1462. DOI: 10.1021/jacs.8b12552.

(325) Fang, W.-Y.; Zha, G.-F.; Qin, H.-L. Making Carbonyls of Amides Nucleophilic and Hydroxyls of Alcohols Electrophilic Mediated by SO2F2 for Synthesis of Esters from Amides. *Org. Lett.* **2019**, *21*, 8657-8661. DOI: 10.1021/acs.orglett.9b03274.

(326) Beckwith, A. L. J.; Raner, K. D. Stereochemistry of the reversible cyclization of .omega.-formylalkyl radicals. *J. Org. Chem.* **1992**, *57*, 4954-4962. DOI: 10.1021/jo00044a034.

(327) Stoll, E. L.; Barber, T.; Hirst, D. J.; Denton, R. M. In situ silane activation enables catalytic reduction of carboxylic acids. *Chem. Commun.* **2022**, *58*, 3509-3512. DOI: 10.1039/D1CC03396D.

(328) Chen, D.; Xu, L.; Yu, Y.; Mo, Q.; Qi, X.; Liu, C. Triflylpyridinium Enables Rapid and Scalable Controlled Reduction of Carboxylic Acids to Aldehydes using Pinacolborane. *Angew. Chem. Int. Ed.* **2023**, *62*, e202215168. DOI: https://doi.org/10.1002/anie.202215168.

(329) Griffin, J. D.; Zeller, M. A.; Nicewicz, D. A. Hydrodecarboxylation of Carboxylic and Malonic Acid Derivatives via Organic Photoredox Catalysis: Substrate Scope and Mechanistic Insight. *J. Am. Chem. Soc.* **2015**, *137*, 11340-11348. DOI: 10.1021/jacs.5b07770.

(330) Harnedy, J.; Maashi, H. A.; El Gehani, A. A. M. A.; Burns, M.; Morrill, L. C. Deconstructive Functionalization of Unstrained Cycloalkanols via Electrochemically Generated Aromatic Radical Cations. *Org. Lett.* **2023**, *25*, 1486-1490. DOI: 10.1021/acs.orglett.3c00219.

(331) Shah, J. A.; Lojko, A. E.; Tang, Z.; Lin, Y.; Scher, E. H.; Barefoot, C. A.; Lipshultz, J. M. Degradative Alcohol Functionalization by Titanocene Photocatalysis. *ACS Catal.* **2025**, *15*, 15315-15323. DOI: 10.1021/acscatal.5c04085.

(332) Moser, A. J.; Sutter, P. E.; Chavez, A. M.; Cruz, S. A.; West, J. G. Mild Hydroalkylation of Terminal Olefins Via Decatungstate/Thiol Cooperative Photocatalysis. *Org. Lett.* **2025**, *27*, 4529-4533. DOI: 10.1021/acs.orglett.5c01088.

(333) Cassani, C.; Bergonzini, G.; Wallentin, C.-J. Photocatalytic Decarboxylative Reduction of Carboxylic Acids and Its Application in Asymmetric Synthesis. *Org. Lett.* **2014**, *16*, 4228-4231. DOI: 10.1021/ol5019294.

(334) Faroux-Corlay, B.; Clary, L.; Gadras, C.; Hammache, D.; Greiner, J.; Santaella, C.; Aubertin, A.-M.; Vierling, P.; Fantini, J. Synthesis of single- and double-chain fluorocarbon and hydrocarbon galactosyl amphiphiles and their anti-HIV-1 activity. *Carbohydr. Res.* **2000**, *327*, 223-260. DOI: https://doi.org/10.1016/S0008-6215(00)00055-0.

(335) Braun, N. A.; Ousmer, M.; Bray, J. D.; Bouchu, D.; Peters, K.; Peters, E.-M.; Ciufolini, M. A. New Oxidative Transformations of Phenolic and Indolic Oxazolines: An Avenue to Useful Azaspirocyclic Building Blocks. *J. Org. Chem.* **2000**, *65*, 4397-4408. DOI: 10.1021/jo000341v.

(336) Nyfeler, E.; Renaud, P. Decarboxylative Radical Azidation Using MPDOC and MMDOC Esters. *Org. Lett.* **2008**, *10*, 985-988. DOI: 10.1021/ol702832x.

(337) Giang Luu, T.; Kim, H.-K. Visible-Light-Driven Copper-Catalyzed Synthesis of Sulfonamides from Aryl-N2BF4 through One-pot Tricomponent Reaction. *Adv. Synth. Catal.* **2023**, *365*, 1671-1677. DOI: https://doi.org/10.1002/adsc.202300197.

(338) McLean, E. B.; Mooney, D. T.; Burns, D. J.; Lee, A. L. Direct Hydrodecarboxylation of Aliphatic Carboxylic Acids: Metal- and Light-Free. *Org. Lett.* **2022**, *24*, 686-691. DOI: 10.1021/acs.orglett.1c04079.

(339) Chang, X.; Cheng, X.; Liu, X.-T.; Fu, C.; Wang, W.-Y.; Wang, C.-J. Stereodivergent Construction of 1,4-Nonadjacent Stereocenters via Hydroalkylation of Racemic Allylic Alcohols Enabled by Copper/Ruthenium Relay Catalysis. *Angew. Chem. Int. Ed.* **2022**, *61*, e202206517. DOI: https://doi.org/10.1002/anie.202206517.

(340) Mao, S.; Chen, Z.; Wang, L.; Khadka, D. B.; Xin, M.; Li, P.; Zhang, S.-Q. Synthesis of Aryl Trimethylstannane via BF3·OEt2-Mediated Cross-Coupling of Hexaalkyl Distannane Reagent with Aryl Triazene at Room Temperature. *J. Org. Chem.* **2019**, *84*, 463-471. DOI: 10.1021/acs.joc.8b02766.

(341) Lu, Y.-C.; West, J. G. Chemoselective Decarboxylative Protonation Enabled by Cooperative Earth-Abundant Element Catalysis. *Angew. Chem. Int. Ed.* **2022**, *62*, e202213055. DOI: 10.1002/anie.202213055.

(342) Ojha, D. P.; Gadde, K.; Prabhu, K. R. Generation of Hydrogen from Water: A Pd-Catalyzed Reduction of Water Using Diboron Reagent at Ambient Conditions. *Org. Lett.* **2016**, *18*, 5062-5065. DOI: 10.1021/acs.orglett.6b02508.

(343) Saget, T.; König, B. Photocatalytic Synthesis of Polycyclic Indolones. *Chem. Eur. J.* **2020**, *26*, 7004-7007. DOI: https://doi.org/10.1002/chem.202001324.

(344) Laha, J. K.; Dayal, N. A Tandem Approach to Functionalized Carbazoles from Indoles via Two Successive Regioselective Oxidative Heck Reactions Followed by Thermal Electrocyclization. *Org. Lett.* **2015**, *17*, 4742-4745. DOI: 10.1021/acs.orglett.5b02265.

(345) Zhao, L.; Huang, G.; Guo, B.; Xu, L.; Chen, J.; Cao, W.; Zhao, G.; Wu, X. Diastereo- and Enantioselective Propargylation of Benzofuranones Catalyzed by Pybox-Copper Complex. *Org. Lett.* **2014**, *16*, 5584-5587. DOI: 10.1021/ol502615y.

(346) Cao, J.; Thor, W.; Yang, S.; Zhang, M.; Bao, W.; Zhu, L.; Yang, W.; Cheng, Y.-K.; Lee, C.-S. Synthesis of the Tricyclic Picrotoxane Motif by an Oxidative Cascade Cyclization. *Org. Lett.* **2019**, *21*, 4896-4899. DOI: 10.1021/acs.orglett.9b01806.

(347) Rathke, M. W.; Cowan, P. J. Procedures for the acylation of diethyl malonate and ethyl acetoacetate with acid chlorides using tertiary amine bases and magnesium chloride. *J. Org. Chem.* **1985**, *50*, 2622-2624. DOI: 10.1021/jo00215a003.

(348) Brillon, D.; Deslongchamps, P. Synthesis of 11-and 12-membered rings by a direct cyclization method. *Can. J. Chem.* **1987**, *65*, 43-55. DOI: 10.1139/v87-010.

(349) Fang, W.; Presset, M.; Guérinot, A.; Bour, C.; Bezzenine-Lafollée, S.; Gandon, V. Copper (II) Triflate as Additive in Low Loading Au (I)--Catalyzed Hydroalkylation of Unactivated Alkenes. *Org. Synth* **2015**, *92*, 117-130.

(350) Craig, R. A., II; Loskot, S. A.; Mohr, J. T.; Behenna, D. C.; Harned, A. M.; Stoltz, B. M. Palladium-Catalyzed Enantioselective Decarboxylative Allylic Alkylation of Cyclopentanones. *Org. Lett.* **2015**, *17*, 5160-5163. DOI: 10.1021/acs.orglett.5b02376.

(351) Xue, F.; Seto, C. T. A Comparison of Cyclohexanone and Tetrahydro-4H-thiopyran-4-one 1,1-Dioxide as Pharmacophores for the Design of Peptide-Based Inhibitors of the Serine Protease Plasmin. *J. Org. Chem.* **2005**, *70*, 8309-8321. DOI: 10.1021/jo0508954.

(352) Piers, E.; Grierson, J. R.; Lau, C. K.; Nagakura, I. Synthesis of β-chloro, β-bromo, and β-iodo α,β-unsaturated ketones. *Can. J. Chem.* **1982**, *60*, 210-223. DOI: 10.1139/v82-033.

(353) Chen, Y.; Hu, X.-T.; Xie, X.-Y.; Li, D.; Zheng, C.-X.; Zhang, Y.-X.; Wang, W.-J.; Zhan, R.; Shao, L.-D. A Practical Approach to 6H-Indol-6-ones Enables the Formal Synthesis of γ-Lycorane. *Synthesis* **2022**, *55*, 289-296. DOI: 10.1055/a-1878-8597.

(354) Arslan, T.; Benner, S. A. Reduction of 2-substituted 3-oxoglutarates mediated by baker's yeast. Variation in enantioselectivity without corresponding variation in diastereoselectivity. *J. Org. Chem.* **1993**, *58*, 2260-2264. DOI: 10.1021/jo00060a048.

(355) Lücke, D.; Campbell, A. S.; Petzold, M.; Sarpong, R. Access to Naphthoic Acid Derivatives through an Oxabenzonorbornadiene Rearrangement. *Org. Lett.* **2023**, *25*, 7349-7353. DOI: 10.1021/acs.orglett.3c02823.

(356) Snider, B. B.; Merritt, J. E.; Dombroski, M. A.; Buckman, B. O. Solvent effects on manganese(III)-based oxidative free-radical cyclizations: ethanol and acetic acid. *J. Org. Chem.* **1991**, *56*, 5544-5553. DOI: 10.1021/jo00019a014.

(357) Helmboldt, H.; Köhler, D.; Hiersemann, M. Synthesis of the Norjatrophane Diterpene (−)-15-Acetyl-3-propionyl- 17-norcharaciol. *Org. Lett.* **2006**, *8*, 1573-1576. DOI: 10.1021/ol060115t.

(358) Li, H.; Dickschat, J. S. Enzymatic Synthesis of Diterpenoids from iso-GGPP III: A Geranylgeranyl Diphosphate Analog with a Shifted Double Bond. *Chem. Eur. J.* **2024**, *30*, e202303560. DOI: https://doi.org/10.1002/chem.202303560.

(359) Hara, R.; Furukawa, T.; Kashima, H.; Kusama, H.; Horiguchi, Y.; Kuwajima, I. Enantioselective Total Synthesis of (+)-Taxusin. *J. Am. Chem. Soc.* **1999**, *121*, 3072-3082. DOI: 10.1021/ja984250f.

(360) Young, D.; Kitching, W.; Wickham, G. Stannylation and germylation of some 4-, 5- and 6-Alkylcyclohex-2-enyl chlorides. *Aust. J. Chem.* **1984**, *37*, 1841-1862.

(361) Wang, B.; Zhang, L.; Fu, K.; Luo, Y.; Lu, W.; Tang, J. An Efficient Synthesis of 1,2,6,7-Tetrahydro-8H-indeno[5,4-b]furan-8-one. *Org. Prep. Proced. Int.* **2009**, *41*, 309-314. DOI: 10.1080/00304940903078053.

(362) Egorova, K. S.; Seitkalieva, M. M.; Posvyatenko, A. V.; Khrustalev, V. N.; Ananikov, V. P. Cytotoxic Activity of Salicylic Acid-Containing Drug Models with Ionic and Covalent Binding. *ACS Med. Chem. Lett.* **2015**, *6*, 1099-1104. DOI: 10.1021/acsmedchemlett.5b00258.

(363) Rackham, M. D.; Brannigan, J. A.; Moss, D. K.; Yu, Z.; Wilkinson, A. J.; Holder, A. A.; Tate, E. W.; Leatherbarrow, R. J. Discovery of Novel and Ligand-Efficient Inhibitors of Plasmodium falciparum and Plasmodium vivaxN-Myristoyltransferase. *J. Med. Chem.* **2013**, *56*, 371-375. DOI: 10.1021/jm301474t.

(364) Ha, M. W.; Lee, H.; Yi, H. Y.; Park, Y.; Kim, S.; Hong, S.; Lee, M.; Kim, M.-h.; Kim, T.-S.; Park, H.-g. Enantioselective Phase-Transfer Catalytic α-Benzylation and α-Allylation of α-tert-Butoxycarbonyllactones. *Adv. Synth. Catal.* **2013**, *355*, 637-642. DOI: https://doi.org/10.1002/adsc.201200976.

(365) Bai, Y.; Chen, W.; Chen, Y.; Huang, H.; Xiao, F.; Deng, G.-J. Copper-catalyzed oxidative cyclization of arylamides and β-diketones: new synthesis of 2,4,5-trisubstituted oxazoles. *RSC Advances* **2015**, *5*, 8002-8005. DOI: 10.1039/C4RA14394A.

(366) Kristensen, S. K.; Laursen, S. L. R.; Taarning, E.; Skrydstrup, T. Ex Situ Formation of Methanethiol: Application in the Gold(I)-Promoted Anti-Markovnikov Hydrothiolation of Olefins. *Angew. Chem. Int. Ed.* **2018**, *57*, 13887-13891. DOI: https://doi.org/10.1002/anie.201809051.

(367) Luque, A.; Groß, J.; Zähringer, T. J. B.; Kerzig, C.; Opatz, T. Vinylcyclopropane [3+2] Cycloaddition with Acetylenic Sulfones Based on Visible Light Photocatalysis. *Chem. Eur. J.* **2022**, *28*, e202104329. DOI: https://doi.org/10.1002/chem.202104329.

(368) Wetter, C.; Jantos, K.; Woithe, K.; Studer, A. Intermolecular Radical Addition and Addition/Cyclization Reactions of Alkoxyamines onto Nonactivated Alkenes. *Org. Lett.* **2003**, *5*, 2899-2902. DOI: 10.1021/ol034994k.

(369) Hatchard, C.; Parker, C. A. A new sensitive chemical actinometer-II. Potassium ferrioxalate as a standard chemical actinometer. *Proc. R. Soc. London, Ser. A* **1956**, *235*, 518-536. DOI: 10.1098/rspa.1956.0102.

(370) Pitre, S. P.; McTiernan, C. D.; Vine, W.; DiPucchio, R.; Grenier, M.; Scaiano, J. C. Visible-Light Actinometry and Intermittent Illumination as Convenient Tools to Study Ru(bpy)3Cl2 Mediated Photoredox Transformations. *Scientific Reports* **2015**, *5*, 16397. DOI: 10.1038/srep16397.

(371) Smith, G. L.; Reutovich, A. A.; Srivastava, A. K.; Reichard, R. E.; Welsh, C. H.; Melman, A.; Bou-Abdallah, F. Complexation of ferrous ions by ferrozine, 2,2′-bipyridine and 1,10-phenanthroline: Implication for the quantification of iron in biological systems. *J. Inorg. Biochem.* **2021**, *220*, 111460. DOI: https://doi.org/10.1016/j.jinorgbio.2021.111460.

(372) Marczenko, Z. Spectrophotometric Determination of Elements; Ellis Horwood, 1976.

(373) Fortune, W. B.; Mellon, M. G. Determination of Iron with o-Phenanthroline: A Spectrophotometric Study. *Industrial & Engineering Chemistry Analytical Edition* **1938**, *10*, 60-64. DOI: 10.1021/ac50118a004.

(374) Yin, H.; Jin, Y.; Hertzog, J. E.; Mullane, K. C.; Carroll, P. J.; Manor, B. C.; Anna, J. M.; Schelter, E. J. The Hexachlorocerate(III) Anion: A Potent, Benchtop Stable, and Readily Available Ultraviolet A Photosensitizer for Aryl Chlorides. *J. Am. Chem. Soc.* **2016**, *138*, 16266-16273. DOI: 10.1021/jacs.6b05712.

(375) Thordarson, P. Determining association constants from titration experiments in supramolecular chemistry. *Chem. Soc. Rev.* **2011**, *40*, 1305-1323. DOI: 10.1039/C0CS00062K.

(376) Wang, B.; Lu, C.; Zhang, S.-Y.; He, G.; Nack, W. A.; Chen, G. Palladium-Catalyzed Stereoretentive Olefination of Unactivated C(sp3)–H Bonds with Vinyl Iodides at Room Temperature: Synthesis of β-Vinyl α-Amino Acids. *Org. Lett.* **2014**, *16*, 6260-6263. DOI: 10.1021/ol503248f.

(377) Nájera, C.; Sansano, J. M. A general method for the synthesis of 2-alkyl substituted 1,3-dienes starting from 2-(chloromethyl)-3-tosylpropene. *Tetrahedron* **1994**, *50*, 5829-5844. DOI: https://doi.org/10.1016/S0040-4020(01)85650-7.

(378) Dang, H. T.; Nguyen, V. T.; Nguyen, V. D.; Arman, H. D.; Larionov, O. V. Efficient synthesis of 3-sulfolenes from allylic alcohols and 1,3-dienes enabled by sodium metabisulfite as a sulfur dioxide equivalent. *Org. Biomol. Chem.* **2018**, *16*, 3605-3609. DOI: 10.1039/C8OB00745D.

(379) Zhang, W.; Baudouin, E.; Cordier, M.; Frison, G.; Nay, B. One-Pot Synthesis of Metastable 2,5-Dihydrooxepines through Retro-Claisen Rearrangements: Method and Applications. *Chem. Eur. J.* **2019**, *25*, 8643-8648. DOI: https://doi.org/10.1002/chem.201901675.

(380) Guibbal, F.; Bénard, S.; Patché, J.; Meneyrol, V.; Couprie, J.; Yong-Sang, J.; Meilhac, O.; Jestin, E. Regioselectivity of thiouracil alkylation: Application to optimization of Darapladib synthesis. *Bioorg. Med. Chem. Lett.* **2018**, *28*, 787-792. DOI: https://doi.org/10.1016/j.bmcl.2017.12.052.

(381) (a) Otera, J.; Ioka, S.; Nozaki, H. Distannoxane as reverse micelle-type catalyst: novel solvent effect on reaction rate of transesterification. *J. Org. Chem.* **1989**, *54*, 4013-4014. DOI: 10.1021/jo00278a002. (b) Otera, J.; Danoh, N.; Nozaki, H. Novel template effects of distannoxane catalysts in highly efficient transesterification and esterification. *J. Org. Chem.* **1991**, *56*, 5307-5311. DOI: 10.1021/jo00018a019.

(382) Nicolaou, K. C.; Wu, T. R.; Sarlah, D.; Shaw, D. M.; Rowcliffe, E.; Burton, D. R. Total Synthesis, Revised Structure, and Biological Evaluation of Biyouyanagin A and Analogues Thereof. *J. Am. Chem. Soc.* **2008**, *130*, 11114-11121. DOI: 10.1021/ja802805c.

(383) Chowdhury, S.; Chauhan, G.; Kumar, A.; Chaturvedi, B.; Behera, C. Copper-Mediated Intramolecular Amidation/C−N-Coupling Cascade Sequence: Straightforward One-Pot Synthesis of N-Aryl γ- and δ-Lactams by Using Amino Acids as Precursors. *Eur. J. Org. Chem.* **2022**, *2022*, e202200850. DOI: https://doi.org/10.1002/ejoc.202200850.

(384) Maza, R. J.; Davenport, E.; Miralles, N.; Carbó, J. J.; Fernández, E. Transition-Metal-Free Allylic Borylation of 1,3-Dienes. *Org. Lett.* **2019**, *21*, 2251-2255. DOI: 10.1021/acs.orglett.9b00531.

(385) Zhu, Y.; Colomer, I.; Thompson, A. L.; Donohoe, T. J. HFIP Solvent Enables Alcohols To Act as Alkylating Agents in Stereoselective Heterocyclization. *J. Am. Chem. Soc.* **2019**, *141*, 6489-6493. DOI: 10.1021/jacs.9b02198.

(386) Rideau, E.; You, H.; Sidera, M.; Claridge, T. D. W.; Fletcher, S. P. Mechanistic Studies on a Cu-Catalyzed Asymmetric Allylic Alkylation with Cyclic Racemic Starting Materials. *J. Am. Chem. Soc.* **2017**, *139*, 5614-5624. DOI: 10.1021/jacs.7b02440.

(387) Morales-Serna, J. A.; García-Ríos, E.; Bernal, J.; Paleo, E.; Gaviño, R.; Cárdenas, J. Reduction of Carboxylic Acids Using Esters of Benzotriazole as High-Reactivity Intermediates. *Synthesis* **2011**, *2011*, 1375-1382. DOI: 10.1055/s-0030-1259988.

(388) Folgueiras-Amador, A. A.; Teuten, A. E.; Salam-Perez, M.; Pearce, J. E.; Denuault, G.; Pletcher, D.; Parsons, P. J.; Harrowven, D. C.; Brown, R. C. D. Cathodic Radical Cyclisation of Aryl Halides Using a Strongly-Reducing Catalytic Mediator in Flow. *Angew. Chem. Int. Ed.* **2022**, *61*, e202203694. DOI: https://doi.org/10.1002/anie.202203694.

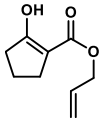
(389) Wang, B.; Zhang, L.; Fu, K.; Luo, Y.; Lu, W.; Tang, J. An Efficient Synthesis of 1, 2, 6, 7-Tetrahydro-8 H-indeno [5, 4-b] furan-8-one. *Org. Prep. Proced. Int.* **2009**, *41*, 309-314.

(390) Hitora, Y.; Takada, K.; Matsunaga, S. On the assignment of the absolute configuration at the isolated methyl branch in miyakosyne A, cytotoxic linear acetylene, from the deep-sea marine sponge Petrosia sp. *Tetrahedron* **2013**, *69*, 11070-11073. DOI: https://doi.org/10.1016/j.tet.2013.11.013.

Appendix A Computational Data

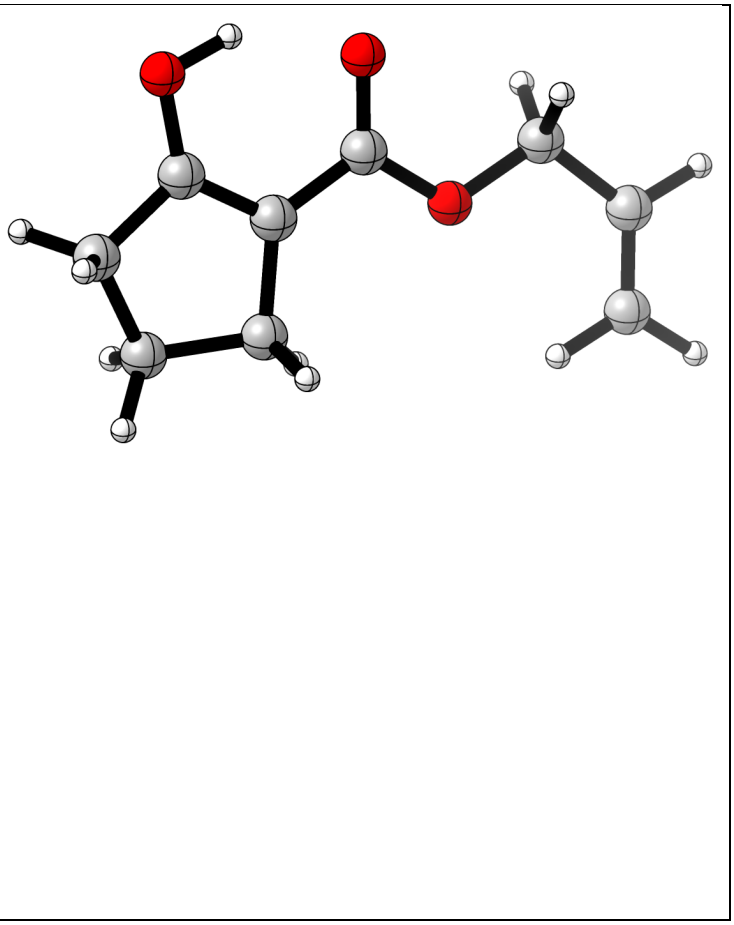
Chapter 3

SM – Ketoester 3.59a (3.59a-I)

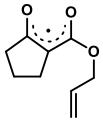


Converged?	Yes	Imaginary Frequencies	None
CBS-QB3 (0 K) =	-574.901370	CBS-QB3 Energy =	-574.889512
CBS-QB3 Enthalpy =	-574.888568	CBS-QB3 Free Energy =	-574.940614

0 1			
C	-3.31945	0.17892	-0.12355
C	-2.20399	-0.82003	-0.03822
C	-0.97836	-0.22949	0.00416
C	-1.09734	1.27573	-0.05595
C	-2.61067	1.51330	0.21508
H	-3.01043	2.35405	-0.35378
H	-2.75596	1.73688	1.27475
H	-0.80097	1.65766	-1.04048
H	-0.46718	1.78157	0.67954
C	0.21001	-1.04858	0.03199
O	0.18863	-2.28017	0.05714
O	1.36315	-0.35065	0.02976
C	2.57601	-1.12274	0.06292
C	3.76239	-0.21375	0.00028
C	3.73495	1.11047	-0.08999
H	4.65238	1.68559	-0.13101
H	2.80034	1.65580	-0.12597
H	4.71515	-0.73783	0.03420
H	2.59361	-1.72573	0.97738
H	2.57801	-1.82784	-0.77506
O	-2.46677	-2.12051	-0.04334
H	-1.59002	-2.57248	-0.00675
H	-3.73469	0.16936	-1.13901
H	-4.13879	-0.06953	0.55588

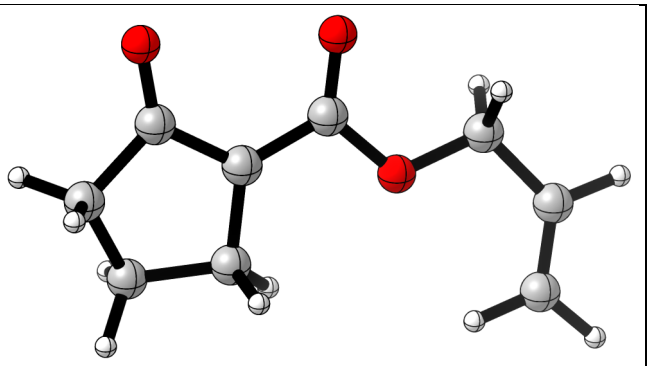


SM• – Same conformer as 3.59a-I (3.59a-II)

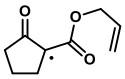


Converged?	Yes	Imaginary Frequencies	None
CBS-QB3 (0 K) =	-574.257026	CBS-QB3 Energy =	-574.244823
CBS-QB3 Enthalpy =	-574.243879	CBS-QB3 Free Energy =	-574.298201

0 2			
C	-3.38791	0.21758	-0.18902
C	-2.44771	-0.99127	-0.09867
C	-1.07700	-0.46605	0.01250
C	-1.08802	1.02460	0.01164
C	-2.55809	1.40699	0.31991
H	-2.84179	2.35648	-0.13553
H	-2.68387	1.51195	1.40093
H	-0.78548	1.38980	-0.98258
H	-0.36401	1.44802	0.71210
C	0.13100	-1.29709	0.06667
O	0.16203	-2.50275	0.13525
O	1.25019	-0.52025	0.03735
C	2.49861	-1.23021	0.09704
C	3.64326	-0.27520	-0.02326
C	3.56045	1.03874	-0.19425
H	4.45274	1.64831	-0.27284
H	2.60448	1.54251	-0.26217
H	4.61782	-0.75449	0.03953
H	2.55028	-1.78537	1.04052
H	2.52614	-1.97827	-0.70283
O	-2.79009	-2.15689	-0.13708
H	-3.66594	0.34292	-1.24250
H	-4.30710	0.02995	0.36727

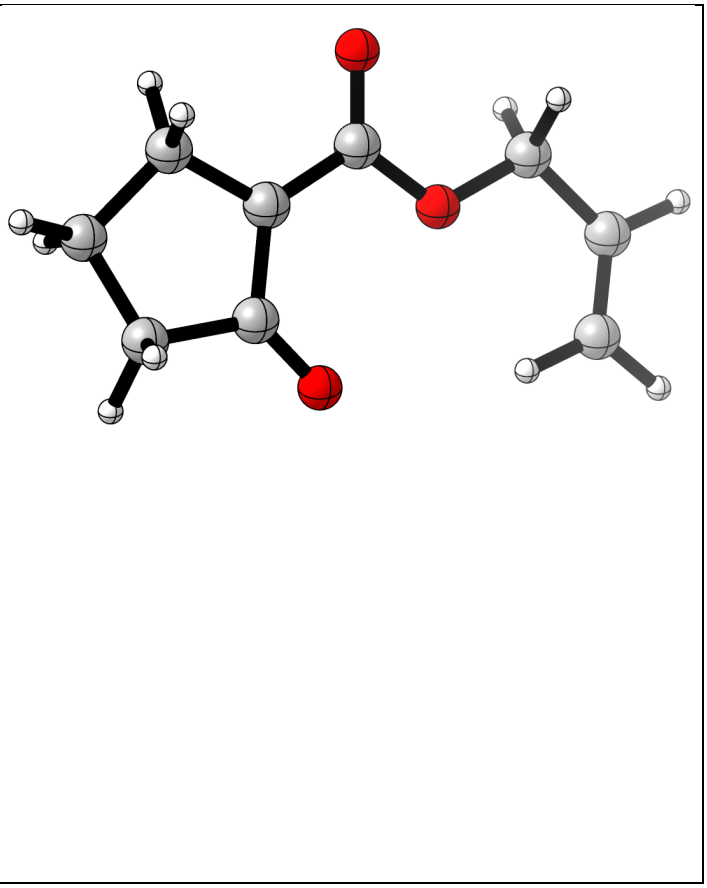


SM• – Lowest energy conformer (3.59a-III)

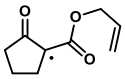


Converged?	Yes	Imaginary Frequencies	None
CBS-QB3 (0 K) =	-574.260280	CBS-QB3 Energy =	-574.248169
CBS-QB3 Enthalpy =	-574.247225	CBS-QB3 Free Energy =	-574.300909

0 2			
C	-2.73275	1.22657	-0.12949
C	-1.21204	1.04429	-0.05895
C	-0.95149	-0.40352	-0.04827
C	-2.23046	-1.16384	-0.09943
C	-3.31630	-0.13185	0.29322
H	-3.46023	-0.15304	1.37690
H	-4.28013	-0.34820	-0.16887
H	-2.20449	-2.05688	0.52975
H	-2.39092	-1.53349	-1.12486
C	0.34131	-1.10372	-0.03364
O	0.42932	-2.31587	-0.03738
O	1.39175	-0.27161	-0.01428
C	2.69595	-0.87650	0.00609
C	3.73492	0.20069	0.03526
C	3.49172	1.50628	0.04328
H	4.30637	2.22086	0.06511
H	2.47929	1.89210	0.02840
H	4.75680	-0.17186	0.05047
H	2.77500	-1.53170	0.88092
H	2.80919	-1.51690	-0.87591
O	-0.39677	1.94904	-0.03381
H	-3.04682	2.07203	0.48401
H	-2.98913	1.46703	-1.16856

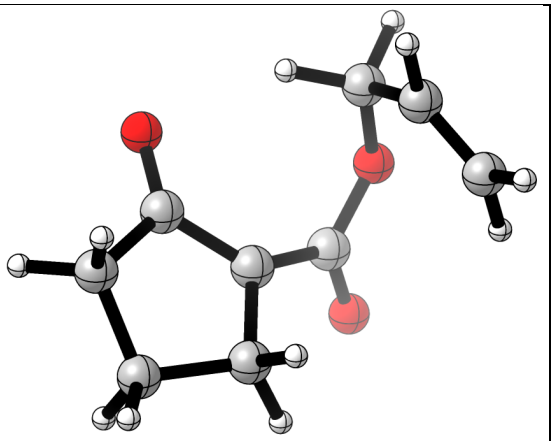


SM• – Leading to major diastereomer 5-exo (3.59a-IVa)

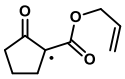


Converged?	Yes	Imaginary Frequencies	None
CBS-QB3 (0 K) =	-574.249752	CBS-QB3 Energy =	-574.237786
CBS-QB3 Enthalpy =	-574.236842	CBS-QB3 Free Energy =	-574.289633

0 2			
C	2.65878	0.62618	0.40157
C	1.23700	1.24399	0.39568
C	0.45482	0.38126	-0.54087
C	1.15650	-0.87732	-0.77808
C	2.44458	-0.85427	0.04698
H	2.27529	-1.46392	0.94328
H	3.26311	-1.31568	-0.50711
O	0.79011	-1.79729	-1.49837
C	-2.45323	-0.79402	0.70862
C	-2.11460	-0.98955	-0.74022
O	-1.85162	0.24051	-1.44311
C	-0.70676	0.93043	-1.28707
O	-0.60909	2.03124	-1.77777
H	-1.28489	-1.68437	-0.87575
H	-2.97416	-1.41172	-1.26769
H	-2.55346	-1.72333	1.26620
C	-2.65604	0.36924	1.31903
H	-2.58977	1.31385	0.79143
H	-2.91189	0.41035	2.37100
H	0.78456	1.19369	1.39796
H	1.20995	2.29229	0.09233
H	3.26147	1.10810	-0.37255
H	3.16936	0.77035	1.35451

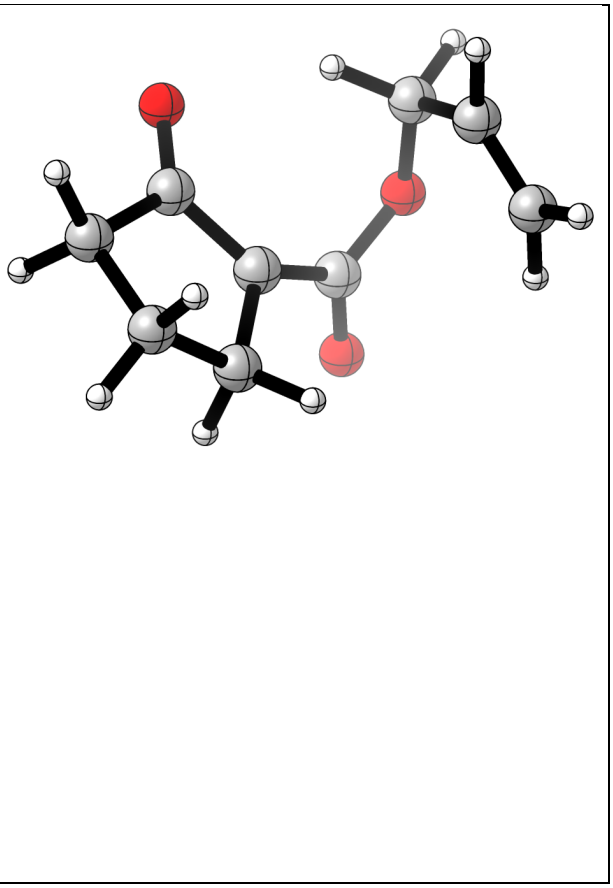


SM• – Leading to minor diastereomer 5-exo & 6-endo (3.59a-IVb)

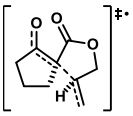


Converged?	Yes	Imaginary Frequencies	None
CBS-QB3 (0 K) =	-574.250323	CBS-QB3 Energy =	-574.238348
CBS-QB3 Enthalpy =	-574.237403	CBS-QB3 Free Energy =	-574.290245

0 2			
C	2.34148	0.46196	0.85000
C	1.24096	1.34363	0.21284
C	0.44136	0.39640	-0.62273
C	1.19955	-0.82857	-0.86161
C	2.54699	-0.68529	-0.15259
H	2.85266	-1.63419	0.29063
H	3.29443	-0.42646	-0.91224
O	0.84639	-1.79116	-1.53144
C	-2.35598	-0.83108	0.77768
C	-2.06669	-1.06991	-0.67536
O	-1.88621	0.14209	-1.43397
C	-0.76037	0.87496	-1.35383
O	-0.71648	1.95632	-1.89242
H	-1.21226	-1.73263	-0.81818
H	-2.92636	-1.54967	-1.15084
H	-2.38972	-1.74016	1.37513
C	-2.58871	0.34604	1.34961
H	-2.58870	1.26964	0.78210
H	-2.80344	0.41927	2.40899
H	0.62758	1.87694	0.94472
H	1.66812	2.11644	-0.44222
H	3.25404	1.02320	1.05402
H	1.98138	0.06224	1.80173

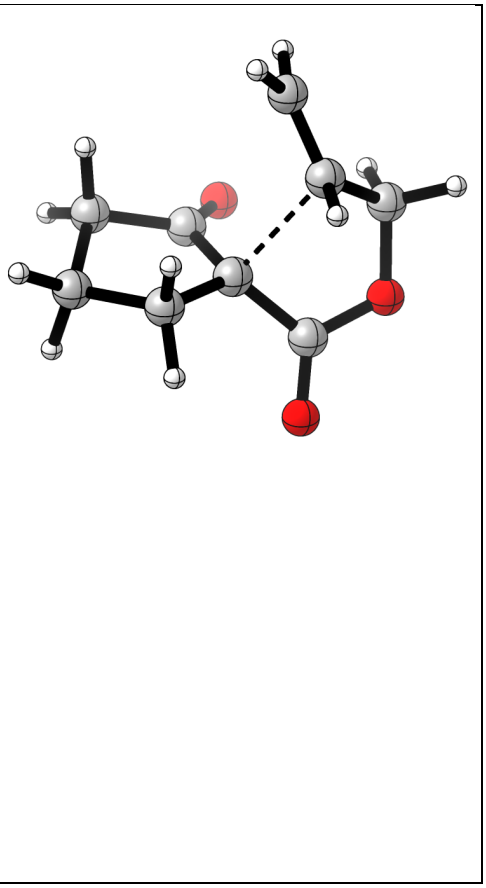


TS• – Major diastereomer 5-exo (3.59a-Va)

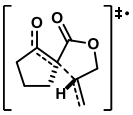


Converged?	Yes	Imaginary Frequencies	One (–474.78)
CBS-QB3 (0 K) =	-574.244078	CBS-QB3 Energy =	-574.233171
CBS-QB3 Enthalpy =	-574.232226	CBS-QB3 Free Energy =	-574.281402

0 2			
C	-2.34333	0.72623	-0.24735
C	-1.00071	0.98380	-0.98412
C	0.07191	0.66174	0.02955
C	-0.55317	-0.03480	1.19202
C	-2.00782	-0.31765	0.82753
H	-2.05067	-1.33692	0.42088
H	-2.63955	-0.29133	1.71584
O	-0.00161	-0.33839	2.23024
C	1.47322	-0.79972	-0.65711
C	2.43995	-0.33222	0.40291
O	2.38017	1.09966	0.54444
C	1.17523	1.64312	0.27670
O	1.01999	2.83521	0.23019
H	2.22267	-0.79789	1.36548
H	3.46992	-0.54984	0.11359
C	0.96021	-2.07433	-0.65623
H	0.47980	-2.48715	-1.53458
H	0.95924	-2.67932	0.24372
H	1.57434	-0.30434	-1.62109
H	-0.91431	0.32706	-1.85786
H	-0.90632	2.01200	-1.33751
H	-2.67608	1.65128	0.23053
H	-3.13307	0.40378	-0.92776

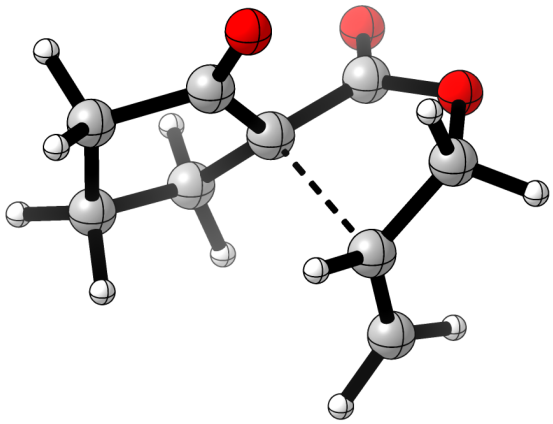


TS• – Minor diastereomer 5-exo (3.59a-Vb)

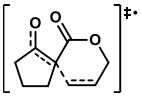


Converged?	Yes	Imaginary Frequencies	One (–454.82)
CBS-QB3 (0 K) =	-574.243877	CBS-QB3 Energy =	-574.232965
CBS-QB3 Enthalpy =	-574.232020	CBS-QB3 Free Energy =	-574.281112

0 2			
C	-2.15694	0.46305	0.54795
C	-0.89151	0.08824	1.35101
C	0.02143	-0.54671	0.33750
C	-0.80991	-1.07741	-0.77429
C	-2.25052	-0.61663	-0.54084
H	-2.71001	-0.29438	-1.47709
H	-2.81309	-1.49036	-0.19069
O	-0.42567	-1.76446	-1.70230
C	1.23346	0.88036	-0.76181
C	2.17598	-0.26793	-1.08067
O	2.33880	-1.13951	0.05862
C	1.23064	-1.29109	0.81206
O	1.23863	-1.96009	1.81176
H	1.79554	-0.85364	-1.91643
H	3.17917	0.09097	-1.31088
H	0.49907	1.11049	-1.52770
C	1.57650	1.88104	0.11305
H	2.40890	1.76991	0.79982
H	0.98002	2.78087	0.19998
H	-0.43432	0.93739	1.86425
H	-1.11531	-0.66251	2.12006
H	-3.04602	0.51507	1.17787
H	-2.02484	1.44733	0.08877

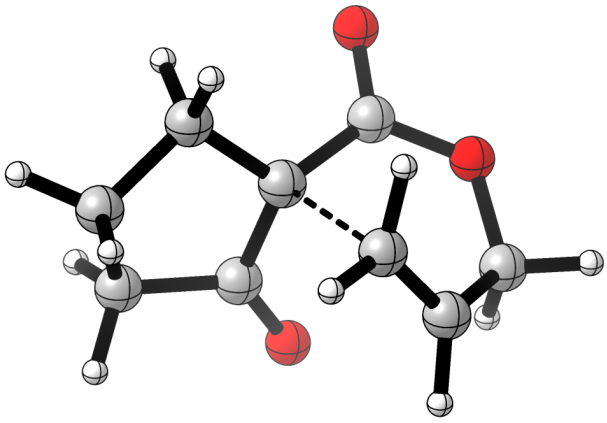


TS• – 6-endo (3.59a-Vc)

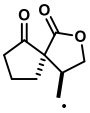


Converged?	Yes	Imaginary Frequencies	One (–496.01)
CBS-QB3 (0 K) =	-574.234013	CBS-QB3 Energy =	-574.223258
CBS-QB3 Enthalpy =	-574.222313	CBS-QB3 Free Energy =	-574.270949

0 2			
C	-0.05278	0.55280	-0.18217
C	0.95848	-0.49840	1.44797
C	1.80013	-1.24060	0.66355
C	2.67323	-0.59156	-0.36057
O	2.38892	0.80369	-0.58632
C	1.14712	1.35636	-0.57861
O	1.04836	2.53108	-0.83454
H	3.73049	-0.60594	-0.07634
H	2.56349	-1.12499	-1.30689
H	1.66729	-2.31274	0.57135
H	1.23392	0.49838	1.77204
H	0.22469	-0.99623	2.07245
C	-0.57473	-0.55385	-1.02065
C	-2.09417	-0.59622	-0.85264
C	-2.38474	0.27578	0.37830
C	-1.23005	1.30116	0.39800
H	-1.44858	2.15755	-0.25160
H	-1.03120	1.71323	1.39075
H	-3.36275	0.75777	0.34116
H	-2.35810	-0.33599	1.28486
H	-2.53343	-0.16336	-1.75970
H	-2.44656	-1.62723	-0.78692
O	0.08095	-1.30069	-1.72348

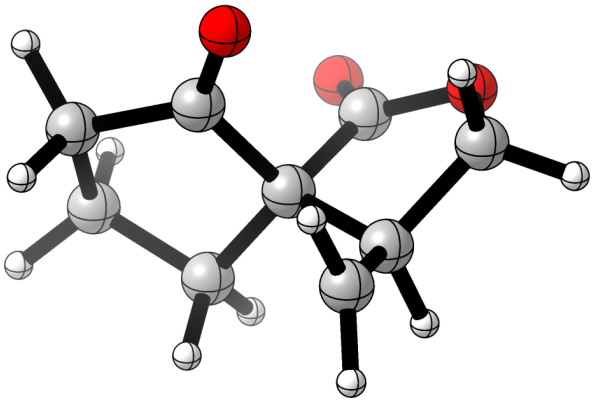


P• – Major diastereomer 5-exo (3.59a-VIa)

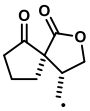


Converged?	Yes	Imaginary Frequencies	None
CBS-QB3 (0 K) =	-574.274630	CBS-QB3 Energy =	-574.263453
CBS-QB3 Enthalpy =	-574.262508	CBS-QB3 Free Energy =	-574.311870

0 2			
C	-2.32208	0.51285	-0.32459
C	-1.02323	0.40240	-1.15139
C	0.10644	0.30872	-0.11387
C	-0.57091	-0.35442	1.11884
C	-2.07505	-0.39706	0.88617
H	-2.32821	-1.44165	0.66348
H	-2.61051	-0.12429	1.79701
O	0.01747	-0.77262	2.08377
C	1.43513	-0.38665	-0.54520
C	2.44335	0.29820	0.40344
O	1.92867	1.63241	0.61842
C	0.60827	1.69312	0.33600
O	-0.03457	2.70006	0.42832
H	2.49694	-0.21253	1.36482
H	3.43832	0.39725	-0.02849
C	1.46846	-1.87012	-0.51025
H	1.59648	-2.44658	-1.41636
H	1.36159	-2.39696	0.42913
H	1.64085	-0.04199	-1.56463
H	-1.03114	-0.51653	-1.74762
H	-0.88951	1.24542	-1.83088
H	-2.45281	1.54542	0.00340
H	-3.20393	0.22554	-0.89951

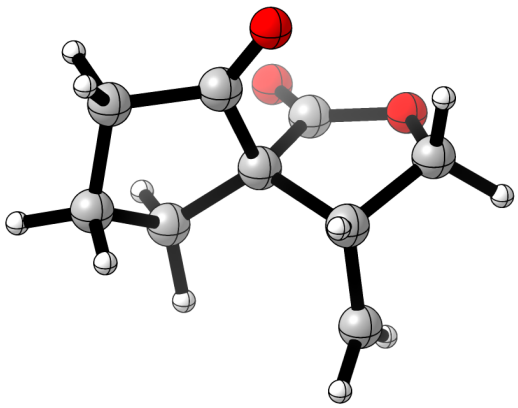


P• – Minor diastereomer 5-exo, high energy conformer (3.59a-VIb)

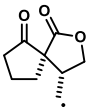


Converged?	Yes	Imaginary Frequencies	None
CBS-QB3 (0 K) =	-574.272083	CBS-QB3 Energy =	-574.260843
CBS-QB3 Enthalpy =	-574.259899	CBS-QB3 Free Energy =	-574.309930

0 2			
C	-2.19466	0.53746	0.38556
C	-0.84257	0.51627	1.12842
C	0.12628	-0.25073	0.21559
C	-0.80371	-1.13200	-0.66946
C	-2.25004	-0.82884	-0.30688
H	-2.89051	-0.89651	-1.18718
H	-2.56998	-1.60761	0.39737
O	-0.42241	-1.88962	-1.52490
C	1.10135	0.56451	-0.72009
C	2.23975	-0.47122	-0.89248
O	2.27366	-1.24049	0.32918
C	1.09577	-1.15803	0.98479
O	0.87901	-1.72519	2.01725
H	2.03673	-1.15022	-1.71991
H	3.21918	-0.01002	-1.01087
H	0.62742	0.75563	-1.68520
C	1.57488	1.84220	-0.12556
H	2.25966	1.83664	0.71503
H	1.19916	2.79672	-0.46964
H	-0.47749	1.51348	1.37823
H	-0.93828	-0.04779	2.06051
H	-3.03326	0.70798	1.06225
H	-2.20992	1.33738	-0.36199

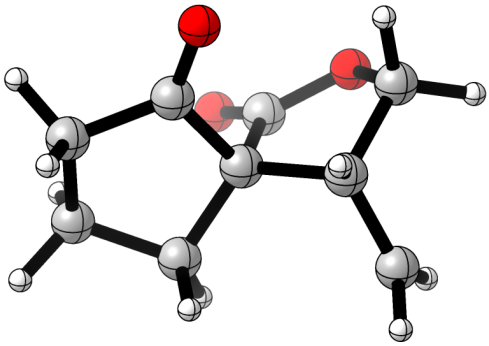


P• – Minor diastereomer, low energy conformer (3.59a-VIIb)

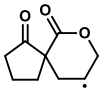


Converged?	Yes	Imaginary Frequencies	None
CBS-QB3 (0 K) =	-574.273413	CBS-QB3 Energy =	-574.262131
CBS-QB3 Enthalpy =	-574.261186	CBS-QB3 Free Energy =	-574.310992

0 2			
C	2.24075	-0.73481	0.32784
C	0.85641	-1.17083	-0.20000
C	-0.07304	0.01866	0.09665
C	0.87171	1.24933	-0.01060
C	2.31641	0.76425	0.00879
H	2.72698	0.95261	-0.99073
H	2.90408	1.35974	0.71011
O	0.50115	2.38878	-0.13488
C	-1.37059	0.22374	-0.75196
C	-2.25540	0.98951	0.25947
O	-1.85091	0.53447	1.57171
C	-0.62089	-0.02128	1.53502
O	-0.07927	-0.47229	2.50471
H	-2.08487	2.06396	0.20110
H	-3.31648	0.76743	0.15522
H	-1.14772	0.86517	-1.60740
C	-1.98931	-1.05089	-1.20842
H	-2.51481	-1.68969	-0.50753
H	-1.84795	-1.41261	-2.21830
H	0.89549	-1.33232	-1.28233
H	0.50832	-2.09496	0.26185
H	2.27848	-0.89160	1.40649
H	3.05155	-1.30637	-0.12678

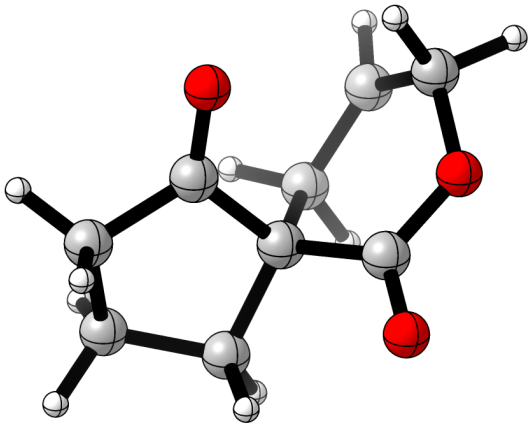


P• – 6-endo, high energy conformer (3.59a-VIc)

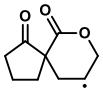


Converged?	Yes	Imaginary Frequencies	None
CBS-QB3 (0 K) =	-574.269706	CBS-QB3 Energy =	-574.258718
CBS-QB3 Enthalpy =	-574.257773	CBS-QB3 Free Energy =	-574.307198

0 2			
C	0.03320	0.38901	0.08214
C	0.68966	-0.49474	1.18222
C	1.97639	-1.08075	0.73250
C	2.72144	-0.45107	-0.38366
O	2.34446	0.92729	-0.62160
C	1.07065	1.35609	-0.50995
O	0.79657	2.47606	-0.85198
H	3.79614	-0.40991	-0.18455
H	2.57278	-0.99692	-1.32345
H	2.35450	-2.00171	1.15788
H	0.83828	0.14977	2.06412
H	-0.00700	-1.27635	1.50787
C	-0.53176	-0.54097	-1.03369
C	-2.05304	-0.46380	-1.01515
C	-2.40240	0.18068	0.33087
C	-1.21715	1.13078	0.59655
H	-1.33354	2.05095	0.02165
H	-1.12160	1.41055	1.64795
H	-3.35622	0.71012	0.31477
H	-2.47053	-0.58531	1.10971
H	-2.34365	0.18968	-1.84759
H	-2.48990	-1.44516	-1.20592
O	0.13272	-1.22429	-1.77068

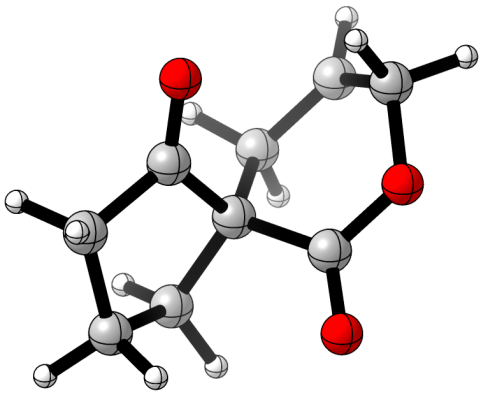


P• – 6-endo, low energy conformer (3.59a-VIIc)

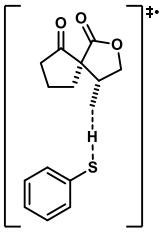


Converged?	Yes	Imaginary Frequencies	None
CBS-QB3 (0 K) =	-574.271290	CBS-QB3 Energy =	-574.260379
CBS-QB3 Enthalpy =	-574.259435	CBS-QB3 Free Energy =	-574.308543

0 2			
C	-0.00953	0.17727	0.26999
C	0.62455	1.33075	-0.53763
O	1.89143	1.17383	-0.96583
C	2.64153	-0.04431	-0.70282
C	2.36305	-0.60717	0.63749
C	1.01921	-0.43688	1.24659
H	1.07729	0.21941	2.12928
H	0.63333	-1.39420	1.62312
H	3.11388	-1.22131	1.11843
H	3.68724	0.24856	-0.81501
H	2.39589	-0.75647	-1.50057
O	0.03742	2.34969	-0.79350
C	-1.30378	0.66068	0.95407
C	-2.41639	0.52009	-0.10427
C	-2.04504	-0.75465	-0.87248
C	-0.53064	-0.88331	-0.74845
O	0.15568	-1.69820	-1.31160
H	-2.33843	-0.77012	-1.92406
H	-2.47627	-1.65146	-0.41086
H	-3.40952	0.46856	0.34506
H	-2.39022	1.38528	-0.76785
H	-1.51138	0.00315	1.80614
H	-1.20926	1.68082	1.32477

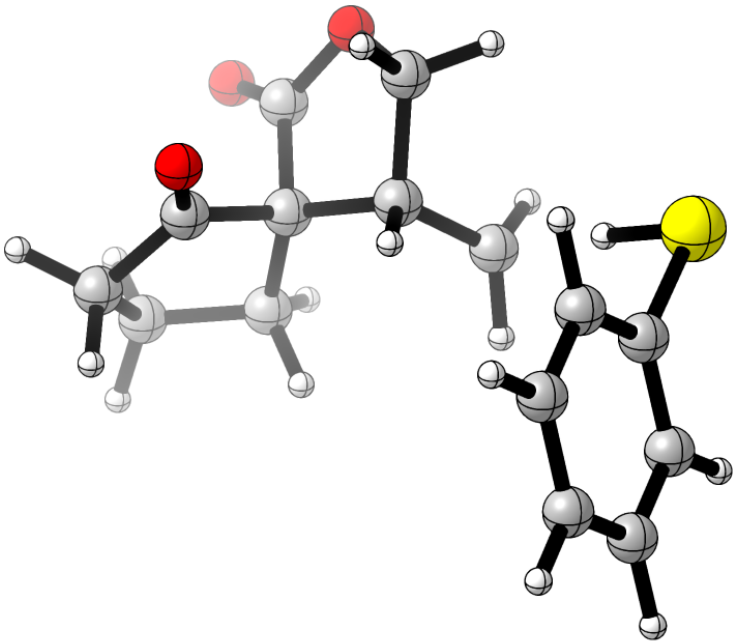


TS• – 5-exo HAT, minor diastereomer (3.59a-VIIIb)



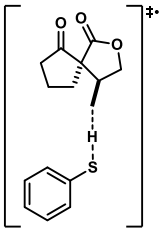
Converged?	Yes	Imaginary Frequencies	One (–361.96)
CBS-QB3 (0 K) =	-1203.819597	CBS-QB3 Energy =	-1203.801469
CBS-QB3 Enthalpy =	-1203.800525	CBS-QB3 Free Energy =	-1203.871750

0 2			
C	3.51876	1.48626	-1.10114
C	2.40803	0.45651	-1.40336
C	2.11343	-0.21544	-0.05081
C	2.38491	0.92153	0.97852
C	3.16371	2.03430	0.28747
H	2.49358	2.90058	0.23024
H	4.01630	2.33291	0.90043
O	1.99515	0.92121	2.11758
C	0.73137	-0.89370	0.20866
C	1.11317	-1.94086	1.27348
O	2.48812	-2.30433	0.99743
C	3.10035	-1.35946	0.25398
O	4.24278	-1.44273	-0.09922
H	1.06470	-1.52385	2.27817
H	0.52097	-2.85265	1.21612
H	0.03791	-0.16223	0.63091
C	0.14458	-1.50815	-1.02360
H	-0.26474	-0.85474	-1.78712
H	0.54914	-2.45192	-1.38049
H	1.50593	0.96896	-1.75398
H	2.70504	-0.26083	-2.16898
H	4.48158	0.97534	-1.06928
H	3.57232	2.26537	-1.86314
C	-3.90489	1.07661	1.48202
C	-3.34835	-0.19353	1.34881
C	-3.34875	-0.83471	0.10462
C	-3.92332	-0.19411	-0.99946
C	-4.47379	1.07757	-0.86196
C	-4.46533	1.71540	0.37760
H	-4.89897	2.70329	0.48342
H	-4.91638	1.56692	-1.72239
H	-3.94188	-0.70047	-1.95687
S	-2.67082	-2.48551	-0.05787



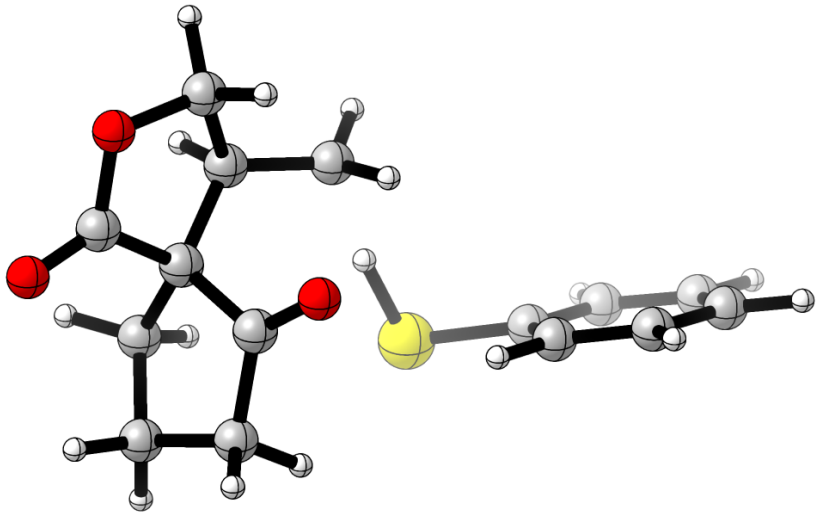
H	-1.37738	-2.09299	-0.52526	
H	-2.91648	-0.69601	2.20570	
H	-3.90078	1.56536	2.44976	

TS• – 5-exo HAT, major diastereomer (3.59a-VIIIa)



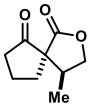
Converged?	Yes	Imaginary Frequencies	One (–478.70)
CBS-QB3 (0 K) =	-1203.821932	CBS-QB3 Energy =	-1203.803928
CBS-QB3 Enthalpy =	-1203.802984	CBS-QB3 Free Energy =	-1203.871746

0 2			
C	2.44498	2.46175	0.23745
C	2.40864	1.43656	-0.91739
C	2.32166	0.06032	-0.23034
C	1.56014	0.35933	1.09074
C	1.52487	1.86328	1.31140
H	0.48347	2.17375	1.16794
H	1.79693	2.10089	2.34168
O	1.05912	-0.48308	1.79480
C	1.74963	-1.12768	-1.04912
C	2.51898	-2.32611	-0.43574
O	3.78513	-1.79608	0.00433
C	3.72320	-0.45348	0.15961
O	4.65384	0.19885	0.53668
H	1.99449	-2.73324	0.42949
H	2.72426	-3.11679	-1.15640
C	0.27095	-1.36082	-1.05507
H	-0.15651	-1.84114	-1.92945
H	-0.20576	-1.59271	-0.10880
H	2.09956	-0.99354	-2.07825
H	1.51531	1.58827	-1.53007
H	3.28031	1.51397	-1.56925
H	3.46455	2.54198	0.61580
H	2.12229	3.45205	-0.08700
C	-5.14609	-0.38076	-0.29925
C	-4.07931	0.18100	-0.99670
C	-2.85020	0.38046	-0.35869
C	-2.69840	0.00452	0.98209
C	-3.76226	-0.57863	1.66512
C	-4.98915	-0.76690	1.03008
H	-5.81784	-1.21152	1.56920
H	-3.63358	-0.87536	2.69995
H	-1.75255	0.16222	1.48634
S	-1.51891	1.16642	-1.26029



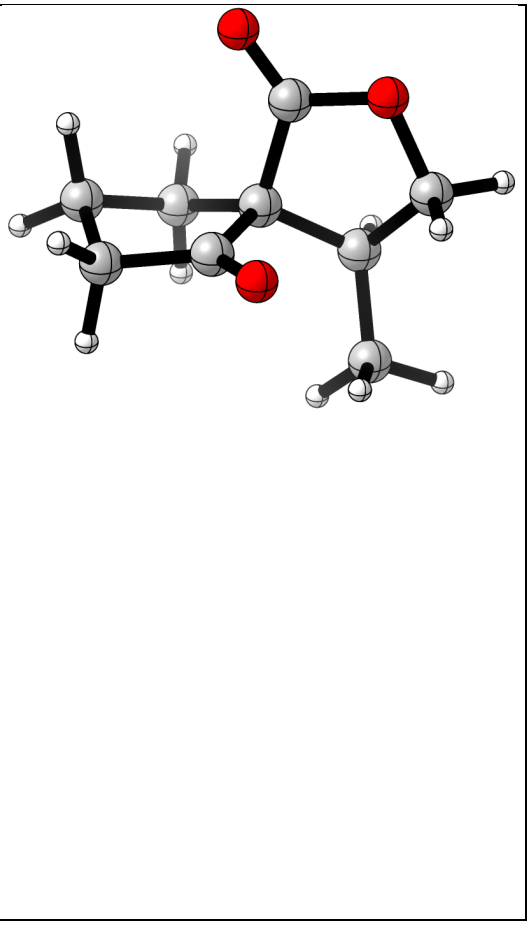
H	-0.60375	0.05206	-1.22508	
H	-4.19113	0.46566	-2.03582	
H	-6.09686	-0.52551	-0.79993	

P – 5-exo, major diastereomer (3.59a-IXa/3.60a)

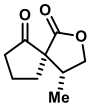


Converged?	Yes	Imaginary Frequencies	None
CBS-QB3 (0 K) =	-574.934121	CBS-QB3 Energy =	-574.923224
CBS-QB3 Enthalpy =	-574.922280	CBS-QB3 Free Energy =	-574.970423

0 1			
C	-2.41085	0.45875	-0.34821
C	-1.09663	0.38343	-1.15415
C	0.02418	0.38033	-0.10090
C	-0.63874	-0.26961	1.14670
C	-2.13683	-0.39189	0.89921
H	-2.34034	-1.45491	0.71591
H	-2.69541	-0.10900	1.79295
O	-0.04644	-0.62258	2.13542
C	1.38732	-0.23542	-0.49016
C	2.35088	0.53347	0.42283
O	1.75333	1.84012	0.60149
C	0.43329	1.80884	0.31226
O	-0.27160	2.77598	0.37521
H	2.44255	0.06160	1.40223
H	3.33877	0.68622	-0.01194
C	1.52806	-1.75436	-0.41121
H	0.81731	-2.25100	-1.07750
H	2.53080	-2.05910	-0.72427
H	1.36430	-2.11948	0.60366
H	1.57997	0.07987	-1.52331
H	-1.05440	-0.55248	-1.72267
H	-0.99430	1.20844	-1.86072
H	-2.59536	1.49496	-0.06044
H	-3.26987	0.10782	-0.92239

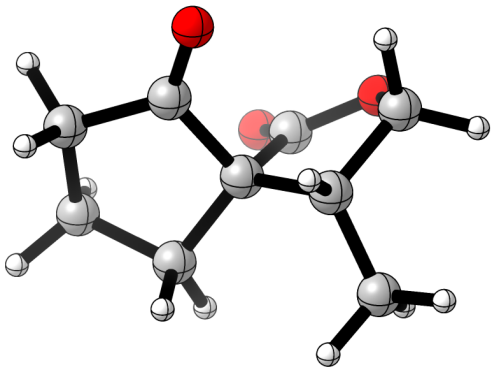


P – 5-exo, minor diastereomer (3.59a-IXb/3.60a')

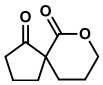


Converged?	Yes	Imaginary Frequencies	None
CBS-QB3 (0 K) =	-574.934119	CBS-QB3 Energy =	-574.923251
CBS-QB3 Enthalpy =	-574.922307	CBS-QB3 Free Energy =	-574.970480

0 1			
C	2.32561	-0.58863	0.54258
C	0.92099	-1.13828	0.21084
C	0.02235	0.10654	0.10012
C	0.99434	1.19588	-0.44116
C	2.42841	0.71001	-0.26843
H	2.82754	0.53698	-1.27520
H	3.03997	1.49301	0.18412
O	0.64826	2.23111	-0.95038
C	-1.28989	0.05614	-0.71551
C	-2.11449	1.15879	-0.02593
O	-1.67606	1.17316	1.35563
C	-0.46737	0.58559	1.48257
O	0.09644	0.47249	2.53465
H	-1.92005	2.14142	-0.45389
H	-3.18576	0.95694	-0.01742
H	-1.10231	0.33555	-1.75505
C	-1.99590	-1.30349	-0.66298
H	-2.93049	-1.26359	-1.22903
H	-1.38154	-2.09552	-1.09619
H	-2.24027	-1.58977	0.36422
H	0.93965	-1.65509	-0.75476
H	0.56585	-1.84443	0.96197
H	2.38154	-0.37105	1.60963
H	3.11320	-1.30377	0.29959

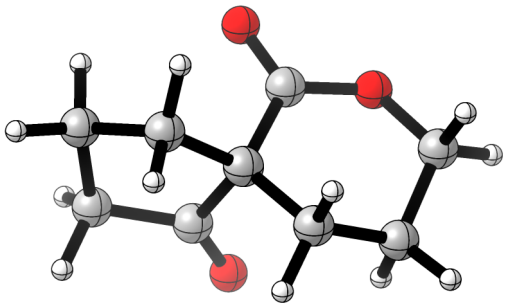


P – 6-endo (3.59a-IXc)



Converged?	Yes	Imaginary Frequencies	None
CBS-QB3 (0 K) =	-574.924887	CBS-QB3 Energy =	-574.914300
CBS-QB3 Enthalpy =	-574.913356	CBS-QB3 Free Energy =	-574.961364

0 1			
C	-0.10377	0.10304	0.15315
C	0.52037	1.28217	-0.61626
O	1.82928	1.24590	-0.94066
C	2.77981	0.36318	-0.29671
C	2.18806	-0.98235	0.06870
C	0.92825	-0.76388	0.90276
H	1.18920	-0.26163	1.84250
H	0.46792	-1.71822	1.17458
H	2.93312	-1.55318	0.63167
H	1.94231	-1.54352	-0.83432
H	3.15421	0.88324	0.59226
H	3.59817	0.27532	-1.01100
O	-0.14611	2.20893	-1.00206
C	-1.25480	0.60798	1.05539
C	-2.51457	0.67692	0.16680
C	-2.35852	-0.49838	-0.80489
C	-0.85895	-0.74134	-0.93103
O	-0.32978	-1.49332	-1.70758
H	-2.79753	-0.34803	-1.79279
H	-2.79107	-1.42300	-0.40245
H	-3.43227	0.61778	0.75505
H	-2.51820	1.61845	-0.38102
H	-1.40301	-0.12321	1.85822
H	-1.02211	1.56713	1.51970

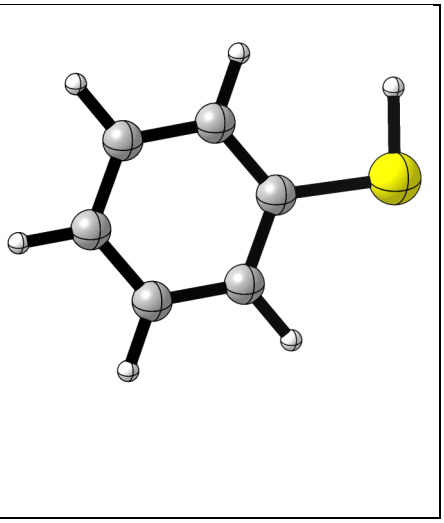


Thiophenol (PhSH)



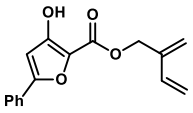
Converged?	Yes	Imaginary Frequencies	None
CBS-QB3 (0 K) =	-629.544155	CBS-QB3 Energy =	-629.537677
CBS-QB3 Enthalpy =	-629.536732	CBS-QB3 Free Energy =	-629.575414

0 1			
C	-1.01067	1.11391	-0.00008
C	0.38160	1.11822	-0.00008
C	1.08416	-0.09024	-0.00003
C	0.37778	-1.29764	-0.00001
C	-1.01347	-1.29118	-0.00006
C	-1.71556	-0.08744	-0.00009
H	-2.79910	-0.08586	-0.00011
H	-1.54913	-2.23385	-0.00006
H	0.91472	-2.23967	0.00008
S	2.86674	-0.17437	-0.00014
H	3.09067	1.14885	0.00082
H	0.91619	2.06120	-0.00015
H	-1.54394	2.05805	-0.00010



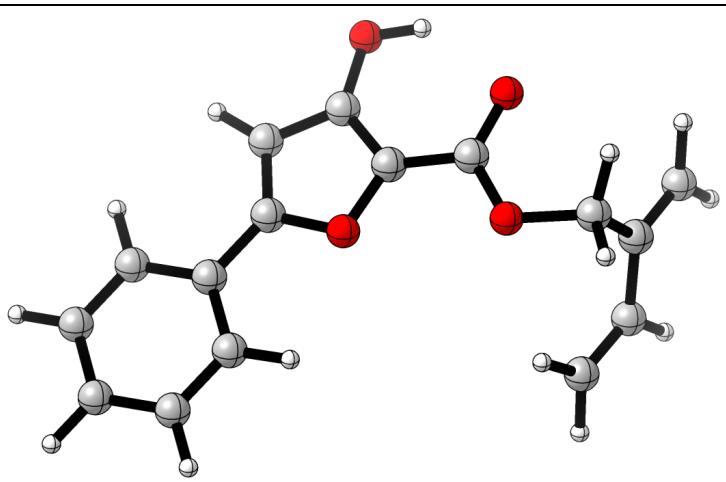
Chapter 4

Furanoate 4.13 SM (4.13-I)



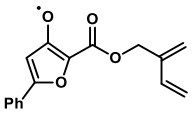
Converged?	Yes	Imaginary Frequencies	None
Zero-point correction		0.270353 (Hartree/Particle)	
Thermal correction to Energy		0.287812	
Thermal correction to Enthalpy		0.288756	
Thermal correction to Gibbs Free Energy		0.222228	
Sum of electronic and zero-point Energies		-918.224177	
Sum of electronic and thermal Energies		-918.206718	
Sum of electronic and thermal Enthalpies		-918.205774	
Sum of electronic and thermal Free Energies		-918.272303	

0 1			
C	3.55045	-0.66938	1.10071
C	4.20951	-0.99765	-0.21957
C	5.16143	-0.18434	-0.72093
H	5.43938	0.73875	-0.22154
H	5.66530	-0.41506	-1.65613
C	3.80003	-2.23122	-0.92071
C	2.78724	-3.03761	-0.54570
H	2.54532	-3.93125	-1.11210
H	2.15777	-2.81135	0.31036
H	4.37791	-2.47463	-1.81145
O	2.11381	-0.38060	0.91637
C	1.78404	0.87063	0.50924
C	0.39449	1.09351	0.22504
C	-0.15461	2.29509	-0.19176
C	-1.55801	2.08443	-0.36836
C	-1.79658	0.76187	-0.05077
O	-0.61408	0.13727	0.31506
C	-3.00577	-0.05686	-0.03288
C	-2.93183	-1.41621	0.32861
C	-4.09211	-2.19928	0.34423
C	-5.33120	-1.63540	0.00074
C	-5.40591	-0.27965	-0.35976
C	-4.24941	0.50711	-0.37678
H	-4.31259	1.55475	-0.65527
H	-6.36135	0.15984	-0.62542
H	-6.22891	-2.24438	0.01356
H	-4.03128	-3.24582	0.62306
H	-1.96927	-1.84093	0.59164
H	-2.27172	2.82419	-0.68912
O	0.50677	3.46399	-0.40029



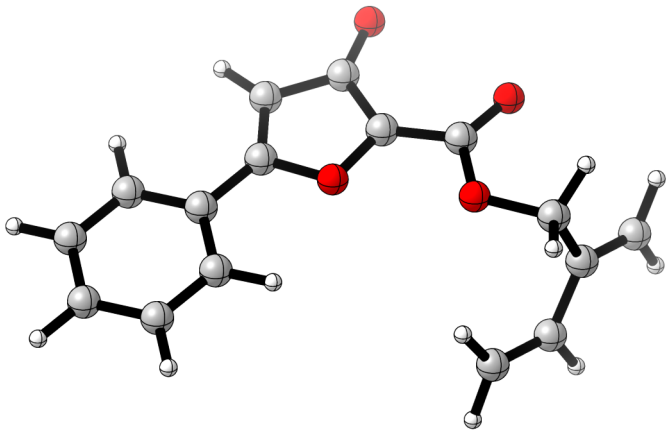
H	1.47132	3.35360	-0.21703	
O	2.61448	1.80858	0.39039	
H	4.02599	0.19380	1.57174	
H	3.55367	-1.52553	1.77731	

SM• – Same Conformer As Closed Shell (4.13-II)



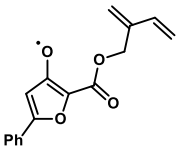
Converged?	Yes	Imaginary Frequencies	None
Zero-point correction		0.256139 (Hartree/Particle)	
Thermal correction to Energy		0.273759	
Thermal correction to Enthalpy		0.274703	
Thermal correction to Gibbs Free Energy		0.206242	
Sum of electronic and zero-point Energies		-917.582194	
Sum of electronic and thermal Energies		-917.564574	
Sum of electronic and thermal Enthalpies		-917.563630	
Sum of electronic and thermal Free Energies		-917.632091	

0 2			
C	3.40160	-0.74794	1.10859
C	4.01388	-1.15030	-0.21398
C	5.06969	-0.47086	-0.70662
H	5.47234	0.40000	-0.19845
H	5.53764	-0.75856	-1.64463
C	3.43818	-2.30667	-0.93006
C	2.32295	-2.97065	-0.56630
H	1.96264	-3.81590	-1.14396
H	1.72981	-2.67115	0.29334
H	3.97863	-2.61673	-1.82362
O	2.01715	-0.27205	0.92270
C	1.86581	1.01588	0.48254
C	0.46781	1.32703	0.18477
C	-0.16742	2.57056	-0.23691
C	-1.59294	2.22092	-0.38415
C	-1.74104	0.90794	-0.07339
O	-0.47840	0.34956	0.27980
C	-2.86489	-0.02095	-0.02617
C	-2.65643	-1.36498	0.33917
C	-3.73972	-2.25125	0.38059
C	-5.03099	-1.80482	0.05945
C	-5.23889	-0.46347	-0.30501
C	-4.16132	0.42616	-0.34805
H	-4.32476	1.46210	-0.62953
H	-6.23593	-0.11643	-0.55330
H	-5.86834	-2.49368	0.09233
H	-3.57798	-3.28606	0.66208
H	-1.65437	-1.69867	0.58491
H	-2.35593	2.91805	-0.68949
O	0.38325	3.69256	-0.42719



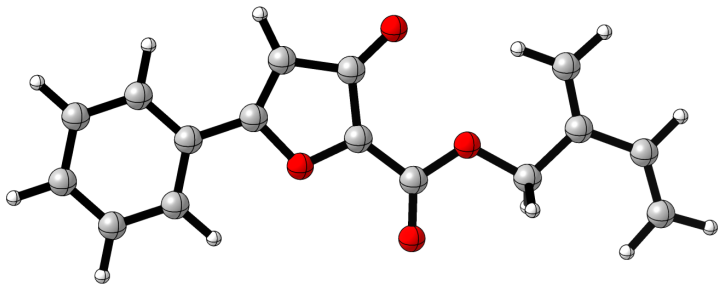
O	2.79566	1.82222	0.36173	
H	3.98704	0.04044	1.58775	
H	3.29027	-1.60144	1.77936	

SM• – Lowest Energy Conformer (4.13-III)



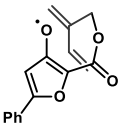
Converged?	Yes	Imaginary Frequencies	None
Zero-point correction		0.255979 (Hartree/Particle)	
Thermal correction to Energy		0.273687	
Thermal correction to Enthalpy		0.274631	
Thermal correction to Gibbs Free Energy		0.206744	
Sum of electronic and zero-point Energies		-917.584790	
Sum of electronic and thermal Energies		-917.567083	
Sum of electronic and thermal Enthalpies		-917.566138	
Sum of electronic and thermal Free Energies		-917.634025	

0 2			
C	-3.68268	-0.73213	0.00005
O	-2.40103	-0.03582	-0.00002
C	-1.26400	-0.77974	0.00007
C	-0.09005	0.09805	-0.00002
C	0.06649	1.54976	-0.00017
C	1.52594	1.75665	-0.00019
C	2.12819	0.53942	-0.00006
C	3.50946	0.07198	0.00000
C	3.78908	-1.30843	0.00019
C	5.11833	-1.74849	0.00025
C	6.17059	-0.81980	0.00013
C	5.89108	0.55774	-0.00006
C	4.56627	1.00360	-0.00012
H	4.35282	2.06831	-0.00027
H	6.70301	1.27669	-0.00015
H	7.19927	-1.16410	0.00018
H	5.33262	-2.81156	0.00040
H	2.96892	-2.01772	0.00028
O	1.13943	-0.48693	0.00005
H	1.99697	2.72585	-0.00029
O	-0.84300	2.42968	-0.00027
O	-1.22927	-2.01645	0.00020
C	-4.77235	0.31180	-0.00004
C	-4.49756	1.63158	-0.00016
H	-3.47632	1.99897	-0.00020
H	-5.30590	2.35878	-0.00023
C	-6.15834	-0.19179	0.00001
C	-6.52196	-1.49075	0.00013
H	-7.56734	-1.78036	0.00016



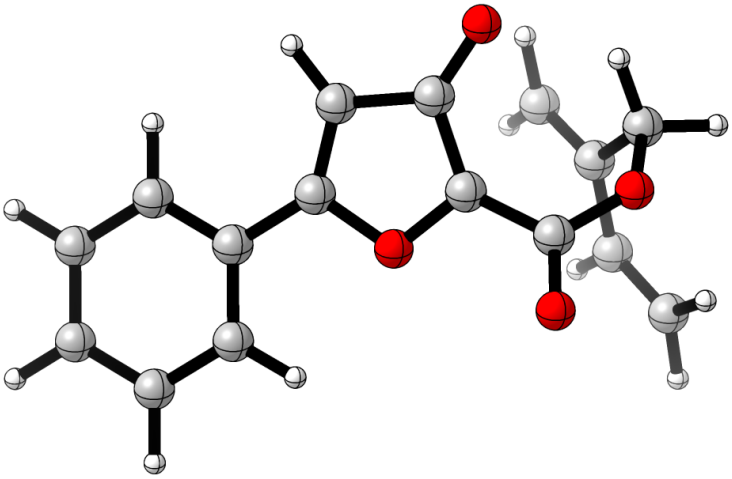
H	-5.79898	-2.30278	0.00020	
H	-6.92940	0.57687	-0.00006	
H	-3.73785	-1.37482	-0.88704	
H	-3.73785	-1.37465	0.88727	

SM• – Leading to 3-epi Hyperolactone C Pathway (4.13-IVb)



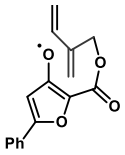
Converged?	Yes	Imaginary Frequencies	None
Zero-point correction		0.256518 (Hartree/Particle)	
Thermal correction to Energy		0.273864	
Thermal correction to Enthalpy		0.274809	
Thermal correction to Gibbs Free Energy		0.208771	
Sum of electronic and zero-point Energies		-917.577046	
Sum of electronic and thermal Energies		-917.559700	
Sum of electronic and thermal Enthalpies		-917.558756	
Sum of electronic and thermal Free Energies		-917.624794	

0 2			
C	-0.83132	0.32387	-0.85086
C	-0.66688	1.74115	-0.54693
C	0.74788	1.87801	-0.17592
C	1.32902	0.65280	-0.27222
C	2.67097	0.13092	-0.04524
C	2.95561	-1.22305	-0.30944
C	4.24781	-1.71670	-0.09275
C	5.25785	-0.86770	0.38578
C	4.97344	0.48345	0.64928
C	3.68527	0.98244	0.43569
H	3.46694	2.02590	0.64231
H	5.75310	1.14034	1.01906
H	6.25818	-1.25308	0.55183
H	4.46668	-2.75875	-0.29824
H	2.16869	-1.86899	-0.68256
O	0.36826	-0.30554	-0.69916
H	1.21209	2.80839	0.10659
O	-1.56007	2.63831	-0.60261
C	-2.76452	-0.00227	1.40850
C	-3.55121	0.53512	0.23023
O	-3.21985	-0.13287	-1.04692
C	-1.94627	-0.48080	-1.39727
O	-1.74392	-1.41650	-2.17292
H	-4.61438	0.31022	0.34142
H	-3.40706	1.60972	0.10867
C	-2.74839	-1.45749	1.66264
C	-3.36271	-2.39594	0.91346
H	-3.91662	-2.15199	0.01130
H	-3.30374	-3.44505	1.18494
H	-2.18295	-1.76336	2.54176



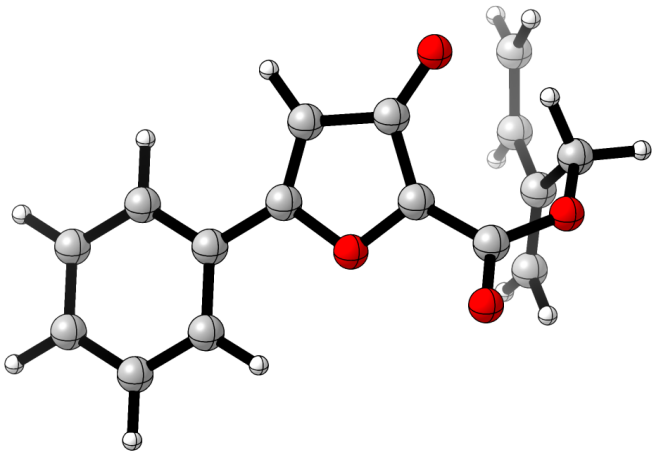
C	-2.14367	0.85733	2.24576	
H	-2.14103	1.92902	2.06425	
H	-1.63251	0.50361	3.13729	

SM• – Leading to Hyperolactone C & 6-Endo Pathway (4.13-IVa)



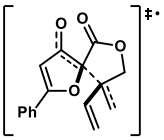
Converged?	Yes	Imaginary Frequencies	None
Zero-point correction		0.256415 (Hartree/Particle)	
Thermal correction to Energy		0.273871	
Thermal correction to Enthalpy		0.274815	
Thermal correction to Gibbs Free Energy		0.207917	
Sum of electronic and zero-point Energies		-917.575158	
Sum of electronic and thermal Energies		-917.557703	
Sum of electronic and thermal Enthalpies		-917.556759	
Sum of electronic and thermal Free Energies		-917.623657	

0 2			
C	0.82655	0.68256	-0.72373
C	0.85784	-0.59336	-1.42749
C	-0.50482	-1.12279	-1.29926
C	-1.24426	-0.22107	-0.60146
C	-2.62977	-0.15353	-0.15329
C	-3.49584	-1.24160	-0.37927
C	-4.82615	-1.17569	0.04503
C	-5.30077	-0.02524	0.69844
C	-4.43832	1.05876	0.92468
C	-3.10504	0.99945	0.50132
H	-2.43165	1.83306	0.66672
H	-4.80384	1.94769	1.42691
H	-6.33345	0.02439	1.02683
H	-5.49128	-2.01418	-0.13011
H	-3.13012	-2.13271	-0.88060
O	-0.43698	0.89730	-0.25674
H	-0.82710	-2.06347	-1.71389
O	1.84659	-1.10536	-2.04052
C	1.78039	1.80740	-0.52997
O	1.39514	2.97557	-0.56561
O	3.09715	1.52144	-0.29753
C	3.54030	0.17688	0.08868
C	2.81784	-0.33563	1.32164
C	2.27880	0.50901	2.22781
H	2.32853	1.58800	2.11338
H	1.77519	0.12837	3.11180
C	2.75165	-1.79670	1.51956
C	3.14668	-2.74016	0.63995
H	3.55369	-2.50800	-0.33974



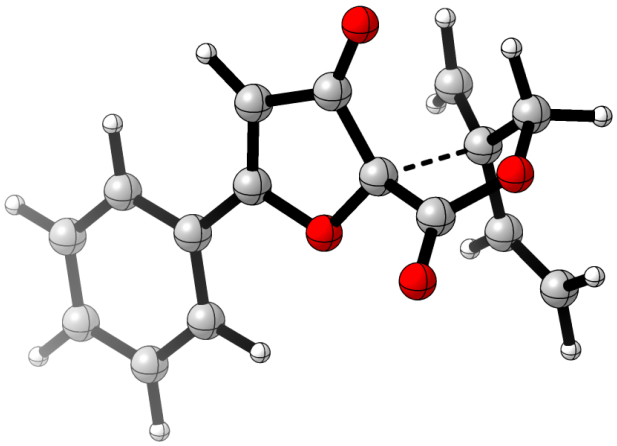
H	3.05173	-3.79361	0.88251	
H	2.33555	-2.10911	2.47637	
H	4.60433	0.30819	0.29298	
H	3.42257	-0.48993	-0.76588	

TS• – 3-epi Hyperolactone C transition state (4.13-Vb)



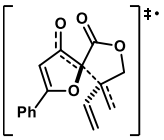
Converged?	Yes	Imaginary Frequencies	One (-598.37)
Zero-point correction			0.254852 (Hartree/Particle)
Thermal correction to Energy			0.271443
Thermal correction to Enthalpy			0.272388
Thermal correction to Gibbs Free Energy			0.209369
Sum of electronic and zero-point Energies			-917.559548
Sum of electronic and thermal Energies			-917.542957
Sum of electronic and thermal Enthalpies			-917.542012
Sum of electronic and thermal Free Energies			-917.605031

0 2			
C	-1.12132	0.31768	-0.49517
C	-0.90441	1.78643	-0.34081
C	0.53716	1.91644	-0.11723
C	1.09869	0.67832	-0.21903
C	2.46755	0.18596	-0.10225
C	3.50657	1.06173	0.26964
C	4.81735	0.58673	0.37265
C	5.09924	-0.76444	0.10687
C	4.06472	-1.63810	-0.26335
C	2.75020	-1.16794	-0.36889
H	1.94241	-1.82903	-0.66237
H	4.28279	-2.67955	-0.47282
H	6.11721	-1.13091	0.18650
H	5.61643	1.26204	0.65817
H	3.28975	2.10492	0.47855
O	0.12901	-0.30006	-0.51071
H	1.03904	2.85157	0.06940
O	-1.79914	2.66387	-0.32964
C	-2.12204	-0.20404	1.27028
C	-3.42029	0.25122	0.60559
O	-3.42658	-0.17453	-0.80196
C	-2.17570	-0.29716	-1.35980
O	-1.98281	-0.87370	-2.42142
H	-4.28630	-0.23725	1.05668
H	-3.52825	1.33722	0.64342
C	-1.82987	-1.66688	1.31016
C	-2.58887	-2.63125	0.75806
H	-3.49253	-2.41533	0.19415
H	-2.30609	-3.67467	0.84932
H	-0.91699	-1.93406	1.83949



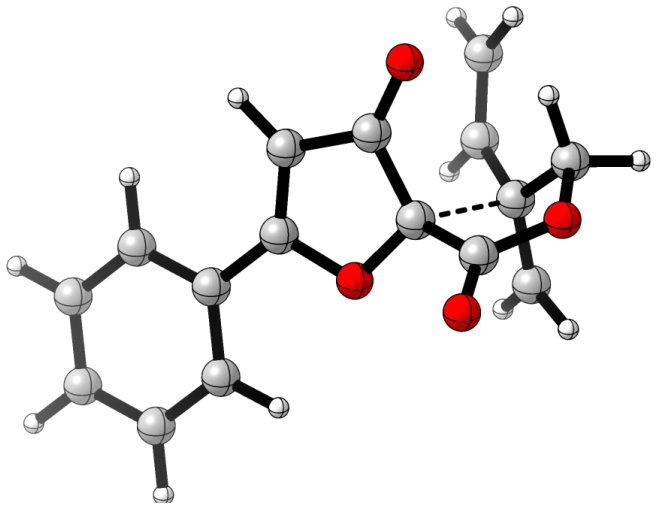
C	-1.58303	0.58606	2.28993	
H	-1.85931	1.63101	2.40004	
H	-0.83765	0.18481	2.96949	

TS• – Hyperolactone C transition state (4.13-Va)



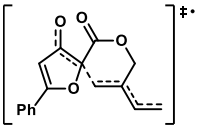
Converged?	Yes	Imaginary Frequencies	One (-586.39)
Zero-point correction			0.254683 (Hartree/Particle)
Thermal correction to Energy			0.271354
Thermal correction to Enthalpy			0.272298
Thermal correction to Gibbs Free Energy			0.209076
Sum of electronic and zero-point Energies			-917.555948
Sum of electronic and thermal Energies			-917.539277
Sum of electronic and thermal Enthalpies			-917.538333
Sum of electronic and thermal Free Energies			-917.601555

0 2			
C	-1.11260	-0.44871	-0.44248
C	-1.04710	0.77342	-1.28904
C	0.36346	1.16457	-1.25791
C	1.05166	0.23069	-0.54559
C	2.45857	0.07828	-0.18947
C	3.38686	1.08341	-0.52612
C	4.73539	0.93057	-0.19088
C	5.16654	-0.22486	0.48361
C	4.24284	-1.22695	0.81985
C	2.89112	-1.07962	0.48575
H	2.16842	-1.84965	0.73115
H	4.57570	-2.12073	1.33611
H	6.21358	-0.34205	0.74220
H	5.44858	1.70484	-0.45167
H	3.05482	1.97805	-1.04405
O	0.19505	-0.78868	-0.08099
H	0.75662	2.03881	-1.74995
O	-2.02095	1.33739	-1.84814
C	-2.22498	0.21101	1.23944
C	-3.48025	-0.06828	0.40919
O	-3.31367	-1.36796	-0.25481
C	-2.02783	-1.61442	-0.68158
O	-1.69106	-2.69452	-1.14576
H	-4.36604	-0.17156	1.03600
H	-3.63964	0.69248	-0.35595
C	-1.83316	-0.74613	2.18826
H	-1.05653	-0.52293	2.91242
H	-2.23078	-1.75709	2.16900
C	-1.82840	1.61832	1.48763
H	-0.99693	1.74171	2.18064



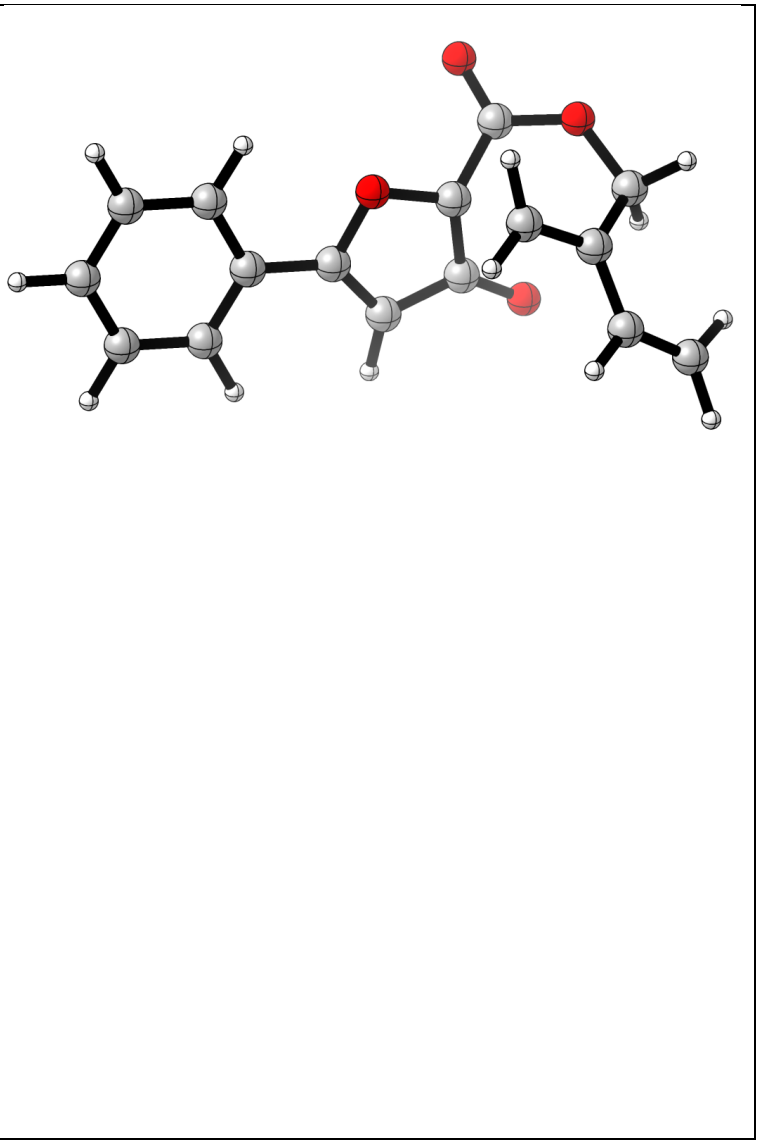
C	-2.40870	2.71090	0.95462	
H	-3.23436	2.66226	0.25208	
H	-2.04887	3.70280	1.20792	

TS• – 6-endo transition state (4.13-Vc)



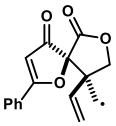
Converged?	Yes	Imaginary Frequencies	One (-515.00)
Zero-point correction			0.255450 (Hartree/Particle)
Thermal correction to Energy			0.272052
Thermal correction to Enthalpy			0.272996
Thermal correction to Gibbs Free Energy			0.209535
Sum of electronic and zero-point Energies			-917.558341
Sum of electronic and thermal Energies			-917.541738
Sum of electronic and thermal Enthalpies			-917.540794
Sum of electronic and thermal Free Energies			-917.604255

0 2			
C	0.76696	0.64538	-0.28722
C	0.85596	-0.58978	-1.09838
C	-0.50636	-1.12993	-1.09278
C	-1.30887	-0.25562	-0.42334
C	-2.73184	-0.24026	-0.10101
C	-3.54001	-1.35212	-0.41081
C	-4.90477	-1.33081	-0.10829
C	-5.47199	-0.20136	0.50692
C	-4.66781	0.90675	0.81660
C	-3.30065	0.89175	0.51473
H	-2.66966	1.74407	0.74069
H	-5.10545	1.78007	1.28775
H	-6.53123	-0.18644	0.74084
H	-5.52509	-2.18764	-0.34776
H	-3.10217	-2.22729	-0.88135
O	-0.57313	0.85754	0.03158
H	-0.79538	-2.04868	-1.57599
O	1.90195	-1.04811	-1.62685
C	1.58427	1.88930	-0.40050
O	1.08320	2.99118	-0.61095
O	2.93889	1.80160	-0.16560
C	3.67666	0.56798	0.11293
C	2.92740	-0.38133	1.02126
C	1.76789	0.05378	1.63567
H	1.60575	1.09646	1.89109
H	1.13479	-0.65965	2.15918
C	3.32317	-1.77557	1.06746
C	4.40896	-2.30251	0.44696
H	5.06756	-1.71022	-0.18166
H	4.65315	-3.35432	0.54785



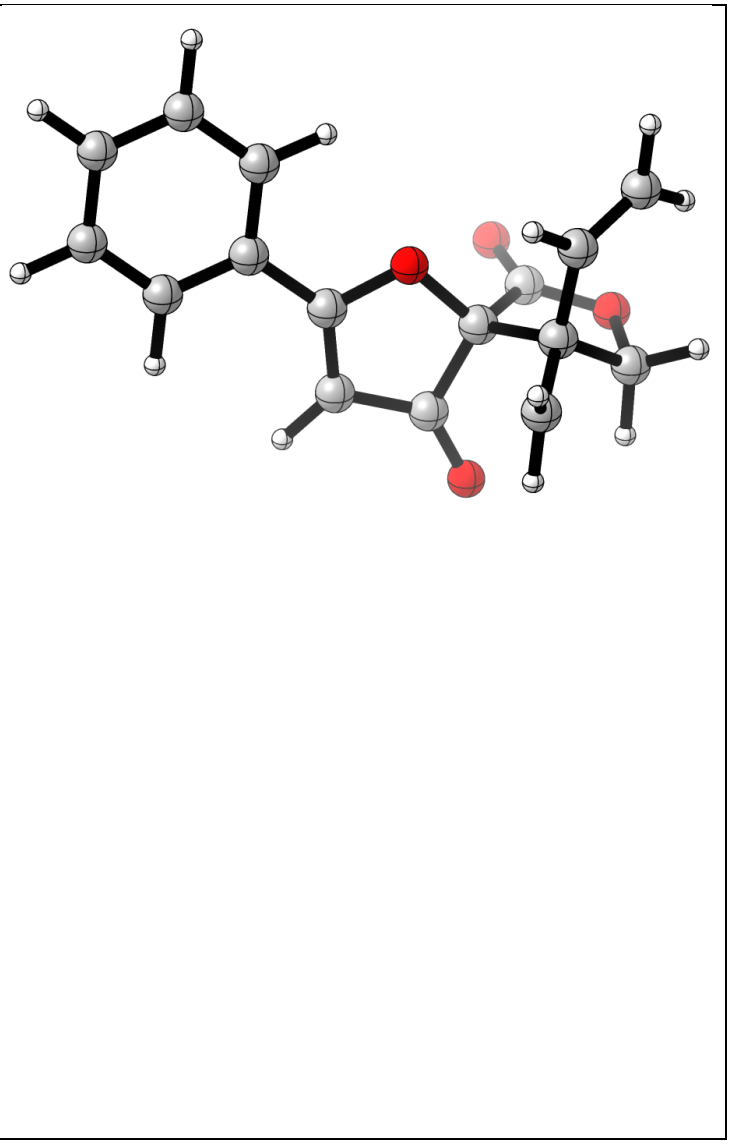
H	2.69828	-2.42401	1.67927	
H	4.61394	0.91784	0.55193	
H	3.87436	0.06827	-0.83846	

P• – 3-epi Hyperolactone C cyclized radical (4.13-VIb)



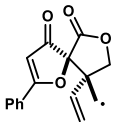
Converged?	Yes	Imaginary Frequencies	None
Zero-point correction		0.255444 (Hartree/Particle)	
Thermal correction to Energy		0.272528	
Thermal correction to Enthalpy		0.273473	
Thermal correction to Gibbs Free Energy		0.209399	
Sum of electronic and zero-point Energies		-917.584873	
Sum of electronic and thermal Energies		-917.567789	
Sum of electronic and thermal Enthalpies		-917.566845	
Sum of electronic and thermal Free Energies		-917.630918	

0 2			
C	-1.18908	-0.26518	0.11671
C	-0.89794	-1.78078	-0.02104
C	0.54992	-1.89277	-0.07467
C	1.08153	-0.63692	-0.01323
C	2.46244	-0.16238	-0.01970
C	2.73040	1.20237	0.20105
C	4.05344	1.65965	0.20336
C	5.10980	0.76139	-0.01569
C	4.84253	-0.60081	-0.23696
C	3.52339	-1.06295	-0.23911
H	3.31799	-2.11446	-0.41434
H	5.65921	-1.29382	-0.40627
H	6.13445	1.11789	-0.01277
H	4.26121	2.70941	0.37870
H	1.90295	1.88024	0.37746
O	0.10953	0.36099	0.06985
H	1.08387	-2.82631	-0.14046
O	-1.78344	-2.65155	-0.07745
C	-2.19669	0.29502	-0.94506
C	-3.52135	-0.07723	-0.22787
O	-3.24726	0.11923	1.21118
C	-1.89547	0.02990	1.45523
O	-1.37637	0.16283	2.54805
H	-4.34542	0.58220	-0.49623
H	-3.78392	-1.12448	-0.38515
C	-1.98597	1.80092	-1.04833
C	-2.69938	2.74136	-0.41107
H	-3.51342	2.50336	0.26900
H	-2.46694	3.79332	-0.54111
H	-1.15128	2.09014	-1.68435



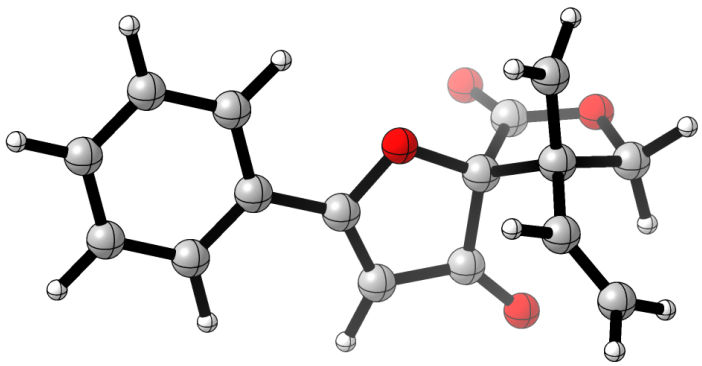
C	-2.07527	-0.35541	-2.28946	
H	-2.29644	-1.41172	-2.40799	
H	-1.77566	0.22508	-3.15445	

P• – Hyperolactone C cyclized radical (4.13-VIa)



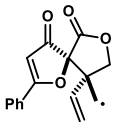
Converged?	Yes	Imaginary Frequencies	None
Zero-point correction		0.255021 (Hartree/Particle)	
Thermal correction to Energy		0.272340	
Thermal correction to Enthalpy		0.273285	
Thermal correction to Gibbs Free Energy		0.208003	
Sum of electronic and zero-point Energies		-917.582628	
Sum of electronic and thermal Energies		-917.565309	
Sum of electronic and thermal Enthalpies		-917.564364	
Sum of electronic and thermal Free Energies		-917.629646	

0 2			
C	-1.17340	-0.27137	-0.19042
C	-1.03259	0.89238	-1.20292
C	0.39398	1.17067	-1.27206
C	1.04261	0.31661	-0.42925
C	2.45867	0.14545	-0.11522
C	3.41702	1.03007	-0.64808
C	4.77080	0.85681	-0.34657
C	5.17576	-0.19949	0.48786
C	4.22199	-1.08190	1.01904
C	2.86473	-0.91248	0.72071
H	2.11606	-1.58975	1.11560
H	4.53586	-1.89916	1.65899
H	6.22717	-0.33304	0.71955
H	5.50810	1.53789	-0.75700
H	3.10553	1.84825	-1.29000
O	0.17306	-0.54058	0.25133
H	0.83335	1.92139	-1.90799
O	-1.99116	1.41598	-1.79402
C	-2.17279	0.01100	0.98529
C	-3.49314	-0.33437	0.25424
O	-3.14608	-1.50833	-0.57670
C	-1.79930	-1.50400	-0.87026
O	-1.23433	-2.34439	-1.54562
H	-4.28350	-0.64448	0.93620
H	-3.82610	0.46057	-0.41356
C	-1.92394	-0.98042	2.09574
H	-1.21890	-0.74453	2.88452
H	-2.31774	-1.99071	2.02626
C	-2.06037	1.42090	1.51857
H	-1.18447	1.58867	2.14620



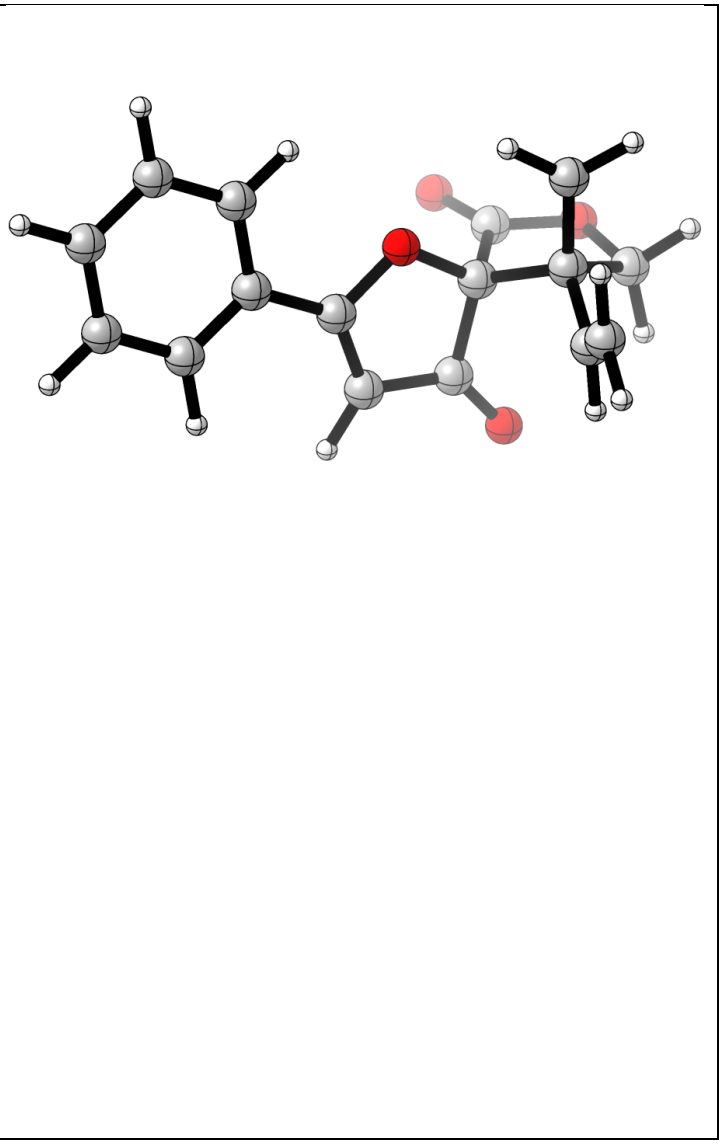
C	-2.91700	2.42861	1.29384	
H	-3.80040	2.32402	0.67112	
H	-2.74504	3.40862	1.72706	

P• – lower energy hyperolactone C cyclized radical (4.13-VIIa)



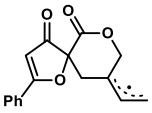
Converged?	Yes	Imaginary Frequencies	None
Zero-point correction		0.255324 (Hartree/Particle)	
Thermal correction to Energy		0.272481	
Thermal correction to Enthalpy		0.273425	
Thermal correction to Gibbs Free Energy		0.208865	
Sum of electronic and zero-point Energies		-917.585271	
Sum of electronic and thermal Energies		-917.568114	
Sum of electronic and thermal Enthalpies		-917.567170	
Sum of electronic and thermal Free Energies		-917.631730	

0 2			
C	-1.22804	-0.32837	0.00526
C	-1.03295	-0.48198	-1.52455
C	0.40144	-0.40702	-1.74102
C	1.00866	-0.19529	-0.53721
C	2.41447	-0.04853	-0.17069
C	3.40324	0.04068	-1.17032
C	4.74778	0.17411	-0.81232
C	5.11297	0.21894	0.54430
C	4.12882	0.13001	1.54142
C	2.78081	-0.00233	1.18806
H	2.00989	-0.08214	1.94590
H	4.41197	0.16012	2.58775
H	6.15721	0.32097	0.82020
H	5.50844	0.24381	-1.58201
H	3.12220	0.01185	-2.21849
O	0.10205	-0.10743	0.52030
H	0.87593	-0.51434	-2.70236
O	-1.96966	-0.63603	-2.32771
C	-2.25777	0.75577	0.43238
C	-3.56363	-0.08156	0.29626
O	-3.18455	-1.44271	0.72335
C	-1.82861	-1.62706	0.58708
O	-1.23076	-2.64851	0.87270
H	-4.35244	0.25844	0.96575
H	-3.91178	-0.13249	-0.73688
C	-2.01657	1.11460	1.87653
H	-2.84613	1.45612	2.48709
H	-1.01311	1.11188	2.28458
C	-2.27993	1.95528	-0.50001
H	-2.53524	1.73425	-1.53644



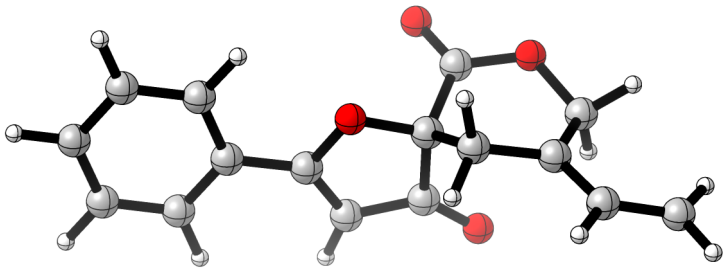
C	-2.01649	3.21746	-0.12748	
H	-1.75770	3.47158	0.89696	
H	-2.05118	4.02907	-0.84737	

P• – 6-endo cyclized radical (4.13-VIc)



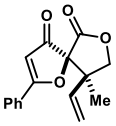
Converged?	Yes	Imaginary Frequencies	None
Zero-point correction		0.257240 (Hartree/Particle)	
Thermal correction to Energy		0.273894	
Thermal correction to Enthalpy		0.274838	
Thermal correction to Gibbs Free Energy		0.210847	
Sum of electronic and zero-point Energies		-917.610350	
Sum of electronic and thermal Energies		-917.593696	
Sum of electronic and thermal Enthalpies		-917.592752	
Sum of electronic and thermal Free Energies		-917.656743	

0 2			
C	0.83038	0.25787	0.03547
C	0.72421	-0.80104	-1.09488
C	-0.69321	-1.09957	-1.21655
C	-1.37173	-0.36598	-0.28575
C	-2.79642	-0.26491	0.01973
C	-3.71842	-1.14145	-0.58568
C	-5.08100	-1.03086	-0.29398
C	-5.53002	-0.04584	0.60275
C	-4.61204	0.82793	1.20658
C	-3.24621	0.72097	0.91873
H	-2.52437	1.39358	1.36765
H	-4.96023	1.59049	1.89445
H	-6.58810	0.03931	0.82693
H	-5.79070	-1.70611	-0.75909
H	-3.37178	-1.90662	-1.27342
O	-0.53375	0.41468	0.50641
H	-1.11005	-1.77383	-1.94624
O	1.70283	-1.24012	-1.72329
C	1.29846	1.60109	-0.55027
O	0.53054	2.46628	-0.94654
O	2.65330	1.78997	-0.56782
C	3.60292	0.68926	-0.34249
C	3.17000	-0.24872	0.75490
C	1.73253	-0.17596	1.19887
H	1.59933	0.56245	2.00289
H	1.38893	-1.14243	1.58273
C	4.06783	-1.16977	1.30999
C	5.40603	-1.30003	0.96147
H	5.87164	-0.67926	0.20166
H	6.03371	-2.04534	1.43612



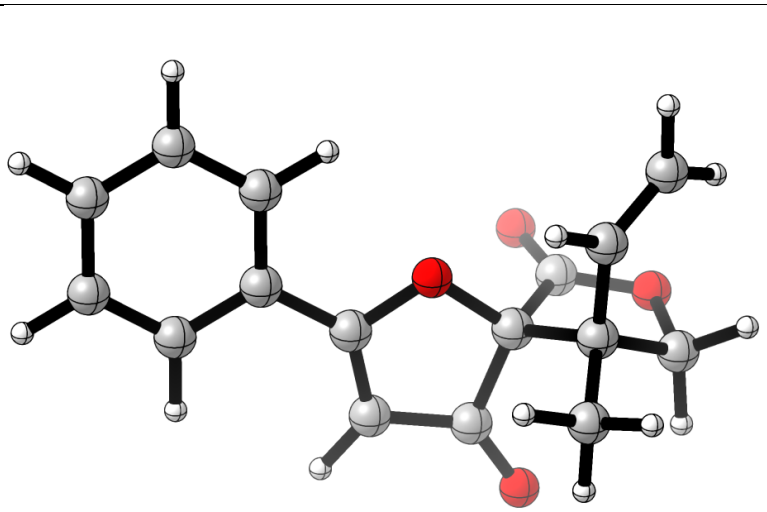
H	3.67420	-1.84165	2.07115	
H	4.53833	1.19810	-0.10013	
H	3.71601	0.14694	-1.28803	

P – 3-epi Hyperolactone C (4.13-VIIIb)



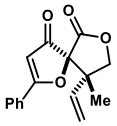
Converged?	Yes	Imaginary Frequencies	None
Zero-point correction		0.270493 (Hartree/Particle)	
Thermal correction to Energy		0.287286	
Thermal correction to Enthalpy		0.288230	
Thermal correction to Gibbs Free Energy		0.225401	
Sum of electronic and zero-point Energies		-918.239946	
Sum of electronic and thermal Energies		-918.223154	
Sum of electronic and thermal Enthalpies		-918.222210	
Sum of electronic and thermal Free Energies		-918.285039	

0 1			
C	-1.17600	-0.26491	0.11753
C	-0.88117	-1.78091	-0.01161
C	0.56765	-1.89140	-0.05792
C	1.09702	-0.63389	-0.01645
C	2.47765	-0.15789	-0.02631
C	2.74359	1.20971	0.17844
C	4.06611	1.66862	0.17751
C	5.12392	0.76909	-0.02886
C	4.85868	-0.59601	-0.23410
C	3.54005	-1.05974	-0.23302
H	3.33620	-2.11357	-0.39573
H	5.67647	-1.29006	-0.39347
H	6.14815	1.12682	-0.02835
H	4.27230	2.72064	0.34075
H	1.91498	1.88847	0.34576
O	0.12341	0.36379	0.03914
H	1.10330	-2.82527	-0.10323
O	-1.76267	-2.65676	-0.05440
C	-2.20965	0.29978	-0.89406
C	-3.51163	-0.07312	-0.15218
O	-3.19759	0.11093	1.28229
C	-1.83890	0.01965	1.48320
O	-1.28468	0.14085	2.56023
H	-4.34604	0.58682	-0.38711
H	-3.78023	-1.11934	-0.30813
C	-2.00475	1.80719	-0.99364
C	-2.71418	2.74692	-0.34949
H	-3.51607	2.50642	0.34408
H	-2.48913	3.79983	-0.48536
H	-1.18268	2.10199	-1.64377



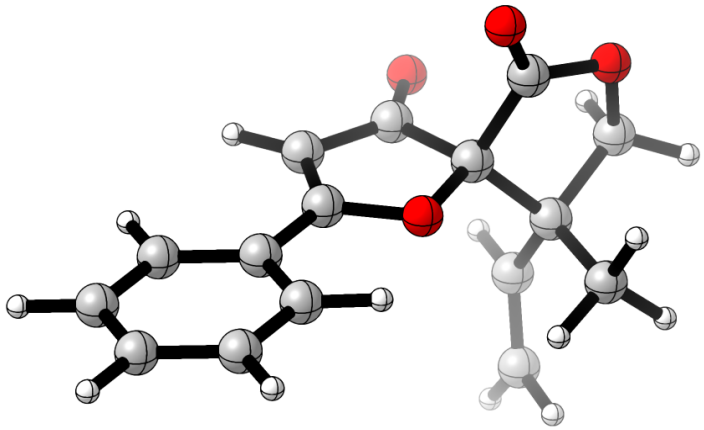
C	-2.11864	-0.33205	-2.28842	
H	-1.13067	-0.14333	-2.72508	
H	-2.28538	-1.41277	-2.25299	
H	-2.86751	0.11649	-2.94928	

P – Hyperolactone C (4.13-VIIIa/3.2)



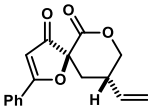
Converged?	Yes	Imaginary Frequencies	None
Zero-point correction		0.270729 (Hartree/Particle)	
Thermal correction to Energy		0.287456	
Thermal correction to Enthalpy		0.288400	
Thermal correction to Gibbs Free Energy		0.225648	
Sum of electronic and zero-point Energies		-918.241181	
Sum of electronic and thermal Energies		-918.224454	
Sum of electronic and thermal Enthalpies		-918.223509	
Sum of electronic and thermal Free Energies		-918.286261	

0 1			
C	1.21332	-0.33854	-0.03110
C	1.00876	-0.71314	1.45891
C	-0.42675	-0.66619	1.67607
C	-1.02656	-0.28123	0.51198
C	-2.42976	-0.07500	0.16373
C	-3.42919	-0.17493	1.15166
C	-4.77041	0.02004	0.81012
C	-5.12184	0.31557	-0.51844
C	-4.12714	0.41490	-1.50402
C	-2.78241	0.22109	-1.16693
H	-2.00291	0.28582	-1.91742
H	-4.39958	0.63864	-2.52952
H	-6.16358	0.46522	-0.78182
H	-5.53933	-0.05693	1.57087
H	-3.15937	-0.39977	2.17883
O	-0.11429	-0.04382	-0.51662
H	-0.90634	-0.90570	2.61064
O	1.94082	-0.98615	2.23566
C	2.24549	0.79221	-0.29640
C	3.54715	-0.05758	-0.29432
O	3.16184	-1.34320	-0.91330
C	1.80821	-1.54785	-0.78495
O	1.20816	-2.52145	-1.20376
H	4.33079	0.37465	-0.91548
H	3.90701	-0.26138	0.71570
C	1.99927	1.37672	-1.69684
H	1.01747	1.85296	-1.75357
H	2.77130	2.11713	-1.92934
H	2.03800	0.59142	-2.46030
C	2.27332	1.83397	0.79991



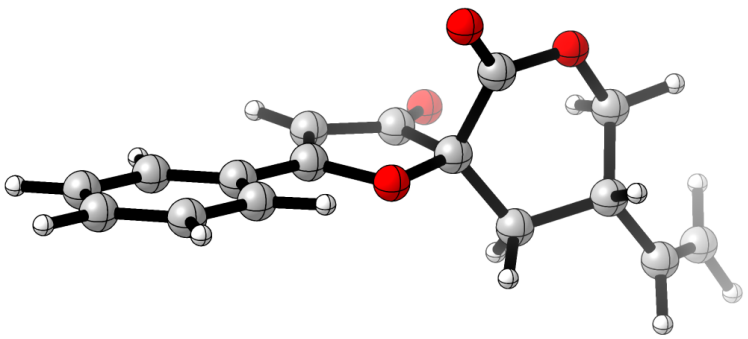
H	2.50925	1.45626	1.79481	
C	2.04164	3.14539	0.63115	
H	1.80210	3.57740	-0.33593	
H	2.08423	3.82870	1.47351	

P – 6-Endo diastereomer E (4.13-VIIIe)



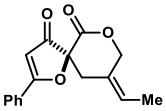
Converged?	Yes	Imaginary Frequencies	None
Zero-point correction		0.271642 (Hartree/Particle)	
Thermal correction to Energy		0.288282	
Thermal correction to Enthalpy		0.289226	
Thermal correction to Gibbs Free Energy		0.225693	
Sum of electronic and zero-point Energies		-918.234614	
Sum of electronic and thermal Energies		-918.217974	
Sum of electronic and thermal Enthalpies		-918.217974	
Sum of electronic and thermal Free Energies		-918.280563	

0 1			
C	0.84233	-0.02404	-0.06911
C	0.61274	-1.55163	0.14243
C	-0.82751	-1.72053	0.22858
C	-1.40981	-0.48580	0.18748
C	-2.81058	-0.07419	0.23347
C	-3.81825	-1.01000	0.53890
C	-5.15686	-0.60854	0.57062
C	-5.49642	0.72792	0.29764
C	-4.49296	1.66111	-0.00712
C	-3.15076	1.26458	-0.03873
H	-2.36350	1.96839	-0.28321
H	-4.75663	2.69057	-0.22312
H	-6.53608	1.03719	0.32127
H	-5.93251	-1.32861	0.80700
H	-3.55634	-2.04084	0.75655
O	-0.48358	0.54990	0.09880
H	-1.32335	-2.67354	0.30966
O	1.53781	-2.37757	0.21415
C	1.23534	0.15232	-1.55514
O	0.40799	0.35050	-2.43529
O	2.56067	0.00253	-1.84184
C	3.54121	-0.09030	-0.74653
C	3.18708	0.95998	0.30548
C	1.82945	0.58404	0.94756
H	1.35222	1.46394	1.38811
H	2.00770	-0.14609	1.74409
C	4.24019	1.12457	1.37628
C	5.36189	0.39534	1.49776
H	5.62148	-0.40107	0.80550
H	6.05983	0.57457	2.30924



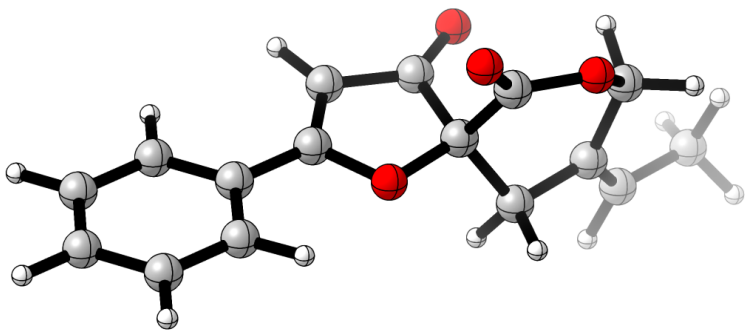
H	4.03131	1.90355	2.10966	
H	4.49895	0.10846	-1.22664	
H	3.51971	-1.10587	-0.33894	
H	3.07174	1.91739	-0.22315	

P – 6-Endo alkene diastereomer C (4.13-VIIIc)



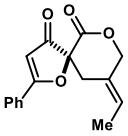
Converged?	Yes	Imaginary Frequencies	None
Zero-point correction		0.270980 (Hartree/Particle)	
Thermal correction to Energy		0.288043	
Thermal correction to Enthalpy		0.288988	
Thermal correction to Gibbs Free Energy		0.224444	
Sum of electronic and zero-point Energies		-918.241831	
Sum of electronic and thermal Energies		-918.224767	
Sum of electronic and thermal Enthalpies		-918.223823	
Sum of electronic and thermal Free Energies		-918.288366	

0 1			
C	-0.78959	0.29547	-0.03290
C	-0.69647	-0.76031	1.10078
C	0.71607	-1.08566	1.21604
C	1.40498	-0.35709	0.28921
C	2.83128	-0.27626	-0.01648
C	3.74026	-1.16919	0.58452
C	5.10429	-1.07789	0.29267
C	5.56778	-0.09587	-0.59995
C	4.66273	0.79418	-1.19952
C	3.29554	0.70657	-0.91135
H	2.58346	1.39156	-1.35716
H	5.02201	1.55436	-1.88434
H	6.62695	-0.02564	-0.82427
H	5.80396	-1.76570	0.75460
H	3.38231	-1.93196	1.26913
O	0.57958	0.44246	-0.49590
H	1.12300	-1.76882	1.94308
O	-1.67666	-1.17603	1.74281
C	-1.25719	1.64489	0.53700
O	-0.49263	2.50835	0.94387
O	-2.61046	1.84446	0.51127
C	-3.56228	0.73649	0.32162
C	-3.12840	-0.24086	-0.75598
C	-1.68652	-0.12564	-1.20524
H	-1.57693	0.64004	-1.98374
H	-1.32742	-1.07424	-1.61509
C	-3.95946	-1.17023	-1.25445
C	-5.40360	-1.36547	-0.86322
H	-4.49409	1.24301	0.06962
H	-3.66563	0.22198	1.28131



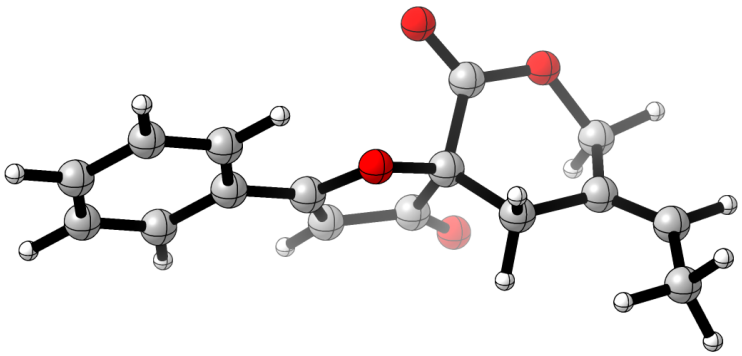
H	-6.04954	-1.36342	-1.74813	
H	-5.76217	-0.59186	-0.17880	
H	-5.53495	-2.33368	-0.36617	
H	-3.56625	-1.86835	-1.99306	

P – 6-Endo alkene diastereomer D (4.13-VIIId)



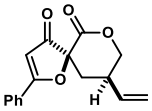
Converged?	Yes	Imaginary Frequencies	None
Zero-point correction		0.271090 (Hartree/Particle)	
Thermal correction to Energy		0.288098	
Thermal correction to Enthalpy		0.289042	
Thermal correction to Gibbs Free Energy		0.224270	
Sum of electronic and zero-point Energies		-918.242484	
Sum of electronic and thermal Energies		-918.225476	
Sum of electronic and thermal Enthalpies		-918.224532	
Sum of electronic and thermal Free Energies		-918.289304	

0 1			
C	-0.89190	-0.21565	0.06705
C	-0.62356	-1.20052	-1.11005
C	0.81727	-1.20136	-1.29740
C	1.36635	-0.29335	-0.43812
C	2.75195	0.10310	-0.20112
C	3.77791	-0.34883	-1.05416
C	5.10218	0.02804	-0.81294
C	5.40876	0.85710	0.28010
C	4.38701	1.30764	1.13083
C	3.05897	0.93412	0.89315
H	2.25819	1.26260	1.54568
H	4.62575	1.94256	1.97690
H	6.43740	1.14726	0.46669
H	5.89219	-0.31899	-1.46977
H	3.54094	-0.98414	-1.90203
O	0.41446	0.36801	0.33015
H	1.33440	-1.83013	-2.00313
O	-1.51229	-1.82006	-1.71992
C	-1.29506	-1.02797	1.31939
O	-0.48098	-1.41147	2.14912
O	-2.62588	-1.30139	1.44330
C	-3.55532	-0.92547	0.35499
C	-3.32932	0.50409	-0.07030
C	-1.87874	0.91324	-0.26864
H	-1.63146	1.75364	0.39014
H	-1.69435	1.24245	-1.29801
C	-4.35962	1.34757	-0.25089
H	-5.36713	0.98183	-0.05373
H	-4.54635	-1.06845	0.78312
H	-3.39435	-1.62110	-0.47223



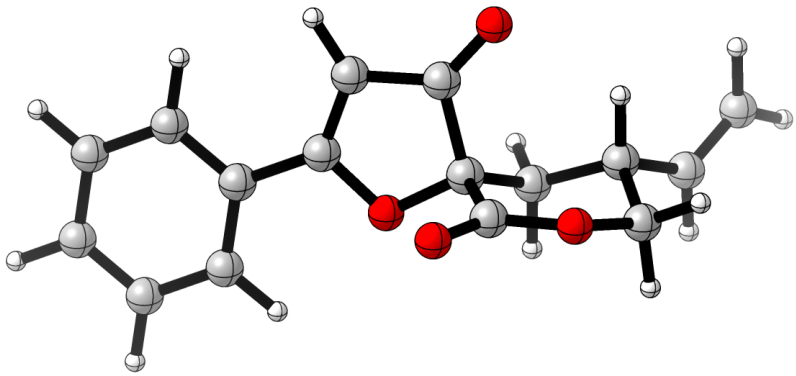
C	-4.25380	2.77720	-0.71884	
H	-3.21795	3.08254	-0.88818	
H	-4.69245	3.45716	0.02033	
H	-4.80577	2.91833	-1.65524	

P – 6-Endo diastereomer F (4.13-VIIIf)



Converged?	Yes	Imaginary Frequencies	None
Zero-point correction		0.271440 (Hartree/Particle)	
Thermal correction to Energy		0.288229	
Thermal correction to Enthalpy		0.289174	
Thermal correction to Gibbs Free Energy		0.225149	
Sum of electronic and zero-point Energies		-918.236172	
Sum of electronic and thermal Energies		-918.219383	
Sum of electronic and thermal Enthalpies		-918.218439	
Sum of electronic and thermal Free Energies		-918.282464	

0 1			
C	-0.84480	0.18342	0.09872
C	-0.63080	-0.69510	1.36861
C	0.80249	-0.92727	1.44416
C	1.39677	-0.33606	0.36766
C	2.79691	-0.25544	-0.04247
C	3.15387	0.53547	-1.15103
C	4.49534	0.62081	-1.54242
C	5.48239	-0.08106	-0.83273
C	5.12659	-0.87105	0.27413
C	3.78859	-0.95905	0.66906
H	3.51529	-1.57191	1.52237
H	5.88944	-1.41268	0.82247
H	6.52158	-0.01277	-1.13687
H	4.77125	1.23374	-2.39344
H	2.38015	1.07773	-1.68213
O	0.48633	0.28392	-0.48464
H	1.28406	-1.47269	2.23880
O	-1.55131	-1.08488	2.10529
C	-1.25103	1.59423	0.56871
O	-0.42815	2.37996	1.02189
O	-2.58074	1.90240	0.55225
C	-3.56379	1.18461	-0.27202
C	-3.25736	-0.31042	-0.41440
C	-1.80403	-0.45797	-0.90425
H	-1.68047	0.03973	-1.87569
H	-1.54205	-1.51274	-1.03428
H	-3.36442	-0.79566	0.56099
C	-4.22147	-0.92068	-1.40326
C	-5.12390	-1.86573	-1.09512
H	-5.20896	-2.25915	-0.08509



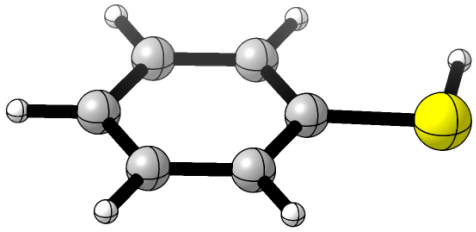
H	-5.79699	-2.27371	-1.84282	
H	-4.15558	-0.54880	-2.42814	
H	-3.58134	1.67229	-1.25456	
H	-4.51565	1.35333	0.22997	

PhSH uM06-2X/LanL2DZ Level

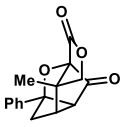


Converged?	Yes	Imaginary Frequencies	None
Zero-point correction		0.100640 (Hartree/Particle)	
Thermal correction to Energy		0.106970	
Thermal correction to Enthalpy		0.107914	
Thermal correction to Gibbs Free Energy		0.069524	
Sum of electronic and zero-point Energies		-242.061981	
Sum of electronic and thermal Energies		-242.055650	
Sum of electronic and thermal Enthalpies		-242.054706	
Sum of electronic and thermal Free Energies		-242.093097	

0 1			
C	-1.60845	1.21420	-0.00095
C	-0.20512	1.21748	-0.00152
C	0.49472	0.00170	0.00083
C	-0.20721	-1.21479	0.00213
C	-1.60889	-1.20984	0.00093
C	-2.31575	0.00322	-0.00020
H	-3.40026	0.00389	-0.00033
H	-2.14486	-2.15313	0.00188
H	0.33426	-2.15564	0.00530
S	2.32308	-0.08458	-0.00367
H	2.55893	1.26514	0.05092
H	0.33019	2.16288	-0.00432
H	-2.14324	2.15825	-0.00199

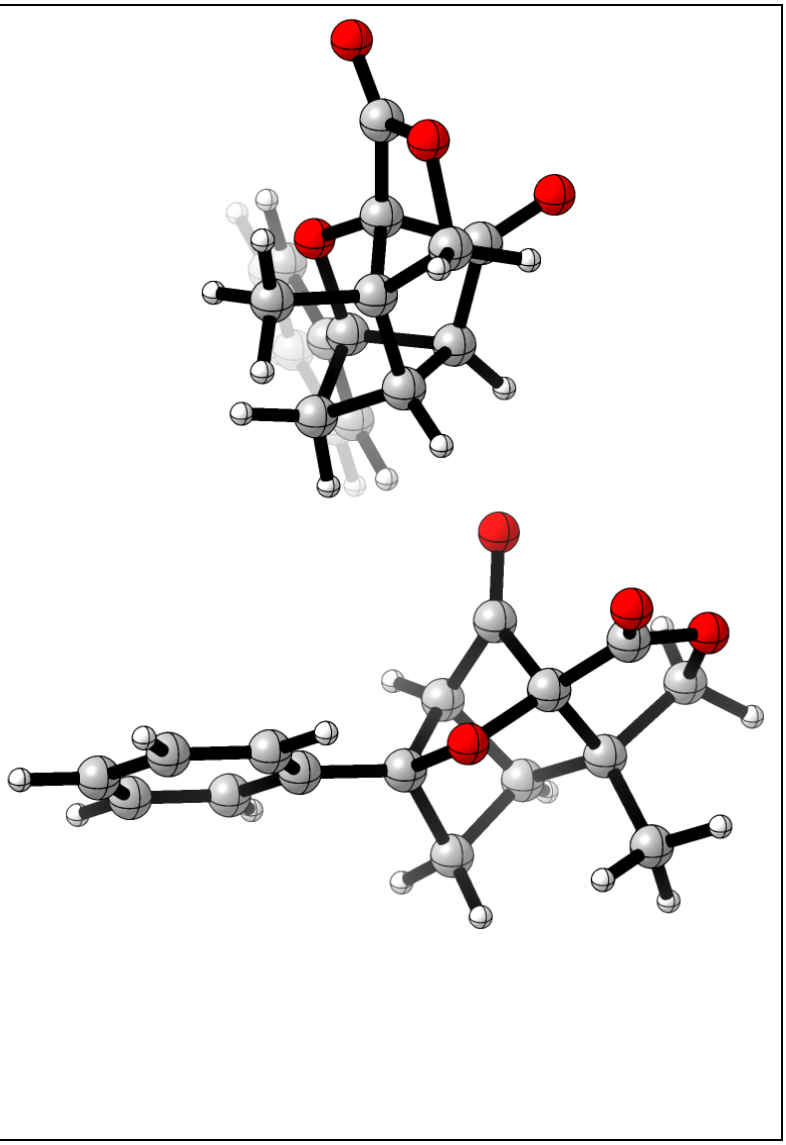


[2+2] Photoproduct from Hyperolactone C (4.123)



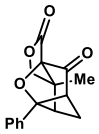
Converged?	Yes	Imaginary Frequencies	None
Zero-point correction		0.273580 (Hartree/Particle)	
Thermal correction to Energy		0.288497	
Thermal correction to Enthalpy		0.289441	
Thermal correction to Gibbs Free Energy		0.231569	
Sum of electronic and zero-point Energies		-918.213584	
Sum of electronic and thermal Energies		-918.198668	
Sum of electronic and thermal Enthalpies		-918.197724	
Sum of electronic and thermal Free Energies		-918.255595	

0 1			
C	-1.36325	0.44597	-0.06309
C	-0.90688	0.27452	1.41741
C	-0.02645	-0.91647	1.18208
H	0.55533	-1.33057	1.99876
C	-0.89176	-1.88189	0.25651
C	-1.99804	-0.94021	-0.32937
C	-3.31982	-0.71496	0.44018
O	-3.64449	0.70422	0.12091
C	-2.49565	1.41731	-0.25637
O	-2.51900	2.57130	-0.63617
H	-4.15278	-1.31412	0.07547
H	-3.23094	-0.81164	1.52647
C	-2.30921	-1.17909	-1.81512
H	-1.50807	-0.80333	-2.45649
H	-2.44149	-2.24963	-2.00893
H	-3.23138	-0.66262	-2.10218
H	-1.25976	-2.82259	0.66372
C	0.32130	-1.90995	-0.72994
H	1.04201	-2.67969	-0.43963
H	0.14500	-1.96456	-1.80330
C	0.74977	-0.53476	-0.15003
C	2.18261	-0.10002	-0.13390
C	2.56566	1.15734	-0.62798
C	3.91622	1.53662	-0.60390
C	4.88805	0.66934	-0.08473
C	4.50560	-0.58653	0.41436
C	3.15920	-0.96925	0.38750
H	2.87232	-1.94263	0.77959
H	5.25221	-1.26015	0.82172
H	5.93107	0.96740	-0.06521



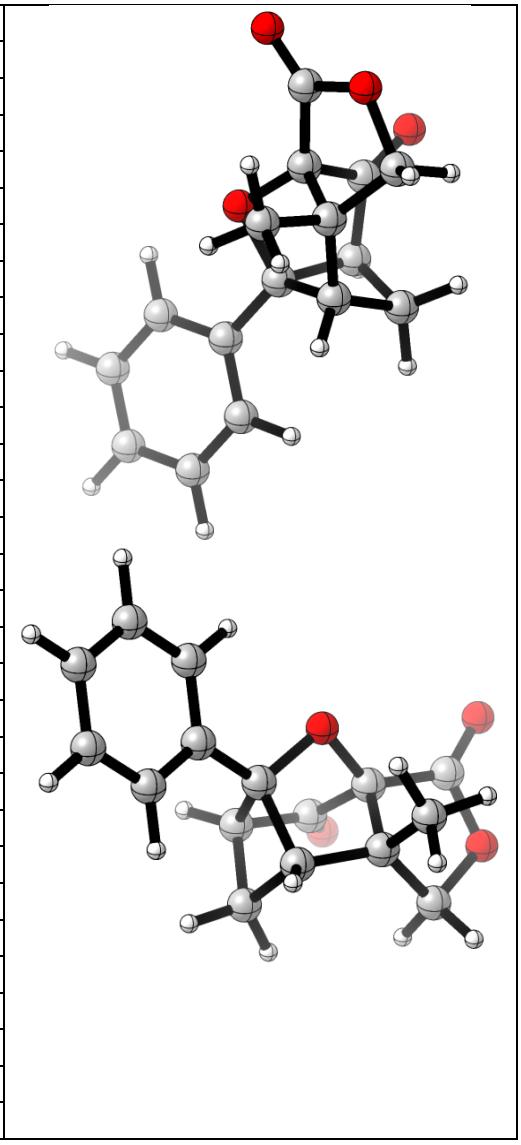
H	4.20706	2.50889	-0.98743	
H	1.80647	1.82200	-1.02219	
O	-0.09858	0.55494	-0.74874	
O	-1.21931	0.91146	2.41373	

Undetected [2+2] Photoproduct from Hyperolactone C (4.124)



Converged?	Yes	Imaginary Frequencies	None
Zero-point correction		0.273685 (Hartree/Particle)	
Thermal correction to Energy		0.288641	
Thermal correction to Enthalpy		0.289585	
Thermal correction to Gibbs Free Energy		0.231698	
Sum of electronic and zero-point Energies		-918.216392	
Sum of electronic and thermal Energies		-918.201436	
Sum of electronic and thermal Enthalpies		-918.200492	
Sum of electronic and thermal Free Energies		-918.258379	

0 1			
C	-1.44097	0.49466	0.13385
C	-1.31620	-0.21673	1.51032
C	0.06651	-0.84241	1.47195
H	0.62086	-0.82280	2.40640
C	-0.11279	-2.17231	0.66853
H	0.77531	-2.80273	0.74859
C	-0.10949	-1.32925	-0.63733
H	0.38612	-1.74334	-1.51465
C	0.63976	-0.15811	0.17554
C	2.10431	0.07914	0.02851
C	2.63027	1.35753	0.28570
C	4.00993	1.58077	0.18342
C	4.87287	0.53175	-0.17078
C	4.34859	-0.74315	-0.43262
C	2.96817	-0.96756	-0.33837
H	2.57111	-1.95487	-0.55962
H	5.01013	-1.55518	-0.71550
H	5.94075	0.70692	-0.24777
H	4.41038	2.57014	0.37754
H	1.95396	2.16334	0.54904
O	-0.13433	1.09844	0.01385
C	-1.42819	-0.59959	-0.97857
C	-2.86397	-1.11685	-0.79822
O	-3.61583	0.14841	-0.53451
C	-2.77316	1.16923	-0.06722
O	-3.14569	2.31142	0.11384
H	-3.30702	-1.55353	-1.69180
H	-3.00322	-1.77869	0.06152
C	-1.27539	0.05595	-2.36512
H	-0.35554	0.64484	-2.41505

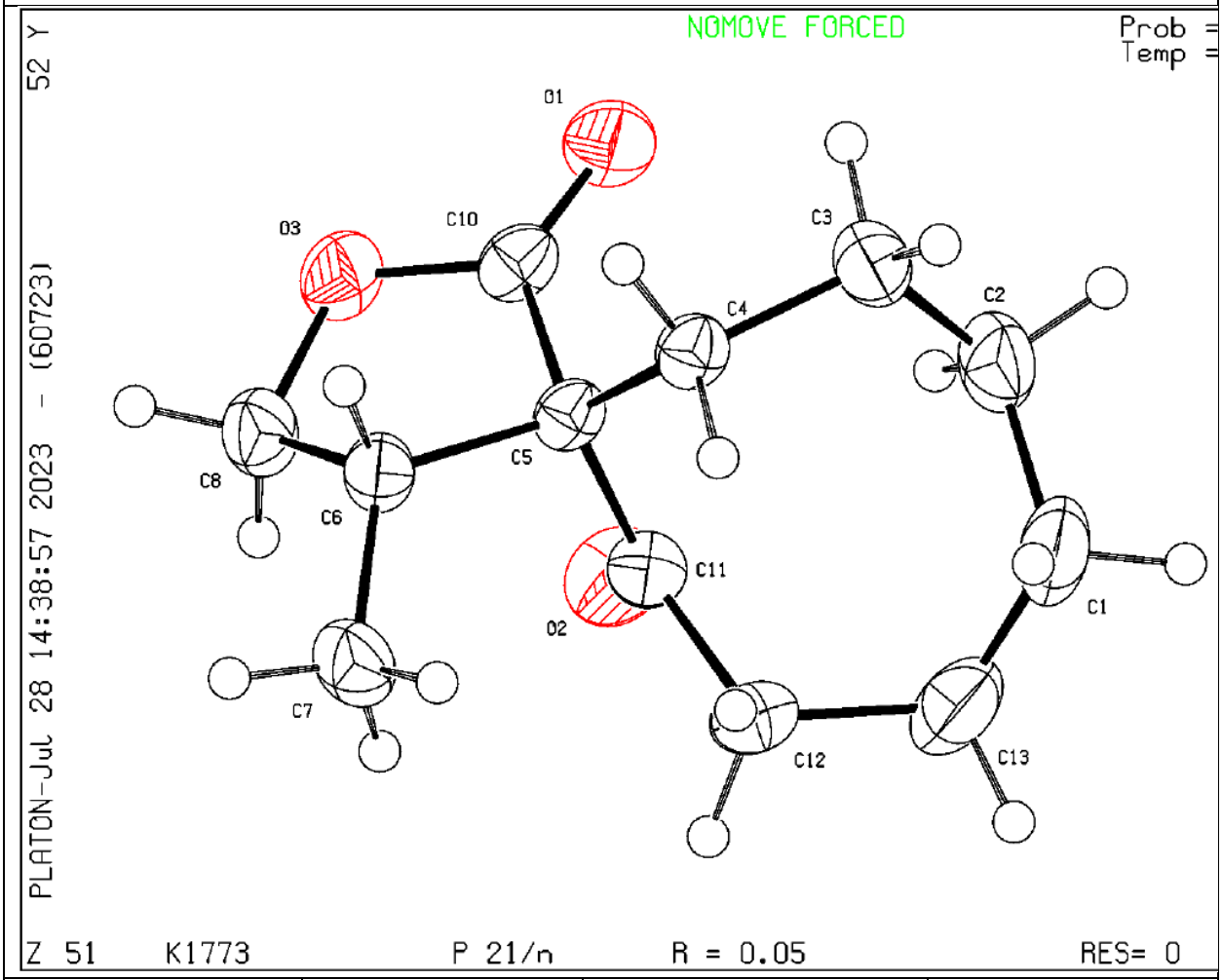


H	-1.23334	-0.72778	-3.12928	
H	-2.11943	0.71430	-2.59688	
H	-0.99756	-2.77040	0.89810	
O	-2.17590	-0.28685	2.38330	

Appendix B Crystallographic Data

3.60d

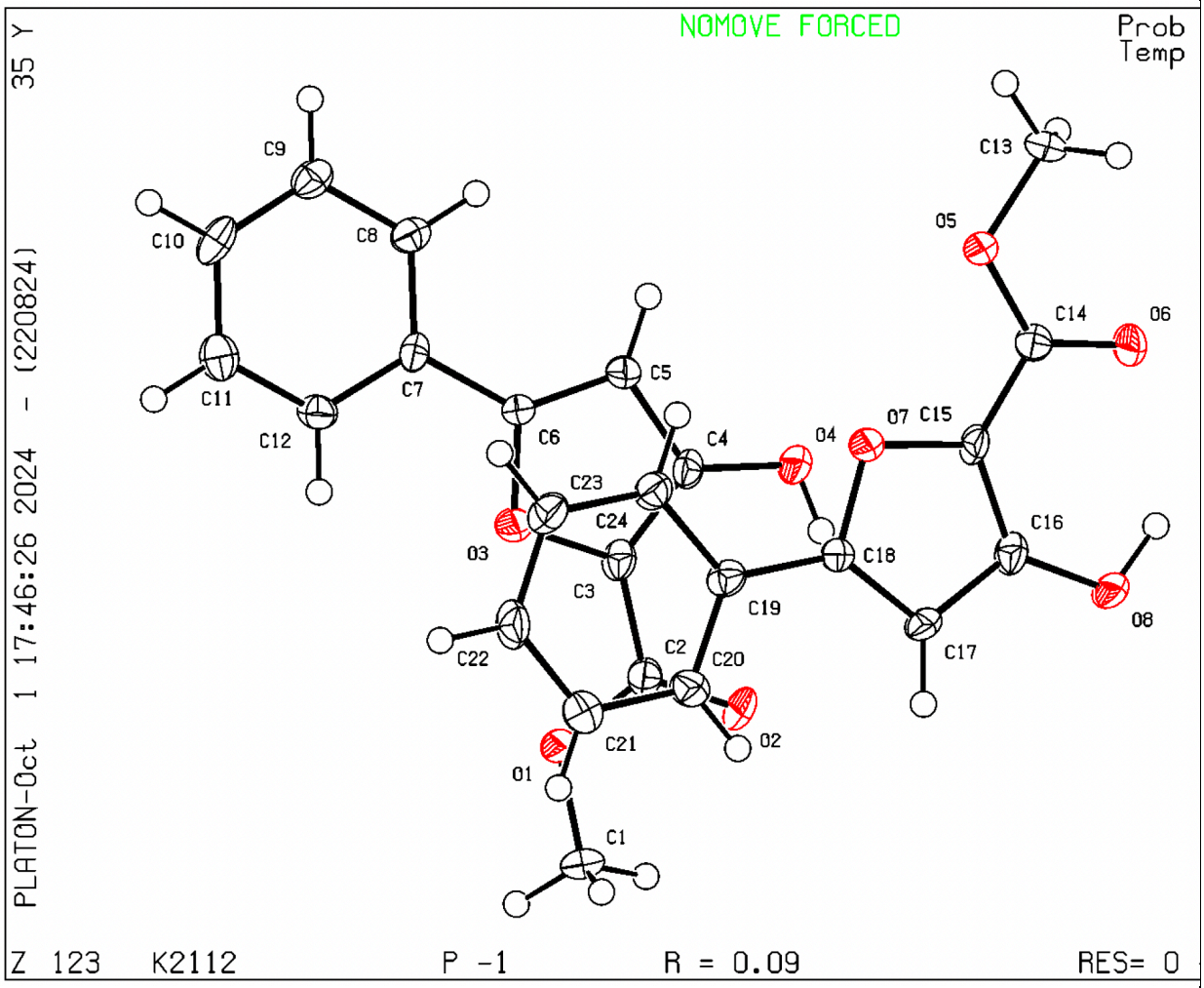
CCDC:



Bond Precision /Å	0.0028	Density /g cm^{-3}	1.251
Wavelength	0.71073	Z	4
a /Å	6.5458(2)	μ /mm^{-1}	0.088
b /Å	18.3578(7)	F(000)	456.0
c /Å	9.3722(3)	h,k,l$_{max}$	8,23,12
α /°	90	Nref	2591
β /°	97.429(3)	T$_{min}$, T$_{max}$	0.702,0.746
γ /°	90	Data Completeness	0.998
Temperature	200 K	θ$_{max}$ /°	27.624
Volume	1116.77(7)	R(reflections)	0.0507(1725)
Space Group	P 21/n	wR2(reflections)	0.1382(2591)
Hall Group	-P 2yn	S	1.038
Empirical Formula	$C_{12}H_{18}O_3$	Npar	137
Formula Weight	210.26		

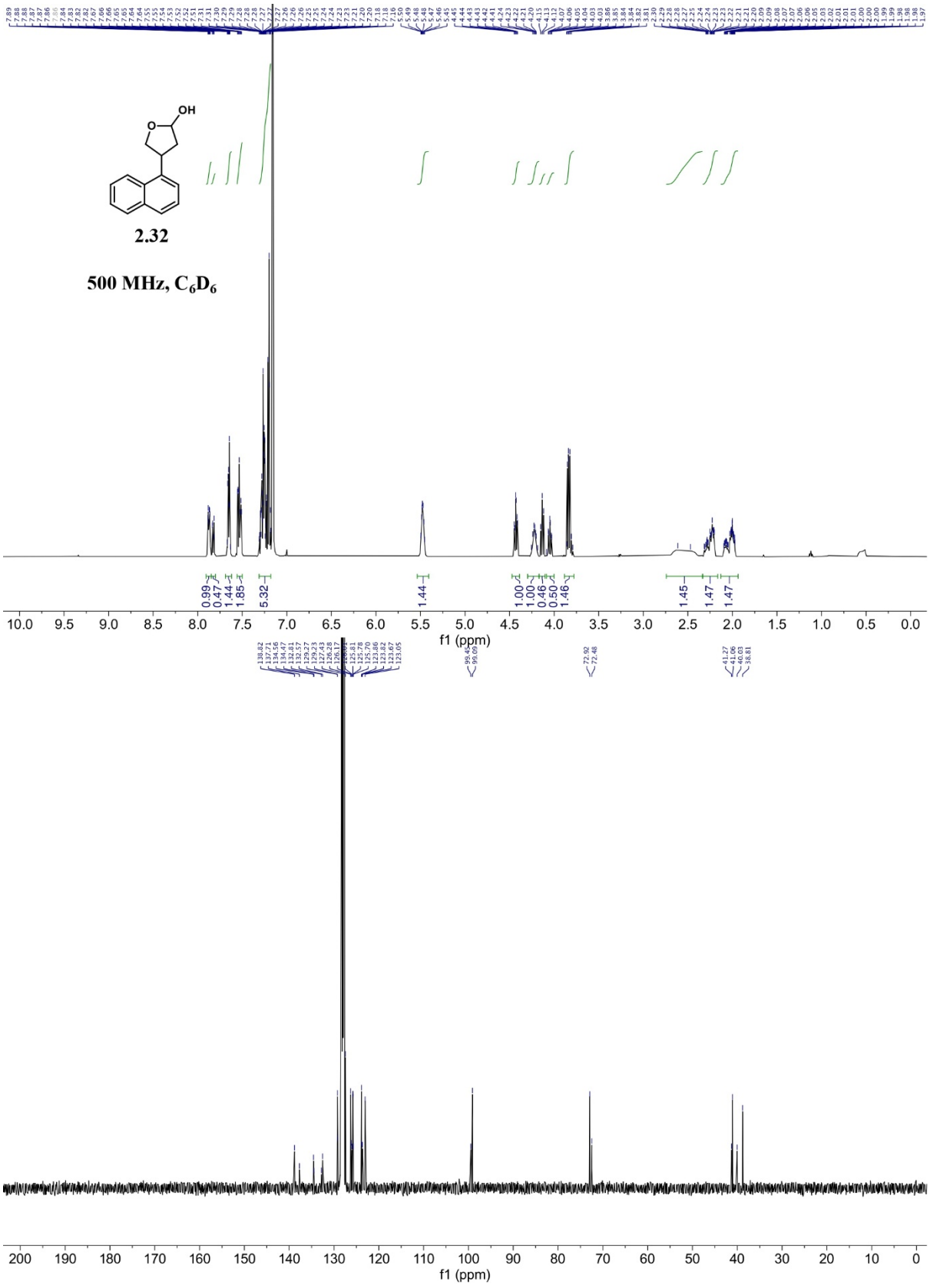
4.82

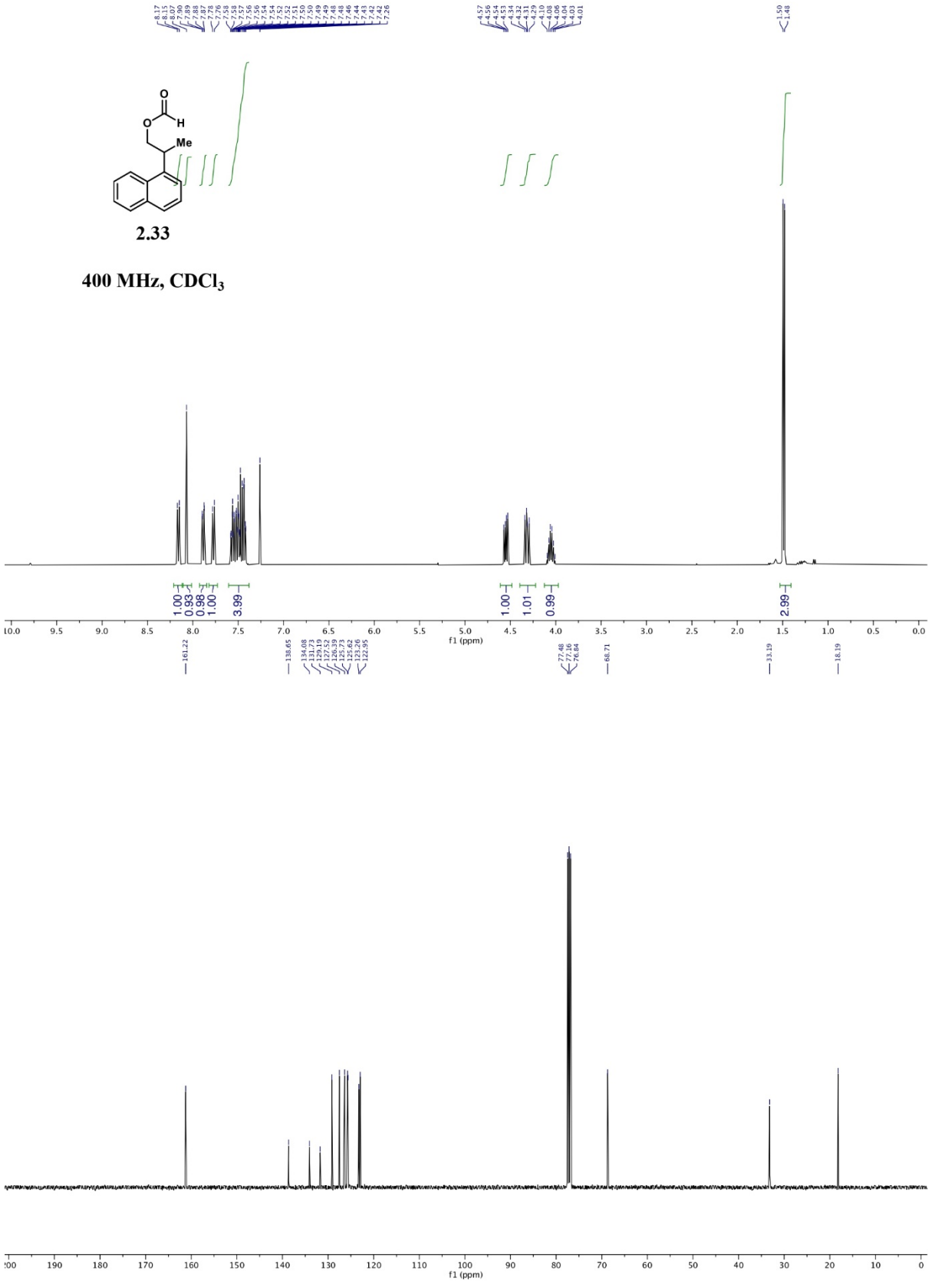
CCDC:



Bond Precision /Å	0.0060	Density /g cm^{-3}	1.441
Wavelength	0.71073	Z	4
a /Å	8.8749 (17)	μ /mm^{-1}	0.109
b /Å	9.8565 (19)	F(000)	456.0
c /Å	12.899 (3)	h,k,l$_{max}$	10,11,15
α /°	68.385 (4)	Nref	3532
β /°	83.348 (4)	T$_{min}$, T$_{max}$	0.585,0.746
γ /°	73.573 (4)	Data Completeness	0.990
Temperature	100 K	θ$_{max}$ /°	25.026
Volume	1006.1 (3)	R(reflections)	0.0949 (2505)
Space Group	P -1	wR2(reflections)	0.2309 (3532)
Hall Group	-P 1	S	1.157
Empirical Formula	$C_{12}H_{10}O_4$	Npar	295
Formula Weight	218.20		

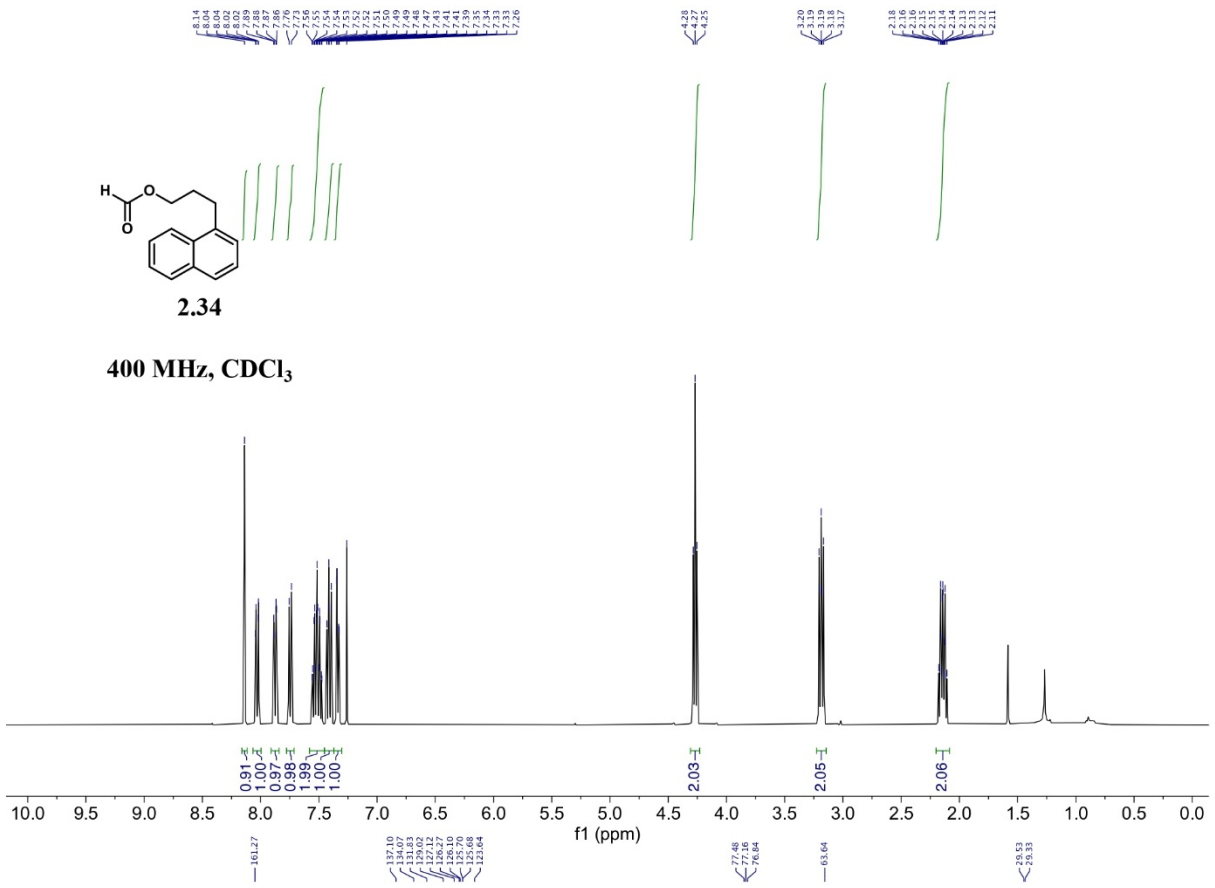
Appendix C NMR Spectra

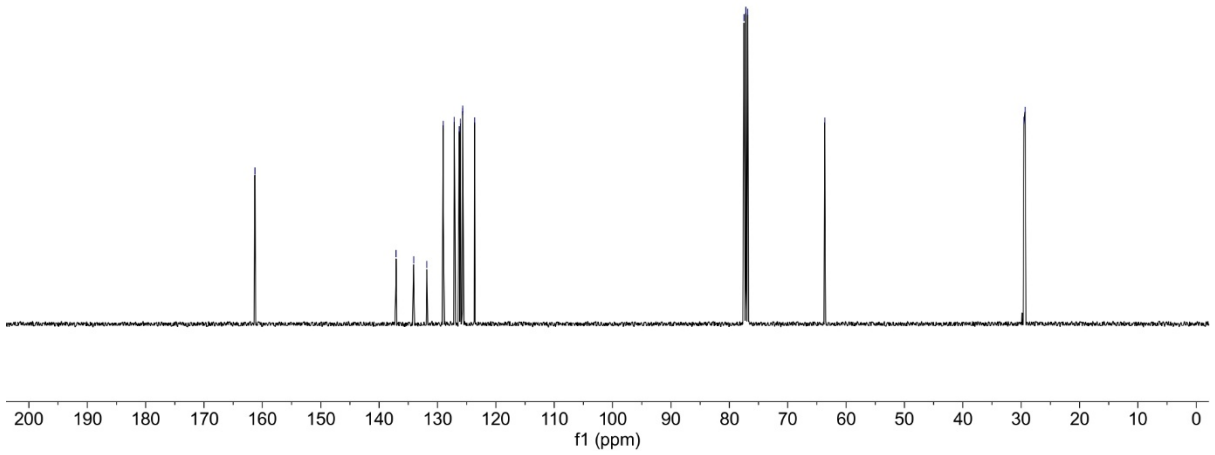


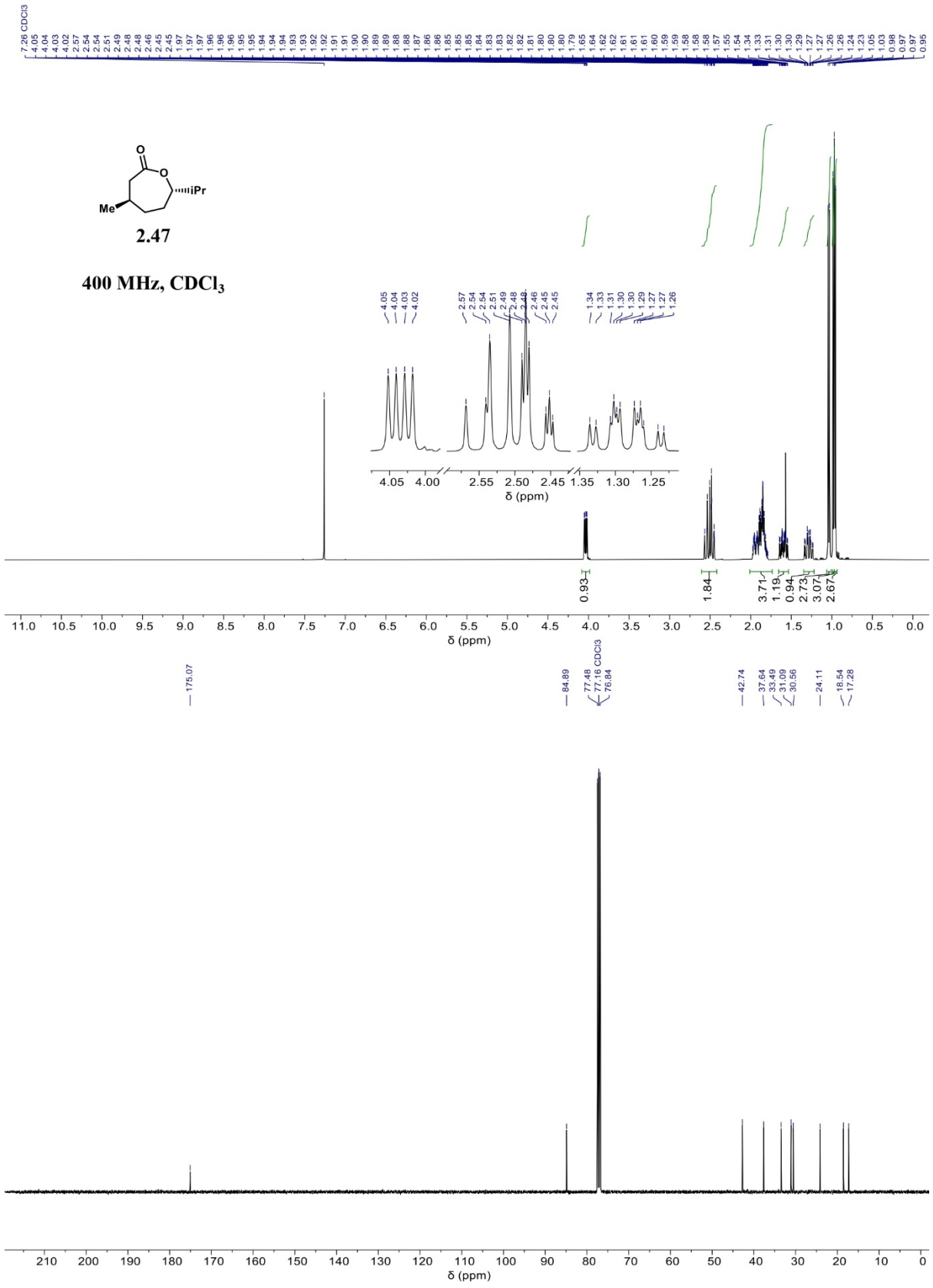


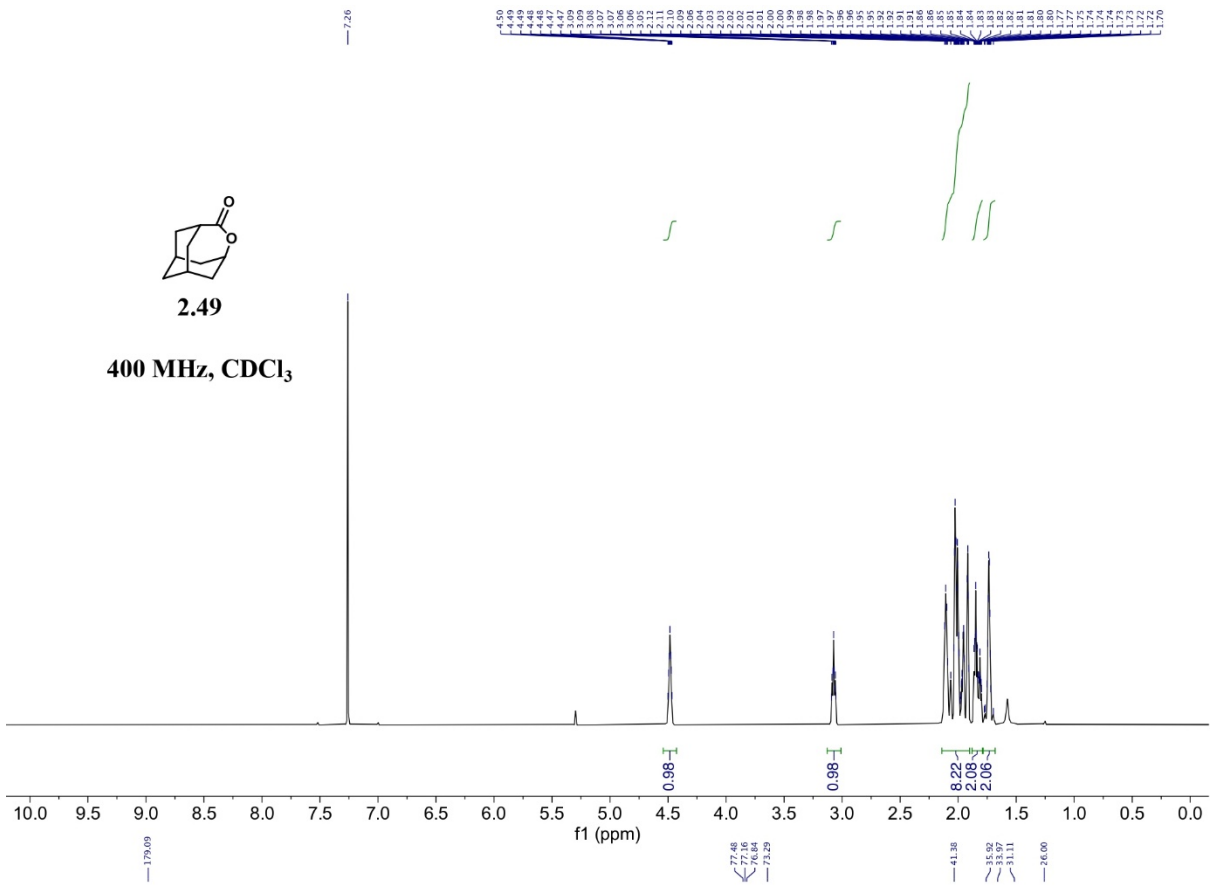
2.33

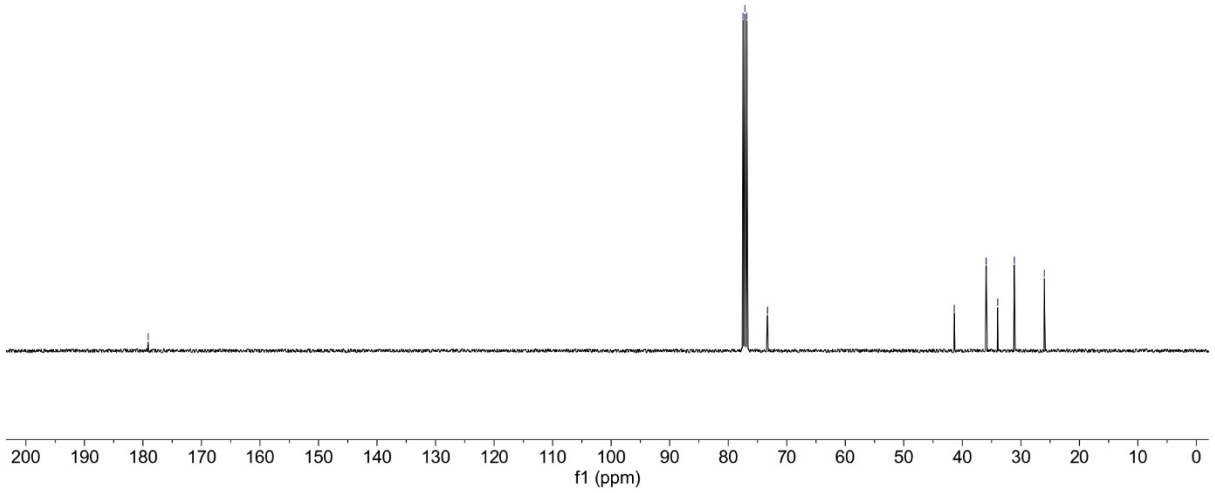
400 MHz, $CDCl_3$

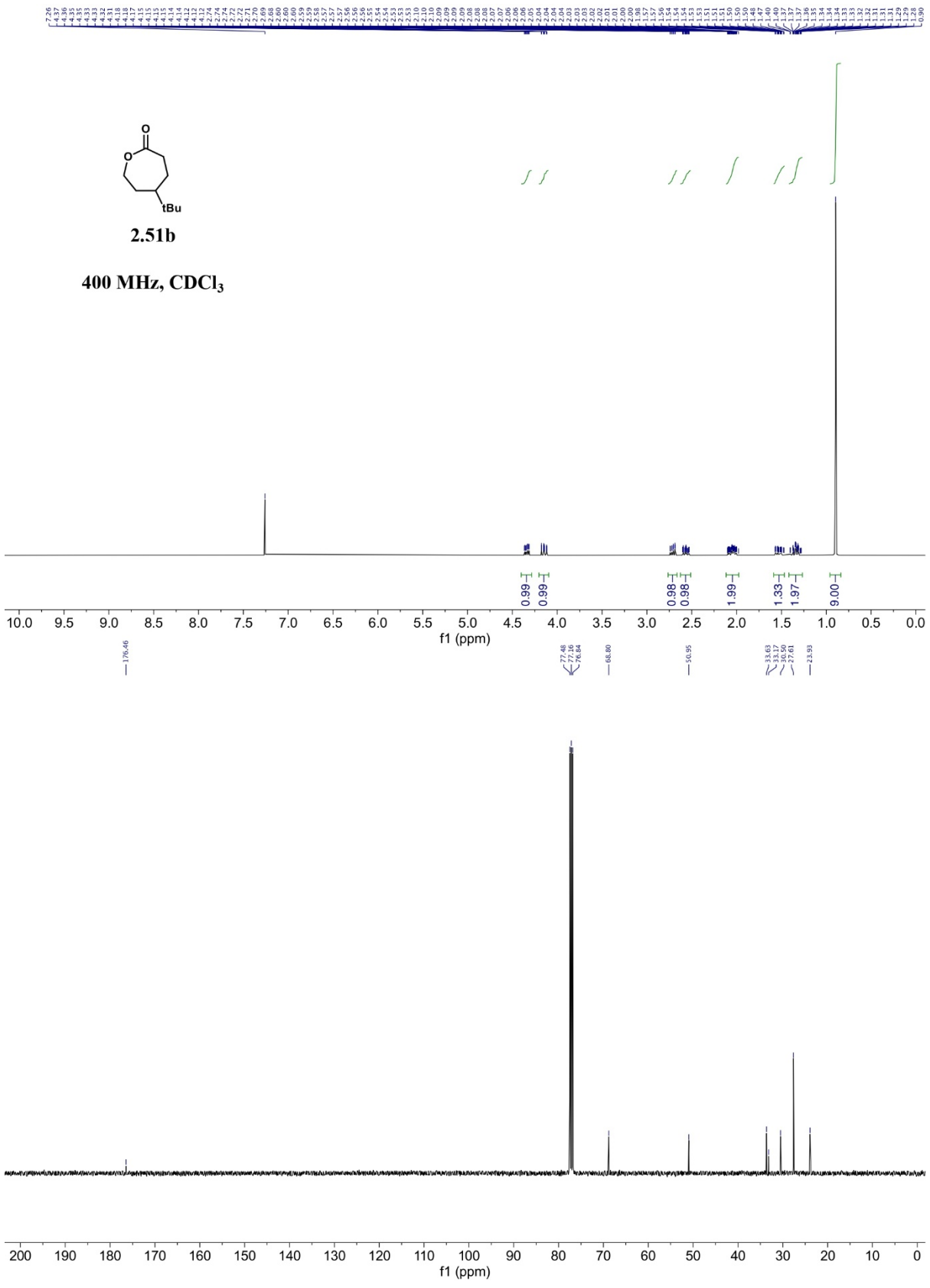

2.34
400 MHz, CDCl3
f1 (ppm)

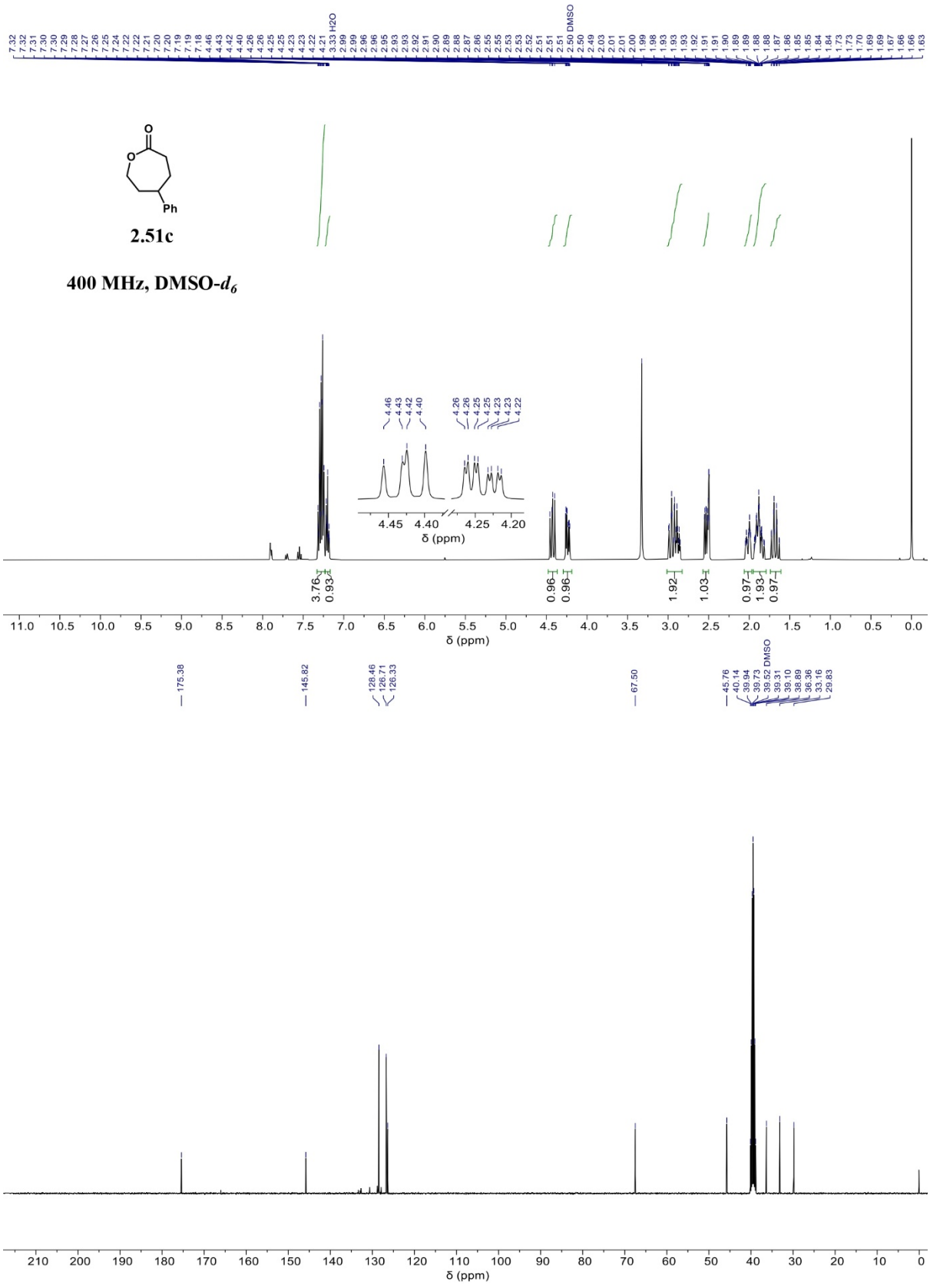

f1 (ppm)

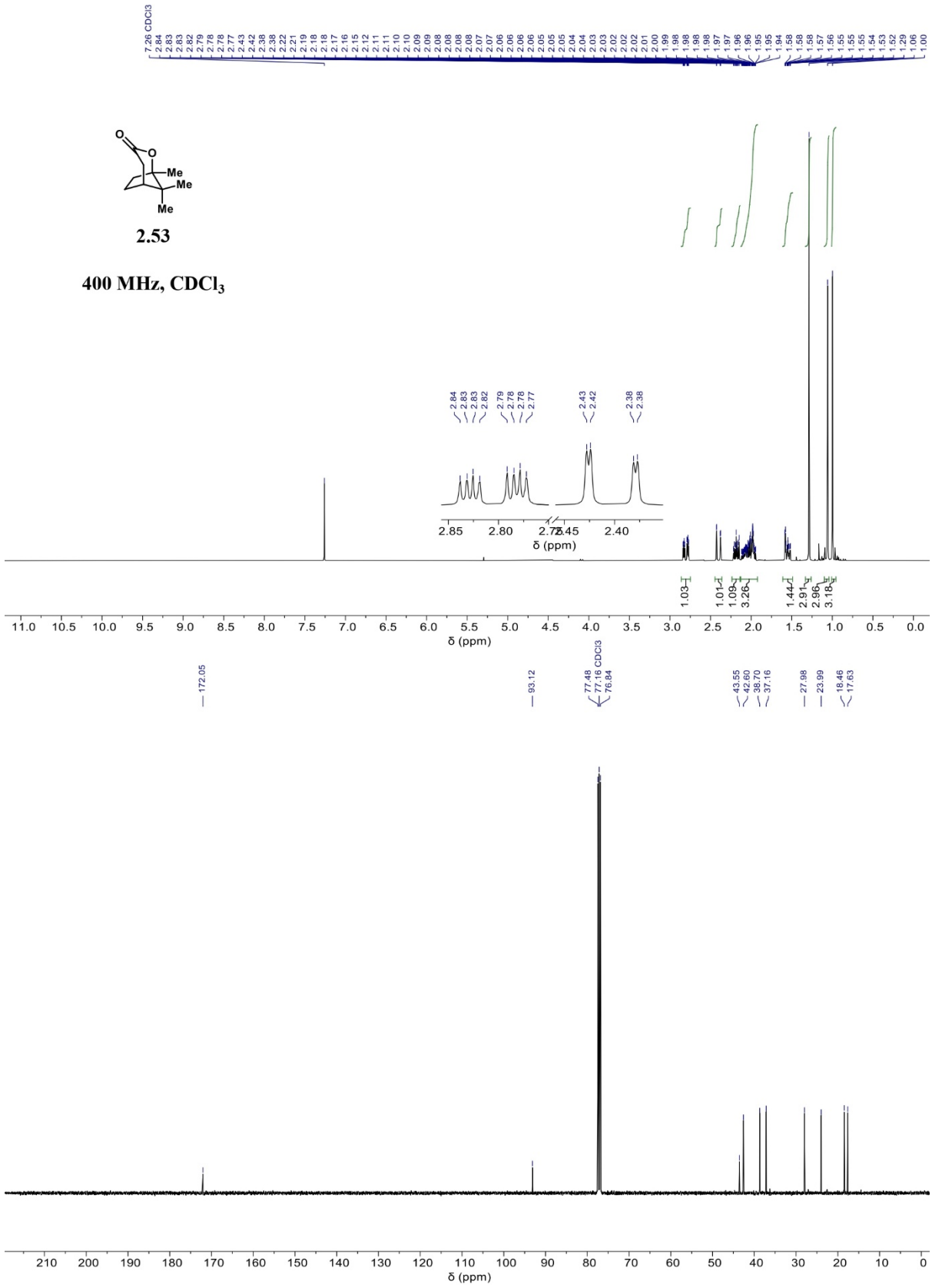

Me
iPr
2.47
400 MHz, CDCl3
δ (ppm)
0.93
1.84
3.71
1.19
0.94
2.73
3.07
2.67
175.07
84.89
77.48
77.16 CDCl3
76.84
42.74
37.64
33.49
31.09
30.56
24.11
18.54
17.28

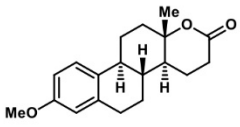

2.49
400 MHz, CDCl3
f1 (ppm)


f1 (ppm)


tBu
2.51b
400 MHz, CDCl3
0.99
0.99
0.98
0.98
1.99
1.33
1.97
9.00
f1 (ppm)
176.46
77.48
77.16
76.84
68.80
50.95
33.63
33.17
31.50
27.61
23.93
f1 (ppm)

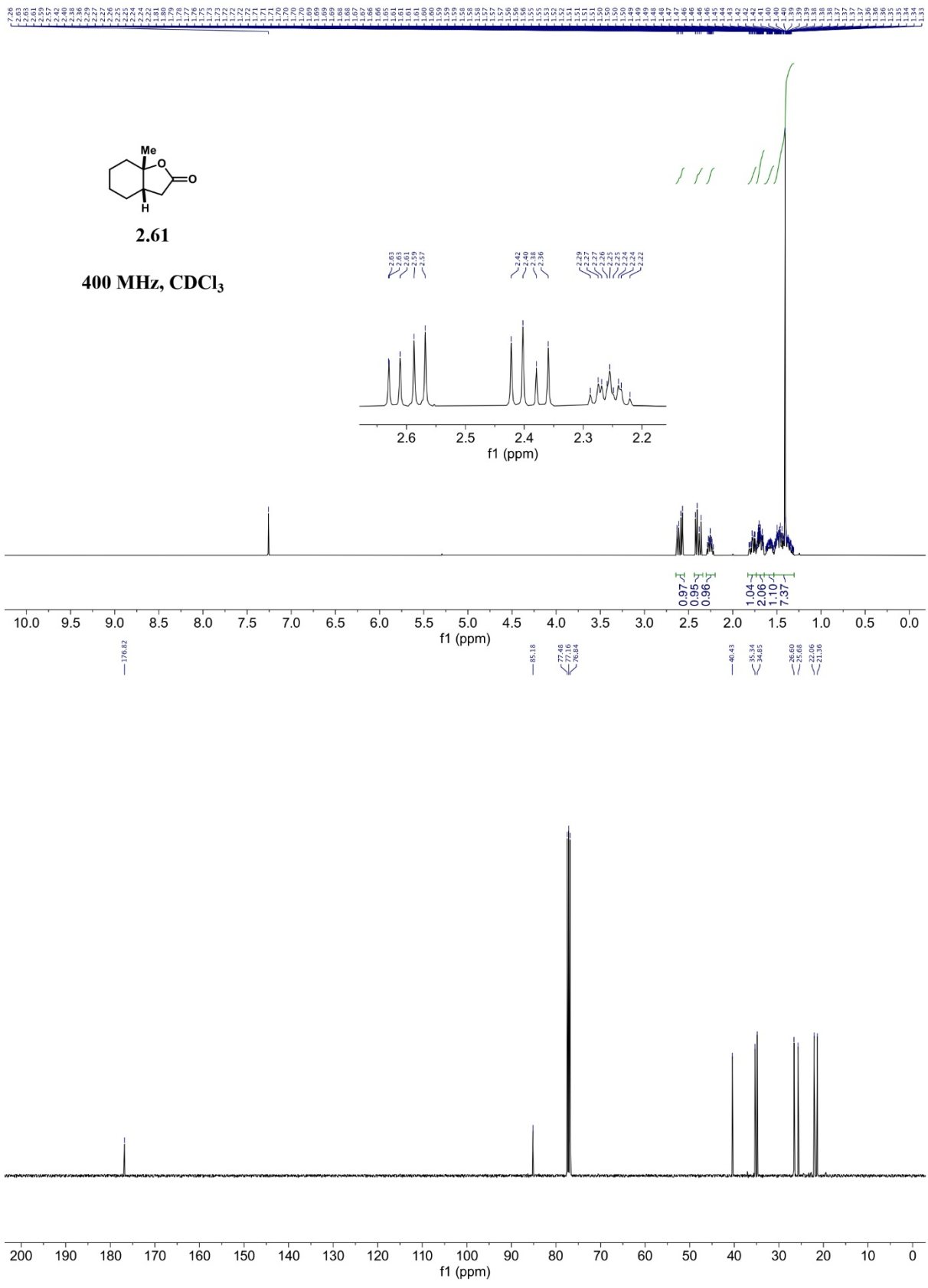

Ph
2.51c
400 MHz, DMSO-d_6
δ (ppm)

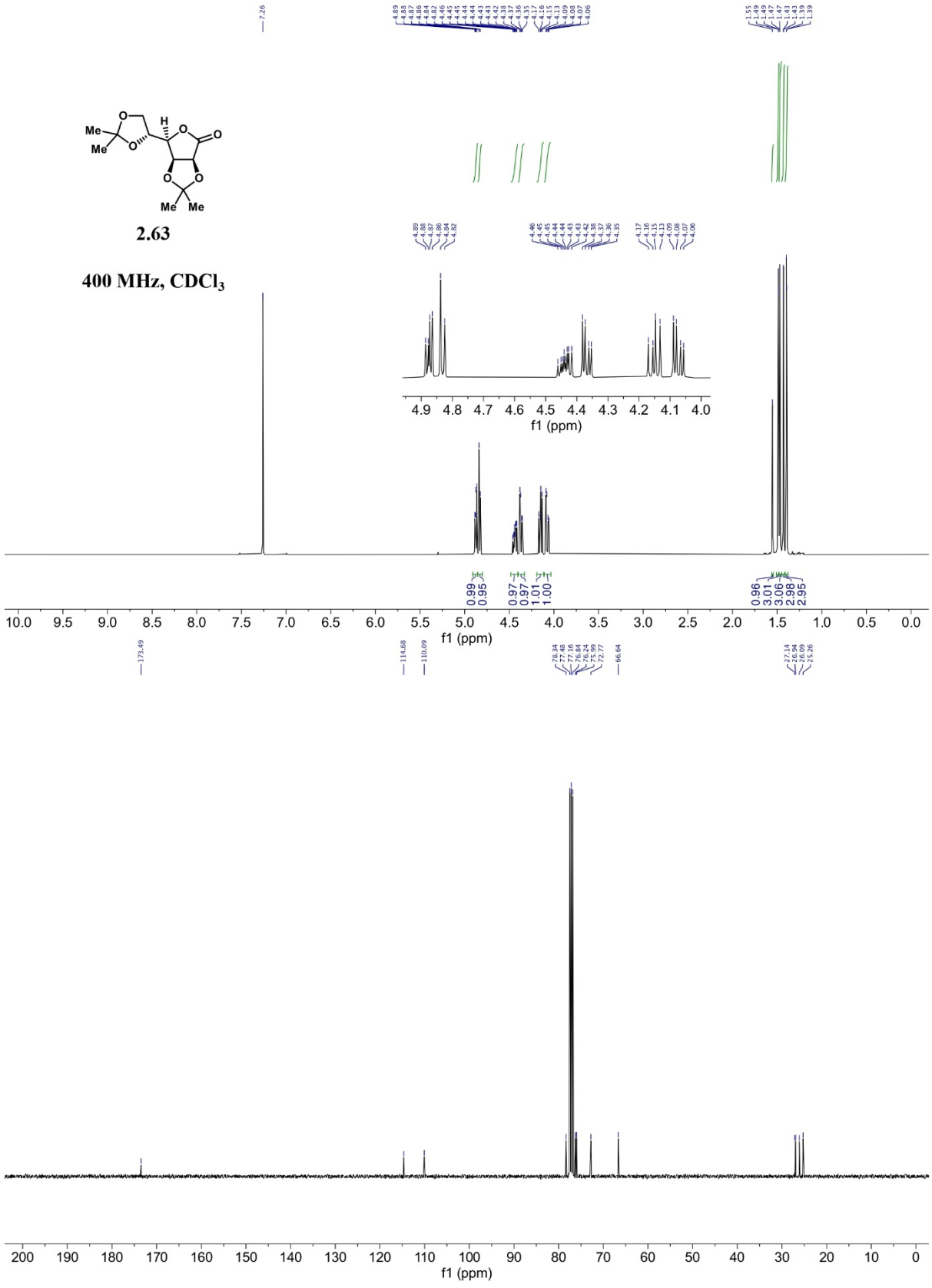

Me
Me
Me
2.53
400 MHz, CDCl3
δ (ppm)
δ (ppm)

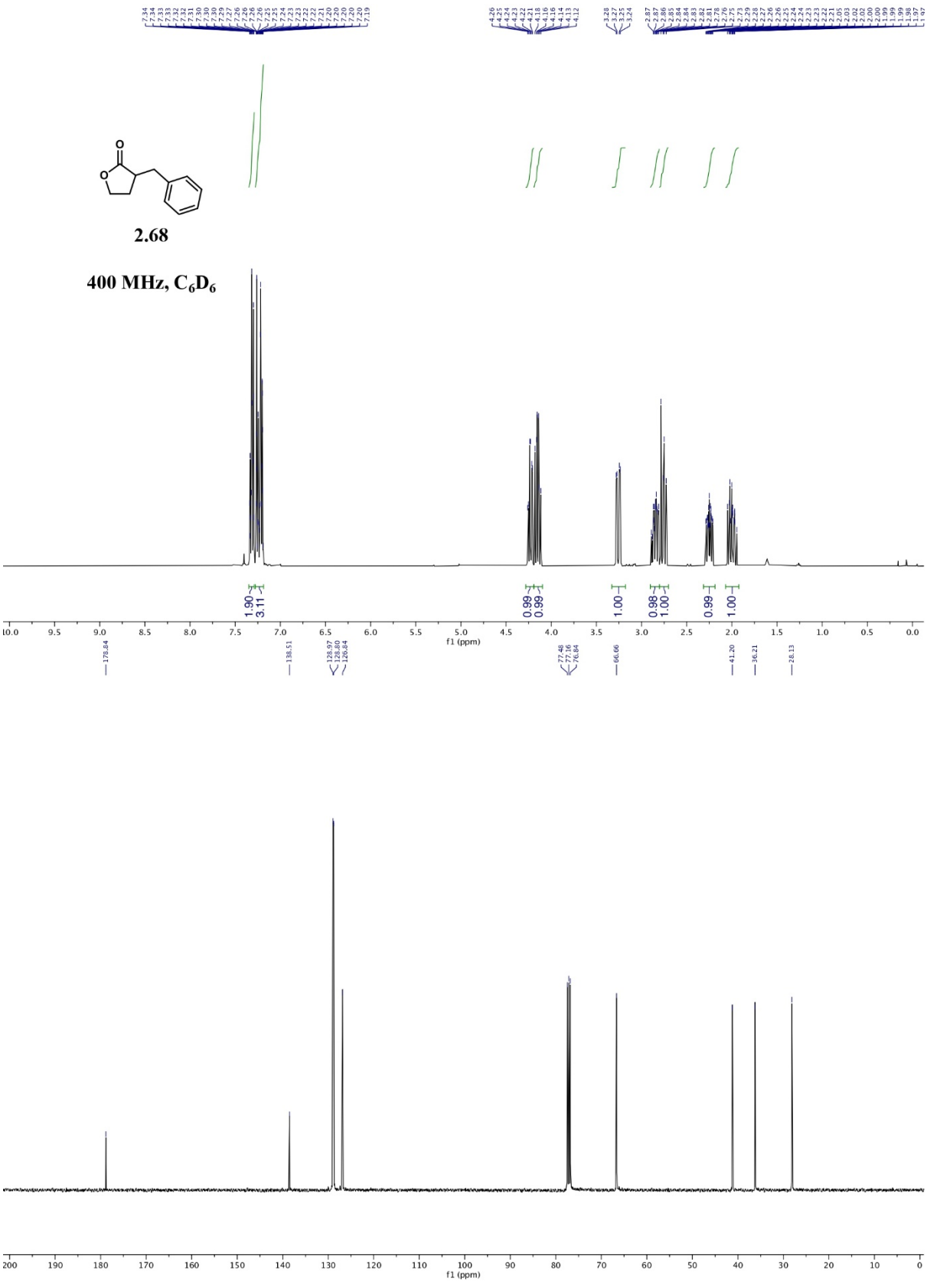


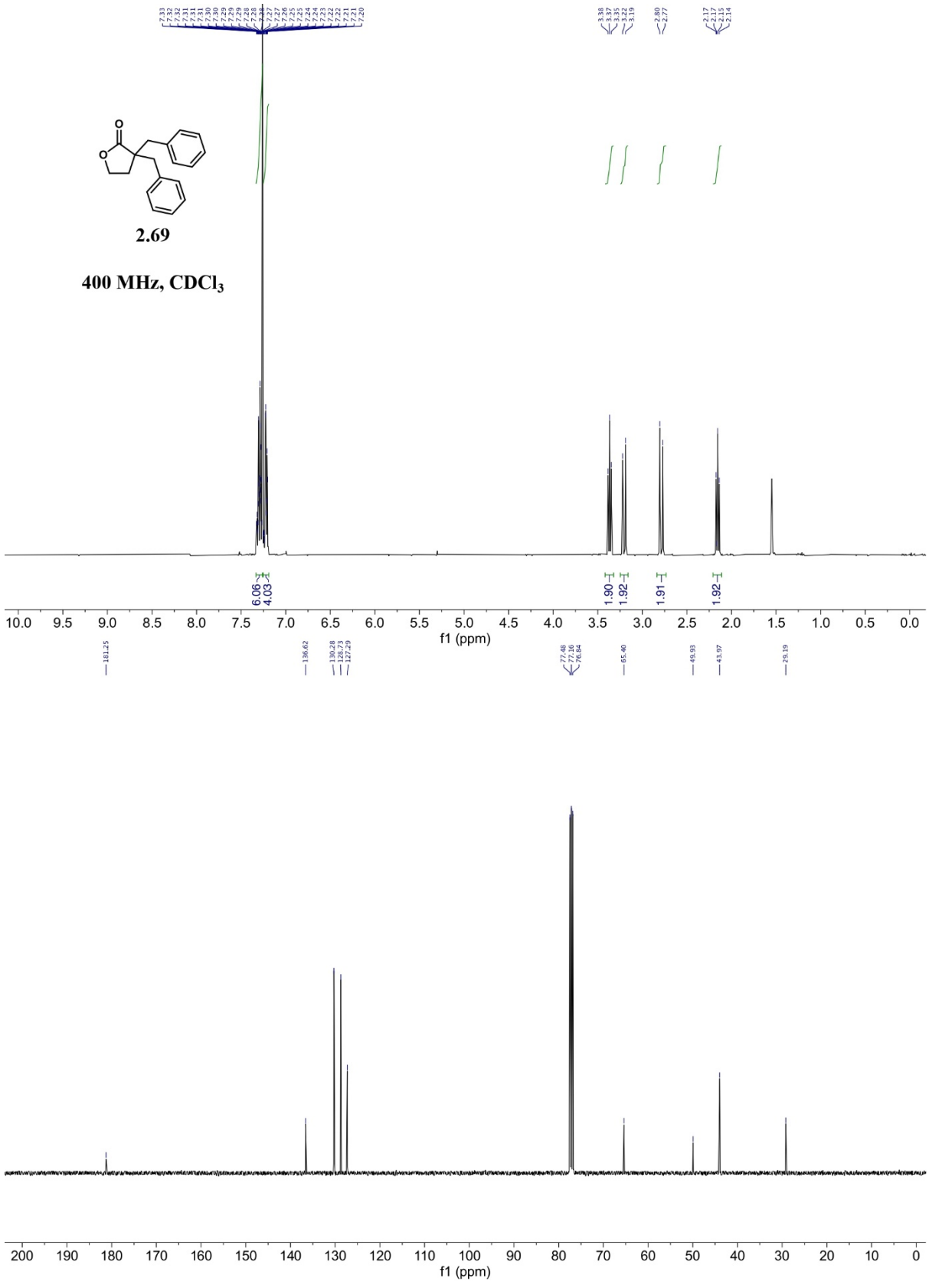
2.56

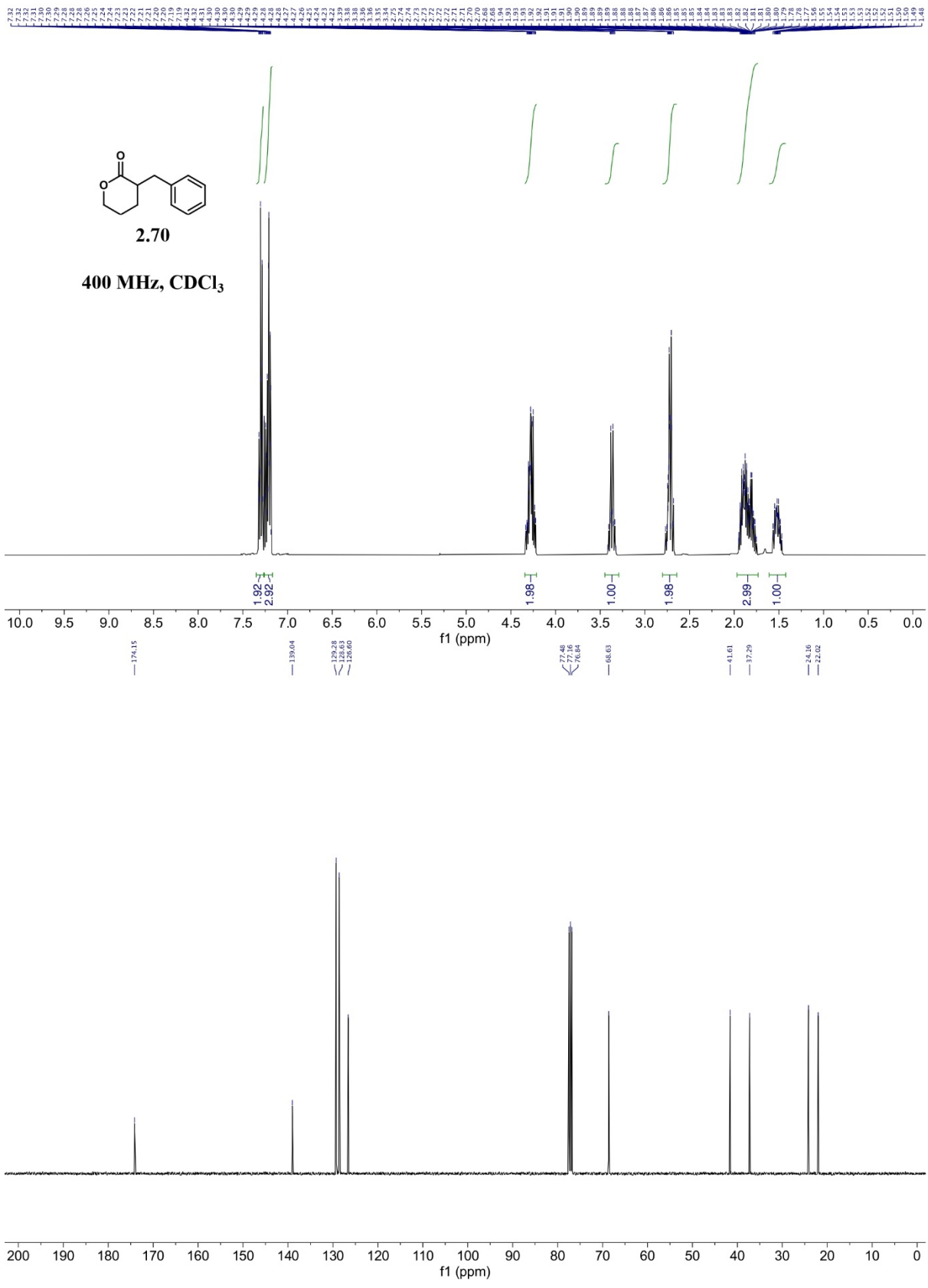
400 MHz, $CDCl_3$

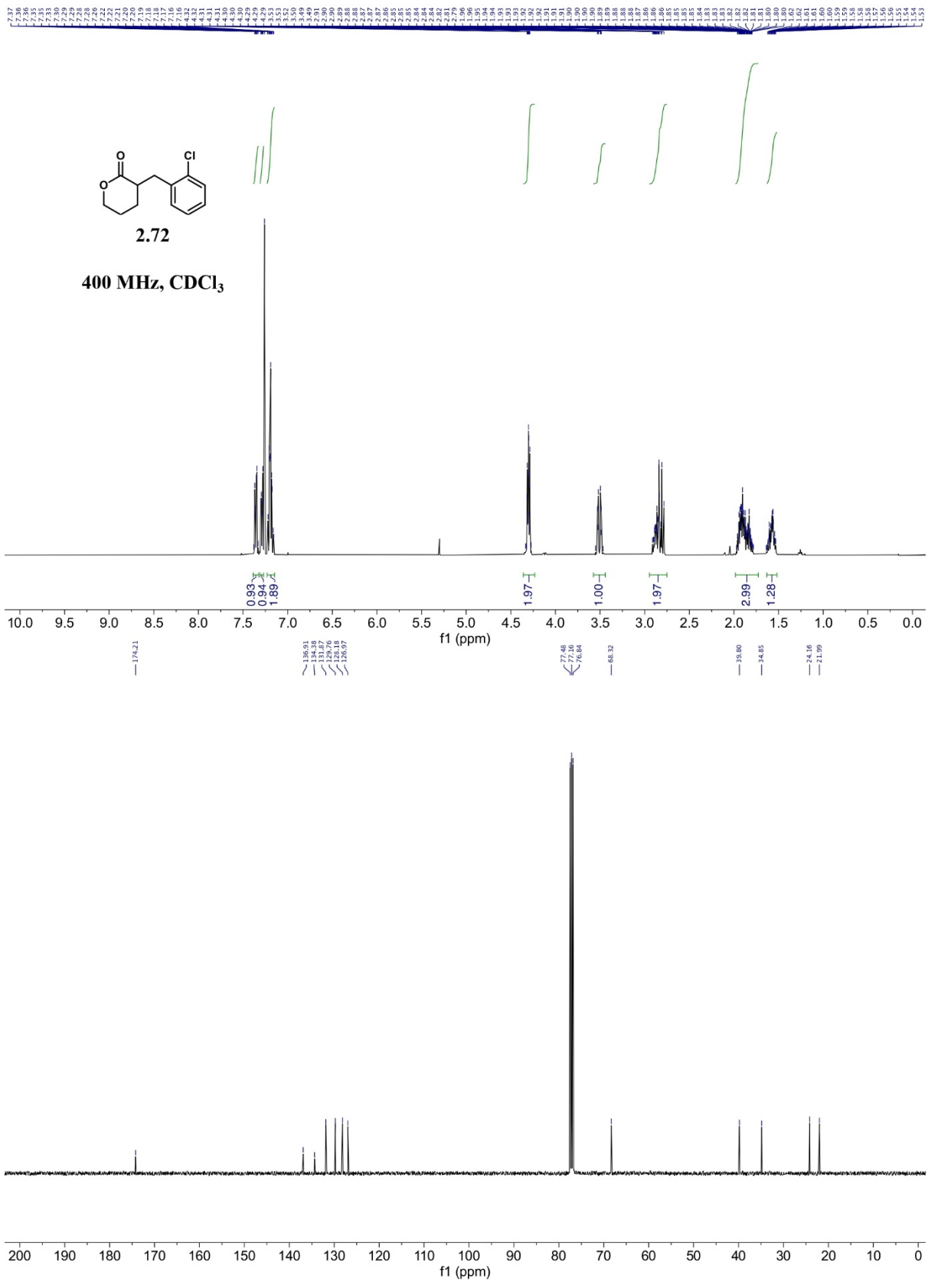

Me
O
O
H
2.61
400 MHz, CDCl3
f1 (ppm)
f1 (ppm)
f1 (ppm)

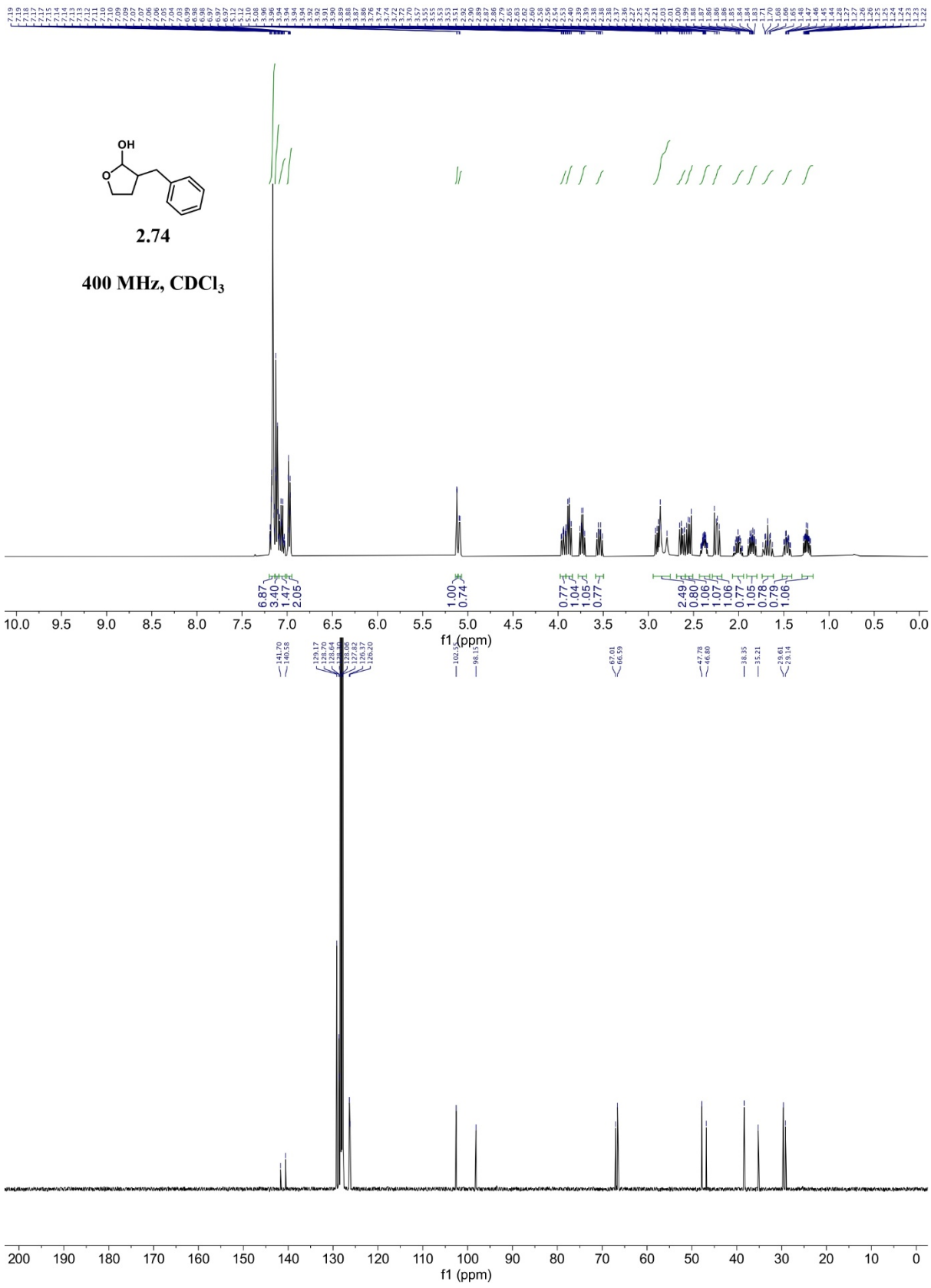

Me
Me
O
O
H
O
O
O
O
Me
Me
2.63
400 MHz, CDCl3
f1 (ppm)
f1 (ppm)
f1 (ppm)

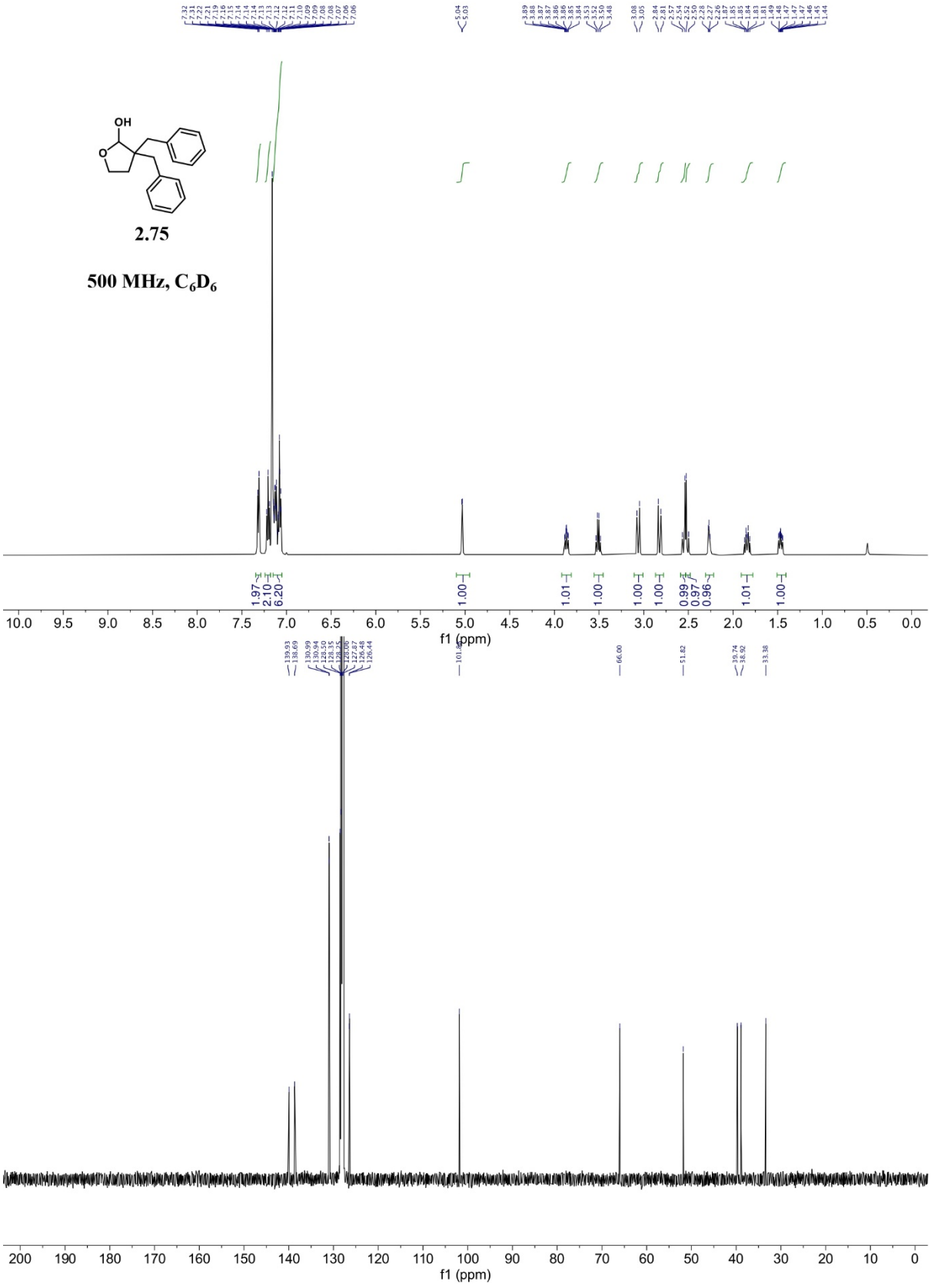

2.68
400 MHz, C6D6
f1 (ppm)

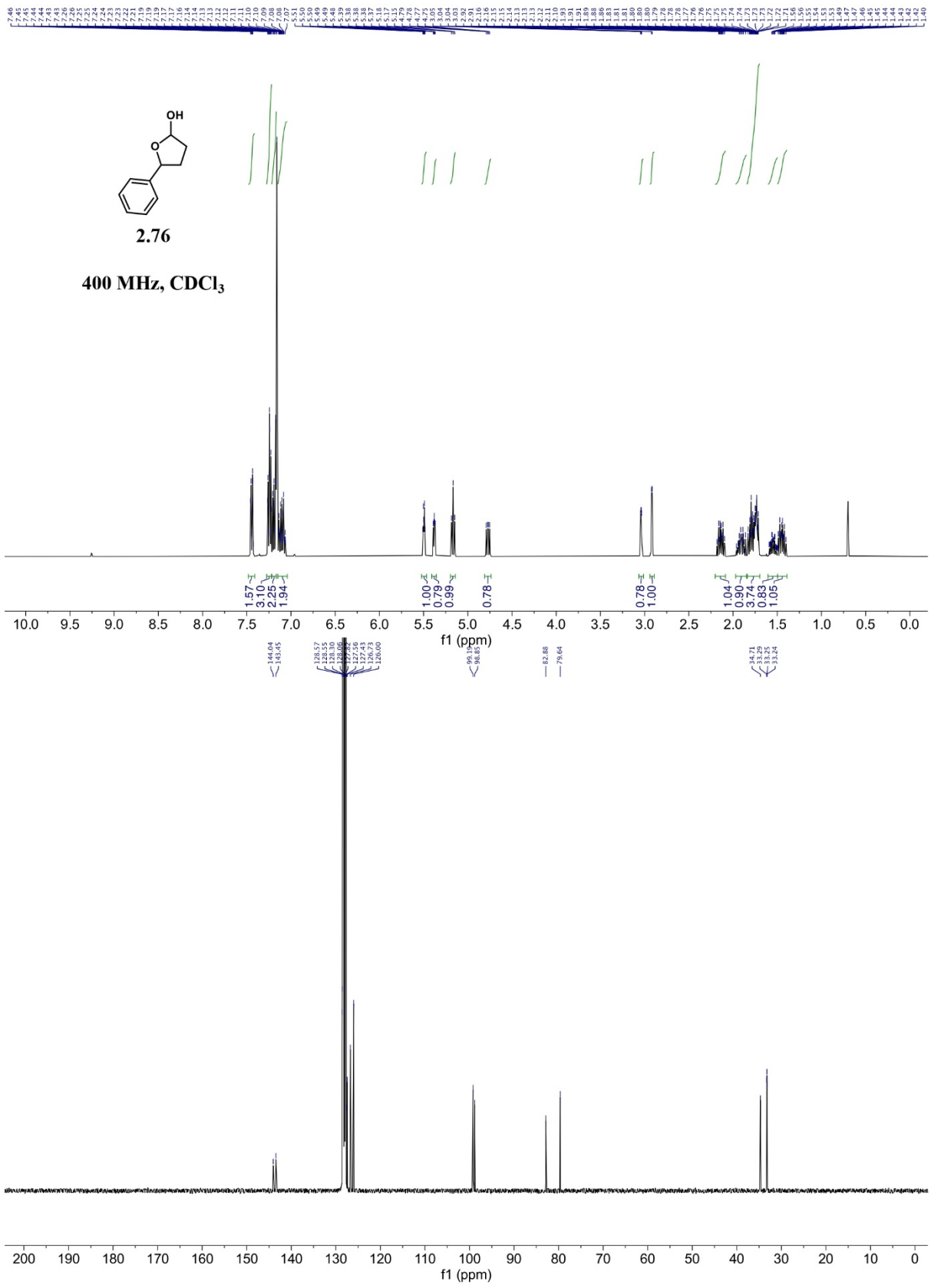

2.69
400 MHz, CDCl3
f1 (ppm)
f1 (ppm)

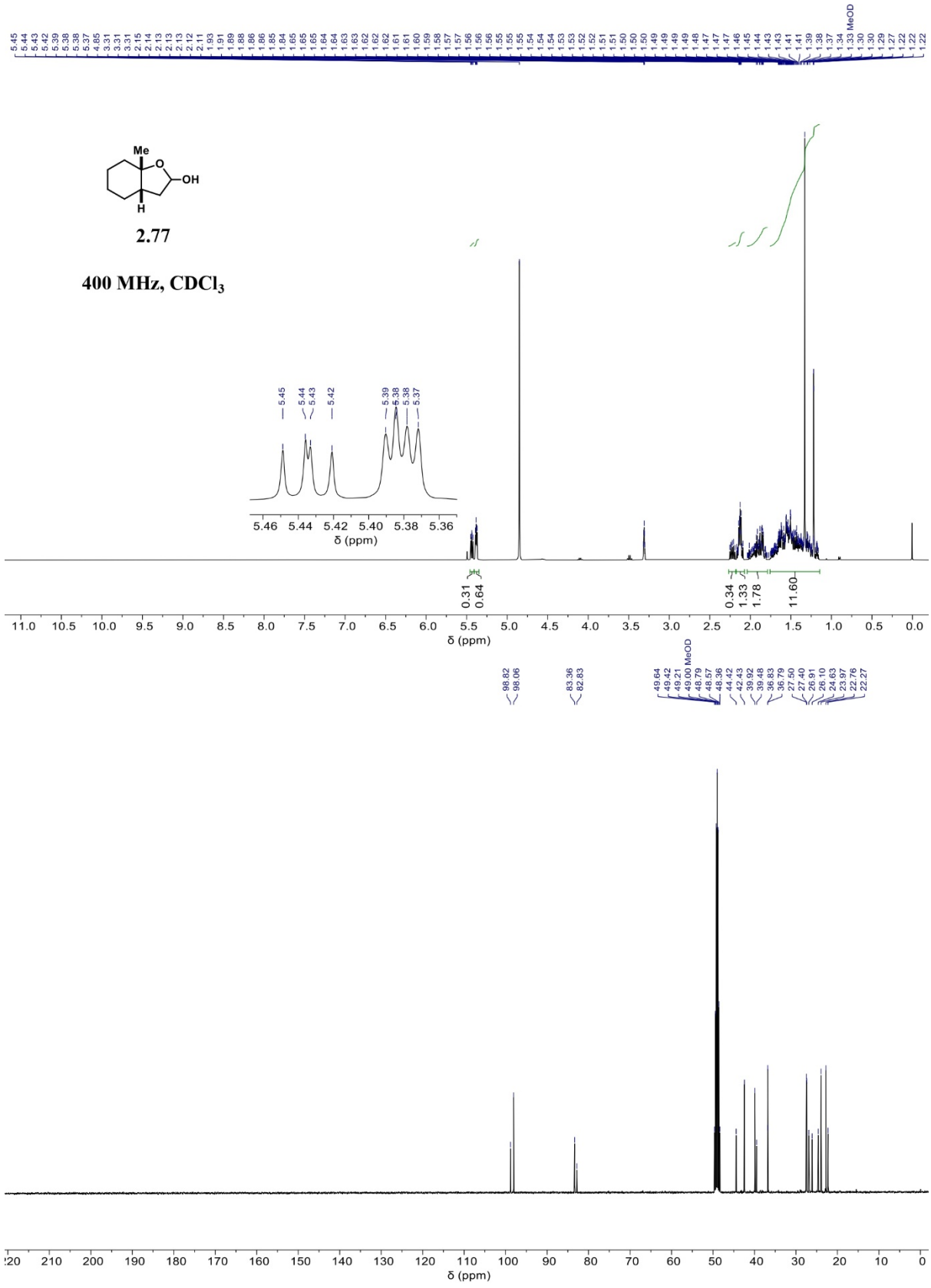

2.70
400 MHz, CDCl3
f1 (ppm)
f1 (ppm)

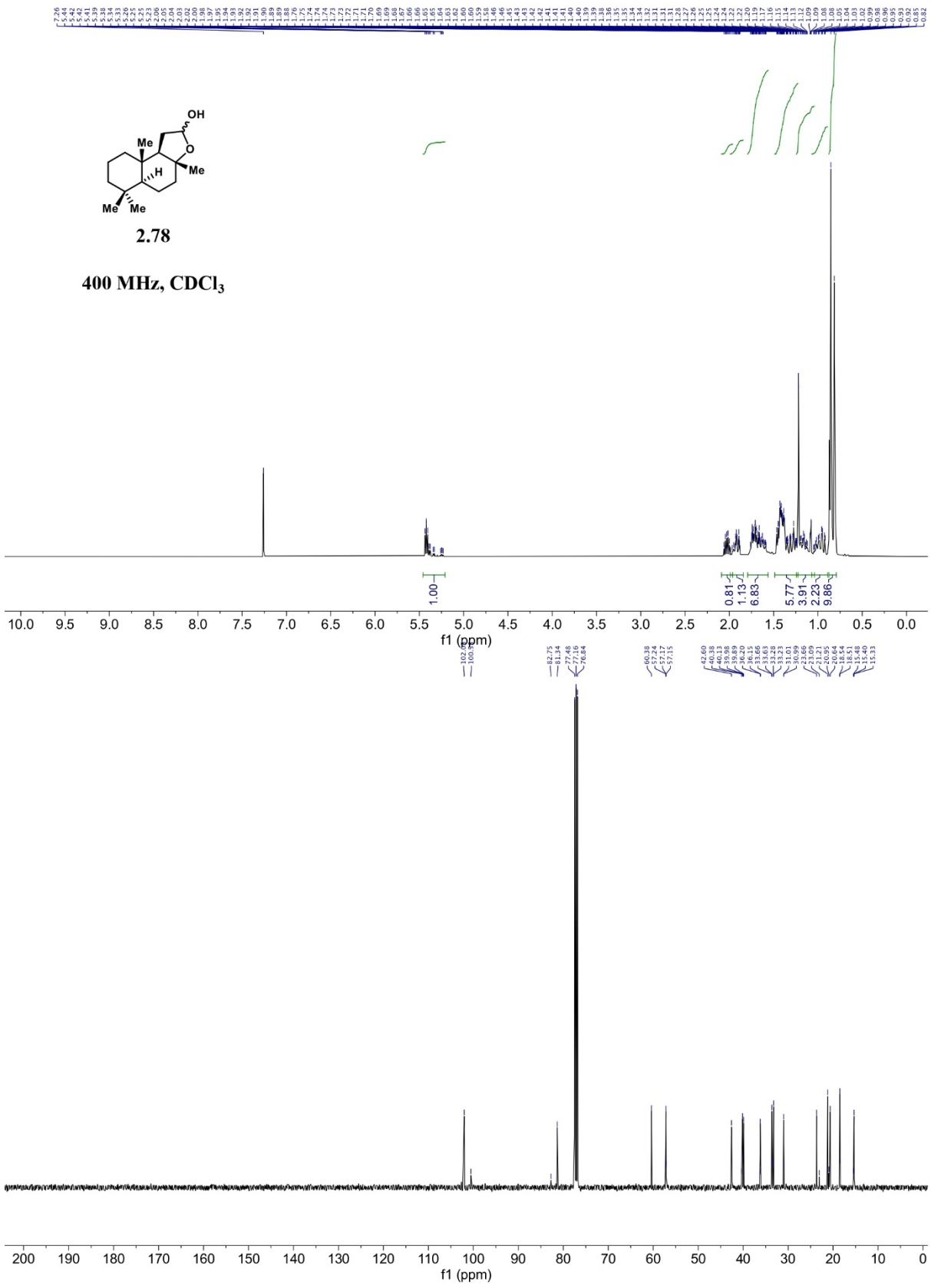

2.72
400 MHz, CDCl3
f1 (ppm)
f1 (ppm)

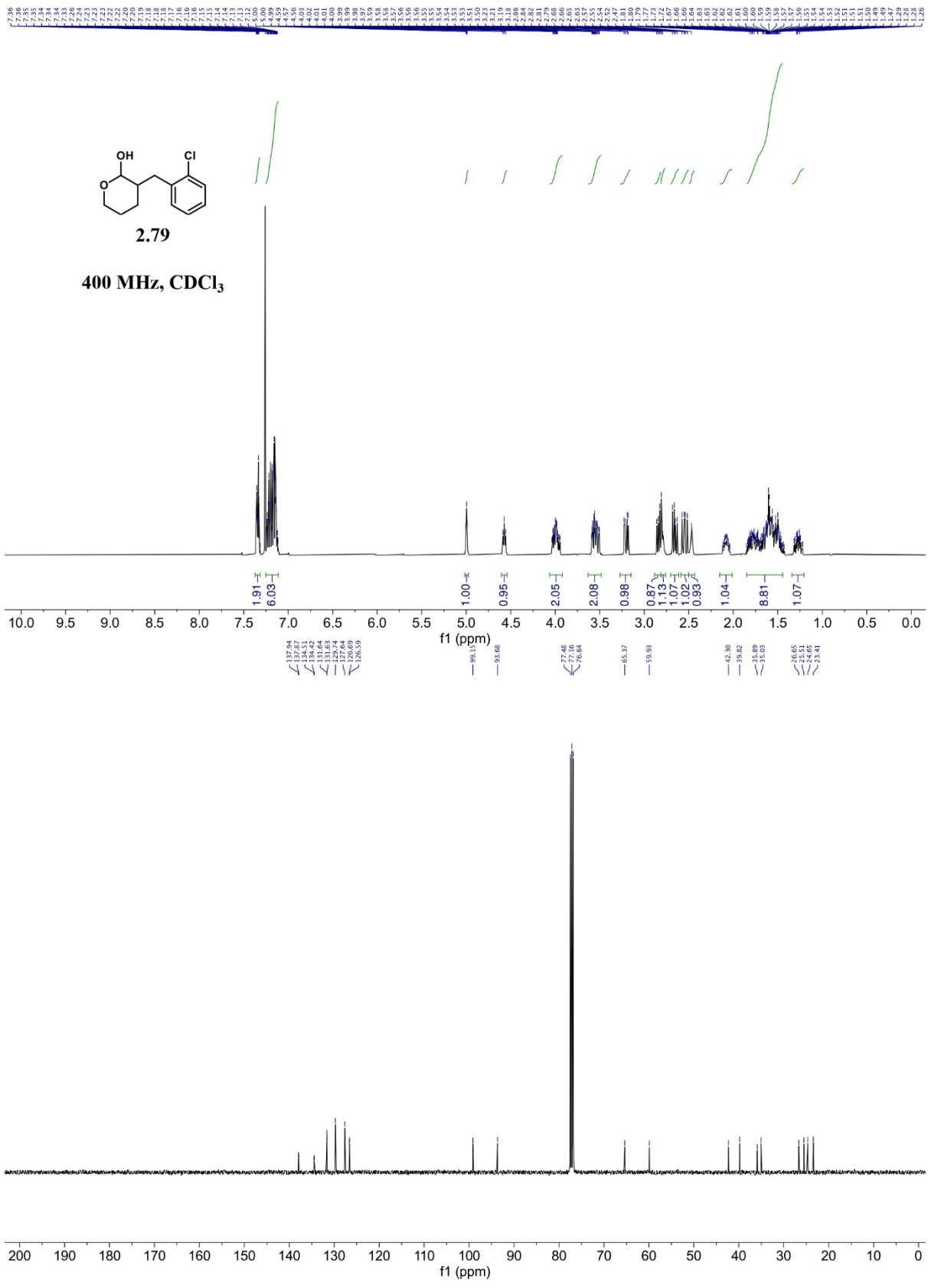

OH
O
2.74
400 MHz, CDCl3
f1 (ppm)
f1 (ppm)

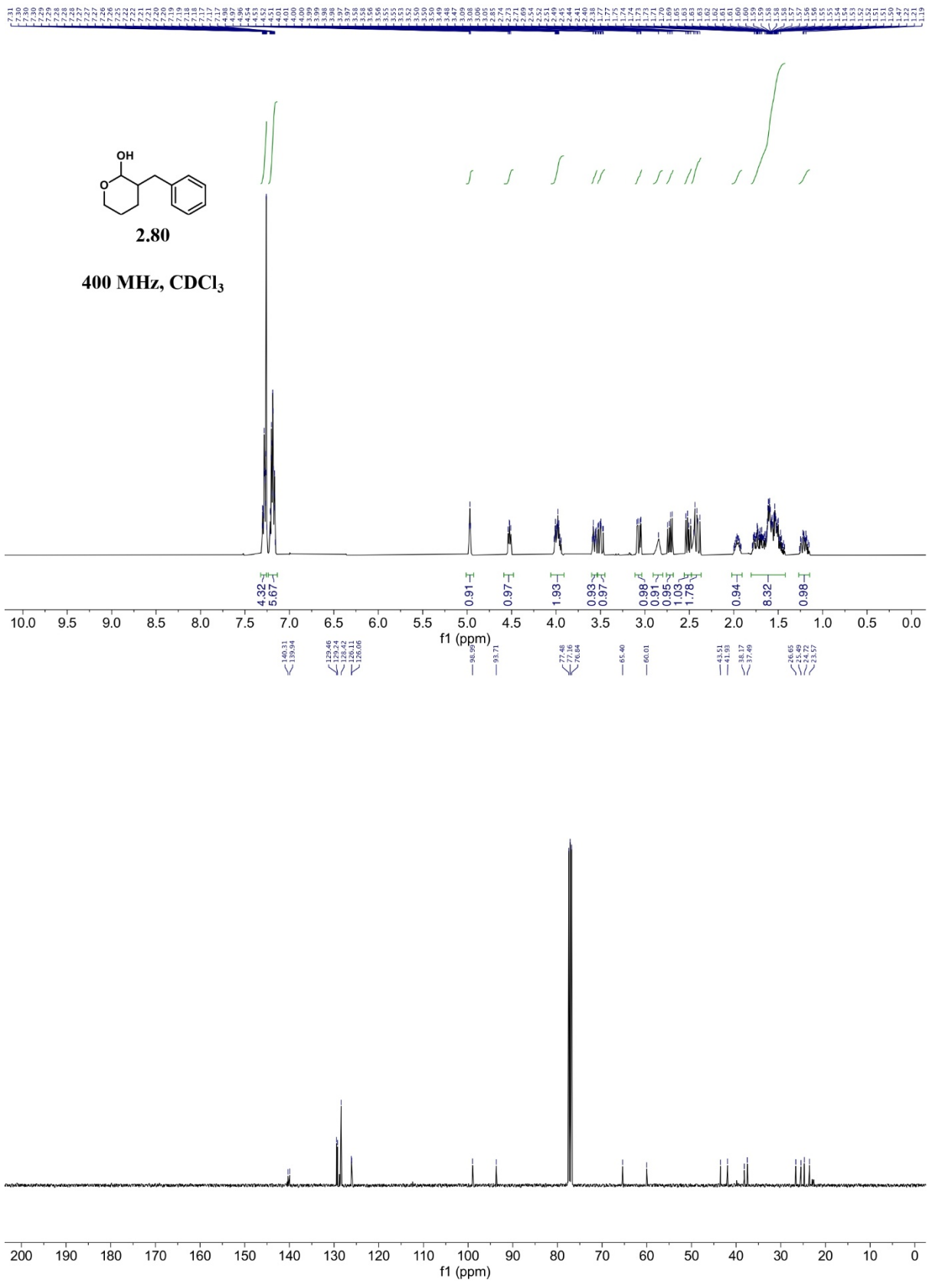

OH
O
2.75
500 MHz, C6D6
f1 (ppm)
f1 (ppm)

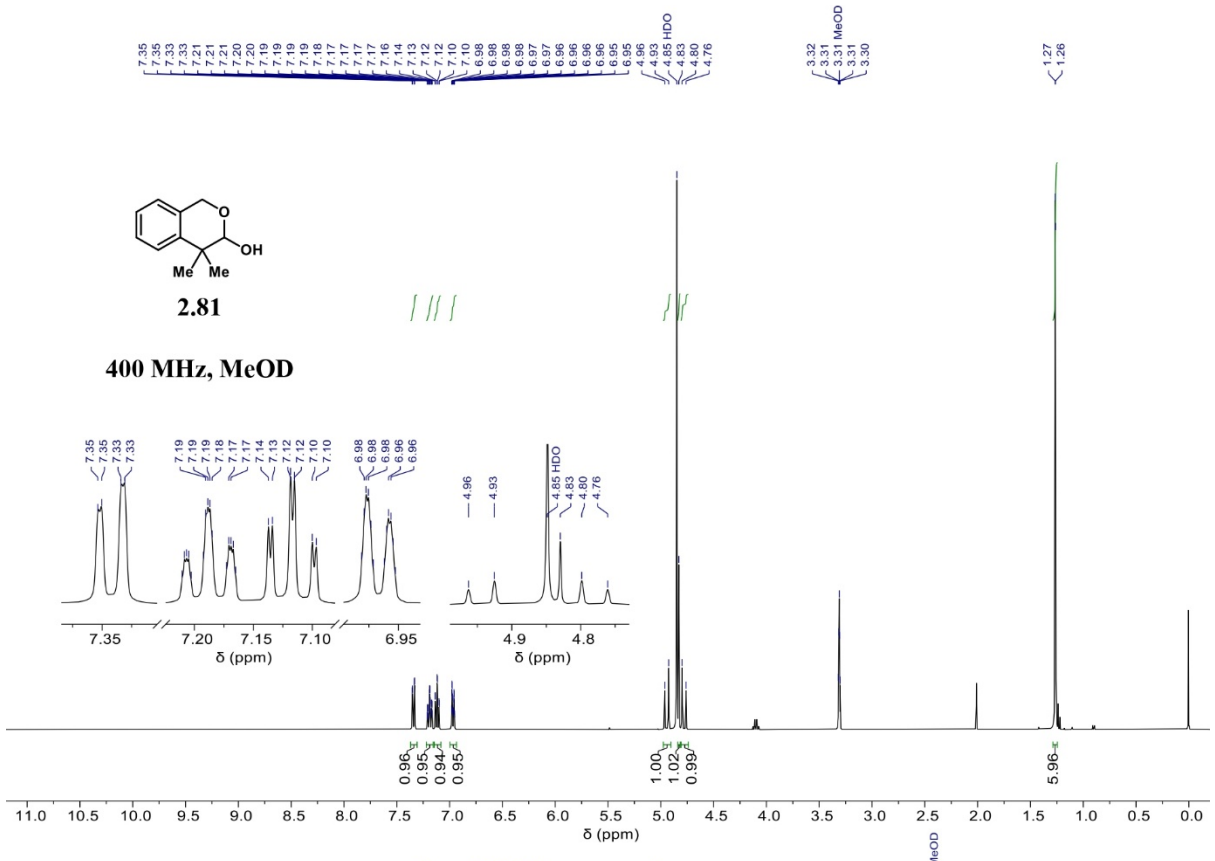

OH
O
2.76
400 MHz, CDCl3
f1 (ppm)
f1 (ppm)

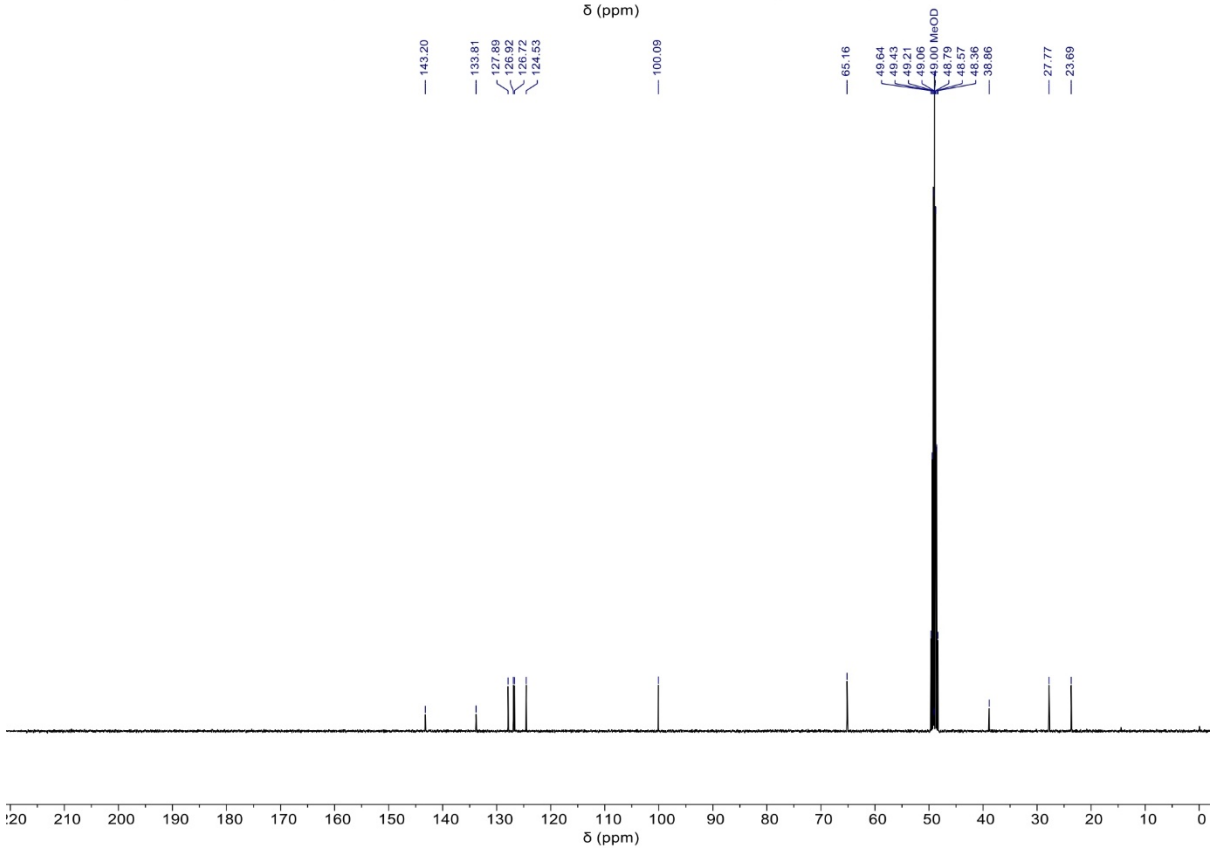

Me
O
OH
H
2.77
400 MHz, CDCl3
δ (ppm)
MeOD

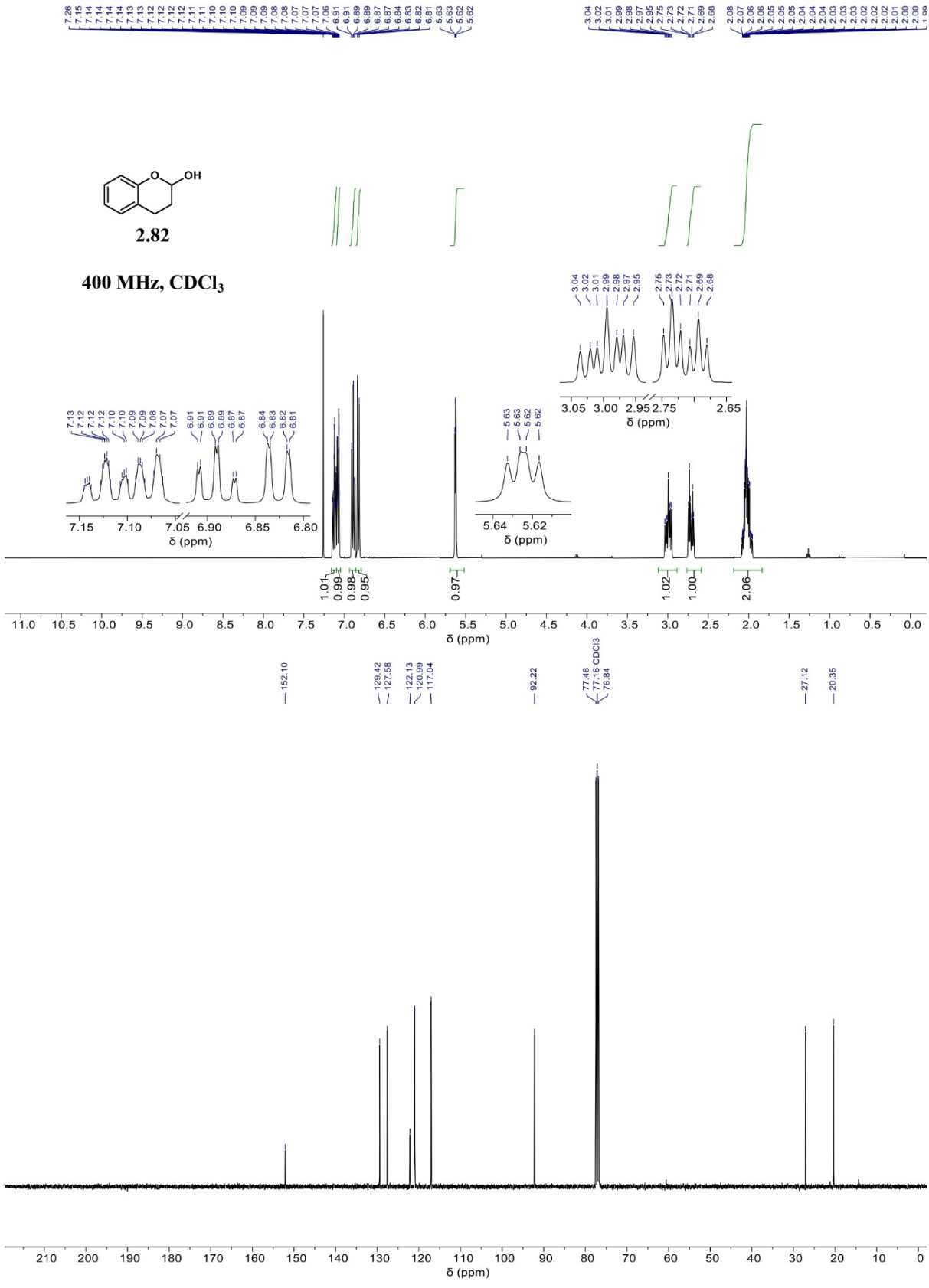

OH
Me
O
Me
H
Me
Me
2.78
400 MHz, CDCl3
1.00
0.81
1.13
6.83
5.77
3.91
2.23
9.86
f1 (ppm)
f1 (ppm)

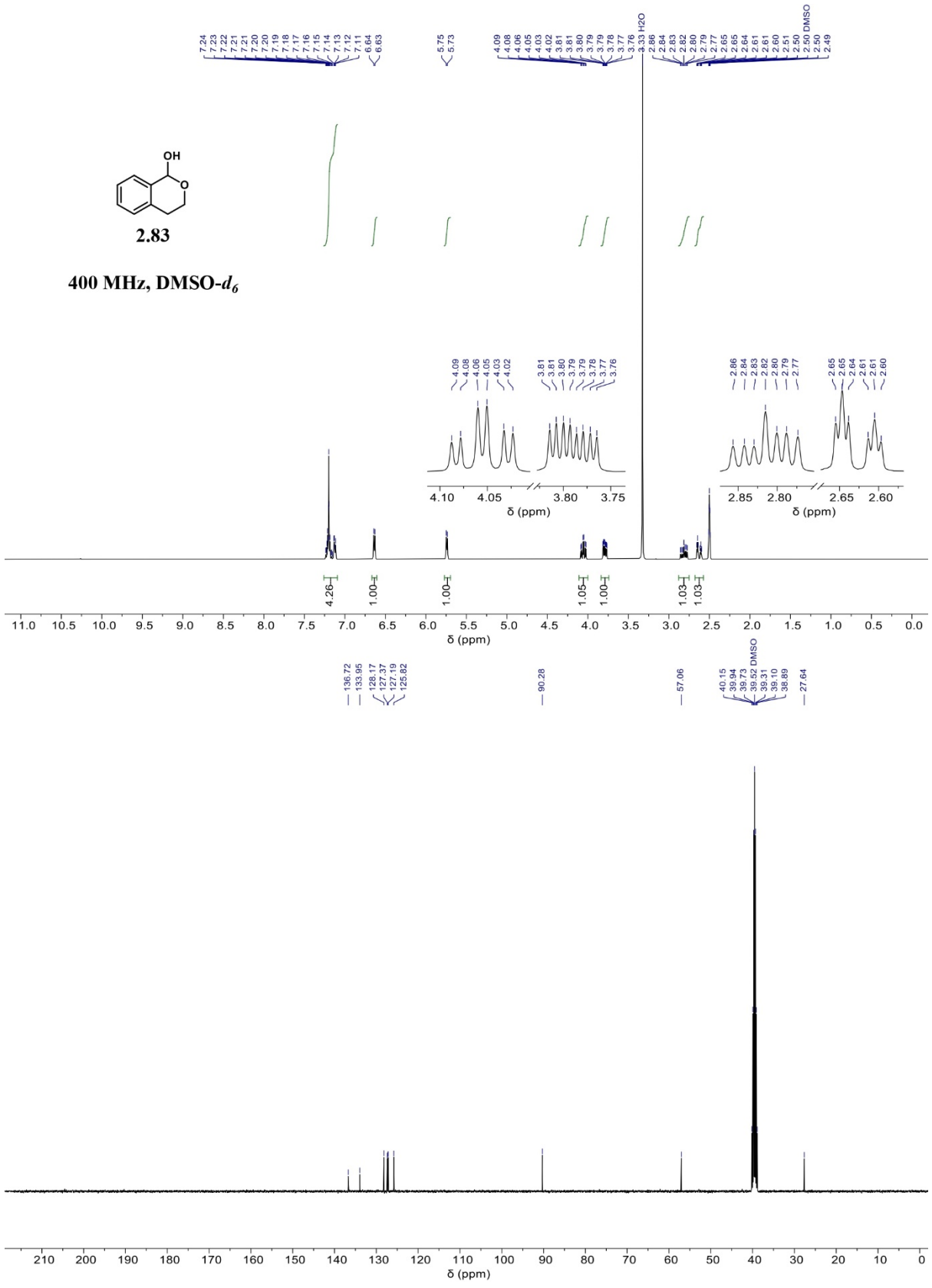

OH
Cl
O
2.79
400 MHz, CDCl3
f1 (ppm)
f1 (ppm)

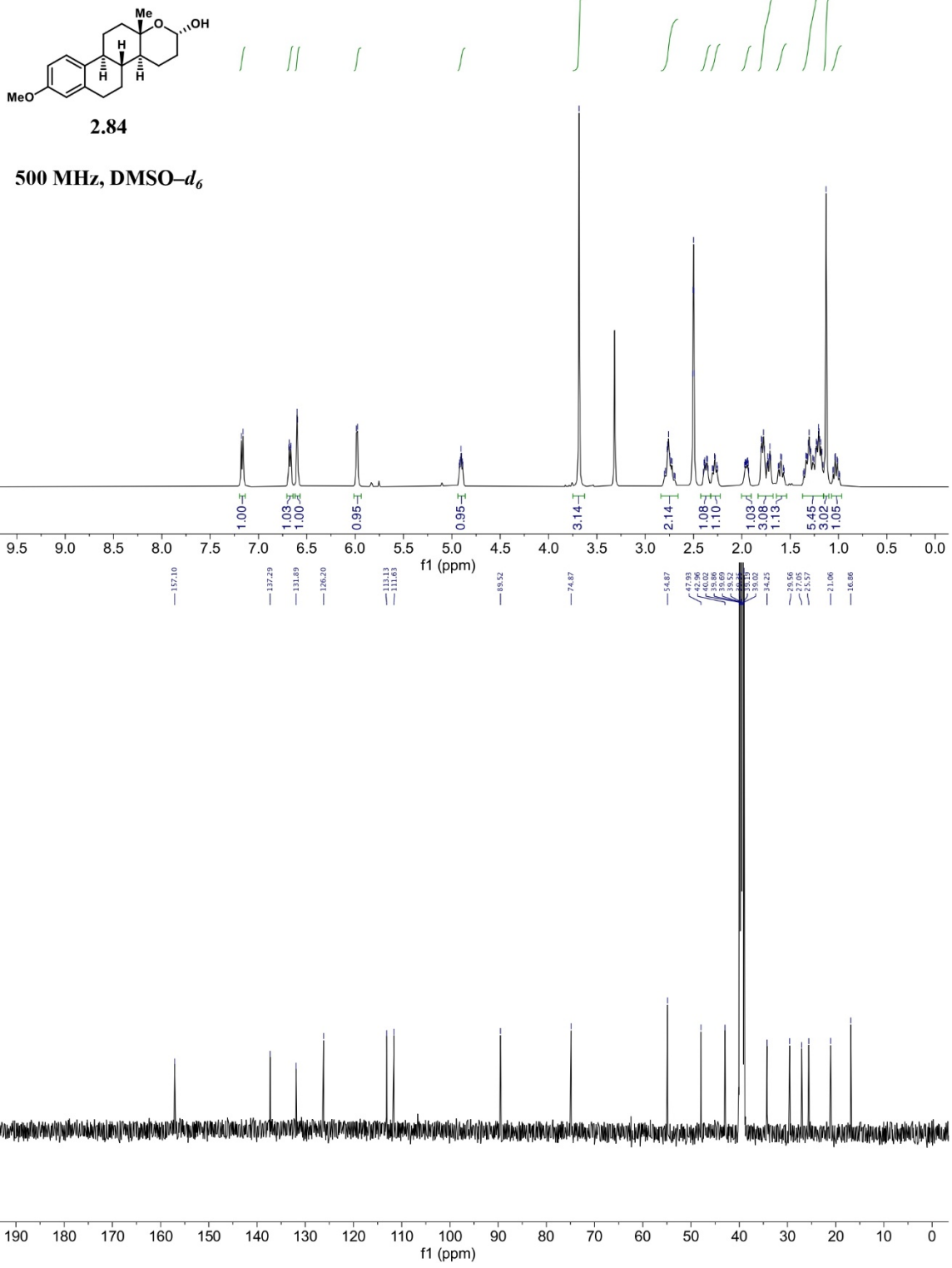

OH
O
2.80
400 MHz, CDCl3
f1 (ppm)
f1 (ppm)

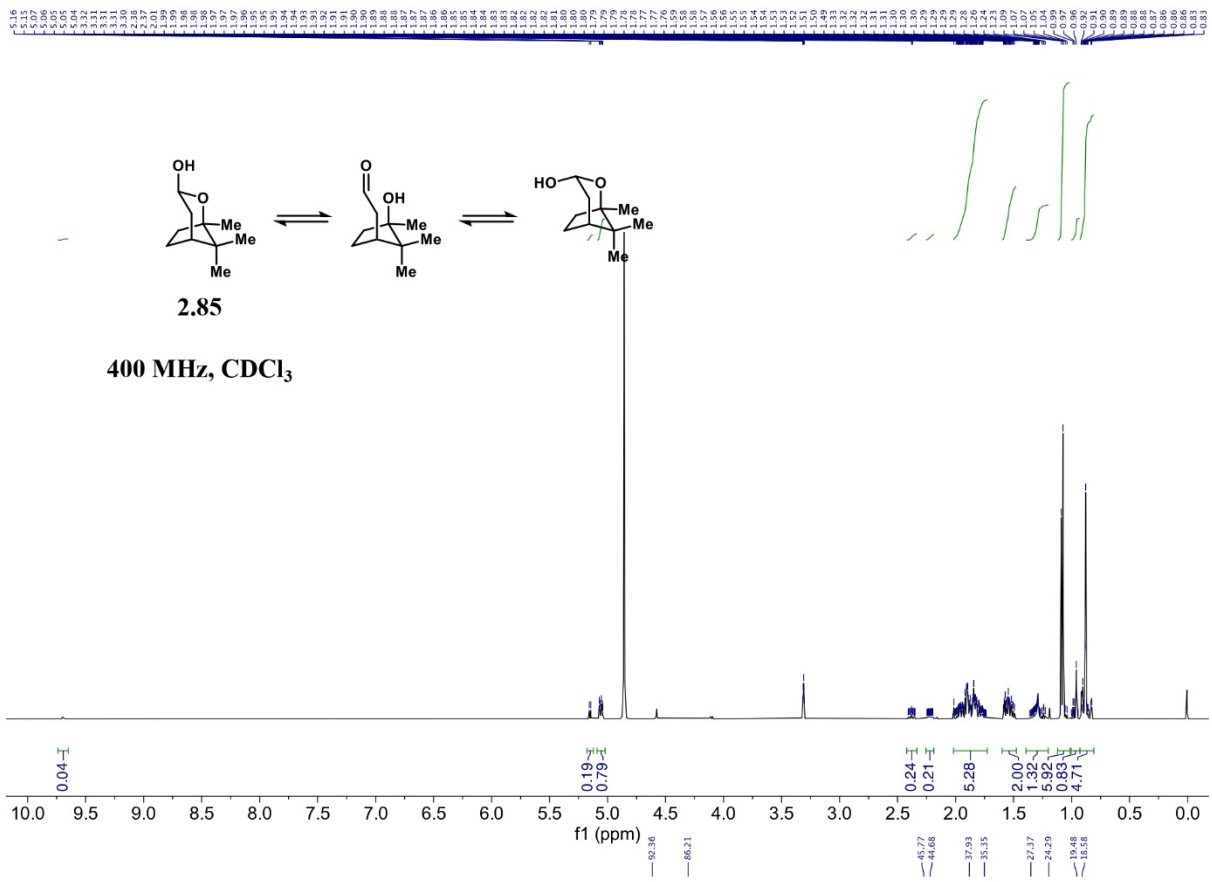

OH
Me Me
2.81
400 MHz, MeOD
δ (ppm)
0.96
0.95
0.94
0.95
1.00
1.02
0.99
5.96

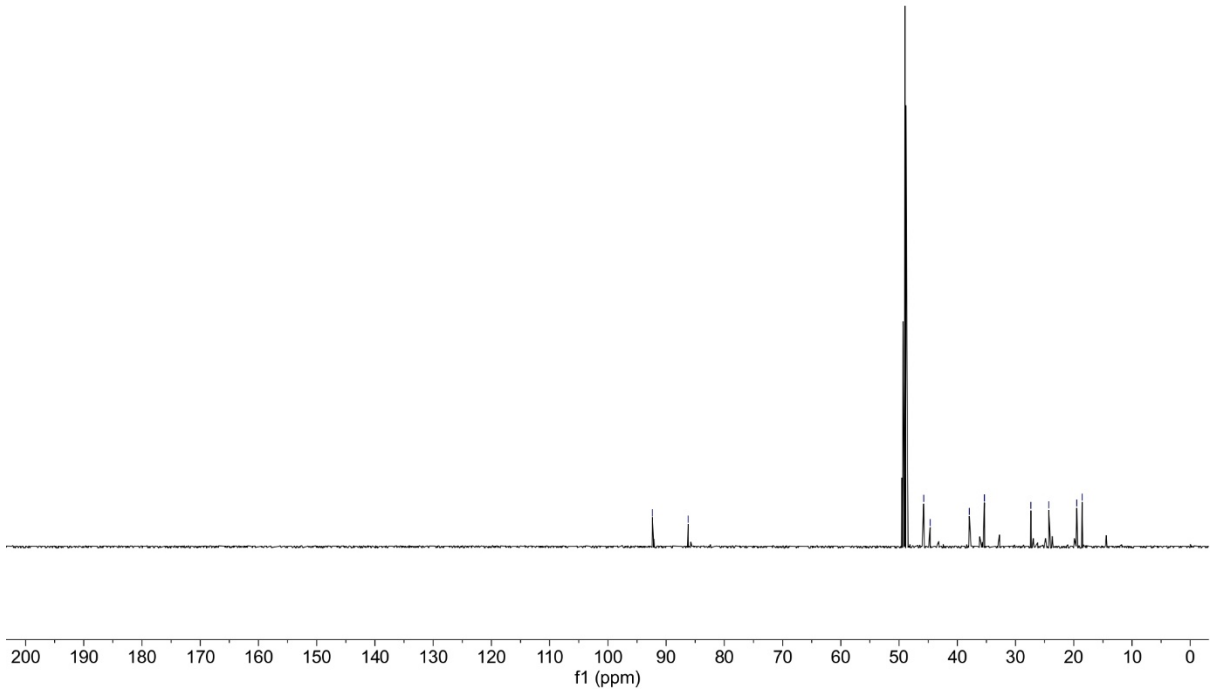

δ (ppm)


2.82
400 MHz, CDCl3
δ (ppm)
152.10
129.42
127.58
122.13
120.99
117.04
92.22
77.48
77.16 CDCl3
76.84
27.12
20.35


OH
O
2.83
400 MHz, DMSO-d_6
δ (ppm)
DMSO
H2O

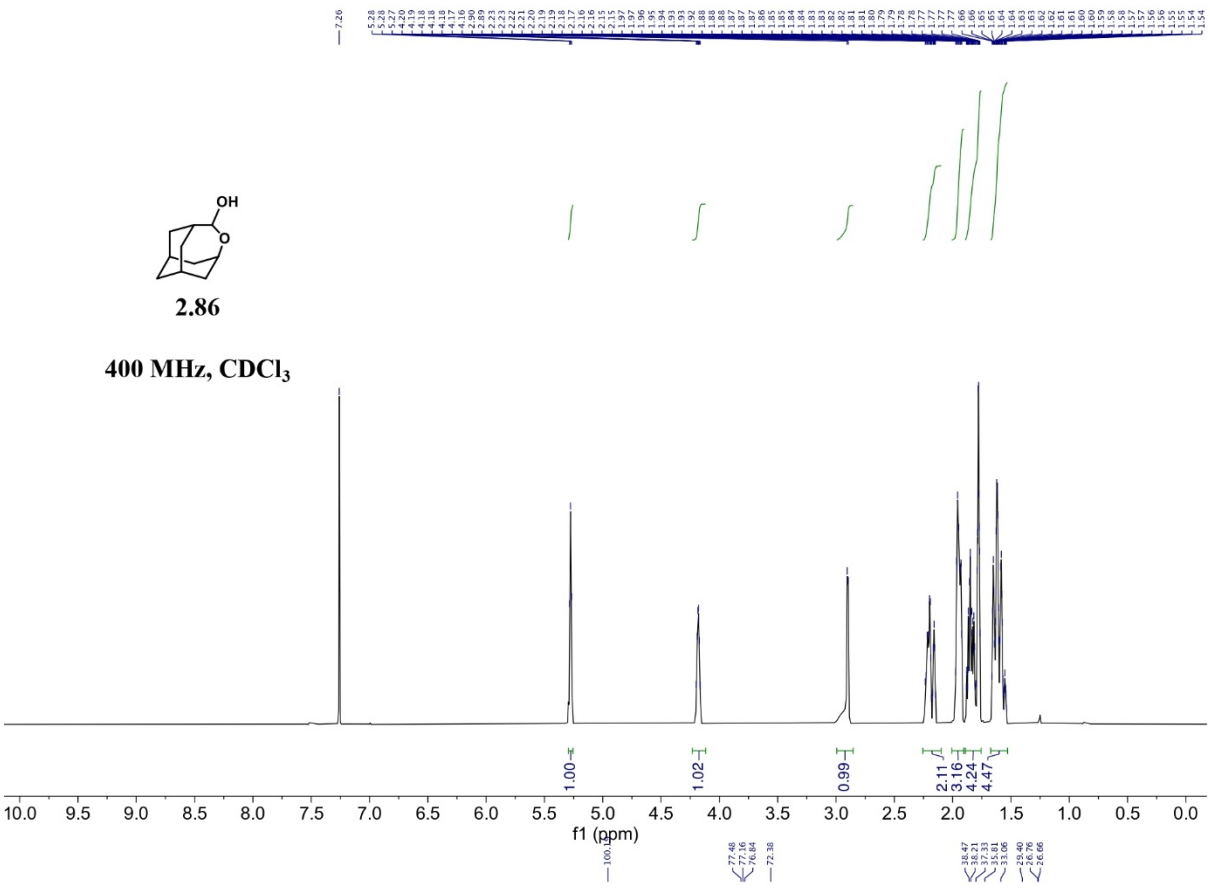

Me
O
OH
H
H
H
MeO
2.84
500 MHz, DMSO–d_6
f1 (ppm)
f1 (ppm)

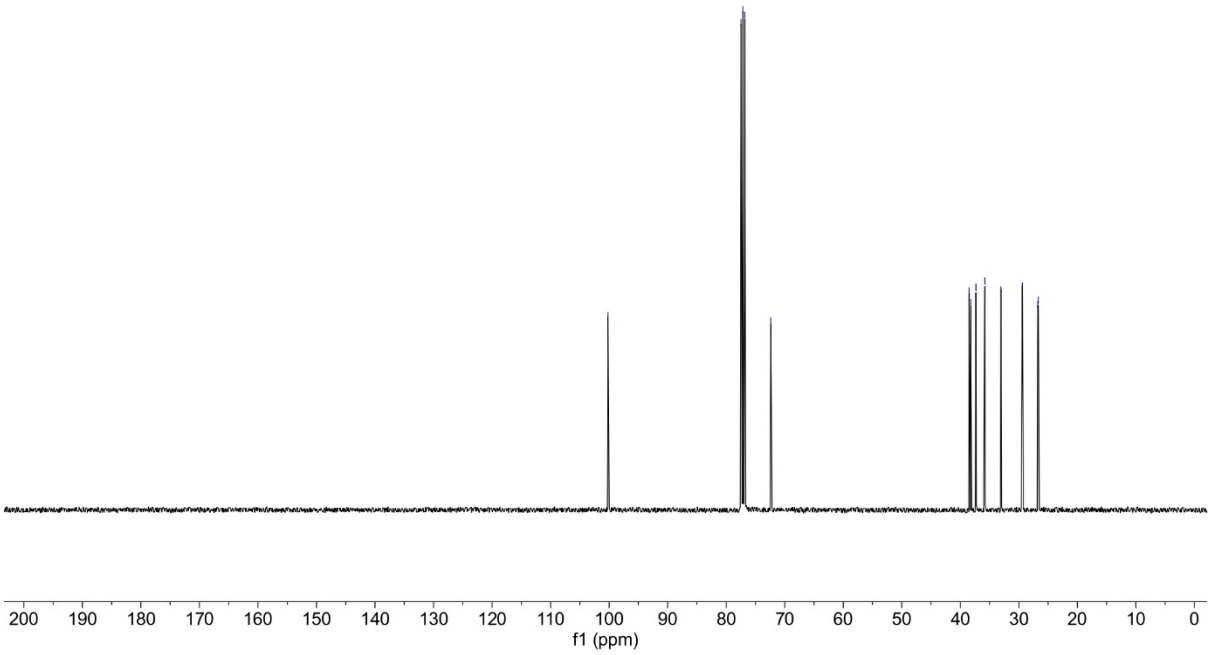

OH
O
Me
Me
Me
O
OH
Me
Me
Me
HO
O
Me
Me
Me
2.85
400 MHz, CDCl3
0.04
0.19
0.79
0.24
0.21
5.28
2.00
1.32
5.92
0.83
4.71
f1 (ppm)
92.36
86.21
45.77
44.68
37.93
35.35
27.37
24.29
19.48
18.58

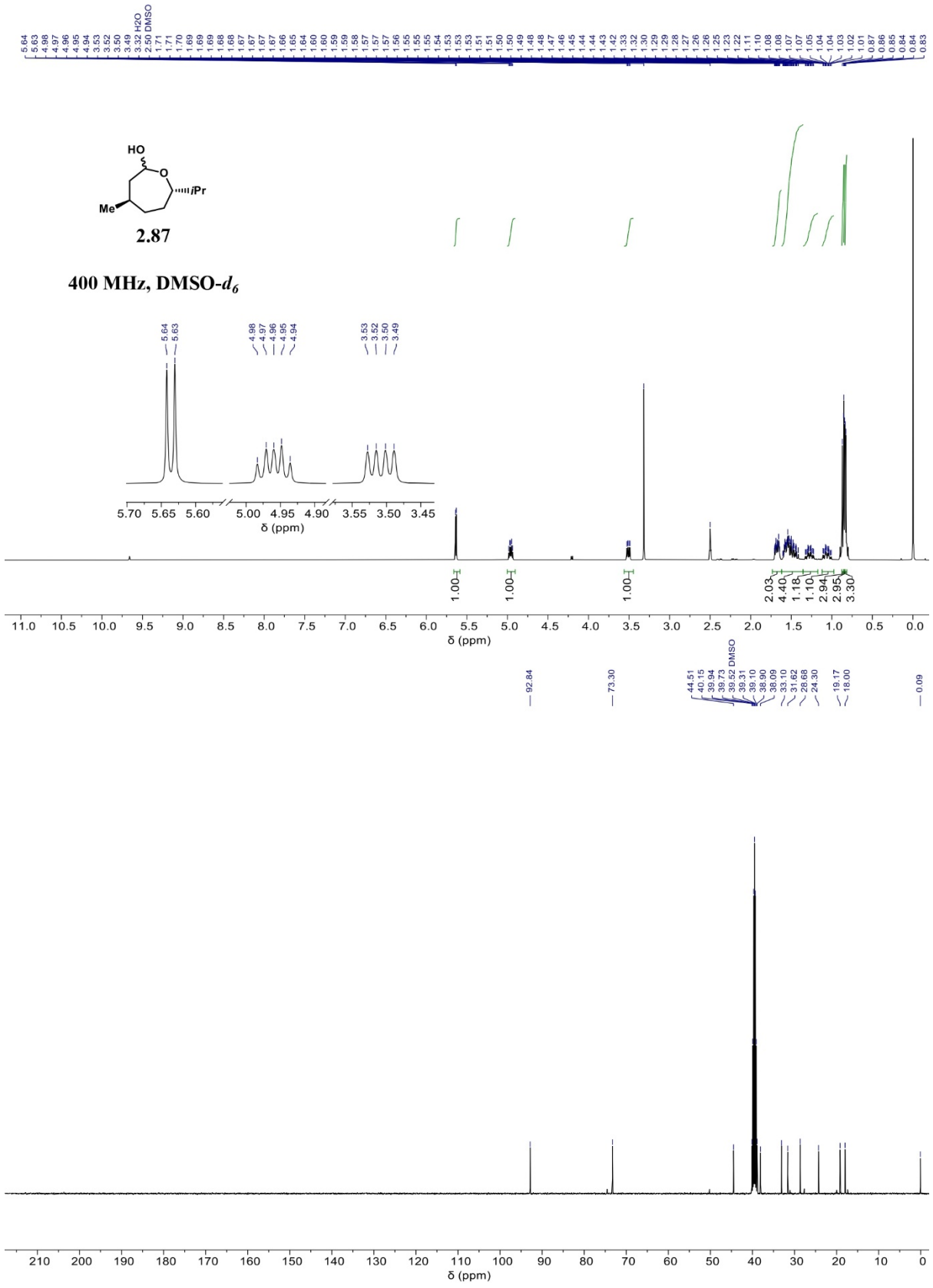

f1 (ppm)

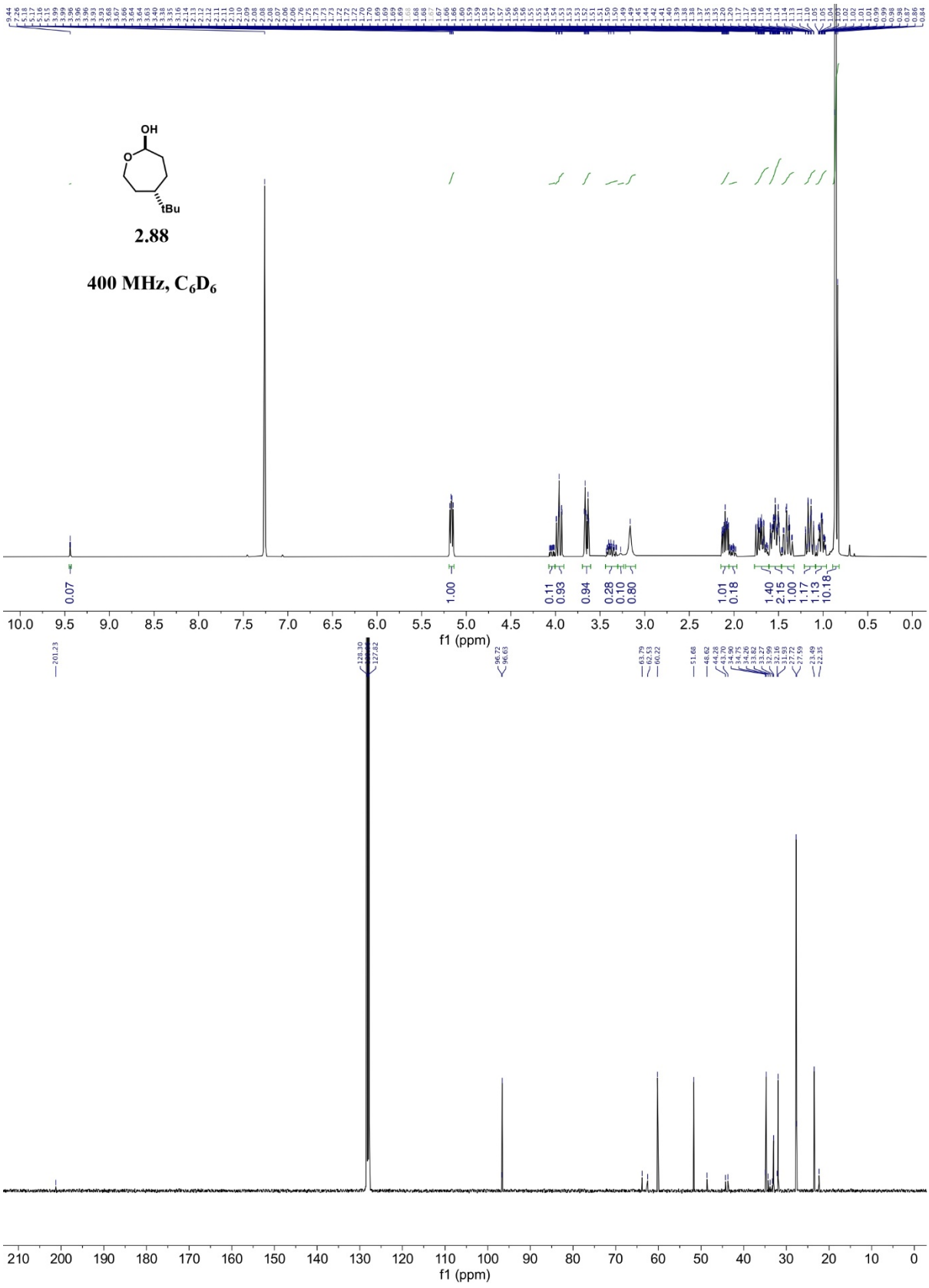
2.86

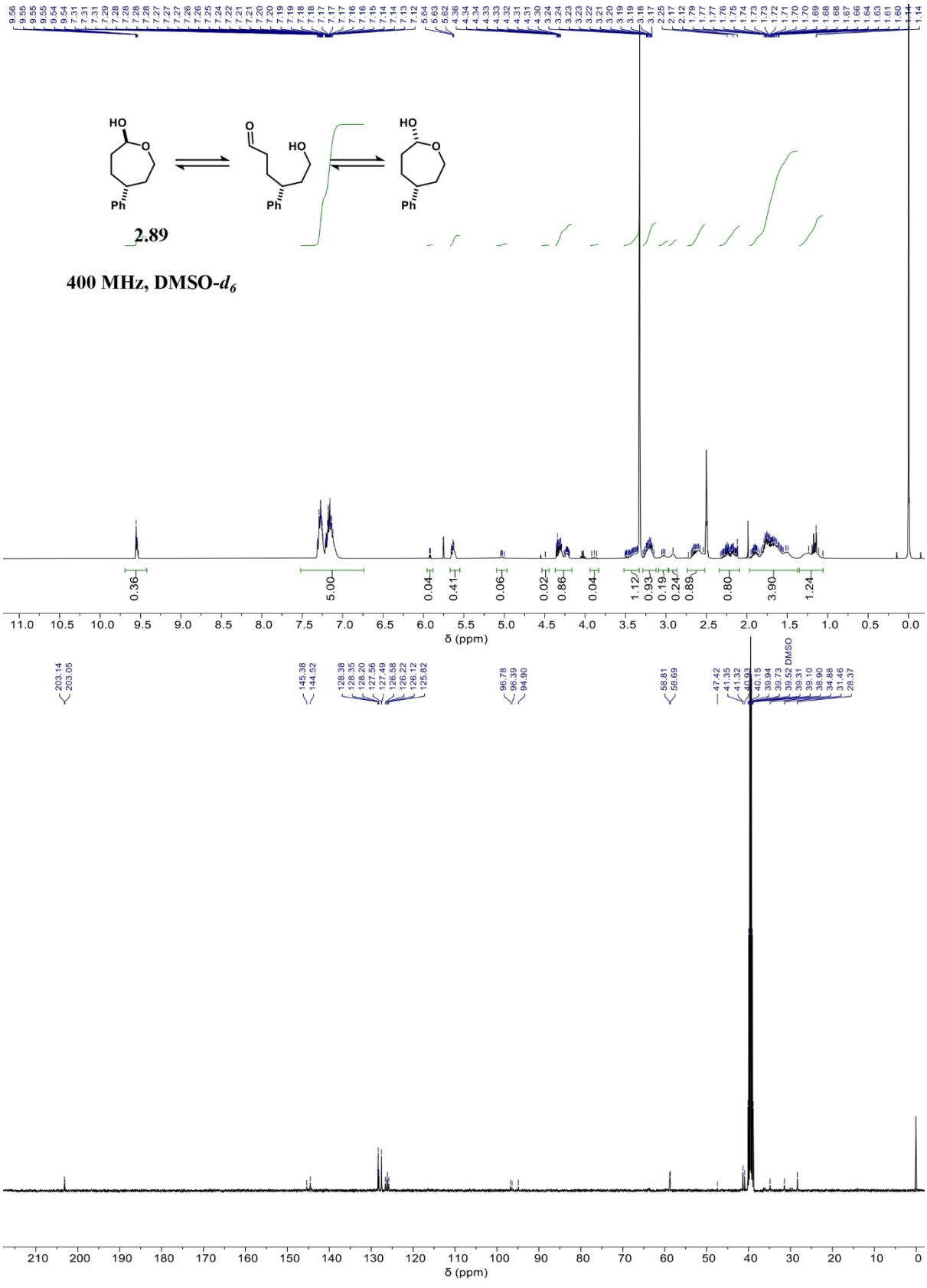
400 MHz, $CDCl_3$





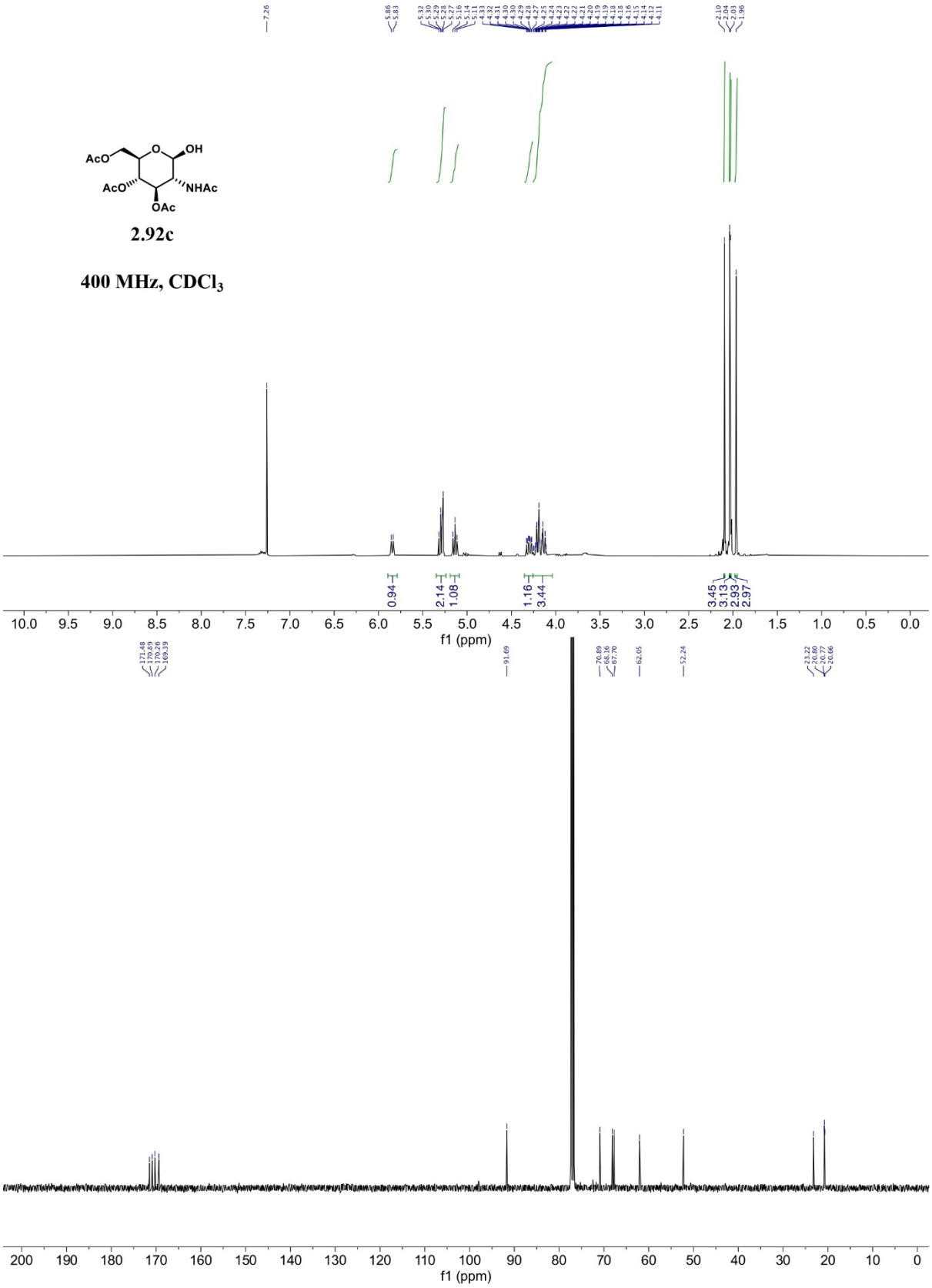

HO
O
iPr
Me
2.87
400 MHz, DMSO-d_6
δ (ppm)
DMSO
H2O

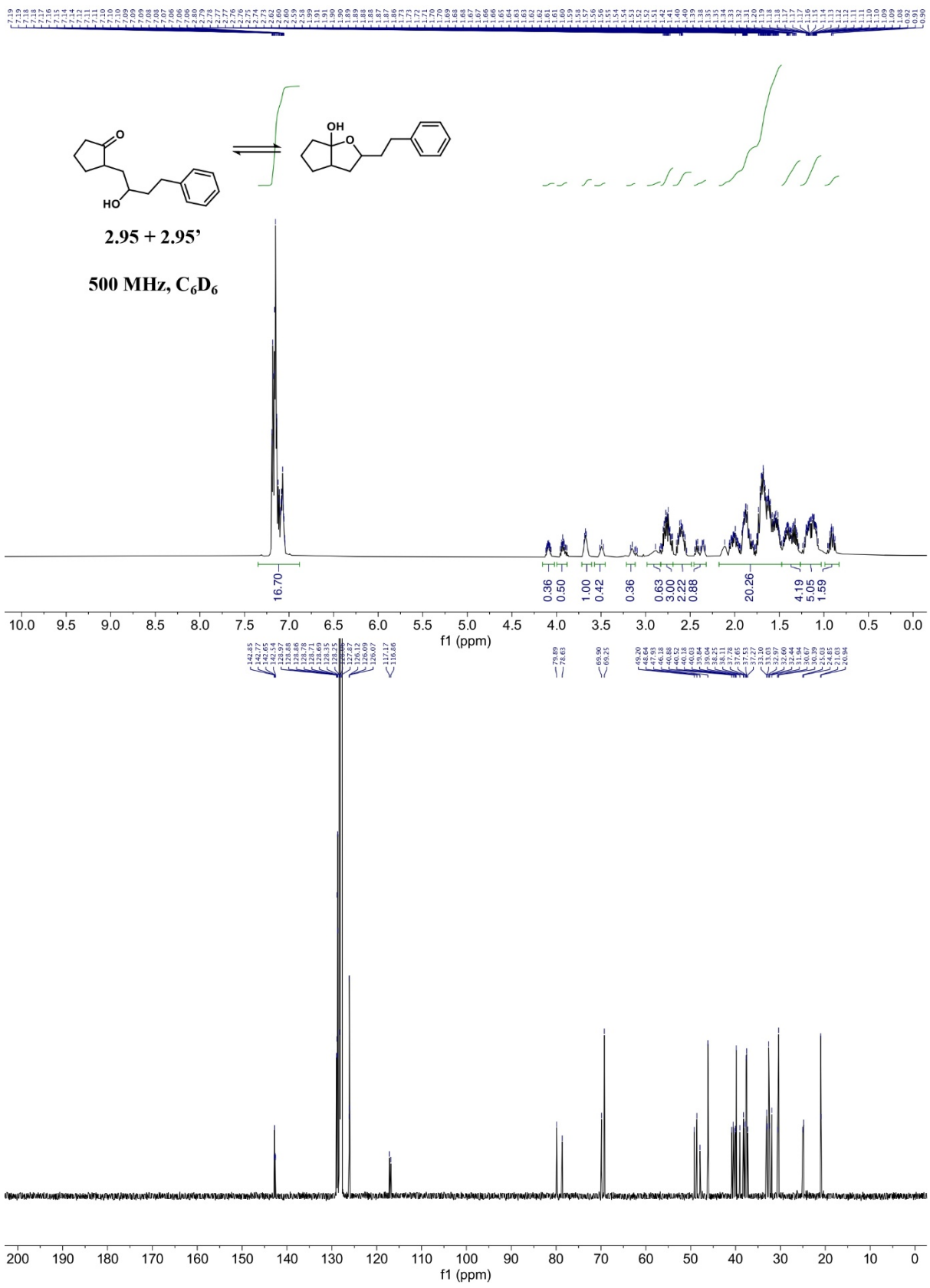

OH
O
tBu
2.88
400 MHz, C6D6
f1 (ppm)
f1 (ppm)

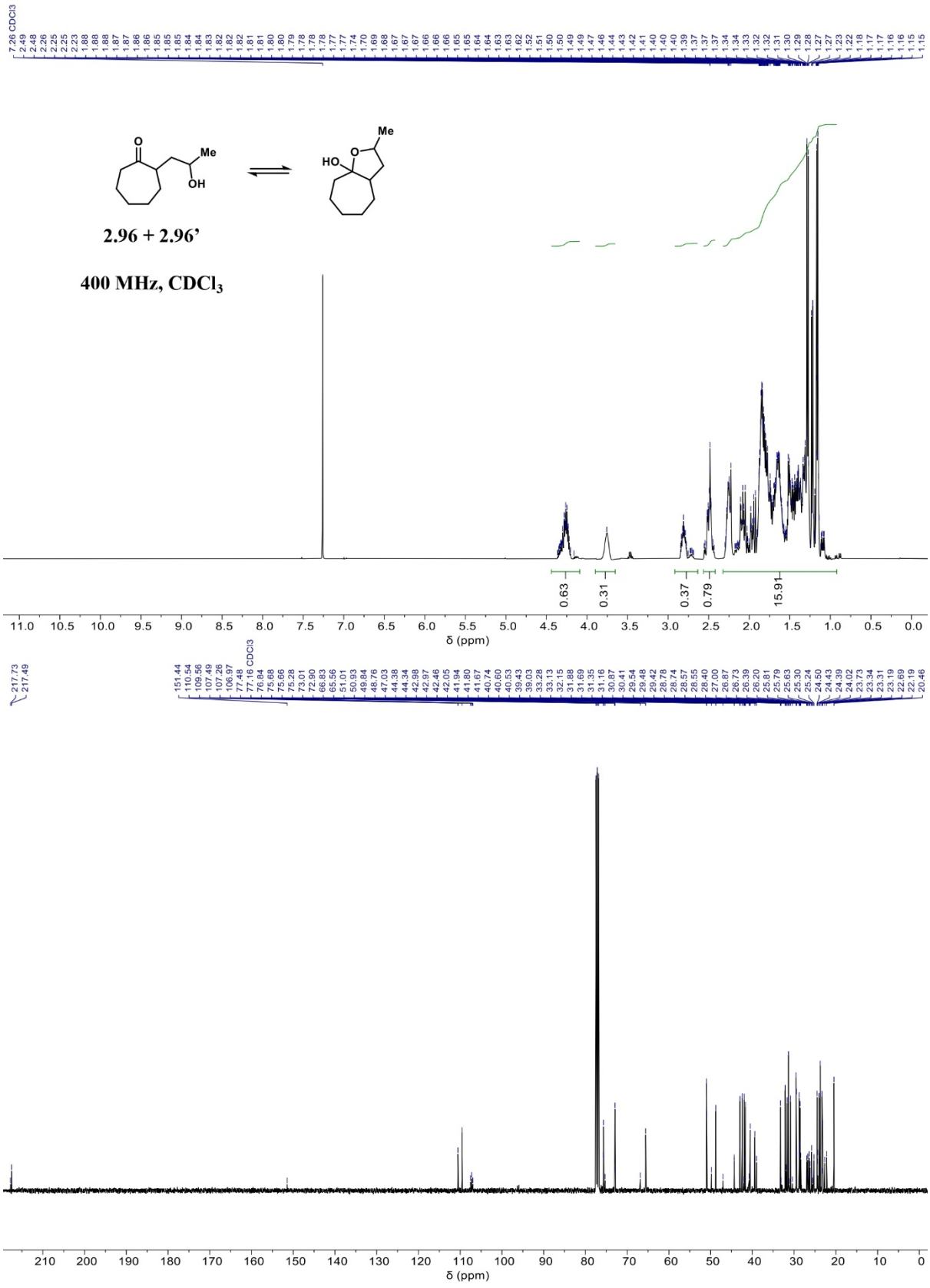

HO
O
Ph
O
HO
Ph
HO
O
Ph
2.89
400 MHz, DMSO-d_6
δ (ppm)
δ (ppm)

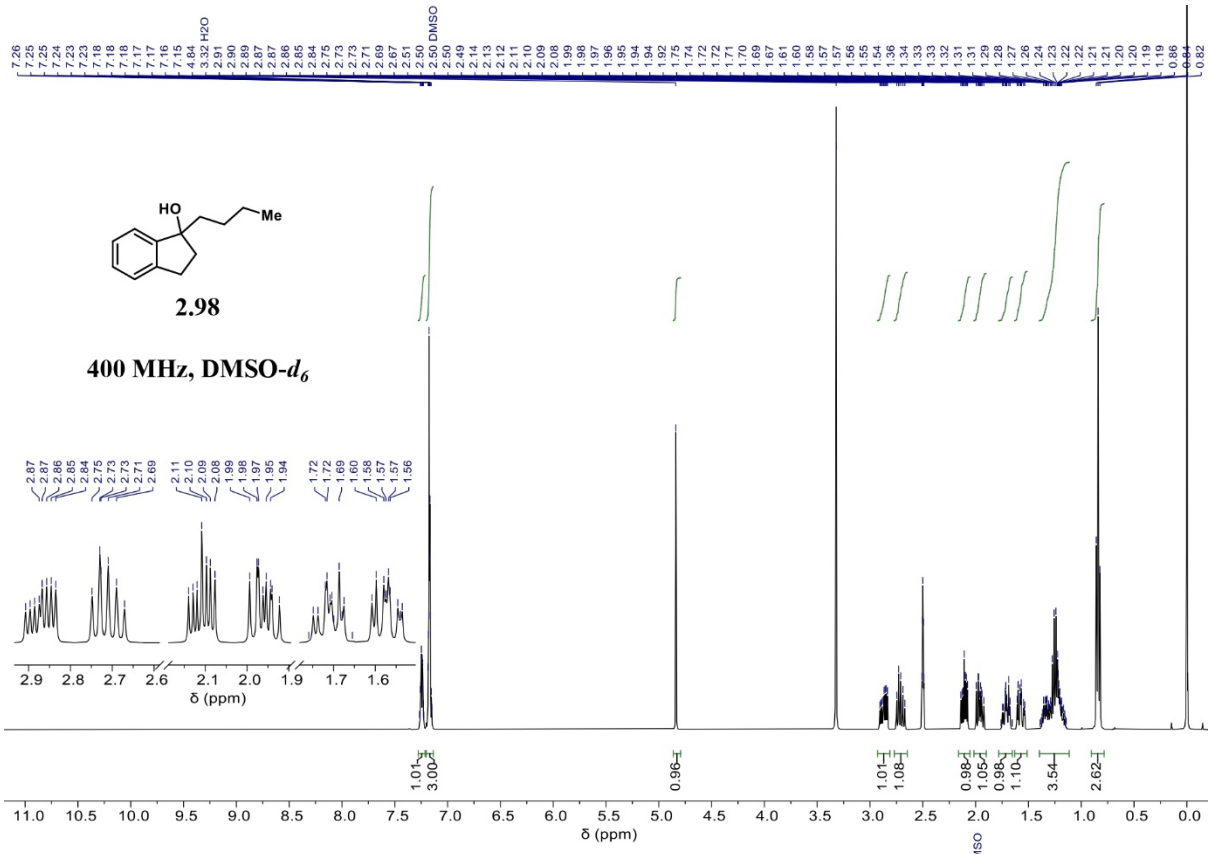
2.92c

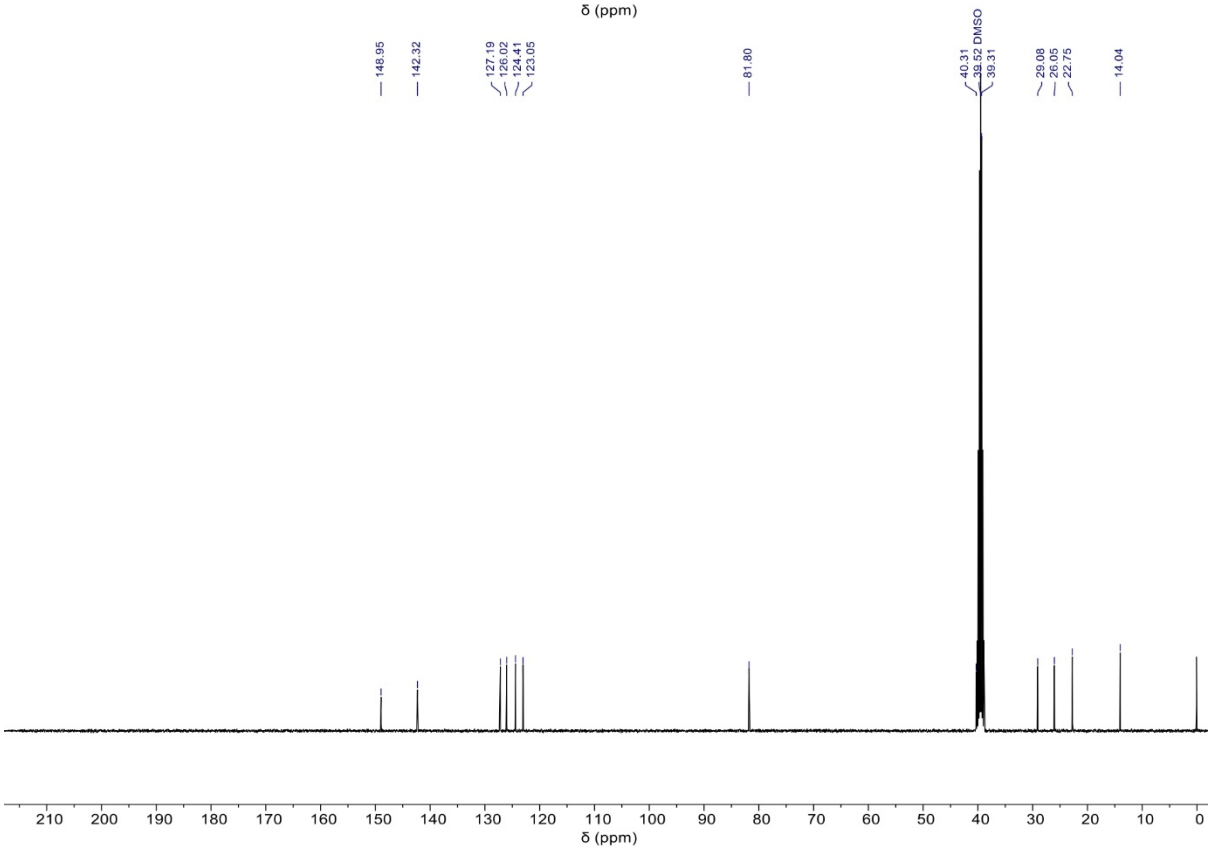
400 MHz, $CDCl_3$

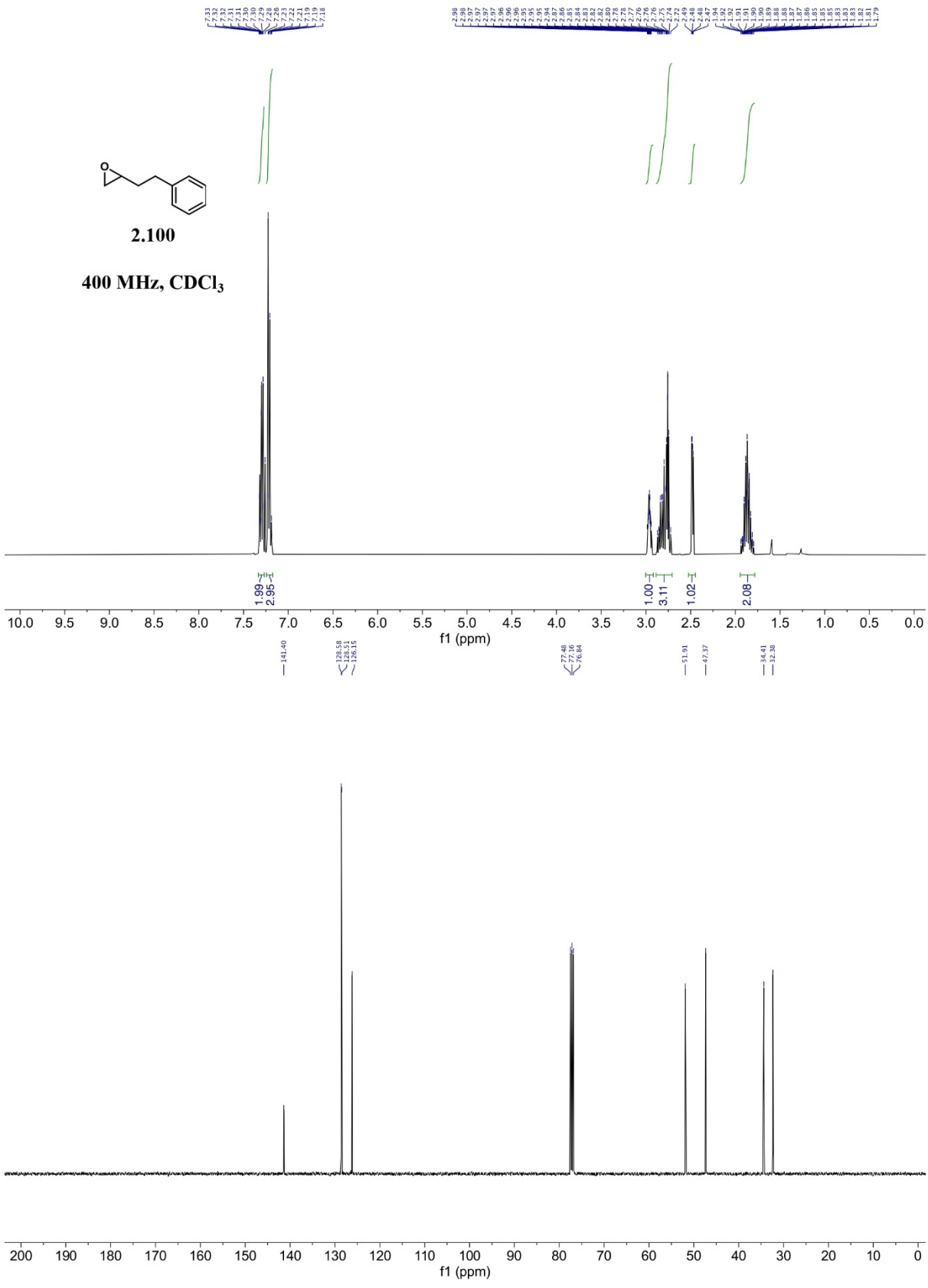



O
HO
OH
O
2.95 + 2.95'
500 MHz, C6D6
16.70
0.36
0.50
1.00
0.42
0.36
0.63
3.00
2.22
0.88
20.26
4.19
5.05
1.59
f1 (ppm)
f1 (ppm)


O
Me
OH
HO
O
Me
2.96 + 2.96'
400 MHz, CDCl3
0.63
0.31
0.37
0.79
15.91
δ (ppm)
δ (ppm)

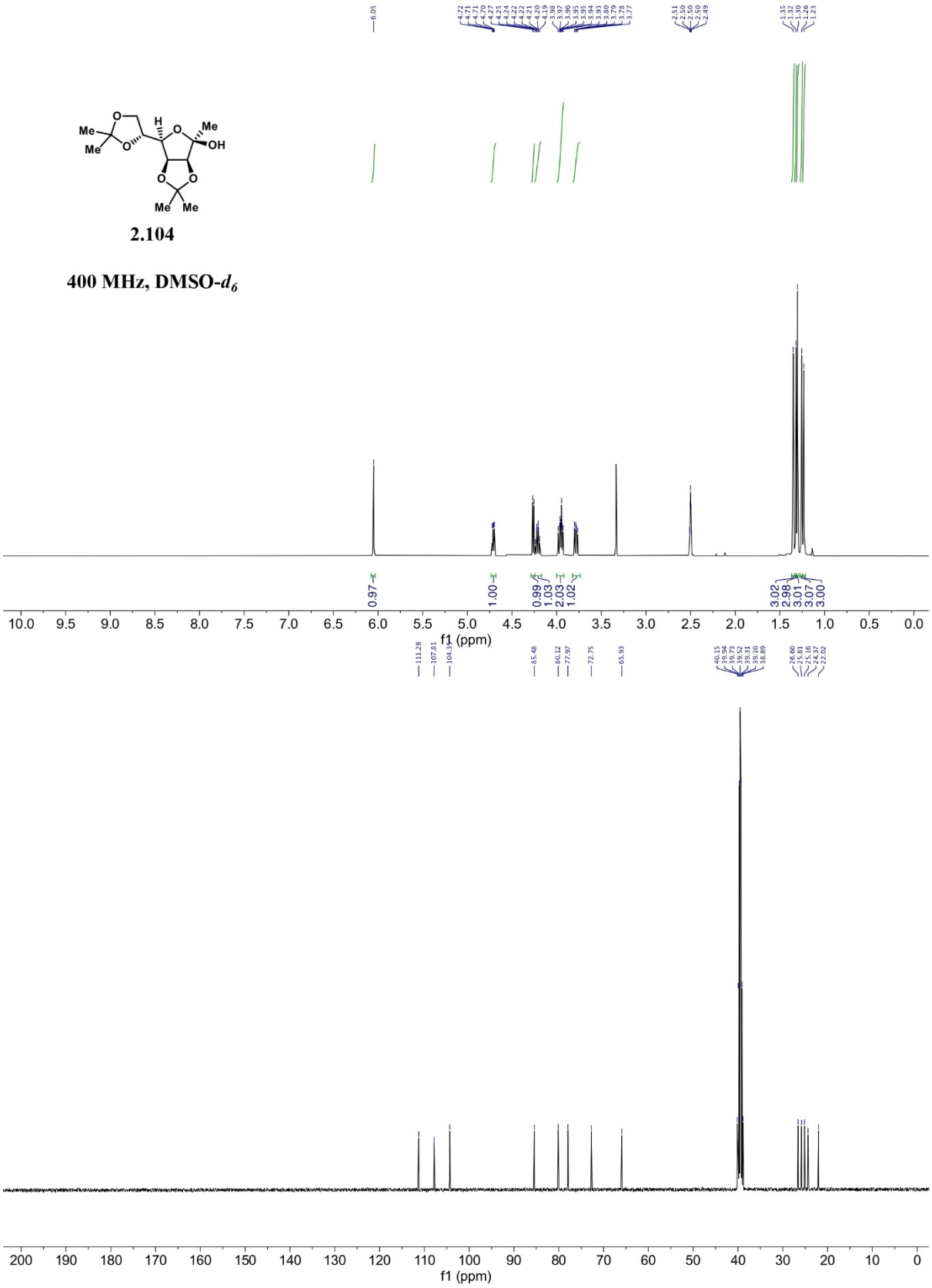

HO
Me
2.98
400 MHz, DMSO-d_6
δ (ppm)

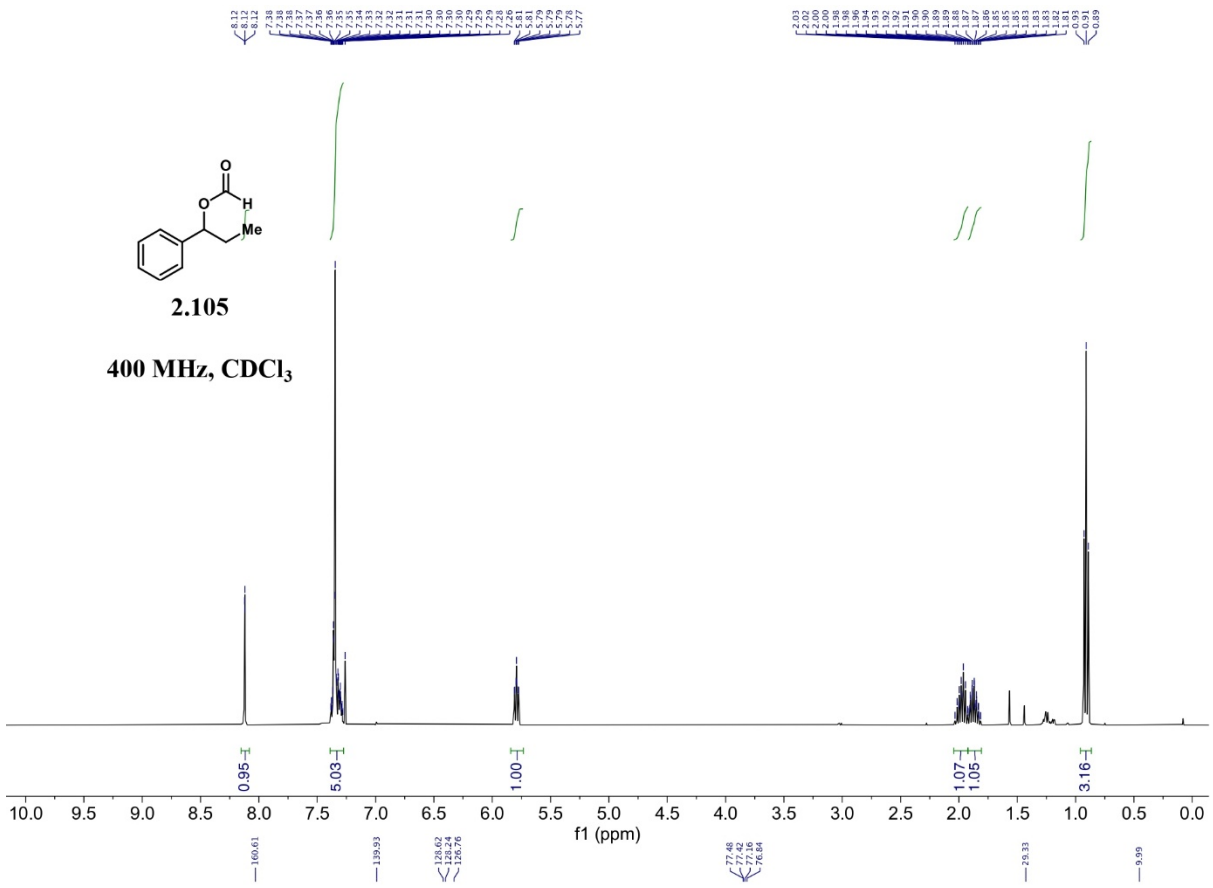

δ (ppm)

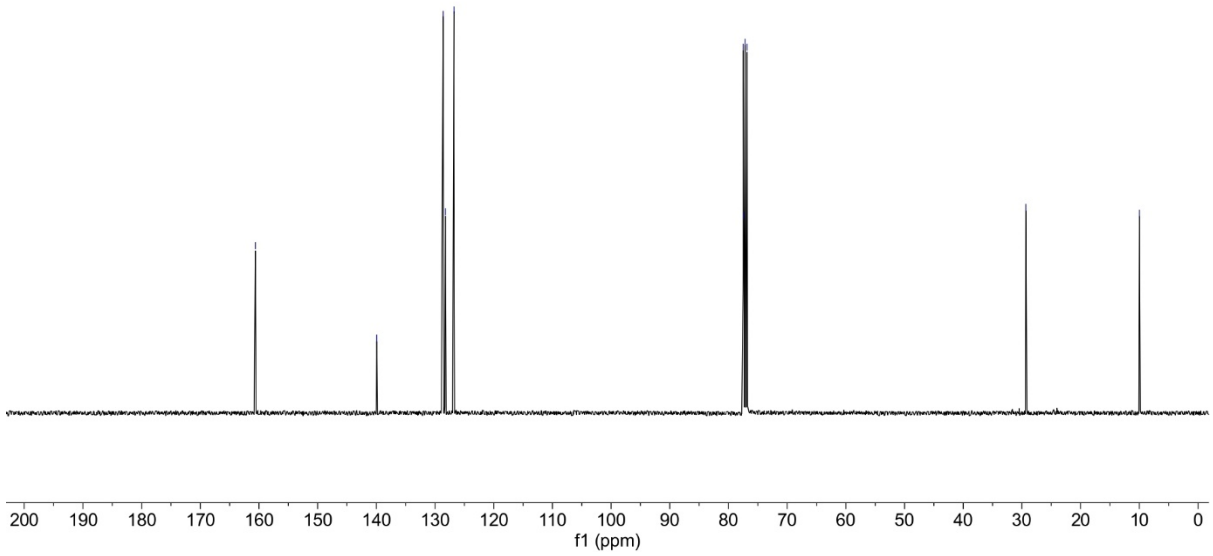

2.100
400 MHz, CDCl3
f1 (ppm)
f1 (ppm)

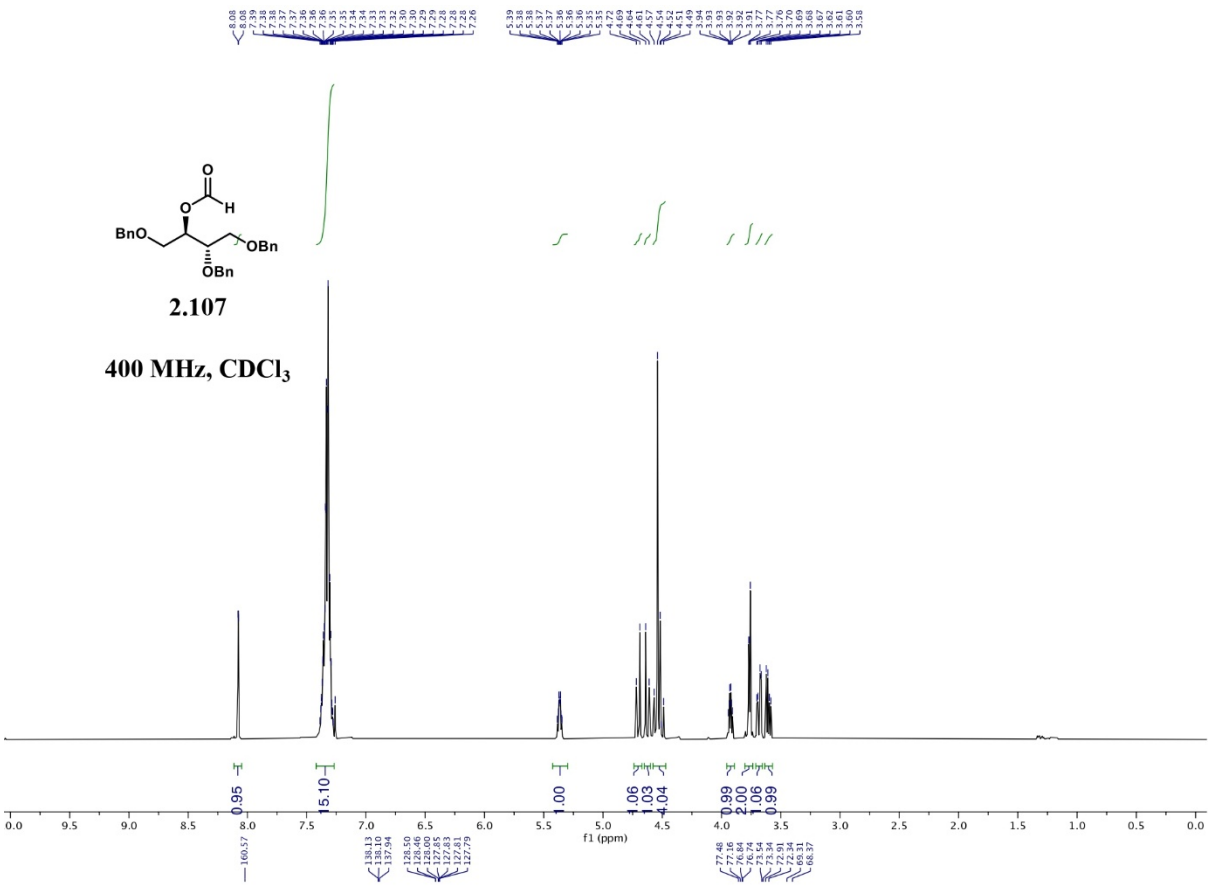
2.104

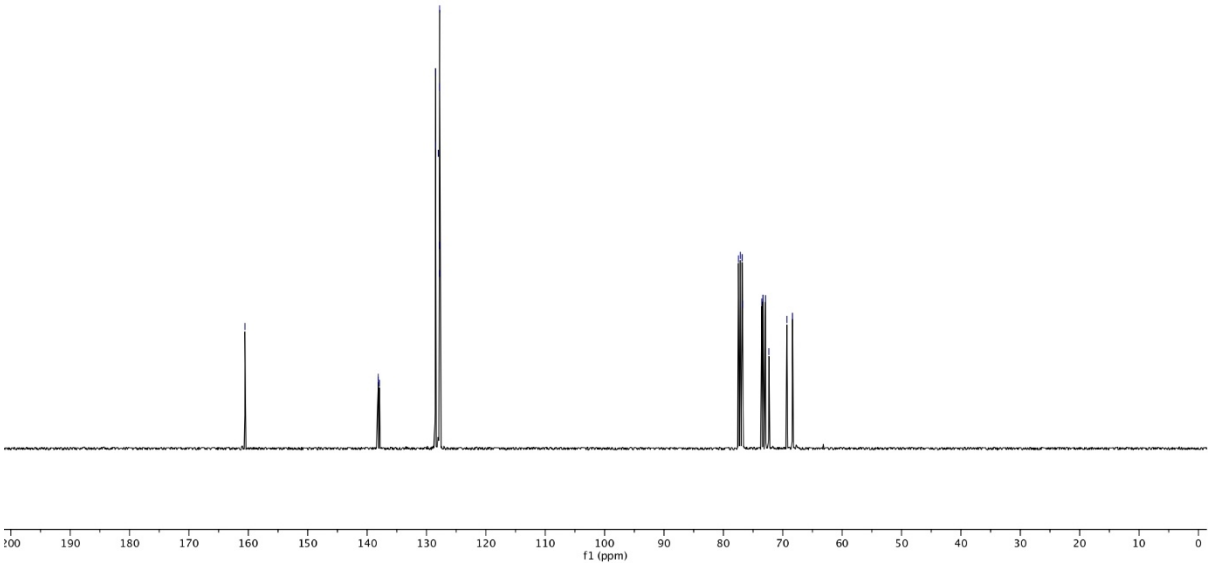
400 MHz, DMSO-d_6




O
O
H
Me
2.105
400 MHz, CDCl3
0.95
5.03
1.00
1.07
1.05
3.16
f1 (ppm)

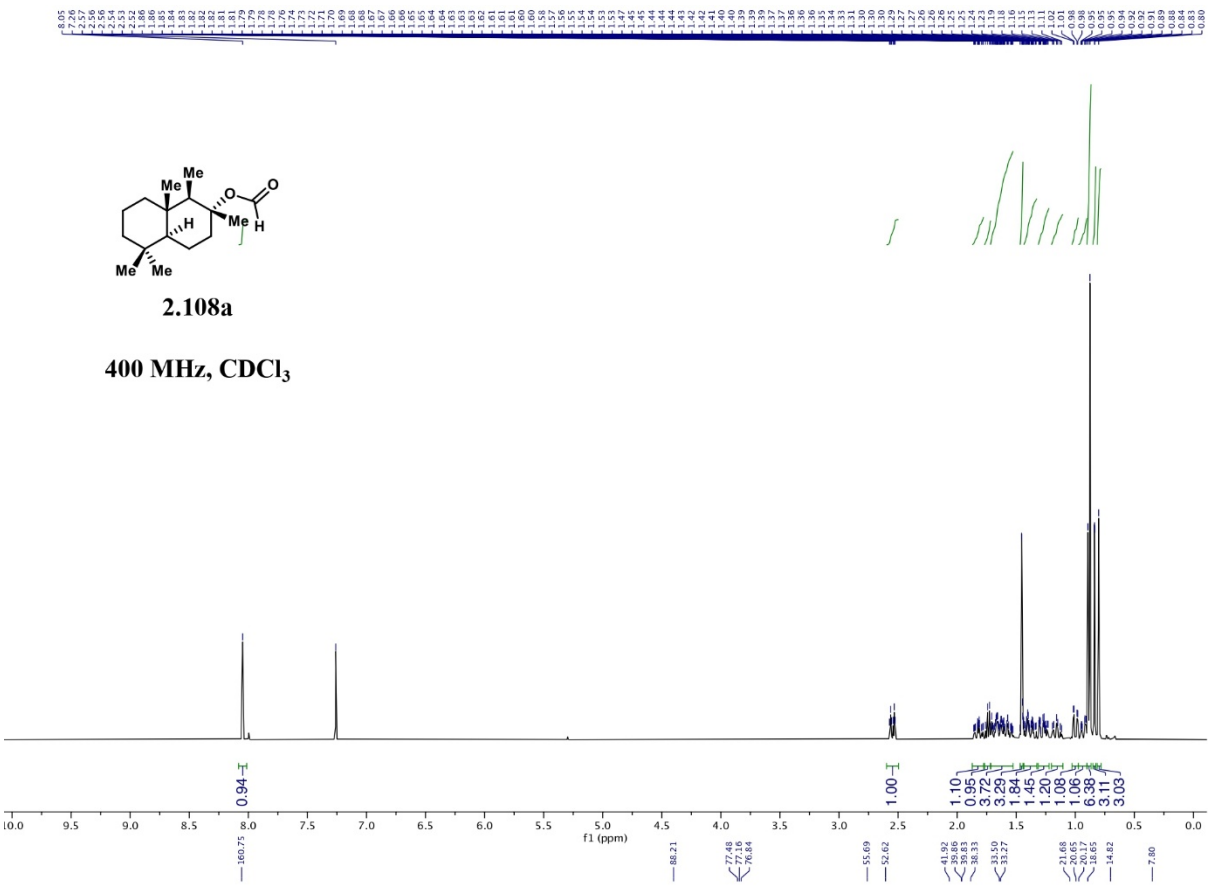

f1 (ppm)

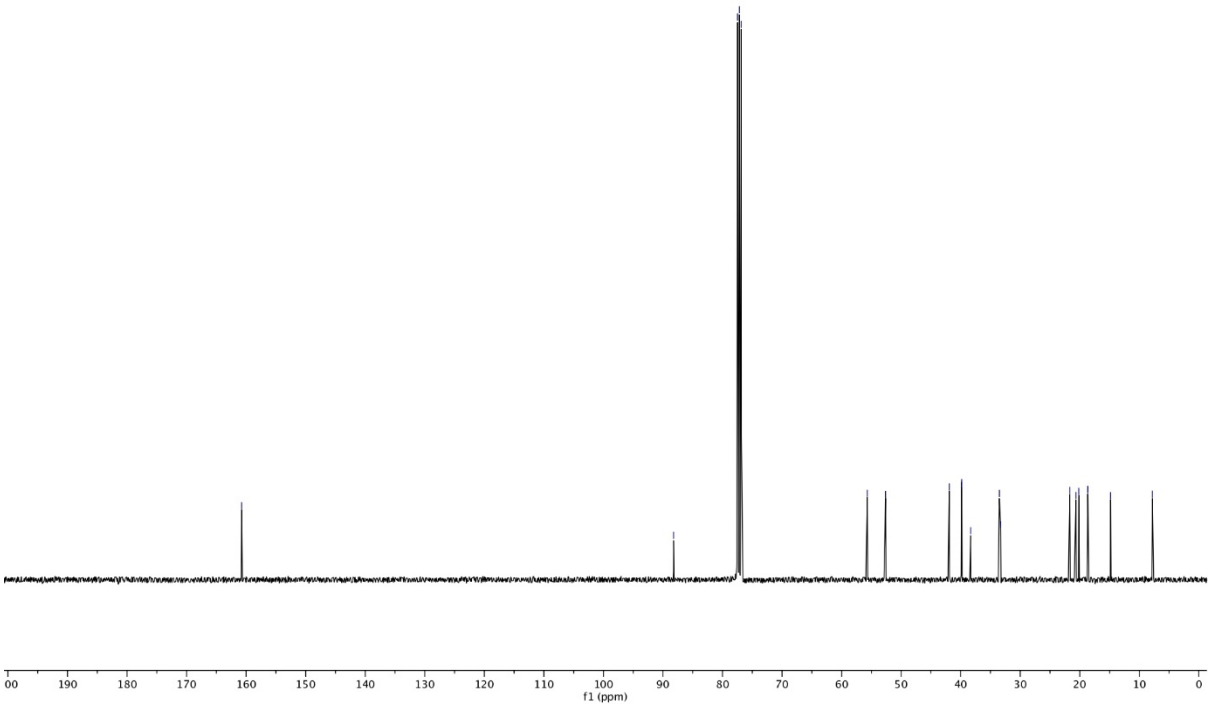

BnO
OBn
OBn
2.107
400 MHz, CDCl3
f1 (ppm)

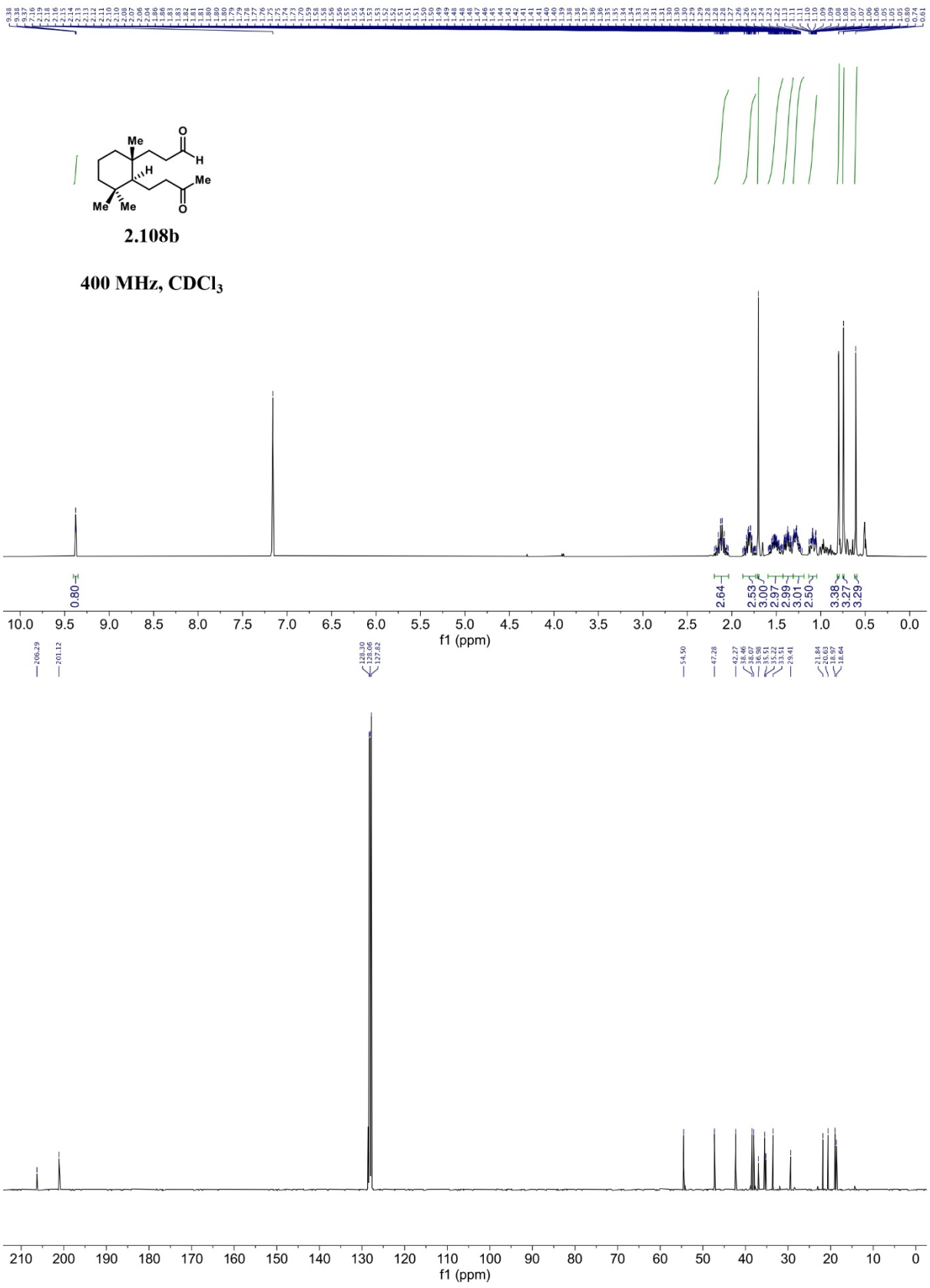

f1 (ppm)

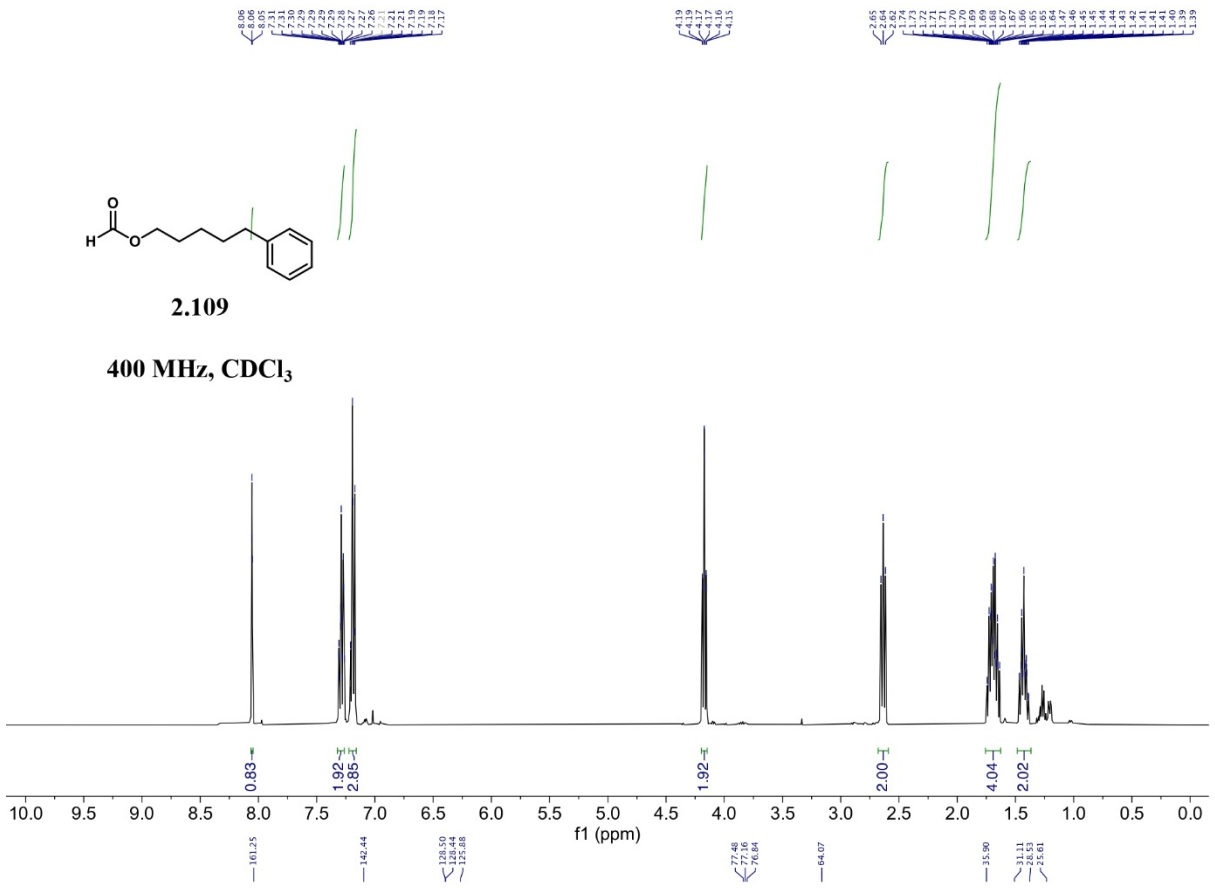
2.108a

400 MHz, $CDCl_3$



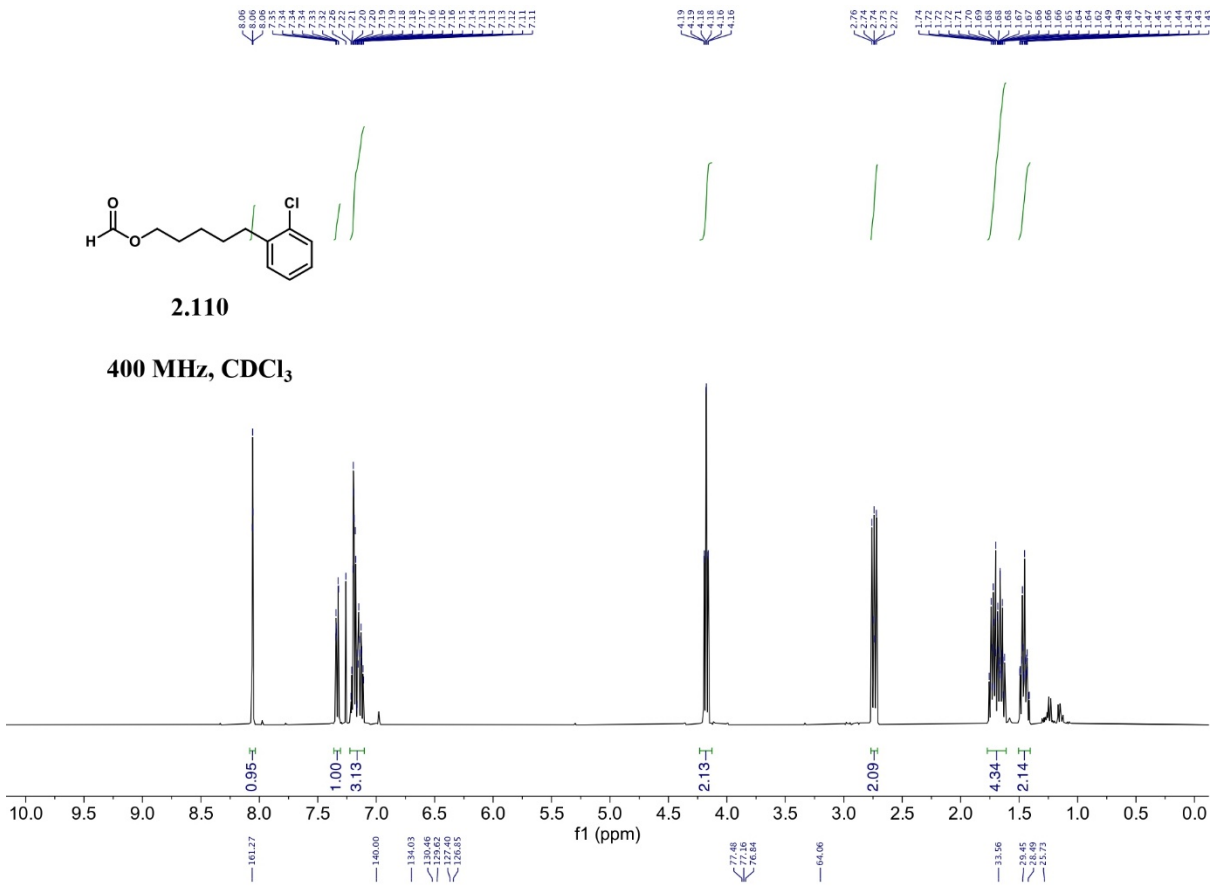


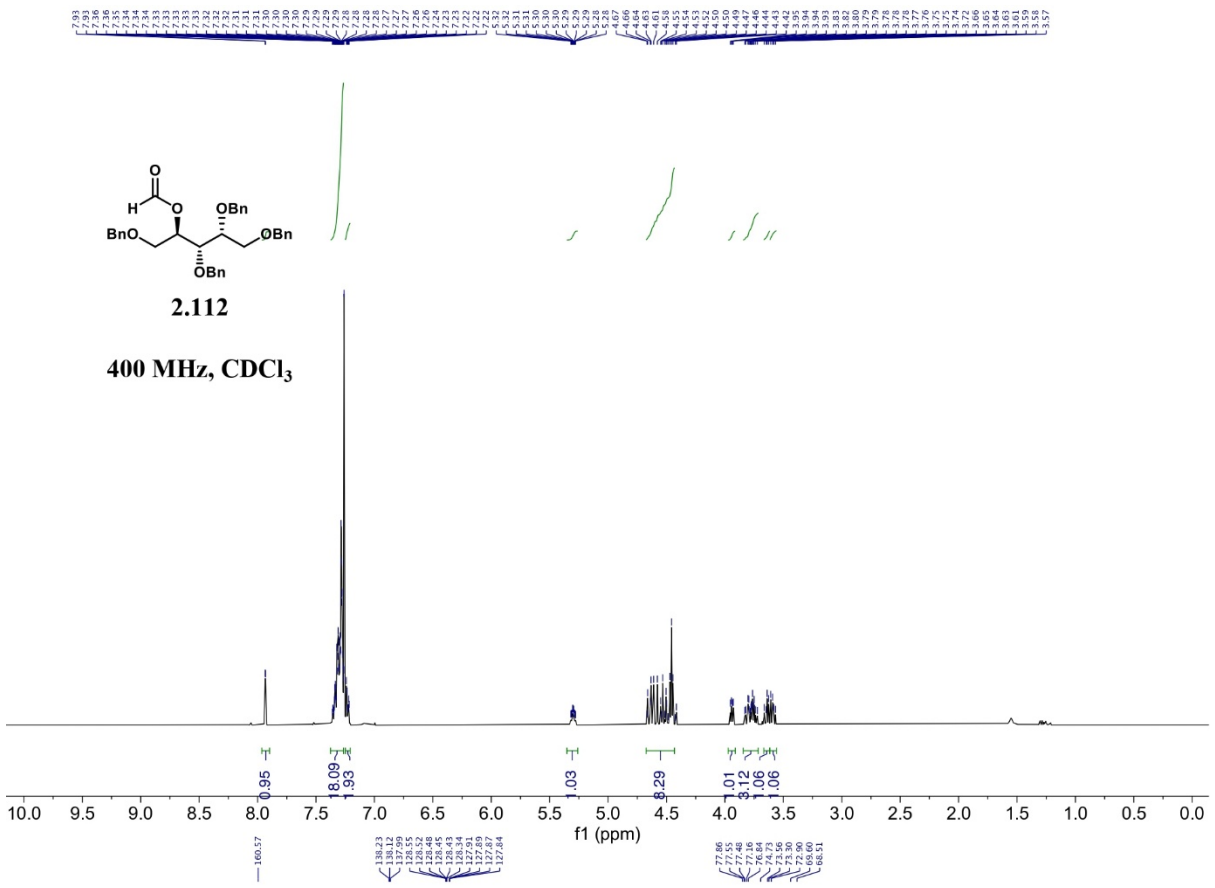

Me
O
H
H
Me
Me
Me
O
2.108b
400 MHz, CDCl3
0.80
2.64
2.53
3.00
2.97
2.99
3.01
2.50
3.38
3.27
3.29
f1 (ppm)
206.29
201.12
128.30
128.06
127.82
54.50
47.28
42.27
38.40
36.07
36.58
35.51
35.22
33.51
29.41
21.84
20.63
18.97
18.64
f1 (ppm)

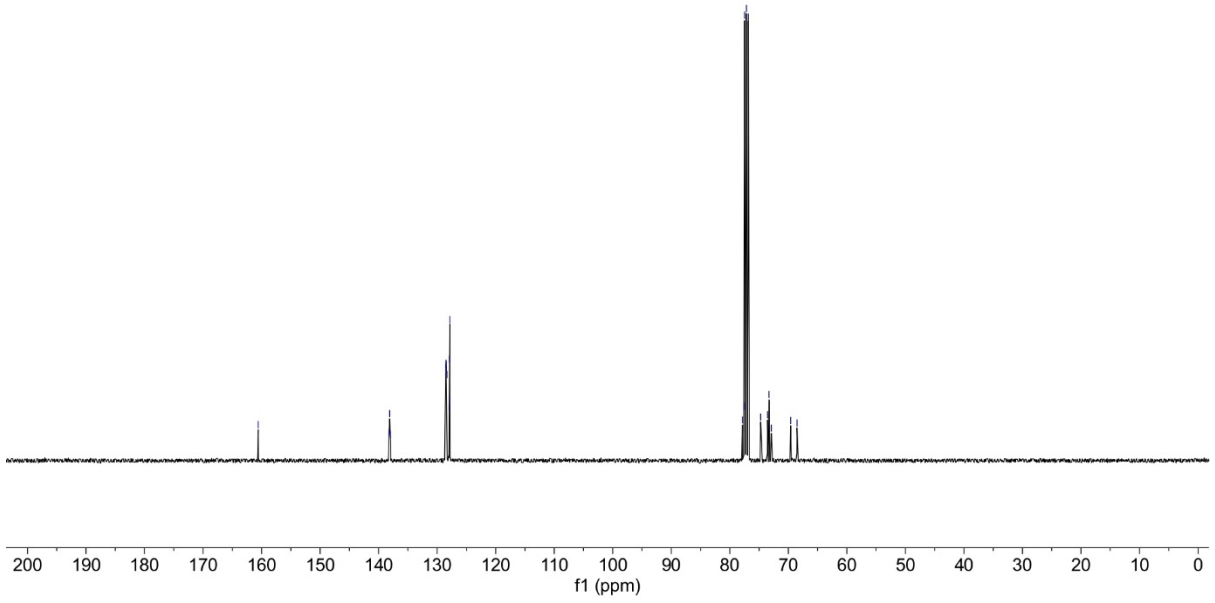


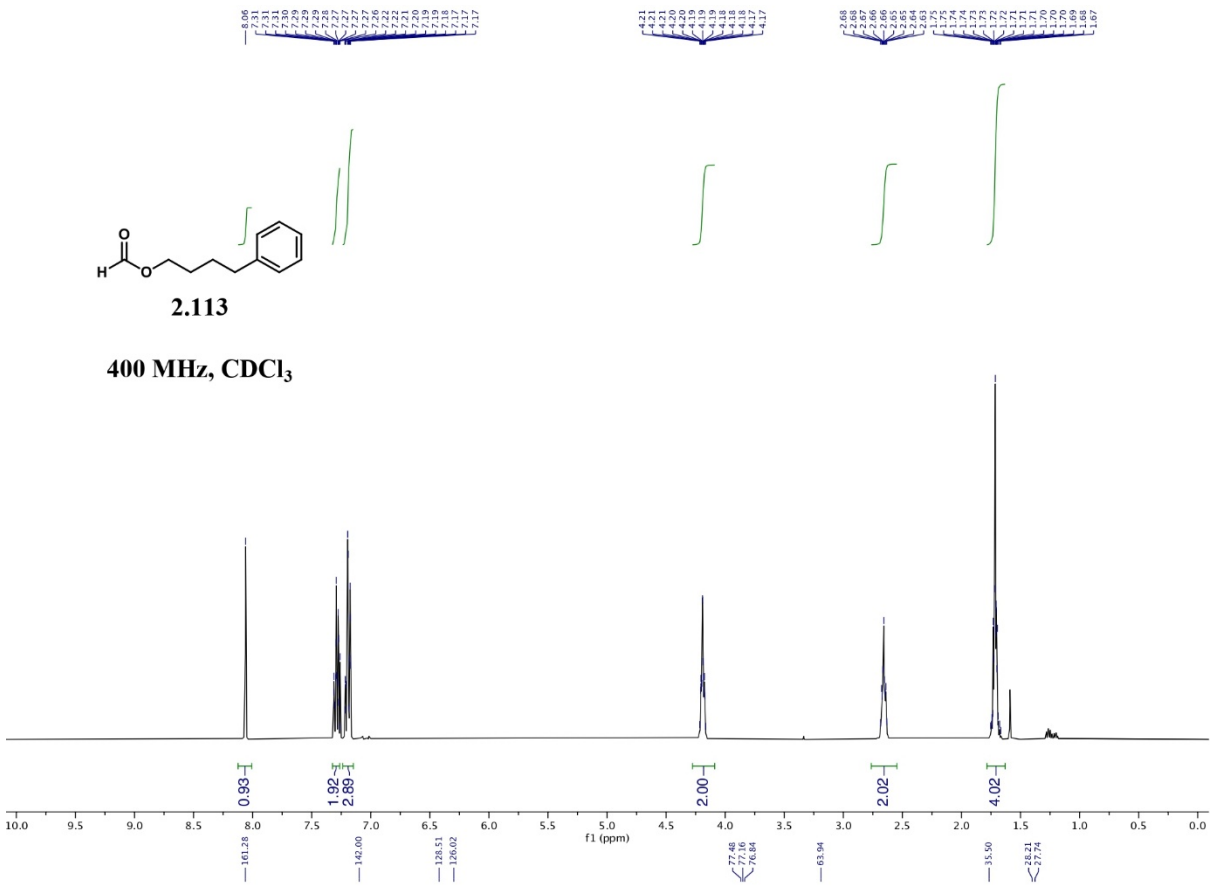
2.109

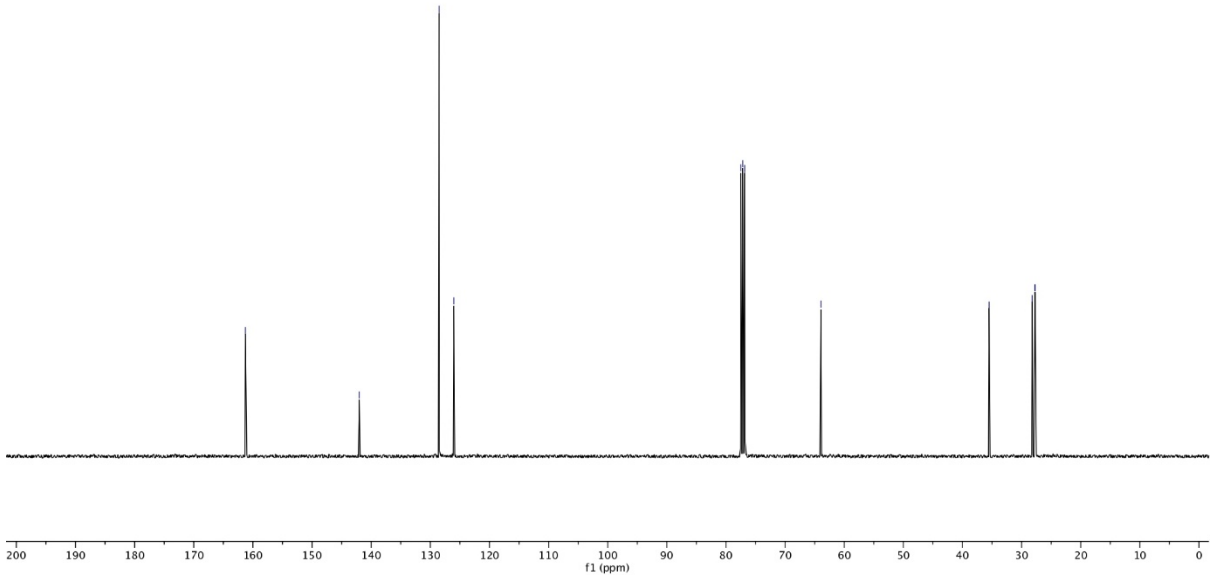
400 MHz, $CDCl_3$

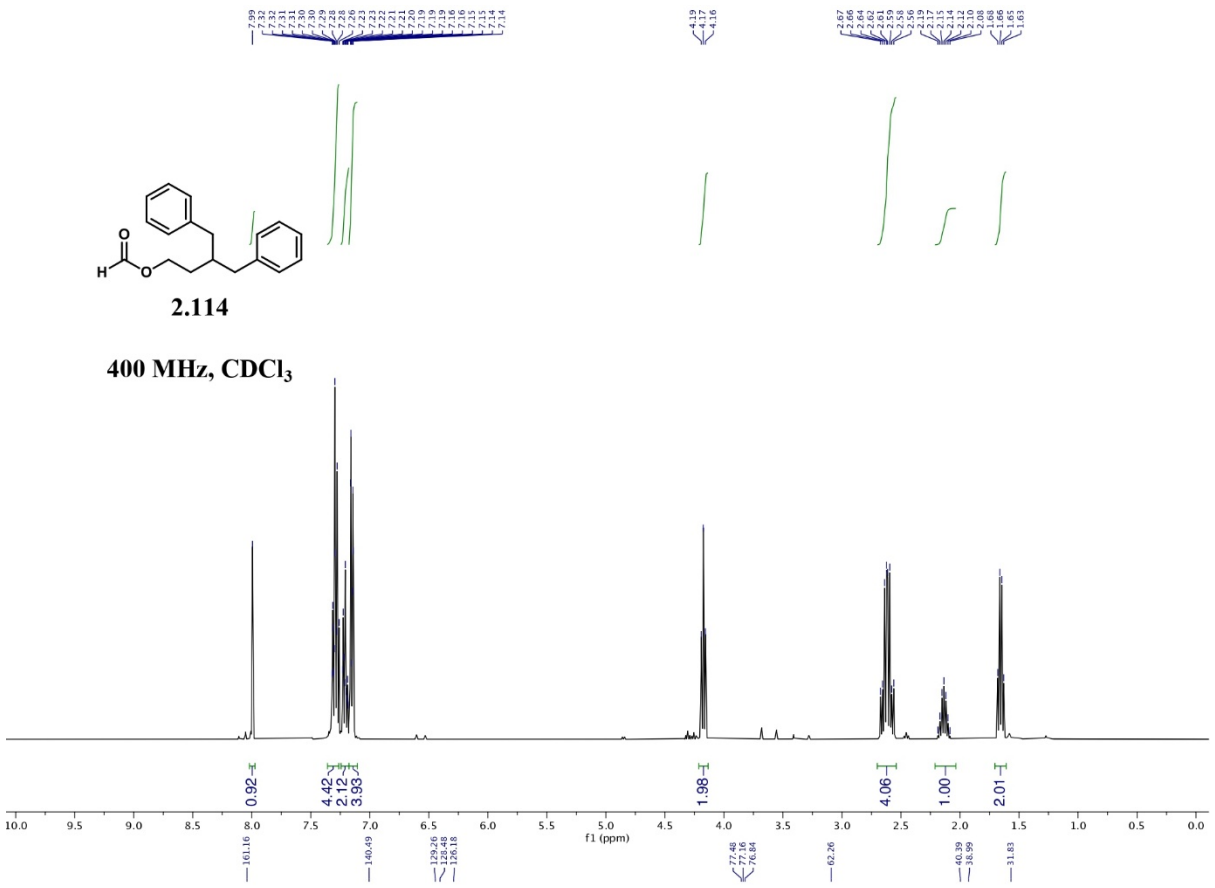

8.06
8.06
8.06
7.35
7.34
7.34
7.34
7.33
7.32
7.32
7.26
7.22
7.21
7.20
7.20
7.19
7.19
7.18
7.18
7.17
7.16
7.16
7.15
7.15
7.14
7.13
7.13
7.13
7.12
7.11
7.11
4.19
4.19
4.18
4.18
4.18
4.16
4.16
2.76
2.74
2.74
2.73
2.72
1.74
1.72
1.72
1.72
1.71
1.70
1.69
1.68
1.68
1.68
1.67
1.67
1.66
1.66
1.66
1.65
1.64
1.64
1.62
1.49
1.49
1.48
1.47
1.47
1.45
1.45
1.44
1.43
1.43
1.41
O
H
O
Cl
2.110
400 MHz, CDCl3
0.95
1.00
3.13
2.13
2.09
4.34
2.14
10.0 9.5 9.0 8.5 8.0 7.5 7.0 6.5 6.0 5.5 5.0 4.5 4.0 3.5 3.0 2.5 2.0 1.5 1.0 0.5 0.0
f1 (ppm)
161.27
140.00
134.03
130.46
129.62
127.40
126.85
77.48
77.16
76.84
64.06
33.96
29.45
28.49
25.73
200 190 180 170 160 150 140 130 120 110 100 90 80 70 60 50 40 30 20 10 0
f1 (ppm)

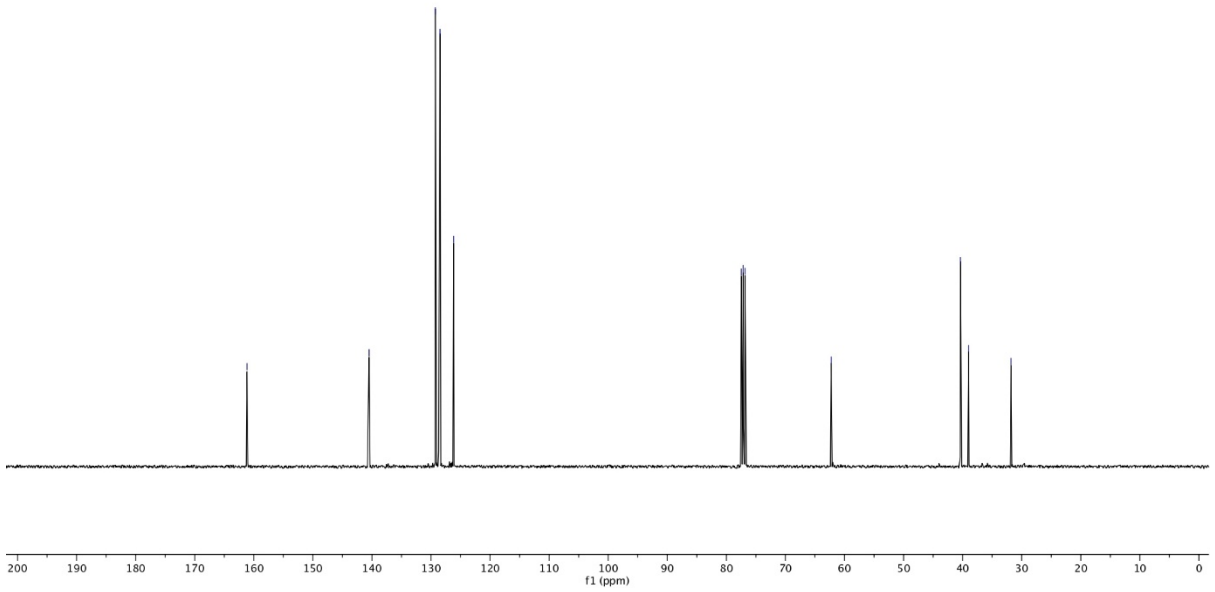

2.112
400 MHz, CDCl3
f1 (ppm)


f1 (ppm)


2.113
400 MHz, CDCl3
0.93
1.92
2.89
2.00
2.02
4.02
f1 (ppm)

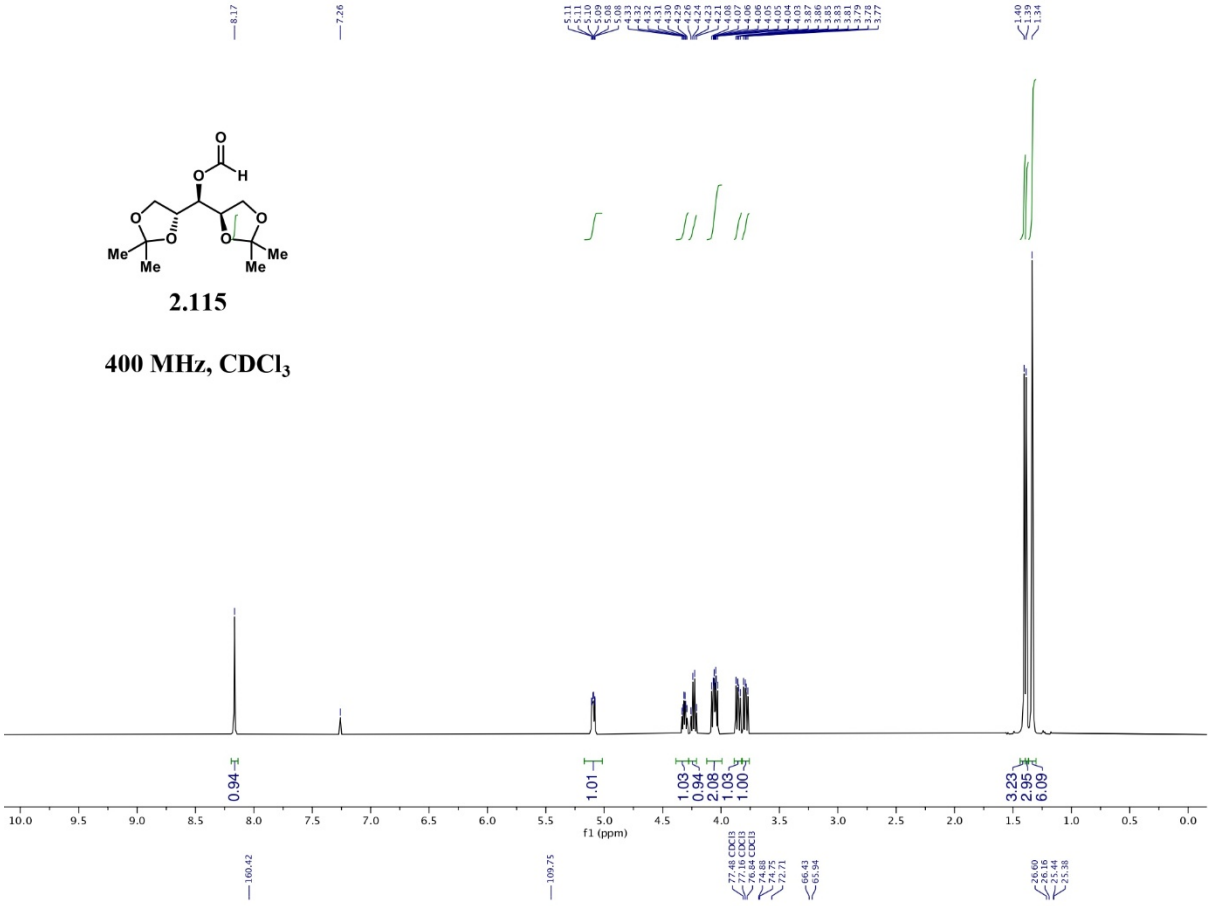

f1 (ppm)

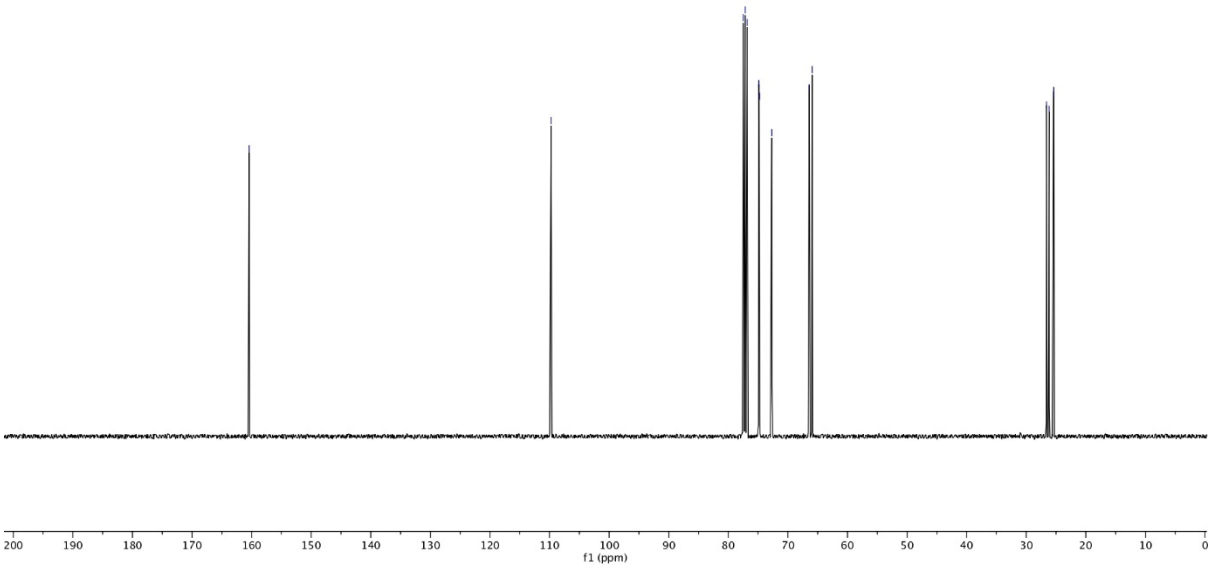

2.114
400 MHz, $CDCl_3$
f1 (ppm)


f1 (ppm)

2.115

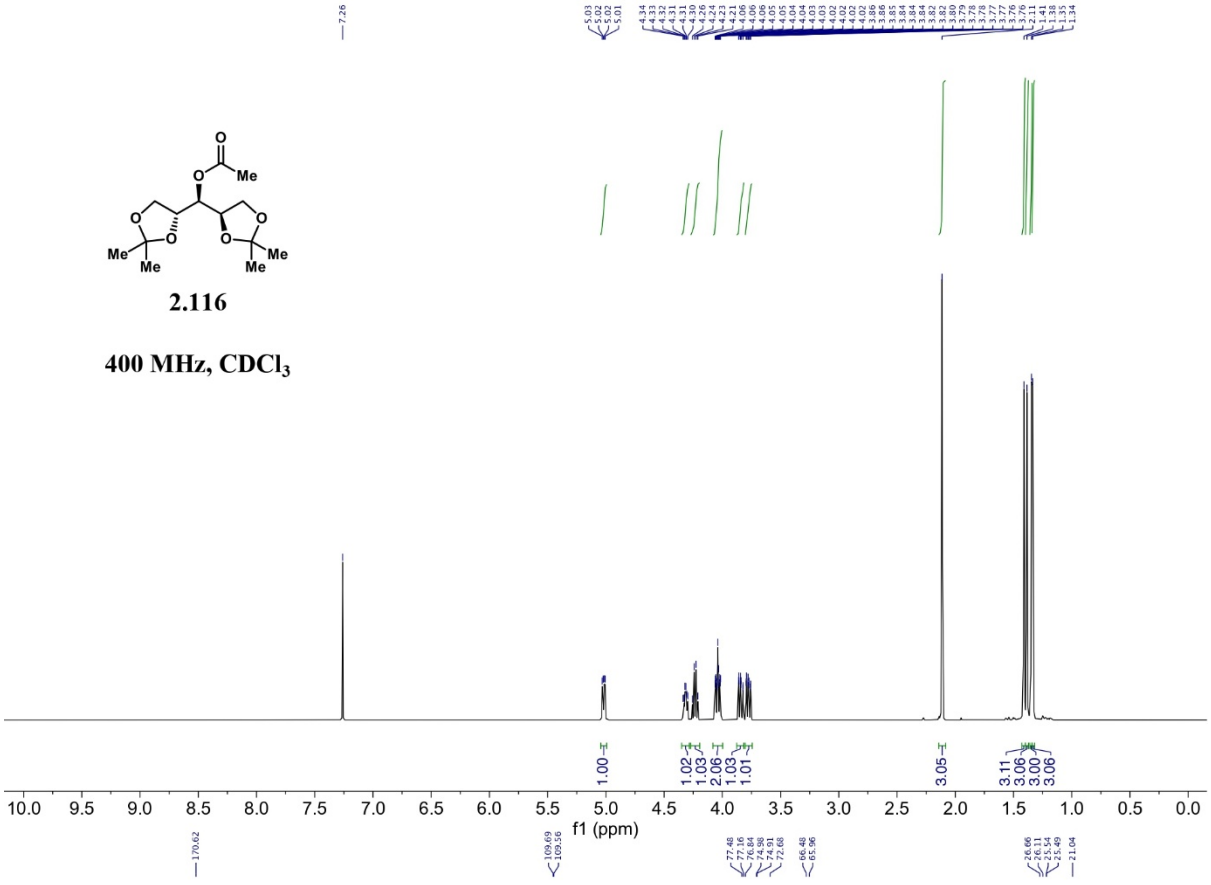
400 MHz, $CDCl_3$

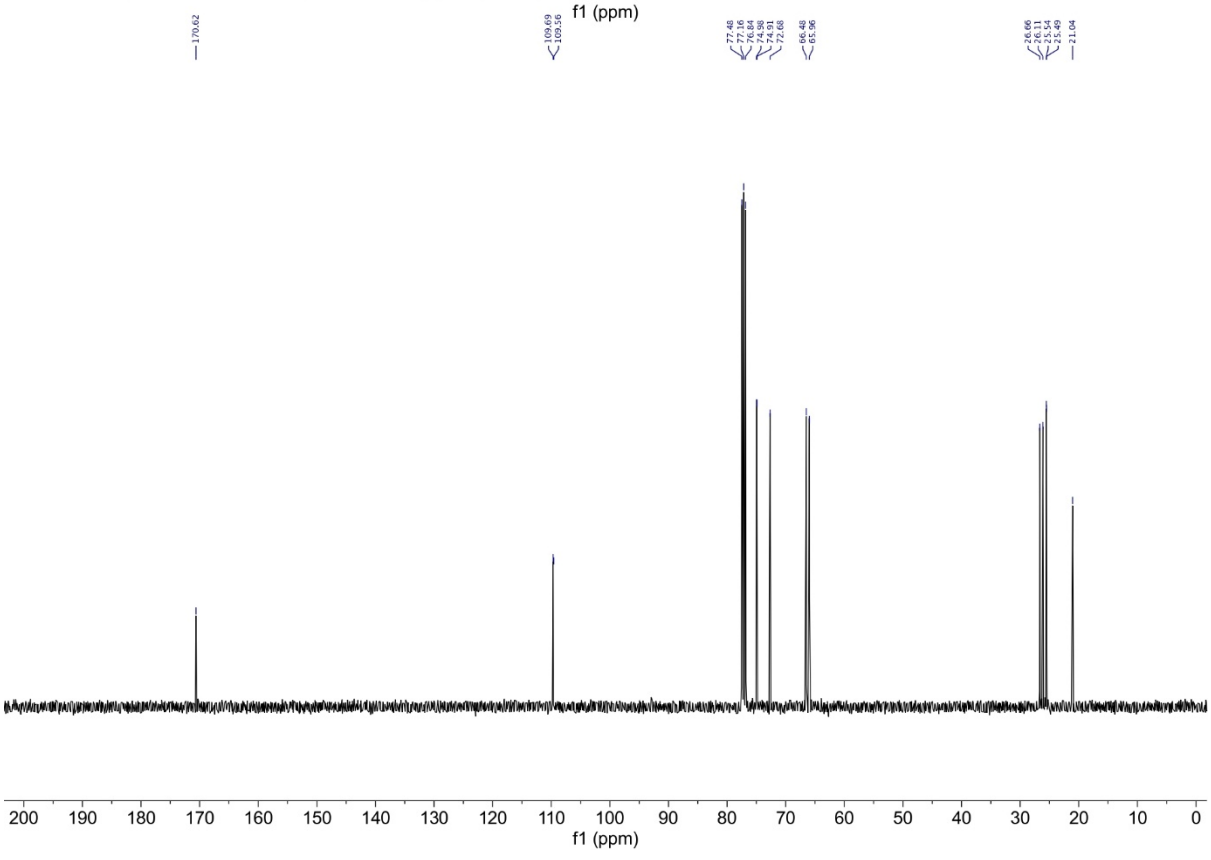




2.116

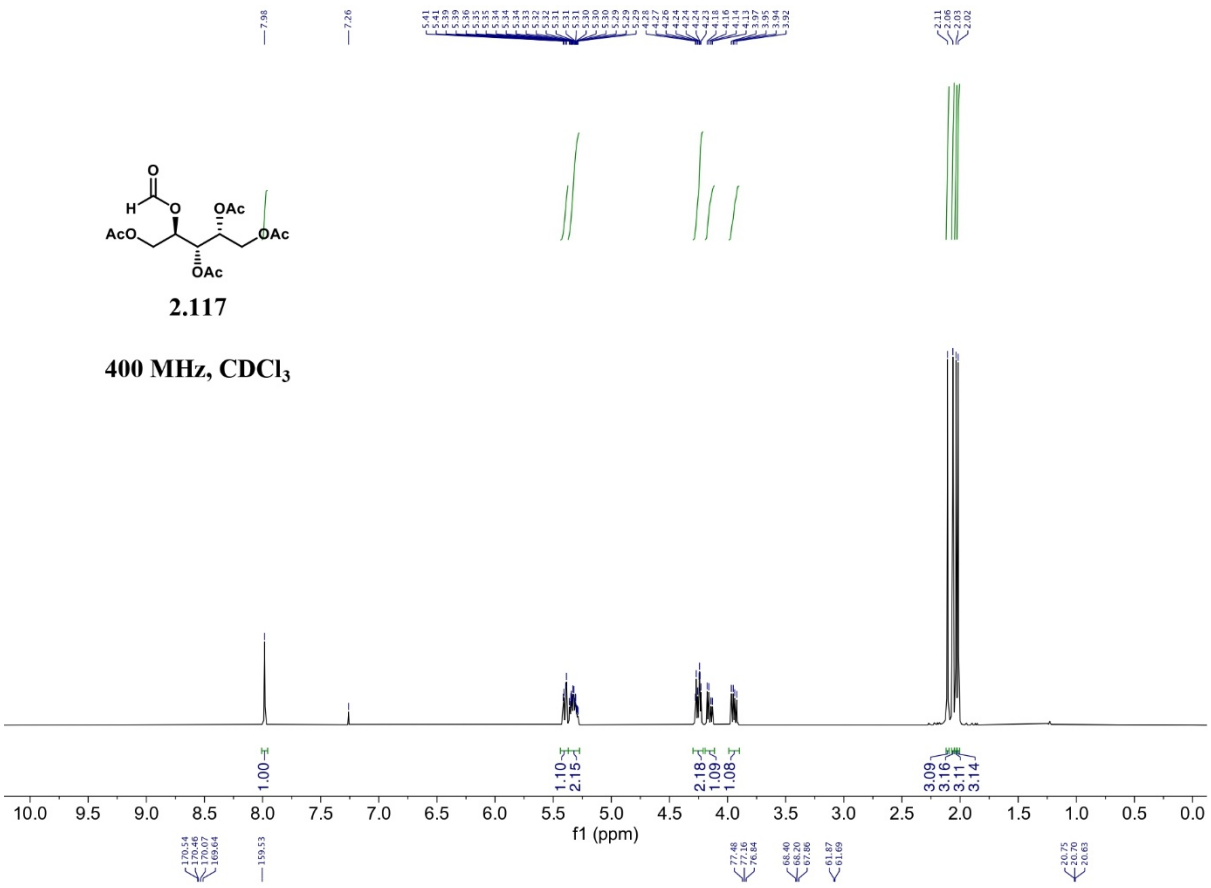
400 MHz, $CDCl_3$

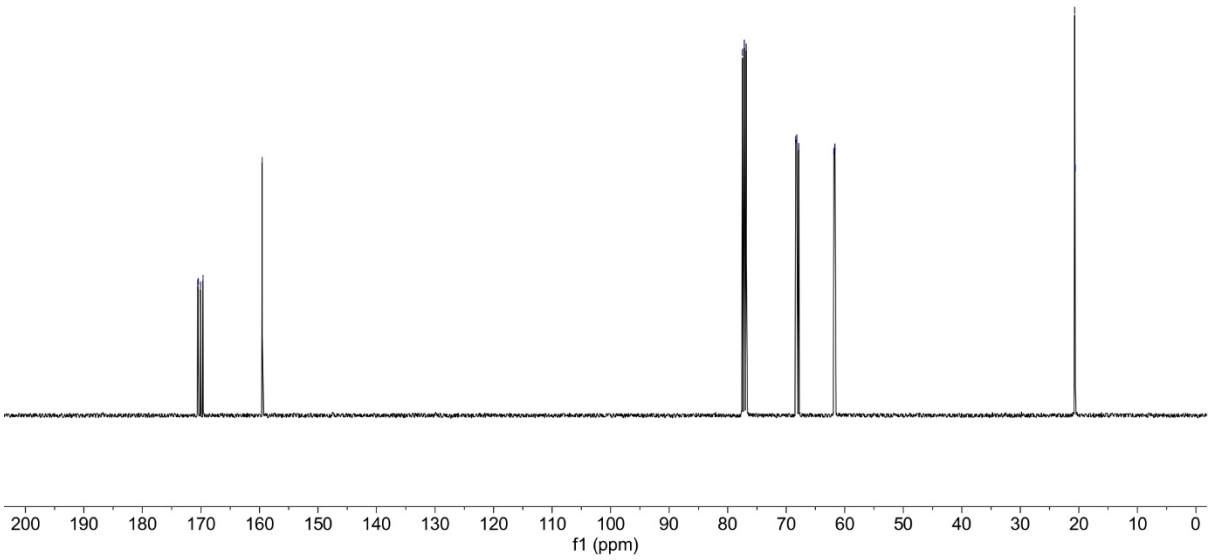


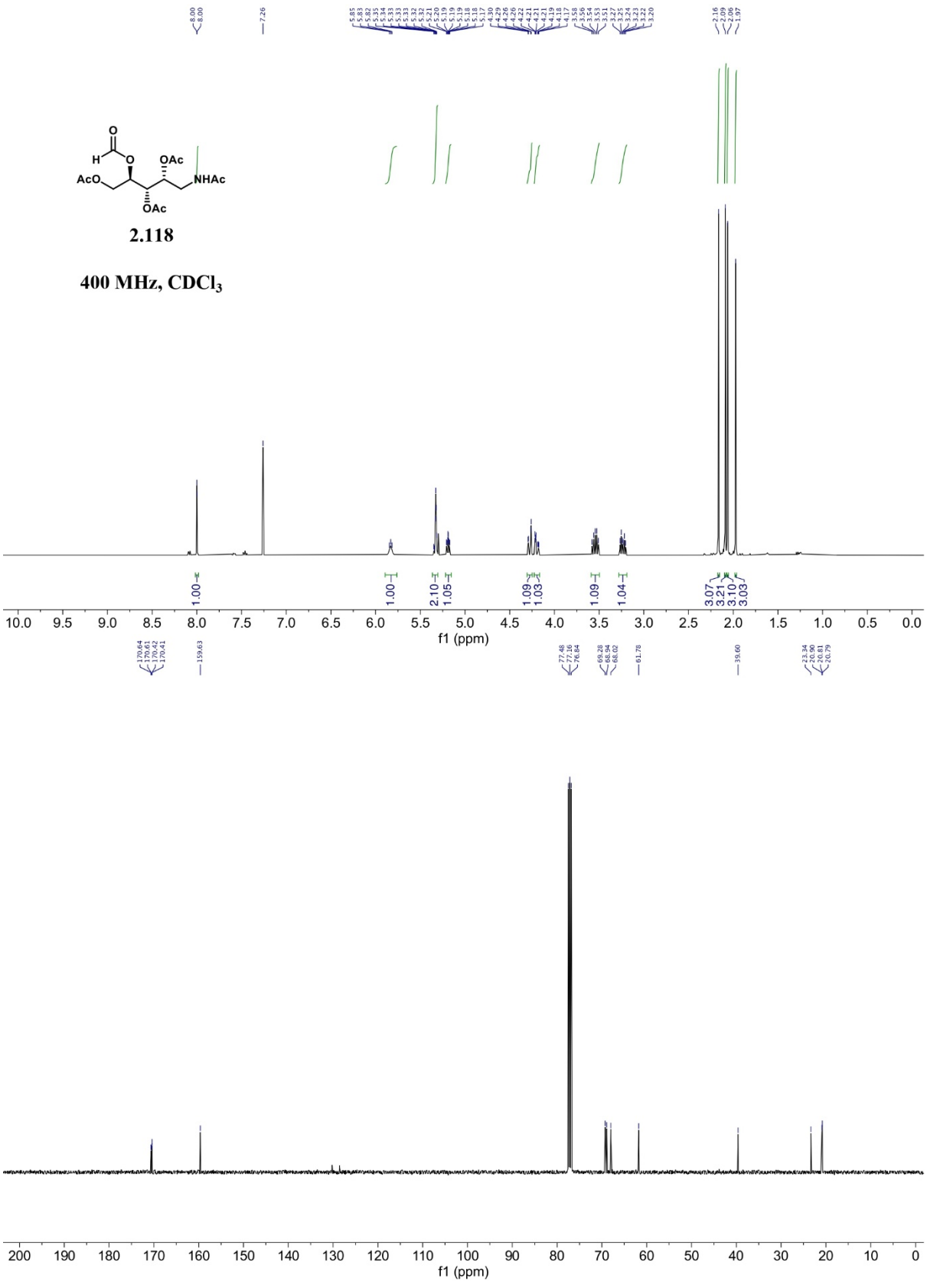


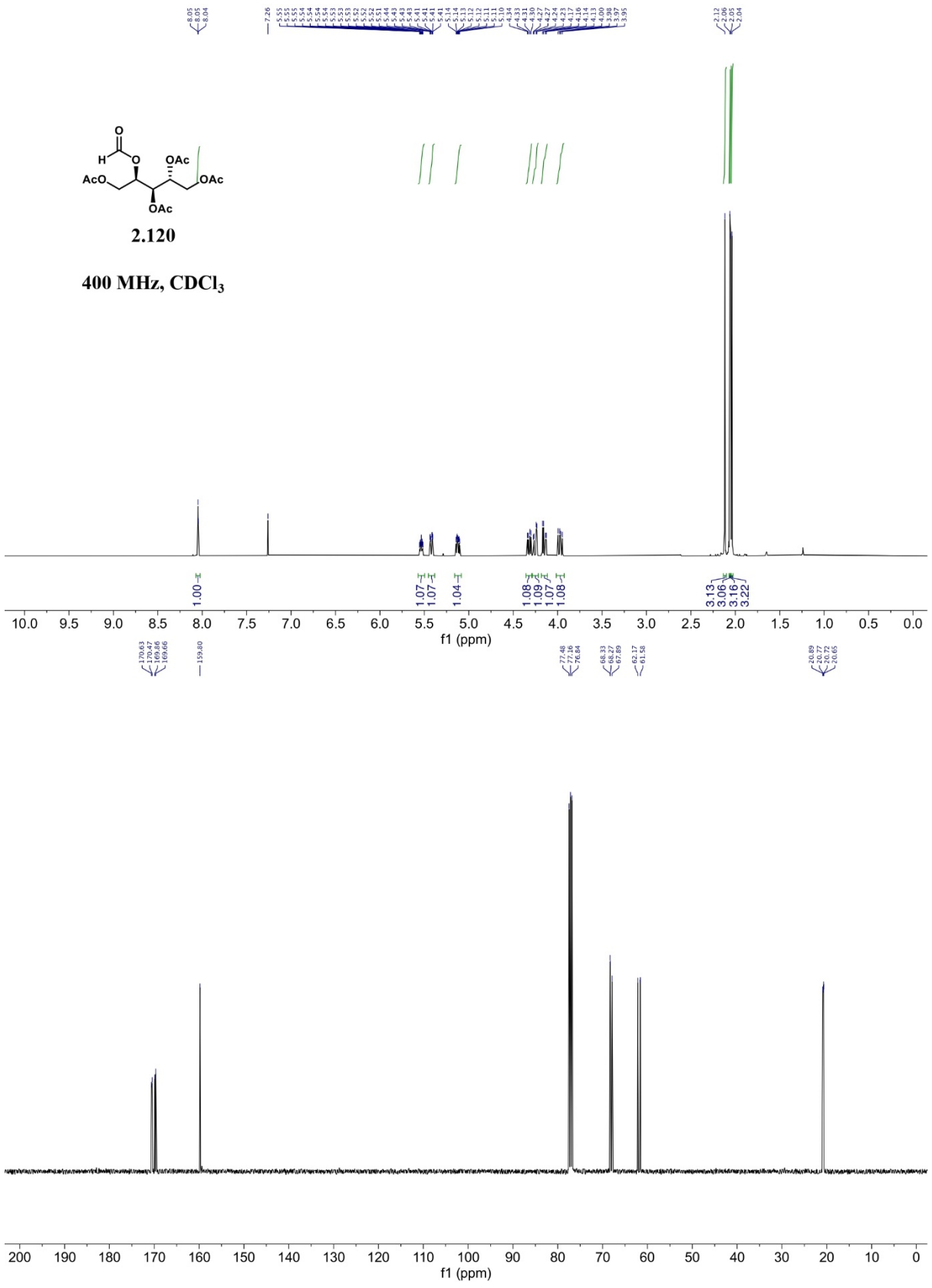
2.117

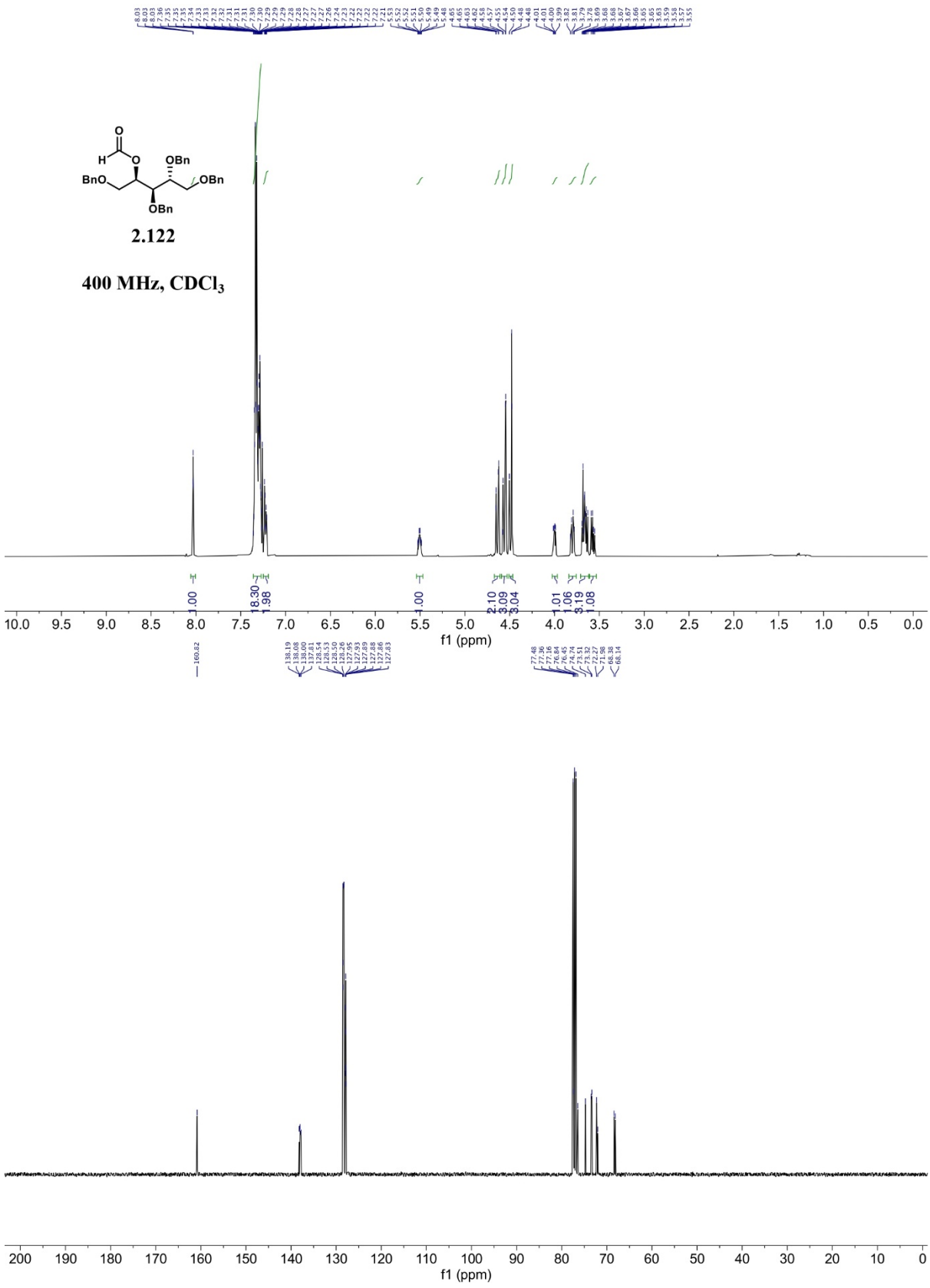
400 MHz, $CDCl_3$

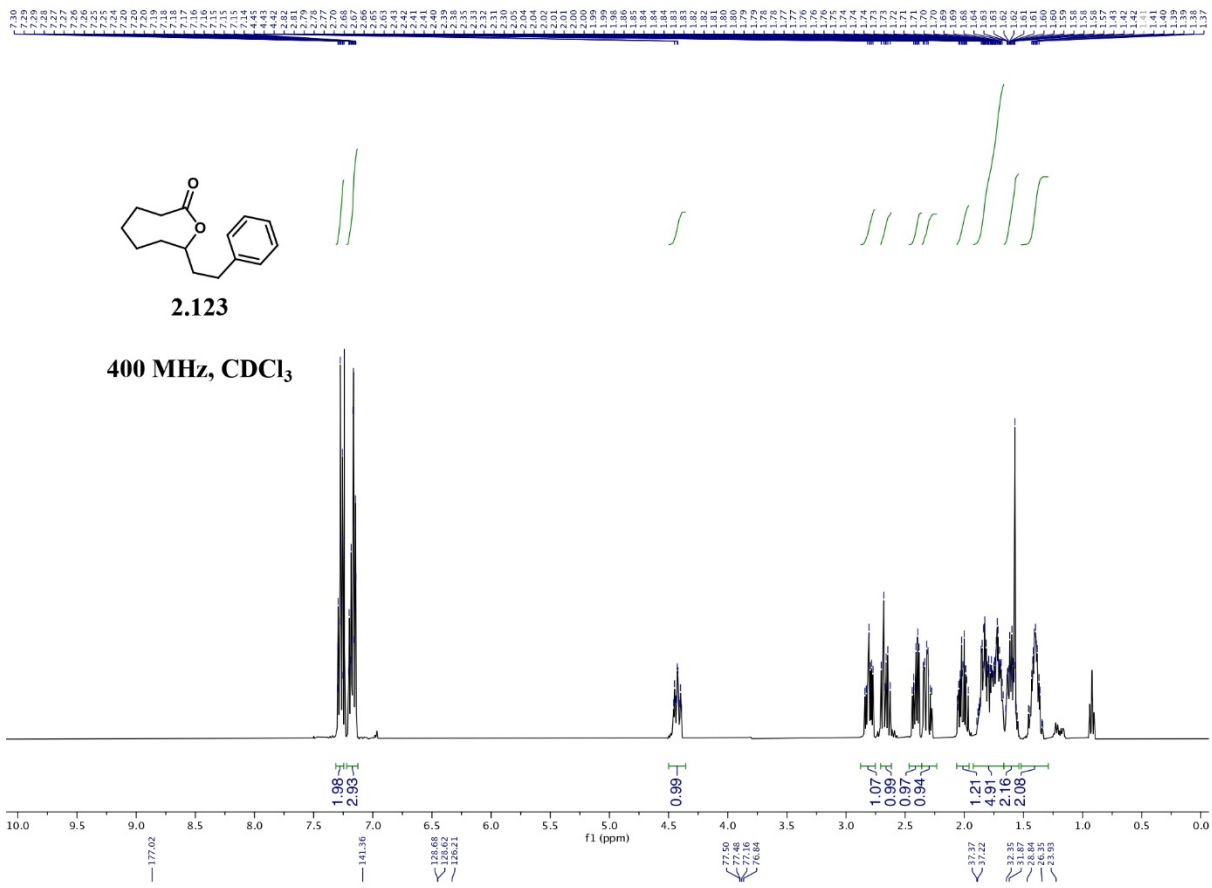


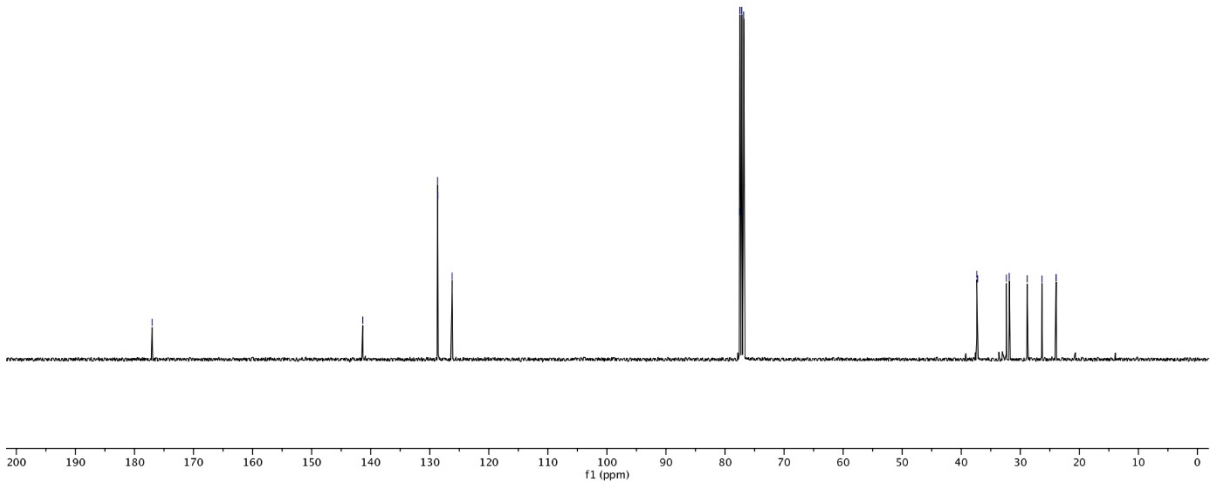


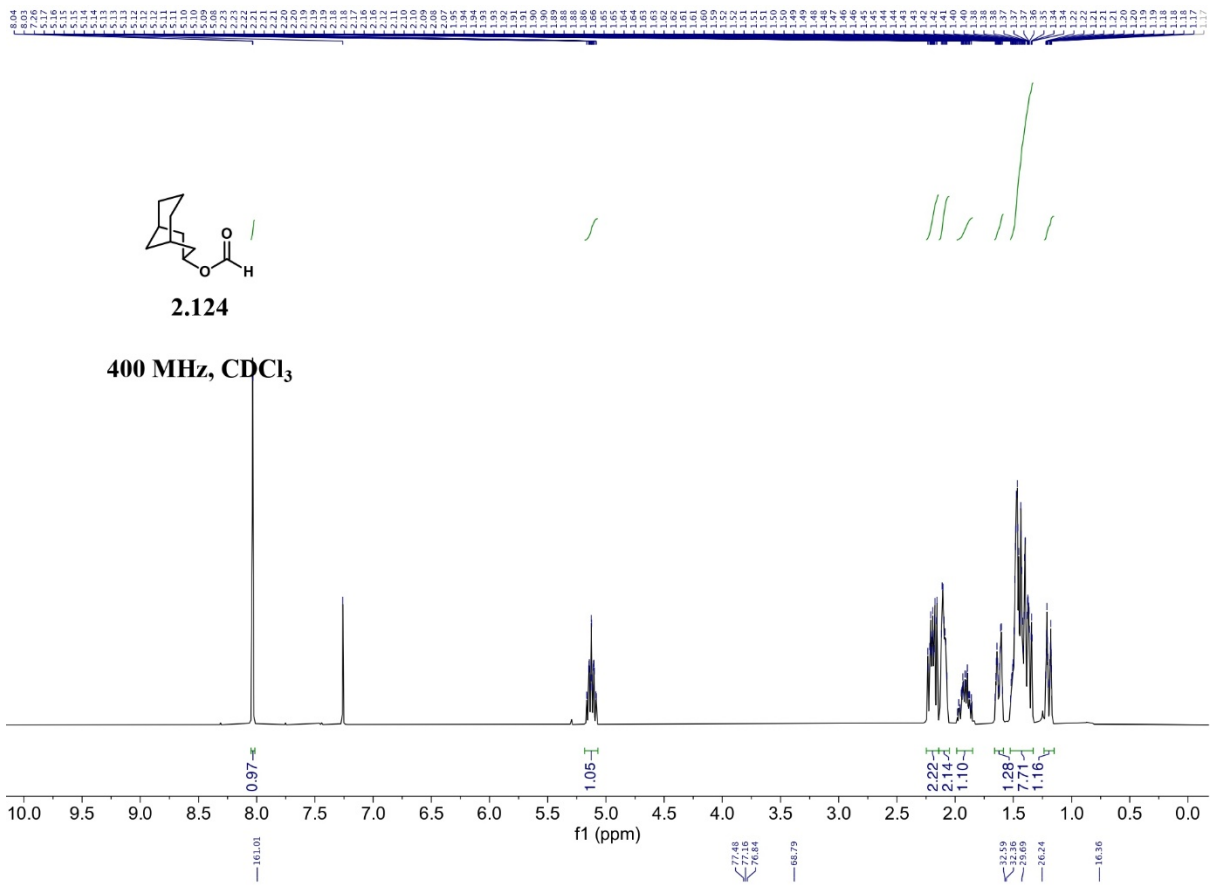

2.118
400 MHz, CDCl3
f1 (ppm)
f1 (ppm)

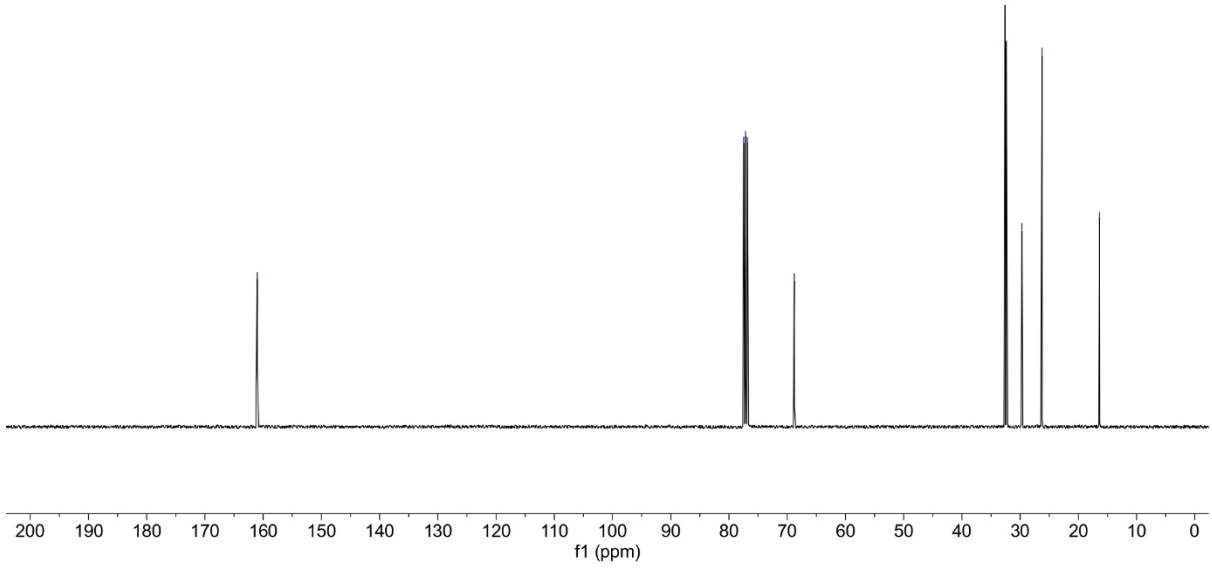

2.120
400 MHz, CDCl3
f1 (ppm)
f1 (ppm)

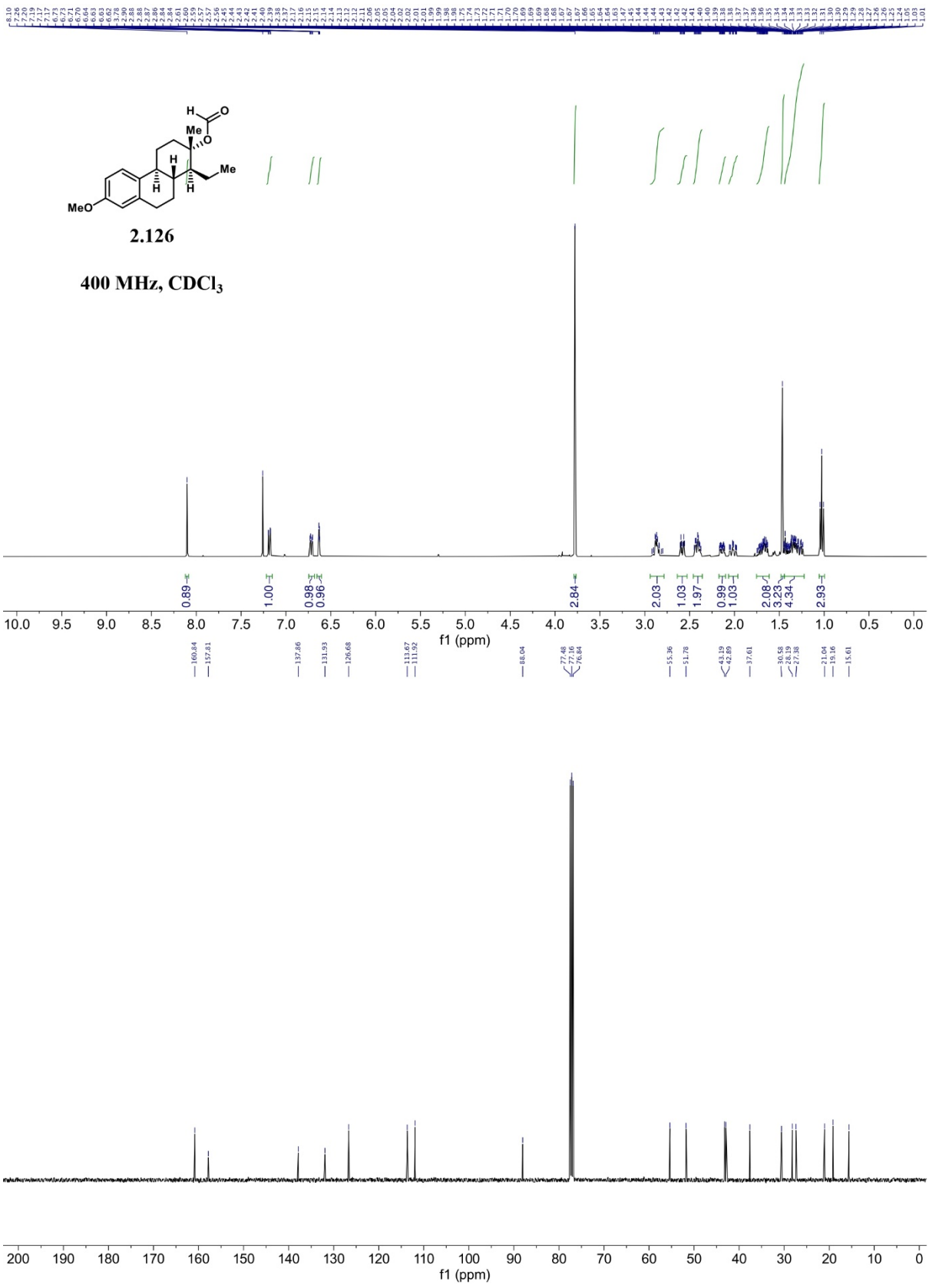

2.122
400 MHz, CDCl3
f1 (ppm)
f1 (ppm)

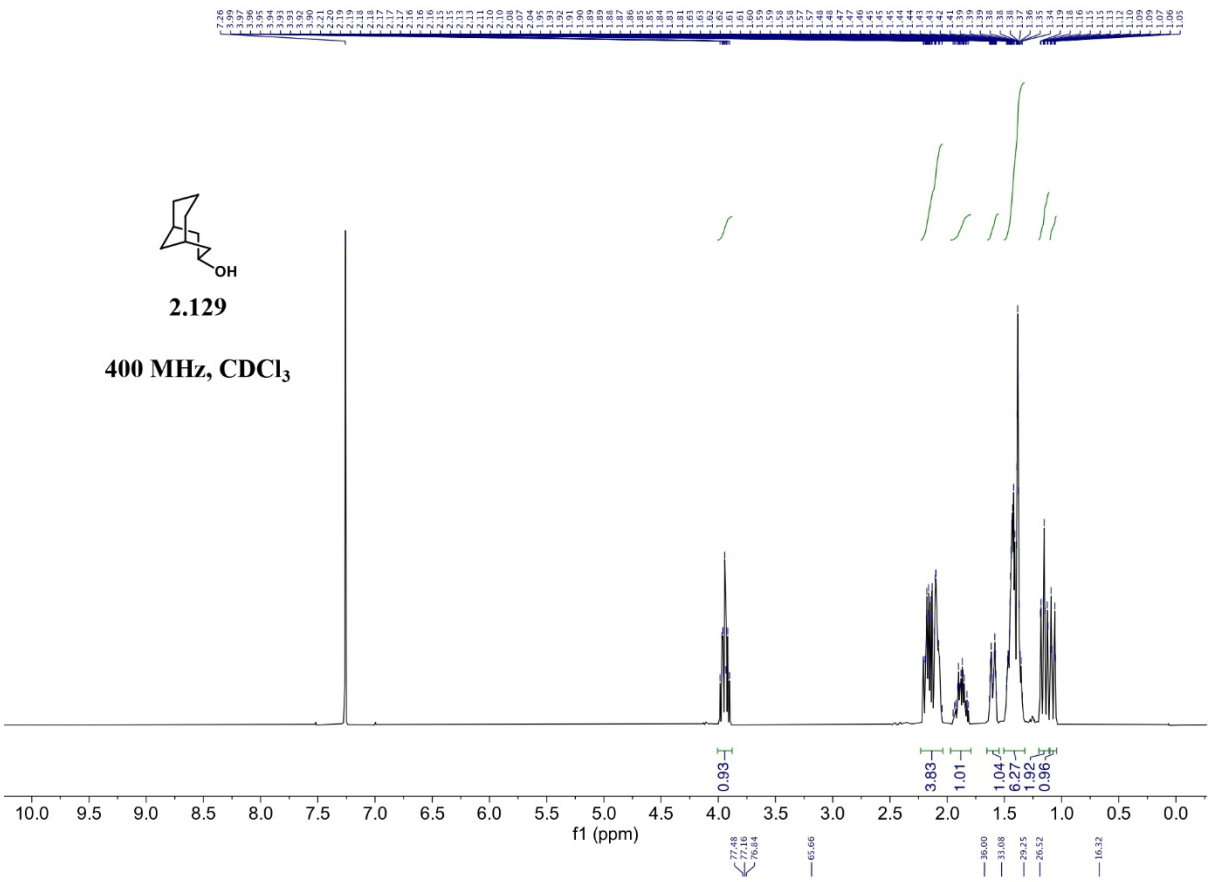

2.123
400 MHz, CDCl3
1.98
2.93
0.99
1.07
0.99
0.97
0.94
1.21
4.91
2.16
2.08
f1 (ppm)

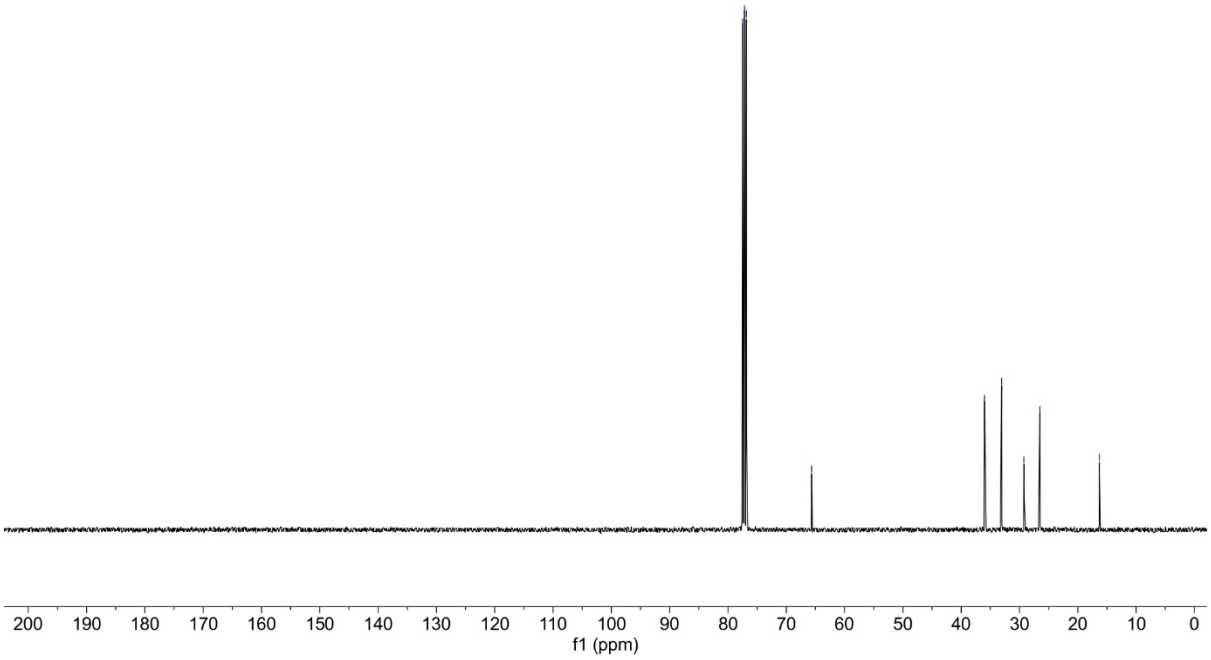

f1 (ppm)


2.124
400 MHz, CDCl3
f1 (ppm)


f1 (ppm)

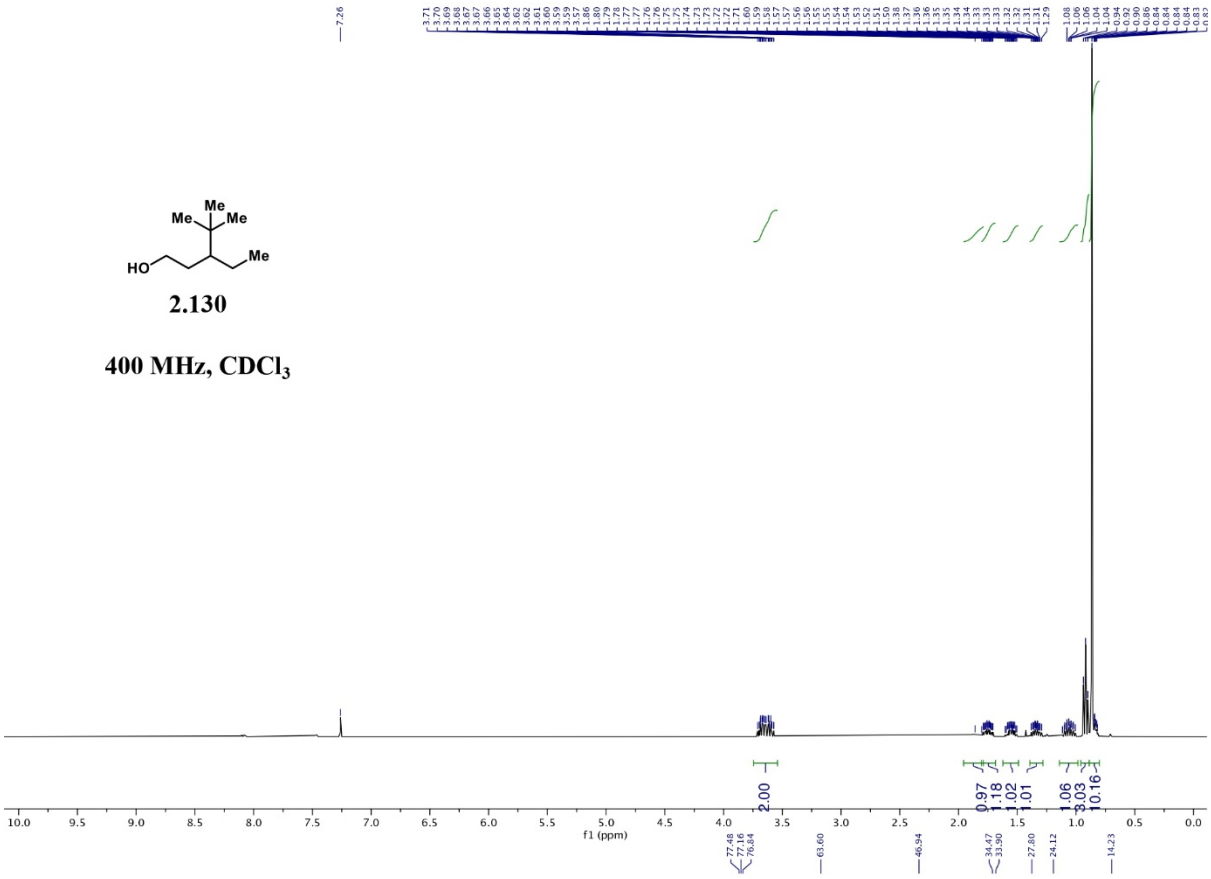

2.126
400 MHz, CDCl3
f1 (ppm)
f1 (ppm)

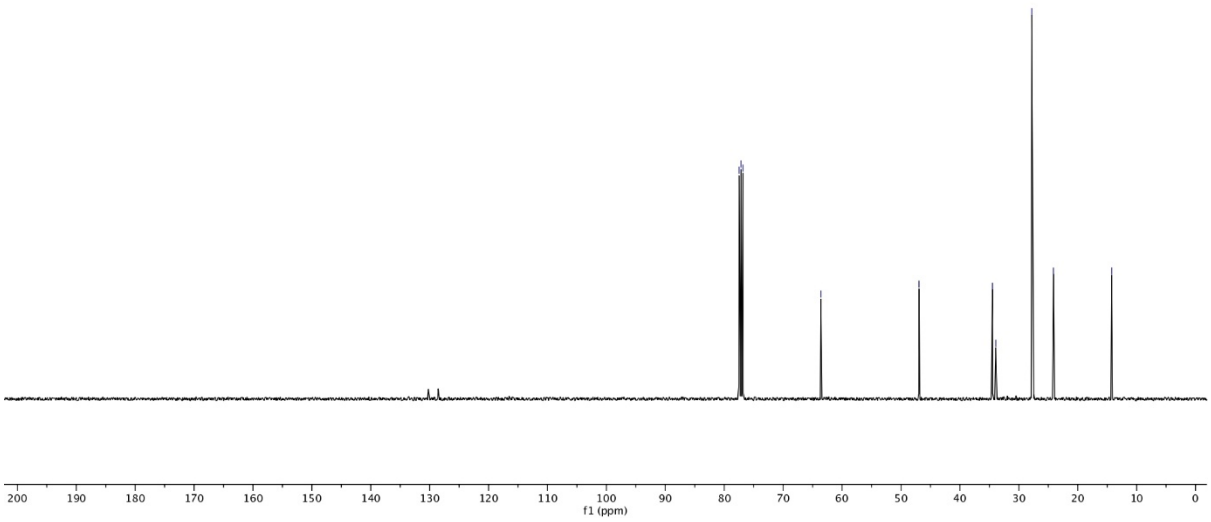

OH
2.129
400 MHz, CDCl3
0.93
3.83
1.01
1.04
6.27
1.92
0.96
f1 (ppm)
77.48
77.16
76.84
65.66
36.00
33.08
29.25
26.52
16.32

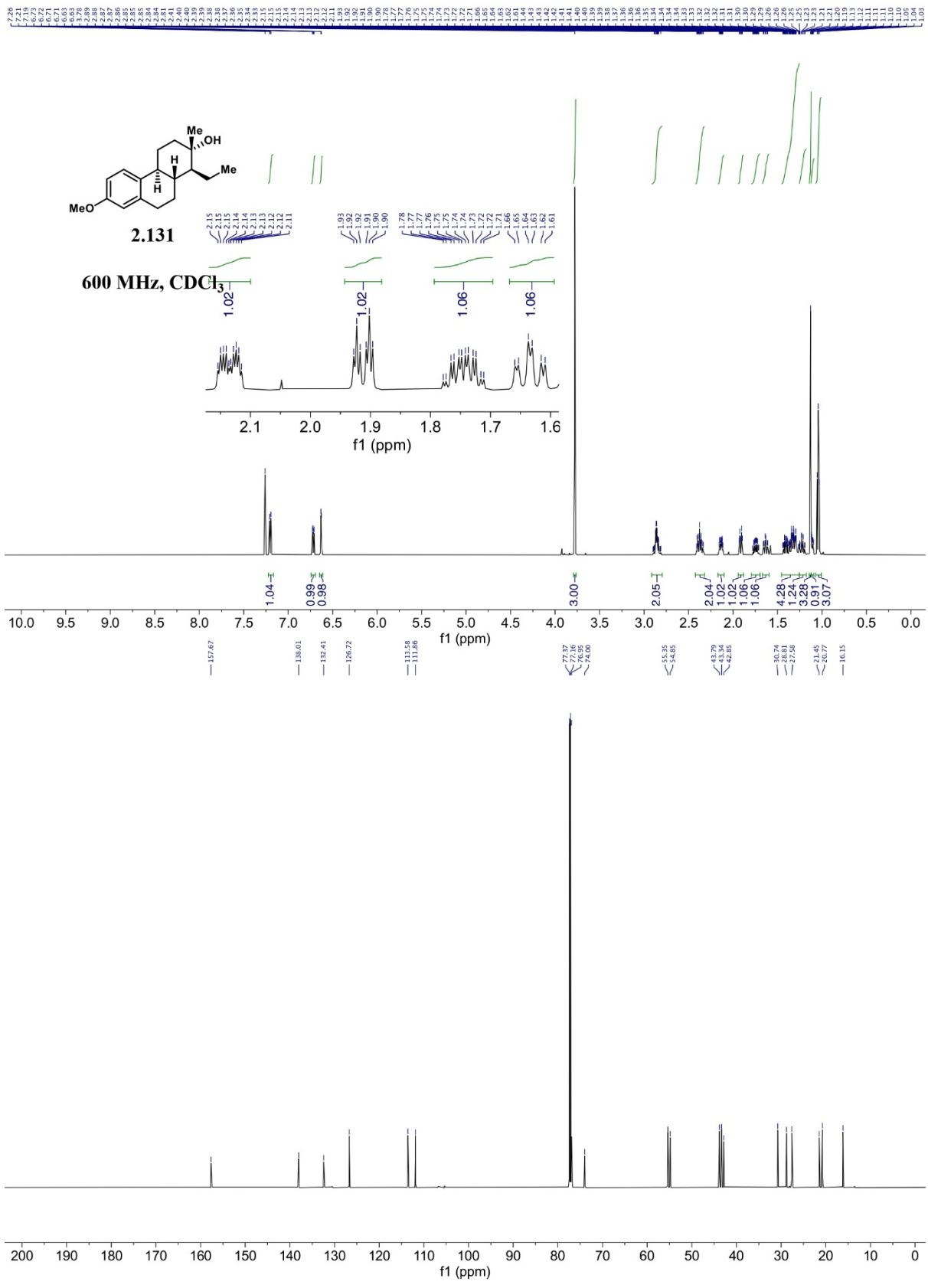

f1 (ppm)

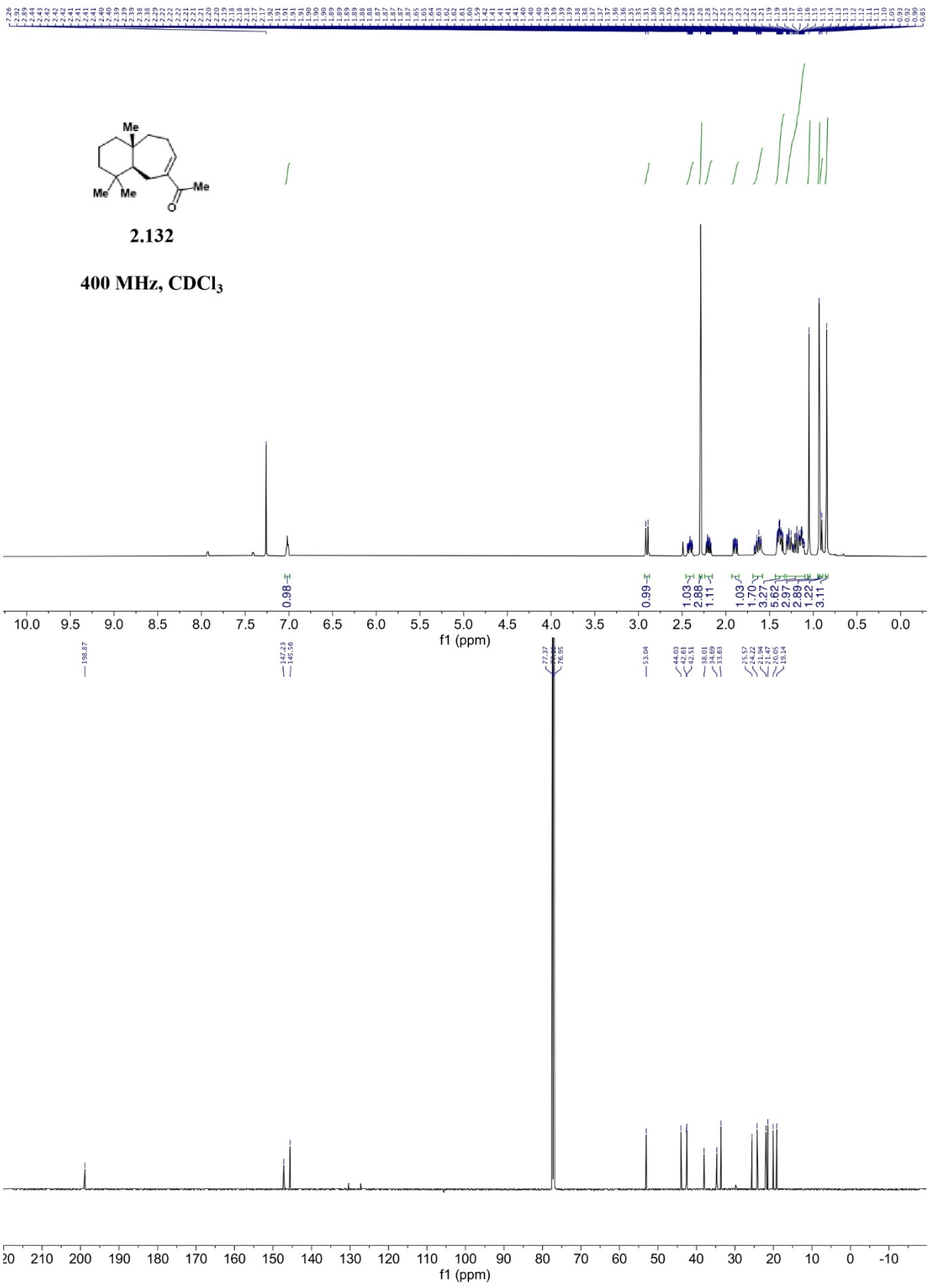
2.130

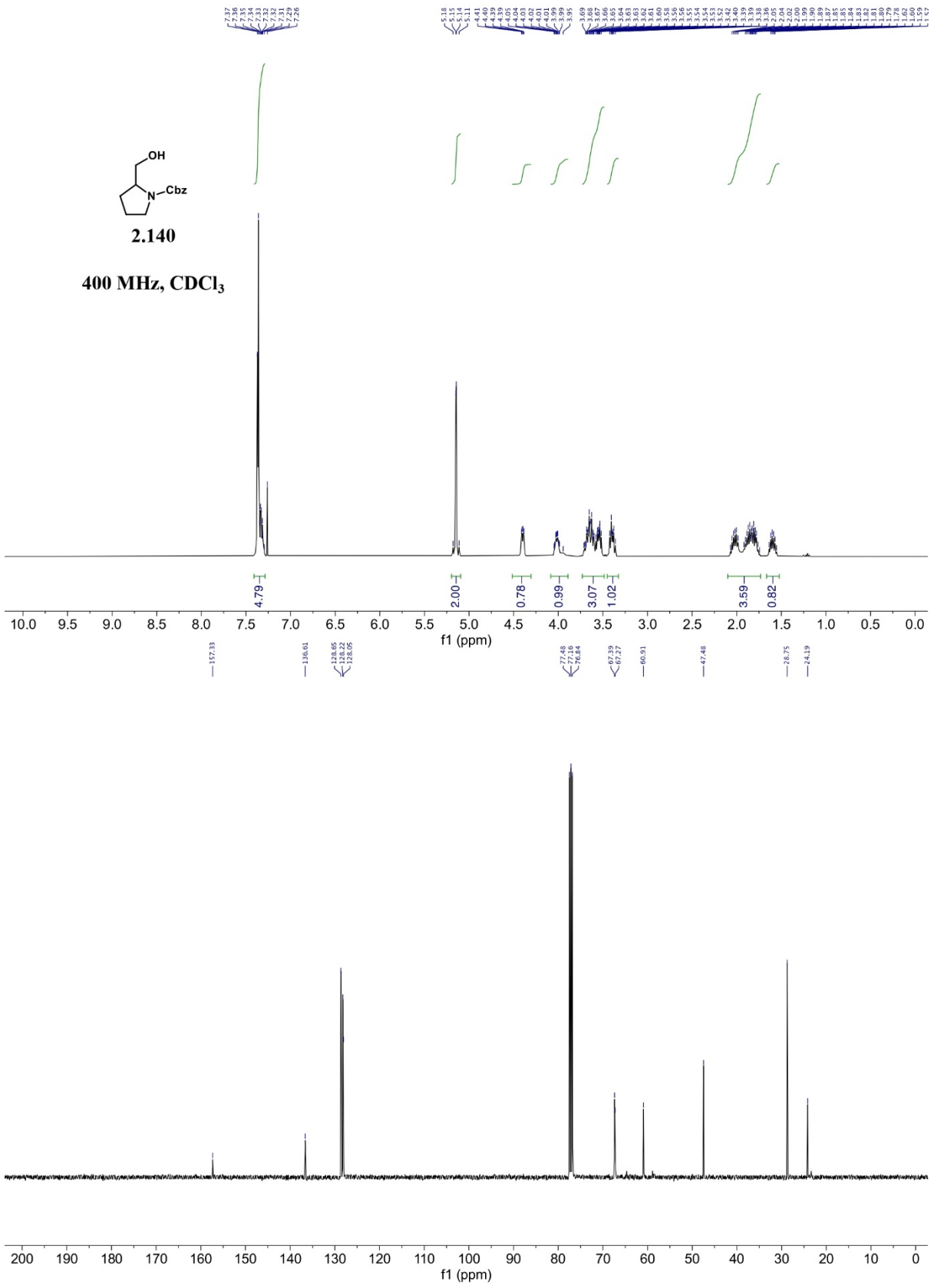
400 MHz, $CDCl_3$

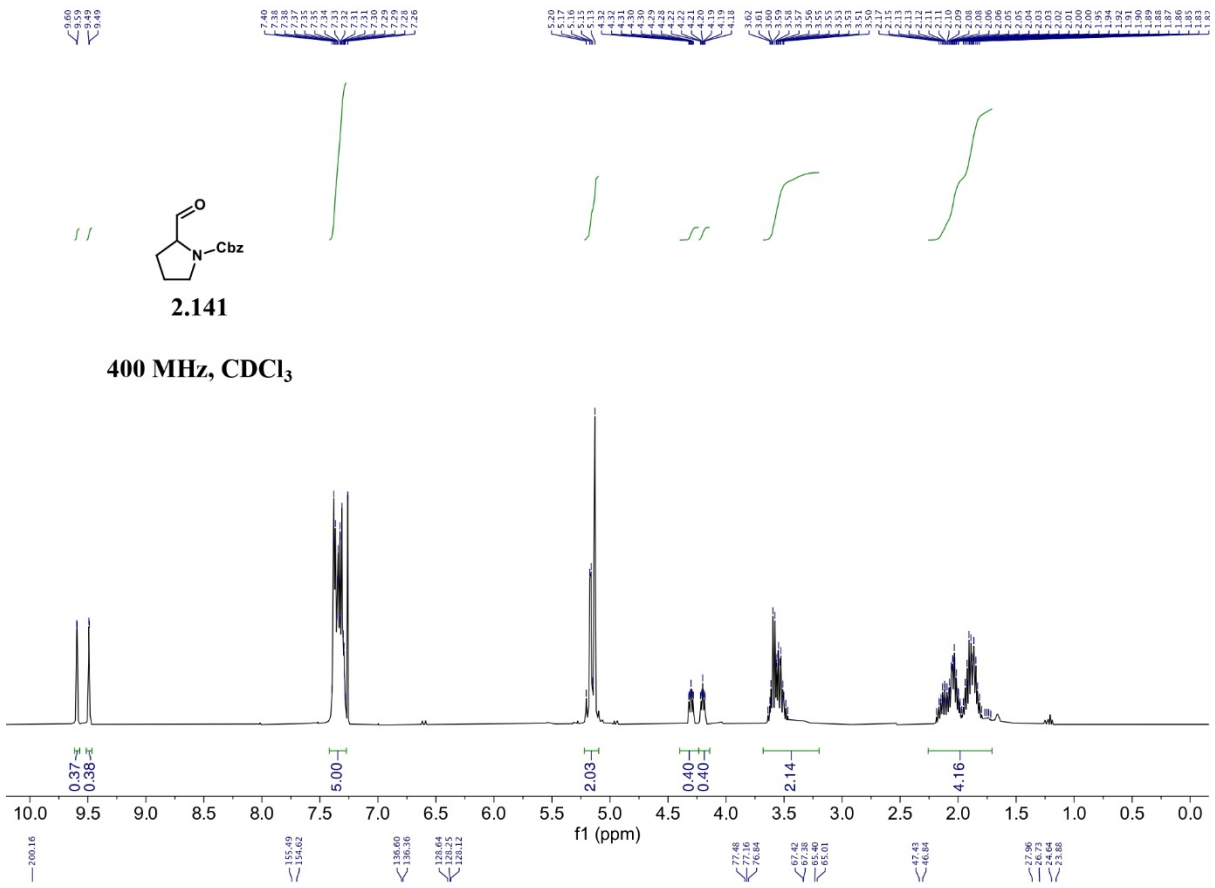





Me
OH
H
H
Me
MeO
2.131
600 MHz, CDCl3
1.02
1.02
1.06
1.06
2.1
2.0
1.9
1.8
1.7
1.6
f1 (ppm)
1.04
0.99
0.98
3.00
2.05
2.04
1.02
1.02
1.06
1.06
4.28
1.24
3.28
0.91
3.07
10.0
9.5
9.0
8.5
8.0
7.5
7.0
6.5
6.0
5.5
5.0
4.5
4.0
3.5
3.0
2.5
2.0
1.5
1.0
0.5
0.0
f1 (ppm)
200
190
180
170
160
150
140
130
120
110
100
90
80
70
60
50
40
30
20
10
0
f1 (ppm)

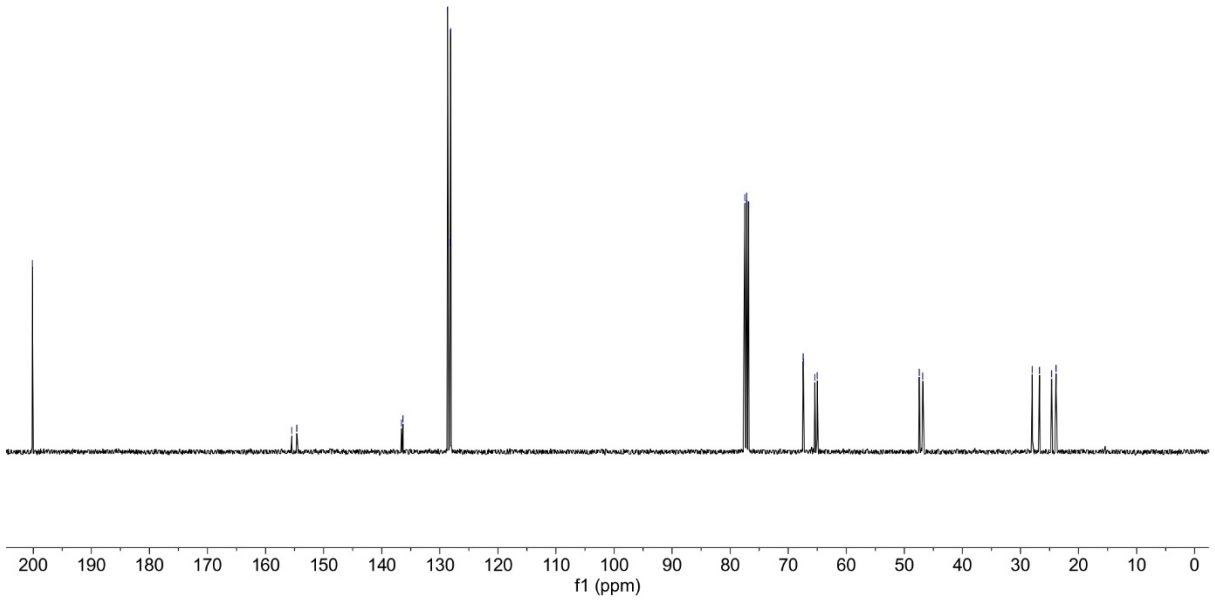

Me
Me
Me
Me
2.132
400 MHz, CDCl3
f1 (ppm)
f1 (ppm)

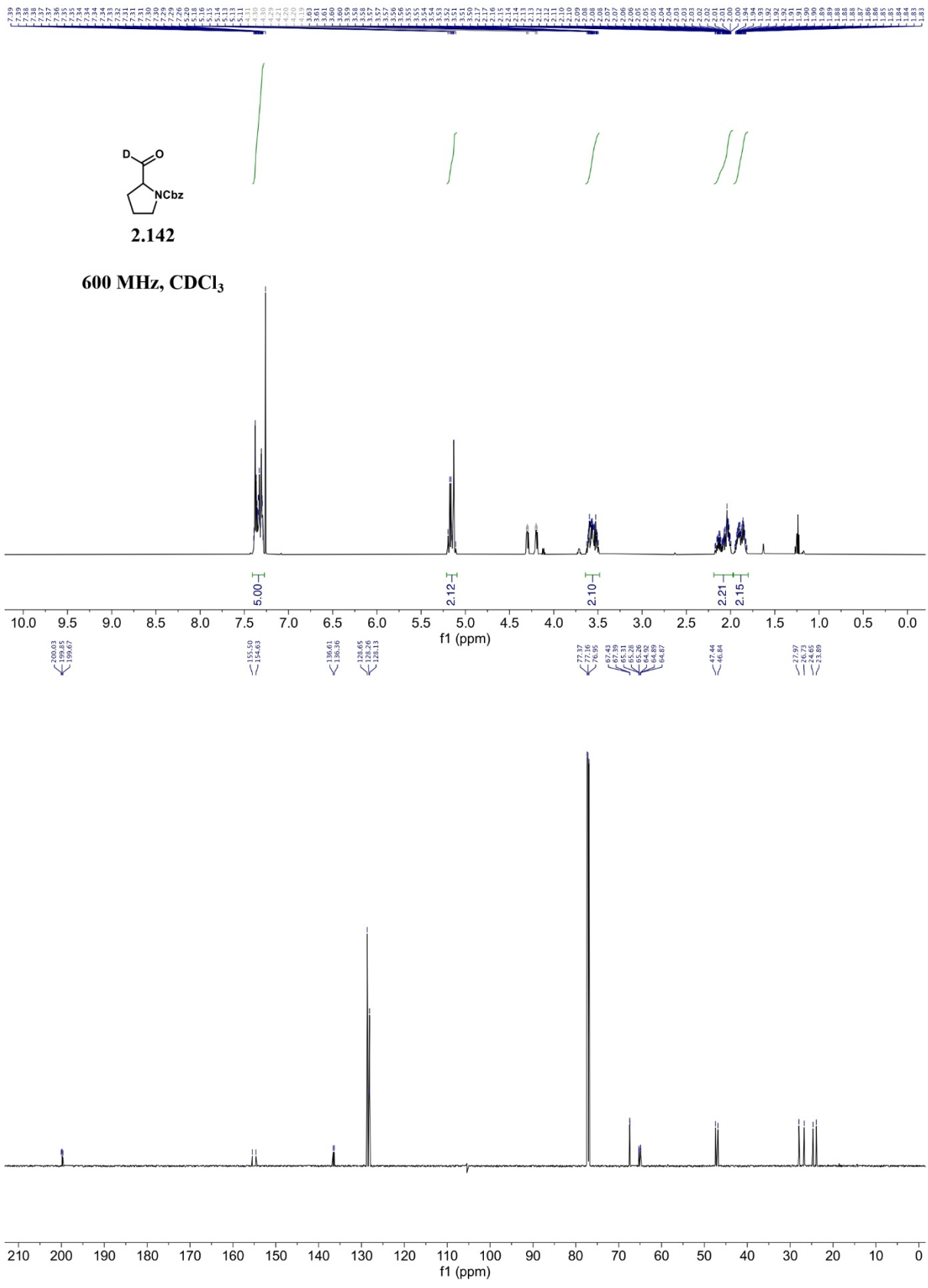

OH
N
Cbz
2.140
400 MHz, CDCl3
f1 (ppm)

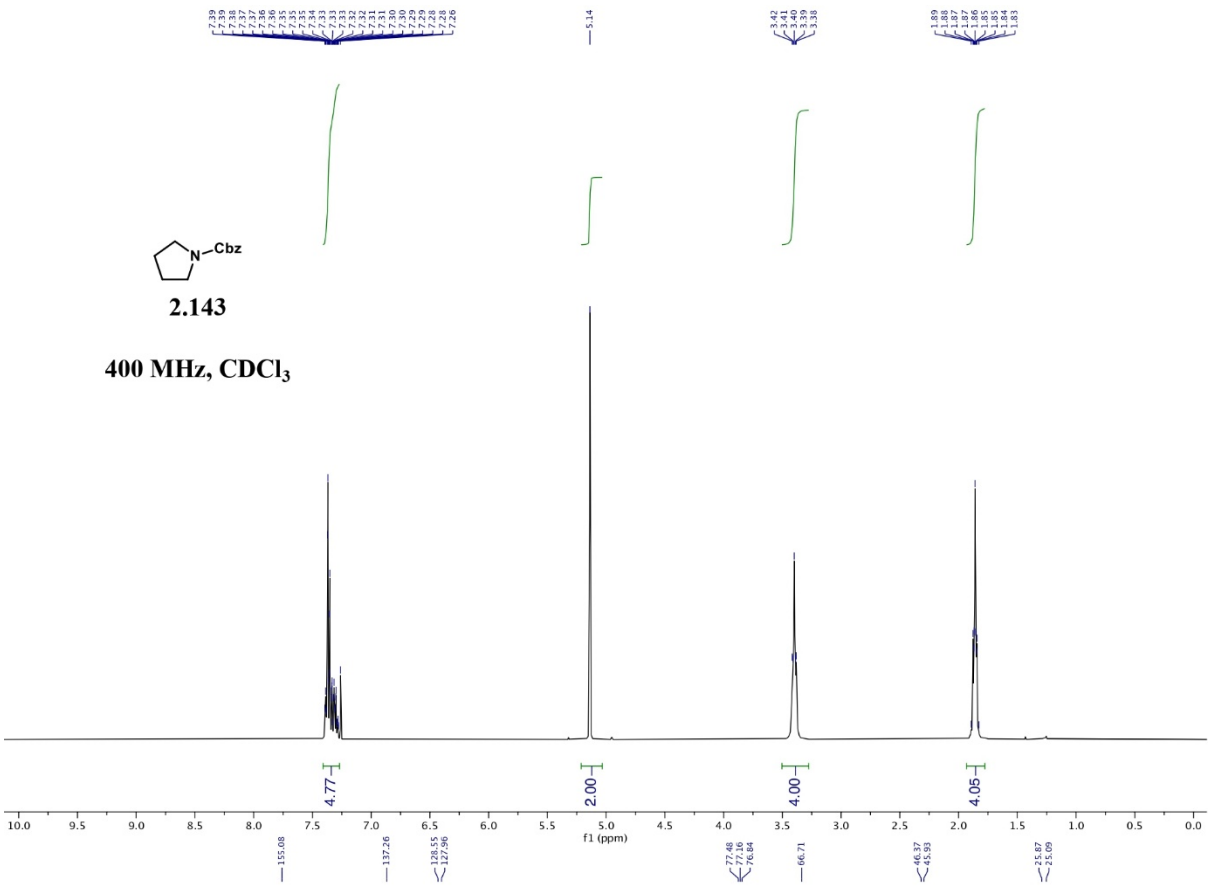


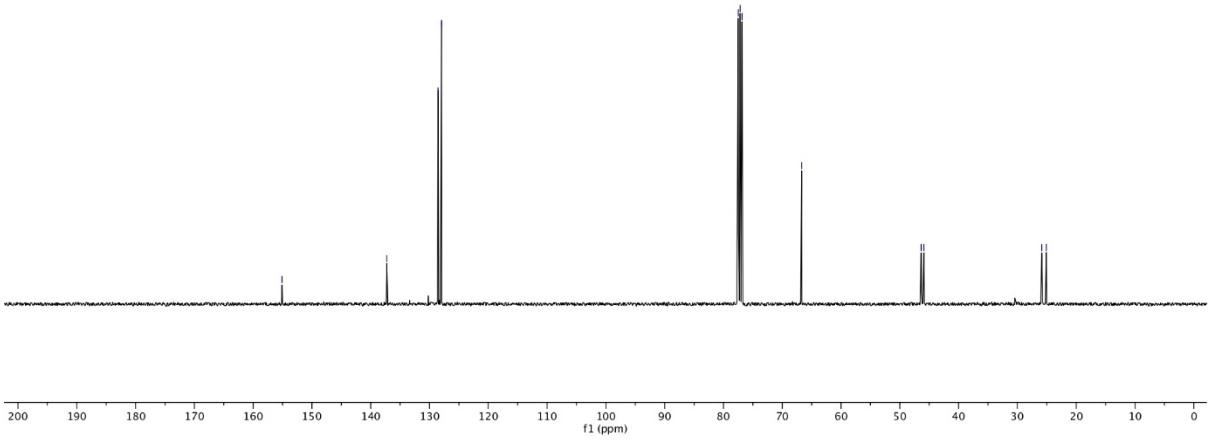
2.141

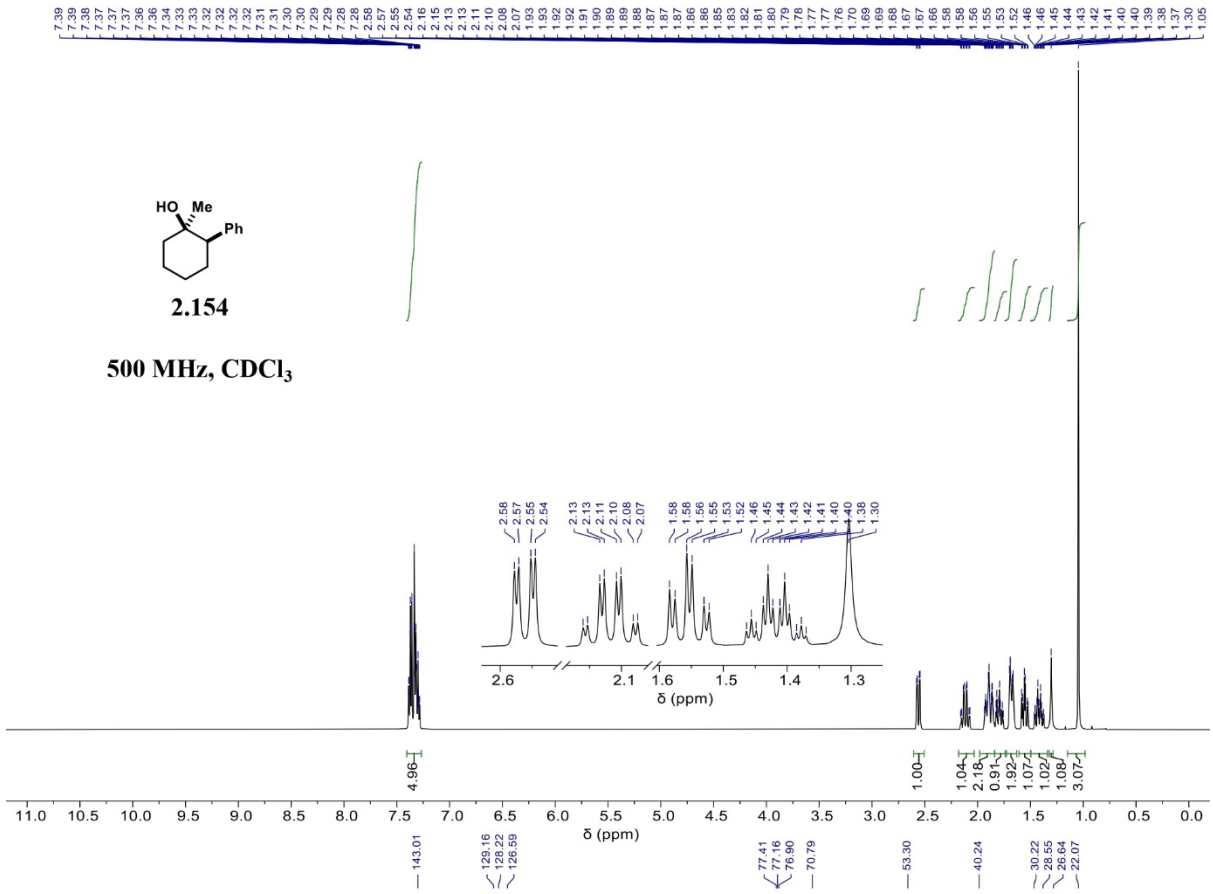
400 MHz, $CDCl_3$




D
O
NCbz
2.142
600 MHz, CDCl3
5.00
2.12
2.10
2.21
2.15
f1 (ppm)
f1 (ppm)

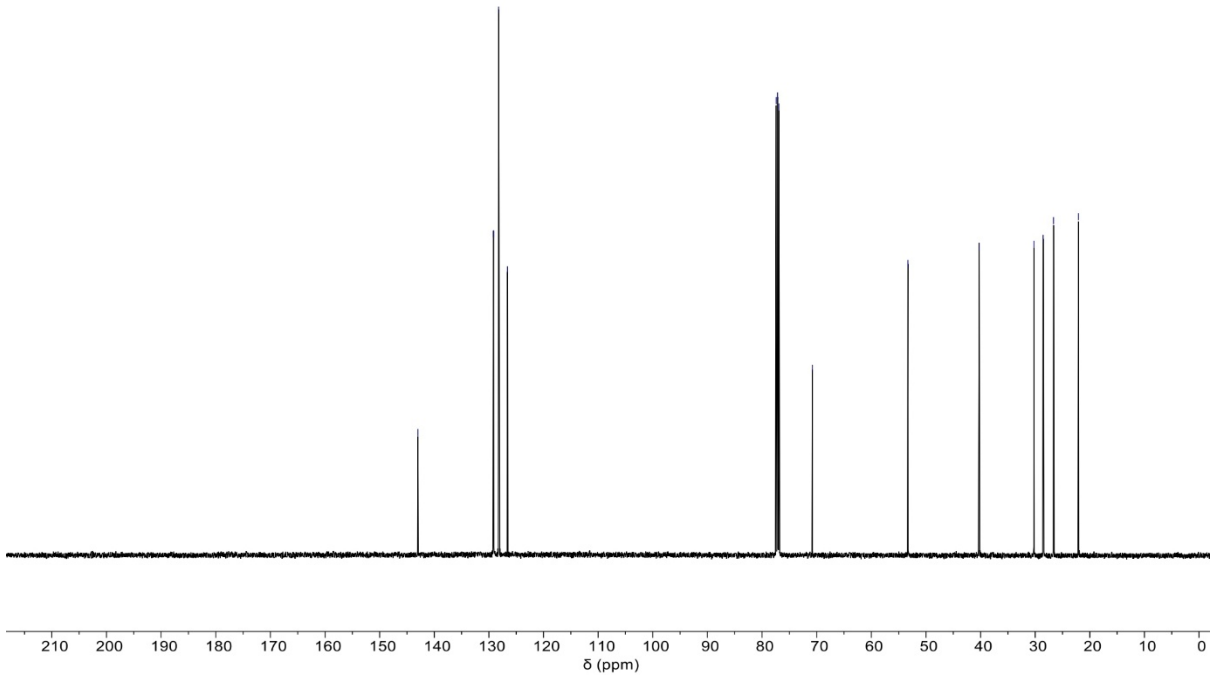

N–Cbz
2.143
400 MHz, CDCl3
4.77
2.00
4.00
4.05
f1 (ppm)

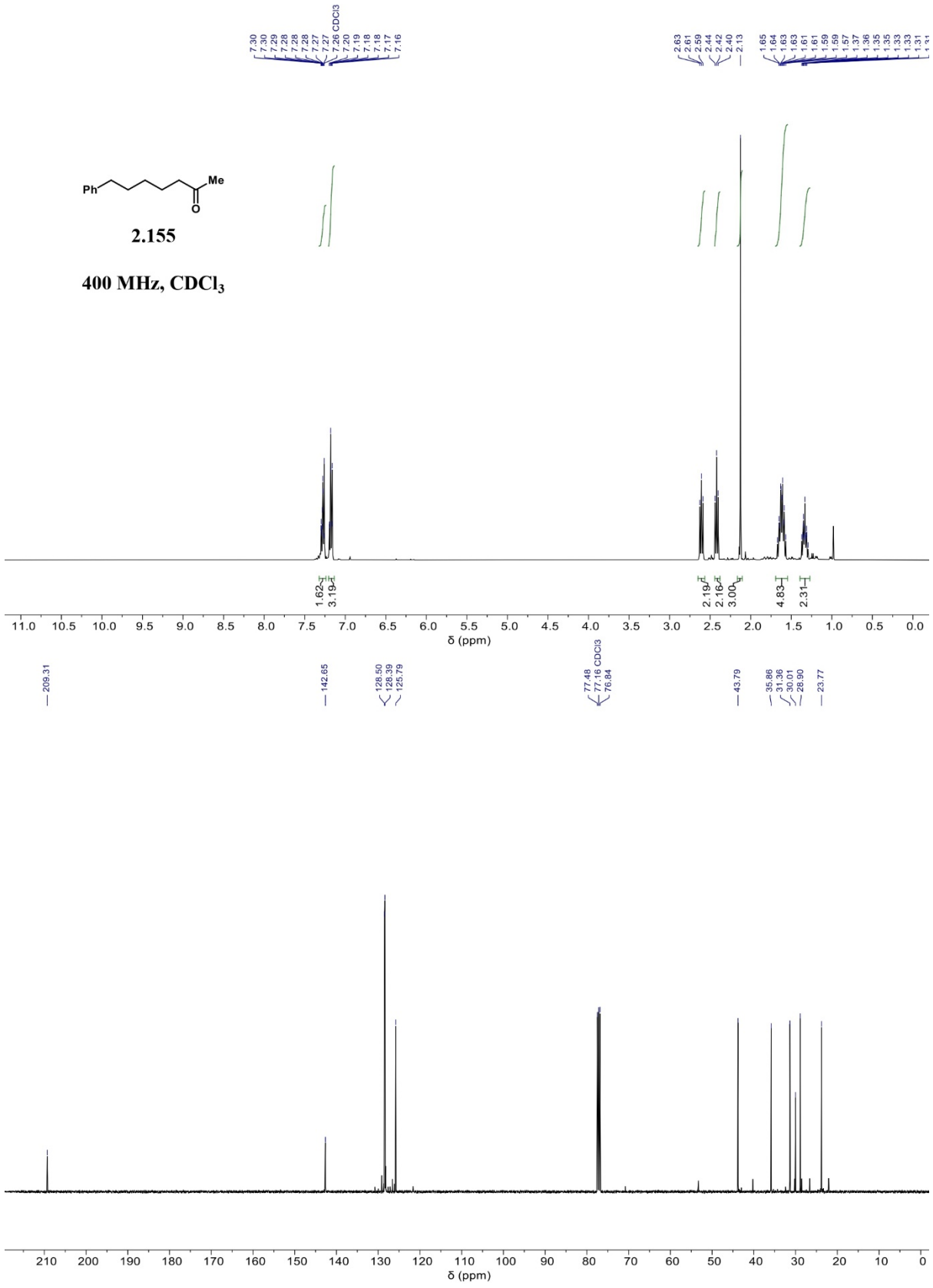

f1 (ppm)

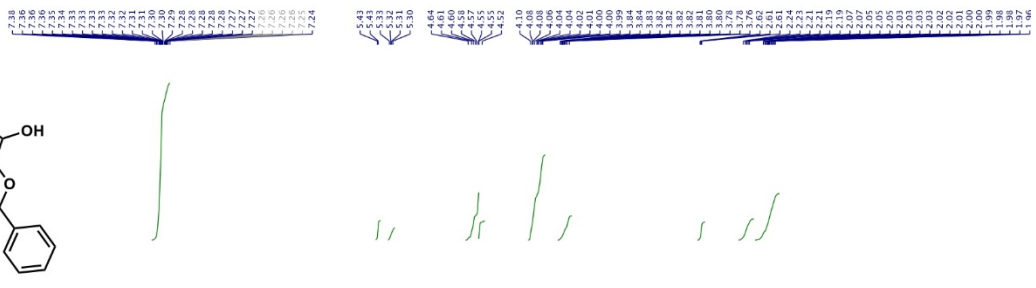


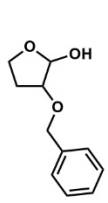
2.154

500 MHz, $CDCl_3$



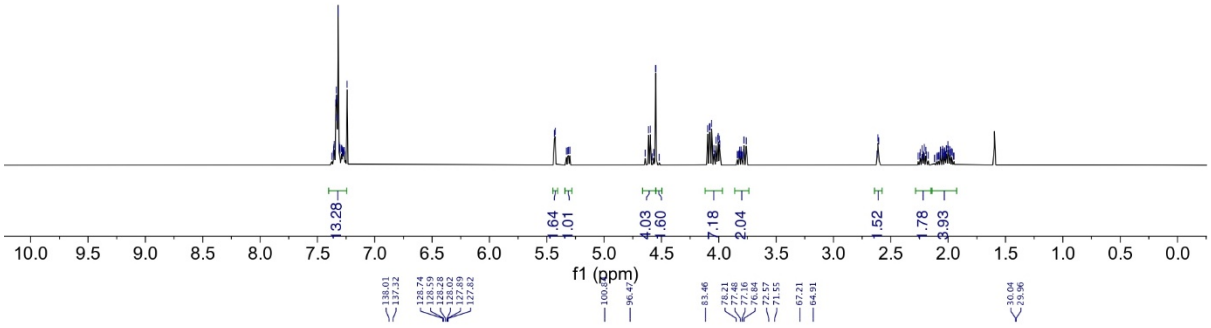

Ph
Me
O
2.155
400 MHz, CDCl3
δ (ppm)
δ (ppm)

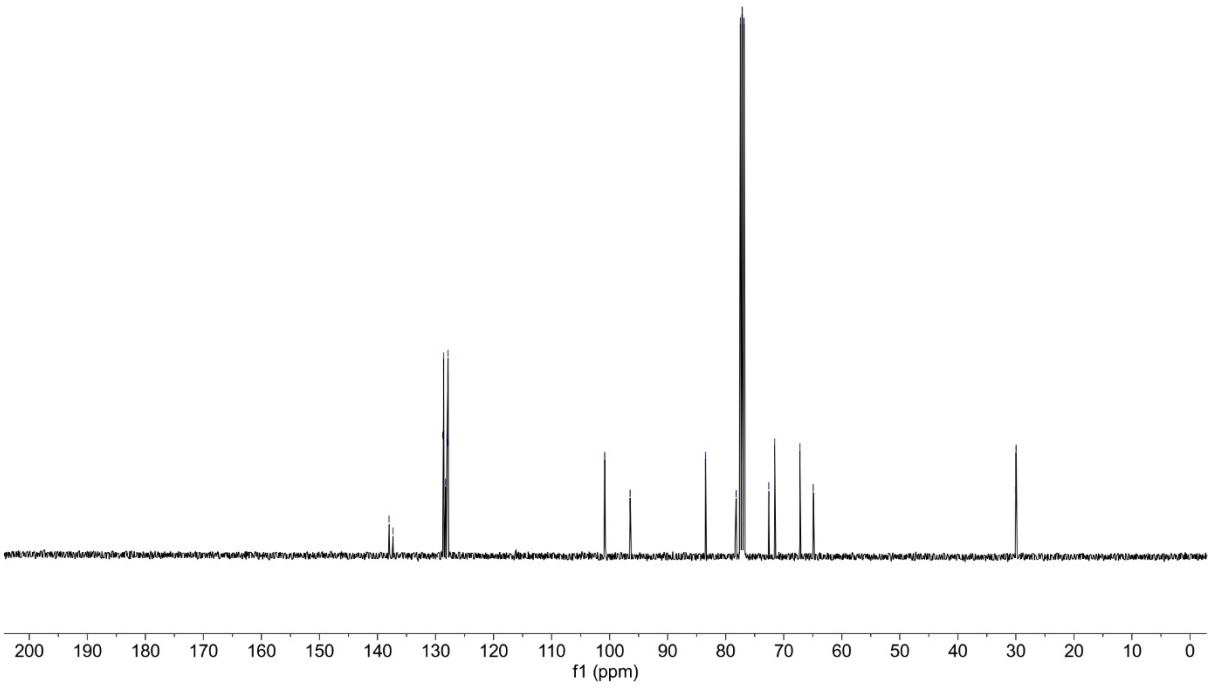


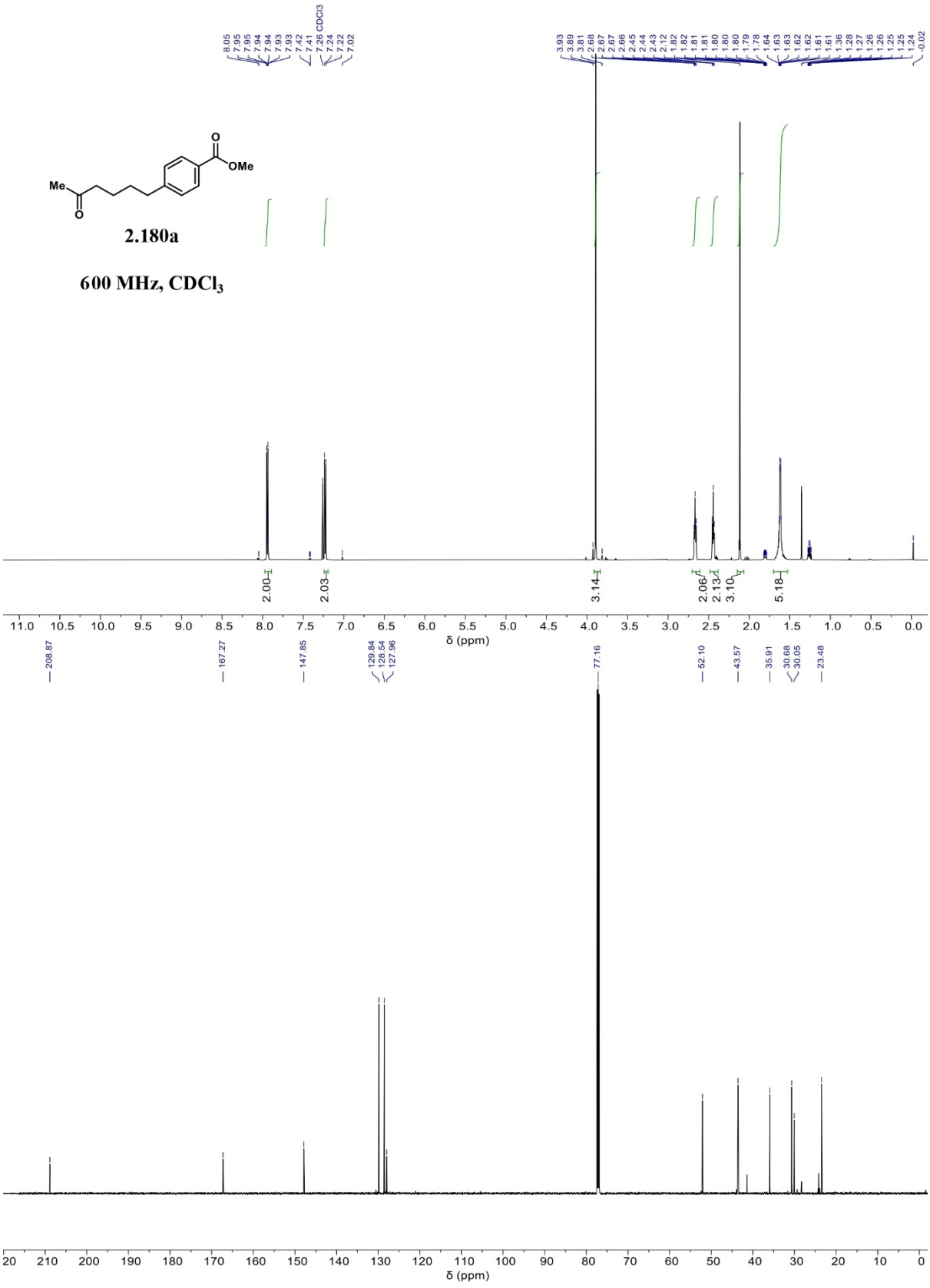


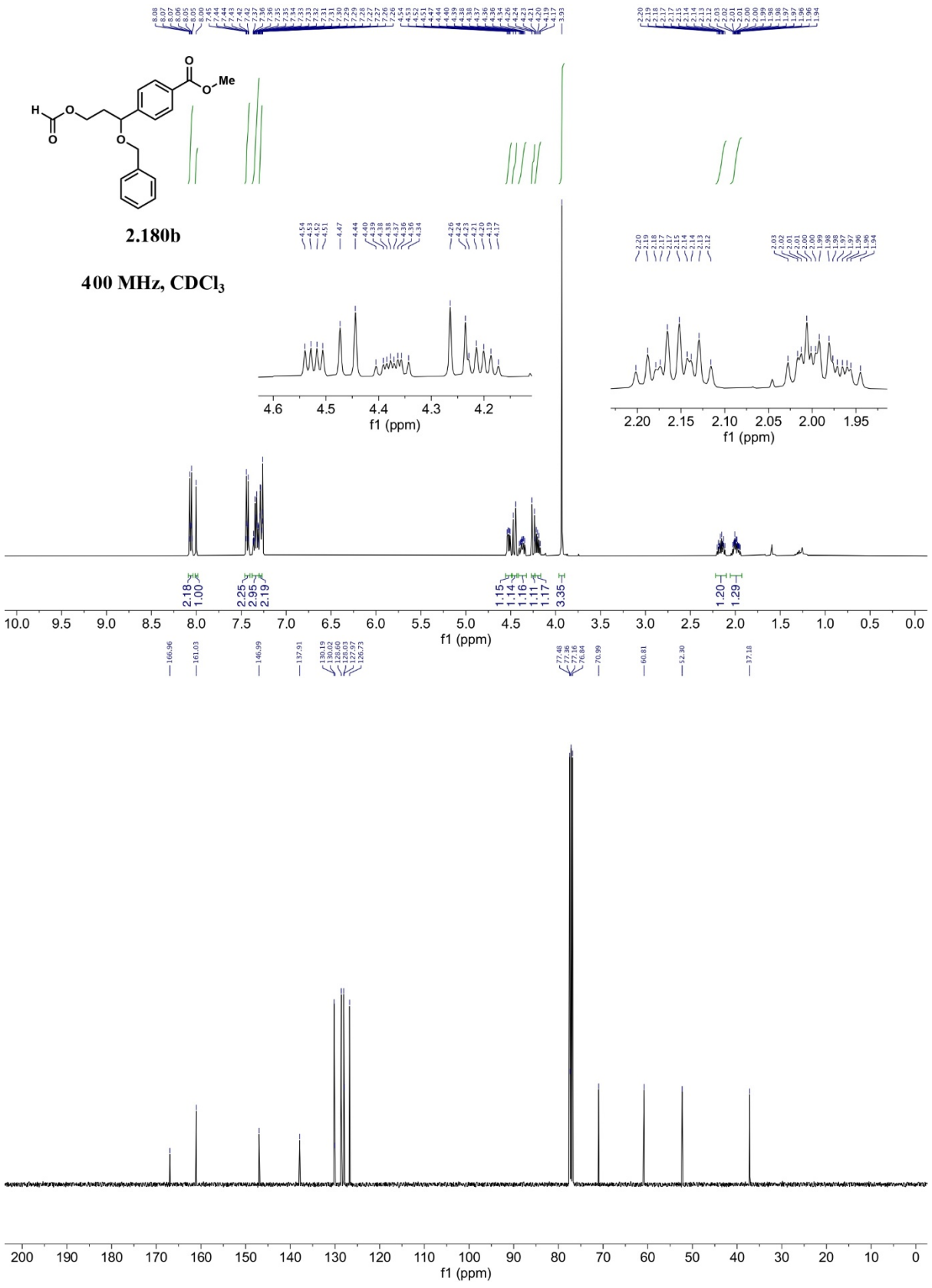
2.179b

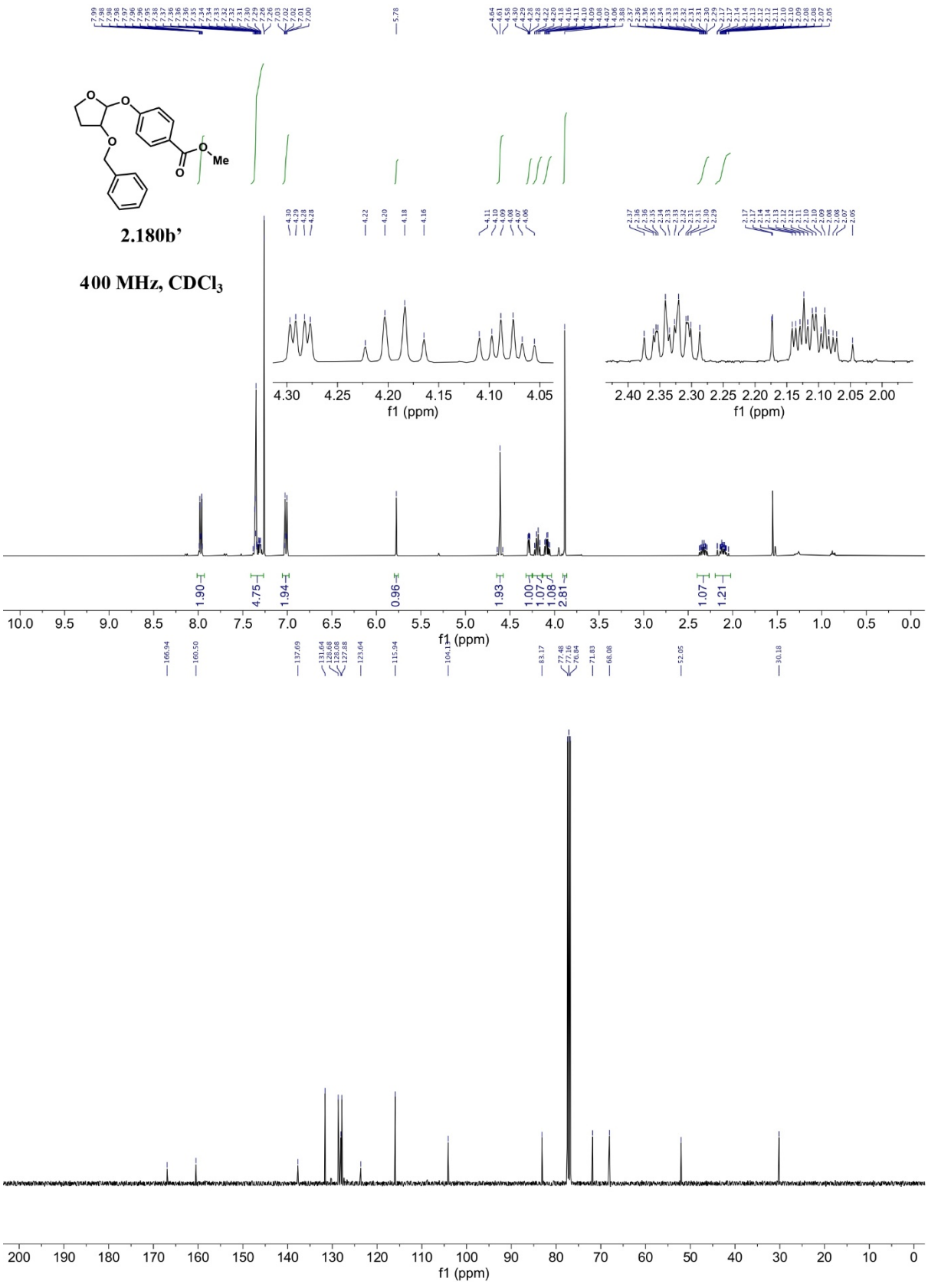
400 MHz, $CDCl_3$

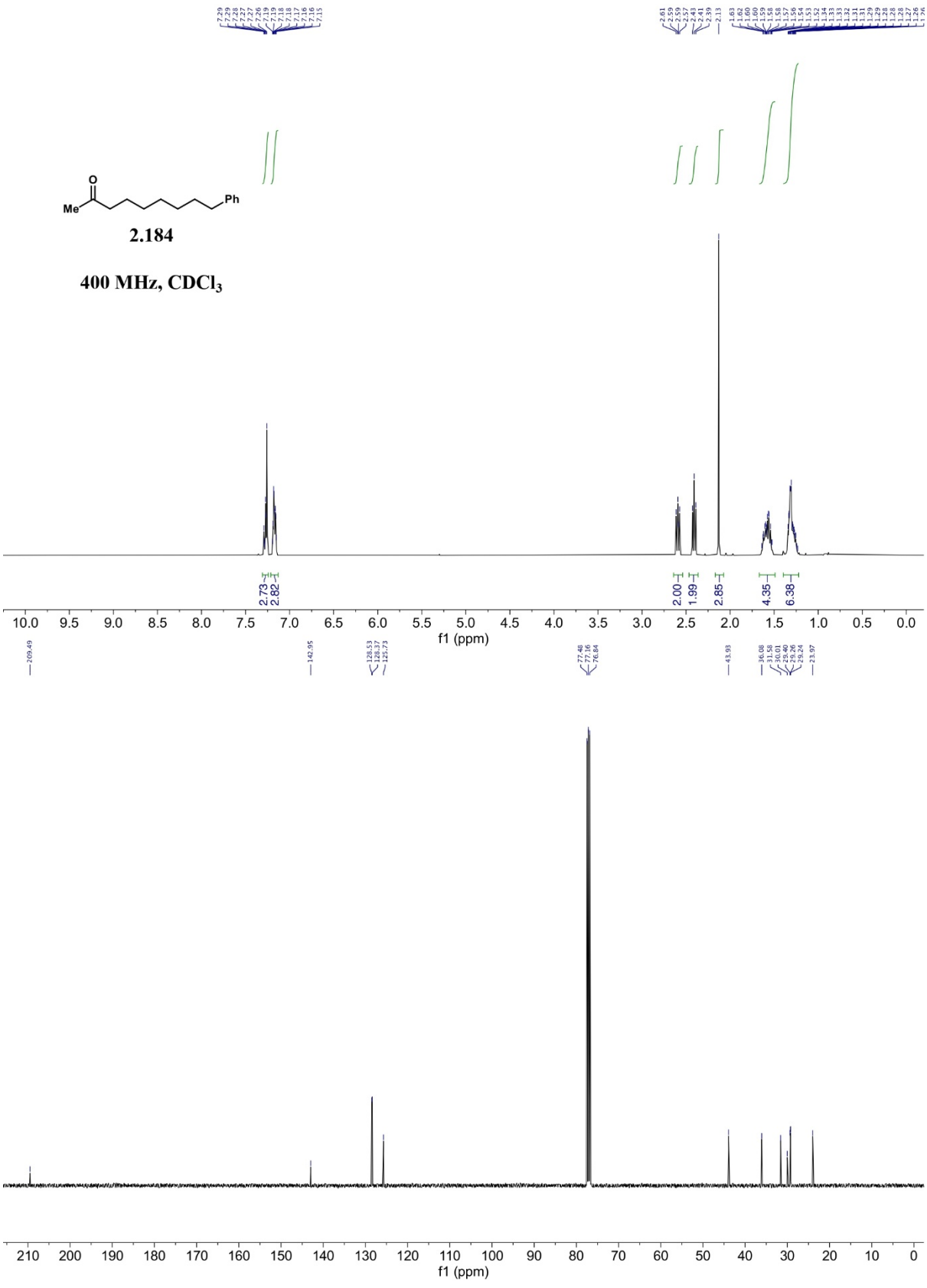


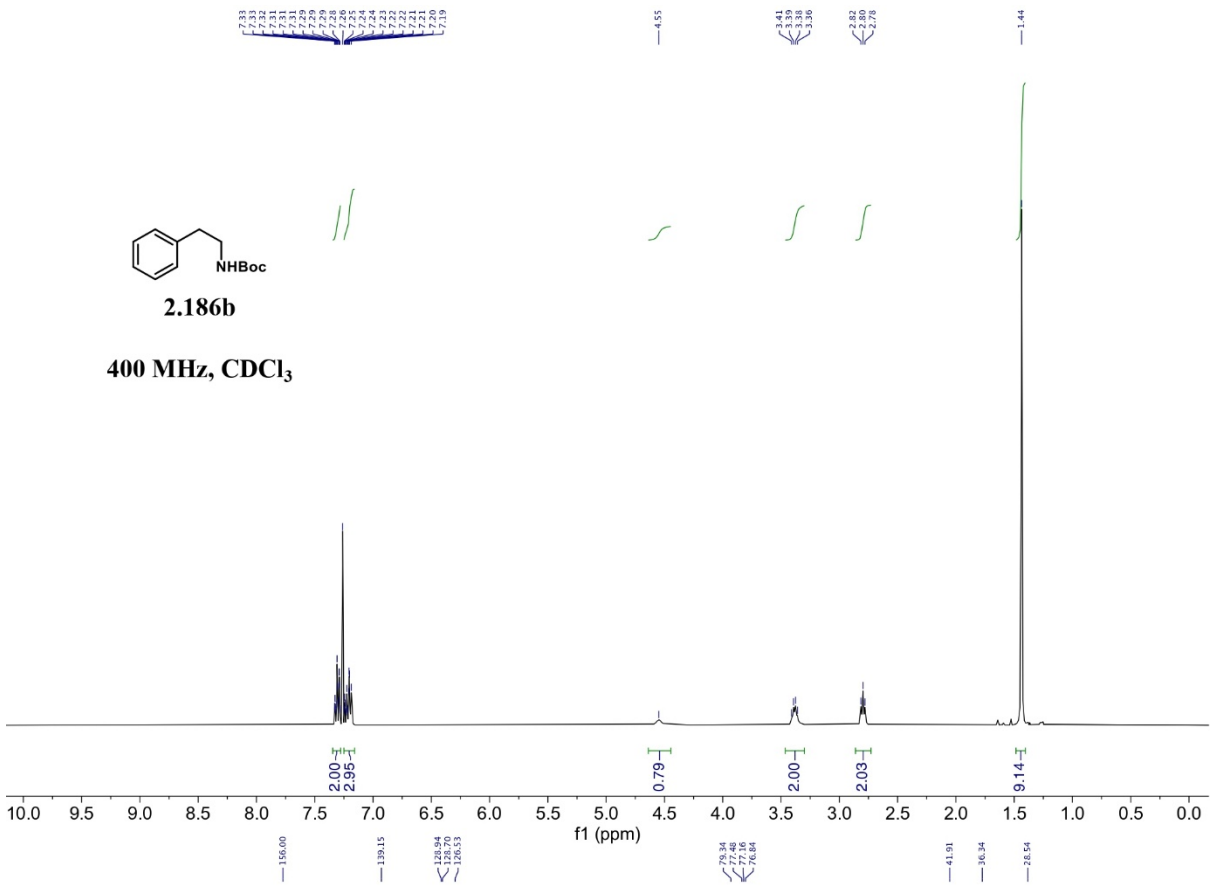


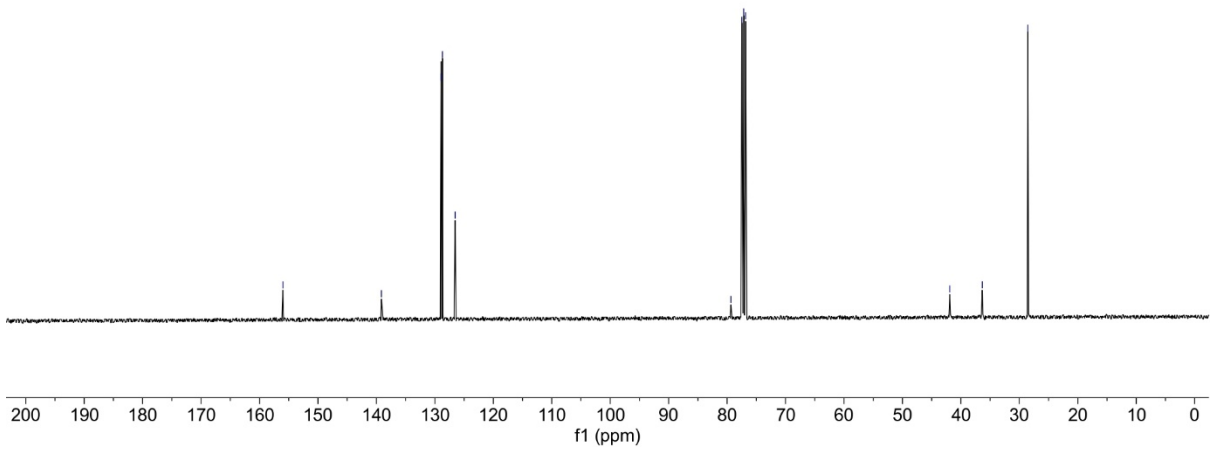

Me
O
O
OMe
2.180a
600 MHz, CDCl3
δ (ppm)
δ (ppm)

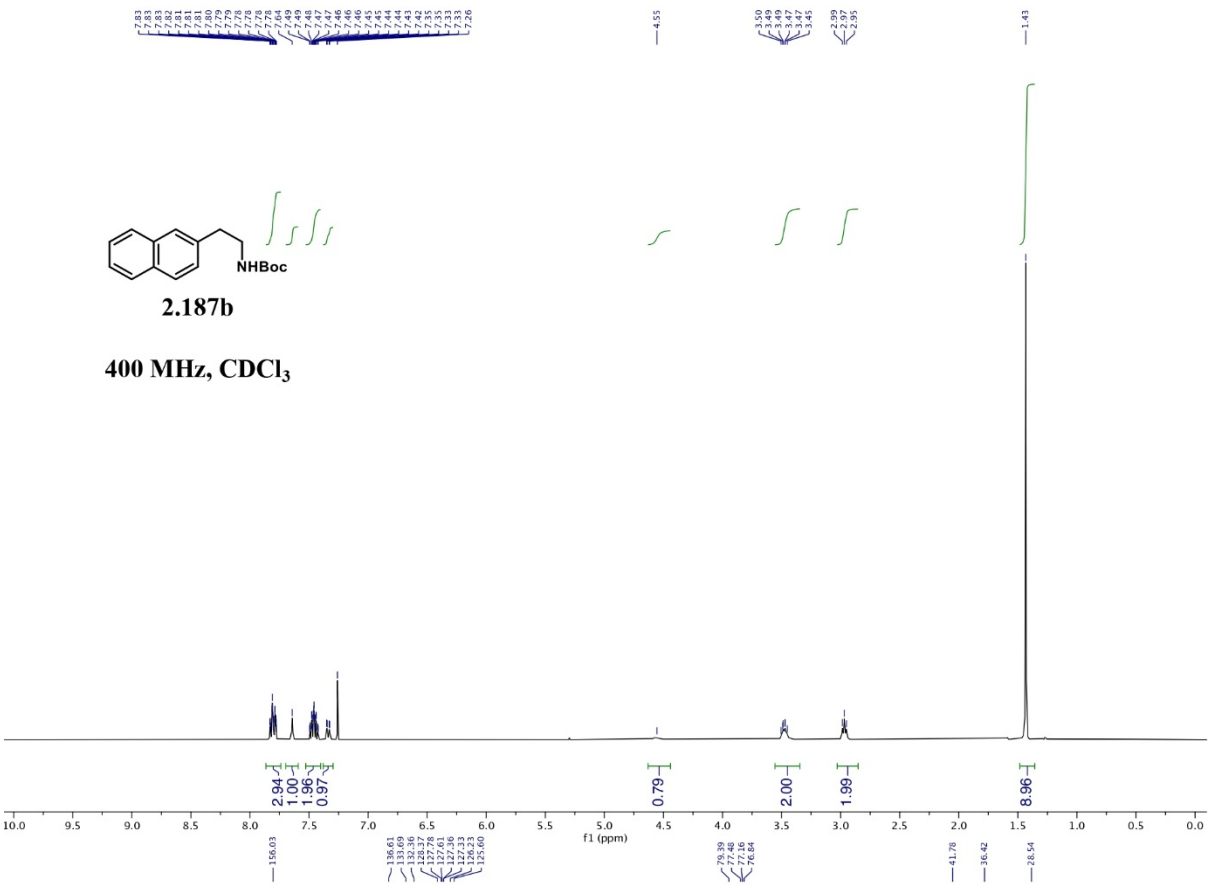

2.180b
400 MHz, CDCl3
f1 (ppm)


2.180b'
400 MHz, CDCl3
f1 (ppm)


Me
O
Ph
2.184
400 MHz, CDCl3
f1 (ppm)
f1 (ppm)

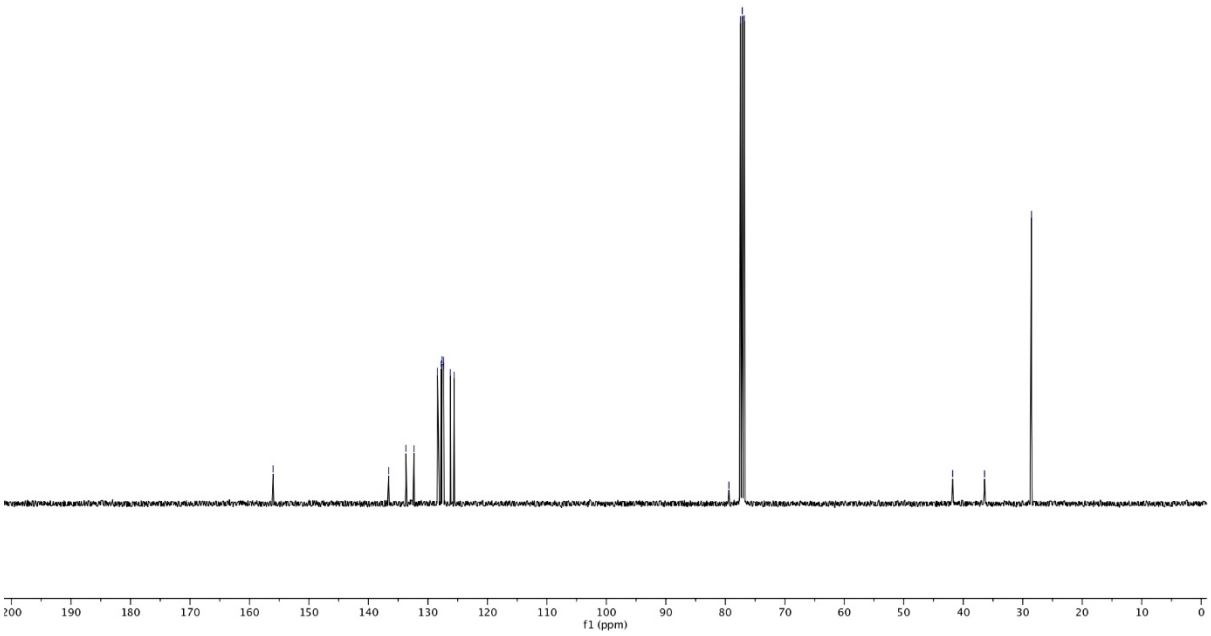

NHBoc
2.186b
400 MHz, CDCl3
f1 (ppm)

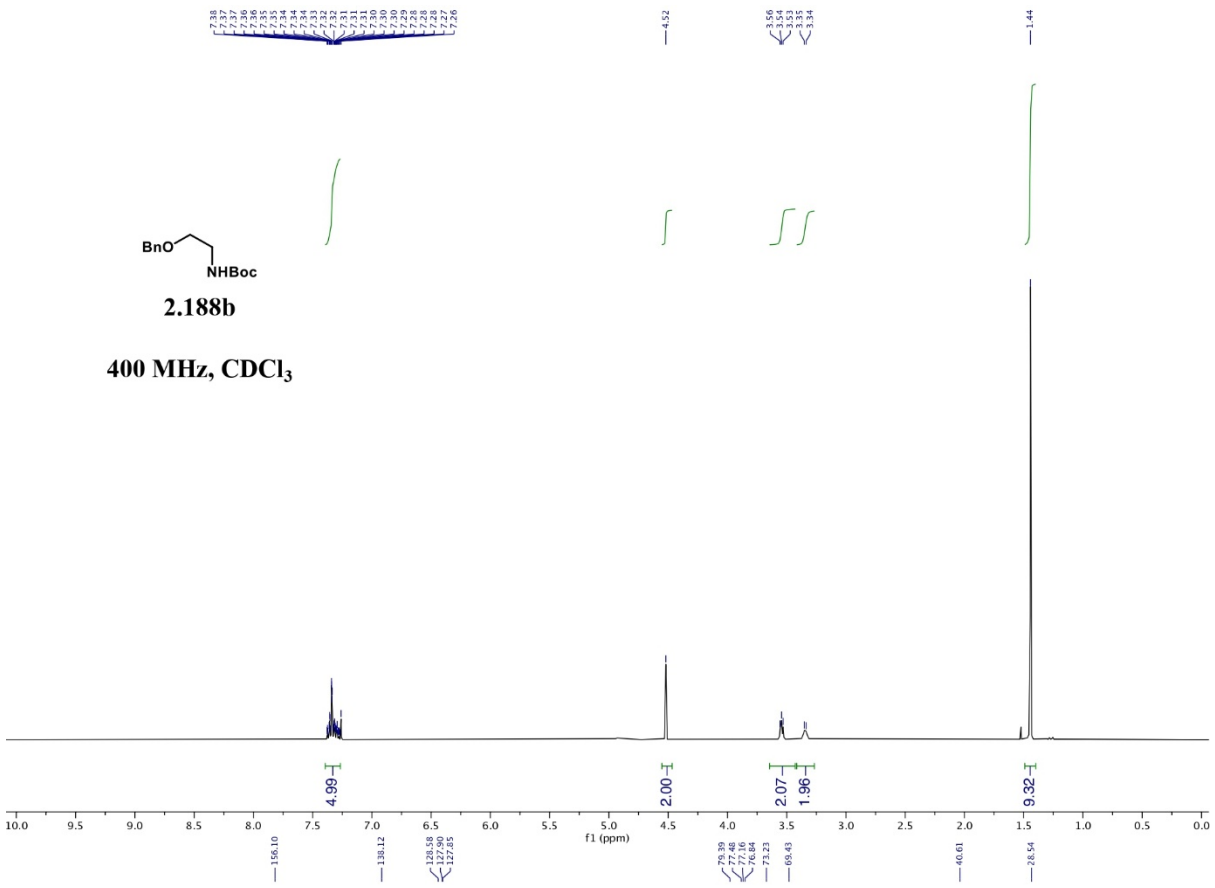

f1 (ppm)



2.187b

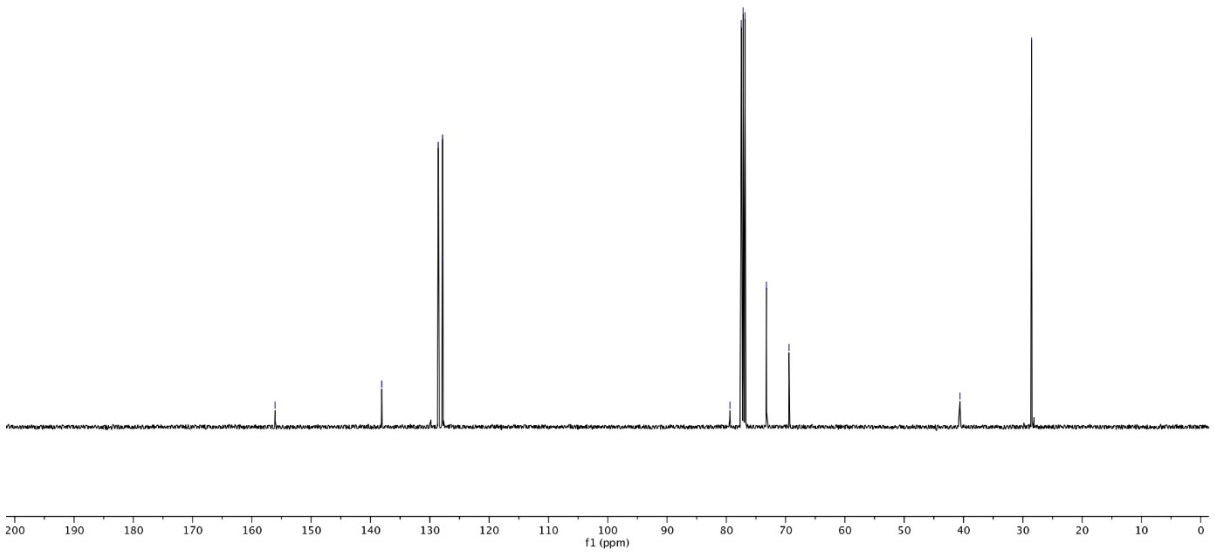
400 MHz, $CDCl_3$

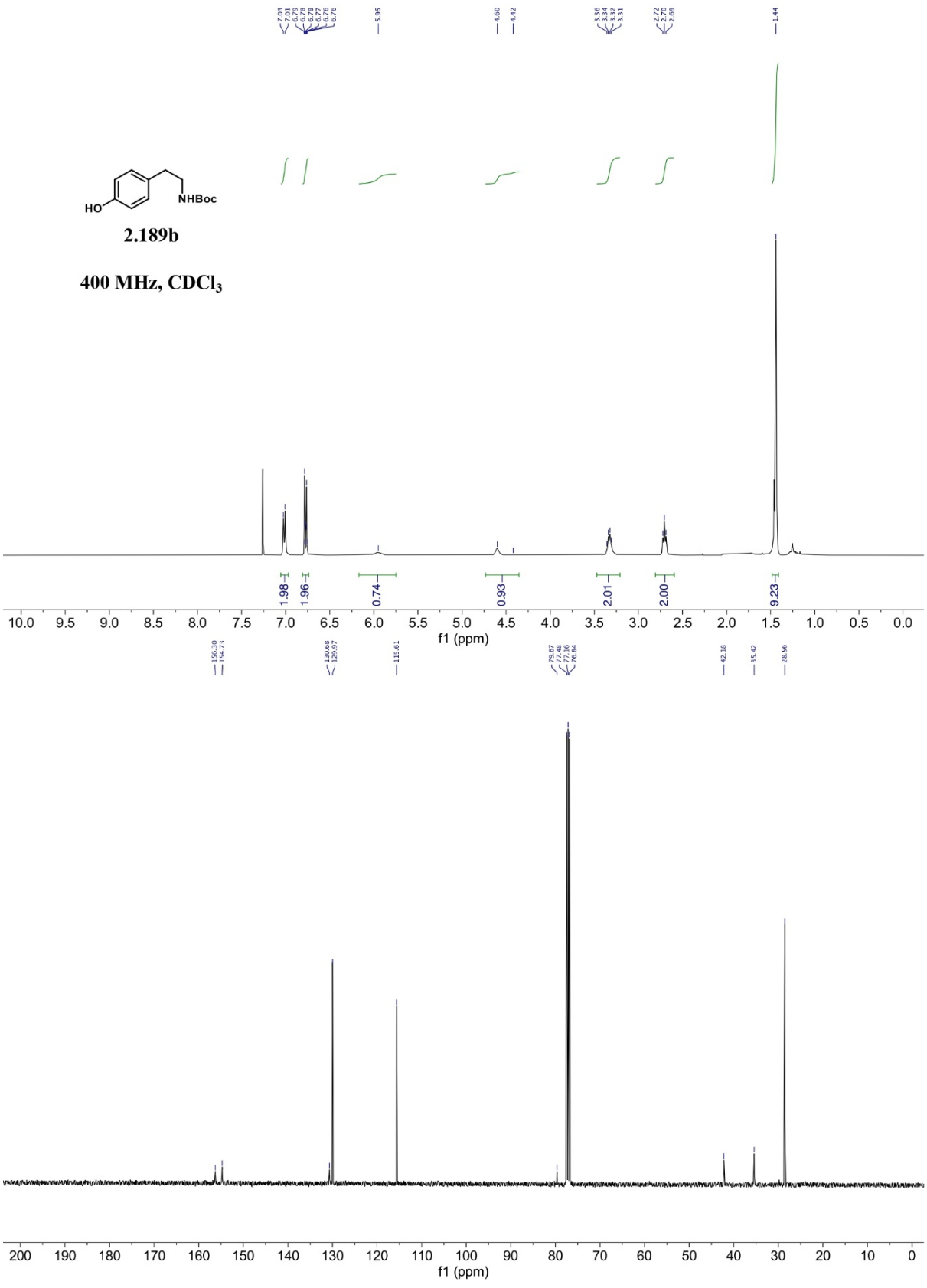


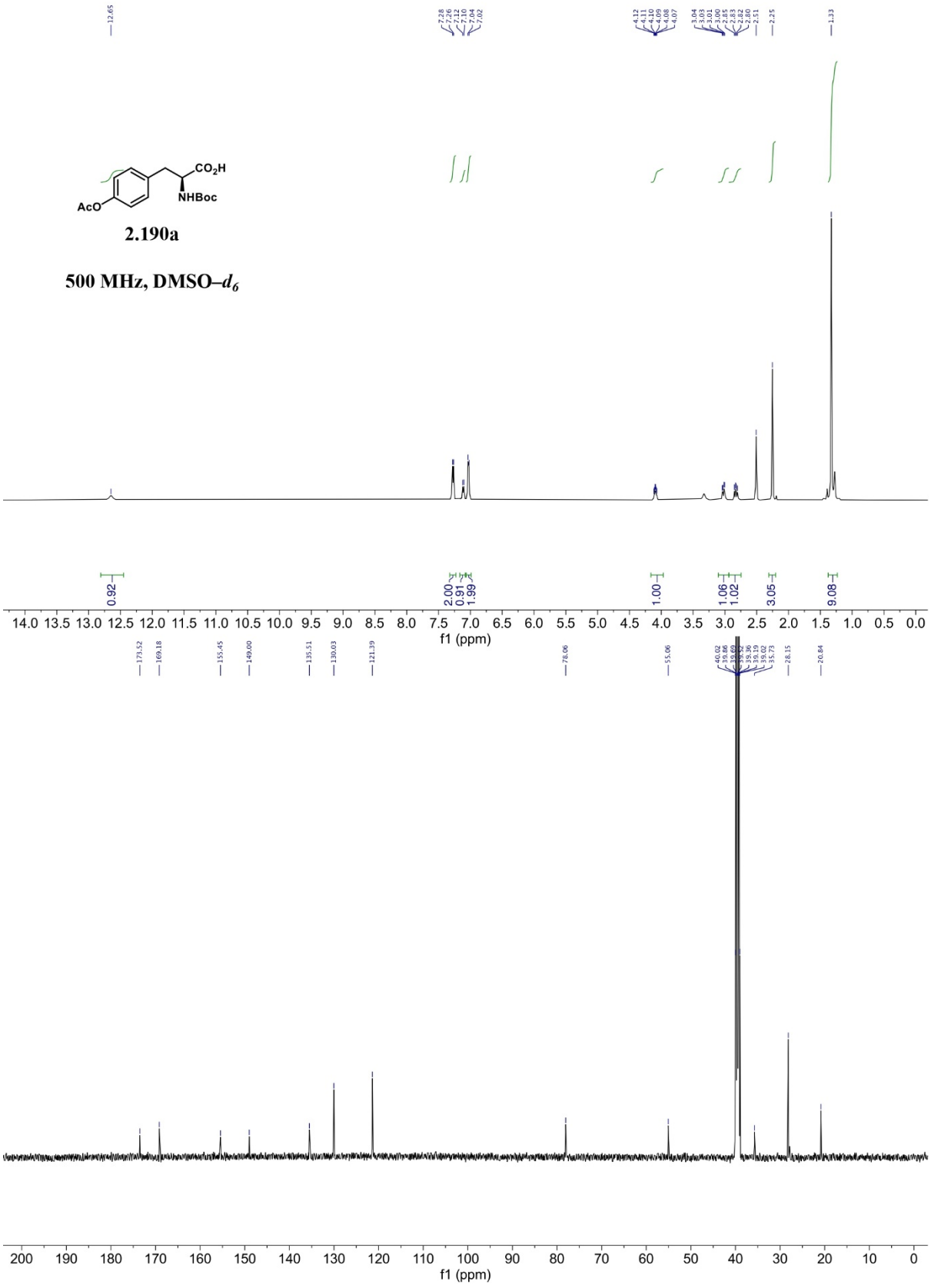


2.188b

400 MHz, $CDCl_3$

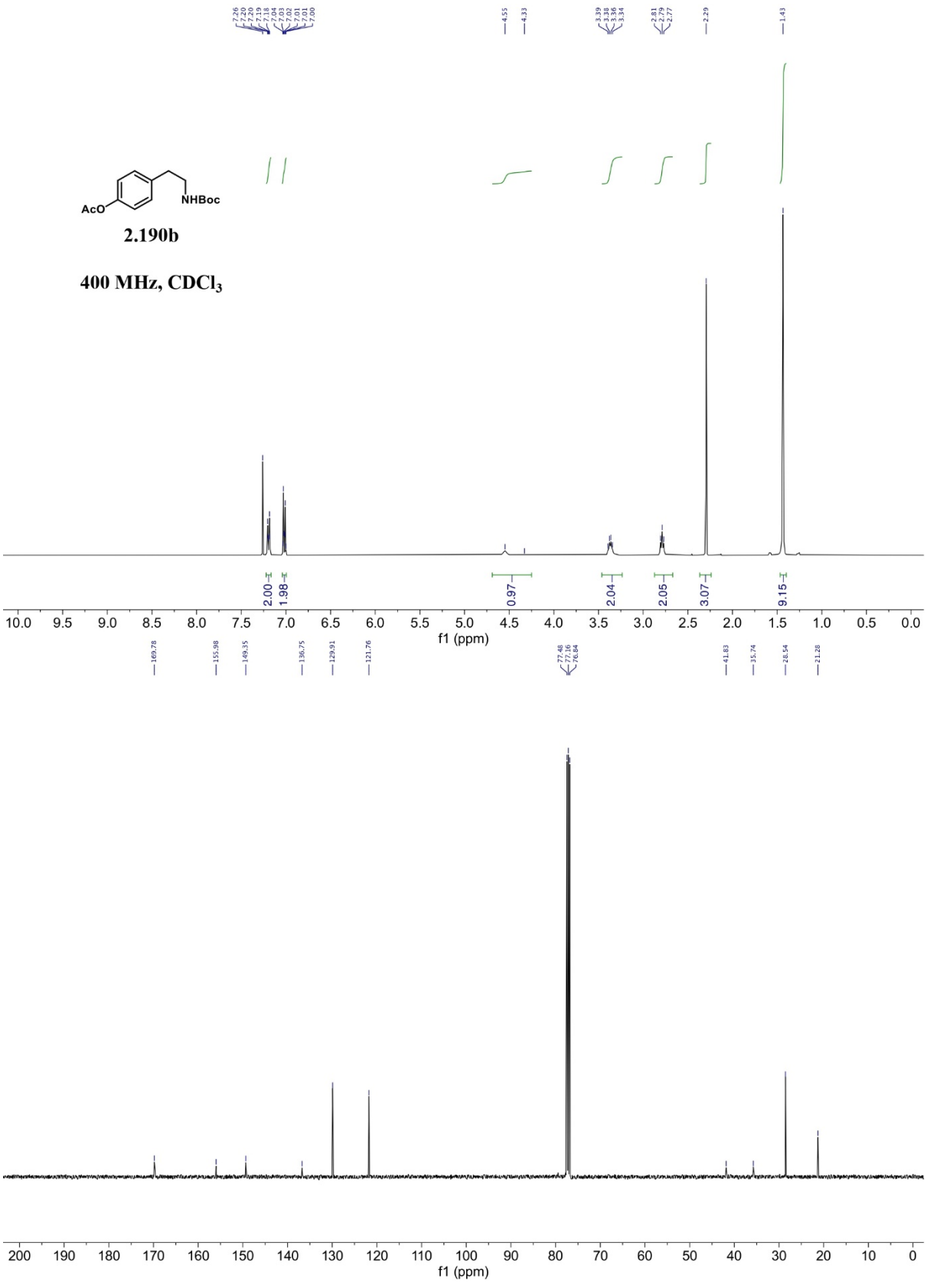


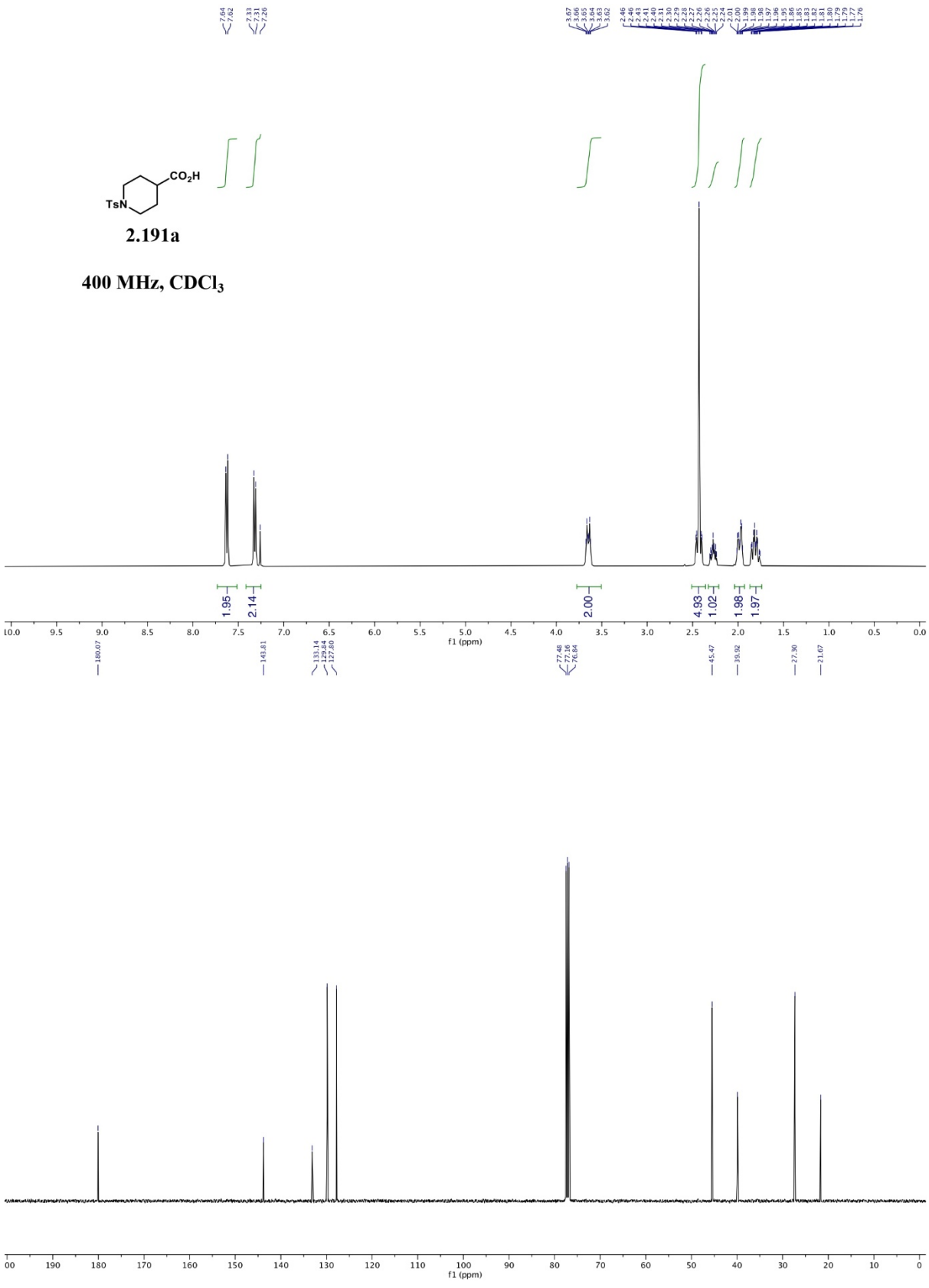

HO
NHBoc
2.189b
400 MHz, CDCl3
f1 (ppm)
f1 (ppm)

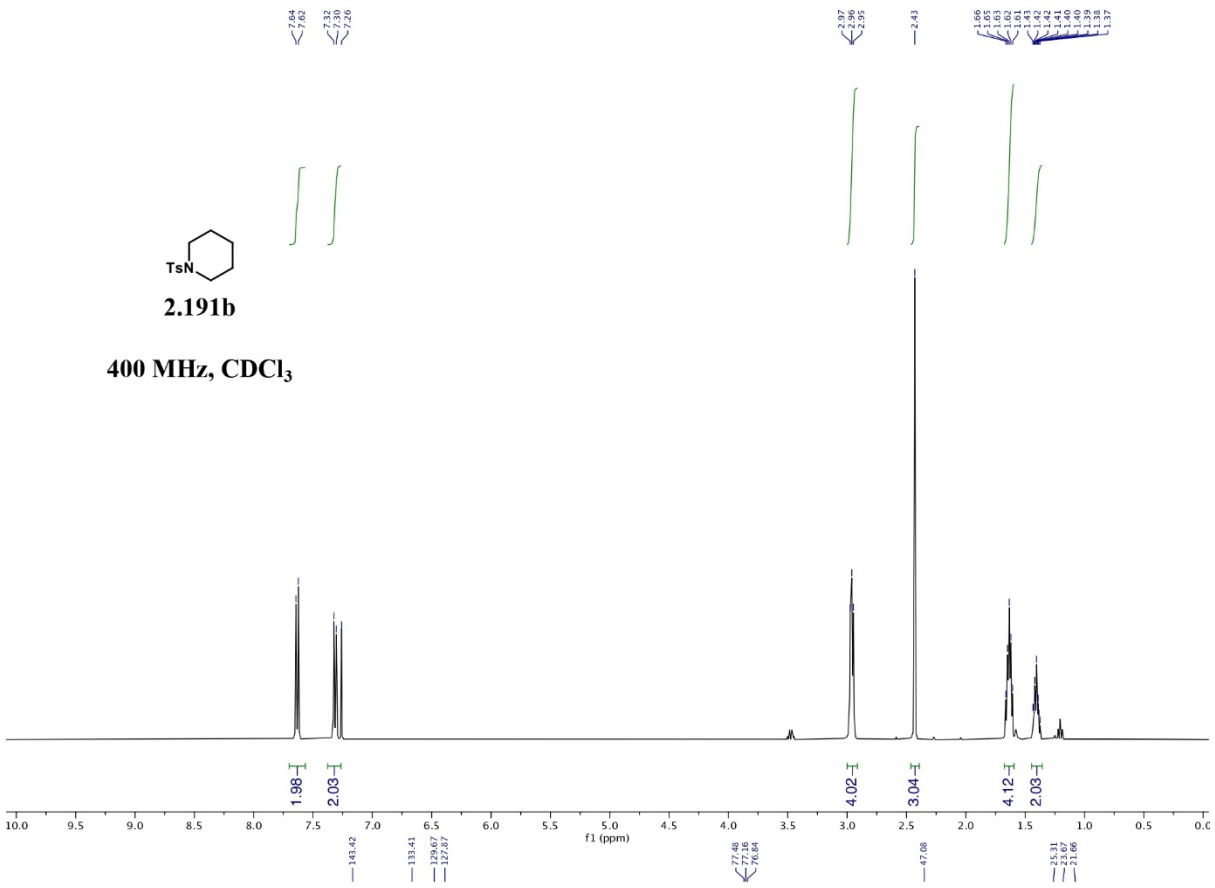


2.190a

500 MHz, DMSO–d_6

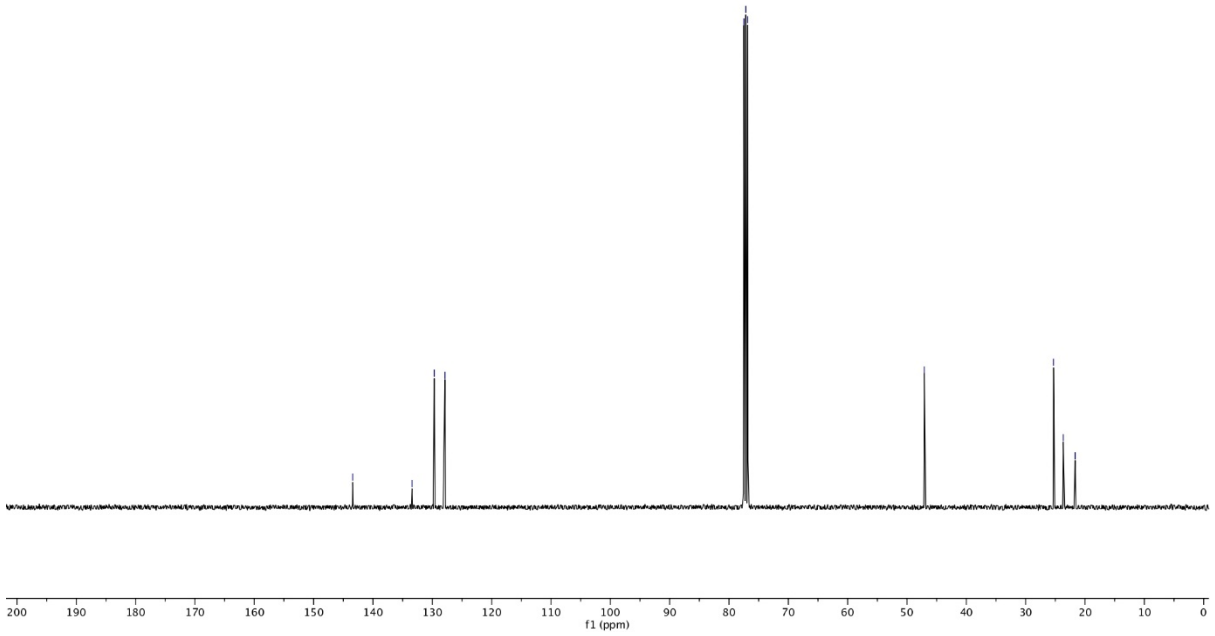

AcO
NHBoc
2.190b
400 MHz, CDCl3
f1 (ppm)
f1 (ppm)

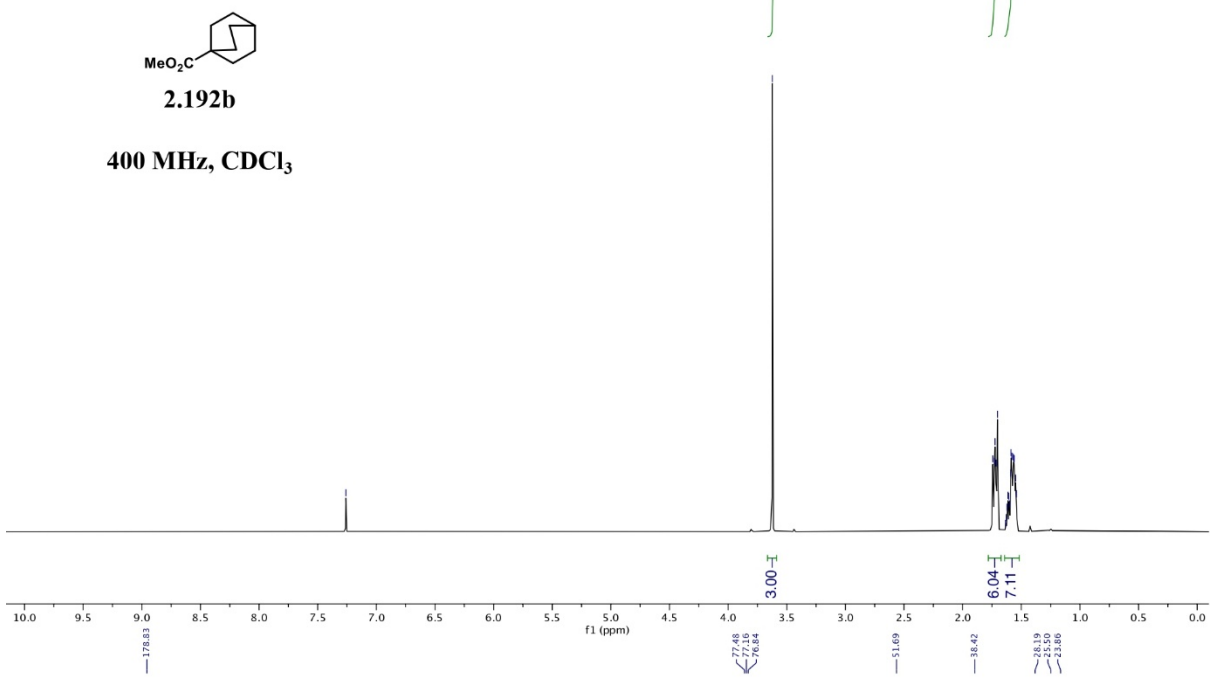

CO2H
TsN
2.191a
400 MHz, CDCl3
f1 (ppm)



2.191b

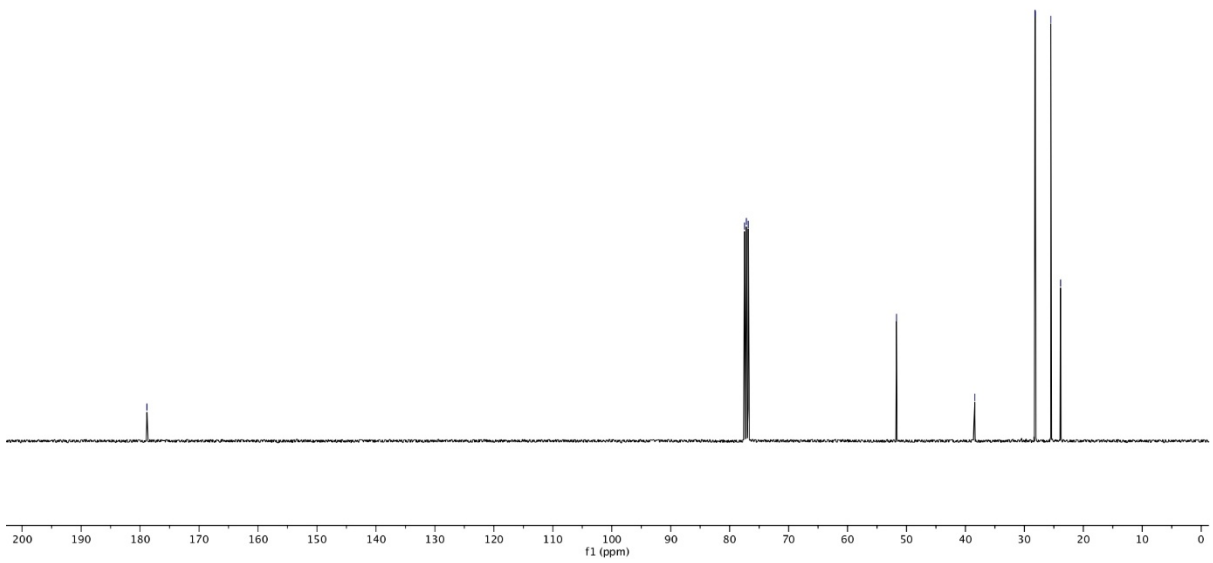
400 MHz, $CDCl_3$

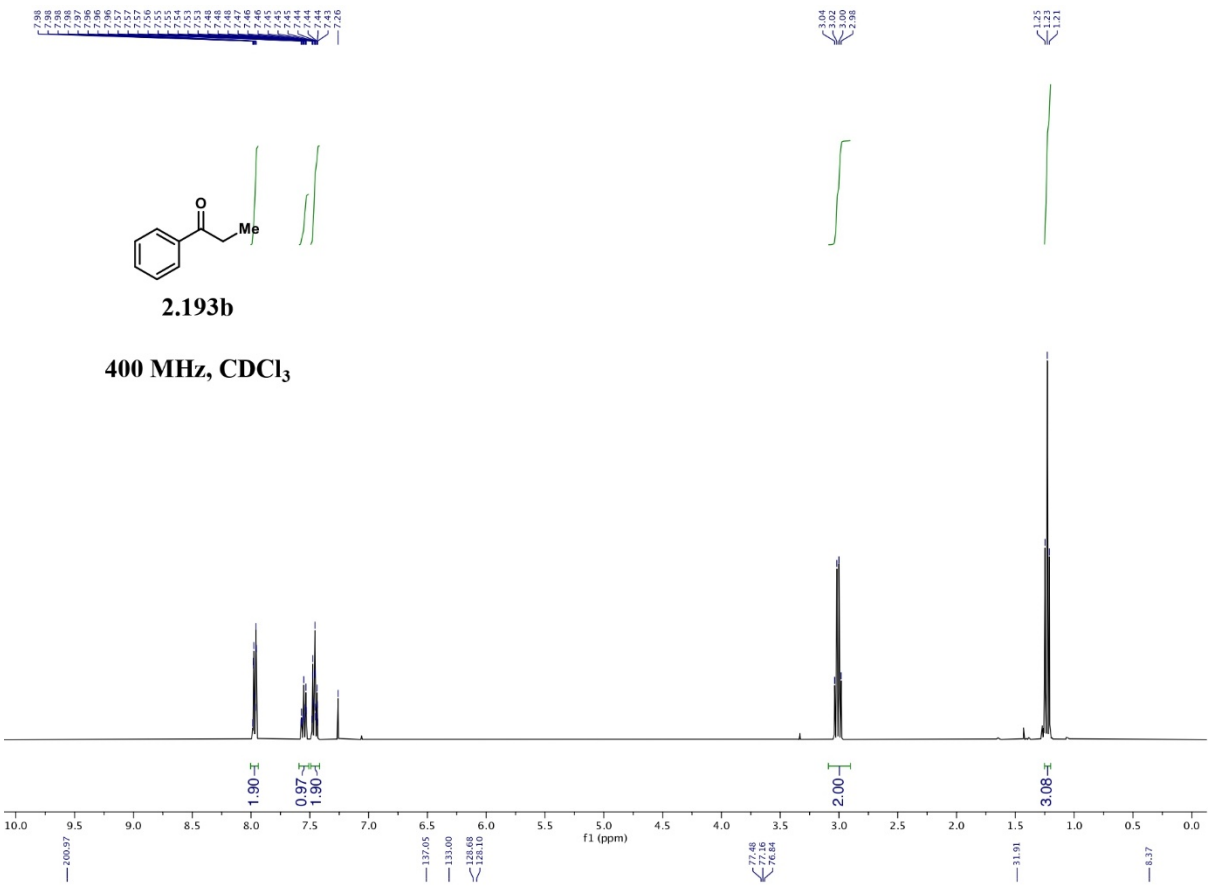


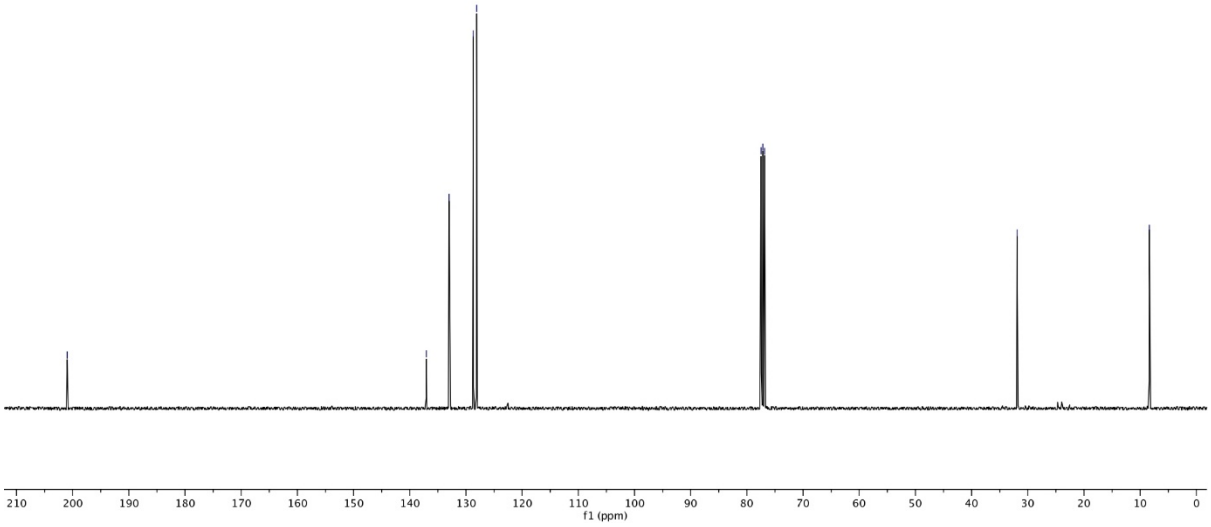


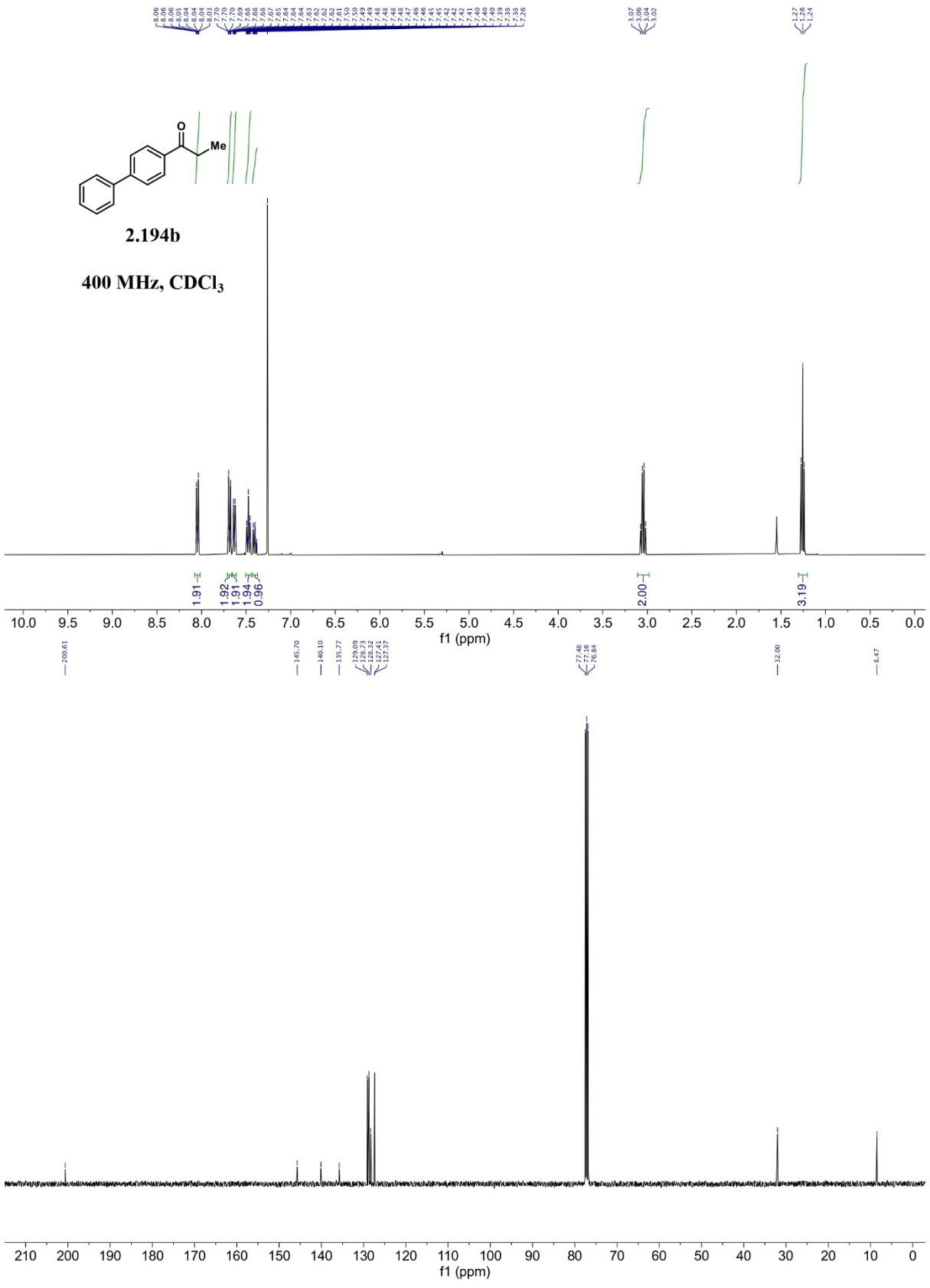
2.192b

400 MHz, $CDCl_3$



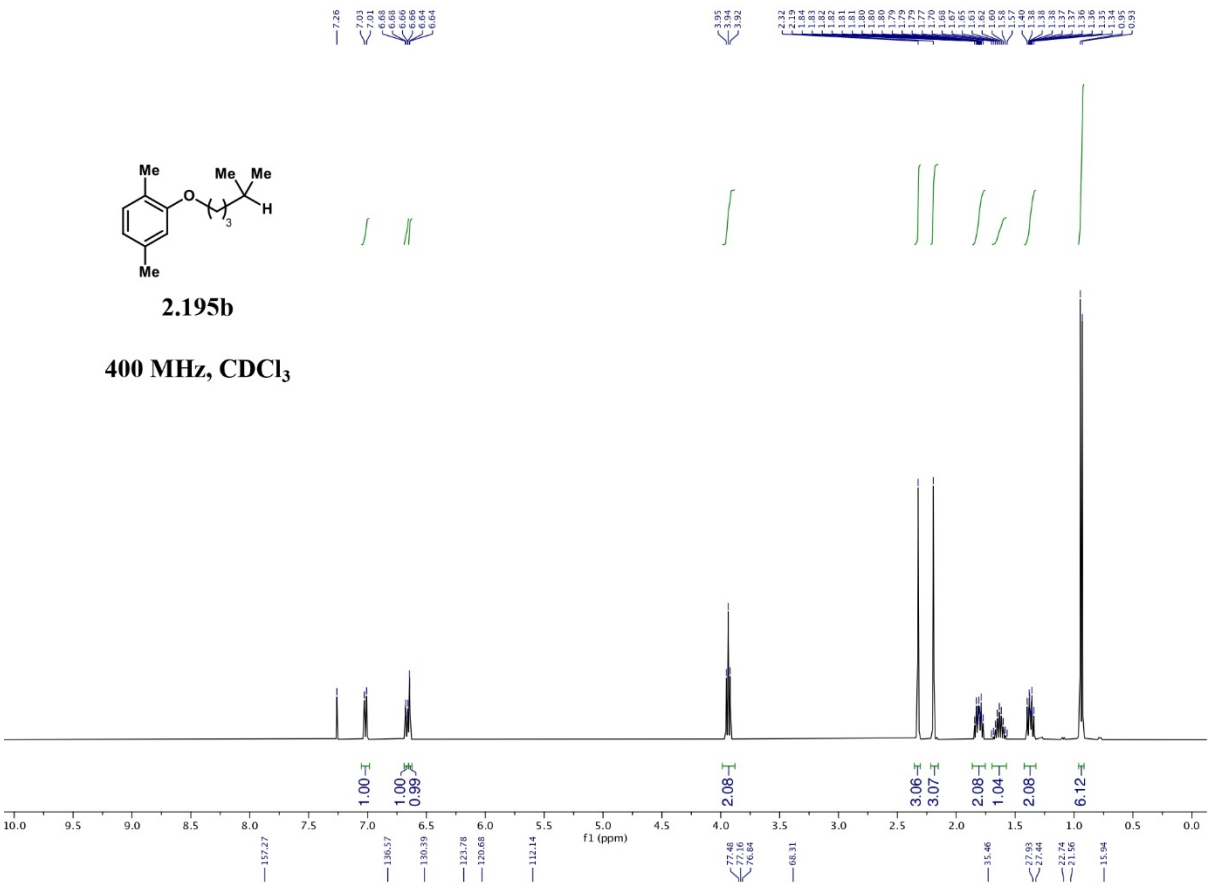

O
Me
2.193b
400 MHz, CDCl3
1.90
0.97
1.90
2.00
3.08
f1 (ppm)

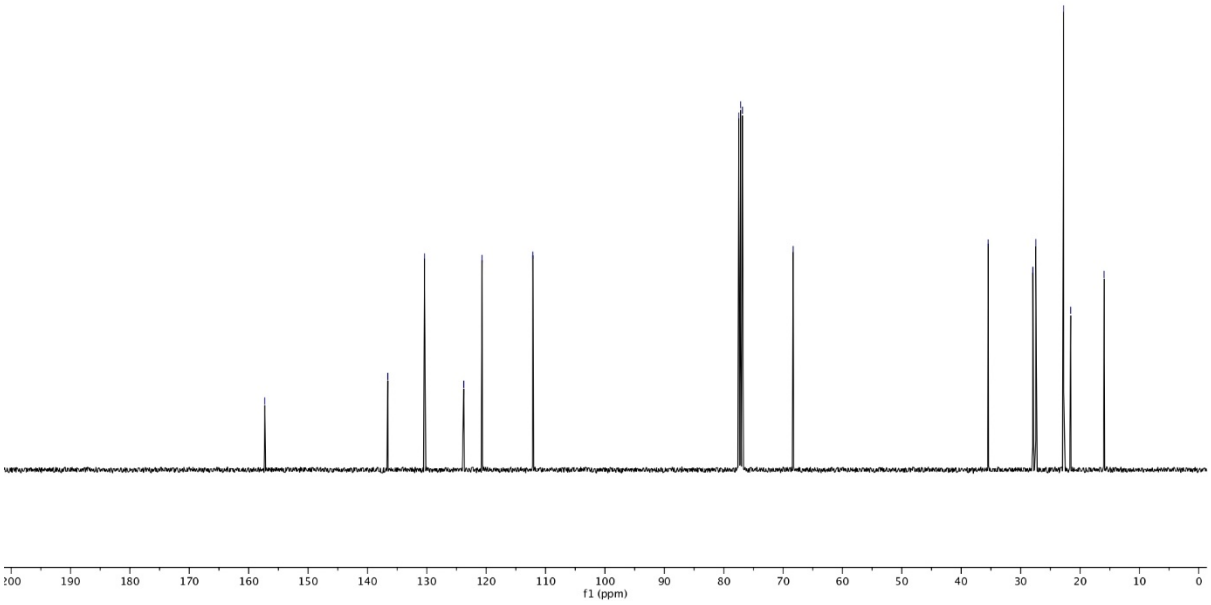

f1 (ppm)


O
Me
2.194b
400 MHz, CDCl3
f1 (ppm)
f1 (ppm)

2.195b

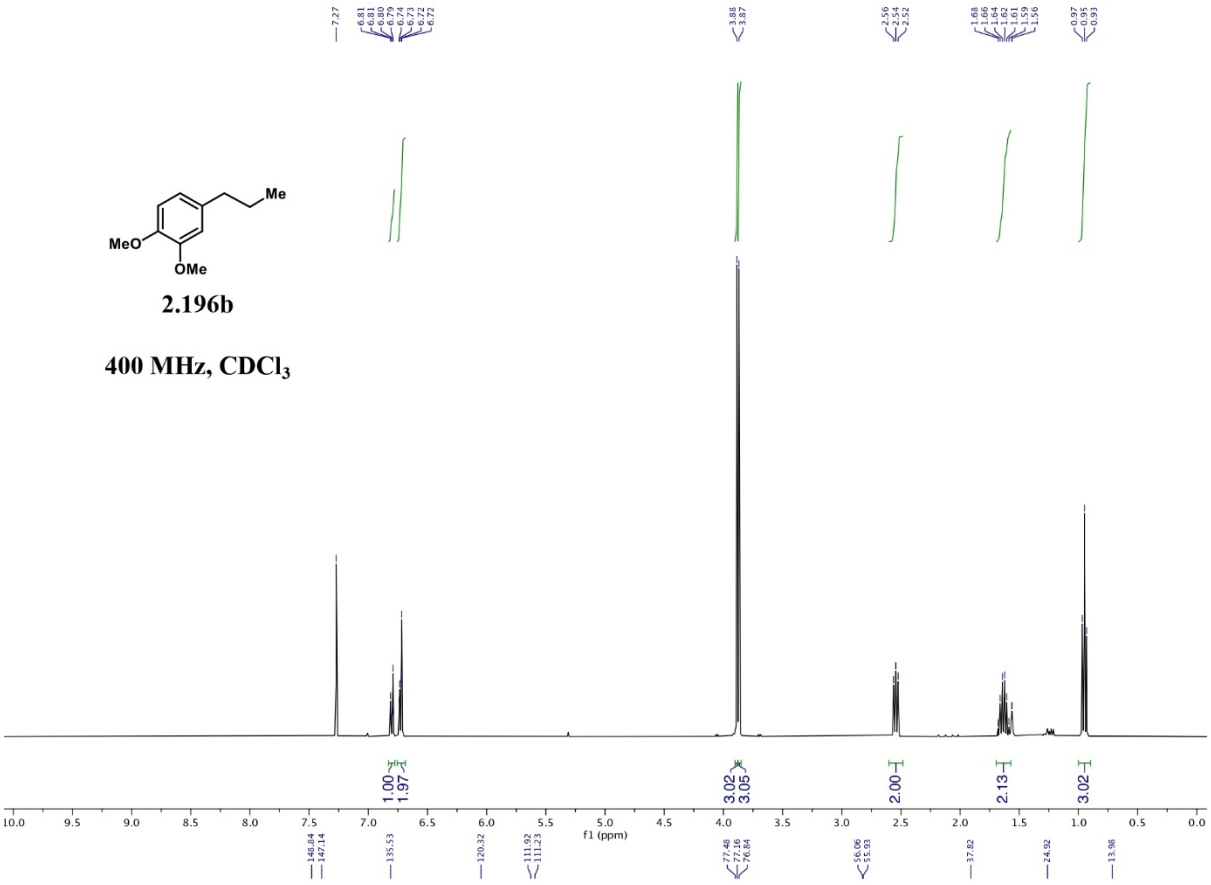
400 MHz, $CDCl_3$

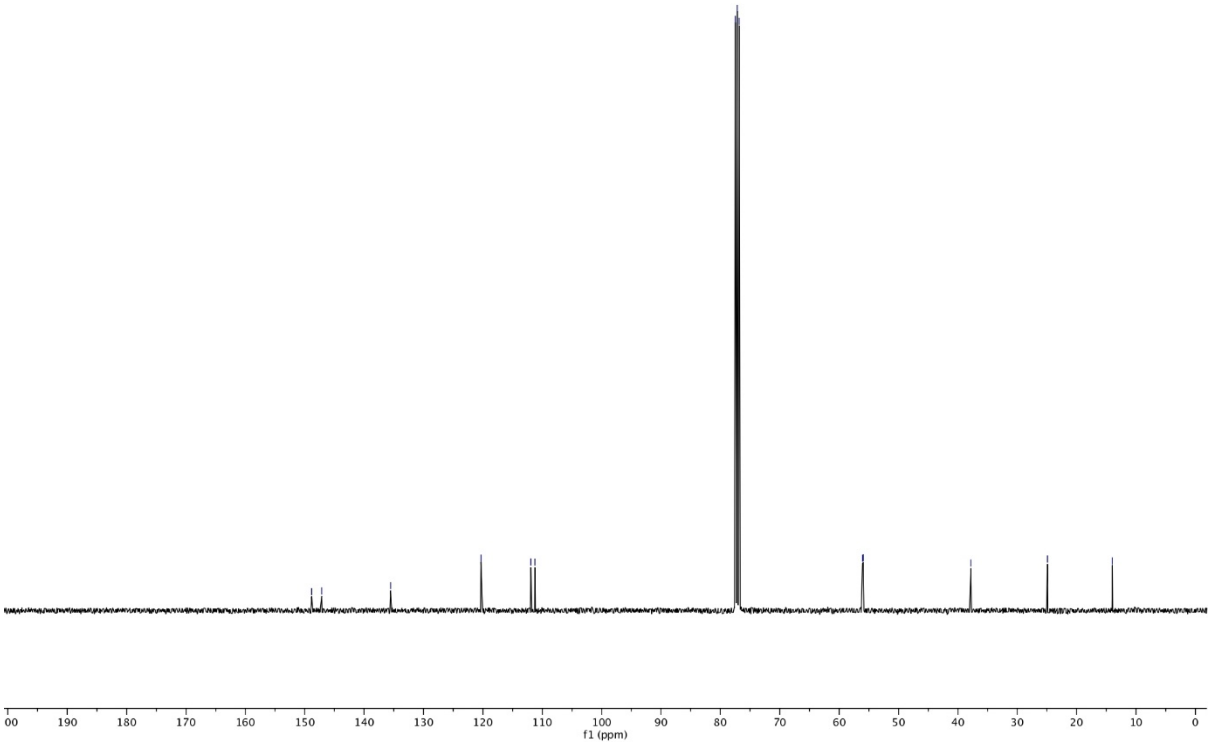


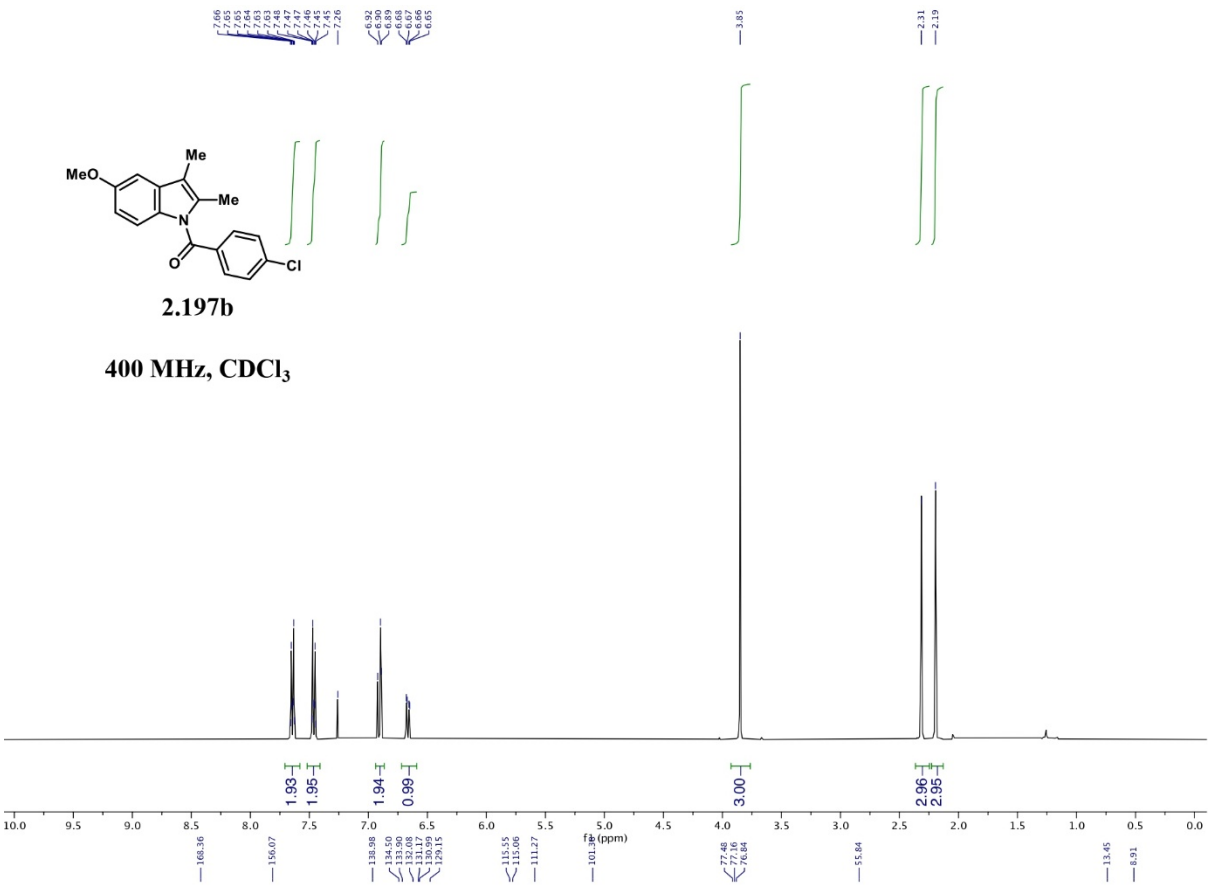


2.196b

400 MHz, $CDCl_3$

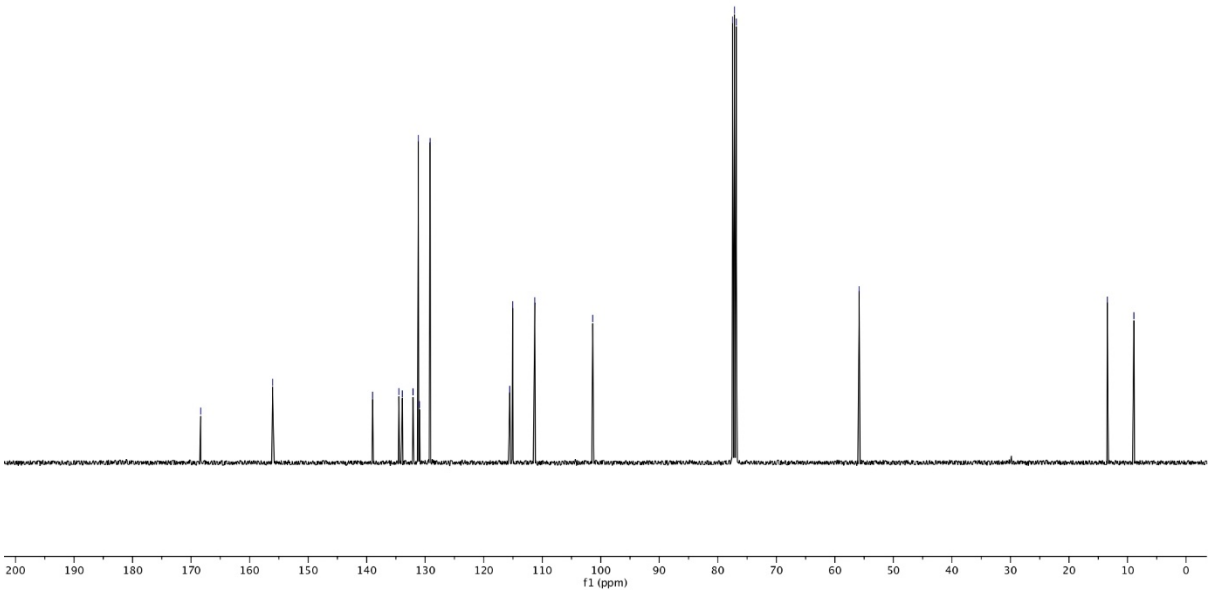


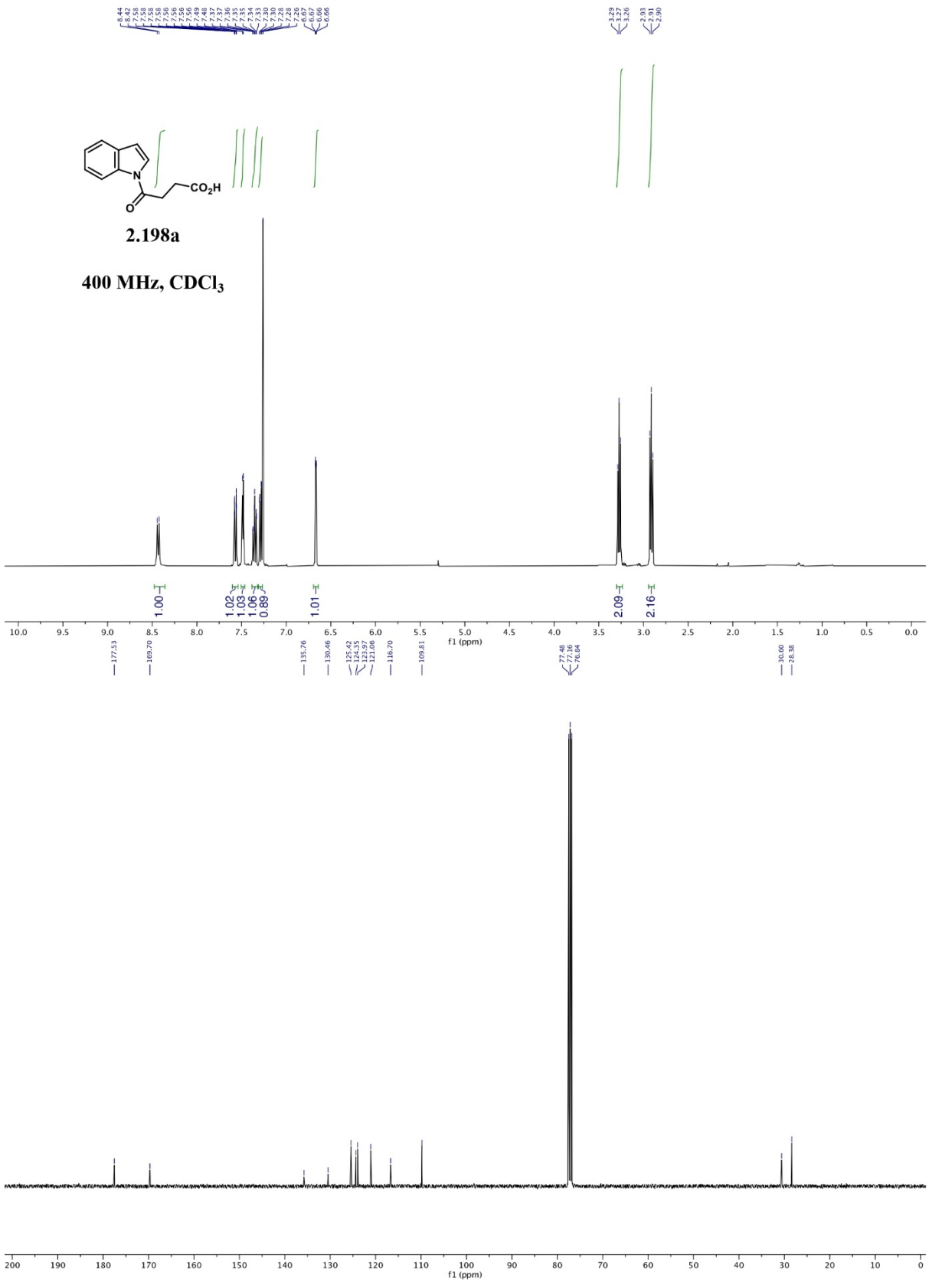


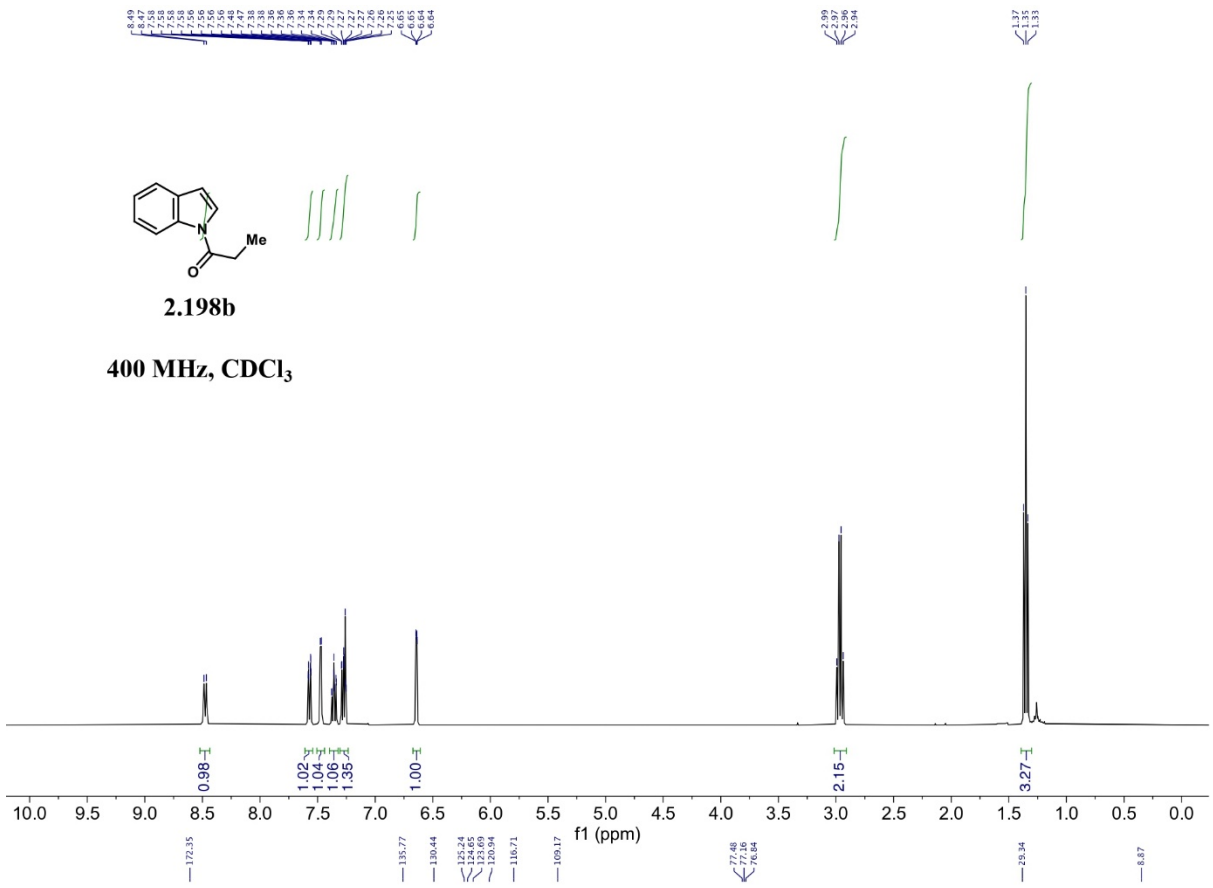


2.197b

400 MHz, $CDCl_3$

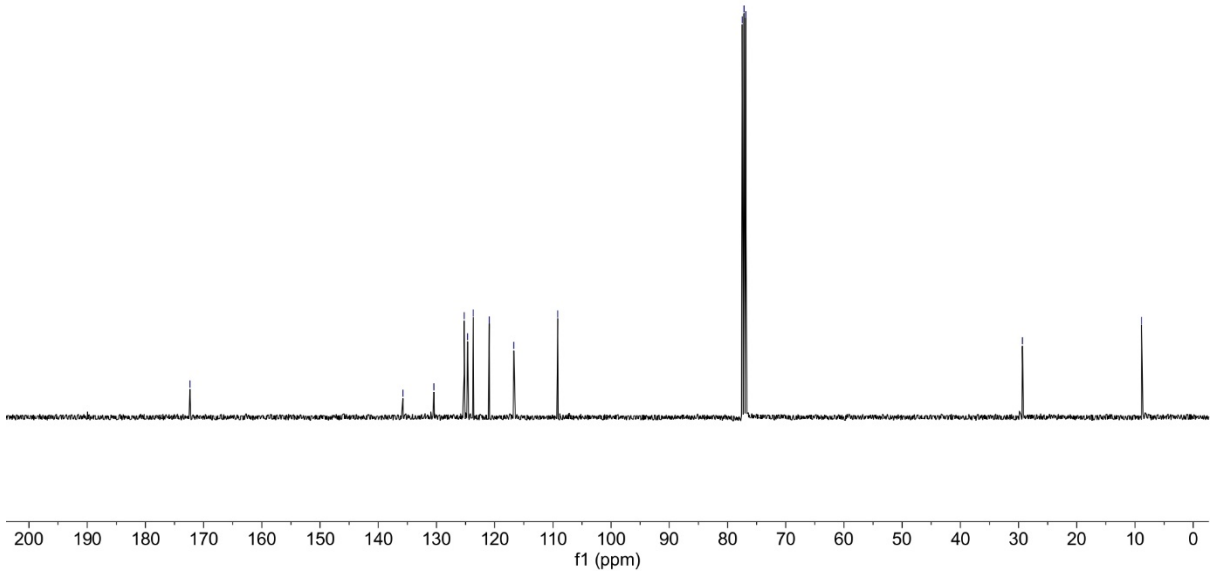


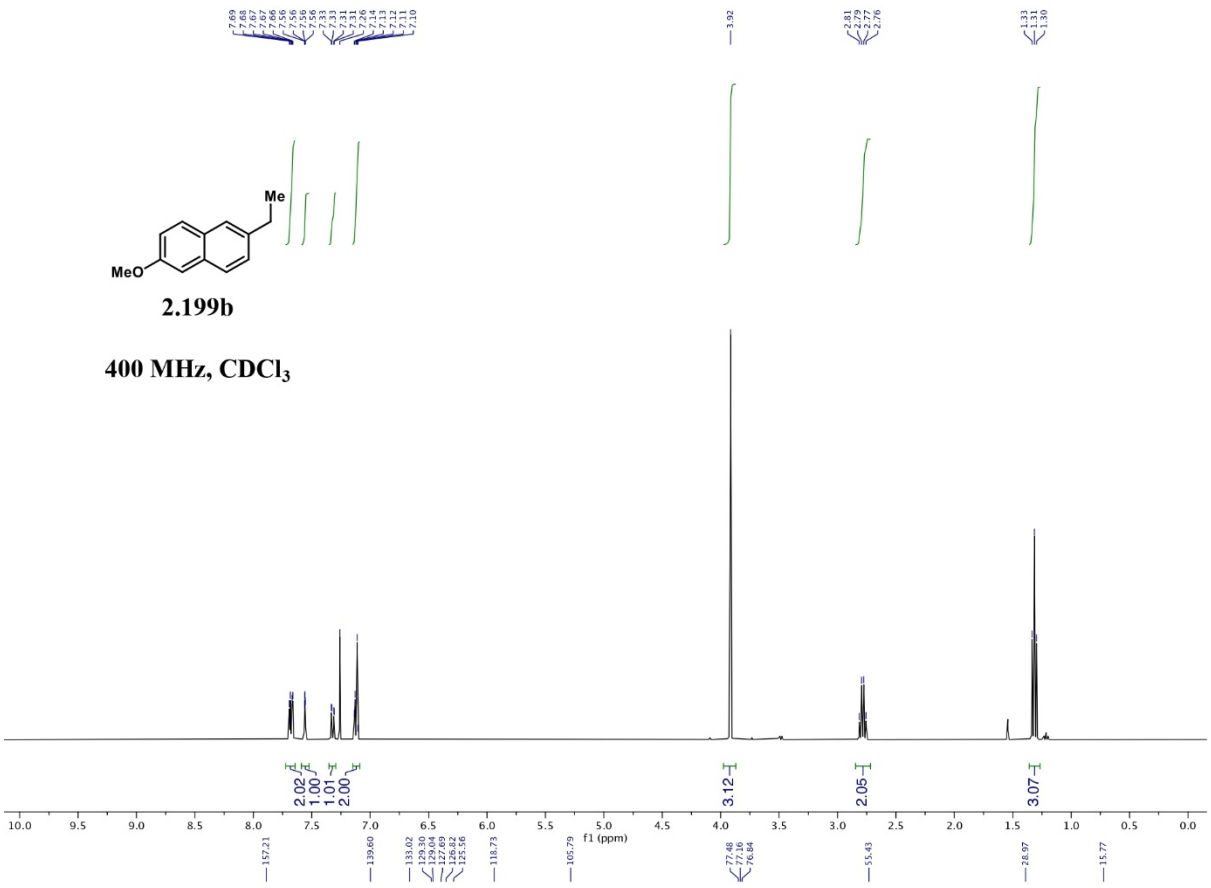

CO2H
O
N
2.198a
400 MHz, CDCl3
f1 (ppm)



2.198b

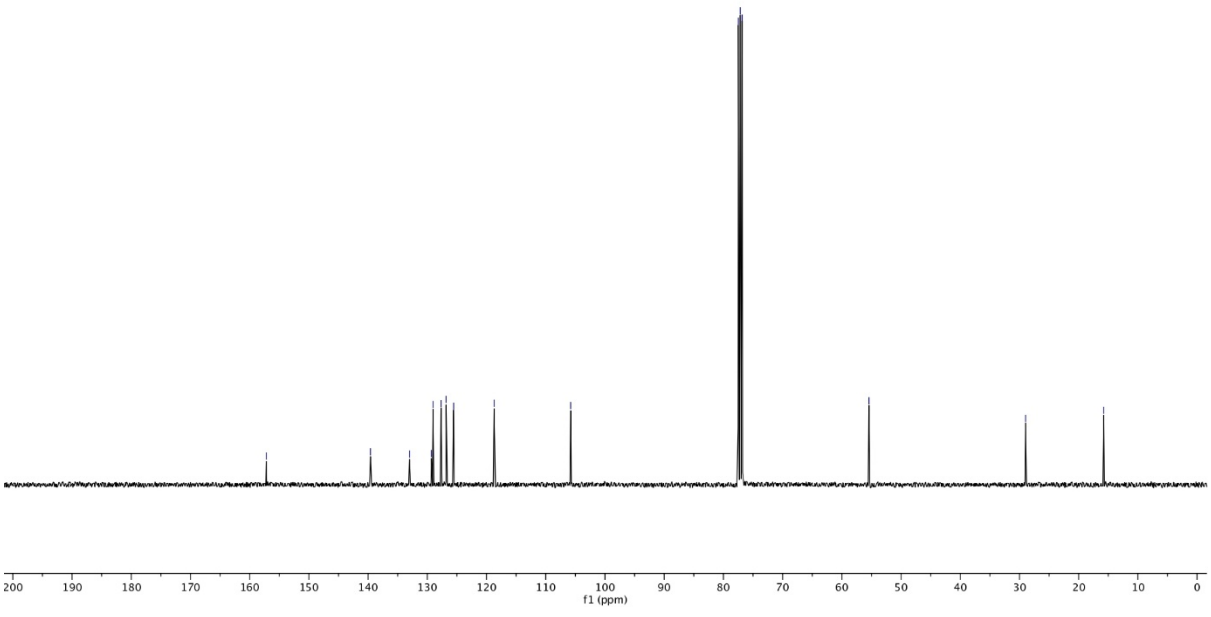
400 MHz, $CDCl_3$





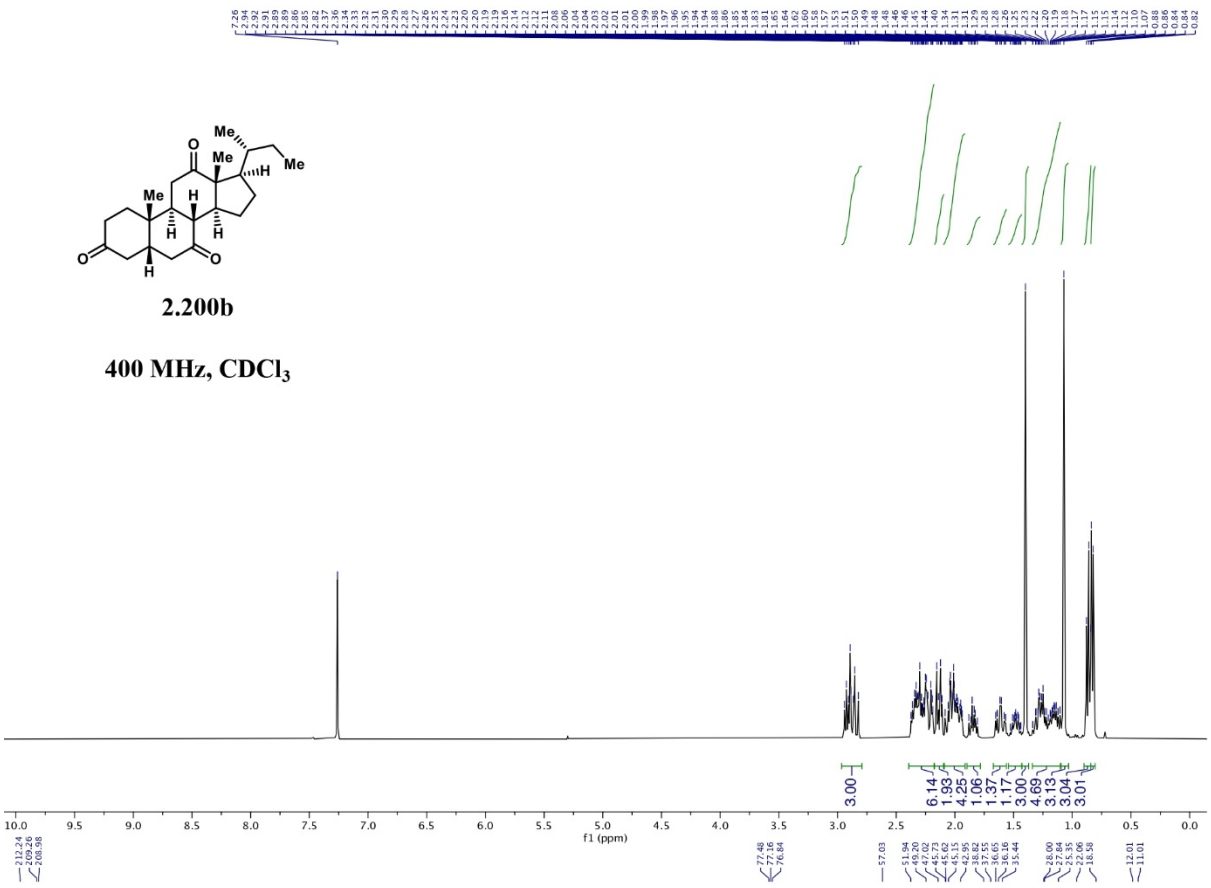
2.199b

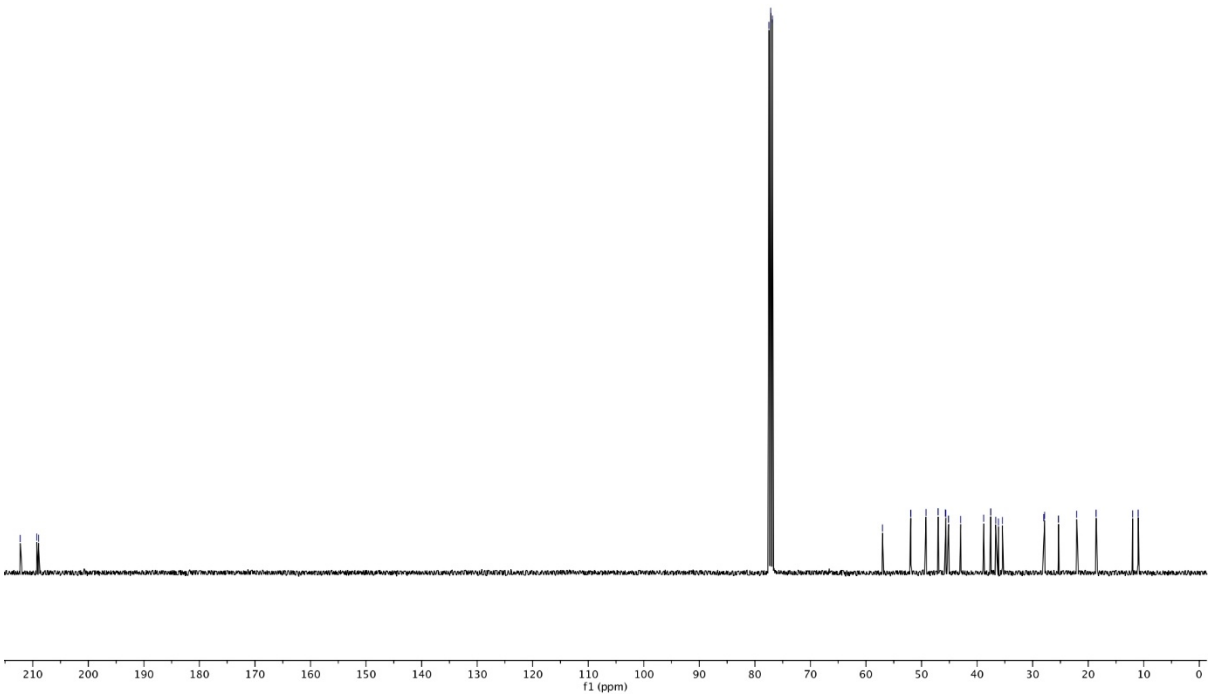
400 MHz, $CDCl_3$

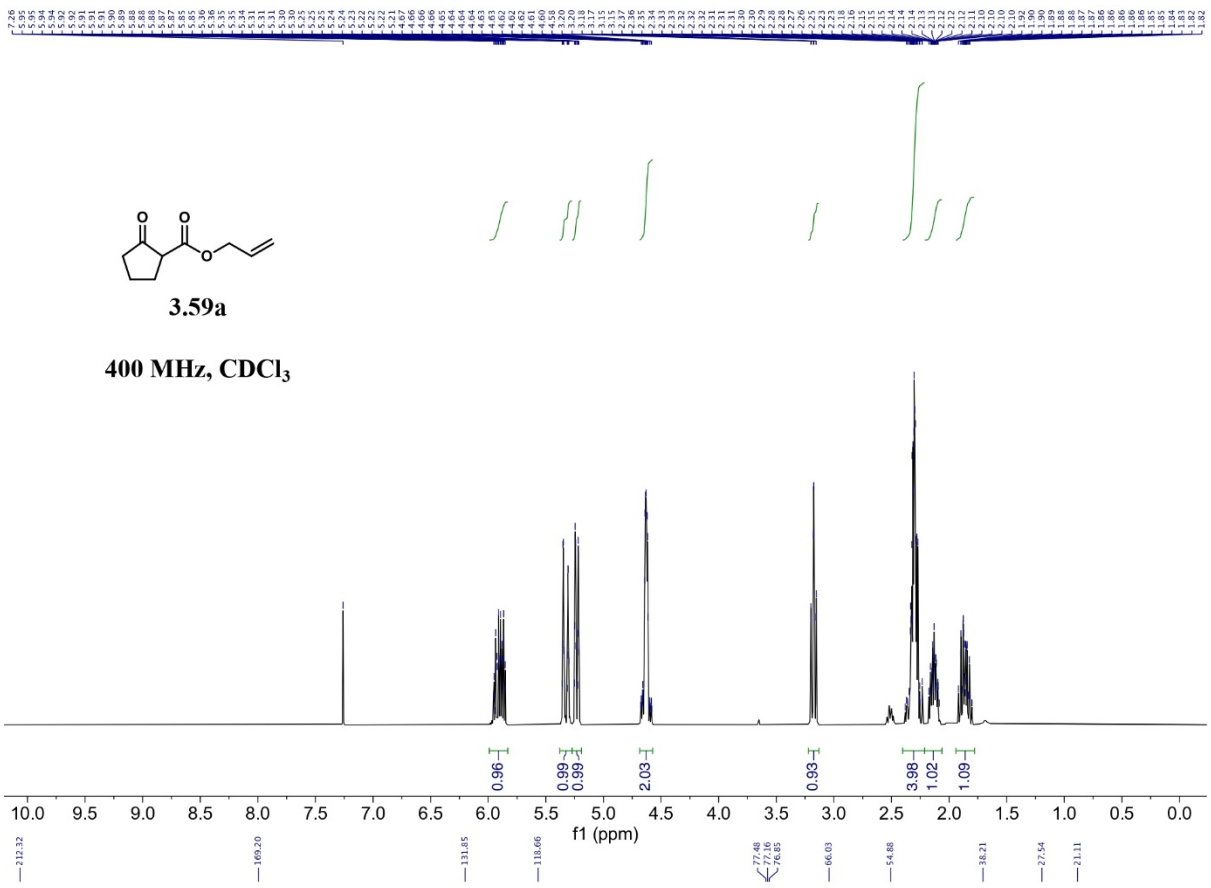


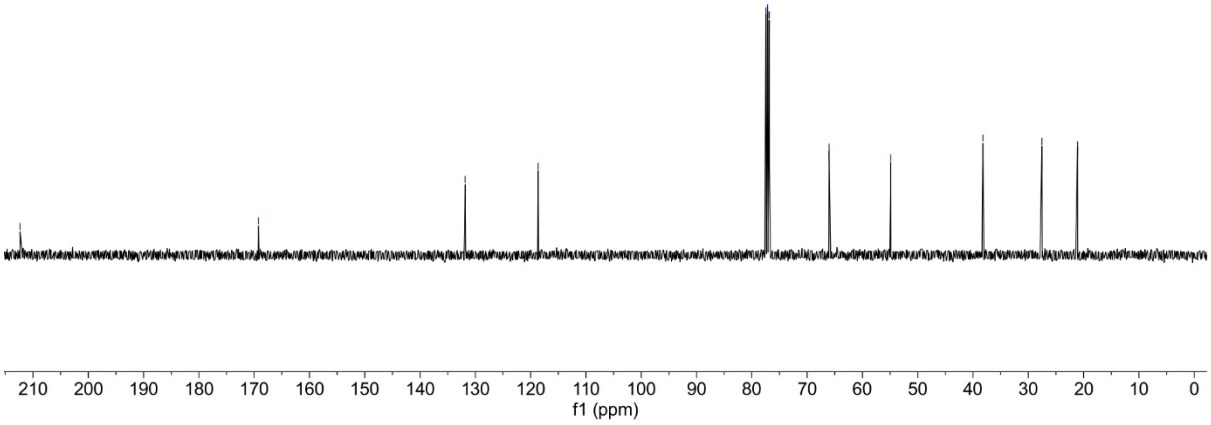
2.200b

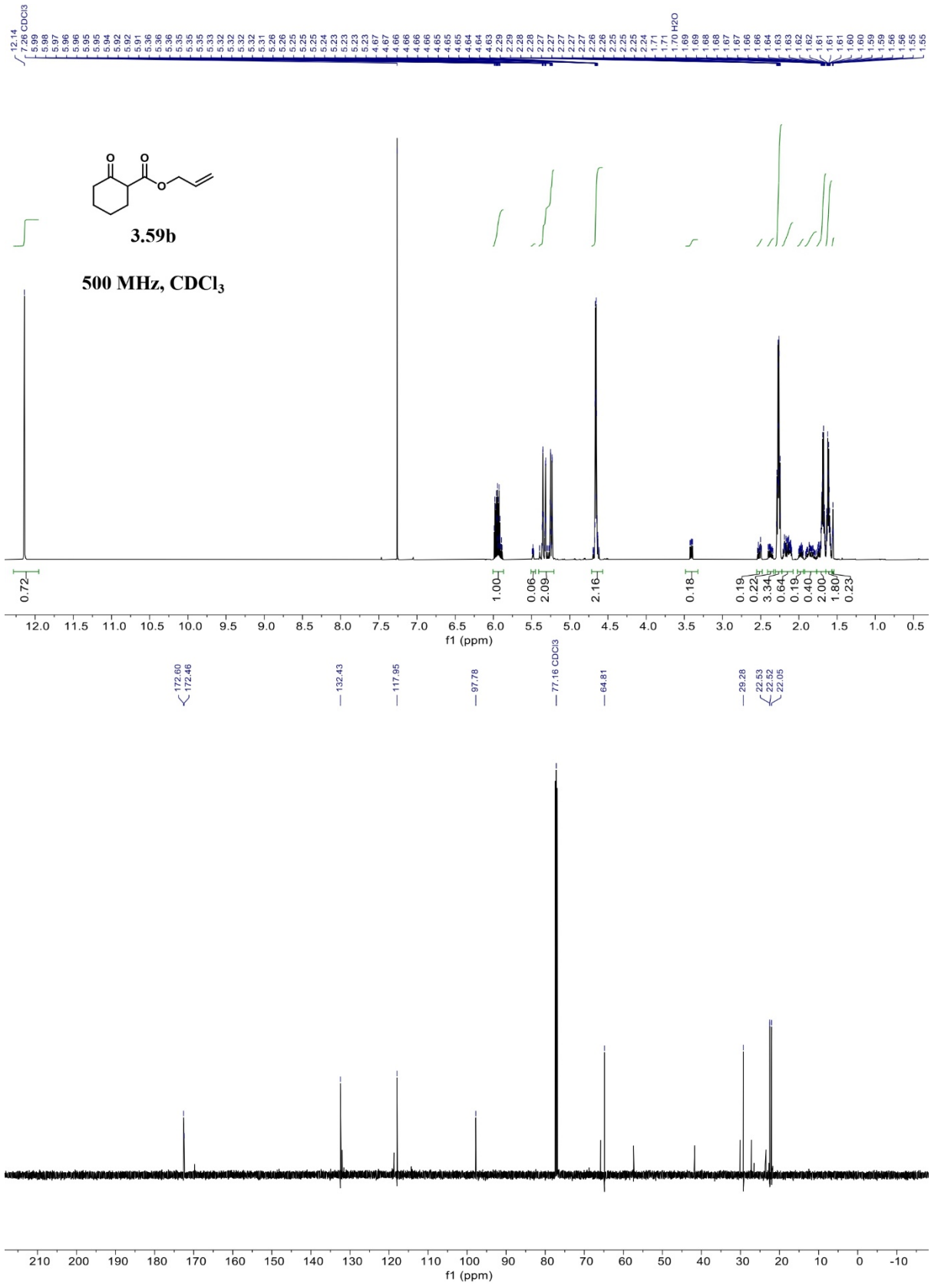
400 MHz, $CDCl_3$

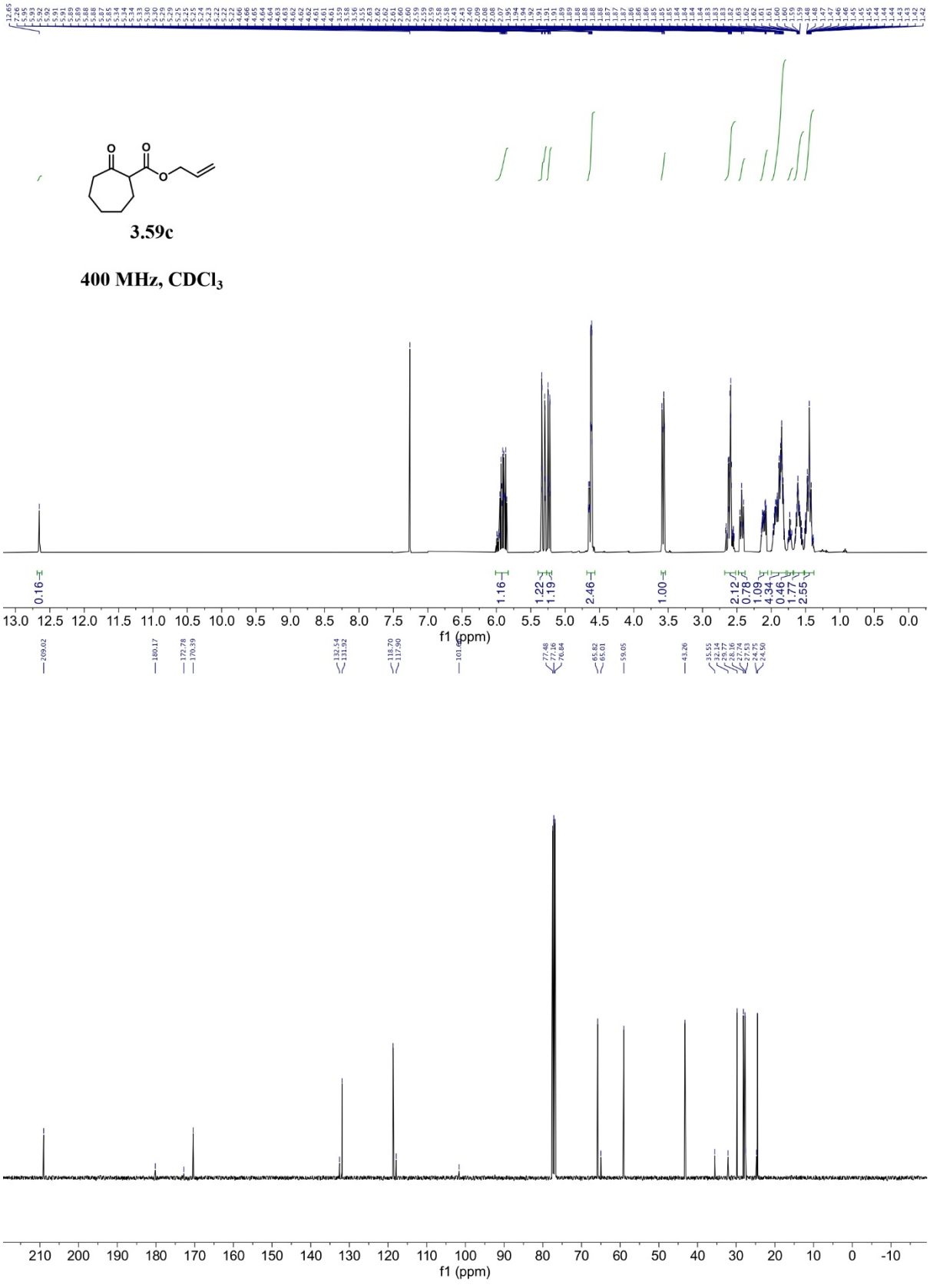


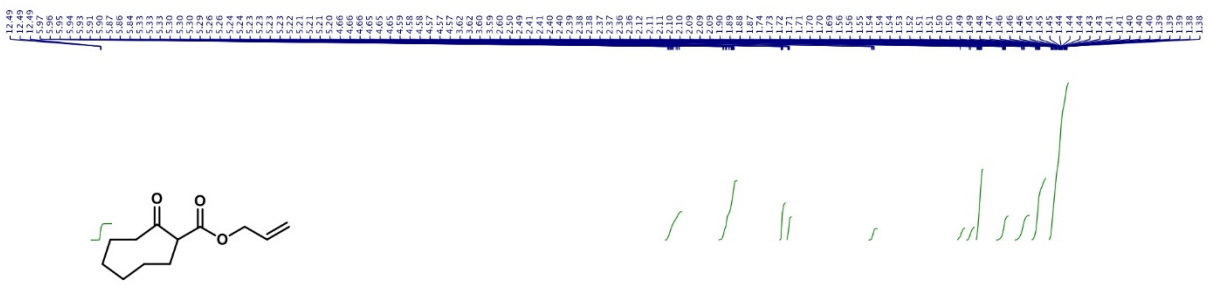



3.59a
400 MHz, CDCl3
0.96
0.99
0.99
2.03
0.93
3.98
1.02
1.09
f1 (ppm)
212.32
169.20
131.85
118.66
77.48
77.16
76.85
66.03
54.88
38.21
27.54
21.11


f1 (ppm)

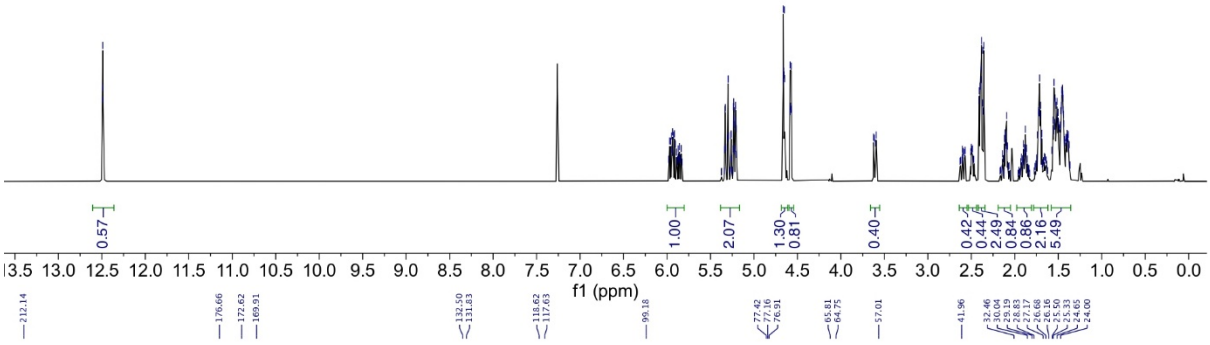

3.59b
500 MHz, CDCl3
f1 (ppm)
f1 (ppm)

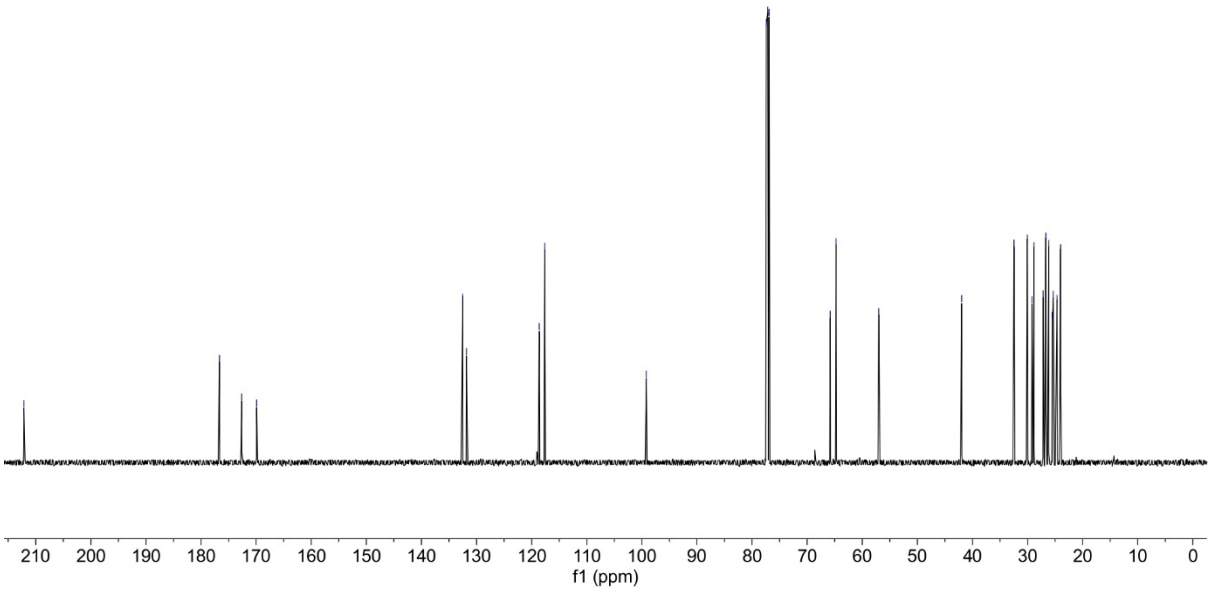

3.59c
400 MHz, CDCl3
f1 (ppm)
f1 (ppm)

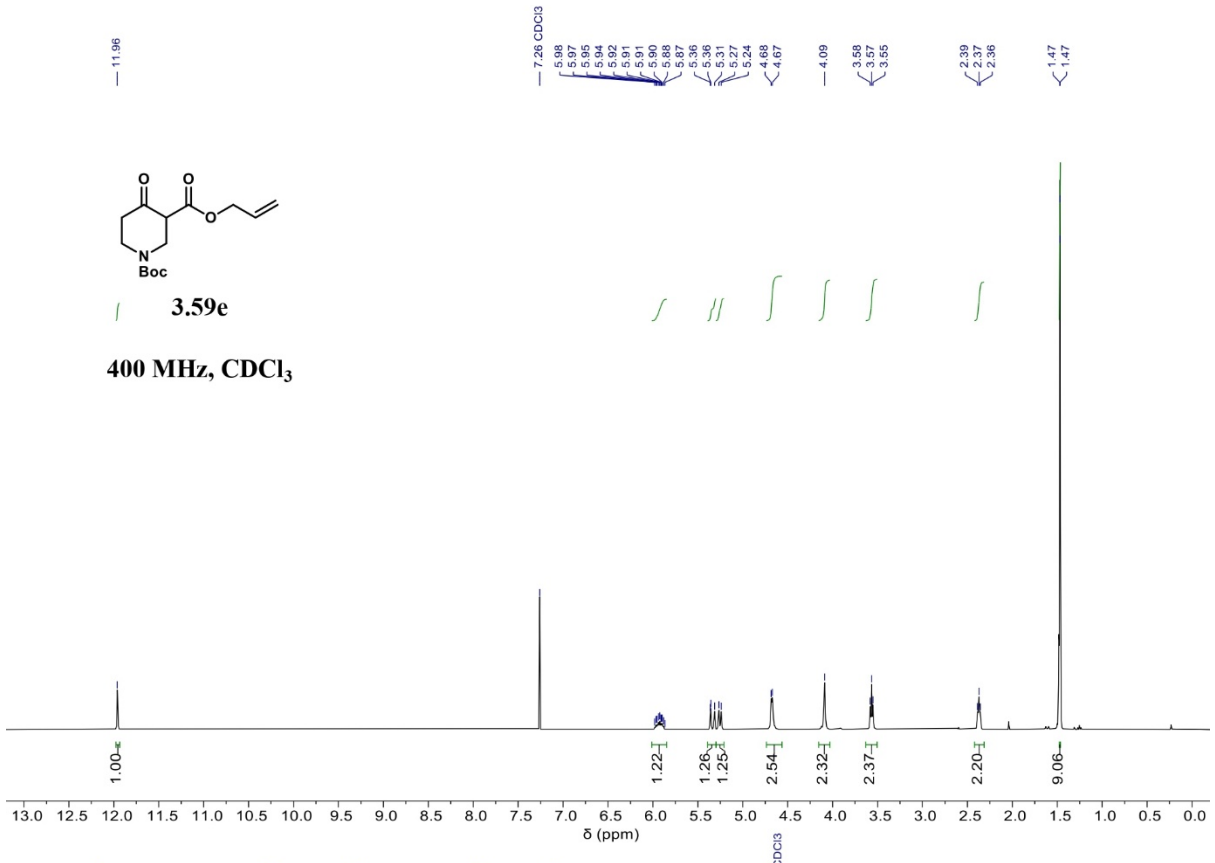


3.59d

500 MHz, $CDCl_3$

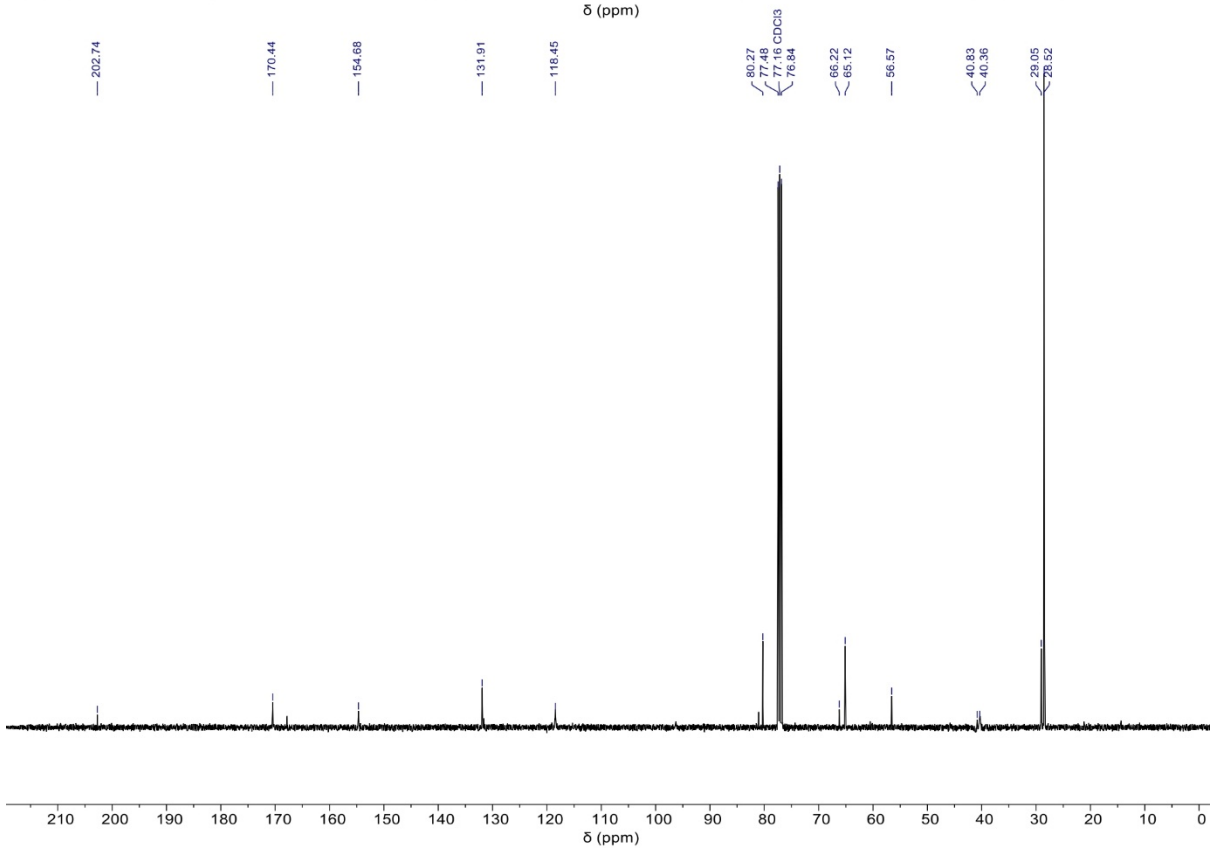


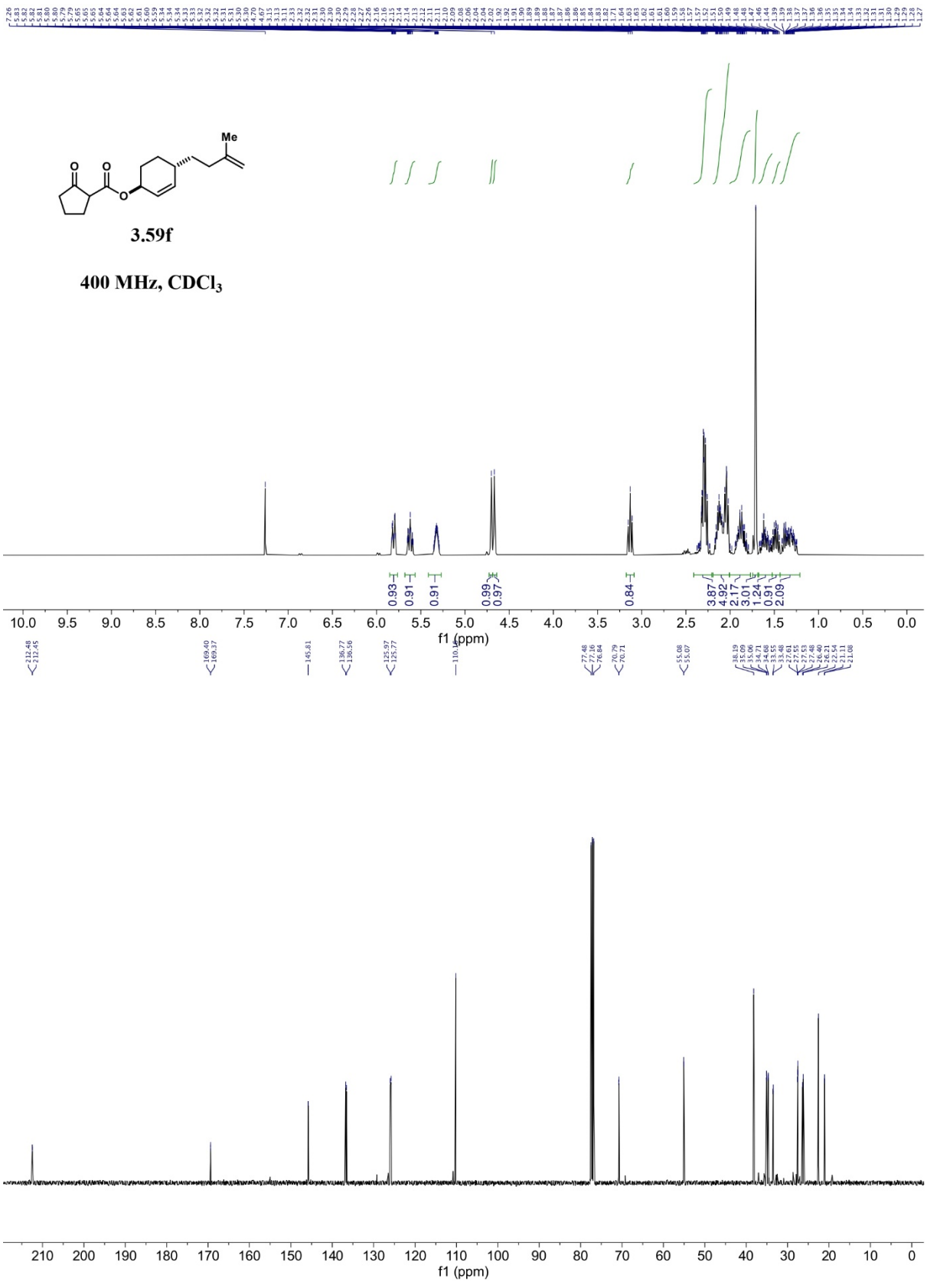


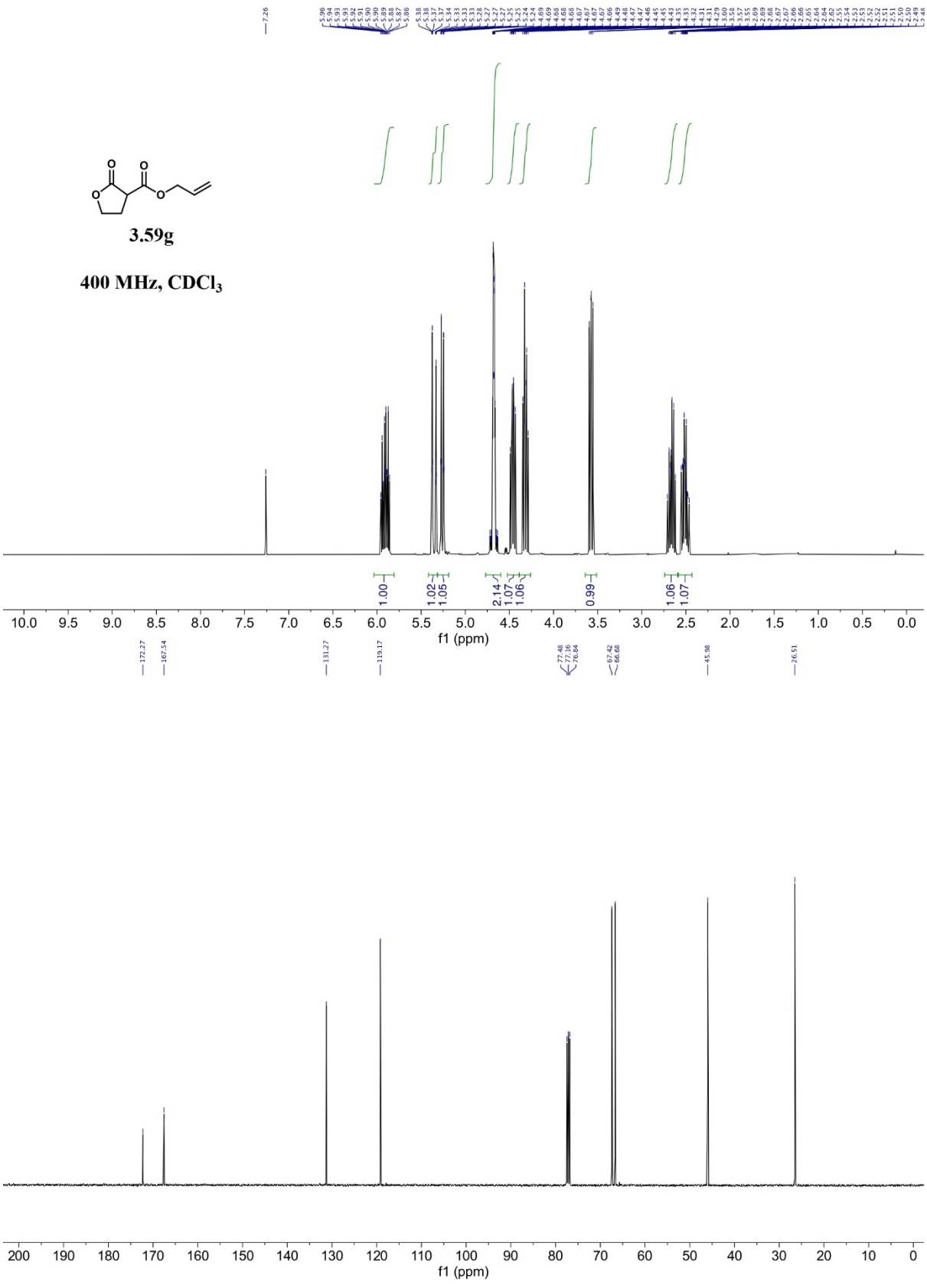


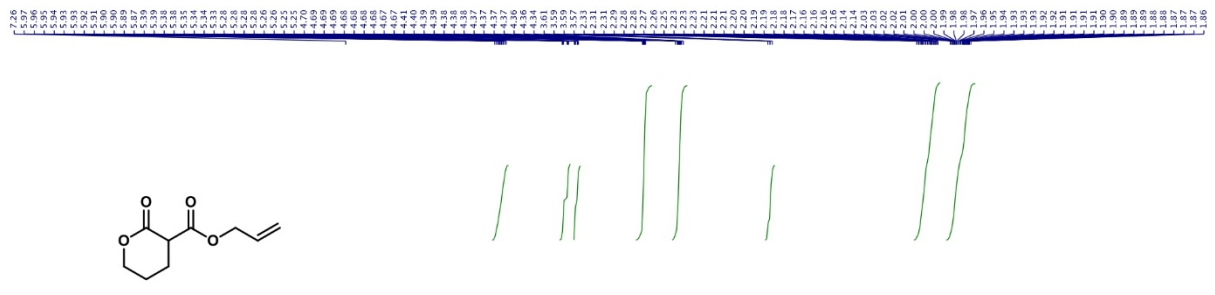
3.59e

400 MHz, $CDCl_3$



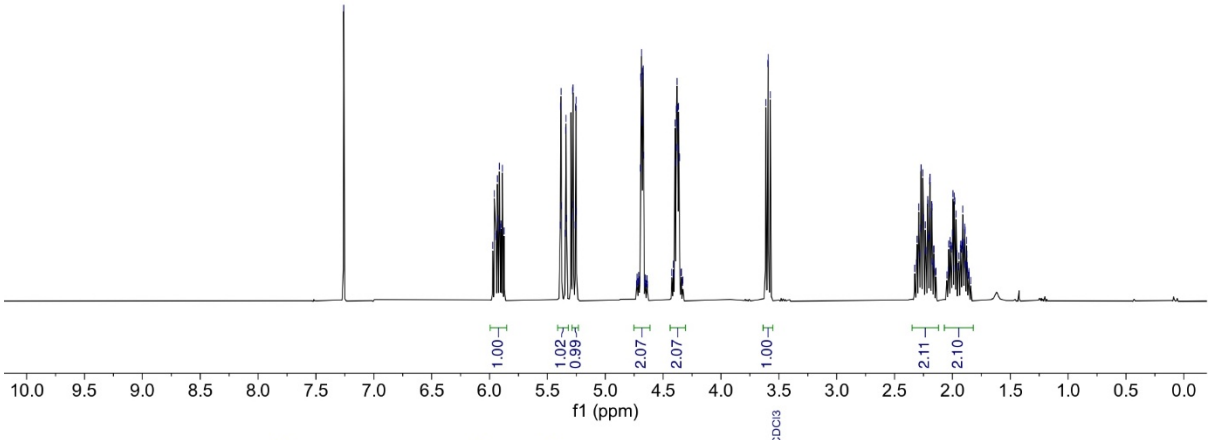

Me
O
O
O
3.59f
400 MHz, CDCl3
0.93
0.91
0.91
0.99
0.97
0.84
3.87
4.92
2.17
3.01
1.24
0.91
2.09
f1 (ppm)

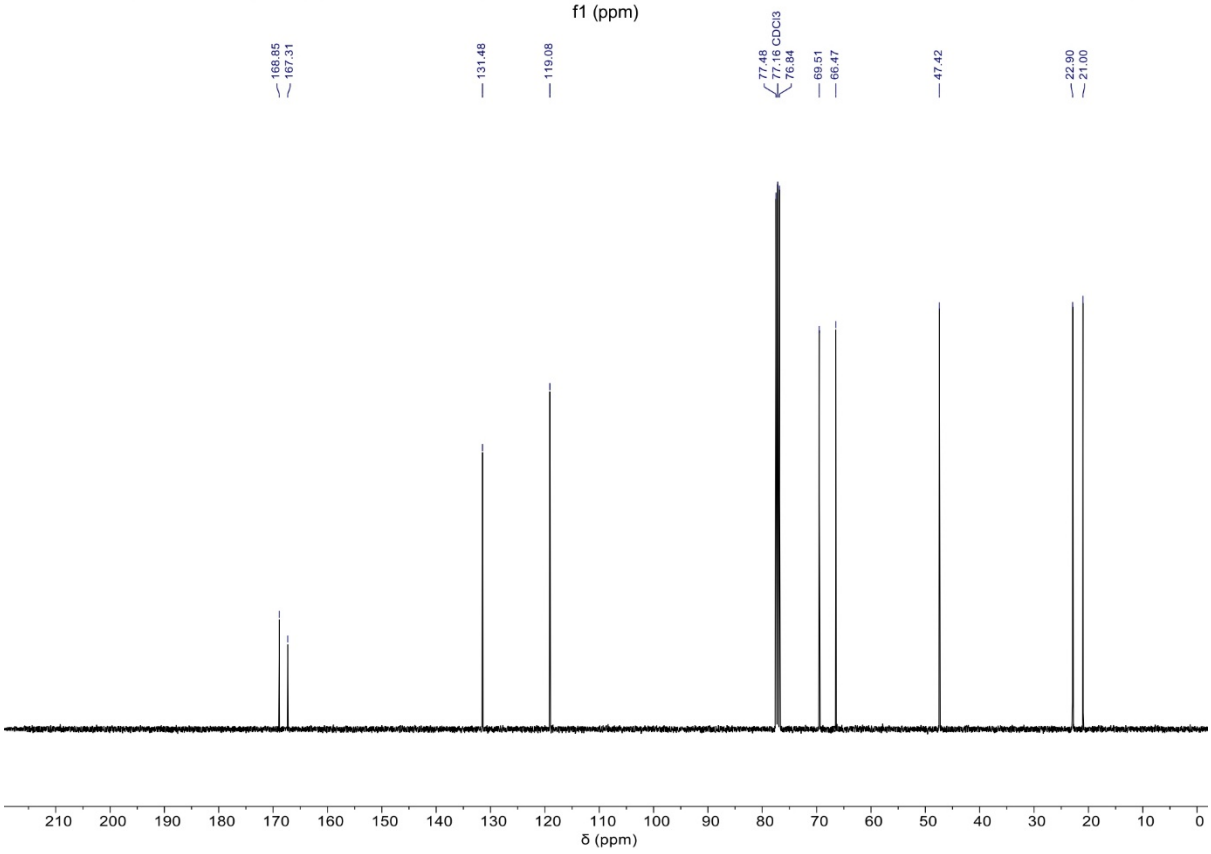

3.59g
400 MHz, CDCl3
f1 (ppm)
f1 (ppm)

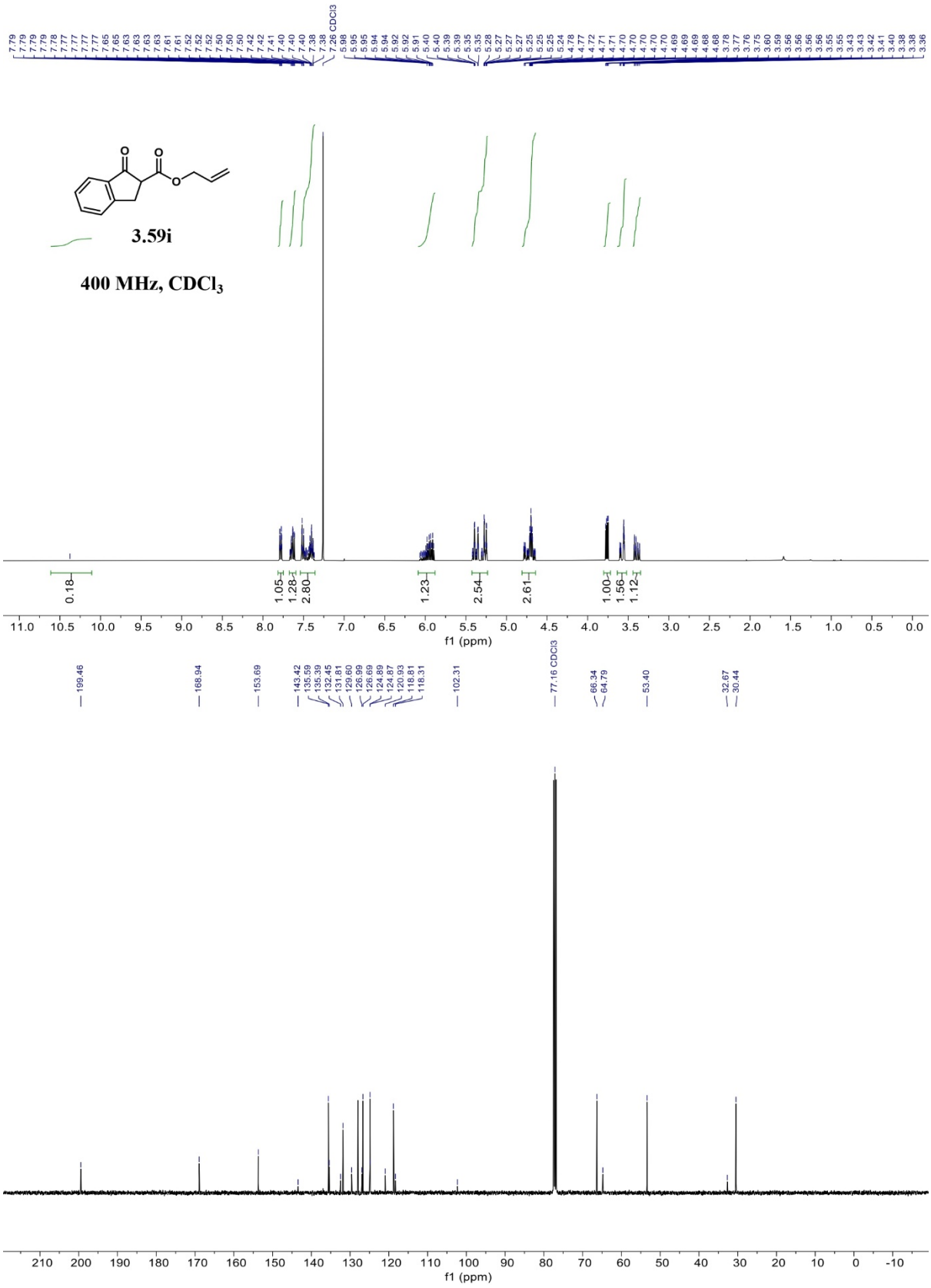


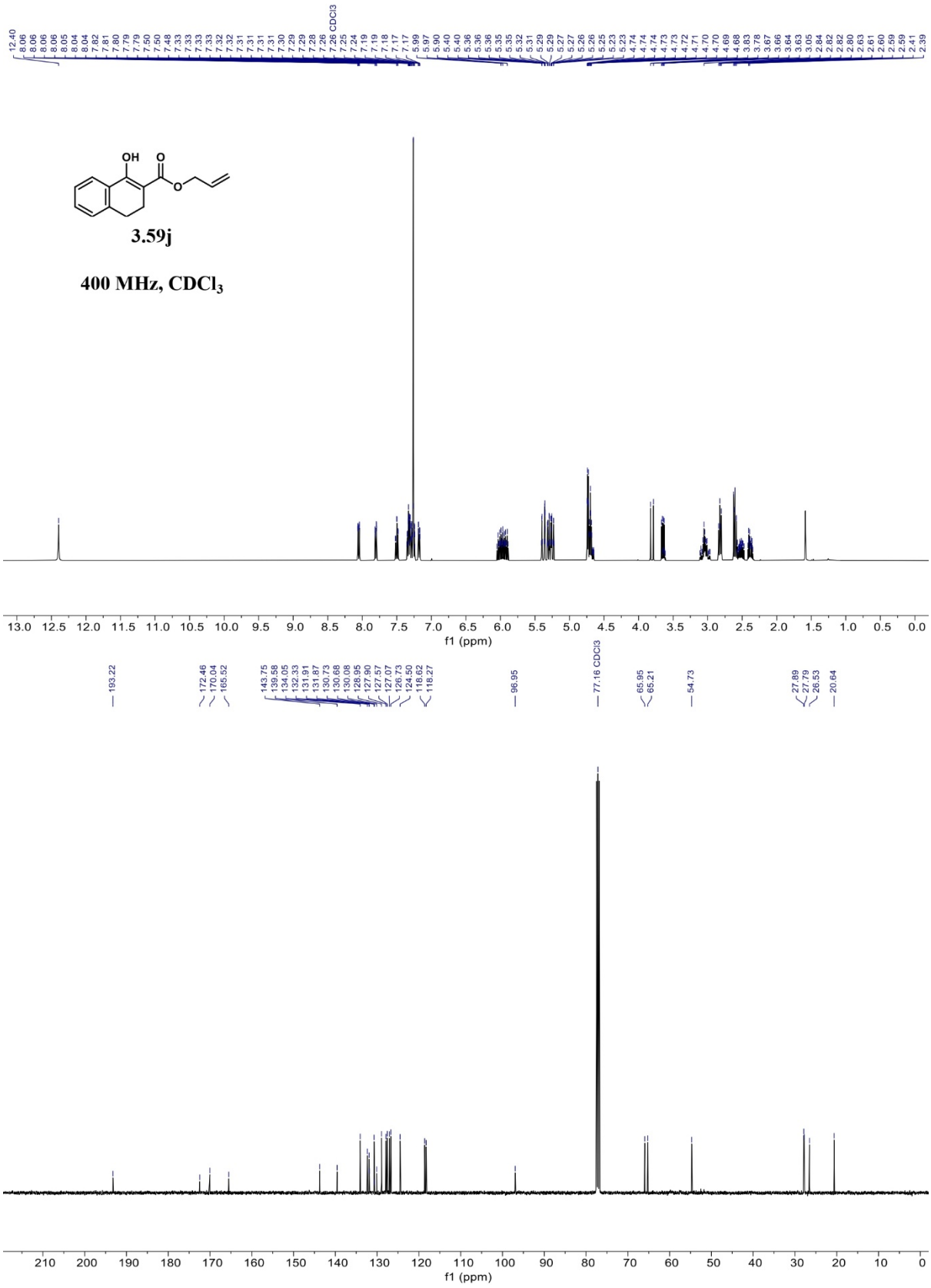
3.59h

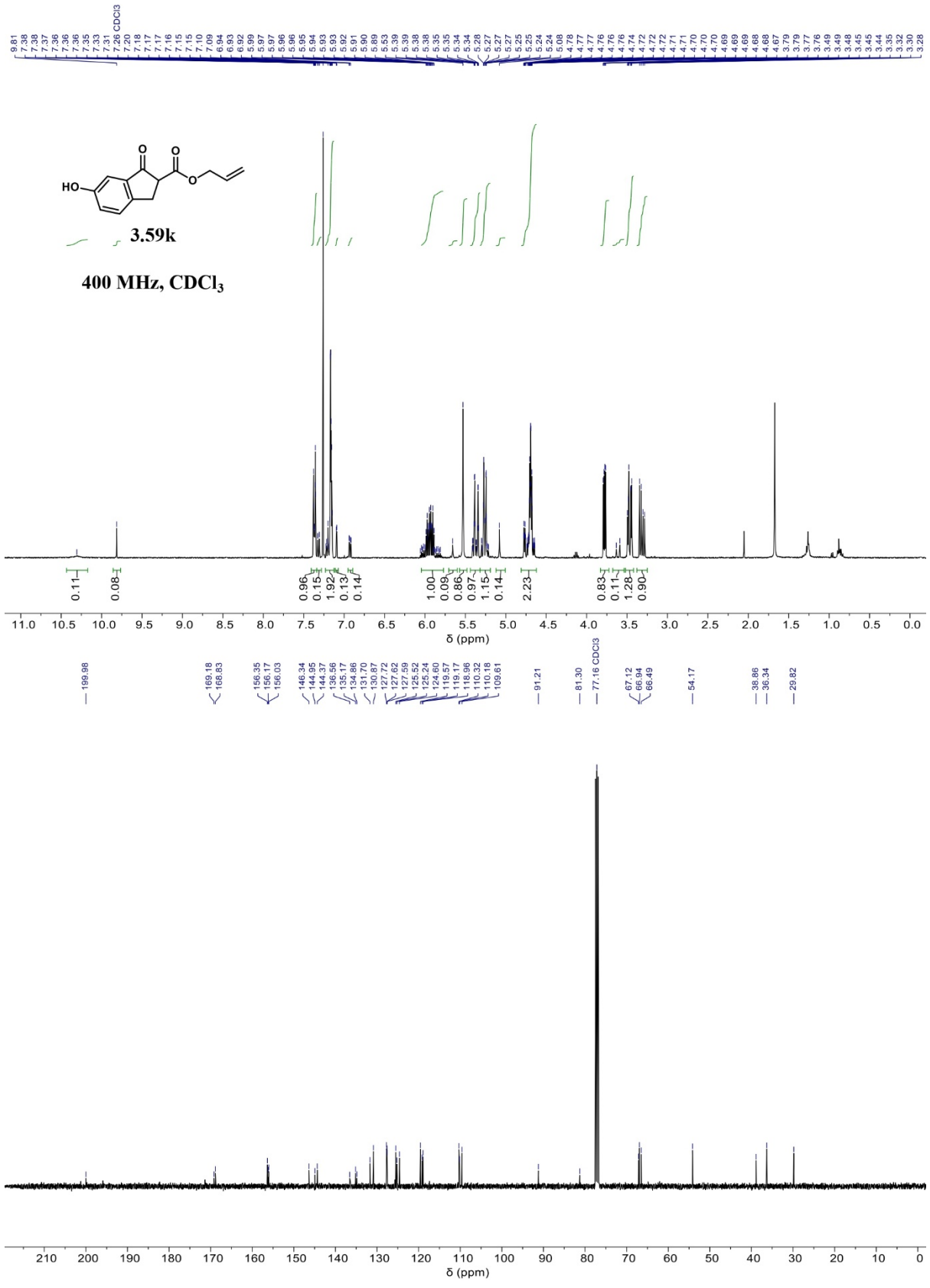
400 MHz, $CDCl_3$

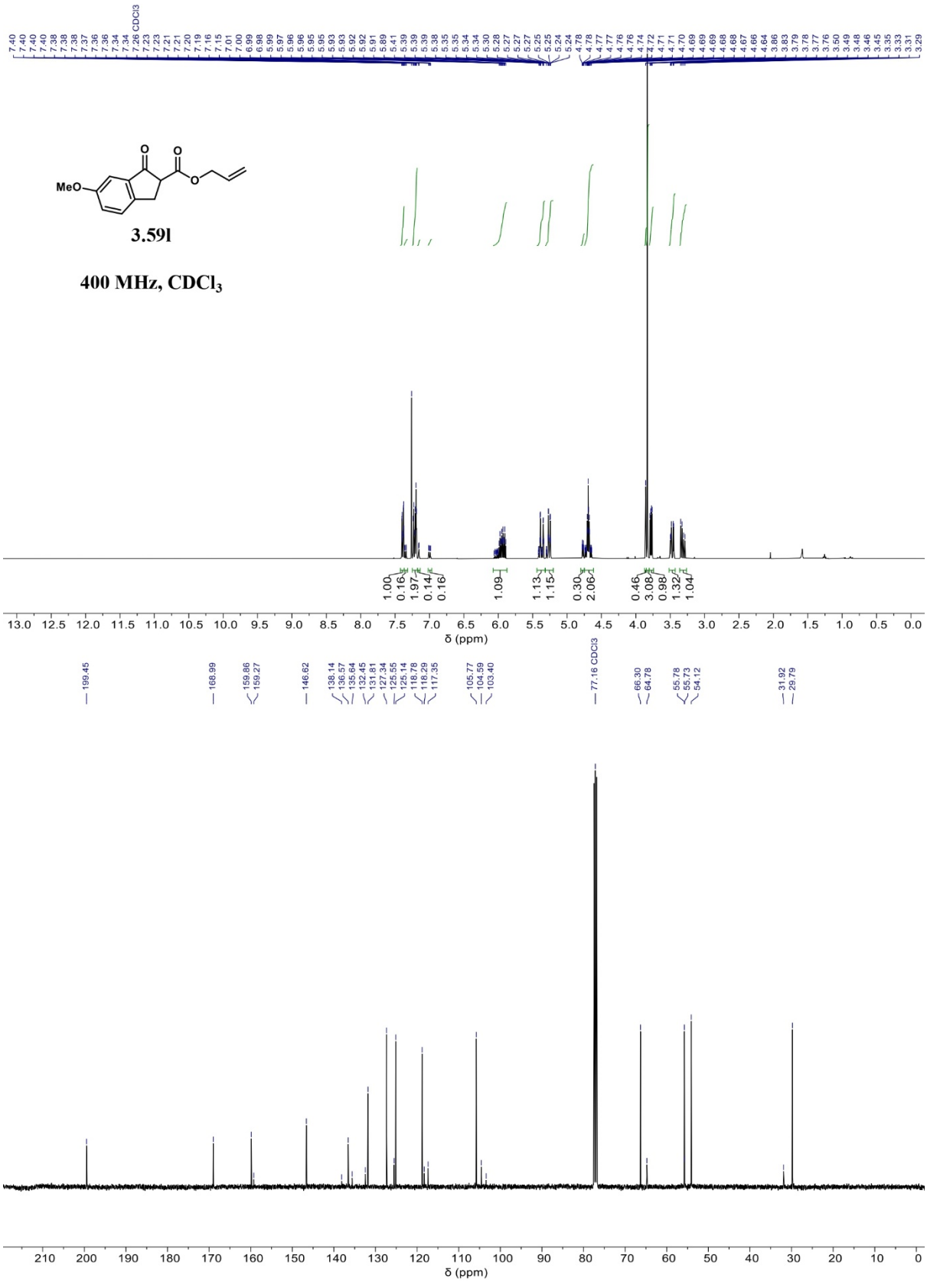


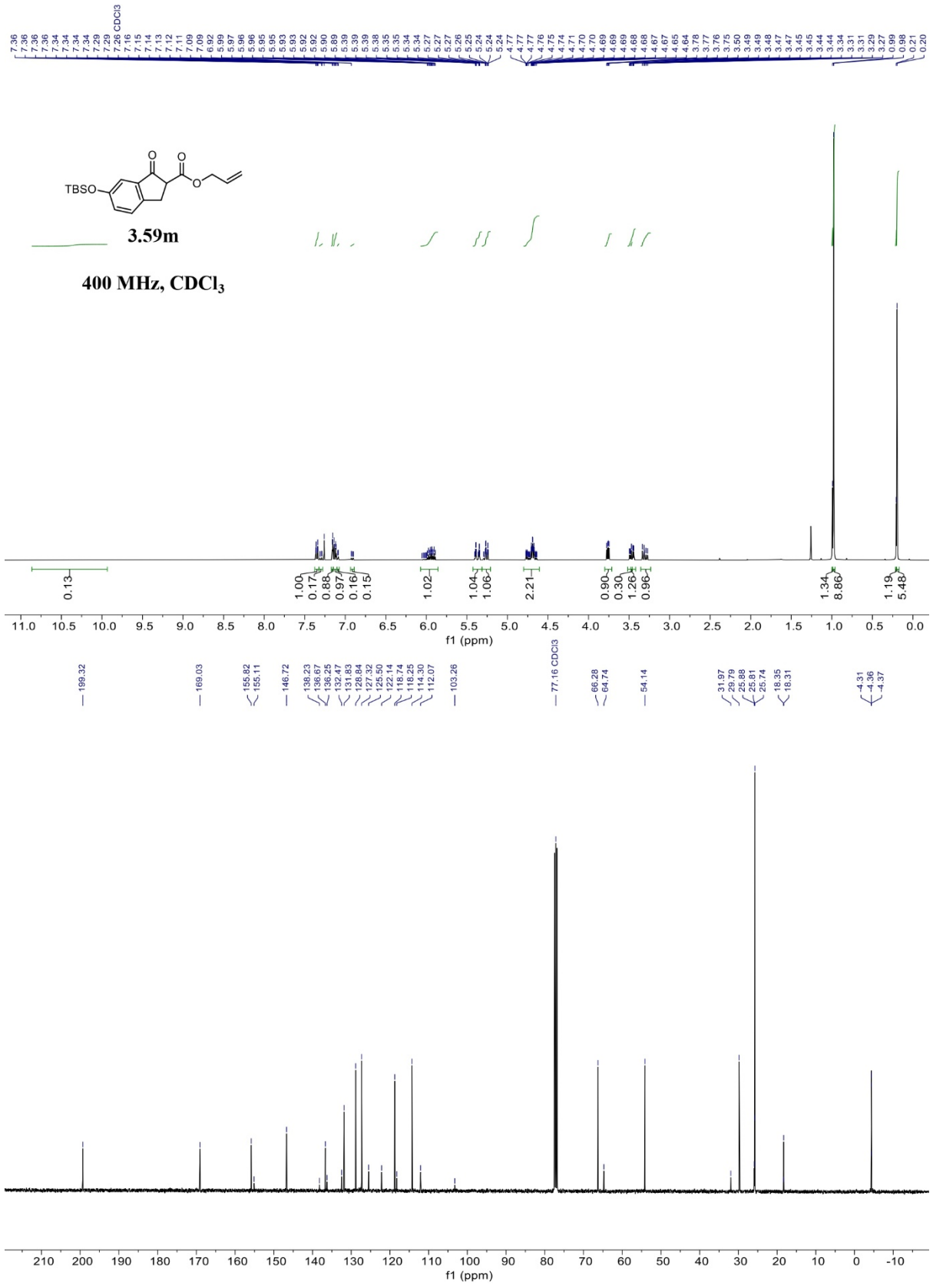


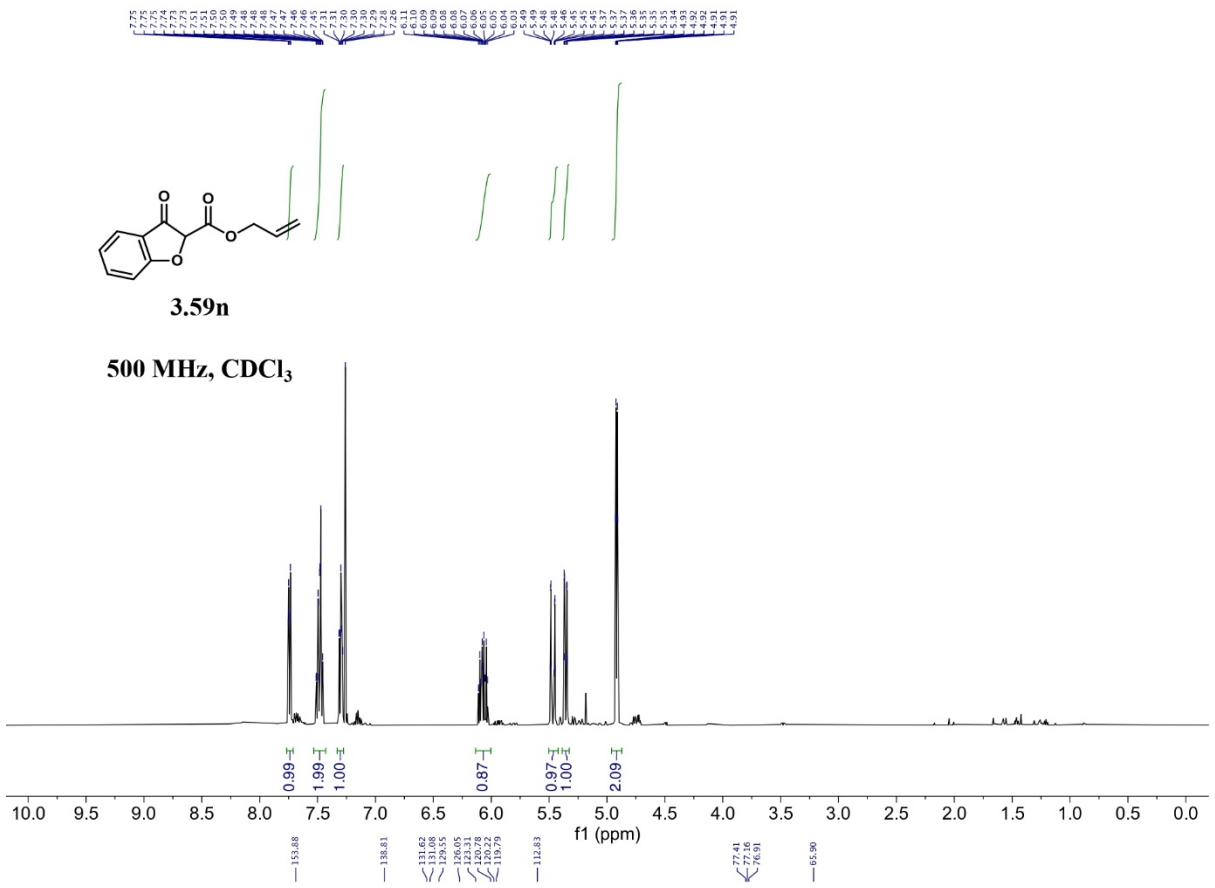

3.59i
400 MHz, CDCl3
f1 (ppm)
f1 (ppm)

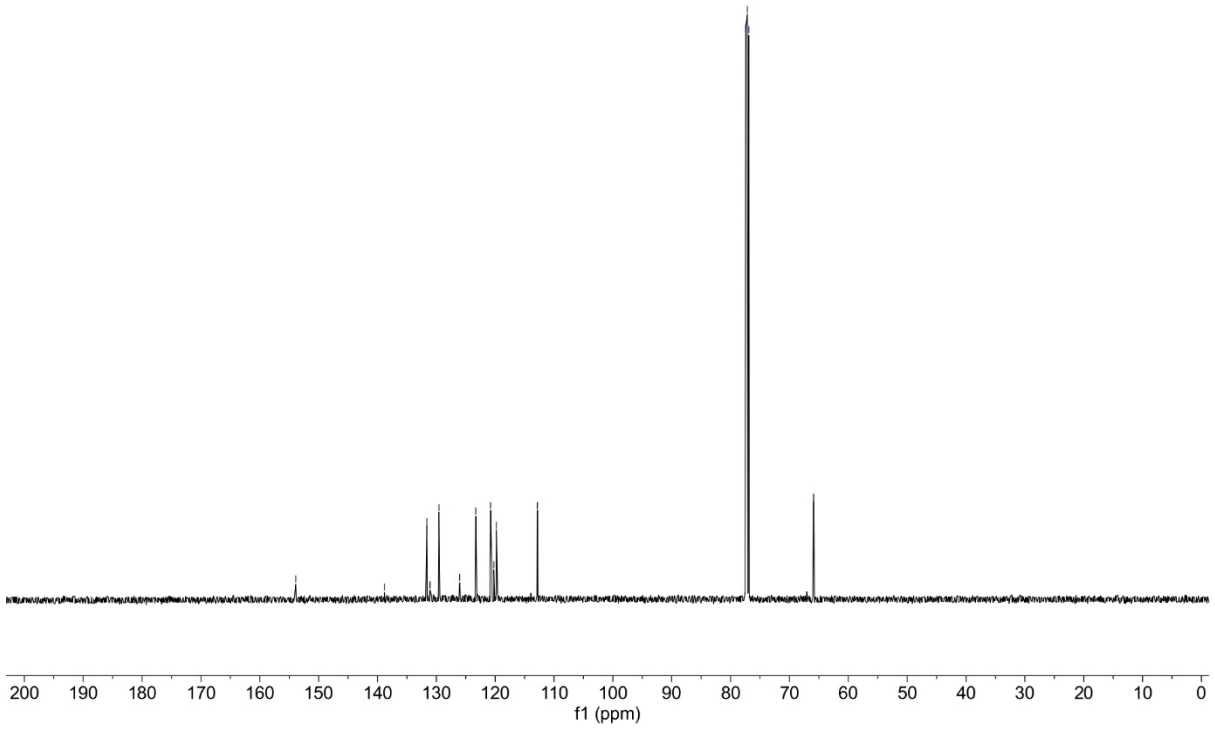

12.40 8.06 8.06 8.06 8.06 8.05 8.04 8.04 7.82 7.81 7.80 7.79 7.79 7.50 7.50 7.48 7.33 7.33 7.33 7.32 7.32 7.31 7.31 7.31 7.31 7.30 7.29 7.29 7.28 7.26 CDCl3 7.25 7.24 7.19 7.19 7.18 7.17 7.17 5.99 5.97 5.90 5.40 5.40 5.36 5.36 5.35 5.35 5.32 5.31 5.29 5.29 5.27 5.27 5.26 5.25 5.23 5.23 4.74 4.74 4.74 4.73 4.73 4.72 4.71 4.70 4.70 4.69 4.68 3.83 3.78 3.67 3.66 3.64 3.63 3.05 2.84 2.82 2.82 2.80 2.63 2.61 2.60 2.59 2.59 2.41 2.39
OH
O
O
3.59j
400 MHz, CDCl3
13.0 12.5 12.0 11.5 11.0 10.5 10.0 9.5 9.0 8.5 8.0 7.5 7.0 6.5 6.0 5.5 5.0 4.5 4.0 3.5 3.0 2.5 2.0 1.5 1.0 0.5 0.0
f1 (ppm)
193.22
172.46 170.04 165.52
143.75 139.58 134.05 132.33 131.91 131.87 130.73 130.68 130.08 128.95 127.90 127.57 127.07 126.73 124.50 118.62 118.27
96.95
77.16 CDCl3
65.95 65.21
54.73
27.89 27.79 26.53
20.64
210 200 190 180 170 160 150 140 130 120 110 100 90 80 70 60 50 40 30 20 10 0
f1 (ppm)

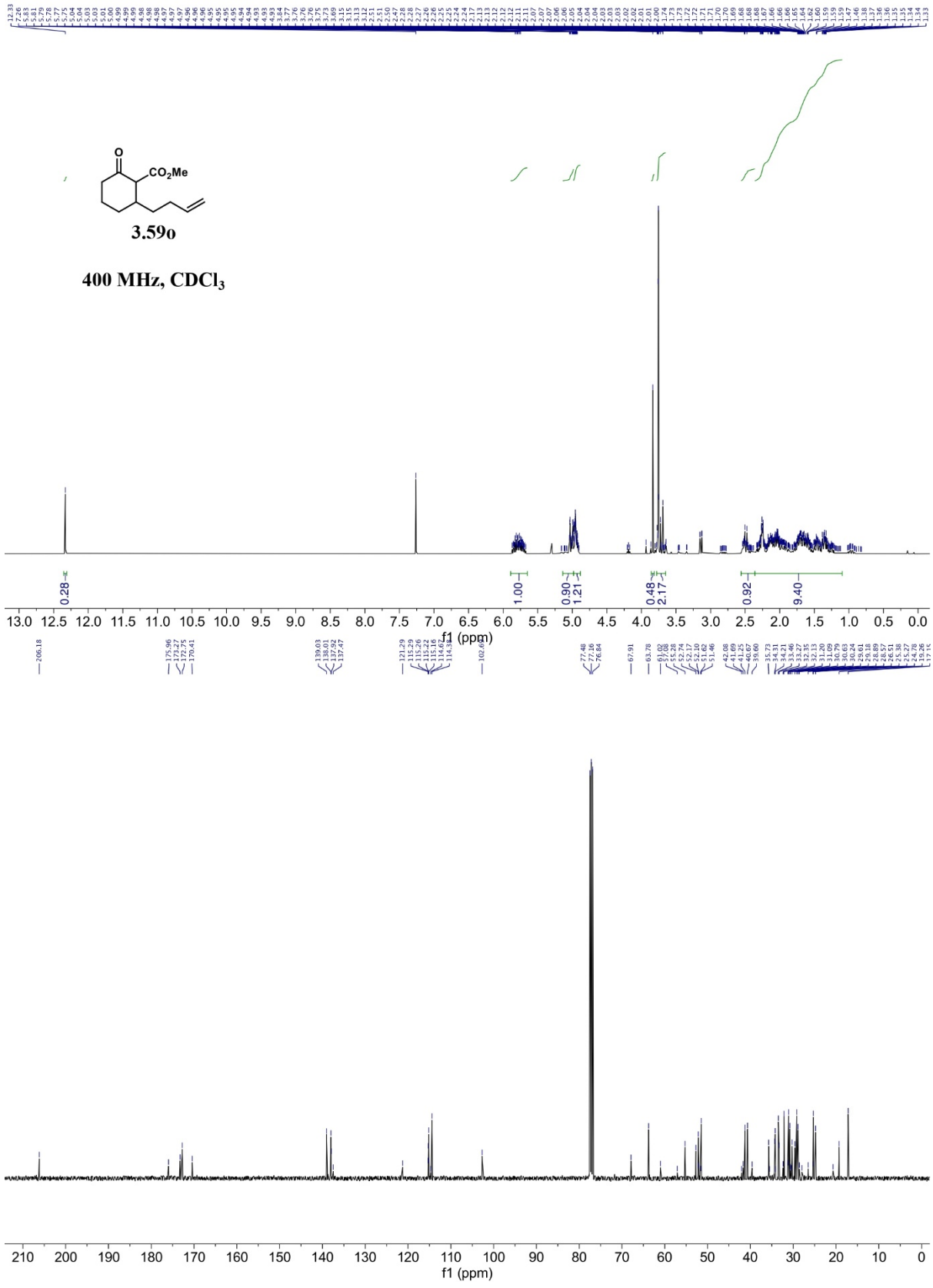

HO
O
O
O
3.59k
400 MHz, CDCl3
δ (ppm)
δ (ppm)

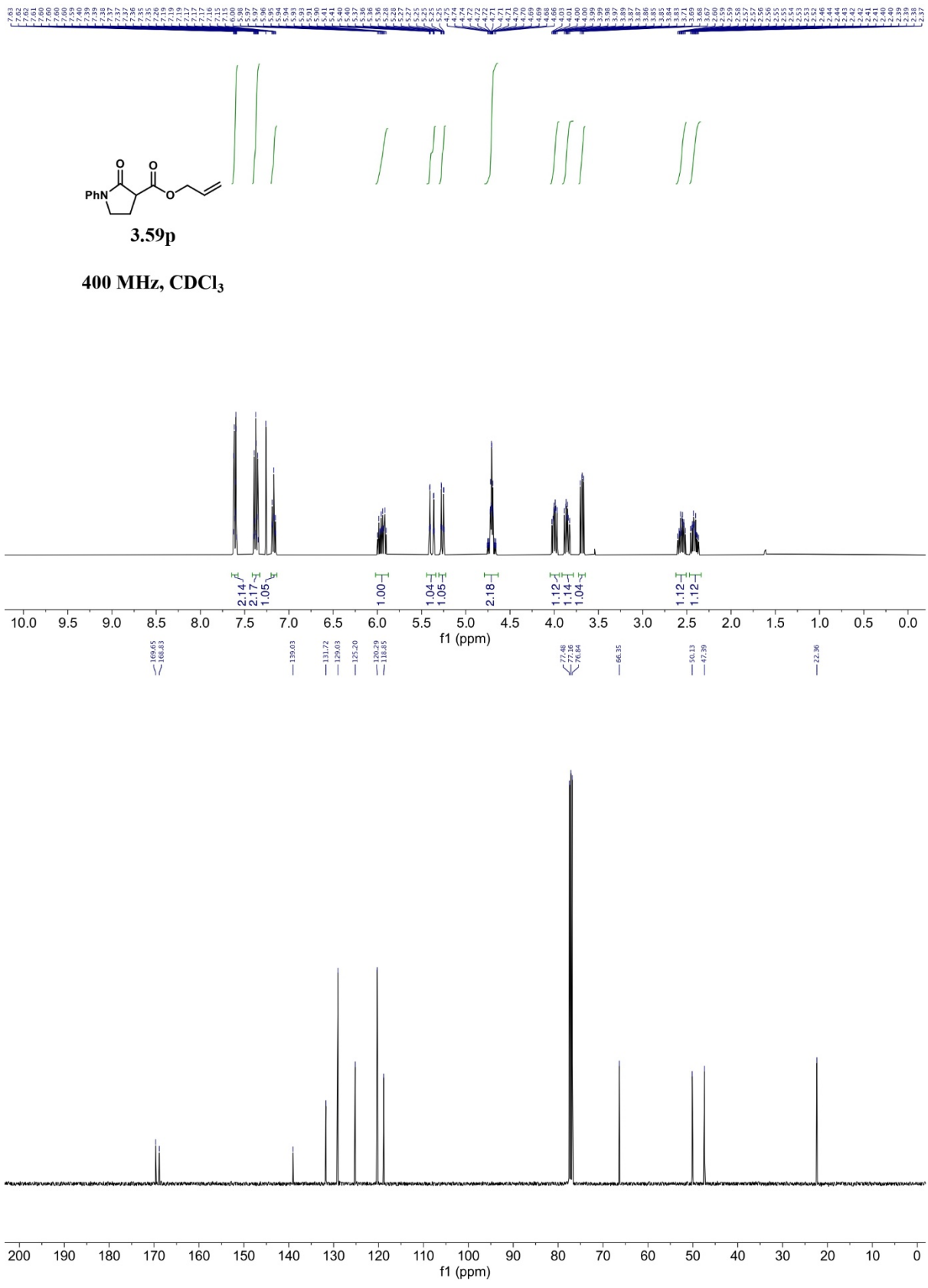

MeO
O
O
O
3.59l
400 MHz, CDCl3
δ (ppm)
δ (ppm)


TBSO
3.59m
400 MHz, CDCl3
f1 (ppm)
f1 (ppm)


3.59n
500 MHz, CDCl3
f1 (ppm)

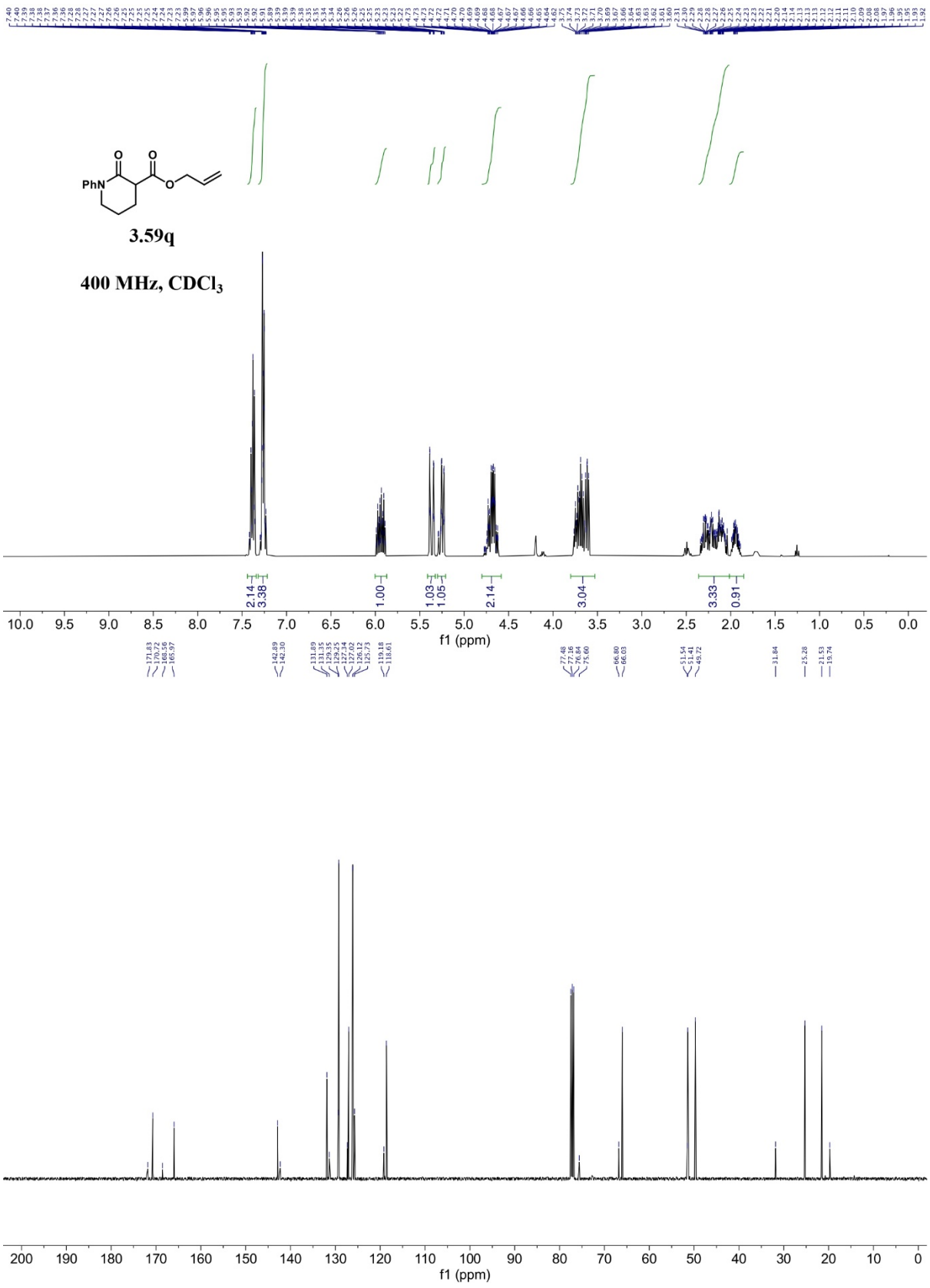

f1 (ppm)

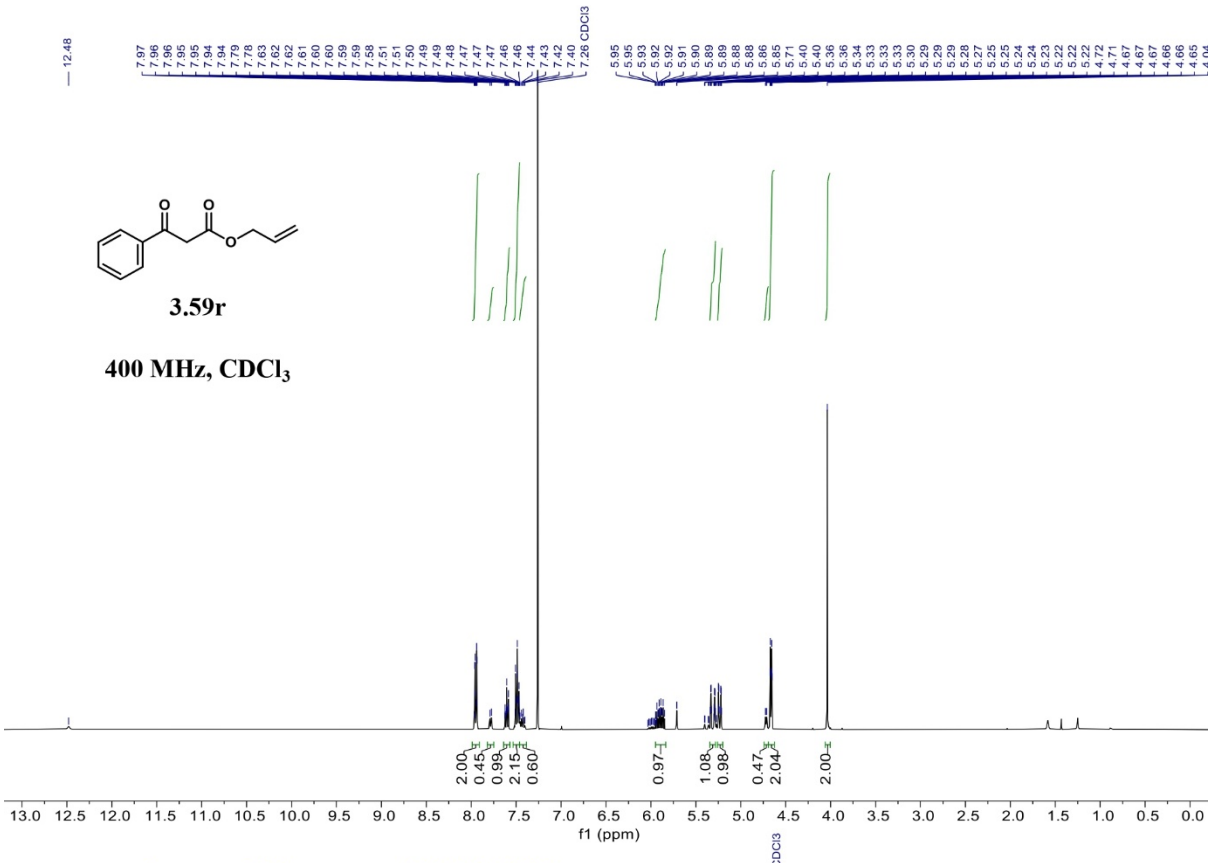

O
CO2Me
3.59o
400 MHz, CDCl3
f1 (ppm)
f1 (ppm)

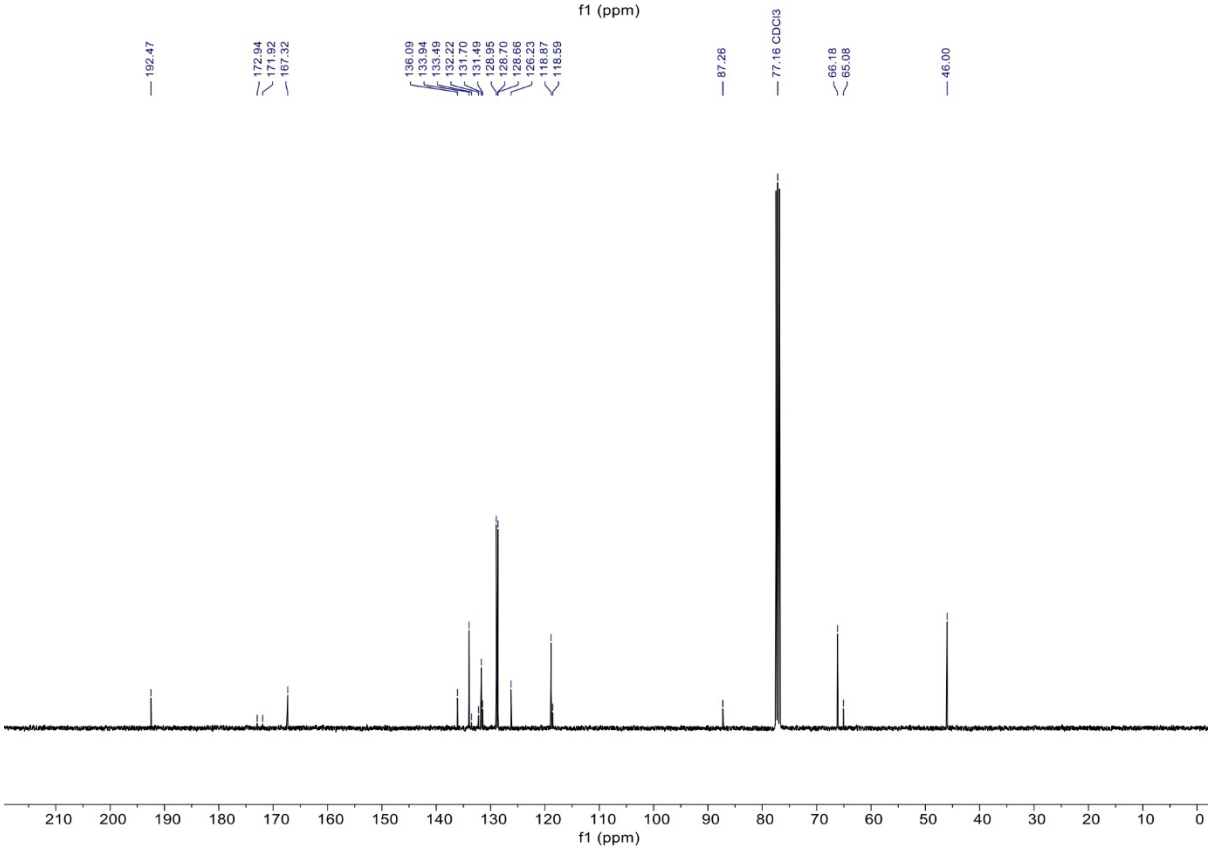


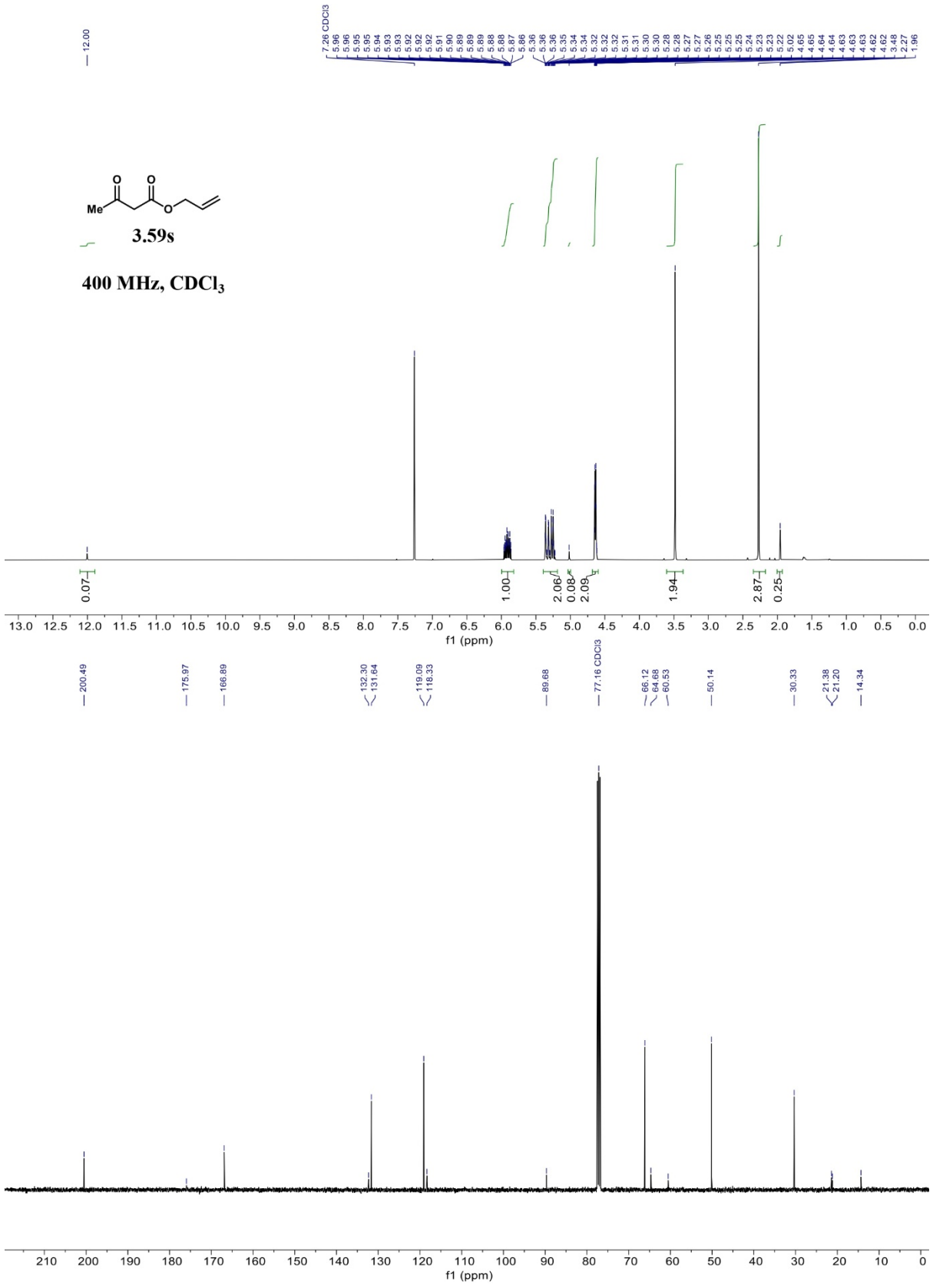
3.59p

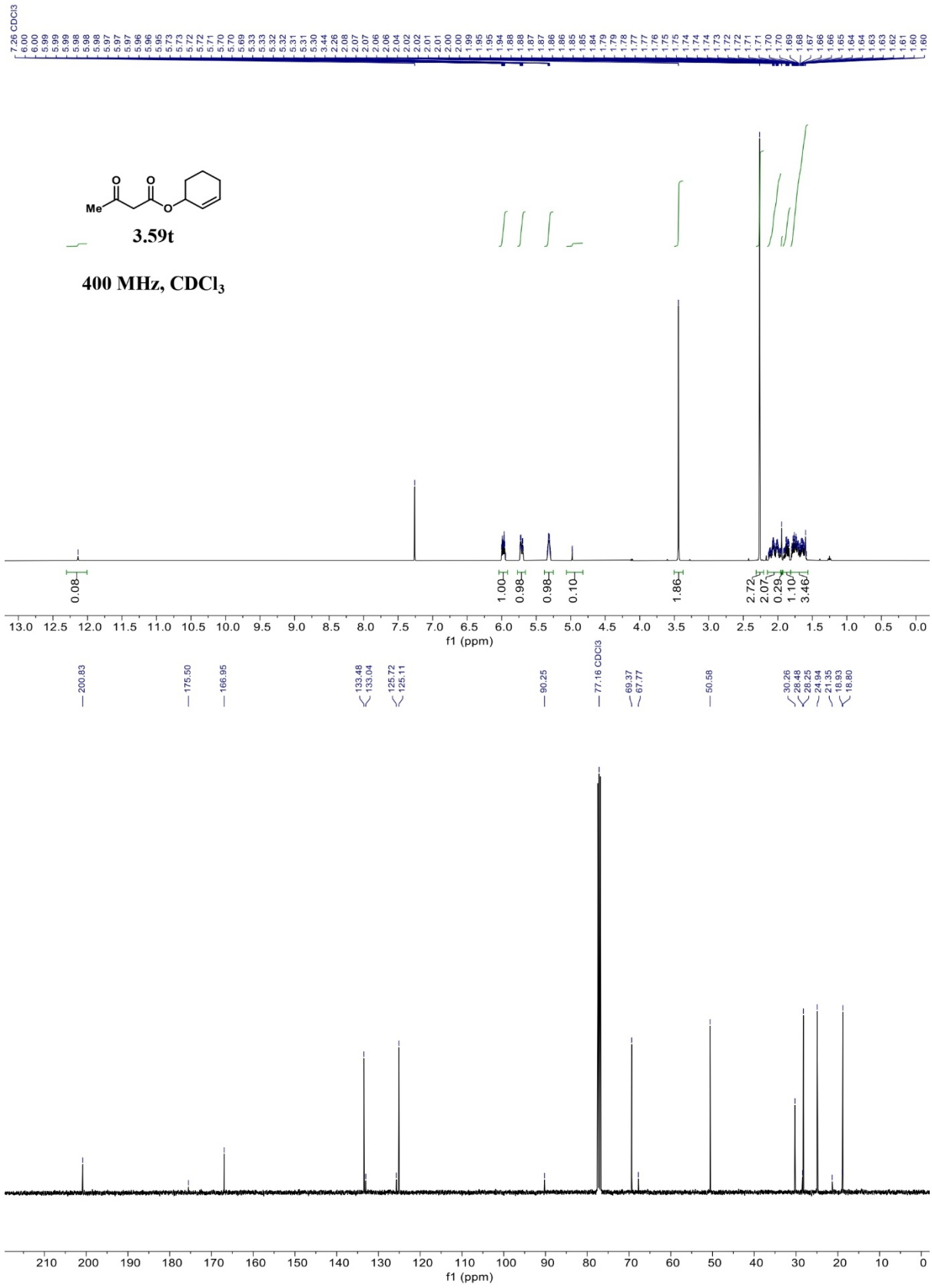
400 MHz, $CDCl_3$

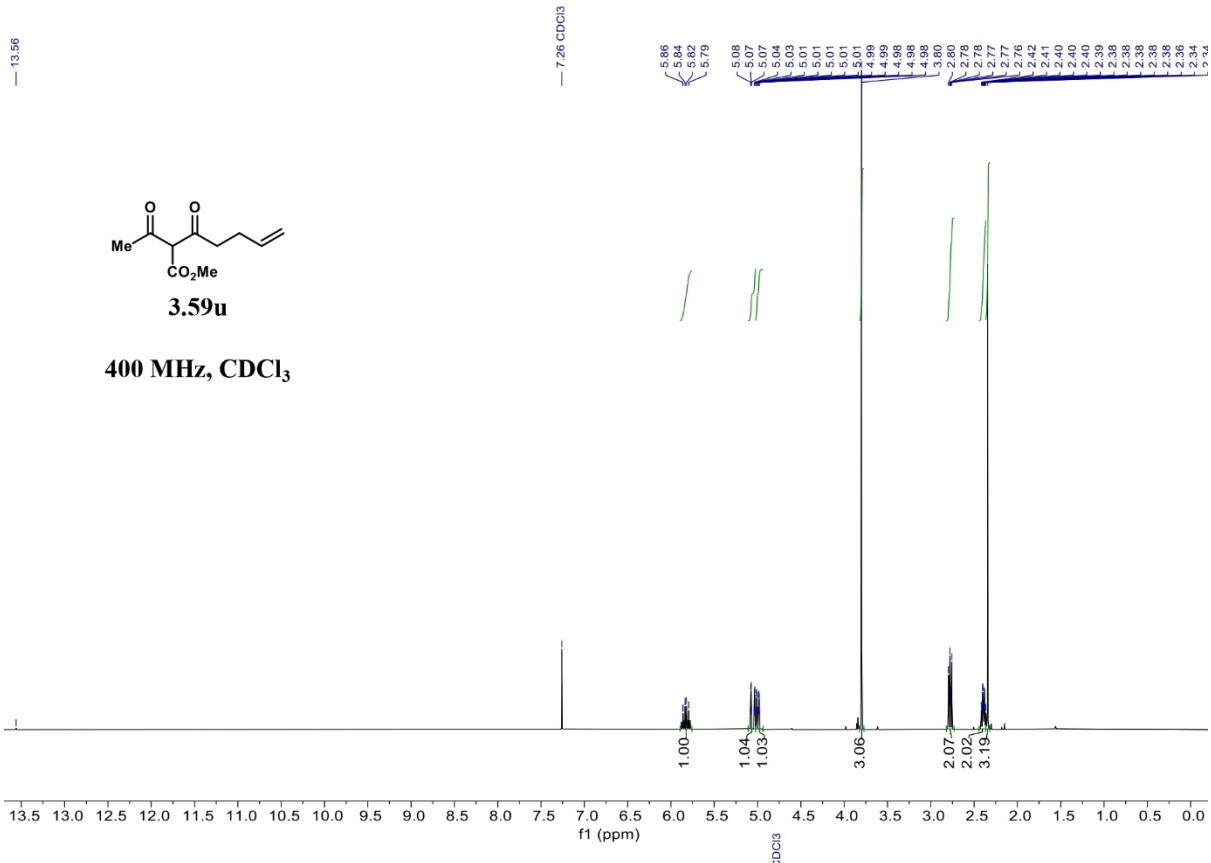

3.59q
400 MHz, CDCl3
f1 (ppm)
f1 (ppm)


12.48
7.97
7.96
7.96
7.95
7.95
7.94
7.94
7.79
7.78
7.63
7.62
7.62
7.61
7.60
7.60
7.59
7.59
7.58
7.51
7.51
7.50
7.49
7.49
7.48
7.47
7.47
7.47
7.46
7.46
7.44
7.43
7.42
7.40
7.26 CDCl3
5.95
5.95
5.93
5.92
5.92
5.91
5.90
5.89
5.89
5.88
5.88
5.86
5.85
5.71
5.40
5.40
5.36
5.36
5.34
5.33
5.33
5.33
5.30
5.29
5.29
5.28
5.27
5.25
5.25
5.24
5.24
5.23
5.22
5.22
5.22
4.72
4.71
4.67
4.67
4.67
4.66
4.66
4.65
3.59r
400 MHz, CDCl3
2.00
0.45
0.99
2.15
0.60
0.97
1.08
0.98
0.47
2.04
2.00
f1 (ppm)


192.47
172.94
171.92
167.32
136.09
133.94
133.49
132.22
131.70
131.49
128.95
128.70
128.66
126.23
118.87
118.59
87.26
77.16 CDCl3
66.18
65.08
46.00
f1 (ppm)

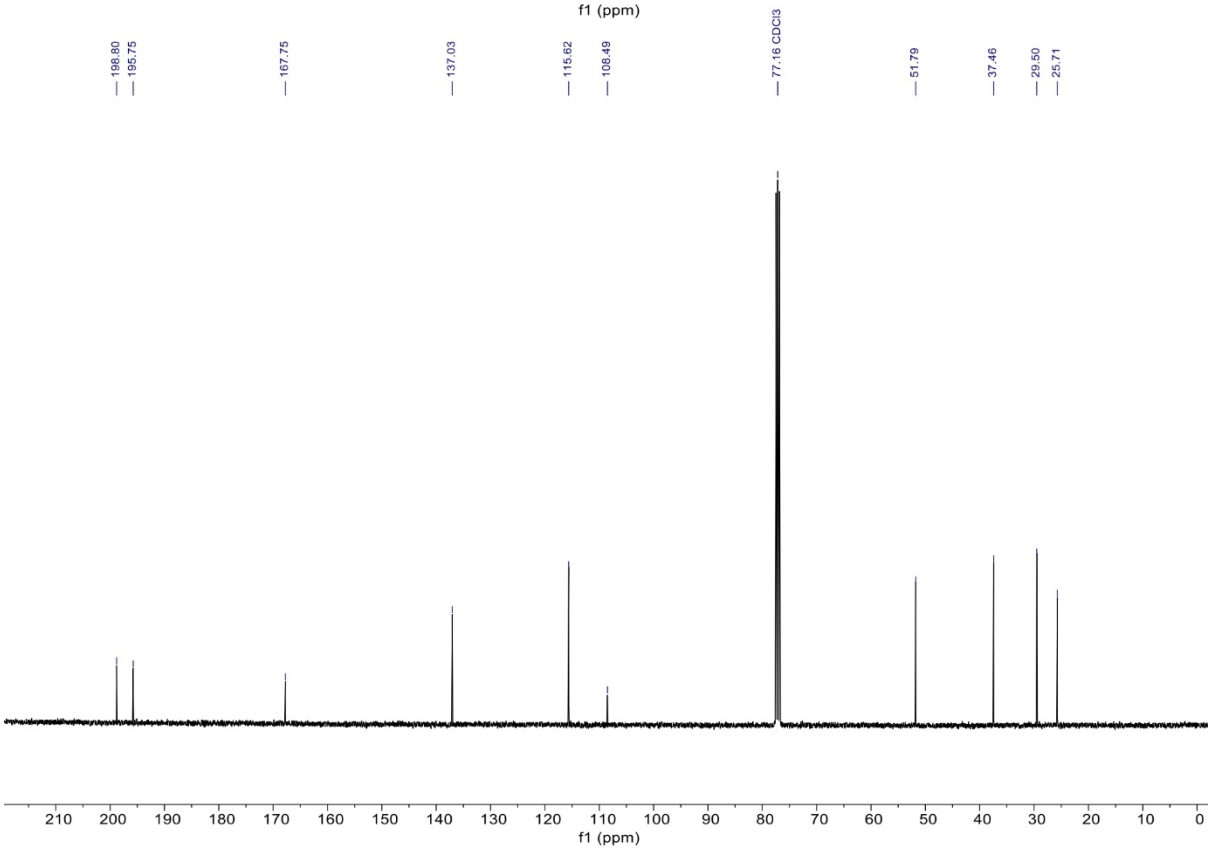

3.59s
400 MHz, CDCl3
f1 (ppm)
f1 (ppm)

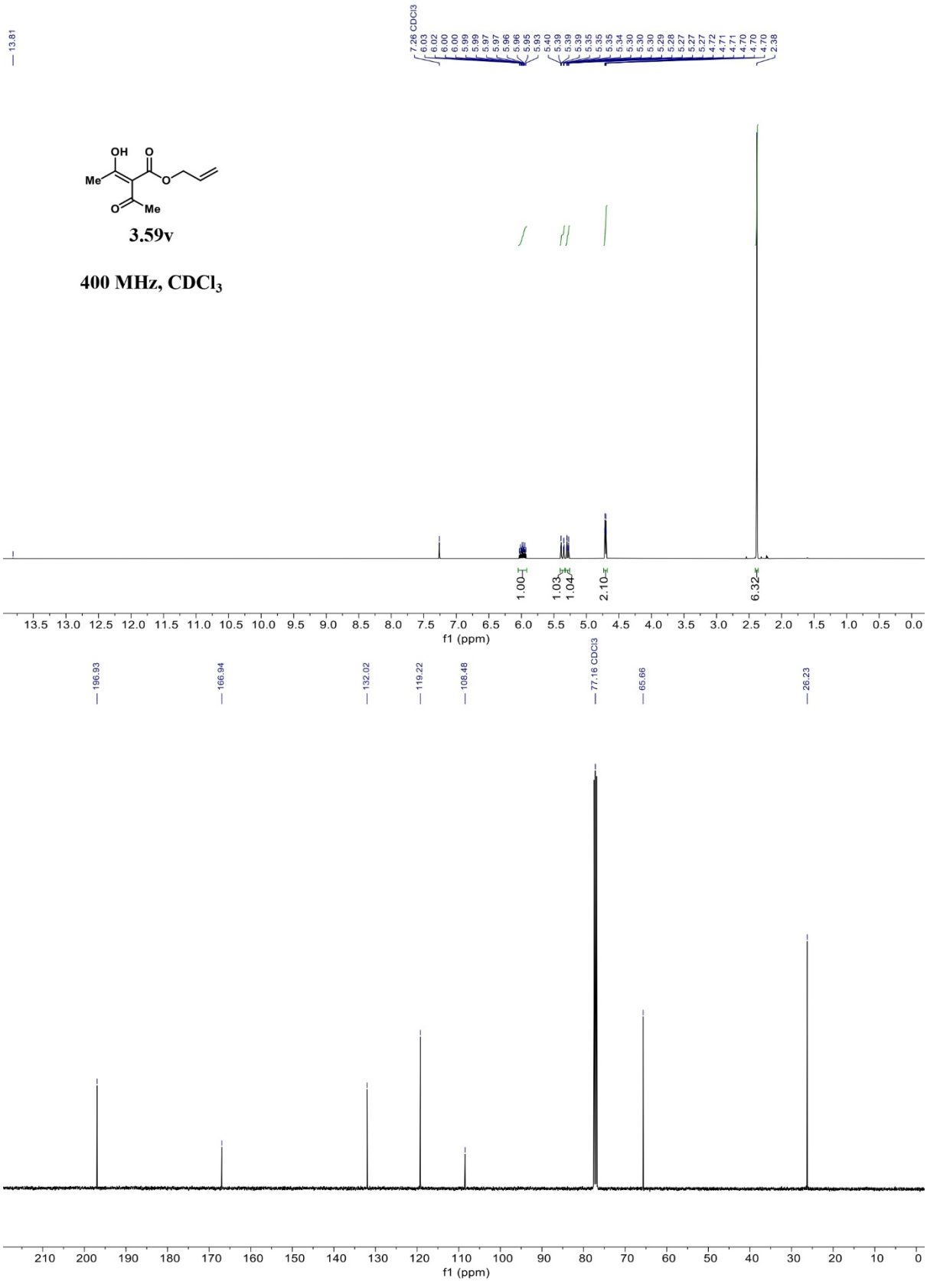

Me
3.59t
400 MHz, CDCl3
f1 (ppm)
f1 (ppm)

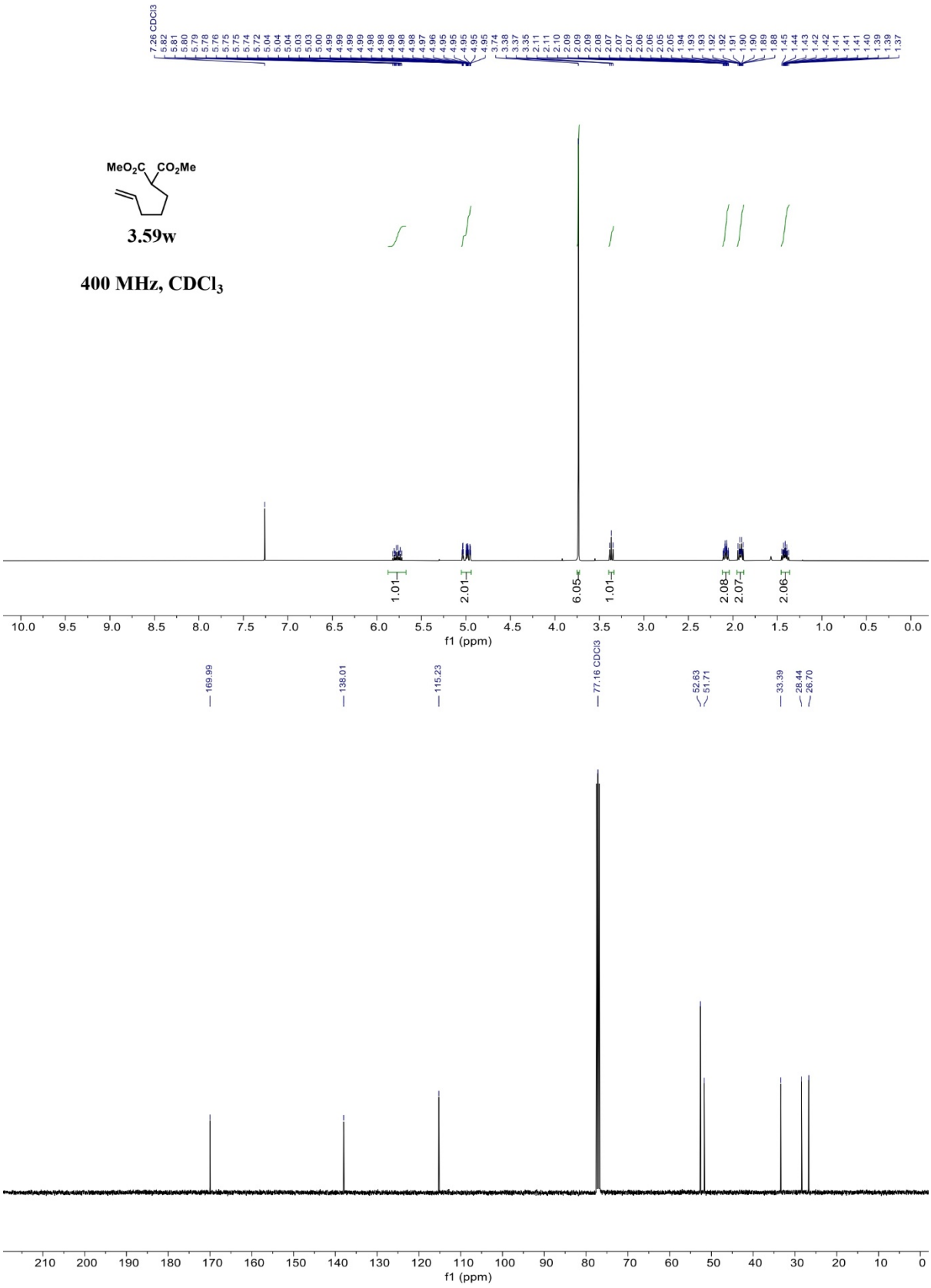


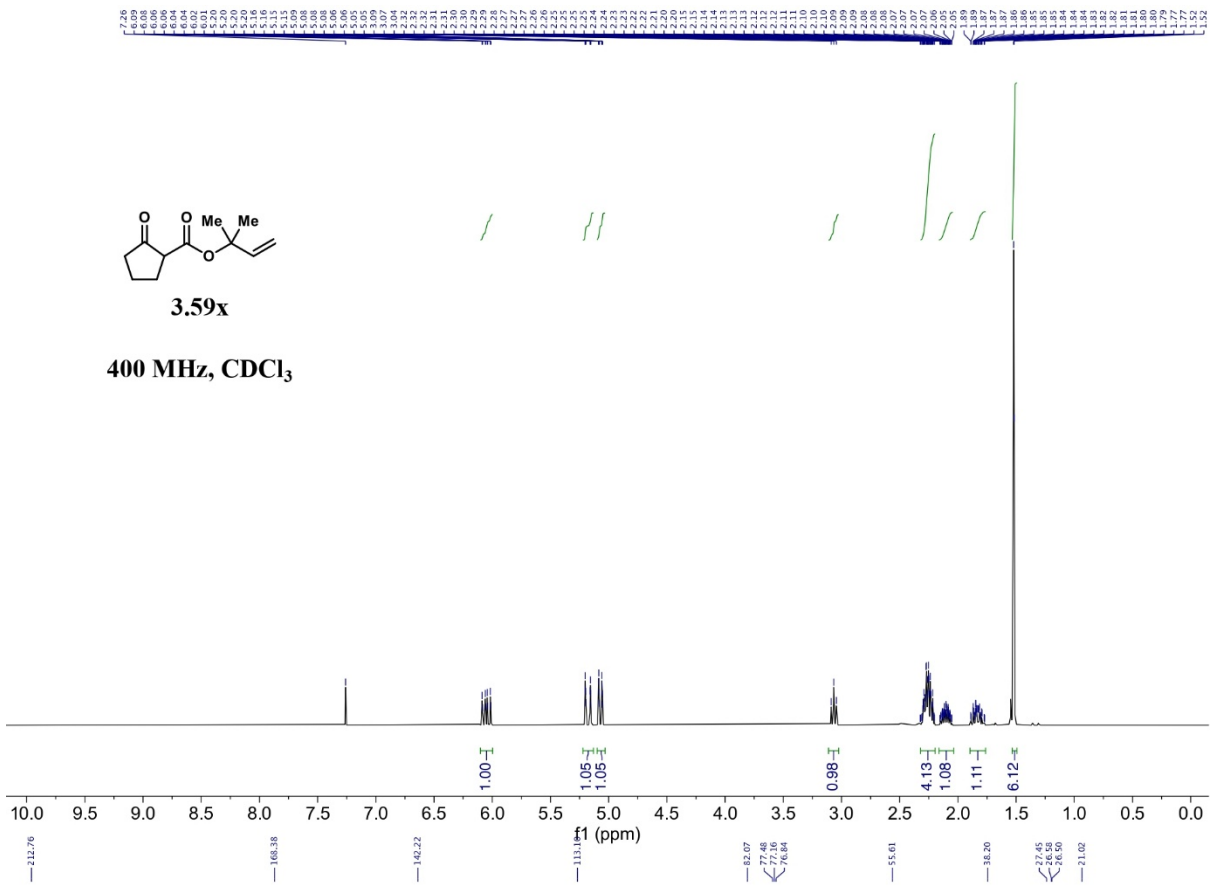
3.59u

400 MHz, $CDCl_3$



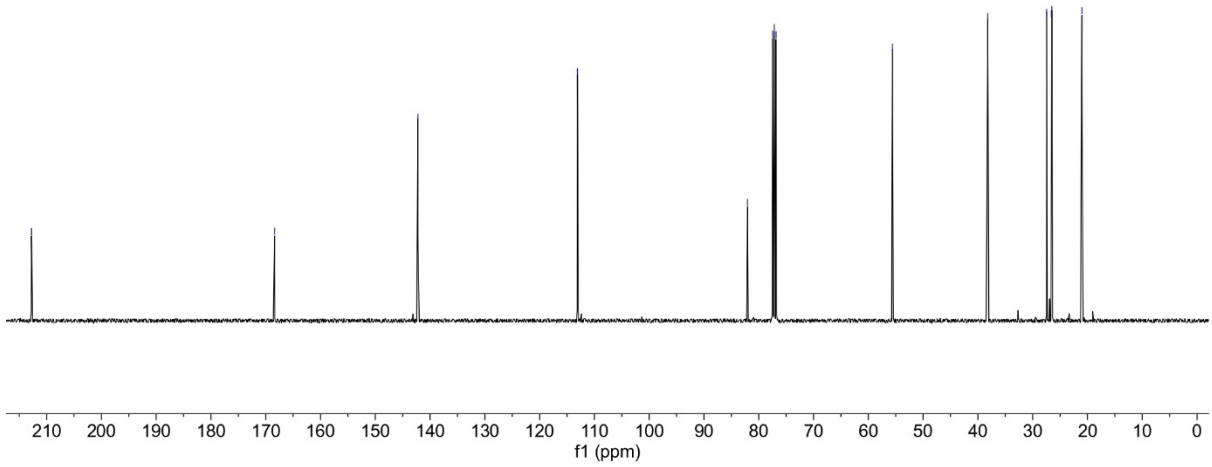

13.81
7.26 CDCl3
6.03
6.02
6.00
6.00
5.99
5.99
5.97
5.97
5.96
5.96
5.95
5.93
5.40
5.39
5.39
5.38
5.35
5.35
5.35
5.34
5.30
5.30
5.30
5.29
5.28
5.27
5.27
5.27
4.72
4.71
4.71
4.70
4.70
4.70
2.38
OH
O
Me
O
O
Me
3.59v
400 MHz, CDCl3
1.00
1.03
1.04
2.10
6.32
f1 (ppm)
196.93
166.94
132.02
119.22
108.48
77.16 CDCl3
65.66
26.23
f1 (ppm)

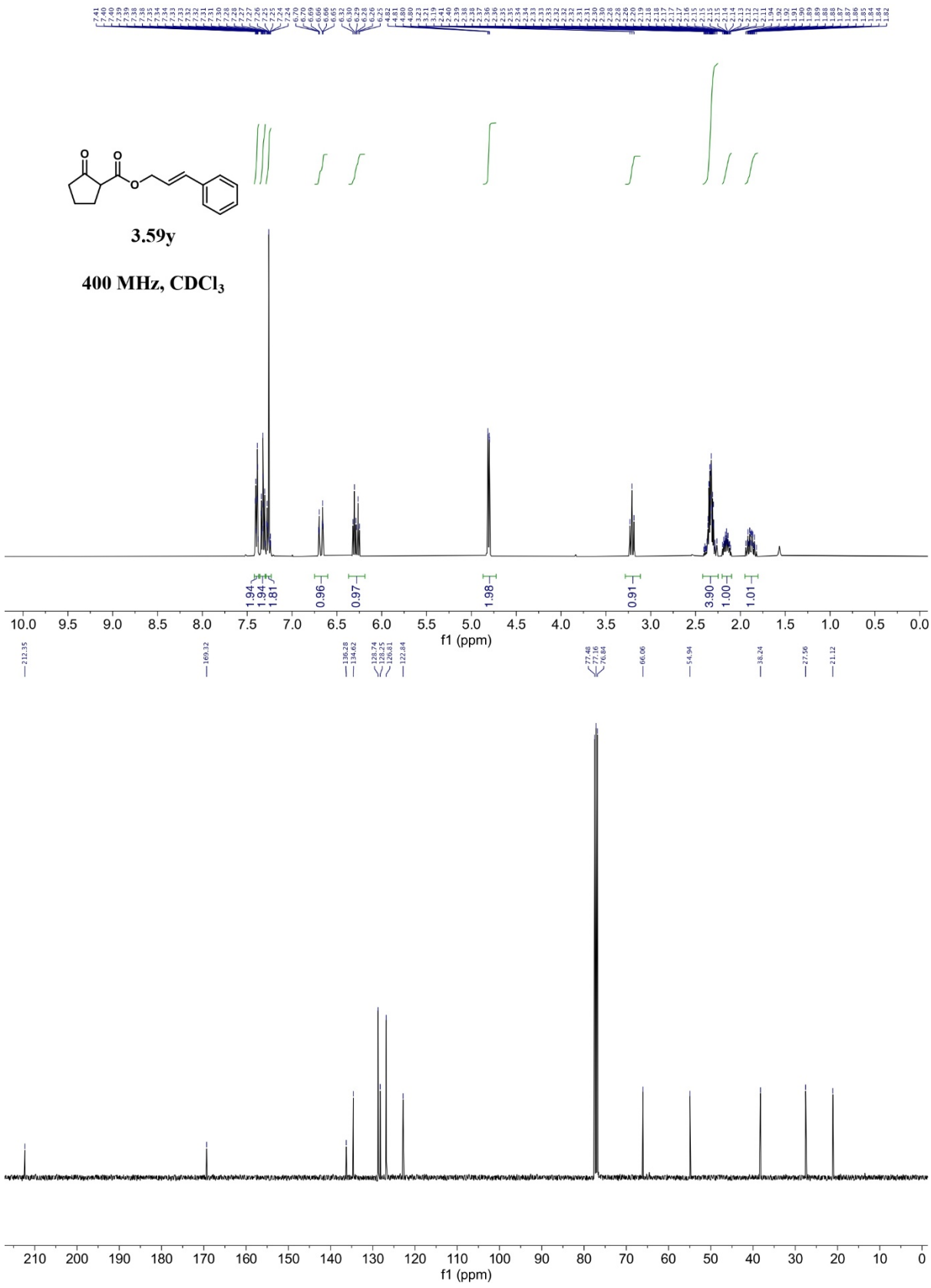

MeO2C CO2Me
3.59w
400 MHz, CDCl3
f1 (ppm)
f1 (ppm)

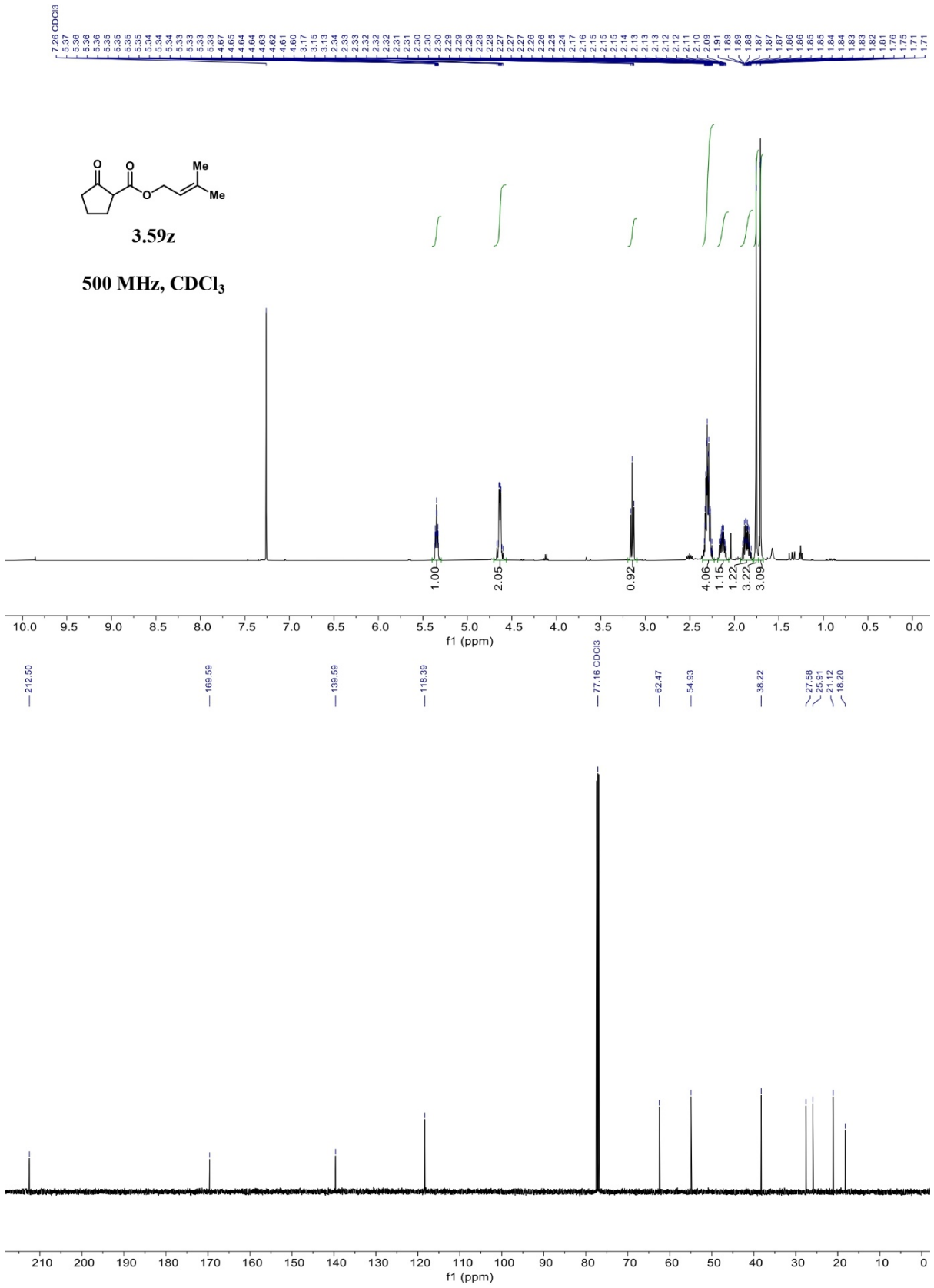


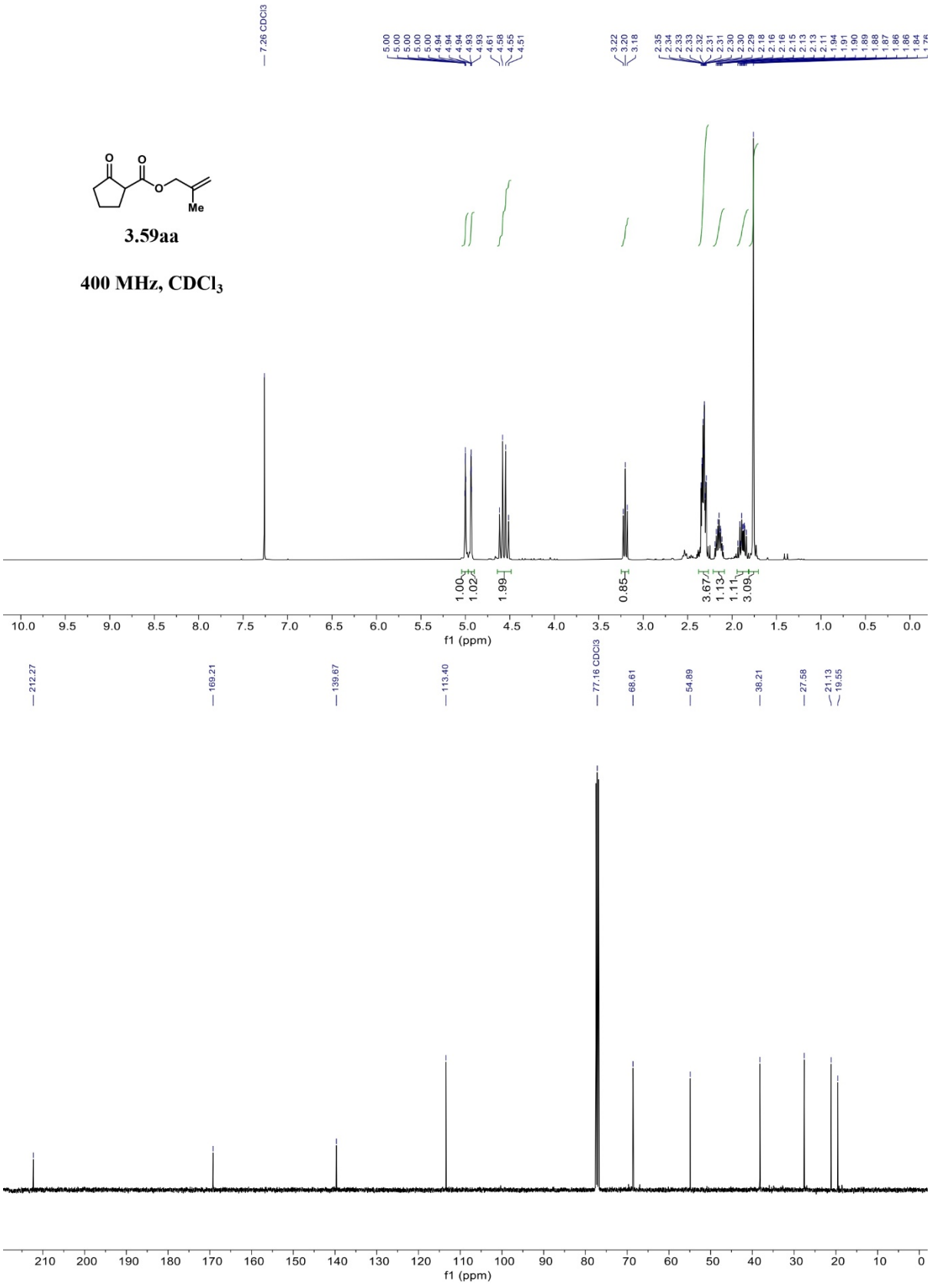
3.59x

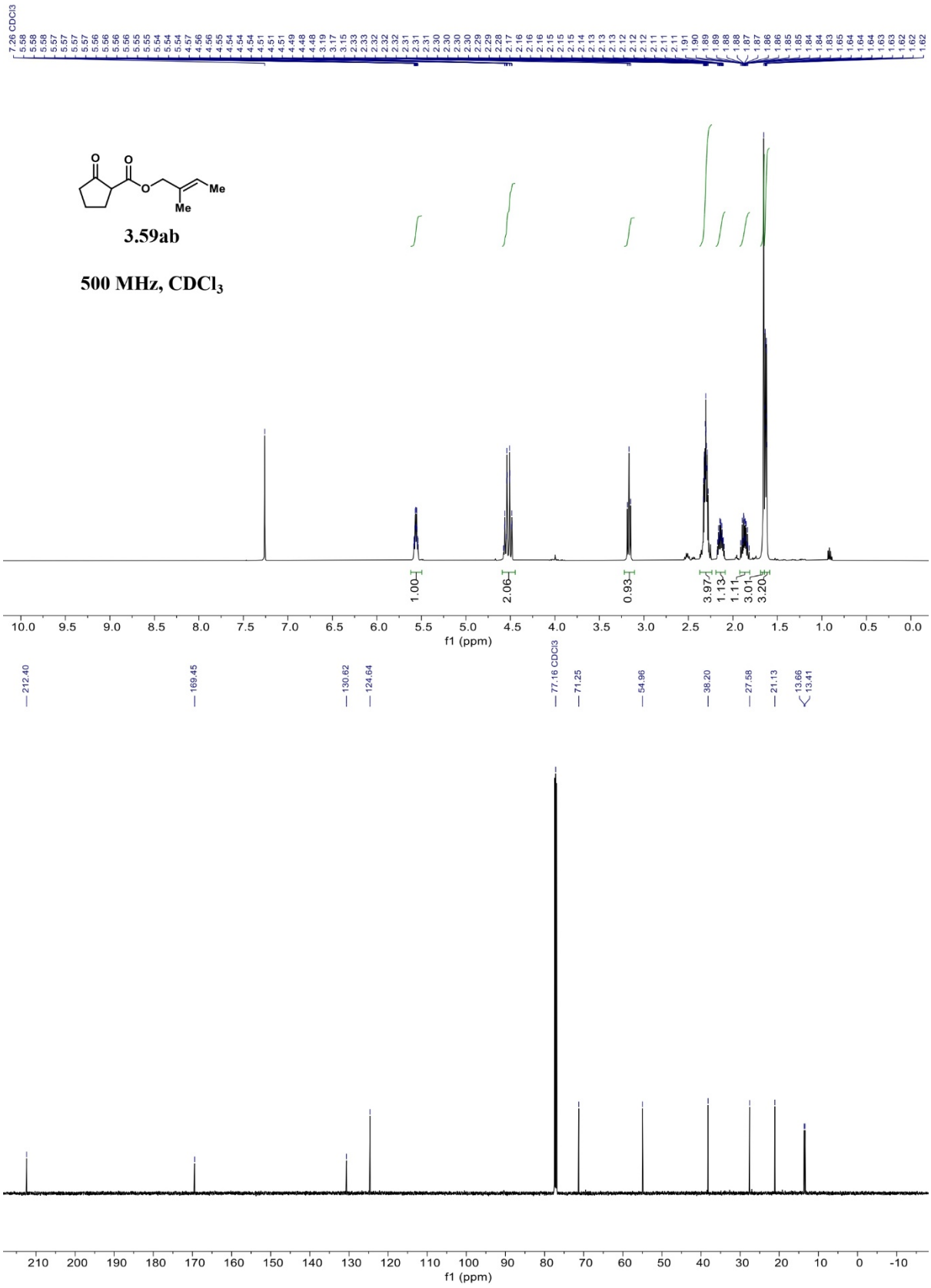
400 MHz, $CDCl_3$

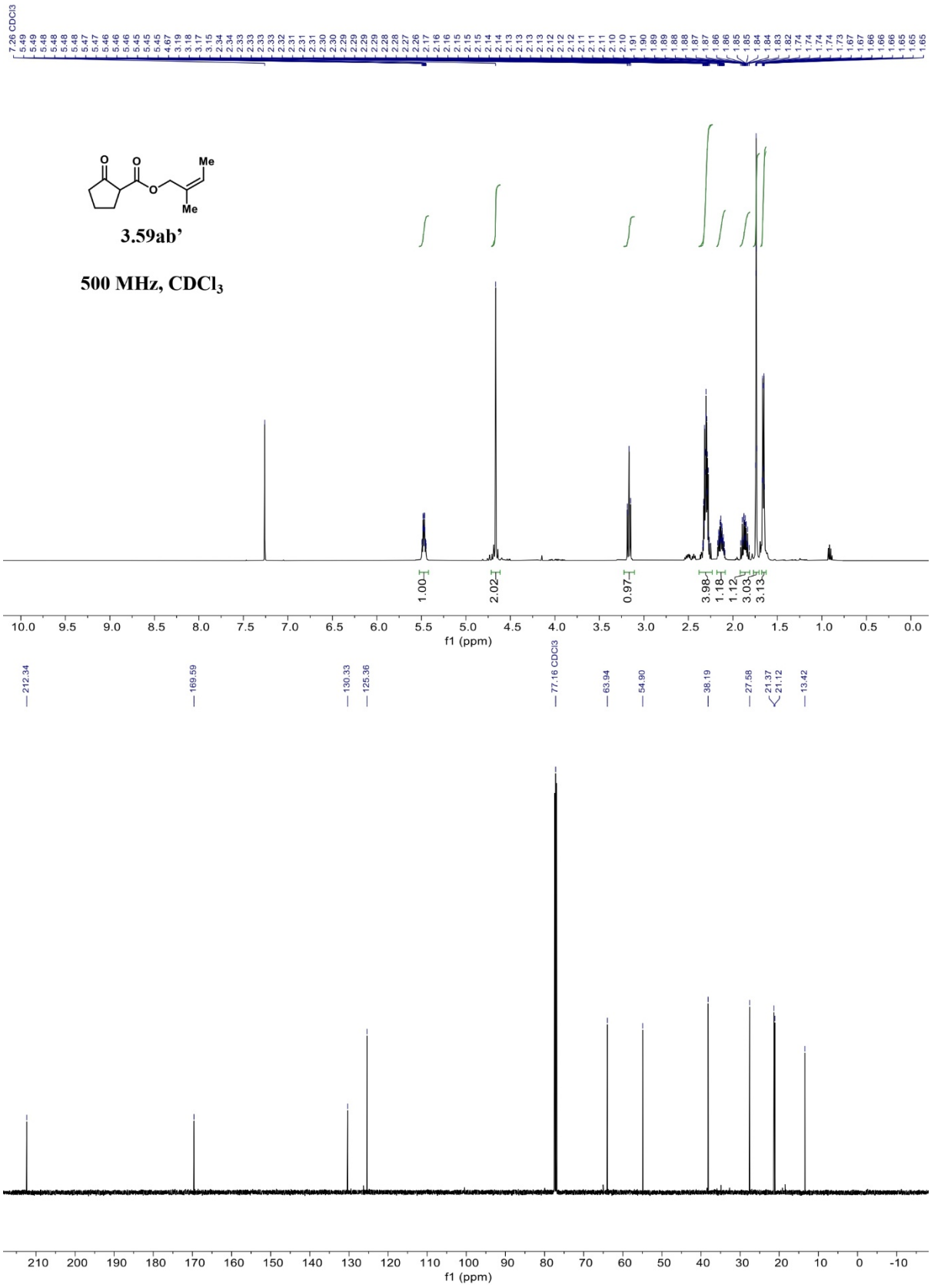


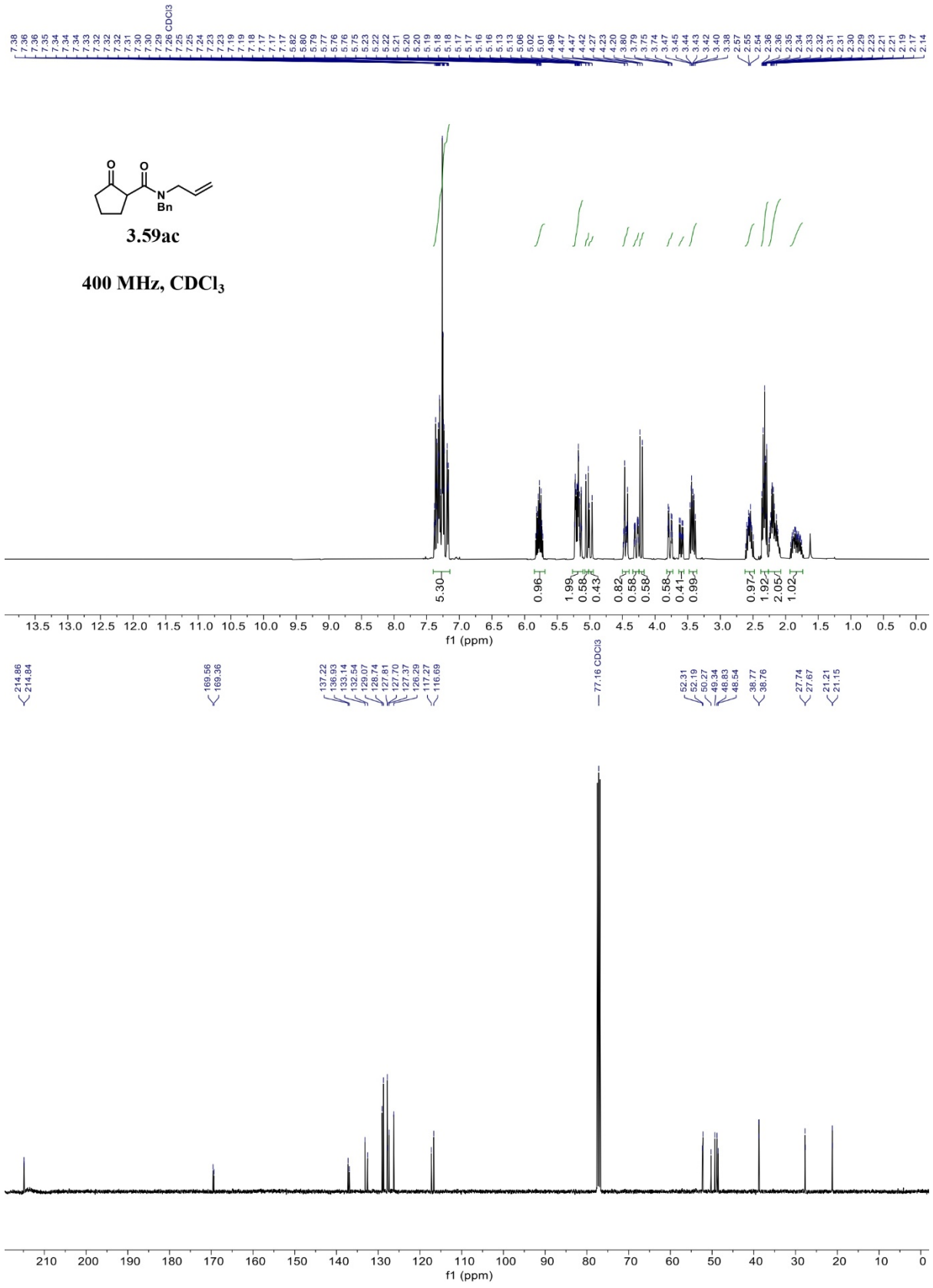

3.59y
400 MHz, CDCl3
f1 (ppm)
f1 (ppm)

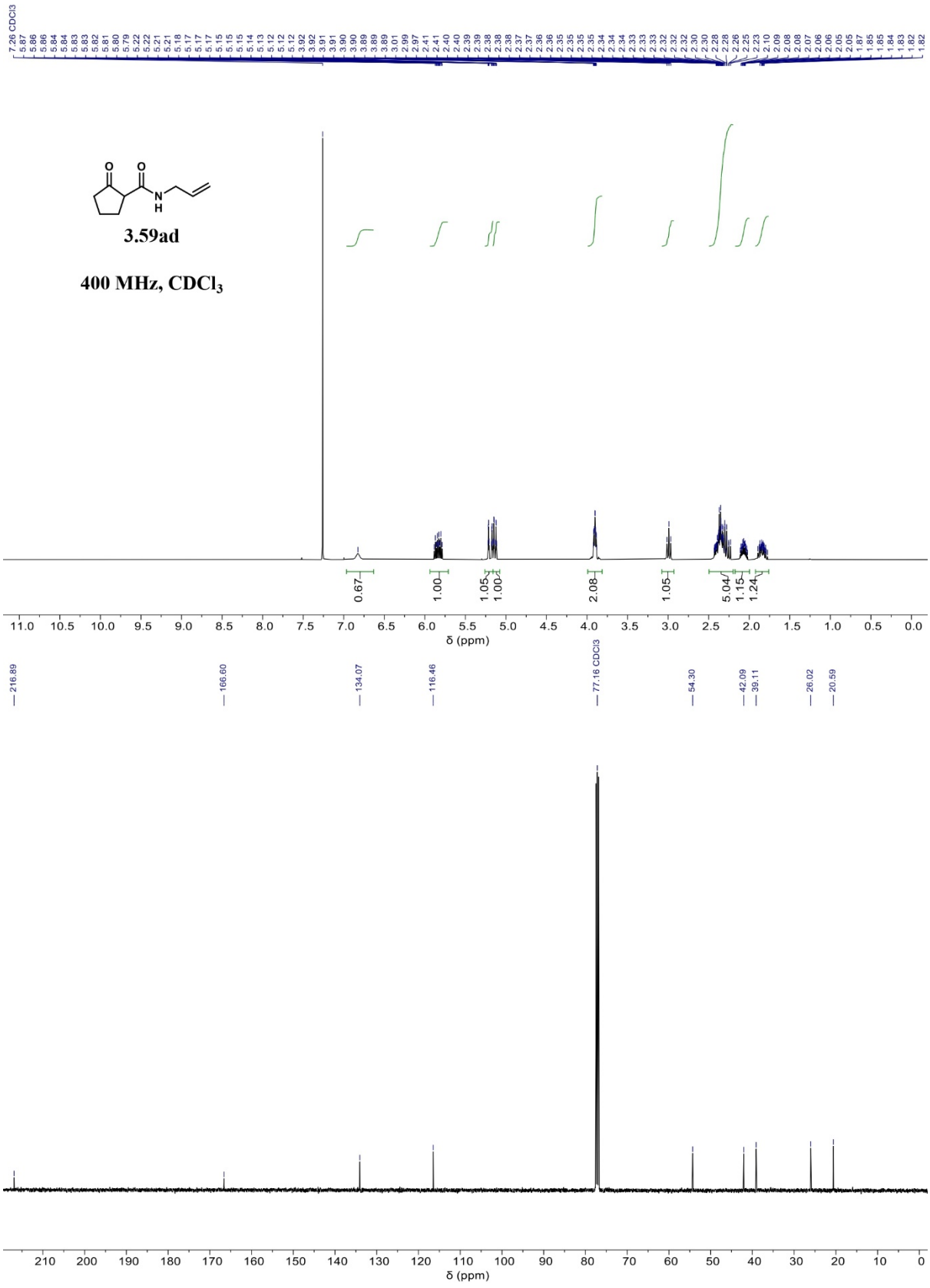

7.26 CDCl3
O
O
O
Me
Me
3.59z
500 MHz, CDCl3
1.00
2.05
0.92
4.06
1.15
1.22
3.22
3.09
f1 (ppm)
212.50
169.59
139.59
118.39
77.16 CDCl3
62.47
54.93
38.22
27.58
25.91
21.12
18.20
f1 (ppm)

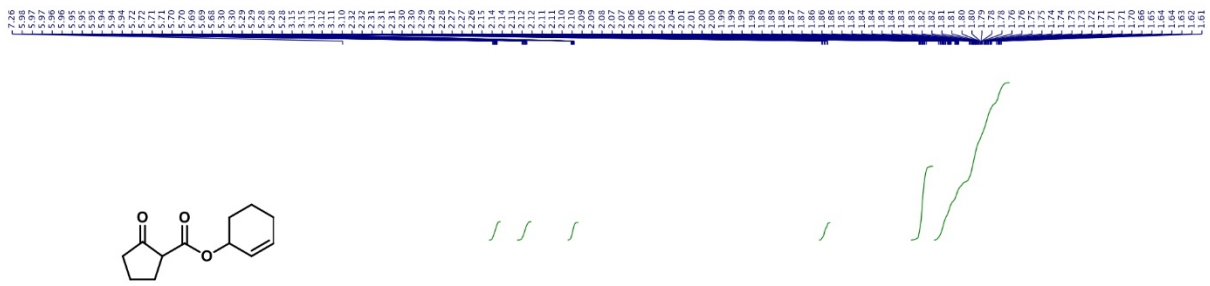

3.59aa
400 MHz, CDCl3
f1 (ppm)
f1 (ppm)


7.26 CDCl3
Me
Me
3.59ab
500 MHz, CDCl3
1.00
2.06
0.93
3.97
1.13
1.11
3.01
3.20
f1 (ppm)
212.40
169.45
130.62
124.64
77.16 CDCl3
71.25
54.96
38.20
27.58
21.13
13.66
13.41
f1 (ppm)


7.26 CDCl3
Me
Me
3.59ab'
500 MHz, CDCl3
1.00
2.02
0.97
3.98
1.18
1.12
3.03
3.13
f1 (ppm)
212.34
169.59
130.33
125.36
77.16 CDCl3
63.94
54.90
38.19
27.58
21.37
21.12
13.42
f1 (ppm)

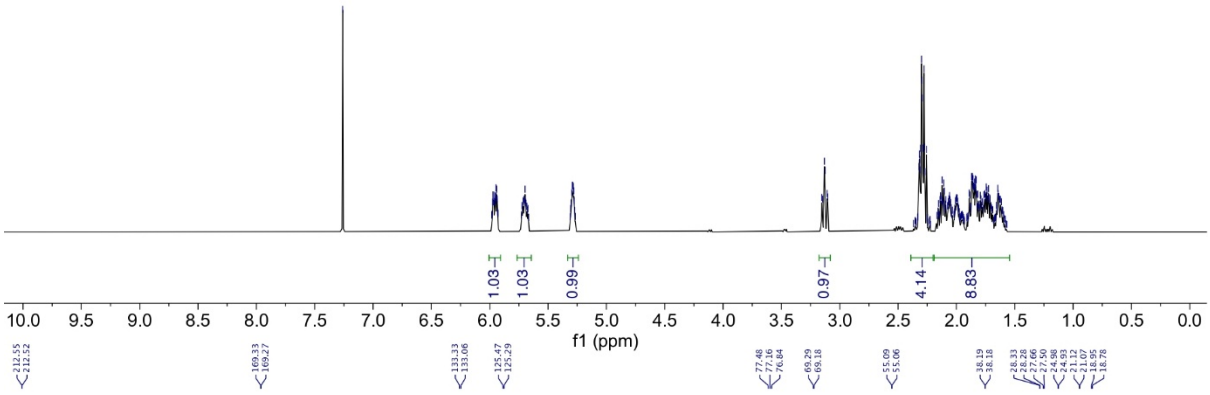

3.59ac
400 MHz, CDCl3
f1 (ppm)
f1 (ppm)

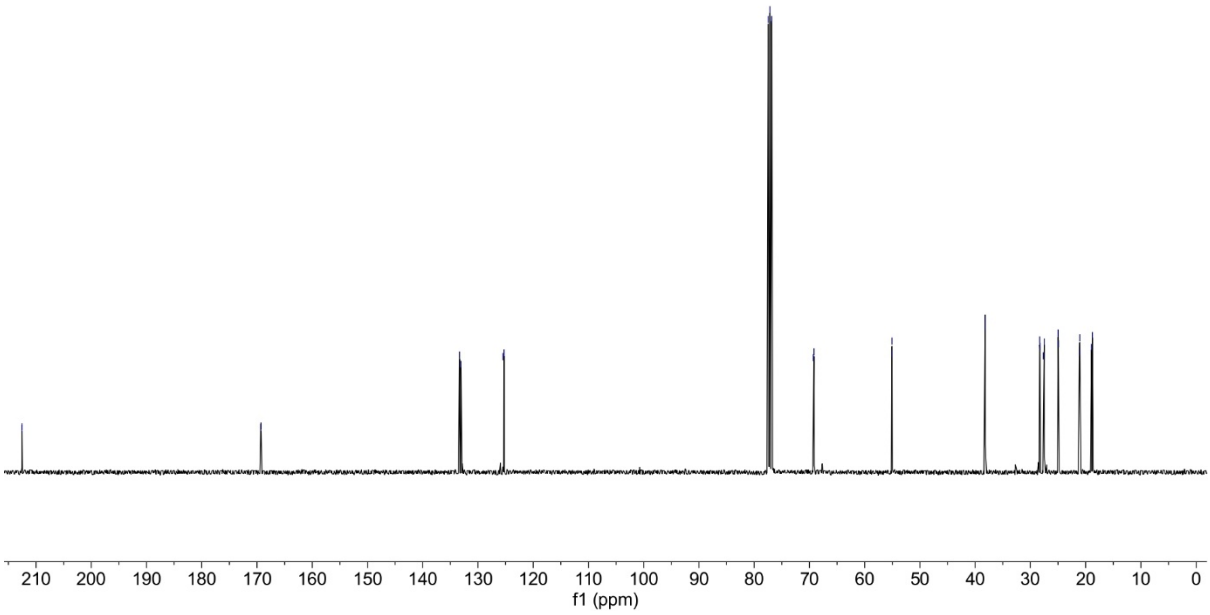

3.59ad
400 MHz, CDCl3
δ (ppm)
δ (ppm)

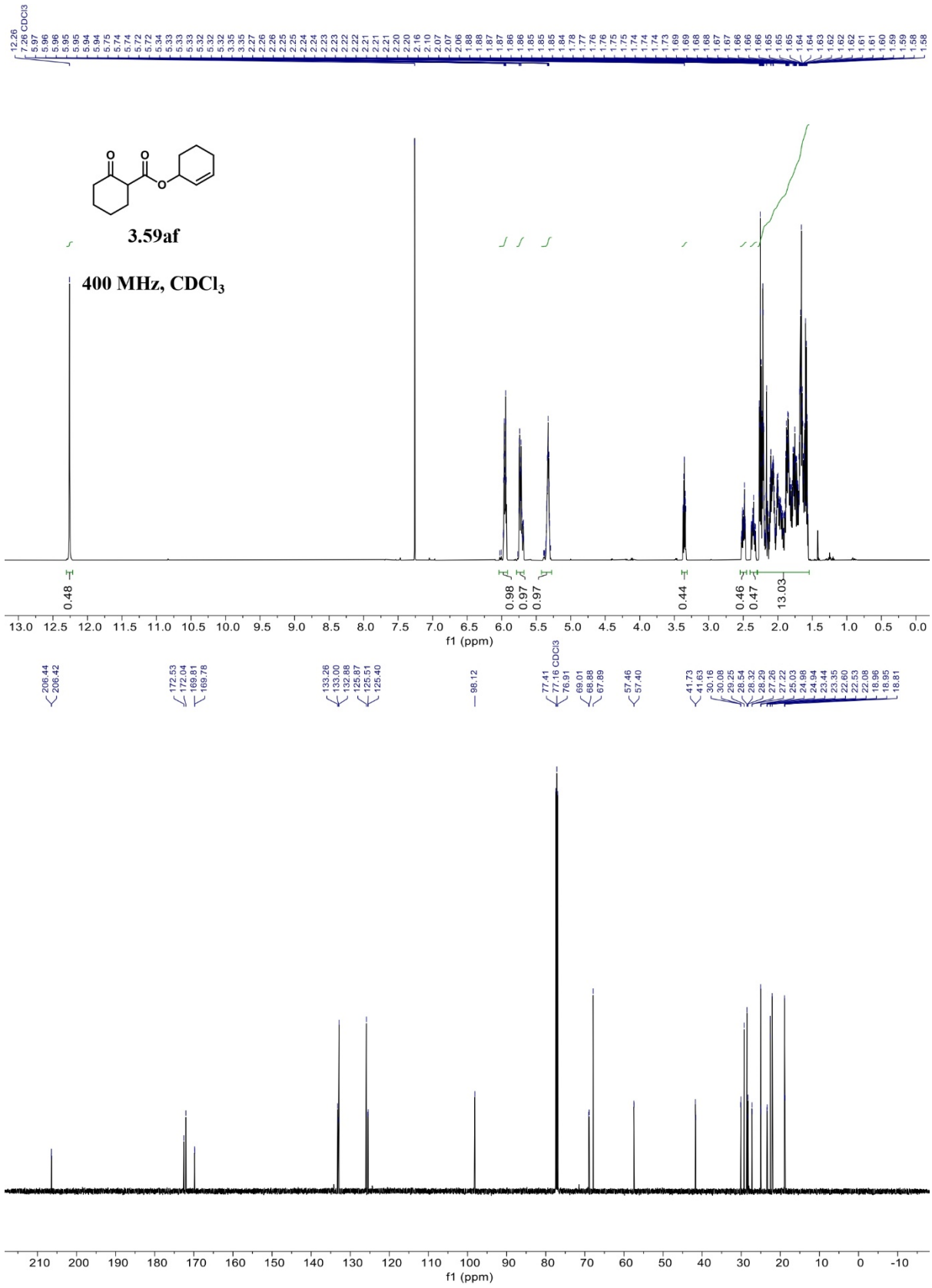


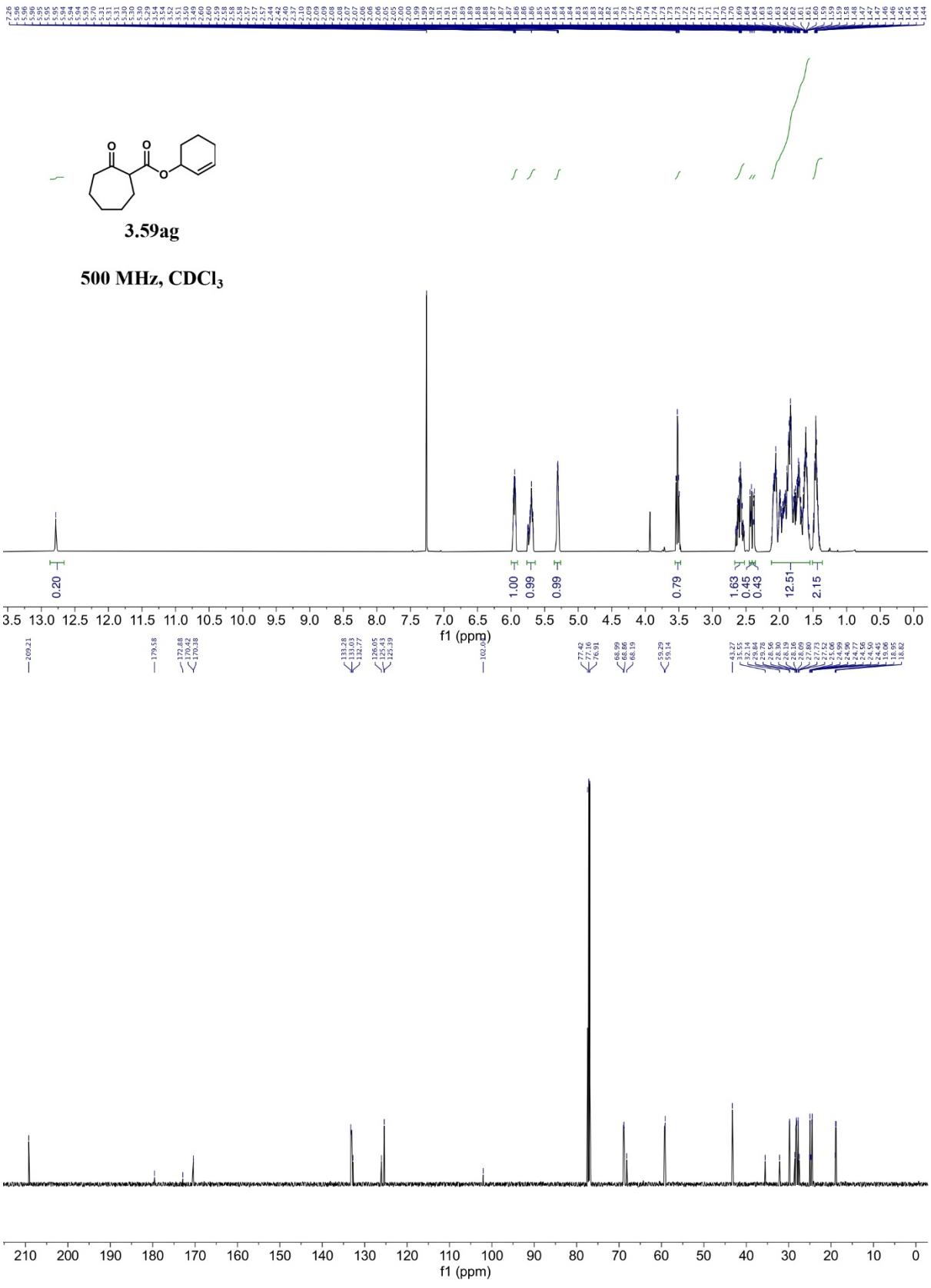
3.59ae

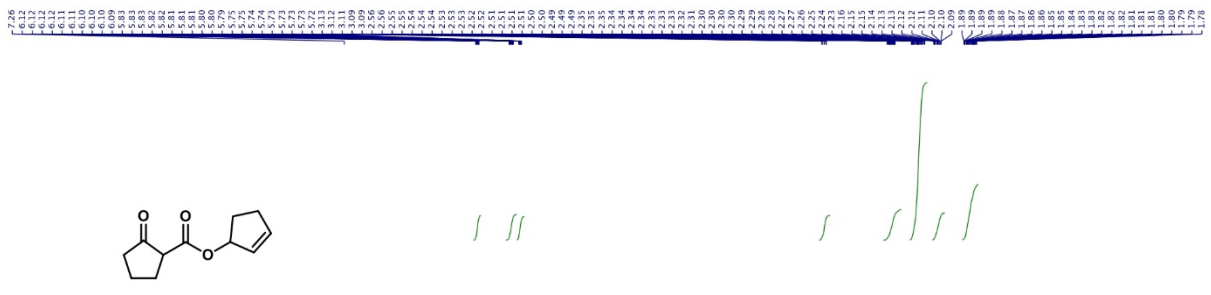
400 MHz, $CDCl_3$





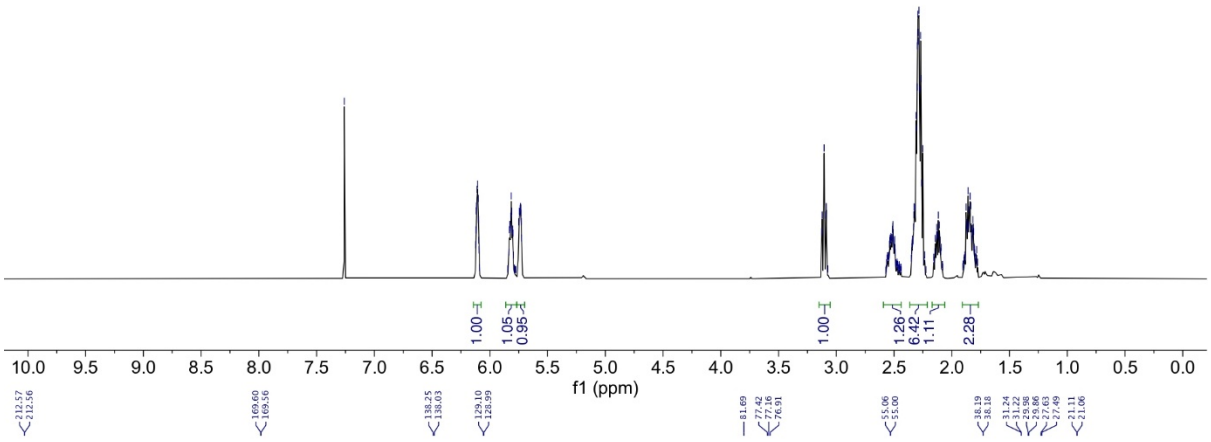

3.59af
400 MHz, $CDCl_3$
f1 (ppm)

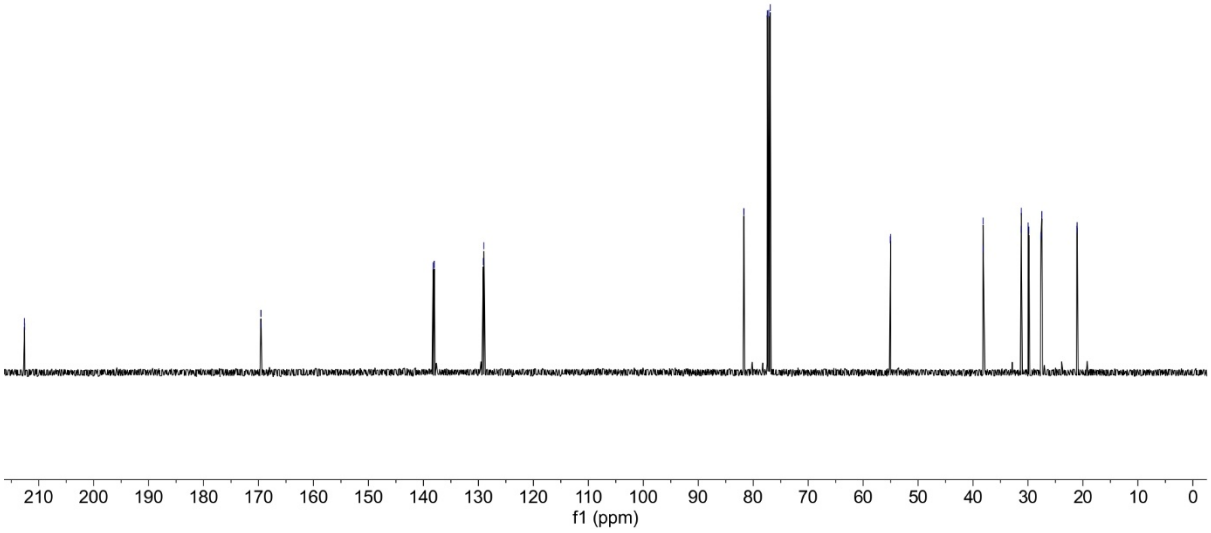

3.59ag
500 MHz, CDCl3
f1 (ppm)
f1 (ppm)

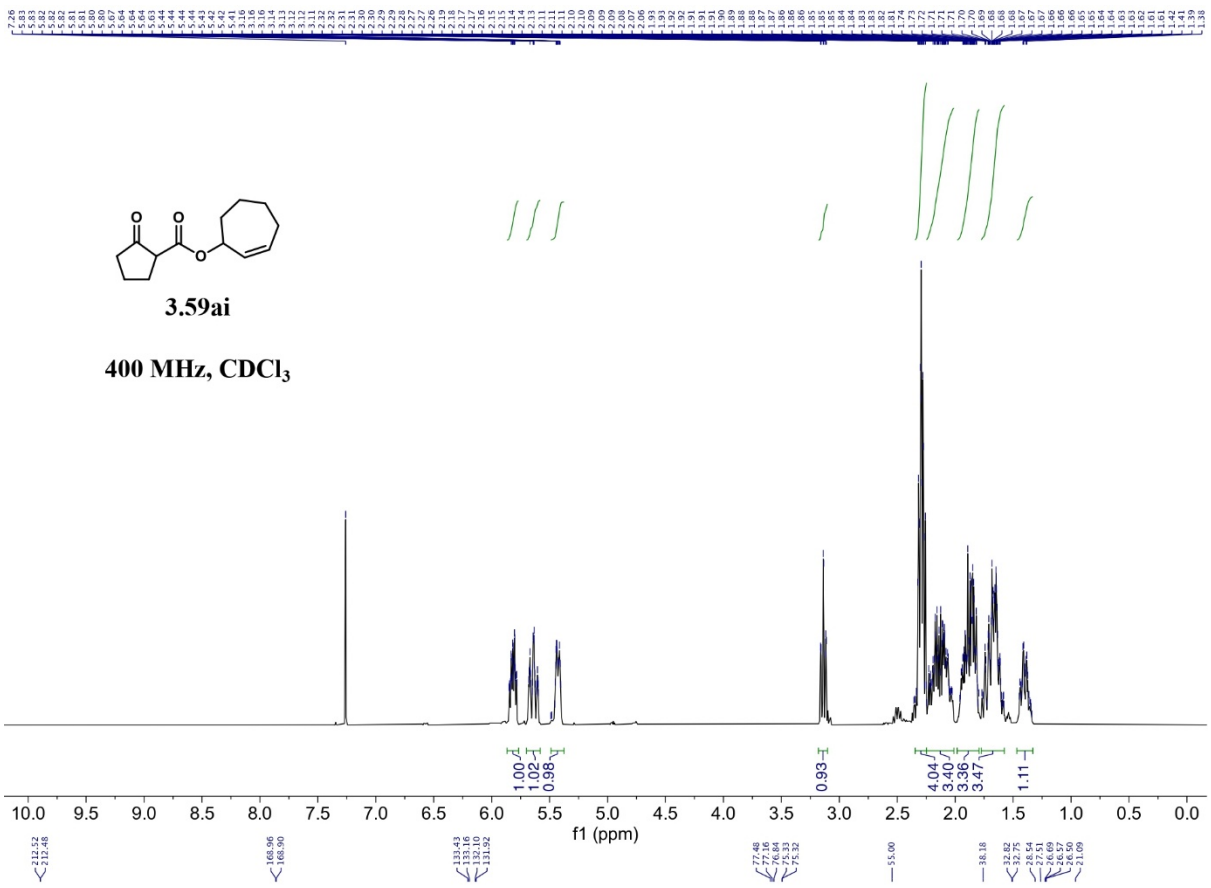


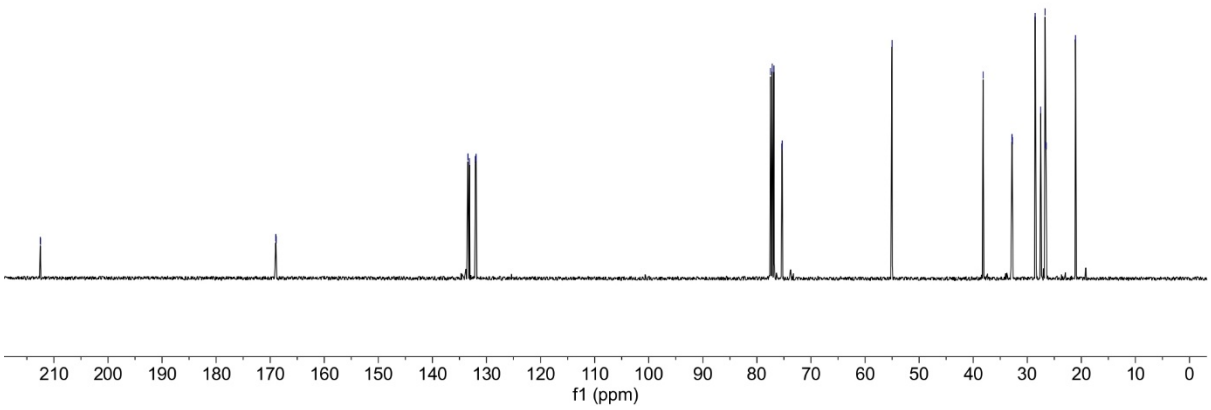
3.59ah

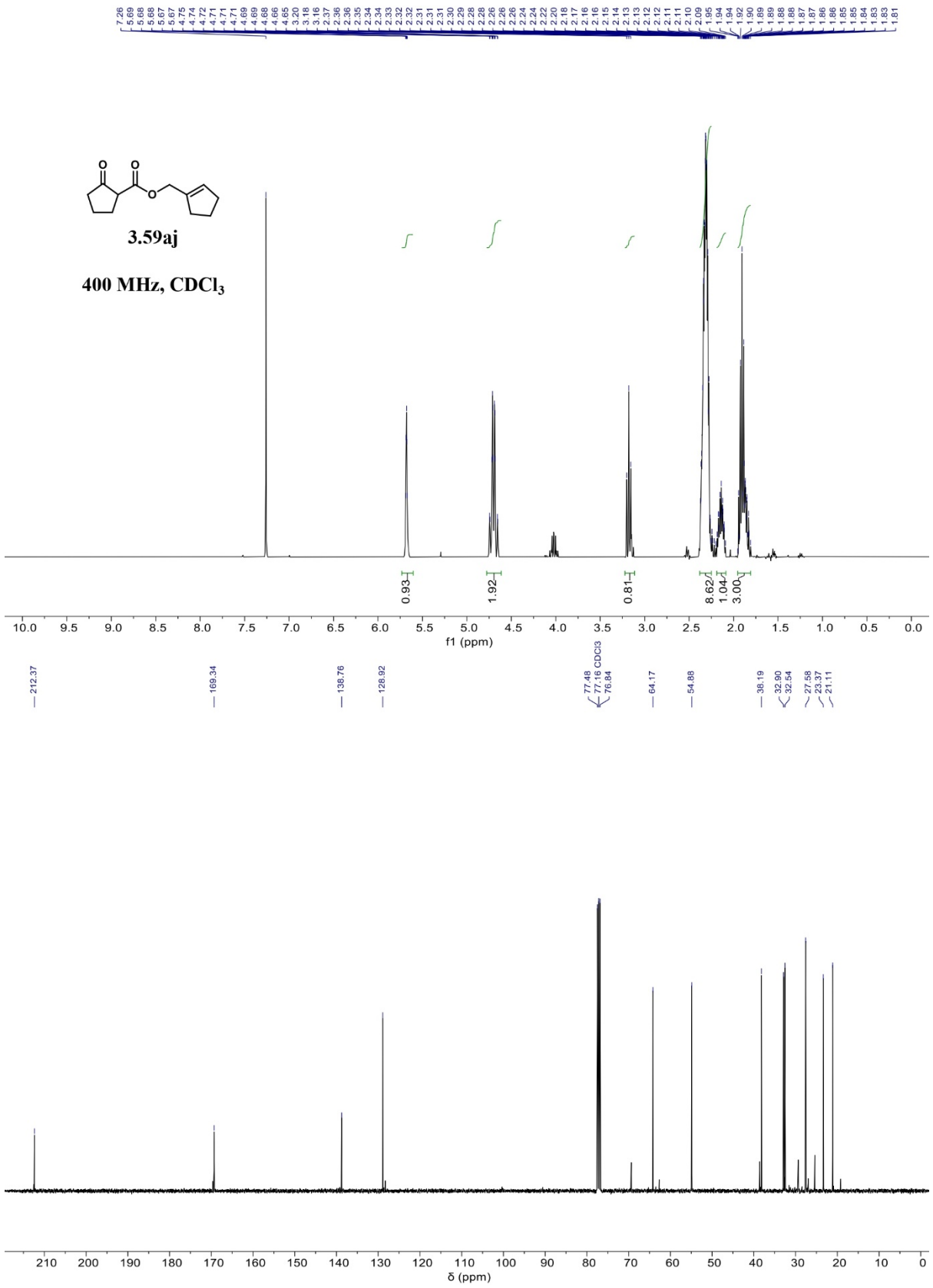
500 MHz, $CDCl_3$

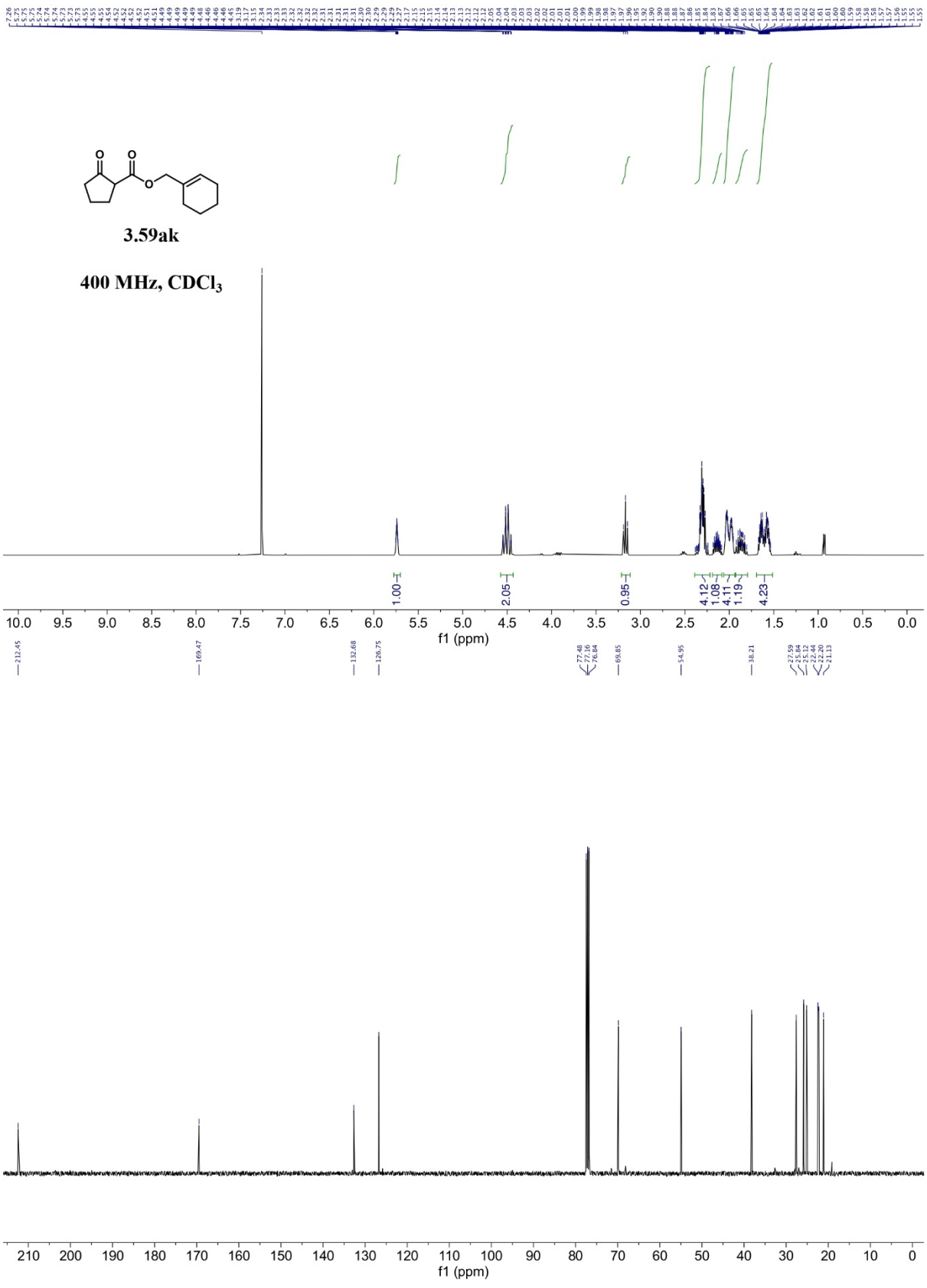


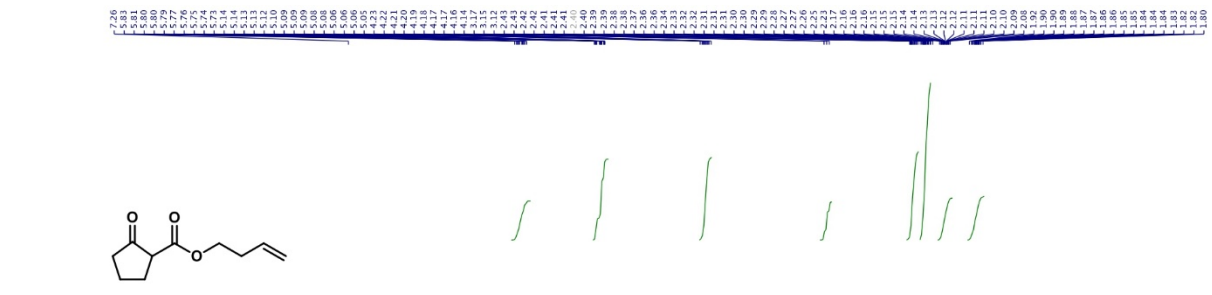



3.59ai
400 MHz, CDCl3
f1 (ppm)


f1 (ppm)

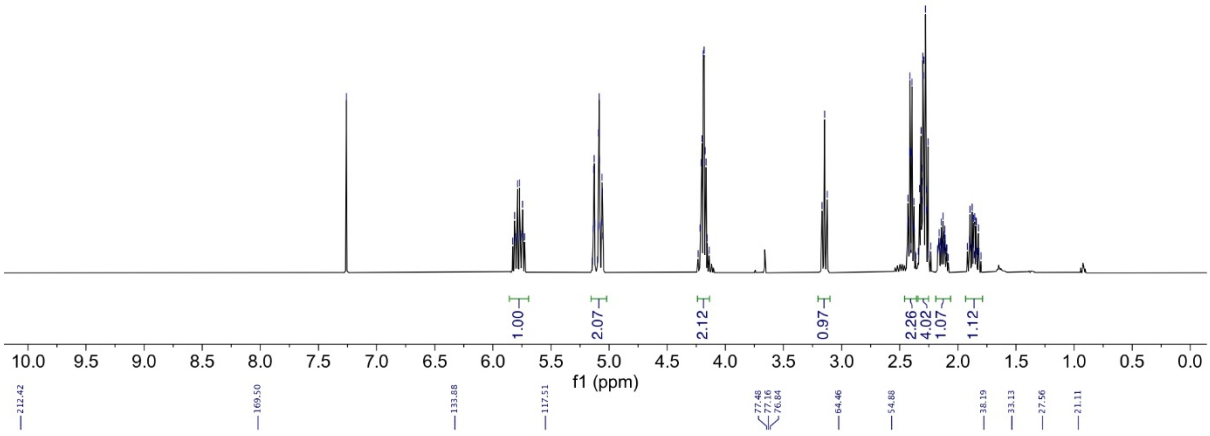

3.59aj
400 MHz, CDCl3
0.93
1.92
0.81
8.62
1.04
3.00
f1 (ppm)
212.37
169.34
138.76
128.92
77.48
77.16 CDCl3
76.84
64.17
54.88
38.19
32.90
32.54
27.58
23.37
21.11
δ (ppm)

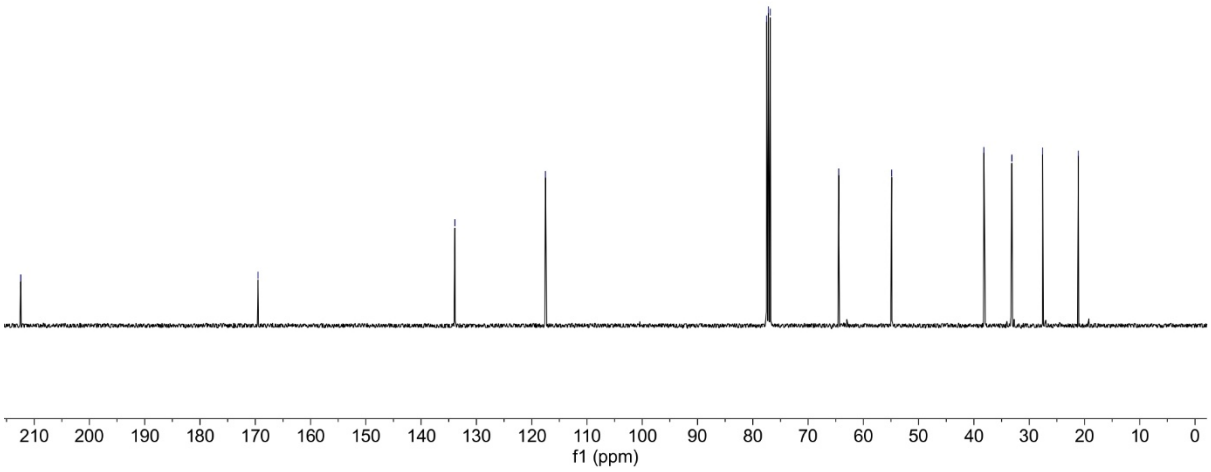

3.59ak
400 MHz, CDCl3
f1 (ppm)

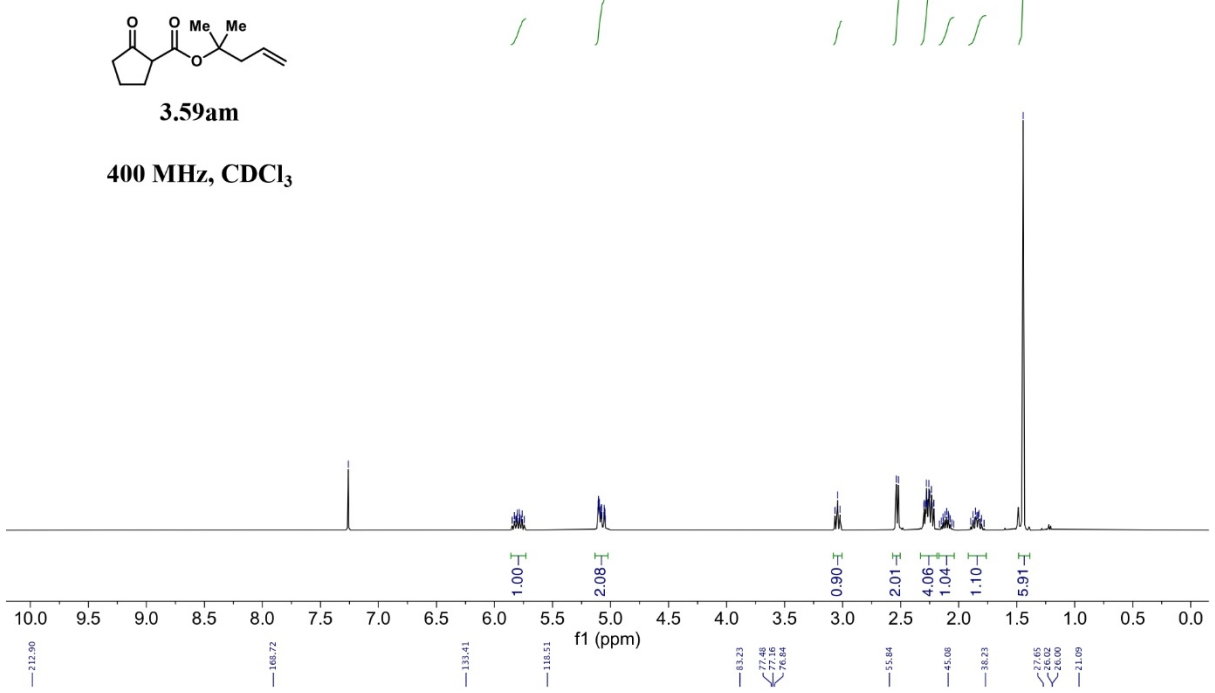


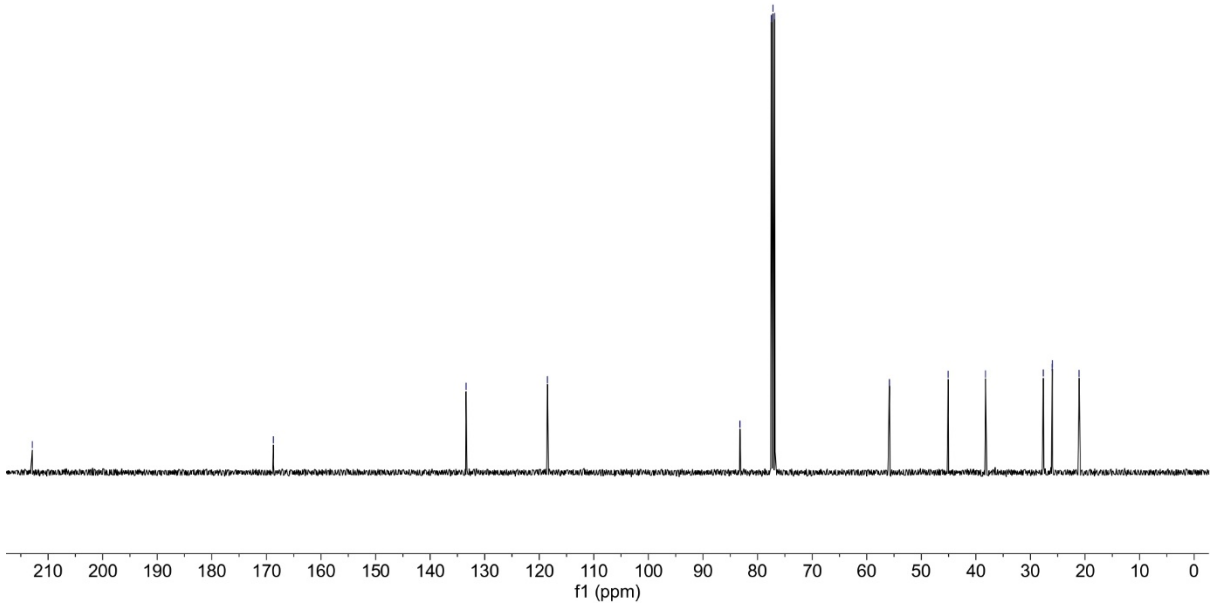
3.59al

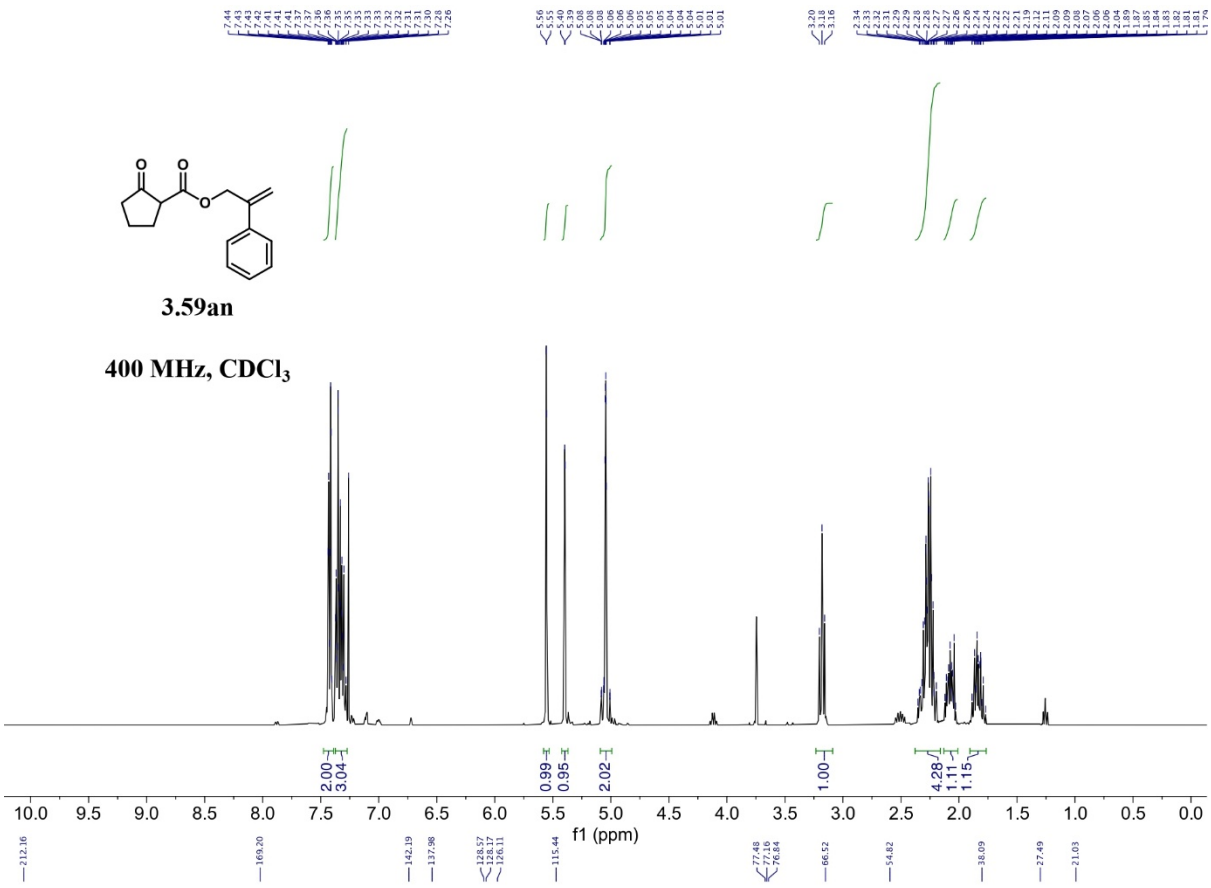
400 MHz, $CDCl_3$





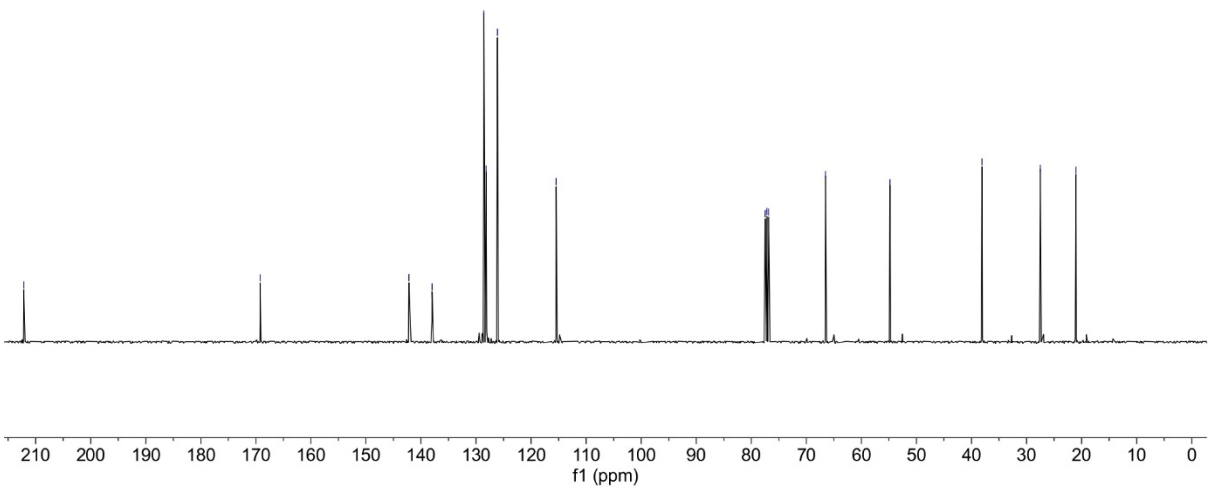

7.26
5.85 5.83 5.82 5.81 5.81 5.80 5.79 5.78 5.78 5.77 5.76 5.74
5.11 5.11 5.10 5.10 5.10 5.09 5.09 5.08 5.08 5.08 5.07 5.06 5.05 5.05 5.05 5.05
3.07 3.04 3.02
2.54 2.52
2.30 2.30 2.29 2.29 2.28 2.28 2.27 2.26 2.26 2.25 2.23 2.23 2.21 2.15 2.14 2.13 2.12 2.10 2.10 2.09 2.09 2.07 1.90 1.88 1.86 1.85 1.84 1.83 1.82 1.81 1.81 1.80 1.44
O
O
Me
Me
O
3.59am
400 MHz, CDCl3
1.00
2.08
0.90
2.01
4.06
1.04
1.10
5.91
10.0 9.5 9.0 8.5 8.0 7.5 7.0 6.5 6.0 5.5 5.0 4.5 4.0 3.5 3.0 2.5 2.0 1.5 1.0 0.5 0.0
f1 (ppm)

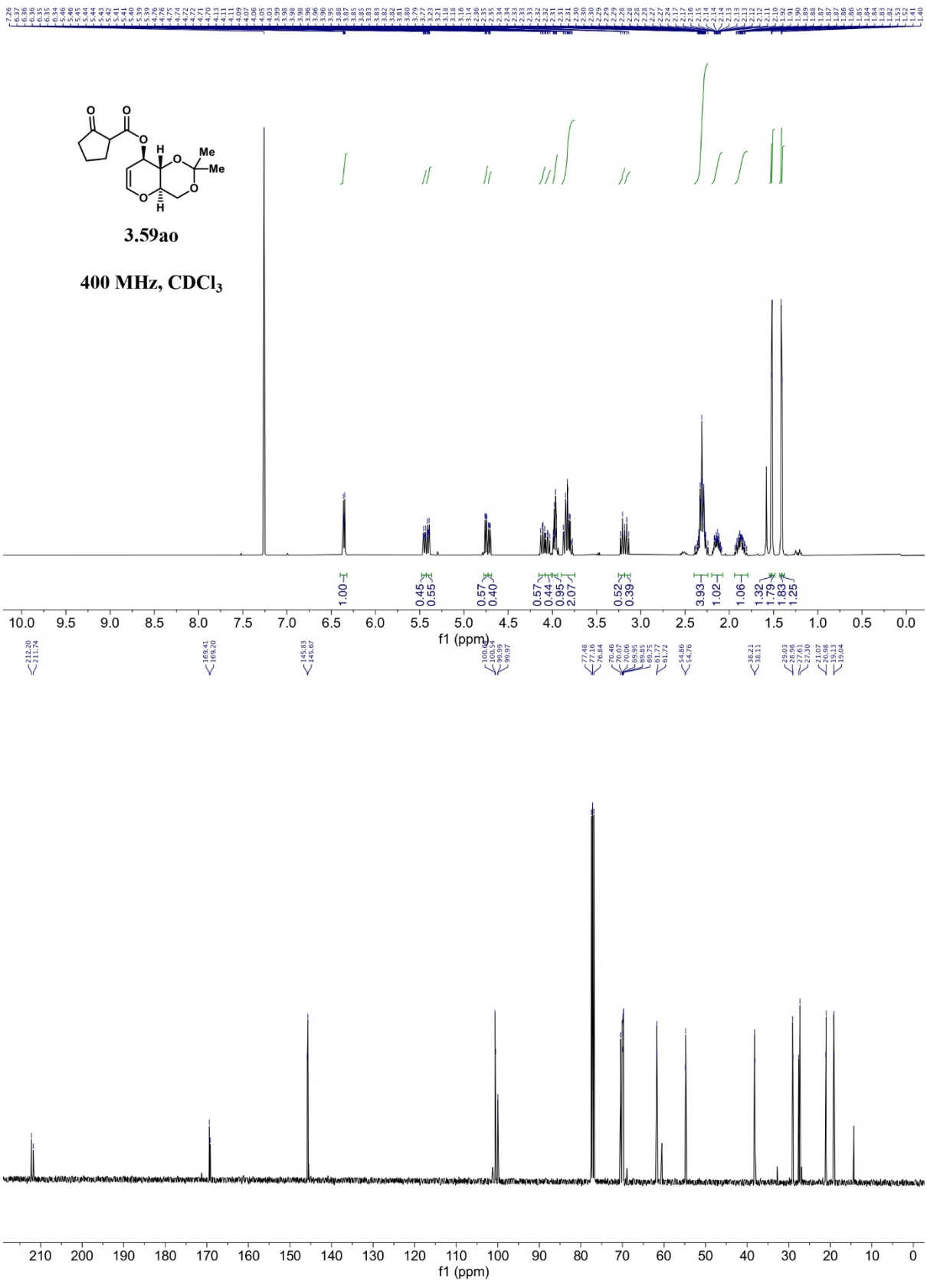

212.90
168.72
133.41
118.51
83.23
77.48
77.16
76.84
55.84
45.08
38.23
27.65
26.02
26.00
21.09
210 200 190 180 170 160 150 140 130 120 110 100 90 80 70 60 50 40 30 20 10 0
f1 (ppm)

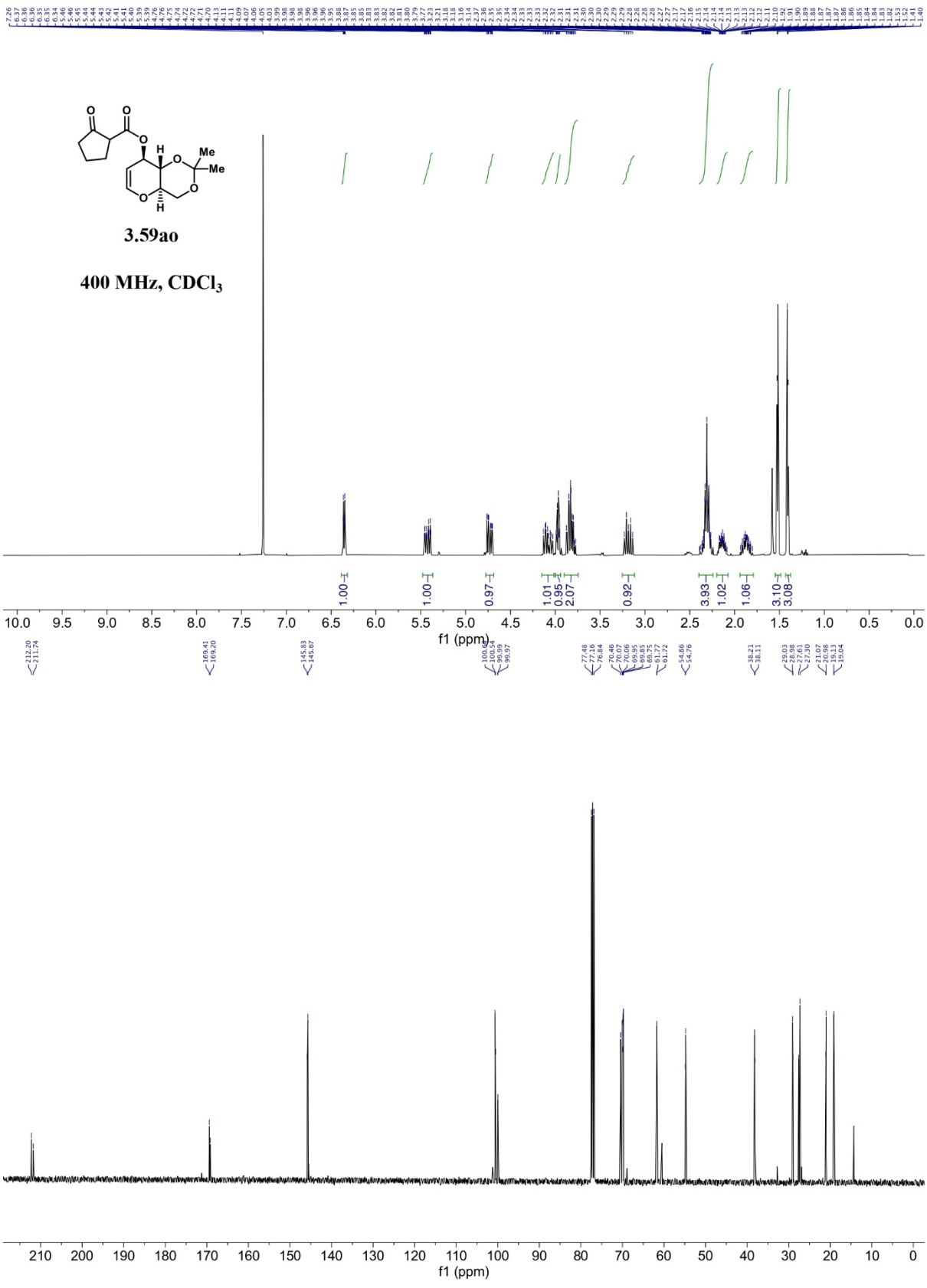


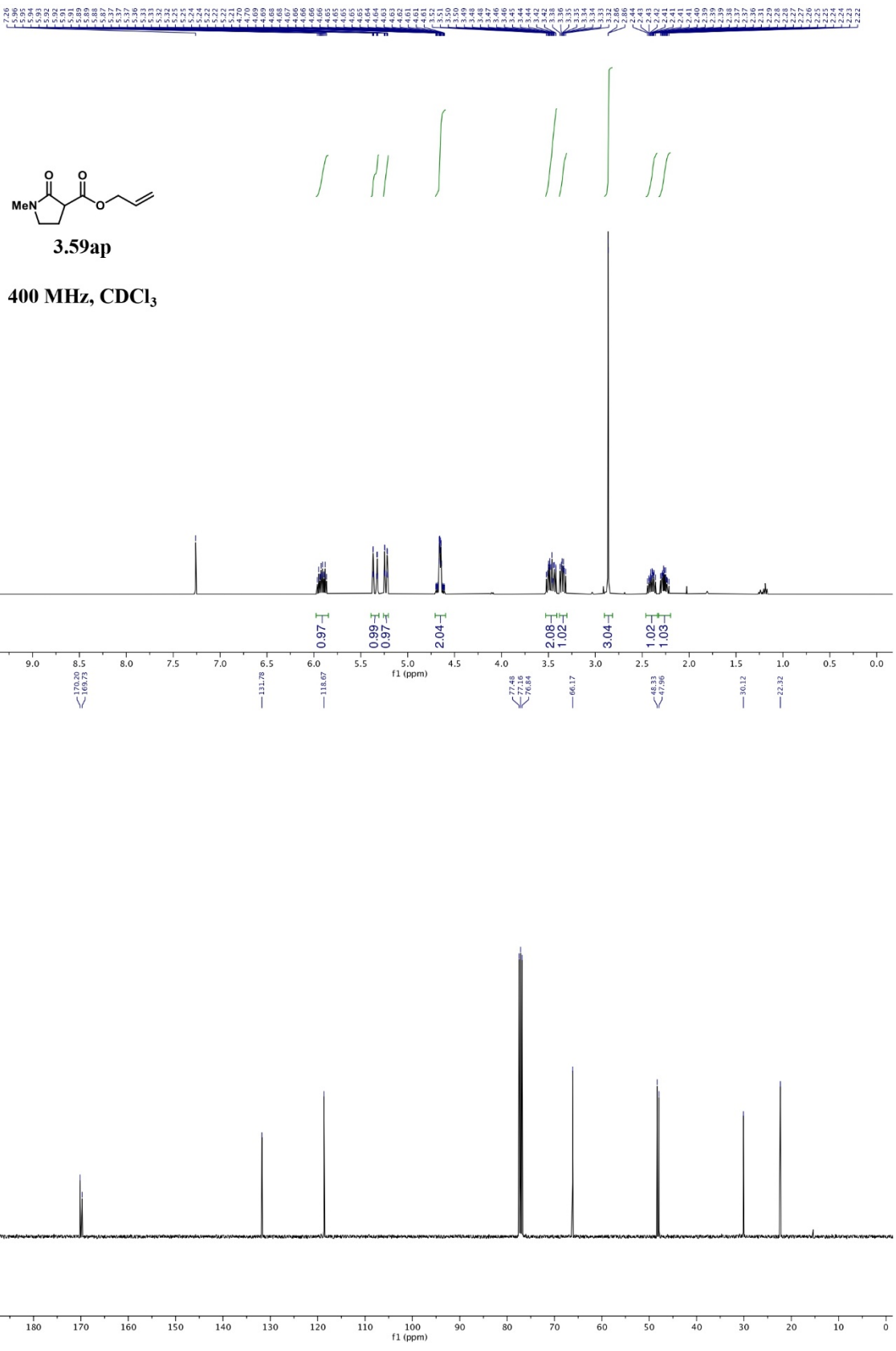
3.59an

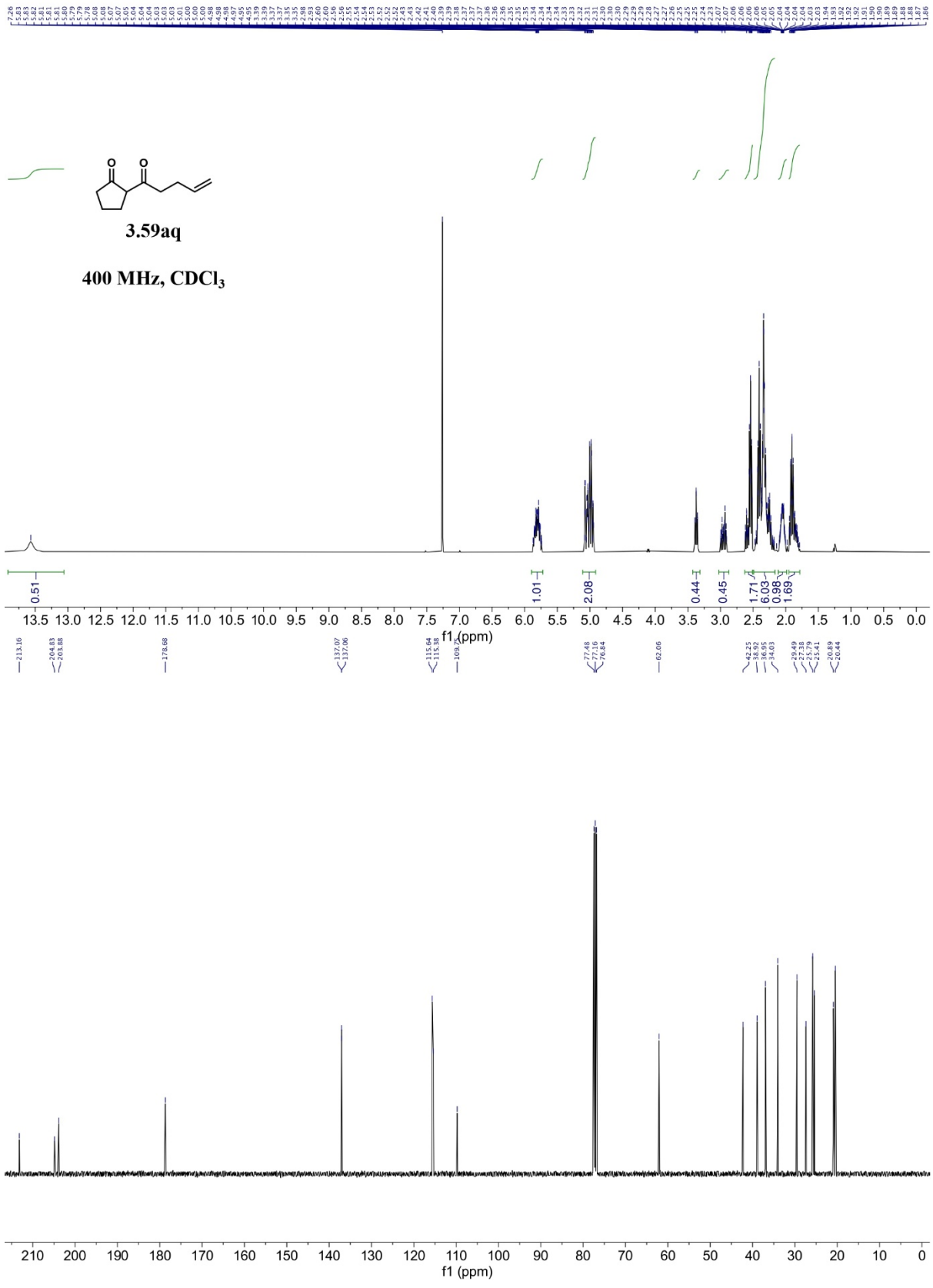
400 MHz, $CDCl_3$

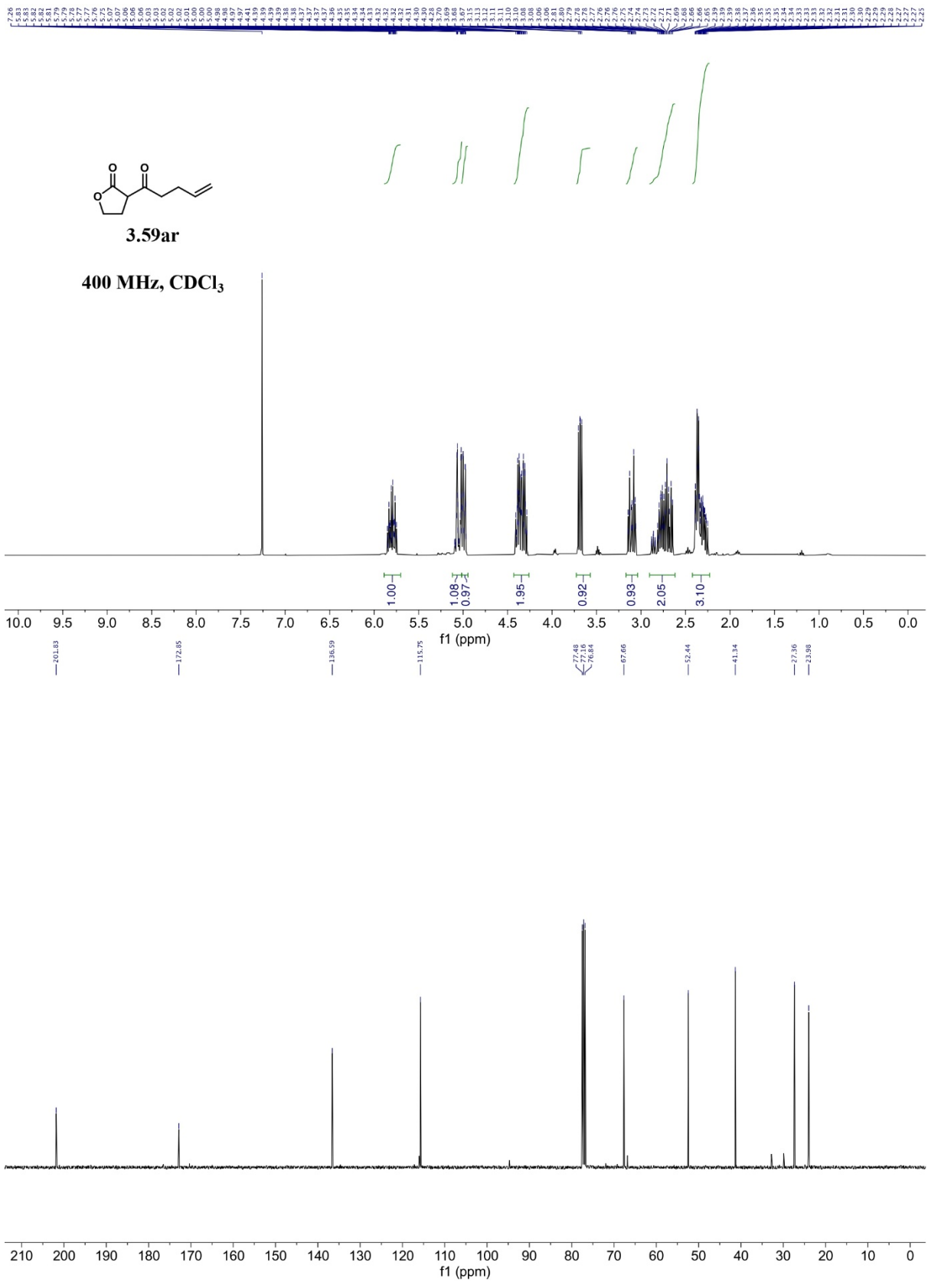


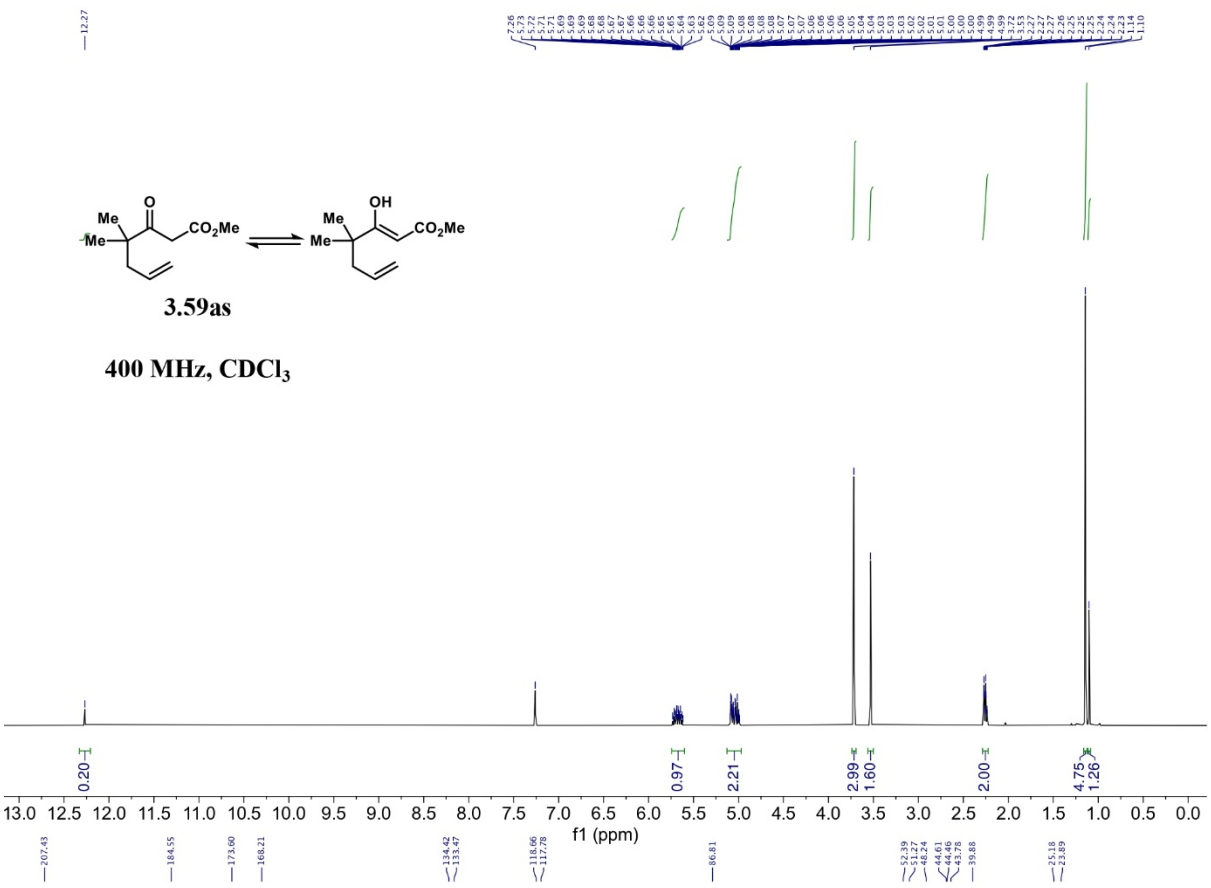

3.59ao
400 MHz, CDCl3
f1 (ppm)
f1 (ppm)

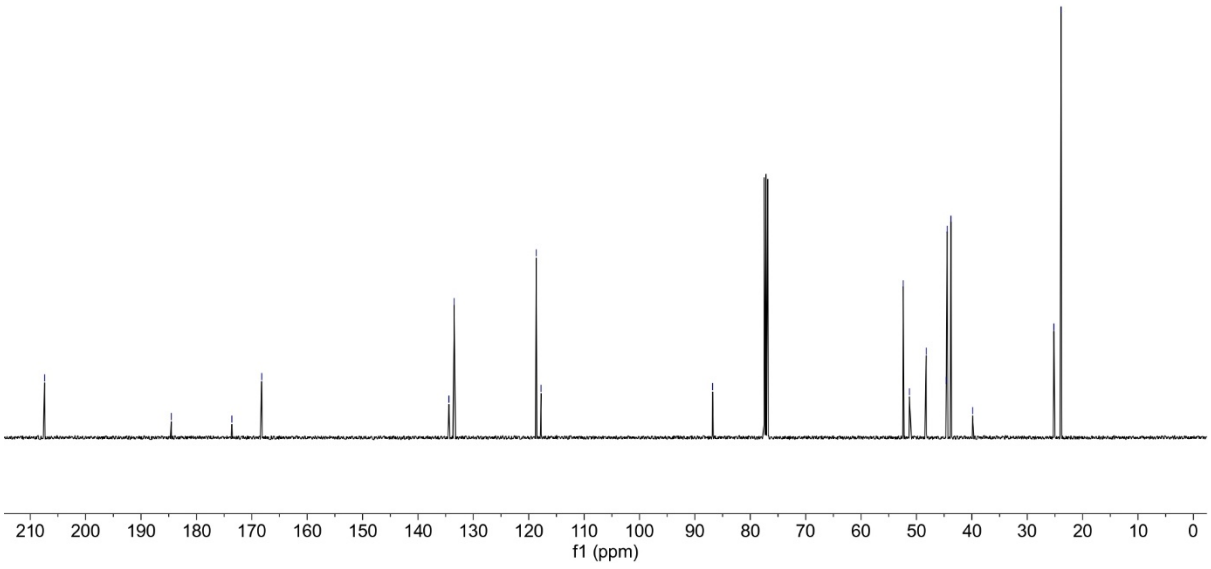

3.59ao
400 MHz, CDCl3
f1 (ppm)
f1 (ppm)

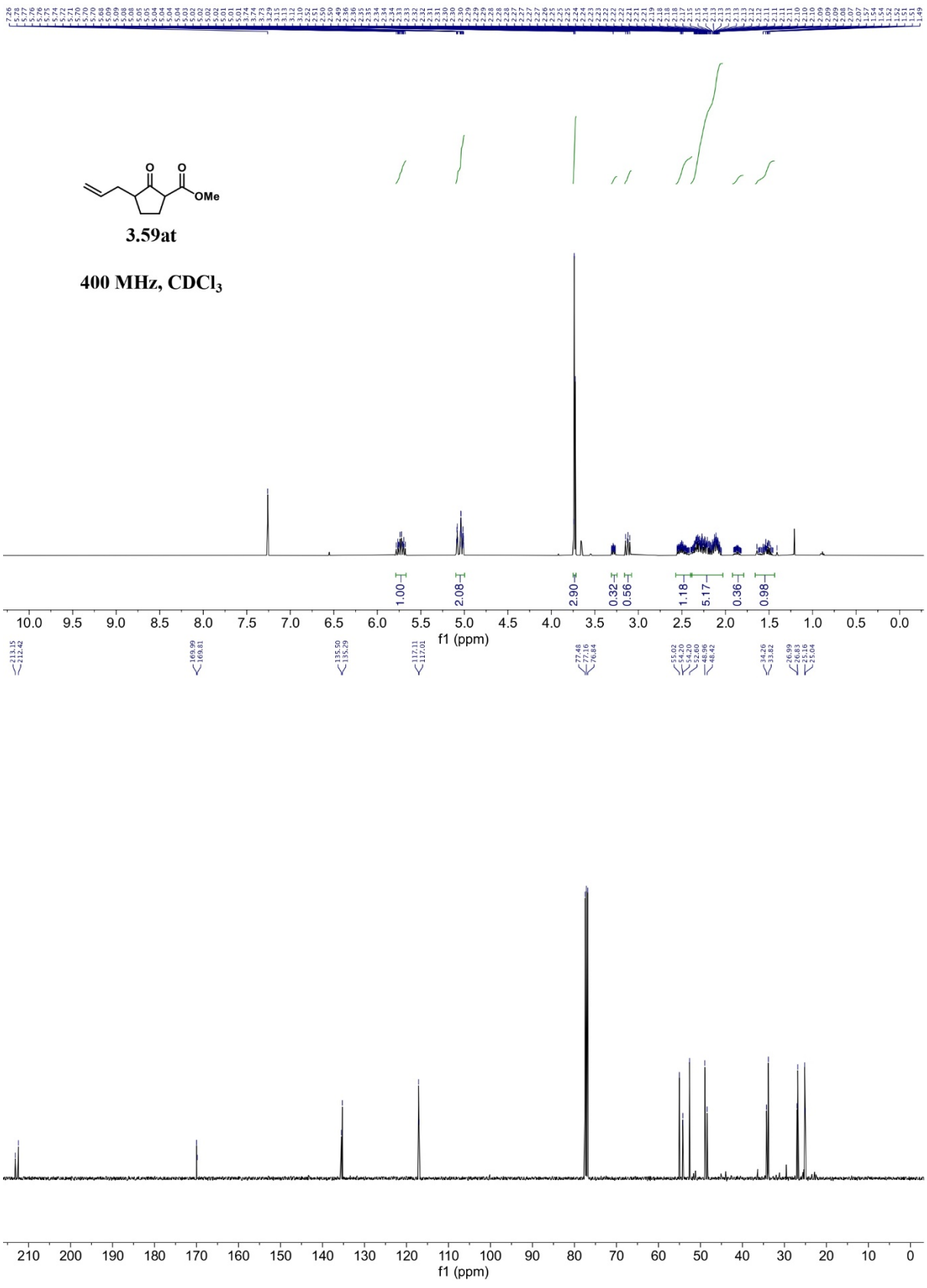

MeN
3.59ap
400 MHz, CDCl3
f1 (ppm)

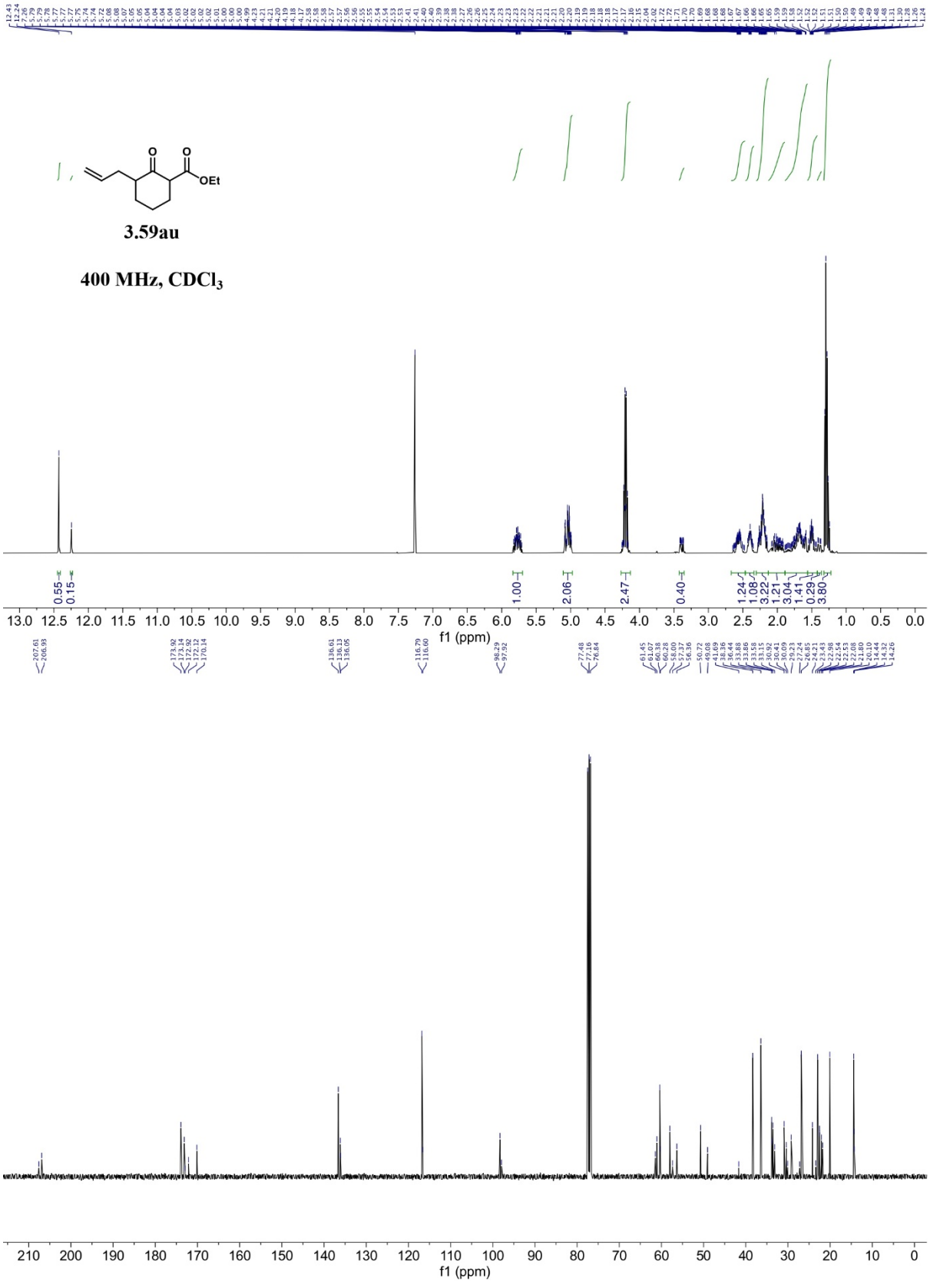

3.59aq
400 MHz, CDCl3
f1 (ppm)

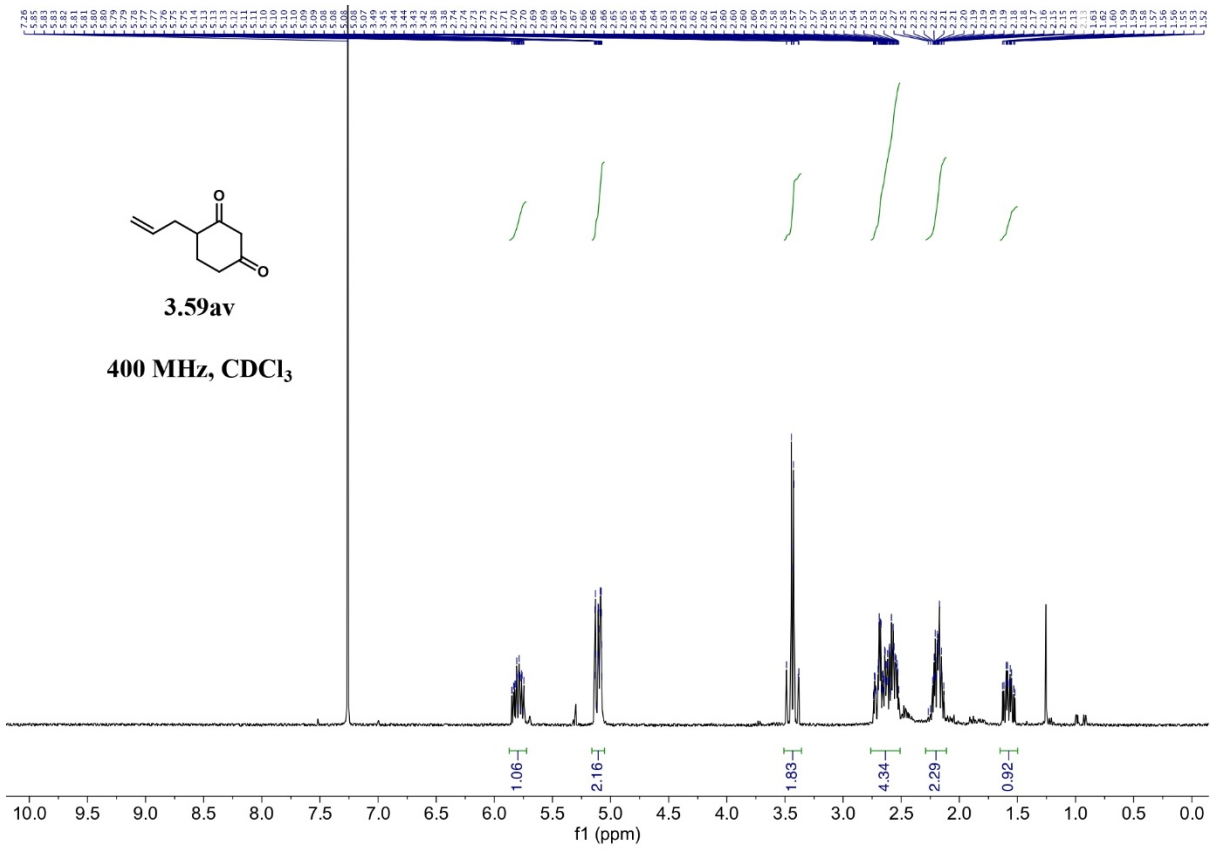

3.59ar
400 MHz, CDCl3
f1 (ppm)
f1 (ppm)

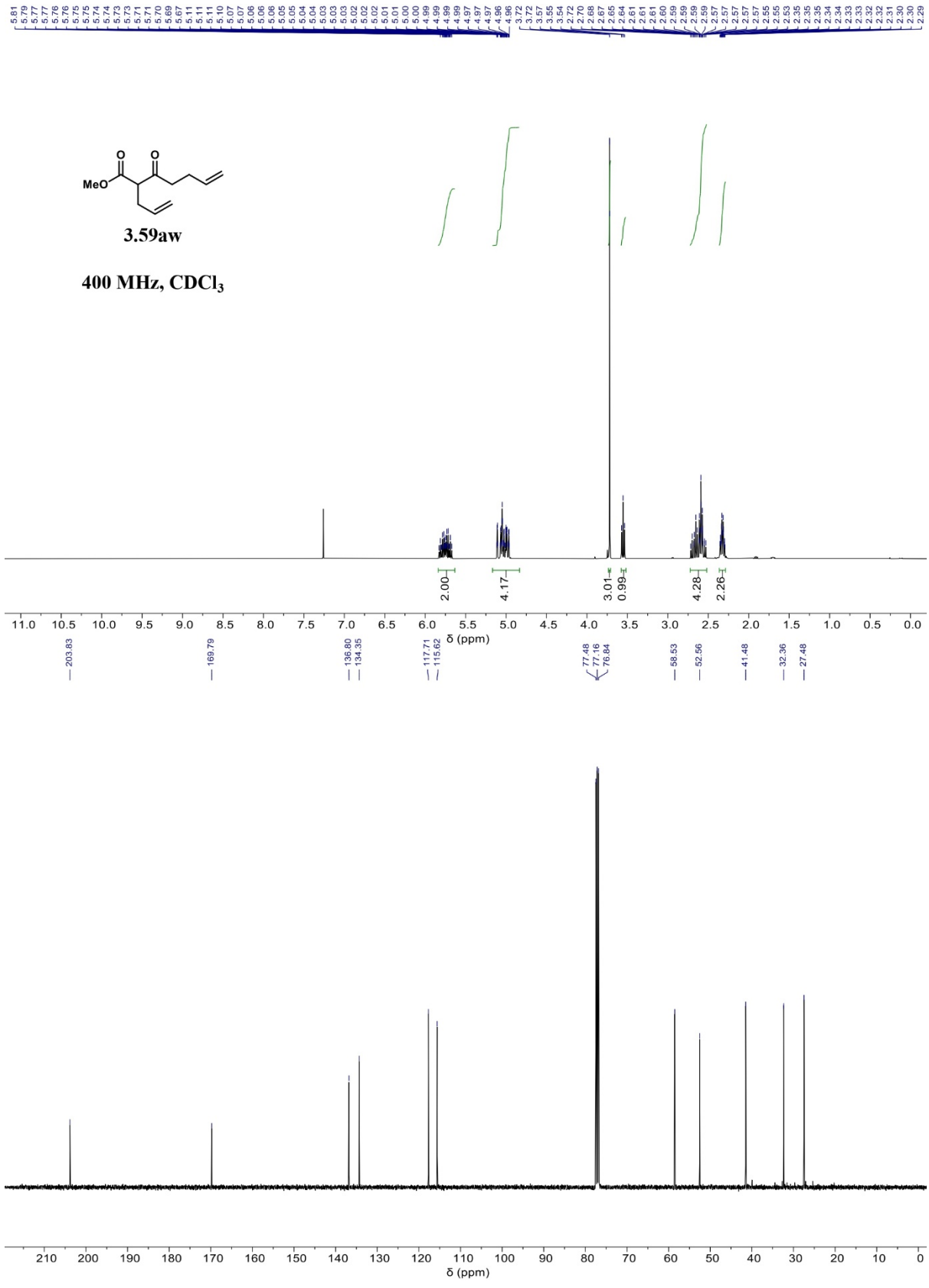

Me
Me
O
CO2Me
Me
Me
OH
CO2Me
3.59as
400 MHz, CDCl3
f1 (ppm)

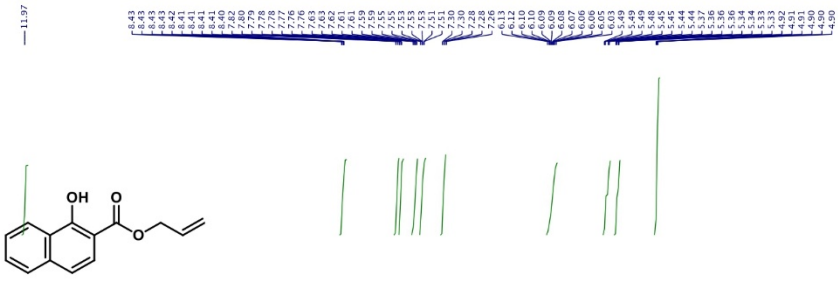

f1 (ppm)


3.59at
400 MHz, CDCl3
f1 (ppm)


OEt
3.59au
400 MHz, CDCl3
f1 (ppm)
f1 (ppm)

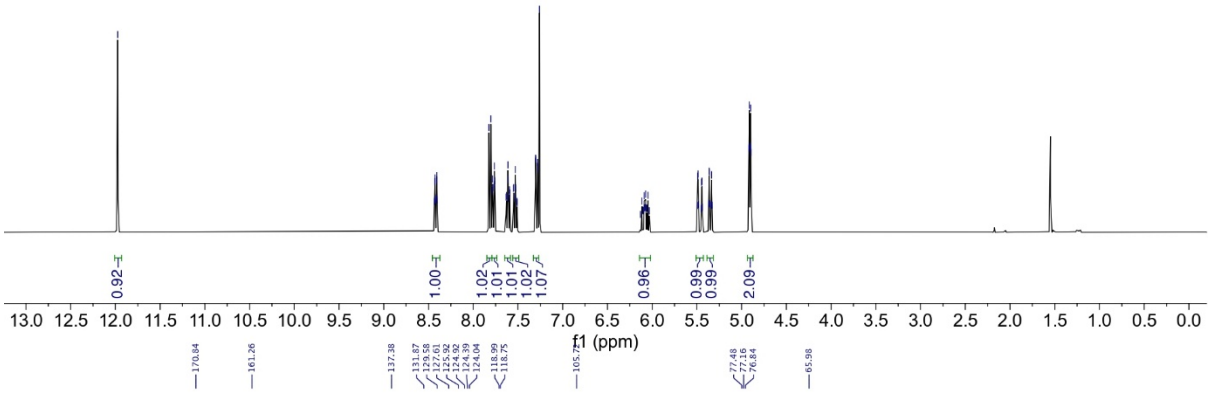

3.59av
400 MHz, CDCl3
1.06
2.16
1.83
4.34
2.29
0.92
f1 (ppm)

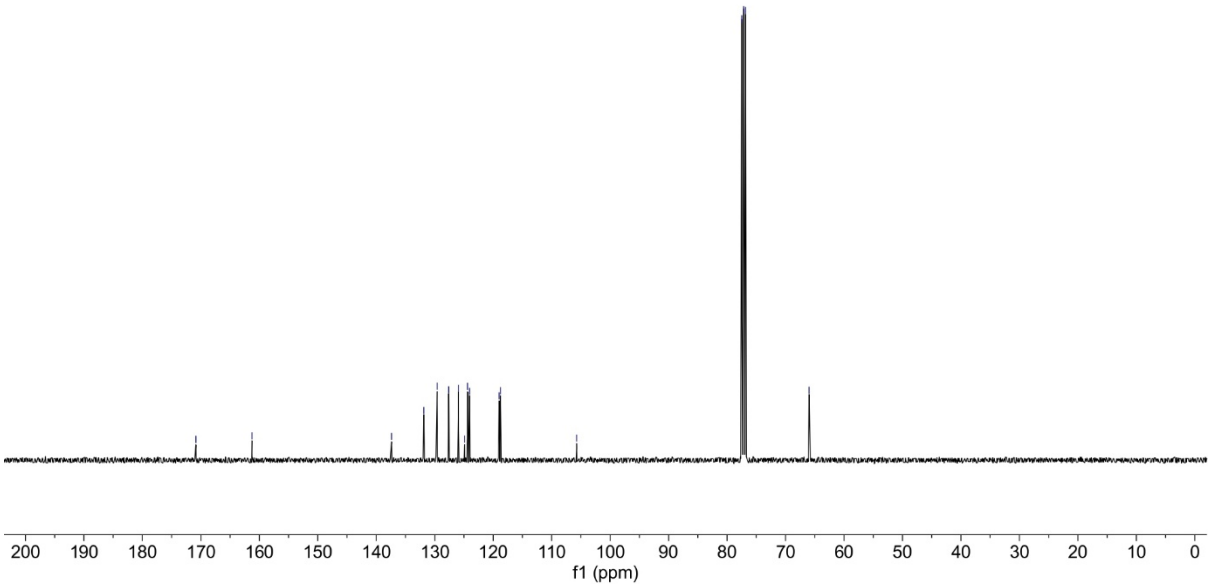

MeO
3.59aw
400 MHz, CDCl3
δ (ppm)

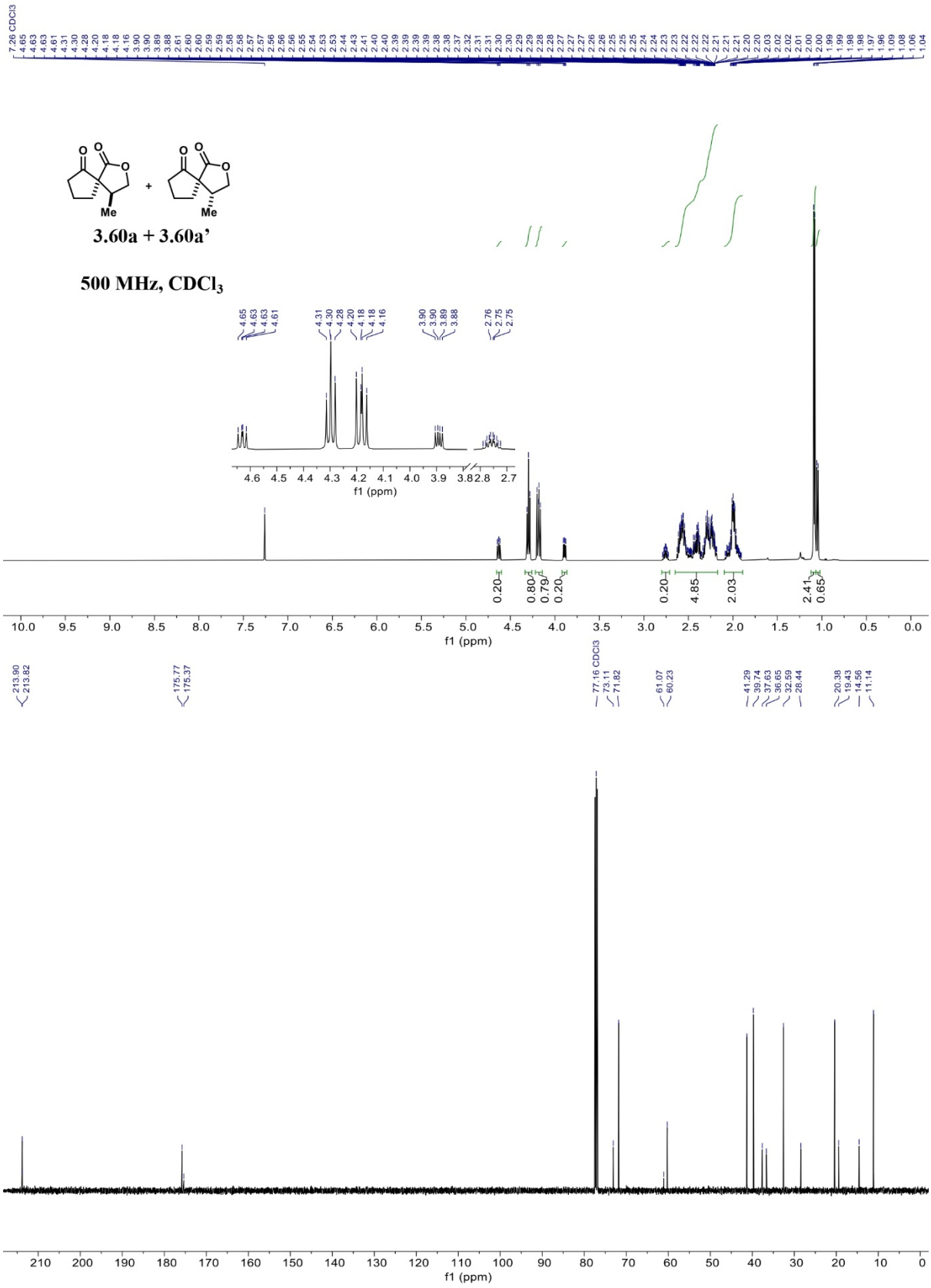


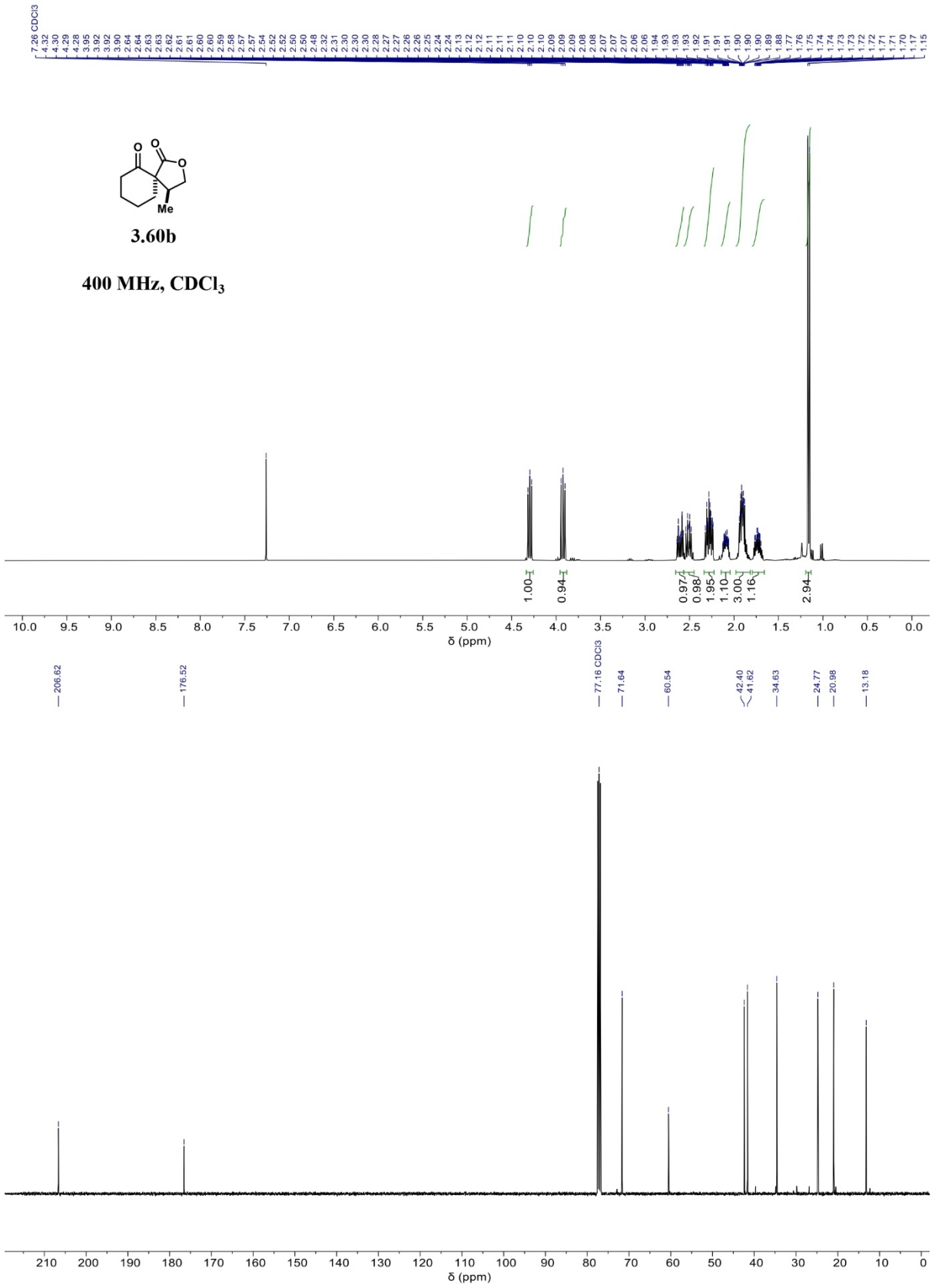
3.59ax

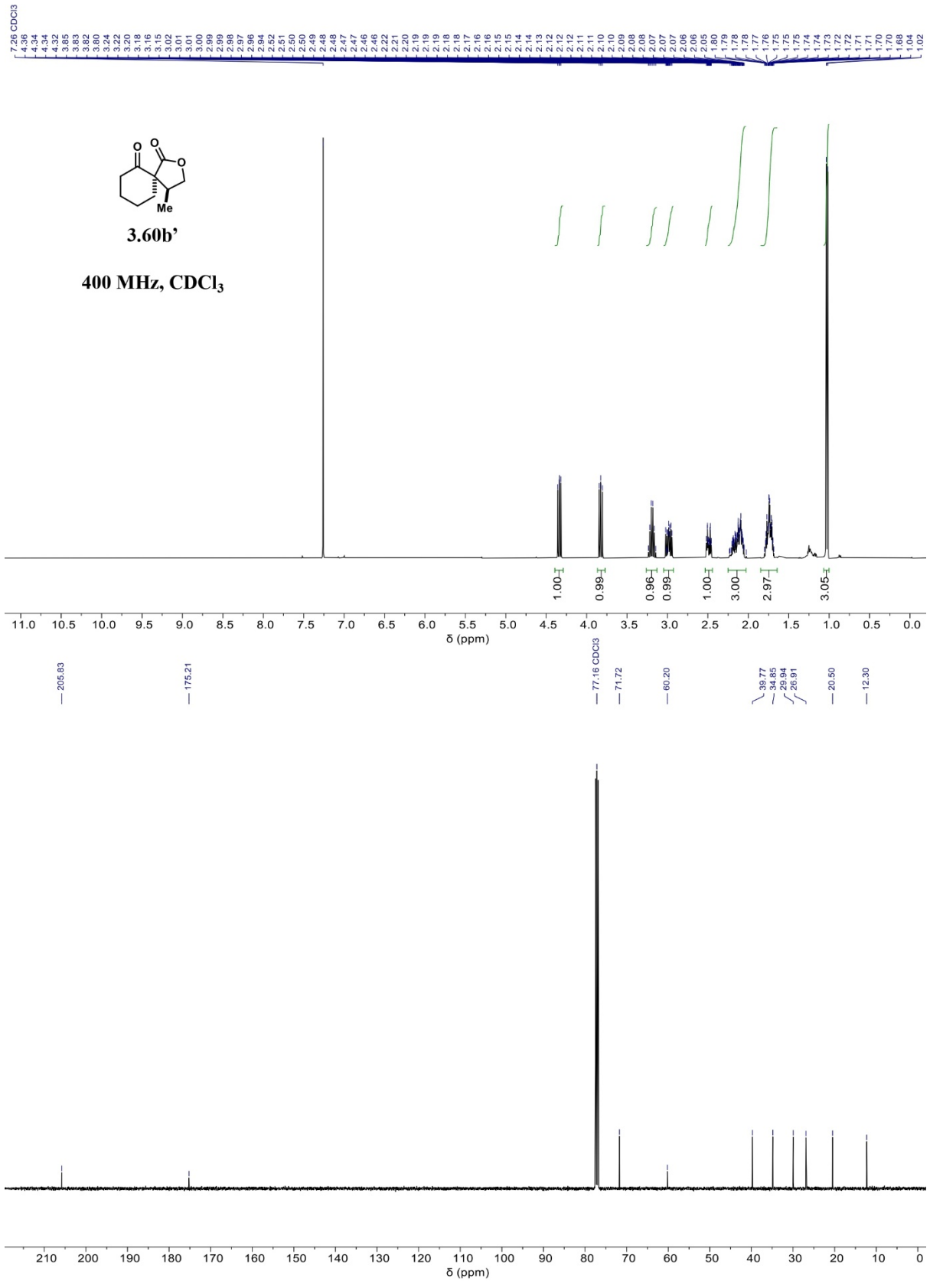
400 MHz, $CDCl_3$

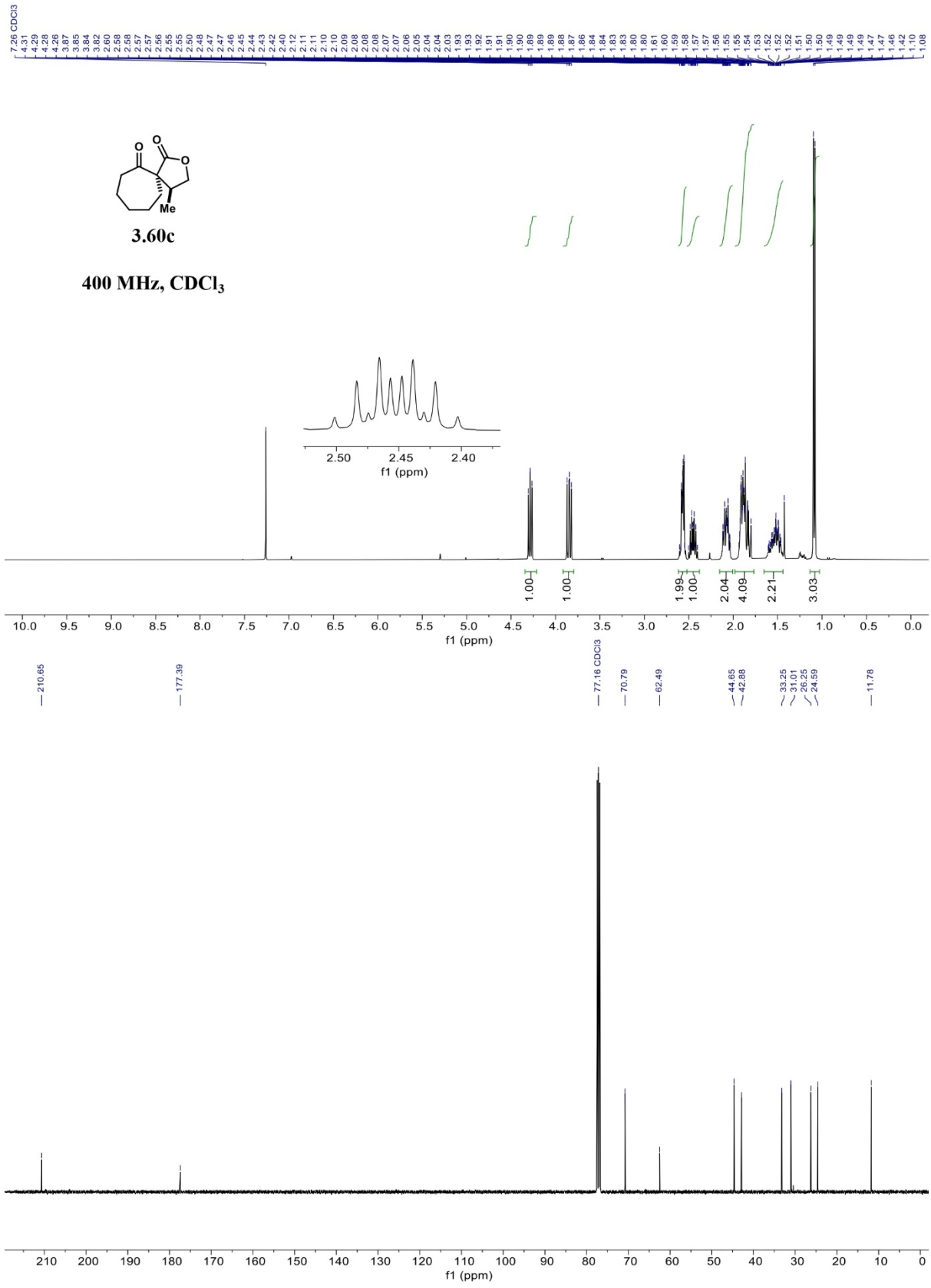


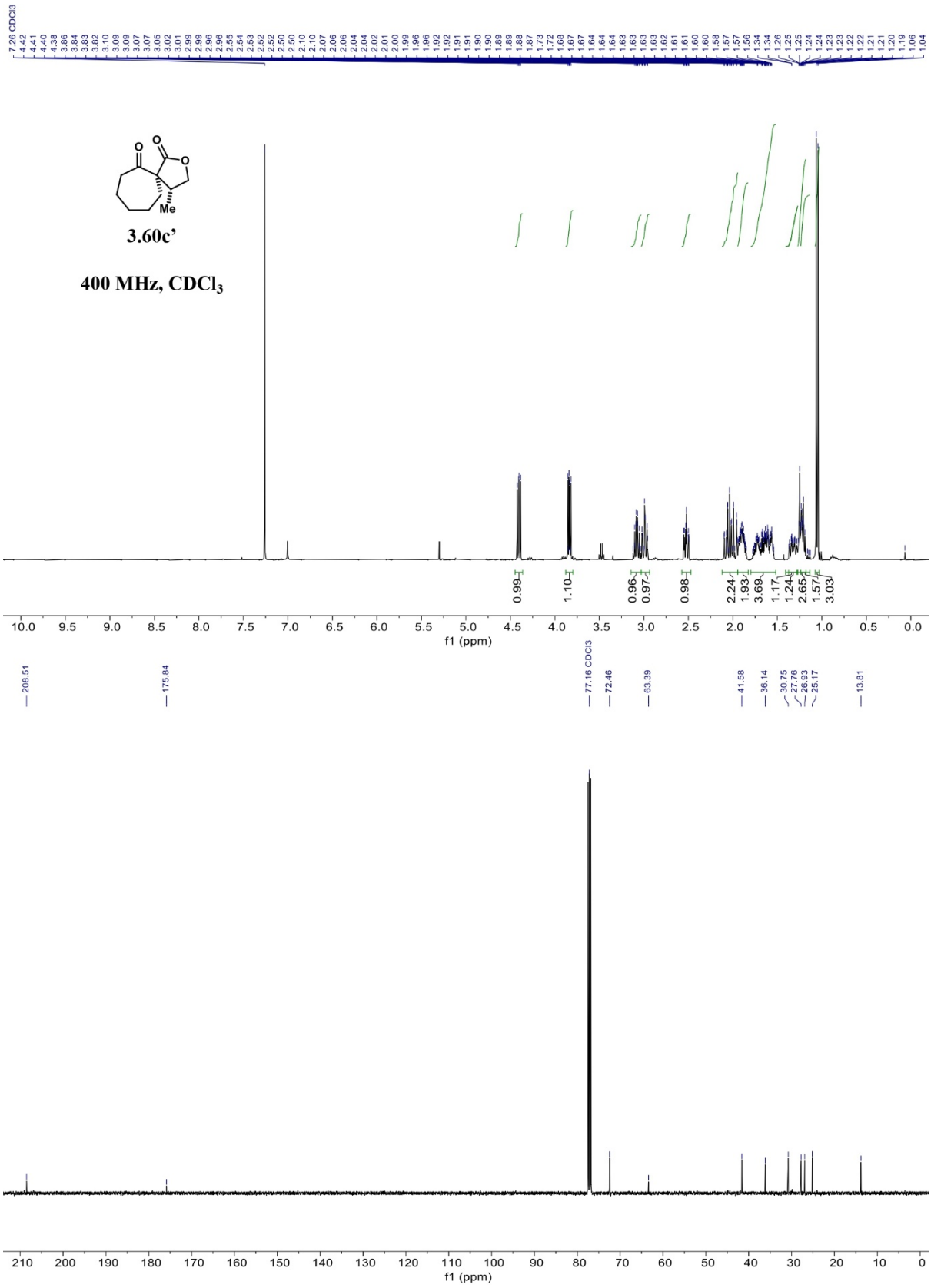


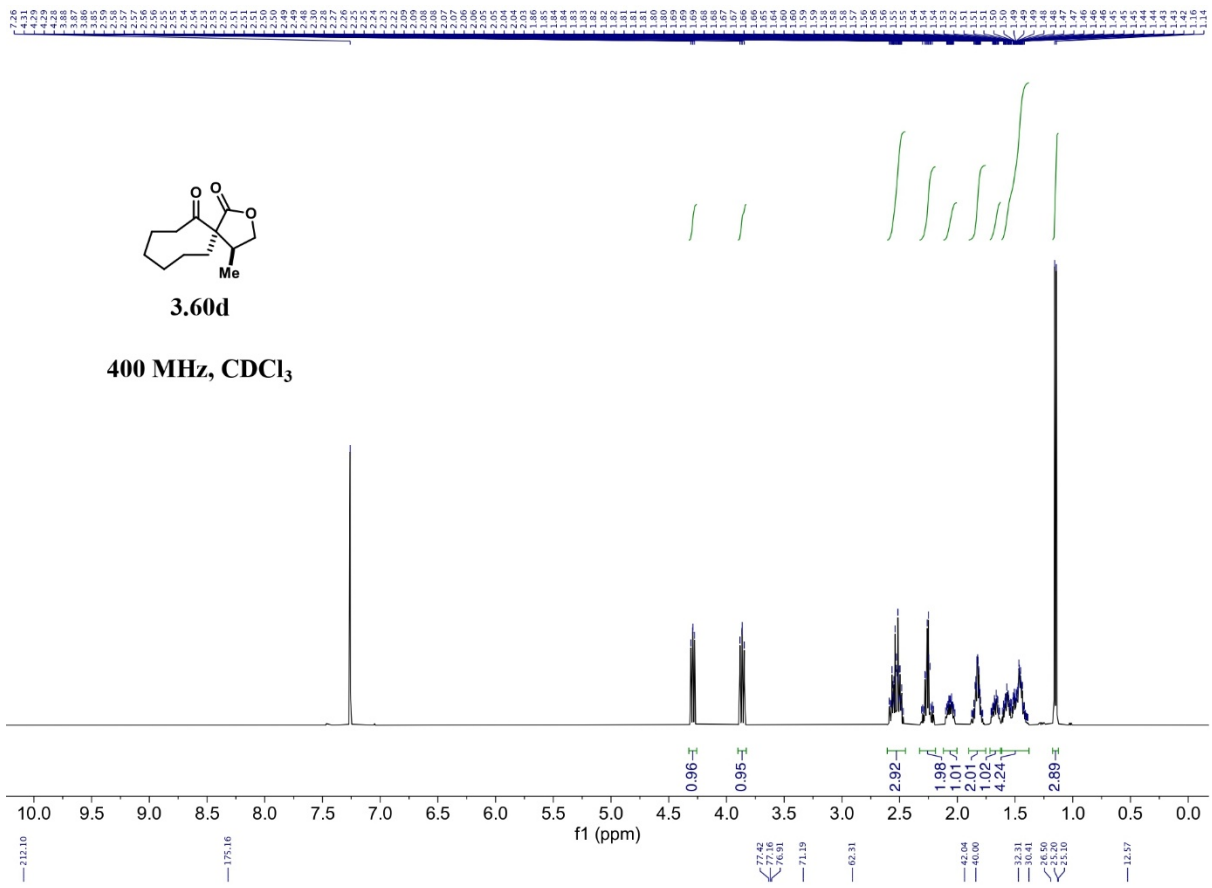

Me
Me
3.60a + 3.60a'
500 MHz, CDCl3
f1 (ppm)
f1 (ppm)

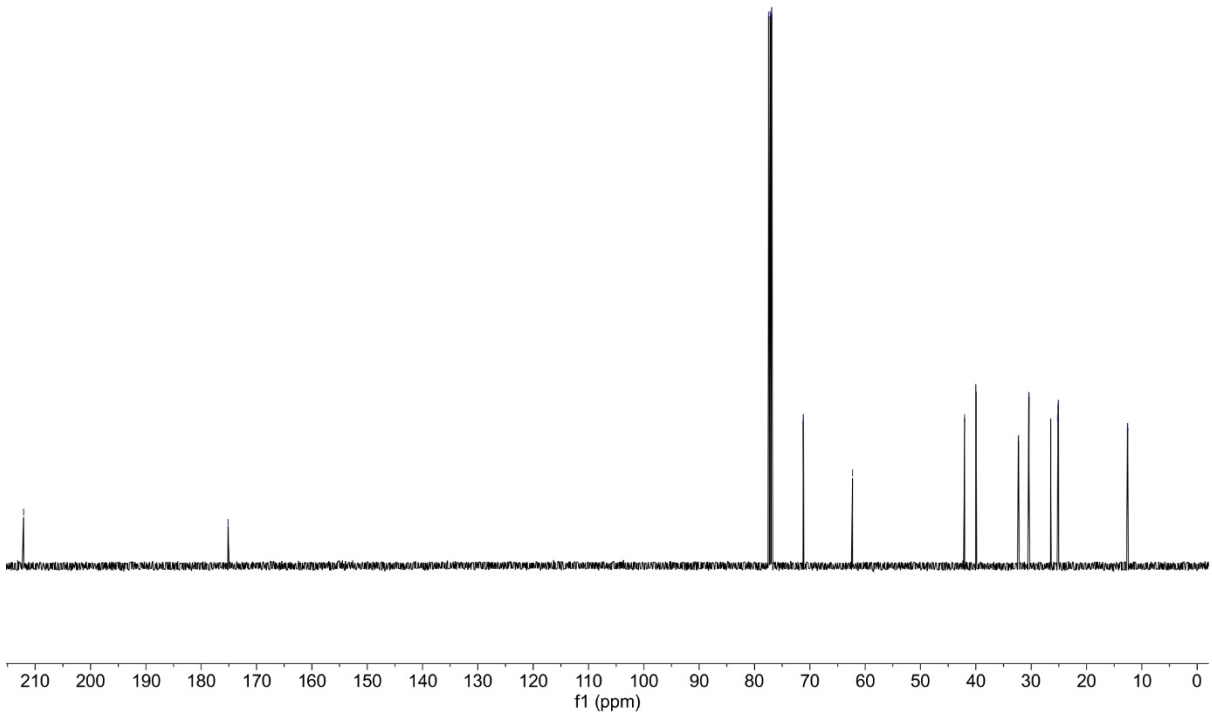

7.26 CDCl3
Me
3.60b
400 MHz, CDCl3
1.00
0.94
0.97
0.98
1.95
1.10
3.00
1.16
2.94
δ (ppm)
206.62
176.52
77.16 CDCl3
71.64
60.54
42.40
41.62
34.63
24.77
20.98
13.18
δ (ppm)

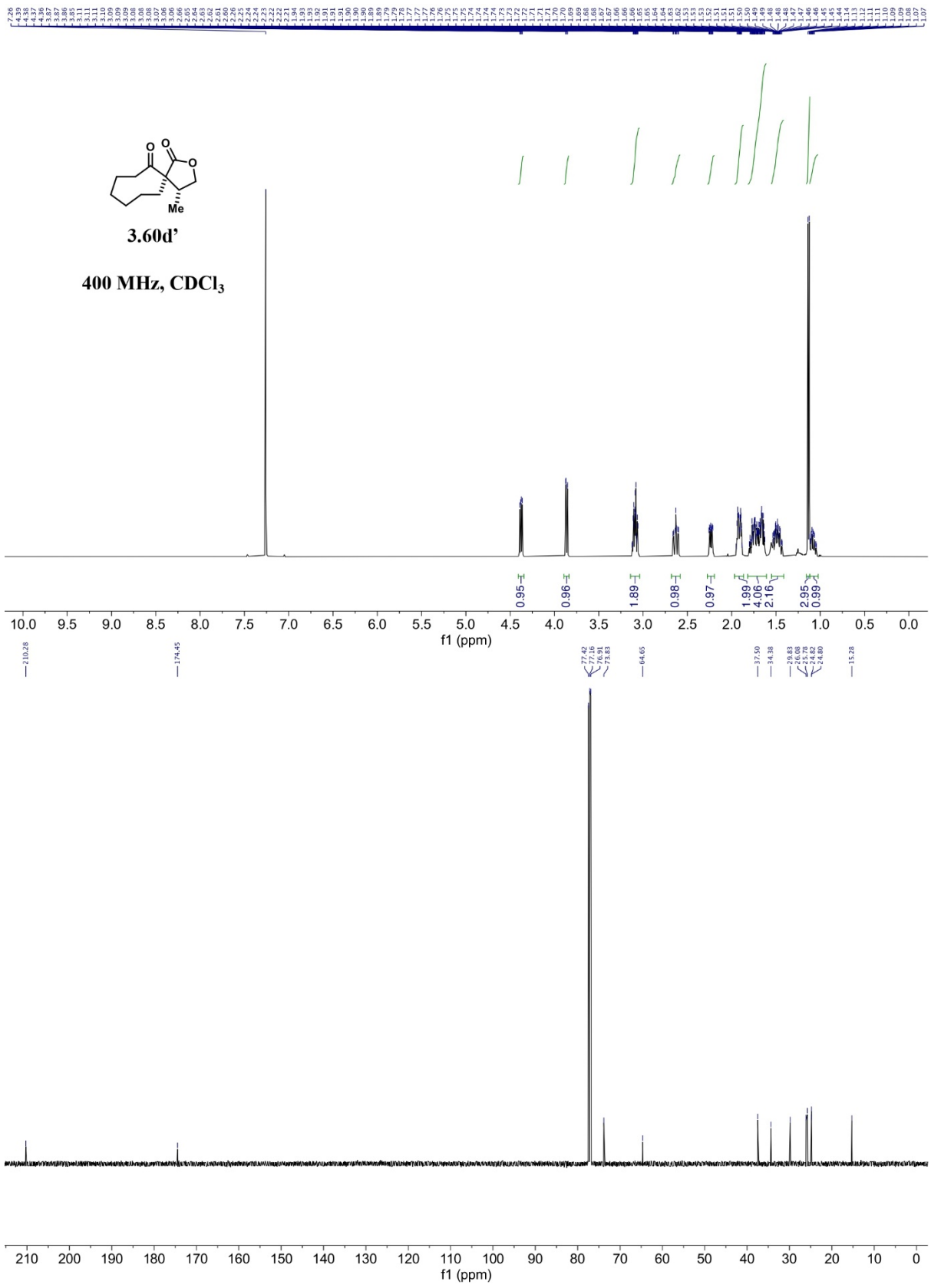

7.26 CDCl3
4.36
4.34
4.34
4.32
3.85
3.83
3.82
3.80
3.24
3.22
3.20
3.18
3.16
3.15
3.02
3.01
3.01
3.00
2.99
2.99
2.98
2.97
2.96
2.94
2.52
2.51
2.50
2.50
2.49
2.48
2.47
2.47
2.46
2.46
2.22
2.21
2.20
2.19
2.19
2.19
2.18
2.18
2.17
2.16
2.16
2.15
2.15
2.14
2.14
2.13
2.12
2.12
2.12
2.11
2.11
2.10
2.10
2.09
2.08
2.08
2.07
2.07
2.07
2.06
2.06
2.05
1.80
1.79
1.78
1.78
1.77
1.76
1.75
1.75
1.75
1.74
1.74
1.73
1.72
1.72
1.71
1.71
1.70
1.70
1.68
1.04
1.02
O
O
O
Me
3.60b'
400 MHz, CDCl3
1.00
0.99
0.96
0.99
1.00
3.00
2.97
3.05
11.0 10.5 10.0 9.5 9.0 8.5 8.0 7.5 7.0 6.5 6.0 5.5 5.0 4.5 4.0 3.5 3.0 2.5 2.0 1.5 1.0 0.5 0.0
δ (ppm)
205.83
175.21
77.16 CDCl3
71.72
60.20
39.77
34.85
29.94
26.91
20.50
12.30
210 200 190 180 170 160 150 140 130 120 110 100 90 80 70 60 50 40 30 20 10 0
δ (ppm)


7.26 CDCl3
4.31 4.29 4.28 4.26 3.87 3.85 3.84 3.82 2.60 2.58 2.58 2.57 2.57 2.56 2.55 2.55 2.50 2.48 2.47 2.47 2.46 2.45 2.44 2.43 2.42 2.40 2.12 2.11 2.11 2.10 2.10 2.09 2.08 2.08 2.08 2.07 2.07 2.06 2.05 2.04 2.04 2.03 1.93 1.93 1.92 1.91 1.91 1.90 1.90 1.89 1.89 1.89 1.88 1.87 1.86 1.84 1.84 1.83 1.80 1.80 1.61 1.60 1.59 1.58 1.57 1.57 1.56 1.55 1.55 1.54 1.53 1.52 1.52 1.52 1.51 1.50 1.50 1.49 1.49 1.49 1.49 1.48 1.47 1.47 1.46 1.42 1.10 1.08
O
O
O
Me
3.60c
400 MHz, CDCl3
2.50 2.45 2.40
f1 (ppm)
1.00 1.00 1.99 1.00 2.04 4.09 2.21 3.03
10.0 9.5 9.0 8.5 8.0 7.5 7.0 6.5 6.0 5.5 5.0 4.5 4.0 3.5 3.0 2.5 2.0 1.5 1.0 0.5 0.0
f1 (ppm)
210.65
177.39
77.16 CDCl3
70.79
62.49
44.65
42.88
33.25
31.01
26.25
24.59
11.78
210 200 190 180 170 160 150 140 130 120 110 100 90 80 70 60 50 40 30 20 10 0
f1 (ppm)


3.60c'
400 MHz, CDCl3
f1 (ppm)
f1 (ppm)

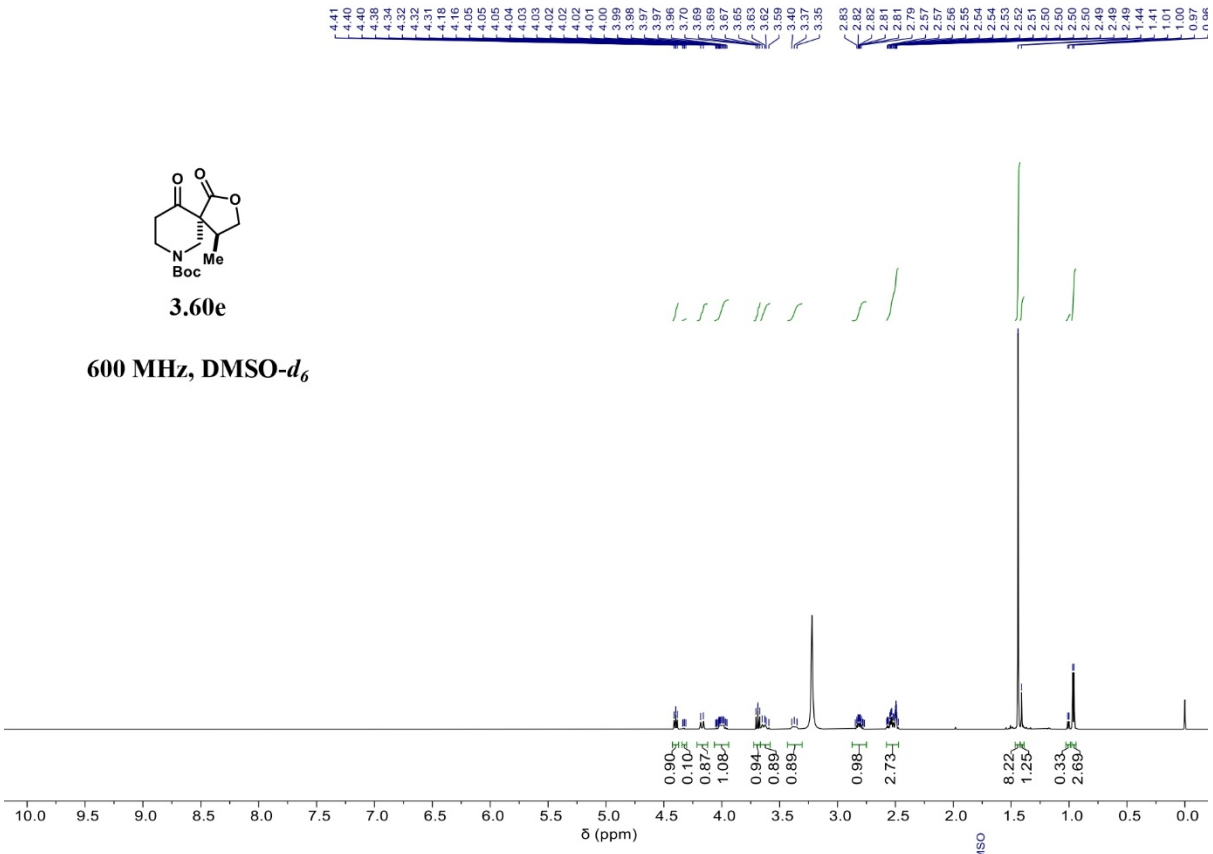

O
O
O
Me
3.60d
400 MHz, CDCl3
0.96
0.95
2.92
1.98
1.01
2.01
1.02
4.24
2.89
f1 (ppm)

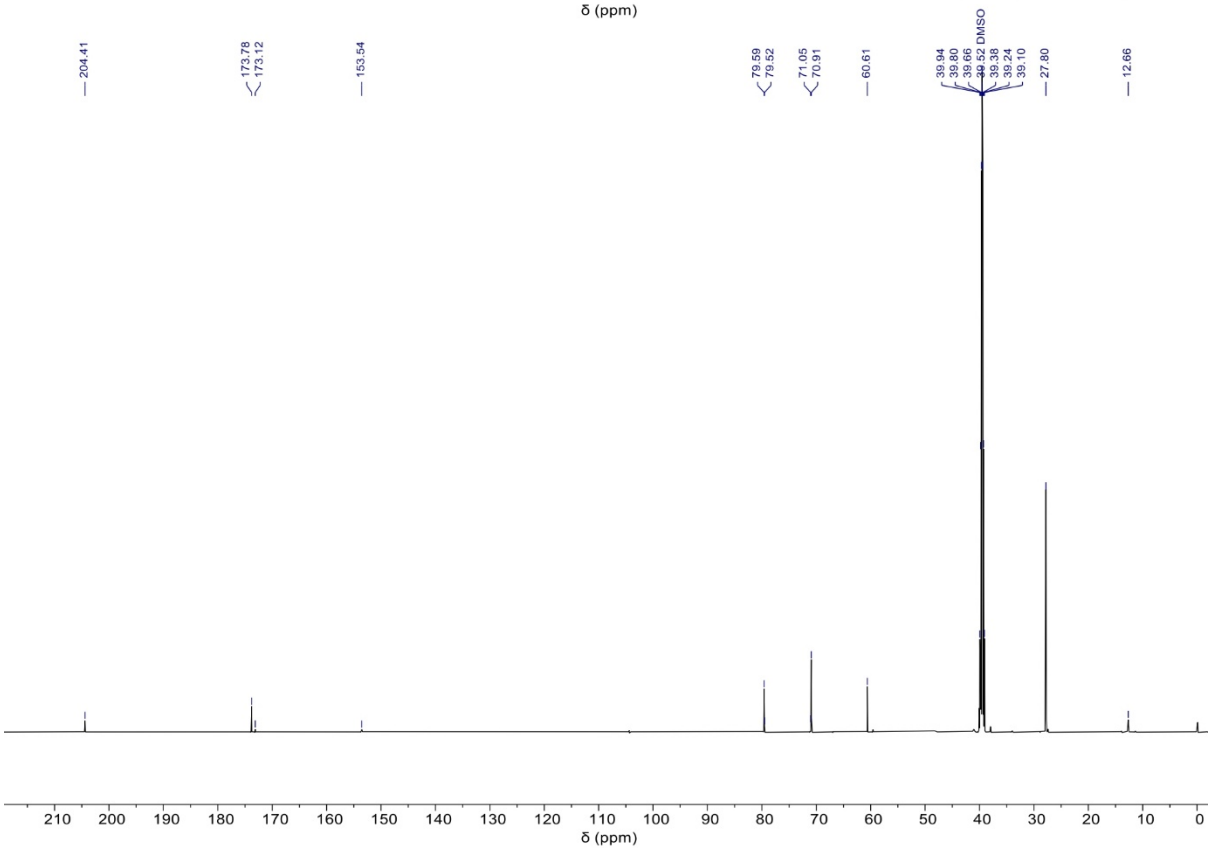

f1 (ppm)

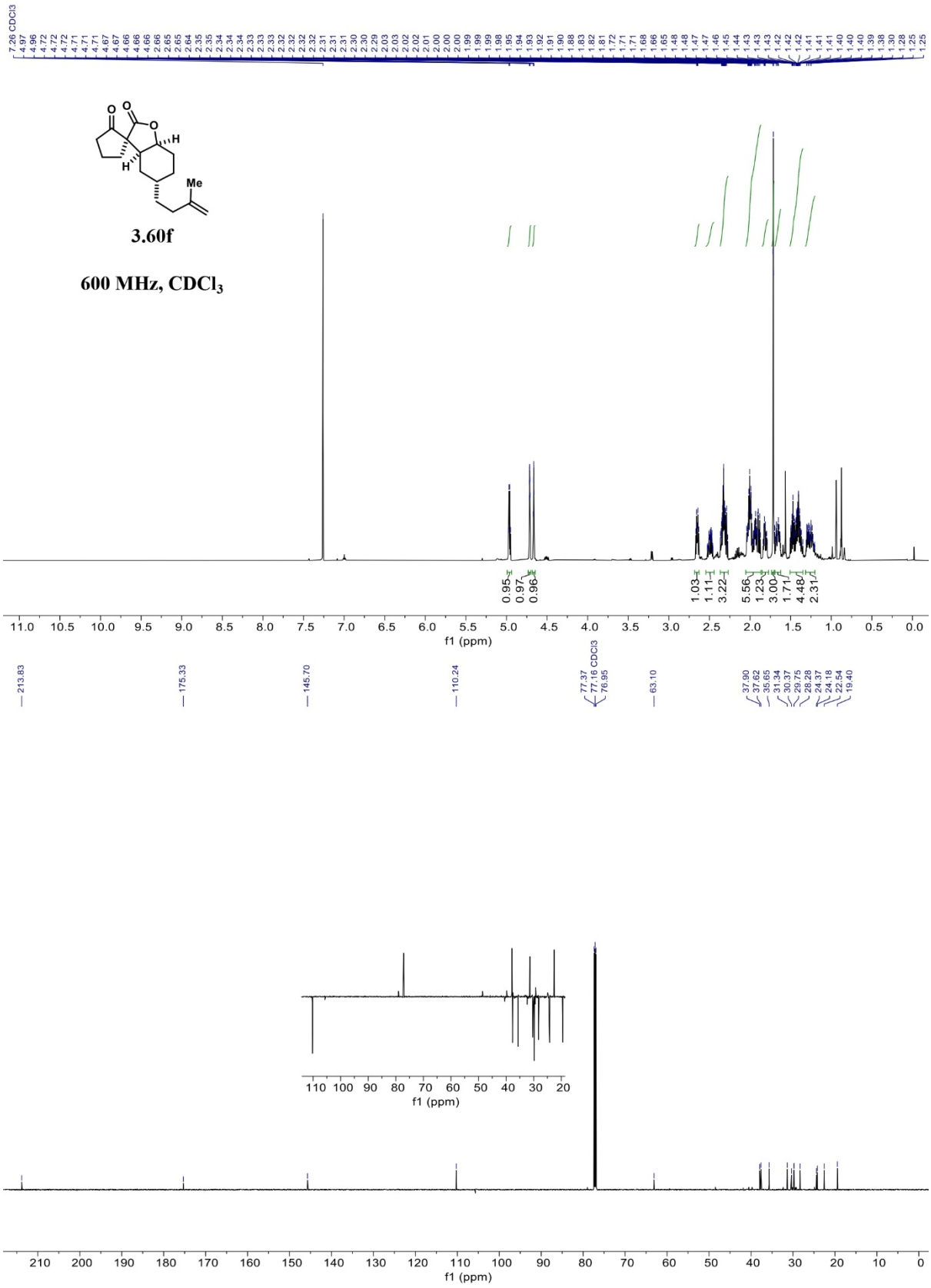

3.60d'
400 MHz, CDCl3
f1 (ppm)
f1 (ppm)

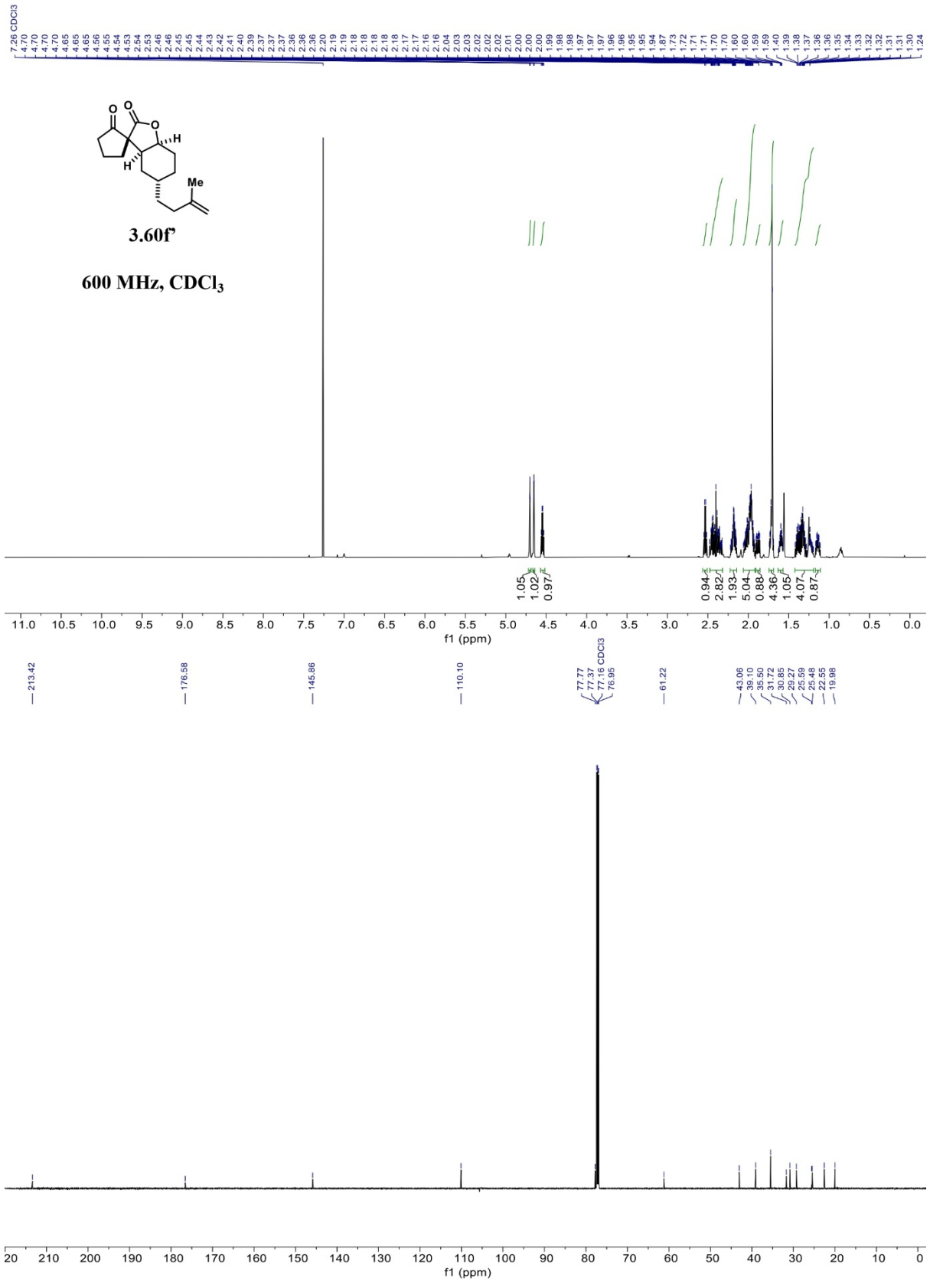
3.60e

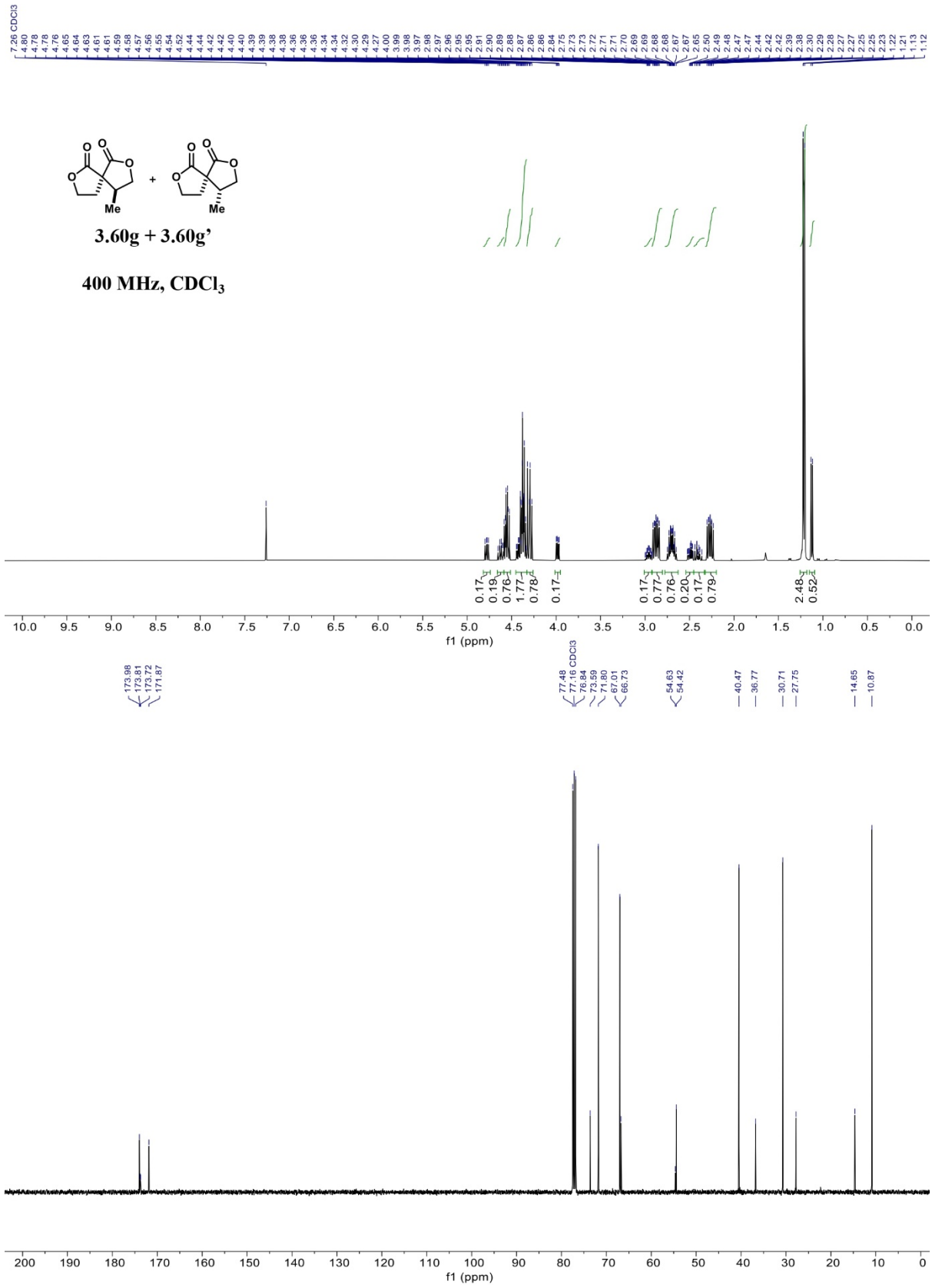
600 MHz, DMSO-d_6

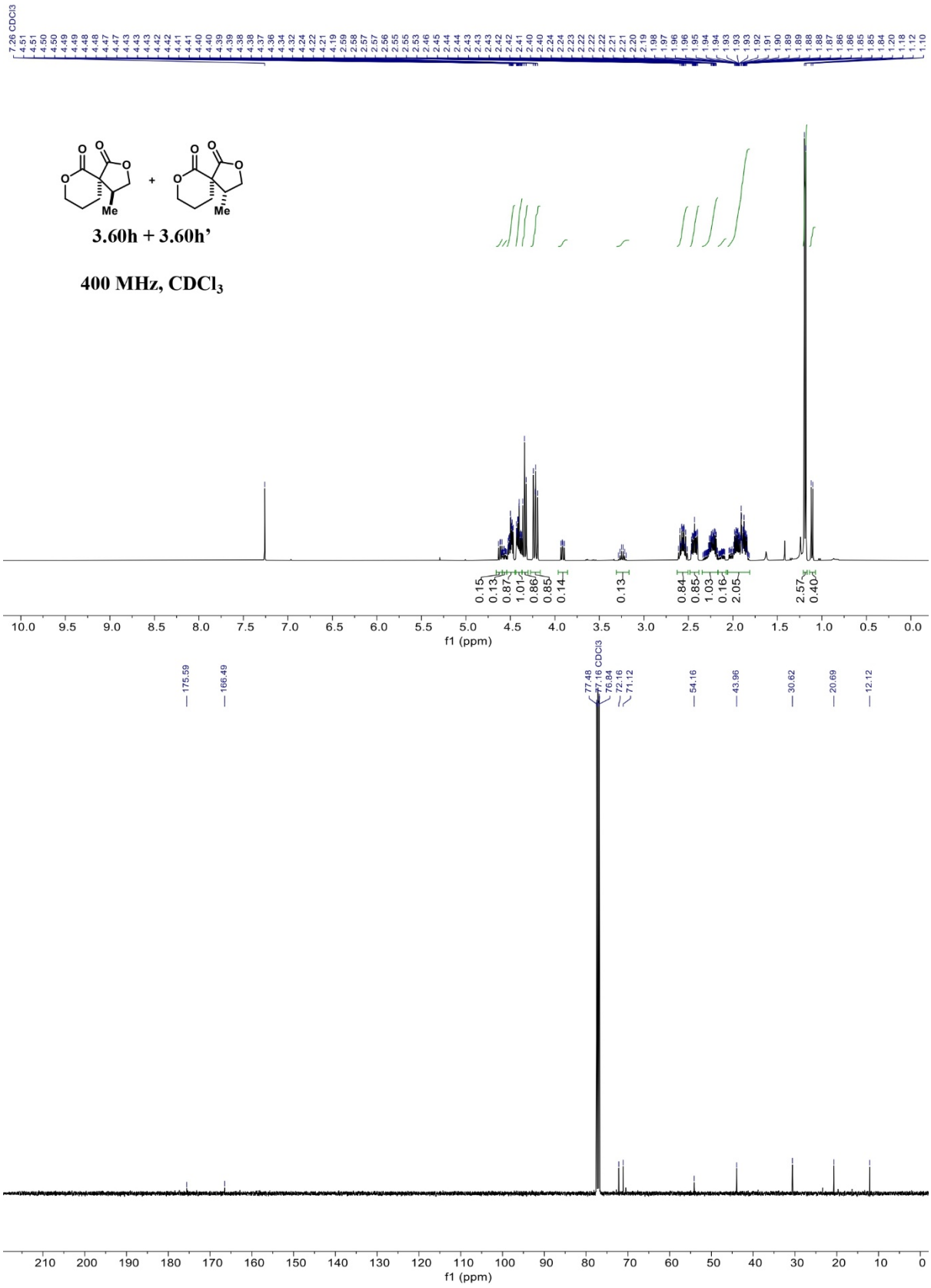


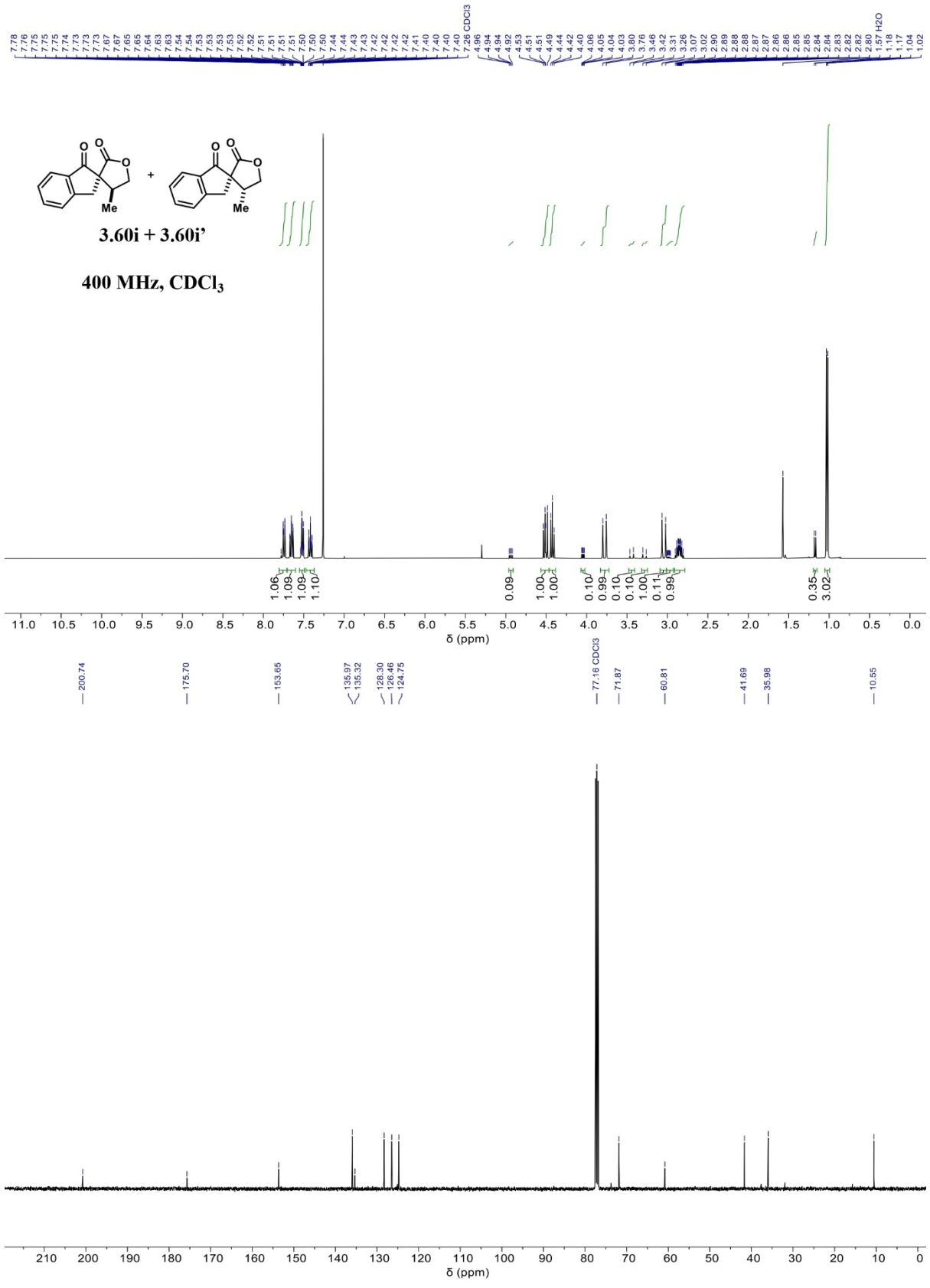


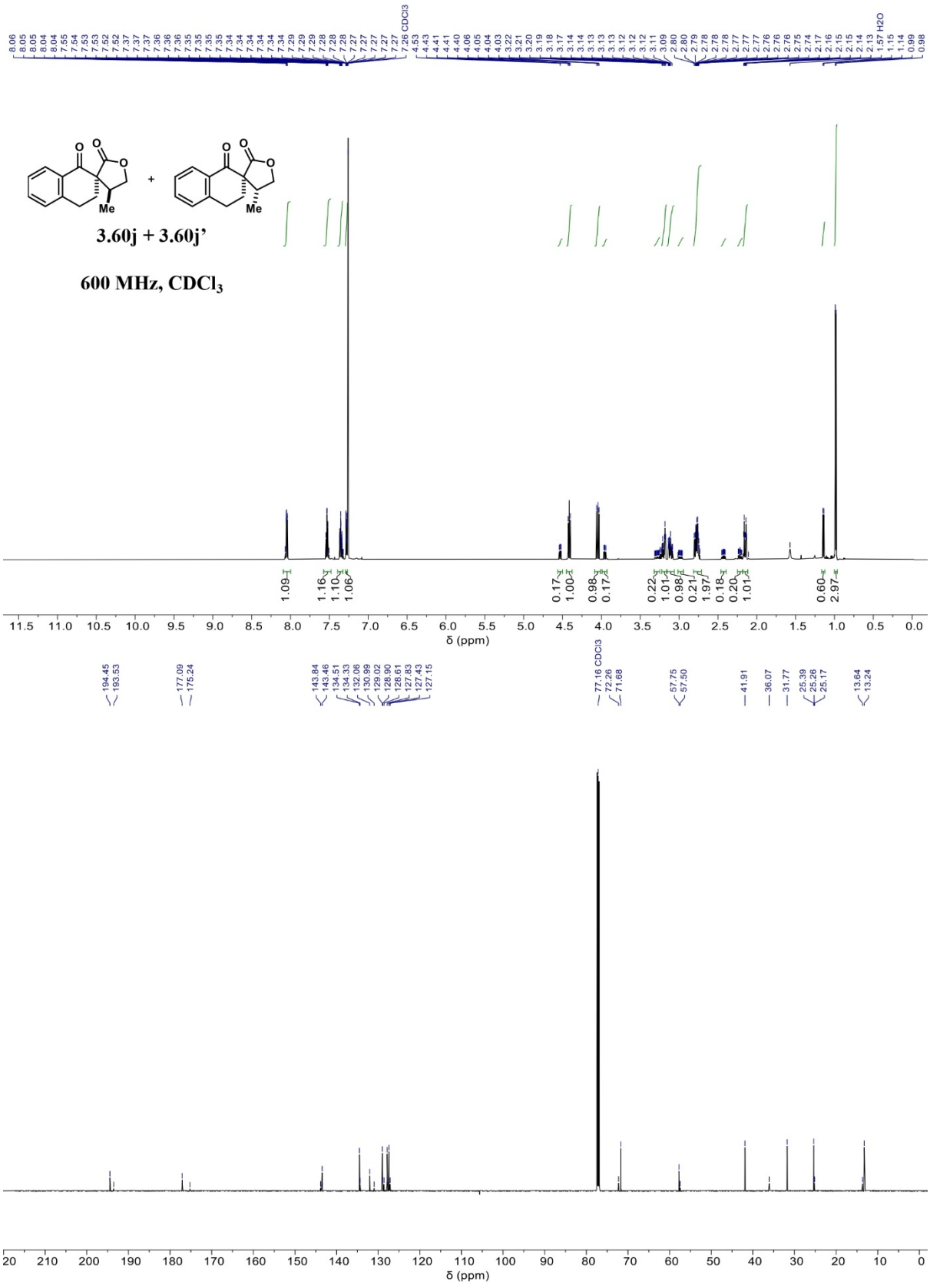

7.26 CDCl3
Me
3.60f
600 MHz, CDCl3
0.95
0.97
0.96
1.03
1.11
3.22
5.56
1.23
3.00
1.71
4.48
2.31
f1 (ppm)
213.83
175.33
145.70
110.24
77.37
77.16 CDCl3
76.95
63.10
37.90
37.62
35.65
31.34
30.37
29.75
28.28
24.37
24.18
22.54
19.40

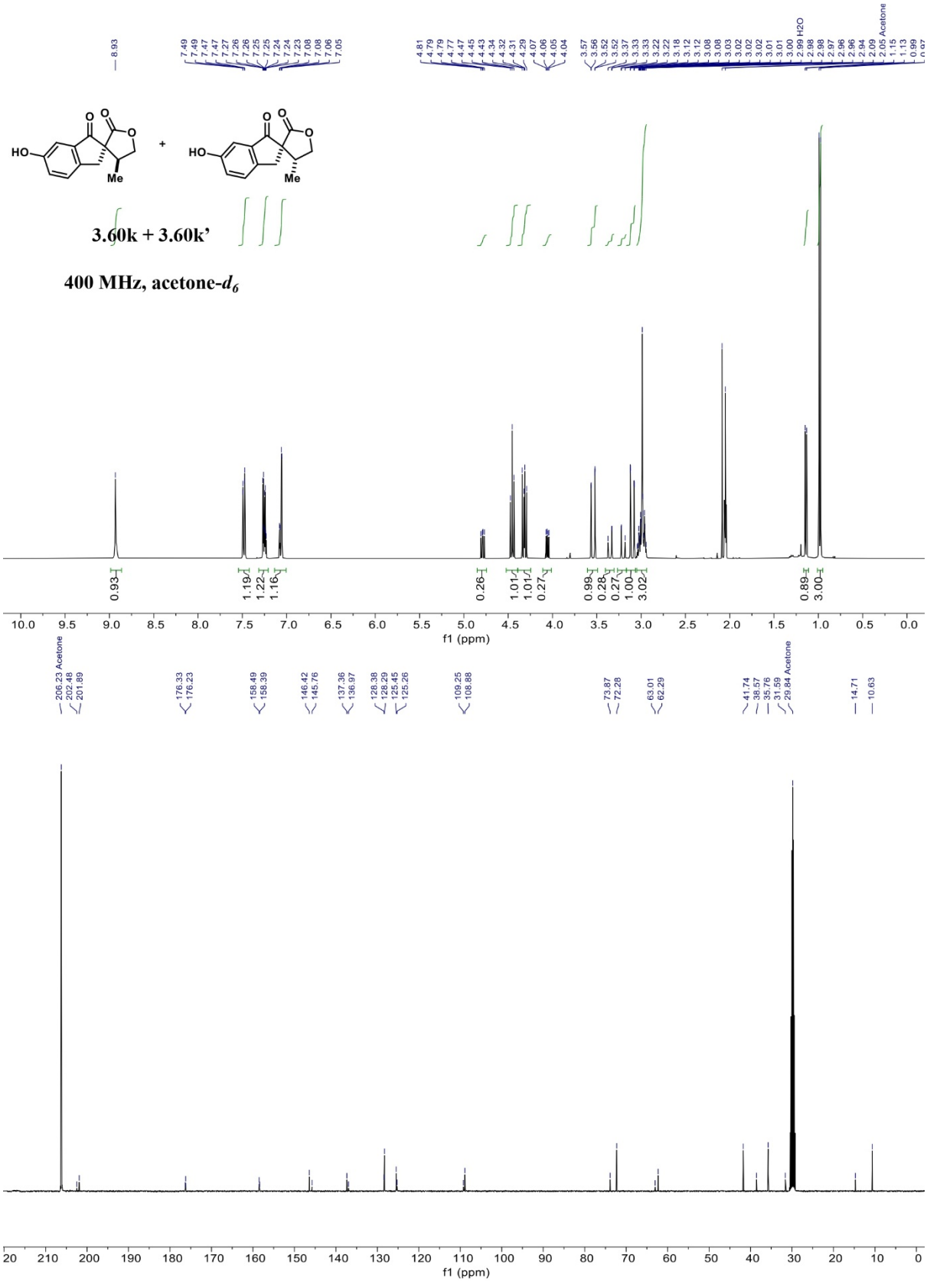

7.26 CDCl3
Me
3.60f'
600 MHz, CDCl3
1.05
1.02
0.97
0.94
2.82
1.93
5.04
0.88
4.36
1.05
4.07
0.87
f1 (ppm)
213.42
176.58
145.86
110.10
77.77
77.37
77.16 CDCl3
76.95
61.22
43.06
39.10
35.50
31.72
30.85
29.27
25.59
25.48
22.55
19.98
f1 (ppm)

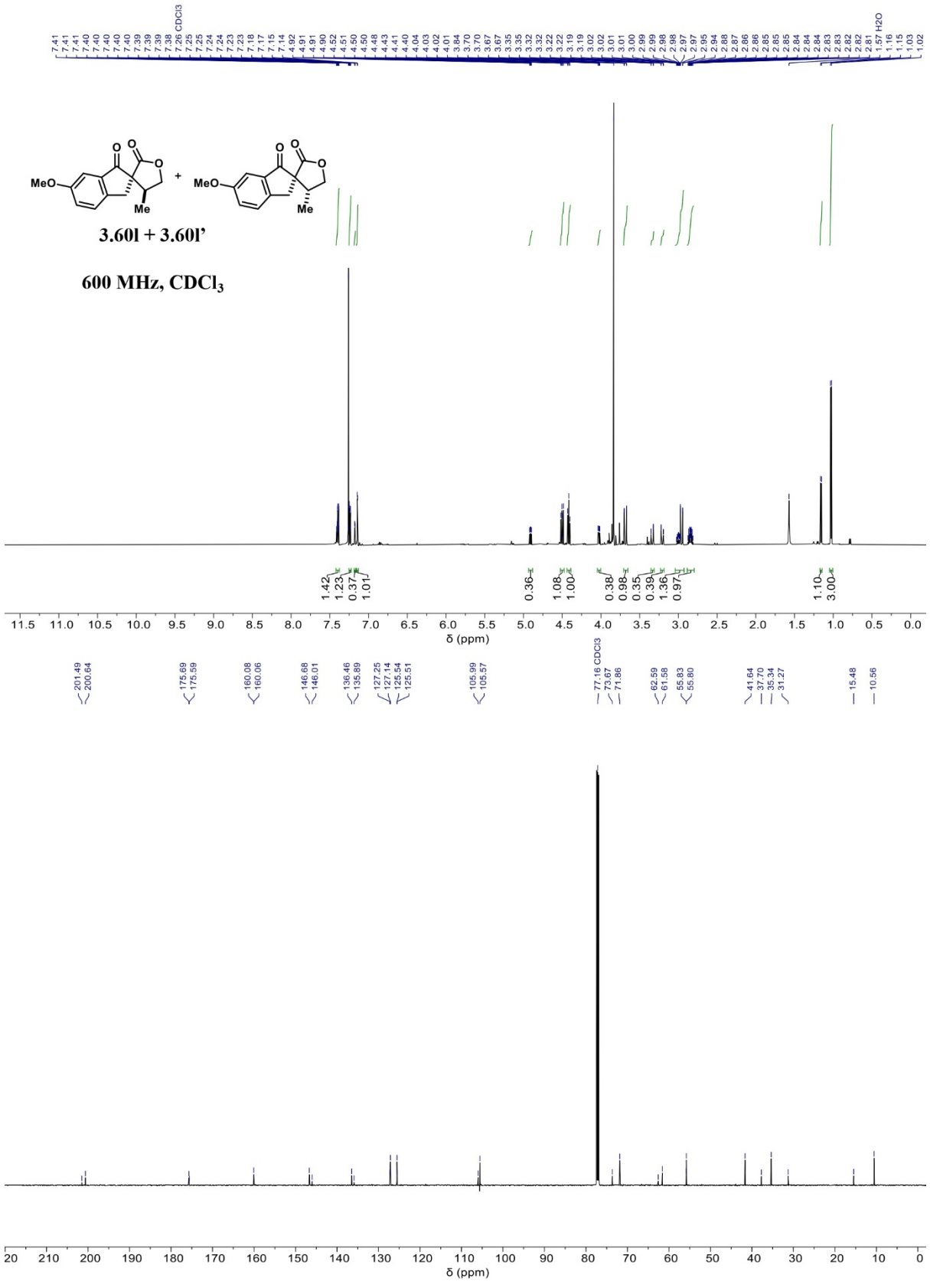

Me
Me
3.60g + 3.60g'
400 MHz, CDCl3
f1 (ppm)
f1 (ppm)

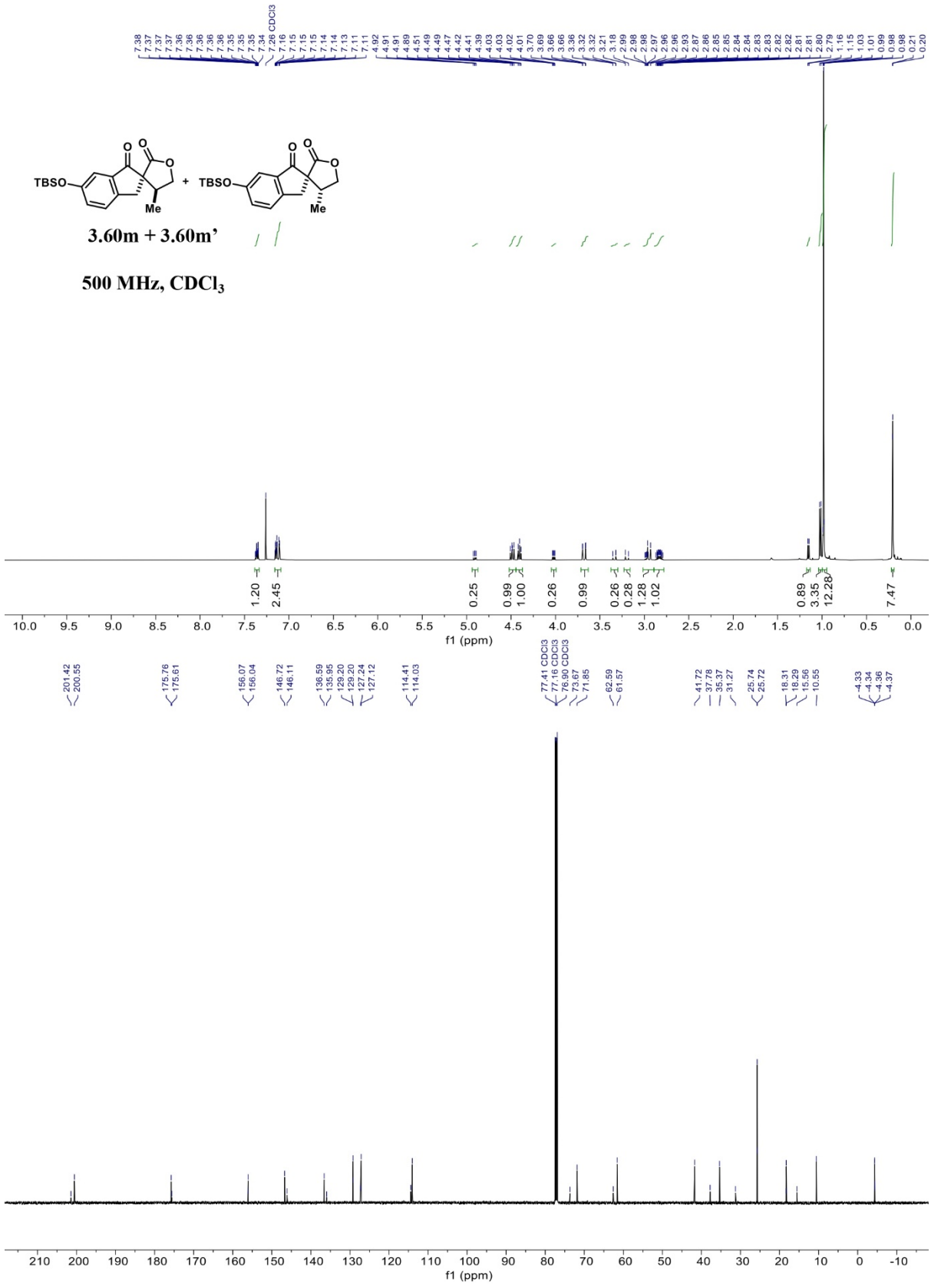

Me
Me
3.60h + 3.60h'
400 MHz, CDCl3
f1 (ppm)
f1 (ppm)

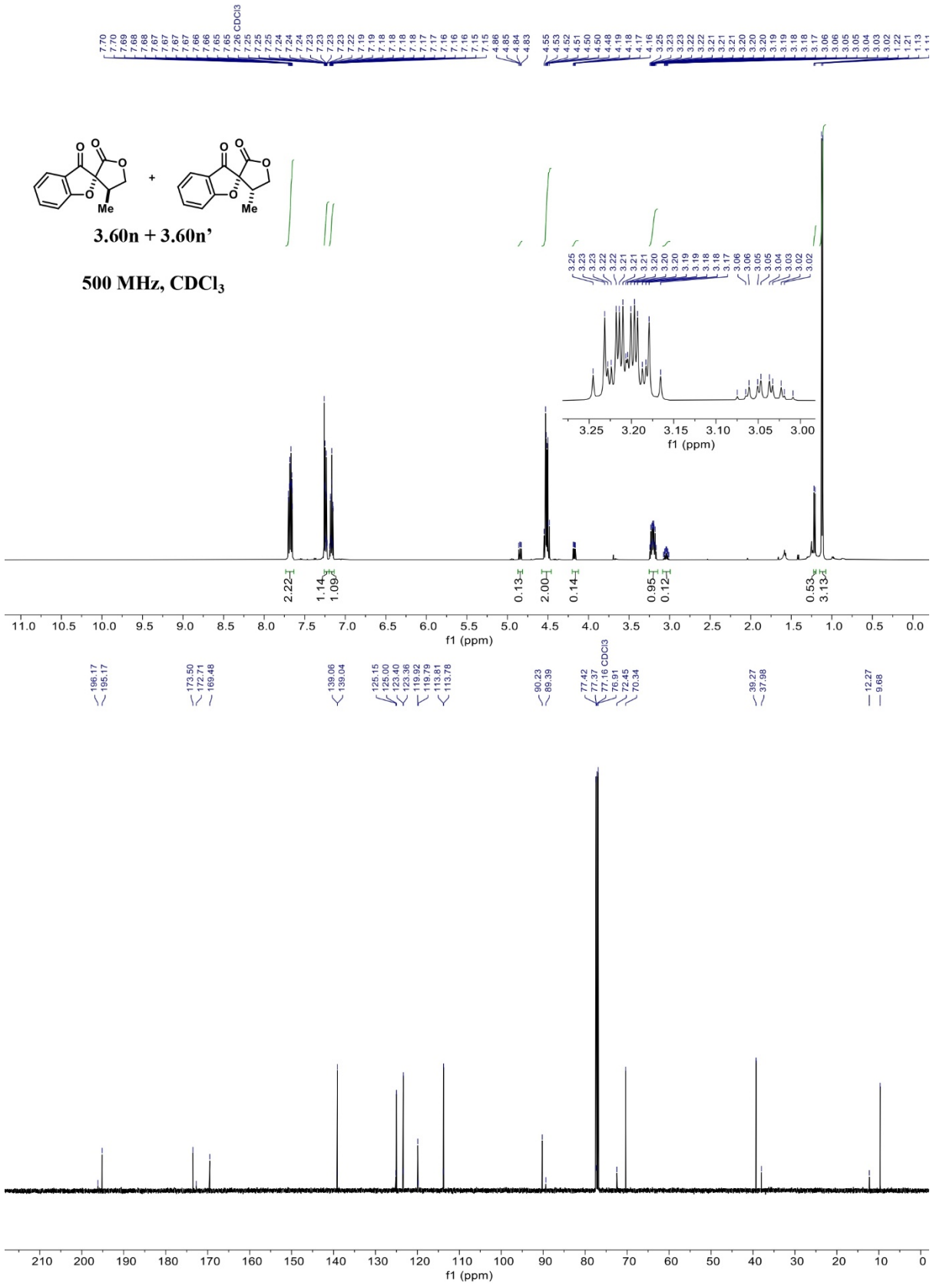

3.60i + 3.60i'
400 MHz, CDCl3
δ (ppm)
δ (ppm)

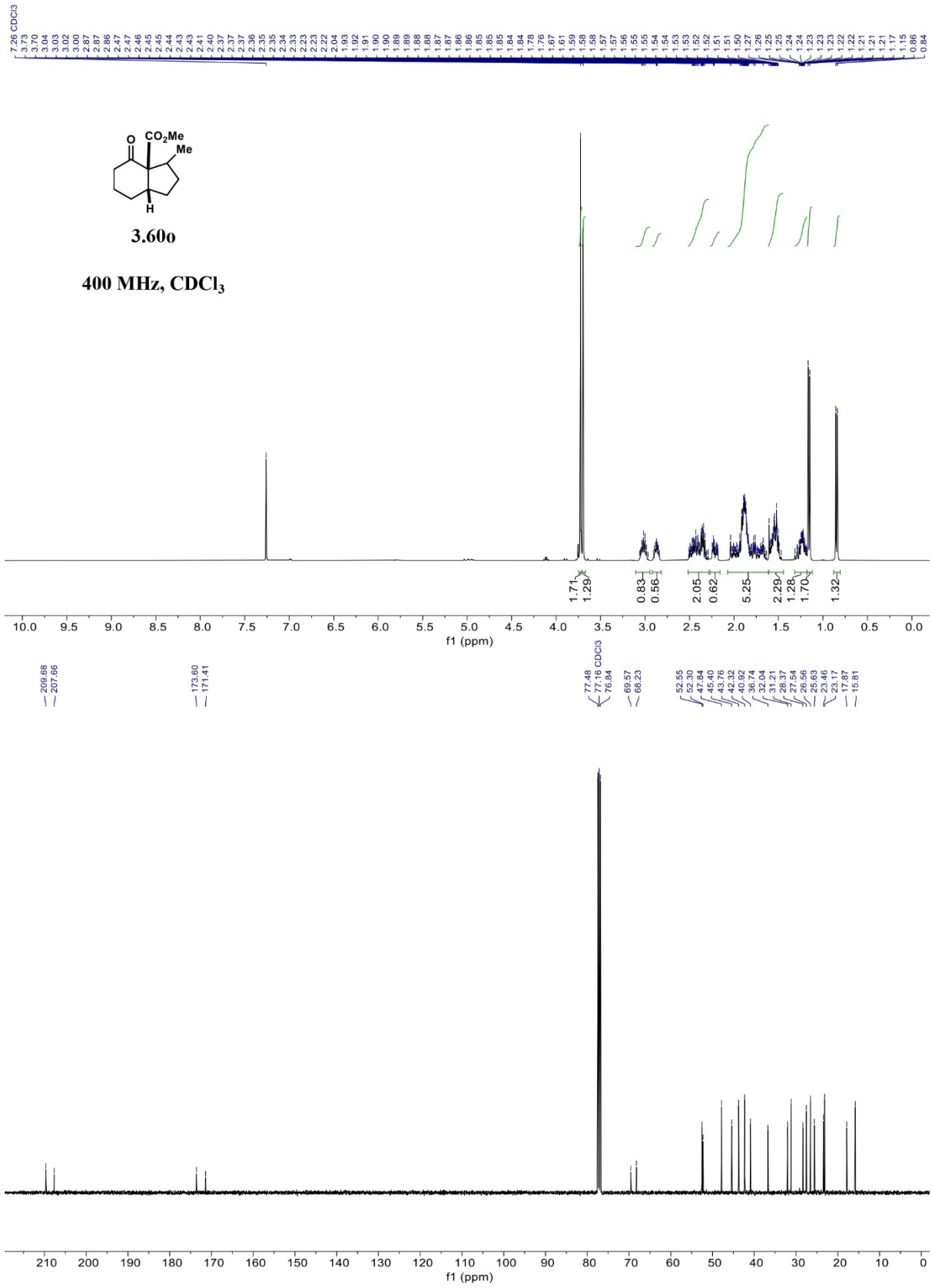

3.60j + 3.60j'
600 MHz, CDCl3
δ (ppm)
δ (ppm)

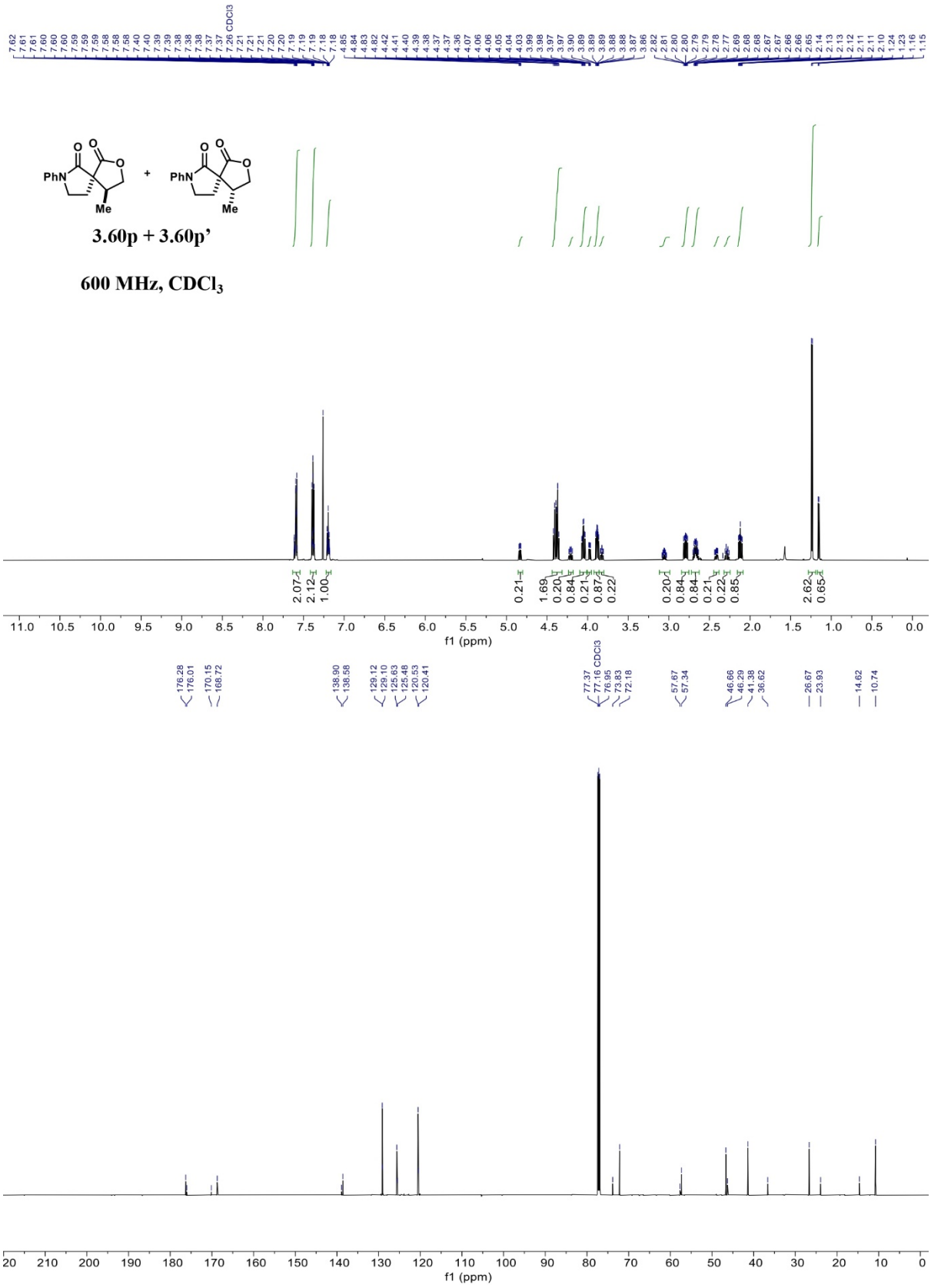

HO
Me
+
HO
Me
3.60k + 3.60k'
400 MHz, acetone-d_6
f1 (ppm)
f1 (ppm)

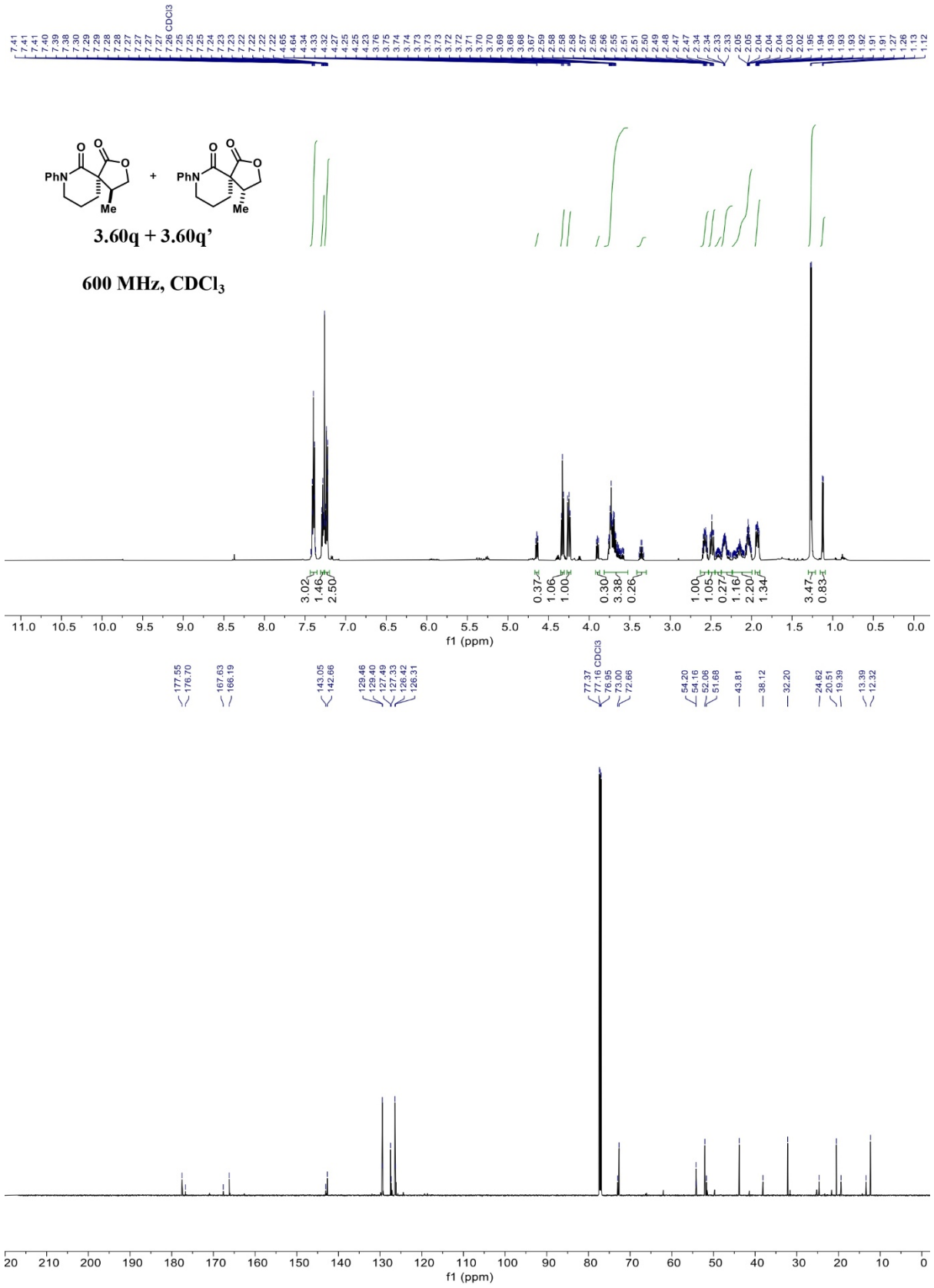

MeO
Me
+
MeO
Me
3.60l + 3.60l'
600 MHz, CDCl3
δ (ppm)
δ (ppm)

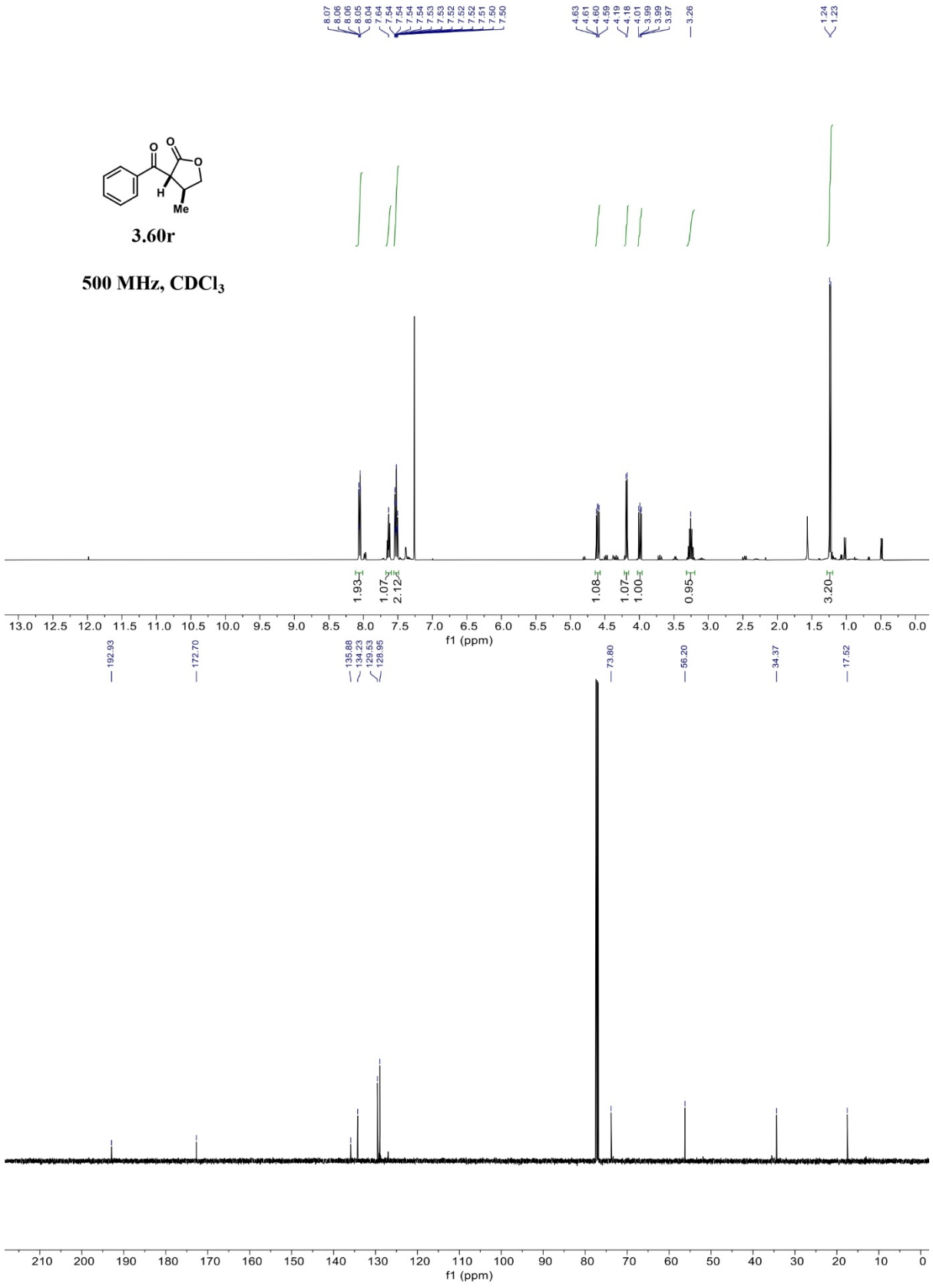

TBSO
Me
+
TBSO
Me
3.60m + 3.60m'
500 MHz, CDCl3
f1 (ppm)
f1 (ppm)

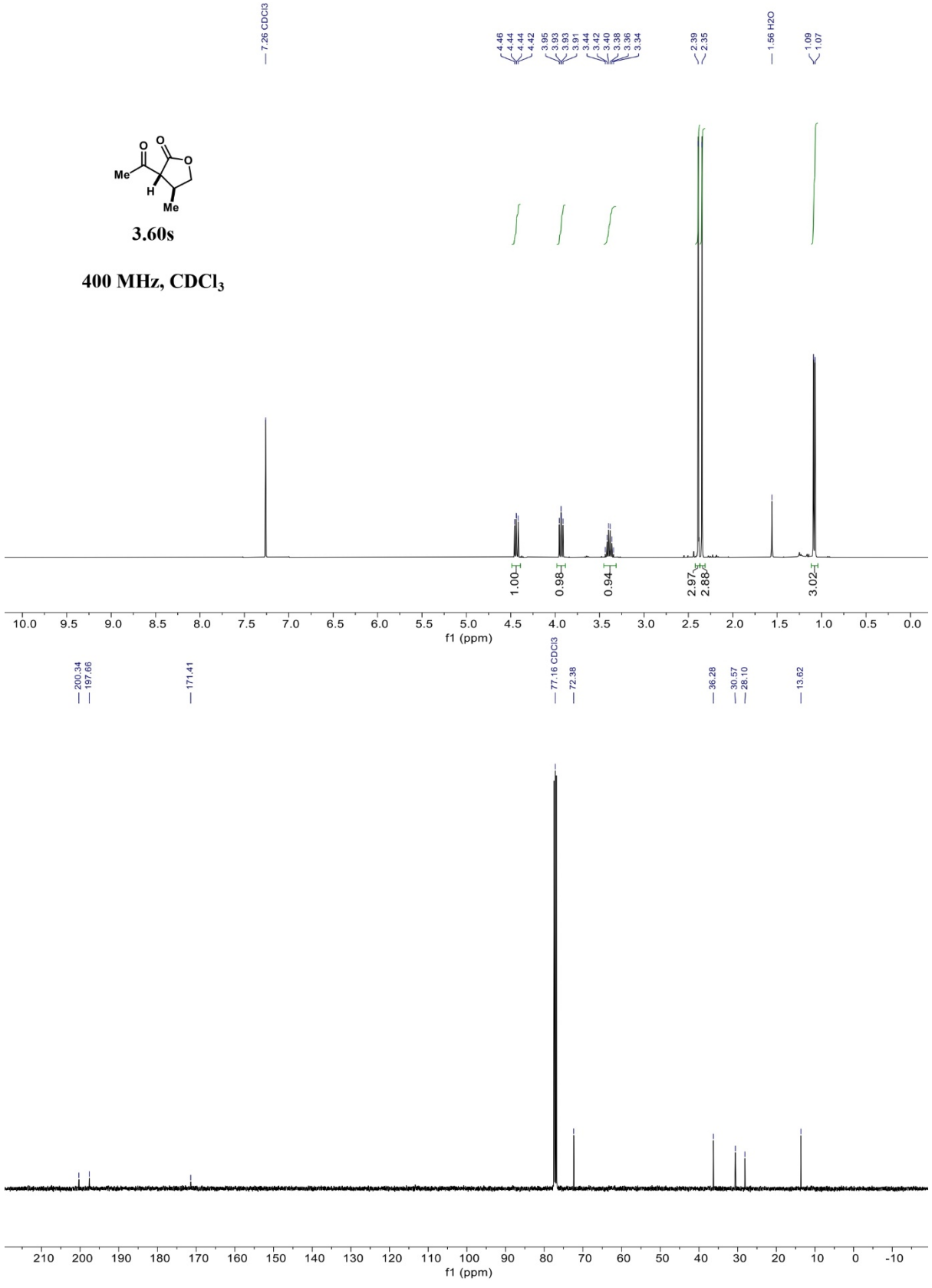

Me
Me
3.60n + 3.60n'
500 MHz, CDCl3
f1 (ppm)
f1 (ppm)

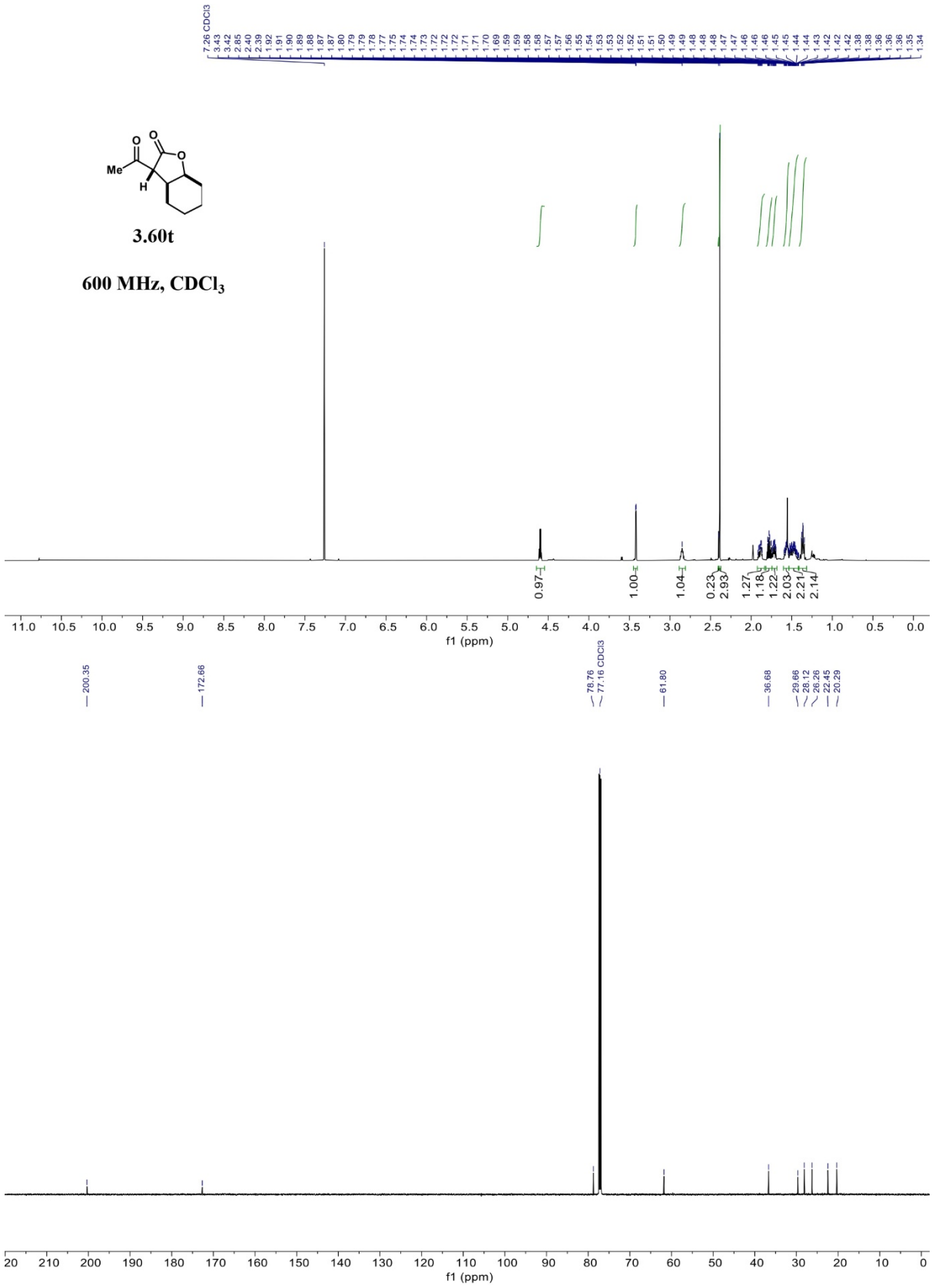

7.26 CDCl3
3.73 3.70 3.04 3.03 3.02 3.00 2.87 2.87 2.86 2.47 2.47 2.46 2.45 2.45 2.44 2.43 2.43 2.41 2.40 2.37 2.37 2.36 2.35 2.35 2.34 2.33 2.23 2.23 2.22 2.04 1.93 1.92 1.91 1.90 1.90 1.89 1.89 1.88 1.88 1.87 1.87 1.86 1.86 1.85 1.85 1.85 1.84 1.84 1.78 1.76 1.67 1.61 1.59 1.58 1.58 1.57 1.57 1.56 1.55 1.55 1.54 1.54 1.53 1.53 1.52 1.52 1.51 1.51 1.50 1.27 1.26 1.25 1.25 1.24 1.24 1.23 1.23 1.23 1.22 1.22 1.21 1.21 1.21 1.17 1.15 0.86 0.84
O
CO2Me
Me
H
3.60o
400 MHz, CDCl3
1.71
1.29
0.83
0.56
2.05
0.62
5.25
2.29
1.28
1.70
1.32
10.0 9.5 9.0 8.5 8.0 7.5 7.0 6.5 6.0 5.5 5.0 4.5 4.0 3.5 3.0 2.5 2.0 1.5 1.0 0.5 0.0
f1 (ppm)
209.68
207.66
173.60
171.41
77.48
77.16 CDCl3
76.84
69.57
68.23
52.55
52.30
47.84
45.40
43.76
42.32
40.92
36.74
32.04
31.21
28.37
27.54
26.56
25.63
23.46
23.17
17.87
15.81
210 200 190 180 170 160 150 140 130 120 110 100 90 80 70 60 50 40 30 20 10 0
f1 (ppm)

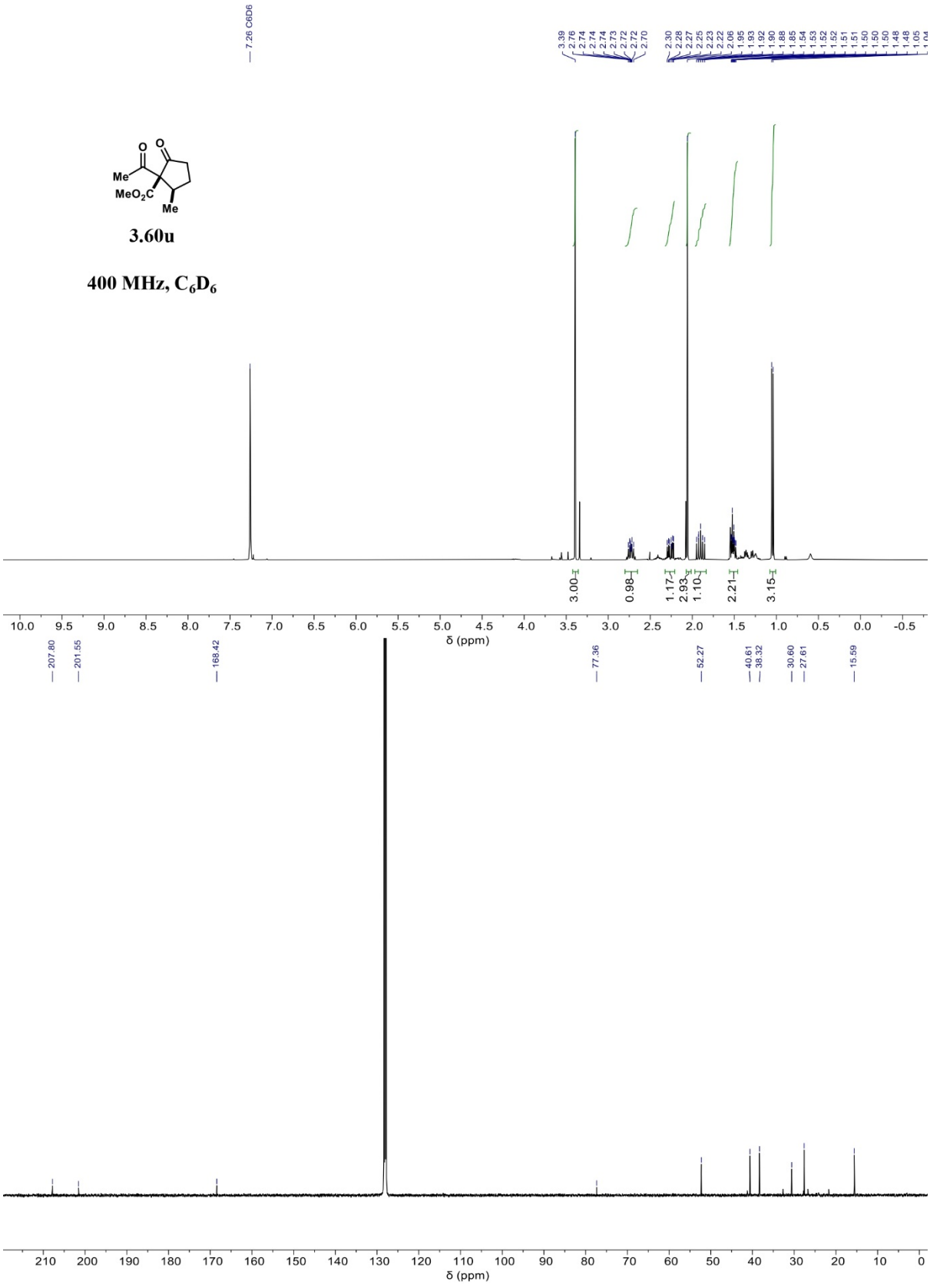

PhN
Me
+
3.60p + 3.60p'
600 MHz, CDCl3
f1 (ppm)
f1 (ppm)

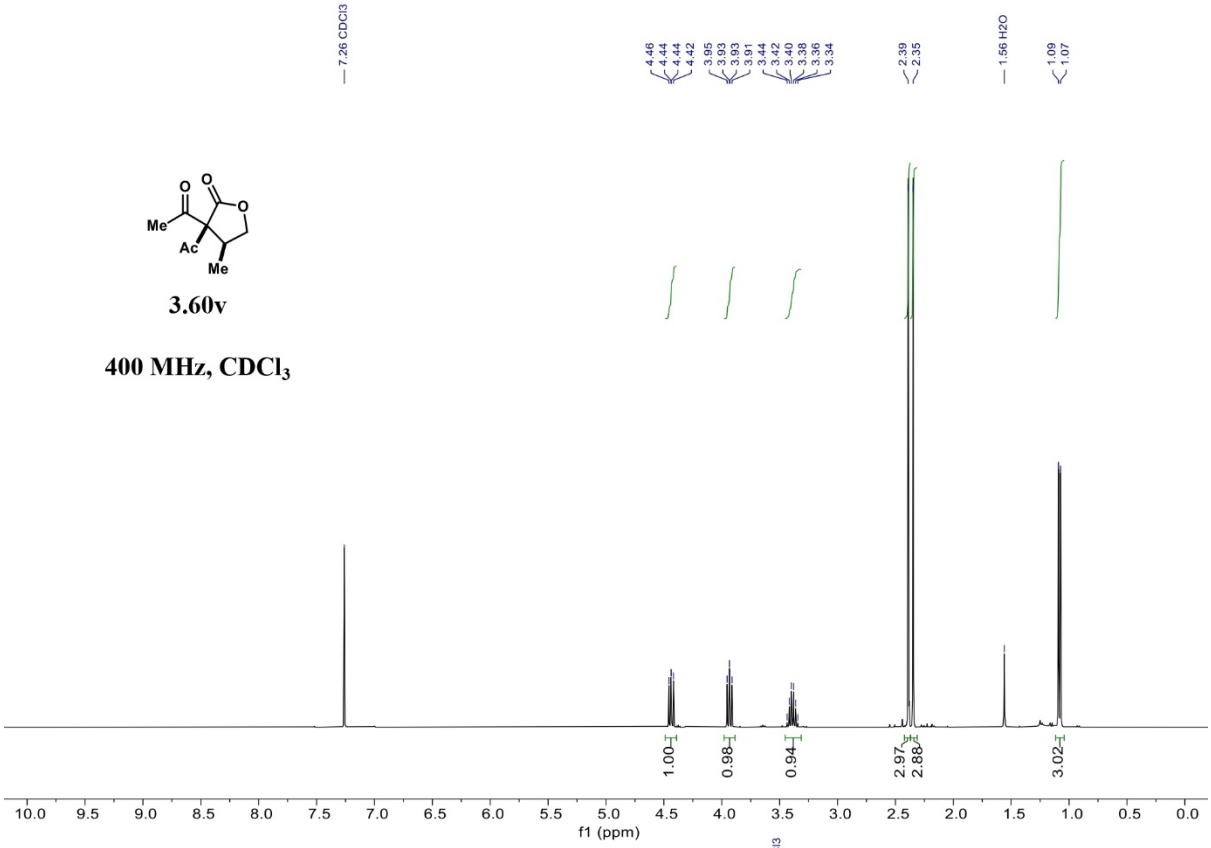

7.41 7.41 7.41 7.40 7.39 7.38 7.30 7.29 7.28 7.28 7.27 7.27 7.27 7.27 7.26 CDCl3 7.25 7.25 7.25 7.24 7.23 7.23 7.22 7.22 7.22 7.22 4.65 4.64 4.34 4.33 4.32 4.27 4.25 4.23 3.76 3.75 3.74 3.74 3.73 3.73 3.73 3.72 3.72 3.71 3.70 3.70 3.69 3.68 3.68 3.67 2.59 2.58 2.58 2.58 2.57 2.56 2.55 2.51 2.51 2.50 2.49 2.48 2.47 2.47 2.34 2.33 2.33 2.05 2.05 2.04 2.04 2.04 2.03 2.02 1.95 1.94 1.93 1.93 1.93 1.92 1.91 1.91 1.27 1.26 1.13 1.12
PhN
Me
+
3.60q + 3.60q'
600 MHz, CDCl3
3.02 1.46 2.50 0.37 1.06 1.00 0.30 3.38 0.26 1.00 1.05 0.27 1.16 2.20 1.34 3.47 0.83
f1 (ppm)
177.55 176.70 167.63 166.19 143.05 142.66 129.46 129.40 127.49 127.33 126.42 126.31 77.37 77.16 CDCl3 76.95 73.00 72.66 54.20 54.16 52.06 51.68 43.81 38.12 32.20 24.62 20.51 19.39 13.39 12.32
f1 (ppm)


8.07
8.06
8.06
8.05
8.04
7.64
7.54
7.54
7.54
7.54
7.53
7.53
7.52
7.52
7.51
7.50
7.50
4.63
4.61
4.60
4.59
4.19
4.18
4.01
3.99
3.99
3.97
3.26
1.24
1.23
O
O
O
H
Me
3.60r
500 MHz, CDCl3
1.93
1.07
2.12
1.08
1.07
1.00
0.95
3.20
f1 (ppm)
192.93
172.70
135.88
134.23
129.53
128.95
73.80
56.20
34.37
17.52
f1 (ppm)


7.26 CDCl3
4.46
4.44
4.44
4.42
3.95
3.93
3.93
3.91
3.44
3.42
3.40
3.38
3.36
3.34
2.39
2.35
1.56 H2O
1.09
1.07
Me
O
O
O
H
Me
3.60s
400 MHz, CDCl3
1.00
0.98
0.94
2.97
2.88
3.02
f1 (ppm)
200.34
197.66
171.41
77.16 CDCl3
72.38
36.28
30.57
28.10
13.62
f1 (ppm)

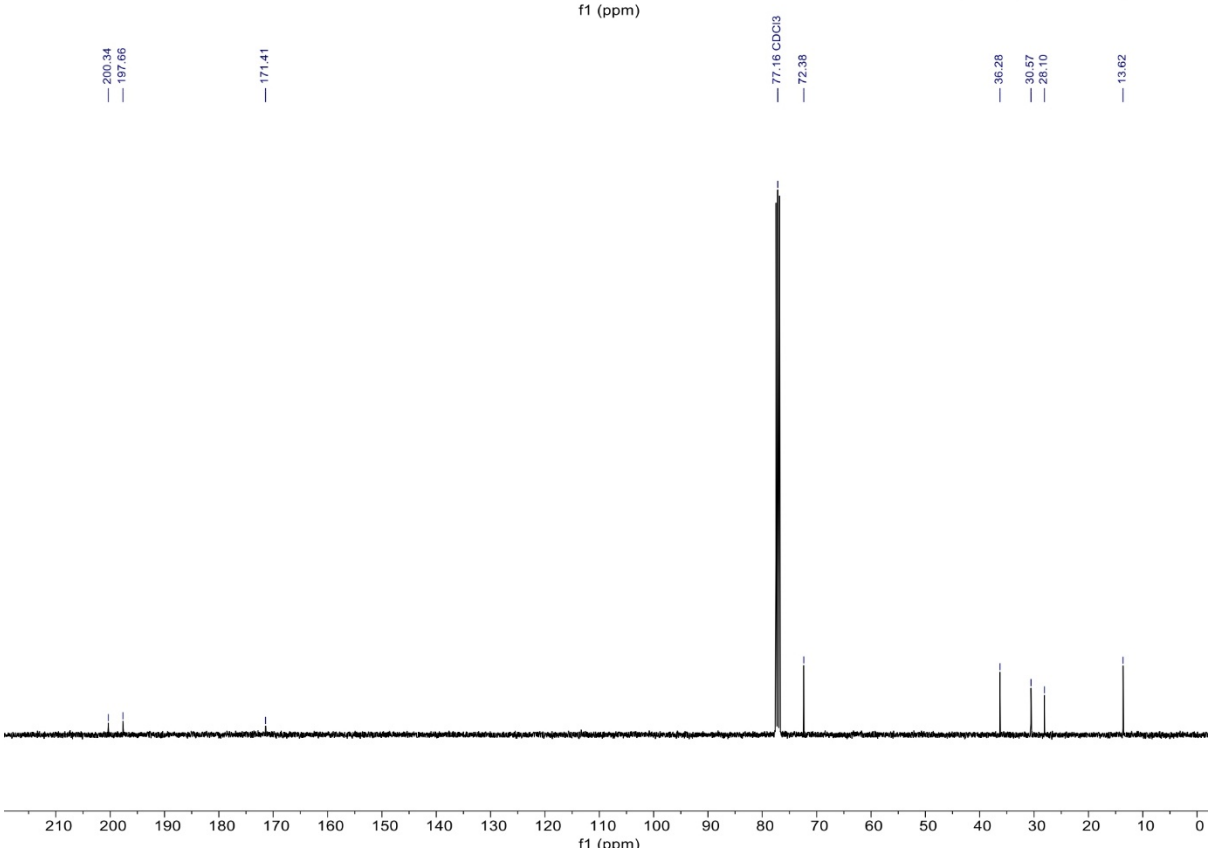

7.26 CDCl3
Me
H
3.60t
600 MHz, CDCl3
0.97
1.00
1.04
0.23
2.93
1.27
1.18
1.22
2.03
2.21
2.14
f1 (ppm)
200.35
172.66
78.76
77.16 CDCl3
61.80
36.68
29.66
28.12
26.26
22.45
20.29
f1 (ppm)

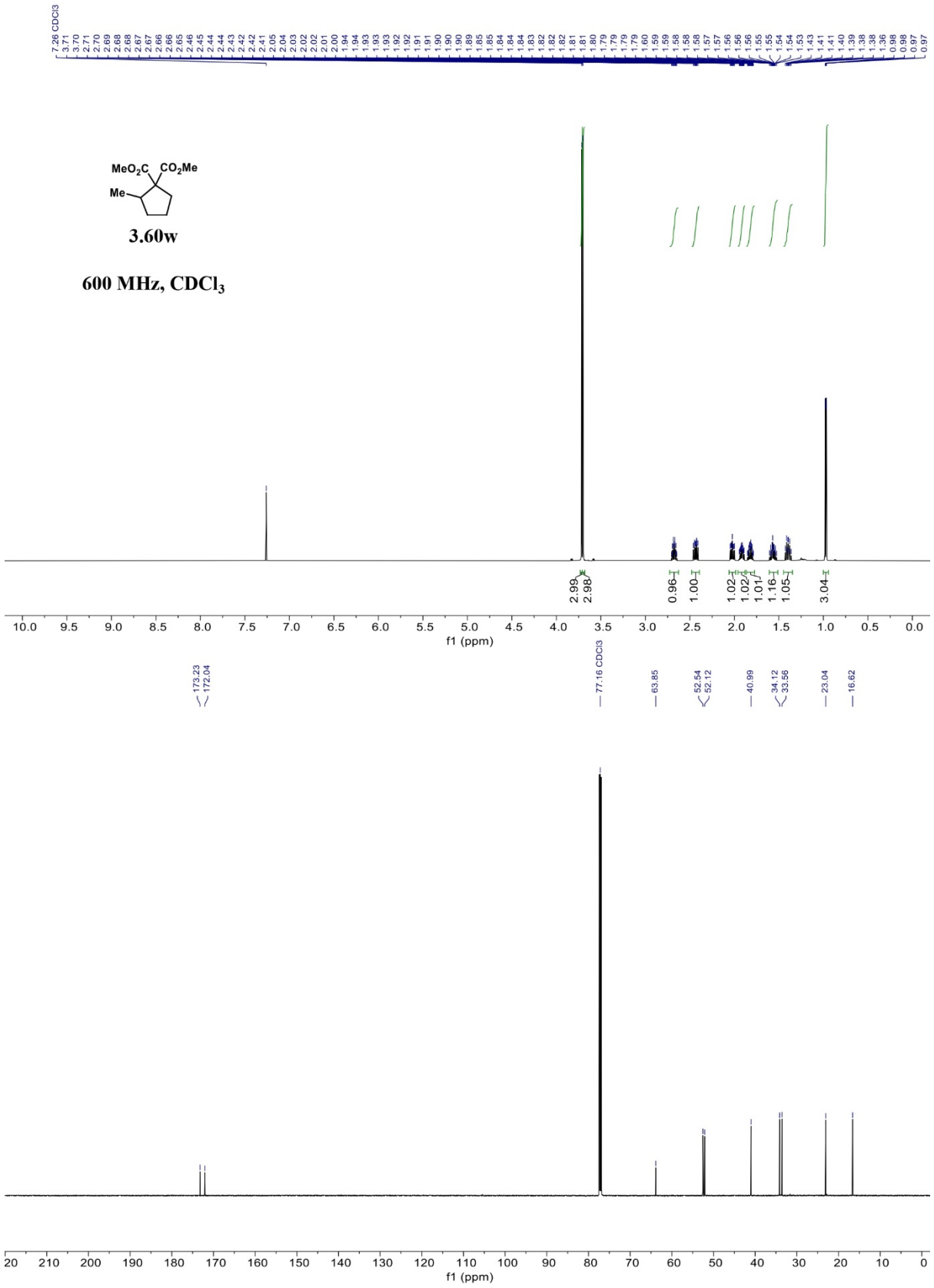

7.26 C6D6
3.39
2.76
2.74
2.74
2.74
2.73
2.72
2.72
2.70
2.30
2.28
2.27
2.25
2.23
2.22
2.06
1.95
1.93
1.92
1.90
1.88
1.85
1.54
1.53
1.52
1.52
1.51
1.51
1.50
1.50
1.50
1.48
1.48
1.05
Me
MeO2C
Me
3.60u
400 MHz, C6D6
3.00
0.98
1.17
2.93
1.10
2.21
3.15
δ (ppm)
207.80
201.55
168.42
77.36
52.27
40.61
38.32
30.60
27.61
15.59
δ (ppm)

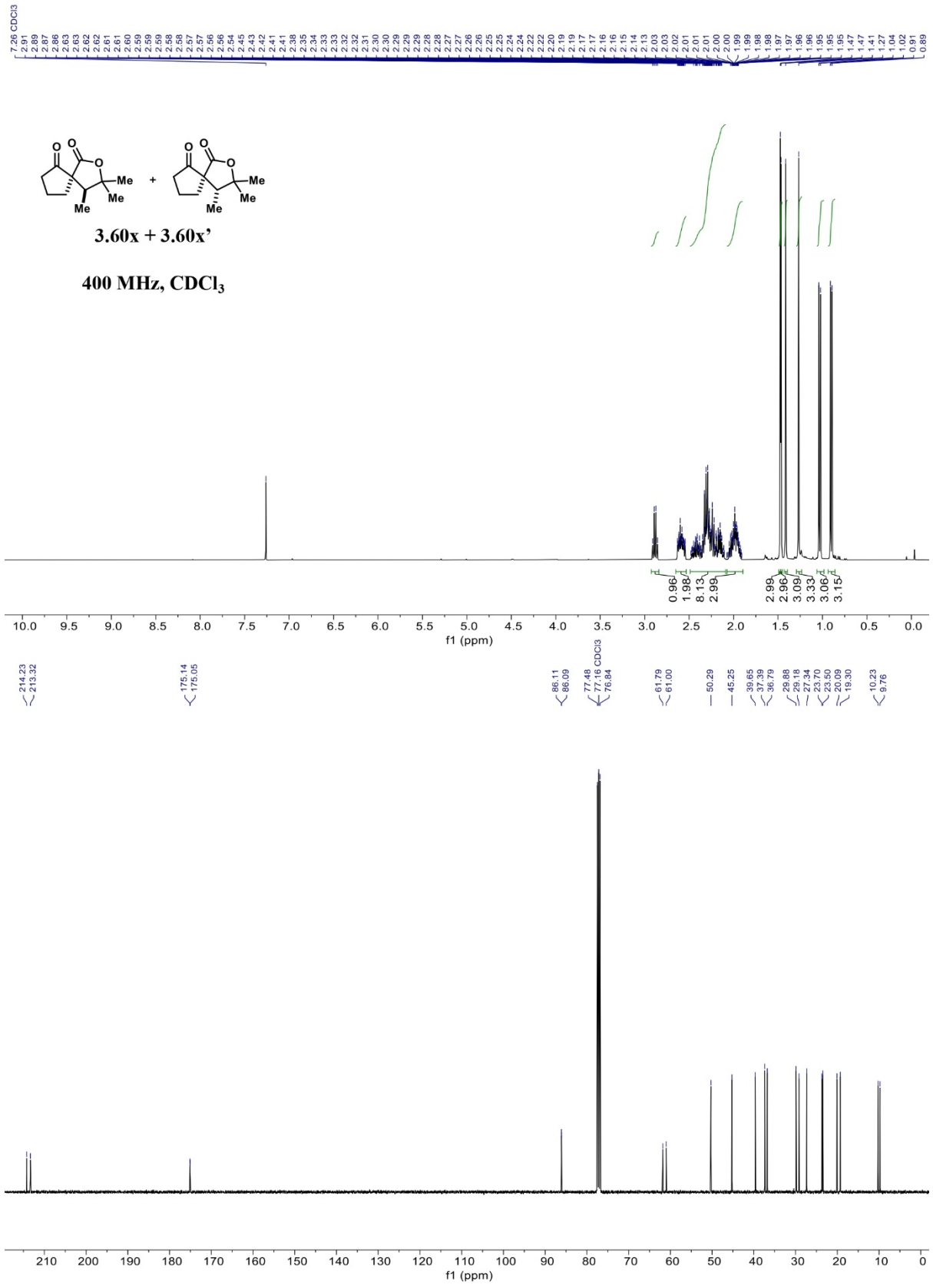


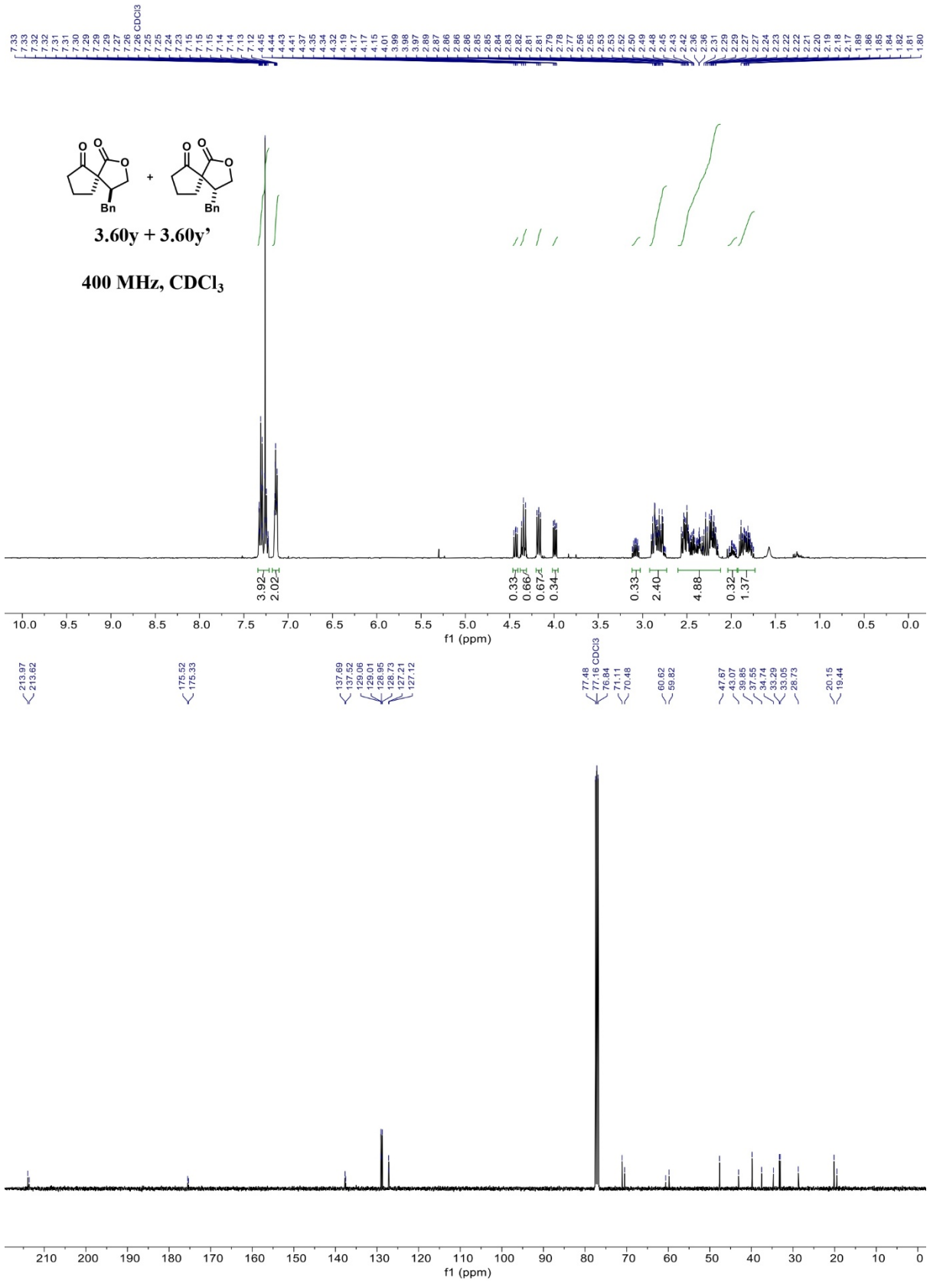
3.60v

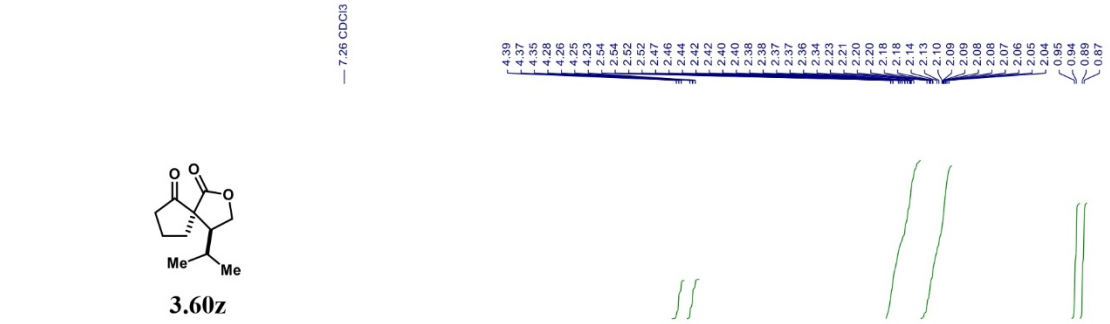
400 MHz, $CDCl_3$




MeO2C CO2Me
Me
3.60w
600 MHz, CDCl3
f1 (ppm)
f1 (ppm)

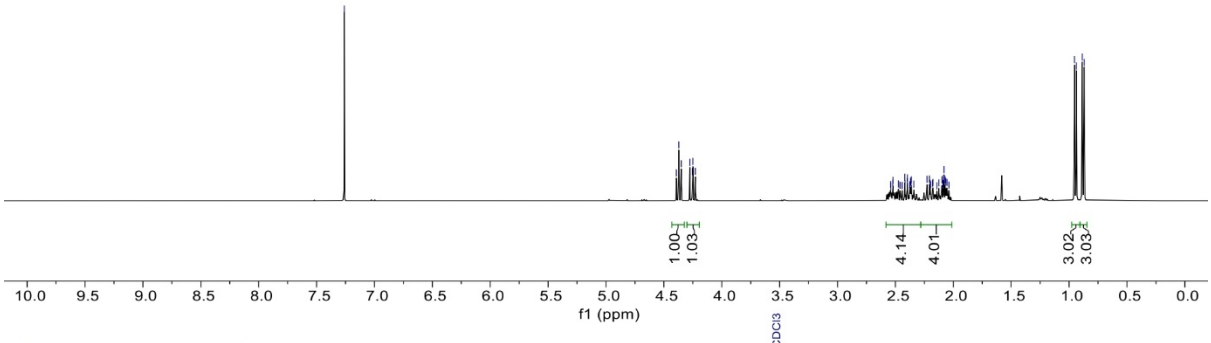

3.60x + 3.60x'
400 MHz, CDCl3
f1 (ppm)
f1 (ppm)

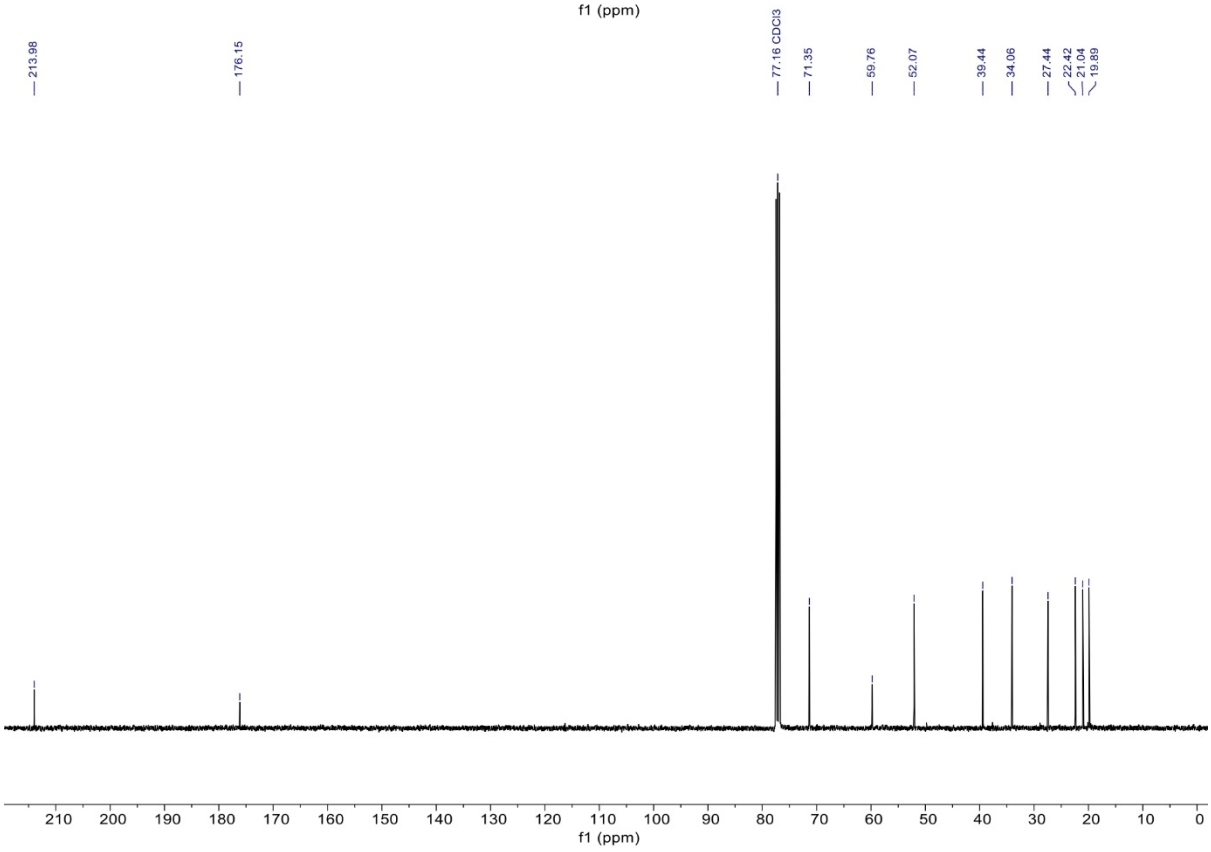

Bn
Bn
3.60y + 3.60y'
400 MHz, CDCl3
f1 (ppm)
f1 (ppm)

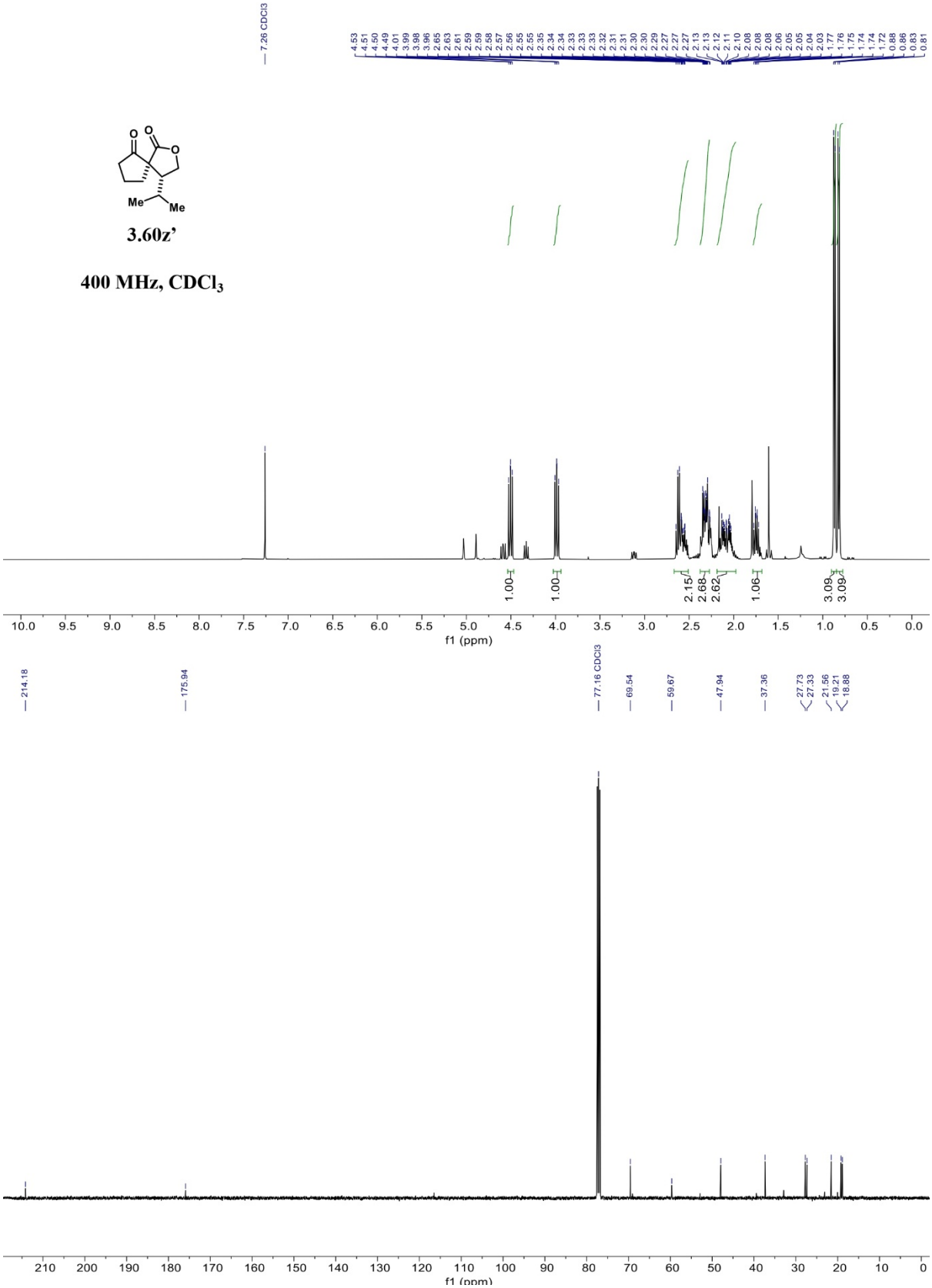


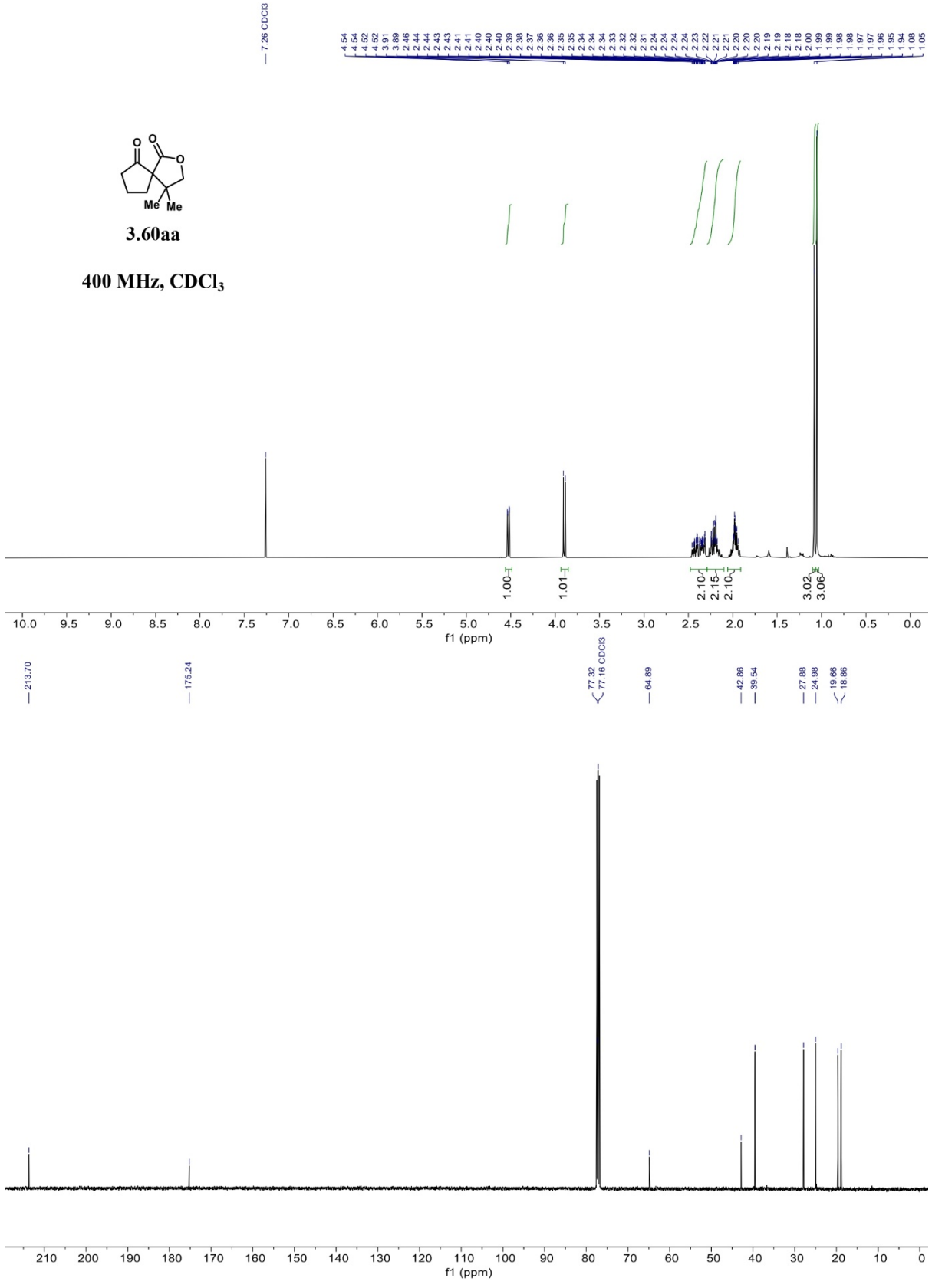
3.60z

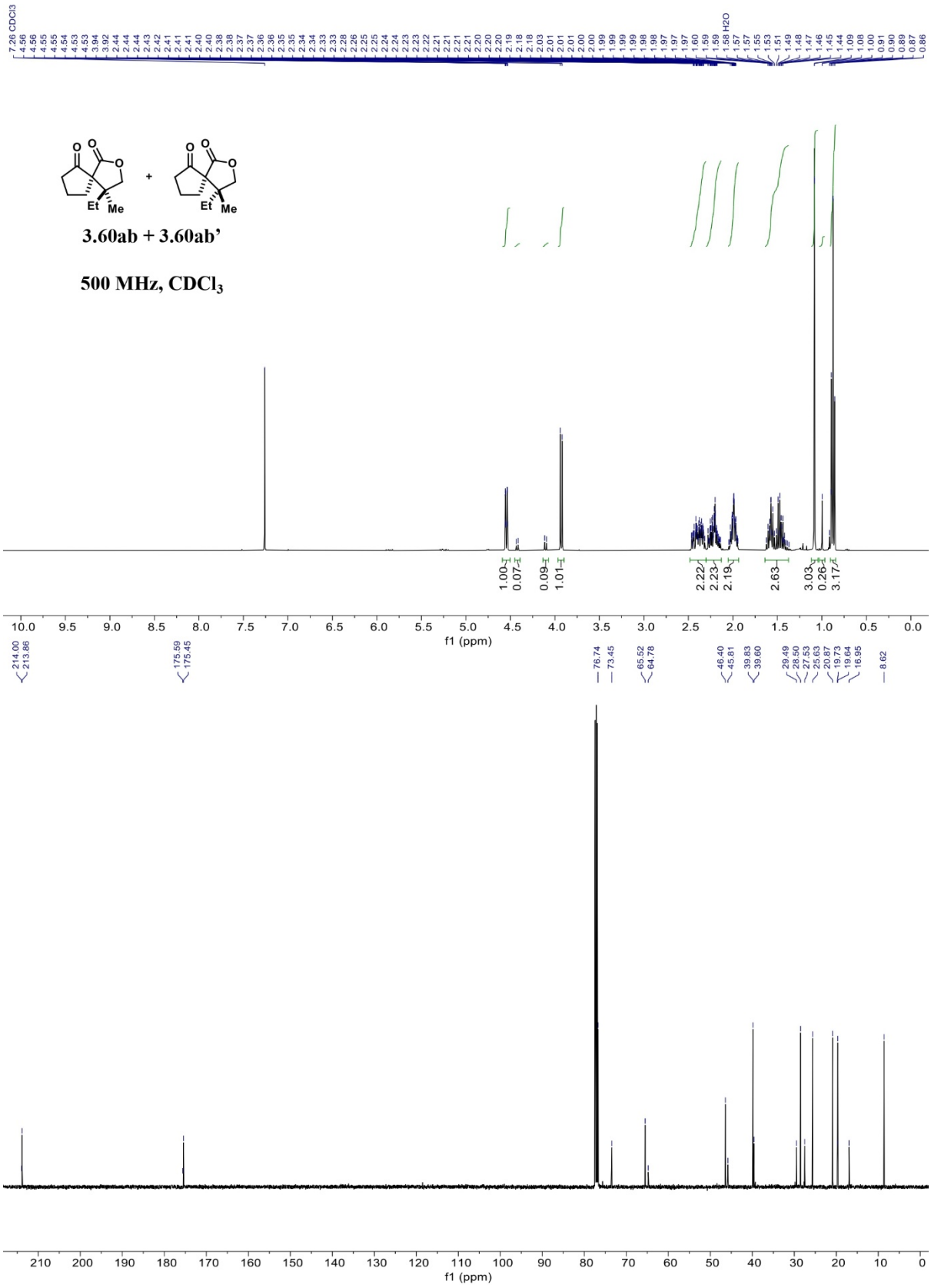
400 MHz, $CDCl_3$

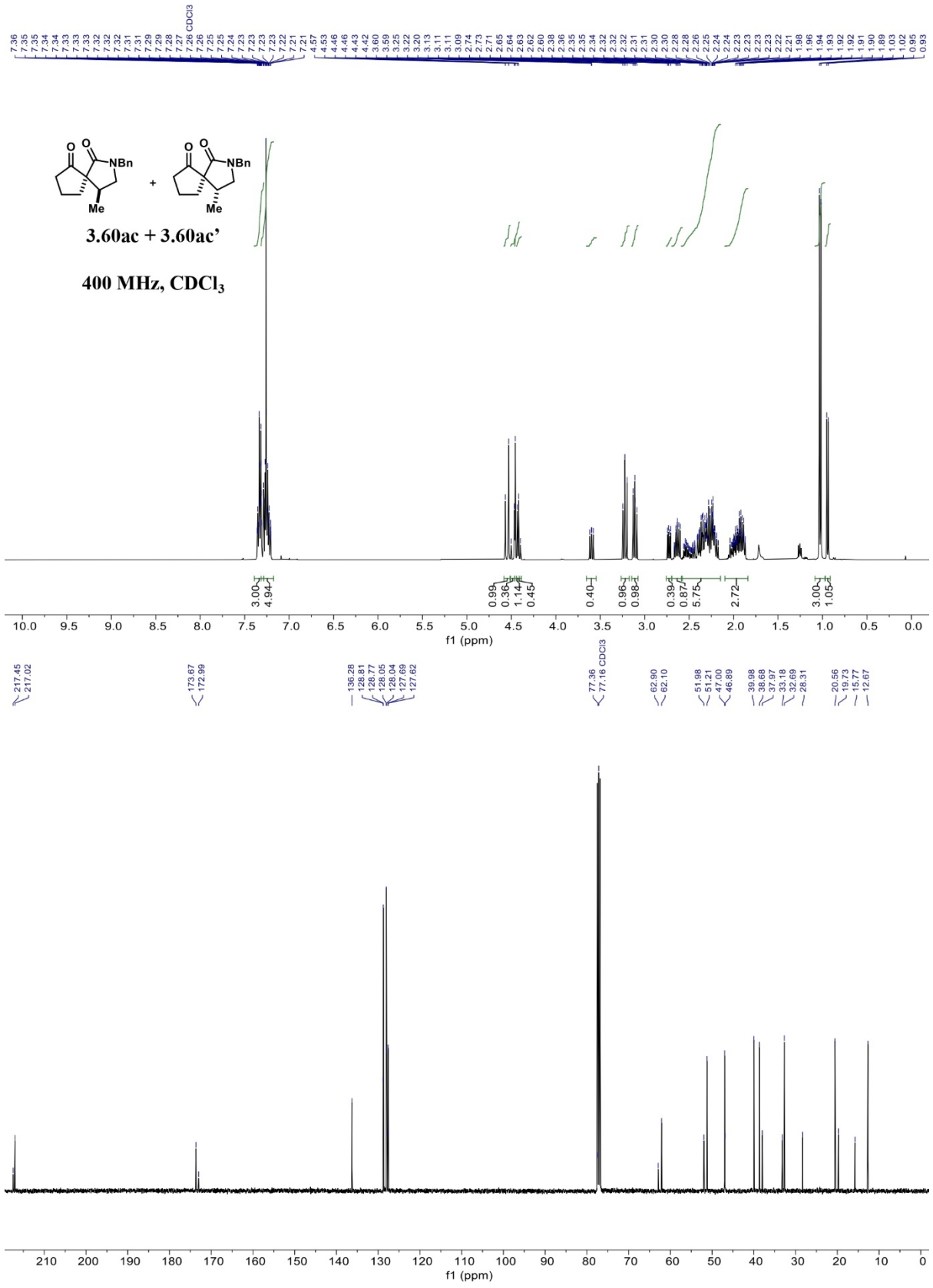


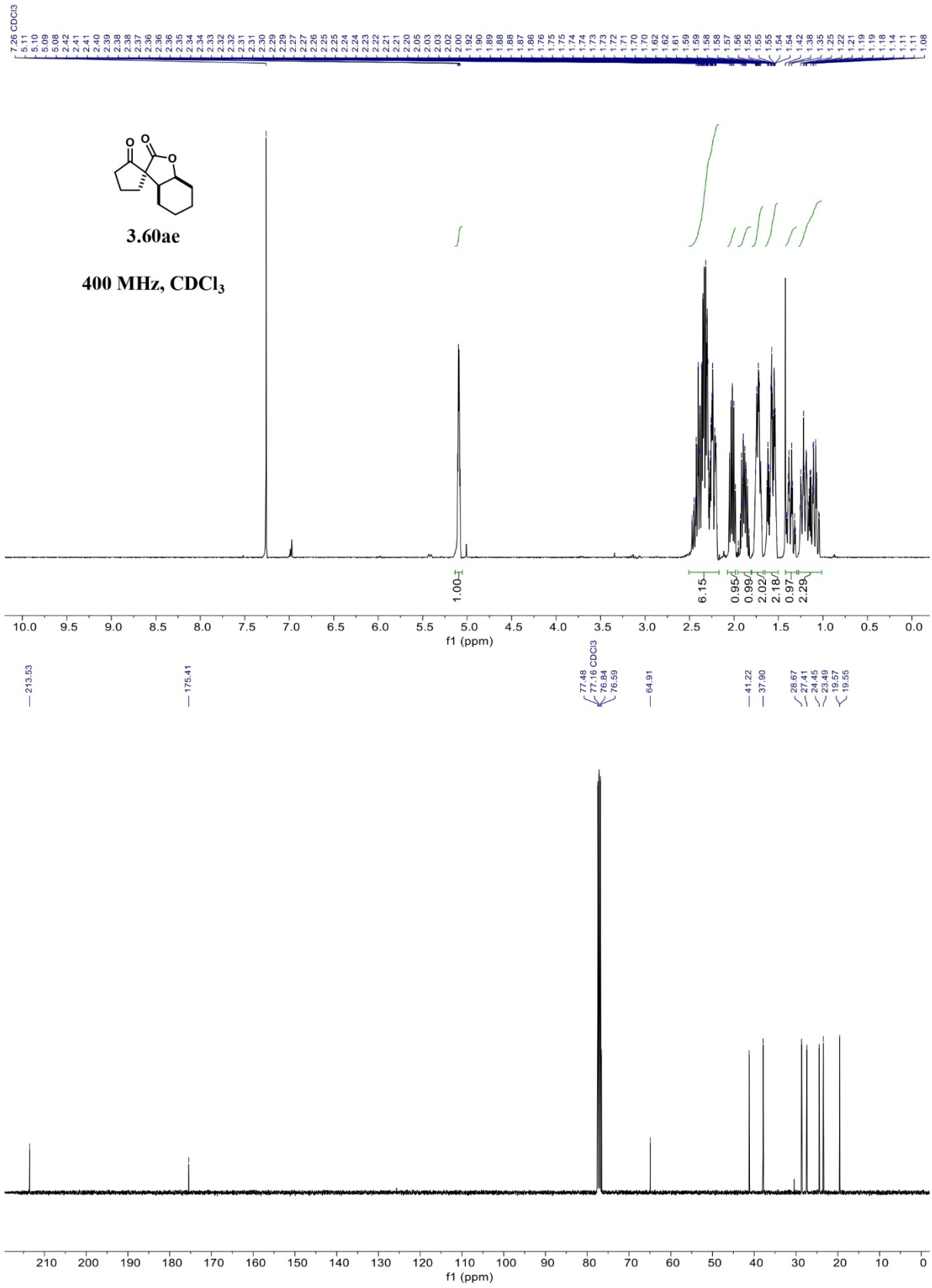


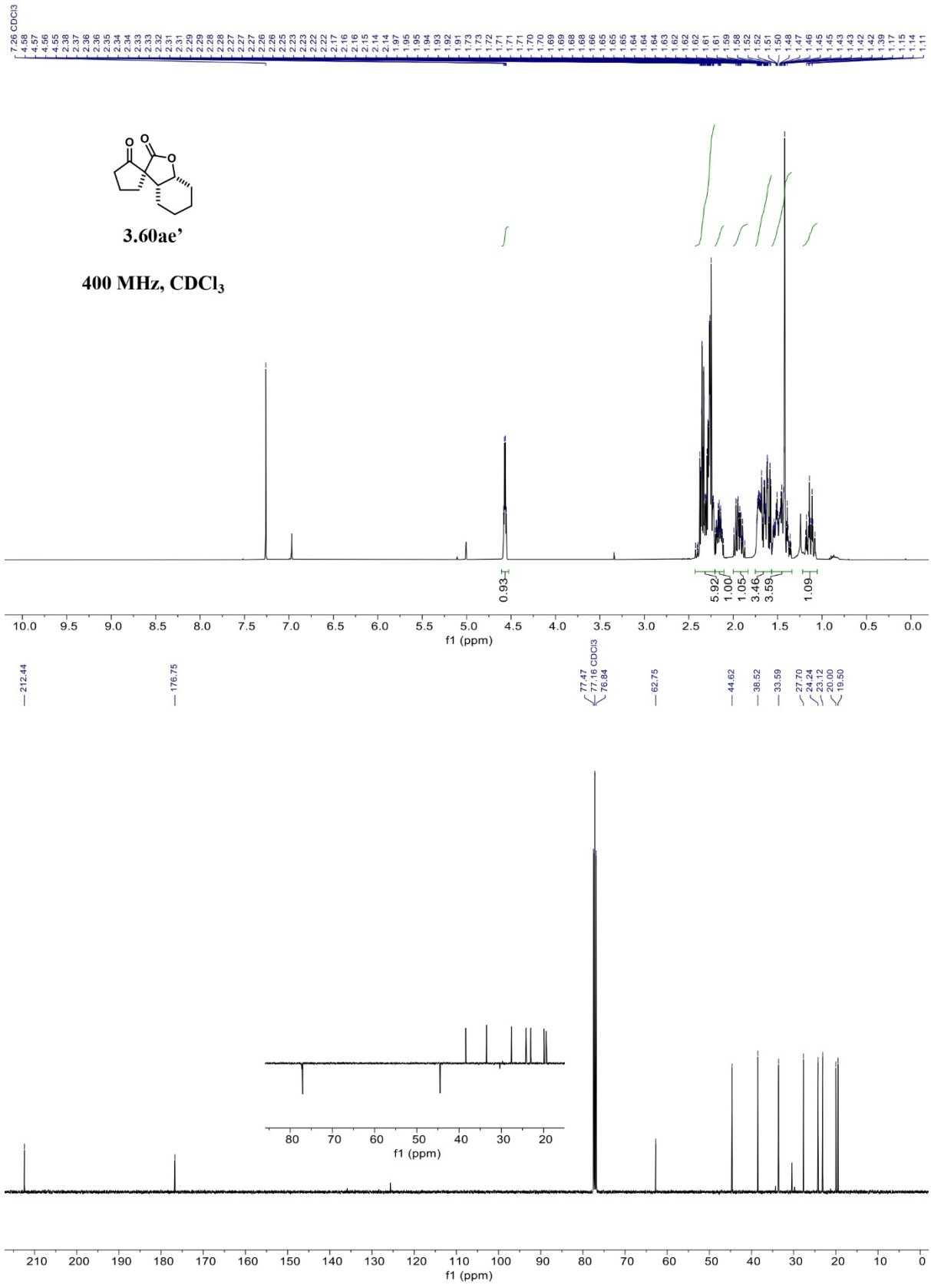

7.26 CDCl3
4.53
4.51
4.50
4.49
4.01
3.99
3.98
3.96
3.65
2.63
2.61
2.59
2.59
2.58
2.57
2.56
2.55
2.55
2.35
2.34
2.34
2.33
2.33
2.32
2.31
2.30
2.30
2.29
2.27
2.27
2.13
2.12
2.11
2.10
2.08
2.08
2.08
2.06
2.05
2.05
2.04
2.03
1.77
1.76
1.75
1.74
1.74
1.72
0.88
0.86
0.83
0.81
O
O
O
Me
Me
3.60z'
400 MHz, CDCl3
1.00
1.00
2.15
2.68
2.62
1.06
3.09
3.09
10.0
9.5
9.0
8.5
8.0
7.5
7.0
6.5
6.0
5.5
5.0
4.5
4.0
3.5
3.0
2.5
2.0
1.5
1.0
0.5
0.0
f1 (ppm)
214.18
175.94
77.16 CDCl3
69.54
59.67
47.94
37.36
27.73
27.33
21.56
19.21
18.88
210
200
190
180
170
160
150
140
130
120
110
100
90
80
70
60
50
40
30
20
10
0
f1 (ppm)

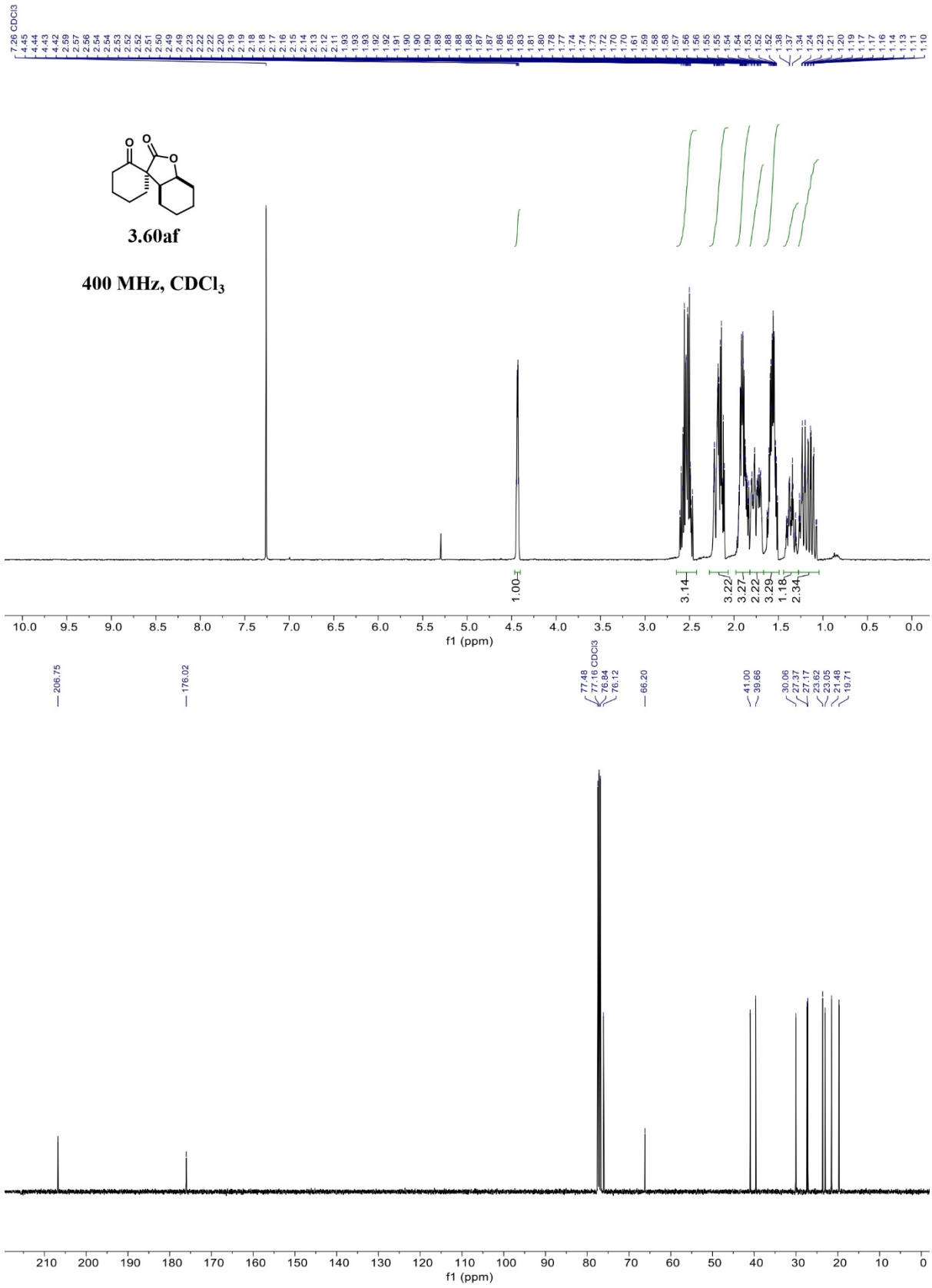

7.26 CDCl3
4.54 4.54 4.52 4.52 3.91 3.89 2.46 2.44 2.44 2.43 2.43 2.41 2.41 2.40 2.40 2.40 2.39 2.38 2.37 2.36 2.36 2.35 2.35 2.34 2.34 2.34 2.33 2.32 2.32 2.31 2.24 2.24 2.24 2.23 2.22 2.21 2.21 2.20 2.20 2.20 2.19 2.19 2.18 2.18 2.00 1.99 1.99 1.98 1.98 1.97 1.97 1.96 1.95 1.94 1.08 1.05
O
O
O
Me
Me
3.60aa
400 MHz, CDCl3
1.00
1.01
2.10
2.15
2.10
3.02
3.06
10.0 9.5 9.0 8.5 8.0 7.5 7.0 6.5 6.0 5.5 5.0 4.5 4.0 3.5 3.0 2.5 2.0 1.5 1.0 0.5 0.0
f1 (ppm)
213.70
175.24
77.32
77.16 CDCl3
64.89
42.86
39.54
27.88
24.98
19.66
18.86
210 200 190 180 170 160 150 140 130 120 110 100 90 80 70 60 50 40 30 20 10 0
f1 (ppm)

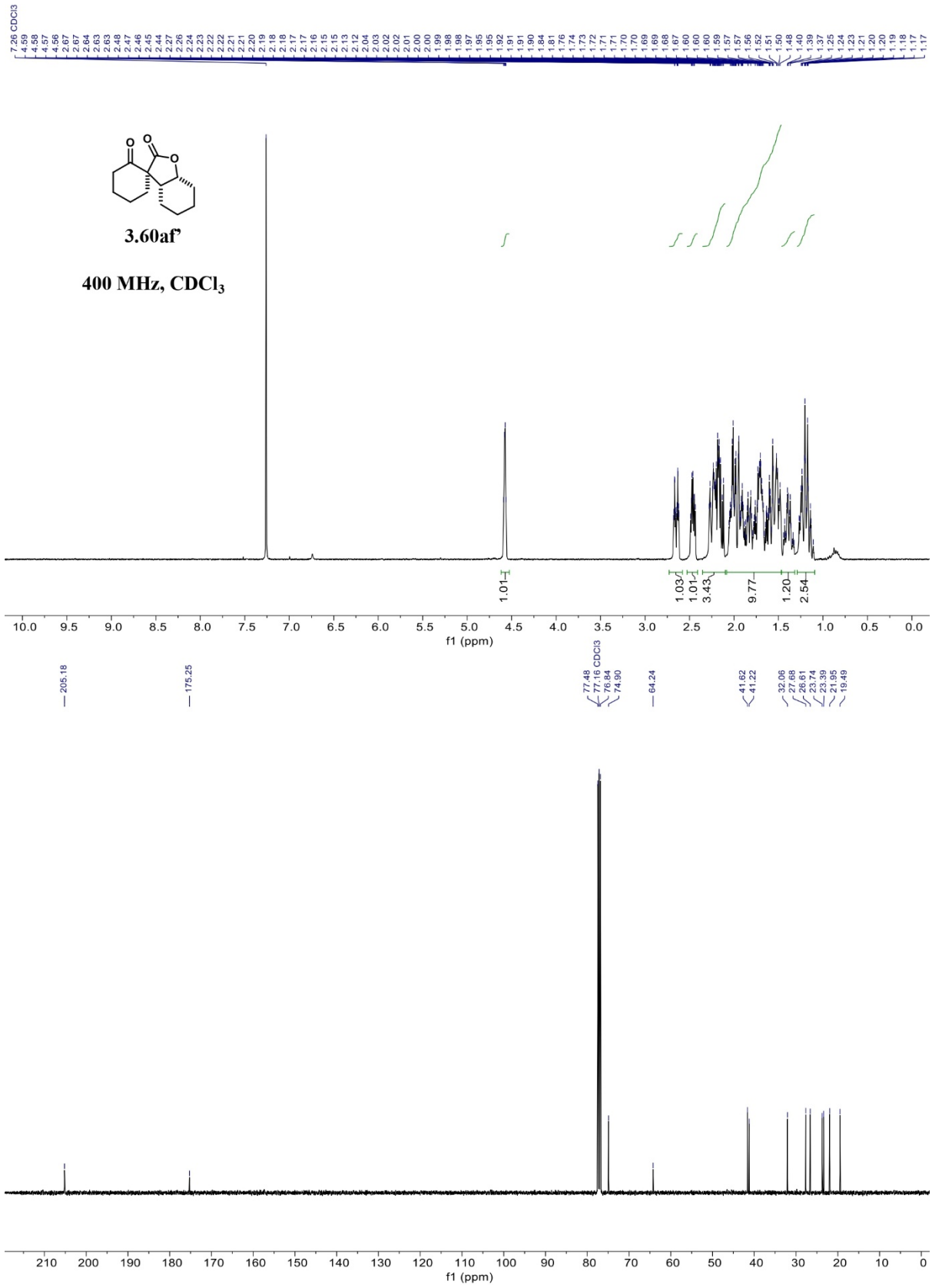

7.26 CDCl3
4.56 4.56 4.55 4.55 4.54 4.54 4.53 3.94 3.92 2.44 2.44 2.44 2.43 2.42 2.41 2.41 2.41 2.40 2.40 2.38 2.38 2.37 2.36 2.36 2.35 2.35 2.34 2.34 2.33 2.33 2.28 2.26 2.25 2.25 2.24 2.24 2.23 2.23 2.22 2.21 2.21 2.21 2.20 2.20 2.20 2.19 2.18 2.03 2.01 2.01 2.00 2.00 1.99 1.99 1.99 1.98 1.98 1.97 1.97 1.60 1.59 1.59 1.58 H2O 1.57 1.57 1.55 1.53 1.51 1.49 1.48 1.47 1.46 1.45 1.44 1.09 1.08 1.00 0.91 0.90 0.89 0.87 0.86
Et Me
Et Me
3.60ab + 3.60ab'
500 MHz, CDCl3
1.00 0.07 0.09 1.01 2.22 2.23 2.19 2.63 3.03 0.26 3.17
f1 (ppm)
214.00 213.86 175.59 175.45 76.74 73.45 65.52 64.78 46.40 45.81 39.83 39.60 29.49 28.50 27.53 25.63 20.87 19.73 19.64 16.95 8.62
f1 (ppm)

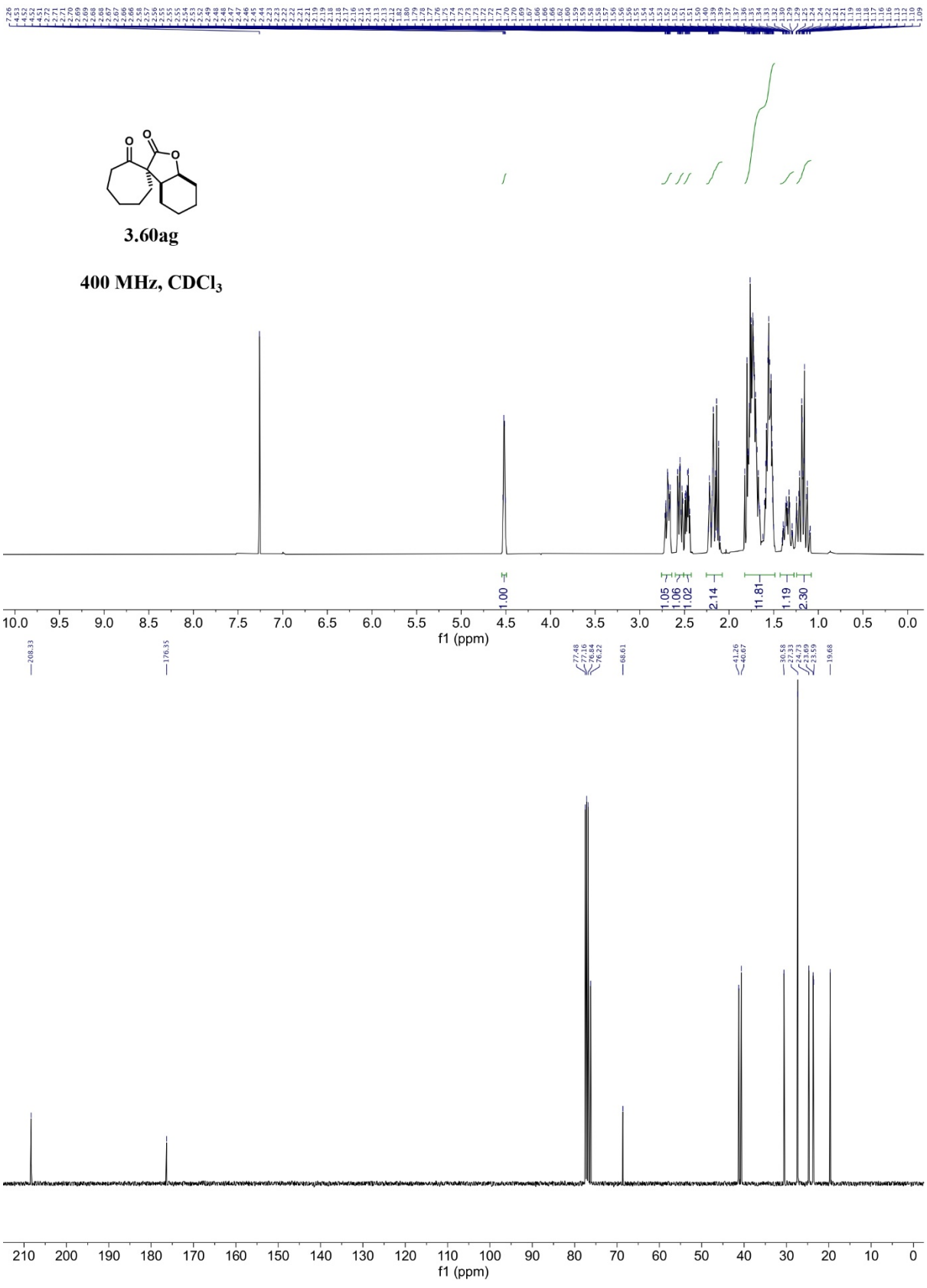

NBn
Me
+
3.60ac + 3.60ac'
400 MHz, CDCl3
f1 (ppm)
f1 (ppm)

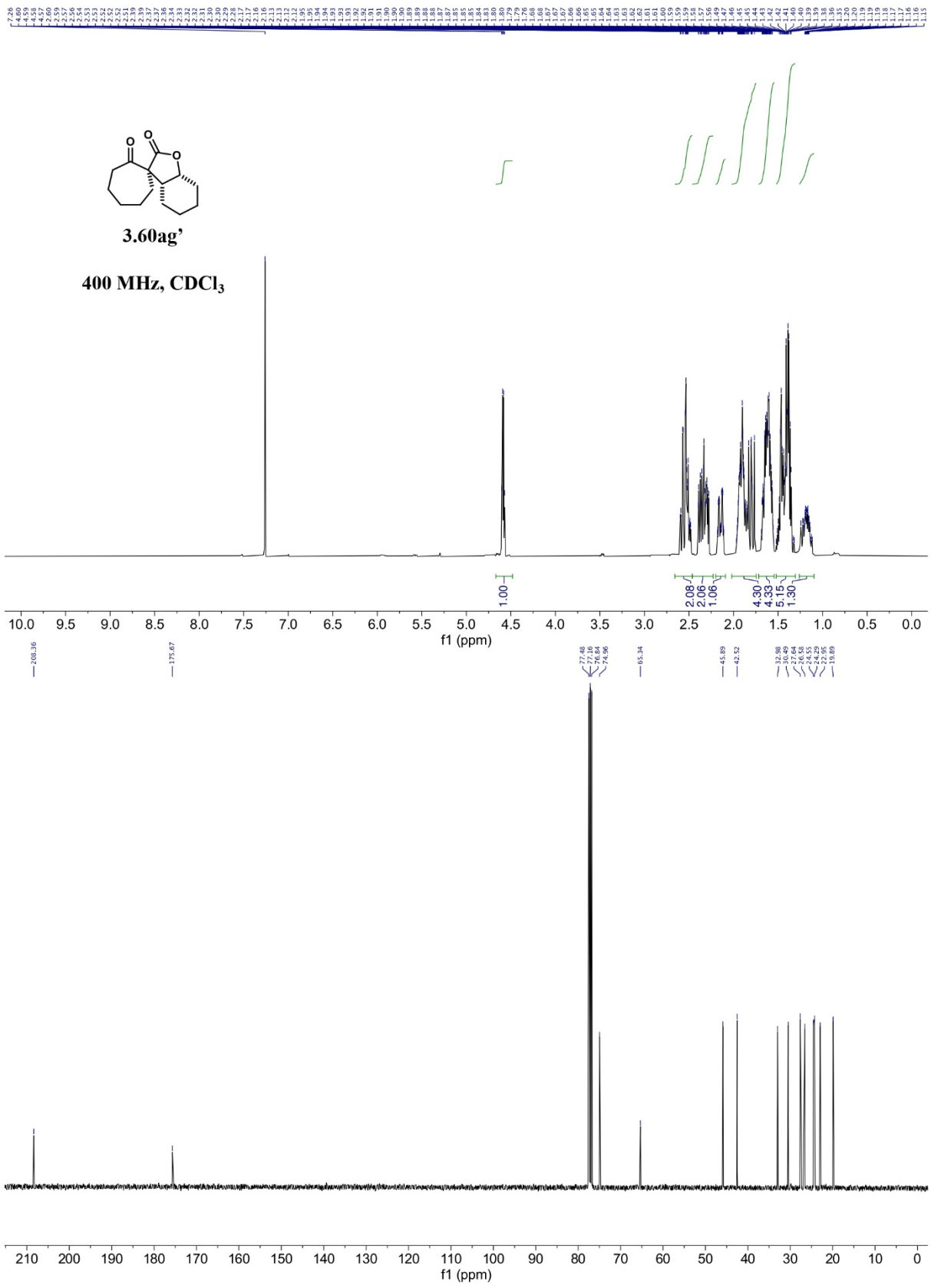

3.60ae
400 MHz, CDCl3
f1 (ppm)
f1 (ppm)

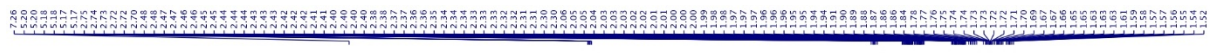

3.60ae'
400 MHz, CDCl3
f1 (ppm)

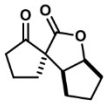

3.60af
400 MHz, CDCl3
f1 (ppm)
f1 (ppm)


3.60af'
400 MHz, CDCl3
f1 (ppm)
f1 (ppm)


3.60ag
400 MHz, CDCl3
1.00
1.05
1.06
1.02
2.14
11.81
1.19
2.30
f1 (ppm)
208.33
176.35
77.48
77.16
76.84
76.22
68.61
41.26
40.67
30.58
27.33
24.73
23.69
23.59
19.68
f1 (ppm)

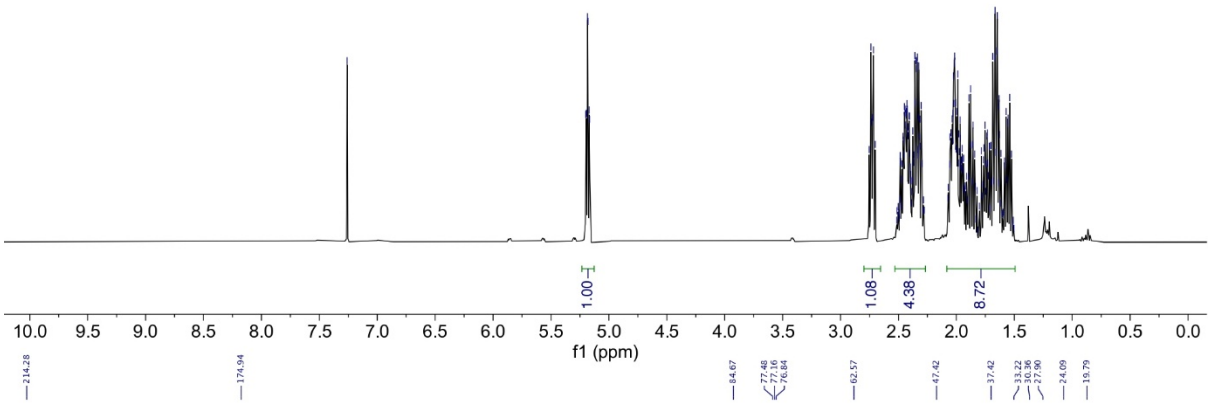

3.60ag'
400 MHz, $CDCl_3$
1.00
2.08
2.06
1.06
4.30
4.33
5.15
1.30
f1 (ppm)
208.36
175.67
77.48
77.16
76.84
74.96
65.34
45.89
42.52
32.98
30.69
27.64
26.58
24.55
24.23
22.95
19.89
f1 (ppm)

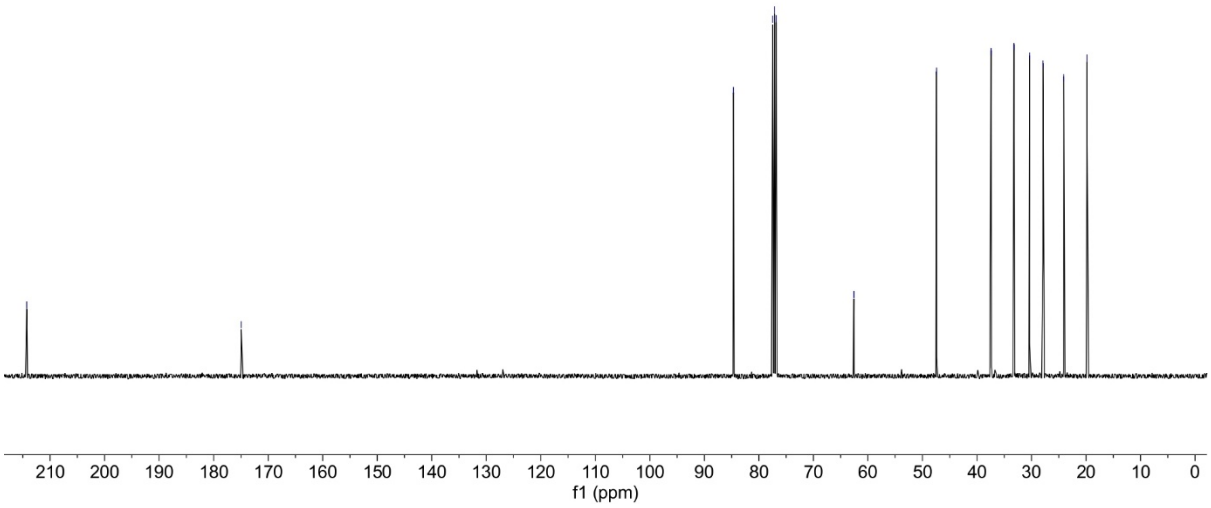


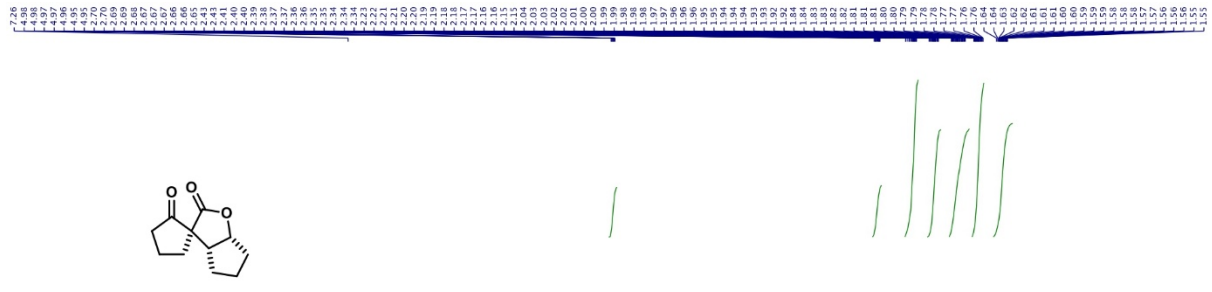


3.60ah

400 MHz, $CDCl_3$

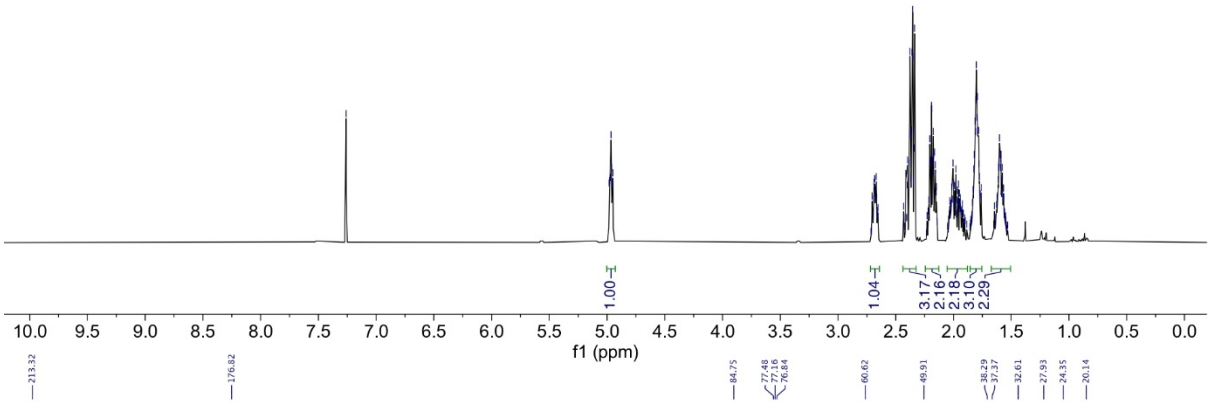


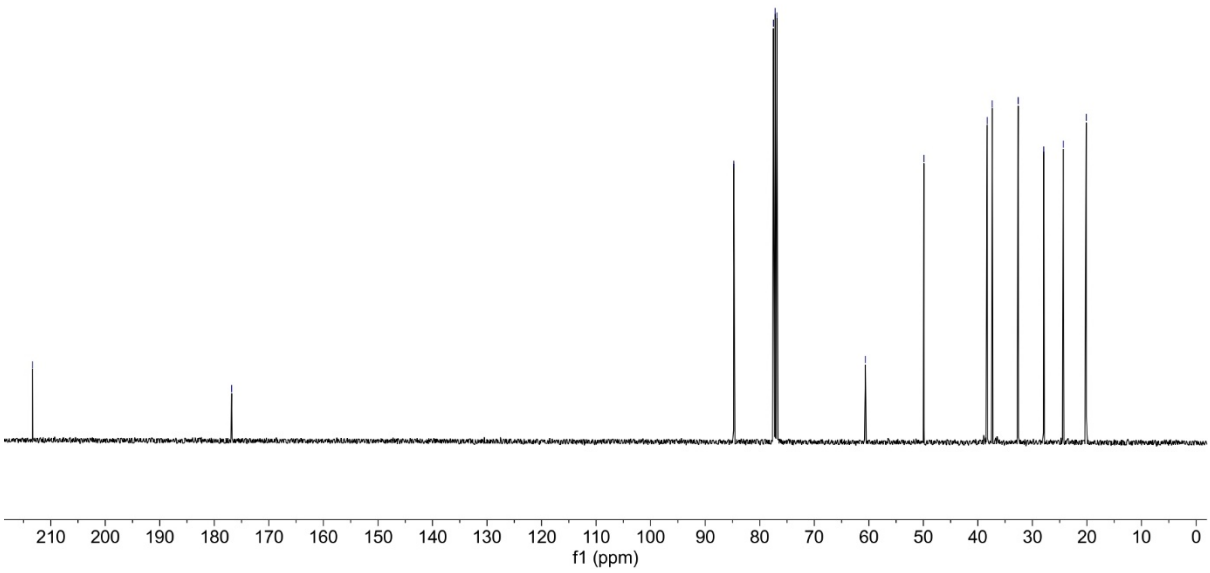


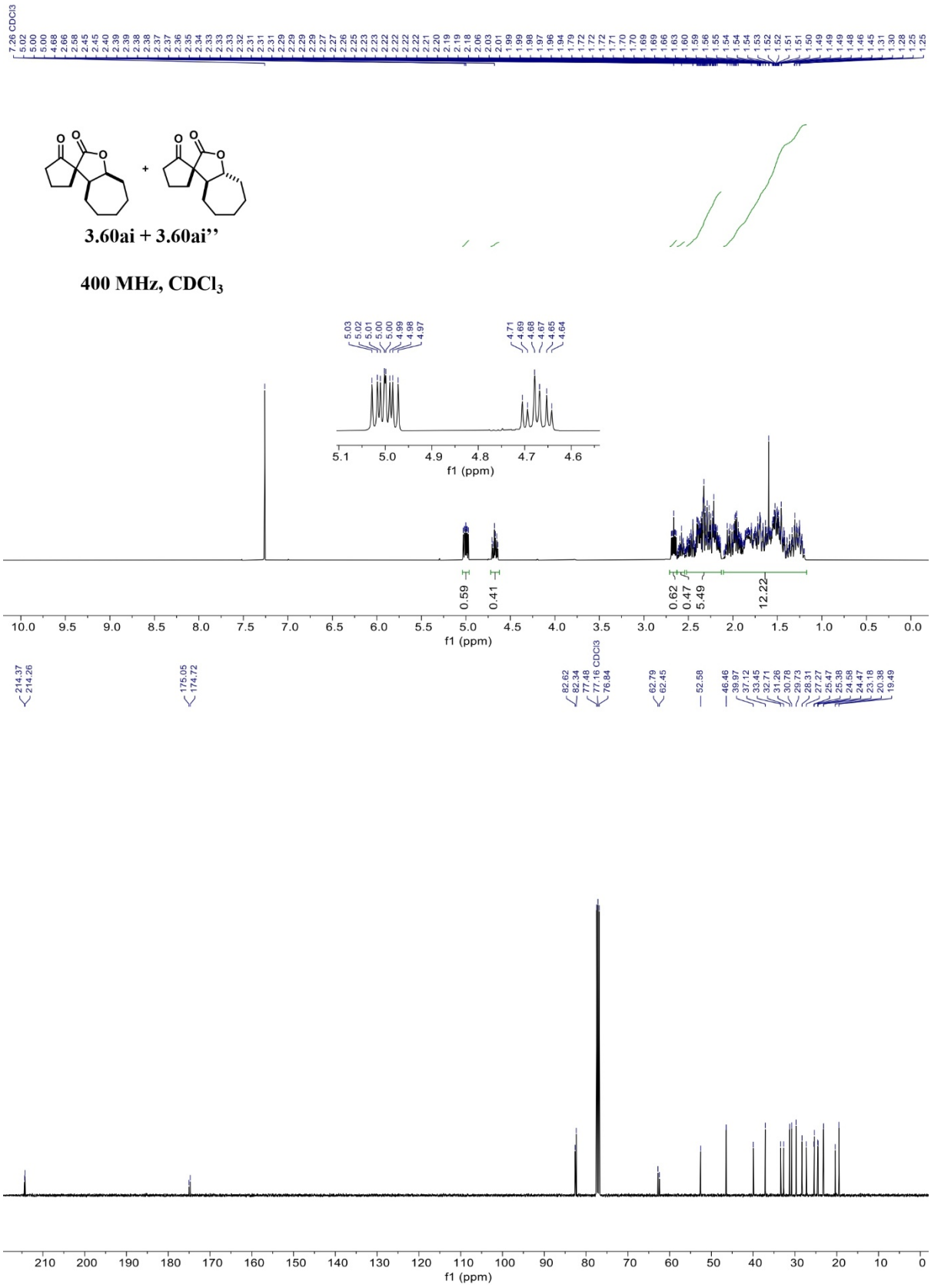


3.60ah'

400 MHz, $CDCl_3$

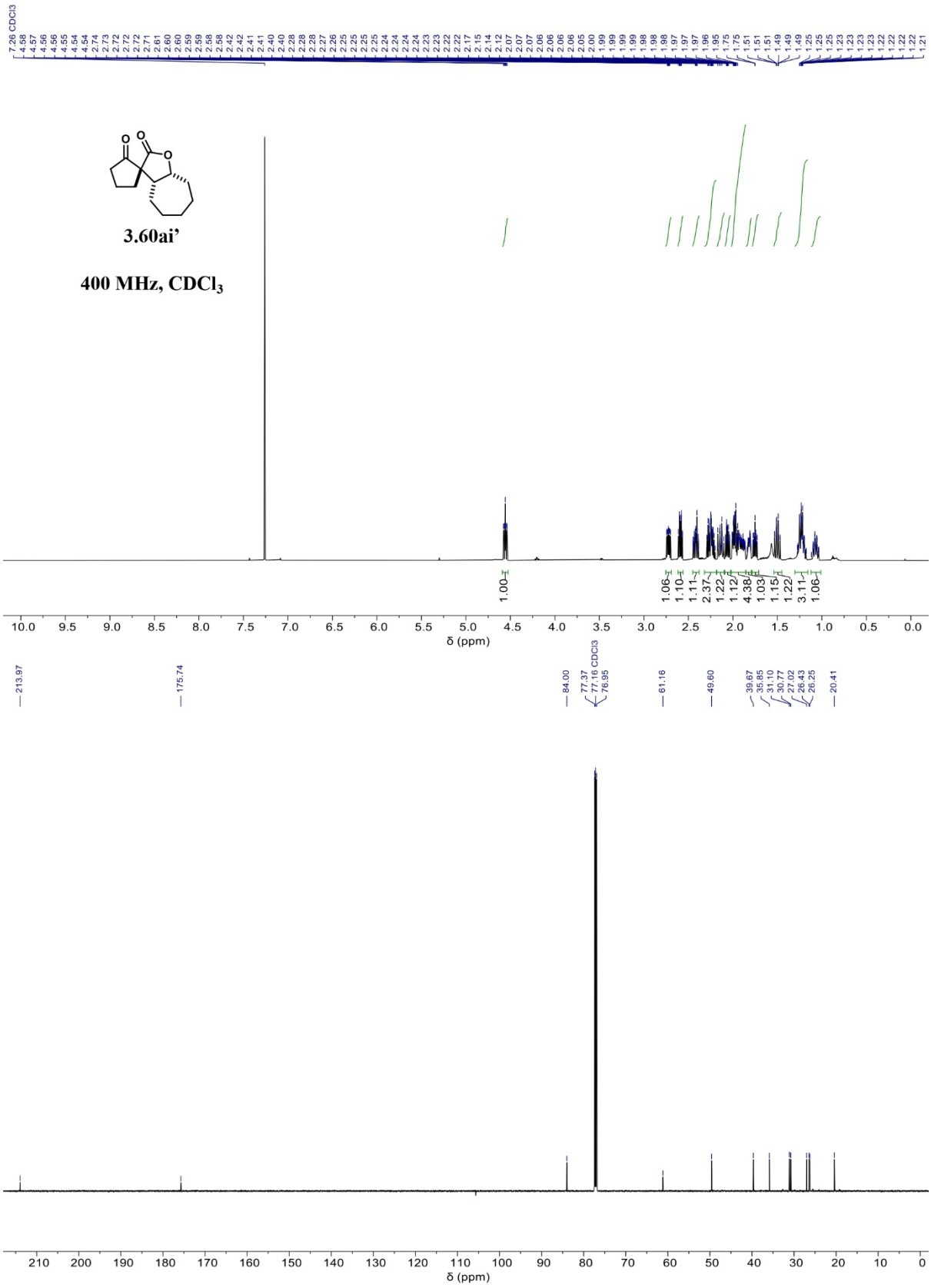


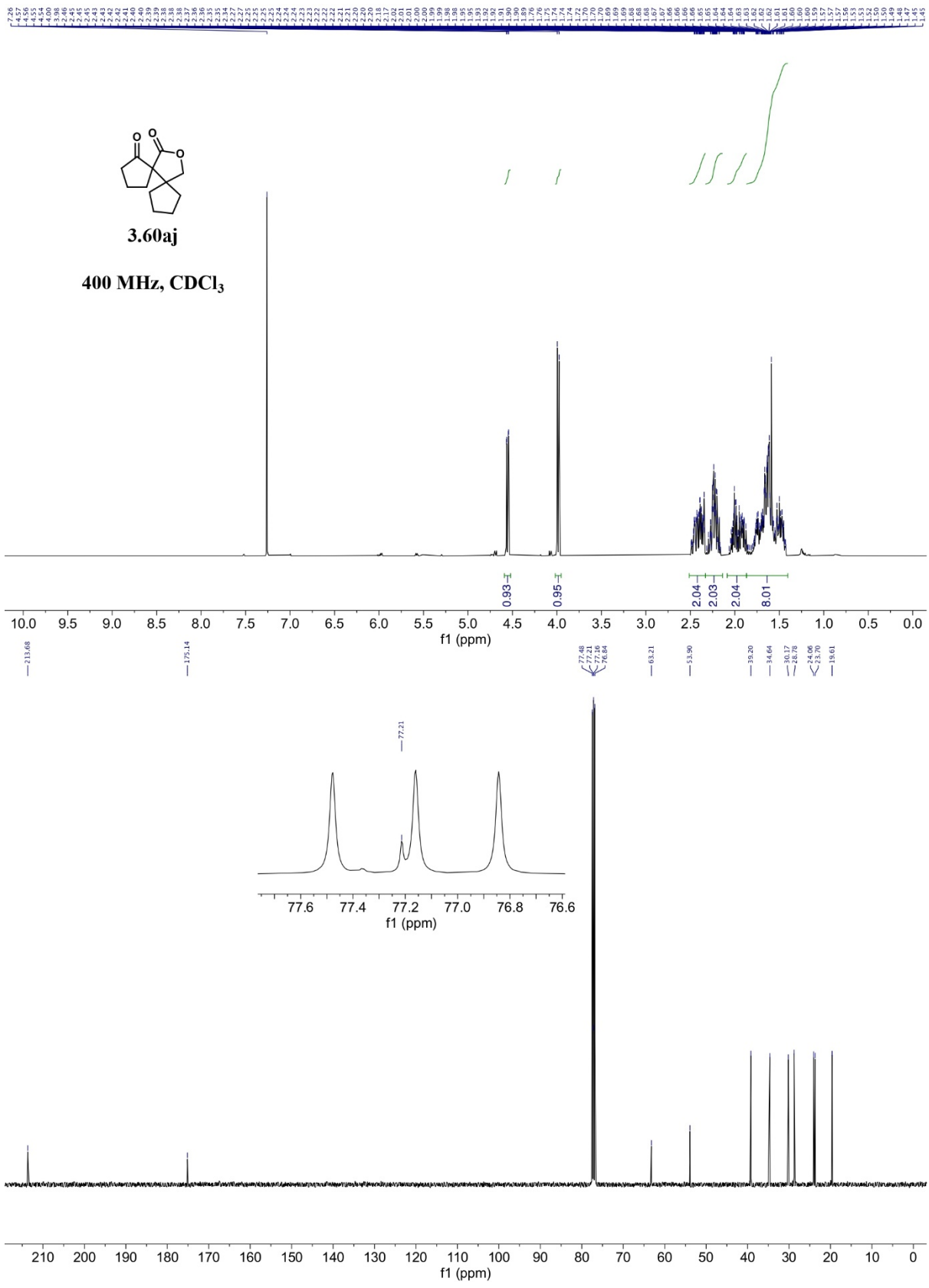


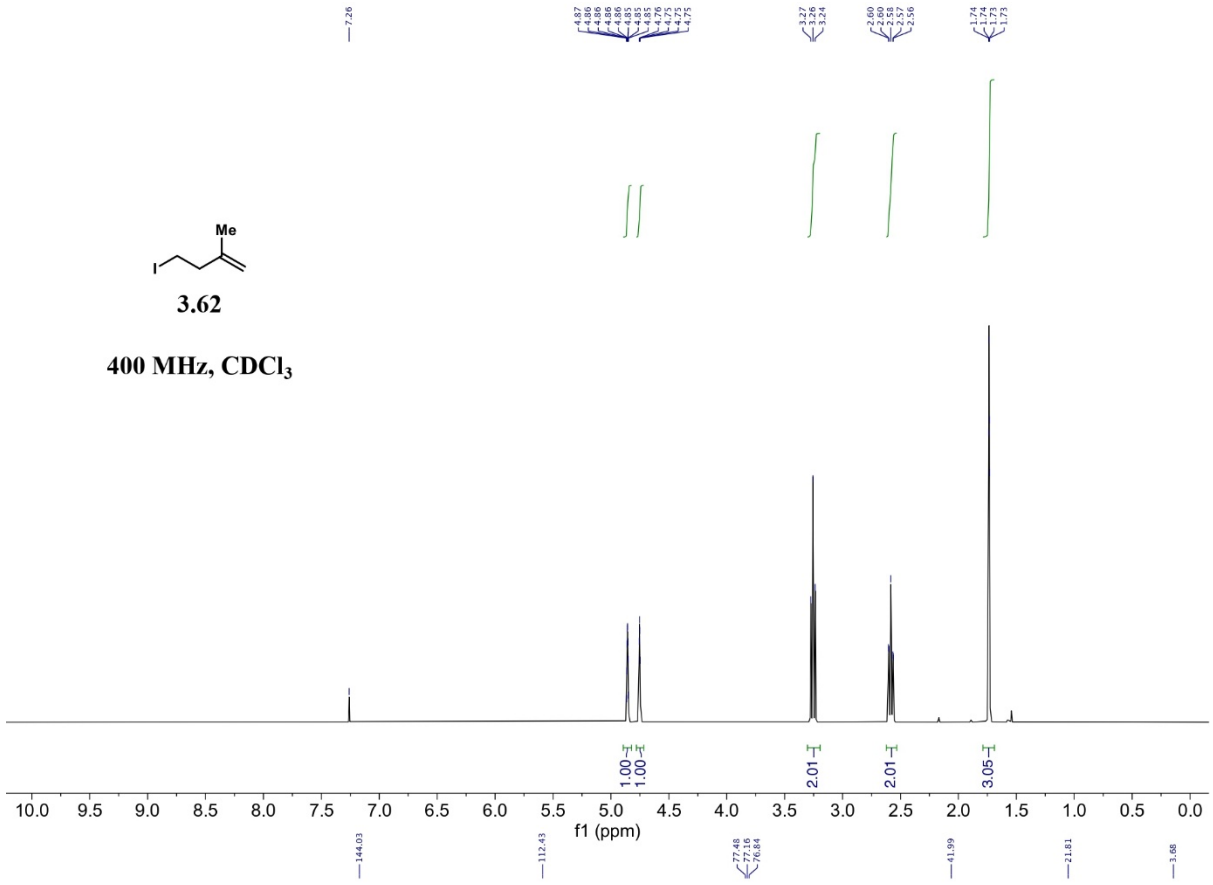


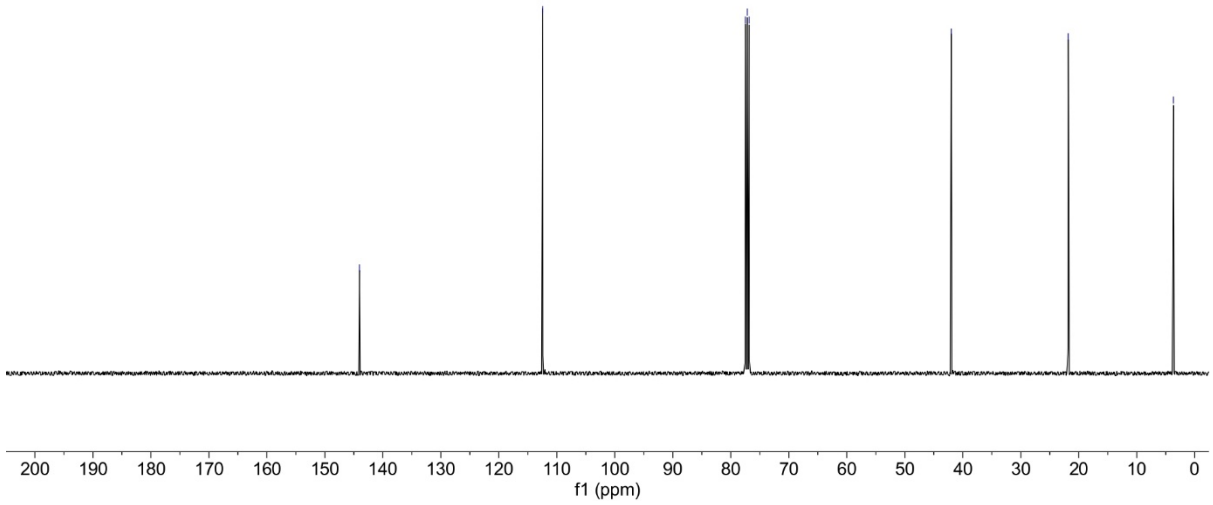
3.60ai + 3.60ai''

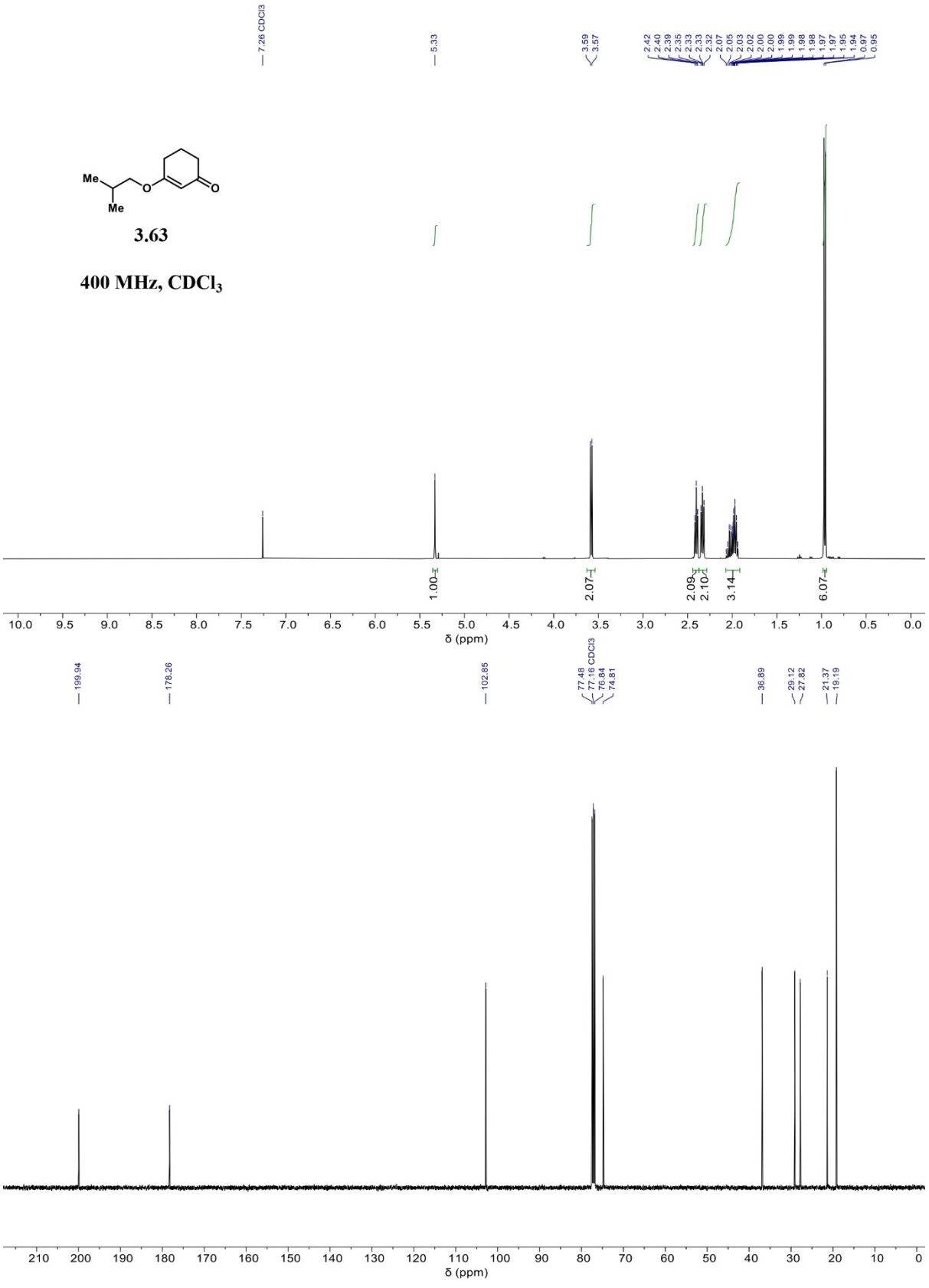
400 MHz, $CDCl_3$


7.26 CDCl3
3.60ai'
400 MHz, CDCl3
δ (ppm)
213.97
175.74
84.00
77.37
77.16 CDCl3
76.95
61.16
49.60
39.67
35.85
31.10
30.77
27.02
26.43
26.25
20.41


3.60aj
400 MHz, CDCl3
0.93
0.95
2.04
2.03
2.04
8.01
f1 (ppm)
213.68
175.14
77.48
77.21
77.16
76.84
63.21
53.90
39.20
34.64
30.17
28.78
24.06
23.70
19.61
77.21
77.6
77.4
77.2
77.0
76.8
76.6
f1 (ppm)
f1 (ppm)

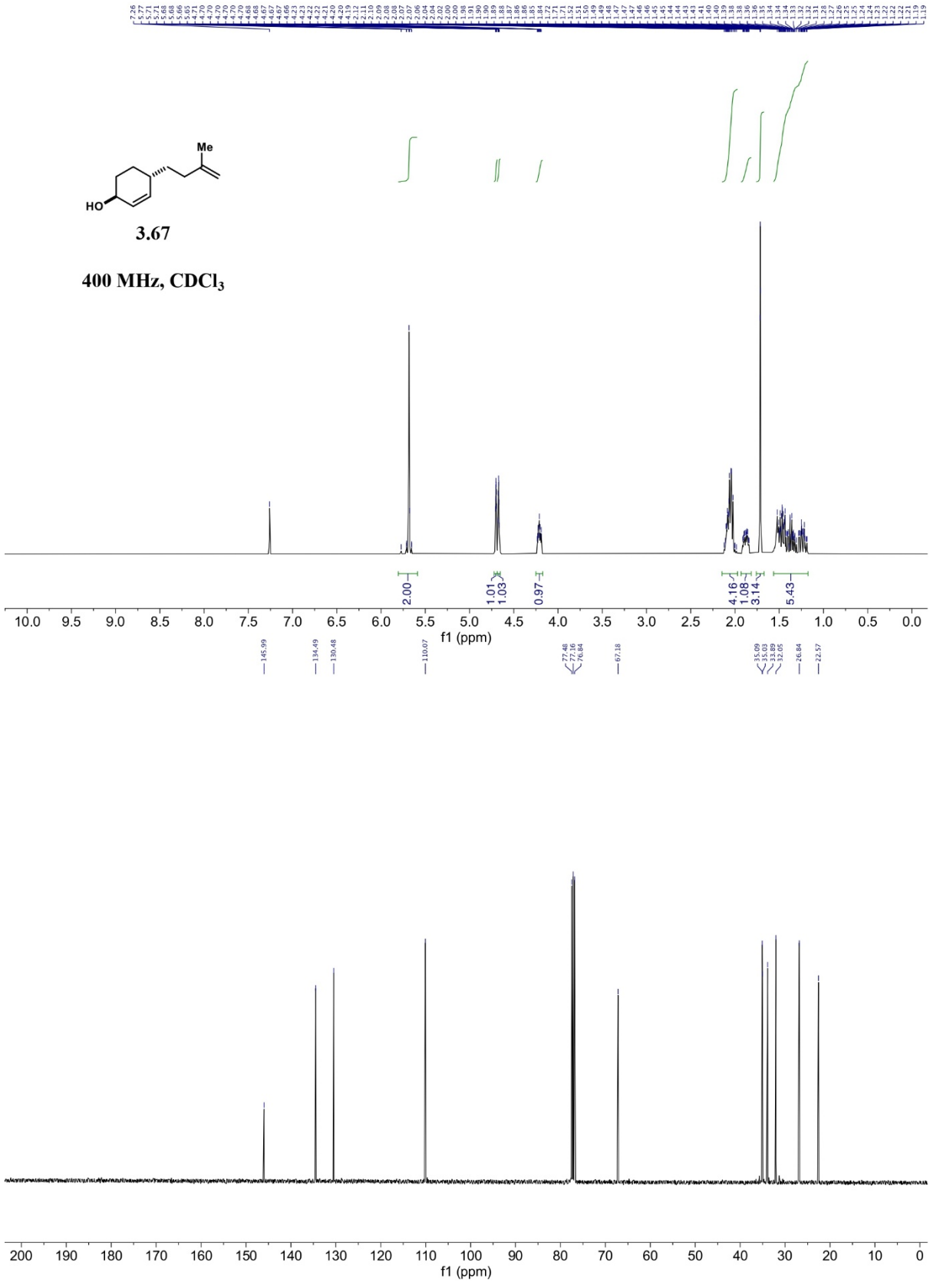

Me
I
3.62
400 MHz, CDCl3
f1 (ppm)

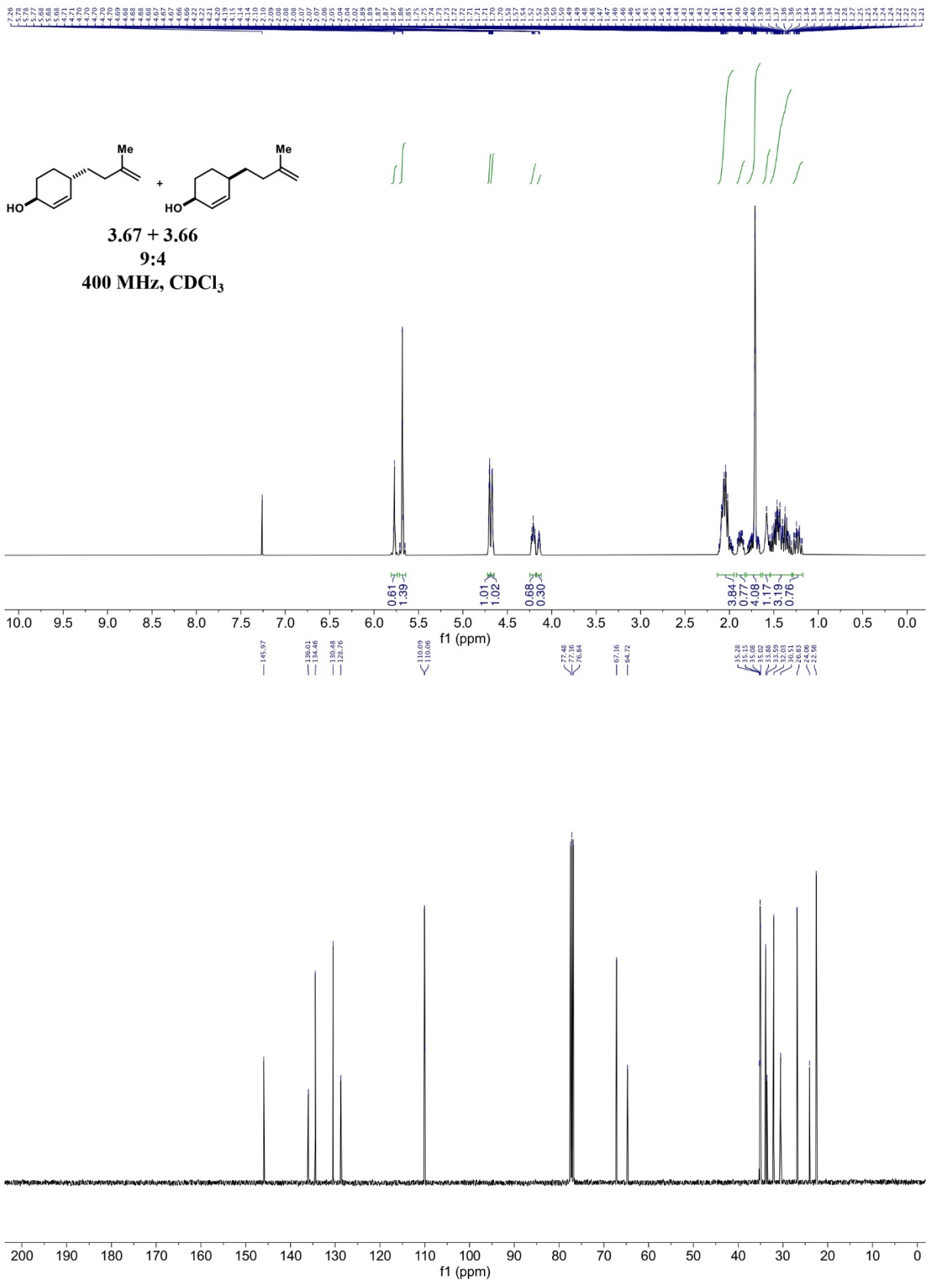

f1 (ppm)

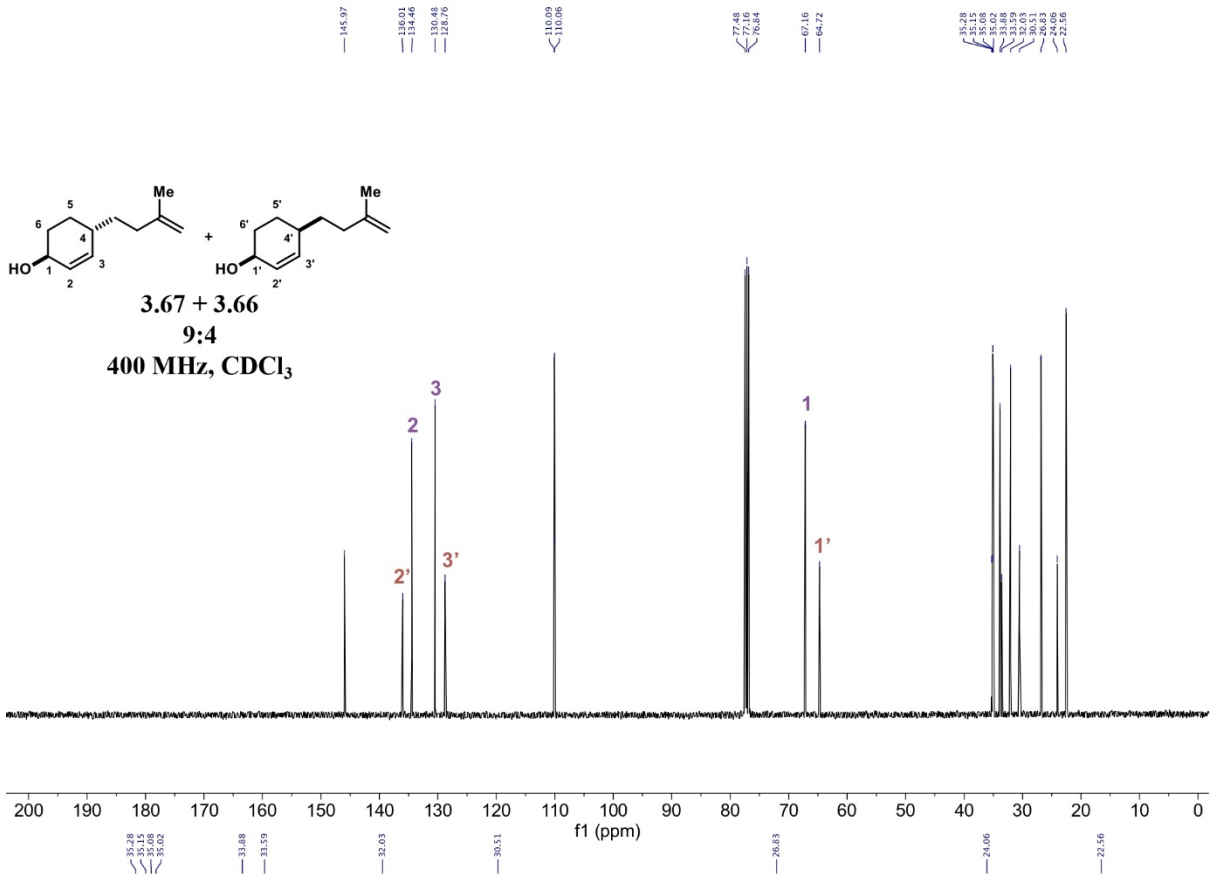


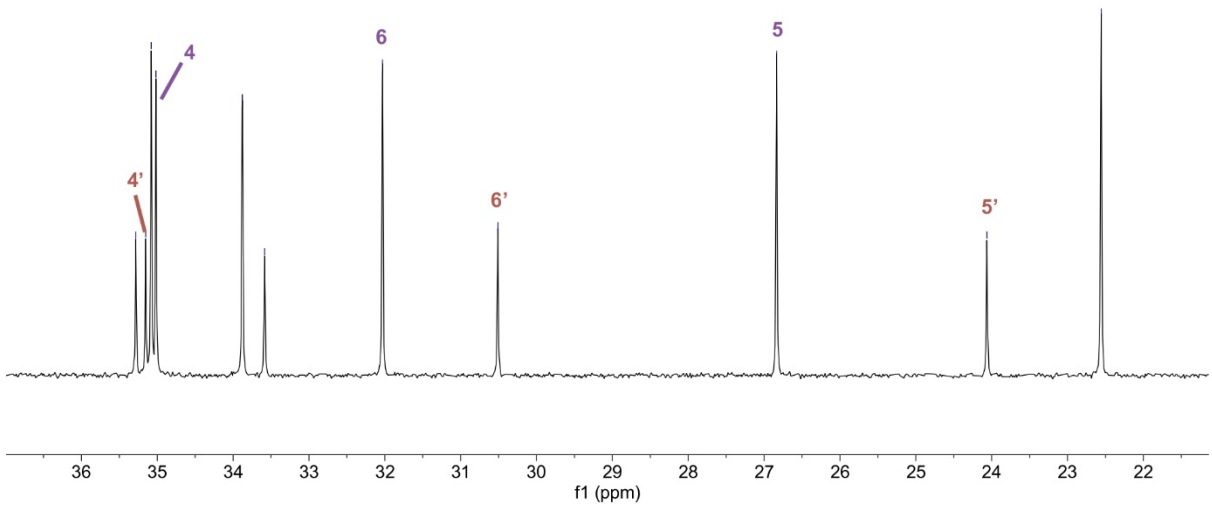
3.63

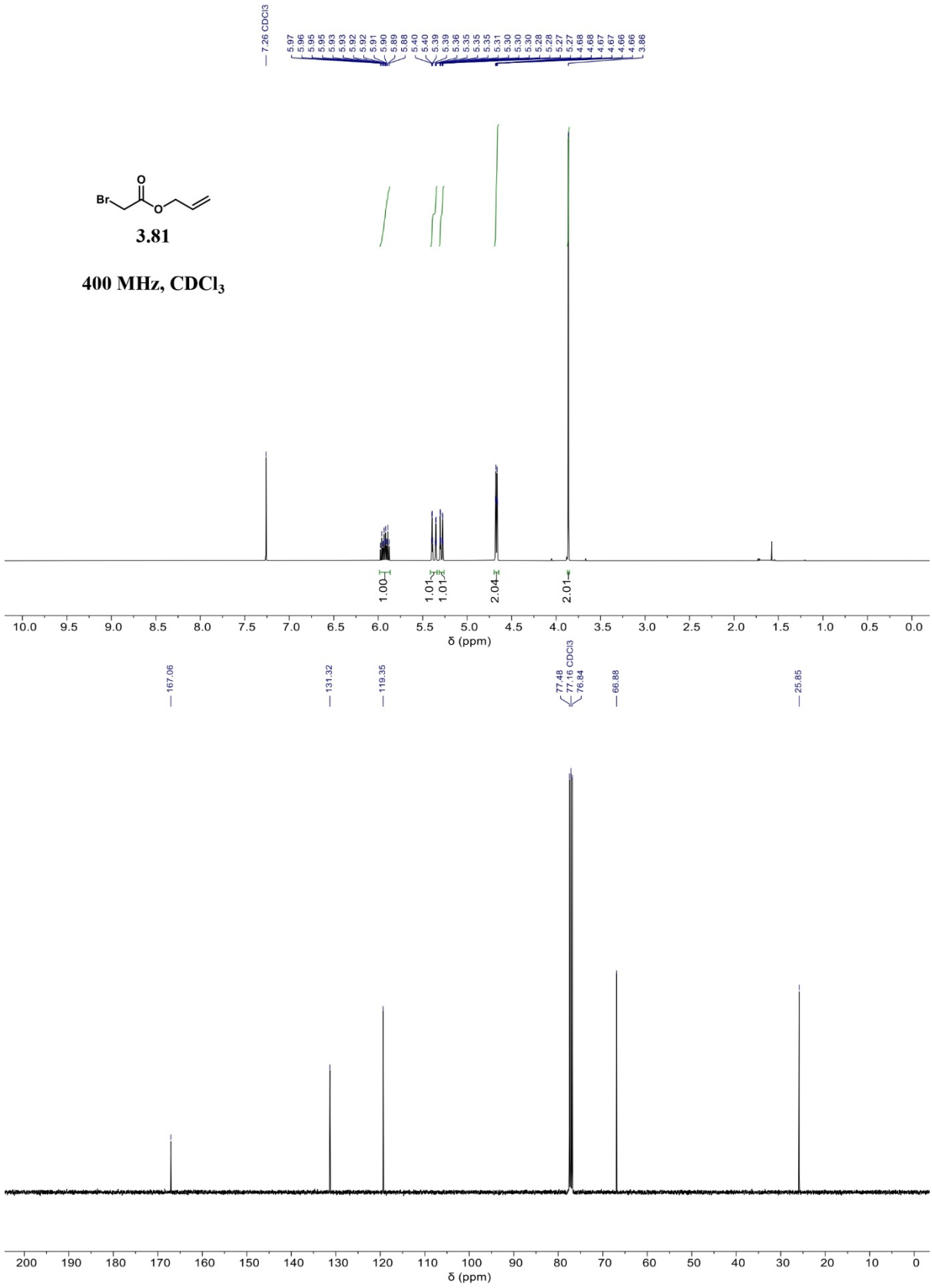
400 MHz, $CDCl_3$

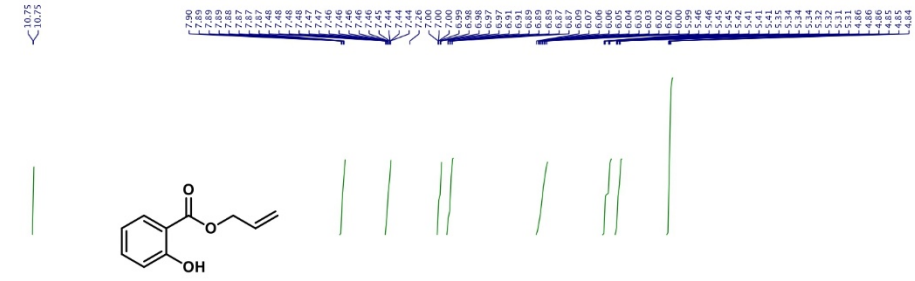

Me
HO
3.67
400 MHz, CDCl3
2.00
1.01
1.03
0.97
4.16
1.08
3.14
5.43
f1 (ppm)
145.99
134.49
130.48
110.07
77.48
77.16
76.84
67.18
35.09
33.69
32.05
26.84
22.57
f1 (ppm)


Me
HO
+
Me
HO
3.67 + 3.66
9:4
400 MHz, CDCl3
f1 (ppm)
f1 (ppm)


145.97
136.01
134.46
130.48
128.76
110.09
110.06
77.48
77.16
76.84
67.16
64.72
35.28
35.15
35.08
35.02
33.88
33.59
32.03
30.51
26.83
24.06
22.56
Me
HO
Me
HO
3.67 + 3.66
9:4
400 MHz, CDCl3
1
2
3
1'
2'
3'
f1 (ppm)

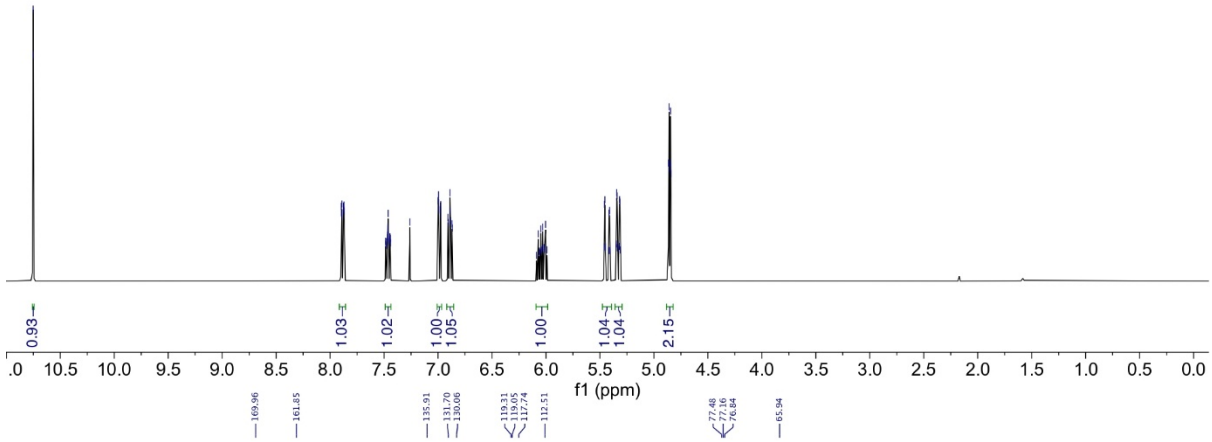

4
6
5
4'
6'
5'
f1 (ppm)

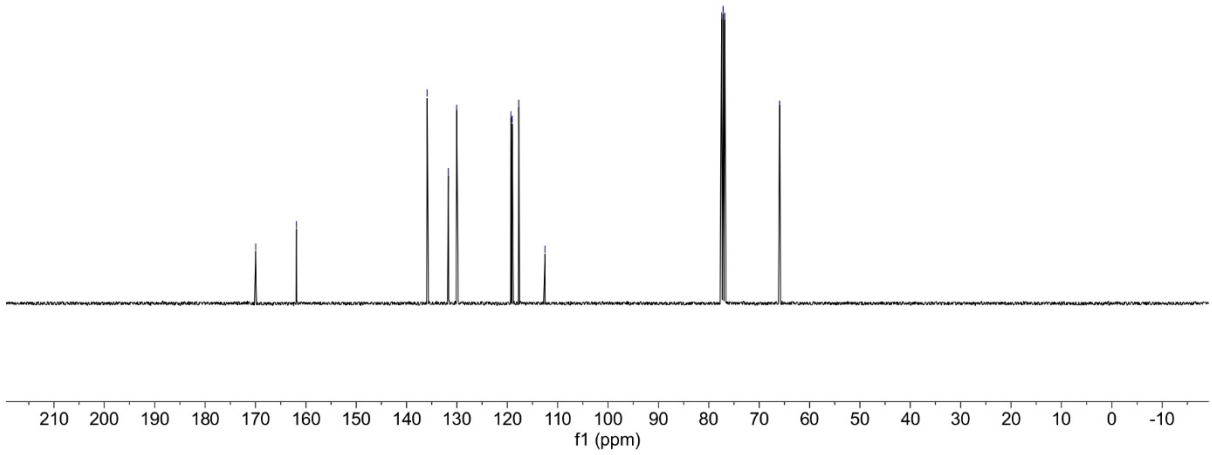

7.26 CDCl3
5.97
5.96
5.95
5.95
5.93
5.93
5.92
5.92
5.91
5.90
5.89
5.88
5.40
5.39
5.39
5.36
5.35
5.35
5.35
5.31
5.30
5.30
5.30
5.29
5.28
5.27
5.27
4.68
4.68
4.67
4.67
4.66
4.66
3.86
Br
O
O
3.81
400 MHz, CDCl3
1.00
1.01
1.01
2.04
2.01
δ (ppm)
167.06
131.32
119.35
77.48
77.16 CDCl3
76.84
66.88
25.85
δ (ppm)

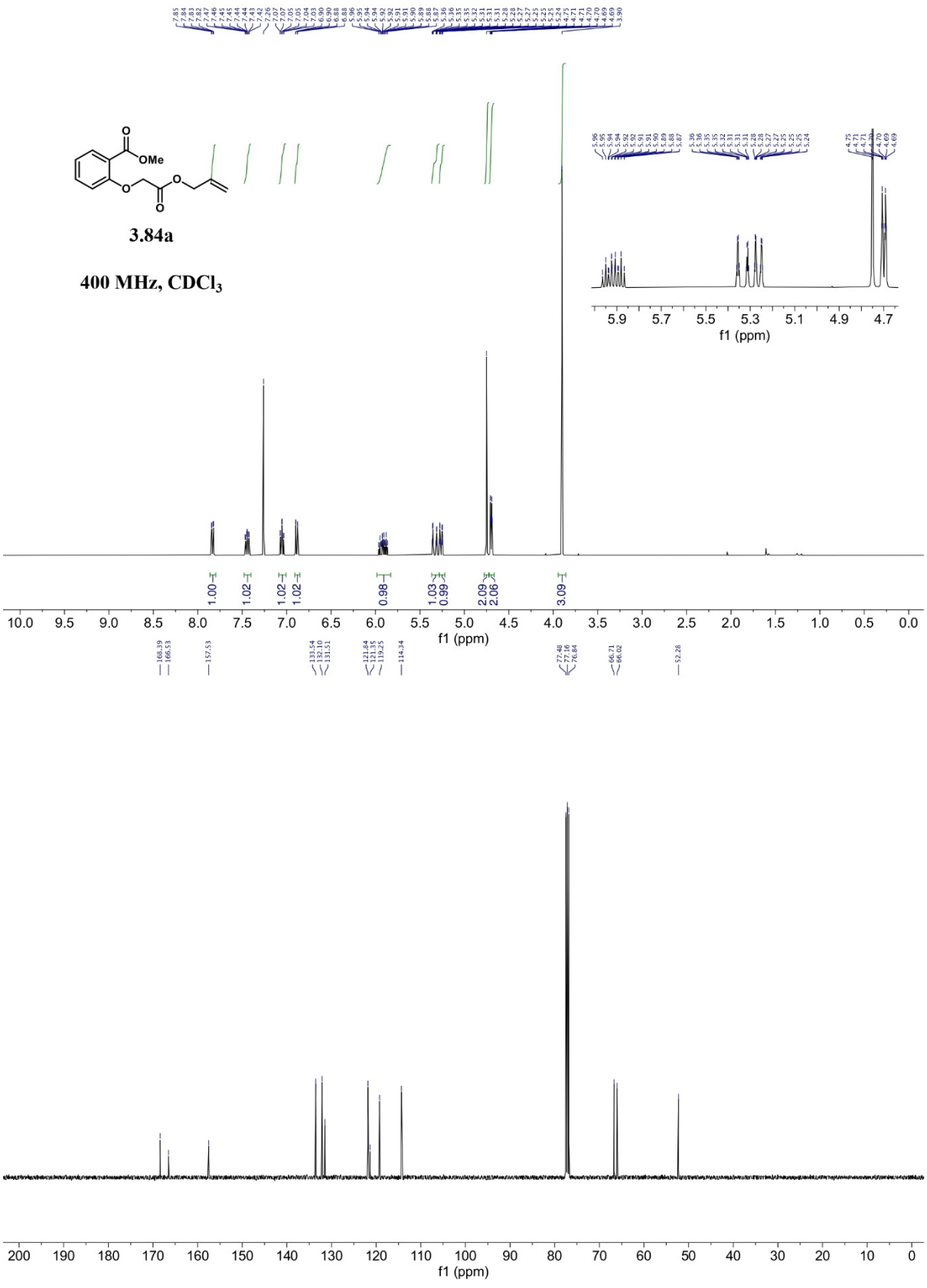


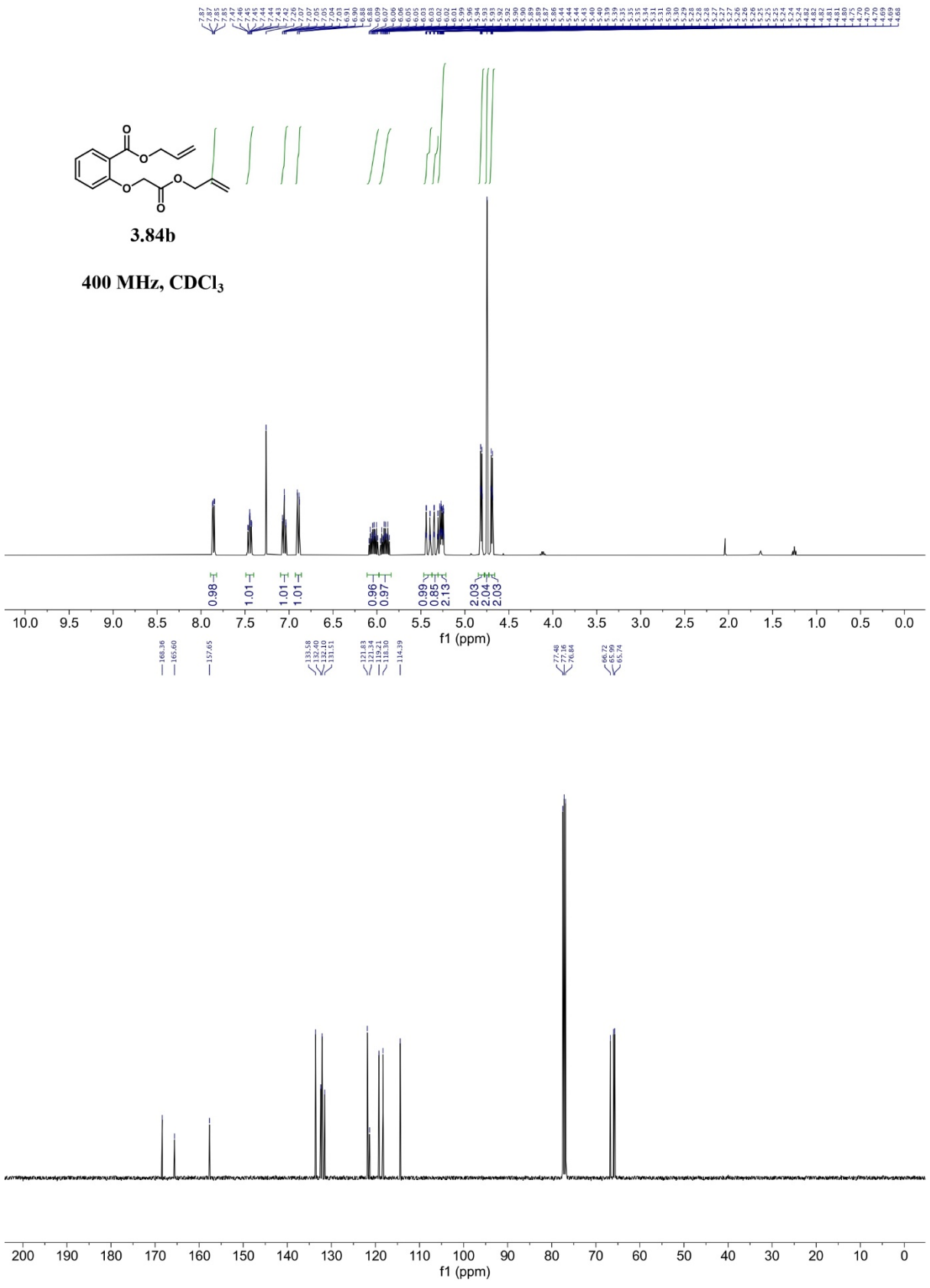
3.83b

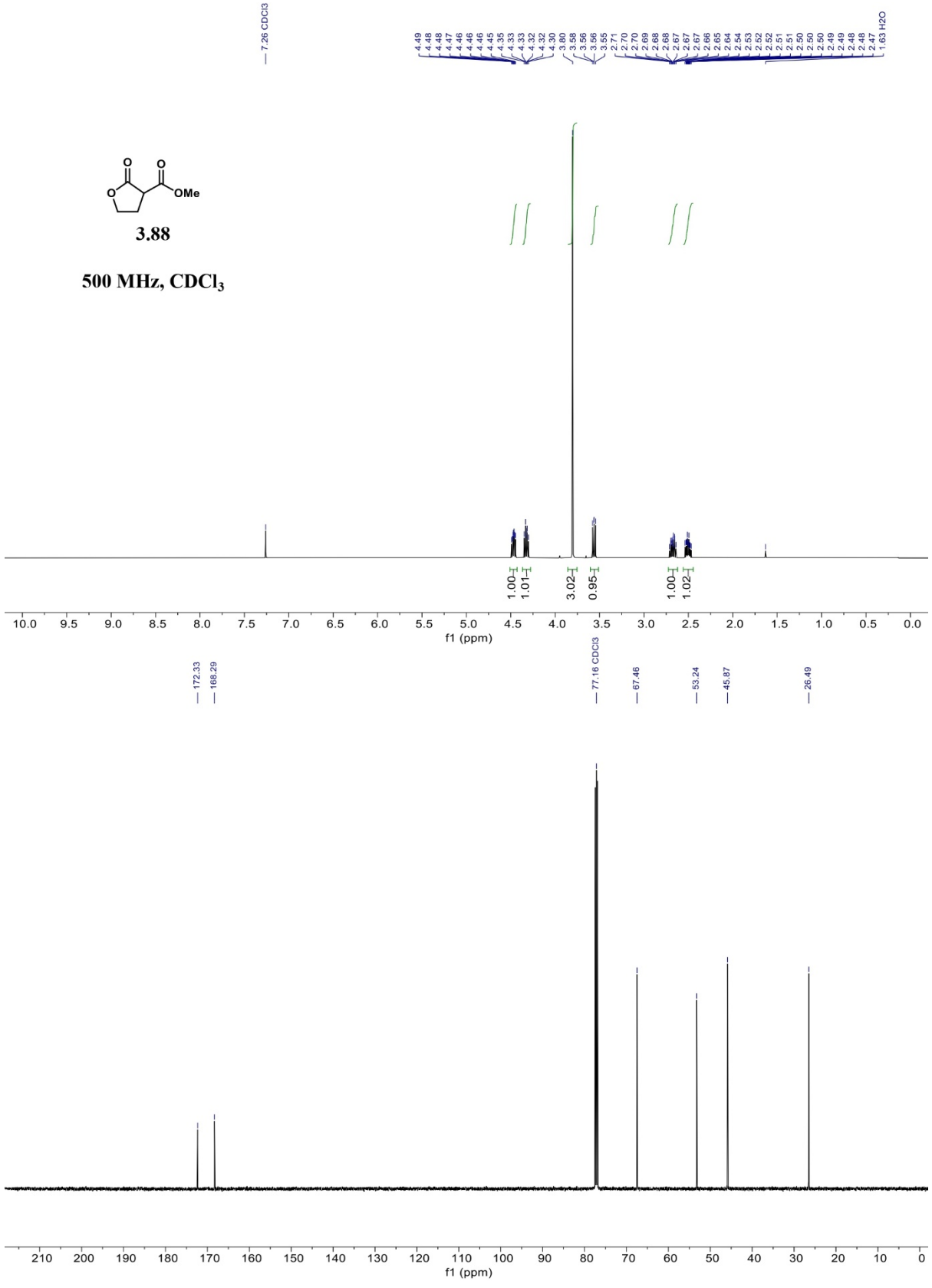
400 MHz, $CDCl_3$

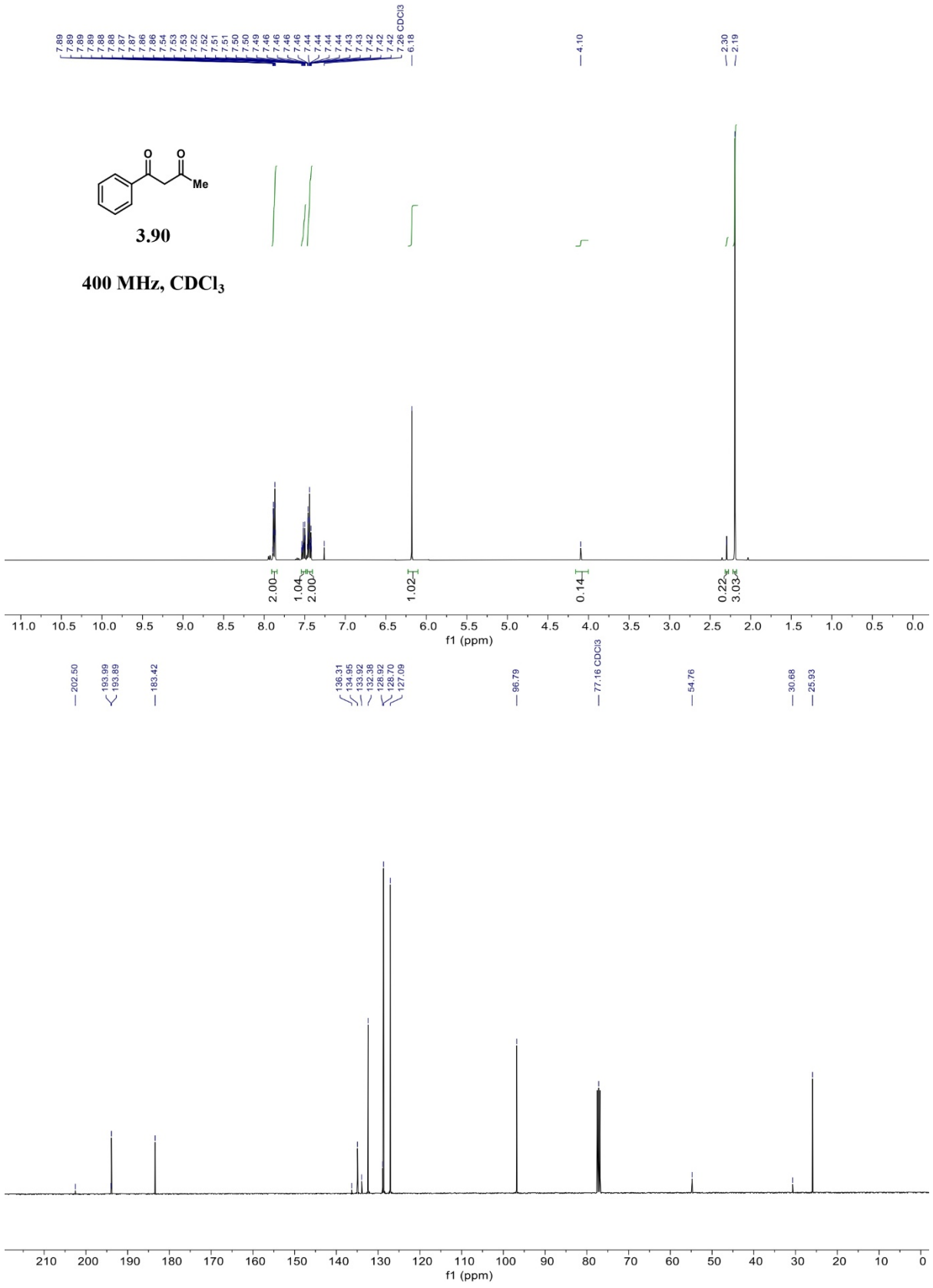


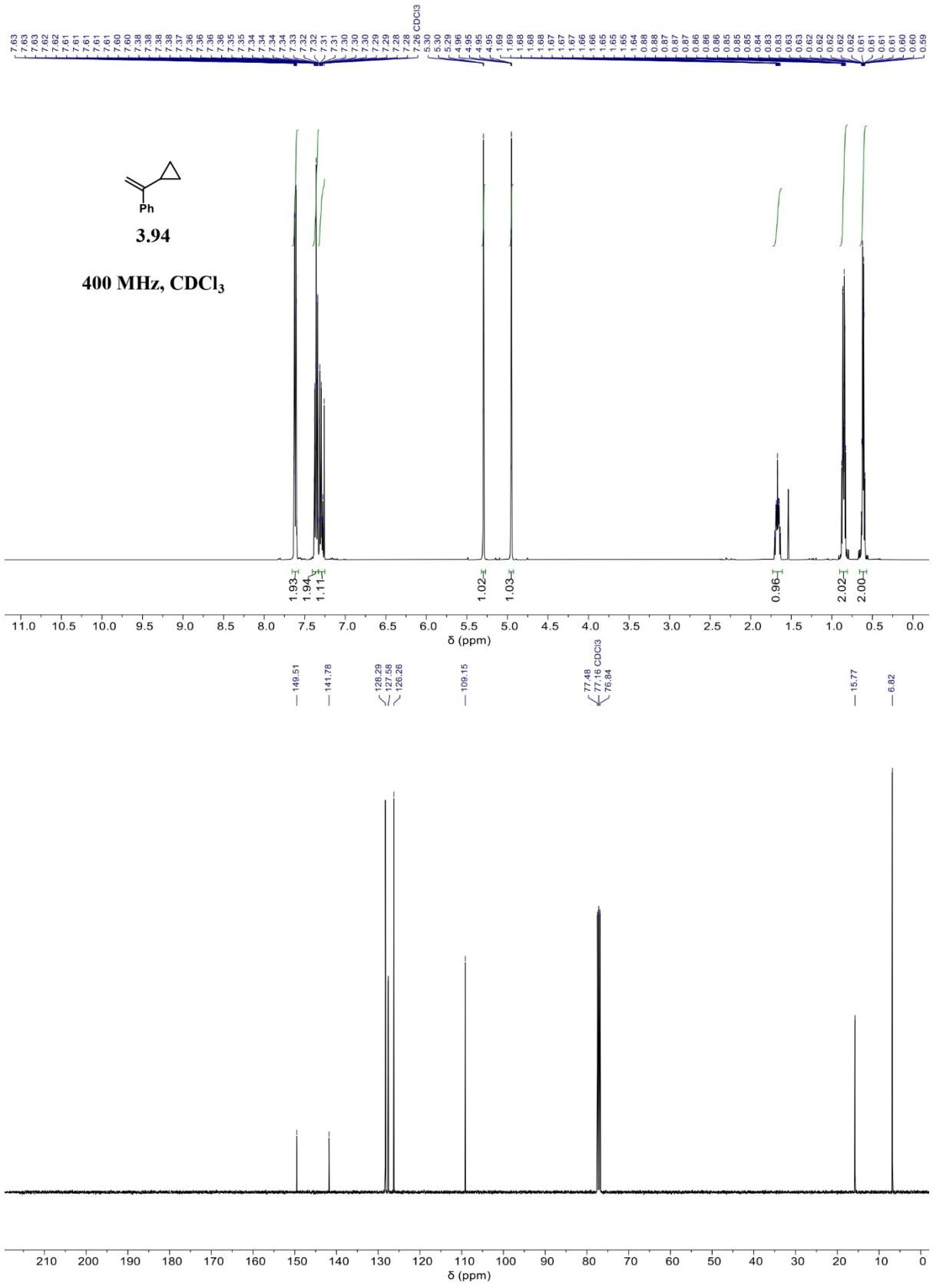


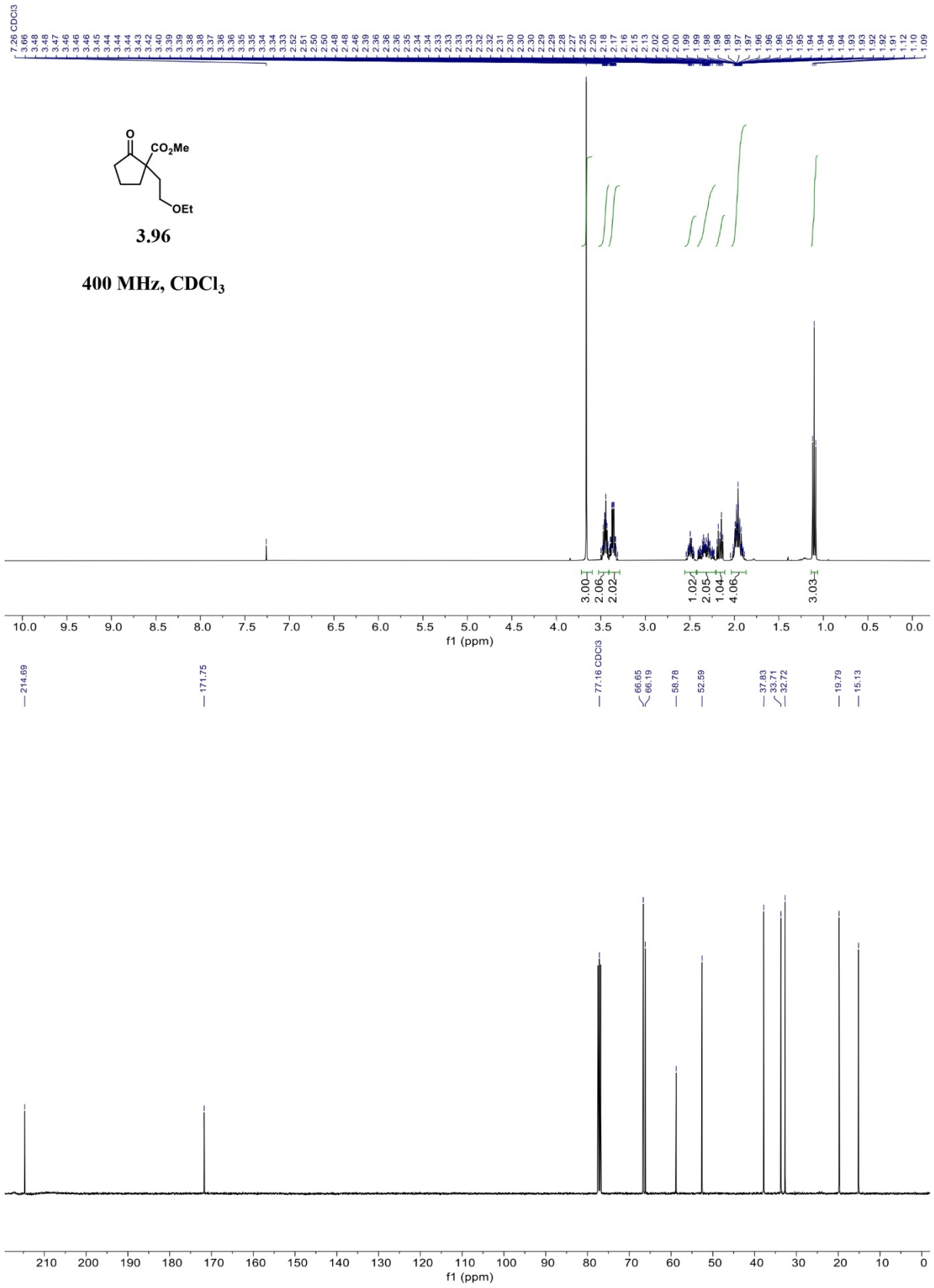

OMe
O
O
O
O
3.84a
400 MHz, CDCl3
f1 (ppm)

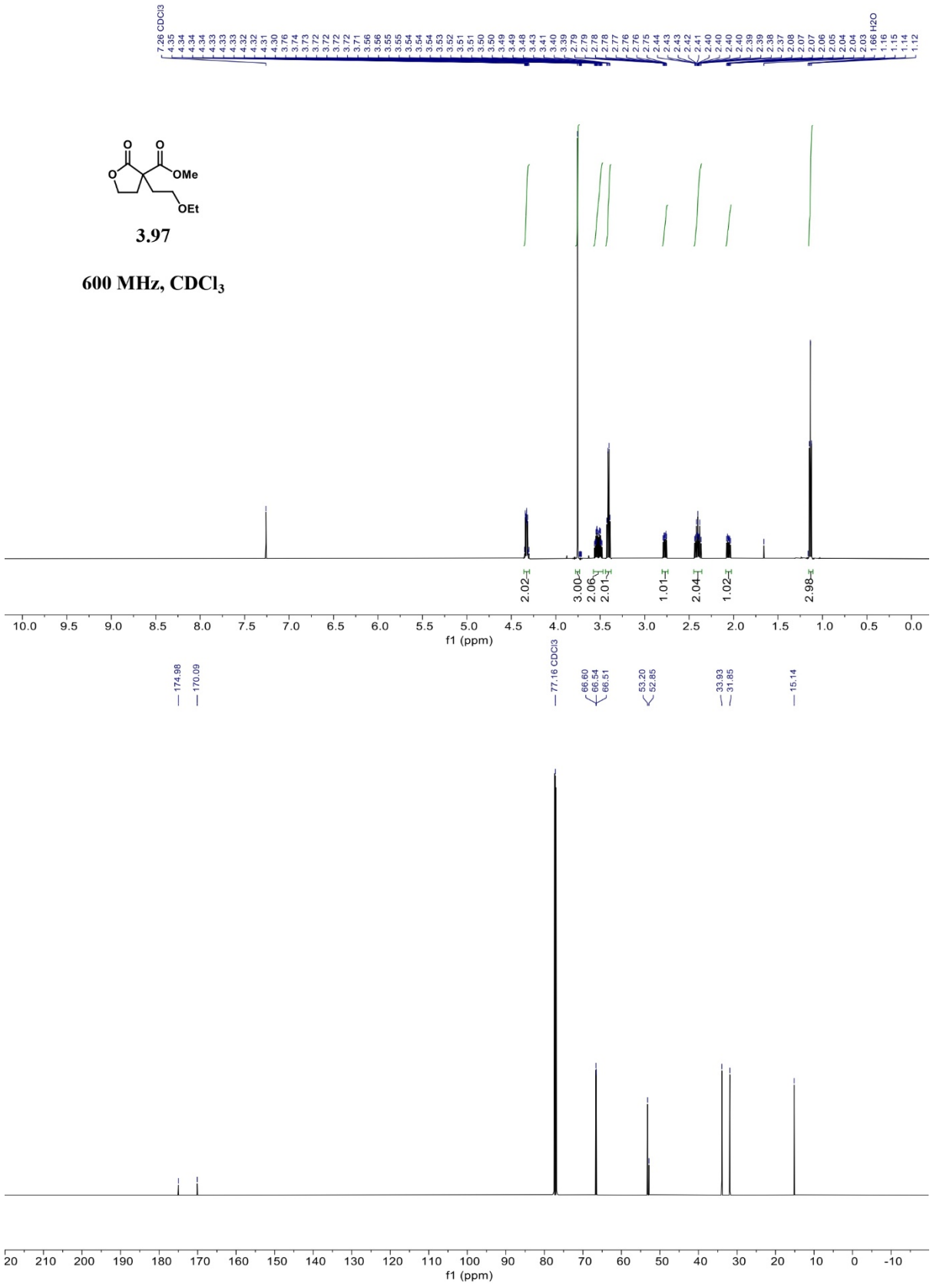

3.84b
400 MHz, CDCl3
f1 (ppm)
f1 (ppm)

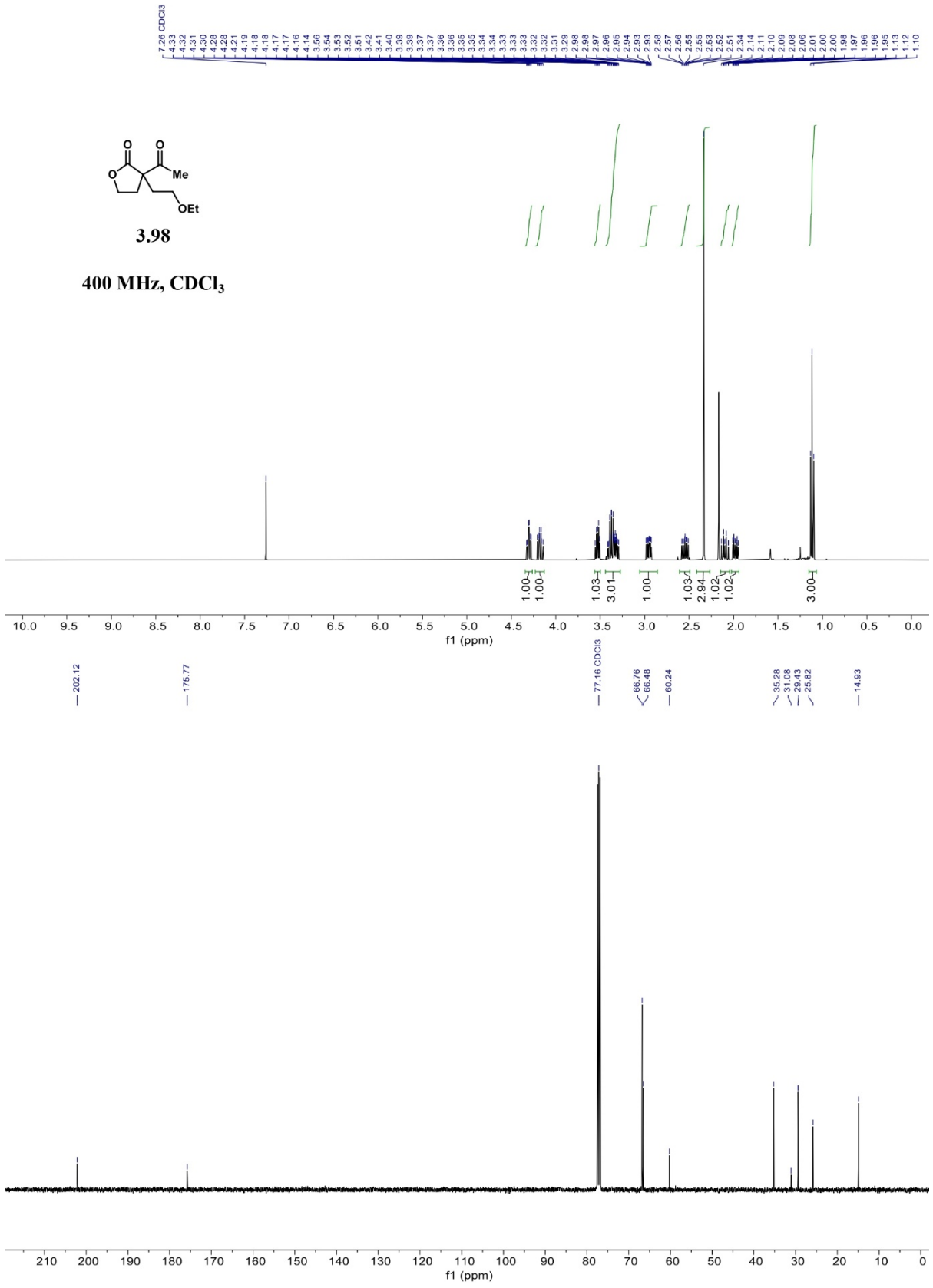

7.26 CDCl3
4.49
4.48
4.48
4.47
4.46
4.46
4.46
4.45
4.35
4.33
4.33
4.32
4.32
4.30
3.80
3.58
3.56
3.56
3.55
2.71
2.70
2.70
2.69
2.68
2.68
2.67
2.67
2.67
2.66
2.65
2.64
2.54
2.53
2.52
2.52
2.51
2.51
2.50
2.50
2.50
2.49
2.49
2.48
2.48
2.47
1.63 H2O
O
O
O
OMe
3.88
500 MHz, CDCl3
1.00
1.01
3.02
0.95
1.00
1.02
f1 (ppm)
172.33
168.29
77.16 CDCl3
67.46
53.24
45.87
26.49
f1 (ppm)

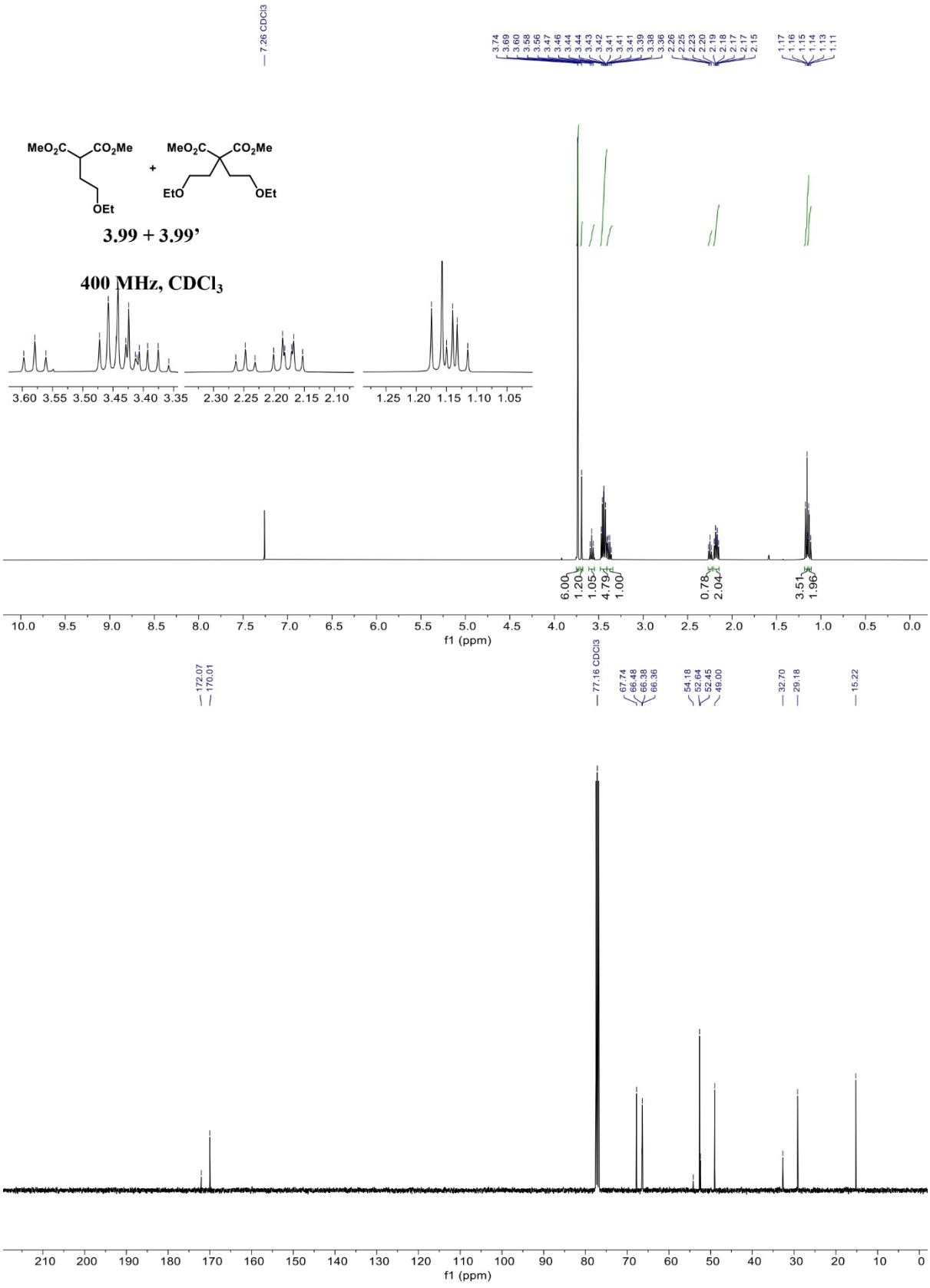

7.89
7.89
7.89
7.89
7.88
7.88
7.87
7.87
7.86
7.86
7.54
7.53
7.53
7.52
7.52
7.51
7.51
7.50
7.50
7.49
7.46
7.46
7.46
7.46
7.44
7.44
7.44
7.43
7.43
7.42
7.42
7.42
7.26 CDCl3
6.18
4.10
2.30
2.19
O
O
Me
3.90
400 MHz, CDCl3
2.00
1.04
2.00
1.02
0.14
0.22
3.03
11.0 10.5 10.0 9.5 9.0 8.5 8.0 7.5 7.0 6.5 6.0 5.5 5.0 4.5 4.0 3.5 3.0 2.5 2.0 1.5 1.0 0.5 0.0
f1 (ppm)
202.50
193.99
193.89
183.42
136.31
134.95
133.92
132.38
128.92
128.70
127.09
96.79
77.16 CDCl3
54.76
30.68
25.93
210 200 190 180 170 160 150 140 130 120 110 100 90 80 70 60 50 40 30 20 10 0
f1 (ppm)

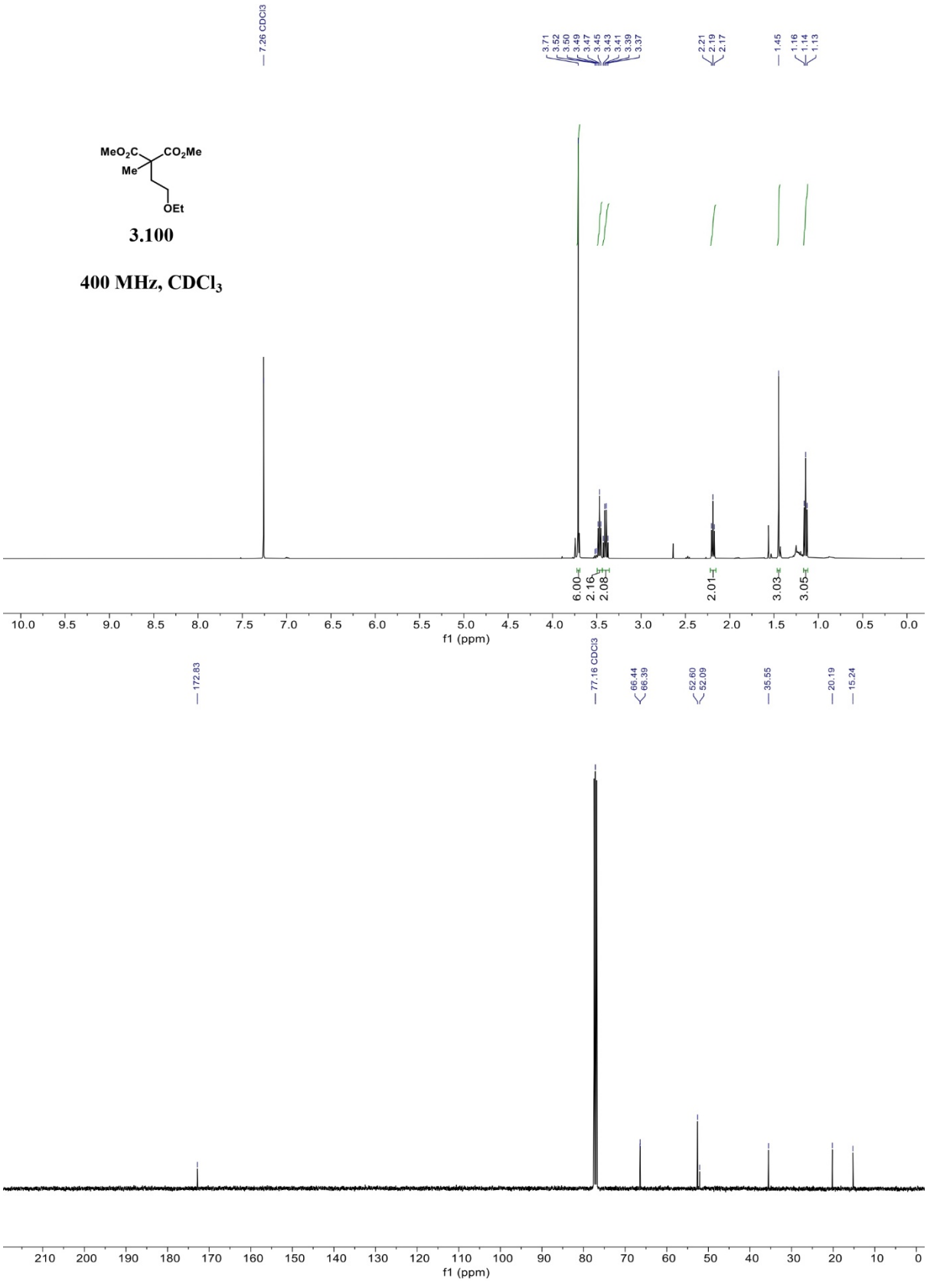

Ph
3.94
400 MHz, CDCl3
δ (ppm)
δ (ppm)

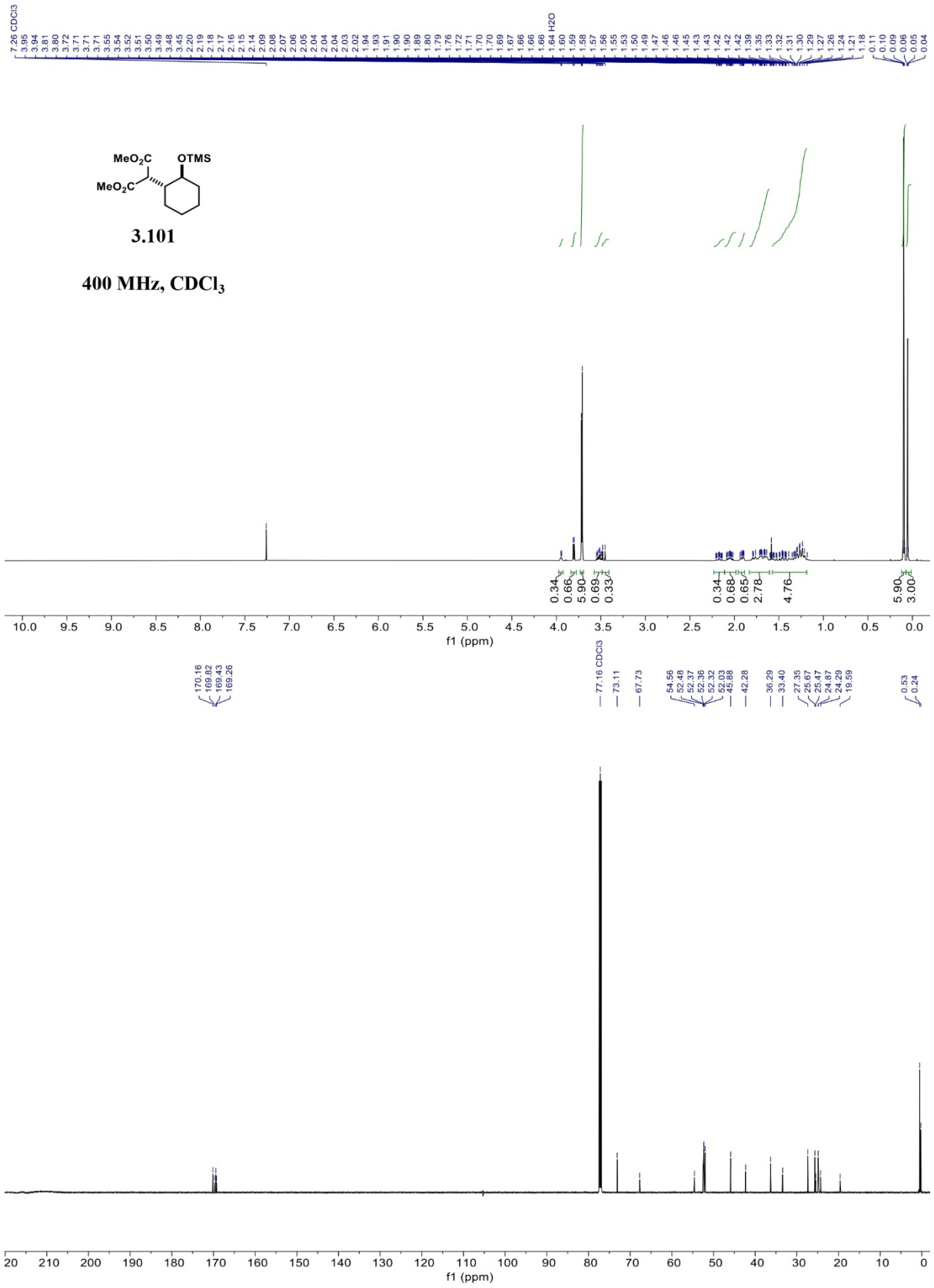

O
CO2Me
OEt
3.96
400 MHz, CDCl3
f1 (ppm)

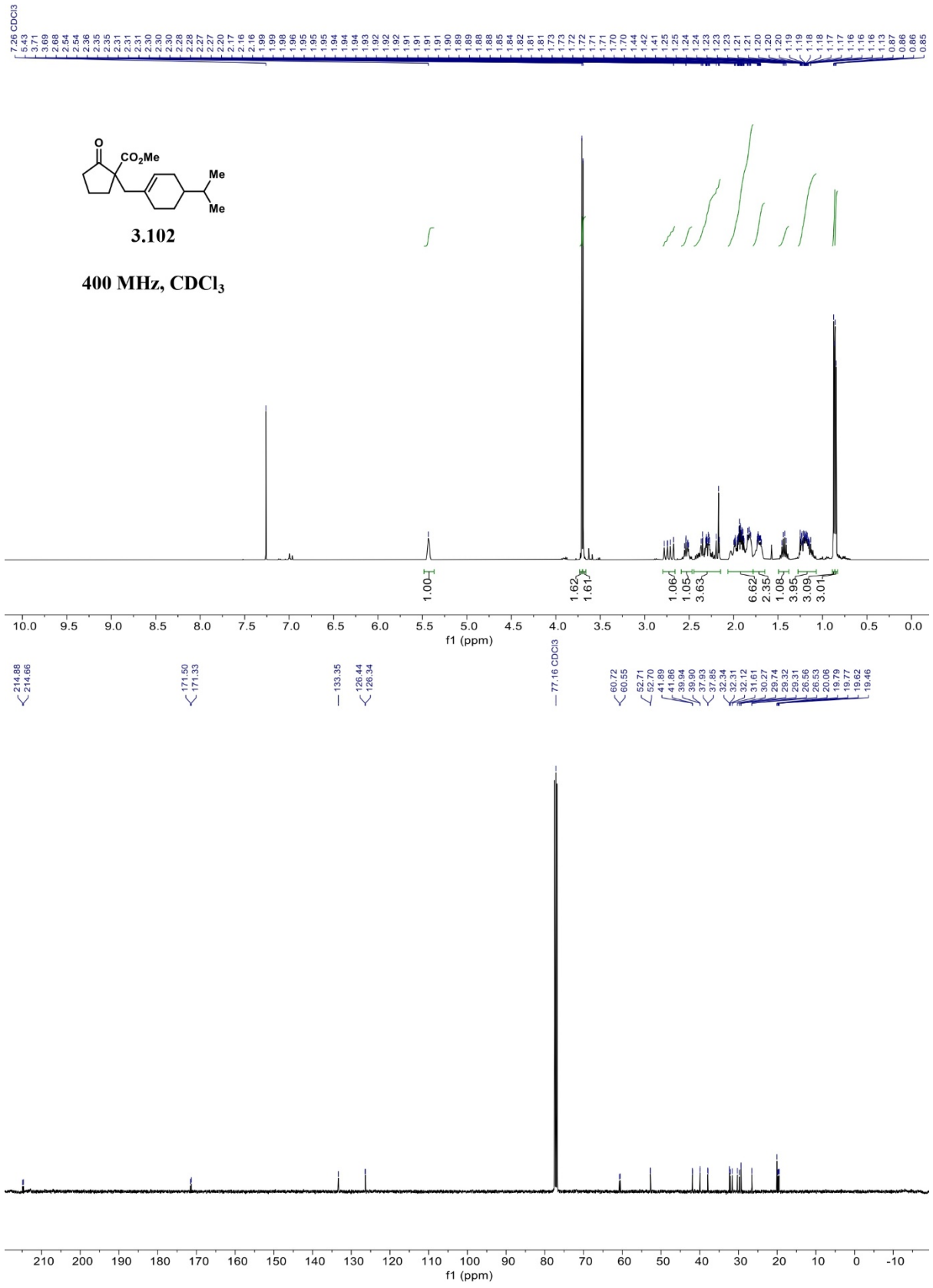

7.26 CDCl3
1.66 H2O
OMe
OEt
3.97
600 MHz, CDCl3
2.02
3.00
2.06
2.01
1.01
2.04
1.02
2.98
f1 (ppm)
174.98
170.09
77.16 CDCl3
66.60
66.54
66.51
53.20
52.85
33.93
31.85
15.14
f1 (ppm)

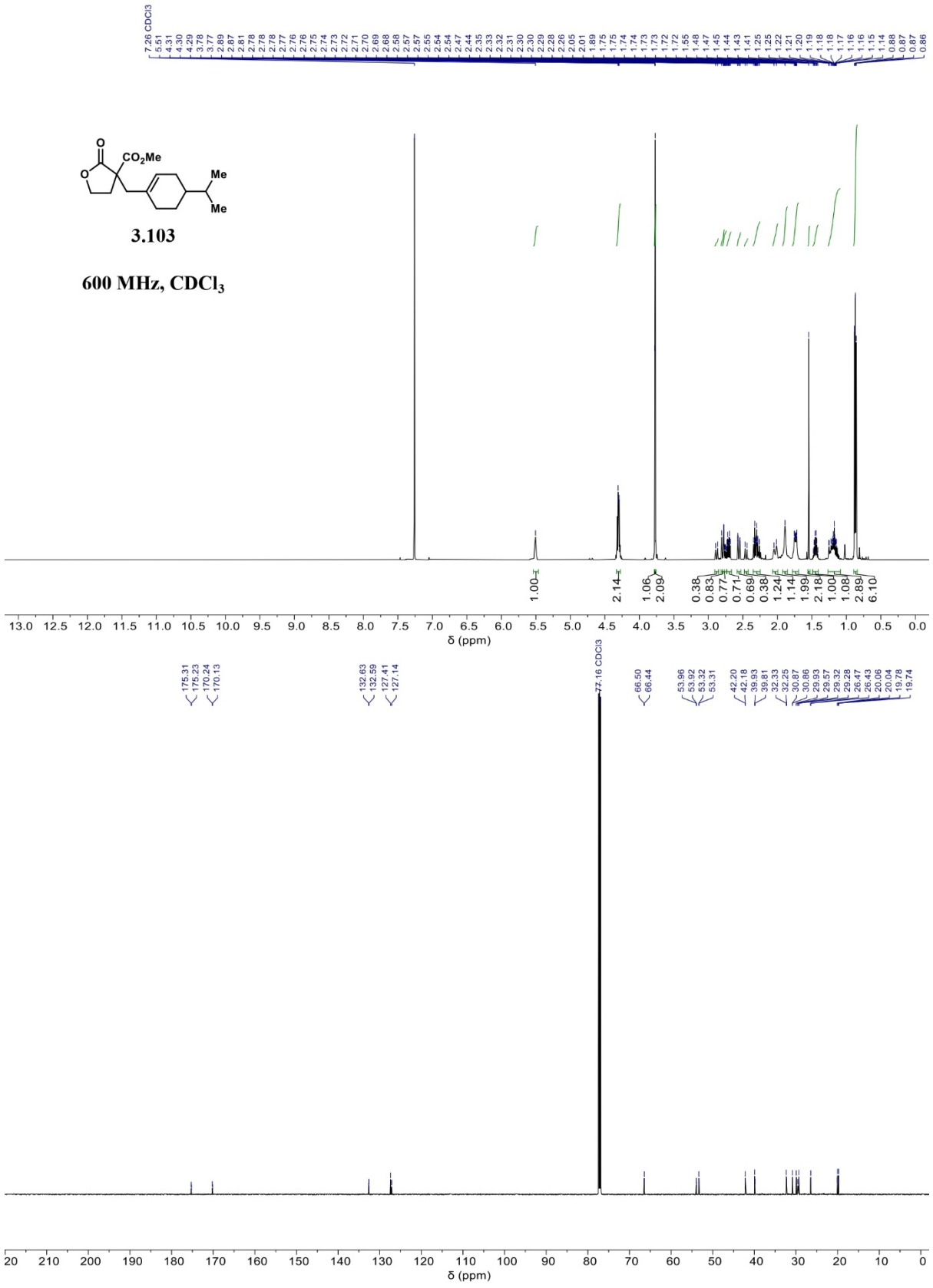

7.26 CDCl3
4.33 4.32 4.31 4.30 4.28 4.28 4.21 4.19 4.18 4.18 4.17 4.17 4.16 4.14 3.56 3.54 3.53 3.52 3.51 3.42 3.41 3.40 3.39 3.39 3.39 3.37 3.36 3.36 3.35 3.35 3.34 3.34 3.33 3.33 3.33 3.32 3.32 3.31 3.29 2.98 2.98 2.97 2.96 2.95 2.94 2.93 2.93 2.58 2.57 2.56 2.55 2.55 2.53 2.52 2.51 2.34 2.14 2.11 2.10 2.09 2.08 2.06 2.01 2.00 2.00 1.98 1.97 1.96 1.96 1.95 1.13 1.12 1.10
O
O
O
Me
OEt
3.98
400 MHz, CDCl3
1.00 1.00 1.03 3.01 1.00 1.03 2.94 1.02 1.02 3.00
10.0 9.5 9.0 8.5 8.0 7.5 7.0 6.5 6.0 5.5 5.0 4.5 4.0 3.5 3.0 2.5 2.0 1.5 1.0 0.5 0.0
f1 (ppm)
202.12
175.77
77.16 CDCl3
66.76
66.48
60.24
35.28
31.08
29.43
25.82
14.93
210 200 190 180 170 160 150 140 130 120 110 100 90 80 70 60 50 40 30 20 10 0
f1 (ppm)

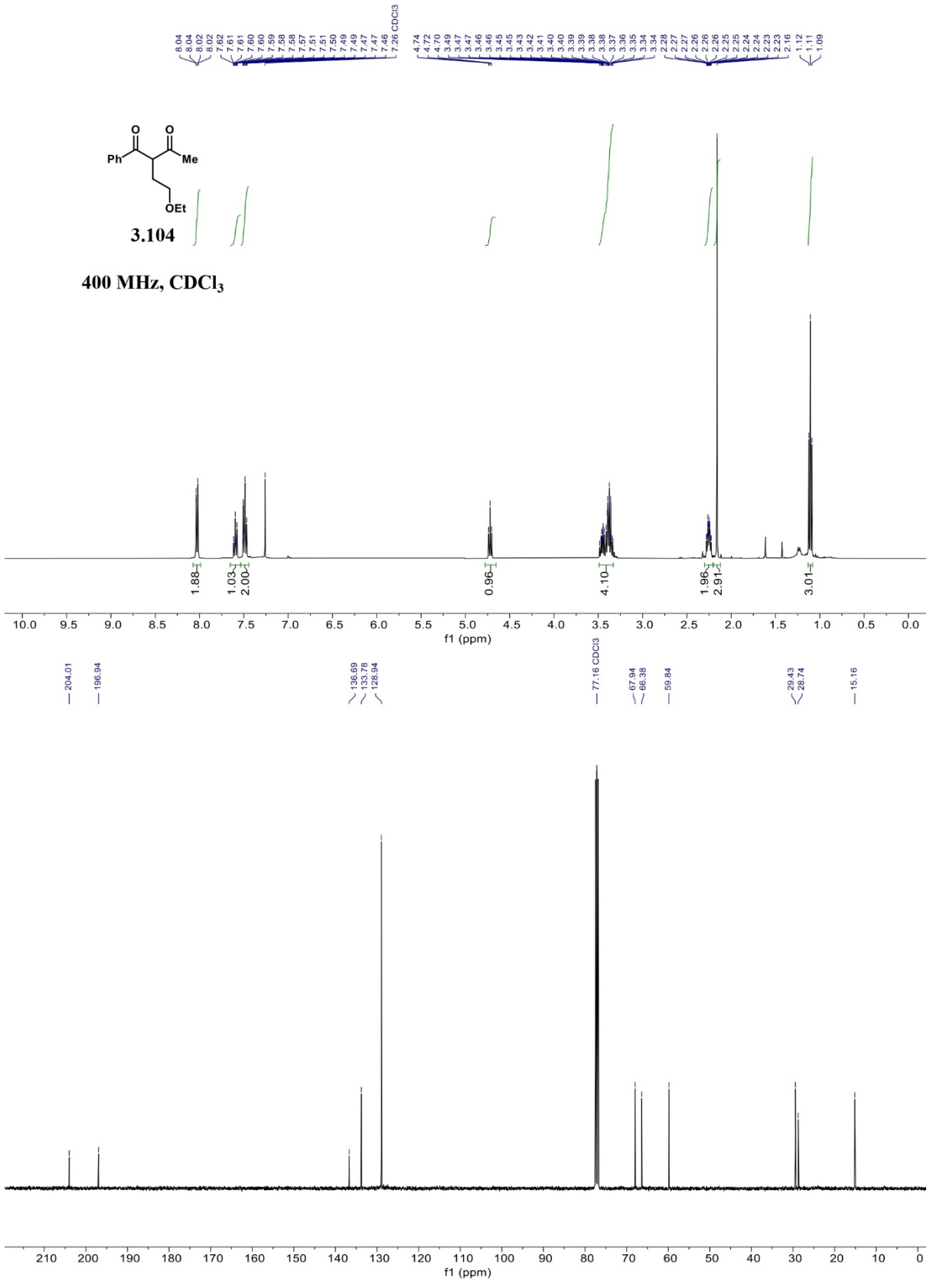

MeO2C
CO2Me
OEt
+
MeO2C
CO2Me
EtO
OEt
3.99 + 3.99'
400 MHz, CDCl3
7.26 CDCl3
3.74
3.69
3.60
3.58
3.55
3.47
3.46
3.44
3.44
3.43
3.42
3.41
3.41
3.41
3.39
3.38
3.36
2.26
2.25
2.23
2.20
2.19
2.18
2.17
2.17
2.15
1.17
1.16
1.15
1.14
1.13
1.11
6.00
1.20
1.05
4.79
1.00
0.78
2.04
3.51
1.96
f1 (ppm)
172.07
170.01
77.16 CDCl3
67.74
66.48
66.38
66.36
54.18
52.64
52.45
49.00
32.70
29.18
15.22
f1 (ppm)

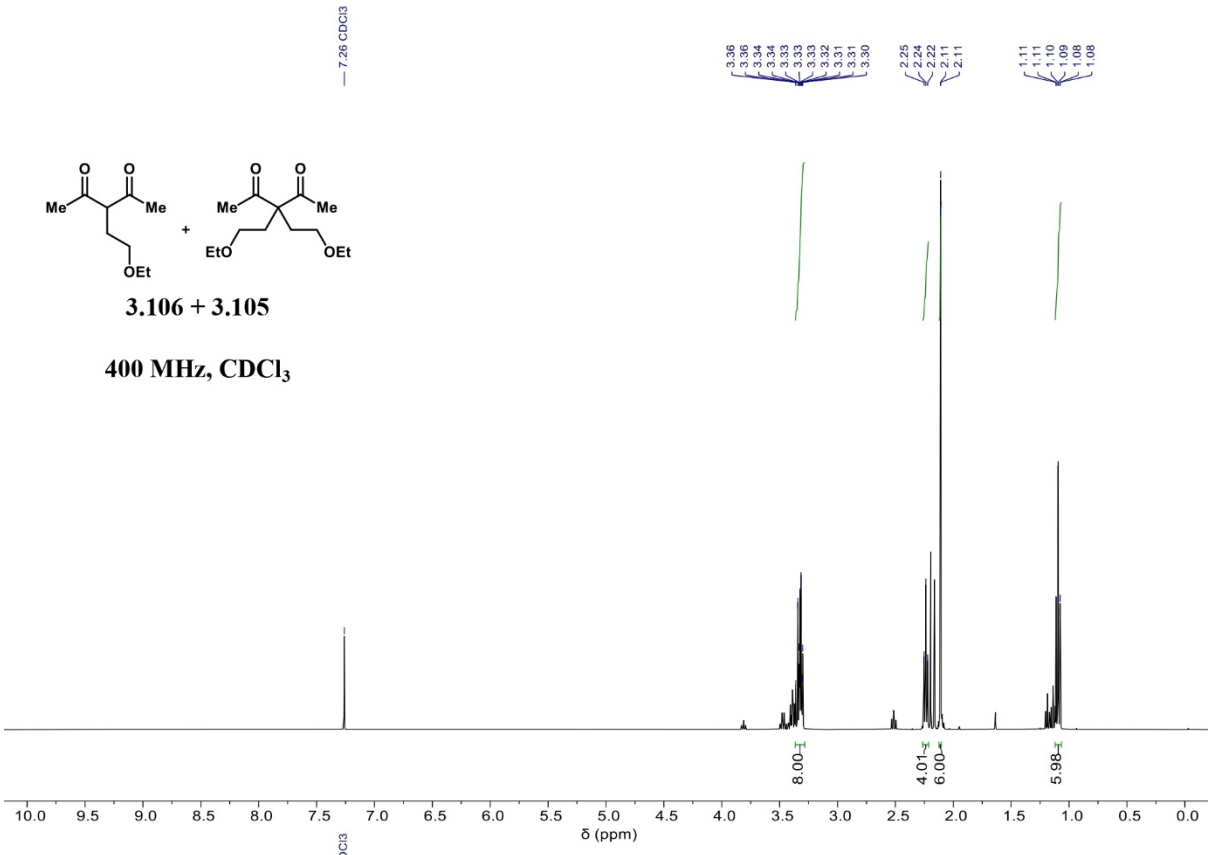

7.26 CDCl3
3.71
3.52
3.50
3.49
3.47
3.45
3.43
3.41
3.39
3.37
2.21
2.19
2.17
1.45
1.16
1.14
1.13
MeO2C
CO2Me
Me
OEt
3.100
400 MHz, CDCl3
6.00
2.16
2.08
2.01
3.03
3.05
f1 (ppm)
172.83
77.16 CDCl3
66.44
66.39
52.60
52.09
35.55
20.19
15.24
f1 (ppm)


MeO2C
OTMS
MeO2C
3.101
400 MHz, CDCl3
f1 (ppm)
f1 (ppm)


CO2Me
Me
Me
3.102
400 MHz, CDCl3
f1 (ppm)
f1 (ppm)

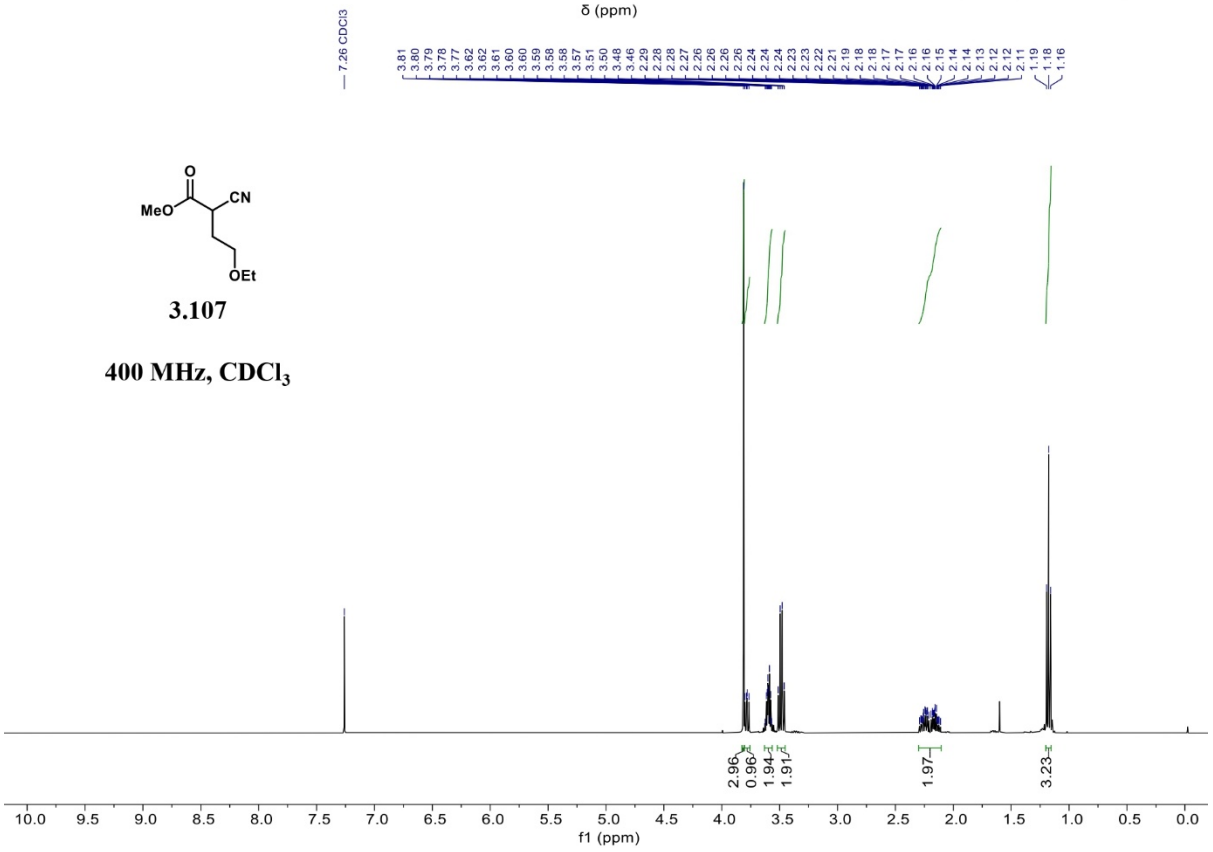

7.26 CDCl3
5.51
4.31
4.30
4.29
3.78
3.77
2.89
2.87
2.81
2.78
2.78
2.78
2.77
2.76
2.76
2.75
2.74
2.73
2.72
2.71
2.70
2.69
2.68
2.58
2.57
2.57
2.55
2.54
2.54
2.47
2.44
2.35
2.33
2.32
2.31
2.30
2.30
2.29
2.28
2.26
2.05
2.01
1.89
1.75
1.75
1.74
1.74
1.73
1.73
1.72
1.72
1.55
1.48
1.47
1.45
1.44
1.43
1.41
1.25
1.25
1.22
1.21
1.20
1.19
1.18
1.18
1.17
1.16
1.16
1.15
1.14
0.88
0.87
0.87
0.86
O
CO2Me
O
Me
Me
3.103
600 MHz, CDCl3
1.00
2.14
1.06
2.09
0.38
0.83
0.77
0.71
0.69
0.38
1.24
1.14
1.99
2.18
1.00
1.08
2.89
6.10
δ (ppm)
175.31
175.23
170.24
170.13
132.63
132.59
127.41
127.14
77.16 CDCl3
66.50
66.44
53.96
53.92
53.32
53.31
42.20
42.18
39.93
39.81
32.33
32.25
30.87
30.86
29.93
29.57
29.32
29.28
26.47
26.43
20.06
20.04
19.78
19.74
δ (ppm)


Ph
Me
OEt
3.104
400 MHz, CDCl3
f1 (ppm)
f1 (ppm)



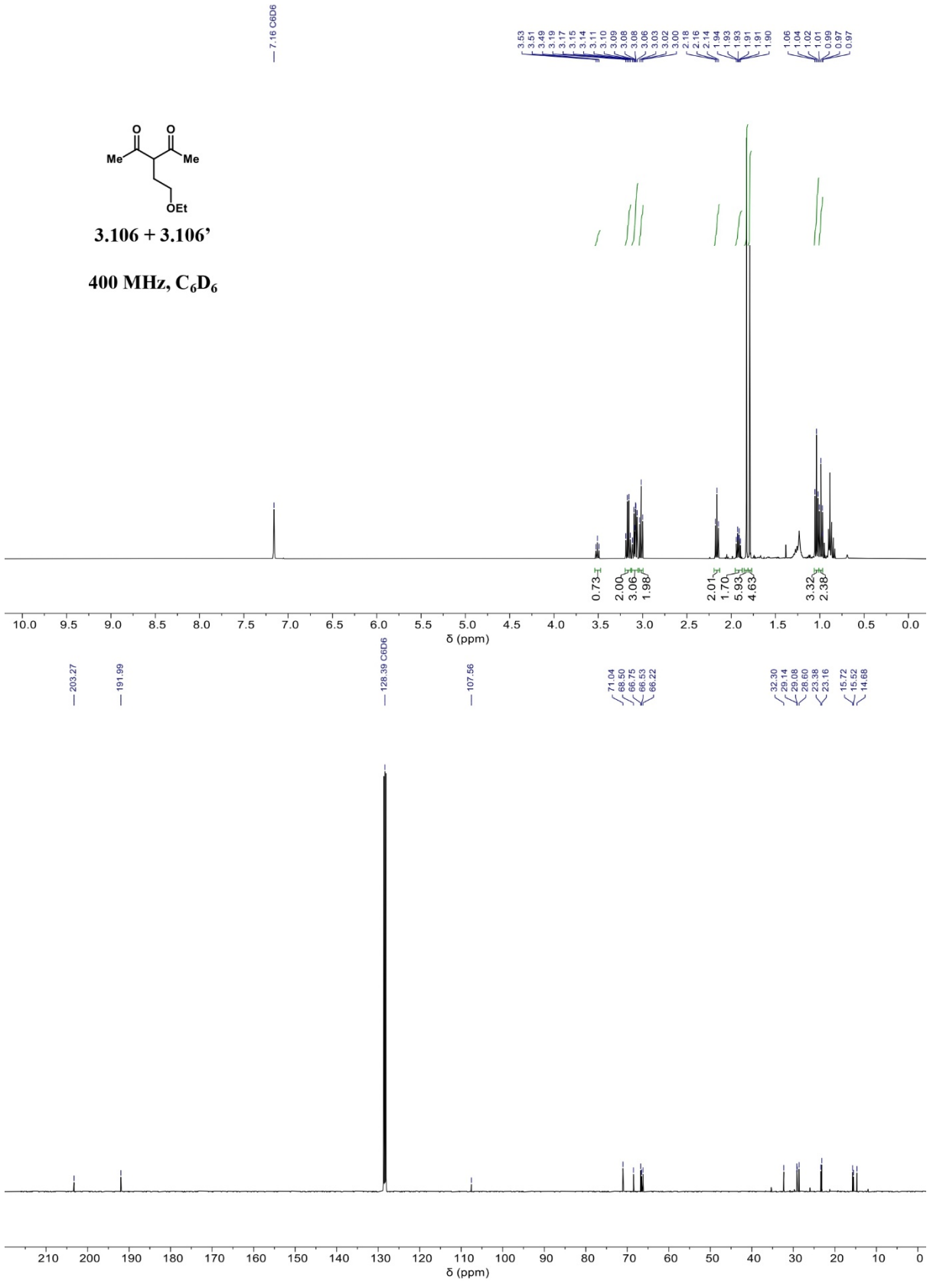
3.106 + 3.105

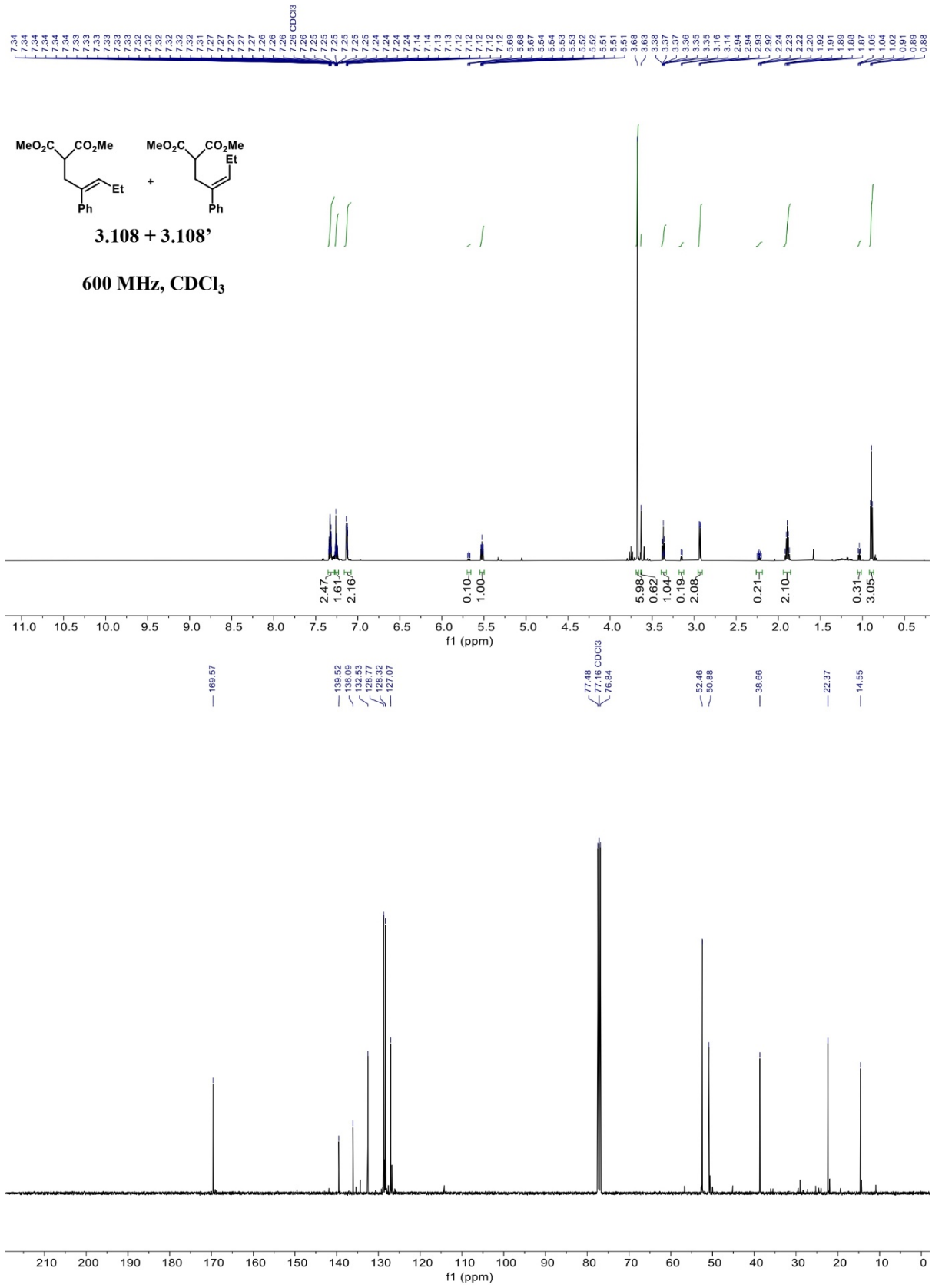
400 MHz, $CDCl_3$

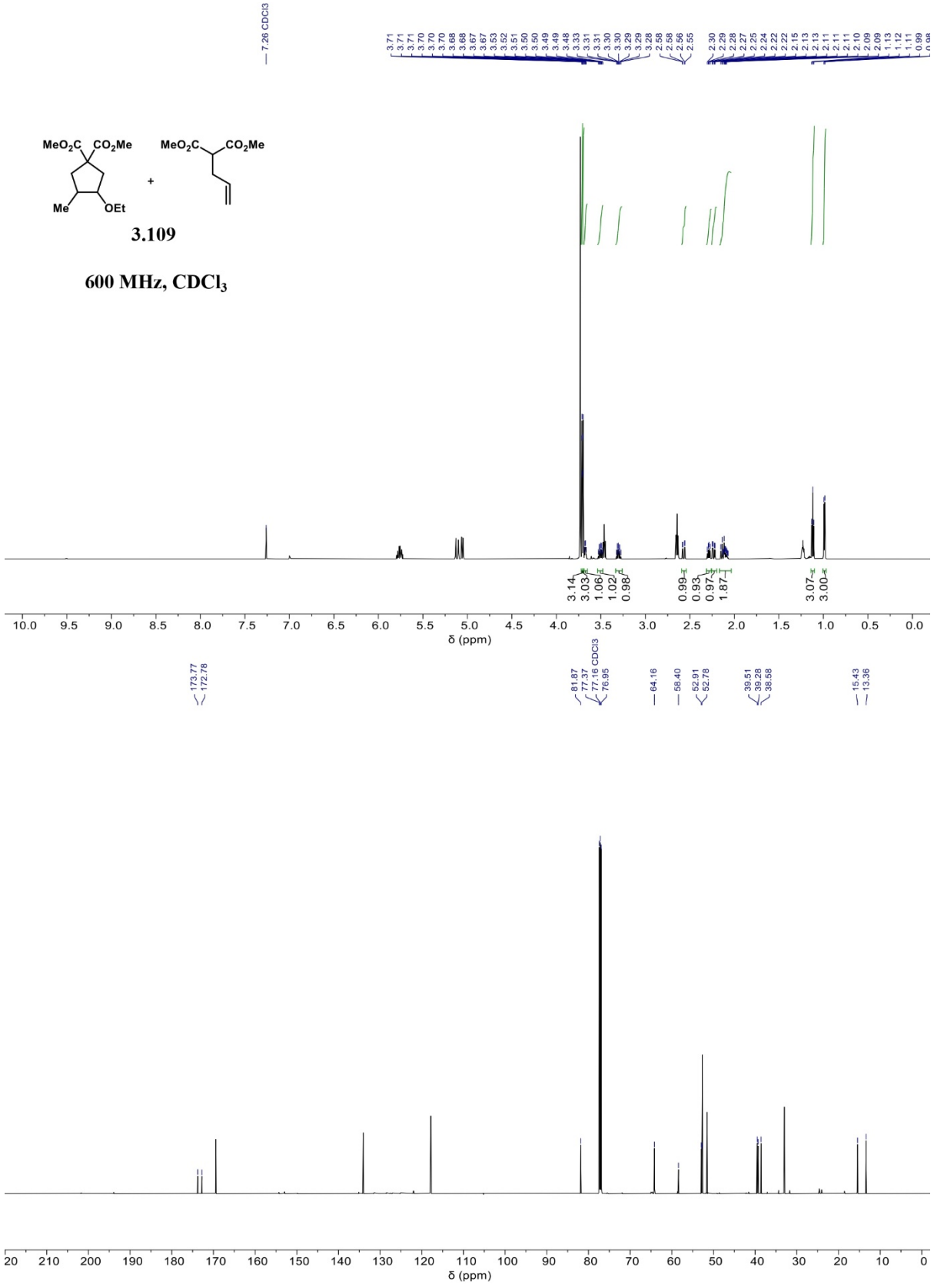


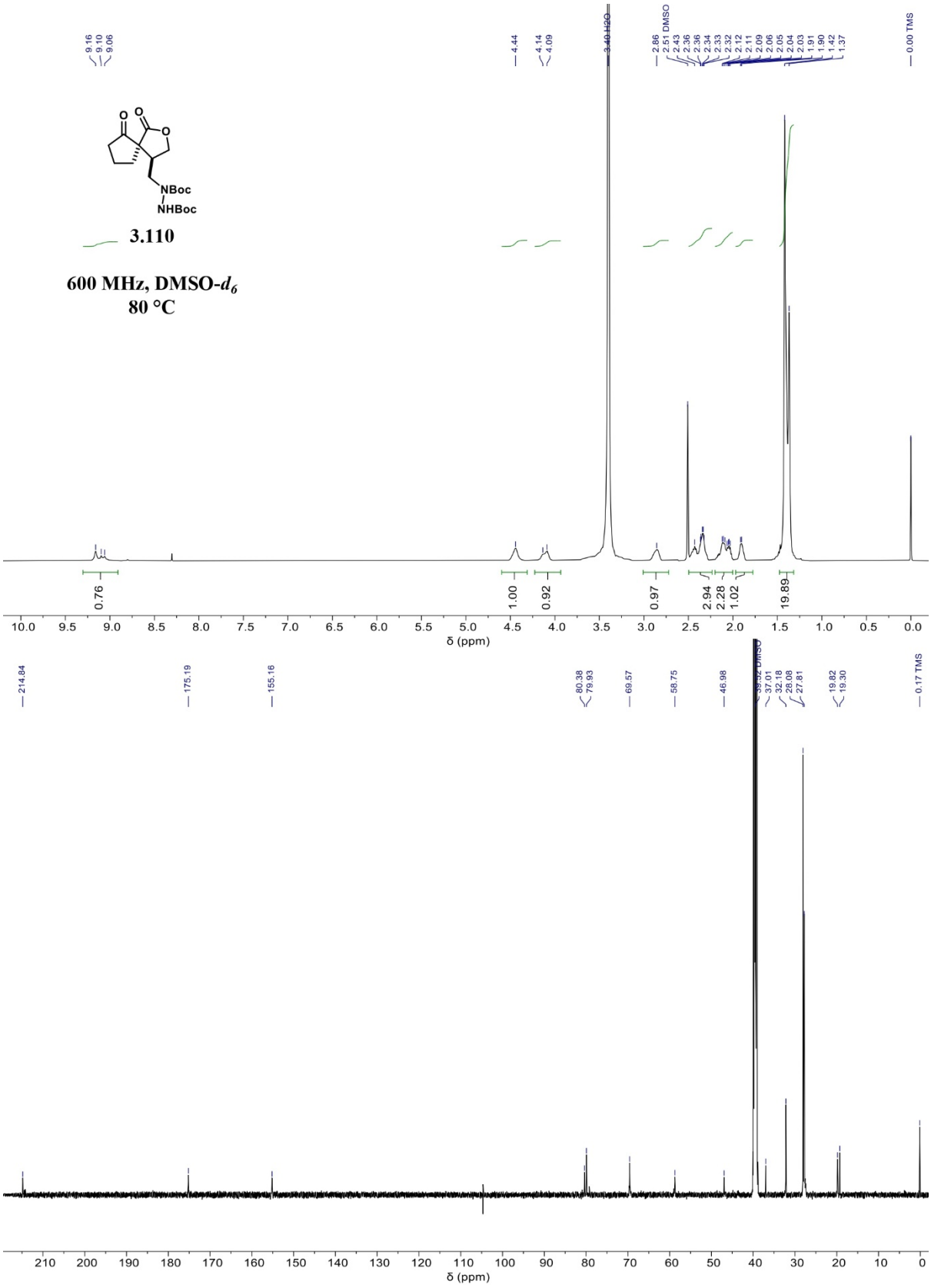
3.107

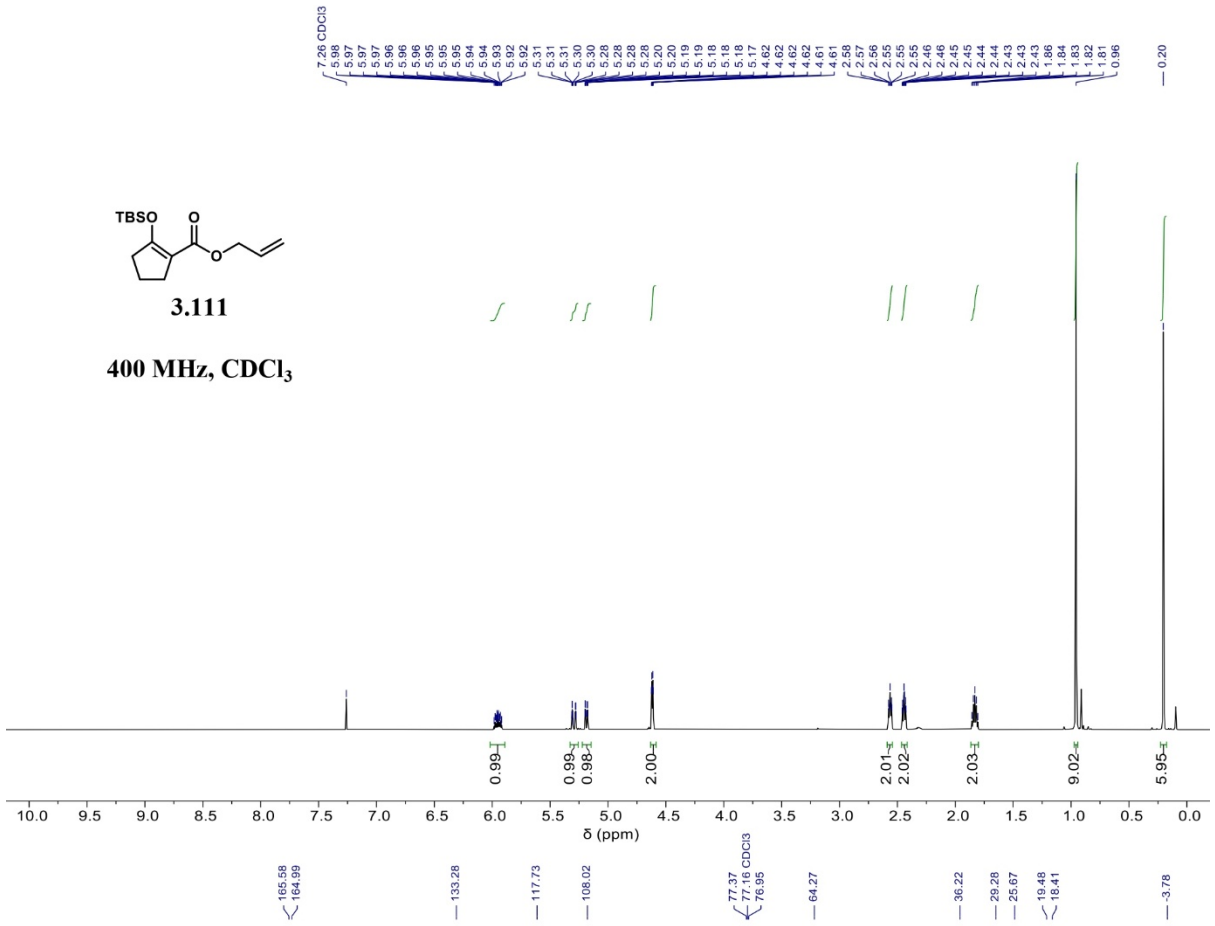
400 MHz, $CDCl_3$

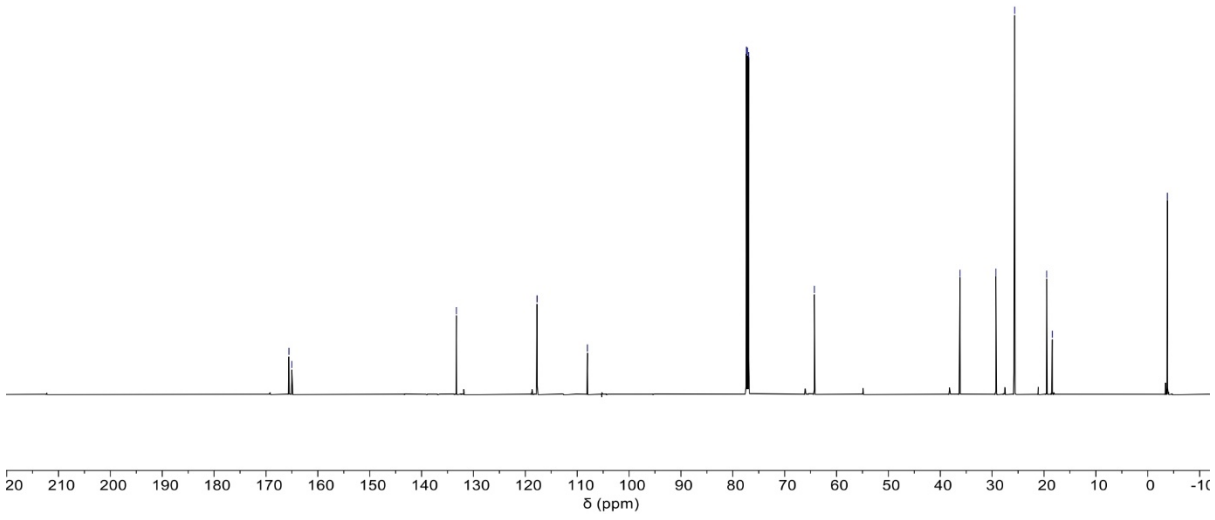

Me
Me
OEt
3.106 + 3.106'
400 MHz, C6D6
δ (ppm)
δ (ppm)

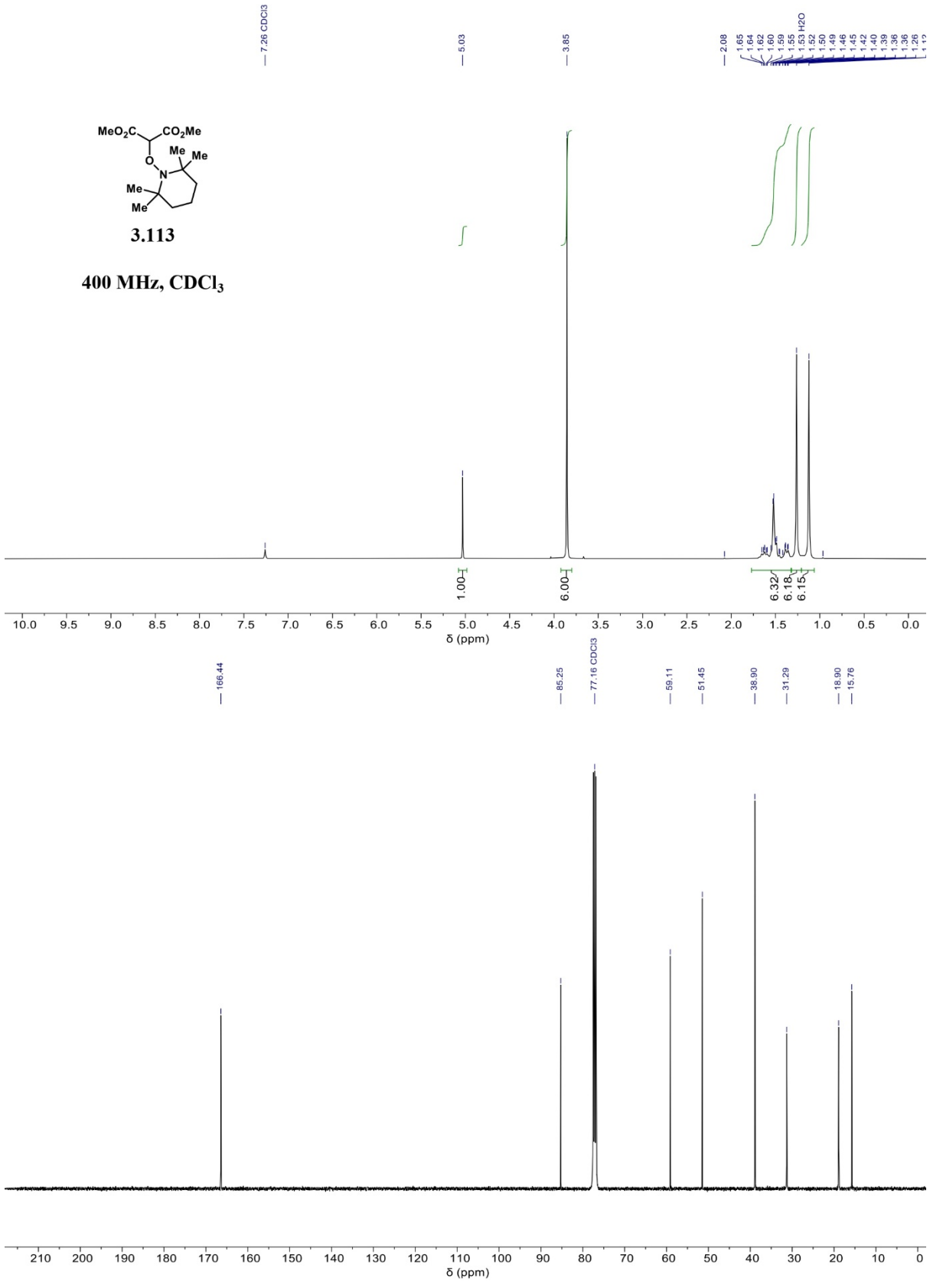

MeO2C
CO2Me
Et
Ph
+
MeO2C
CO2Me
Et
Ph
3.108 + 3.108'
600 MHz, CDCl3
f1 (ppm)
f1 (ppm)

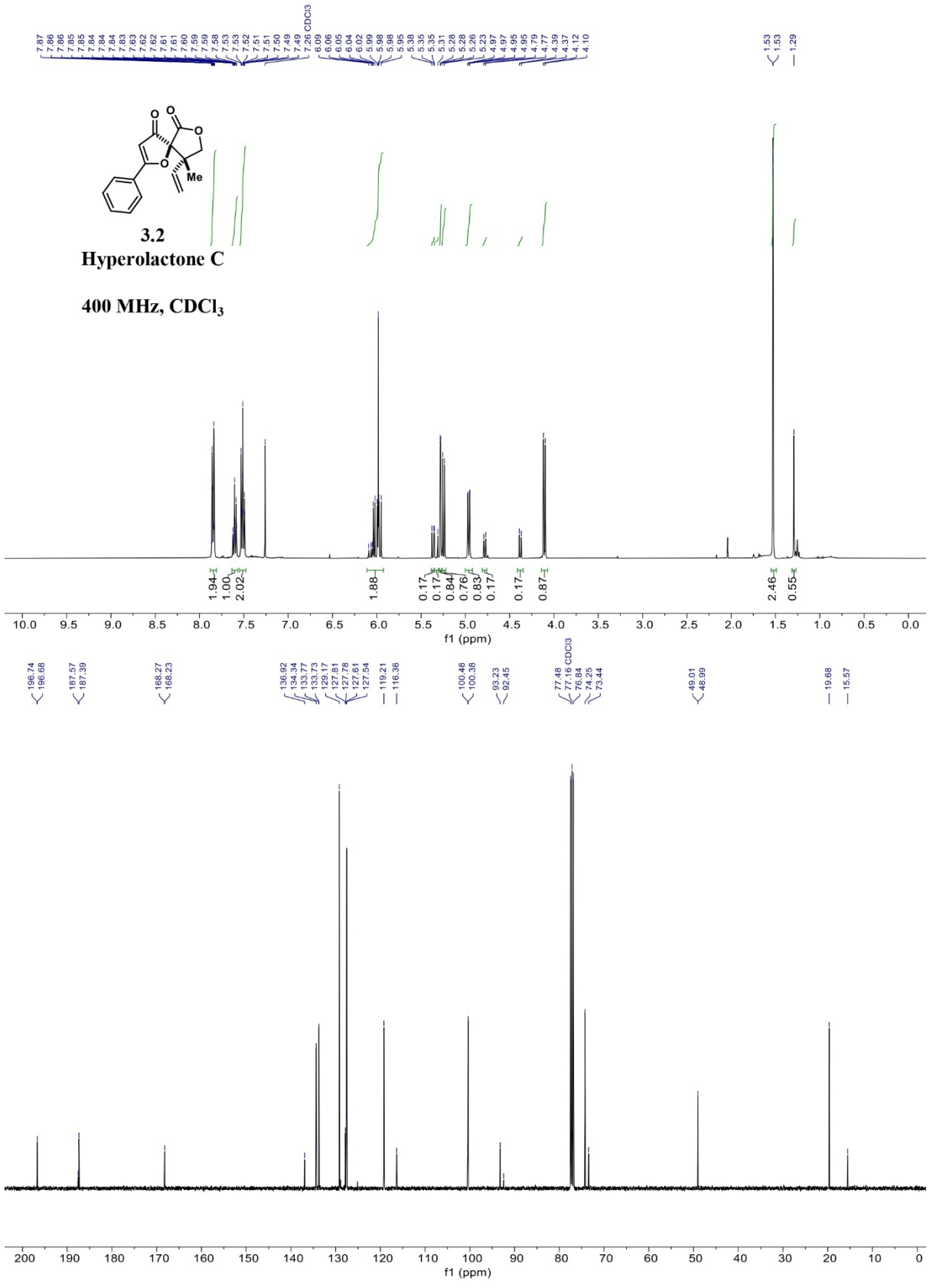

MeO2C
CO2Me
Me
OEt
+
MeO2C
CO2Me
3.109
600 MHz, CDCl3
δ (ppm)
δ (ppm)

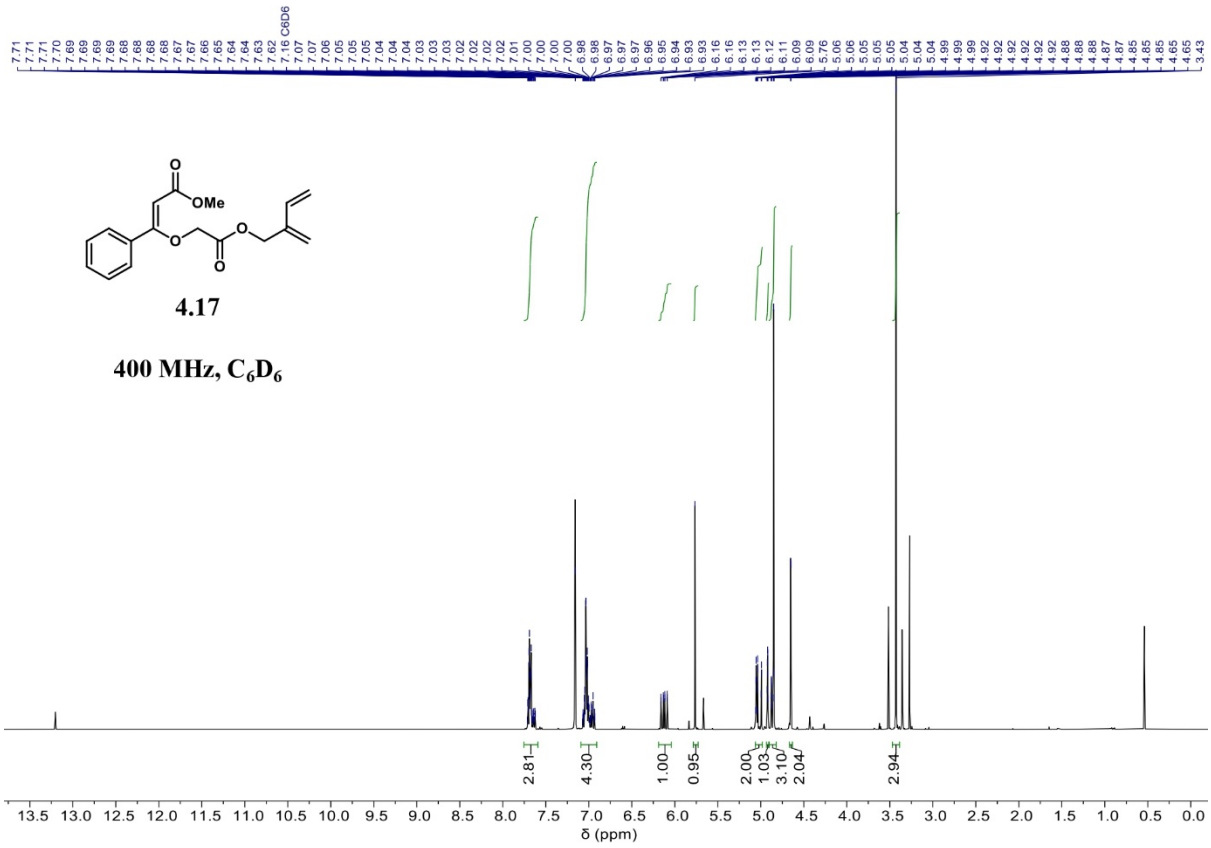

9.16
9.10
9.06
4.44
4.14
4.09
3.40 H2O
2.86
2.51 DMSO
2.43
2.36
2.36
2.34
2.33
2.32
2.12
2.11
2.09
2.06
2.05
2.04
2.03
1.91
1.90
1.42
1.37
0.00 TMS
NBoc
NHBoc
3.110
600 MHz, DMSO-d_6
80 °C
0.76
1.00
0.92
0.97
2.94
2.28
1.02
19.89
δ (ppm)
214.84
175.19
155.16
80.38
79.93
69.57
58.75
46.98
39.52 DMSO
37.01
32.18
28.08
27.81
19.82
19.30
0.17 TMS
δ (ppm)


7.26 CDCl3
TBSO
O
O
3.111
400 MHz, CDCl3
δ (ppm)


δ (ppm)

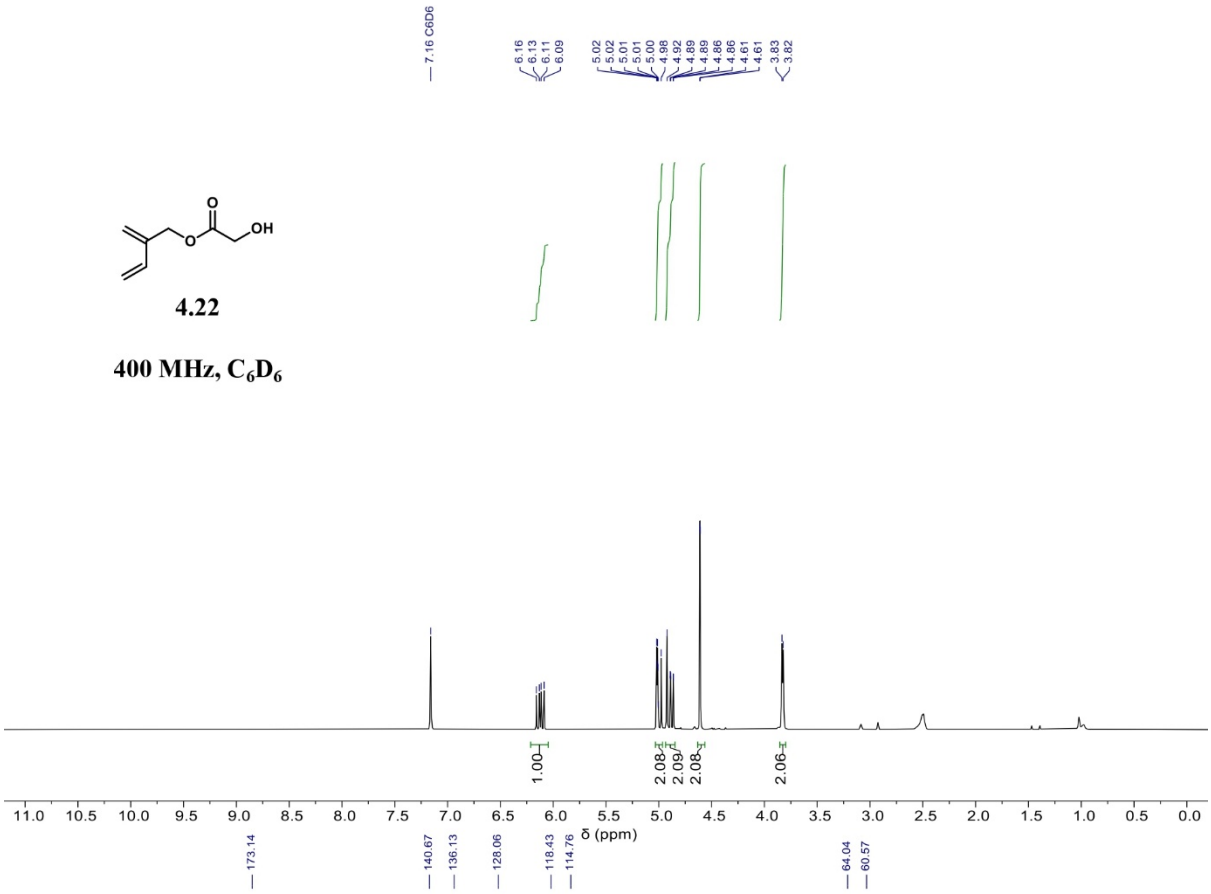

MeO2C
CO2Me
Me
Me
O
N
Me
Me
3.113
400 MHz, CDCl3
7.26 CDCl3
5.03
3.85
2.08
1.65
1.64
1.62
1.60
1.59
1.55
1.53 H2O
1.52
1.50
1.49
1.46
1.45
1.42
1.40
1.39
1.36
1.36
1.26
1.00
6.00
6.32
6.18
6.15
δ (ppm)
166.44
85.25
77.16 CDCl3
59.11
51.45
38.90
31.29
18.90
15.76
δ (ppm)

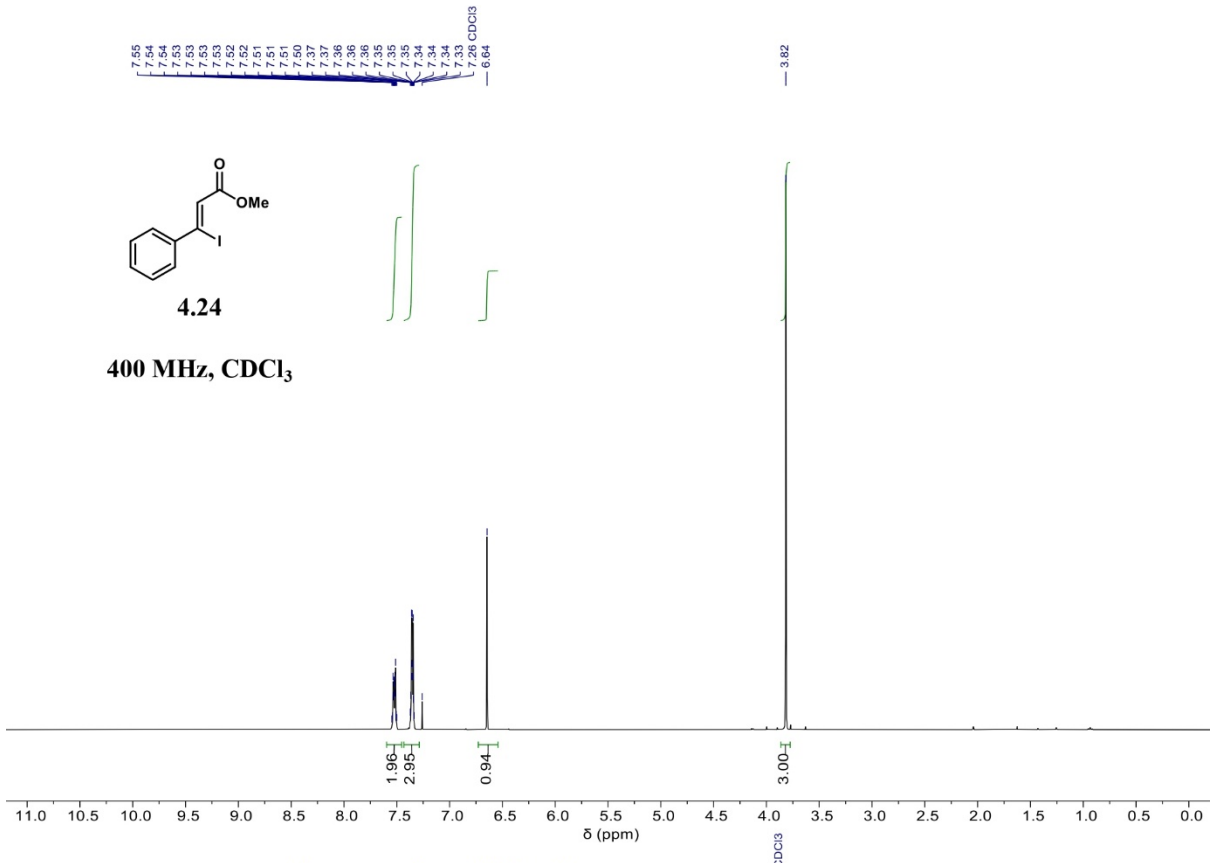

7.87 7.86 7.86 7.85 7.85 7.84 7.84 7.84 7.83 7.63 7.62 7.62 7.61 7.61 7.60 7.59 7.59 7.58 7.53 7.52 7.51 7.51 7.50 7.49 7.49 7.26 CDCl3 6.09 6.06 6.05 6.04 6.02 5.99 5.98 5.98 5.95 5.38 5.35 5.35 5.31 5.28 5.28 5.26 5.23 4.97 4.97 4.95 4.95 4.79 4.77 4.39 4.37 4.12 4.10
1.53 1.53 1.29
Me
3.2
Hyperolactone C
400 MHz, CDCl3
1.94 1.00 2.02 1.88 0.17 0.17 0.84 0.76 0.83 0.17 0.17 0.87 2.46 0.55
10.0 9.5 9.0 8.5 8.0 7.5 7.0 6.5 6.0 5.5 5.0 4.5 4.0 3.5 3.0 2.5 2.0 1.5 1.0 0.5 0.0
f1 (ppm)
196.74 196.68 187.57 187.39 168.27 168.23 136.92 134.34 133.77 133.73 129.17 127.81 127.78 127.61 127.54 119.21 116.36 100.46 100.38 93.23 92.45 77.48 77.16 CDCl3 76.84 74.25 73.44 49.01 48.99 19.68 15.57
200 190 180 170 160 150 140 130 120 110 100 90 80 70 60 50 40 30 20 10 0
f1 (ppm)


OMe
O
O
O
O
4.17
400 MHz, C6D6
C6D6
2.81
4.30
1.00
0.95
2.00
1.03
3.10
2.04
2.94
δ (ppm)

4.22

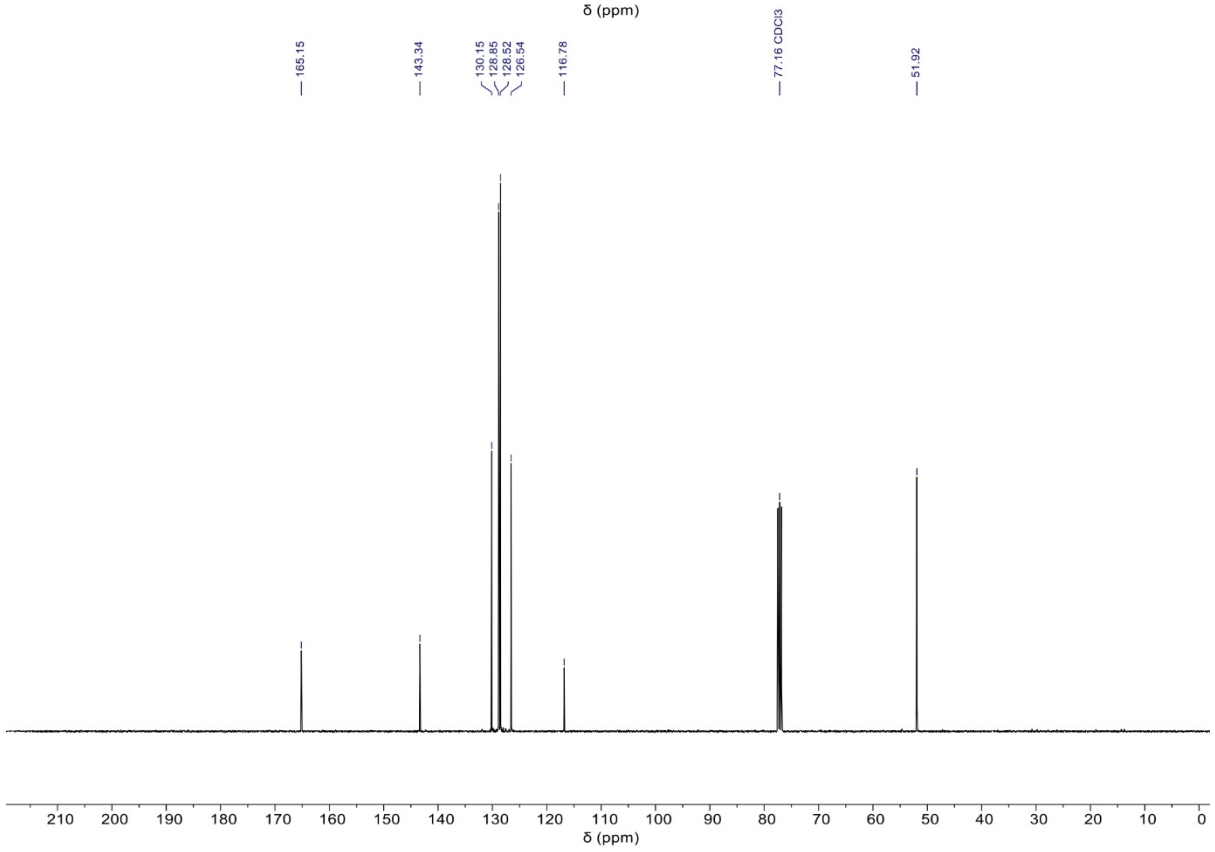
400 MHz, C_6D_6

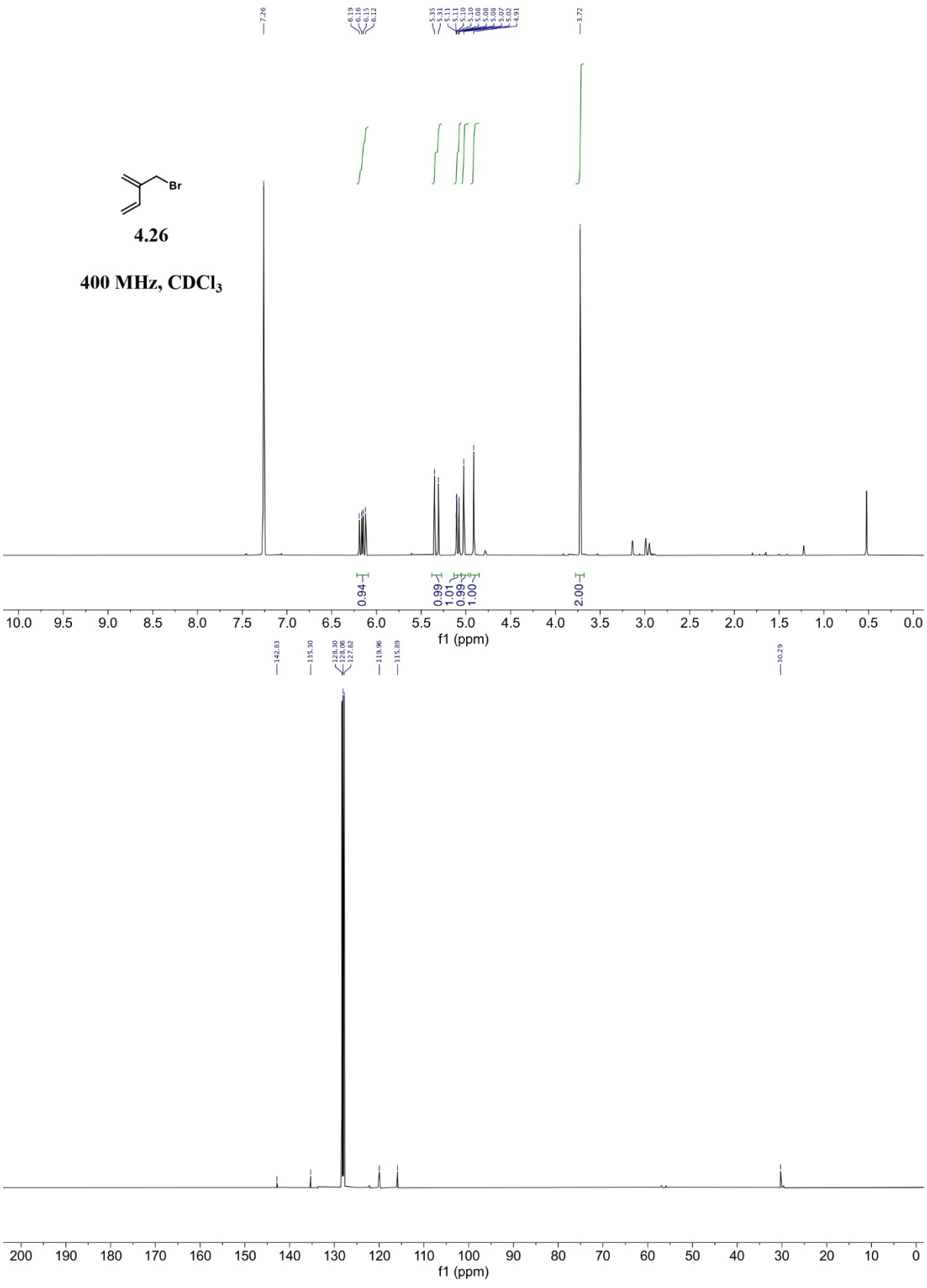


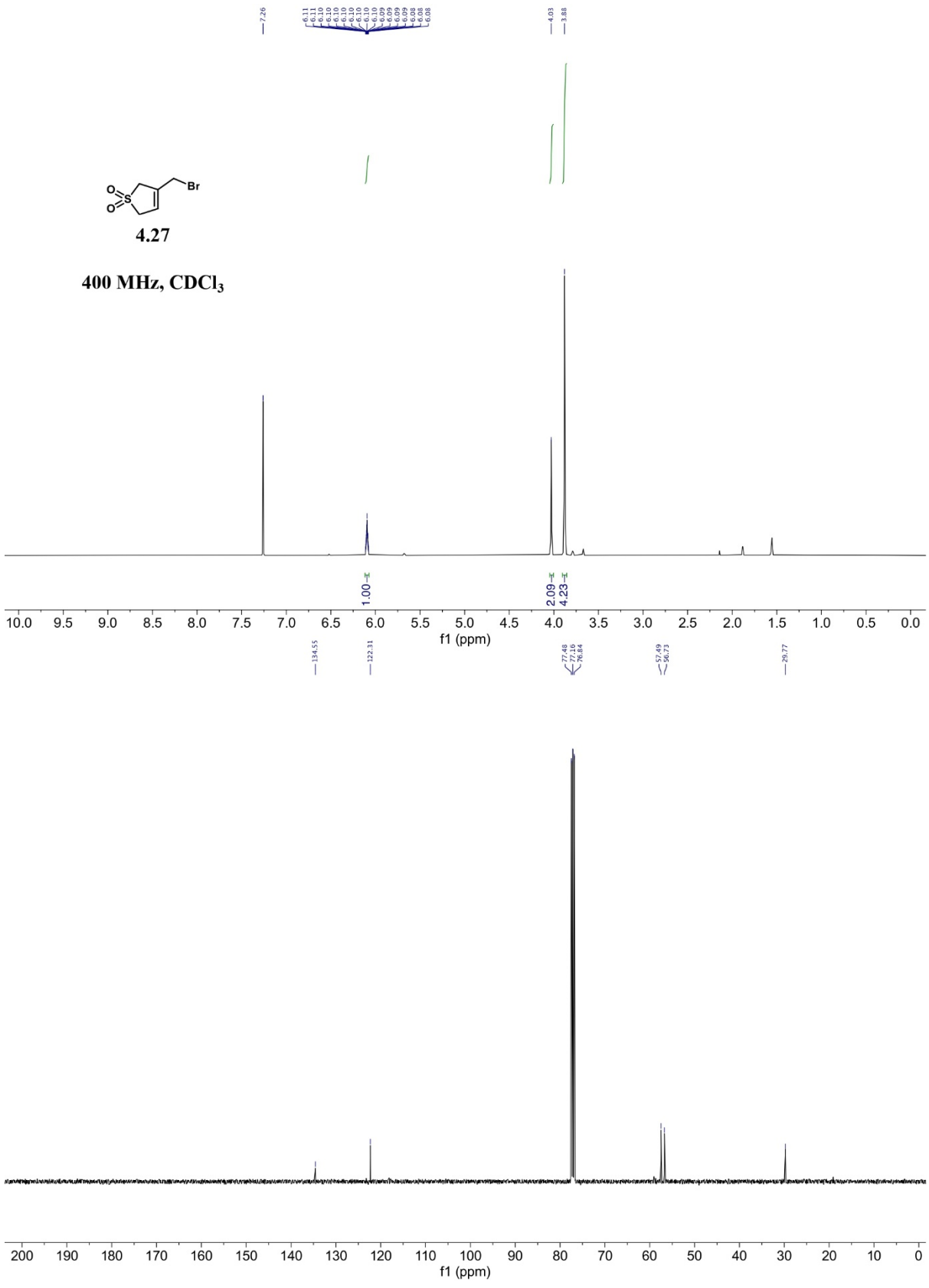


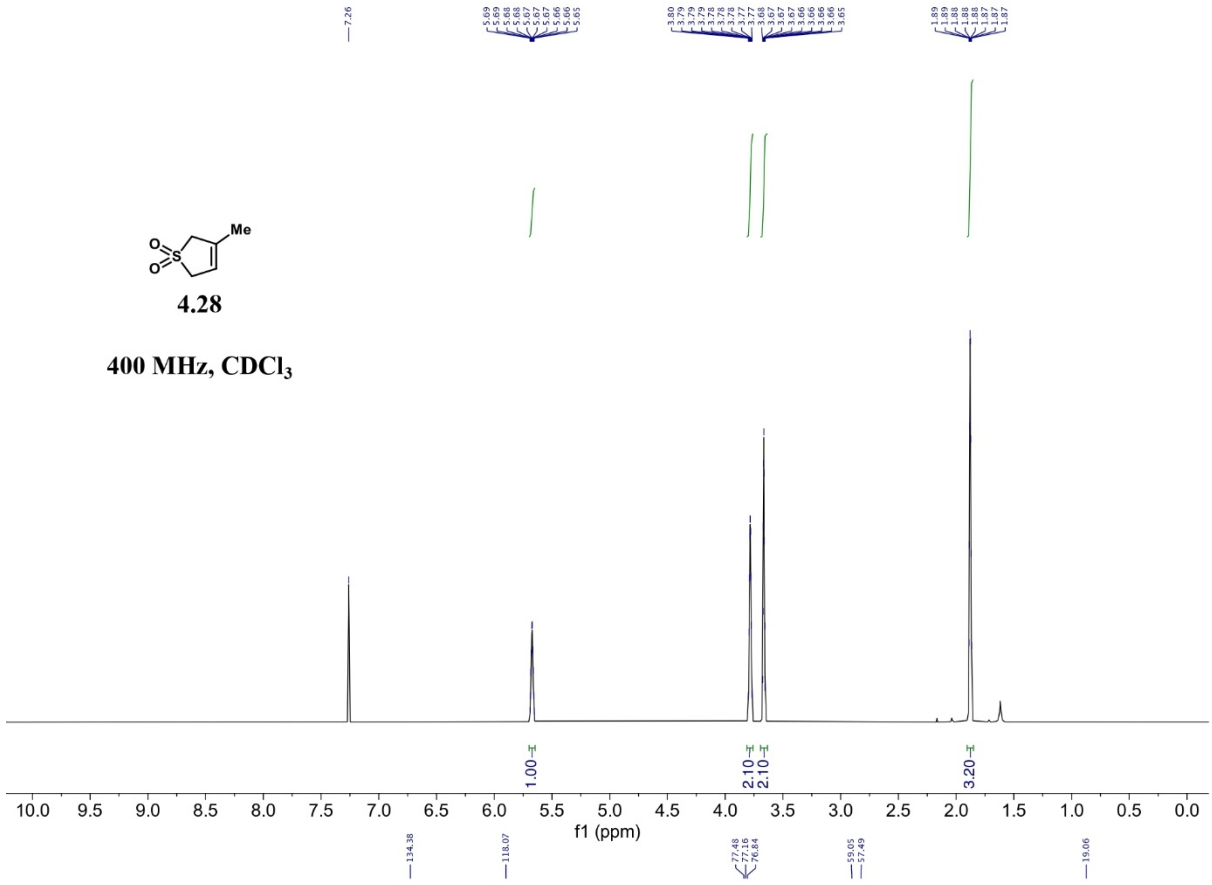
4.24

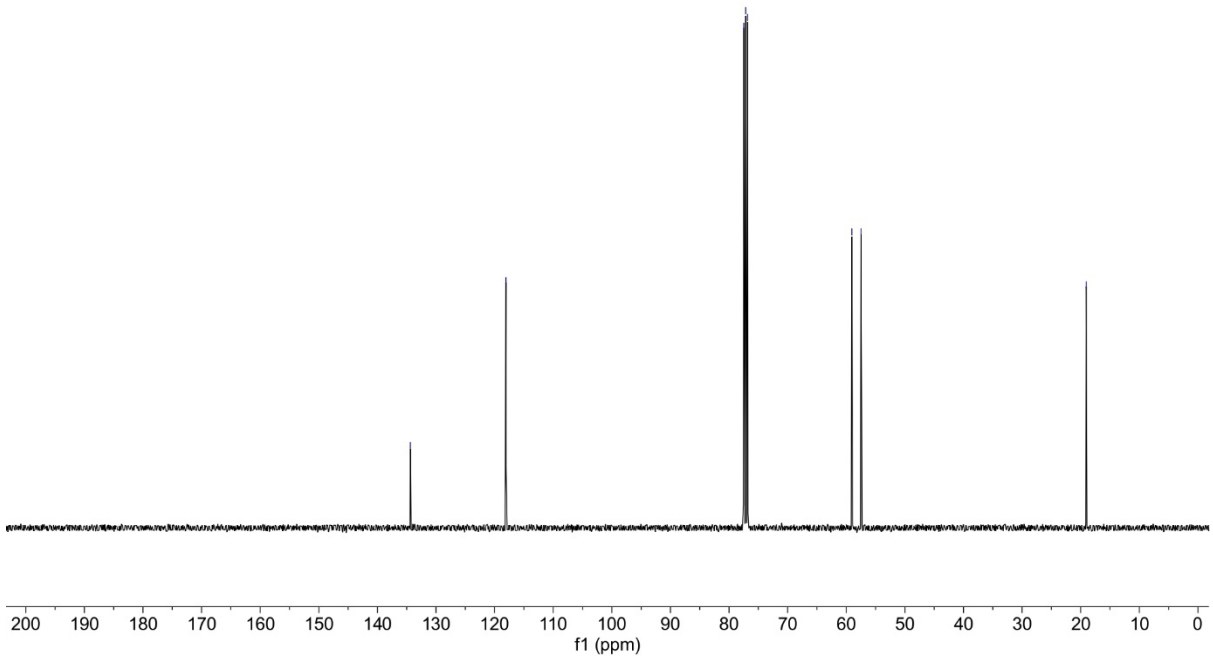
400 MHz, $CDCl_3$

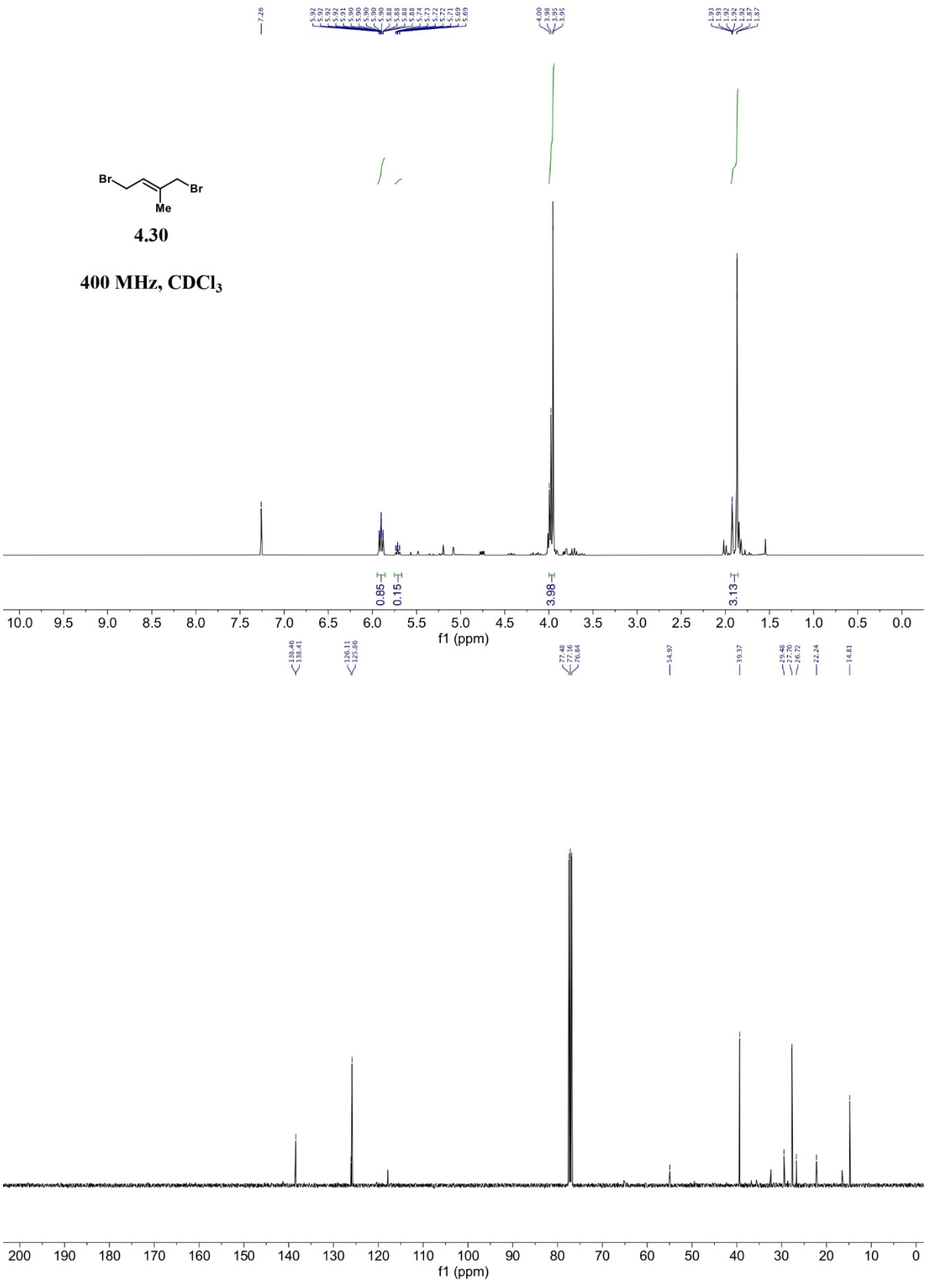


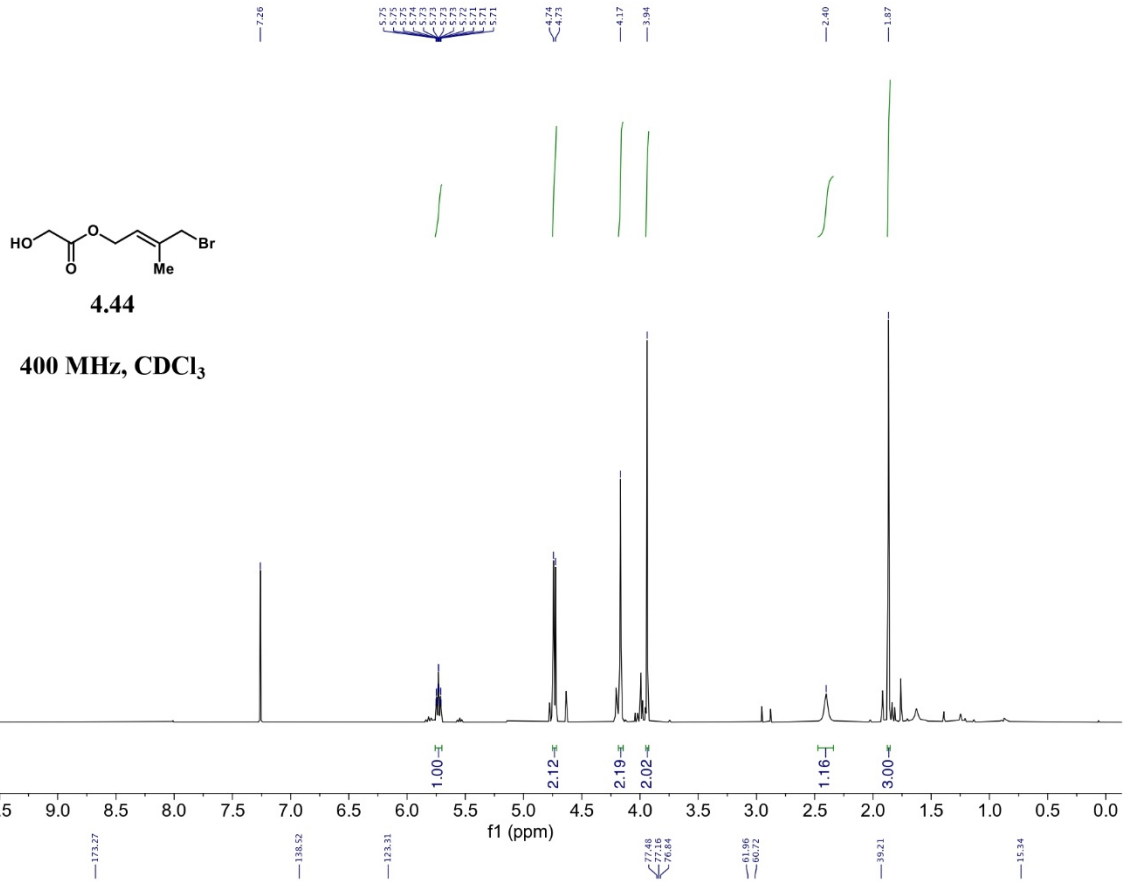

Br
4.26
400 MHz, CDCl3
7.26
6.19
6.16
6.15
6.12
5.35
5.31
5.11
5.10
5.10
5.08
5.08
5.07
5.02
4.91
3.72
0.94
0.99
1.01
0.99
1.00
2.00
f1 (ppm)
142.83
135.30
128.30
128.06
127.82
119.96
115.89
30.29
f1 (ppm)

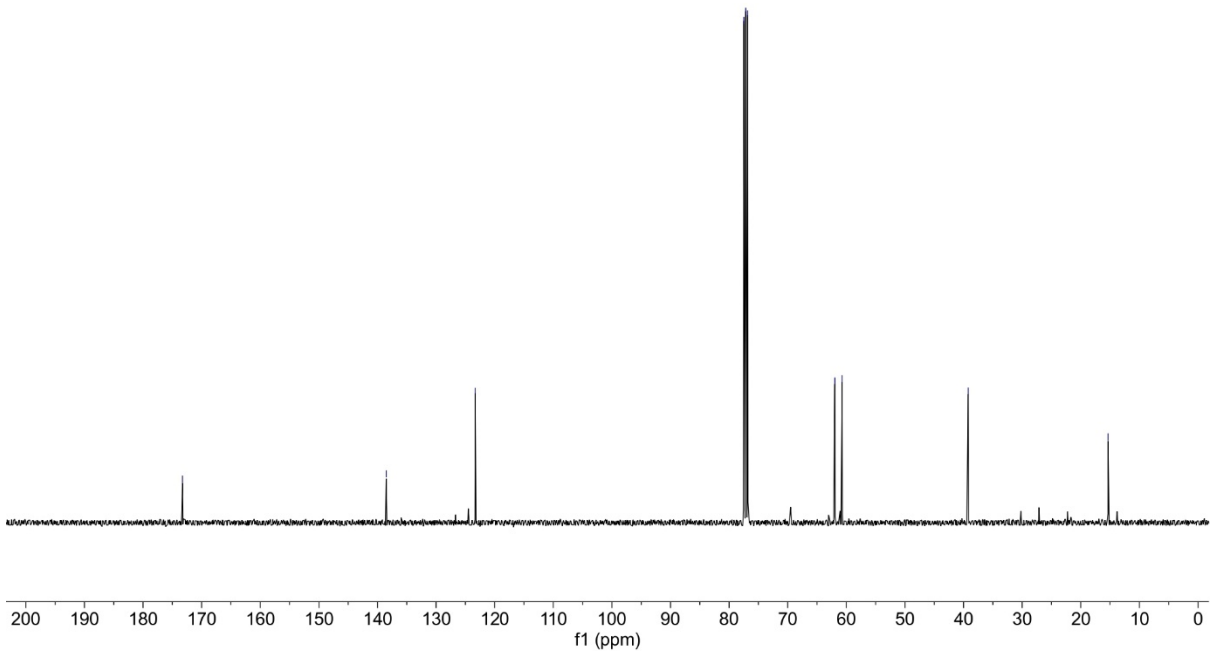

Br
4.27
400 MHz, CDCl3
f1 (ppm)
f1 (ppm)

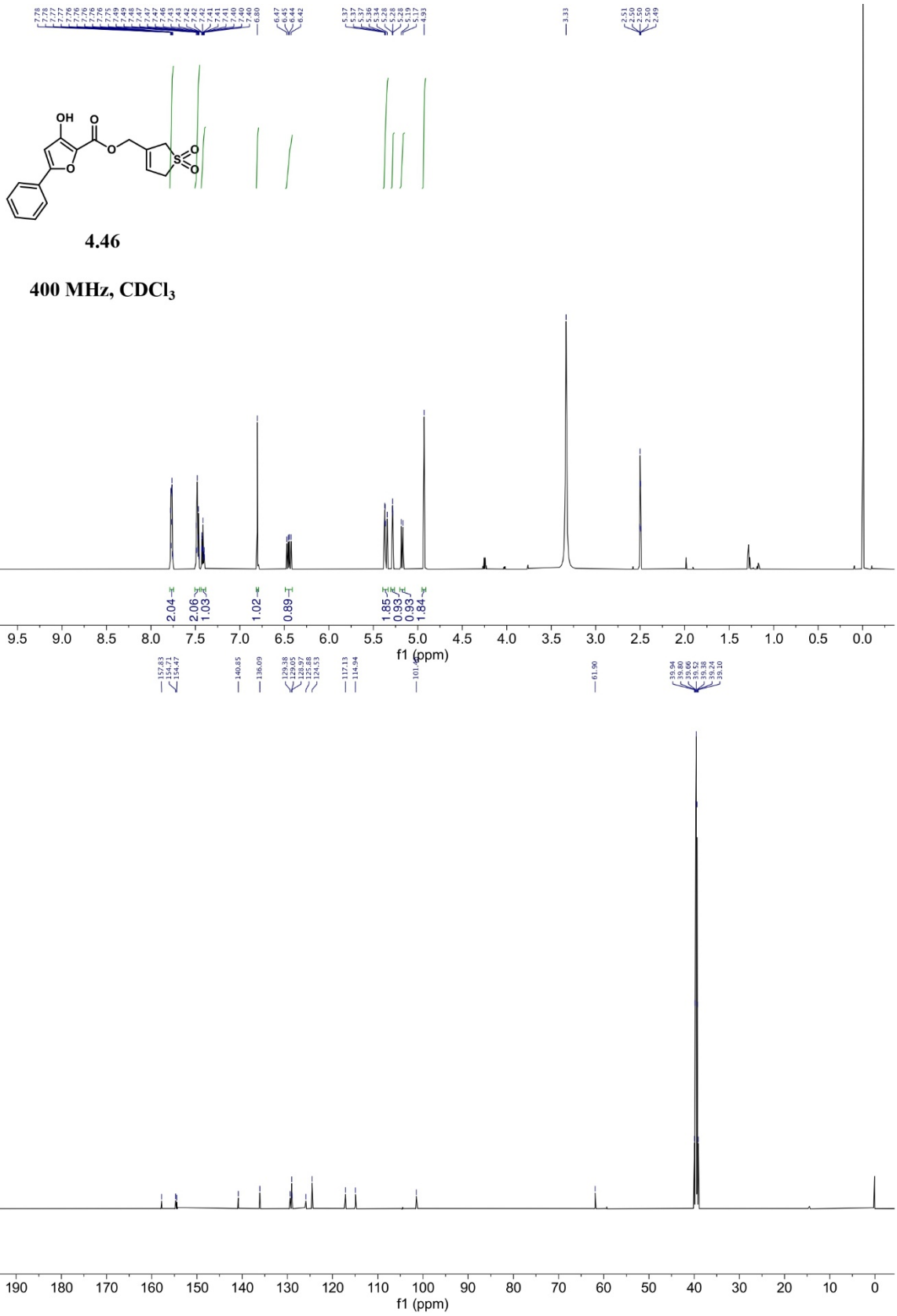

Me
O
O
S
4.28
400 MHz, CDCl3
7.26
5.69
5.68
5.67
5.66
5.65
3.80
3.79
3.78
3.77
3.68
3.67
3.66
3.65
1.89
1.88
1.87
1.87
1.87
1.87
1.00
2.10
2.10
3.20
10.0 9.5 9.0 8.5 8.0 7.5 7.0 6.5 6.0 5.5 5.0 4.5 4.0 3.5 3.0 2.5 2.0 1.5 1.0 0.5 0.0
f1 (ppm)

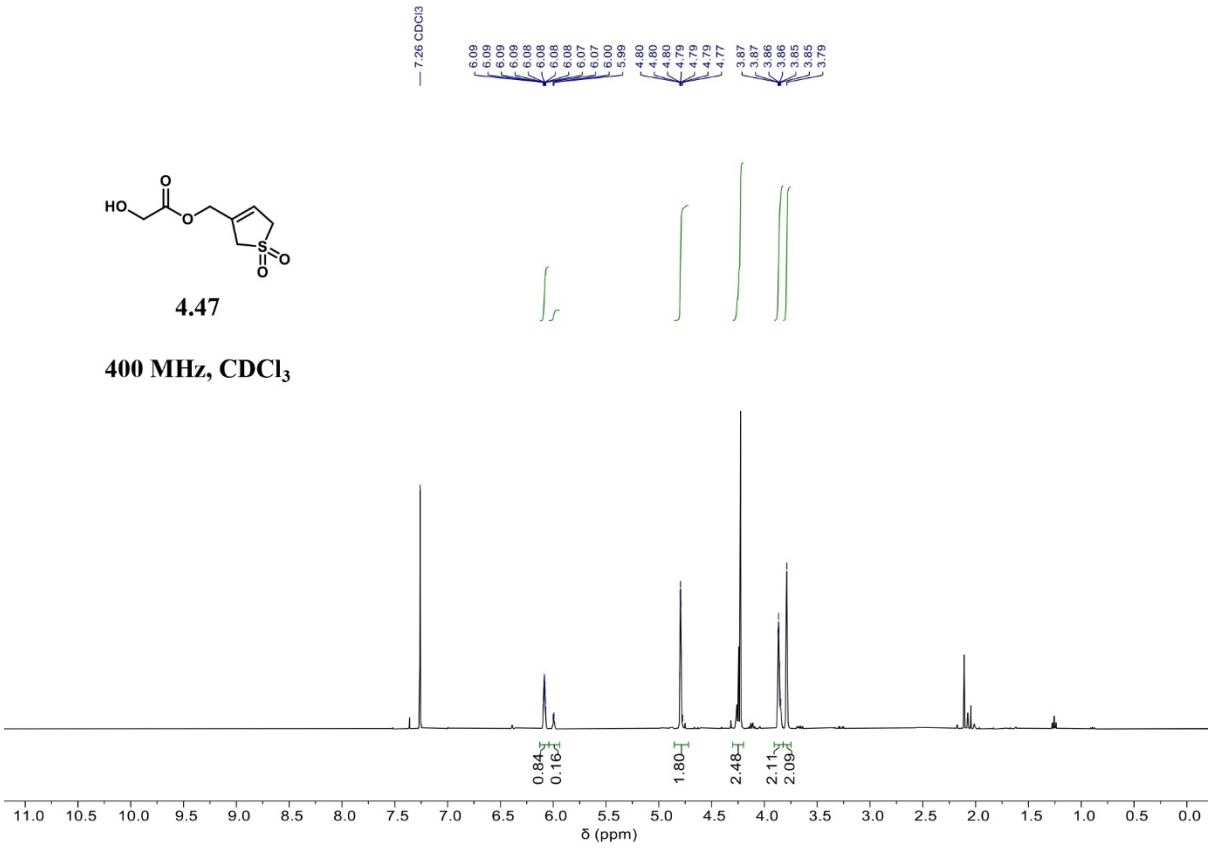

134.38
118.07
77.48
77.16
76.84
59.05
57.49
19.06
200 190 180 170 160 150 140 130 120 110 100 90 80 70 60 50 40 30 20 10 0
f1 (ppm)


Br
Br
Me
4.30
400 MHz, CDCl3
f1 (ppm)
f1 (ppm)


HO
O
O
Br
Me
4.44
400 MHz, CDCl3
7.26
5.75
5.75
5.75
5.74
5.73
5.73
5.73
5.73
5.72
5.71
5.71
5.71
4.74
4.73
4.17
3.94
2.40
1.87
1.00
2.12
2.19
2.02
1.16
3.00
f1 (ppm)

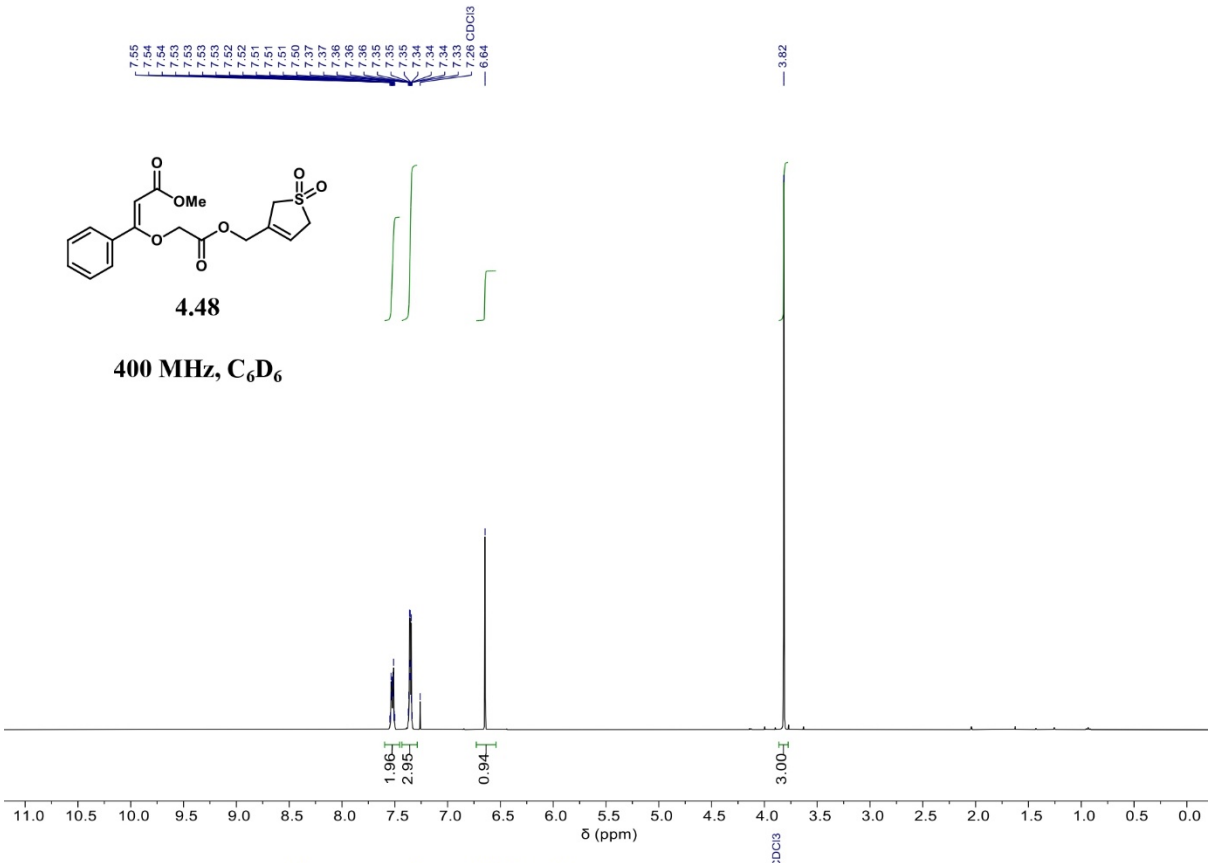

173.27
138.52
123.31
77.48
77.16
76.84
61.96
60.72
39.21
15.34
f1 (ppm)

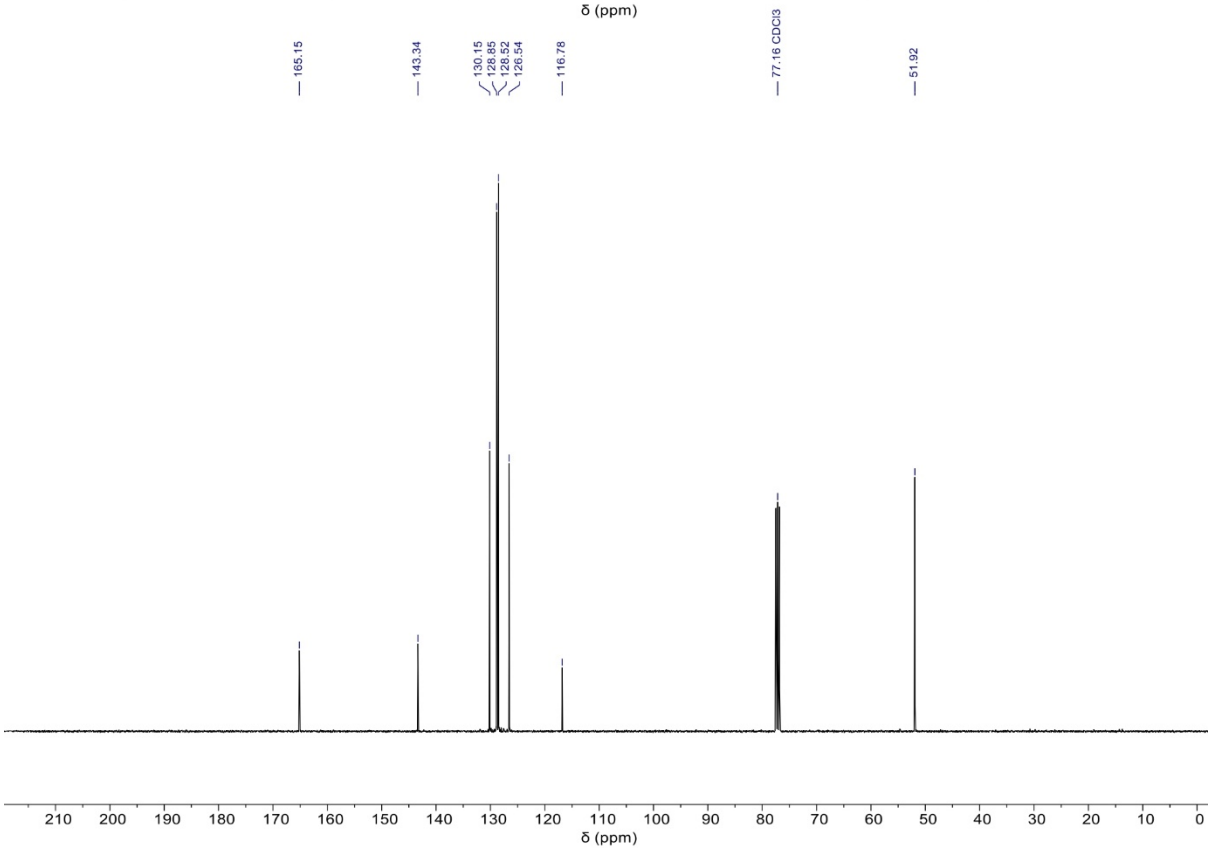

OH
O
O
O
O
S
O
O
4.46
400 MHz, CDCl3
f1 (ppm)
f1 (ppm)

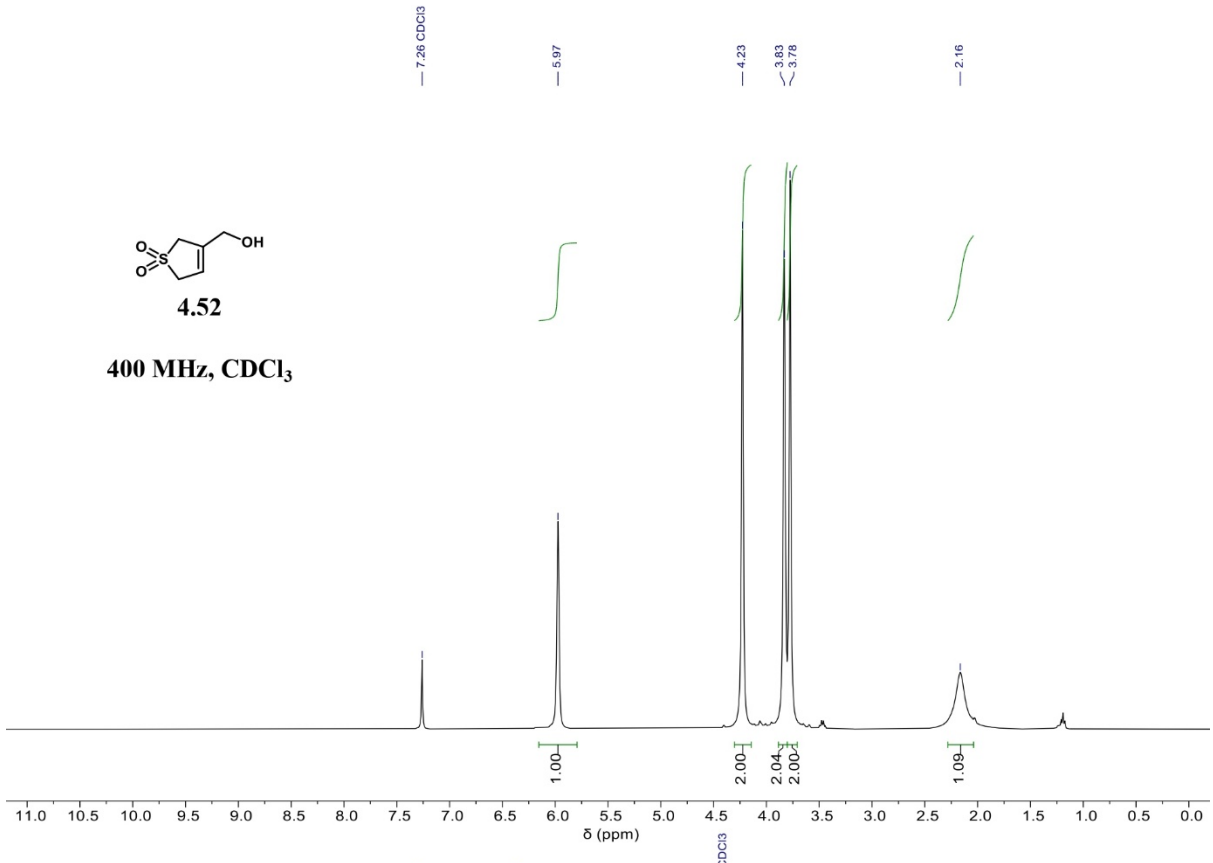


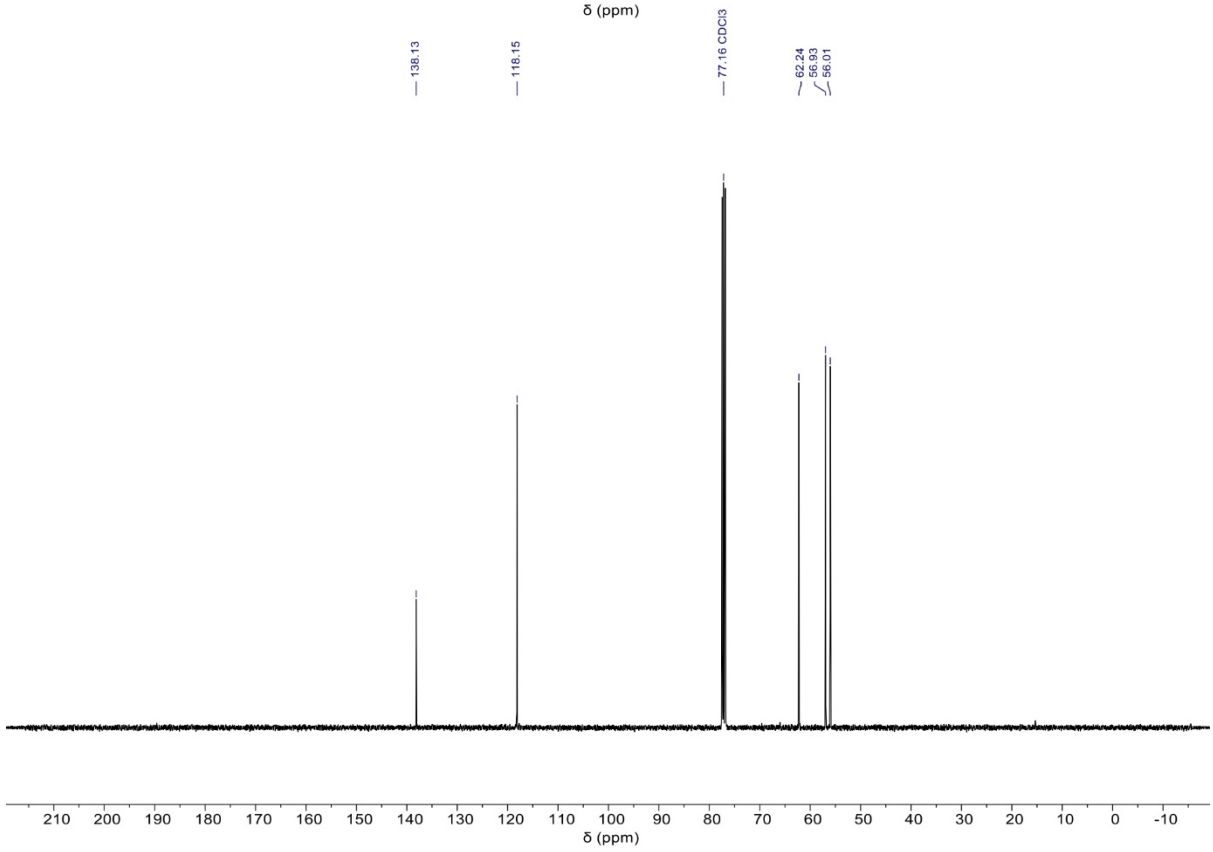
4.47

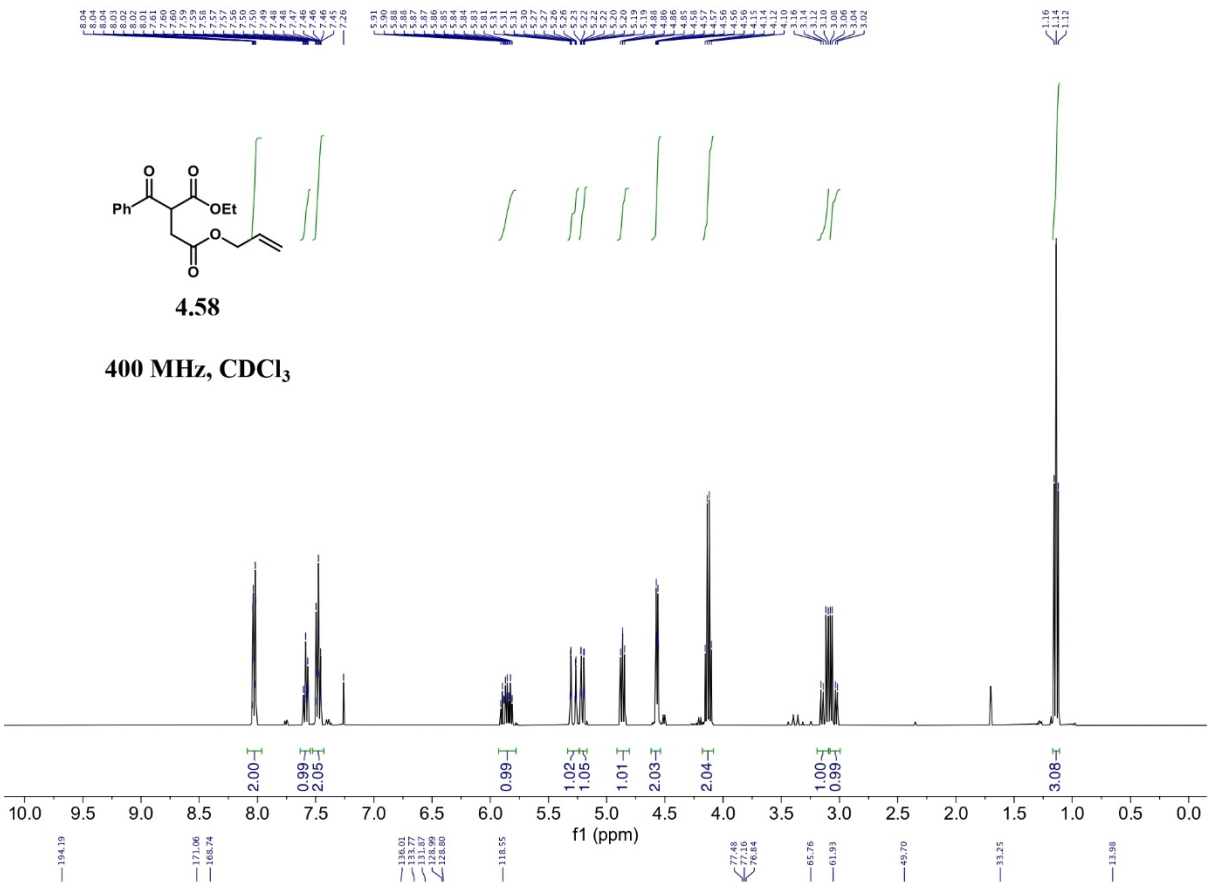
400 MHz, $CDCl_3$


7.55
7.54
7.54
7.53
7.53
7.53
7.53
7.52
7.52
7.51
7.51
7.51
7.50
7.37
7.37
7.36
7.36
7.36
7.35
7.35
7.35
7.34
7.34
7.34
7.33
7.26 CDCl3
6.64
3.82
O
OMe
O
S
O
O
O
O
O
4.48
400 MHz, C6D6
1.96
2.95
0.94
3.00
11.0 10.5 10.0 9.5 9.0 8.5 8.0 7.5 7.0 6.5 6.0 5.5 5.0 4.5 4.0 3.5 3.0 2.5 2.0 1.5 1.0 0.5 0.0
δ (ppm)


165.15
143.34
130.15
128.85
128.52
126.54
116.78
77.16 CDCl3
51.92
210 200 190 180 170 160 150 140 130 120 110 100 90 80 70 60 50 40 30 20 10 0
δ (ppm)

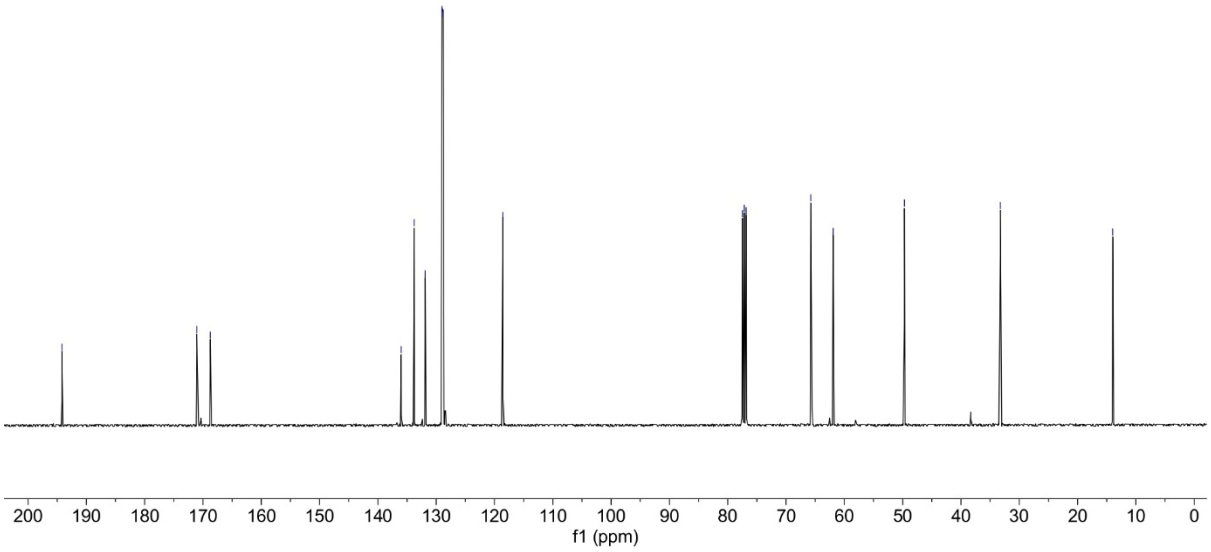

7.26 CDCl3
5.97
4.23
3.83
3.78
2.16
OH
4.52
400 MHz, CDCl3
1.00
2.00
2.04
2.00
1.09
δ (ppm)

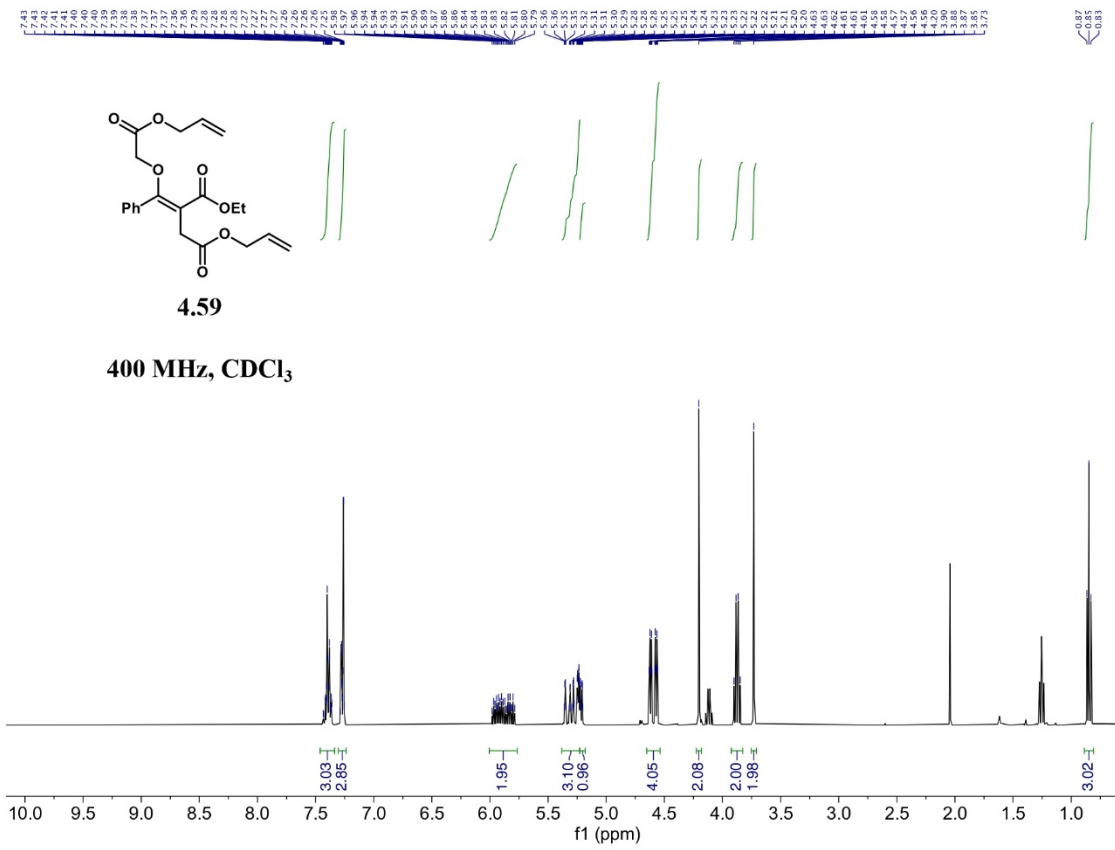

138.13
118.15
77.16 CDCl3
62.24
56.93
56.01
δ (ppm)



4.58

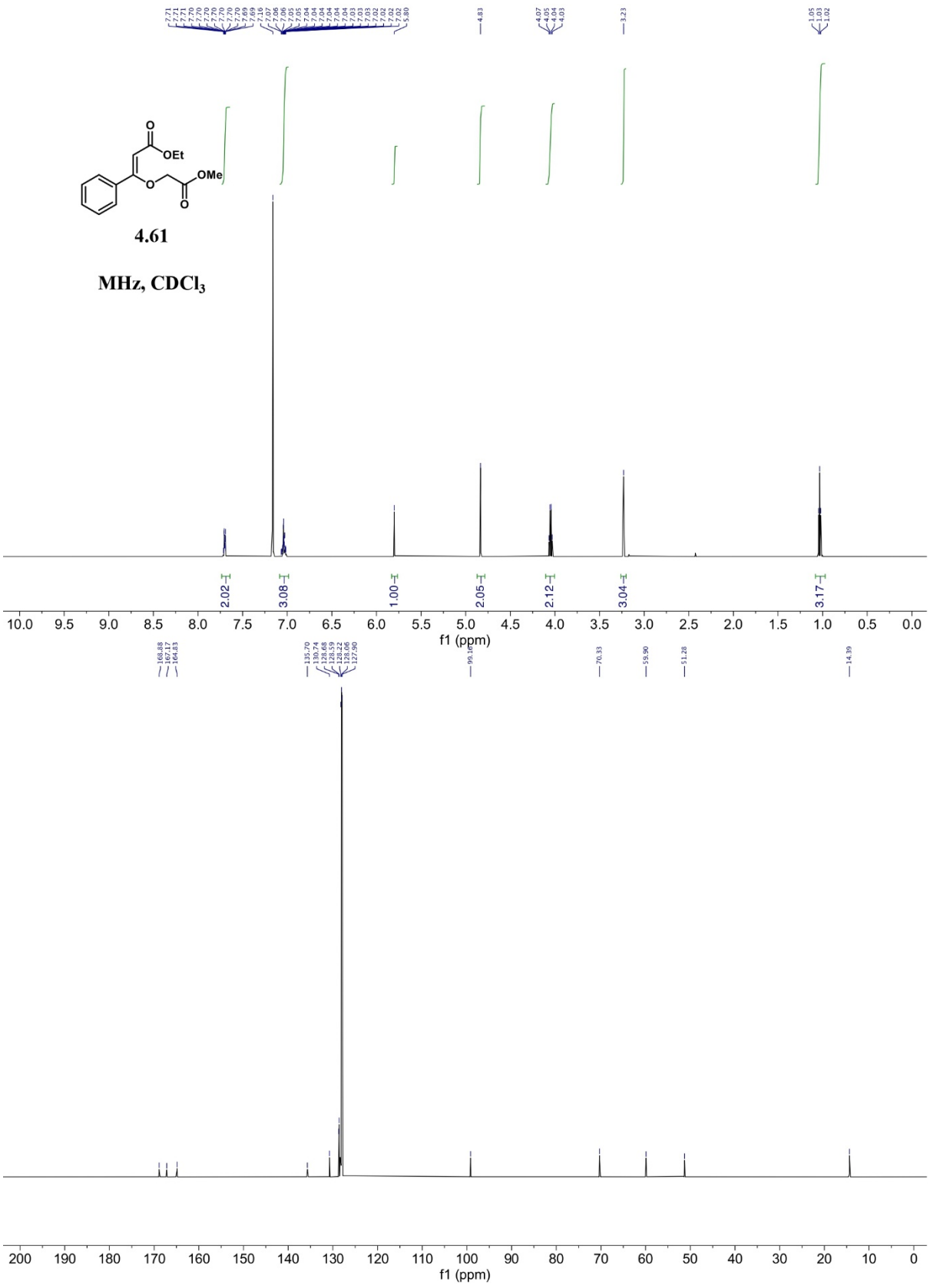
400 MHz, $CDCl_3$

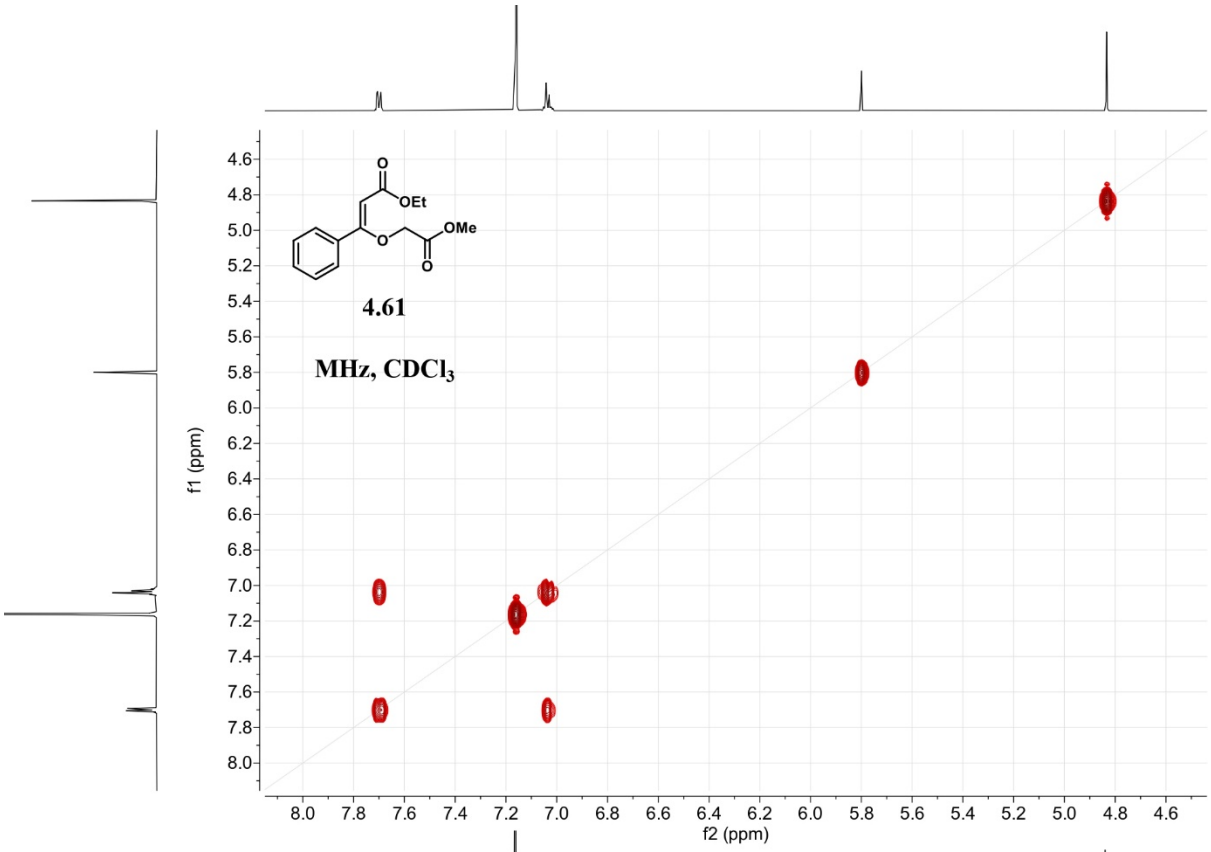


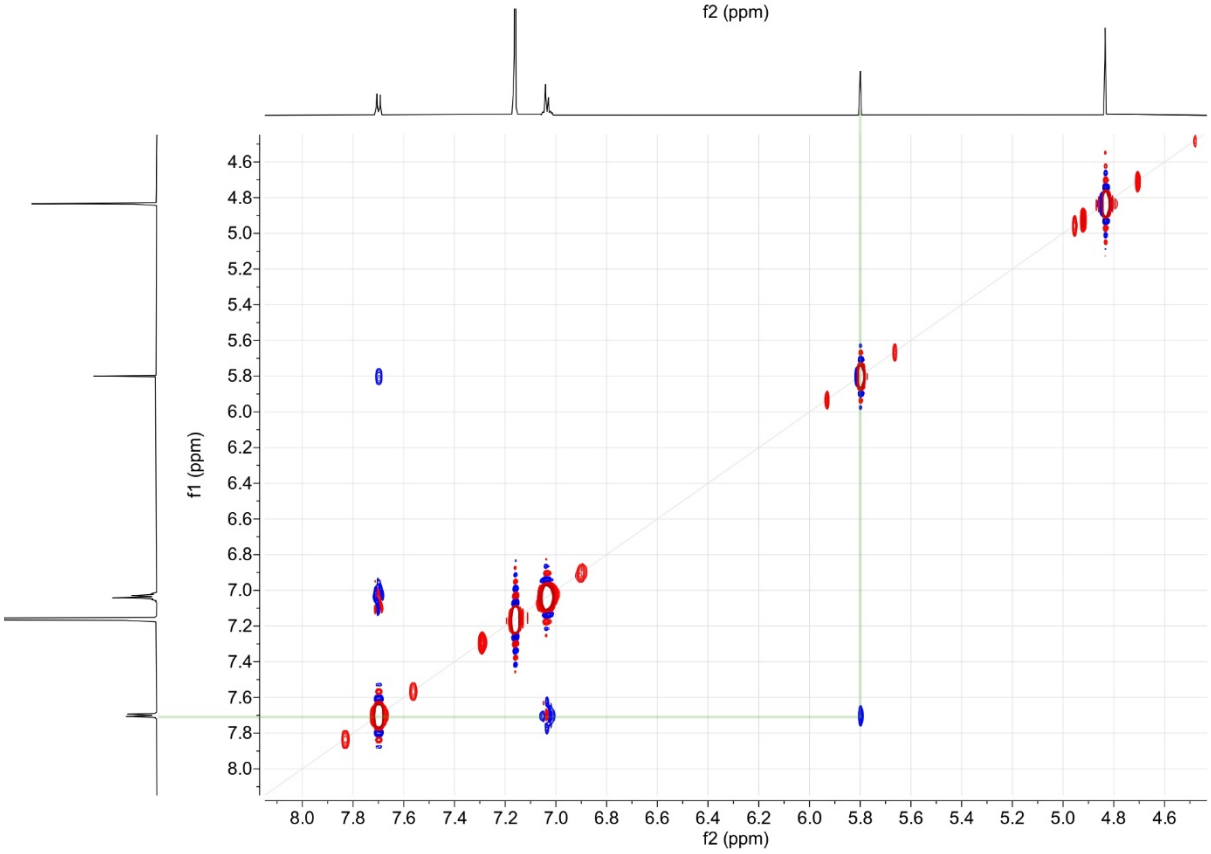


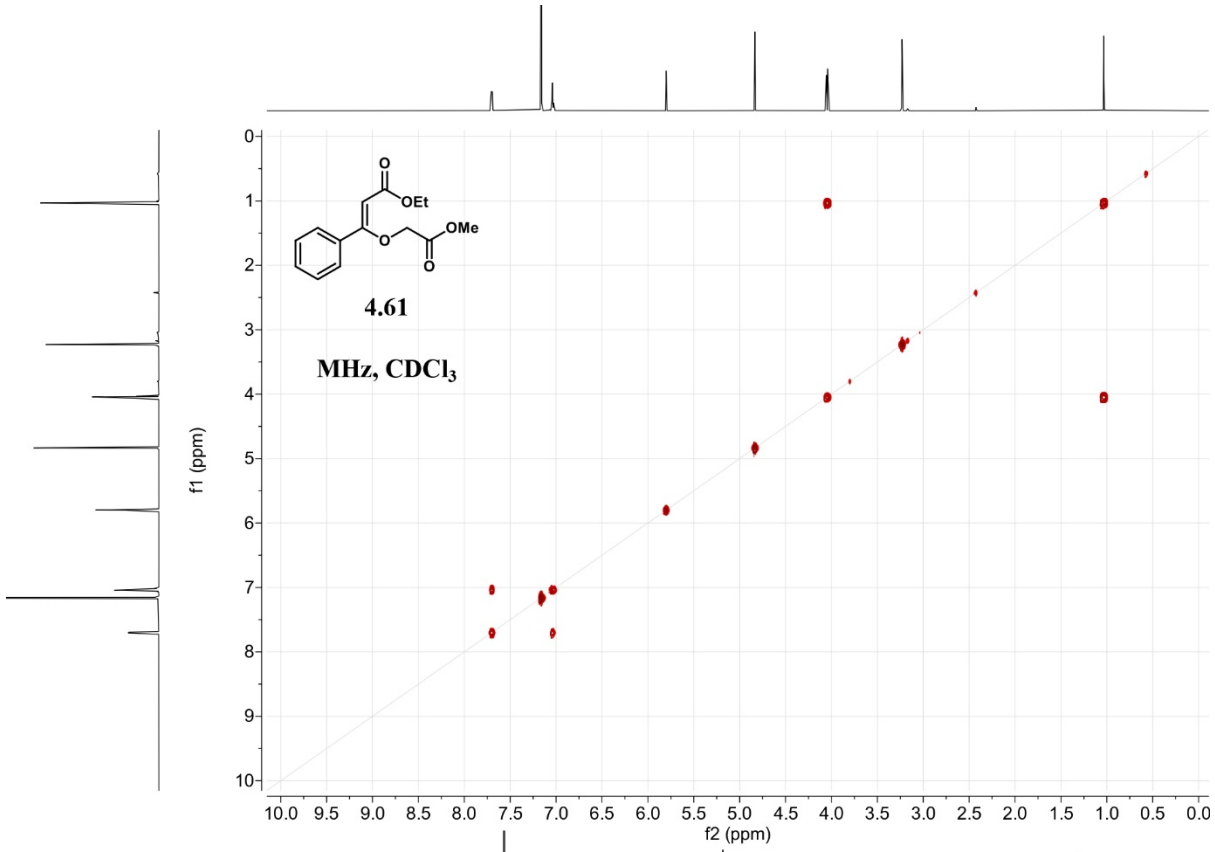
4.59

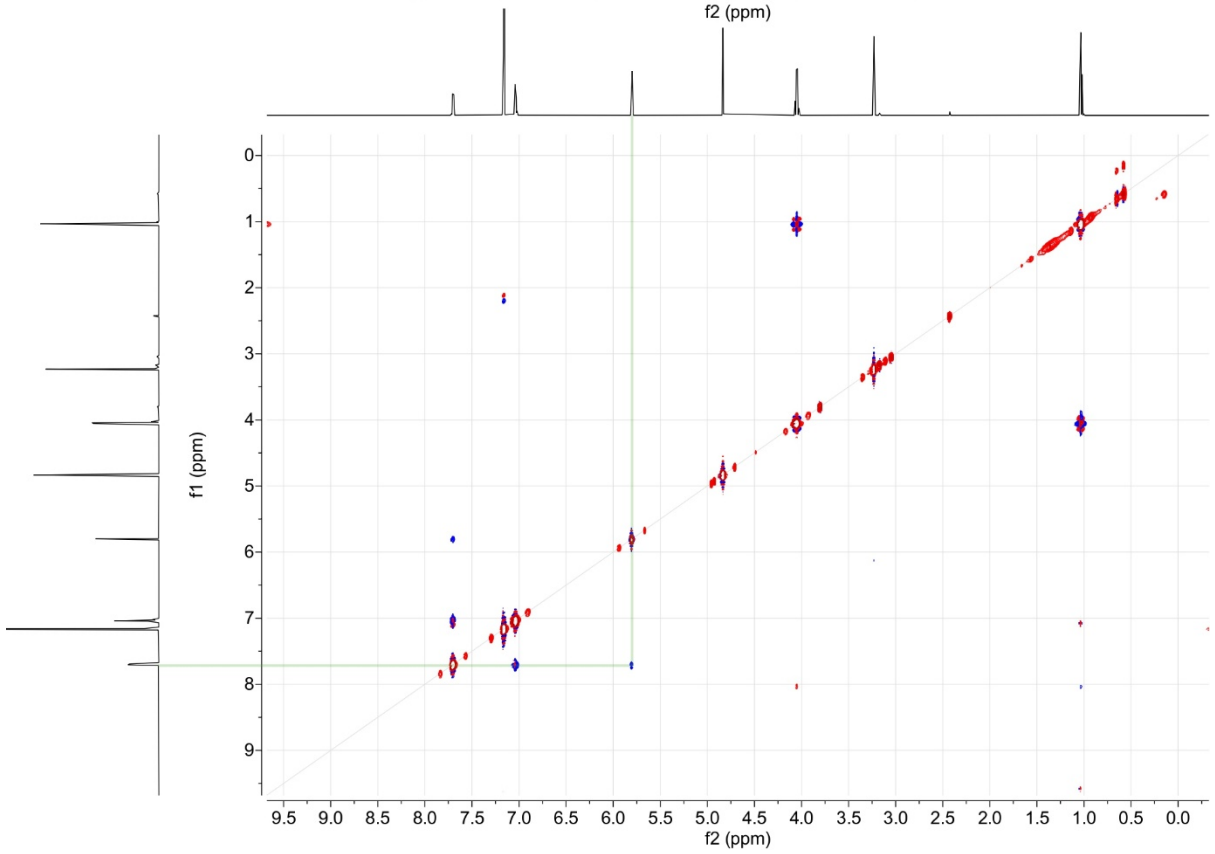
400 MHz, $CDCl_3$

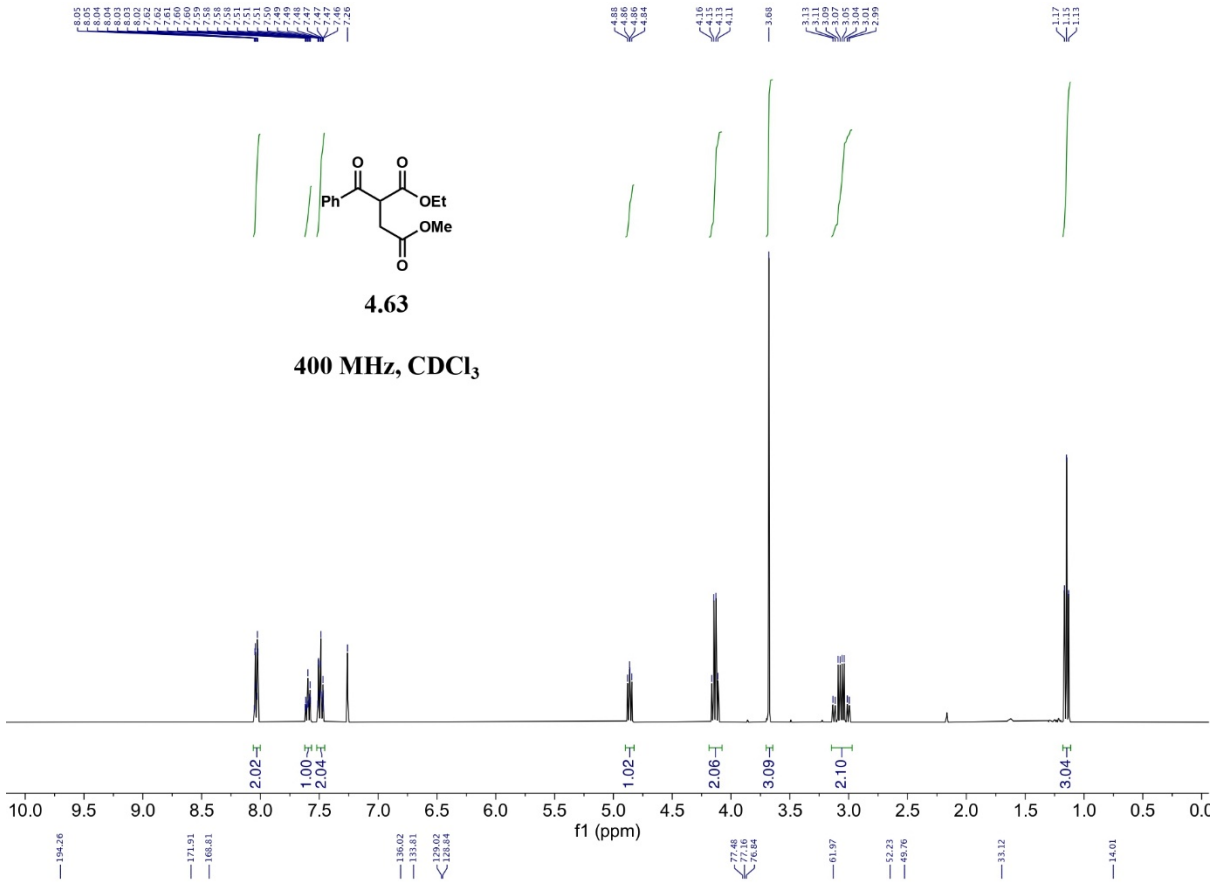

OEt
OMe
O
O
O
O
4.61
MHz, CDCl3
f1 (ppm)
f1 (ppm)


OEt
OMe
4.61
MHz, CDCl3
f1 (ppm)
f2 (ppm)


f1 (ppm)
f2 (ppm)

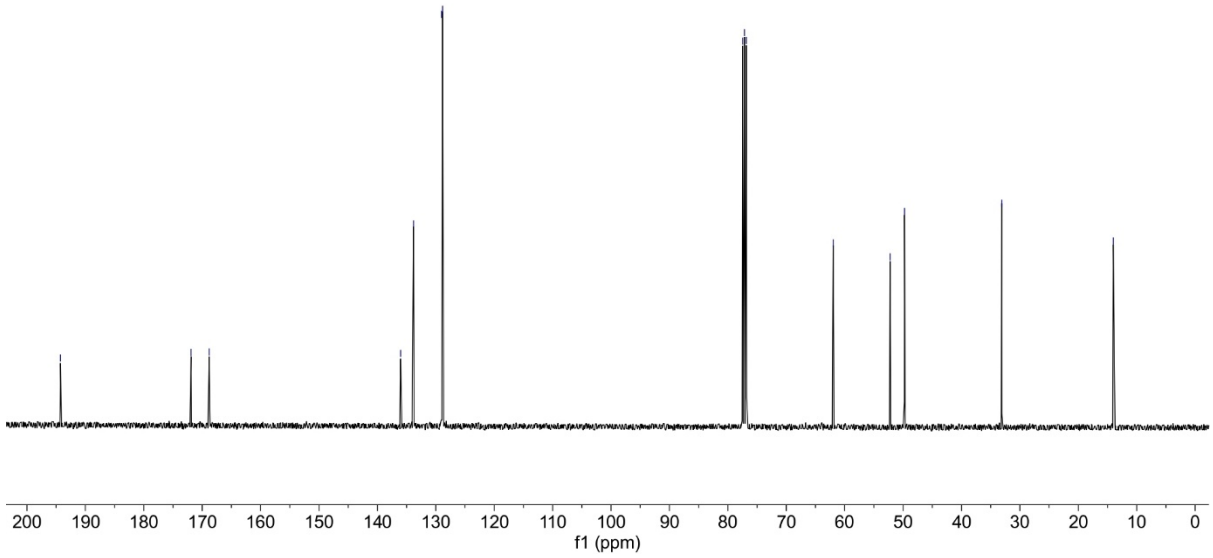

OEt
OMe
4.61
MHz, CDCl3
f1 (ppm)
f2 (ppm)

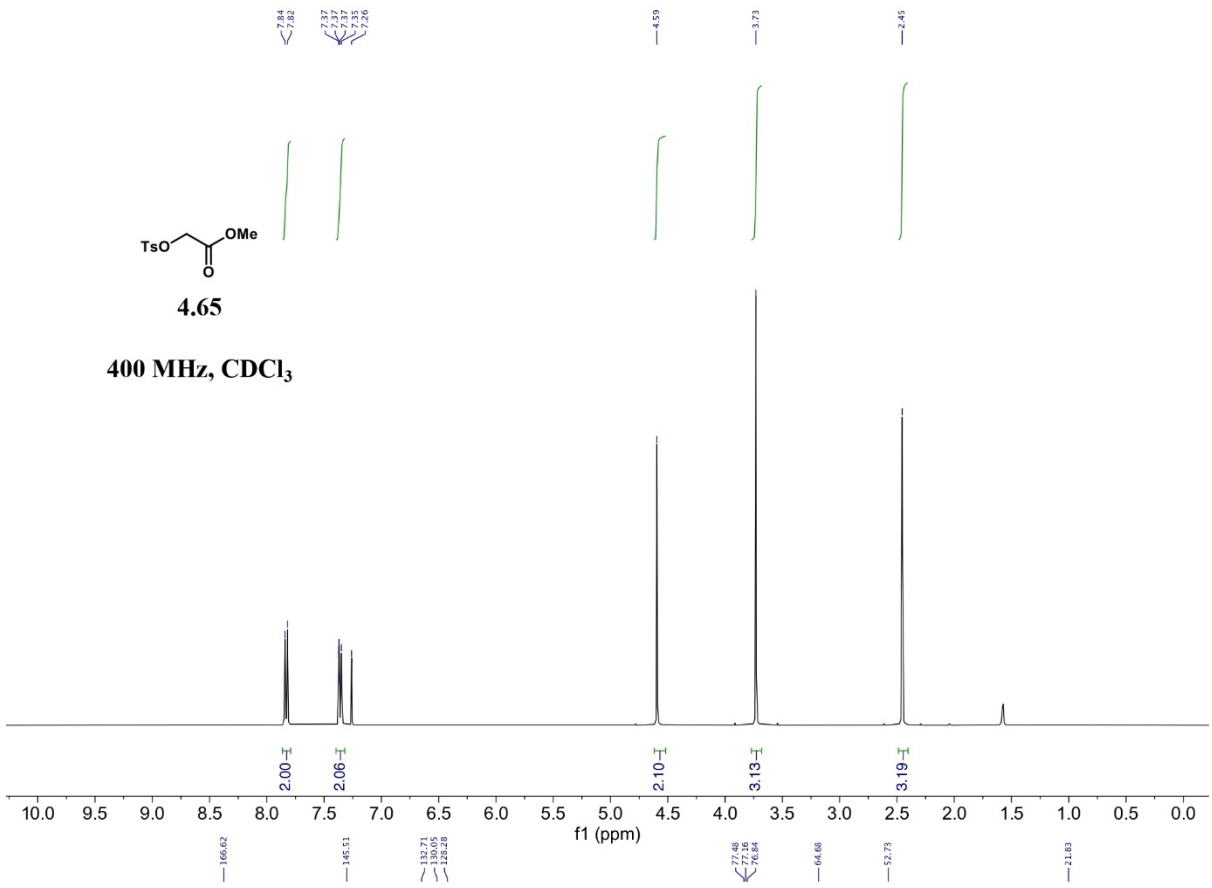

f1 (ppm)
f2 (ppm)



4.63

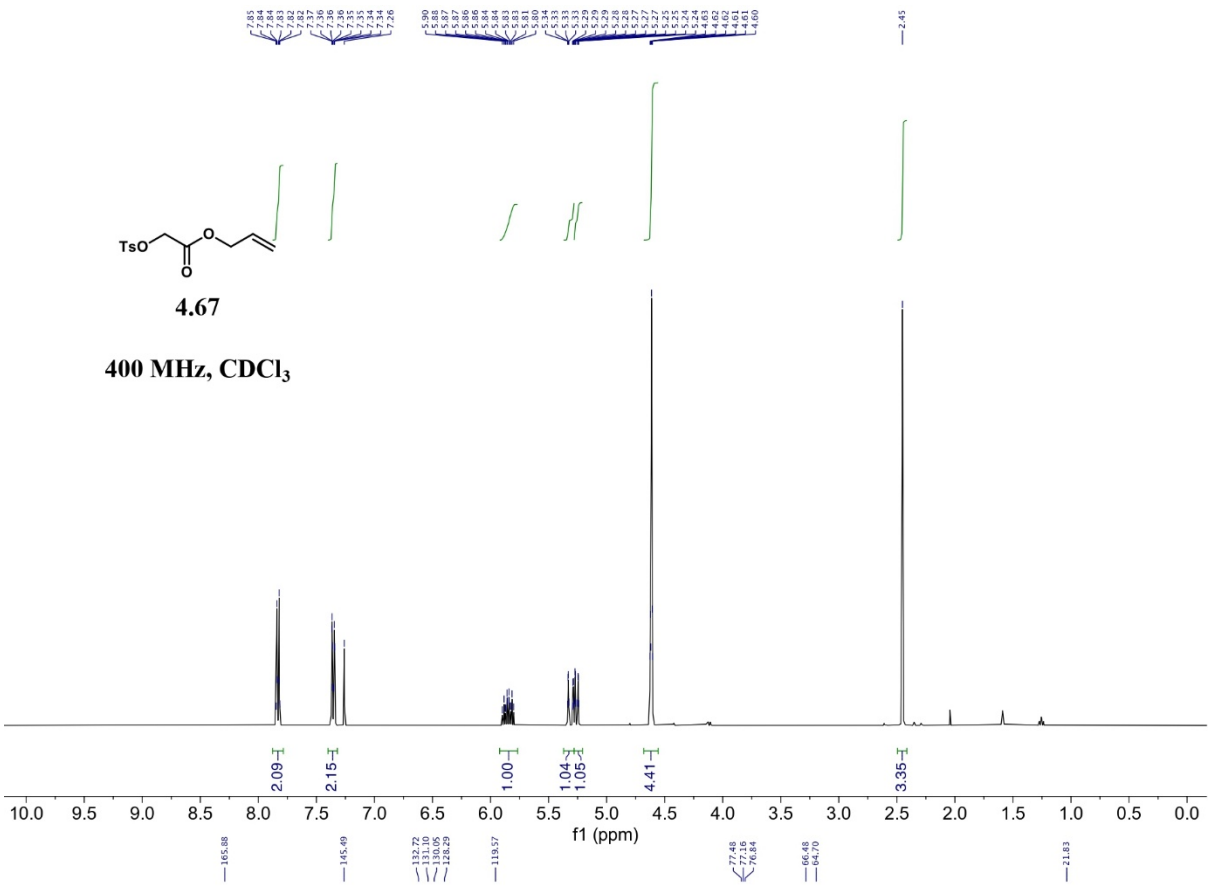
400 MHz, $CDCl_3$

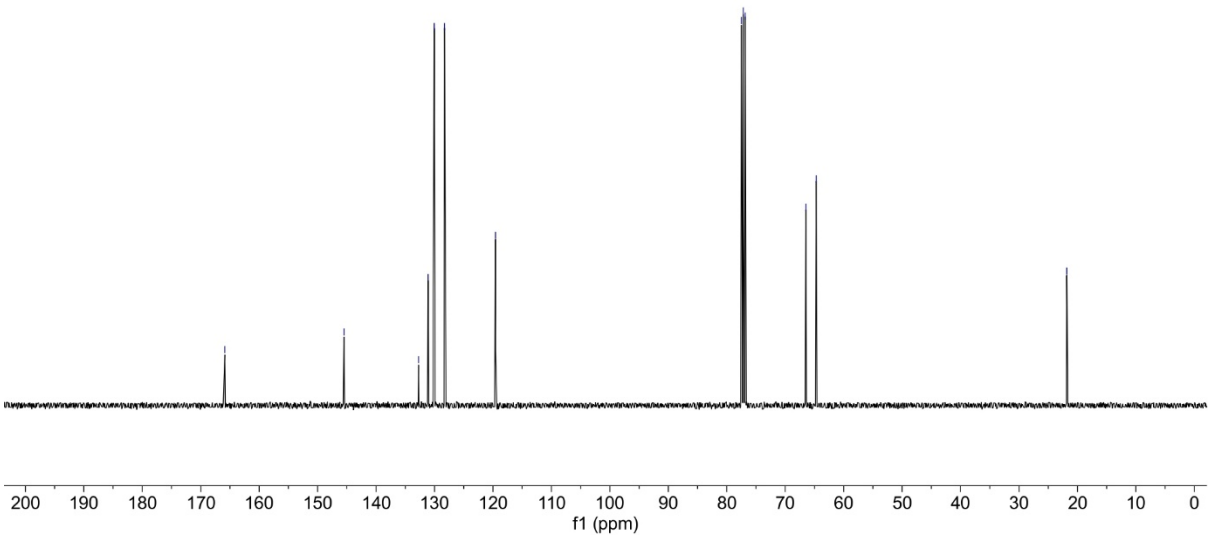


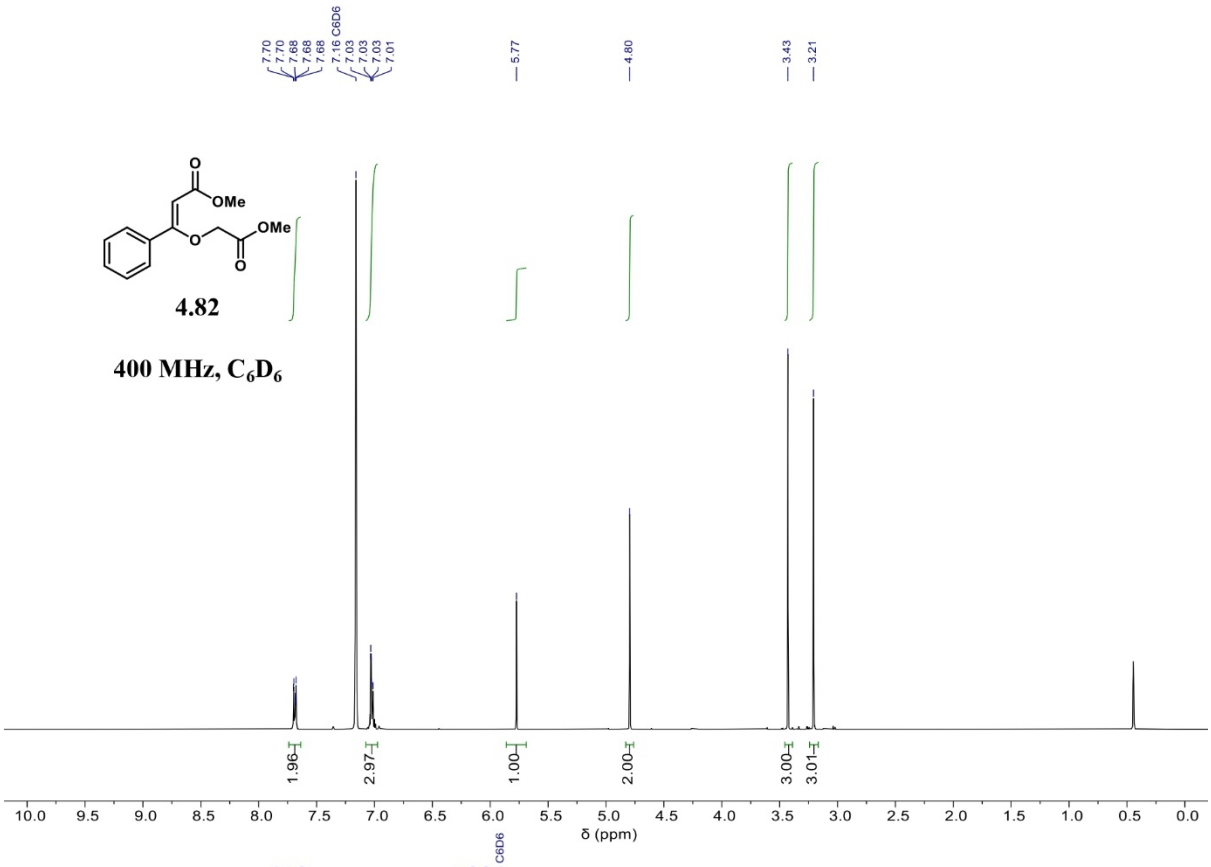


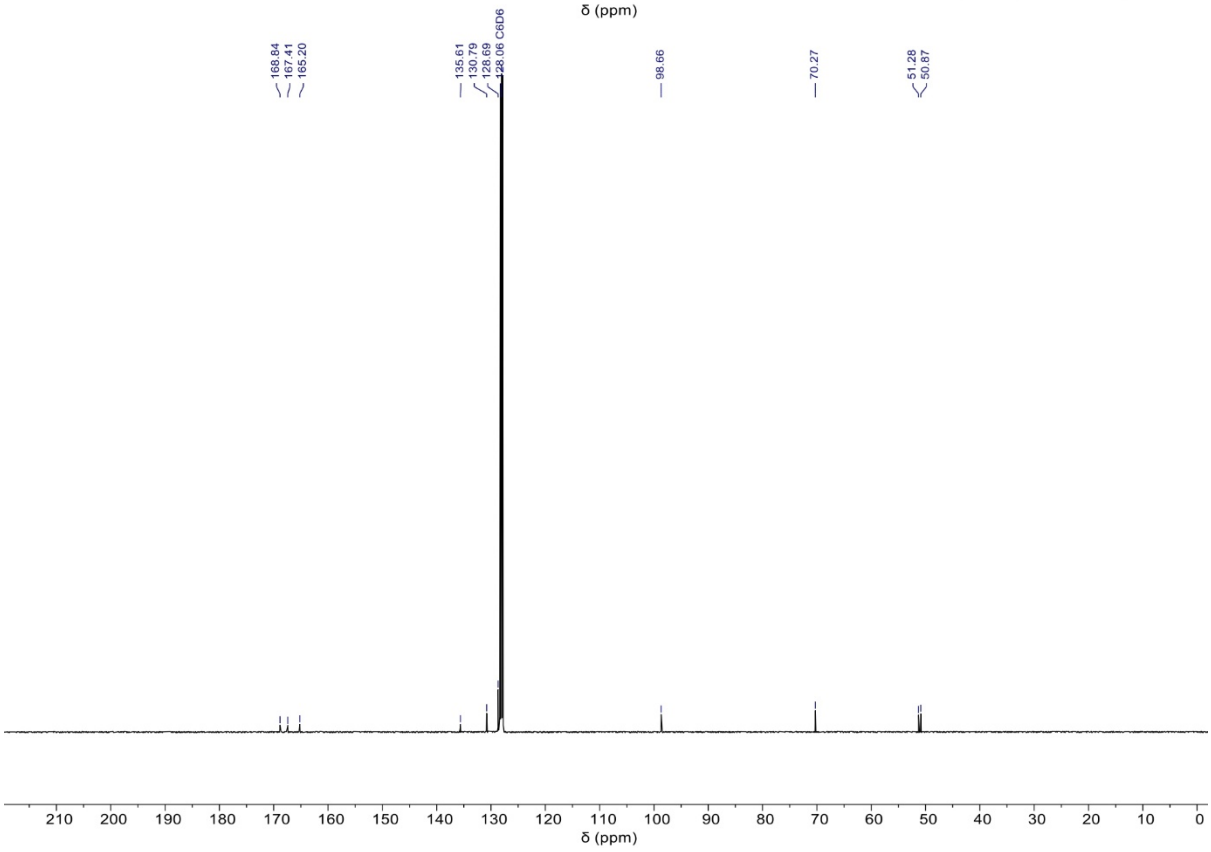
4.65

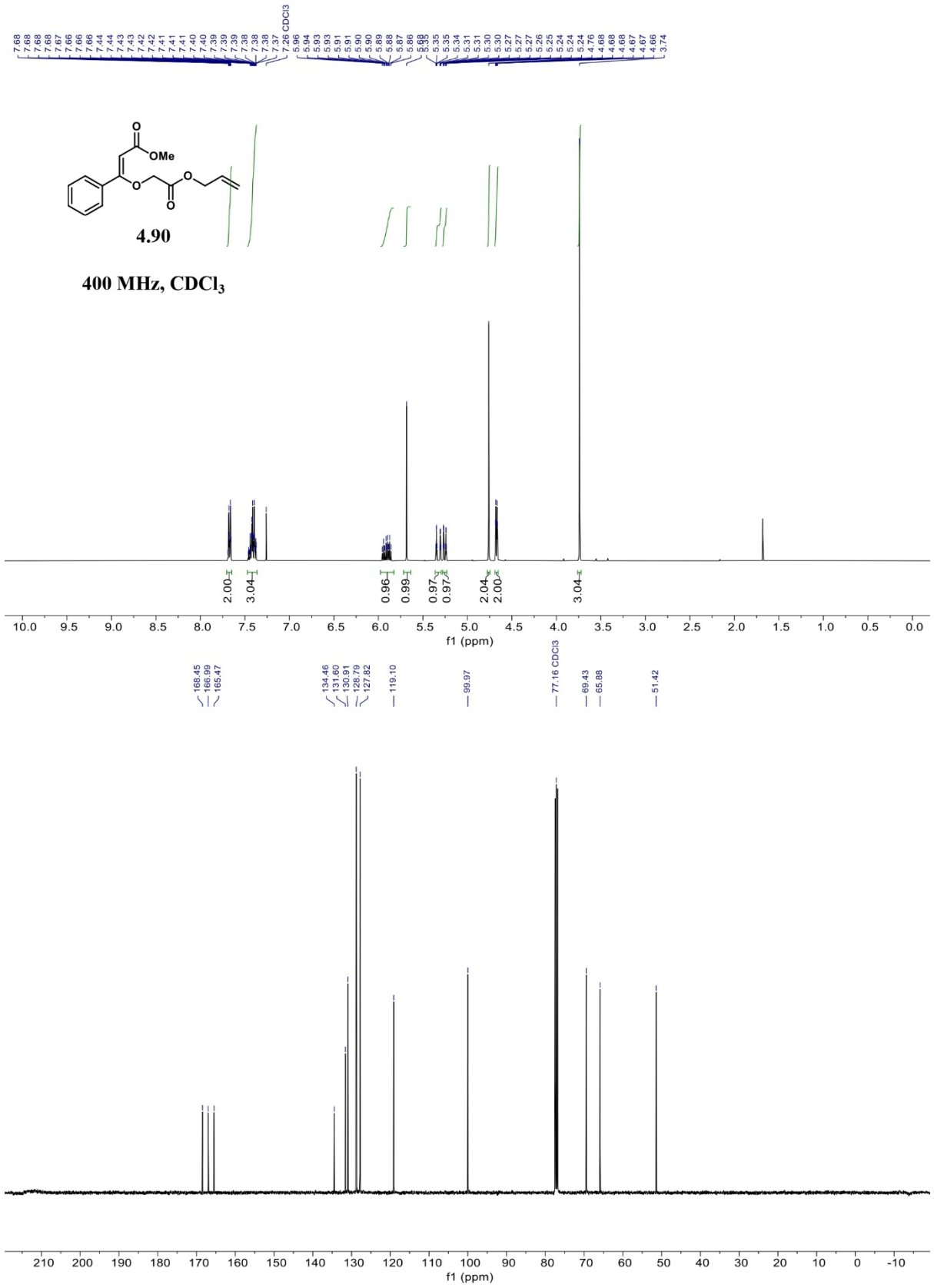
400 MHz, $CDCl_3$

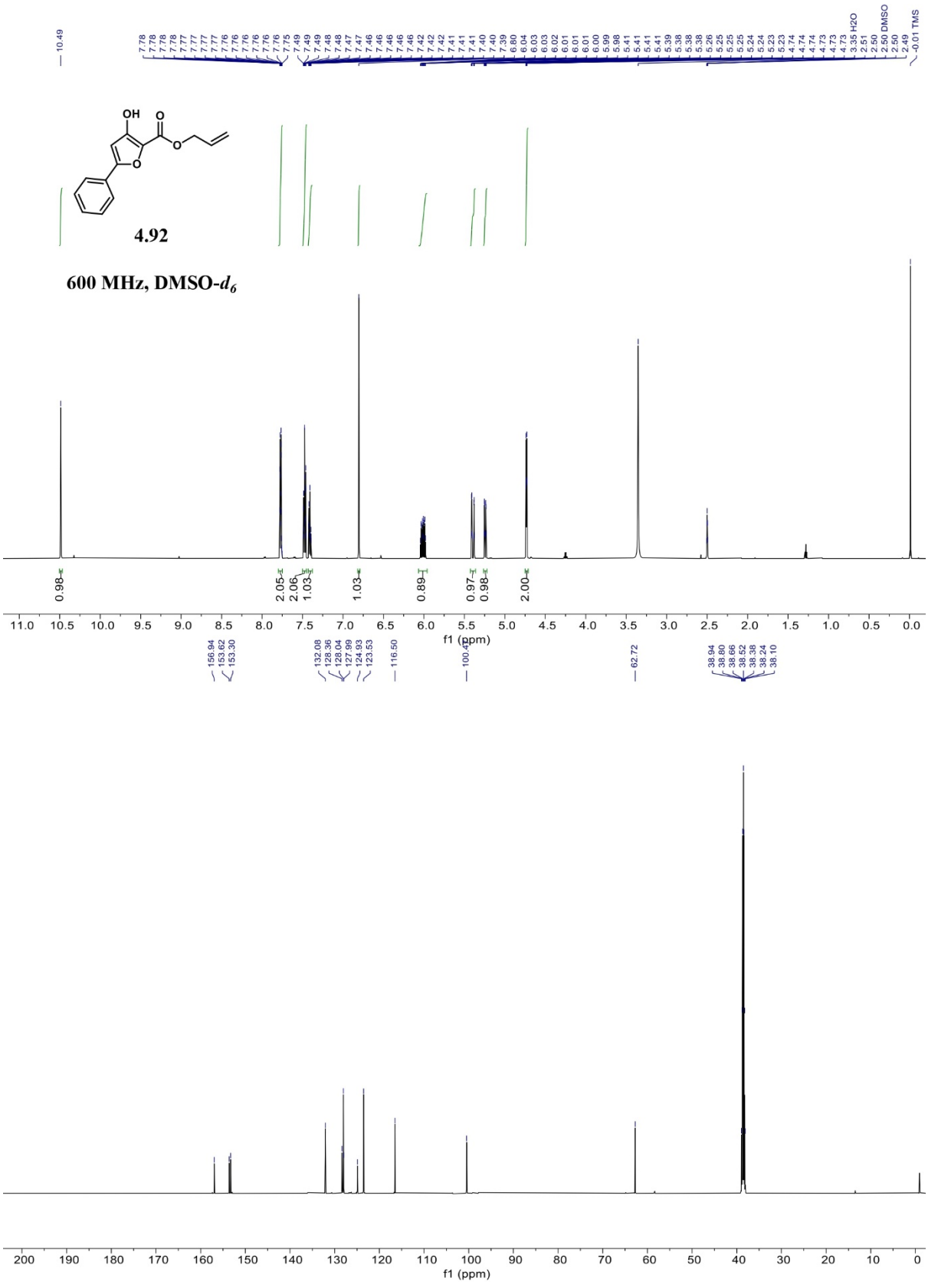

TsO
O
O
4.67
400 MHz, CDCl3
f1 (ppm)

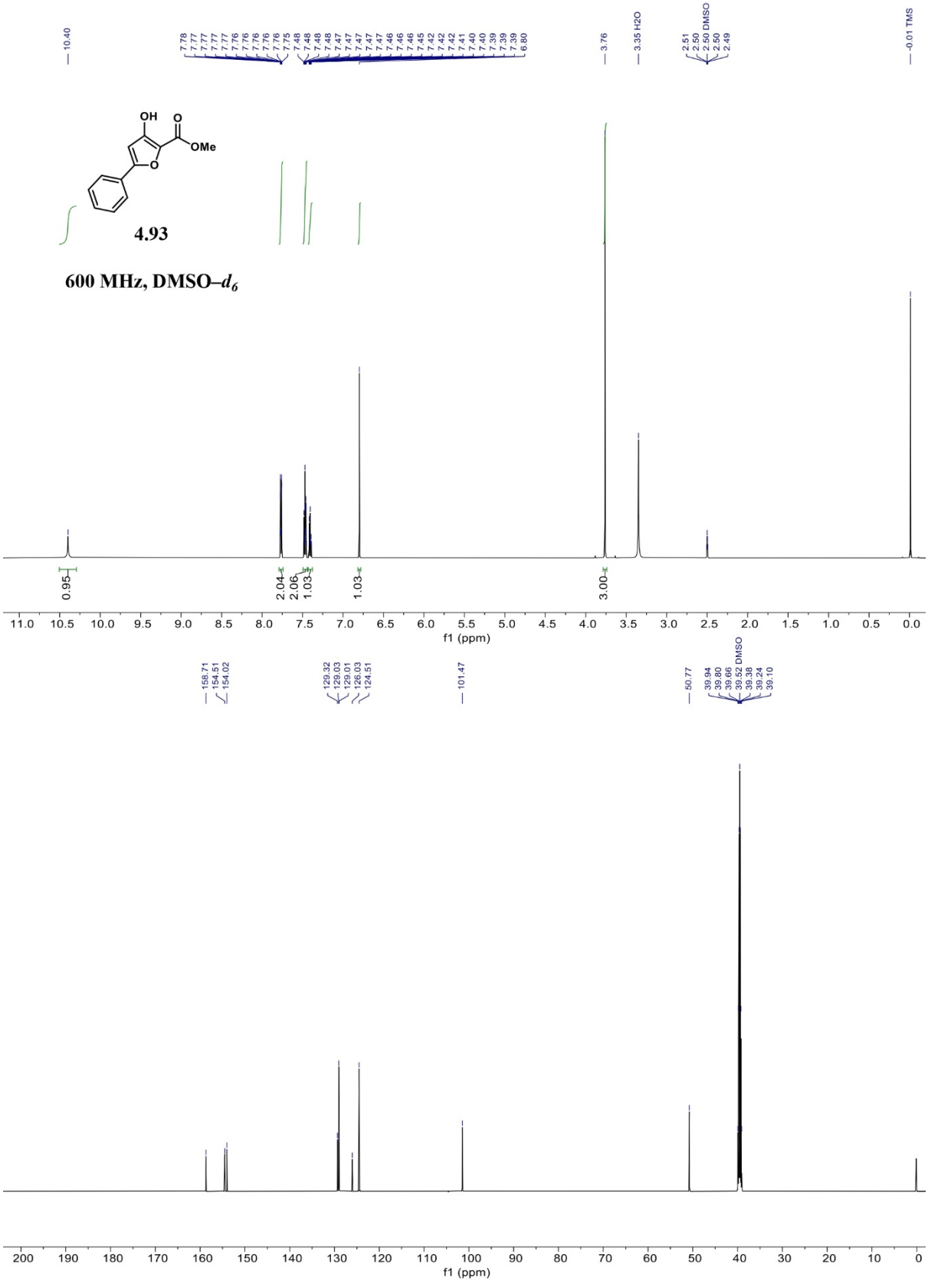

f1 (ppm)

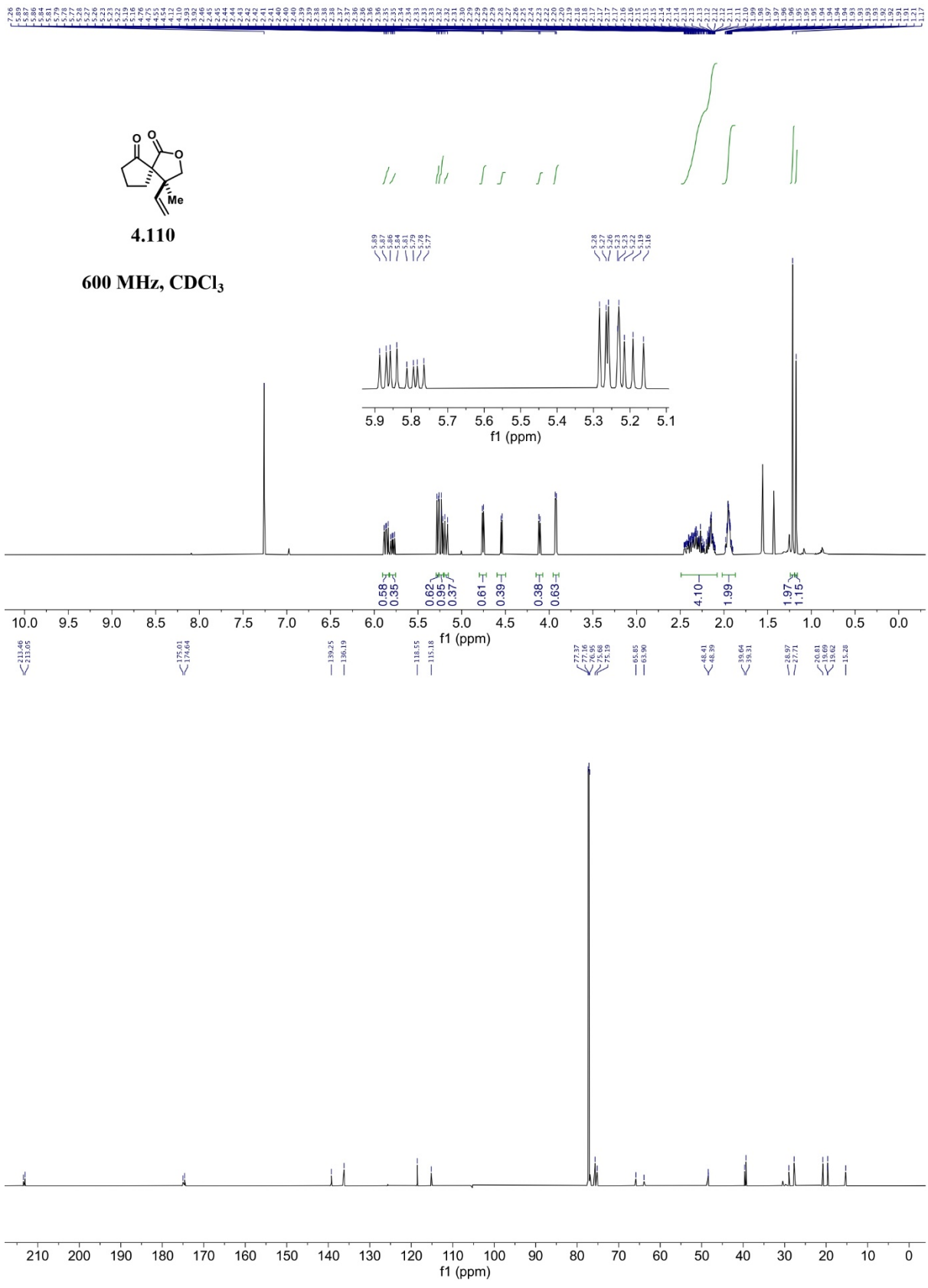

7.70
7.70
7.68
7.68
7.68
7.16 C6D6
7.03
7.03
7.03
7.01
5.77
4.80
3.43
3.21
OMe
OMe
O
O
O
O
4.82
400 MHz, C6D6
1.96
2.97
1.00
2.00
3.00
3.01
δ (ppm)

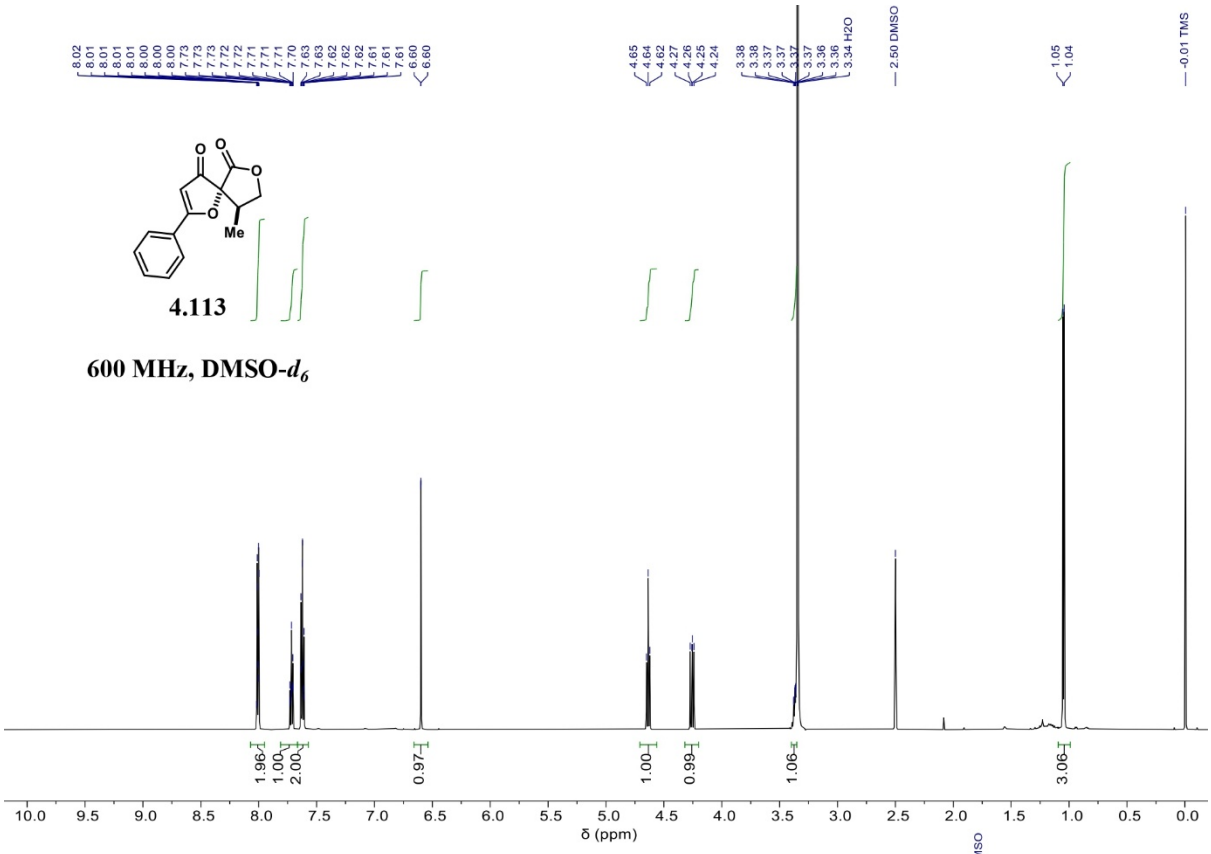

168.84
167.41
165.20
135.61
130.79
128.69
128.06 C6D6
98.66
70.27
51.28
50.87
δ (ppm)

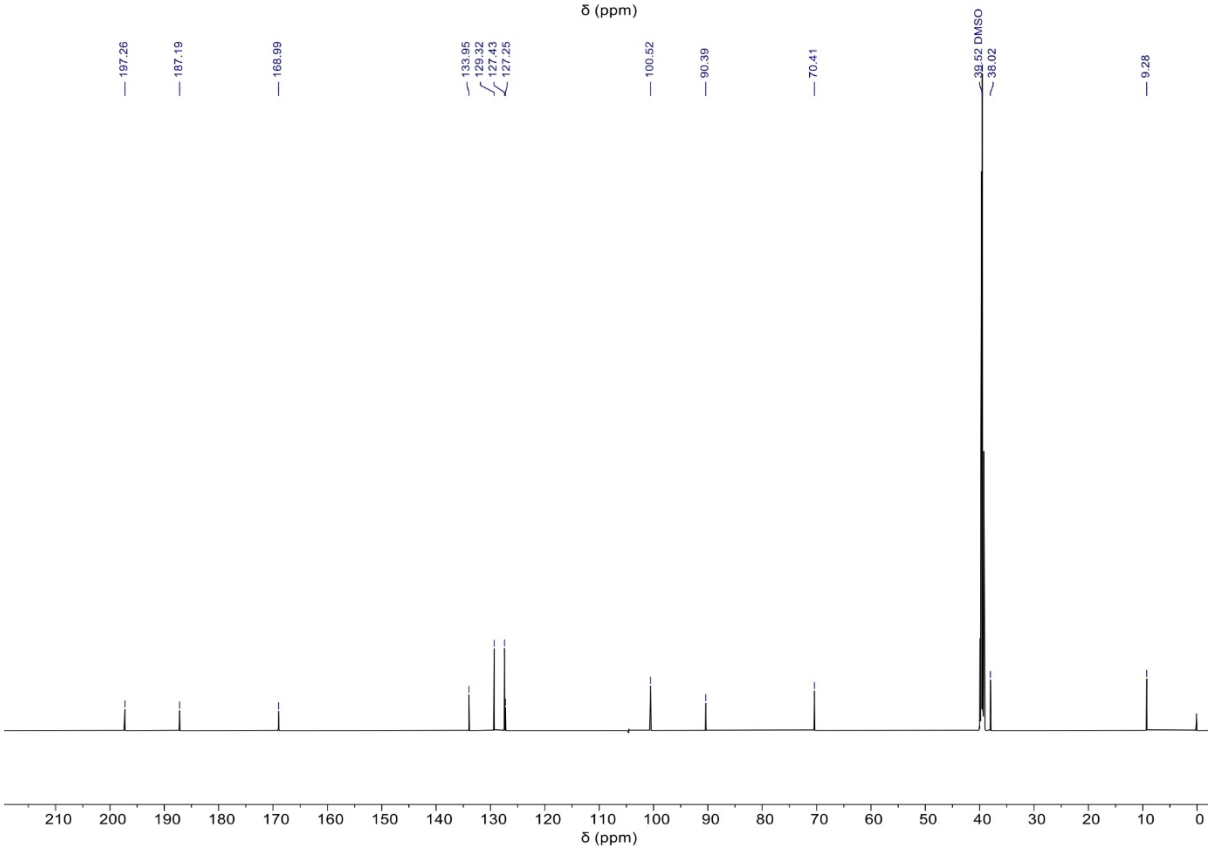

4.90
400 MHz, CDCl3
f1 (ppm)
f1 (ppm)

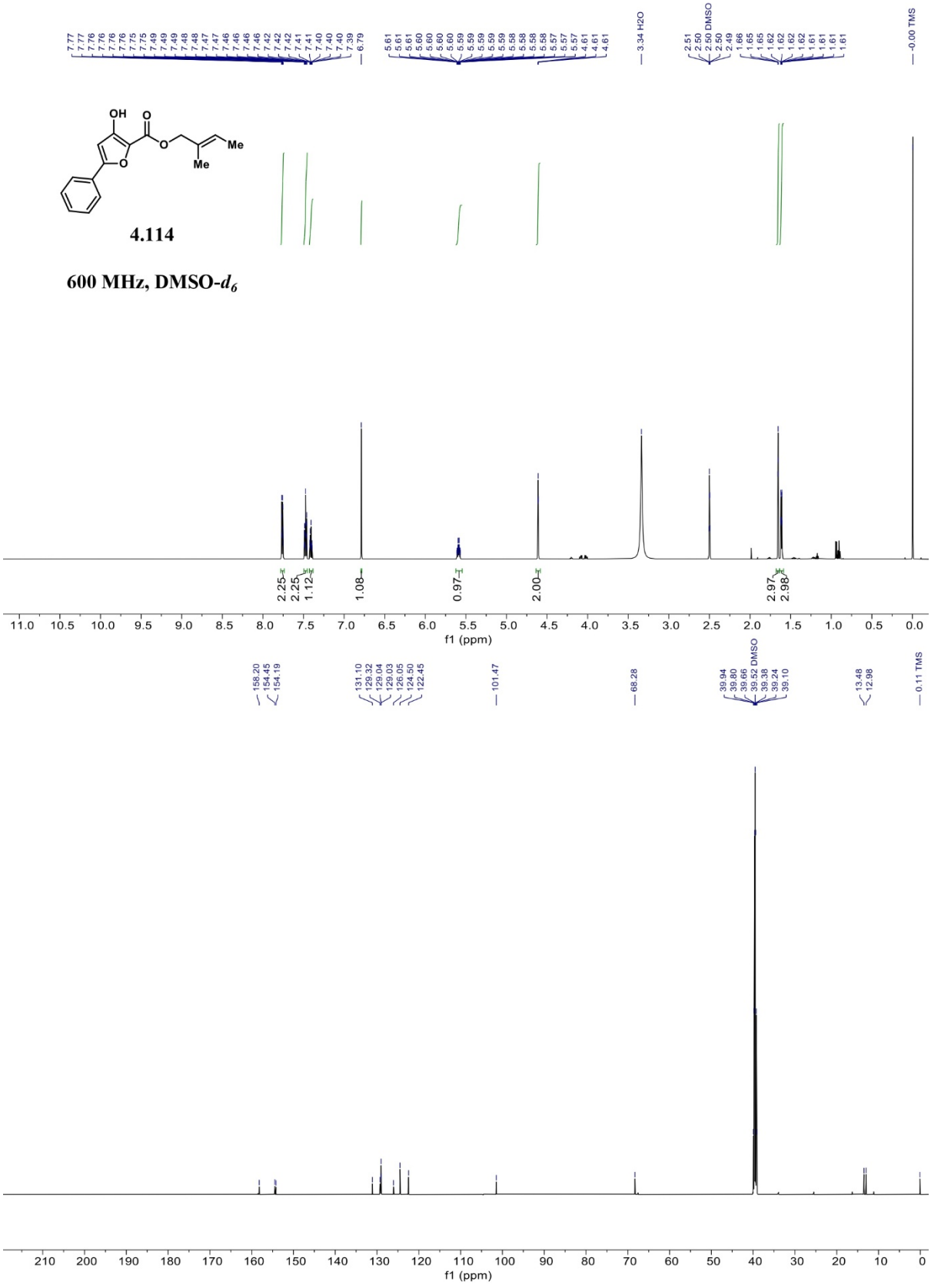

4.92
600 MHz, DMSO-d_6
f1 (ppm)
f1 (ppm)

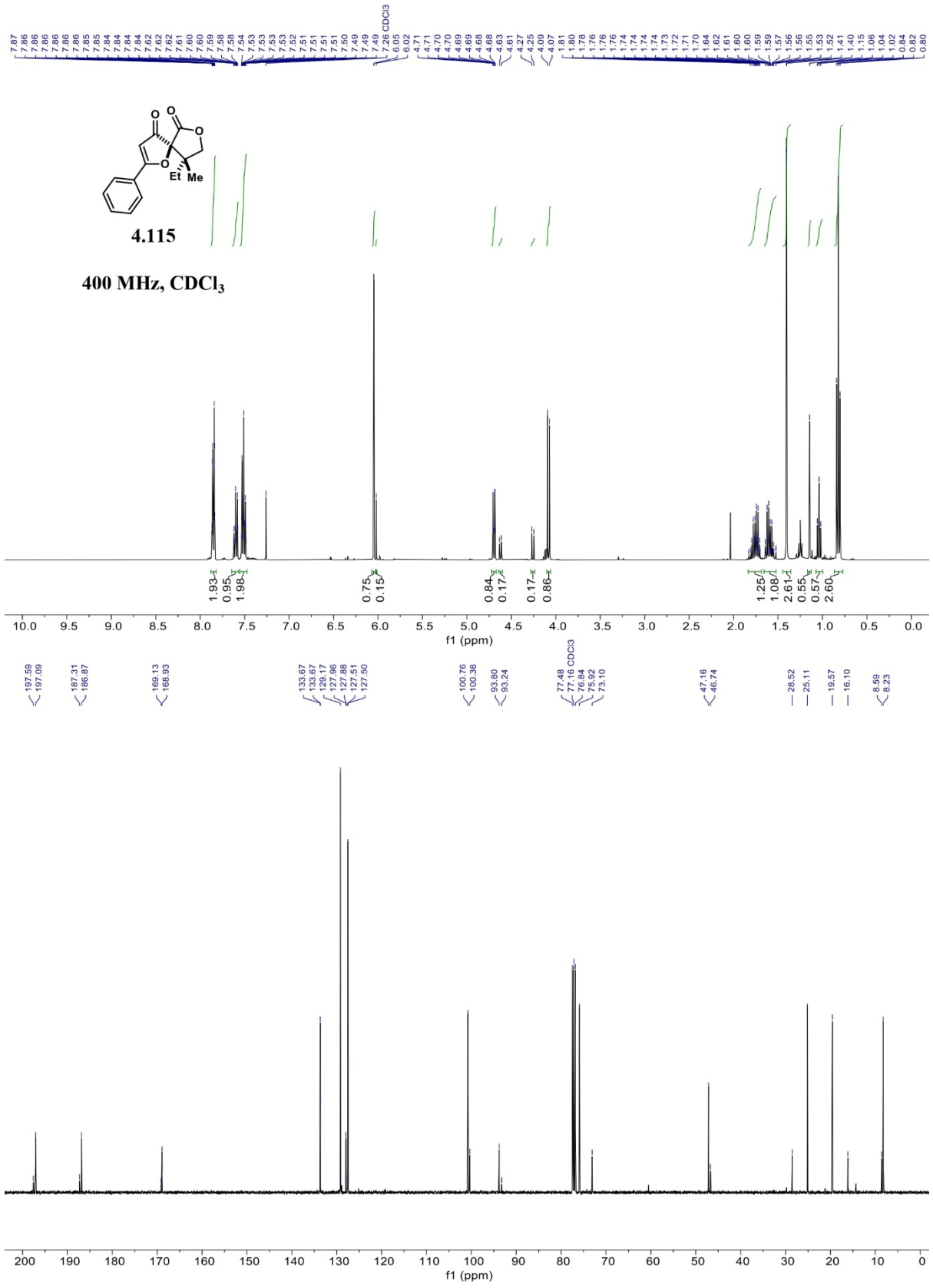

10.40
7.78
7.77
7.77
7.77
7.77
7.76
7.76
7.76
7.76
7.76
7.75
7.48
7.48
7.48
7.48
7.47
7.47
7.47
7.47
7.47
7.46
7.46
7.46
7.45
7.42
7.42
7.42
7.41
7.40
7.40
7.39
7.39
7.39
6.80
3.76
3.35 H2O
2.51
2.50
2.50 DMSO
2.50
2.49
0.01 TMS
OH
O
OMe
O
4.93
600 MHz, DMSO–d_6
0.95
2.04
2.06
1.03
1.03
3.00
11.0 10.5 10.0 9.5 9.0 8.5 8.0 7.5 7.0 6.5 6.0 5.5 5.0 4.5 4.0 3.5 3.0 2.5 2.0 1.5 1.0 0.5 0.0
f1 (ppm)
158.71
154.51
154.02
129.32
129.03
129.01
126.03
124.51
101.47
50.77
39.94
39.80
39.66
39.52 DMSO
39.38
39.24
39.10
200 190 180 170 160 150 140 130 120 110 100 90 80 70 60 50 40 30 20 10 0
f1 (ppm)

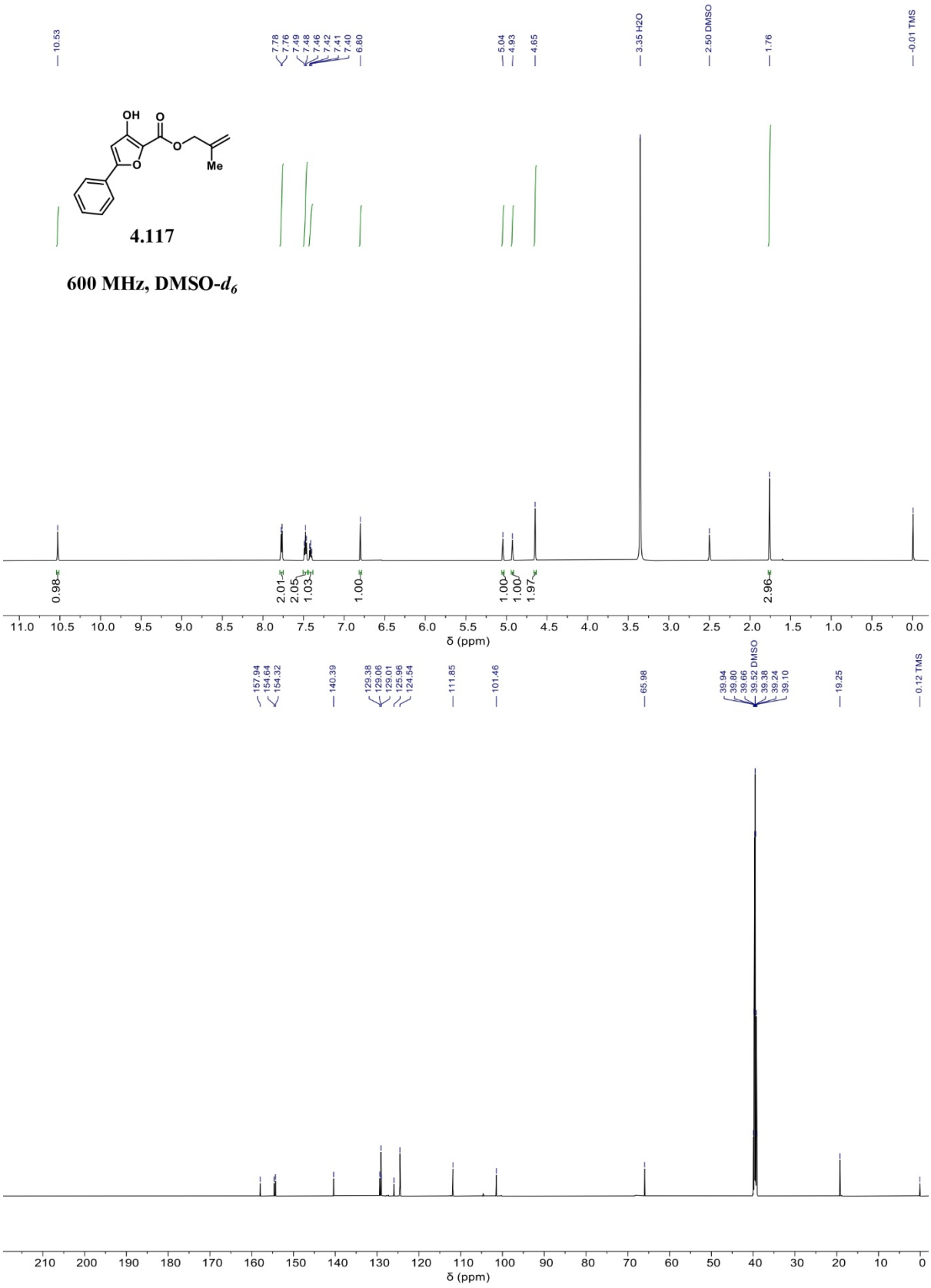

Me
4.110
600 MHz, CDCl3
f1 (ppm)


8.02
8.01
8.01
8.01
8.01
8.00
8.00
8.00
7.73
7.73
7.73
7.72
7.72
7.71
7.71
7.71
7.70
7.63
7.63
7.62
7.62
7.62
7.61
7.61
7.61
6.60
6.60
4.65
4.64
4.62
4.27
4.26
4.25
4.24
3.38
3.38
3.37
3.37
3.37
3.37
3.36
3.34 H2O
2.50 DMSO
1.05
1.04
0.01 TMS
O
O
O
O
O
Me
4.113
600 MHz, DMSO-d_6
1.96
1.00
2.00
0.97
1.00
0.99
1.06
3.06
10.0 9.5 9.0 8.5 8.0 7.5 7.0 6.5 6.0 5.5 5.0 4.5 4.0 3.5 3.0 2.5 2.0 1.5 1.0 0.5 0.0
δ (ppm)


197.26
187.19
168.99
133.95
129.32
127.43
127.25
100.52
90.39
70.41
39.52 DMSO
38.02
9.28
210 200 190 180 170 160 150 140 130 120 110 100 90 80 70 60 50 40 30 20 10 0
δ (ppm)

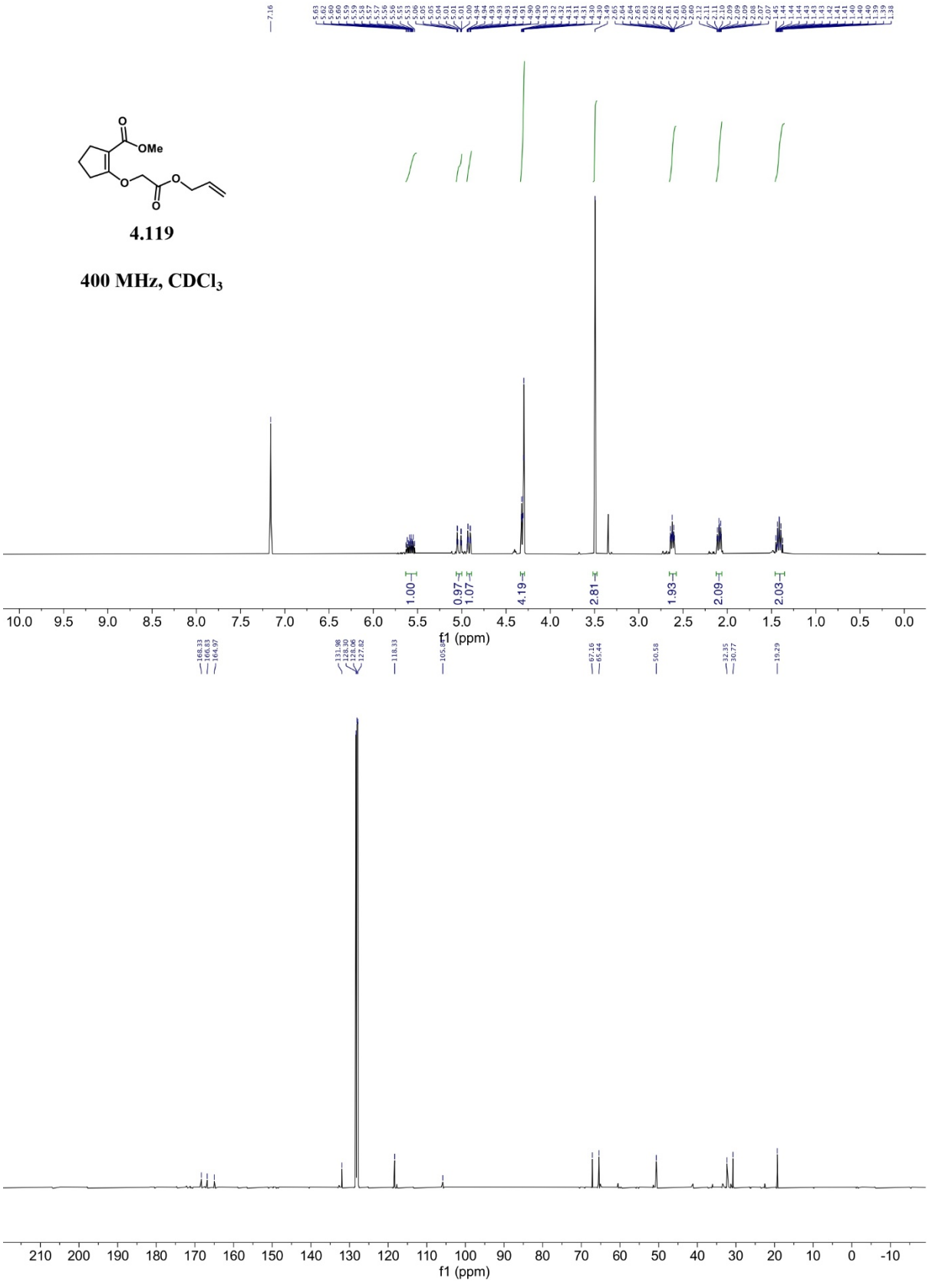

OH
O
O
O
Me
Me
4.114
600 MHz, DMSO-d_6
f1 (ppm)
f1 (ppm)

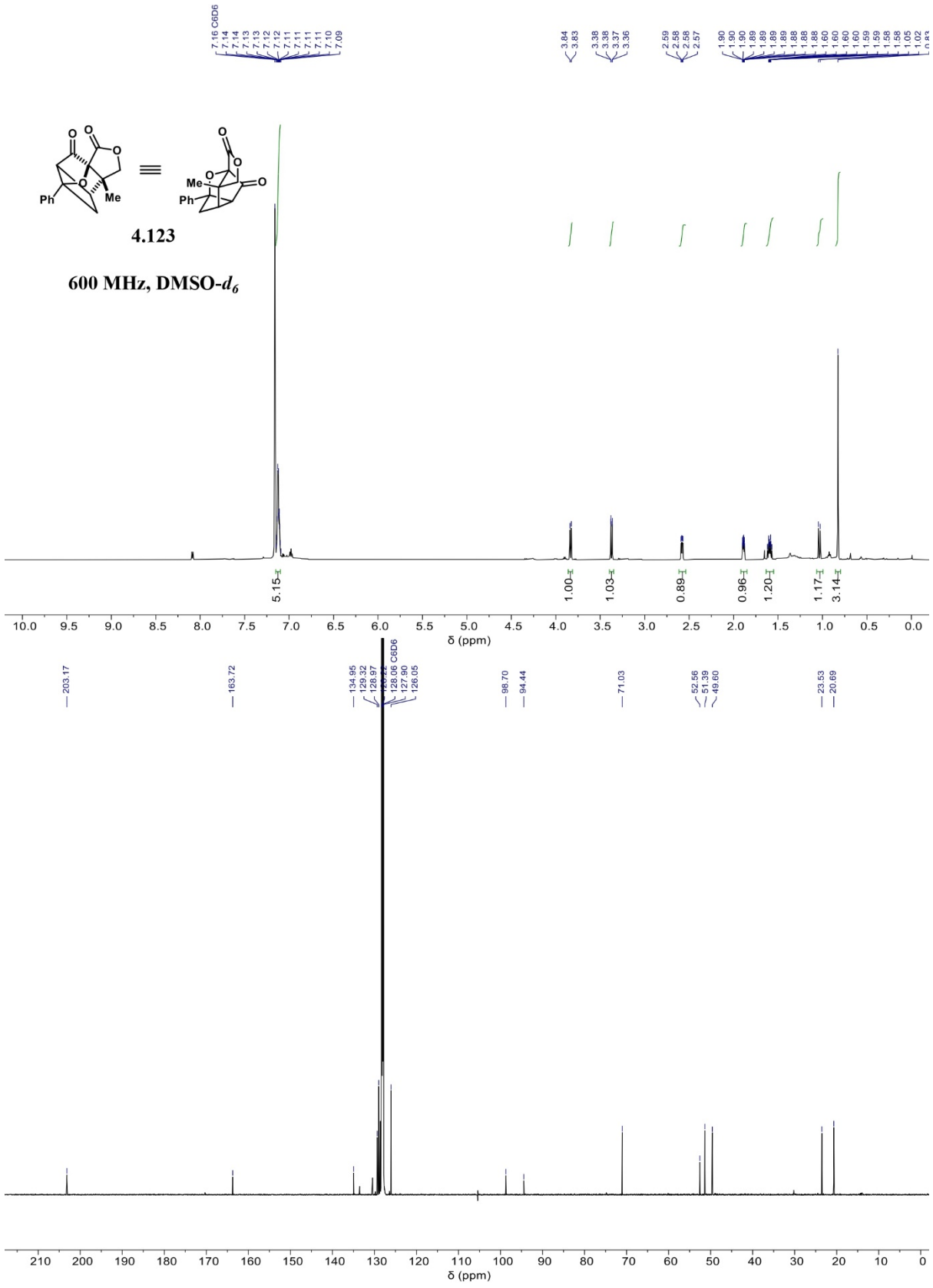

4.115
400 MHz, CDCl3
f1 (ppm)
f1 (ppm)

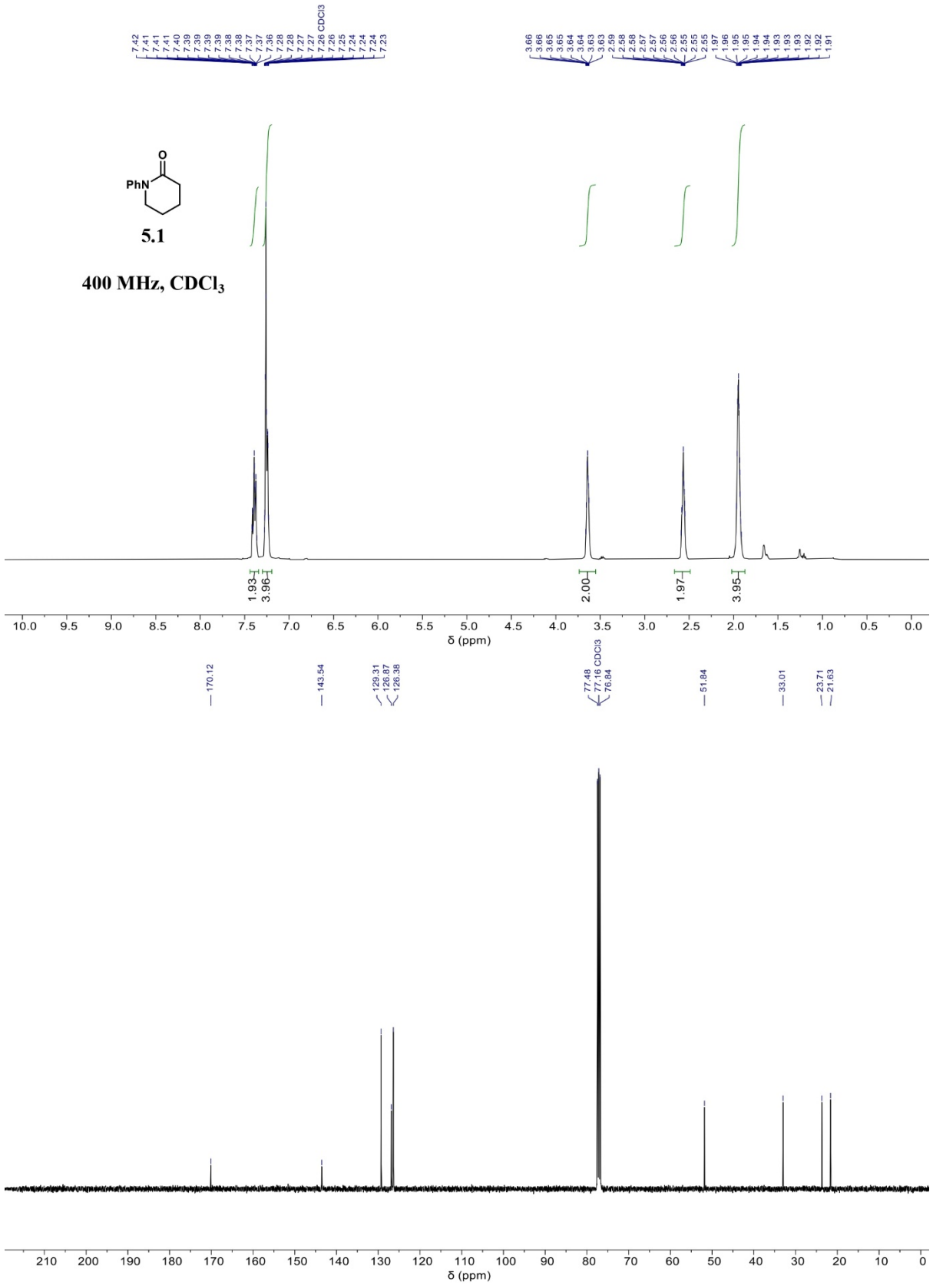

10.53
7.78
7.76
7.49
7.48
7.46
7.42
7.41
7.40
6.80
5.04
4.93
4.65
3.35 H2O
2.50 DMSO
1.76
-0.01 TMS
OH
O
O
O
Me
4.117
600 MHz, DMSO-d_6
0.98
2.01
2.05
1.03
1.00
1.00
1.00
1.97
2.96
δ (ppm)
157.94
154.64
154.32
140.39
129.38
129.06
129.01
125.96
124.54
111.85
101.46
65.98
39.94
39.80
39.66
39.52 DMSO
39.38
39.24
39.10
19.25
0.12 TMS
δ (ppm)

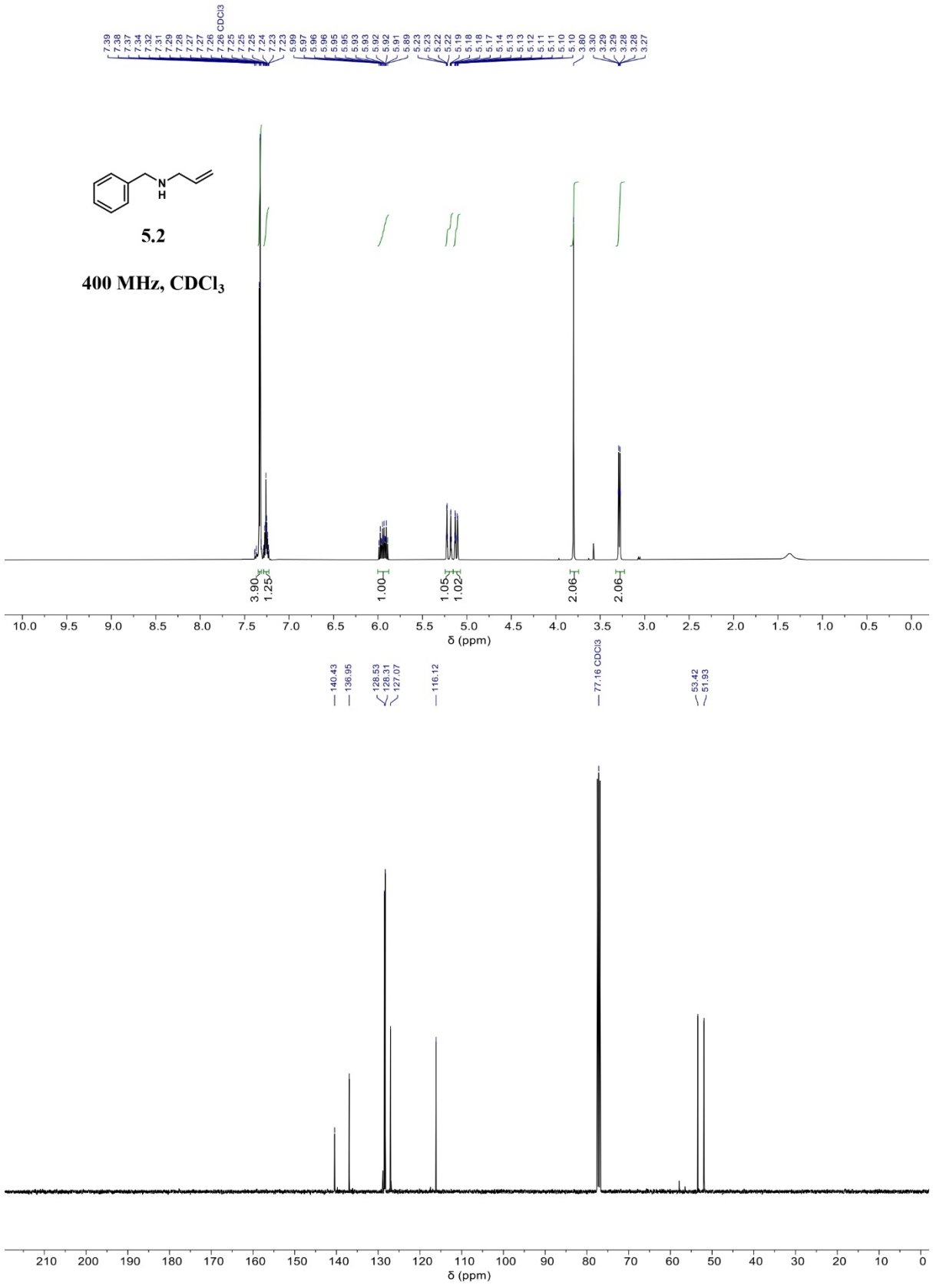
4.119

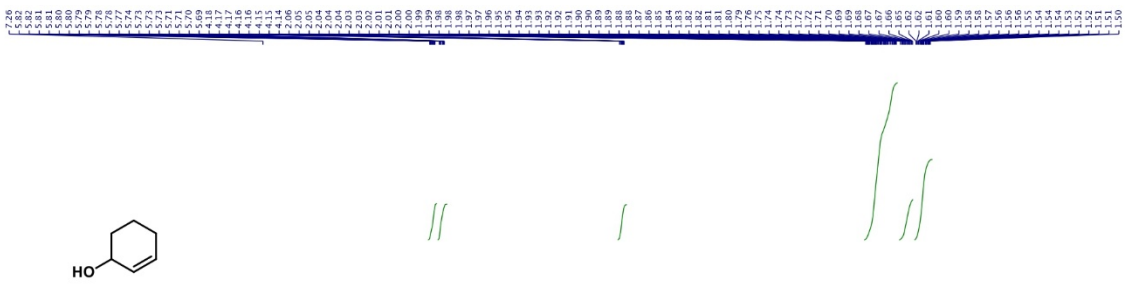
400 MHz, $CDCl_3$




4.123
600 MHz, DMSO-d_6
δ (ppm)
δ (ppm)

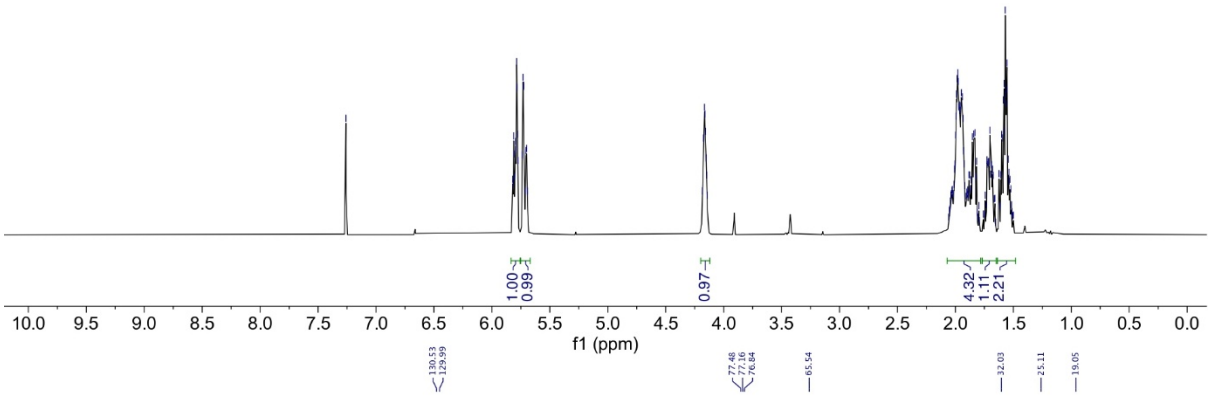

7.42
7.41
7.41
7.41
7.40
7.39
7.39
7.39
7.38
7.38
7.37
7.37
7.36
7.28
7.27
7.27
7.26 CDCl3
7.26
7.25
7.24
7.24
7.23
3.66
3.66
3.65
3.65
3.64
3.64
3.63
3.63
2.59
2.58
2.58
2.57
2.57
2.56
2.56
2.55
2.55
2.55
1.97
1.96
1.95
1.95
1.94
1.94
1.93
1.93
1.93
1.92
1.92
1.91
O
PhN
5.1
400 MHz, CDCl3
1.93
3.96
2.00
1.97
3.95
δ (ppm)
170.12
143.54
129.31
126.87
126.38
77.48
77.16 CDCl3
76.84
51.84
33.01
23.71
21.63
δ (ppm)

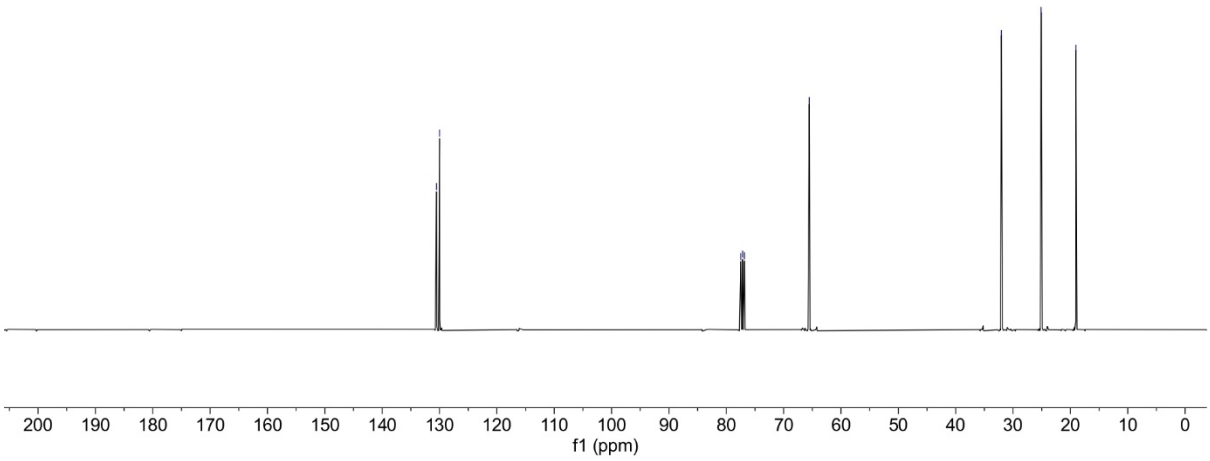

7.39 7.38 7.37 7.34 7.32 7.31 7.29 7.28 7.27 7.27 7.26 CDCl3 7.26 7.25 7.25 7.24 7.23 7.23 5.99 5.97 5.96 5.96 5.95 5.95 5.93 5.93 5.92 5.92 5.91 5.89 5.23 5.23 5.22 5.22 5.19 5.18 5.18 5.17 5.14 5.13 5.13 5.12 5.11 5.11 5.10 5.10 3.30 3.30 3.29 3.29 3.28 3.28 3.27
N
H
5.2
400 MHz, CDCl3
3.90
1.25
1.00
1.05
1.02
2.06
2.06
δ (ppm)
140.43
136.95
128.53
128.31
127.07
116.12
77.16 CDCl3
53.42
51.93
δ (ppm)

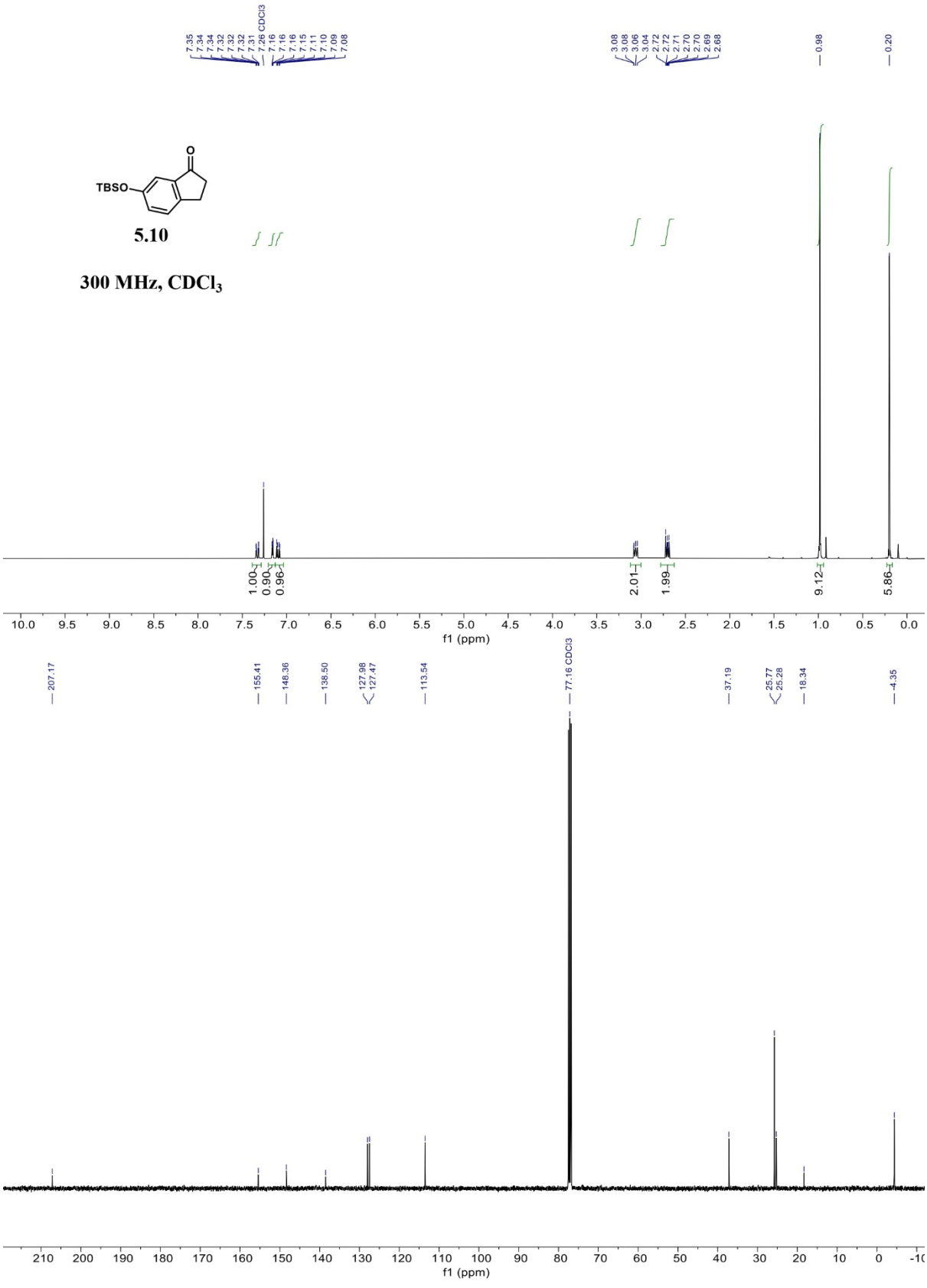


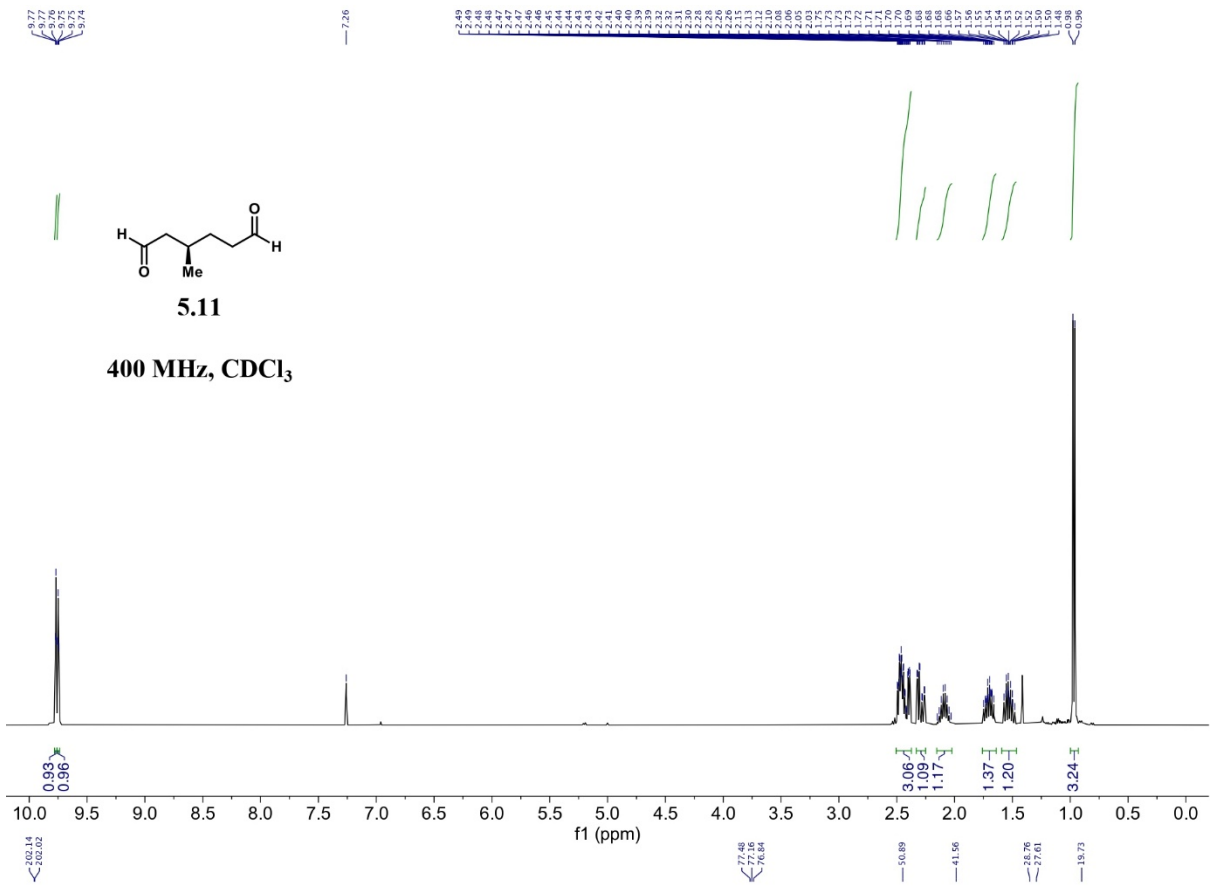
5.3

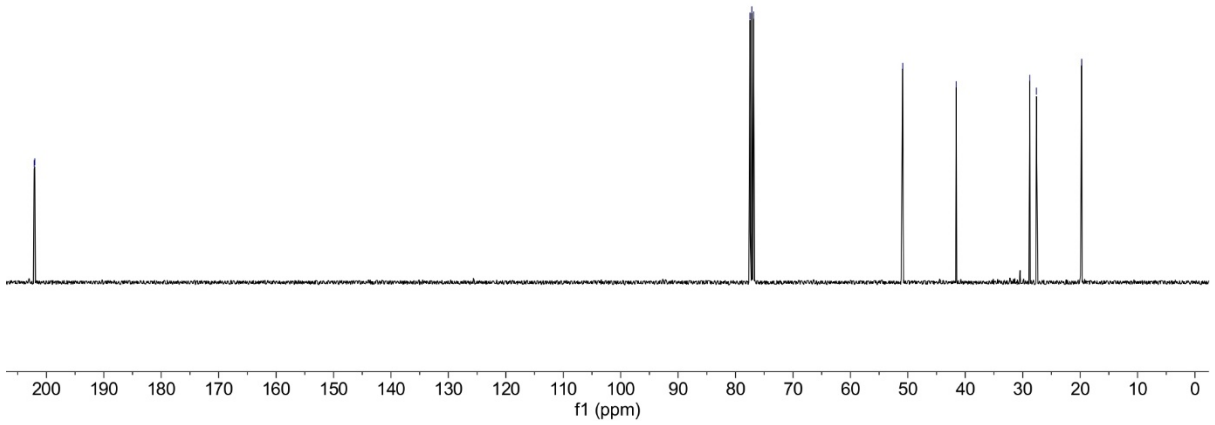
400 MHz, $CDCl_3$

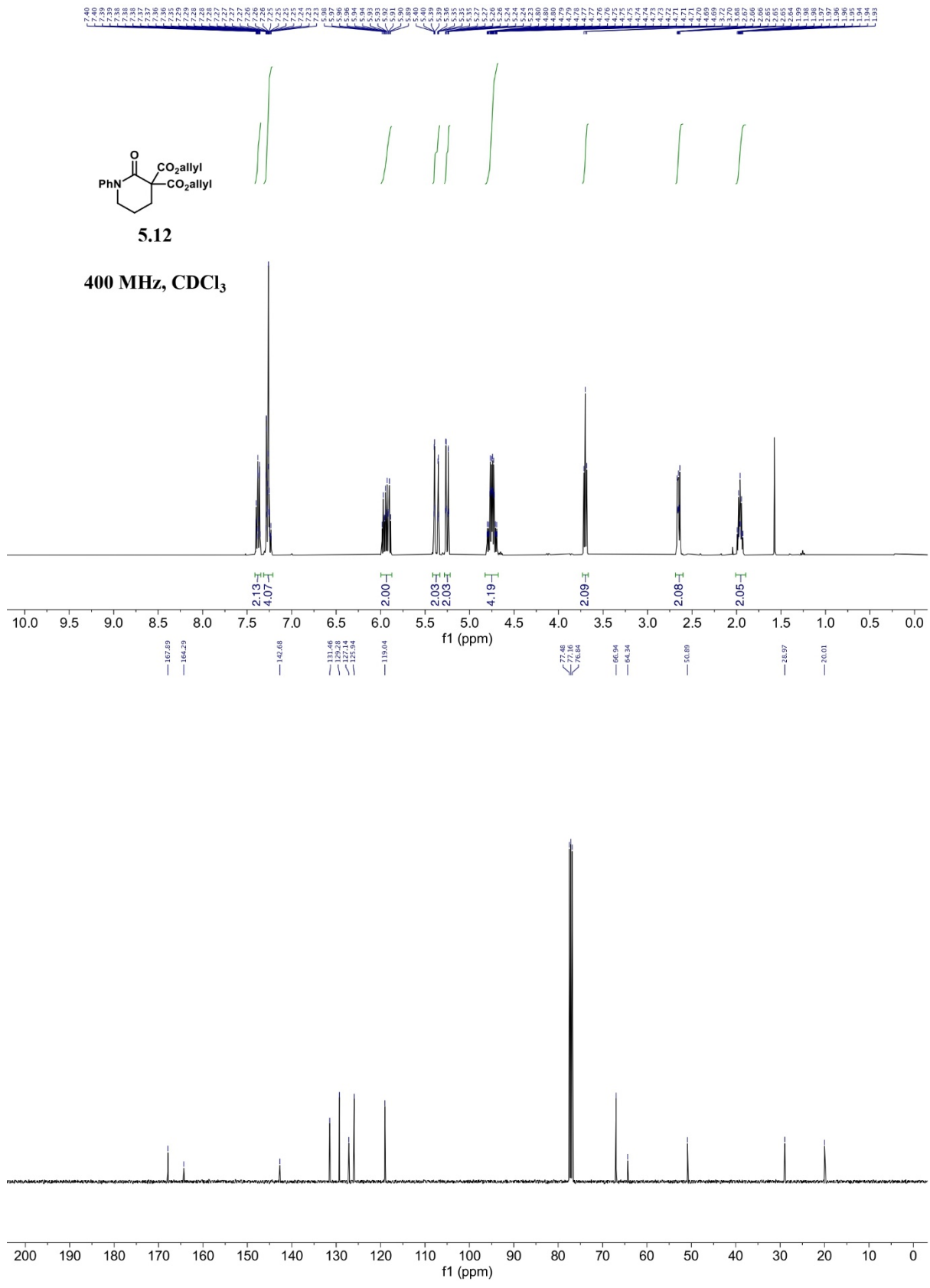


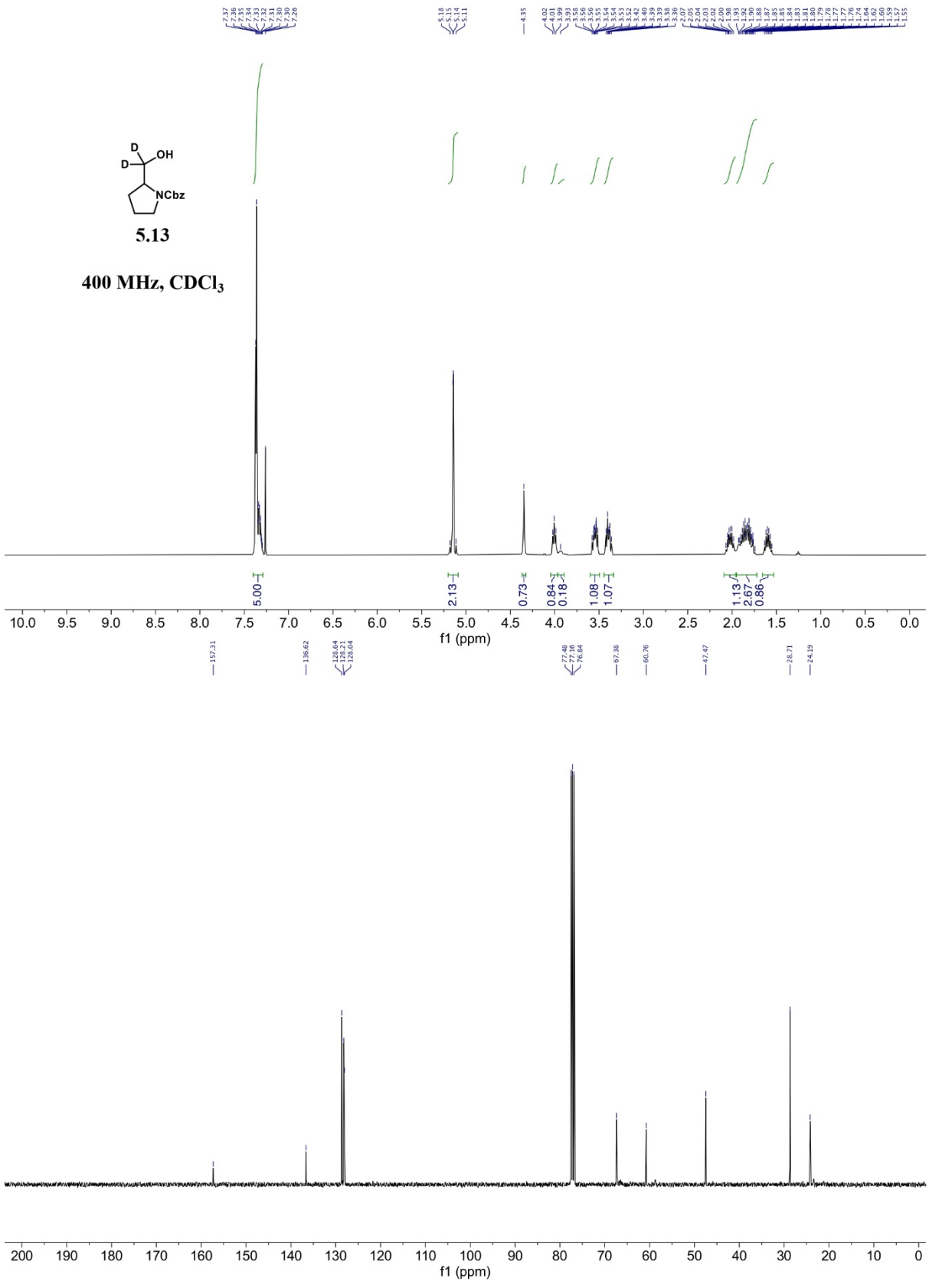



7.35
7.34
7.34
7.32
7.32
7.32
7.31
7.26 CDCl3
7.16
7.16
7.16
7.15
7.11
7.10
7.09
7.08
3.08
3.08
3.06
3.04
2.72
2.72
2.71
2.70
2.70
2.69
2.68
0.98
0.20
TBSO
O
5.10
300 MHz, CDCl3
1.00
0.90
0.96
2.01
1.99
9.12
5.86
f1 (ppm)
207.17
155.41
148.36
138.50
127.98
127.47
113.54
77.16 CDCl3
37.19
25.77
25.28
18.34
-4.35
f1 (ppm)


H
O
O
H
Me
5.11
400 MHz, CDCl3
f1 (ppm)


f1 (ppm)


CO2allyl
CO2allyl
PhN
O
5.12
400 MHz, CDCl3
f1 (ppm)
f1 (ppm)


D
D
OH
NCbz
5.13
400 MHz, CDCl3
f1 (ppm)
f1 (ppm)